



Sam Boggs, Jr.

Petrology of Sedimentary Rocks

SECOND EDITION

CAMBRIDGE

CAMBRIDGE

www.cambridge.org/9780521897167

This page intentionally left blank

PETROLOGY OF SEDIMENTARY ROCKS

SECOND EDITION

Petrology of Sedimentary Rocks is an advanced textbook describing the physical, chemical, and biologic properties of the major types of sedimentary rocks, as revealed by petrographic microscopy, geochemical techniques, and field study. It covers the mineralogy, chemistry, textures, and sedimentary structures that characterise sedimentary rocks, and relates these features to the depositional origin of the rocks and their subsequent alteration by diagenetic processes during burial. In addition to detailed sections on siliciclastic rocks (sandstones, shales, conglomerates) and carbonate rocks (limestones and dolomites), it also discusses evaporites, cherts, iron-rich sedimentary rocks, phosphorites, and carbonaceous sedimentary rocks such as oil shales.

This Second Edition maintains the fundamental structure of the original book, and presents a comprehensive treatment of sedimentary petrography and petrology. It has been thoroughly updated to include new concepts and ideas, and cutting-edge techniques such as cathodoluminescence imaging of sedimentary rocks and backscattered electron microscopy. Numerous photographs and diagrams illustrate characteristic features while an extensive and up-to-date reference list provides a useful starting point for additional literature research.

This textbook is designed for advanced undergraduate and graduate courses in sedimentary petrology. It is also a key reference for researchers and professional petroleum geoscientists wanting to develop an understanding of the petrologic characteristics of sedimentary rocks and their geological significance.

SAM BOGGS, Jr. received his Ph.D. from the University of Colorado and worked in the petroleum industry for a number of years before joining the University of Oregon, where he taught sedimentology and related subjects for more than 30 years, and where he continues his research in sedimentary petrology as a Professor Emeritus. He has also worked part-time as a research geologist for the US Geological Survey. Professor Boggs is a member of the Society for Sedimentary Geology (SEPM), the American Association of Petroleum Geologists, and the Geological Society of America. He is the author of two other books for Cambridge University Press – *Backscattered Scanning Electron Microscopy and Image Analysis of Sediments and Sedimentary Rocks* (1998) and *Application of Cathodoluminescence Imaging to Study of Sedimentary Rocks* (2006), as well as the author of four other books.

PETROLOGY OF
SEDIMENTARY ROCKS

SECOND EDITION

SAM BOGGS, JR.

University of Oregon



CAMBRIDGE
UNIVERSITY PRESS

CAMBRIDGE UNIVERSITY PRESS
Cambridge, New York, Melbourne, Madrid, Cape Town, Singapore,
São Paulo, Delhi, Dubai, Tokyo

Cambridge University Press
The Edinburgh Building, Cambridge CB2 8RU, UK

Published in the United States of America by Cambridge University Press, New York

www.cambridge.org

Information on this title: www.cambridge.org/9780521897167

© S. Boggs, Jr. 2009

This publication is in copyright. Subject to statutory exception and to the provision of relevant collective licensing agreements, no reproduction of any part may take place without the written permission of Cambridge University Press.

First published in print format 2009

ISBN-13 978-0-511-71933-2 eBook (NetLibrary)

ISBN-13 978-0-521-89716-7 Hardback

Cambridge University Press has no responsibility for the persistence or accuracy of urls for external or third-party internet websites referred to in this publication, and does not guarantee that any content on such websites is, or will remain, accurate or appropriate.

Dedicated to my father, Sam Boggs, Senior,
for all he gave.

Contents

<i>Preface</i>	<i>page ix</i>
Part I Principles	1
Chapter 1 Origin, classification, and occurrence of sedimentary rocks	3
Part II Siliciclastic sedimentary rocks	19
Chapter 2 Sedimentary textures	21
Chapter 3 Sedimentary structures	63
Chapter 4 Sandstones	111
Chapter 5 Conglomerates	165
Chapter 6 Mudstones and shales	194
Chapter 7 Provenance of siliciclastic sedimentary rocks	220
Chapter 8 Diagenesis of sandstones and shales	268
Part III Carbonate sedimentary rocks	311
Chapter 9 Limestones	313
Chapter 10 Dolomites	382
Chapter 11 Diagenesis of carbonate rocks	408
Part IV Other chemical/biochemical sedimentary rocks and carbonaceous sedimentary rocks	459
Chapter 12 Evaporites, cherts, iron-rich sedimentary rocks, and phosphorites	461
Chapter 13 Carbonaceous sedimentary rocks	527
<i>References</i>	556
<i>Index</i>	596

Preface

As indicated in the first edition, this book emphasizes the properties of sedimentary rocks rather than sedimentary processes. Thus, it focuses on description and discussion of mineralogic and chemical composition, as well as the textures and sedimentary structures that characterize sedimentary rocks. Further, it discusses application of insights derived from study of rock properties to interpretation of their origin, including provenance (sediment source), depositional environments, and diagenesis. Part I of the book deals with basic principles related to the origin, classification and occurrence of sedimentary rocks. Part II describes and discusses the siliciclastic sedimentary rocks such as sandstones. Part III describes the carbonate sedimentary rocks (e.g. limestones), and Part IV discusses other chemical sedimentary rocks and carbonaceous sedimentary rocks such as oil shales. The book is aimed at advanced undergraduate and graduate students; however, professional geologists may also find the book useful.

Sedimentary petrology is a broad scientific discipline that encompasses study of all kinds of sedimentary rocks, including those that constitute a relatively small volume of total sedimentary rocks. These volumetrically minor rock types nonetheless provide valuable insight into Earth history, and some are economically significant. Thus, the book gives significant coverage to minor rock types such as cherts, phosphorites and iron-rich sedimentary rocks, as well as to more abundant sedimentary rocks such as sandstones, shales and limestones, which make up the bulk of the sedimentary rock record.

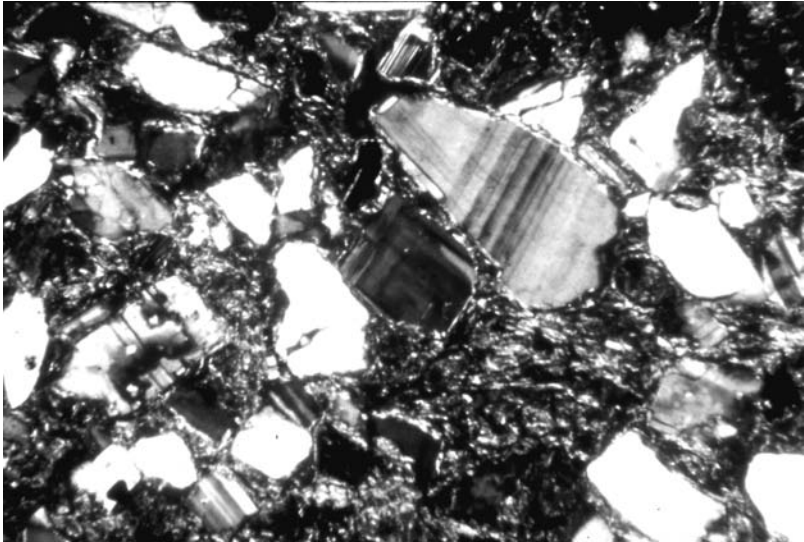
Petrologic study requires application of suitable techniques for field and laboratory observation and analysis. Several kinds of studies, such as measuring and describing sedimentary structures, are carried out in the field before specimens are collected for further analysis. In the laboratory, petrographic microscopy is a venerable, basic tool for studying the composition and texture of sedimentary rocks; however, it is being supplemented increasingly by a variety of other tools and techniques (see Chapter 1). Electron microscopy, cathodoluminescence microscopy, X-radiography, electron probe microanalysis, Fourier analysis and various kinds of spectroscopic analyses are examples of techniques that allow further optical, geochemical and physical characterization of sedimentary rocks. This book discusses applications of many of these techniques and furnishes references to

numerous published monographs that provide further in-depth discussion of analytical methods.

During preparation of *Petrology of Sedimentary Rocks*, I drew heavily upon the published work of numerous researchers. I wish to acknowledge the value of their contributions and to thank other individuals, including reviewers and editors, who contributed to the book.

Part I

Principles



Photomicrograph of a poorly sorted, Pleistocene volcanoclastic sandstone, Japan Sea

1

Origin, classification, and occurrence of sedimentary rocks

1.1 Introduction

Sedimentary rocks form at low temperatures and pressures at the surface of Earth owing to deposition by water, wind, or ice. By contrast, igneous and metamorphic rocks form mainly below Earth's surface where temperatures and pressures may be orders of magnitude higher than those at the surface, although volcanic rocks eventually cool at the surface. These fundamental differences in the origin of rocks lead to differences in physical and chemical characteristics that distinguish one kind of rock from another. Sedimentary rocks are characterized particularly by the presence of layers, although layers are also present in some volcanic and metamorphic rocks, and by distinctive textures and structures. Many sedimentary rocks are also distinguished from igneous and metamorphic rocks by their mineral and chemical compositions and fossil content.

Sedimentary rocks cover roughly three-fourths of Earth's surface. They have special genetic significance because their textures, structures, composition, and fossil content reveal the nature of past surface environments and life forms on Earth. Thus, they provide our only available clues to evolution of Earth's landscapes and life forms through time. These characteristics of sedimentary rocks are in themselves reason enough to study sedimentary rocks. In addition, many sedimentary rocks contain minerals and fossil fuels that have economic significance. Petroleum, natural gas, coal, salt, phosphorus, sulfur, iron and other metallic ores, and uranium are examples of some of the extremely important economic products that occur in sedimentary rocks.

Many different terms are used to describe the study of sedimentary rocks, including stratigraphy, sedimentation, sedimentology, and paleontology. This book deals with **sedimentary petrology**, which is that particular branch of study concerned especially with the composition, characteristics, and origins of sediments and sedimentary rocks. The book focuses on the physical, chemical, and biological characteristics of the principal kinds of sedimentary rocks; however, it is concerned also with the relationship of these properties to depositional conditions and provenance (sediment sources). I have attempted, where appropriate, to identify major problems and concerns regarding the origin of particular kinds of sedimentary rocks or particular properties of these rocks. Where controversy surrounds the origin, as with the origin of dolomites and iron-formations, different points of view are examined.

In this opening chapter of the book, I give a brief, generalized discussion of the origin, classification, occurrence, and study of sedimentary rocks. I also examine the tectonic setting of sediment accumulation. The composition of siliciclastic sedimentary rocks, in particular, is strongly influenced by tectonic provenance and the kinds of depositional basins and depositional conditions present in the tectonic setting. Therefore, it seems appropriate in this opening chapter to consider tectonic setting and basin architecture as a framework for discussion in succeeding chapters.

Chapters 2 and 3 examine the sedimentary textures and structures that are common to many kinds of sedimentary rocks. Chapter 4 describes the characteristics of sandstones, Chapter 5 discusses conglomerates, and Chapter 6 describes the characteristic features of shales and mudrocks. The extremely important topic of sediment provenance is discussed in Chapter 7, followed in Chapter 8 by discussion of diagenesis of siliciclastic sedimentary rocks. Chapters 9–13 deal with the chemical/biochemical sedimentary rocks. Chapter 9 describes limestones, Chapter 10 discusses dolomites, and Chapter 11 examines the diagenesis of these carbonate rocks. Chapter 12 describes the characteristics of evaporites, cherts, phosphorites, and iron-rich sedimentary rocks and discusses some of the controversial aspects of their origin. The final chapter of the book, Chapter 13, discusses the organic-rich, carbonaceous sedimentary rocks such as oil shales and coals.

1.2 Origin and classification of sedimentary rocks

As mentioned, all sedimentary rocks originate in some manner by deposition of sediment through the agencies of water, wind, or ice. They are the product of a complex, sequential succession of geologic processes that begin with **formation of source rocks** through intrusion, metamorphism, volcanism, and tectonic uplift. Physical, chemical, and biologic processes subsequently play important roles in determining the final sedimentary product. **Weathering** causes the physical and chemical breakdown of source rocks, leading to concentration of resistant particulate residues (mainly silicate mineral and rock fragments) and formation of secondary minerals such as clay minerals and iron oxides. At the same time, soluble constituents such as calcium, potassium, sodium, magnesium, and silica are released in solution. Soluble constituents are constantly carried from weathering sites in surface (and ground) waters that discharge ultimately into the ocean. **Explosive volcanism** may also contribute substantial quantities of particulate (pyroclastic) debris, including feldspars, volcanic rock fragments, and glass.

In time, particulates are removed from the land by erosion, and undergo **transportation** by water, wind, or ice to depositional basins at lower elevations. Within depositional basins, transport of particulates eventually stops when the particles are **deposited** below wave base. Soluble constituents delivered to basins by surface waters, or added to ocean water by water–rock interactions along mid-ocean spreading ridges, may eventually accumulate in basin waters in concentrations sufficiently high to cause their removal by inorganic processes. In many cases, however, precipitation of dissolved constituents is aided in some way by biologic processes. Also, plant or animal organic residues, which wash in from land or originate within the depositional basins, may be deposited along with land-derived detritus or chemical/biochemical precipitates.

After deposition of particulate sediment or chemical/biochemical precipitates, burial takes place as this sediment is covered by successive layers of younger sediment. The increased temperatures and pressures encountered during burial bring about **diagenesis** of the sediment, leading to solution and destruction of some constituents, generation of some new minerals in the sediment, and eventually consolidation and lithification of the sediment into sedimentary rock.

This highly generalized succession of sedimentary processes leads to generation of four fundamental kinds of constituents – terrigenous siliciclastic particles, chemical/biochemical constituents, carbonaceous constituents, and authigenic constituents – which, in various proportions, make up all sedimentary rock.

1. Terrigenous siliciclastic particles

The processes of terrestrial explosive volcanism and rock decomposition owing to weathering generate gravel- to mud-size particles that are either individual mineral grains or aggregates of minerals (rock fragments or clasts). The minerals are mainly silicates such as quartz, feldspars, and micas. The rock fragments are clasts of igneous, metamorphic, or older sedimentary rock that are also composed dominantly of silicate minerals. Further, fine-grained secondary minerals, particularly iron oxides and clay minerals, are generated at weathering sites by recombination and crystallization of chemical elements released from parent rocks during weathering. These land-derived minerals and rock fragments are subsequently transported as solids to depositional basins. Because of their largely extrabasinal origin and the fact that most of the particles are silicates, we commonly refer to them as terrigenous siliciclastic grains, although some pyroclastic particles may originate within depositional basins. These siliciclastic grains are the constituents that make up common sandstones, conglomerates, and shales.

2. Chemical/biochemical constituents

Chemical and biochemical processes operating within depositional basins may lead to extraction from basin water of soluble constituents to form minerals such as calcite, gypsum, and apatite, as well as formation of calcareous and siliceous tests or shells of organisms. Some precipitated minerals may become aggregated into silt- or sand-size grains that are moved about by currents and waves within the depositional basin. Carbonate ooids and pellets are familiar examples of such aggregate grains. There is no commonly accepted group name for precipitated minerals and mineral aggregates, analogous to the term siliciclastic; they are referred to here simply as chemical/biochemical constituents. These constituents are the materials that make up intrabasinal sedimentary rocks such as limestones, cherts, evaporites, and phosphorites.

3. Carbonaceous constituents

The preserved, carbonized residues of terrestrial plants and marine plants and animals, together with the petroleum bitumens, make up a third category of sedimentary constituents.

Humic carbonaceous materials are the woody residues of plant tissue and are the chief components of most coals. **Sapropelic** residues are the remains of spores, pollen, phyto- and zooplankton, and macerated plant debris that accumulate in water. They are the chief constituents of cannel coals and oil shales. **Bitumens** are solid asphaltic residues that form from petroleum through loss of volatiles, oxidation, and polymerization.

4. Authigenic constituents

Minerals precipitated from pore waters within the sedimentary pile during burial diagenesis constitute a fourth category of constituents. These secondary, or authigenic, constituents may include silicate minerals such as quartz, feldspars, clay minerals, and glauconite and nonsilicate minerals such as calcite, gypsum, barite, and hematite. They may be added during burial to any type of sedimentary rock but are never the dominant constituents of sedimentary rocks.

Depending upon the relative abundance of siliciclastic, chemical/biochemical, and carbonaceous constituents, we recognize three fundamental types of sedimentary rocks (Fig. 1.1): siliciclastic (terrigenous) sedimentary rocks, chemical/biochemical sedimentary rocks, and carbonaceous sedimentary rocks. As shown in Fig. 1.1, each of these major groups of sedimentary rocks can be further subdivided on the basis of grain size and/or mineral composition. Thus, the siliciclastic sedimentary rocks are divided by grain size into conglomerates/breccias, sandstones, and mudrocks (shales), each of which can be classified on a still finer scale on the basis of composition. The chemical/biochemical sedimentary rocks are divided by composition into carbonates, evaporites, cherts, ironstones and iron-formations, and phosphorites. Carbonaceous sedimentary rocks may be separated by composition into oil shales, impure coals, coals, and bitumens.

Although we recognize many types of sedimentary rocks on the basis of composition and grain size, only three of these rock types are volumetrically important. As discussed in greater detail below, mudrocks (shales), sandstones, and limestones make up the bulk of all sedimentary rocks in the rock record. The compositions, textures, and structures of sandstones and limestones make them particularly important as indicators of past depositional conditions. Therefore, I have placed major emphasis in this book on these two important groups of rocks.

1.3 Distribution of sedimentary rocks in space and time

Sedimentary rocks and sediments range in age from Precambrian to modern. The ages of the oldest known sedimentary rocks (in Greenland and northern Quebec, Canada) have been determined by iron isotope analyses to be about 3.7–3.8 billion years (e.g. Dauphas *et al.*, 2007). The first rocks that formed on Earth were probably basic volcanic rocks. Sedimentary rocks began to form once Earth's atmosphere and oceans had developed owing to degassing of Earth's interior.

The area of Earth's surface covered by sedimentary rocks has increased progressively with time as the area of volcanic rocks has been successively reduced by erosion (Fig. 1.2).

Composition		Group name	Particle size	Principal constituents	Main rock types
~15% Carbonaceous residues	<50% Terrigenous siliciclastic grains	or siliciclastic rocks	>2 mm	Rock fragments	Conglomerates and breccias
			1/16–2 mm	Silicate minerals and rock fragments	Sandstones
			<1/16 mm	Silicate minerals	Shales (mudrocks)
	>50% Chemical/biochemical constituents	Chemical/biochemical rocks	Variable	Carbonate minerals, grains; skeletal fragments	Carbonate rocks (limestones and dolomites)
				Evaporite minerals (sulfates, chlorides)	Evaporites (rock salt, gypsum, anhydrite)
				Chalcedony, opal, siliceous skeletal remains	Siliceous rocks (cherts and related rocks)
				Ferruginous minerals	Ironstones and iron-formations
				Phosphate minerals	Phosphorites
	>15% Carbonaceous residues	Carbonaceous rocks	Variable	Siliciclastic or chemical–biochemical constituents: carbonaceous residues	Oil shales Impure coals
				Carbonaceous residues	Humic coals Cannel coals Solid hydrocarbons (bitumens)

Figure 1.1 Classification of sedimentary rocks.

Sedimentary rocks now cover about 80 percent of the total land area of Earth (Ronov, 1983). They also cover most of the floor of the ocean, above a basement of volcanic rocks. According to Ronov, sedimentary rocks make up about 11 percent of the volume (9.5 percent of mass) of Earth’s crust and 0.1 percent of the volume (0.05 percent of mass) of the total Earth. Average thickness of Earth’s sedimentary shell is 2.2 km, but thickness varies widely in different parts of the continents and ocean basins.

Most of the volume of sedimentary rocks of Earth’s crust (about 70 percent) is concentrated on the continents, which make up about 29 percent of Earth’s surface (Ronov, 1983). About 13 percent of sedimentary rocks occur on the continental shelf and continental slope, which together make up about 14 percent of Earth’s surface. Approximately 17 percent of the total volume of sedimentary rocks occurs on the floors of the oceans, which constitute about 58 percent of Earth’s surface.

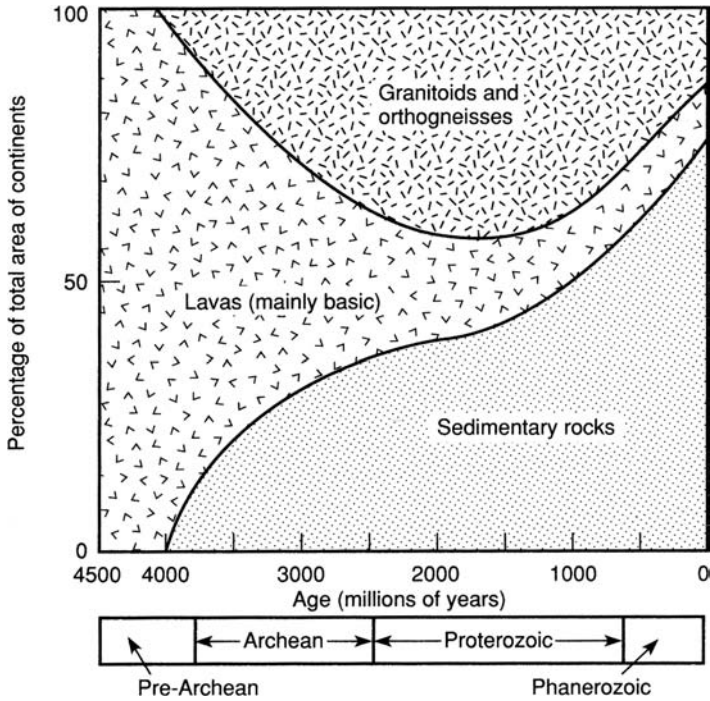


Figure 1.2 Percent of continents covered by most important groups of rocks as a function of age. (After Ronov, A. B., 1983, *The Earth's Sedimentary Shell*: American Geological Institute Reprint Series 5, Fig. 17, p. 31. Reproduced by permission.)

As mentioned, the rocks that make up Earth's sedimentary shell are mainly shales, sandstones, and carbonate rocks. Past estimates, by different workers, of the relative proportion of these rock types in the total sedimentary pile have varied significantly. Estimates by Ronov (1983), on the basis of data obtained by direct measurement of the distribution of the most important rock types, suggest that shales make up about 50 percent of the sedimentary rocks on the continents, sandstones 24 percent, carbonate rocks 24 percent, evaporites about 1 percent, and siliceous rocks (cherts) about 1 percent. In this tabulation, Ronov has apparently lumped iron-rich sedimentary rocks with carbonate rocks, possibly under the assumption that the iron-rich rocks formed by alteration of siderites (iron carbonates). Phosphorites and carbonaceous sedimentary rocks are omitted from the tabulation because their overall volume is quite small compared to that of the other sedimentary rocks. Conglomerates are probably included with sandstones.

The distribution of sedimentary rock types by age is shown in Fig. 1.3. Note that the relative volume of preserved shale per unit age has not changed significantly since early/middle (Archean) Precambrian time. Also, the volume of sandstone of various ages is fairly constant, although the proportion of different sandstone types (graywackes, arkoses, quartzitic sands) has changed somewhat through time. The most notable changes in volume of

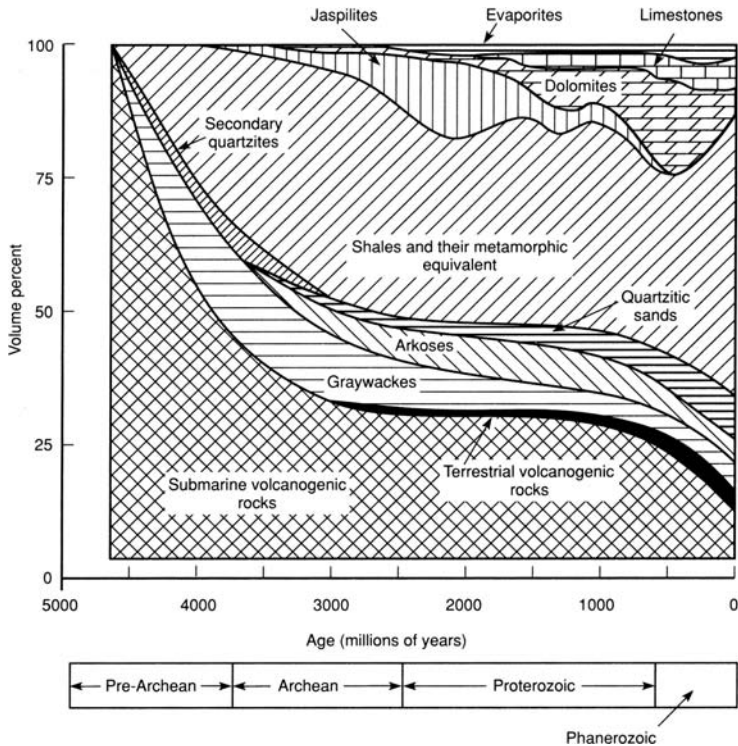


Figure 1.3 Volume percent of sedimentary rocks as a function of age. (After Ronov, A. B., 1983, *The Earth's Sedimentary Shell*: American Geological Institute Reprint Series 5, Fig. 19, p. 33. Reproduced by permission.)

preserved sediment per unit age are the marked decrease in iron-rich sedimentary rocks (jaspilites) after late Precambrian time and the significant increase in carbonate rocks and evaporites after the Precambrian.

1.4 Recycling of sedimentary rocks

Figure 1.4 depicts the mass of total sedimentary rocks graphed as a function of age of the rocks. This graph shows a very strong trend of increasing mass of sedimentary rock per unit time from the Precambrian into the Cenozoic. This trend reflects both rates of sedimentation and rates of erosion. Keep in mind that the volume of older sedimentary rocks has been progressively reduced through time by erosion. Thus, the volume of sediments shown for a given age in Fig. 1.4 does not represent the total volume of sediment deposited during that period of time. Rather, it is the preserved remnant of that original volume.

The particles that made up the first sedimentary rocks that formed on Earth were derived by erosion of basic volcanic rocks. Through time, the area of Earth's surface covered by sedimentary rocks increased as the area covered by basic volcanic rocks decreased

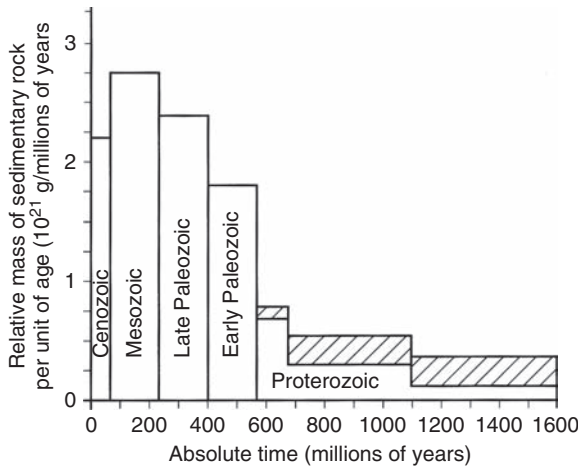


Figure 1.4 Relative volume of sedimentary rocks on the continents per unit of age. Crosshatched areas denote metamorphosed equivalents of the sedimentary rocks of late Proterozoic age. (After Ronov, A. B., 1983, *The Earth's Sedimentary Shell*: American Geological Institute Reprint Series 5, Fig. 8, p. 14. Reproduced by permission.)

(Fig. 1.2). Some of these early formed sedimentary rocks were ultimately uplifted after burial and lithification to become the source rocks for a new generation of sedimentary rocks. These sedimentary rocks, in turn, were subsequently uplifted and exposed to become the source rocks for a still younger generation of sedimentary rocks, and so on. The constituents that make up younger sedimentary rocks have thus been recycled through the processes of uplift, weathering, and erosion. The number of times that sedimentary rock of a particular type has been recycled is a function of both the tectonic setting of the rocks within a continental mass and the relative susceptibility of the rocks to destruction by weathering and erosion. Tectonic setting (and climate) governs the intensity of the weathering/erosion process; rock type determines the relative ease of destruction. In general, evaporites are the most soluble and most easily destroyed sedimentary rocks. Limestones are next, dolomites are third, and shales, sandstones, and volcanogenic sediments are fourth (Garrels and McKenzie, 1971). Owing to the greater susceptibility of evaporite rocks to destruction, Garrels and McKenzie suggest that such rocks may have been recycled up to 15 times in the last three billion years. Carbonate rocks have been recycled about 10 times and shales and sandstones 5 times.

Garrels and McKenzie suggest two possible models to account for recycling of sedimentary rocks through time. The **constant mass model** assumes an early degassing of the Earth. All the water of the hydrosphere and atmosphere was presumably released at this time, along with all the CO₂, HCl, and other acid gases that could react with primary igneous rock to form sedimentary rock. The total volume of sedimentary rock was thus created very early in Earth's history. Since that time, no completely new sediment has been created because no new acid gases have been released to create them. Through time, these early formed

sediments have been recycled owing to erosion and destruction by metamorphism, with concomitant recycling of CO₂ and HCl. The **linear accumulation model** assumes that water, CO₂, and HCl are being continuously degassed from Earth's interior at a linear rate. New sedimentary rocks have thus continued to form through time by breakdown of primary igneous rock. Therefore, the mass of sediments has grown linearly through time from zero to the currently existing mass. This model represents the extreme opposite conditions to those assumed in the constant mass model. It is possible, of course, that the real recycling process may have combined elements of the two models. That is, an early high rate of degassing may have been followed by a continuously decreasing, possibly irregular, rate of degassing.

In any case, either model could account for the volume of preserved sediment that now exists. What is important in studying the petrology of sedimentary rocks is to keep in mind that the recycling process has brought about some important changes in sedimentary rocks through time. For example, the mineralogy of siliciclastic sedimentary rocks must have been affected through time as chemically and mechanically less-stable minerals and rock fragments were selectively destroyed as they moved through several cycles of uplift, weathering, erosion, transportation, deposition, and diagenesis – moving sediments toward a state of greater compositional maturity (more quartz rich). Textural properties such as shape, roundness, and grain size must also have been affected by multiple cycling, resulting, for example, in enhanced rounding of detrital grains. Recycling of sediments has also produced changes through time in the bulk chemical composition of sedimentary rocks, particularly in the amounts of major elements such as Fe, Mn, Ca, Mg, K, Na, and Si. The patterns of chemical change as a function of time are complex and not easily generalized.

1.5 Tectonic setting of sediment accumulation

1.5.1 Introduction

The physical, chemical, and biological properties of sedimentary rocks are strongly influenced by the nature of sediment source areas (provenance) and the conditions of the depositional environment. The characteristics of source areas and depositional environments, in turn, are the result of the tectonic and geologic history of the region in which the sediments accumulate. For example, source rock types are intimately related to the regional tectonic setting; e.g. volcanic source rocks originate mainly within magmatic arc settings, plutonic igneous rocks are more characteristic of continental block provenances, and metamorphic and sedimentary source rocks typically occur in orogenic belts characterized by collision tectonics. Furthermore, the topographic expression and relief of source areas are controlled by uplift and deformation. Similarly, such aspects of the depositional environment as basin size and geometry, water depth, proximity to source areas, and rate of basin subsidence are influenced by the position of the depositional environment within the regional tectonic framework.

Tectonism, through its influence on provenance and depositional environments, thus exerts an important, indirect control on sedimentation patterns and sedimentary rock characteristics. We will examine more closely the nature of this relationship in appropriate sections of the book.

1.5.2 Plate tectonics and depositional basins

From about the 1860s to the 1960s, geological thought regarding the relationship of tectonics and sedimentation focused on the geosynclinal theory. This theory proposed that geosynclines are relatively narrow, elongate sediment-filled troughs that were located along the margins of continents or possibly within continents. Shallow-marine deposits putatively accumulated in these troughs to great thickness as a result of continued subsidence of the geosyncline caused by sediment loading or by downbuckling of Earth's crust owing to lateral compression generated by shrinking of the Earth.

While some geologists were still thinking and debating about geosynclines as late as the 1950s, a quiet geological revolution was under way that was soon to have a profound effect on every aspect of geological thinking. Spearheaded by geologists such as Harry Hess, Robert Dietz, and J. Tuzo Wilson, the concept of seafloor spreading and plate tectonics emerged in the late 1950s and early 1960s. Although the plate tectonics theory is now familiar to all geologists, the concept of spreading ridges, moving crustal plates, and subduction zones forced some dramatic new ideas about tectonics and sedimentation upon a reluctant generation of geologists weaned on geosynclinal concepts. Eventually, most geologists abandoned the geosynclinal concept in favor of the plate tectonics theory.

What became important to sedimentologists was developing a better understanding of the relationship between global tectonic settings and patterns of sedimentation. Central to all of this was the need to formulate models of depositional basins that are consistent with the characteristics of sedimentary rocks in the geologic record. Sedimentary basins are now commonly classified in terms of (1) the type of crust on which the basins rest, (2) the position of the basins with respect to plate margins, and (3) for basins lying close to a plate margin, the type of plate interactions occurring during sedimentation (e.g. Miall, 1990, p. 501).

Several classifications of sedimentary basins that take into account these criteria have been proposed. Perhaps the most comprehensive basin model is that of Busby and Ingersoll (1995), who classify depositional basins into 5 major types and 26 subtypes (Table 1.1). Figure 1.5 illustrates several of the more important types of depositional basins. A summary of major characteristics of these basins and the kinds of sedimentary rocks deposited in the basins is given in Boggs (2006, pp. 554–568), and is not repeated herein. The factors that control or affect depositional processes and the resulting sediment characteristics include:

1. The lithology of the parent rock (e.g. granite, metamorphic rock) in the sediment source area, which controls the composition of sediment derived from these source rocks.
2. The relief, slope, and climate of the source area, which controls the rate of sediment denudation, the survivability of unstable minerals, and the rate at which sediment is delivered to depositional basins. The climate of the depositional basin is also important because it affects sedimentary processes such as transport of sediment by wind, water, or ice.
3. The rate of basin subsidence, together with rates of sea-level rise or fall, determines the **accumulation space** – the space available at any time in which sediments can accumulate.
4. The size and shape of the basins, which places limits on the volume of sediments that can accumulate.

Table 1.1 Major kinds of sedimentary basins and their tectonic setting

Divergent settings

Terrestrial rift valleys:	Rifts within continental crust commonly associated with bimodal volcanism. Modern example: Rio Grand rift (New Mexico)
Proto-oceanic rift troughs:	Incipient oceanic basins floored by new oceanic crust and flanked by young rifted continental margins. Modern example: Red Sea

Intraplate settings

Continental rises and terraces:	Mature rifted continental margins in intraplate settings at continental–oceanic interfaces. Modern example: East Coast of USA
Continental embankments:	Progradational sediment wedges constructed off edges of rifted continental margins. Modern example: Mississippi Gulf Coast
Intracratonic basins:	Broad cratonic basins floored by fossil rifts in axial zones. Modern example: Chad Basin (Africa)
Continental platforms:	Stable cratons covered with thin and laterally extensive sedimentary strata. Modern example: Barents Sea (Asia)
Active ocean basins:	Basins floored by oceanic crust formed at divergent plate boundaries unrelated to arc-trench systems (spreading still active). Modern example: Pacific Ocean
Oceanic islands, aseismic ridges and plateaus:	Sedimentary aprons and platforms formed in intraoceanic settings other than magmatic arcs. Modern example: Emperor-Hawaii seamounts
Dormant ocean basins:	Basins floored by oceanic crust, which is neither spreading nor subducting (no active plate boundaries within or adjoining basin). Modern example: Gulf of Mexico

Convergent settings

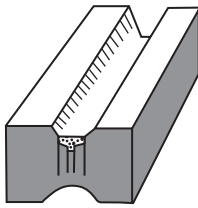
Trenches:	Deep troughs formed by subduction of oceanic lithosphere. Modern example: Chile Trench
Trench-slope basins:	Local structural depressions developed on subduction complexes. Modern example: Central America Trench
Forearc basins:	Basins within arc-trench gaps. Modern example: Sumatra
Intraarc basins	Basins along arc platform, which includes superposed and overlapping volcanoes. Modern example: Lago de Nicaragua
Backarc basins:	Oceanic basins behind intraoceanic magmatic arcs (including interarc basins between active and remnant arcs), and continental basins behind continental-margin magmatic arcs without foreland foldthrust belts. Modern example: Marianas
Retroarc foreland basins:	Foreland basins on continental sides of continental-margin arc-trench systems (formed by subduction-generated compression and/or collision). Modern example: Andes foothills

Table 1.1 (*cont.*)

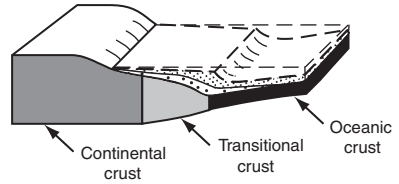
Remnant ocean basins:	Shrinking ocean basins caught between colliding continental margins and/or arc-trench systems, and ultimately subducted or deformed within suture belts. Modern example: Bay of Bengal
Peripheral foreland basins:	Foreland basins above rifted continental margins that have been pulled into subduction zones during crustal collisions (primary type of collision-related forelands). Modern example: Persian Gulf
Piggyback basins:	Basins formed and carried atop moving thrust sheets. Modern example: Peshawar Basin (Pakistan)
Foreland intermontane basins (broken forelands):	Basins formed among basement-cored uplifts in foreland settings. Modern example: Sierras Pampeanas basins (Argentina)
<i>Transform settings</i>	
Transensional basins:	Basins formed by extension along strike-slip fault systems. Modern example: Salton Sea (California)
Transpressional basins:	Basins formed by compression along strike-slip fault systems. Modern example: Santa Barbara Basin (California) (foreland)
Transrotational basins:	Basins formed by rotation of crustal blocks about vertical axes within strike-slip fault systems. Modern example: Western Aleutian forearc (?)
<i>Hybrid settings</i>	
Intracontinental wrench basins:	Diverse basins formed within and on continental crust due to distant collisional processes. Modern example: Qaidam Basin (China)
Aulacogens:	Former failed rifts at high angles to continental margins, which have been reactivated during convergent tectonics, so that they are at high angles to orogenic belts. Modern example: Mississippi embayment
Impactogens:	Rifts formed at high angles to orogenic belts, without preorogenic history (in contrast with aulacogens). Modern example: Baikal rift (Siberia) (distal)
Successor basins:	Basins formed in intermontane settings following cessation of local orogenic or taphrogenic activity. Modern example: Southern Basin and Range (Arizona)

Basin classification – modified after Dickinson, 1974, 1976, and Ingersoll, 1988. *Source:* Ingersoll, R. V. and C. J. Busby, 1995, Tectonics of sedimentary basins, in Busby, C. J. and R. V. Ingersoll (eds.), *Tectonics of Sedimentary Basins*: Blackwell Science, Oxford, Table 1.1, p. 3, Table 1.2, p. 5.

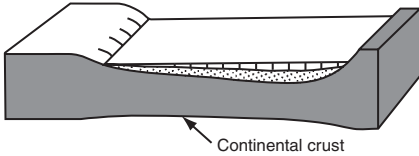
Reproduced by permission.



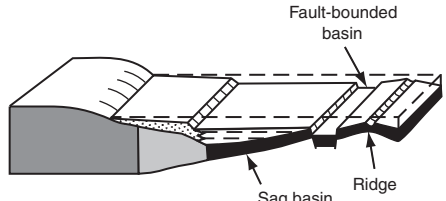
A. Rift graben



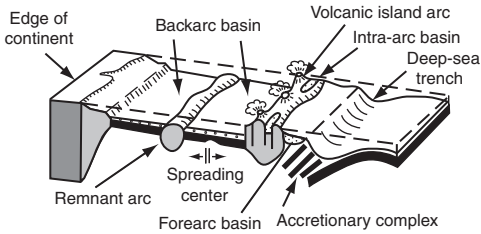
B. Passive-margin basins (continental rises and terraces)



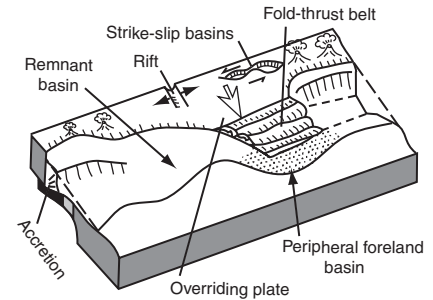
C. Intracratonic basin



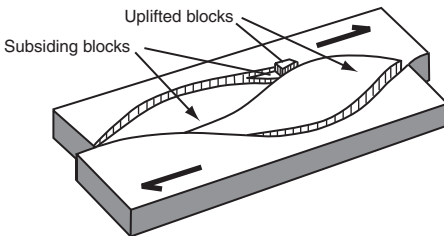
D. Basins floored by oceanic crust



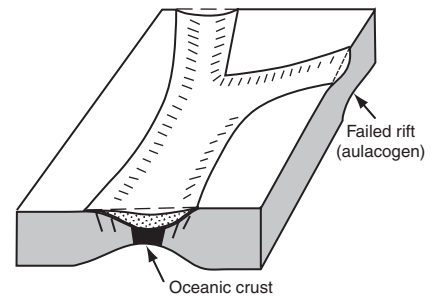
E. Subduction-related basin



F. Collision-related basins



G. Transform-fault-related basin



H. Aulacogen

Figure 1.5 Schematic representation of selected kinds of tectonically formed basins. (After Boggs, S., 2006, *Principles of Sedimentology and Stratigraphy*, 4th edn.: Prentice Hall, Upper Saddle River, NJ., Fig. 16.3, p. 556. Reproduced by permission.)

A close relationship exists between the tectonic setting of the sediment source area(s), the characteristics of the depositional basin, and the kinds of sedimentary rocks that accumulate in the basins. Tectonic setting governs the kinds of source rocks available to furnish sediment to depositional basins and thus the **composition** of sediments furnished to these basins. The physical characteristics of basins and the nature of depositional processes within basins, such as water depth and velocity, influence the characteristics of the deposited sediment, e.g., size and shape of sediment grains and kinds of sedimentary structures. Therefore, understanding the relationship between sedimentary rock characteristics and depositional processes is essential to interpretation of sediment source areas (provenance), paleogeography, and paleoenvironments in order to unravel Earth history.

1.6 Study of sedimentary rocks

1.6.1 Field study

Geologists can gain indispensable clues to geologic history through field studies of stratification styles, bedding characteristics, and sedimentary structures. It is in the field also that samples are collected for all subsequent laboratory analyses. Depending upon the objectives of the investigation, field studies of sedimentary rocks can range from simple reconnaissance descriptions of principal rock types to detailed geophysical investigations. The more common types of field studies performed by a single investigator or small groups of investigators include: mapping the distribution of formations or rock types (geologic mapping); determining lateral and vertical changes in lithofacies or biofacies; measuring the thickness of rock units; describing textural properties and sedimentary structures; measuring the orientation of directional sedimentary structures such as cross-bedding; identifying mineral components of rocks; studying modern sedimentation processes such as sediment transport and deposition; and collecting samples for later laboratory analysis. Numerous books have been published over the years that describe the various methods of field study and mapping. Recent examples of such books include Assaad *et al.* (2004), Bhattacharyya (2000), Stow (2005), and Tucker (2003).

Sampling is a critically important aspect of field work because the value of interpretations based on laboratory analyses of sedimentary rocks is uniquely dependent upon the sampling technique used in the field. Exhaustive laboratory analysis of samples is useless if samples are not representative of the unit investigated. In fact, improperly collected samples are worse than useless because they can lead to erroneous conclusions. Griffith (1971) philosophized that sampling is like religion: “*Everybody is for it, but few seem to practice it.*” Field sampling is performed to obtain samples for laboratory analysis of many different rock properties, such as chemical and mineral composition, isotopic composition, grain size, grain shape, and fossil content. Sampling methods vary with the intended purpose of the analysis and the type of rock being sampled. For example, the technique used to collect samples from a vertical exposure of heterogeneous, layered, consolidated sedimentary rock will differ from the method used to sample the surface layer of a relatively homogeneous,

unconsolidated modern beach or fluvial deposit. An investigator may be concerned primarily with differences between beds in the layered rocks but interested only in spatial variations within the surface layer of the unconsolidated deposits. A paleontologist may take spot samples from several different beds in a layered sequence if the object is to establish differences in fossil assemblages from bed to bed, but may take a channel sample across all the beds if concerned only with the total assemblage of fossils in the beds. It is hardly possible to overemphasize the importance of using the proper sampling technique for a given situation. The problem of selecting the proper technique is compounded if the investigator at the time of sample collection has only a hazy notion of the intended purpose of the samples.

Detailed discussion of the theory and practice of sampling is beyond the scope of this book. The serious student or investigator will, however, make an effort to become familiar with sampling methods before beginning a sampling project. Lewis and McConchie (1994, pp. 48–60) provide a concise description of sampling techniques and sampling equipment, as well as an extended bibliography dealing with sampling. Thompson (2002) presents a more comprehensive, rigorous discussion of sampling theory. Shorter articles that describe specific aspects of sampling, such as sampling stream deposits or lake sediments, may be found by accessing appropriate library databases such as **GeoRef** and **GeoBase**.

1.6.2 *Laboratory study*

Petrographic microscopy has been an essential tool for petrologic study since Henry Clifton Sorby pioneered a new branch of geology, “microscopical petrography,” in 1849; however, petrographic microscopy is only one of the many techniques available for laboratory study of sedimentary rocks. Some techniques, such as sieve and pipette analyses for sediment grain-size determination, are time-tested methods that have been around for several decades. Other techniques such as X-radiography of sedimentary structures, grain-shape studies involving computer-assisted Fourier analysis, electron microscopy of very small particles – including backscattered electron microscopy, cathodoluminescence studies of carbonates and silicates, and chemical analysis of sediments by techniques such as X-ray fluorescence and ICP (inductively coupled argon plasma emission spectrometry) are comparatively recent developments.

It is not feasible here to attempt description of the various laboratory methods of studying sedimentary rocks; however, several available books discuss these methods in detail. Carver (1971) is a dated but still useful volume that contains numerous papers dealing with textural and mineralogical analysis of sediments and sedimentary rocks. Tucker (1988) is a more recent, multi-author volume that also describes textural analysis and petrographic microscopical techniques, as well as more specialized techniques such as electron microscopy and cathodoluminescence microscopy. Useful atlases that depict the characteristics of sedimentary rocks as seen under the petrographic microscope include Adams and Mackenzie (1998), MacKenzie and Adams (1994), Scholle (1978, 1979), and Scholle and Ulmer-Scholle (2003).

Krinsley *et al.* (1998) evaluate the use of backscattered electron microscopy (BSE) in the study of sediments and sedimentary rocks, especially study of fine-grained rocks. Boggs and

Krinsley (2006) discuss application of cathodoluminescence imaging to study of sedimentary rocks, particularly provenance analysis. Chemical analysis of minerals and rocks has become routine by using electron probe microanalysis (EPMA); e.g. Reed and Romanenko (1995). More sensitive chemical analysis at low trace-element concentration levels is possible by using techniques such as secondary mass spectrometry (SIMS) and laser-ablation-inductively coupled plasma mass spectrometry (LA-ICP-MS); see for example MacRae (1995) and Ridley and Lichte (1998). Many of these techniques are summarized in Boggs and Krinsley (2006; ch. 3). Many issues of the *Journal of Sedimentary Petrology* also contain notes and full-length articles describing special methods for measuring or analyzing sedimentary rock properties.

1.6.3 Basin analysis

In recent years, it has become popular to refer to detailed stratigraphic and sedimentologic analysis of depositional systems as **basin analysis**. Basin analysis may include aspects of magnetostratigraphy, seismic stratigraphy, sequence stratigraphy, and radiometric age dating, as well as more conventional stratigraphic and petrologic analysis, including provenance study. Such comprehensive analysis is rarely possible for an individual investigator but is becoming increasingly important in larger research efforts. Numerous books are available that provide detailed information about basin analysis. See, for example, Allen and Allen (2005), Busby and Ingersoll (1995), and Miall (2000).

Further reading

- Allen, P. A. and J. R. Allen, 2005, *Basin Analysis: Principles and Applications*, 2nd edn.: Blackwell Publishing, Malden, MA.
- Bhattacharyya, A., 2000, *Analysis of Sedimentary Successions: a Field Manual*: A. A. Balkema, Rotterdam.
- Boggs, S., Jr. and D. Krinsley, 2006, *Application of Cathodoluminescence Imaging to Study of Sedimentary Rocks*: Cambridge University Press, Cambridge.
- Busby, C. J. and R. V. Ingersoll (eds.), 1995, *Tectonics of Sedimentary Basins*: Blackwell Science, Cambridge, MA.
- Krinsley, D. H., K. Pye, S. Boggs, Jr., and N. K. Tovey, 1998, *Backscattered Scanning Electron Microscopy and Image Analysis of Sediments and Sedimentary Rocks*: Cambridge University Press, Cambridge.
- MacKenzie, W. S. and A. E. Adams, 1994, *A Colour Atlas of Rocks and Minerals in Thin Section*: Manson Publishing, London.
- Miall, A. D., 2000, *Principles of Sedimentary Basin Analysis*, 3rd edn.: Springer-Verlag, New York.
- Stow, D. A. V., 2003, *Sedimentary Rocks in the Field: A Color Guide*: Elsevier, Burlington, MA.
- Tucker, M. (ed.), 1988, *Techniques in Sedimentology*: Blackwell Scientific, Oxford.

Part II

Siliciclastic sedimentary rocks



De Chelly Sandstone (Permian) exposed in Canyon de Chelly, Arizona

2

Sedimentary textures

2.1 Introduction

Few subjects in the field of sedimentology have been researched more thoroughly than sedimentary textures. This strong interest in sedimentary textures has apparently arisen out of the conviction of many workers that sedimentary texture is a valuable tool for environmental analysis. The sizes, shapes, and arrangement (fabric) of siliciclastic grains have been examined and reexamined over a period of decades in an effort to establish through empirical and experimental studies the validity of this assumption. Unfortunately, this goal of environmental interpretation remains elusive, and many problems still beset investigators who attempt to use sedimentary texture as a tool for environmental analysis. Nonetheless, texture is a fundamental attribute of siliciclastic sedimentary rocks. Along with other properties of these rocks, it helps to characterize and distinguish them from other types of rocks and it aids in their correlation. Furthermore, the texture of sedimentary rocks affects such derived properties of these rocks as porosity, permeability, bulk density, electrical conductivity, and sound transmissibility. These derived properties are of particular interest to petroleum geologists, hydrologists, and geophysicists.

Sedimentary texture encompasses three fundamental properties of sedimentary rocks: grain size, grain shape (form, roundness, and surface texture [microrelief] of grains), and fabric (grain packing and orientation). Grain size and shape are properties of individual grains. Fabric is a property of grain aggregates. The characteristics of each of these properties are explored in this chapter.

2.2 Grain size

2.2.1 Grain-size scales

Natural siliciclastic particles range in size from clay to boulders. Because of this wide range of sizes, the most useful grade scales for expressing particle size are logarithmic or geometric scales that have a fixed ratio between successive elements of the series. The grade scale most widely used by sedimentologists is the **Udden–Wentworth scale** (Wentworth, 1922). Each value in this scale is either two times larger than the preceding value or one-half as large, depending upon the sense of direction (Table 2.1). The Udden–Wentworth scale extends from

Table 2.1 *Udden–Wentworth grain-size scale for sediments and the equivalent phi (ϕ) scale*

		US Standard sieve mesh	Millimeters	Phi (ϕ) units	Wentworth size class
GRAVEL			4096	-12	
			1024	-10	Boulder
			256	-8	
			64	-6	Cobble
			16	-4	
		5	4	-2	Pebble
		6	3.36	-1.75	
		7	2.83	-1.5	Granule
		8	2.38	-1.25	
		10	2.00	-1.0	
SAND		12	1.68	-0.75	
		14	1.41	-0.5	Very coarse sand
		16	1.19	-0.25	
		18	1.00	0.0	
		20	0.84	0.25	
		25	0.71	0.5	Coarse sand
		30	0.59	0.75	
		35	0.50	1.0	
		40	0.42	1.25	
		45	0.35	1.5	Medium sand
		50	0.30	1.75	
		60	0.25	2.0	
		70	0.210	2.25	
		80	0.177	2.5	Fine sand
		100	0.149	2.75	
		120	0.125	3.0	
		140	0.105	3.25	
		170	0.088	3.5	Very fine sand
		200	0.074	3.75	
	MUD	SILT	230	0.0625	4.0
270			0.053	4.25	
325			0.044	4.5	Coarse silt
			0.037	4.75	
			0.031	5.0	
			0.0156	6.0	Medium silt
			0.0078	7.0	Fine silt
CLAY			0.0039	8.0	Very fine silt
			0.0020	9.0	
			0.00098	10.0	Clay
			0.00049	11.0	
			0.00024	12.0	
			0.00012	13.0	
			0.00006	14.0	

< 1/256 mm (0.0039 mm) to > 256 mm and is divided into four major size categories (clay, silt, sand, and gravel). Some of these major size categories can be further subdivided, as shown in Table 2.1.

Although the Udden–Wentworth scale adequately expresses the wide range of particle sizes found in natural sediments and sedimentary rocks, it does not lend itself especially well to the purposes of graphical plotting and statistical calculations. Because the magnitude of each size class in the scale is different, and because many of the size classes are in fractions of millimeters, the scale is difficult to work with when graphing. This problem can be avoided in part by plotting the logarithm to base 10 of the millimeter sizes. This procedure yields even-size divisions, but the divisions have fractional values. The phi (ϕ) scale is a

logarithmic scale to base 2 that overcomes this problem of fractional size classes by allowing grain-size classes to be expressed in integers. The scale is based on the relationship

$$\phi = \log_2 S \quad (2.1)$$

where ϕ is phi size and S is grain size in millimeters. Equivalent phi and millimeter sizes are shown in Table 2.1. Note that increasing absolute value of negative phi numbers indicates increasing millimeter size, whereas increasing positive phi numbers indicate decreasing millimeter size.

2.2.2 Measuring grain size

Methods

Several methods for measuring the grain size of siliciclastic particles are available, with the choice of methods depending upon the sizes of the particles and their state of consolidation (Table 2.2). Some of these measurement techniques have been used for several decades; others are comparatively new. The principal methods of interest are described below.

Unconsolidated sediment

Older, conventional techniques for measuring the grain size of unconsolidated **sandy sediment** include **sieving** (see discussion in Folk, 1974, pp. 33–35 and Ingram, 1971) and

Table 2.2 *Methods of measuring sediment grain size*

Type of sample	Sample grade	Method of analysis
Unconsolidated sediment and disaggregated sedimentary rock	Boulders Cobbles Pebbles	Manual measurement of individual clasts
	Granules Sand Silt	Sieving, settling-tube analysis, image analysis
	Clay	Pipette analysis, sedimentation balances, Sedigraph, laser diffractometry, electro-resistance size analysis (e.g. Coulter Counter)
Lithified sedimentary rock	Boulders Cobbles Pebbles	Manual measurement of individual clasts
	Granules Sand Silt	Thin-section measurement, image analysis
	Clay	Electron microscopy

sedimentation methods that involve measuring the fall time of particles through water in a settling tube (Galehouse, 1971; Syvitski *et al.*, 1991, pp. 45–63). Fall time can be equated empirically to particle diameter. More recently, automated settling tubes (so-called rapid sediment analyzers) have been developed that allow grain size of sandy sediment to be measured rapidly and easily. The weight of sediment accumulating in a pan at the bottom of the settling tube, or change in pressure of the water column as sediment settles, is automatically measured as a function of time. The resulting data are simultaneously recorded on an X - Y plotter or chart recorder as a cumulative curve. When the curve is properly calibrated, grain size can be read from it. The latest development in rapid sediment analysis is to feed the output from the analyzer directly into a microcomputer which, with appropriate software, digitizes the data. The computer then calculates grain-size statistics and produces various kinds of grain-size graphs or charts (e.g. Poppe *et al.*, 1985).

Most methods for measuring the grain size of **fine-size sediment** (fine silt and clay) are based in some way upon **Stokes' law**

$$D = \frac{\sqrt{V}}{\sqrt{C}} \quad (2.2)$$

where D is particle diameter in centimeters, V is settling velocity, and C is a constant that equals $(\rho_s - \rho_f)g/18\eta$, in which ρ_s is the density of the settling grains, ρ_f is density of the fluid, η is viscosity of the fluid, and g is gravitational acceleration.

The standard, conventional way of measuring particle size on the basis of Stokes' law is by **pipette analysis** (e.g. Galehouse, 1971). Fine, unconsolidated sediment is stirred into a suspension in a measured volume of distilled water in a settling tube. Uniform-size aliquots of this suspension are withdrawn with a pipette at specified times, evaporated to dryness in an oven, and weighed. These weight data can then be used in a modified version of Stokes' law to calculate particle diameter

$$D = \frac{\sqrt{x/t}}{\sqrt{C}} \quad (2.3)$$

where x is the depth in cm to which particles have settled in a given time (withdrawal depth), t is the elapsed time in seconds, and $x/t = V$ (settling velocity).

Because pipette analysis is such a laborious and time-consuming process, several automated techniques for measuring the grain size of fine-grained sediment have now been developed, most of which are also based on Stokes' law. These methods require the use of sophisticated (and expensive) equipment that may not be available in every sedimentology laboratory.

Sedimentation balances are a type of automated settling tube for fine sediment that work on much the same principle as rapid sediment analyzers for sandy sediment; fine sediment is continuously weighed as it collects on a pan at the bottom of the settling tube. The **Sedigraph** is an automated particle size analyzer that determines the size of particles dispersed in a liquid by measuring the attenuation of a finely collimated X-ray beam as a

function of time and height in a settling suspension. The transmitted X-ray intensity increases with time as particles settle out of suspension and thereby decrease X-ray absorption. X-Ray intensity is electronically transferred into concentration values and indicated linearly on the Y-axis of an X-Y chart recorder (Stein, 1985; Coakley and Syvitski, 1991). The data output can be either a printout of size statistics or be in a graphical form specified by the analyst.

A **laser-diffraction size analyzer** operates on the principle that particles of a given size diffract light through a given angle, the angle increasing with decreasing size (e.g. McCave *et al.*, 1986). According to McCave *et al.*, a narrow beam of monochromatic light from an He-Ne laser is passed through a sediment suspension and the diffracted light focused onto a detector. This process senses the angular distribution of scattered light energy. "A lens placed between the illuminated sample with the detector at its focal point focuses the undiffracted light to a point at the center and leaves only the surrounding diffraction pattern, which does not vary with particle movement. Thus, a stream of particles can be passed through the beam to generate a stable diffraction pattern. By using a computer, it is possible to optimize the size distribution accounting for the light-energy distribution." For additional discussion of laser-diffraction size analysis, see Agrawal *et al.* (1991), Sperazza (2004), and Blott (2004).

Electro-resistance size analyzers such as the Coulter Counter or Electrozone Particle Counter measure grain size on the basis of the principle that a particle passing through an electrical field maintained in an electrolyte will displace its own volume of the electrolyte and thus cause a change in the field. Particles are dispersed in a suitable electrolyte and forced to flow through an aperture one at a time. As each particle passes through the aperture, the properties of the field change. These changes are scaled and counted as voltage pulses. The magnitude of each pulse is proportional to particle volume, and the number of pulses is a function of particle concentration. By counting the number of pulses of various magnitudes, the volume percentages of particles of different sizes can be determined (Swift *et al.*, 1972; Milligan and Kranck, 1991; McTainsh, 1997). By interfacing microcomputers to the particle size analyzer, through appropriate amplifiers and software, great speed and high resolution in data collection can be achieved.

These various methods of measuring the grain size of fine-grained unconsolidated sediment may give slightly different results because they are based on somewhat different principles. For a comparison of the results of size analysis by some of these techniques, see Singer *et al.* (1988), Grewal (1991), Konert (1997), and Beuselinck (1998).

Consolidated sedimentary rock

The grain size of consolidated sedimentary rocks that cannot be adequately disaggregated cannot be measured by the various techniques described above. The conventional technique for measuring sand- and coarse-silt-size grains in consolidated rocks is measurement in thin sections by use of a petrographic microscope fitted with an ocular micrometer. The grain size determined in this way is the section diameter of randomly oriented grains, which is commonly smaller than the maximum diameter of the grains. This phenomenon is

sometimes referred to as the **corpuscle effect** (Burger and Skala, 1976), meaning that grains cut marginally in a thin-section plane have smaller apparent diameters. Thin-section measurements do not yield the same results as sieve analysis, which measures the intermediate diameter of grains. Therefore, thin-section grain-size measurements are commonly corrected in some way to make them agree more closely with sieve data (Friedman, 1962; Burger and Skala, 1976; Piazzola and Cavaroc, 1991; Johnson, 1994).

A more sophisticated (and expensive) method of measuring the size of particles in thin section is available by using so-called **image analysis** (Ehrlich *et al.*, 1984; Schäfer and Teyssen, 1987; Kennedy and Mazzullo, 1991; Van den Berg *et al.*, 2003). With this system, a television camera with a special viewing tube is mounted on a petrographic microscope. The camera feeds an image to a high-resolution television monitor and to a video digitizer (analog/digital converter) that converts the analog television signal to digital form and that is controlled by a microprocessor (e.g. microcomputer or minicomputer). The television camera views the grains through the microscope and projects an image of the grains onto the monitor or onto a digitizer tablet. A grain to be measured is encircled on the monitor or digitizer table with the cursor or a pen stylus. The boundary of the grain is “seen” as pixel units. Pixels are electronically digitized arrays or squares, and each pixel is defined by two spatial coordinates (X, Y) and a gray-level intensity value, which is a measure of brightness. The area of the particle in pixel units can then be calculated from a special formula (e.g. Kennedy and Mazzullo, 1991). A conversion factor is used to convert the data from square pixels to square micrometers, from which the diameter of the particle is calculated. Fine silt- and clay-size particles in consolidated rocks can also be studied by using an **electron microscope**, although the electron microscope is not routinely used as a tool for grain-size measurement.

Image analysis is especially useful for measuring the size of grains in consolidated rocks where the grains cannot be measured by sieving or settling-tube methods. The method can be applied equally well to measurement of loose grains in unconsolidated sediment (Kennedy and Mazzullo, 1991; Francus, 1998).

2.2.3 Reducing and displaying grain-size data

Graphical methods

The measurement techniques described in Table 2.2 yield large amounts of data that must be reduced in some way before meaningful comparison can be made between different sediment samples. The techniques for reducing and presenting grain-size data include both graphical and statistical or quasistatistical methods. Graphical presentation of grain-size data commonly involves plotting the data on bivariate diagrams in which either individual weight percent of each grain-size class or cumulative weight percent is plotted against phi size (Fig. 2.1). **Histograms** (Fig. 2.1A) are bar diagrams constructed by plotting individual weight percent (frequency) along the ordinate and the phi size of each size class along the abscissa. Such diagrams provide an easily visualized pictorial representation of the grain-size distribution, but their shape is affected by the phi-size intervals selected for

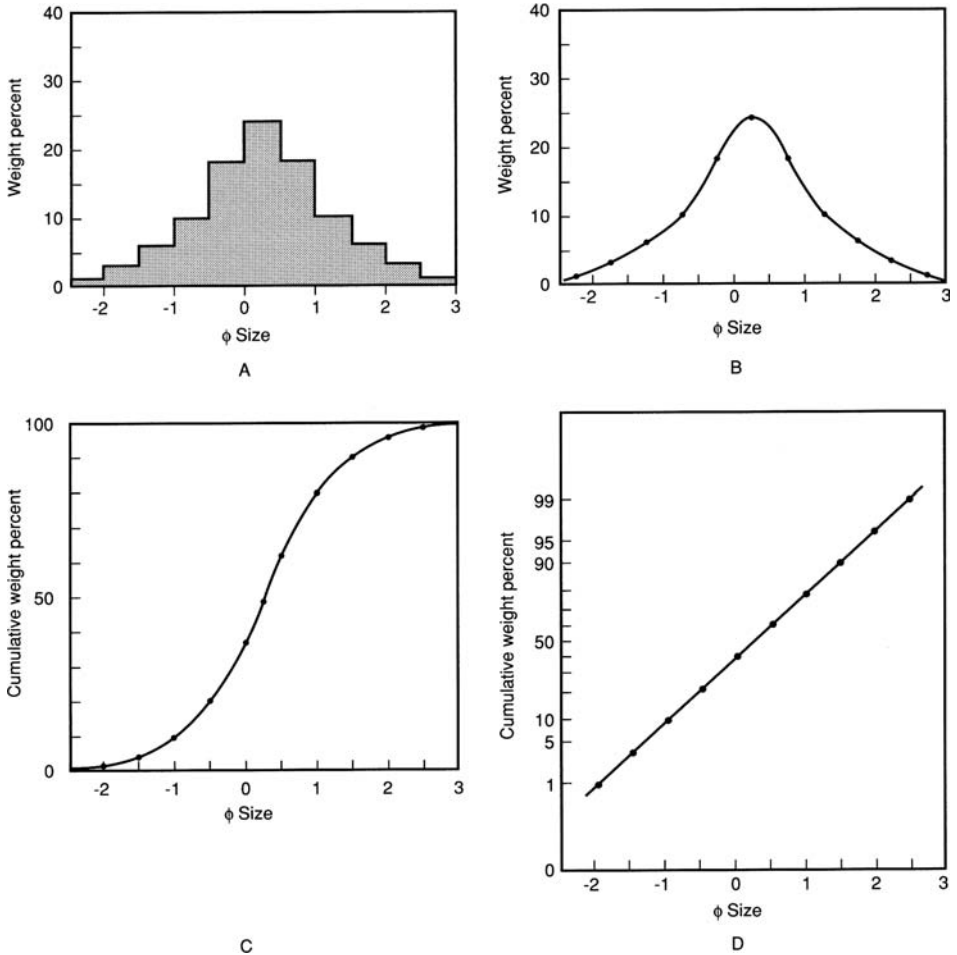


Figure 2.1 A hypothetical, nearly log-normal grain-size distribution plotted as a histogram (A), a frequency curve (B), a cumulative curve with an arithmetic ordinate (C), and a cumulative curve with a log-probability ordinate (D).

plotting ($1/4$, $1/2$, etc.). A **frequency curve** is similar to a histogram except that the bar diagram is replaced by a smooth curve (Fig. 2.1B). Crude frequency curves can be constructed by connecting the midpoints of each size class in a histogram with a line. More accurate frequency curves can allegedly be constructed by a technique described by Folk (1974) involving graphical differentiation of the cumulative curve. A **cumulative curve** is generated by plotting cumulative weight percent frequency against phi size. Cumulative curves can be constructed that use either an arithmetic scale (Fig. 2.1C) or a log-probability scale (Fig. 2.1D) for the ordinate. Plotting a cumulative curve on a probability ordinate yields a straight line if the grain-size values have a log-normal distribution (explained below).

Mathematical methods

General statement

Although graphical plots provide a convenient visual method for evaluating the grain-size distribution of a given sample, comparison of large numbers of such plots can be very cumbersome. Also, the average grain-size and sorting of samples cannot be determined very accurately by visual inspection of grain-size graphs. To avoid these difficulties, mathematical methods that permit statistical treatment of grain-size data can be used to derive parameters that describe grain-size distributions mathematically.

Average grain size

Three mathematical measures can be used to describe the average size of grains in a sediment sample. The **mode** is the most frequently occurring particle size in a population of grains. The modal diameter corresponds to the diameter of grains represented by the peak of a frequency curve or the steepest point (inflection point) of a cumulative curve. The **median size** represents the midpoint of the grain-size distribution. Half of the grains by weight in the sample are larger than the median and half are smaller. The median corresponds to the 50th percentile diameter on the cumulative curve (Fig. 2.2). The **mean size** is the arithmetic average of all the particle sizes in a sample. The true arithmetic mean size of grains in a sediment sample cannot be calculated from the data obtained by most grain-size measurement techniques, other than manual measurement of individual clasts, because such measurements do not yield the sizes of individual particles. An approximation of the mean size can be calculated from formula 1, Table 2.3. The graphic mean size (Table 2.3) is obtained by calculating the average of the 16th, 50th, and 84th percentile diameters determined from the cumulative curve (Fig. 2.2).

Grain-size sorting

The sorting of a grain population is a measure of the range of grain sizes present and the magnitude of the spread or scatter of these sizes around the mean size. Sorting can be

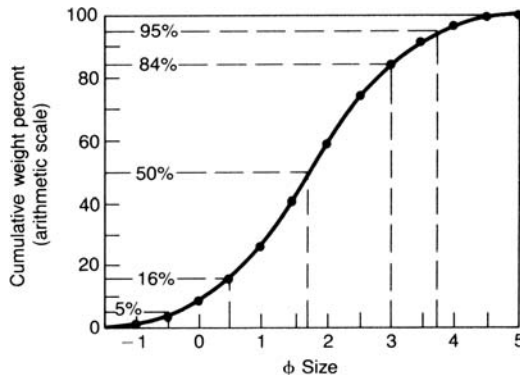


Figure 2.2 Method for calculating percentile values from a cumulative curve.

Table 2.3 Formulas for calculating grain-size statistical parameters by graphical methods

Graphic mean	$M_z = \frac{16 + 50 + 84}{3}$	(1)
Inclusive graphic standard deviation	$i = \frac{84}{4} + \frac{16}{6.6} + \frac{95}{5}$	(2)
Inclusive graphic skewness	$SK_i = \frac{(\frac{84}{2} + \frac{16}{84} + \frac{2}{16} + \frac{50}{16})}{2} + \frac{(\frac{95}{2} + \frac{5}{95} + \frac{2}{5} + \frac{50}{5})}{2}$	(3)
Graphic kurtosis	$K_G = \frac{(\frac{95}{2.44} + \frac{5}{75} + \frac{25}{25})}{2.44}$	(4)

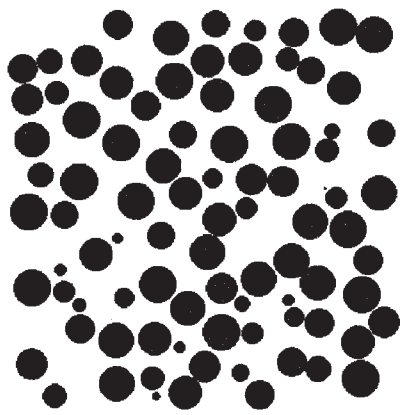
Source: Folk, R. L. and W. C. Ward, 1957. Brazos River bar: A study in the significance of grain-size parameters: *J. Sediment. Petrol.*, **27**, 3–26.

estimated by using a hand lens or microscope and reference to a visual estimating chart such as that shown in Fig. 2.3 (see Jerram, 2001).

More accurate determination of sorting requires mathematical treatment of grain-size data. The mathematical expression of sorting is standard deviation. In conventional statistics, one standard deviation encompasses approximately the central 68 percent of the area under the frequency curve (Fig. 2.4). The conventional formula for calculating standard deviation cannot be used with grain-size data; however, a formula for calculating the approximate standard deviation of a grain-size distribution by graphical-statistical methods is given in Table 2.3: formula 2 yields standard deviation expressed in phi units (phi standard deviation). Verbal terms for sorting corresponding to various values of graphic phi standard deviation are given below, after Folk (1974).

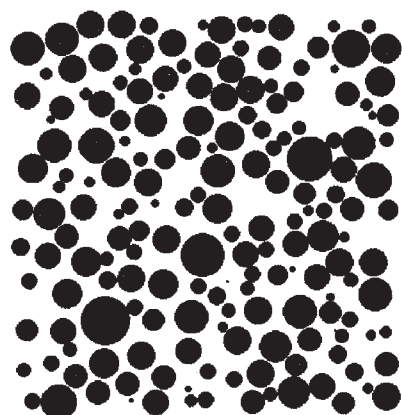
Phi standard deviation	Verbal sorting
< 0.35	Very well sorted
0.35 to 0.50	Well sorted
0.50 to 0.70	Moderately well sorted
0.70 to 1.00	Moderately sorted
1.00 to 2.00	Poorly sorted
2.00 to 4.00	Very poorly sorted
> 4.00	Extremely poorly sorted

Skewness is an additional measure of grain-size sorting that reflects sorting in the tails of the distribution. When plotted as a frequency curve, the grain-size distributions of most natural sediments do not yield a perfect bell-shaped curve such as the idealized curve shown in Fig. 2.4. That is, they do not exhibit a normal, or log-normal, grain-size distribution (even distribution of sizes about the mean size). Instead, they display an asymmetrical or skewed distribution. When an excess of fine particles is present in a sample, the frequency curve has a fine-size “tail” and the grain-size distribution is said to be fine-skewed, or positively skewed (fine sediment has positive phi values; Fig. 2.5A). When a coarse tail is present, the grain population is coarse-skewed, or negatively skewed (Fig. 2.5B). The numerical value



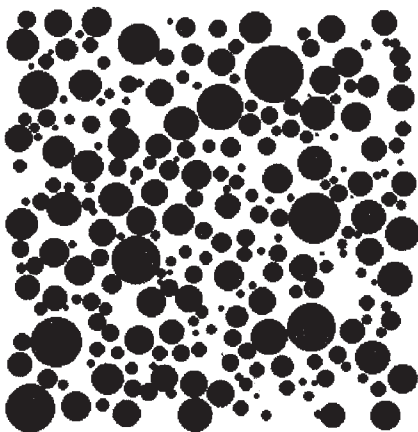
Very well sorted

$\phi = 0.0$



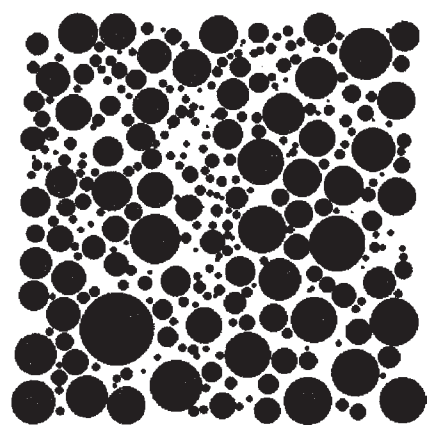
Well sorted

$\phi = 0.36$



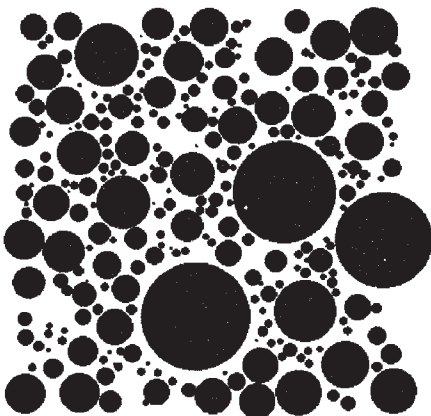
Moderately well sorted

$\phi = 0.67$



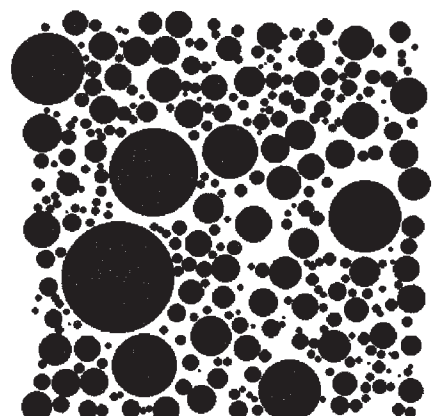
Moderately sorted

$\phi = 0.74$



Poorly sorted

$\phi = 1.06$



Poorly sorted

$\phi = 1.15$

Figure 2.3 Textural comparison chart showing degree of sorting. Each section is labeled with its verbal sorting description according to Folk (1968). (After Jerram (2001), Visual comparators for degree of grain-size sorting in two and three-dimensions: *Comput. Geosci.*, 27, Fig. 5, p. 490. Reproduced by permission of Pergamon Press, Elsevier Science Ltd.)

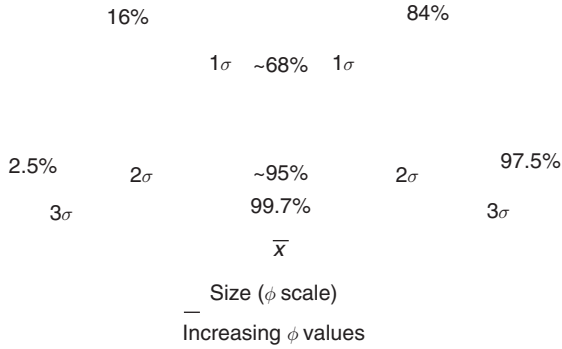


Figure 2.4 Frequency curve for a normal distribution showing the relation of standard deviation (σ) to the population mean (\bar{x}). One standard deviation (1σ) accounts for approximately 68 percent of the area under the curve, two standard deviations (2σ) account for approximately 95 percent, and three standard deviations (3σ) account for 99.7 percent.

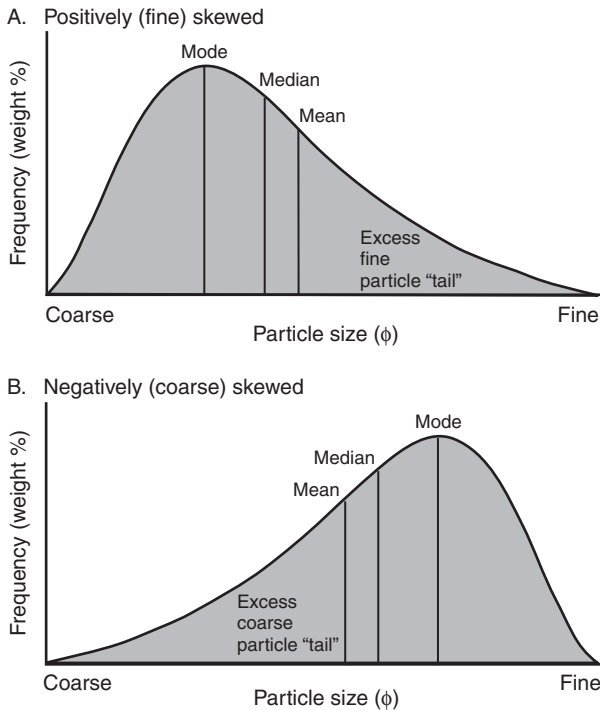


Figure 2.5 Skewed grain-size frequency curves, illustrating the difference between positive (fine) and negative (coarse) skewness. Note the difference between these skewed, asymmetrical curves and the normal frequency curve shown in Fig. 2.4.

of skewness (+ or -) can be calculated by using the graphic skewness formula shown in Table 2.3. The more this numerical value deviates from zero, the greater the skewness. Verbal skewness is related to calculated values of skewness as follows (Folk, 1974).

Calculated skewness	Verbal skewness
> +0.30	Strongly fine skewed
+ 0.30 to +0.10	Fine skewed
+0.10 to -0.10	Near symmetrical
-0.10 to -0.30	Coarse skewed
< -0.30	Strongly coarse skewed

The sharpness or peakedness of a grain-size frequency curve is referred to as **kurtosis**. Sharp-peaked curves are said to be leptokurtic; flat-peaked curves are platykurtic. Sharp-peaked curves indicate better sorting in the central portion of the grain-size distribution than in the tails, and flat-peaked curves indicate the opposite. A formula for calculating graphic kurtosis is given in Table 2.3.

The mean size, standard deviation, skewness, and kurtosis of a grain-size distribution can be calculated directly, without reference to cumulative curve plots, by the **moment method**. This method of deriving grain-size statistical parameters has been known since the 1930s but was not used extensively until computers became readily available to facilitate the involved computations. These computations involve multiplying a weight (weight frequency in percent) by a distance (from the midpoint of each size grade to the arbitrary origin of the abscissa). Equations for computing moment statistics are given in Table 2.4, and a sample computation form using 1/2 size classes is given in Table 2.5.

2.2.4 Applications and significance of grain-size data

Preceding discussion of sediment grain size focuses on discussion of techniques for measuring grain size and the various methods of presenting and studying grain-size data.

Table 2.4 Formulas for calculating grain size by the moment method

Mean (1st moment)	$\bar{x} = \frac{fm}{n}$	(1)
Standard deviation (2nd moment)	$= \sqrt{\frac{f(m - \bar{x})^2}{100}}$	(2)
Skewness (3rd moment)	$Sk = \frac{f(m - \bar{x})^3}{100^3}$	(3)
Kurtosis (4th moment)	$K = \frac{f(m - \bar{x})^4}{100^4}$	(4)

f = Weight percent (frequency) in each grain-size grade present. m = Midpoint of each grain-size grade in phi values. n = Total number in sample; 100 when f is in percent.

Table 2.5 Form for computing moment statistics using 1/2 size classes

Class interval ()	m Midpoint ()	f Weight %	fm Product	$(m-\bar{x})^2$		$(m-\bar{x})^3$		$(m-\bar{x})^4$	
				Deviation	squared	Deviation	cubed	Deviation	quadrupled
0-0.5	0.25	0.9	0.2	-2.13	4.54	-9.67	-8.70	20.60	18.54
0.5-1.0	0.75	2.9	2.2	-1.63	2.66	-4.34	-12.59	7.07	20.50
1.0-1.5	1.25	12.2	15.3	-1.13	1.28	-1.45	-17.69	1.63	19.89
1.5-2.0	1.75	13.7	24.0	-0.63	0.40	-0.25	-3.43	0.16	2.19
2.0-2.5	2.25	23.7	53.3	-0.13	0.02	0.00	0.00	0.00	0.00
2.5-3.0	2.75	26.8	73.7	0.37	0.13	0.05	1.34	0.02	0.54
3.0-3.5	3.25	12.2	39.7	0.87	0.76	0.66	8.05	0.57	6.95
3.5-4.0	3.75	5.6	21.0	1.37	1.88	2.57	14.39	3.52	19.71
>4.0	4.25	2.0	8.5	1.87	3.50	6.55	13.10	12.25	24.50
Total		100.0	237.9				-5.53		112.82

Source: McBride, E. F., Mathematical treatment of size distribution, in Carver, R. E. (ed.), *Procedures in Sedimentary Petrology*, Table 2, p. 119. © 1971, John Wiley and Sons, Inc. Reprinted by permission of John Wiley and Sons, Inc., New York.

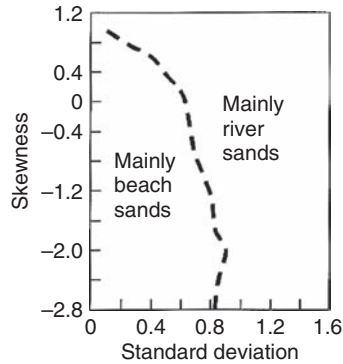


Figure 2.6 Grain-size bivariate plot of moment skewness vs. moment standard deviation, showing the fields in which most beach and river sands plot. [Redrawn from Friedman, G. M., 1967, Dynamic processes and statistical parameters for size frequency distributions of beach and river sands: *J. Sediment. Petrol.*, **37**, Fig. 5, p. 334, reproduced by permission of SEPM.]

All of this has importance mainly if grain-size data provide information that is useful in evaluating the economic significance of sedimentary rocks or in interpreting some aspect of Earth history. Geologists recognize, for example, that grain size and sorting affect the porosity and permeability of sedimentary rocks and thus the ability of these rocks to transmit and store fluids. Accordingly, these rock properties hold significant interests for petroleum and groundwater geologists.

Much of what has been written and published about grain size over the past half century has, however, focused on the usefulness of grain-size data for interpreting depositional environments. Geologists have assumed that grain-size characteristics reflect depositional conditions and processes and thus depositional environments. Sediments from each sedimentary environment allegedly exhibit uniquely different grain-size properties that distinguish them from sediments of different environments. It has been further assumed that once sediments from modern environments have been typed or “fingerprinted” by grain-size characteristics, this information can be extrapolated to interpretation of ancient depositional environments.

Two principal types of graphical plots have been used extensively in environmental analysis: two-component variation diagrams and log-probability plots. Friedman (1967, 1979) popularized use of two-component grain-size variation diagrams in which one statistical parameter is plotted against another, for example, skewness versus standard deviation (Fig. 2.6) or mean grain size versus standard deviation. These methods putatively allow separation of the plots into major environmental fields, such as beach environments and river environments.

Several workers (e.g. Visher, 1969; Sagoe and Visher, 1977) have suggested that the shapes of grain-size cumulative curves plotted on log-probability paper have environmental significance. Such curves typically display two or three straight-line segments rather than the single straight line predicated for a normally distributed population (e.g. Fig. 2.7). These curve segments are interpreted by the above workers to represent subpopulations of grains transported simultaneously by different transport modes; that is, by traction, saltation, and

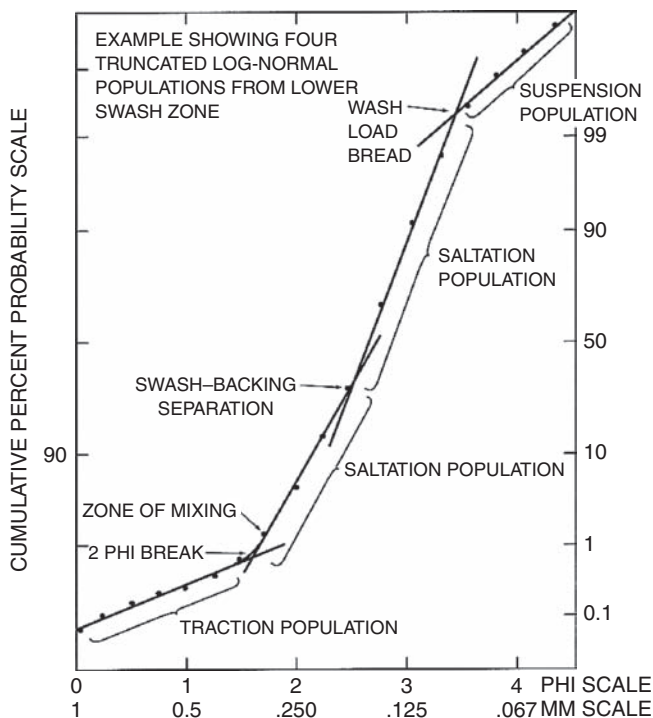


Figure 2.7 Relation of sediment transport dynamics to populations and truncation points in a grain-size distribution as revealed by plotting grain-size data as a cumulative curve on probability paper. [After Visher, G. S., 1969, Fig. 4, p. 1079, reproduced by permission of SEPM]

suspension. Differences in curve shapes and the locations of truncation points of the curve segments allegedly allow discrimination of sediments from different environments.

Although some workers have reported success by using these methods for typing and differentiating sediments from several modern environments (e.g. beach, river, dune), many other researchers found that these methods failed to identify the correct environment in an unacceptably high number of cases (e.g. Sedimentation Seminar, 1981). Consequently, researchers subsequently turned to other methods for interpreting grain-size data.

Some achieved success in grain-size environmental analysis by using more sophisticated multivariate statistical techniques such as factor analysis and discriminant function analysis (e.g. Stokes *et al.*, 1989; Syvitski, 1991b); however, these techniques have not been widely applied. Furthermore, some of the assumptions used in these statistical methods have also come under criticism (e.g. Forrest and Clark, 1989). One statistical method that has received modest attention is the so-called **log-hyperbolic distribution**. The hyperbolic distribution was formally introduced to geologists by Barndorff-Nielsen (1977) and subsequently discussed and amplified by Bagnold and Barndorff-Nielsen (1980) and Barndorff-Nielsen *et al.* (1982), as well as others. The principle involved in log-hyperbolic distributions is discussed briefly below.

Most geologists assume that the sizes of grains in natural sediments tend toward a normal distribution when the logarithm of grain size is plotted as a frequency curve. Thus, we say that sediments have a log-normal distribution, or a log-normal probability density function. This assumption is made even though we know that most natural sediments have grain-size distributions that exhibit some degree of skewness. If a truly log-normal population of grains is plotted on double log (log–log) paper so that the logarithms of both the grain size and frequency are plotted, or the logarithm to base e or base 10 of the frequency is plotted against phi size on arithmetic scales, the resulting curve is a parabola with continuously inward-curving tails. Barndorff-Nielsen (1977) and Bagnold and Barndorff-Nielsen (1980) maintain that when the size distribution of natural sediment, such as dune sand, is plotted on log–log plots and a curve is fitted to these data, the resulting curve actually has the shape of a hyperbola, whose straight-line asymptotes or “tails” extend to include the smallest measurable frequencies. They suggest that “granular size distributions occurring in nature do not conform to the ‘normal’ probability function, but to a different, ‘hyperbolic,’ probability function” (Bagnold and Barndorff-Nielsen, 1980). They further suggest that not only is the hyperbolic probability function a better descriptor of natural grain populations than the normal probability function, but that it holds the potential to discriminate between sediments from different environments.

The papers by Barndorff-Nielsen and his co-workers were followed by the appearance of several papers from other workers who have attempted to use the log-hyperbolic function in environmental analysis. Some (e.g. Christiansen, 1984; Vincent, 1986) reported that parameters from the log-hyperbolic distributions gave much better environmental discrimination than did those from normal probability distributions; however, some other researchers (e.g. Fieller *et al.*, 1984; Wyrwoll and Smyth, 1985) did not share this optimism. Christiansen and Hartmann (1991) provide a more recent discussion of the hyperbolic distribution.

Although analysis of grain-size data has not proven to be a consistently reliable technique for interpreting depositional environments, grain-size data have many other useful applications. As summarized by Syvitski, 1991a, grain-size data can be used:

1. To interpret coastal stratigraphy and sea-level fluctuations
2. To trace glacial sediment transport and the cycling of glacial sediments from land to sea
3. By marine geochemists to understand the fluxes, cycles, budgets, sources, and sinks of chemical elements in nature
4. To understand the mass physical (geotechnical) properties of seafloor sediment, i.e. the degree to which these sediments are likely to undergo slumping, sliding, or other deformation.

Details of these applications are available in Syvitski (1991a).

2.3 Grain shape

2.3.1 Methods of expressing shape

Numerous parameters or measures have been suggested to describe the shapes of particles (see reviews by Barrett, 1980 and Illenberger, 1991). As used herein, particle **shape** is taken

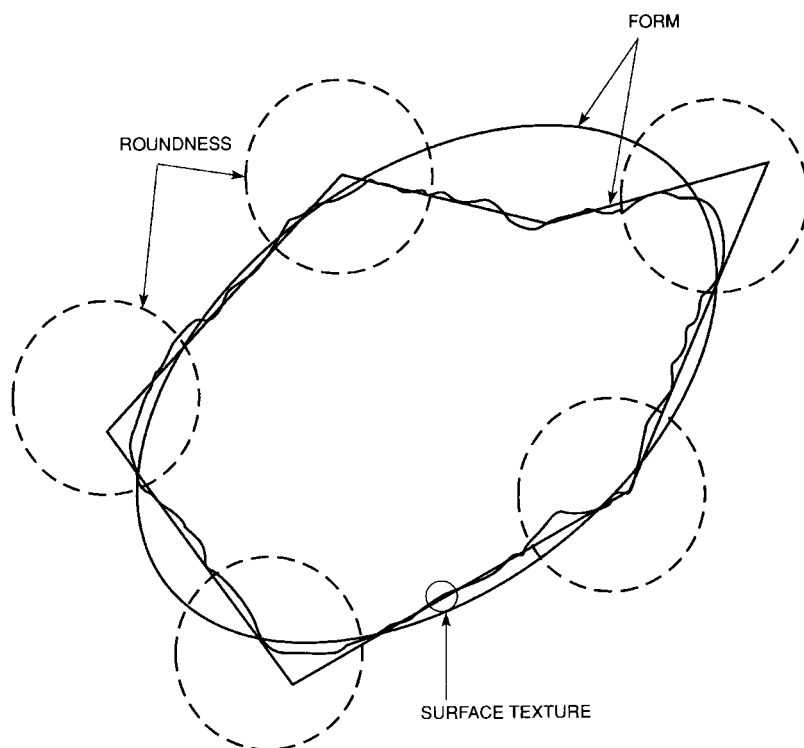


Figure 2.8 The hierarchical relationship of form, roundness, and surface texture. The heavy, solid line is the particle outline. (From Barrett, J.P., 1980, The shape of rock particles, a critical review: *Sedimentology*, 27, Fig. 2, p. 293, reprinted by permission of Elsevier Science Publishers, Amsterdam.)

to encompass all aspects of the external morphology of particles, including form, roundness, and surface texture. **Form** refers to the gross, overall morphology or configuration of particles. Most measures of form consider the three-dimensional shape of the grains. **Roundness** is a measure of the sharpness of the corners of a grain, and is commonly measured in two dimensions only. **Surface texture** refers to microrelief features, such as scratches and pits, that appear on the surfaces of clastic particles, particularly particles that have undergone transport. Changes in form or roundness brought about by abrasion during sediment transport or solution or cementation during diagenesis can affect surface texture by creating new grain surfaces. Thus, the three aspects of shape can be thought of as constituting a hierarchy, where form is a first-order property, roundness a second-order property superimposed on form, and surface texture a third-order property superimposed on both the corners of a grain and the surfaces between the corners (Barrett, 1980; Fig. 2.8). These three shape properties of grains are independent parameters. One property can vary without necessarily affecting the others, although dramatic changes in form or roundness are likely also to affect surface texture.

2.3.2 Particle form

The gross morphology or overall shape of particles has proven to be a difficult parameter to quantify with great precision and accuracy. Several measures of form were proposed by early workers, including flatness, elongation, and sphericity (Barrett, 1980; Illenberger, 1991). Particular emphasis has been given to the sphericity of grains, that is, the degree to which the shape of grains approaches the shape of a sphere (Wadell, 1932). Practical determination of sphericity involves measurement of the three orthogonal axes of particles and calculation of a sphericity value based on the relative lengths of these axes. The assumption is made that the more nearly equal the lengths of the three axes, the more nearly the particle approaches the shape of a sphere. Examples of mathematical relationships generated for the purpose of calculating sphericity include those for determining so-called intercept sphericity (ψ_I) (Krumbein, 1941).

$$\psi_I = \sqrt[3]{\frac{D_S D_I}{D_L^2}} \quad (2.4)$$

and maximum projection sphericity (ψ_p) (Sneed and Folk, 1958)

$$\psi_p = \sqrt[3]{\frac{D_S^2}{D_L D_I}} \quad (2.5)$$

where D_S refers to the length of the short particle axis, D_I the length of the intermediate axis, and D_L the length of the long axis.

Alternative expressions of particle form, in addition to sphericity, are provided by the venerable shape classification of Zingg (1935) and that of Sneed and Folk (1958). Zingg's shape classification is derived by plotting on a bivariate diagram the ratio of the intermediate to long particle axis versus the ratio of the short to intermediate particle axis (Fig. 2.9A). Four shape fields, or four types of particle shapes, are identified: roller, bladed, oblate, and equant. This shape measure is somewhat similar to sphericity; note, however, that a particle with a particular value of (intercept) sphericity (Krumbein, 1941) can fall in more than one of Zingg's shape fields (Fig. 2.9B). Sneed and Folk (1958) classify form on a triangular diagram in which ratios of particle axes are plotted in such way as to create ten form fields (Fig. 2.10). End member particle shapes are compact, platy, and elongated. As in the case of Zingg's shape fields, note that lines of equal (maximum projection) sphericity plotted on this diagram can cross several form fields.

More recently, Illenberger (1991) presented a triangular shape diagram (Fig. 2.11) in which a sphericity parameter called the Corey shape index, defined as S/\sqrt{IL} , is plotted against a disc-rod index $[(L-I)/(L-S)]$, where L , I , and S refer to the lengths of the long, intermediate, and short axes, respectively. The end members of shape are spheres, discs, and rods. Illenberger maintains that this triangular plot is the most effective shape diagram.

Measuring the length of particle axes of loose, gravel-size particles is relatively easy; however, such measurements become much more difficult when performed on sand-size

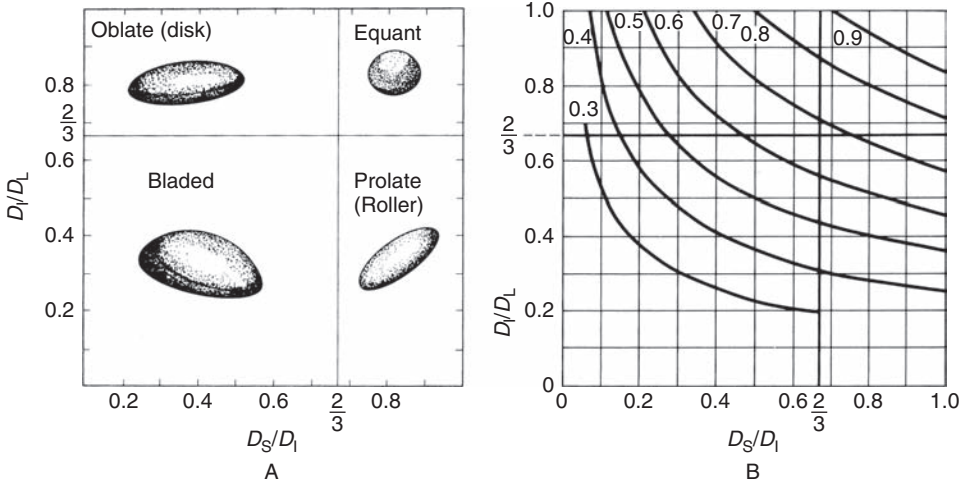


Figure 2.9 A. Classification of pebble shapes after Zingg (1935). B. Relation between intercept sphericity and Zingg shape fields. The curves represent lines of equal sphericity. (A. From Blatt, H., G. Middleton, and R. Murray, 1980, *Origin of Sedimentary Rocks*, 2nd edn.: Prentice-Hall, Upper Saddle River, NJ, Fig. 3.20, p. 80, reprinted by permission. B. After Pettijohn, F. J., 1975, *Sedimentary Rocks*: Harper Collins, New York, NY, Fig. 3.19, p. 54, reprinted by permission.)

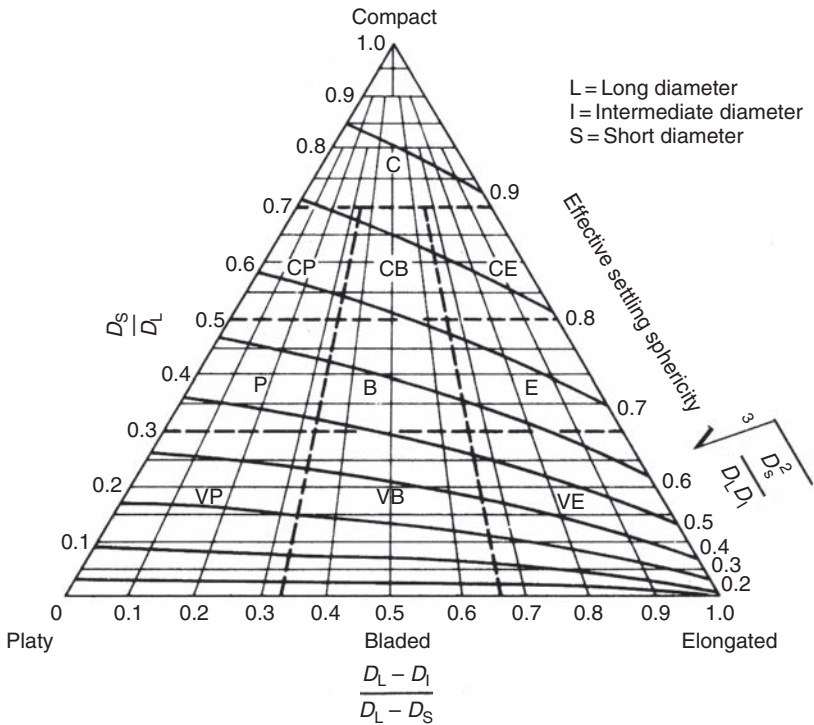


Figure 2.10 Classification of pebble shapes after Sneed and Folk (1958); V = very, B = bladed, C = compact, E = elongated, P = platy. (After Sneed, E. D. and R. L. Folk, 1958, *Pebbles in the Lower Colorado River, Texas, a study of particle morphogenesis*: *J. Geol.*, **66**, Fig. 2, p. 119, reprinted by permission of University of Chicago Press.)

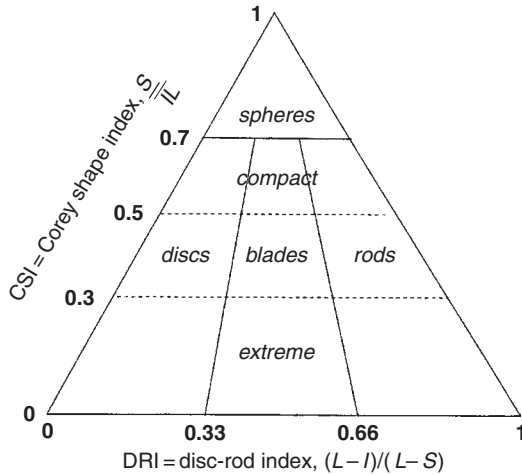


Figure 2.11 The Corey shape index (CSI) plotted against the disc-rod index (DRI) on a triangular diagram. (After Illenberger, W. K., 1991, Pebble shape (and size!): *J. Sediment. Petrol.*, **61**, Fig. 3, p. 761, reproduced by permission of SEPM, Tulsa, OK.)

and smaller grains. Two dimensions of a loose, sand-size particle (commonly the long and intermediate axes) can be measured rather easily under a microscope; however, it is difficult (although not impossible) and time consuming to measure the third dimension. This problem of axes measurement is severely compounded when we deal with consolidated sedimentary rocks that cannot be disaggregated. As viewed in thin section, only two dimensions of a particle are visible and, owing to the corpuscle effect referred to in the discussion of grain size, these dimensions rarely correspond exactly to the short, long, or intermediate axes of the particle.

Because of this problem of determining the three-dimensional shape of small particles, especially in consolidated rocks, it would be useful to find a method of expressing particle shape in two dimensions. Mathematical methods involving Fourier analysis offer one solution to the problem of characterizing two-dimensional shape. These methods, which appear to allow good characterization of two-dimensional particle shape, are discussed subsequently in greater detail.

2.3.3 Particle roundness

Several methods for measuring and expressing particle roundness have been proposed (reviewed by Dobkins and Folk, 1970; Barrett, 1980; and Diepenbroek *et al.*, 1992). Wadell (1932) is credited with introducing the most widely used mathematical expression for roundness. He defined roundness as the arithmetic mean of the roundness of the individual corners of a grain in the plane of measurement (a two-dimensional measure). The roundness of individual corners is given by the ratio of the radius of curvature of the

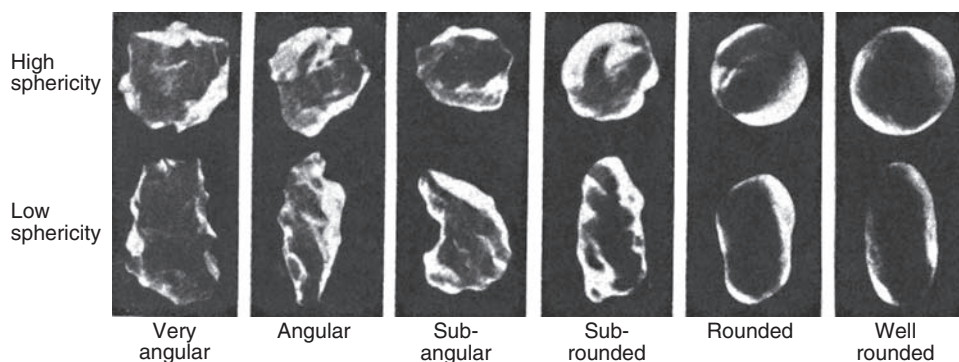


Figure 2.12 Grain images for estimating the roundness of sedimentary particles. (After Powers, 1953, A new roundness scale for sedimentary particles: *J. Sediment. Petrol.*, **23**, Fig. 1, p. 118, reproduced by permission of SEPM, Tulsa, OK.)

corners to the radius of the maximum-size circle that can be inscribed within the outline of the grain in the plane of measurement. The degree of Wadell roundness (R_w) is thus expressed as

$$R_w = \frac{\sum(r/R)}{N} = \frac{\sum(r)}{RN} \quad (2.6)$$

where r is the radius of curvature of individual corners (the radius of a circle that fits within the corner), R is the radius of the maximum inscribed circle, and N is the number of corners. Measuring the values of r and R in loose grains or in thin section (by using a microscope or by using a concentric-circle protractor to measure the radii of projected images) is a very laborious process – so much so, that most previous investigators have not been willing to spend the necessary time. Therefore, many investigators resort to visual estimates of grain roundness aided by the use of visual estimation charts. Several such charts have been proposed; however, the roundness scale of Powers (1953; Fig. 2.12) appears to be most widely used. Although visual estimates of grain roundness can be done quite rapidly, reproducibility of results, even by the same operator, can be quite low. To obtain more accurate results, investigators have turned to Fourier techniques for roundness analysis (e.g., Diepenbroek *et al.*, 1992). Fourier techniques are discussed below.

2.3.4 Another method for analyzing and quantifying two-dimensional particle shape: Fourier shape analysis

General statement

Owing to the problems inherent in measuring sphericity and roundness and the inability of these parameters to delineate the shapes of particles with a high degree of accuracy, some geologists have sought more exact, mathematical methods for characterizing particle shape. Several such methods are possible (Clark, 1981); however, most workers have focused on

measuring particle shape by Fourier analysis, which appears to work well for describing the regular shapes of most natural particles. Highly irregular or strongly embayed particles are less amenable to Fourier analysis. Because of the potential that Fourier analysis holds for accurate measurement of particle shape, it is described below in greater detail than were the preceding techniques for shape measurement.

Fourier analysis

General principles

The fundamentals of Fourier analysis of particle shape were introduced to geologists particularly in the papers of Schwarcz and Shane (1969) and Ehrlich and Weinberg (1970). Applications and amplifications of the method have appeared in numerous subsequent papers. The problem in mathematical approaches to shape analysis is to find an exact method for describing, and regenerating, the (two-dimensional) outline of a grain. This problem can be attacked by cutting and unrolling the outline of a grain, as shown in Fig. 2.13. When unrolled in this way, it can be seen that the outline of the grain is a periodic function, somewhat resembling the shape of a sine wave.

The simplest periodic function is given by

$$y = A \sin (\omega x + \phi) \quad (2.7)$$

where A is amplitude, ω is (angular) frequency, and ϕ is initial phase, which characterizes the initial position of the point x . Furthermore,

$$\omega = 2\pi/T \quad \text{and} \quad T = 2\pi/\omega \quad (2.8)$$

where T is the period. [In the course of a period T , x sweeps through an angle of 2π radians.] This function is called a harmonic of amplitude A , frequency ω , and initial phase ϕ . If the simplest case is assumed, where $A = 1$, $\omega = 1$, and $\phi = 0$ (0 phase angle), this function gives a normal sine curve $y = \sin x$, as shown in Fig. 2.14A. If in this example a phase angle of 90 degrees ($\pi/2$) is used instead of 0, we get the cosine curve $y = \cos x$. The graph of the cosine function is the same as that of the sine shifted to the left by an amount of 90 degrees ($\pi/2$).

If, instead of plotting the ordinary sine curve $y = \sin x$, we plot $y = \sin 2x$, $y = \sin 3x$, etc., we deform the sine curve by uniform compression along the x axis (Tolstov, 1976). Figure 2.14B shows the harmonic $y = \sin 3x$, of period $T = 2\pi/3$. In addition to uniform compression (or expansion) along the x axis, a shift along the x axis occurs if we change the initial phase (phase angle). Thus, Fig. 2.14C represents the harmonic

$$y = \sin (3x + \pi/3) \quad (2.9)$$

with a period $2\pi/3$ and an initial phase $\pi/3$. Finally, a change in the amplitude of the sine curve can also be effected. Thus the harmonic

$$y = 2 \sin (3x + \pi/3) \quad (2.10)$$

has the form shown in Fig. 2.14D.

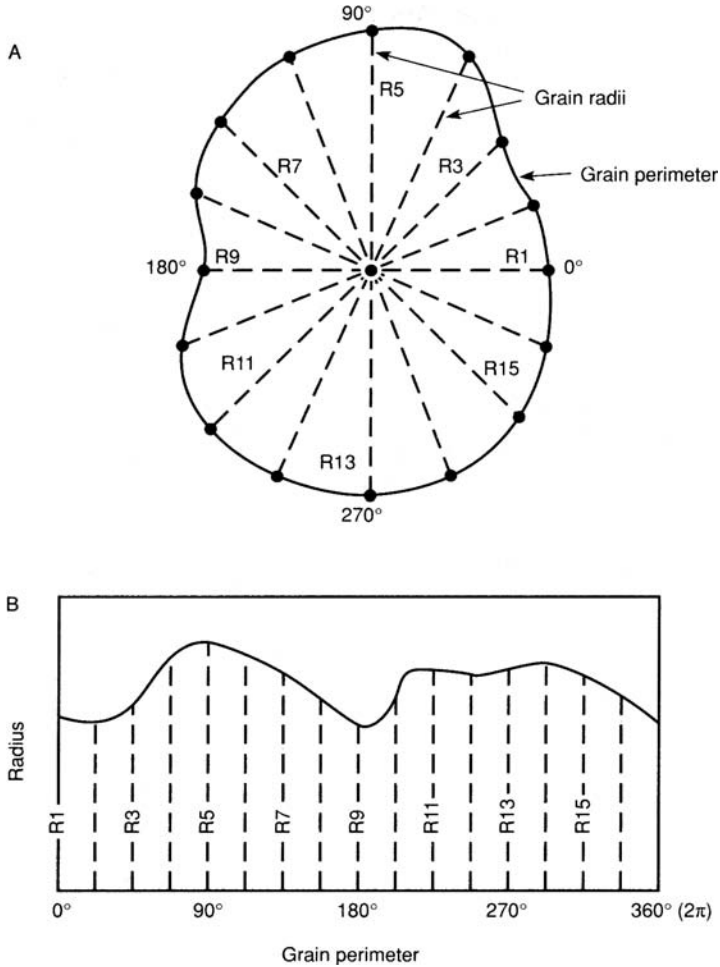


Figure 2.13 Method of “unrolling” a grain to produce a periodic wave. A. Grain outline showing radii measured from grain center to points on the grain perimeter. B. Unrolled grain outline as constructed from radii measurements. Note that the form of the unrolled grain is a crude sine wave.

A mathematical theorem owing to Fourier shows that any periodic function with frequency ω can be represented as a superposition of harmonic vibrations of frequencies $\omega, 2\omega, 3\omega, \dots$ with various amplitudes (harmonics 1, 2, 3...). Consider, for example, Fig. 2.15. The dashed line in Fig. 2.15A has the form of a square “wave.” Figure 2.15B shows three harmonics of a sine wave. If these three harmonics are superimposed (added graphically), the result is the heavy, solid line in Fig. 2.15A. Note that this solid curve has the approximate shape of the square curve. If additional, higher-order harmonics are superimposed, a more exact approximation of the square curve can be achieved.

This representation of a curve shape by superimposition of successive harmonics of a periodic function is the basis for Fourier analysis of particle shape. The shape of the curve

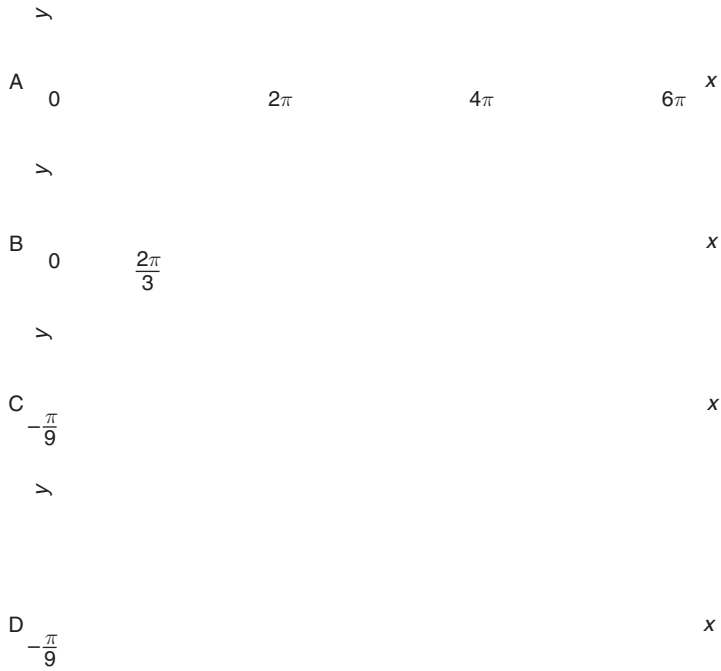


Figure 2.14 Harmonics of a sine wave. (After Tolstov, G. P., 1976, *Fourier Series*, Dover Publications, New York, NY, Fig. 4, p. 4, reprinted by permission.)

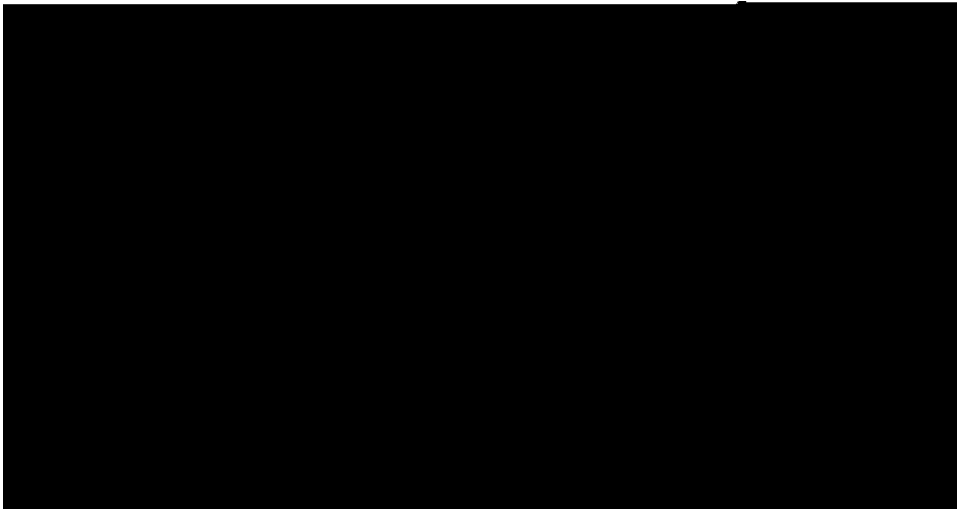


Figure 2.15 Fourier synthesis of a square wave by addition of successive harmonics of a sine wave. (After Borowitz, S. and A. Beiser, 1966, *Essentials of Physics*: Addison-Wesley Publishing Co., Fig. 25.17, reprinted by permission of Pearson Education, Upper Saddle River, NJ.)

formed by unrolling the outline of a particle, as shown in Fig. 2.13, can be synthesized quite faithfully by superimposition of the harmonics of the periodic sine function. As described by Ehrlich and Weinberg (1970), grain shape can be estimated by a closed Fourier series by expansion of the periphery radius of a grain as a function of angle about the grain's center of gravity. To accomplish this, the image of a grain is projected onto a polar grid or a digitizing tablet. The center of the grain is then determined. Finding the center can be done graphically, but a more accurate center (center of gravity) can be found by calculation (Ehrlich and Weinberg, 1970). A number of points are then picked along the periphery of the grain and the locations of these points expressed in polar coordinates about the center of gravity.

The radius $R(\theta)$ is determined by the relationship

$$R(\theta) = R_0 + \sum_{n=1}^{\infty} R_n \cos(n\theta - \phi_n) \quad (2.11)$$

where θ is the polar angle measured from an arbitrary reference line. R_0 is equivalent to the average radius determined from measuring all the radii from the center of gravity to the peripheral points. The remainder of the equation (which is a function of the harmonic amplitude R_n) represents the length to be added to the average radius at each angle θ . Thus R_n is the amplitude at each frequency, n is the harmonic order or number, and ϕ_n is the phase angle.

Each successive harmonic curve represented by this periodic function has a distinctive shape, if you think of the ends of the curves as being joined. The "zeroth" harmonic is simply the R_0 value in Equation 2.11 and is thus a centered circle with an area equal to the total area of the grain (based on the average radius). The curve of the first harmonic has the shape of an offset circle, the second is a figure eight, and the third is a trefoil. The shapes of the first 20 harmonics are illustrated in Fig. 2.16. The shape of a particle can be adequately represented

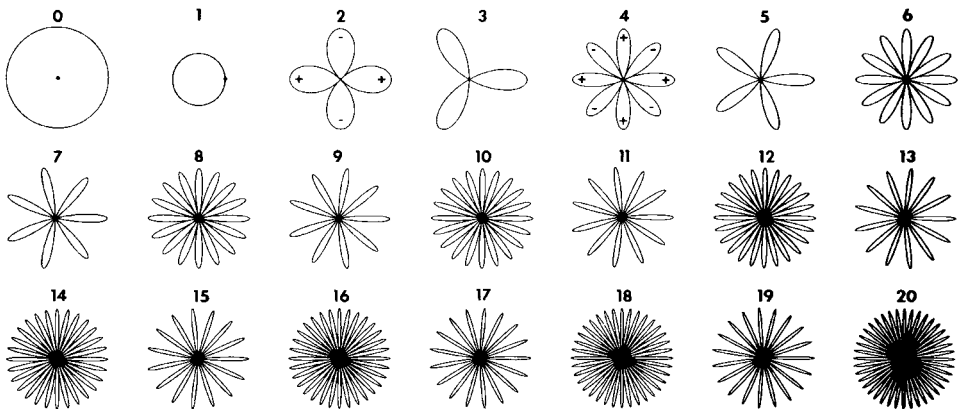


Figure 2.16 Graphic representation of the first 20 Fourier harmonics. (From Eppler, D. T., R. Ehrlich, D. Nummendahl, and P. H. Schulz, 1983, Sources of shape variation in lunar impact craters: Fourier shape analysis: *Geol. Soc. Am. Bull.*, **94**, Fig. 1, p. 275.)

by an average radius and 24 harmonic amplitudes representing the relative contribution of each fixed lobate form (harmonic) to the approximation of the outline (Ehrlich *et al.*, 1987). The first few harmonics are sufficient to define the gross shape of the particles (form); successively higher-order harmonics add to the refinement of this shape and allow discrimination of smaller-scale features such as roundness.

Once the harmonics have been calculated, the outline of the grain can be regenerated by superimposing all of the harmonic shapes, as illustrated in the simpler example in Fig. 2.15. Obviously, it would be very difficult to superimpose curves by visual graphic addition. This entire operation is tailor-made for computer application. The periphery points are first digitized in polar coordinates. These data are then fed into a computer, which, with proper software, calculates the Fourier equation and adds the harmonic shapes together to regenerate the particle shape. In early applications, the grain outline was digitized manually by placing a polar grid over the outline or by some type of electronic “pencil-follower” technique. More recently, the automated techniques of image analysis, involving television cameras and mini- or microcomputers, have been adopted. The technique is similar to that described in the preceding discussion of grain-size analysis. The grain image is captured by means of a video camera. Information about the grain outline is extracted through “frame grabbers” to acquire a series of x, y coordinates of the grain boundary. See Clark (1987) and Telford *et al.* (1987) for details.

2.3.5 Significance of form and roundness

General statement

In spite of the considerable preoccupation that geologists have displayed in measuring the form and roundness of natural particles, these parameters have not proven to be especially reliable guides to the provenance and transport histories of siliciclastic sediment. On the other hand, it is commonly conceded that shape does have an influence on the settling velocity of particles in a fluid and that departure of a grain from a spherical shape causes a decrease in settling velocity. Le Roux (2004) examines this relationship more closely and presents a hydrodynamic classification of grains on the basis of shape. Also, shape (form) is known to affect the transportability of particles moving by traction. For example, gravel-size particles that have a roller shape are transported preferentially over blade-shaped particles, which in turn are more transportable than disc-shaped particles (Swanson, 1972). Even the transportability of silt-size particles is allegedly influenced by shape, including roundness (e.g. Mazzullo *et al.*, 1992); that is, more-rounded grains are transported preferentially. See Pye (1994) for a different point of view.

The failure of sphericity and roundness, as measured by conventional techniques, to serve as dependable guides to source and depositional environments rests in part on the fact that many natural variables interact to produce the characteristics of a particular deposit. A single parameter such as roundness or sphericity may not be a sensitive enough measure to identify these variables. A more important reason may be, as suggested by Barrett (1980), that even

the best of the commonly used procedures for determining sphericity and roundness are limited by observational subjectivity and low discriminating power. For example, measurement of the three axes of a particle does not provide a unique characterization of particle form. Particles with quite different form may have the same numerical sphericity when measured in this manner. On the other hand, measurement of grain shape by Fourier analysis leads to more exact characterization of (two-dimensional) shape, and may thus hold greater potential for provenance and environmental interpretation.

Significance of Fourier shape

Because the shapes of particles can be characterized very exactly by Fourier analysis, shape studies based on this technique may provide a more reliable method for studying the source and transport histories of particles than do studies based on roundness and sphericity. An immediate problem is encountered in interpreting Fourier results, however, because the data obtained do not directly represent any physical property of the grains. Fourier data are in the form of amplitudes of the various harmonics. Thus, to compare the shapes of two grains, an investigator compares the amplitudes of each harmonic of the two grains, which in total represent the shape of the grains. These individual amplitudes have no easily visualized relationship to the actual shapes of the grains, and, in fact, interpretation is not related to the physical properties of the grain except in a crude way (Clark, 1981). Nonetheless, this method of comparing amplitudes is the principal technique used in interpretative Fourier studies.

Because large numbers of grains are commonly studied in environmental and provenance analysis, the harmonic amplitudes must be presented in some condensed form. This data reduction is commonly done by plotting as a histogram the “mean amplitude spectrum” as a function of number frequency (Fig. 2.17). The mean amplitude spectrum is obtained by averaging the amplitudes of a particular harmonic, say the fifth, as determined from all the grains analyzed from a particular sample. Visual inspection of the histograms makes it

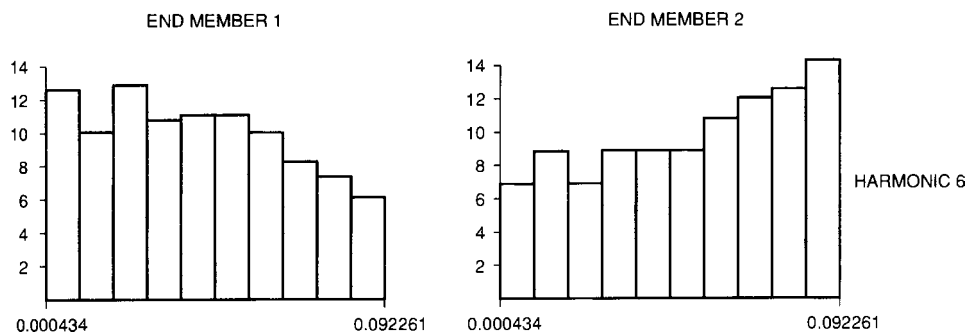


Figure 2.17 Mean amplitude spectra for harmonic 6 of two populations of grains. End member 1 represents a population of grains that are on the average smooth and round. Grains in end member 2 are largely angular and irregular in shape. [After Mazzullo, and Anderson, 1987, Analysis of till and glacial-marine sands, in Marshall, J. R. (ed.), *Clastic Particles*, Fig. 2, p. 319. Copyright 1987 by Van Nostrand Reinhold. All rights reserved.]

possible to distinguish differences owing to gross form (lower order harmonics) and finer-scale features of shape, such as roundness and surface texture (?) (higher order harmonics).

When investigating the shapes of large numbers of grains in numerous samples, the huge amount of data generated in 20 or more harmonics of each grain in each sample makes cumbersome the analysis of each harmonic separately. It becomes desirable to determine which one or which few harmonics may yield the most useful information about shape for the purposes of a particular study, so that all harmonics need not be studied in equal detail. An investigator can then concentrate on statistical analysis of the data from perhaps four or five harmonics, rather than 20 or more. The problem is to select those four or five harmonics that make the most useful or meaningful contribution to the particle's shape.

Full *et al.* (1984) suggest a method for selecting the most useful harmonics for more-detailed study by plotting against harmonic number a parameter called relative entropy. Entropy, in this context, refers to so-called information entropy and is concerned with the frequency distributions of values. Interested readers are referred to Full's paper for further details.

Applications of Fourier techniques to provenance analysis

Since the introduction to geologists of Fourier shape analysis in the late 1960s and early 1970s, several investigators have applied this technique to the problem of interpreting sediment source; see, for example, Mazzullo and Magenheimer (1987) and Torley (2001). The fundamental assumption in these applications is that the shapes of quartz grains from different sources are sufficiently different and distinctive, as revealed by Fourier shape analysis, that the separate sources can be differentiated and identified. Ehrlich *et al.* (1980) suggest that both provenance and process history (degree of abrasion) can be evaluated by Fourier techniques.

Application of Fourier shape analysis to environmental studies

Although the techniques of Fourier shape analysis have been used by geologists since the late 1960s, surprisingly few attempts have apparently been made to apply the technique to interpretation of ancient sedimentary environments. The technique of "fingerprinting" modern sediments from many known environments, so widely used in grain-size studies, has evidently not caught on with workers using Fourier shape analysis. At this time, to my knowledge, no investigator has published data on the Fourier shape characteristics of quartz grains from a wide range of modern environments, such as beach, shoreline dune, inland dune, fluvial, alluvial fan, continental shelf, delta, etc., that can be used by other investigators as a basis for environmental interpretation of ancient sedimentary rocks. One reason why relatively few "fingerprinting" studies of modern quartz sands have been made may be that the effects of diagenesis (solution, overgrowth cementation, etc.) may make the shape characteristics of quartz sands in modern environments a questionable model for quartz sands in ancient sedimentary rocks. For two examples of the application of Fourier technique to sediment transport and environmental analysis see Mazzullo and Ehrlich (1983) and Mazzullo *et al.* (1986).

Problems with highly irregular-shaped grains

Standard (closed-form) Fourier analysis does not work for highly irregular or strongly embayed grains, where radii from the grain center may intersect the grain perimeter more than once. For example, many grains that have undergone intensive chemical leaching during diagenesis or weathering would fall into this category of highly irregular particles.

Closed-form Fourier analysis analyzes the change in radial distance of points on a grain's perimeter to its centroid (Erlich and Weinberg, 1970). Torley (2001) proposed a new method of Fourier analysis for highly irregular grains that analyses changes in curvature around the perimeter of a grain's outline rather than distance of points on the perimeter from the centroid. According to Torley, this new method allows analysis of irregular-shaped grains that would be rejected by closed-form Fourier analysis.

Some workers, notably Orford and Whalley (1983, 1987) and Whalley and Orford (1986), have urged the use of the fractal dimension of particles as a method of analyzing the shapes of these irregular particles. The fractal dimension of an object is defined as the degree to which a line fills a two-dimensional space (Whalley and Orford, 1986). The greater the wiggleness of a line, the greater its fractal dimension, which can range in numerical value from 1 for a point or a straight line to values approaching 2 for an extremely wiggly line.

2.3.6 SEM analysis of grain surface texture

Geologists have long recognized through observation with a standard binocular light microscope that the surfaces of some pebbles and mineral grains are either polished or roughened (frosted); however, the details of surface texture could not be recognized at such low magnification. It was not until the 1960s, when electron microscopes became available, that the surface texture of grains could be studied in detail. With the appearance of the scanning electron microscope (SEM) in the late 1960s, the technique for studying surface texture at high magnifications became routine. With the aid of the electron microscope, geologists were able to identify a variety of microrelief markings on grain surfaces, such as V-shaped pits (Fig. 2.18A and B), grooves (striations), conchoidal fractures, and abrasion features. More than 40 such microfeatures have been identified (e.g. Mahaney, 2002, p. 27). Interested readers may view many of these features in the photo atlases of Krinsley and Dornkamp (1973) and Mahaney (2002).

Numerous applications of SEM analysis of surface textural features have been suggested (Krinsley and Trusty, 1986; Mahaney, 2002, p. 10); however, the main objective of this research has been identification of sedimentary environments from grain surface micro-textures. Hundreds of research papers about surface textural analysis have been published since the 1960s (see extensive bibliography in Mahaney, 2002), many of which deal with environmental interpretation.

Application of SEM analysis of grain surface texture as an environmental tool lies in the assumption that surface texture, being easier to modify than either particle form or roundness, is more likely than either form or roundness to preserve the imprint of the last depositional

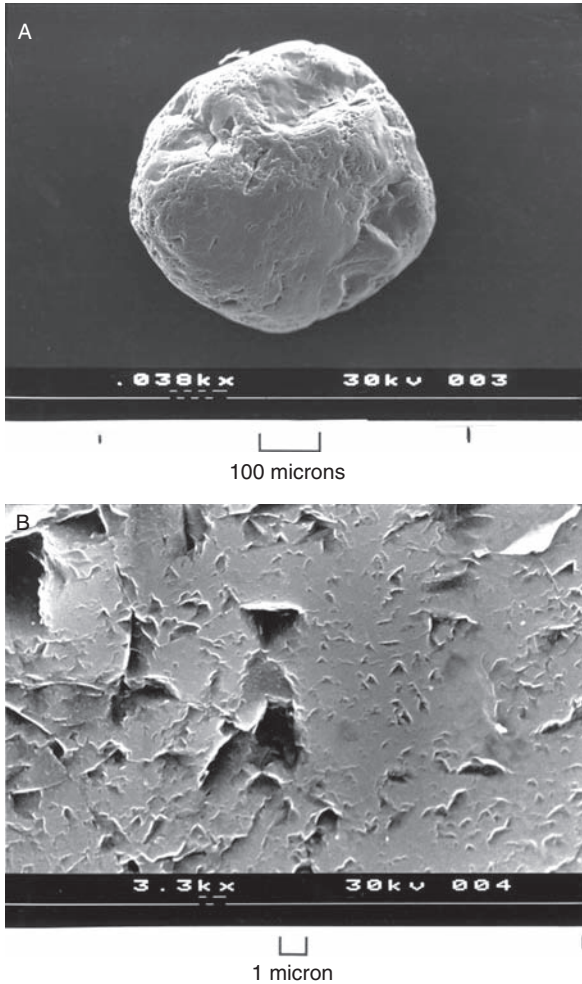


Figure 2.18 A. Electron micrograph of surface markings on a quartz grain from a late Pleistocene high-energy beach deposit near Norwich, Norfolk, England. B. Enlarged portion of the extreme right edge of the grain in A. Note abundant V-shaped markings, which are characteristics of quartz grains from high-energy beaches. [Photograph courtesy of David Krinsley.]

environment. Owing to its superior hardness and chemical stability, quartz is commonly considered to be the most appropriate material to record the surface textural features produced in each environment. The assumption is made that the energy conditions within each environment will tend to produce surface textural features that reflect that environment and that these features will differ from environment to environment. Thus, different textural features are produced by the grinding and sliding motion of glaciers, the collision and abrasion of grains in breaking waves of the beach surf zone, and the traction and saltation movement of grains by wind or river water.

The surface textures of many thousands of quartz grains from known modern environments have now been studied by a host of investigators, together with experimentally formed textures produced by grinding or other laboratory techniques to mimic glacial, eolian, or subaqueous transport. Unfortunately, few if any of the textural features are unique to a particular environment. Likewise, several different kinds of markings can be produced in the same environment. Although the same type of surface features can be produced in more than one environment, some markings tend to be relatively more abundant in some environments than in others. For example, mechanical V-shaped pits are particularly common on quartz grains from high-energy subaqueous environments on beaches and in rivers. Parallel grooves (striations) and step features are common on grains from glacial environments, and grains with low relief and abundant abrasion features (rubbed or worn grain surfaces) are characteristic of wind-blown transport.

Nonetheless, environmental analysis of surface features on quartz grains from ancient sedimentary rocks must be made on a statistical basis, looking at relative abundances of particular features rather than absolute abundances (e.g. Mahaney *et al.*, 2001). Environmental analysis has not yet progressed very far beyond identifying a few major environments: glacial, high-energy beach (littoral), eolian, fluvial. Features produced during diagenesis and soil formation (pedogenic sands) can also be identified.

Advantages and limitations of surface textural analysis

The major advantage of SEM analysis of surface textures is that SEM imagery allows a researcher to study small-scale shape features that cannot be resolved by any other shape-study technique. Even Fourier analysis characterizes only relatively large “bumps” on a grain periphery – those bumps that subtend angles of 7.5° or more when measured from the grain center (Ehrlich *et al.*, 1987). Furthermore, the SEM permits direct observation of surface features in contrast to Fourier analysis, which “sees” grain shapes only indirectly. Another advantage of SEM imagery is that surface texture changes more readily during transport and abrasion than do roundness and sphericity and thus may be a more sensitive indicator of environment. At the same time, quartz is sufficiently durable that a grain that has passed through several environments may retain some diagnostic markings from each environment. Thus, surface texture may reveal multiple episodes in the transport history, making it possible for a researcher to trace its passage through these environments.

On the other hand, the fact that quartz retains its surface markings for some time could lead to incorrect interpretations. For example, quartz sand deposited on the continental shelf from a melting iceberg would bear the textural imprint of glaciation. If such a sand was buried quickly before shelf processes had an opportunity to imprint markings characteristic of a subaqueous environment, the surface texture of the quartz would indicate that the last depositional environment was a glacial setting on land. Another weakness of SEM textural analysis is that the technique is less quantitative than Fourier analysis; it is, in fact, a semiquantitative or qualitative technique in many ways. Because of this fact, operator error and the reproducibility of data can be problems. To take advantage of the best

features of both SEM imagery and Fourier analysis, many investigators are now using these two techniques together.

2.3.7 Concept of textural maturity

Sedimentologists often use the term textural maturity in reference to the textural characteristics of a particular sediment. Folk (1951) suggested that textural maturity of sandstones encompasses three textural properties: (1) the amount of clay-size sediment in the rock, (2) the sorting of the framework grains, and (3) the rounding of the framework grains. He visualized four stages of textural maturity: immature, submature, mature, and supermature (Fig. 2.19). Any sandstone containing considerable clay, say more than 5 percent, is in the immature stage. Also, the framework grains in immature sediments are poorly sorted and poorly rounded. Presumably, immature sediments have not undergone sufficient sediment transport and reworking to remove fine-size material and produce sorting and rounding of grains. With additional sediment transport and reworking, sediments enter the submature stage, in which the sediments are characterized by low clay content but grains are still not well sorted or well rounded. This stage is followed by the mature stage, in which clay

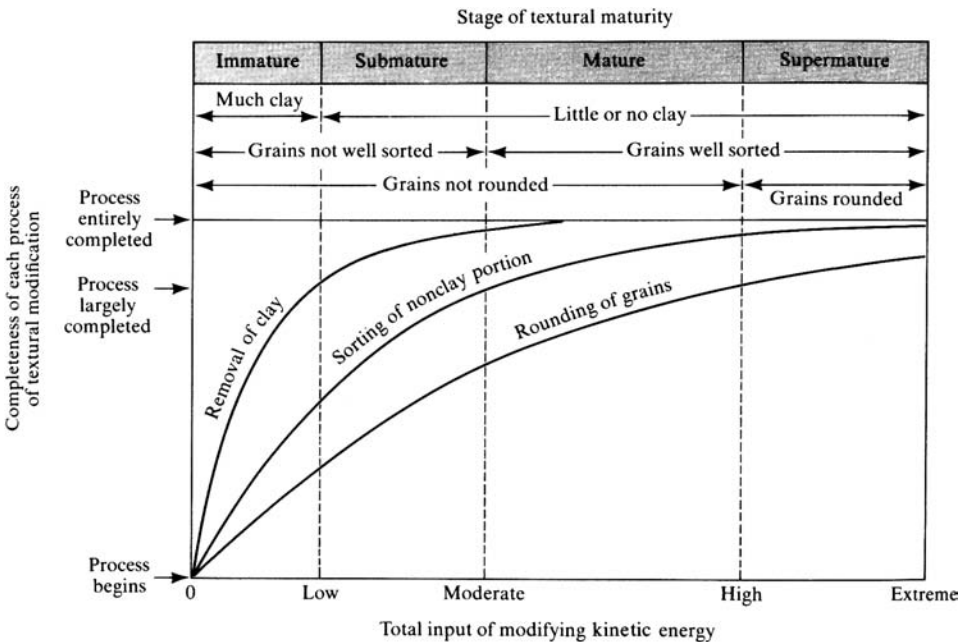


Figure 2.19 Textural maturity classification of Folk. Textural maturity of sands is shown as a function of input of kinetic energy. (From Folk, R. L., 1951, Stages of textural maturity in sedimentary rocks: *J. Sediment. Petrol.*, 21, Fig. 1, p. 128, reproduced by permission of SEPM, Tulsa, OK.)

content is low and framework grains become well sorted but are not yet well rounded. Sediments in the supermature stage are essentially clay-free, and framework grains are both well sorted and well rounded.

The textural maturity concept is a useful one for characterizing sediments; however, to attribute progressive increase in textural maturity primarily to increasing total input of modifying kinetic energy is probably overly simplistic. Matlack *et al.* (1989) have shown, for example, that the vadose infiltration of clays into sandy sediments is influenced by several variables in addition to the hydrologic conditions and depositional processes within a depositional environment. These additional factors may include grain size of the sand, size and shape of clay particles, and concentration of suspended sediment. Another significant difficulty with the concept stems from the likelihood that much of the clay-size material in many sandstones is of diagenetic origin. Therefore, its presence may have little or nothing to do with the spectrum of energy expended during transport and deposition. Also, the particles in many mature to supermature sandstones may have been recycled one or more times. Thus, the total expenditure of energy necessary to produce rounding may not have come in a single depositional cycle.

2.3.8 Fabric

General concept

The properties of grain size and shape have to do with the characteristics of individual grains. Fabric refers to the textural characteristics displayed by aggregates of grains. Fabric encompasses two properties of grain aggregates: grain packing and grain orientation. Grain packing is a function of the size and shape of grains and the postdepositional physical and chemical processes that bring about compaction of sediment. Grain orientation is mainly a function of the physical processes and conditions operating at the time of deposition; however, original grain orientation can be modified after deposition by the activities of organisms (bioturbation) and to some extent by the processes of compaction during diagenesis.

Grain packing

Interest in the packing of sediments dates back to the late nineteenth century (see summary by Griffith, 1967, p. 166). Griffith points out that most early investigators were primarily concerned with the theoretical and experimental treatment of packing (e.g. the in-depth study of the packing of spheres done by Graton and Fraser, 1935). Serious study of packing in natural sediments did not begin until the late 1930s.

Numerous definitions for packing have been proposed. For example, Kahn (1956, p. 390) defined packing simply as the “mutual spatial relationship among ... grains.” The AGI *Glossary of Geology* (Bates and Jackson, 1980, p. 449) refers to packing as “the manner of arrangement or spacing of the solid particles in a sediment or sedimentary rock...; specifically, the arrangement of clastic grains entirely apart from any authigenic grains that may

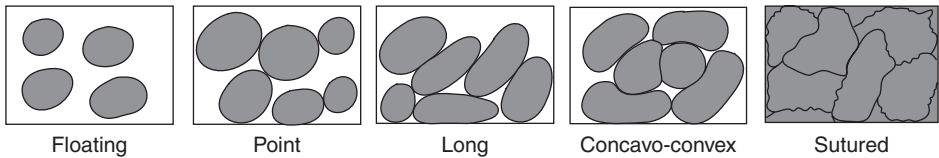


Figure 2.20 Diagrammatic illustration of principal kinds of grain contacts: Point (tangential), long, concavo–convex, and sutured. (Based on Taylor, J. M., 1950, Pore-space reduction in sandstones: *Am. Assoc. Pet. Geol. Bull.*, **34**, pp. 701–716.)

have crystallized between them.” Pandalai and Basumallick (1984, p. 87) suggest that packing is “the effective utilization of space by mutual arrangement of the constituent grains of an aggregate.”

Whatever its definition, packing is regarded to be a function of several variables or properties, including particle size and sorting, particle shape, and particle orientation or arrangement. Several early attempts were made to reduce the concept of packing to an operational level, such that packing can be measured and specified in terms of specific properties of individual grains or sets of grains (e.g. Griffith 1967, p. 166; Pandalai and Basumallick 1984, p. 88; Pettijohn *et al.* 1987, p. 86). Two packing indices in common use now are the **contact index** (= average number of contacts/grain) and the **tight packing index** (= average number of long, concavo–convex and sutured contacts/grain); see McBride (1991). Long, concavo–convex, and sutured contacts are illustrated in Fig. 2.20.

Packing is of special interest to geologists concerned with the porosity and permeability of sediments and with changes in these parameters as a function of burial depth and sediment compaction. Packing is also of interest to geophysicists concerned with petrophysical rock properties and the geomechanical behavior of rocks. See Hecht (2004) for a discussion of geomechanical models for clastic grain packing.

Particle orientation

General statement

Platy, flaky, or elongated particles in sedimentary rocks commonly display some degree of orientation that reflects the nature of the depositional process. For example, small platy or flaky particles settling from suspension onto a flat bed in the absence of current flow are commonly deposited with their flattened dimensions parallel to bedding surfaces (Fig. 2.21A). Small elongated grains settling under the same conditions also tend to have their long dimensions oriented approximately parallel to the bedding surface; however, the grains may have any orientation (random arrangement) within the bedding plane (Fig. 2.21B). Small or large particles transported and deposited by traction currents or by sediment gravity flows generally display an orientation that reflects the flow direction of the depositing current. Thus, particles may be oriented with long or flattened dimensions parallel to bedding but have orientations within the bedding plane that are either parallel to current flow (Fig. 2.21C) or perpendicular to current flow

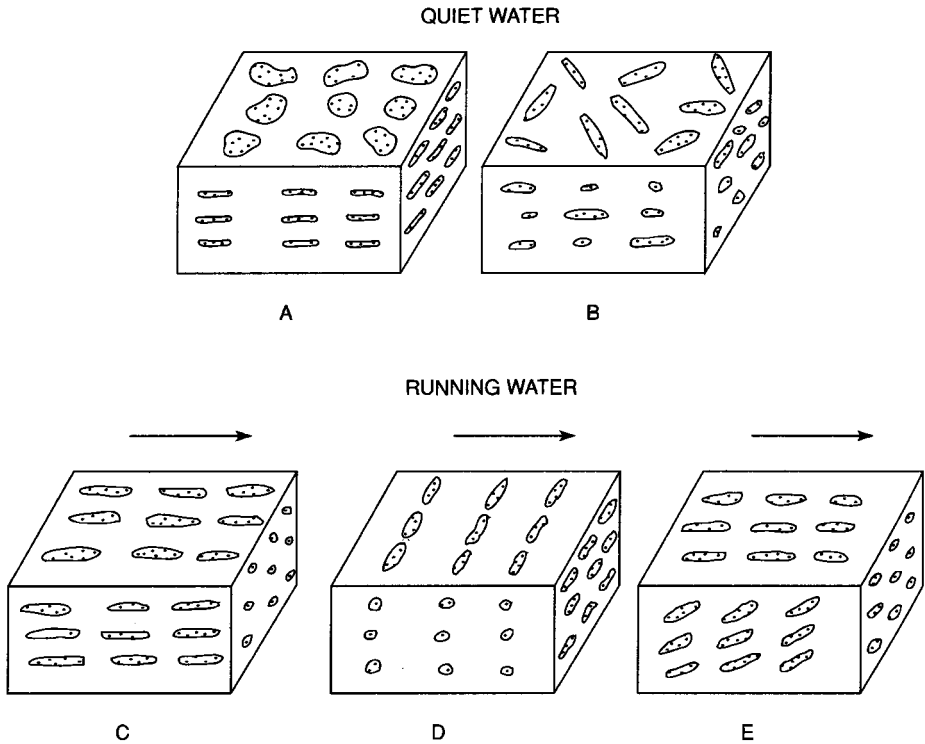


Figure 2.21 Hypothetical, schematic arrangement of grains in sediments. A. Platy or flaky grains deposited in quiet water on a flat bed. B. Elongated grains deposited in a random arrangement in quiet water. C. Elongated grains deposited under current flow with long dimensions parallel to current flow. D. Elongated grains deposited under current flow with long dimensions perpendicular to current flow. E. Elongated grains deposited in an imbricated arrangement under current flow. Arrows indicate direction of current flow,

(Fig. 2.21D), depending upon particle size and the nature of the flow. On the other hand, under some conditions of flow, the particles may lie at an angle to bedding surfaces in a shingled arrangement called imbrication (Fig. 2.21E).

The primary interest in particle orientation arises from its potential usefulness in paleocurrent analysis. In the absence of distinctive directional sedimentary structures in a deposit, particle orientation may provide the only clue to paleocurrent directions. Particle orientation is also believed to have an effect on the permeability of sedimentary rocks to fluid movement and thus is of interest to hydrologists and petroleum geologists. A few investigators have suggested that particle orientation may have significance in paleoenvironmental studies; however, use of particle orientation as an environmental tool is not fully developed. Orientation analysis has been applied to the orientation of clasts and mineral grains in siliciclastic sedimentary rocks, clasts and shells in carbonate rocks, and even to waterlogged wood.

Methods of studying orientation

The orientation of pebble- and cobble-size particles can be measured comparatively easily. If pebbles have a prolate (elongated) shape, the orientation (compass bearing) and dip (plunge) of the long particle axis is commonly measured. The orientation of plate- or disc-shaped particles is generally not expressed in terms of the long axis; instead, the orientation of the L–I plane (the plane containing the long and intermediate axes; often called the *ab* plane) is specified. The bearing of the strike of the L–I plane and the amount and direction of dip of the plane are all needed to completely describe the orientation of such pebbles.

Measuring the orientation of sand-size and smaller particles is more difficult. Application of image analysis techniques provides one solution to the problem of determining the orientation of elongated grains in thin sections (e.g. Schäfer and Teyssen, 1987; Krinsley *et al.*, 1998, p. 157.).

Displaying orientation data

Once the orientation of a statistically significant number of grains (perhaps 100 or more) has been measured, the orientation data are commonly plotted on a fabric diagram (Fig. 2.22). If we imagine a particle located in its properly oriented position in the center of a sphere and the particle axes elongated to intersect the sphere, each axis would cut the sphere in two places – one in the upper hemisphere and one in the lower. Commonly only the lower hemisphere is used in such projections, as shown in Fig. 2.22A. The points where the axes cut the lower hemisphere are then projected onto the equatorial plane of the hemisphere, as seen from directly above (Fig. 2.22B). The geographic positions of the points within the four quadrants of the equatorial plane indicate the bearing of the axes (e.g. point L in Fig. 2.22B indicates that the long particle axis is oriented NW–SE and is dipping SE; point I indicates that the intermediate axis is oriented NE–SW and is dipping SW). The relative distance of the points from the center of the hemisphere shows the amount of dip of the axes. Points located near the center indicate axes with high dips; those near the edge imply low dips (e.g. point I has a dip of 15°; point S has a dip of 45°). We may plot the orientation of one or more axes to specify the orientation of the particle. Commonly, we plot the long axes of prolate particles or the short axis of plate- or disc-shaped particles. Figure 2.22C is a “point” diagram showing the orientations of the long axes of 75 prolate pebbles. Note that the long axes of most of these pebbles are oriented NW–SE, and most dip to the SE at inclinations ranging from horizontal to about 75°. For easier visualization of particle orientation, point diagrams are often contoured as shown in Fig. 2.22D. The contours generally represent the percentage of particles that fall in each one percent area of the hemisphere (percent per one percent area).

Interpretation of orientation data

Interpretation of grain-orientation data involves an understanding of how particles behave under different transport and depositional conditions. Numerous studies of particle orientation, particularly the orientation of pebble-size particles, have been reported since the 1930s.

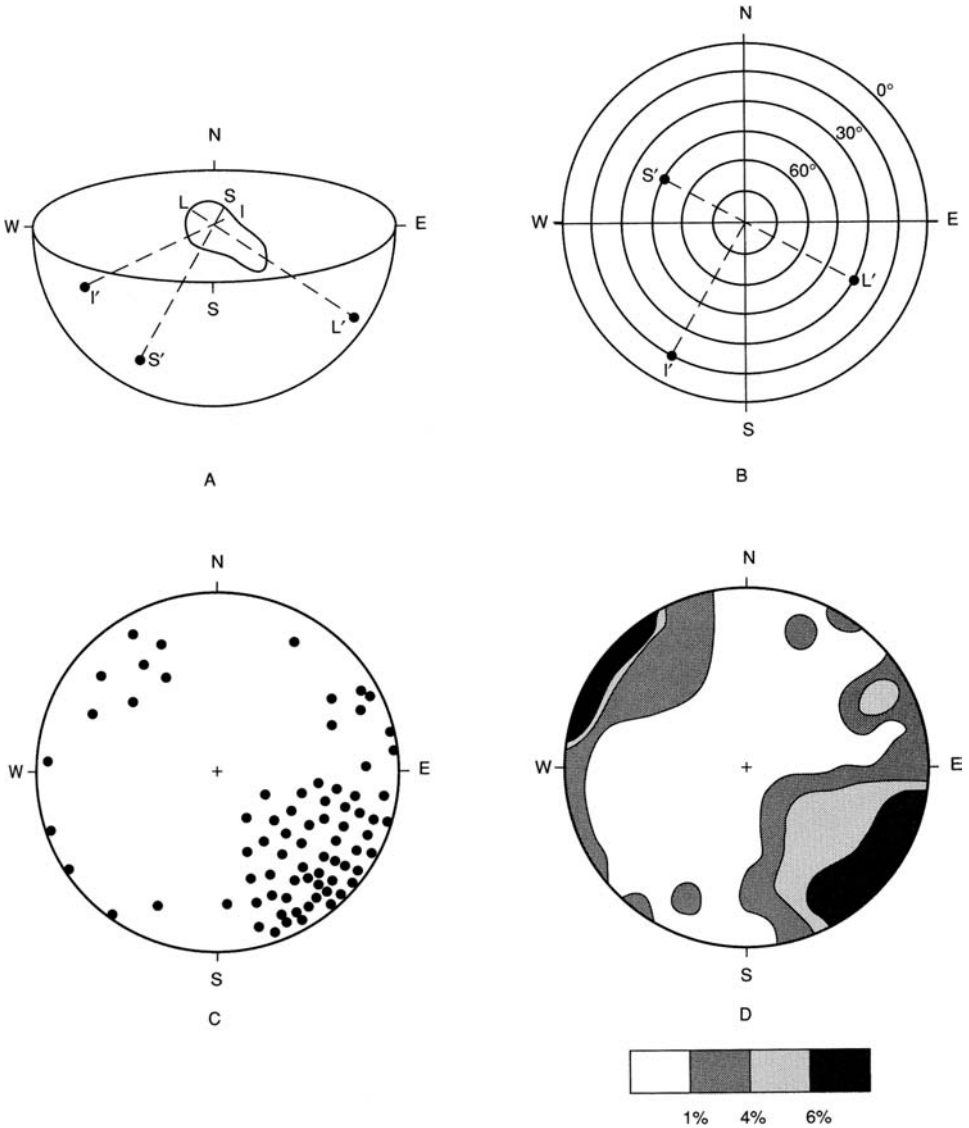


Figure 2.22 Method of graphically displaying particle orientations by using fabric diagrams. A. Extension of the long (L), intermediate (I), and short (S) axes of a particle to intersect the lower hemisphere at points L, I, and S. B. Projection of L, I, and S onto the equatorial plane of the lower hemisphere, as seen from directly above. C. A point diagram showing the projections of the long axes of 75 prolate particles. D. The point diagram contoured to show the percent points per one percent area of the diagram.

Table 2.6 *Particle imbrication and orientation in various kinds of sedimentary deposits*

Type of deposit	Imbrication direction and dip	Orientation of long axes of prolate clasts or L-I planes of blade- or disc-shaped clasts	Remarks
Gravels			
Fluvial gravel	Dip upstream 10°–30°	Dominantly transverse to flow; less commonly parallel to flow	Parallel orientation possibly related to high flow velocities and increasing pebble concentration on the bed
Glacial deposits	Poorly imbricated	Strong preferred orientation parallel to direction of ice flow	Parallel orientation weaker in basal lodgment till; water-laid glacial gravels may have random fabric
Lahars	Weak imbrication with low-angle upflow dips	Variable; both flow-parallel and flow-transverse orientations reported	Clast fabrics complex and variable
Debris flows	Poorly imbricated	Slight tendency toward flow-parallel orientation	Weak orientation
Turbidites	Dip upflow at about 10°	Flow-parallel orientations dominant	Stronger clast orientation than in debris flows
Beach gravel	Dip seaward at angles exceeding foreslope angle	Variable; ranging from parallel to perpendicular to 45° to beach trend	Some clasts may dip landward
Sands	Commonly dip upstream 10°–20°; less commonly dip downstream	Dominant flow-parallel orientation, but transverse orientation possible	Sediment size, sorting, transport mode, and flow velocity may all affect orientation

Data from various sources.

These studies suggest that particle orientation may be a function of several variables, including the nature of flow (e.g. current flow versus sediment gravity flow), bed slopes, flow velocity, particle size, particle shapes, and packing density (the number of particles that touch each other during transport). Unfortunately, the ways in which these different variables interact are not well understood. From the standpoint of paleocurrent analysis, we are particularly interested in (1) the orientation (and dip) of the long axes of prolate (elongated) particles or the L-I plane of less elongated particles, and (2) the direction and amount (dip) of imbricated particles. Several empirical studies and a limited number of experimental investigations have addressed these problems of interpretation. [Table 2.6](#) summarizes orientation data for various kinds of sediment deposits.

2.4 Porosity and permeability

2.4.1 General statement

Porosity and permeability are important secondary, or derived, properties of sedimentary rocks that are controlled in part by the textural attributes of grain size, shape, packing, and arrangement. Because porosity and permeability are, in turn, controlling parameters in the movement of fluids through rocks and sediment, they are of particular interest to petroleum geologists, petroleum engineers, and hydrologists concerned with groundwater supplies and liquid waste management. Porosity and permeability also play an extremely important role in the diagenesis of sediments by regulating the flow through rocks of fluids that promote dissolution, cementation, and authigenesis of minerals.

2.4.2 Porosity

Porosity is defined as the ratio of pore space in a sediment or sedimentary rock to the total volume of the rock. It is commonly expressed in percent as

$$\text{porosity (\%)} = V_p/V_b \quad 100 \quad (2.12)$$

Where V_p is pore volume and V_b is bulk volume. This formula yields the **total** or **absolute porosity**. Petroleum geologists and hydrologists are often more interested in the effective porosity, which is the ratio of the interconnected pore space to the bulk volume of a rock.

$$\text{effective porosity (\%)} = IV_p/V_b \quad 100 \quad (2.13)$$

where IV_p is interconnected pore volume. It is the effective porosity, commonly several percent less than total porosity, that controls the movement of fluids through rock.

In terms of origin, porosity may be either **primary** (depositional) or **secondary** (post-depositional). Primary porosity can be of three types: (1) **intergranular** or **interparticle** – pore space that exists between or among framework grains, such as siliciclastic particles and carbonate grains (ooids, fossils, etc.), (2) **intragranular** or **intraparticle** – pore space within particles, such as cavities in fossils and open space in clay minerals, and (3) **intercrystalline** – pore space between chemically formed crystals, as in dolomites. Secondary porosity may include (1) **solution porosity** caused by dissolution of cements or metastable framework grains (feldspars, rock fragments) in siliciclastic sedimentary rocks or dissolution of cements, fossils, framework crystals, etc. in carbonate or other chemically formed rocks; (2) **intercrystalline porosity** arising from pore space in cements or among other authigenic minerals, and (3) **fracture porosity**, owing to fracturing of any type of rock by tectonic forces or other processes such as compaction and desiccation.

Porosity can be measured by a variety of techniques ranging from the purely qualitative to quantitative. Qualitative “estimates” of porosity can be made by scanning a rock specimen with a hand lens or under the microscope. Somewhat more quantitative estimates can be made by point counting techniques with a petrographic microscope. Before preparing a thin section for porosity analysis, the specimen is impregnated with a colored (commonly blue)

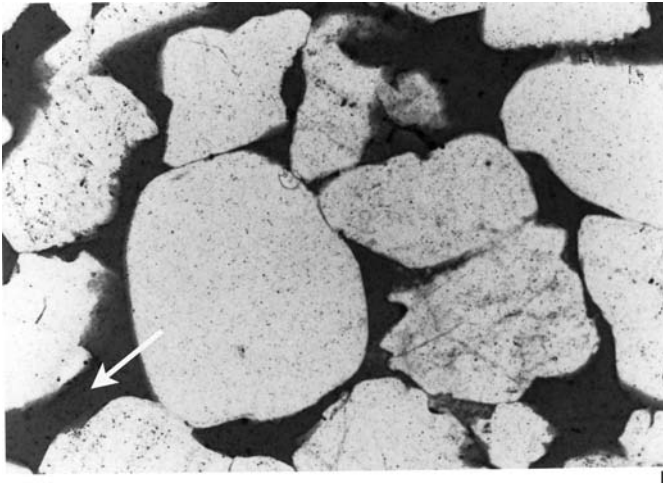


Figure 2.23 Quartz-rich sandstone impregnated with (blue) epoxy resin (arrow) to reveal porosity. Miocene, Louisiana. The field of view is 1.3 mm wide. (Photograph courtesy of D. W. Houseknecht.)

epoxy resin. Impregnation prevents the pores from becoming damaged during thin-section grinding, and the colored dye makes the pores easily visible under the microscope (Fig. 2.23). Point counts of 500 or more points provide a semiquantitative estimate of porosity. More-accurate measurements of porosity can be made in the laboratory with a variety of instrumental techniques (Monicard, 1980). Most of these techniques determine the effective porosity of a specimen by first measuring the pore volume. Pore volume is calculated by determining the volume of fluid or gas that can be forced into the rock to completely fill the pores. The porosity is then calculated by Equation 2.13, with IV_p considered to be equal to the volume of fluid forced into the pores. An alternative technique is to determine pore volume indirectly by first determining the grain volume of a specimen. The grain volume is determined by dividing the dry weight of the specimen by the rock grain density (about 2.65 in the case of a quartz-rich sandstone). The pore volume is the grain volume subtracted from the bulk volume. This method works reasonably well for clean quartz sandstones and limestones but is less accurate for rocks with highly variable compositions, owing to the difficulty of determining rock grain density.

Petroleum geologists are often required to determine the porosity of particular rock units in well bores after drilling is completed. If the well has not been cored, and thus samples of these rock units are not available, indirect methods for determining porosity must be used. These methods involve semiquantitative measurements of porosity from various types of instrumental well logs or petrophysical logs (electric logs, sonic logs, neutron logs, etc.). Discussion of these techniques is beyond the scope of this book. Details are available in numerous references, such as Asquith and Krygowski (2004).

The porosity of sedimentary rocks is affected by numerous variables. Some of these variables are physical characteristics, such as grain size, sorting, shape, packing, and grain

arrangement, that are the result, at least in part, of depositional processes. Other factors that affect porosity are caused by postdepositional processes such as compaction (which can rearrange packing), solution, and cementation. Freshly deposited, unconsolidated sediment may have porosities of 40–50 percent, or higher. During diagenesis, this initial porosity can be reduced to essentially zero, depending upon depth of burial, by a combination of compaction and cementation. On the other hand, depending upon geochemical conditions, diagenetic solution of cements and framework grains can generate considerable secondary porosity. The ultimate porosity of a rock thus depends upon both the initial depositional conditions and the diagenetic history of the rock. Additional details of porosity and porosity changes in sedimentary rocks are explored in appropriate sections of subsequent chapters, particularly [Chapters 9](#) and [12](#).

2.4.3 Permeability

Permeability is commonly defined as the ability of a medium to transmit a fluid. Rock permeability can be thought of more simply as the property of a rock that permits the passage of a fluid through the interconnected pores of the rock. The French scientist Henri Darcy performed much original work on fluid flow through porous media around 1856. Subsequent workers have quantified the passage of fluids through porous substances and formulated an equation for fluid flow that is commonly called **Darcy's law**. This equation is expressed as

$$Q = K(P_1 - P_2)A / \mu L \quad (2.14)$$

where Q is the flow rate, K is the permeability constant or permeability of the flow medium, $P_1 - P_2$ is the pressure drop across length L of the medium, A is the cross-sectional area of the medium, and μ is the viscosity of the fluid measured in centipoises. From this equation, it can be seen that the rate of flow of a fluid through a porous rock is directly proportional to the rock permeability and indirectly proportional to the fluid viscosity. Strictly speaking, Darcy's law applies when only one fluid is present in the rock and no chemical reaction takes place between the fluid and the rock.

The qualitative permeability of a rock (poor, fair, good) can be guessed by techniques such as putting a drop of water on the rock and noting the rate at which the water is absorbed into the rock. Quantitative permeability is determined in the laboratory with an instrument that can measure the rate of flow of a fluid of known viscosity across a sample of cross-section A and length L . These values are then plugged into the above equation to yield the mathematical value of K . Permeability is expressed in darcies or millidarcies (0.001 darcy). A darcy is defined as a unit of permeability equivalent to the passage of one cubic centimeter of fluid of one centipoise viscosity flowing in one second under a pressure differential of one atmosphere through a porous medium having an area of cross-section of one square centimeter and a length of one centimeter.

Permeability is a complex function of particle size, sorting, shape, packing, and orientation of sediments. The exact relationship of permeability to each of these variables is still not

fully understood, and no attempt is made here to develop a rigorous treatment of these relationships. In a very general way, permeability is believed to decrease with decreasing particle size (owing to the decrease in pore diameters and increase in capillary pressures) and decreasing sorting. It may possibly decrease with increasing particle sphericity (perhaps owing to tighter packing of spheres) and increasingly tighter or denser packing (which may reduce pore size). Also, permeability is affected by particle orientation; that is, permeability seems generally to be greater parallel to an oriented fabric, e.g. parallel to bedding planes, than perpendicular to an oriented fabric, although this may not be true in every case. Permeability also tends to increase with increasing effective porosity, but it may not be positively correlated with total porosity. Interested readers may wish to consult the voluminous literature on petroleum geology (e.g. publications of the American Association of Petroleum Geologists) that deals with this subject.

Further reading

- Asquith, G. and D. Krygowski, 2004, *Basic Well Log Analysis*, 2nd edn.: American Association of Petroleum Geologists, Tulsa, OK.
- Krinsley, D. H., K. Pye, S. Boggs, Jr., and N. K. Tovey, 1998, *Backscattered Electron Microscopy and Image Analysis of Sediments and Sedimentary Rocks*: Cambridge University Press, Cambridge.
- Mahaney, W. C., 2002, *Atlas of Sand Grain Surface Textures and Applications*: Oxford University Press, New York.
- Marshall, J. R. (ed.), 1987, *Clastic Particles*: Van Nostrand Reinhold, New York, NY.
- Syvitski, J. P. M. (ed.), 1991, *Principles, Methods, and Application of Particle Size Analysis*: Cambridge University Press, Cambridge.

3

Sedimentary structures

3.1 Introduction

Study of sedimentary structures has captured the interest of geologists for decades. Some sedimentary structures such as cross-bedding and ripple marks were recognized as early as the late eighteenth century, and perhaps well before. Progress in identification, description, classification, and interpretation of sedimentary structures has been especially rapid since the 1950s, and the fundamental origin of most sedimentary structures is now reasonably well understood. Nonetheless, empirical study of modern and ancient sediments and experimental investigation of the mechanisms that form sedimentary structures continue. Geologists are especially interested in understanding how specific sedimentary structures are related to such aspects of ancient depositional environments as relative water energy, water depth, and current flow directions. Investigation of the origin and significance of bedforms such as ripples and dunes has been a particularly active field of research.

Many sedimentary structures originate by physical processes involving moving water or wind that operate at the time of deposition. Others are formed by physical processes such as gravity slumping or sediment loading that deform unconsolidated sediment after initial deposition (soft-sediment deformation). Still other structures are of biogenic origin, formed by the burrowing, boring, browsing, or sediment-binding activities of organisms. Some types of bedding, the laminated bedding of evaporites for example, are generated by primary chemical precipitation processes. A few other structures, such as concretions, form by chemical processes operating within sediment during burial and diagenesis; thus, they are regarded to be secondary in origin. Short discussions of the processes that act to form the major kinds of sedimentary structures are given in appropriate parts of this chapter; however, detailed analysis of the sedimentary processes involved in the formation of sedimentary structures is beyond the intended scope of the book. Other topics covered in this chapter include classification of sedimentary structures and a description of the major kinds of structures. Finally, methods for studying sedimentary structures and the usefulness of sedimentary structures in paleocurrent analysis are discussed.

Readers who wish to have more information on sedimentary structures may turn to a variety of additional sources. For example, a rigorous treatment of the mechanisms of sediment transport involved in generation of bedforms and other types of structures is

given in Allen (1982). More recent books dealing with physically formed sedimentary structures include Collinson and Thompson (1989), Dimicco and Hardie (1994), and Ricci-Lucci (1995). Several older volumes are also very useful, e.g. Pettijohn and Potter (1964) and Harms *et al.* (1982). Biogenic activities important to the formation of sedimentary structures are discussed in numerous books, such as Donovan (1994), Bromley (1996), Hasiotis (2002), McIlroy (2004), and Miller (2006). Recent textbook chapters that discuss sedimentary structures include those of Boggs (2006) and Prothero and Schwab (2004). Other pertinent references are listed under further reading at the end of this chapter.

3.2 Major kinds of sedimentary structures

Sedimentary structures may be classified purely on the basis of their morphological or descriptive characteristics or on the basis of presumed mode of origin. Neither of these methods is entirely satisfactory. Descriptive classification provides little or no information about the genesis of structures; also, it is somewhat awkward trying to fit all structures into a few descriptive categories. On the other hand, genetic classifications are subjective and can be misleading. Some structures can form by more than one process or by a mixture of processes and hence can be classified under different genetic categories.

The classification shown in Table 3.1 attempts a compromise by listing primary sedimentary structures under both morphological and genetic headings. In any case, this table provides a reference point for further discussion of the major kinds of sedimentary structures. The structures are discussed mainly under the descriptive headings shown in Table 3.1; however, some kinds of structures are further subdivided for discussion by genetic category.

3.3 Bedding and bedforms

3.3.1 Nature of bedding

All sedimentary rocks occur in beds of some kind. **Beds** are tabular or lenticular layers of sedimentary rock having characteristics that distinguish them from strata above and below. Beds are a function of and are distinguished by the composition, size, shape, orientation, and packing of sediment. Beds are separated by **bedding planes** or **bounding planes** into units that may range widely in thickness. Although the term bed is used in an informal sense for any sedimentary layer, most workers formally designate as beds only those layers thicker than 1 cm, as suggested by McKee and Weir (1953). Layers thinner than 1 cm are **laminae**. On the other hand, Campbell (1967) suggested that beds have no limiting thickness and can range in thickness from a few millimeters to a few tens of meters. Figure 3.1 shows a commonly used classification of bed thickness.

Beds may be characterized internally by the presence of features such as laminae, a lens of pebbles, or a band of chert (Fig. 3.2). A distinct discontinuity, such as an erosional surface, that is present between two beds of similar composition is called an **amalgamation surface**;

Table 3.1 (cont.)

GENETIC CLASSIFICATION	Depositional structures			Erosional structures		Deformation structures					Biogenic structures		
	Suspension-settling and current- and wave-formed structures	Wind-formed structures	Chemically and biochemically precipitated structures	Scour marks	Tool marks	Slump structures	Load and founder structures	Injection (fluidization) structures	Fluid-escape structures	Desiccation structures	Impact structures (rail, hail, spray)	Bioturbation structures	Biostratification structures
MORPHOLOGICAL CLASSIFICATION													
BEDDING-PLANE MARKINGS													
Groove casts; striations; bounce, brush, prod, and roll marks					X								
Flute casts				X									
Parting lamination	X												
Load casts							X						
Tracks, trails, burrows†												X	
Mudcracks and syneresis cracks									X				
Pits and small impressions										X			
Rill and swash marks	X												
OTHER STRUCTURES													
Sedimentary sills and dikes								X					

* Not wholly stratification structures.

† Not wholly bedding-plane markings.

beds separated by such a discontinuity are called **amalgamated beds**. Beds may also display internal variations in grain size and color.

Most bedding planes that separate sedimentary layers represent a plane of nondeposition, an abrupt change in depositional conditions, or an erosion surface, although the processes or events that produce the bedding plane may not affect the entire bedding plane at one moment. Some bedding planes may be postdepositional features created by processes such as intense burrowing of some layers by organisms. Features resembling bedding or bedding planes may also be created by diagenesis or weathering, although these features are probably not true bedding. Bedding surfaces may have a variety of configurations as shown in Fig. 3.3. Thus, the beds enclosed by these bounding surfaces may likewise have various

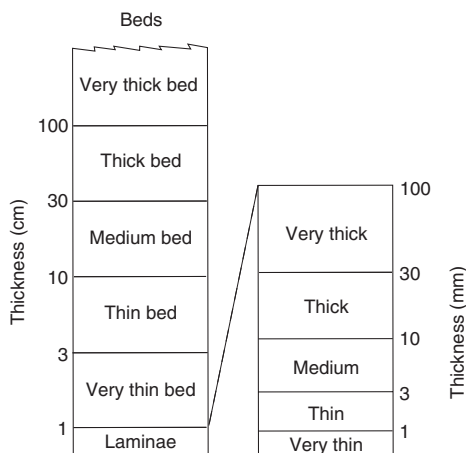


Figure 3.1 Terms used for describing the thickness of beds and laminae. (Modified from McKee, E. D. and G. W. Weir, 1953, Terminology for stratification and cross-stratification in sedimentary rocks: *Geol. Soc. Am. Bull.*, **64**, Table 2, p. 383; and Ingram, R. L., 1954, Terminology for the thickness of stratification and parting units in sedimentary rocks: *Geol. Soc. Am. Bull.*, **65**, Fig. 1, p. 937.)

geometric forms as seen in cross-section, forms such as uniform-tabular, lens-shaped, wedge-shaped, or irregular. Beds that contain internal layers that are essentially parallel to the bounding bedding surfaces are said to be **planar-stratified**. Groups of similar planar beds are called **bedsets** (Fig. 3.4). Simple bedsets are characterized by similar compositions, textures, and internal structures; **composite bedsets** consist of groups of beds that differ in these characteristics but that are genetically associated. Beds displaying internal layers deposited at a distinct angle to the bounding surfaces are **cross-stratified**. A cross-stratified bed is sometimes referred to as a set of cross-strata, and a succession of such sets is called a **coset**.

3.3.2 Laminated bedding

Many sandstones and shales, as well as some nonsiliciclastic sedimentary rocks such as evaporites, display internal laminations that are essentially parallel to bedding surfaces (Fig. 3.5). Individual laminae in these planar-stratified beds may range in thickness from a few grain diameters to as much as 1 cm. The laminae are distinguished on the basis of differences in grain size, clay and organic matter content, mineral composition, and in rare cases microfossil content of the sediment. Color changes may accentuate the presence of some laminae.

Some laminated bedding forms as a result of suspension settling of fine-size sediment in a variety of depositional environments (lakes, tidal flats, subtidal shelves, deep-sea environments). The laminae in many shales and evaporites, for example, may have formed by such suspension settling mechanisms. The presence of suspension-deposited laminae in

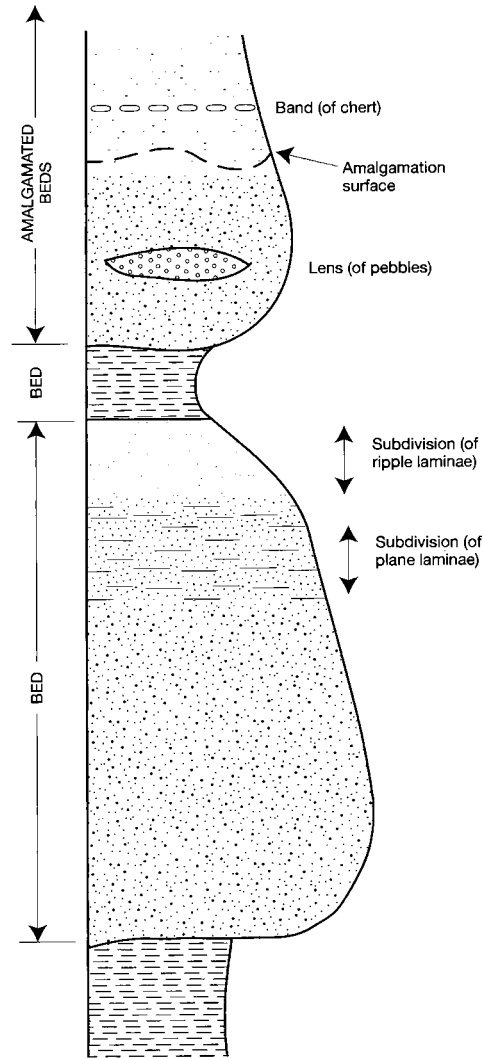


Figure 3.2 Informal subdivision of beds on the basis of internal structures. (After Boggs, 2006, *Principles of Sedimentology and Stratigraphy*, 4th edn., Prentice-Hall, Upper Saddle River, NJ, Fig. 4.2, p. 77, reproduced by permission. Based in part on Blatt H., G. Middleton, and R. Murray, 1980, *Origin of Sedimentary Rocks*, 2nd edn., Prentice-Hall, Upper Saddle River, NJ, Fig. 5.1, p. 130.)

fine-grained sediments suggests slow deposition in quiet-water environments where organic activity (bioturbation) at and below the depositional interface was not intense enough to destroy the lamination.

On the other hand, the laminae in some shales and most laminae in sandstones probably formed by traction transport mechanisms. For example, many laminated deep-sea mud deposits are now being interpreted as the products of dilute, low-velocity turbidity current

	PARALLEL		NONPARALLEL	
EVEN	Even, parallel	Discontinuous, even, parallel	Even, nonparallel	Discontinuous, even, nonparallel
WAVY	Wavy, parallel	Discontinuous, wavy, parallel	Wavy, nonparallel	Discontinuous, wavy, nonparallel
CURVED	Curved, parallel	Discontinuous, curved, parallel	Curved, nonparallel	Discontinuous, curved, nonparallel

Figure 3.3 Descriptive terms used for the configuration of bedding surfaces. (After Campbell, C. V., 1967, Lamina, lamina set, bed, and bedset: *Sedimentology*, 8, Fig. 2, p. 18, reprinted by permission of Elsevier Science Publishers, Amsterdam.)

THE NATURE OF BEDDING				
Grain size	Structure and features	Individual bed limits	Types of groups of beds (cosets or bedsets)	Bedding type
Gravel Sand	Layers or strata		Simple	Simple layered gravel
	Bedding planes and bounding surfaces		Simple	Plane laminated sand
	Layers and laminae Erosional bounding surfaces	Cross laminae	Simple	Simple cross-bedded or cross-laminated (ripple-bedded)
Sand-silty mud	Cross-beds	Cross strata	Composite	Interbedded sand/mud
	Nonerosional bounding surfaces		Composite	Lenticular bedded sand
			Simple	Laminated
Silt-mud	Laminae			Coarsening upwards

Increasing grain size, mud + gravel

Coarsening upwards of several bedsets

Figure 3.4 Diagram illustrating the terminology of bedsets. (After Collinson J.D. and D.B. Thompson, 1989, *Sedimentary Structures*: Chapman and Hall, London, Fig. 2.2, p. 7, reprinted by permission of Springer-Verlag.)

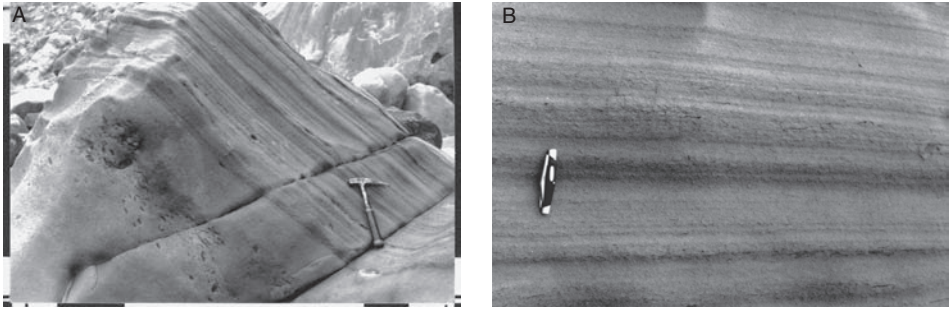


Figure 3.5 A. Laminated sandstone lying above a massive sandstone unit that contains rip-up clasts. B. Close-up view of laminae in the laminated part of A.

flows. The laminae are believed to result from the spillover of the dilute upper parts of channelized turbidity currents (Hesse and Chough, 1980; Stow and Bowen, 1980); however, the exact mechanism that produces the lamination is still speculative. Parallel laminae are very common in many sandstones and have been attributed to a variety of causes, including swash and backwash on beaches, wind transport, transport by steady-flow currents in the upper-flow regime, phases of upper-flow-regime and lower-flow-regime transport during turbidity current flow, sheet flow – the oscillatory equivalent of plane-bed transport in the upper-flow regime – and transport in the lower-flow regime.

3.3.3 Graded bedding

Graded beds are strata characterized by gradual but distinct vertical changes in grain size (Fig. 3.6A). Beds that display gradation from coarser particles at the base to finer particles at the top are said to have **normal grading**. Those that grade from finer particles at the base to coarser at the top have **reverse grading** or **inverse grading**. Grading can occur in beds of almost any thickness, even in laminae, but is most common in beds ranging from a few centimeters to a few meters. Bouma (1962, pp. 48–51) describes an “ideal” graded-bed sequence, in rocks of probable turbidity current origin, that consists of five distinct divisions. This complete sequence of units grades upward from a massive, well-graded basal portion (unit A) through a lower unit characterized by parallel laminae (B), a ripple cross-laminated middle unit (C), an upper unit with parallel laminae (D), and a topmost nearly structureless mud unit (E) (Fig. 3.7[1]A). This idealized complete sequence is now commonly referred to as a Bouma sequence; Fig. 3.6A shows a nearly complete Bouma sequence. Bouma points out, however, that many graded sequences may be truncated at the top, base, or both, and thus do not contain all of the units found in the ideal sequence. In fact, many graded beds display no visible internal structures except size grading.

Hsü (1989, p. 117) claims that Bouma’s unit D rarely occurs and that most turbidites can be divided into only two units: a lower horizontally laminated unit (unit A + B, Fig. 3.7[2]) and an upper cross-laminated unit (unit C). Unit E may be pelagic shale and thus may not be

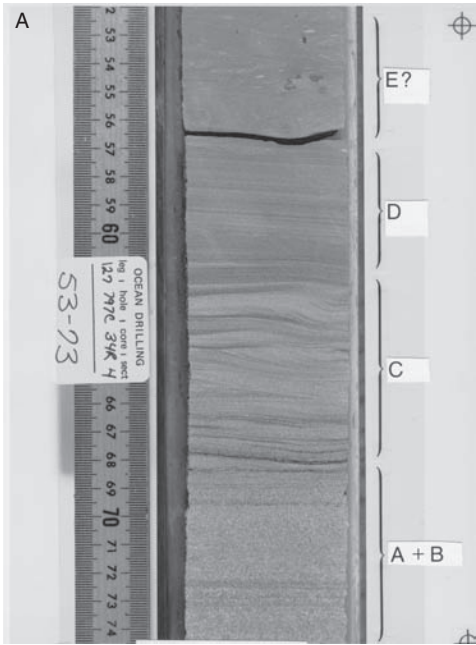


Figure 3.6 A. Graded bedding in Miocene deep-sea sandstone (core) from ODP Leg 127, Site 797, Japan Sea. Note the nearly complete Bouma sequence (units A through E) in this core, and compare with Fig. 3.7. (Photograph courtesy of the Ocean Drilling Program, Texas A & M University.) B. Rhythmically bedded, graded turbidites from the Tyee Formation (Eocene), northern Oregon Coast Range.

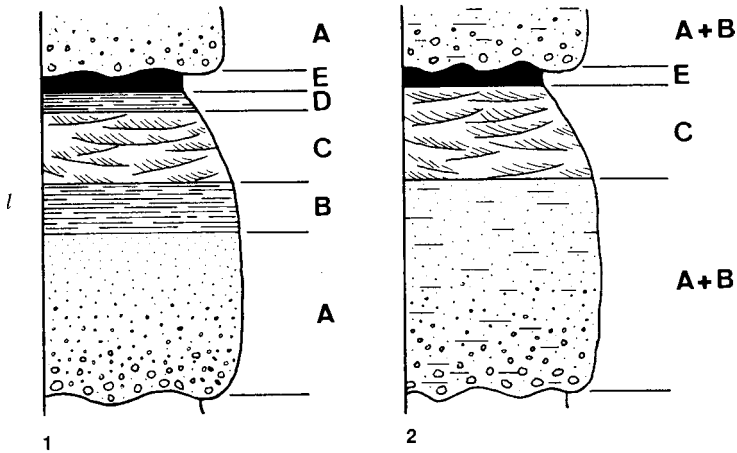


Figure 3.7 Ideal sequence of sedimentary structures in graded-bed units, as proposed by Bouma (1) and Hsü (2). Note in Hsü's model that Bouma's units A and B are combined and unit D is omitted. (After Hsü, 1989, *Physical Principles in Sedimentology*; Springer-Verlag, Berlin, Fig. 7.8, p. 116, reprinted by permission.)

part of a turbidite flow unit. The differences between Bouma's model and Hsü's model can be seen by comparing Figures 3.7(1) and 3.7(2).

Normal graded bedding can result from any process (e.g. turbidity currents, storm activity on shelves, periodic silting on delta distributaries, deposition in the last phases of a flood, settling of volcanic ash after an eruption) that produces a suspension of sediments of various sizes, which may then settle according to size. Some graded beds may have formed through the bioturbation activities of organisms. Most graded beds in the geologic record, especially graded beds that display complete Bouma sequences (Fig. 3.7), have been attributed to deposition from waning turbidity currents. Nelson (1982) has shown, however, that some shallow-water sediments deposited under the influence of storm-wave surges may also develop graded units that display Bouma sequences. Deep-sea fan deposits are commonly made up of thin, graded sandstone or siltstone beds of turbidite origin with interbeds of pelagic or hemipelagic shale. The graded units repeat one after another, producing what is commonly called rhythmic bedding (Fig. 3.6B).

Inverse grading, although less common than normal grading, occurs in some sediments, particularly in sediment-gravity-flow deposits such as debris flows and possibly some turbidites (e.g. resedimented conglomerates). There is still considerable disagreement about the causes of reverse grading. It has been attributed, among other causes, to (1) dispersive pressures owing to interparticle collisions, (2) kinetic sieving – the process whereby smaller particles fall downward through layers of coarser particles when agitated, and (3) the strength loss that clays undergo on deformation – for example, the lowermost, most strongly sheared layers of debris flows are weakest and support relatively small clasts compared to the uppermost layers. Naylor (1980) reviews these and other ideas to explain reverse grading.

3.3.4 Massive bedding

The term massive bedding is applied to beds of sedimentary rock that contain few or no visible internal laminae. Truly massively bedded sediments are rare. Many massive appearing beds have been shown actually to contain internal structures when examined after etching and staining or by X-radiography techniques. Nonetheless, massive beds do occur, both in graded and nongraded units. They appear to be most common in sandstones (Fig. 3.8).

The origin of massive beds is difficult to explain. Presumably, massive bedding is generated in the absence of fluid-flow traction transport, either by some type of sediment gravity flow or by rapid deposition of material from suspension. For example, turbidites deposited from highly concentrated flows may be massively bedded, particularly at the base. Arnott and Hand (1989) demonstrated experimentally that under upper plane-bed conditions of transport in the presence of a heavy rain of suspended sand (typical of turbidity currents) the formation of laminations is suppressed. This finding suggests that rapid aggradation can account for the massive character of Bouma A divisions of turbidites. The deposits of some grain flows, fluidized or liquefied flows, and debris flows may also appear massive. Nonetheless, extremely thick, massive beds are particularly difficult to explain, inasmuch as the deposits of single sediment gravity flows tend to be much thinner, although some thick, massive beds may be the product of truly catastrophic sediment gravity flows. Some very thick units may actually be amalgamated units, which formed by the “welding” together of the deposits of several successive sediment gravity flows consisting of sediments having about the same grain size and general characteristics. Other massive beds may be of secondary origin, formed either by the homogenizing activities of bioturbating organisms or by postdepositional sediment liquefaction owing to shocking or other mechanisms.

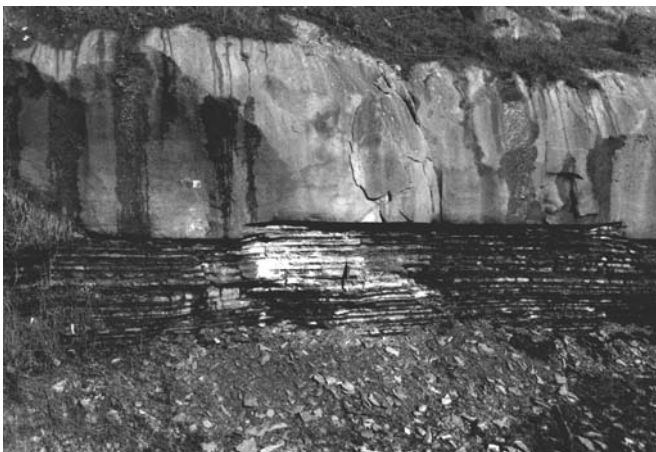


Figure 3.8 Massive-bedded sandstone (upper part of photograph) lying above thin, parallel-bedded siltstone and shale. Fluornoy Formation (Eocene), southwestern Oregon.

3.3.5 Cross-bedding

Cross-bedding is one of the commoner structures in sedimentary rocks. Although it is most abundant in sandstones, it can occur in any kind of rock made up of grains capable of undergoing traction transport. Thus, cross-bedding has been reported in limestone, salt deposits, ironstones, and phosphorites. Cross-beds, described in the simplest possible terms, are strata in which internal layers, or foresets, dip at a distinct angle to the surfaces that bound the sets of cross-beds. (Cross-bedding is called cross-lamination if thickness of the foresets is less than 10 mm.) The bedding surfaces themselves may be either planar surfaces or surfaces that are curved in some manner. Thus, one common, simple method of classifying cross-bedding is to characterize it as either **tabular cross-bedding**, having bounding surfaces that are planar, or **trough cross-bedding**, having bounding surfaces that are curved (Figs 3.9–3.11). Bedding that is markedly trough-shaped or scoop-shaped has also been referred to as **festoon bedding**.

Tabular cross-bedding is formed mainly by the migration of large-scale two-dimensional bedforms (dunes). (The geometry of two-dimensional [2-D] bedforms can be described by one transect parallel to flow, whereas three-dimensional [3-D] bedforms must be defined in three dimensions [Ashley, 1990].) Individual beds range in thickness from a few tens of centimeters to a meter or more, but bed thicknesses up to 10 meters have been reported. Trough cross-bedding originates by migration of 3-D bedforms, either small current ripples that produce small-scale cross-bed sets or large-scale ripples (dunes) that produce much larger-scale cross-bed sets. Trough cross-bedding formed by migration of large-scale ripples commonly ranges in thickness to a few tens of centimeters and in width from less than one meter to more than four meters. Cross-bedding can also form by filling of scour pits and

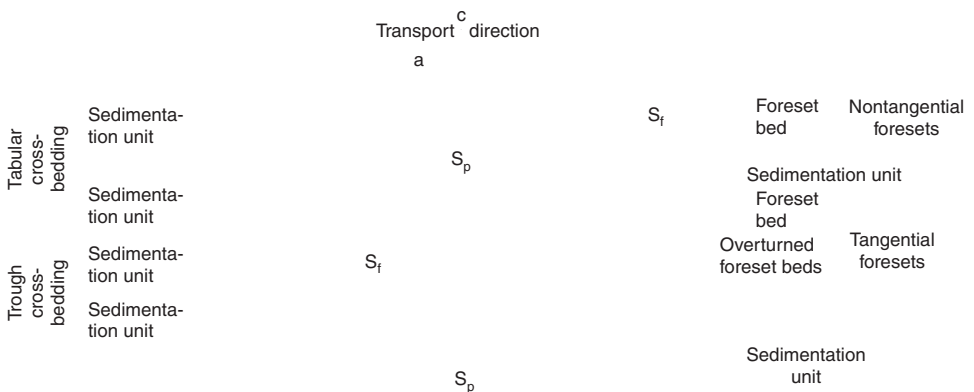


Figure 3.9 Terminology and defining characteristics of two fundamental types of cross-bedding. Symbols: (a), direction parallel to the average sediment transport direction; (c), direction perpendicular to (a) and the transport plane (bed) in which (a) lies; (S_p), the principal bedding surface or bedding plane; (S_f), the foreset surface of cross-bedding. (After Potter, P.E. and F.J. Pettijohn, 1977, *Paleocurrents and Basin Analysis*, 2nd edn., Springer-Verlag, Berlin, Fig. 4.1, p. 91, reprinted by permission.)



Figure 3.10 Multiple sets of small-scale planar cross-beds (between arrows) with tangential foresets. Coin for scale. Coaledo Formation (Eocene), southwestern Oregon.

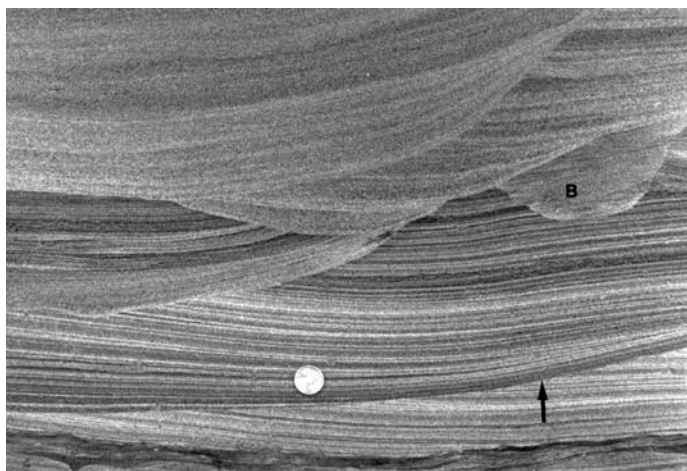


Figure 3.11 Three intersecting sets of small-scale trough cross-beds in fine, laminated sandstone. The area marked (B) may be a burrow. Probable hummocky cross-stratification (arrow) is shown in the lower part of the photograph; see also Figure 3.17. Coin for scale. Coaledo Formation (Eocene), southwestern Oregon.

channels, deposition on the point bars of meandering streams, and deposition on the inclined surfaces of beaches and marine bars. Cross-bedding formed under different environmental conditions (fluvial, eolian, marine) can be very similar in appearance and thus may be difficult to differentiate in ancient deposits.

Some cross-stratified units contain inclined surfaces that separate adjacent foresets, with similar orientations, and truncate the lower foreset laminae. Collinson (1970) referred to

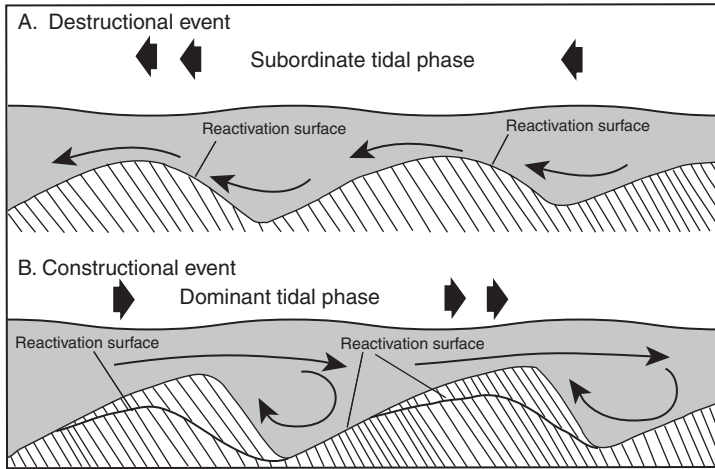


Figure 3.12 Schematic representation of reactivation surfaces in rippled sand caused by erosion of previously formed ripples during a subordinate tidal phase (destructural event) followed by renewed deposition during a dominant tidal phase (constructural event). (Based on Klein, 1970, Depositional and dispersal dynamics of intertidal sand bars: *J. Sediment. Petrol.*, **40**, Fig. 28, p. 1118.)

these surfaces as **reactivation surfaces**. Reactivation surfaces have been attributed to modification of previously formed ripples (or larger bedforms) by several mechanisms, including (1) erosion during a decrease in water depth owing to wave action or flow around the bedforms, (2) erosion during a change in current flow direction, as during a tidal reversal (Fig. 3.12), and (3) modification at constant water depth and flow direction owing either to erosion resulting from random interaction of bedforms or to erosion in the lee of an advancing bedform.

3.3.6 Ripple cross-lamination

Ripple cross-lamination is a type of cross-stratification that has the general appearance of waves when viewed in outcrop sections cut normal to the wave (ripple) crests (Fig. 3.13). Ripple cross-lamination forms when deposition takes place very rapidly during migration of current or wave ripples. A series of cross-laminae is produced owing to superimposition of one ripple on another as the ripples migrate. The ripples succeed one another upward in such a manner that the crests of vertically succeeding ripples are out of phase and appear to be advancing or climbing in a downcurrent direction; thus, this structure is sometimes called **climbing-ripple lamination**. In outcrop sections cut at orientations other than normal to ripple crests, the laminae may appear horizontal or trough-shaped, depending upon the orientation and the shape of the ripples.

Ripple cross-lamination forms under conditions where abundant sediment is present, particularly sediment in suspension, which quickly buries and preserves rippled layers.



Figure 3.13 Ripple cross-lamination (arrow). Note truncation of underlying parallel-laminated fine sand by ripple cross-lamination. Coin for scale. Coaledo Formation (Eocene), southwestern Oregon.

Abundant sediment supply is combined with enough traction transport to produce ripples and to cause the ripples to migrate, but not enough to cause complete erosion of laminae from the stoss (upcurrent) side of the ripples. In some deposits, ripple laminae are in phase, indicating that the ripples did not migrate. Ripple cross-lamination of this type forms under conditions where a balance is achieved between traction transport and sediment supply so that ripples do not migrate despite a growing sediment surface. According to Ralph Hunter (personal communication), in-phase laminae form by climbing ripples that climb essentially vertically. Such a process could occur under two possible kinds of conditions: (1) the ripples are oscillating ripples and remain active but nonmigrating during deposition or (2) the ripples are inactive and are being passively draped by suspension settling, in which case the ripple amplitude gradually decreases upward; that is, the ripples are damped. The conditions of rapid sedimentation required to produce ripple cross-lamination occur in a variety of environments, including fluvial floodplains, point bars, river deltas subject to periodic flooding, and environments of turbidite sedimentation.

3.3.7 Flaser and lenticular bedding

Flaser bedding is a special type of ripple cross-lamination in which thin streaks of mud occur between sets of ripple laminae (Fig. 3.14). The mud streaks tend to occur in the ripple troughs but may partly or completely cover the crests. Flaser bedding appears to form under fluctuating depositional conditions marked by periods of current activity, when traction transport and rippling of fine sands takes place, alternating with periods of quiescence, when mud is deposited. Repeated episodes of current activity result in



Figure 3.14 Flaser bedding in tidal-flat sediments of the North Sea. (After Reineck, H. E., 1967, Layered sediments of tidal flats, beaches, and shelf bottoms of the North Sea, in Lauff, G. H. (ed.), *Estuaries*: American Association for the Advancement of Science, Washington, DC, Fig. 8, p. 195, reproduced by permission.)



Figure 3.15 Lenticular bedding in tidal flats of the North Sea. Sand lenses are wave ripples. (After Reineck, H. E. and I. B. Singh, 1975, *Depositional Sedimentary Environments*: Springer-Verlag, New York, NY, Fig. 176, p. 103, reproduced by permission.)

erosion of previously deposited ripple crests, allowing new rippled sands to bury and preserve rippled beds with mud flasers in the troughs (Reineck and Singh, 1980). The term **lenticular bedding** is used instead of flaser bedding for interbedded mud and ripple cross-laminated sand in which the ripples or sand lenses are discontinuous and isolated in both vertical and lateral directions (Fig. 3.15). Lenticular bedding appears

to form in environments that favor deposition of mud over sand, whereas flaser bedding forms under conditions that favor deposition of sand over mud. Both structures are common in the deposits of tidal flats and some subtidal environments where conditions of current flow or wave activity, which cause sand deposition, alternate with slack-water conditions that favor mud deposition. Flaser and lenticular bedding may also form in marine and lacustrine delta-front environments, where fluctuations in sediment supply and current velocity are common; and possibly on shallow-marine shelves owing to storm-related transport of sand into deeper-water zones of mud deposition.

3.3.8 Hummocky cross-stratification

Hummocky cross-stratification is a type of cross-stratification originally called “truncated wave-ripple laminae” by Campbell (1966). It was later renamed hummocky cross-stratification by Harms *et al.* (1975). This structure is characterized by undulating sets of cross-laminae that are both concave-up (swales) and convex-up (hummocks). The cross-bed sets cut into each other with curved erosional surfaces (Figs. 3.16, 3.17). Hummocky cross-stratification

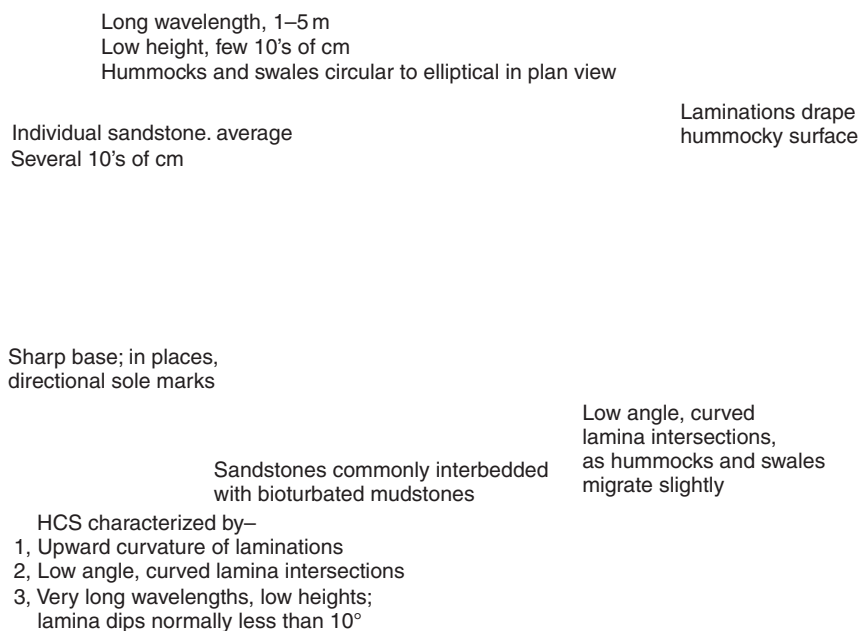


Figure 3.16 Schematic diagram of hummocky cross-stratification. (From Walker, R. G., 1984, Shelf and shallow marine sands, in Walker, R. G. (ed.), *Facies Models*, 2nd edn.: Geoscience Canada Reprint Series 1, Fig. 11, p. 149, reprinted by permission of the Geological Association of Canada.)

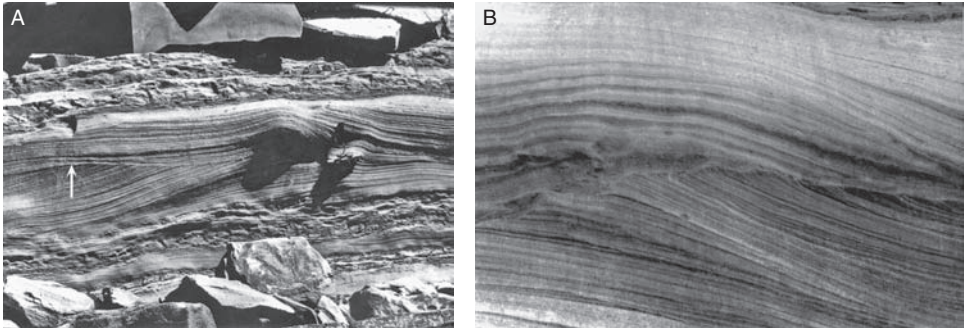


Figure 3.17 A. Hummocky cross-stratification in Coaledo Formation (Eocene) sandstones, southwest Oregon. The arrow points to a line marking the erosion surface between underlying, truncated laminae and overlying draped laminae. B. Detail of the erosional contact between underlying hummock and overlying draped laminae in a hummocky cross-stratified unit, Coaledo Formation.

commonly occurs in sets 15–20 cm thick. Spacing of hummocks and swales is from a few tens of centimeters to several meters. The lower bounding surface of a hummocky unit is sharp and is commonly an erosional surface. Current-formed sole marks may be present on the base. Hummocky cross-stratification seems to occur typically in fine sandstone to coarse siltstone that commonly contain abundant mica and fine carbonaceous plant debris.

Most workers agree that hummocky cross-stratification forms in some manner under the action of waves and that it appears to be particularly common in ancient sediments deposited on the shoreface and shelf. The exact process or processes by which hummocky cross-stratification is formed is, however, still speculative. A principal reason for uncertainty about the origin is that few unequivocal examples of this structure have been observed in modern sediments, although Greenwood and Sherman (1986) report possible hummocky cross-stratification in modern surf-zone deposits in the Canadian Great Lakes. Duke *et al.* (1991) and Cheel and Leckie (1993) suggest that hummocky cross-stratification originates by a combination of unidirectional and oscillatory flow related to storm activity. Although the exact mechanism by which this structure forms remains an open question, hummocky cross-stratification is generally regarded to be a fairly reliable indicator of deposition in shelf and shoreface environments.

3.3.9 Ripple marks

Ripples of various sizes are among the most common sedimentary structures in modern sedimentary environments, where they form in both siliciclastic and carbonate sediments. Experimental and empirical studies have firmly established that ripples occur owing to traction transport of granular materials under either unidirectional current flow or oscillatory

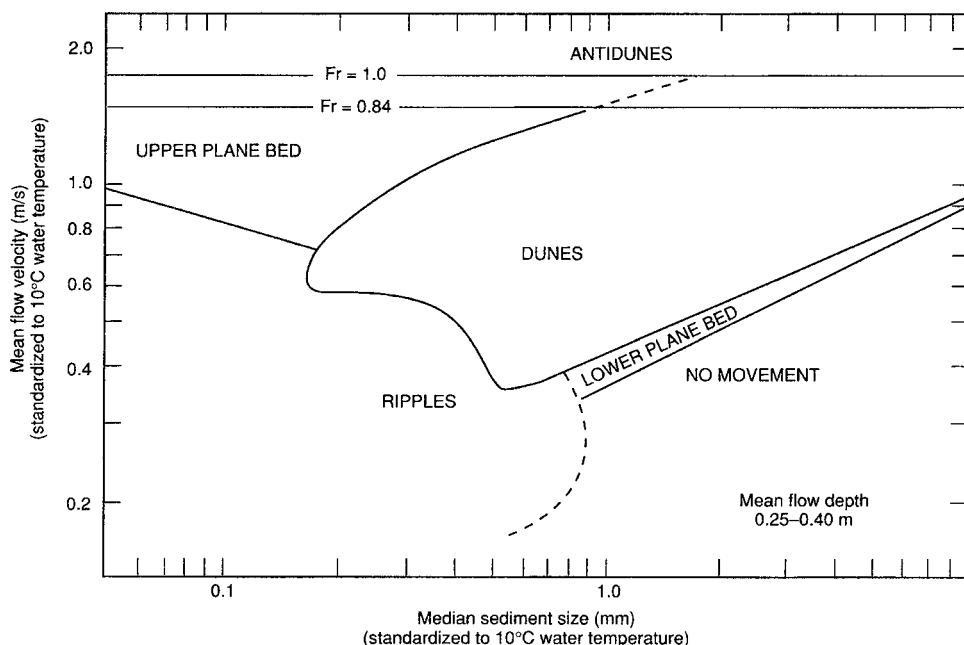


Figure 3.18 Plot of mean flow velocity against median sediment size showing the stability fields of bed phases. Note that the recommended terminology for bedforms is (1) lower plane bed, (2) ripples, (3) dunes (all large-scale ripples), (4) upper plane bed, and (5) antidunes. Fr = Froude number. (After Southard, J. B. and L. A. Boguchwal, 1990, *Bed configurations in steady unidirectional water flows. Part 2. Synthesis of flume data: J. Sediment. Petrol.*, **60**, Fig. 3, p. 664, reprinted by permission of the Society for Sedimentary Geology, Tulsa, OK.)

flow (wave action). They are most common in sand-size sediment but can occur in finer and coarser sediment.

Experimental work has shown that a progression of bedforms develop in granular materials undergoing traction transport as flow conditions change from lower-flow regime to upper-flow regime (e.g. Southard and Boguchwal, 1990). At low-flow velocities, only small ripples (0.05–0.2 m in length and 0.005–0.03 m in height) form. With increase in flow velocity, small ripples are replaced by much larger ripples. Under natural conditions, these larger ripples may reach lengths ranging from 0.5 m to more than 100 m and heights to tens of meters. Earlier workers tended to group these large ripples into two types: sand waves (low, long-wavelength bedforms) and dunes (higher, shorter-wavelength bedforms). More recent workers recommended that large bedforms have only one name, **dune**; they can be referred to as **subaqueous dunes** when it is important to distinguish them from eolian dunes (Ashley, 1990). At the higher flow velocities that bring flow conditions into the upper-flow regime, dunes are eroded and destroyed and a phase of plane-bed sediment transport occurs. Still higher flow velocities may produce **antidunes**, which migrate in an upcurrent direction. **Figure 3.18**, which shows the kinds of bedforms that develop as a function of mean flow

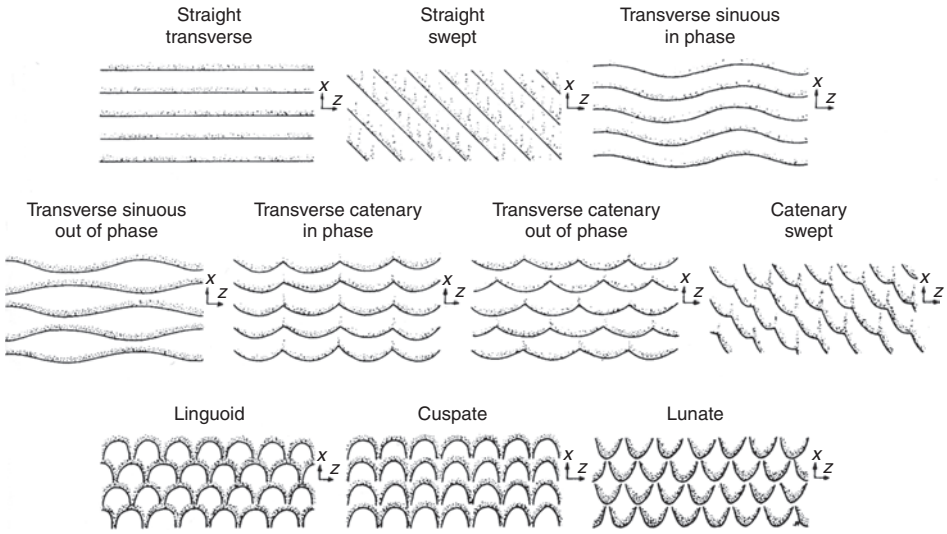


Figure 3.19 Idealized classification of current ripples on the basis of plan-view shape. Flow is from bottom to top in each case. (After Allen, 1968, *Current Ripples: Their Relation to Patterns of Water Motion*: North Holland Publ. Co., Amsterdam, Fig. 4.6, p. 65, reprinted by permission of Elsevier Science Publishers.)

velocity and mean sediment size, summarizes much of the past experimental work on bedform configuration.

When flow velocities eventually diminish, bedforms tend to be destroyed in the reverse order in which they are produced; therefore, ripples, especially large ripples and antidunes, have low preservation potential. Thus, preserved large ripples (ripple marks) are rarely abundant in ancient sedimentary rocks, although small-scale ripple marks are moderately common.

Ripples developed under unidirectional current flow are asymmetrical in cross-sectional shape, with a gently sloping upcurrent stoss side and a more steeply sloping lee side. Ripples of this type are called **current ripples**. In plan view, the crests of current ripples may have a variety of shapes: **straight**, **sinuous**, **catenary**, **linguoid**, and **lunate** (Fig. 3.19). Ripples developed under wind flow are also asymmetrical in cross-sectional shapes, but the crests are predominantly straight. Ripples generated by wave action tend to be symmetrical in cross-sectional shape unless a unidirectional bottom current is superimposed on the oscillatory flow during ripple formation. Wave-formed ripples are called **oscillation ripples** or **wave ripples**. Figure 3.20A schematically illustrates the typical plan-view shape of oscillation ripples compared to that of current ripples. Figure 3.20 B shows a photograph of oscillation ripples.

Ripple marks in ancient sedimentary rocks furnish extremely useful information about paleoflow conditions and paleocurrent directions. Ripple marks are not, however, indicators of unique depositional environments. Because they can form under

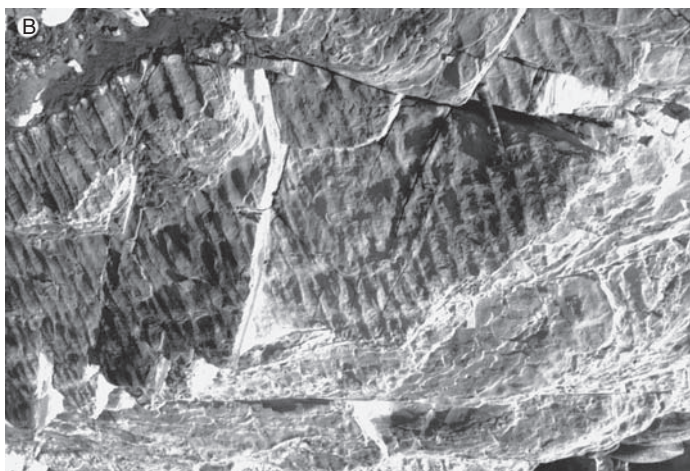
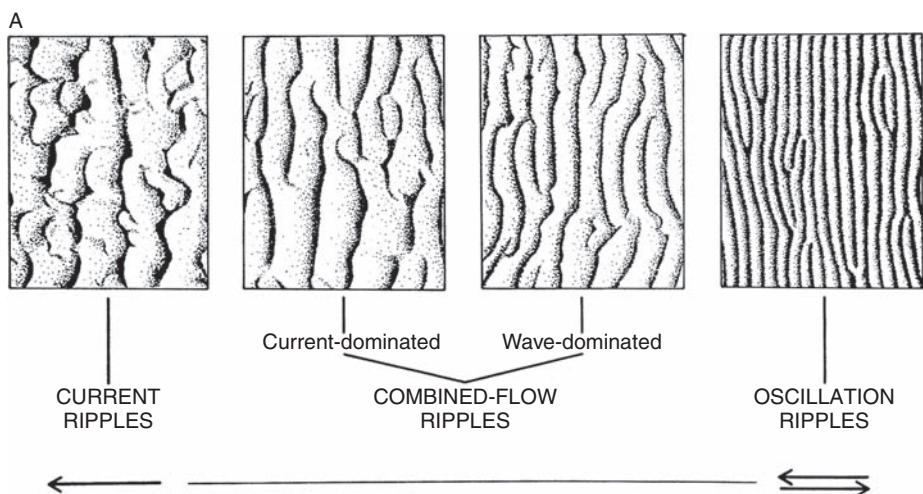


Figure 3.20 A. Plan-view shape of oscillation ripples. The shapes of typical current ripples and combined-flow ripples are shown also for comparison. (After Harms, J. C., J. B. Southard, and R. G. Walker, 1982, *Structures and Sequences in Clastic Rocks*: SEPM Short Course 9, Fig. 2–19, pp. 2–48, reprinted by permission of SEPM, Tulsa, OK.) B. Multiple sets of oscillation ripples on the upper surface of upturned, fine sandstone beds, Elkton Siltstone (Eocene), southwestern Oregon. Note hammer (upper right corner) for scale.

unidirectional currents (in both shallow and deep water), by wind transport, and by wave action great care must be used in interpreting depositional environments on the basis of these bedforms. See Boggs (2006, pp. 81–86) for a short synopsis of the origin and significance of bedforms.

3.4 Irregular stratification

3.4.1 *General statement*

Several kinds of sedimentary structures are recognized that display features of bedding or stratification, but which do not show the regular stratification of the structures discussed above. Many of these structures appear to have formed from regular bedding or stratification that was deformed or altered during or after deposition but prior to consolidation (penecontemporaneous deformation). Presumably, deformation occurs by physical processes that involve soft-sediment slumping, loading, squeezing, or partial liquefaction. Structures of this putative origin are commonly referred to as **deformation structures**. Other irregular stratification structures appear to have formed as a result of erosion of unconsolidated beds followed by an episode of sedimentation. Structures of this kind are called simply **erosion structures**. One type of irregular stratification structure, stromatolites, is produced as an original bedding structure through the activities of organisms and is thus a biogenic structure.

3.4.2 *Deformation structures*

Convolute bedding and lamination

Convolute bedding, or convolute lamination, is the name applied to complexly folded or intricately crumpled beds or laminations that are commonly, although not invariably, confined to a single sedimentation unit. Strata above and below this unit may show little or no evidence of deformation. In cross-section, the deformed strata appear as small-scale anticlines and synclines (Fig. 3.21). Axial planes of some folds may lean in the paleocurrent direction, as determined by other structures in the deposit. Convolute

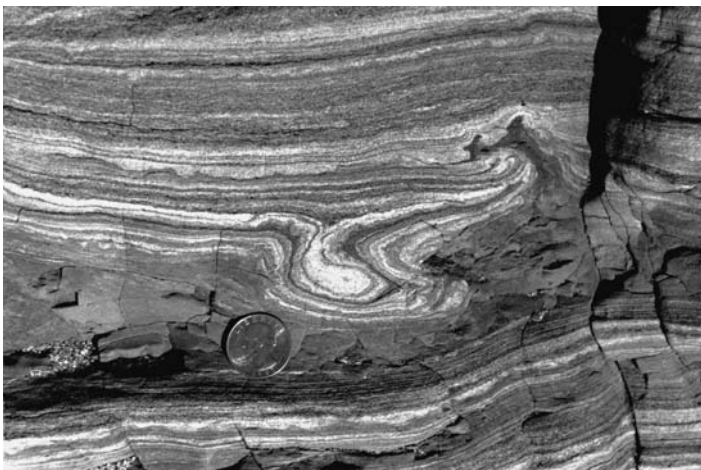


Figure 3.21 Convolute laminae in laminated siltstone overlying a thin mudstone unit. Elkton Siltstone (Eocene), southwestern Oregon.

bedding is most common in fine sand- to silt-size siliciclastic sediment but also can occur in carbonates. Each individual lamina can generally be traced from fold to fold; however, the laminae can be truncated by erosional surfaces, which may also be convoluted. Convolutions tend to increase in complexity and amplitude upward from the base or from undisturbed laminae in the lower part of the unit. They may either die out in the top part of the unit or be truncated by the upper bedding surface.

Although commonly confined to beds less than about 25 cm in thickness, convoluted units ranging up to several meters thick have been reported in both subaqueous and eolian sediments. The lateral extent of units containing convolute lamination can apparently be considerable. In one example, a convoluted unit only 12 cm thick is reported to occur over an area of about 750 km² (Sutton and Lewis, 1966). Convolute lamination is particularly common in turbidites but can occur also in a variety of other sediments, including intertidal-flat, deltaic, river-floodplain, point-bar, and eolian deposits.

The origin of convolute bedding and lamination is not fully understood. Allen (1982, vol. II, pp. 351–352) suggests that convolute lamination may form at three different stages with respect to the time of sedimentation: **postdepositional convolute lamination** arises some time after the start of burial, **metadepositional convolute lamination** arises just before or immediately after deposition ceases, and **syndepositional convolute lamination** forms episodically to continuously during deposition. The mechanisms or processes that cause convolute lamination to form are, however, poorly understood. Most workers agree that it is caused in some way by deformation of hydroplastic or liquefied sediment, but little agreement exists regarding the actual deformation mechanism (although it is probably not slumping in most cases). For additional discussion of the origin of these structures, see Allen (1982, vol. II, pp. 351–354) and Potter and Pettijohn (1977, pp. 207–208).

Flame structures

Flame structures are flame-shaped projections of mud that extend upward from a shale unit into an overlying bed of different composition, commonly sandstone (Fig. 3.22). Individual “flames” may range in height from a few millimeters to several centimeters. In some examples of the structure, the flames extend more or less directly upward into the overlying layer. In others, the crests of the flames are overturned or bent downward, commonly all in the same direction. Flame structures are probably caused by squeezing of low-density, water-saturated muds upward into denser sand layers owing to the weight of the sand. The oriented, overturned crests of some flames suggest that slight horizontal (downslope or downcurrent) movement or drag may take place between the mud and sand layers during the process of loading and squeezing. The orientation direction of overturned flame crests is commonly consistent with the paleocurrent direction suggested by other, associated sedimentary structures.

Ball and pillow structures and pseudonodules

The name ball and pillow structure (Potter and Pettijohn, 1977, p. 201) is applied to the basal portion of sandstone beds, which overlie shales, that are broken into masses of various sizes



Figure 3.22 Multiple sets of small-scale flame structures in a thinly bedded and laminated siltstone–mudstone sequence. Elkton Siltstone (Eocene), southwestern Oregon. Note hammerhead for scale.

packed vertically and laterally in a mud matrix (Fig. 3.23). These sand masses somewhat resemble the structure of pillow lavas and may have “pillow,” “hassock,” “kidney,” or “ball” shapes. The underlying shale is squeezed between pillows and may extend as tongues into the overlying sandstone. In some deposits, the sand masses may become detached from the overlying sand and be completely surrounded by shale, forming a laterally extensive layer of nearly uniform-size sand balls that may superficially resemble concretions (Allen, 1982, vol. II, p. 359). These isolated sand masses are commonly called **pseudonodules**. Individual pillows tend to be curled upward, that is, concave upward and convex downward. If they contain internal laminations, the laminations may be deformed, but they conform roughly to the boundaries of the pillows (Fig. 3.23).

Ball and pillow structures and pseudonodules are probably caused by the breakup and foundering of semiconsolidated sand or limy sediment when underlying muds become temporarily liquefied or partially liquefied. As in the formation of flame structures, lower-density mud is pushed upward into higher-density sand. Kuenen (1958) produced structures in the laboratory that closely resemble natural ball and pillow structures by applying a shock to a layer of sand overlying a thixotropic clay, momentarily liquefying the clay. Under such conditions, the overlying sand breaks up and the pieces sink into the partially liquefied clay, becoming somewhat rounded and upward-curved as they sink.

Synsedimentary folds, faults, and rip-up clasts

Unconsolidated sediment may move downslope under the influence of gravity as slumps, slides, or flows. Structures produced by such penecontemporaneous deformation may be caused by two types of movement. The first of these is a décollement type of movement in which the lateral displacement is concentrated along a sole, producing beds that are tightly folded and piled into nappe-like structures (Fig. 3.24). Such structures are referred to as

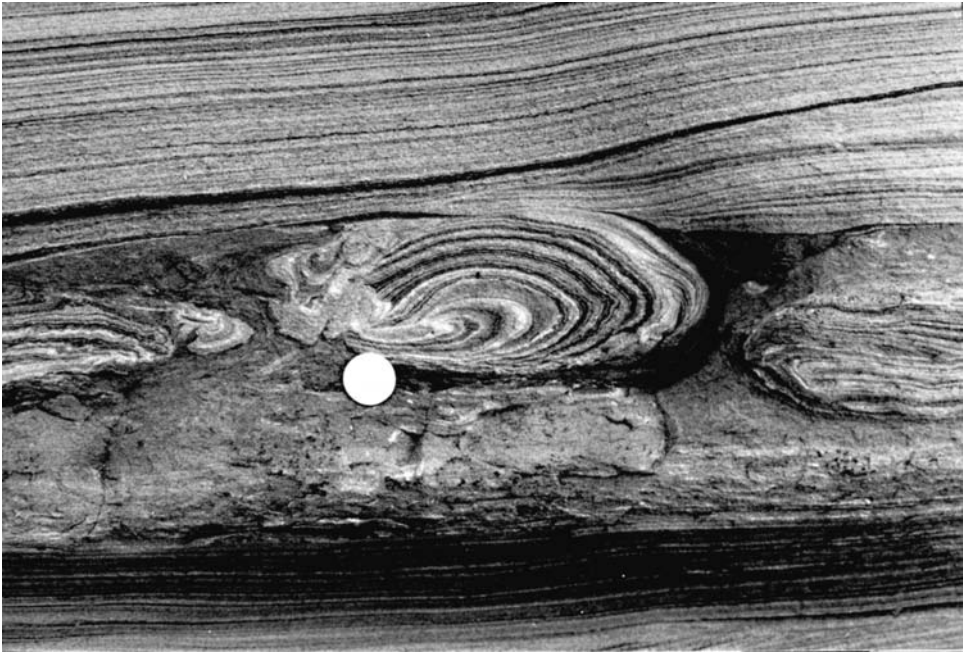


Figure 3.23 Ball and pillow structure. The balls are composed of laminated fine sandstone and are enclosed within a thin mudstone layer. Coaledo Formation (Eocene), southwestern Oregon.

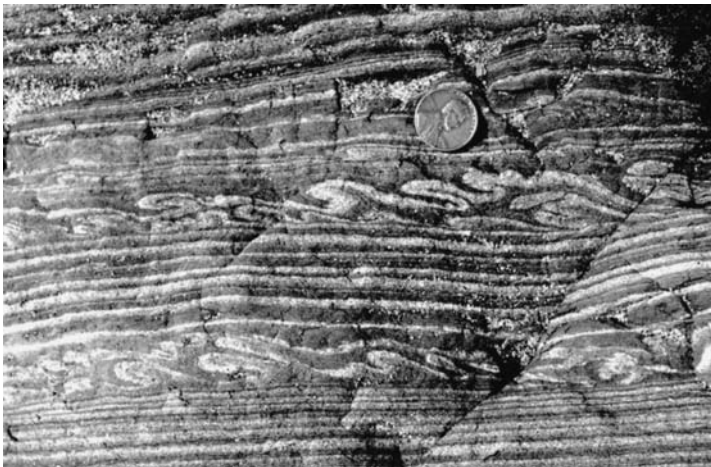


Figure 3.24 Small-scale syndimentary folds in a thick sand laminae (white) in a laminated and thinly bedded mudstone–sandstone sequence. Elkton Siltstone (Eocene), southwestern Oregon.

syndimentary folds. Slump structures of this type may involve sediments in several beds, and the structures are commonly faulted.

Thicknesses of units characterized by slump structures may range from less than 1 m to more than 50 m. Slump units are commonly bounded above and below by strata that show no evidence of deformation. Such units must be examined with care, however, to be sure that they are indeed the product of penecontemporaneous deformation and not the result of deformation of incompetent shale or other beds caught between competent sandstone or carbonate beds during tectonic folding. Slump structures commonly occur in mudstones and sandy shales and less commonly in sandstones, limestones, and evaporites. They typically form in sediments deposited in environments where rapid sedimentation and oversteepened slopes lead to instability: glacial sediments; varved silts and clays of lacustrine origin; eolian dune sands; turbidites; delta and reef-front sediments; subaqueous dune sediments; and sediments from the heads of submarine canyons, continental slopes, and the walls of deep-sea trenches.

The second type of penecontemporaneous deformation produced by slumping or flowing is the product of pervasive movement that involves the interior of the transported mass. This movement produces a chaotic mixture of different types of sediments, such as broken mud layers embedded in sandy sediment. If muddy and sandy sediment are both capable of flowing during such transport, the result is a streaked, “migmatitic” mixture (Pettijohn *et al.*, 1987, p. 117). If, on the other hand, the clay is cohesive and resistant to flow, it will break into fragments, which become incorporated into and surrounded by sand flowing as a slurry (Fig. 3.25). Shale clasts of this type in sandstone units are sometimes called **rip-up clasts**, although this term is more commonly used for shale clasts ripped up by currents, e.g. turbidity currents. The clasts may range from a few millimeters in size to several tens of



Figure 3.25 Large rip-up clasts in a massive, coarse channel sandstone. Elkton Siltstone (Eocene), southwestern Oregon. Note well-preserved laminae in some of the clasts.

centimeters. They may be angular or subrounded and may be bent or curled. Rip-up clasts appear to be particularly common in turbidites, but they occur also in debris flows and other types of sediment gravity flows and in fluvial sandstones.

Dish and pillar structures

Some sandstone and siltstone beds are characterized in cross-sectional exposures by the presence of thin, dark-colored, subhorizontal, flat to concave-upward clayey laminations (Fig. 3.26). In plan view, these features are polygonal, circular, oval, or elliptical. Because the shapes of these clayey laminations superficially resemble the shapes of saucers or other shallow dishes, they are called **dish structures** (e.g. Stauffer, 1967). Dish structures typically occur in laterally extensive, thick beds that may, or may not, be devoid of other structures. Individual dishes range from 1 to 50 cm in width but commonly are only a few millimeters thick. They may also occur in thinner beds (<0.5 m), where they may cut across primary flat lamination or other lamination (e.g. convolute lamination). The laminae forming dishes are generally darker in color than the surrounding sediment (Fig. 3.26) and commonly contain more clay, silt, or organic matter. Dish structures are particularly common in turbidites and



Figure 3.26 Dish structures (long arrow) and pillar structures (short arrow) in siliciclastic sediments of the Jackfork Group, southeast Oklahoma. (From Lowe, 1975, Water escape structures in coarse-grained sediment: *Sedimentology*, 22, Fig. 8, p. 175, reprinted by permission of Elsevier Science Publishers.)

other high-concentration flow deposits, but they have also been reported in deltaic, alluvial, lacustrine, and shallow-marine sediments and in volcanic ash layers.

Pillar structures commonly occur in association with dishes (Fig. 3.26). They are vertical to near-vertical cross-cutting columns and sheets of structureless or swirled sand that cut through either massive or laminated sands that commonly also contain dish structures and convolute lamination. Pillars range in size from tubes a few millimeters in diameter to large structures greater than 1 m in diameter and several meters in length.

Dish structures and pillars have generally been considered water-escape structures – formed as a result of rapid deposition with subsequent escape of water from the sediment during compaction and consolidation. Lowe and LoPiccolo (1974) suggested that during gradual compaction and dewatering, semipermeable laminations act as partial barriers to upward-moving water carrying fine sediment. The fine particles are retarded by the laminations and added to them, forming the dishes. Some of the water is forced horizontally beneath the laminations until it finds an easier escape route upward. This forceful upward escape of water forms the pillars. Allen (1982, vol. II, pp. 373–374) proposed an alternative explanation for formation of dish structures. He suggested that dishes may occur from a kind of stoping process within a water-saturated bed that is slightly cohesive, but far from completely consolidated. Shallow, horizontal water-filled cavities must exist in the lower part of a bed (created as a result of sedimentation after liquefaction of zones where sand has remained cohesionless or by forceful injection of external water into a bed). Each such shallow, water-filled cavity is a potentially unstable system under the influence of gravity. Slightly cohesive sand above the cavities will fail and collapse en masse into the cavities, creating subhorizontal failure surfaces, the dishes. As the sand masses are released one after the other from the roofs of the cavities, the cavities will progress upward through the bed, creating a series of dishes. If dish structures form in this manner, as suggested by Allen, they are not, strictly speaking, water-escape structures.

3.4.3 Erosion structures: channels and scour-and-fill structures

Channels are sediment-filled troughs that show a U- or V-shape in cross-section and that cut across previously formed beds or laminations (Fig. 3.27A). Channels exposed in outcrops commonly range in width and depth from a few centimeters to a few meters; rarely, they may reach tens of meters across. The long profiles of channels are rarely exposed in outcrops but can, in some cases, be defined by mapping or drilling. Channels are generally filled with sediment that is texturally different, commonly coarser, than that of the beds they truncate. Channels are probably eroded principally by currents, but some may be the result of erosion by sediment gravity flows. They are particularly common in fluvial and tidal sediments but occur also in turbidite sediments, where the long dimensions of the channels tend to be parallel to paleocurrent direction determined by other structures.

Scour-and-fill structures, also called **cut-and-fill structures**, resemble channels but tend to be somewhat smaller, more asymmetrical in cross-sectional shape, and shorter in length. They may be filled with material that is either coarser or finer than the substrate into

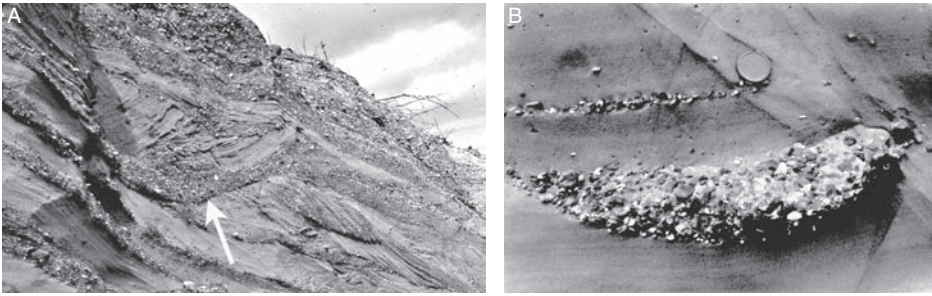


Figure 3.27 A. Channel (arrow) in fine sandstone, filled with fine sand and pebbles. Coquille Formation (Pleistocene), southern Oregon coast. B. Small channel filled with gravel, showing a lenslike form in cross-section. The sandstones at Flora Lake (Miocene), southwestern Oregon.

which they are cut (Fig. 3.27B). They are most common in sandy sediment, where they probably form owing to current scour and subsequent backfilling as current velocity decreases. In contrast to channels, several scour-and-fill structures may occur closely spaced in a row. They are particularly prevalent in sediments of fluvial origin and can occur in river, alluvial-fan, or glacial-outwash-plain environments. Genetically, scour-and-fill structures are related to flute casts (Section 3.5.1), which occur on the soles of beds.

3.4.4 Biogenic structures: stromatolitic bedding

Stromatolites are laminated structures commonly composed of fine silt- or clay-size, more rarely sand-size, carbonate sediment. They have also been reported in siliciclastic sediment, but such occurrences are rare. Some stromatolites are composed of nearly flat laminations that may be difficult to differentiate from laminations of other origins. Most stromatolites are hemispherical bodies made up of laminations that are curved, crinkled, or deformed to various degrees (Fig. 3.28). The term thrombolite was proposed by Aitken (1967) for structures that resemble stromatolites in external form and size but lack laminations. The laminations of stromatolites are generally less than 1 mm thick and are caused by variations in the concentrations and properties of fine calcium carbonate minerals, fine organic matter, and detrital clay and silt.

Stromatolites are organosedimentary structures formed largely by the trapping and binding activities of blue-green algae (cyanobacteria). They are known from rocks of Precambrian age and are forming today in many localities. Modern stromatolites are confined mainly to the shallow subtidal, intertidal, and supratidal zones of the ocean, but they have been found also in lacustrine environments. Owing to the requirements of blue-green algae to carry on photosynthesis, stromatolites are restricted to environments with adequate light for photosynthesis. The laminated structure forms as a result of trapping of fine sediment in the very fine filaments of algal mats. Once a thin layer of sediment covers a mat, the algal filaments grow up and around sediment grains to form a new mat, a process



Figure 3.28 Stromatolites in limestones of the Helena Formation (Precambrian), Glacier National Park, Montana.

that is repeated many times to produce the laminated structure. Stromatolites are most common in carbonate rocks, but have been reported from siliciclastic rocks.

3.5 Bedding-plane markings

3.5.1 *Markings generated by erosion and deposition*

General statement

Bedding-plane markings may occur either on the tops of beds or the undersides (soles) of beds. **Sole markings** are particularly common, typically consisting of positive-relief casts and various kinds of irregular markings, especially on the soles of sandstones and other coarser-grained sedimentary rocks that overlie shales. Many sole markings are generated by a two-stage process that involves initial erosion of a cohesive mud substrate to produce grooves or depressions, followed by an episode of deposition during which the grooves or depressions are filled by coarser-grained sediment. After burial and lithification, the coarser-grained sediment remains welded or amalgamated to the base of the overlying bed. After tectonic uplift, weathering processes may remove the softer underlying shale, exposing the sole of the overlying bed and the sole markings (Fig. 3.29). Erosional markings

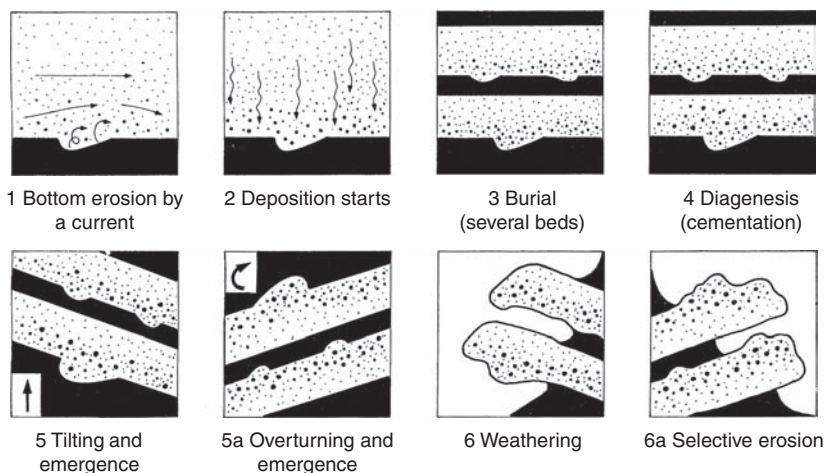


Figure 3.29 Suggested stages of development of sole markings owing to erosion of a mud bottom followed by deposition of coarser sediment. The diagram illustrates also how the sole markings appear as positive-relief features on the base of the infilling bed after tectonic uplift and subaerial weathering – and suggests how sole markings can be used to tell top and bottom of overturned beds. (From Ricci-Lucchi, F., 1995, *Sedimentographica. A Photographic Atlas of Sedimentary Structures*, 2nd edn.: Columbia University Press, New York, NY, Fig. 5, p. 4, reproduced by permission.)

are particularly common on the soles of turbidite sandstones, but they can form in any environment where the requisite conditions of an erosive event followed quickly by a depositional event are met, e.g. fluvial, tidal-flat, and shelf environments.

Tool-formed erosional structures

General statement

The erosional event that initiates the process of forming erosional sole markings can result from the action of current-transported objects that intermittently or continuously make contact with the bottom. Such contact may simultaneously deform (compress) the soft bottom sediment and gouge depressions or grooves in the sediment. The “tools” can be pieces of wood, the shells of organisms, pebbles or clasts, or any similar object that can be rolled or dragged along the bottom by normal currents or turbidity currents. Filling of these tool-formed grooves or depressions by coarser sediment generates positive-relief casts on the base of the overlying bed.

Groove casts

The most common tool-formed structures are probably groove casts. These structures are elongate, nearly straight ridges (Fig. 3.30) that result from the infilling of grooves produced by some object dragged over a mud bottom in continuous contact with the bottom. Typical groove casts are a few millimeters to a few tens of centimeters wide, with a relief of a few millimeters to a few centimeters. Much larger groove casts are known. Groove casts are



Figure 3.30 Large intersecting groove casts on the base of a graded turbidite sandstone. The knife near the center of the photograph is about 10 cm long. Fluornoy Formation (Eocene), southwestern Oregon.

markedly elongated parallel to the paleocurrent direction; therefore, they can be used to determine the sense of paleoflow, although it is generally not possible to distinguish the upcurrent from the downcurrent direction. A special kind of groove cast called chevrons is made up of continuous V-shaped crenulations that close in a downstream direction. Thus, this type of groove cast can be used to determine the true paleoflow direction. Dzulnyski and Walton (1965) suggest that chevrons are formed by tools moving just above the sediment surface, but not touching the surface, causing rucking-up of the sides of the groove.

Bounce, brush, prod, roll, and skip marks

These markings are related in origin to groove casts, but they are produced by tools that make intermittent contact with the bottom rather than continuous contact. Brush and prod marks are positive-relief features produced by the infilling of small gouge marks. They are asymmetrical in cross-section, with the deeper, broader part of the mark oriented downcurrent. By contrast, bounce marks are roughly symmetrical. Roll and skip marks are formed either by a saltating tool or by rolling of a tool over the surface, producing a continuous track. The postulated genesis of these structures is illustrated diagrammatically in Fig. 3.31.

Current-formed erosional structures

General statement

Under some conditions, currents are capable of eroding depressions in muddy or sandy substrates independently of the action of tools. Current scour owing to eddies and associated

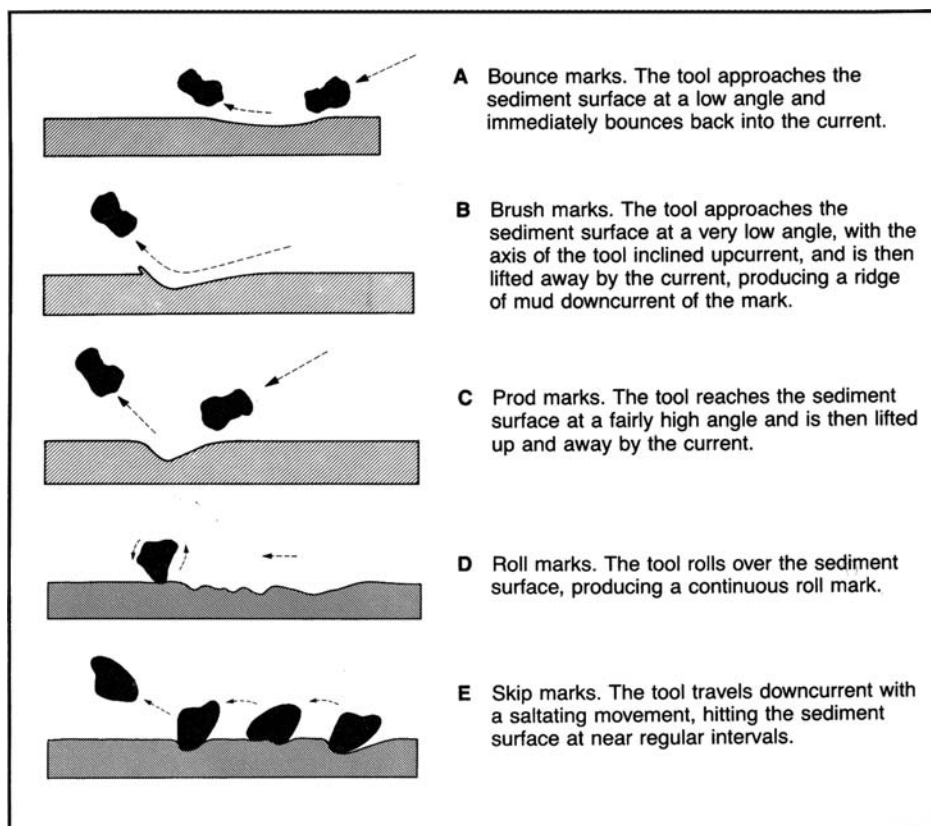


Figure 3.31 Postulated development in a cohesive mud bottom of (A) bounce marks, (B) brush marks, (C) prod marks, (D) roll marks, and (E) skip marks, which formed by the action of tools making contact with the bottom in various ways. These tool-formed depressions are subsequently filled with coarser sediment to produce positive-relief casts. (After Reineck, H. E. and I. B. Singh, 1980, *Depositional Sedimentary Environments*, 2nd edn., Springer-Verlag, Berlin, Figs. 125, 127, 129, 132, 131, p. 82, 83, reprinted by permission.)

velocity fluctuations behind obstacles, or by chance eddy scour, commonly generates asymmetrical, somewhat elongated depressions with the steepest and deepest side of the depression upstream and the more gentle side downstream. Filling of such depressions produces a positive-relief sole marking with an abrupt upstream end and a gradually tapering downstream end. Thus, current-formed structures generally make good paleocurrent indicators because they show the unique direction of current flow.

Flute casts

Flute casts are elongated welts or ridges that have at one end a bulbous nose that flares out toward the other end and merges gradually with the surface of the bed (Fig. 3.32). Flute casts



Figure 3.32 Flute casts covering the entire base (sole) of a turbidite sandstone bed. Note also the large groove cast in the lower part of the photograph (running under the hammer). The paleocurrent direction is from the upper right toward the lower left. Hornbrook Formation (Cretaceous), northern California.

tend to occur in swarms, with all of the flutes oriented in roughly the same direction, but they can occur singly. All of the flutes on the base of a given bed are generally about the same size, but great variation in size from one bed to another is possible. Flute casts can range in width from a few centimeters to more than 20 cm, in height or relief from a few centimeters to more than 10 cm, and in length from a few centimeters to a meter or more. The plan-view shape of flutes varies from nearly streamlined, bilaterally symmetrical forms to more elongate and irregular forms, some of which are highly twisted. Flute casts are particularly common on the soles of turbidite sandstones, but they occur also in sediments from shallow-marine and nonmarine environments. Less commonly, they have been reported on the soles of limestone beds.

Current crescents

These structures, also called obstacle scours, are common in modern environments, particularly sandy beach environments. They occur as narrow semicircular or horseshoe-shaped troughs, which form around small obstacles such as pebbles or shells owing to current scour (Fig. 3.33). They can form also in muddy sediment. They are relatively uncommon in ancient sedimentary rocks, where they typically occur as positive-relief casts on the soles of sandstone beds. They are most characteristic of ancient fluvial sandstones with shale interbeds, but they have also been reported in turbidites. Similar structures can form in modern eolian sediments as a result of wind transport of sand around obstacles. Wind-produced current crescents, as well as those produced in beach sands, are rarely preserved in ancient sedimentary rocks.

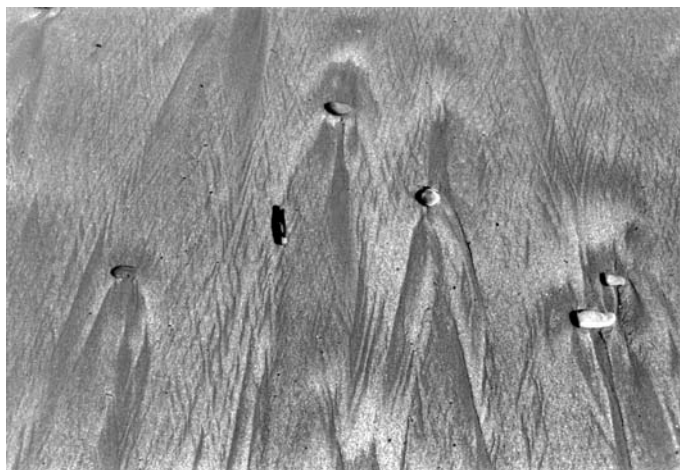


Figure 3.33 Current crescents formed downflow from pebbles on a modern beach, southern Oregon coast. The knife (near center of photograph) is about 10 cm long.



Figure 3.34 Load casts on the base of a large sandstone boulder. Some of the load casts may be modified organic traces. Unknown formation, southern Oregon coast. The knife (left side of photo) is about 10 cm long.

3.5.2 Sole markings generated by deformation: load casts

Load casts are rounded knobs or irregular protuberances on the soles of sandstone beds that overlie shales. They differ in appearance from flute casts because they lack the regular form and orientation of flutes. Where load casts are present, they tend to cover the entire surface of the sole (Fig. 3.34). They can range in size from a few centimeters to a few tens of centimeters, and the casts on a single sole may display considerable variation in size.

Load casts appear to be most common on the soles of turbidite sandstones, but have been reported in deposits from a variety of environments, including fluvial, lacustrine, deltaic, and shallow-marine. They have been found also in pyroclastic sequences. Load casts originate owing to the gravitational instability arising from the presence of beds of greater density lying above beds of lower density and low strength. Hydroplastic or uncompacted muds with excess pore pressures or muds liquefied by an externally generated shock can be deformed by the weight of the overlying sand, which may sink unequally into the incompetent mud. Such loading allows protrusions of sand to sink down into the mud, creating positive-relief features on the bases of the beds. Load casts are closely related genetically to ball and pillow structures and flame structures. Flute and groove casts, as well as ripples, may be modified by loading, a process that tends to exaggerate their relief and destroy original shapes. The presence of load casts on the bases of some beds and not on others appears to reflect the state of the underlying hydroplastic mud. They apparently will not form on the bases of sandstone beds deposited on muds that have already been compacted or dewatered prior to deposition of the sand.

3.5.3 *Markings generated by organisms: trace fossils*

Bed-surface markings attributed to the activities of fossil organisms have long been recognized. Such organically produced markings are now commonly called **trace fossils**, but they have been referred to also as **ichnofossils** and **Lebensspuren**. These markings are believed to result from the burrowing, boring, feeding, resting, and locomotion activities of organisms, which can produce a variety of trails, shallow depressions, and open burrows and borings in muds or other semiconsolidated sediments. Filling of trails or other shallow depressions with sediment of different size or packing creates structures that show up as positive-relief features on the soles of overlying beds (Fig. 3.35A). Filled burrows or borings show up as rounded markings on the top surface of underlying beds. Burrows and borings commonly extend down into beds and thus may appear in cross-sectional exposures of beds

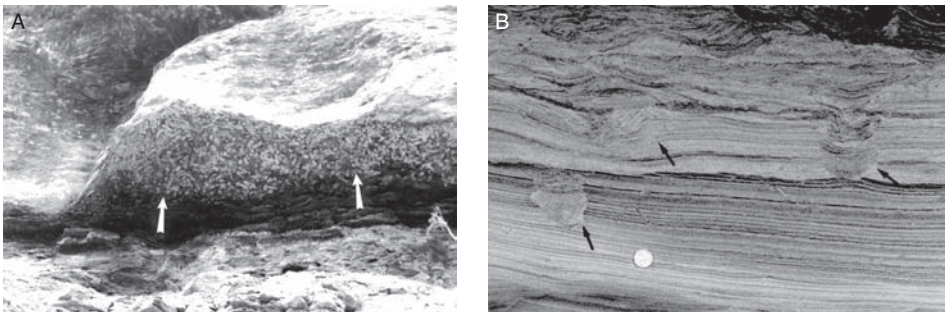


Figure 3.35 Organic markings (trace fossils). A. Copious organic traces (arrows) on the base of a massive sandstone bed. Bateman Formation (Eocene), southwestern Oregon. B. Shallow burrows (arrows) that cut across laminated fine sandstone. Coaledo Formation (Eocene), southwestern Oregon.

as filled tubes (Fig. 3.35B). Therefore, filled burrows and borings are not exclusively bedding-plane structures.

Four broad categories of biogenic structures are recognized: (1) **bioturbation structures** (burrows, tracks, trails, root penetration structures) arising from organic activity that tends to penetrate, mix, or otherwise disturb sediment, (2) **bioerosion structures** (borings, scrapings, bitings), (3) **biostratification structures** (stromatolites, graded bedding of biogenic origin), and (4) **excrement** (coprolites, such as fecal pellets or fecal castings). Not all geologists regard biostratification structures as trace fossils (see Section 3.4.4 above for a discussion of stromatolites), and these structures are not commonly included in published discussions of trace fossils.

Trace fossils have been classified also in various other ways, although classification is a complex and controversial procedure. See the discussion in Bromley (1996), Magwood (1992), and Pickerill (1994). On the basis of morphology, trace fossils have been grouped into such categories as tracks, trails, burrows, borings, and bioturbate texture (mottled bedding). On the basis of behavior (ethological classification), they can be divided into resting traces, crawling traces, grazing traces, feeding traces or structures, and dwelling structures. Trace fossils can even be classified in terms of type of preservation by use of such terms as full relief, semirelief, concave, and convex.

Geologists have become increasingly interested in trace fossils in the past few decades owing to their potential usefulness in paleoenvironmental and paleoecological interpretation. Numerous full-length books and extended research papers dealing with trace fossils have been published. See, for example, Maples and West (1992), Donovan (1994), Bromley (1996), Hasiotis *et al.* (2002), and McIlroy (2004). Trace fossils have special usefulness in paleoenvironmental analysis because they are biogenic features that clearly formed in place. In contrast to body fossils, trace fossils other than excrement cannot be transported from one environment to another and cannot be reworked from older rocks.

Although similar trace fossils may be produced by different organisms, certain associations of biogenic structures tend to characterize particular sedimentary facies. These facies, in turn, can be related to depositional environments. Seilacher (1964) introduced the term **ichnofacies** for sedimentary facies characterized by a particular association of trace fossils. Trace fossils can form under both subaerial and subaqueous conditions. In subaerial environments, organisms such as insects, spiders, worms, millipedes, snails, and lizards produce various types of burrows and tunnels; vertebrate organisms leave tracks; and plants leave root traces. In subaqueous environments, the principal factors that appear to influence their distribution are water salinity, water depth, oxygenation state of the water, and consistency of the substrate (hard or soft bottom). Numerous organisms such as worms, crustaceans, insects, bivalves, gastropods, fish, birds, amphibians, mammals, and reptiles produce traces in freshwater fluvial or lacustrine environments. Trace fossils of continental deposits are grouped into the *Scoyenia* ichnofacies (Frey *et al.*, 1984), which consists of a rather nondistinctive, low-diversity suite of invertebrate and vertebrate tracks, trails, and burrows. See Hasiotis *et al.* (2002) for extended discussion of terrestrial trace fossils.

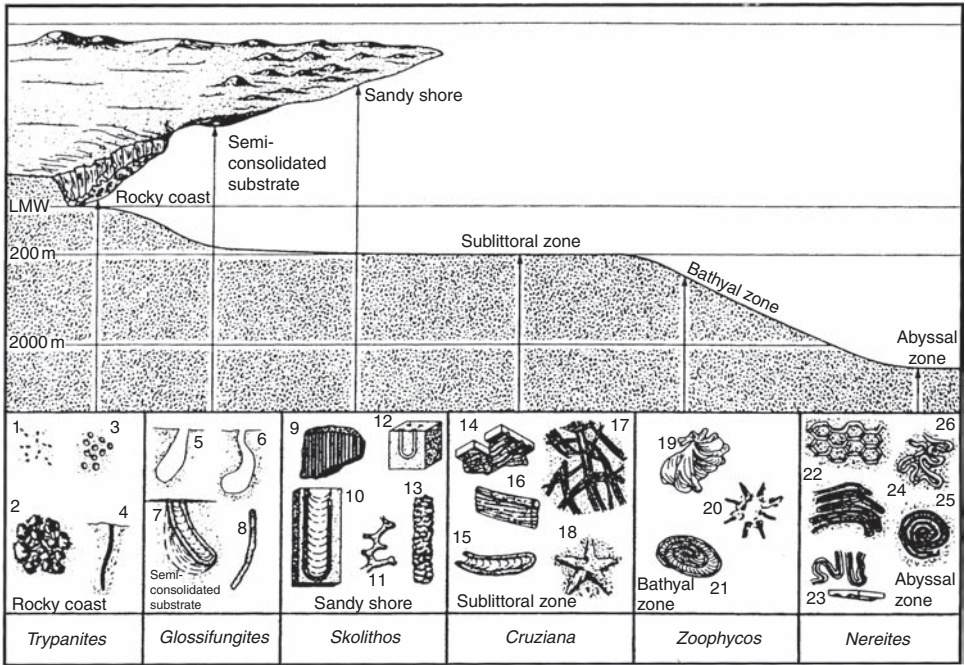


Figure 3.36 Schematic representation of the relationship of characteristic trace fossils to sedimentary facies and depth zones in the ocean. Borings of 1, *Polydora*; 2, *Entobia*; 3, echinoid borings; 4, *Trypanites*; 5,6, pholadid burrows; 7, *Diplocraterion*; 8, unlined crab burrow; 9, *Skolithos*; 10, *Diplocraterion*; 11, *Thalassinoides*; 12, *Arenicolites*; 13, *Ophiomorpha*; 14, *Phycodes*; 15, *Rhizocorallium*; 16, *Teichichnus*; 17, *Crossopodia*; 18, *Asteriacites*; 19, *Zoophycos*; 20, *Lorenzina*; 21, *Zoophycos*; 22, *Paleodictyon*; 23, *Taphrhelminthopsis*; 24, *Helminthoidea*; 25, *Spirohaphe*; 26, *Cosmorhaphe*. (From Ekdale, A. A., R. G. Bromley, and S. B. Pemberton, 1984, *Ichnology: Trace Fossils in Sedimentology and Stratigraphy*: SEPM Short Course 15, Fig. 15.2, p. 187, reprinted by permission of SEPM, Tulsa, OK. Modified from Crimes, T. P., 1975, The stratigraphical significance of trace fossils, in Crimes, T. P., and J. C. Harper, (eds.), *The Study of Trace Fossils*, Springer-Verlag, New York, NY, Fig. 7.2, p. 118.)

Marine trace fossils, produced largely by invertebrate organisms and some fish, are grouped into seven marine ichnofacies (Fig. 3.36), each named from a representative trace fossil: *Teredolites*, *Trypanites*, *Glossifungites*, *Skolithos*, *Cruziana*, *Zoophycos*, and *Nereites*. The *Teredolites* ichnofacies, not shown in Fig. 3.36, occurs only in woody material. The *Trypanites* ichnofacies is characteristic of hard, fully indurated substrates, and the *Glossifungites* ichnofacies typically occurs in firm, but uncemented, substrates. The remaining marine ichnofacies are all soft-sediment ichnofacies whose distribution appears to be controlled mainly by water depth, as illustrated in Fig. 3.36.

Each major depth zone in the ocean tends to be characterized by a distinctive association of trace fossils (Fig. 3.36). On rocky coasts and pebbly shores, trace fossils are largely rock

borings (*Trypanites* ichnofacies), which serve as dwelling structures for suspension-feeding organisms (Fig. 3.36, 1–4). Other structures in this ichnofacies include rasping and scraping traces made by feeding organisms, holes drilled by predatory gastropods, and microborings made by algae and fungi. Nearshore environments characterized by firm bottom sediment consisting largely of uncemented, dewatered, cohesive mud are inhabited by organisms that produce the *Glossifungites* ichnofacies of Frey and Seilacher (1980). The trace fossils of this environment are mainly vertical, U-shaped, and branched dwelling burrows of suspension feeders or carnivores such as shrimp, crabs, worms, and pholadid bivalves (Fig. 3.36, 5–8). The high-energy littoral zone or intertidal zone of sandy coasts, characterized by harsh conditions of intermittent exposure and large fluctuations in temperature and salinity, is host to a variety of organisms that burrow into the sandy bottom for escape. Thus, vertical and U-shaped dwelling burrows, such as the *Skolithos*, *Diplocraterion*, *Arenicolites*, and *Ophiomorpha* burrows shown in Figure 3.36, 9–13 typify the *Skolithos* ichnofacies of this zone.

It is now recognized that trace-fossil depth zones may overlap. For example, some trace fossils originally believed to be exclusively shallow-water forms, such as *Ophiomorpha*, have been found in sediments from greater depths. Also, some supposedly deep-water trace fossils such as *Zoophycos* have turned up in beds that, on the basis of associated coal or algal limestone, are clearly shallow-water deposits (Hallam, 1981). These inconsistencies suggest that factors other than water depth and food supply (oxygen levels, for example) may be involved in controlling the distribution of trace fossils. Also, not all environments at a particular depth may harbor organisms capable of leaving traces. For example, highly saline waters or highly reducing (euxinic) conditions, where low oxygen levels and the production of hydrogen sulfide gas create a toxic environment, may preclude or greatly reduce organic activity.

3.5.4 Bedding-plane markings of miscellaneous origin

A variety of generally small-scale markings of miscellaneous origin can occur on the tops (mainly) of beds: these include mudcracks, syneresis cracks, raindrop and hailstone imprints, bubble imprints, rill marks, swash marks, and parting lineation. **Mudcracks** are common in modern environments and may be preserved on the top or bottom bedding surfaces of ancient sedimentary rocks as positive-relief fillings of the original cracks (Fig. 3.37). They can occur in both siliciclastic and carbonate muds, and indicate subaerial exposure and desiccation. They may occur in association with **raindrop imprints** and **hailstone imprints**, which are craterlike pits with slightly raised rims that are commonly less than 1 cm in diameter. These imprints can be confused with **bubble imprints**, caused by bubbles breaking on the surface of sediments. **Syneresis cracks** resemble mudcracks but tend to be discontinuous and vary in shape from polygonal to spindle shaped or sinuous (Plummer and Gostin, 1981). They commonly occur in thin mudstones interbedded with sandstones as either positive-relief features on the bases of sandstones or negative-relief features on the tops of the mudstones. Syneresis cracks are believed to be subaqueous

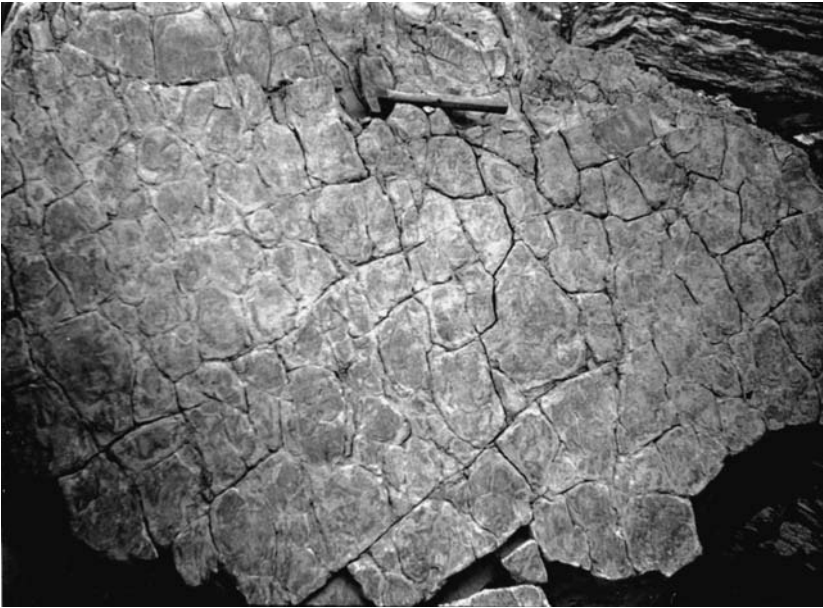


Figure 3.37 Mudcracks on the upper surface of a Miocene mudstone bed, Bangladesh. (Photograph courtesy of E. M. Baldwin.)

shrinkage cracks, formed in clayey sediment by loss of pore water from clays that have flocculated rapidly or that have undergone shrinkage of swelling-clay mineral lattices owing to changes in salinity of surrounding water (Burst, 1965). **Rill marks** are small dendritic channels or grooves that form on beaches by discharge of pore waters at low tide by small streams debouching onto a sand or mud flat. They have very low preservation potential and are seldom found in ancient sedimentary rocks. **Swash marks** are thin, arcuate lines or small ridges on a beach formed by concentrations of fine sediment and organic debris owing to wave swash; they mark the farthest advance of wave uprush. They likewise have low preservation potential.

Parting lamination, also called **current lamination**, forms primarily on the bedding surfaces of parallel-laminated sandstones, although it is reported to form also on the backs of ripples and dunes. It consists of subparallel ridges and grooves a few millimeters wide and many centimeters long (Fig. 3.38); the length of the ridges is generally 5–20 times greater than their width (Allen, 1982, vol. I, p. 261). Relief on the ridges is commonly on the order of the diameter of the sand grains. Parting lamination appears to be most common in deposits composed of medium sand or coarse silt. Detailed study of parting lamination by several investigators has revealed that the trend of the ridges and grooves is commonly in good agreement with the preferred grain orientation in the deposits, indicating that the linear fabric of current lamination is parallel to current flow direction. Parting lamination occurs in newly deposited sands in modern beach, fluvial, and tidal-run-off environments. It is most



Figure 3.38 Parting lamination in sandstone. Paleocurrent flow was approximately parallel to the bottom of the photograph. Haymond Formation, Texas. (Photograph courtesy of E. F. McBride.)

common in ancient deposits in thin, evenly bedded sandstones, probably of shallow-marine origin. It has been described also in turbidite sandstones. Its origin is obviously related to current flow and grain orientation, probably turbulent flow in the upper flow regime plane-bed phase. A more rigorous explanation of the origin of parting lamination is given by Allen (1982, vol. I, pp. 262–265).

3.6 Other structures

3.6.1 Sandstone dikes and sills

Sandstone dikes are tabular bodies of sandstone that fill fractures in any kind of host rock. They range in thickness from a few centimeters to 10 meters or more. Most sandstone dikes lack internal structures except oriented mica flakes and elongated particles that may be aligned parallel to the dike walls. They are apparently formed from liquefied sand forcefully injected upward into fractures, although examples are known where sand appears to have been injected downward into fractures. **Sandstone sills** are features of similar appearance and origin except that they are sand bodies that have been injected between beds of other rock. Sandstone sills may be difficult to differentiate from normally deposited sandstone

beds unless they can be traced into sandstone dikes or traced far enough to show a cross-cutting relationship with other beds. For example, Archer (1984) describes sandstone sills in Ordovician deep-sea deposits of western Ireland that are virtually identical to normally deposited beds. She discusses also some of the criteria that can be used to distinguish clastic sills from normal beds.

The sands that form sandstone dikes and sills must have been in a highly water-saturated, liquefied state at the time of injection, and injection seems to have been essentially instantaneous. Although some sandstone dikes and sills may have been injected into host rocks before they were completely consolidated, others could have formed much later – considerably later than the time of lithification of the host. Pettijohn *et al.* (1987) suggest that host rocks that have been injected early tend to be contorted, whereas those injected after lithification are sharp-edged and straight-walled. Sandstone dikes and sills appear to have relatively little sedimentological significance, although they may be of some value in working out the tectonic history of a region; e.g. sand-filled cracks imply episodes of tensional deformation.

3.6.2 Structures of secondary origin

Most structures discussed in preceding sections of this chapter, with the exception of some sandstone dikes and possibly convolute lamination, appear to have formed at or very shortly after deposition of the host sediment. Thus, these structures are commonly called primary sedimentary structures. A few kinds of structures occur in sedimentary rocks that clearly postdate deposition and are thus secondary sedimentary structures. The majority of these secondary structures are of chemical origin, formed by precipitation of mineral substances in the pores of semiconsolidated or consolidated sedimentary rock or by chemical replacement processes. Some secondary structures appear to form through processes involving pressure and solution.

Concretions are perhaps the most common secondary structure. These structures are typically composed of calcite; however, concretions made of other minerals (e.g. dolomite, hematite, siderite, chert, pyrite, gypsum) are known also. Concretions form by precipitation of minerals around a center, building up a globular mass. Some concretions have a distinct nucleus, such as a shell or shell fragment, but many do not. When cut open, concretions may display concentric banding around the center or may display little or no internal structure. They range in shape from nearly spherical bodies (Fig. 3.39) to disc-shaped, cone-shaped, and pipe-shaped bodies; and in size from less than a centimeter to as much as 3 m. Some concretions may be syndepositional in origin, growing in the sediment as it accumulates; however, most concretions are probably postdepositional, as shown in many cases by original bedding structures, such as laminations, that pass through the concretions. Some early workers suggested that concretions grow displacively in sediments, pushing aside sedimentary layers as they grow. Many concretions, however, appear to have formed simply by precipitation of minerals in the pore spaces of the sediment. Concretions are especially common in sandstones and shales but can occur in other sedimentary rocks.



Figure 3.39 Multiple spherical concretions in sandstones of the Coaledo Formation (Eocene), southwestern Oregon.

An unusual type of concretion was reported by Boggs (1972) that has as its nucleus a large rhombic-shaped prism, with pyramidal terminations, composed of calcite. In some specimens, the nucleus extends through the concretion and projects at either end (Fig. 3.40). Exceptional specimens of these rhombic prisms exceed 4 cm in width and 25 cm in length. Careful study of the nuclear prisms revealed that they are actually pseudomorphs after an earlier mineral. The concretionary calcite that surrounds the rhombic prisms clearly formed later than the prisms as shown by distinctly different $\delta^{13}\text{C}$ values in the concretionary calcite and the nucleus. The identity of the parent mineral was solved in the early 1980s, when a German research vessel reported crystals of **ikaite** in a core from the seabed off Bransfield Strait, Antarctica (Suess *et al.*, 1982). Ikaite is a little-known hydrated calcium carbonate mineral ($\text{CaCO}_3 \cdot 6\text{H}_2\text{O}$) discovered and named in 1963. It is now believed to be the parent mineral of these unusual pseudomorphs (Shearman and Smith, 1985). According to Shearman and Smith, ikaite crystallizes at temperatures near 0°C and breaks down at normal temperatures to form calcium carbonate and water. The calcium carbonate is then redistributed to form the calcite pseudomorphs. Aside from their unusual nature, these ikaite pseudomorphs (formerly called glendonites), not all of which are enclosed in concretionary calcite, may prove to be important as paleothermometers.

Nodules are closely related to concretions. They are small, irregularly rounded bodies that commonly have a warty or knobby surface. They generally have no internal structure except the preserved remnants of original bedding or fossils. Common minerals that make up nodules include chert, apatite (phosphorite), anhydrite, pyrite, and manganese. Some so-called nodules (e.g. manganese and phosphorite nodules) are forming now on the seafloor and are syndepositional in origin (these might better be

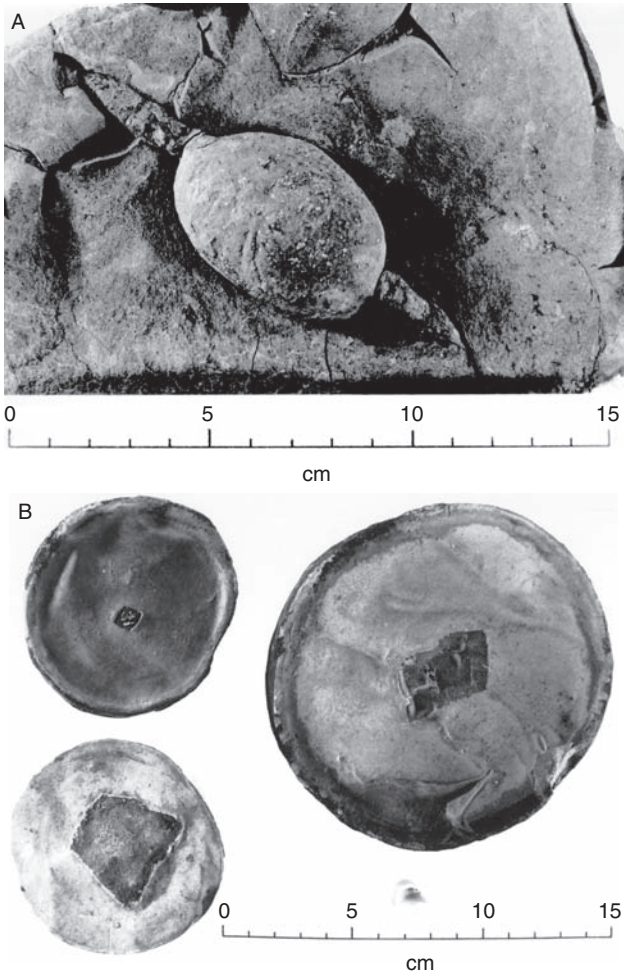


Figure 3.40 Ikaite concretion. A. A complete specimen with ikaite nucleus still intact, shown in place within host mudstone. B. Cross-sectional views of three concretions showing typical rhombic cross-sectional shape of ikaite nuclei. Astoria Formation (Miocene), northwestern Oregon.

called concretions). Other nodules (e.g. chert nodules in limestones) are clearly post-depositional. Postdepositional nodules appear to form by partially or completely replacing minerals of the host rock rather than by simple precipitation of mineral into available pore space.

Sand crystals are very large euhedral or subhedral crystals of calcite, barite, or gypsum that are filled with detrital sand inclusions (Fig. 3.41). They appear to form during diagenesis by growth in incompletely cemented sands. **Rosettes** are radially symmetric, sand-filled crystalline aggregates or clusters of crystals that somewhat resemble the shape

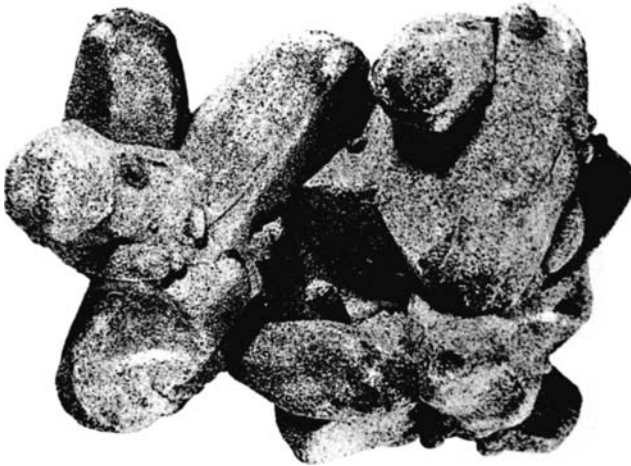


Figure 3.41 Sand crystals, Miocene sandstone, Badlands, South Dakota. Length of specimen about 15 cm. (From Pettijohn, F. J., 1975, *Sedimentary Rocks*: Harper and Row, New York, NY, Fig. 12.3, p. 467, reprinted by permission.)

of a rose. They are commonly composed of barite, pyrite, or marcasite and form by cementation processes.

Color banding, sometimes referred to as Liesegang banding, is a type of rhythmic layering resulting from the precipitation of iron oxide in fluid-saturated sediments to form thin, closely spaced, commonly curved layers. Layers having various shades of red, yellow, or brown alternate with white or cream layers. Color banding may resemble primary bedding or lamination, but can almost always be distinguished by careful study (e.g. color banding may cut across primary stratification).

Stylolites are suture- or stylus-like seams, as seen in cross-section, in generally homogeneous, thick-bedded sedimentary rocks (Fig. 3.42). The seams result from the irregular, interlocking penetration of rock on each side of the suture. They are typically only a few centimeters thick, and they are generally marked by concentrations of difficultly soluble constituents such as clay minerals, iron oxide minerals, and fine organic matter. Stylolites are most common in limestones, but occur also in sandstones, quartzites, and cherts. Although many ideas were advanced by early workers to explain stylolites, they are now regarded to form as a result of pressure solution. These structures are discussed in further detail in [Chapter 11](#).

Cone-in-cone structure is a type of structure rarely mentioned in recent sedimentological literature. It consists of nested sets of small concentric cones, composed, in most examples, of calcium carbonate, with individual cones ranging in height mainly from 10 mm to 1 cm (Fig. 3.43). Sides of the cones are slightly ribbed or fluted, and some have fine striations that resemble slickensides. Cone-in-cone structure generally occurs in thin, persistent layers of fibrous calcite, commonly in association with concretions; it is also

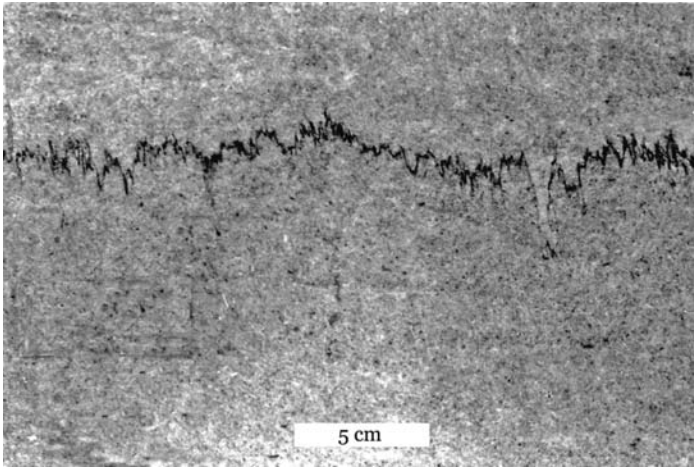


Figure 3.42 Sharp-peaked, sutured stylolites in a polished limestone slab. Age and location unknown. University of Oregon collection.

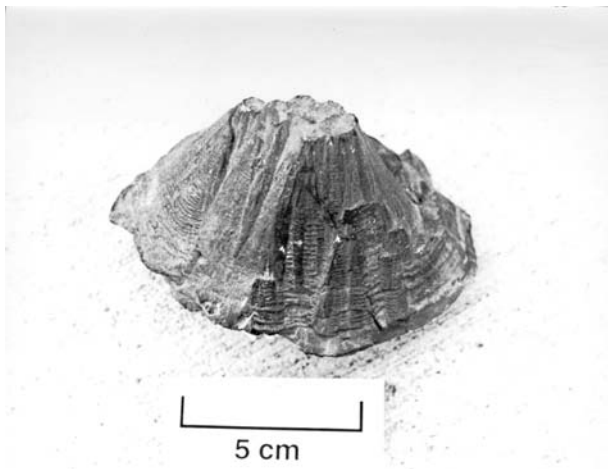


Figure 3.43 Large specimen showing typical cone-in-cone structure. Age and locality of specimen unknown.

known in pyrite concretions (Carstens, 1985). The structure is most common in shales and marly limestones. Considerable difference of opinion about the origin of cone-in-cone structure emanated from early workers (see review by Franks, 1969). Most recent workers appear to believe that cone-in-cone is an early diagenetic structure that forms by growth of fibrous crystals in the enclosing sediment while it is still in a plastic state (Woodland, 1964; Franks, 1969).

3.7 Methods for studying sedimentary structures

3.7.1 General statement

Sedimentary structures provide important information about depositional conditions and depositional environments. Also, many sedimentary structures have directional significance, making them useful indicators of paleocurrent direction. Analysis of sedimentary structures thus plays a crucial role in basin analysis. Basin analysis is a broad term that encompasses all of the various methods of study (geophysical, geochemical, sedimentologic, stratigraphic) that are focused on the evaluation of depositional systems. Information gained from such evaluation may have economic significance in petroleum and mineral exploration and significance to interpretation of geologic and tectonic history, including plate reconstructions, regional historical geology, and paleogeography. Because study of sedimentary structures constitutes such an important part of environmental interpretation and basin analysis, much work has gone into developing suitable methods for their study. See, for example, Collinson and Thompson, 1989, pp. 186–195 and Miall, 1990, pp. 315–327.

Most study of sedimentary structures takes place in the field where structures are exposed in outcrop and can be studied and photographed. Replicas of structures, called peels, may also be made in the field and taken back to the laboratory for further study. Also, samples of sediment buried on land and in subaqueous environments can be obtained by suitable coring devices, such as box corers, for subsequent laboratory study. X-Radiography techniques are particularly useful for revealing faint structures in such cores.

3.7.2 Paleocurrent analysis

Determining paleoflow (paleocurrent) directions is an important aspect of much field study. Directional sedimentary structures, such as cross-bedding and ripple marks, provide reliable information for determining paleocurrent directions. The orientation of directional sedimentary structures (e.g. the dip direction of cross-bed foresets) is determined in the field with a Brunton compass by taking measurements from as many different outcrops as practical. If directional structures have been tilted owing to tectonic uplift of their host beds, a correction must be made for this tilt (e.g. Collinson and Thompson, 1989, p. 200).

The orientation of directional structures in a particular bed or outcrop may display considerable scatter. Directional data must, therefore, be treated statistically to reveal primary and secondary paleocurrent trends. Depositing paleocurrents may have flowed in a single direction (unidirectional), two directions (bidirectional), or three or more directions (polydirectional). Corresponding paleocurrent data are thus said to be **unimodal** (e.g. river sediment), **bimodal** (e.g. tidal sediment), or **polymodal** (e.g. shoreline sediment). Geologists commonly plot paleocurrent data on so-called **rose diagrams** to reveal the

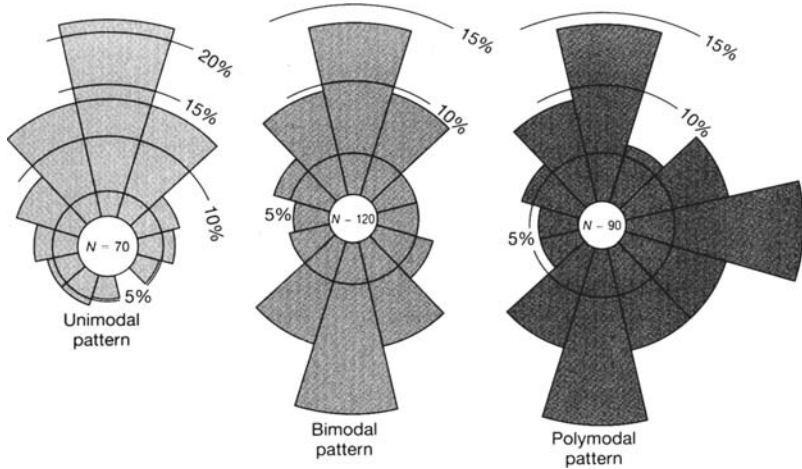


Figure 3.44 Hypothetical paleocurrent data plotted as rose diagrams. N = the number of measurements (directions) taken in the field. (After Boggs, S., Jr., 2006, *Principles of Sedimentology and Stratigraphy*, 4th edn., Prentice-Hall, Upper Saddle River, NJ, Fig. 4.43, p. 115, reproduced by permission.)

paleocurrent direction(s) (Fig. 3.44). Paleocurrents generally have their greatest usefulness when plotted on a regional scale to reveal regional paleocurrent patterns.

Further reading

- Allen, J. R. L., 1982, *Sedimentary Structures: Their Character and Physical Basis*: Elsevier, Amsterdam, vol. 1, vol. II.
- Bhattacharyya, A. and C. Chakraborty, 2000, *Analysis of Sedimentary Successions: A Field Manual*: A. A. Balkema, Rotterdam.
- Demicco, R. V. and L. A. Hardie, 1994, *Sedimentary Structures and Early Diagenetic Features of Shallow Marine Carbonate Deposits*: SEPM Atlas Series 1.
- Donovan, S. K., 1994, *The Palaeobiology of Trace Fossils*: John Hopkins University Press, Baltimore, MD.
- Hasiotis, S. T. and J. C. Van Wagoner, 2002, *Continental Trace Fossils*: Society for Sedimentary Geology, SEPM Short Course Notes 52.
- Hopkins, S. K. (ed.), 1994, *The Palaeobiology of Trace Fossils*: John Hopkins University Press, Baltimore, MD.
- Maples, C. G. and R. W. West (eds), 1992, *Trace Fossils: The Paleontological Society. Short Courses in Paleontology 5*, University of Tennessee, Knoxville, TN.
- McIlroy, D., 2004, *The Application of Ichnology to Palaeoenvironmental and Stratigraphic Analysis*: Geological Society of London, London.
- Miller, W. (ed.), 2006, *Trace Fossils, Problems, Prospects*: Elsevier, Amsterdam.
- Pettijohn, F. J. and P. E. Potter, 1964, *Atlas and Glossary of Primary Sedimentary Structures*: Springer-Verlag, New York, NY.
- Ricci-Lucchi, F., 1995, *Sedimentographica: A Photographic Atlas of Sedimentary Structures*, 2nd edn.: Columbia University Press, New York, NY.

4

Sandstones

4.1 Introduction

Sandstones make up nearly one-quarter of the sedimentary rocks in the geologic record. They are common rocks in geologic systems of all ages, although their abundance and composition vary from system to system. They are distributed throughout the continents of Earth, and they form under a wide range of depositional conditions in a variety of depositional environments. Sandstones contain many kinds of sedimentary textures and structures that have potential environmental significance, as discussed in the preceding two chapters.

Particle composition is also an important aspect of these rocks; it is a fundamental physical property of sandstones and is the chief property used in their classification. Also, particle composition has significant value in interpreting the provenance history of siliciclastic deposits (Chapter 7). Particle composition may also influence the economic importance of sandstones as oil and gas reservoirs because particle composition has an important effect on the course of diagenesis in sandstones (Chapter 8) and thus on the ultimate porosity and permeability of these rocks.

Because of the relatively coarse grain size of sandstones, their particle composition can generally be determined with reasonable accuracy by using a standard petrographic microscope. Therefore, petrographic microscopy has remained for many years the primary tool for studying the composition of sandstones. Newer tools for studying particle composition are available also. X-ray diffraction techniques are used to determine the mineralogy of very fine-grained sediments. The electron microprobe can provide accurate chemical compositions of individual mineral grains (e.g. Reed and Romanenko, 1995), and X-ray fluorescence and ICP (inductively coupled argon plasma emission spectrometry; e.g. Ridley and Lichte, 1998) allow rapid and relatively inexpensive chemical analysis of bulk samples. Cathodoluminescence petrography is being used increasingly to study cements in sandstones and the provenance of quartz and other minerals (e.g. Boggs and Krinsley, 2006). The scanning electron microscope (SEM) allows study of mineral grains at high magnification. The ability to study minerals in the SEM by using back-scattered electron image analysis (e.g. Krinsley *et al.*, 1998) is a particularly useful innovation. Chemical compositions of particular features (and thus mineral identification) can also be determined with an X-ray attachment to the SEM (energy-dispersive X-ray spectrometer), commonly referred to as XRD analysis (e.g. Goldstein *et al.*, 2003).

Sand- and coarse silt-size particles in sandstones constitute the **framework fraction** of the sandstones. Sandstones may also contain various amounts of **matrix** (material $< \sim 0.03$ mm) and **cement**, which are present within interstitial pore space among the framework grains. **Authigenic minerals** that replace some framework grains, matrix, or cement are also present in many sandstones, as well as empty pore space (**porosity**). The composition of the framework fraction is the major emphasis of this chapter; however, discussion of matrix and cement is also included. Thus, in the present chapter, I describe the mineralogy of the important detrital and authigenic constituents of sandstones and briefly consider their chemical composition. The classification of sandstones and the petrographic characteristics of the major groups of sandstones are also discussed.

4.2 Particle composition

4.2.1 Detrital constituents

General statement

Sandstones are composed of a very restricted suite of major detrital minerals and rock fragments, plus a variety of minerals that may be present in accessory amounts (Table 4.1). Detrital constituents are defined as those derived by mechanical–chemical disintegration of a parent rock. Most detrital constituents in sandstones are terrigenous siliciclastic particles that are generated through the process of weathering, explosive volcanism, and sediment transport from parent rocks located outside the depositional basin. Some volcanoclastic particles may, however, originate from volcanic centers located within basins. A few detrital constituents in sandstones may be nonsiliciclastic particles, such as skeletal fragments or carbonate clasts, formed within the depositional basin by mechanical disruption of reef masses or other consolidated or semiconsolidated carbonate bodies. Sandstones may also contain intrabasinal biogenic remains that accumulated at the depositional site, as organisms died, along with detrital sediment.

Owing to the wide variety of igneous, metamorphic, and sedimentary rocks that may constitute source materials for detrital sediment, sandstones could theoretically contain an extensive suite of major minerals. The fact that they do not can be attributed to the processes of chemical weathering and physical and chemical attack during transport, deposition, and burial that tend to destroy or degrade chemically unstable and mechanically weak sand-size grains. Thus, the framework grains of most sandstones are composed predominantly (commonly > 90 percent) of quartz, feldspars, and rock fragments. Clay minerals may be abundant in some sandstones as matrix constituents; however, the detrital origin of such clay minerals is often difficult to establish. Coarse micas, especially muscovite, make up a few percent of the framework grains of many sandstones. Finally, heavy minerals may constitute a small percentage of the detrital constituents of sandstones, particularly the chemically stable heavy minerals such as zircon, tourmaline, and rutile.

Numerous references that describe the silicate minerals are available. One of the earlier English-language descriptions of the physical and optical properties of the detrital minerals

Table 4.1 *Common minerals and rock fragments in siliciclastic sedimentary rocks***Major minerals** (abundance > ~1–2%)

Stable minerals (greatest resistance to chemical decomposition)

Quartz – makes up approximately 65% of average sandstone, 30% of average shale; 5% of average carbonate rock

Less stable minerals

Feldspars – include K-feldspars (orthoclase, microcline, sanidine, anorthoclase) and plagioclase feldspars (albite, oligoclase, andesine, labradorite, bytownite, anorthite); make up about 10–15% of average sandstone, 5% of average shale, <1% of average carbonate rock

Clay minerals and fine micas – clay minerals include the kaolinite group, illite group, smectite group (montmorillonite a principal variety), and chlorite group; fine micas are principally muscovite (sericite) and biotite; make up approximately 25–35% of total siliciclastic minerals, but may comprise >60% of the minerals in shales

Accessory minerals (abundances < ~1–2%)

Coarse micas – principally muscovite and biotite

Heavy minerals (specific gravity > ~2.9)

Stable nonopaque minerals – zircon, tourmaline, rutile, anatase

Metastable nonopaque minerals – amphiboles, pyroxenes, chlorite, garnet, apatite, staurolite, epidote, olivine, sphene, zoisite, clinozoisite, topaz, monazite, plus about 100 others of minor importance volumetrically

Stable opaque minerals – hematite, limonite

Metastable opaque minerals – magnetite, ilmenite, leucoxene

Rock fragments (make up about 10–15% of the siliciclastic grains in average sandstone and most of the gravel-size particles in conglomerates; shales contain few rock fragments)

Igneous rock fragments – may include clasts of any igneous rock, but fragments of fine-crystalline volcanic rock and volcanic glass are most common in sandstones

Metamorphic rock fragments – include metaquartzite, schist, phyllite, slate, argillite, and less commonly gneiss clasts

Sedimentary rock fragments – any type of sedimentary rock possible in conglomerates; clasts of fine sandstone, siltstone, shale, and chert are most common in sandstones; limestone clasts are comparatively rare in sandstones

Chemical cements (abundance variable)

Silicate minerals – predominantly quartz; others may include chalcedony, opal, feldspars, and zeolites

Carbonate minerals – principally calcite; less commonly aragonite, dolomite, siderite

Iron oxide minerals – hematite, limonite, goethite

Sulfate minerals – anhydrite, gypsum, barite

Note: Stability refers to chemical stability.

is that of Milner (1962). More recent references, most of which contain photomicrographs of detrital minerals and other constituents of sandstones, include Adams *et al.* (1984), Johnsson (1993), MacKenzie and Guilford (1980), and Scholle (1979). Pettijohn *et al.* (1987, pp. 19–21) provide a bibliography of petrographic manuals and encyclopedias that includes

many non-English titles. The works of Deer and others (1997) on rock-forming minerals are excellent general references for the silicate minerals. Principal journals that focus on sedimentary petrology include the *Journal of Sedimentary Research* (formerly *Journal of Sedimentary Petrology*), published by SEPM (The Society for Sedimentary Geology), *Sedimentology*, published by the International Association of Sedimentologists, and *Sedimentary Geology*, published by Elsevier.

Silica minerals

General statement

The silica minerals are the most abundant minerals in most sandstones. Quartz is the dominant silica mineral. Cristobalite and tridymite are high-temperature varieties of quartz that are uncommon in most sandstones. Chalcedony (fibrous quartz) and opal (amorphous and crystalline silica) may be present in chert grains, a common rock fragment in sandstones, and opal may be present as a cement. The most important characteristics of the silica minerals are summarized in [Table 4.2](#).

Quartz

The principal crystalline varieties of SiO_2 are quartz, cristobalite, and tridymite. Cristobalite and tridymite are metastable, high-temperature polymorphs of quartz that transform slowly with time to quartz. As mentioned, detrital cristobalite and tridymite rarely occur (or are rarely recognized) in detrital sediments. By contrast, quartz is an extremely stable mineral, and it is a dominant mineral constituent in most sandstones. It commonly makes up about two-thirds of the average sandstone (Blatt, 1982), although its actual modal abundance may range from less than 5 percent (rare) to more than 95 percent. Its relative abundance in most source rocks, coupled with its chemical resistance to weathering and mechanical resistance to abrasion during transport, account for its abundance in sandstones.

Quartz is distinguished optically by its uniaxial positive sign, although quartz that has undergone deformation may yield a biaxial figure with a small $2V$ (up to 8–10 degrees). It has low birefringence with gray interference colors in sections cut perpendicular to the optic axis. Sections cut parallel to the optic axis show white to straw yellow (in thicker sections) interference colors. In this orientation, quartz may display a flash figure, which breaks up and quickly leaves the field of view upon slight rotation of the microscope stage.

Many quartz grains display undulatory extinction, a pattern of sweeping extinction as the stage is rotated. Undulatory extinction is caused by deformation of quartz after crystallization, which results in displacement of the C crystallographic axis in the optic plane of the grain. Extinction angles, measured by rotation of a microscope stage, may be as great as 30 degrees. Quartz having an extinction angle greater than about 5 degrees is called **undulatory quartz**; quartz with extinction angles of 5 degrees or less is **nonundulatory quartz**. Intensely strained quartz grains may also be marked by the presence of trains of minute bubbles forming thin lines across the grains. These bubble trains are called **Böhm lamellae**.

Many quartz grains contain inclusions, either bubbles or mineral inclusions. The bubbles, also called **vacuoles**, are filled with liquid, liquid and gas, or gas alone. They are distributed

Table 4.2 *Characteristics of detrital silica (SiO₂) minerals***Quartz**

Most abundant detrital SiO₂ mineral; uniaxial (+), but can have biaxial (–) flash figure when cut nearly parallel to *c*-axis; low birefringence in sections cut perpendicular to optic axis; white to straw yellow interference colors in parallel sections. Occurs as single grains (monocrystalline quartz) and composite grains (polycrystalline quartz).

Monocrystalline quartz – consists of single quartz crystals that may be characterized by:

Undulatory extinction – ranging to 30°. Quartz with more than 5° undulatory extinction is called undulatory quartz; quartz with 5° or less undulatory extinction is nonundulatory quartz.

Inclusions

Liquid inclusions – liquid- or gas-filled bubbles

Vacuoles – nonoriented bubbles

Böhm lamellae – bubbles oriented along strain lines

Mineral inclusions (microlites) – tourmaline or rutile particularly common

Polycrystalline quartz – quartz grains composed of aggregates of two or more quartz crystals (composite quartz); some rock fragments (chert, quartzite, quartz-rich sandstone) are also considered to be polycrystalline quartz grains by some authors.

Cristobalite and tridymite

High-temperature varieties of SiO₂ best identified by X-ray methods; metastable and invert slowly with time and temperature to quartz; rare as detrital minerals in most sandstones, but may be present in volcanoclastic sandstones

Chalcedony and microcrystalline quartz

Chalcedony is composed of sheaflike bundles of radiating, thin fibers of quartz that average ~0.1 mm but range from ~20 μm to 1 mm. Microcrystalline quartz consists of aggregates of nearly equant crystals that are commonly < 5 μm but range to ~20 μm. Both may appear brownish in plain light owing to the presence of minute, liquid-filled bubbles. Chalcedony and microquartz are the principal minerals that make up chert, which may also contain opal.

Opal

Opal-A is a hydrous, cryptocrystalline form of cristobalite with submicroscopic pores containing water; isotropic under crossed polarizing prisms; may appear brownish in plain light. Opal-A is metastable and inverts in time to opal-CT and eventually quartz. Rare as a detrital mineral in most sandstones, but may occur as a cement, particularly in volcanoclastic sandstones.

randomly through the quartz, in contrast to the oriented bubble trains of Böhm lamellae, and may be extremely abundant or very sparse. Tiny mineral inclusions are common in quartz, and include apatite, rutile, tourmaline, zircon, magnetite, micas, chlorite, and feldspars.

Detrital quartz grains, particularly small grains, tend to be subangular; however, grains that have undergone an episode of intensive eolian transport, or polycyclic grains that have undergone several episodes of transport and deposition, may be well rounded, with all traces of original crystal faces or original angularity removed. Such rounded quartz grains that undergo secondary silica cementation during diagenesis may assume crystalline outlines

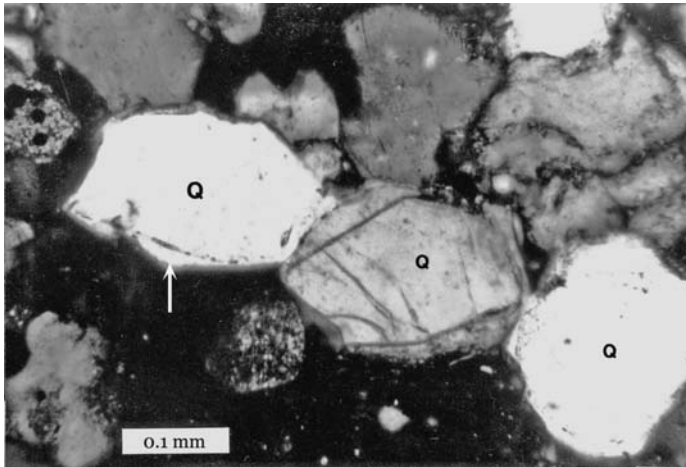


Figure 4.1 Detrital quartz grains (Q) that developed crystal faces owing to formation of overgrowths (arrow). Deadwood Formation (Cambrian–Ordovician). South Dakota. Crossed nicols.

owing to precipitation of silica **overgrowths** onto the rounded grains in the presence of open pore space (Fig. 4.1). The original rounded grain outline is commonly revealed by the presence of small specks of hematite, clay, or other material. Not all quartz overgrowths are marked by such inclusions; therefore, it may be necessary to use cathodoluminescence petrography to identify the overgrowths (e.g. Boggs and Krinsley, 2006, p. 88).

Although quartz occurs preferentially in sandstones as individual sand-size crystals (**monocrystalline quartz**), detrital **polycrystalline quartz** is extremely common in some sediments. Polycrystalline quartz, also called composite quartz, is quartz made up of aggregates of two or more crystals (Fig. 4.2). The character of polycrystallinity can vary enormously. The individual crystals within a polycrystalline grain may be equant or elongate in shape, fine grained or coarse grained, all about the same size or variable in size, and have crystal boundaries that are relatively straight or sutured to various degrees. Young (1976) has shown that polycrystalline quartz can develop from monocrystalline quartz during metamorphism. Under the influence of increasing pressure and temperature, nonundulatory monocrystalline quartz changes progressively to undulatory quartz, polygonized quartz (quartz that shows distinct zones of extinction with sharp boundaries), and finally to polycrystalline quartz. The polycrystalline quartz initially consists of elongated original crystals characterized by sutured boundaries. With increasing metamorphism, grains recrystallize to form small, new crystals. Some of these new crystals may grow larger at the expense of others until the smaller crystals are replaced by a few large crystals. These large crystals are characterized by polyhedral outlines, lack of undulose extinction, smooth crystal–crystal boundaries, and interfacial angles of 120 degrees at triple junctions.

Polycrystalline quartz grains can also form in plutonic igneous rocks. The exact nature of the polycrystalline grains putatively depends upon the type of igneous or metamorphic rock from which the grains were ultimately derived. In addition to polycrystalline quartz grains

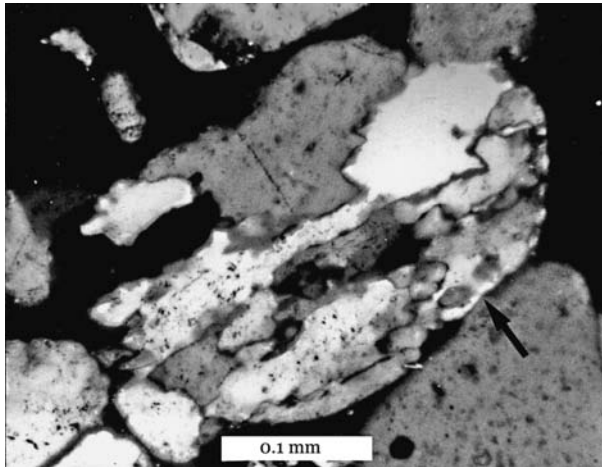


Figure 4.2 Large, well-rounded polycrystalline quartz grain (arrow) that displays sutured internal boundaries between composite crystals, indicating a probable early stage in development of metamorphic polycrystalline quartz. Unknown formation. Crossed nicols.

that originate as single grains in metamorphic or plutonic igneous rocks, clasts of quartzite, chert, and quartz-rich sandstone are considered by some authors (e.g. Pettijohn *et al.*, 1987, p. 30) to be polycrystalline quartz grains.

Quartz may be derived from igneous rocks, especially acid plutonic rocks, various kinds of metamorphic rocks, and sedimentary rocks. Owing to the increase in the volume of sedimentary rocks through time (Chapter 1), the principal source for detrital quartz in more recent geologic time has probably been sedimentary rocks.

Chalcedony

Chalcedony is a fibrous variety of quartz containing submicroscopic pores. Water may be present in the pore spaces or in the form of hydroxyl (Nesse, 1986, p. 254). Some chalcedony may contain cristobalite. Chalcedony typically displays a “feathery” texture owing to alignment of quartz fibers in a parallel or spherulitic pattern (Fig. 4.3). The fibers are a few micrometers thick, up to a millimeter long, and average about 0.1 mm (Folk, 1974, p. 80). Chalcedony commonly contains very tiny bubbles or inclusions that cause it to appear brownish in transmitted light (uncrossed nicols).

Opal

Opal is SiO_2 that contains a few percent water. It consists of mixtures of amorphous and crystalline silica. The amorphous silica commonly consists of very small (0.1–0.5 nm), closely packed spherical masses. The crystalline material consists of extremely small crystals of cristobalite or tridymite. Water is contained in submicroscopic pores. Amorphous opal (opal-A) is metastable and transforms in time to opal-CT (disordered cristobalite/tridymite) and eventually to quartz. Opal is isotropic under crossed polarizing prisms, making it

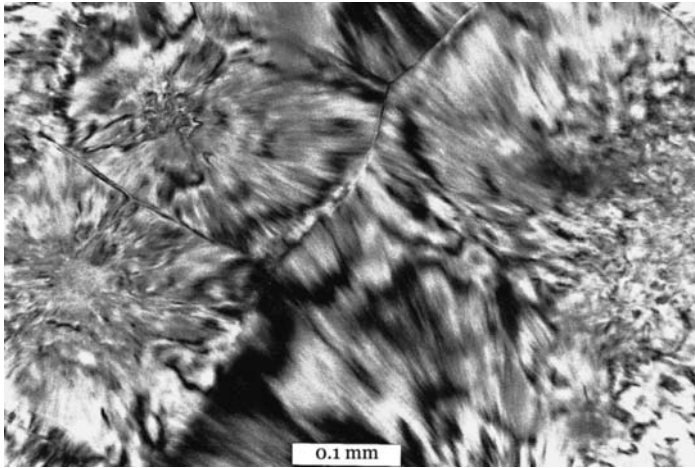


Figure 4.3 Fibrous to feathery texture of chalcedony. Unknown formation. Crossed nicols.

relatively easy to identify in thin section. It is rare as a detrital mineral, and occurs mainly in sandstones as an uncommon secondary cement.

Feldspars

General characteristics and occurrence

Feldspars are the most common framework mineral in sands and sandstones after quartz. Data on the feldspar content of Holocene and Pleistocene sands of North America compiled by Pettijohn *et al.* (1987, p. 35) indicate that feldspars make up about 22 percent of the average river sand and 10 percent of the average beach and dune sand. The overall average content of feldspars in these Holocene and Pleistocene sands is about 15 percent, but their range of abundance extends from less than 1 percent to more than 75 percent. Feldspars make up about 10–15 percent of the average ancient sandstone, but their reported abundance in sandstones ranges from zero to as much as 60 percent. Sandstones containing more than 25 percent feldspar are considered feldspar-rich.

Feldspars are commonly divided into two main groups: alkali feldspars (potassium feldspars) and plagioclase feldspars. Both groups are well represented in detrital sediments. Potassium feldspars are generally regarded to be more abundant than plagioclase feldspars in the average sandstone; however, sandstones derived from source areas rich in volcanic rocks may contain more plagioclase than potassium feldspar. Sodic plagioclase tends to be more abundant in sandstones than calcic plagioclase. Some important characteristics of detrital feldspars are summarized in [Table 4.3](#).

Alkali feldspars

Alkali feldspars form a group of minerals in which the chemical composition can range through a complete solid solution series from $K(AlSi_3O_8)$ through $(K,Na)(AlSi_3O_8)$ to

Table 4.3 *Characteristics of detrital feldspars***Alkali (potassium–sodium) feldspars**

Complete solid-solution series from $K(AlSi_3O_8)$ (orthoclase, sanidine, microcline) to $Na(AlSi_3O_8)$ (anorthoclase); all biaxial (–) with low negative relief

Orthoclase – a common detrital feldspar characterized by birefringence lower than quartz and 2V ranging from $\sim 40^\circ$ to 75° ; extinction angle $\sim 13^\circ$ – 21° ; twinned (Carlsbad twins most common) or untwinned; may appear cloudy owing to alteration products; distinguished from quartz most easily by staining

Sanidine – a high-temperature feldspar, with similar appearance to orthoclase, derived mainly from volcanic rocks; distinguished from orthoclase by smaller 2V (0° – 47°); extinction angle $\sim 5^\circ$ – 21° ; commonly has fewer alteration products than orthoclase

Microcline – a common detrital feldspar distinguished particularly by distinctive cross-hatch twinning with twin lamellae approximately at right angles; 2V commonly larger than 65° (range 50° – 85°); extinction angle $\sim 5^\circ$ – 15° ; may be cloudy owing to the presence of alteration products

Anorthoclase – comparatively rare in sandstones; extinction angle $\sim 5^\circ$ – 20° ; distinguished from microcline by finer-scale cross-hatch twinning and smaller 2V ($\sim 43^\circ$ – 54°)

Perthite – alkali feldspars characterized by platy intergrowths of albite

Plagioclase feldspars

Complete solid-solution series ranging from $NaAlSi_3O_8$ (albite) to $CaAl_2Si_2O_8$ (anorthite); composition commonly expressed as percent anorthite (An) molecule. Large 2V, which ranges with composition from about 50° to 105° ; biaxial (+) or (–); extinction angles vary as a function of composition and temperature of crystallization and may range from $\sim 3^\circ$ to 60° ; indices of refraction also vary with composition. Twinned or untwinned; if albite twinning present, easily distinguished from alkali feldspars. If untwinned, distinguished by large 2V, extinction angles, or by staining.

Plagioclase from igneous rocks may display compositional zoning. Very common in sandstones derived from volcanic and metamorphic rocks but may also be derived from plutonic igneous rocks. [Check published references such as Nesse (1986) for details of extinction angles, 2Vs, and indices of refraction.] Members of the series are

Albite (An_0 – An_{10})

Oligoclase (An_{10} – An_{30})

Andesine (An_{30} – An_{50})

Labradorite (An_{50} – An_{70})

Bytownite (An_{70} – An_{90})

Anorthite (An_{90} – An_{100})

Note: Data on extinction angles and 2Vs mainly from Nesse, 1986.

$Na(AlSi_3O_8)$. Because potassium-rich feldspars are such common members of this group, geologists often refer to all of these feldspars as potassium feldspars, or K-feldspars. A more accurate name is potassium–sodium feldspars. Orthoclase, sanidine, and microcline all have the chemical formula $KAlSi_3O_8$, but may contain various amounts of sodium. Anorthoclase is a sodium-rich alkali feldspar that can have the end-member formula $NaAlSi_3O_8$; however,

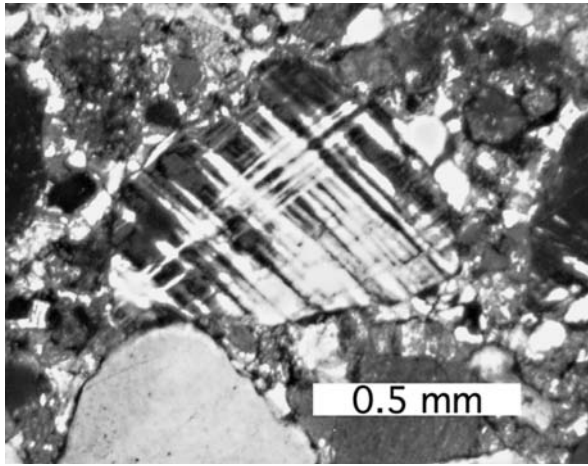


Figure 4.4 Microcline grain (center of photograph) with well-developed grid twinning. Fountain Formation (Pennsylvanian), Colorado. Crossed nicols.

it may contain considerable potassium and thus grade to microcline or one of the other potassium feldspars. Orthoclase and microcline appear to be by far the most abundant potassium feldspars in sandstones.

Orthoclase has lower birefringence than quartz, but can appear very similar in thin sections. Thus, it can be confused with quartz and misidentified unless its optic sign is checked (biaxial negative with a large $2V$), cleavage faces are apparent, or the orthoclase is clouded with alteration products, particularly if the alteration products are arranged in faint lines parallel to crystal directions. The most reliable technique for distinguishing between orthoclase and quartz is to stain the orthoclase (e.g. Houghton, 1980). Determining the chemical composition by use of the electron microprobe is likewise a reliable (but expensive) way of identifying orthoclase. **Sanidine** is a high-temperature feldspar, which occurs in lavas and some intrusive rocks, that closely resembles orthoclase. Orthoclase may be distinguished from sanidine by careful optical examination (orthoclase has a higher $2V$, may have a slightly higher extinction angle, and may contain microperthitic textures).

Microcline is generally easy to recognize in thin section owing to the common presence of its distinctive “grid” twinning, with the two sets of twin lamellae approximately at right angles to each other (Fig. 4.4). The lamellae are commonly tapered. Some microcline is untwinned (Nesse, 1986, p. 271). Untwinned microcline may be misidentified as orthoclase or quartz. **Anorthoclase** can have grid twinning resembling microcline; however, the twinning is on a much finer scale and anorthoclase has a smaller $2V$ and extinction angle. **Perthite** is microcline or orthoclase characterized by patchy intergrowths of albite (described below) in the form of small strings, lamellae, blebs, films, or irregular veinlets (Fig. 4.5). It forms by exsolution of sodium-rich albite from the potassium feldspar.

The alkali feldspars are derived particularly from alkali and acid igneous rocks and are especially abundant in syenites, granites, granodiorites, and their volcanic equivalents.

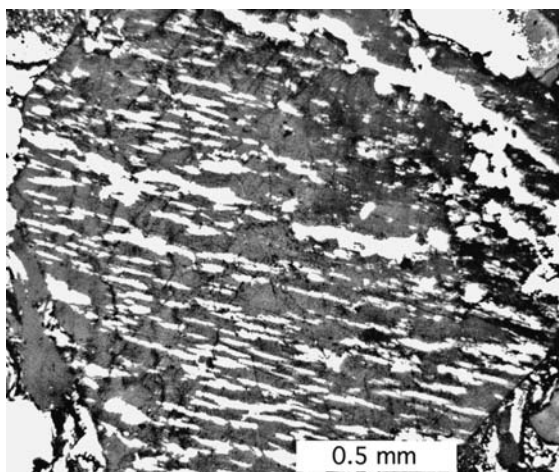


Figure 4.5 Large K-feldspar grain with abundant perthitic lamellae. Unknown formation. Crossed nicols.

They occur also in pegmatites and acid and intermediate-composition metamorphic rocks such as gneisses.

Plagioclase feldspars

The plagioclase feldspars constitute a solid-solution series ranging in composition from $\text{NaAlSi}_3\text{O}_8$ (albite) through $\text{CaAl}_2\text{Si}_2\text{O}_8$ (anorthite). As mentioned, sodic plagioclases appear to be more abundant in sandstones than calcic plagioclases. Many plagioclase grains are characterized by distinctive albite twinning, with twin lamellae that are straight and parallel (Fig. 4.6). When such twinning is present, plagioclase is easily distinguished from other feldspars and quartz. Unfortunately for the purpose of identification, much plagioclase is untwinned, especially plagioclase from metamorphic source rocks. Some plagioclase displays either oscillatory or progressive zoning (Chapter 7). Untwinned and unzoned plagioclase can be identified by staining (Houghton, 1980) or by electron microprobe analysis. In the past, many sedimentary petrographers have not bothered to identify the individual plagioclase feldspars within the series. The growing usefulness of feldspars in provenance determination has, however, made identification of the individual plagioclases important. Determination of the identity of loose grains of plagioclase can be done by refractive-index methods. In thin section, the approximate composition of plagioclase can be determined on the basis of extinction angles by the so-called Michel-Lévy method. See, for example, Jones and Bloss (1980, p. 17–3). Very accurate determination of the composition of plagioclase feldspars is now done routinely with the electron probe microanalyzer. The principal source for detrital plagioclase is probably basic and intermediate lavas, where it occurs as phenocrysts. It may also be derived from basic intrusive rocks and is a very common constituent of many metamorphic rocks, where its composition is related to the metamorphic grade of the host rock.

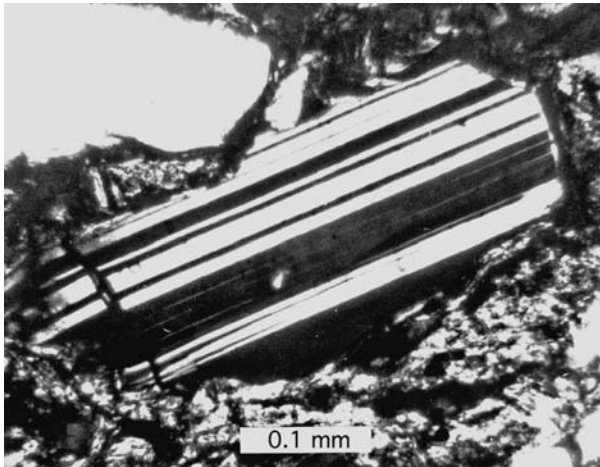


Figure 4.6 Large, twinned plagioclase grain from Miocene deep-sea sandstone, Ocean Drilling Program Leg 127, Site 796, Japan Sea, 326 m below seafloor. Crossed nicols.

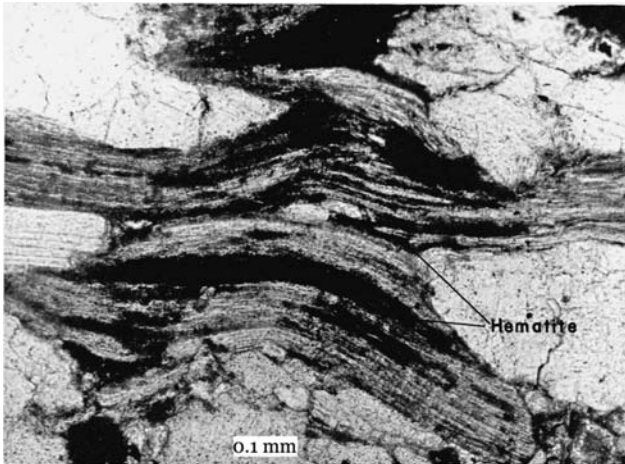


Figure 4.7 Large mica (biotite) grain cut normal to basal section. Hematite replaces biotite along some cleavage planes (black). Mintum Formation (Pennsylvanian), Colorado. Plane polarized light.

Coarse micas

The principal coarse micas that occur as detrital grains in sandstones are **muscovite** and **biotite**. These minerals are complex hydrous, potassium, aluminum sheet silicates; biotite contains in addition iron and magnesium. **Chlorite**, which occurs as detrital grains in some cases, is a hydrous, magnesium, iron, aluminum sheet silicate that resembles the micas in many respects. The micas are distinguished from other minerals by their platy or flaky habit. Also, their layered appearance in sections cut normal to the basal plane somewhat resembles the grain in “birds-eye” maple (Fig. 4.7). Muscovite is colorless in thin section. Biotite is

normally yellow, brown, or green, but may be leached pale yellow or almost colorless. Muscovite has very weak or no pleochroism; however, flakes of biotite cut normal to the basal plane commonly are strongly pleochroic and have parallel extinction. Muscovite and biotite have moderately high birefringence in second-order reds, blues, and greens. In addition to its dark color and pleochroism, biotite is distinguished from muscovite by its lower $2V$ (0–25 vs. 30–47 degrees). Chlorite is generally green and pleochroic. It is commonly distinguished by anomalous interference colors, particularly in blues, but also in gray–blue, russet brown, or khaki yellow.

Micas and chlorite are derived primarily from metamorphic rocks, but biotite occurs also in basic intrusive and volcanic rocks and in granites. Muscovite occurs also in granites and pegmatites. Coarse micas rarely form more than about two percent of the framework grains of sandstones and commonly much less. Muscovite is chemically more stable than biotite and is much more abundant in sandstones on the average than biotite. Coarse detrital chlorite is less abundant than biotite, possibly as a result of the greater tendency of chlorite to degrade mechanically to finer-size grains. Detrital micas are rarely rounded, and they are commonly deposited with their flattened dimension parallel to bedding. Owing to their sheetlike shape and consequent low settling velocity, they tend to be hydraulic equivalents of finer grains and thus are commonly deposited in very fine sands and silts rather than in coarser sands (Doyle *et al.*, 1983).

Clay minerals

Clay minerals are common in sandstones as matrix constituents. They occur also within argillaceous rock fragments. Because of their fine grain size, clay minerals cannot easily be identified under the petrographic microscope. Accurate identification requires X-ray diffraction methods or use of the scanning electron microscope or the electron probe micro-analyzer. Therefore, clay minerals are rarely identified during routine petrographic study of sandstones. In most cases, they are simply lumped together with fine-size (<0.03 mm) quartz, feldspars, and micas as “matrix.” Furthermore, there is growing evidence that much of the matrix of sandstones may be authigenic, derived during diagenesis by chemical precipitation of clay minerals into pore space or alteration of framework grains to clays. The clay minerals are not discussed further at this point in the book, but are considered in detail in [Chapter 6](#).

Heavy minerals

Most sandstones contain small quantities of sand-size accessory minerals. Most of these minerals have specific gravities that exceed 2.85 and are thus called heavy minerals. Because of their generally low abundance in sandstones and siliciclastic sediments, heavy minerals are usually concentrated for study by disaggregating the sandstones and then separating the heavy minerals from the light-mineral fraction by using heavy liquids (e.g. Lindholm, 1987, pp. 214–217). After washing and drying, a grain mount of the heavy minerals is prepared for microscopic study. The heavy grains are sprinkled on a warmed glass slide covered with a thin layer of resin or epoxy and then covered with a cover

Table 4.4 *Detrital heavy minerals in sandstones*

Nonopaque heavy minerals	
Ultrastable	Rutile, tourmaline, zircon, anatase (uncommon)
Stable	Apatite, garnet (iron-poor), staurolite, monazite, biotite
Moderately stable	Epidote, kyanite, garnet (iron-rich), sillimanite, sphene, zoisite
Unstable	Hornblende, actinolite, augite, diopside, hypersthene, andalusite
Very unstable	Olivine
Relative stability not well established	Ankerite, barite, brookite, cassiterite, chloritoid, chondrite, clinozoisite, corundum, chromite, dumortierite, fluorite, glaucophane, lawsonite, magnesite, monazite, phlogopite, pitotite, pleonaste, pumpellyite, siderite, spinel, spodumene, topaz, vesuvianite, wolframite, xenotime, zoisite (many of the minerals in this group are uncommon as detrital grains in sandstones)
Opaque heavy minerals	
Stable to moderately stable	Magnetite, ilmenite, hematite, limonite, pyrite, leucoxene

Note: Relative stabilities of the nonopaque minerals, excluding those for which relative stability is not well established (after Pettijohn *et al.*, 1987, p. 262). Stability refers to chemical stability.

slide. Identification of heavy minerals in grain mounts can be challenging for beginning petrographers, and considerable experience is generally required before the grains can be identified rapidly and accurately.

Heavy minerals are commonly divided into two groups on the basis of optical properties: opaque and nonopaque (Table 4.4). **Opaque heavy minerals** include magnetite, ilmenite, hematite and limonite, pyrite, and leucoxene. Opaque minerals are difficult to identify with an ordinary petrographic microscope, and few petrographers attempt to do so. The **non-opaque heavy minerals** encompass a very large group of more than 100 minerals, of which olivine, clinopyroxenes, orthopyroxenes, amphiboles, garnet, epidote, clinozoisite, zoisite, kyanite, sillimanite, andalusite, staurolite, apatite, monazite, rutile, sphene (titanite), tourmaline, and zircon are particularly common.

The average heavy-mineral content of sandstone is commonly reported to be about 1 percent or less. The heavy-mineral content of some modern sands, e.g. beach sands, can be considerably higher. The lower average content in ancient sandstones reflects selective destruction of heavy minerals by chemical weathering, sediment transport, and diagenetic processes. Thus, ancient sandstones tend to be enriched in the more stable heavy minerals.

The most stable heavy minerals (**ultrastable minerals**) are zircon, tourmaline, and rutile. Zircon and tourmaline are particularly resistant to both chemical decomposition and mechanical abrasion and, like quartz, can survive multiple recycling. Thus, the presence of abundant, rounded zircon and tourmaline in a sandstone that contains few if any other heavy minerals is suggestive of sediment recycling or of an episode of intensive chemical

leaching or mechanical abrasion. Hubert (1962) proposed a **zircon–tourmaline–rutile (ZTR) index** as a measure of mineralogic maturity of heavy-mineral assemblages in sandstones. The ZTR index is the percentage of combined zircon, tourmaline, and rutile grains among the transparent, nonmicaceous, detrital heavy minerals. Hubert's data for selected formations suggest the ZTR index is highest for quartzose sandstones and may be least for feldspathic sandstones.

The amount of study and interest lavished on heavy minerals in the past, judged by published papers, is greatly out of proportion to their generally low abundance in sandstones. The primary reason for this past interest is that they were once considered to have great significance in correlation and provenance studies. Currently, they play only a minor role in correlation. They are still thought to be useful indicators of sediment provenance (Chapter 7). That belief is probably the principal reason for their continued study today (see review by Morton, 1984). They are used also for characterization of petrologic provinces. Finally, some heavy minerals have economic value.

Rock fragments

Kinds of rock fragments

Rock fragments are detrital particles made up of two or more mineral grains. Depending upon source-rock composition, almost any kind of rock fragment can be present in a sandstone; however, clasts of fine-crystalline or fine-grained parent rocks are generally most abundant. The most common igneous rock fragments are volcanic rock fragments and glass. Metamorphic clasts include schist, phyllite, slate, and quartzite. Common sedimentary rock fragments are shale, fine sandstone and siltstone, and chert. Clasts of limestone and coarse plutonic and metamorphic rock are less common. Figure 4.8 shows examples of some common types of detrital rock fragments.

Identifying rocks fragments

Correct identification of individual kinds of rock fragments is important to sandstone classification and especially to provenance determination (Chapter 7). Identification of some types of rock fragments can be extremely difficult, particularly if the fragments become physically deformed or chemically altered during burial diagenesis. Table 4.5 lists the principal types of rock fragments that occur in sandstones and provides some specific criteria that can be used in their identification.

Occurrence of rock fragments

Rock fragments are common constituents of both modern sediments and ancient sandstones and conglomerates. They make up about 10–20 percent of the framework grains in average sandstones. Their range in abundances in ancient sandstones is very broad, however, and extends from less than 1 percent in some quartzose sandstones to well above 50 percent in some lithic sandstones. The abundance of rock fragments in ancient sandstones is a function of several factors, which include the lithology of their

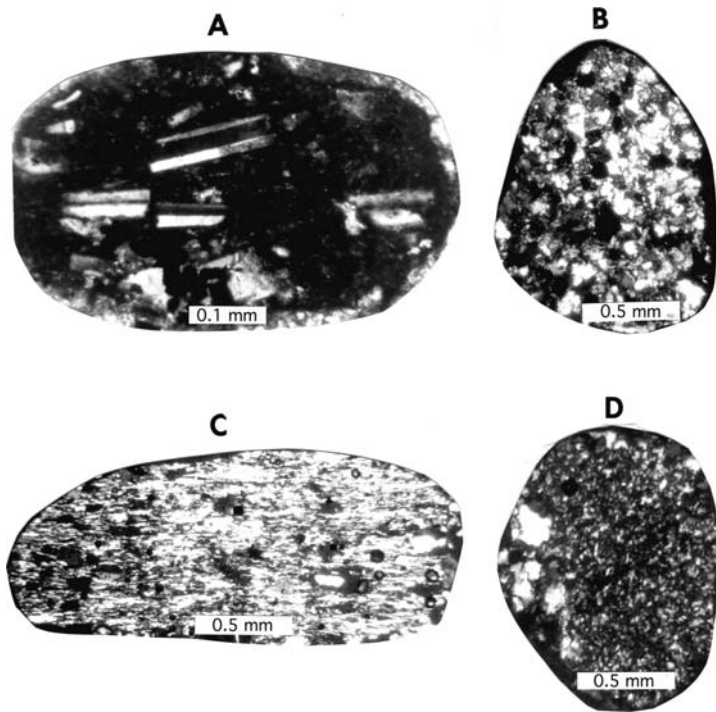


Figure 4.8 Examples of several kinds of common detrital rock fragments. A. Volcanic clast with plagioclase phenocrysts, Miocene deep-sea sandstone, ODP Leg 127, Site 796, Japan Sea, 387 m below seafloor. B. Sandstone clast, Taiwan shelf sand. C. Metamorphic clast, Taiwan shelf sand. D. Chert clast, Taiwan shelf sand. Crossed nicols.

source rocks, their chemical and mechanical durability, and their transport and diagenetic history.

On the whole, we find fewer rock fragments in compositionally mature (quartz-rich) sandstones than in immature sandstones. Chert and quartzite clasts are the most chemically stable and mechanically durable clasts. Shale and schist fragments may be less durable mechanically, and limestone fragments are probably the least stable chemically.

Skeletal remains

Skeletal particles, generally in low abundances, are common grains in many sandstones. These skeletal remains may be broken fragments of larger fossils or the unbroken remains of smaller fossils or microfossils. Because of the usefulness of fossils in paleoenvironmental and paleoecological studies, it is often desirable to identify the types of fossils present. Identifying fossils and fossil fragments in thin sections can be an exercise in futility for the uninitiated. Fortunately, excellent picture-atlas volumes are available that greatly aid in identification (see, for example, Scholle and Ulmer-Scholle, 2003). Identification of fossils

Table 4.5 *Principal kinds of rock fragments in sandstones (identification based on textures, fabrics, and mineralogy of fragments)*

Igneous rock fragments – igneous textures

Volcanic rock fragments – aphanitic and porphyritic textures

Felsic grains – characterized by an anhedral, microcrystalline mosaic, either granular or seriate (commonly porphyritic; grain size varies gradually or in a continuous series); composed mainly of quartz and feldspar; derived principally from silicic volcanic rocks, either lavas or tuffs

Microlitic grains – contain subhedral to euhedral feldspar crystals in felted or pilotaxitic (groundmass of holocrystalline rock in which lath-shaped crystals, commonly plagioclase, are arranged in a glass-free mesostasis and generally interwoven in an irregular fashion), trachytic (feldspar crystals in groundmass have a subparallel arrangement corresponding to flow lines), or hyalopilitic (needlelike crystals of the groundmass are set in a glassy mesostasis) patterns of microlites (microscopic crystals); derived from lavas of intermediate composition

Lathwork grains – characterized by plagioclase laths forming intergranular and insertal (triangular patches of interstitial glass between feldspar laths) textures; derived mainly from basaltic lavas

Vitric to vitrophyric grains and glass shards – composed of glass or altered glass; alteration products may be phyllosilicates, zeolites, feldspars, silica minerals, or combinations of these in microcrystalline aggregates

Hypabyssal and plutonic igneous rock fragments – hypabyssal types are fine crystalline, subhedral, commonly low in quartz and rich in feldspars; plutonic fragments are fine- to coarse-crystalline, anhedral granular; commonly composed of quartz and feldspar; derived mainly from acid igneous rocks; not common in sandstones owing to coarse crystal size

Sedimentary rock fragments – fragmental or microgranular textures

Epiclastic sandstone-siltstone grains – fragmental textures composed dominantly of silt- to fine-sand-size quartz and feldspar; may display cement or interstitial clay (matrix)

Volcaniclastic grains – fragmental textures; zoned plagioclase, embayed quartz, glass shards; may be difficult to differentiate from some epiclastic sandstone grains or some volcanic rock fragments

Shale clasts – fragmental textures; dominantly clay- and silt-size particles

Chert – mainly microgranular texture; composed entirely of quartz, chalcedony, opal; may be confused with silicified volcanic fragments

Carbonate grains – microgranular texture; composed of calcite or dolomite; may contain microfossils or fossil fragments

Metamorphic rock fragments – foliated or nonfoliated fabrics

Grains with tectonite fabric – grains showing schistose, semischistose, or slaty fabric resulting from preferred orientation of recrystallized mineral grains

Metasedimentary grains – characterized by presence of quartz and mica; include schist, phyllite, slate; slate possibly distinguished from shale by mass-extinction effect

Metaigneous grains – mainly metavolcanic; contain abundant feldspars or mineral assemblages that include chlorite and amphiboles

Grains with nonfoliated fabric – mainly microgranular textures; may include hornfelsic grains (containing metamorphic minerals), metaquartzite clasts (composed mainly of quartz with strongly sutured contacts), and marble fragments (coarse-crystalline carbonate)

Table 4.5 (cont.)

Indeterminate microgranular grains – very fine-grained fragments in which individual mineral grains are difficult to distinguish and textures are indeterminate; could be igneous, metamorphic, or sedimentary
Indeterminate microphanerite grains – individual minerals large enough to identify, but identity of clasts (gneiss, granite, etc.) difficult to establish; not common in sandstones

Source: Based on Dickinson, 1970.

is particularly important in carbonate rocks (Chapter 9), in which fossils and fossil fragments are commonly abundant.

Organic matter

Organic matter can occur in sandstones as clay- to silt-size particles or as fragments ranging to several centimeters in size. These organic substances are derived through the breakdown of plant and animal tissue; thus, they can be considered a kind of detrital particle. Some organic material, particularly woody and leafy material and mineral charcoal, originates on land and is subsequently transported into depositional basins. Other particulate organic material originates within depositional basins by disintegration of marine or freshwater organisms.

In plain light in thin sections, organic material appears as black (opaque), brownish translucent, or brownish transparent particles. Darkness of the color is related to increasing organic carbon content (Pettijohn *et al.*, 1987, p. 52). Larger, elongated carbonaceous or woody fragments are commonly oriented parallel or subparallel to bedding, and the fragments may show evidence of compaction and flattening owing to diagenesis. In sandstones that contain abundant silt- to sand-size carbonaceous detritus, the carbonaceous material may be concentrated in layers. These organic-rich layers show up as thin, dark laminae that superficially resemble heavy-mineral laminae.

Sandstones commonly contain less than about 0.1 percent organic matter (Chapter 13). Sandstones deposited in oxygenated environments are particularly depleted in organic matter, which is destroyed by oxidation. Rare sandstones, such as some graywackes, that were deposited under more strongly reducing conditions may contain a few percent organic matter. Mudrocks (shales) commonly contain much higher amounts of organic matter than do sandstones. These higher concentrations probably result both because fine organic matter tends to be deposited preferentially with clay- and silt-size sediment and because the lower permeability of muds, compared to sands, inhibits entry of oxygen-bearing fluids into these sediments. Organic-rich sedimentary rocks that contain extremely high concentrations (>10–20 percent) of organic matter are discussed in detail in Chapter 13.

Organic matter deposited in sediments undergoes complex chemical change during diagenesis. Some of the organic matter in shales, for example, is believed to be converted into liquid petroleum and natural gas at higher burial temperatures as a result of these processes

(Chapter 13). This petroleum may subsequently be introduced into sandstones by migration from the shale source rocks.

4.2.2 Authigenic minerals

General statement

Authigenic minerals are minerals that form in place within sediments either shortly after deposition, while sediment is still in an unconsolidated state, or during burial and diagenesis. They may include minerals from most of the major mineral groups: quartz and the other silica minerals, feldspars, carbonates, iron silicates (glauconite and chamosite), clay minerals, iron and manganese oxides, sulfides, and sulfates. They can occur as cements, crystallize in pore space as new minerals that do not act as cements, or form by replacement of original detrital minerals or rock fragments.

Authigenic minerals in sandstones can be distinguished from detrital minerals by several criteria: (1) they tend to be smaller than the associated framework grains, although some may grow to sand size, (2) they may display either well-developed, euhedral crystal faces or, alternatively, show highly irregular, intricate grain outlines that could not have survived transport, (3) they may display definitive replacement textures such as transected grain boundaries or caries texture (bitelike embayments; Chapter 8), or (4) they may exhibit cementation textures such as syntaxial rims or drusy (void-filling) texture (Chapter 8). Electron microprobe analysis, to determine chemical composition, and other instrumental techniques such as cathodoluminescence are being used also to identify some authigenic minerals.

Unless authigenic minerals form quite early, while sediment is still very close to the depositional interface, they provide little or no useful information about depositional conditions. They do, however, reflect the conditions of the diagenetic environment and in this way provide an understanding of the course of diagenesis. Because many authigenic minerals act as cements, they aid the process of lithification during burial. In so doing, they have a strong effect on the porosity and permeability of sediments and thereby influence the movement of fluids through the rocks and subsequent diagenetic processes. For example, sandstones that undergo early cementation may resist intrastratal solution, so that unstable minerals are preserved. Because authigenic minerals are diagenetic in origin, the formation of these minerals is discussed in greater detail in Chapter 8.

4.2.3 Framework grains versus matrix and cement

Preceding discussion in this chapter suggests that sandstones are composed principally of three fundamental kinds of constituents: framework grains, matrix, and cement. In addition, replacement minerals and open pore space may be present. **Framework grains** are coarse silt- and sand-size (0.03–2.0 mm) detrital particles that include quartz, feldspars, coarse micas, and heavy minerals. **Matrix** is finer-grained material that fills interstitial

spaces among framework grains. The upper size limit of material in sandstones considered to be matrix is arbitrary and debatable; however, a maximum size of 0.03 mm appears to be favored by many workers. The most common matrix minerals in sandstones are fine silica minerals, feldspars, micas, clay minerals, and chlorite. Matrix may make up trace amounts to a few tens of percent of the total rock volume. Siliciclastic rocks that contain more matrix-size material than framework grains are generally considered to be shales or mudrocks.

Cements are authigenic minerals that fill interstitial areas that were originally open pore spaces. Cement crystals may be any size up to or larger than the sizes of the individual pores they fill. A single crystal of calcite, for example, can fill several adjacent pores. Cements visible under a petrographic microscope rarely make up more than about 30 percent of the total volume of sandstones and commonly are much less abundant. Several minerals may act as cements in sandstones; however, clay minerals, carbonate minerals, and quartz are particularly common cements; see, for example, Morad (1998a) and Worden and Morad (2003).

Because some cements can be composed of very fine-size crystals, an investigator may find it extremely difficult, by standard petrographic examination, to differentiate between matrix and fine-grained cements such as clay-mineral cements. In fact, the difference between such fine-grained cements and matrix tends to become a matter of semantics if the matrix is authigenic. Earlier workers assumed that most matrix in sandstones was detrital; that is, it was sedimented along with framework grains at the time of deposition. That point of view has undergone considerable revision. It now appears that most transport and depositional processes separate clay-size grains from coarser detritus, so that most sand when initially deposited contains very little if any matrix.

Current views suggest that much, if not most, matrix in sandstones originates (1) by postdepositional infiltration of clay into interstitial spaces, particularly in fluvial deposits or (2) as an authigenic filling owing to diagenetic alteration of unstable rock fragments, feldspars, and ferromagnesian minerals. With respect to infiltration, Matlack *et al.* (1989) conclude on the basis of experimental work that vadose infiltration of muddy water through sand is an effective mechanism for emplacing clay into sand. They suggest that this infiltration occurs most effectively in environments characterized by high suspended-sediment concentration, fluctuating water levels, and minimum sediment reworking by waves or currents.

Alteration of framework grains during diagenesis may also produce significant amounts of clay matrix and cement. Alteration takes place mainly by dissolution and replacement of framework grains, and the alteration products are reconstituted as clay minerals, chlorite, micas, and fine quartz and feldspar. In particular, the matrix in so-called graywackes is now believed to be largely authigenic.

Recognition of authigenic clay cements and matrix may be extremely difficult by routine petrographic examination. Coarser-grained clays deposited in the form of radiating crystals that line interstitial voids (drusy texture; Fig. 4.9) may be identifiable as cements under the petrographic microscope. On the other hand, much authigenic clay is

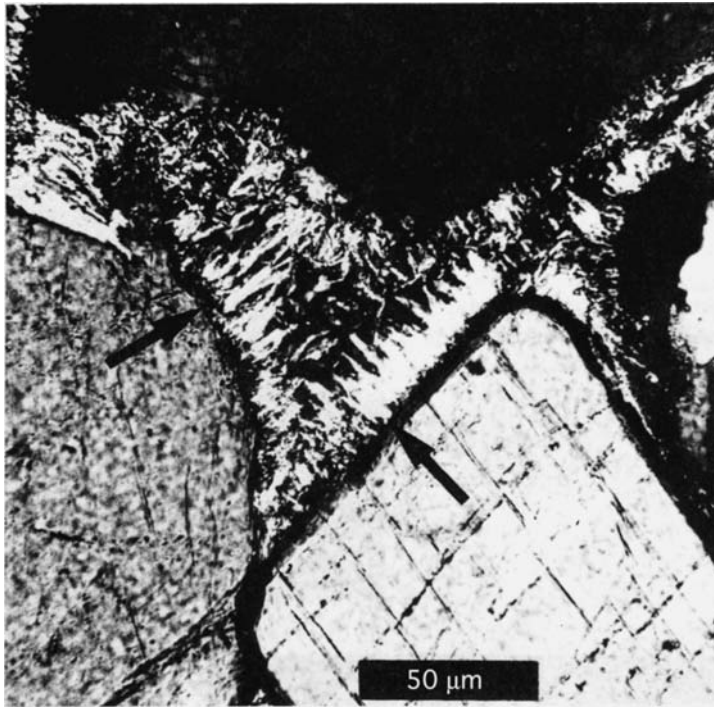


Figure 4.9 Photomicrograph of coarse clay-mineral cement with drusy texture (arrows) filling pore space among framework grains. Cuchara Formation (Eocene), Colorado. Ordinary light. (From Walker, T.R., *et al.*, 1978, Diagenesis in first-cycle desert alluvium of Cenozoic age, southwestern United States and northwestern Mexico: *Geol. Soc. Am. Bull.*, **89**, Fig. 8A, p. 27. Photograph courtesy of T.R. Walker.)

so fine sized that it shows up during petrographic examination as an indistinguishable part of the interstitial matrix. At higher magnification under the scanning electron microscope, authigenic clays may be distinguishable from detrital clays. Walker *et al.* (1978) show, for example, that authigenic clays in fluvial sandstones have a characteristic boxwork texture (Fig. 4.10), whereas mechanically infiltrated clays consist of clay platelets oriented parallel to grain surfaces (Fig. 4.11). Moraes and De Ros (1990) report significant amounts of mechanically infiltrated clays in Jurassic sandstones of northeastern Brazil. According to these authors, mechanically infiltrated clays can be identified in ancient rocks on the basis of several criteria: (1) ridges and bridges between grains, (2) geopetal fabric, (3) loose aggregates, (4) isopachous clay coatings (coatings that do not completely surround grains) or tangentially accreted lamellae, (5) massive aggregates, and (6) shrinkage patterns developed during diagenesis. The matrix of sandstones that have undergone extreme diagenesis or incipient metamorphism may not, however, preserve these distinctions between authigenic clays and infiltrated clays.

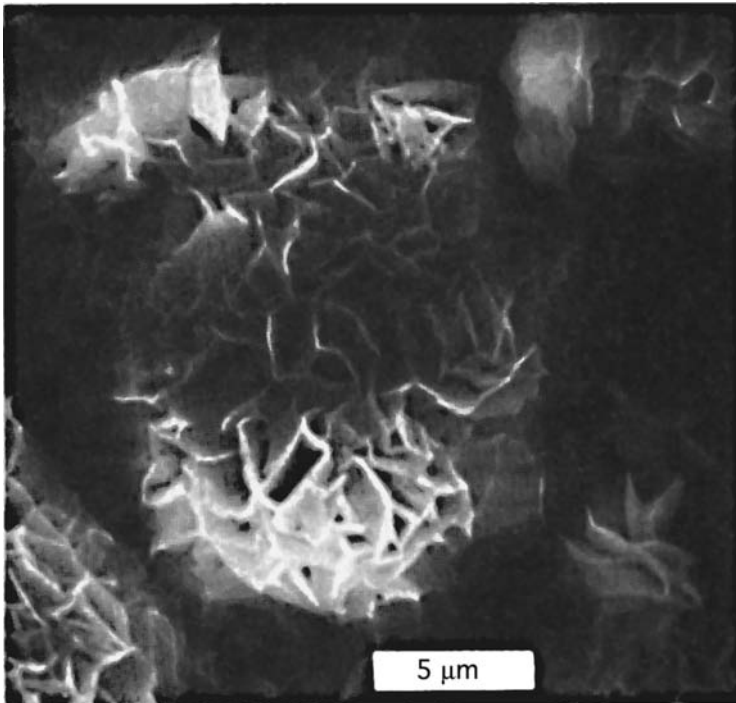


Figure 4.10 Electron micrograph showing typical boxwork structure of authigenic clay minerals. Gila Group (Pliocene–Pleistocene), Tuscon, Arizona. (From Walker T.R. *et al.*, 1978, Diagenesis in first-cycle desert alluvium of Cenozoic age, southwestern United States and northwestern Mexico: *Geol. Soc. Am. Bull.*, **89**, Fig. 8C, p. 27. Photograph courtesy of T. R. Walker.)

Philosophically and pragmatically, it is difficult to distinguish between fine-grain silicic cements and authigenic matrix. Is there a difference? Dickinson (1970) attacked this problem by grouping the interstitial constituents of sandstones into six categories:

1. **Cement** – easily recognizable authigenic calcite, chalcedony, zeolites, or other minerals not common in the framework.
2. **Phyllosilicate cement** – clay-mineral or mica cements displaying growth patterns in open pores. Dickinson suggests five textural characteristics of clay cements that may allow their distinction from inhomogeneous matrix:
 - a. clear transparency of clay cements, indicating absence of minute detritus or murky impurities
 - b. dominance of a single mineral type
 - c. radial arrangement of crystal platelets, projecting inward from surrounding framework grains (drusy texture)
 - d. medial sutures within the interstitial clays, indicating lines of junction of radially arranged crystals
 - e. concentric color zonation, indicating successive compositional changes in minerals grown in voids from interstitial fluids as coatings built on framework grains.
3. **Protomatrix** – unrecrystallized, detrital clay in weakly consolidated rocks.

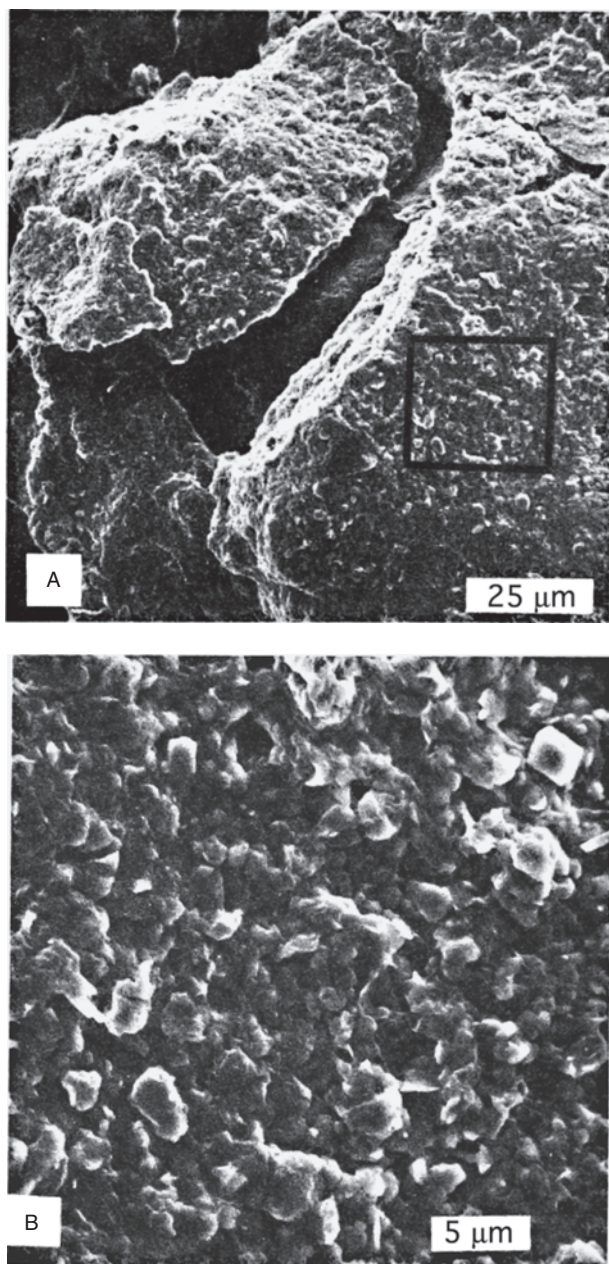


Figure 4.11 A. Electron micrograph of infiltrated clay particles showing clay platelets oriented parallel to grain surfaces. B. Enlargement of area outlined in A. Gila Group (Pliocene–Pleistocene), Red Rock, New Mexico. (From Walker T. R. *et al.*, 1978, Diagenesis in first-cycle desert alluvium of Cenozoic age, southwestern United States and northwestern Mexico: *Geol. Soc. Am. Bull.*, **89**, Fig. 1E and 1F, p. 20. Photograph courtesy of T. R. Walker.)

4. **Orthomatrix** – recrystallized detrital clay or protomatrix, recognized by relict detrital textures and inhomogeneity, in contrast to the homogeneity of clay cements.
5. **Epimatrix** – authigenic interstitial materials grown in originally open interstices but lacking the homogeneity of clay cements.
6. **Pseudomatrix** – discontinuous matrix-like material formed by squeezing and flowing of weak detrital grains, such as shale or phyllite fragments, into adjacent pore spaces. Dickinson suggests that pseudomatrix can be recognized by
 - a. flame-like wisps of mashed rock fragments that extend into pore spaces between rigid framework grains
 - b. deformation of internal fabric of lithic fragments to form concentric drape lines that conform to the margins of confining, rigid grains
 - c. irregular distribution of matrix, forming large matrix-filled patches in the framework (which are separated by areas nearly free of matrix); true matrix should more or less fill all pore spaces.

Dickinson's classification of interstitial components is valuable in the sense that it helps us to understand the various possible origins of interstitial materials. The classification is, however, extremely difficult to apply in practice. It is highly doubtful, for example, if even an experienced petrographer using a petrographic microscope can routinely distinguish protomatrix, orthomatrix, and epimatrix, or unambiguously distinguish these matrix types from clay cement. On the other hand, recognition of pseudomatrix can often be made by careful examination. Therefore, this term is a very useful one and has gained general acceptance by geologists.

4.3 Chemical composition

4.3.1 Significance

Geologists are interested in the chemical composition of sandstones, but they generally regard chemical composition to be less useful than mineralogy as a means of characterizing sandstones and evaluating their provenance and depositional environments. Nonetheless, sandstone geochemistry has a number of important applications. For example, major-element chemistry can provide information about the tectonic setting of sandstone accumulation ([Chapter 7](#)), allowing distinction among sandstones derived from oceanic island arc, continental island arc, active continental margin, and passive margin settings (Bhatia, 1983; Roser and Korsch, 1986). Major- and trace-element chemistry have been used to evaluate sedimentation rates and depositional environments in orogenic belts (Sugisaki, 1984). Major-element chemistry has been utilized also to infer the original clastic assemblages in deeply buried and altered sedimentary rocks and to help clarify the processes that produced the sediments (Argast and Donnelly, 1987). Trace elements also have value in some kinds of provenance studies (see discussion in [Chapter 7](#)).

4.3.2 Expressing chemical composition

It is customary in reporting the results of chemical analyses to express major elements as oxides and report abundances in weight percent of the total oxides. [Table 4.6](#) is an example

Table 4.6 Average chemical composition of sandstones reported by Argast and Donnelly (1987)

	Source (n)								
	1 (11)	2 (23)	3 (30)	4 (16)	5 (18)	6 (12)	7 (119)	8 (12)	9 (59)
SiO ₂ (wt.%)	86.5	67.8	65.6	56.9	56.2	68.4	70.6	37.3	50.3
TiO ₂	0.53	0.95	0.91	1.42	0.89	0.69	0.64	0.34	0.64
Al ₂ O ₃	5.71	15.4	15.1	12.3	15.3	13.5	12.6	7.91	14.0
Fe ₂ O ₃ (t)	2.69	6.46	6.09	6.18	6.48	5.30	4.97	3.18	6.40
MnO	0.02	0.07	0.15	0.11	0.07	0.09	0.08	0.10	0.13
MgO	0.69	1.73	1.82	4.20	2.35	1.68	1.51	1.07	3.25
CaO	0.05	0.42	1.94	5.82	5.74	2.38	1.61	26.0	9.90
Na ₂ O	0.02	1.07	0.87	1.92	1.28	3.15	2.76	0.92	–
K ₂ O	1.55	2.74	3.03	1.90	2.80	2.62	2.20	0.51	2.09
P ₂ O ₅	0.02	0.16	0.17	0.17	0.17	0.18	0.02	0.10	0.21
V (ppm)	51	123	159	100	126	71	79	103	–
Cr	55	82	88	225	71	55	44	31	–
Ni	19	231	58	130	49	30	8	5	49
Zn	29	52	104	84	114	69	–	66	91
Rb	60	123	133	72	125	93	–	10	79
Sr	29	134	113	233	168	310	110	879	267
Y	17	31	40	21	35	36	37	15	29
Zr	417	238	260	191	187	333	413	58	118

Note: Iron is reported as total Fe₂O₃; n is the number of samples in each average. No reported value is shown with a dash.

Source:

- 1 Shawangunk Formation, near Ellenville, New York (quartz arenite)
- 2 Millport Member of the Rhinestreet Formation, Elmira, New York (lithic arenite/wacke)
- 3 Oneota Formation, Unadilla, New York (lithic arenite/wacke)
- 4 Cloridorme Formation, St. Yvon and Gros Morne, Quebec (lithic arenite/wacke)
- 5 Austin Glen Member of Normanskill Formation, Poughkeepsie, New York (lithic arenite/wacke)
- 6 Rennselaer Member of the Nassau Formation, near Grafton, New York (feldspathic arenite/wacke)
- 7 Rennselaer Member, averages of analyses from Ondrick and Griffiths (1969) (feldspathic arenite/wacke)
- 8 Rio Culebrinas Formation, La Tosca, Puerto Rico (fossiliferous volcanoclastics)
- 9 Turbidites from DSDP site 379A (lithic arenites/wacke).

of the general form used in reporting chemical analyses. Note from this table that trace elements are not reported as oxides; instead, their abundances are given in actual concentration units, in this case parts per million (ppm). The concentrations of elements present in even lower abundances are given in parts per billion (ppb). As suggested by Table 4.6, the

major chemical elements in sandstones are silicon, aluminum, iron (expressed either as Fe_2O_3 or FeO), magnesium, calcium, sodium, potassium, titanium, manganese, and phosphorus. Silicon is the most abundant element in sandstones, commonly followed by aluminum and iron. The relative abundance of calcium, magnesium, sodium, and potassium vary considerably in different sandstones, but these elements are commonly much more abundant than manganese, titanium, and phosphorus.

4.3.3 Relation of chemical composition to mineralogy

The **silicon** content of sandstones is a function of all the silicate minerals present, but obviously is most strongly influenced by the presence of quartz. Therefore, SiO_2 values are particularly high in quartz-rich sandstones. **Aluminum** is contained mainly in feldspars, micas, and clay minerals. Because of the abundance of aluminum in fine micas and clay minerals, sandstones containing abundant clay matrix commonly have much higher aluminum contents than those with little or no matrix. **Iron** is a common constituent of many minerals, and may be present both in the ferrous (Fe^{2+}) and ferric (Fe^{3+}) states. Ferrous iron is particularly important in chlorites (and to a lesser extent in some other clay minerals such as smectites), biotites, carbonates (siderite, ankerite), and sulfides (pyrite and marcasite). Ferrous iron may occur also in some volcanic rock fragments and in minor quantities in some silicate minerals such as feldspars. Ferric iron is most abundant in the iron-oxide minerals hematite, goethite, and lepidochrochite and in glauconites. Iron is an important constituent also of many heavy minerals such as magnetite; however, the content of such minerals is so low in most sandstones that they do not greatly affect the bulk chemical composition of the sandstones.

Sodium and **potassium** are contained especially in alkali feldspars and muscovite. They are present also in illite and smectite clay minerals and most zeolite minerals. **Calcium** is contributed to sandstones in calcitic plagioclases, calcite cements, and, to a minor extent, smectite clay minerals. Calcite cements probably account for most of the calcium in sandstones that are particularly enriched in calcium. **Magnesium** is contained particularly in chlorite, smectite clay minerals, and dolomite cements. Because dolomite cements in sandstones are much less common on the average than calcite cements, calcium is generally more abundant than magnesium in sandstones. As [Table 4.6](#) indicates, however, magnesium may exceed calcium in an occasional sandstone. **Titanium** and **manganese** each commonly make up less than one percent of the chemical constituents in sandstones. Titanium is contained in some clay minerals and in the heavy minerals ilmenite, rutile, brookite, and anatase. Manganese probably occurs mainly as a substitute for iron in the iron oxide minerals, but minor amounts of manganese oxides occur also. **Phosphorus** is a common element in sandstones but seldom exceeds a few tenths of one percent in abundance. Its principal source is detrital and authigenic apatite. Numerous other elements may be present in sandstones in trace amounts including, as shown in [Table 4.6](#), V, Cr, Ni, Zn, Rb, Sr, Y, and Zr. The **trace-element** composition of sandstones is mainly a function of detrital mineral composition. Therefore, some trace elements contained in specific detrital minerals are

useful in provenance studies, as discussed above. On the other hand, trace elements can be added to sandstones at the depositional site and during diagenesis. Thus, considerable caution is necessary in interpreting provenance on the basis of trace-element abundances in bulk samples.

The preceding discussion clearly suggests that chemical composition of sandstones is strongly correlated with mineral composition, particularly detrital mineral composition. We should expect, therefore, that mineralogically different kinds of sandstones will show considerable variation in chemical composition.

4.4 Relationship of particle and chemical composition to grain size

Sandstones are composed of mixtures of mineral grains and rock fragments, but mineral grains dominate in most sandstones. Mudrocks commonly contain few rock fragments. Particle composition in sediments may vary considerably as a function of particle size. A relationship between particle size and composition of sandstones has long been recognized (e.g. P. Allen, 1945; Hunter, 1967). In a study of Illinois River sands, for example, Hunter (1967) reported that the percentage of feldspar and heavy minerals increases with decreasing grain size, whereas the amount of quartz, rock fragments, chert, and quartzite decreases. Odom *et al.* (1976) also reported a strong relationship between feldspar content and grain size in quartz-rich sandstones. They found that feldspars are concentrated especially in the < 0.125 mm size fraction and that a nearly linear inverse relationship exists between feldspar abundance and grain size in some sandstones.

With respect to heavy minerals, Rittenhouse pointed out in 1943 that heavy minerals in stream sediments are sorted by density and size. That is, fine-size heavy minerals tend to occur with much coarser, lower-density quartz grains – the concept of **hydraulic equivalent size** (the size of a larger or smaller grain that settles with a given mineral grain under the same conditions). In general, the higher the specific gravity of the heavy minerals, the smaller the heavy minerals will be with respect to the size of the quartz grains with which they occur. Rittenhouse proposed use of the **hydraulic ratio** to express the quantity of any given mineral in a sediment. The hydraulic ratio is equal to the weight of a heavy mineral in a given size class divided by the weight of light minerals in the hydraulic equivalent class, multiplied by 100.

These examples all point out a basic sedimentologic tenet as applied to the petrologic study of siliciclastic sediments: comparison of composition between samples of different sediments can be made only if sediments of approximately the same grain size are compared. Ingersoll *et al.* (1984) suggest that the problems inherent in grain size–composition relationships can be minimized in point counts of sandstones by assigning the sand-sized crystals and grains within larger rock fragments to the category of the crystals or grains, rather than to the category of rock fragments. This technique is the so-called **Gazzi–Dickinson** point-counting method. On the other hand, some geologists (e.g. Suttner and Basu, 1985) believe that use of the Gazzi–Dickinson method obscures provenance information (see discussion in Chapter 7, Section 7.6.2). Furthermore, it may not adequately address

the composition changes when few rock fragments are present and the sizes of particles are very different.

Because the chemical composition of siliciclastic sedimentary rocks is closely related to the mineral composition of these rocks, as discussed, chemical composition varies as a function of grain size along with variations in mineralogy. Pettijohn (1975, p. 270) points out, for example, that SiO_2 abundance decreases progressively from fine sands to fine clays, whereas the Al_2O_3 content systematically increases.

4.5 Classification of sandstones

4.5.1 Introduction

In the broadest sense, sandstones can be separated into two groups: **epiclastic** and **volcaniclastic**. Epiclastic deposits are formed from fragments of pre-existing rocks derived by weathering and erosion. Thus, they are composed mainly of silicate minerals and various kinds of igneous, metamorphic, and sedimentary rock fragments. Volcaniclastic deposits are those especially rich in volcanic debris, including glass. Many volcaniclastic deposits consist principally of pyroclastic materials such as ash or lapilli, derived directly through explosive volcanism. On the other hand, some material in volcaniclastic deposits may be epiclastic debris derived by weathering of older volcanic rock. Epiclastic and volcaniclastic deposits can be further classified on the basis of their composition. Unfortunately, there is little agreement among geologists about sandstone classification, particularly classification of epiclastic sandstones.

4.5.2 Classification of epiclastic sandstone

Parameters for classification

The framework grains in most sandstones are dominated by quartz, feldspars, and rock fragments, as indicated in the preceding discussion. Many other minerals may be present in a given sandstone, but the abundances of these other minerals are so low in most sandstones that they can be ignored for the purpose of sandstone classification. Some sandstones contain **matrix** in addition to sand-size framework grains. As mentioned, matrix is defined as material less than about 0.03 mm (30 microns) in size. Thus, it is not a framework constituent. Rather, it occupies the interstitial spaces among sand-size grains. The matrix content of sandstones may range from zero to several tens of percent.

Owing to the simple framework composition of sandstones (mainly quartz, feldspars, rock fragments), classification of sandstones ought to be a fairly straightforward process. Practice has proven differently! Sedimentologists have had a difficult time indeed developing a single sandstone classification scheme that is acceptable to most workers in the field. According to Friedman and Sanders (1978, p. 190), more than 50 classifications for sandstones have been published since the late 1940s in ten countries and seven languages.

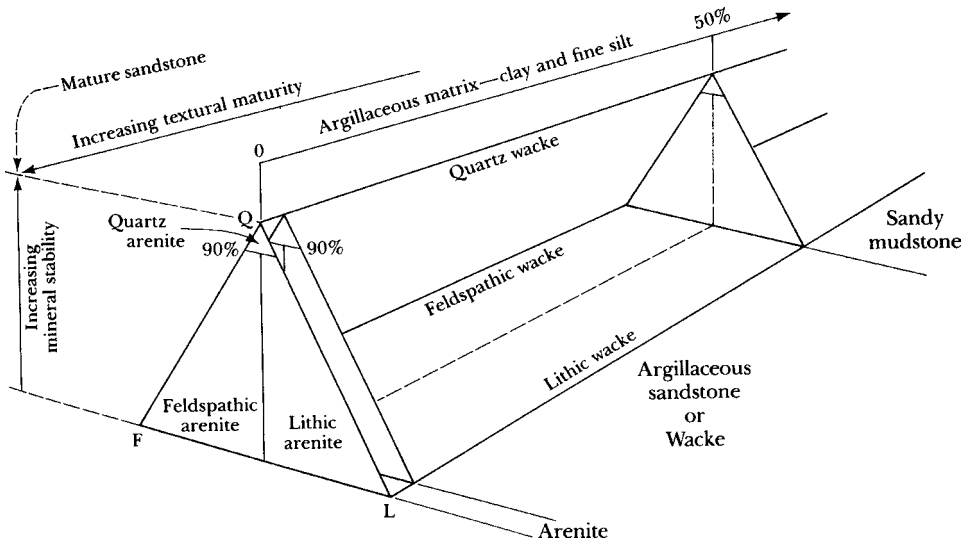


Figure 4.12 Classification of sandstones on the basis of three mineral components: Q = quartz, chert, quartzite fragments; F = feldspars; L = unstable lithic grains (rock fragments). Points within the triangle represent relative proportions of Q, F, L end members. Percentage of argillaceous matrix is represented by a vector extending toward the rear of the diagram. The term *arenite* is restricted to sandstones essentially free of matrix (<5%); sandstones containing matrix are *wackes*. (After Williams, H., F.J. Turner, and C.M. Gilbert, 1982, *Petrography, an Introduction to the Study of Rocks in Thin Sections*, 2nd edn.: W.H. Freeman, San Francisco, Fig. 31.1, p. 327. Modified from Dott, R.H., Jr., 1964, Wacke, graywacke, and matrix – what approach to immature sandstone classification? *J. Sediment. Petrology*, **34**, Fig. 3, p. 629, reprinted by permission of SEPM, Tulsa, OK.)

Examples of classifications

I shall not attempt herein to trace the history of sandstone classification; however, two fundamental types of classifications have emerged: those based upon both the composition of framework grains and the abundance of matrix, and those based entirely upon the composition of framework grains. Gilbert's classification (in Williams *et al.*, 1982, p. 327), shown in Fig. 4.12, is an example of the first type of classification. A principal feature of this classification is its simplicity. Sandstones are divided into two broad groups: **arenites**, containing little or no matrix (<5 percent), and **wackes**, containing perceptible matrix. Combining the matrix parameter with composition (QFL, see Fig. 4.12 for explanation) yields six kinds of sandstones: quartz arenites and wackes, feldspathic arenites and wackes, and lithic arenites and wackes.

The two classifications shown in Fig. 4.13 are examples of the second type of classification. These classifications divide sandstones into seven or eight compositional types; however, the classifications do not use matrix as a classification parameter. Note that Fig. 4.13B allows even finer subdivision of sandstones by erecting "daughter" compositional triangles on the main composition diagram.

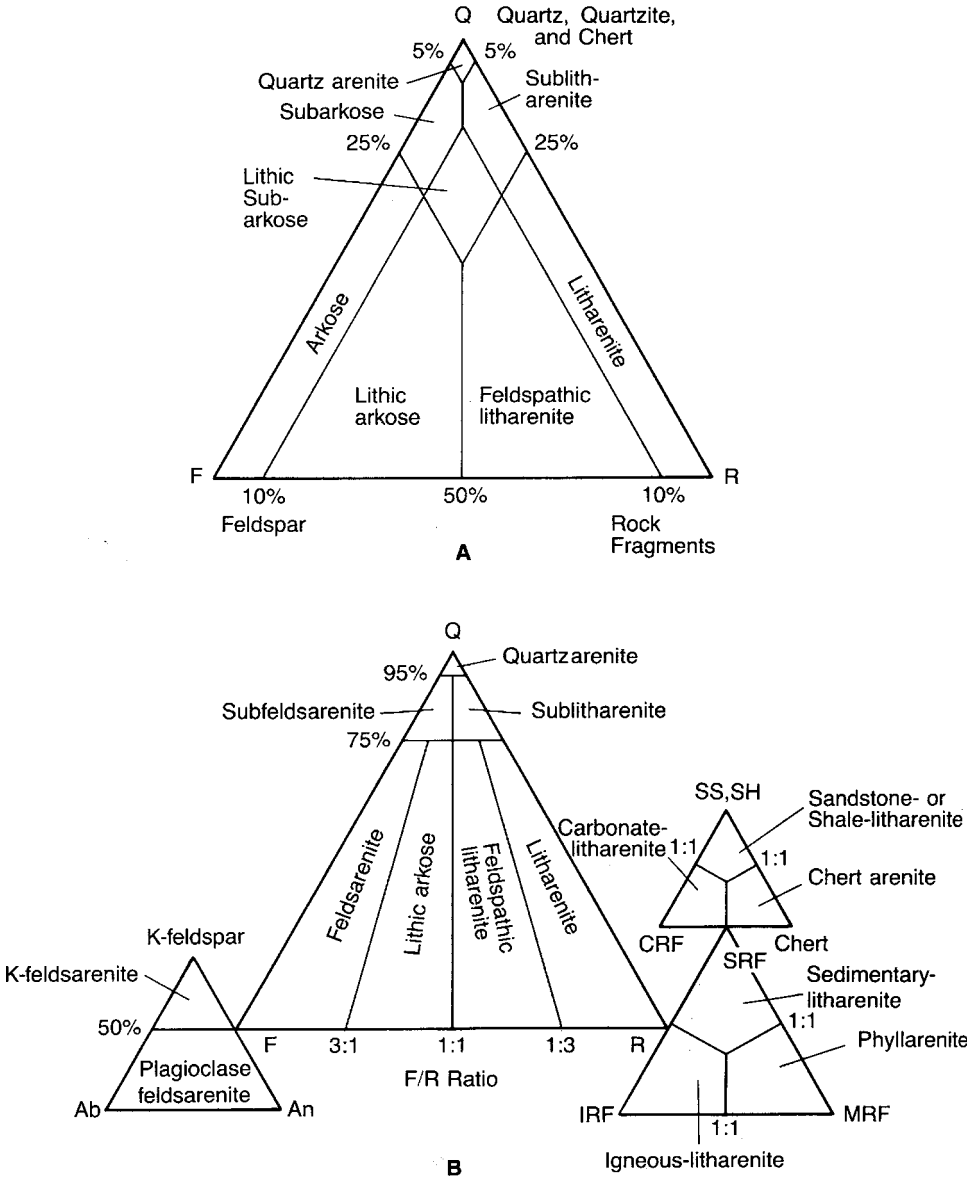


Figure 4.13 Classification of sandstones according to (A) McBride (1963) and (B) Folk *et al.* (1970). In Folk's classification, chert is included with rock fragments at the R pole, and granite and gneiss fragments are included with feldspars at the F pole. SS = sandstone, SH = shale, CRF = carbonate rock fragments, SRF = sedimentary rock fragments, IRF = igneous rock fragments, MRF = metamorphic rock fragments. (A, from McBride, E. F., 1963, A classification of common sandstones: *J. Sediment. Petrology*, **34**, Fig. 1, p. 667, reprinted by permission of SEPM. B, from Folk, R. L., P. B. Andrews, and D. W. Lewis, 1970, Detrital sedimentary rock classification and nomenclature for use in New Zealand: *New Zealand J. Geol. Geophys.*, **13**, Fig. 8, p. 955, and Fig. 9, p. 959, British Crown copyright, reprinted by permission.)

Two common sandstone names that do not appear in many formal classifications require some additional explanation. The term **arkose** is used in some sandstone classifications and is in general use by many geologists. The exact meaning of this term is elusive because the term has been defined in different ways. It has been applied to any sandstone containing conspicuous amounts of feldspars, as seen in hand specimens, to sandstones containing more than 20 percent, more than 25 percent, or more than 30 percent feldspars, and to sandstones derived from granitic source rocks. Probably the most widely accepted definition for an arkose is a feldspathic sandstone containing more than 25 percent feldspars. Presumably, an arkose also has a lower rock-fragment content than feldspar content.

The term **graywacke** is a much-maligned term that is still used by many geologists. Some workers have suggested that the name be abandoned, but it manages to survive. In general, the name graywacke is applied to dark-gray, greenish-gray, or black, matrix-rich, well-indurated sandstones. According to Crook (1970), the origin of the term goes back to Werner in 1787. The name was originally given to rocks on the basis of their field characteristics, but the term has subsequently been defined in various other ways. Hence, the suggestion that it be abandoned.

4.6 Petrography and chemistry of epiclastic sandstones

4.6.1 Major petrographic divisions

The preceding discussion indicates that epiclastic sandstones can be divided by particle composition into three major groups: quartz-rich sandstones (quartz arenites and wackes), feldspar-rich sandstones (feldspathic arenites and wackes), and rock-fragment-rich sandstones (lithic arenites and wackes). These major sandstone clans may differ in more than just particle composition. They may show also detectable variations in texture, types of cements, matrix content, and bulk chemistry.

4.6.2 Quartz arenites

General characteristics

Quartz arenites are composed of >90–95 percent siliceous grains (quartz, chert, quartzose rock fragments). They are commonly white or light gray, but may be stained red, pink, yellow, or brown by iron oxides. They are generally well lithified and well cemented with silica or carbonate cement; however, some are porous and friable. Quartz arenites typically occur in association with assemblages of rocks deposited in stable cratonic environments such as eolian, beach, and shelf environments. Thus, they tend to be interbedded with shallow-water carbonates and, in some cases, feldspathic sandstones.

Most quartz arenites are texturally mature to supermature according to Folk's (1951) textural maturity classification, but quartz arenites with low maturity exist. Cross-bedding is particularly characteristic of these rocks, and ripple marks are moderately common. Fossils are rarely abundant in these sandstones, possibly owing to poor preservation or to the eolian

origin of some quartz arenites, but both fossils and carbonate grains may be present. Also, trace fossils such as burrows of the *Skolithos* facies may be locally abundant in some shallow-marine quartz arenites. Quartz arenites are common in the geologic record. Pettijohn (1963) estimates that they make up about one-third of all sandstones.

Particle composition

Quartz arenites have the simplest particle composition of all sandstones. Siliceous grains in these sandstones range in abundance from 90 percent to more than 99 percent. Quartz dominates the siliceous constituents; however, a few percent chert, metaquartzite clasts, or siliceous sandstones/siltstone clasts may be included. Most quartz in quartz arenites is monocrystalline. Polycrystalline grains commonly make up less than 10 percent (generally about two percent) of the framework grains. The low content of polycrystalline grains in quartz arenites has been attributed to size reduction of these grains. Polycrystalline quartz grains apparently break up to form smaller monocrystalline grains owing to sediment transport and other processes involved in grain recycling. Quartz arenites tend to be characterized by high percentages of nonundulatory monocrystalline quartz, which may be due to relative enrichment in nonundulose quartz over time owing to selective destruction of less stable undulose quartz by mechanical and chemical processes operating during successive sedimentary cycles.

Feldspars make up trace amounts to as much as 5 percent of the framework constituents in many quartz arenites. Chert and silicic rock fragments, both metaquartzite clasts and sandstone/siltstone clasts, occur in some quartz arenites in amounts that rarely exceed 1 percent. Unstable rock fragments are very rare. Micas, commonly muscovite, occur in amounts that generally do not exceed about 0.5 percent. Heavy minerals are common in most quartz arenites, but generally make up no more than about 0.5 percent of total framework grains. The most common heavy minerals are the ultrastable types zircon, tourmaline, and rutile; therefore, the ZTR index of heavy minerals in quartz arenites is commonly very high. The ultrastable heavy minerals are commonly well rounded. Less common heavy minerals include magnetite, sphene, epidote, monazite, apatite, leucoxene, garnet, hypersthene, and hornblende. Minor amounts of secondary pyrite are present in some quartz arenites.

Cements

Most quartz arenites are well cemented with silica, carbonate, or hematite cement. Quartz appears to be by far the most common cement and is typically present as syntaxial overgrowths on detrital quartz cores. When syntaxial overgrowths are picked out by a line of bubbles or impurities (e.g. Fig. 4.14), they are easy to see. Application of cathodoluminescence petrography may be necessary to identify overgrowths not marked by such a line of impurities. Microquartz and opal cements occur in some quartz arenites but are much rarer than syntaxial overgrowths. Opal is distinguished by its isotropic character. Microquartz cement occurs as equidimensional microquartz or fibrous chalcedony, and more than one generation of cement may be present (Boggs, 2006, p. 100). In some pores, microquartz may display well-developed drusy texture.

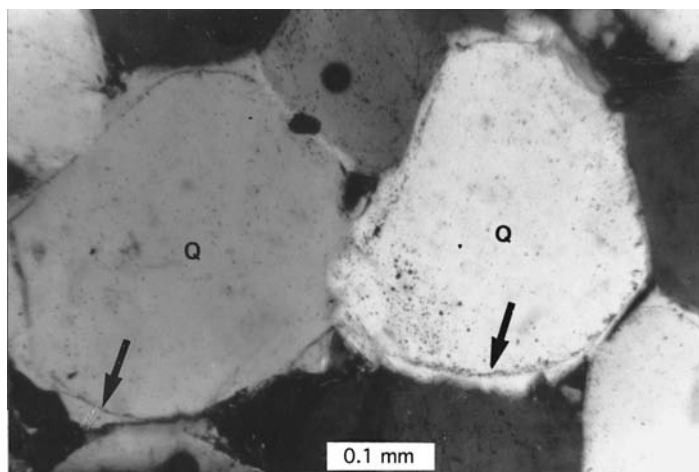


Figure 4.14 Photograph of two quartz grains (Q) with overgrowths. Note that original grain outlines are clearly marked by a line of impurities (arrows) and that the grain on the right is almost completely surrounded by the overgrowth. Quartz arenites of the Deadwood Formation (Cambrian–Ordovician), South Dakota. Crossed nicols.

Calcite is the most common carbonate cement in quartz arenites, but dolomite and, less commonly, siderite may occur also. Calcite cement can occur as a mosaic of small crystals within a single pore, but typically it forms single, large crystals that completely fill a pore. In fact, in some portions of a sandstone, a single crystal may fill the pore spaces among several grains, thus enclosing parts or all of several grains to form a poikilitic texture.

Matrix

Quartz arenites typically contain very minor amounts of matrix; many are matrix free. On the other hand, some quartz wackes have more than 10 percent matrix. The small amount of matrix present in most quartz arenites is probably best explained as the product of diagenesis. The matrix consists mainly of fine-size quartz, feldspars, micas, and clay minerals, which likely form diagenetically by alteration of detrital feldspars and rock fragments. Abundant matrix in quartz wackes is probably not the product of diagenesis but may originate by some kind of special depositional conditions, such as conditions where quartz sands are blown into a lagoon or other quiet-water environment or are washed over during a storm. Alternatively, abundant matrix might result from bioturbation by organisms that mix mud from an underlying or adjacent layer into a clean quartz sand or by vadose infiltration of clays into sands (e.g. Matlack *et al.*, 1989).

Texture

Quartz arenites tend to be texturally mature to supermature; however, some are submature to immature. They are typically well sorted with low matrix content, as discussed. Subrounded to well-rounded grains predominate in many examples (Fig. 4.15). On the other hand, some

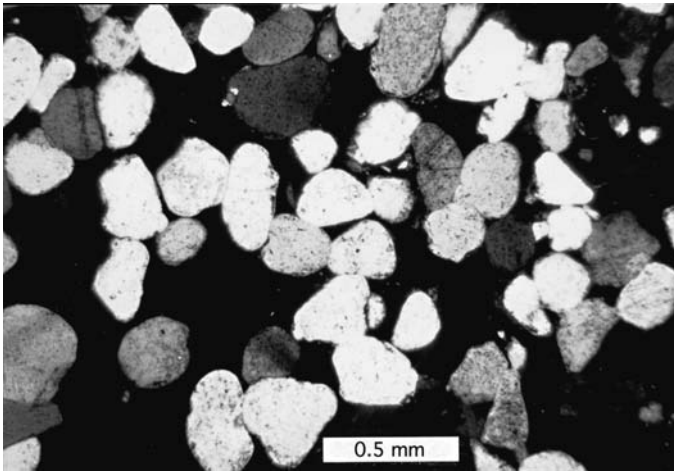


Figure 4.15 Quartz arenites with subrounded to well-rounded, well-sorted grains. Navajo Formation (Jurassic), Utah. Crossed nicols.

quartz arenites are more poorly sorted and may contain high percentages of subangular to angular grains. Some quartz arenites exhibit textural inversions (Folk, 1974, p. 145) such as a combination of poor sorting and high rounding, a lack of correlation between roundness and size, such as small round grains and larger angular grains, or mixtures of rounded and angular grains within the same size fraction. These textural inversions probably result from mixing of grains from different sources, erosion of older sandstones, or environmental variables such as wind transport of rounded grains into a quiet-water environment. Angular grains may result also from diagenetic development of secondary overgrowths.

Chemical composition

Owing to their rather restricted mineral composition, the bulk chemical composition of quartz arenites varies within very narrow limits. On the average, SiO_2 makes up 96–97 percent of the chemical components of quartz arenites; Al_2O_3 , Fe_2O_3 , FeO , MgO , and CaO together make up most of the remaining few percent of the chemical constituents. Other elements are commonly present in trace amounts. Rare extreme variations from these averages result mainly from differences in cement and matrix content rather than differences in particle composition. Thus, significant amounts of calcite or dolomite cement are reflected in abnormally high calcium and magnesium abundances, hematite cements increase the iron content of samples, high clay matrix content is reflected in higher than normal aluminum content, and so on.

Field characteristics

Quartz arenites tend to occur in sheetlike units, many of regional extent, which may range in thickness from a few meters to several hundred meters. Thickness of individual units can

vary considerably from place to place. The Jurassic Navajo Formation of the US Colorado Plateau, for example, reaches a thickness of 425 m in some areas, but thins to about 5 m in other localities. Quartz arenites may occur in dominantly nonmarine stratigraphic sections or dominantly marine sections. In marine sections, they are typically present in association with shallow-water limestones, dolomites, and, less commonly, feldspathic sandstones. On the other hand, some quartz arenites are associated with siliceous shales and cherts, suggesting a deeper-water origin (e.g. Bond and Devay, 1980). In nonmarine sections, they may occur in association with fluvial, lithic or feldspathic sandstones, siltstones, conglomerates, and evaporites.

Cross-bedding is a prominent feature of some quartz arenites, and some units display giant-scale sets of cross-beds several meters thick that have foreset dips of 20 to 35 degrees near the top of each bed. Other quartz arenites consist of thick-bedded, massive-appearing units that lack cross-beds or that display only indistinct cross-beds with low-angle foresets. Parallel-laminated quartz arenites are common also, and ripple marks are present in some units. Body fossils may be present in some beds, but are rare in most. On the other hand, bioturbation features and trace fossils can be locally abundant.

Origin

The extreme compositional maturity of quartz arenites requires that these sandstones originate under rather specialized conditions. If quartz arenites are first-cycle deposits, they must form under weathering, transport, and depositional conditions so vigorous that most grains chemically and mechanically less stable than quartz are eliminated (see, for example, Johnsson *et al.*, 1988). Conceivably, extreme chemical leaching under hot, humid, low-relief weathering conditions, prolonged transport by wind, intensive reworking in the surf zone or tidal zone (reworking by reversing tides), or a combination of these factors might be adequate to generate a first-cycle quartz arenite. Stream transport is known to produce little rounding of sand-size quartz grains, whereas wind transport is an effective rounding agent. Therefore, the well-rounded and well-sorted character of many quartz arenites, plus the common presence of large-scale sets of cross-beds with high-angle foresets, suggests that many quartz arenites are eolian deposits. On the other hand, many other quartz arenites are clearly of marine origin, as shown by their association with carbonates or other marine deposits. These marine quartz arenites may have been deposited in beach or barrier-island settings; however, the effectiveness of surf action in rounding of sand-size quartz is still not well known. Ferree *et al.* (1988) conclude that both modern beach sand and ancient beach sandstones have frameworks that are mineralogically more mature than their fluvial counterparts. They suggest that breakdown of rock fragments on beaches where wave power is high tends to enrich the sand in quartz and is an important factor in increasing compositional maturity of the sands.

Suttner *et al.* (1981) suggest that first-cycle quartz arenites cannot be produced under “average” conditions. A unique combination of extreme climatic conditions, transportation, and low sedimentation rates are required to produce such a sandstone. These authors conclude that most quartz arenites in the geologic record are multicycle deposits. Less

intensive weathering/transport processes operating through several sedimentation cycles may be able to selectively remove less stable grains to produce a quartz arenite. To account for the extreme grain rounding, many quartz arenites may have been subjected to an episode of wind transport during at least one of these cycles, although not necessarily the last cycle. On the other hand, Johnsson *et al.* (1988) report that definite first-cycle quartz arenites are forming in the Orinoco River basin in Venezuela and Colombia. They cite two conditions that are necessary to produce first-cycle quartz arenites: an environment of intense chemical weathering and a mechanism to provide extended time over which weathering can operate (e.g. temporary storage on extensive alluvial plains).

Occurrence and examples

Quartz arenites are present in geologic systems ranging in age from Precambrian to Tertiary. Even some Holocene eolian, coastal plain, and fluvial sands are quartz-rich. At least 60 formations composed totally or in part of quartz arenites are known from North America alone, and many may occur in other parts of the world. Distribution of North American quartzites by age is skewed toward those of Precambrian, Cambrian, and Ordovician ages. Some well-known examples include the Precambrian Barabo Quartzite of Wisconsin and the Sioux Quartzite of Minnesota, the Cambrian Franconia Sandstone of the upper Mississippi Valley and the Potsdam Sandstone of New York, the Ordovician St. Peter Sandstone of the upper Mississippi Valley, and the Eureka Quartzite of Utah, Nevada, and California.

Other well-known quartz arenites include the Silurian Tuscarora Quartzite of Pennsylvania and New Jersey, the Devonian Oriskany Sandstone of Pennsylvania, the Pennsylvanian Tensleep Sandstone of Wyoming, the Permian Coconino Sandstone of the Colorado Plateau, the Triassic Wingate Sandstone and Jurassic Navajo Sandstone of the Colorado Plateau, and parts of the Cretaceous Dakota Formation of the Colorado Plateau and the Great Plains. See Pettijohn *et al.* (1987, pp. 179–184) for additional examples of quartz arenites from North America, Europe, and other parts of the world. For a well-described case history of a fairly typical quartz arenite, the Ordovician Kinnikinic Quartzite of Idaho, see James and Oaks (1977).

4.6.3 Feldspathic arenites

General characteristics

Feldspathic arenites contain less than 90 percent quartz grains, more feldspar than unstable rock fragments, and minor amounts of other minerals such as micas and heavy minerals. They may contain as little as 10 percent feldspar grains, but most feldspathic arenites show greater feldspar enrichment. In fact, rare feldspar values exceeding 80 percent have been reported (e.g. Crook, 1960). As discussed, sandstones that contain more than about 25 percent feldspar are commonly called arkoses. Some feldspathic arenites are colored pink or red owing to the presence of K-feldspars or iron oxides; others are light gray to white. They are

typically medium to coarse grained and may contain high percentages of subangular to angular grains. Matrix content may range from trace amounts to more than 15 percent, and sorting of framework grains can range from moderately well sorted to poorly sorted. Thus, feldspathic sandstones are commonly texturally immature or submature.

Feldspathic arenites are not especially characterized by any particular kinds of sedimentary structures. Bedding may range from essentially structureless to parallel laminated or cross-laminated. Fossils may be present in marine examples. Feldspathic arenites typically occur in cratonic or stable shelf settings, where they are associated with conglomerates, shallow-water quartz arenites or lithic arenites, carbonate rocks, and evaporites. Less typically, they occur in sedimentary successions that were deposited in unstable basins or other deeper-water, mobile-belt settings. Feldspathic arenites of the latter type, which are matrix rich and well indurated owing to deep burial, are often called **feldspathic graywackes**.

The abundance of feldspathic arenites in the geologic record is not well established. Pettijohn (1963) estimates that arkoses make up about 15 percent of all sandstones. Feldspathic arenites in total are probably more abundant than 15 percent, especially if feldspathic graywackes are included.

Particle composition

Quartz is the dominant particle constituent in most feldspathic arenites and typically makes up about 50–60 percent of the framework grains. Reported quartz abundances range from about 10 percent to more than 75 percent. Quartz tends to be less abundant in plagioclase-rich feldspathic arenites than in K-feldspar-rich feldspathic arenites. Most quartz is monocrystalline. Polycrystalline quartz grains generally make up less than 6 or 7 percent of the framework constituents

Total feldspar content of feldspathic arenites can range from as little as 10 percent to more than 75 percent of grains; a more typical range is 20 to 40 percent. Available data indicate that feldspathic arenites in which K-feldspars exceed plagioclase feldspars are most common; however, plagioclase is the dominant feldspar in many sandstones, particularly those from mobile-belt settings. Microcline is a common K-feldspar in many feldspathic arenites; however, K-feldspar identified as orthoclase equals or exceeds microcline in some feldspathic sandstones. Plagioclase is typically sodic, in the range of An₅ to An₅₀, with oligoclase and andesine being most common; however, calcic plagioclases have been reported. Both twinned and untwinned, and zoned and unzoned plagioclase occur. The feldspars in feldspathic arenites may range from fresh, unaltered grains to those showing various degrees of alteration to sericite or kaolinite. Feldspar grains may also be stained with hematite and partially replaced by calcite or other minerals. [Figure 4.16](#) shows a fairly typical K-feldspar-rich arkose.

Coarse muscovite and biotite are common minor constituents of feldspathic arenites. Muscovite is generally unaltered, but may be stained with hematite or limonite. Biotite grains may show alteration to hematite or chlorite. Heavy minerals commonly make up only 1 or 2 percent of the framework grains. In contrast to the quartz arenites, the heavy minerals in feldspathic arenites may include unstable or metastable types such as olivine, pyroxenes,

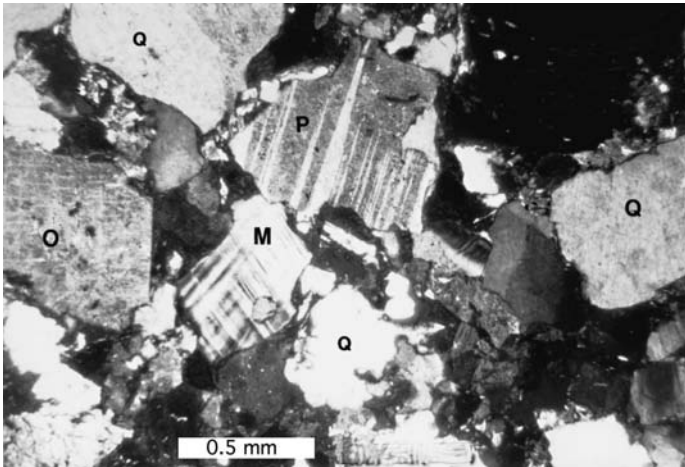


Figure 4.16 Poorly rounded feldspars (M = microcline, O = orthoclase, P = plagioclase) and quartz (Q) in a feldspathic arenite. Belt (Precambrian) facies, Montana. Crossed nicols.

amphiboles, magnetite, epidote, garnet, and kyanite, as well as ultrastable rutile, tourmaline, and zircon. Therefore, the ZTR index of heavy minerals in many of these sandstones is typically lower than that in quartz arenites. On the other hand, some feldspathic arenites contain very restricted suites of heavy minerals, possibly owing to destruction of less stable heavy minerals by intrastratal solution during diagenesis. Rock fragments are common but are much less abundant than feldspars. These fragments may include quartzose clasts (mainly metaquartzite) and various kinds of less stable plutonic igneous, volcanic, metamorphic, and sedimentary clasts. Rock fragments, especially volcanic rock fragments, appear to be most abundant in plagioclase-rich feldspathic arenites. Feldspathic arenites can grade compositionally into lithic arenites.

Cements

Carbonate cements appear to be the most common cements in feldspathic arenites and range from trace amounts to more than 20 percent of total constituents. Carbonate cements are typically calcite, but may include dolomite. The cement may occur as a mosaic of smaller crystals but more commonly occurs as large, single crystals that entirely fill pores or even surround grains. Other cements, which generally occur in minor amounts, may include silica (quartz overgrowths), authigenic feldspars (overgrowths), hematite, and sulfate minerals such as barite, pyrite, and clay minerals.

Matrix

The matrix content of feldspathic arenites may range from trace amounts to more than 15 percent of total constituents. Many of these sandstones contain very little matrix and have correspondingly higher amounts of cement, commonly carbonate cement. The matrix in

many feldspathic arenites appears to consist mainly of sericite and kaolinite, typically stained with hematite. It is probably derived by alteration of biotite or other iron-bearing minerals. In others, the matrix materials may include also chlorite, fine quartz, feldspar, and organic matter. Although some matrix in feldspathic arenites may be detrital, or may have been introduced by vadose infiltration, much of it is probably derived by diagenetic alteration of feldspars, micas, and ferromagnesian minerals. Therefore, the matrix content of these rocks is probably not a reliable indicator of depositional conditions.

Texture

Feldspathic arenites are typically coarse grained, but grain size can range from coarse silt or very fine sand to very coarse sand. Several investigators have reported that the feldspar content of feldspathic arenites tends to increase with decreasing grain size of the sediment. This inverse correlation of increasing feldspar abundance with decreasing grain size may reflect the tendency of feldspars to break into smaller fragments (owing to the presence of twin planes, etc.) during sediment transport.

Sorting of framework constituents in feldspathic arenites can range from moderately well sorted to poorly sorted; moderate sorting is most common. Both quartz and feldspars in feldspathic arenites are typically angular to subangular (e.g. Fig. 4.16); subrounded to well-rounded quartz is less common. Owing to the presence of matrix in many feldspathic arenites and generally poor rounding of these grains, most feldspathic arenites are texturally immature to submature.

Chemical composition

Feldspathic arenites contain markedly less silica and considerably more aluminum, sodium, and potassium than do quartz arenites. Silica content is influenced both by quartz abundance and the abundance of rock fragments, feldspars, and other silicates. Aluminum content is affected particularly by feldspars, micas, and clay minerals, all of which are commonly more abundant in feldspathic arenites than in quartz arenites. Iron in both the oxidized (ferric) and reduced (ferrous) states is common in feldspathic arenites. The high content of sodium and potassium in feldspathic arenites compared to that in quartz arenites is a function mainly of the greater content of sodium and potassium feldspars in these rocks. Calcium and magnesium abundances are influenced particularly by the content of carbonate cements.

Field characteristics

As defined in this book, feldspathic arenites include all sandstones that contain less than 90 percent quartz and more feldspars than rock fragments. Thus, they encompass both classic arkoses (25 percent or more feldspars) and sandstones that are less feldspar rich, some of which may be considered graywackes by some workers. Feldspathic arenites may be deposited under a wide range of conditions, ranging from nonmarine to deep marine (turbidite). Therefore, feldspathic arenites may display considerable variation in their field characteristics.

Many feldspathic arenites were deposited in fluvial, lacustrine, or transitional marine environments. These arkoses are typically red or pink and tend to form thick (to 2000 m or more), wedge-shaped units adjacent to ancient uplifts. These so-called aprons, or fans, commonly become thinner and finer grained basinward, where the arkoses may interfinger with finer-grained lacustrine or marine deposits. Arkoses may be interbedded with a variety of nonmarine to marine deposits including conglomerates, shales, limestones, and evaporites. Individual arkose beds may range in thickness from a few centimeters to several meters and tend to be poorly sorted, irregularly bedded, and laterally discontinuous. Trough cross-bedding is common. Other evidence of fluvial deposition such as cut-and-fill structures and plant fossils may be present. Feldspathic arenites deposited in marine environments tend to have less feldspar than nonmarine arkoses and are better sorted, more evenly bedded and laterally continuous. Also, they may contain marine fossils. Feldspathic arenites deposited by turbidity currents may display graded bedding and sole markings of various types.

Origin

Feldspathic arenites originate mainly by weathering of feldspar-rich crystalline rocks, either plutonic igneous rocks or feldspar-rich metamorphic rocks. Therefore, most feldspathic arenites are probably first-cycle deposits. Most reported feldspathic arenites contain considerably more K-feldspar than plagioclase; however, several plagioclase feldspathic arenites are known. These plagioclase-rich feldspathic arenites are derived mainly from volcanic sources. Most plagioclase in these sandstones is sodic, commonly oligoclase and andesine. The feldspar composition of feldspathic arenites thus suggests that most of these sandstones were derived from acid (felsic) to intermediate crystalline rocks.

Rarely, plagioclase arenites contain calcic plagioclase, indicating derivation from more basic igneous rocks. The preservation of large quantities of feldspars during the process of weathering appears to require that feldspathic arenites originate either (1) under very cold or very arid climatic conditions where chemical weathering processes are inhibited or (2) in warmer, more humid climates where marked relief of local uplifts allows rapid erosion of feldspars before they can be decomposed. Dickinson (1984) suggest that feldspar-rich sandstones are derived especially from fault-bounded, uplifted basement areas in continental-block provenances, where high relief and rapid erosion of uplifted sources gives rise to quartzo-feldspathic sands of classic arkosic character. These sandstones may accumulate in basins related to transform ruptures of continental blocks, incipient rift blocks, or zones of wrench tectonism within continental interiors. Some feldspathic arenites, particularly plagioclase-rich arenites, could conceivably be derived from dissected magmatic-arc settings, where they might be deposited in forearc or backarc basins.

As discussed, most feldspathic arenites, particularly arkoses, appear to have been deposited as clastic wedges or fans very close to their sources. Pettijohn *et al.* (1987, p. 152) suggest that some arkoses are *in situ*, or residual, deposits that formed essentially in place by disintegration of coarse crystalline rocks. These residual deposits tend to have very poor sorting, high detrital matrix content, and very angular grains. Residual arkosic debris shifted

downslope short distances by mass-transport processes probably has much the same characteristics as that of residual arkoses. On the other hand, arkosic sediment transported greater distances by traction currents is “cleaned up.” Thus, transported arkoses display better sorting and various degrees of grain rounding. Less detrital matrix is likely present in these transported arkoses than in residual arkoses, but the transported arkoses may contain considerable diagenetic matrix. Arkosic material transported into marine environments undergoes additional sorting and perhaps mixing of sediment from other sources, which may dilute the feldspar content below that typical of residual arkoses. Feldspathic sediments may be retransported by turbidity currents into deep water.

Occurrence and examples

Feldspathic arenites are present in geologic formations ranging in age from Precambrian to Holocene. They do not appear to be especially characteristic of any particular geologic period. In contrast to the quartz arenites, they tend to be of local rather than regional extent. They apparently formed whenever and wherever tectonic processes generated marked uplifts of crystalline basement rocks, allowing rapid erosional stripping of these tectonic blocks and accumulation of thick, localized deposits of arkosic debris in adjacent, subsiding basins. Some formations contain feldspathic arenites only at their bases. These basal feldspar-rich units grade upward into either lithic arenites or quartz arenites.

Some well-known examples of feldspathic arenites include the Precambrian Torridon sandstones of Scotland, the Silurian Clinton Formation of Pennsylvania (USA), the Devonian Old Red Sandstone of England, the Pennsylvanian Minturn and Fountain formations of Colorado, the Triassic Newark Group of Connecticut, and the Paleocene Swauk Formation (a plagioclase-rich arkose) of Washington.

4.6.4 Lithic arenites

General characteristics

Lithic arenites are an extremely diverse group of rocks that are characterized by generally high content of unstable rock fragments. Classified according to Fig. 4.12, any sandstone that contains less than 90 percent quartz (plus chert and quartzite) and unstable rock fragments in excess of feldspars is a lithic arenite. Colors may range from light gray (“salt and pepper”) to uniform, medium to dark gray. Many lithic arenites are poorly sorted; however, sorting ranges from well sorted to very poorly sorted. Quartz and many other framework grains are generally poorly rounded. Lithic arenites tend to contain substantial amounts of matrix, most of which may be of secondary origin. They may range from irregularly bedded, laterally restricted, cross-stratified fluvial units to evenly bedded, laterally extensive, graded, marine turbidite units. They occur in association with fluvial conglomerates and other fluvial deposits and in association with generally deeper-water, marine conglomerates, pelagic shales, cherts, and submarine basalts.

Classified as mentioned, lithic arenites include many sandstones that are called graywackes. Some authors (e.g. Pettijohn *et al.*, 1987) consider graywackes to be distinctly

different from lithic arenites (or feldspathic arenites) and treat them as different groups of rocks. The origin, meaning, and usage of the term graywacke remain controversial. Even the spelling of the term varies: greywacke vs. graywacke. Although consistent usage of the term graywacke is still lacking, it appears to be used mainly for sandstones that are dark gray or dark green, well indurated or lithified, and matrix rich. The matrix, often referred to as a chloritic “paste,” tends to pervade the rock and obscure the boundaries of rock fragments and other grains, making identification of grains difficult. Most graywackes appear to be turbidites and thus are associated with deep-water deposits of various types.

As indicated, graywackes are defined largely on the basis of field characteristics and matrix content, rather than on particle composition, and they all look very much alike in overall field appearance. When examined petrographically, they turn out to be mainly lithic wackes or feldspathic wackes. Graywackes that classify as quartz wackes are rare. In this book, I do not treat graywackes as a separate group of sandstones. Rather, I regard them to be special types of either lithic or feldspathic arenites and include them in discussion of these sandstone types. Some workers have suggested that we abandon any precise definition of graywacke, and simply use these terms for imprecise field descriptions (e.g. Dickinson, 1970). Pettijohn (1963) estimates that lithic arenites and graywackes together make up nearly one-half of all sandstones.

Particle composition

Sandstones that classify as lithic arenites may have highly variable compositions. The quartz-grain content of lithic arenites can range from less than 1 percent to more than 70 percent, and no particular range of quartz values seems typical. Available data suggest that the percentage of polycrystalline quartz is much higher (up to about 10 percent) than that in either feldspathic arenites or quartz arenites. Feldspar content may range from less than 1 percent to more than 25 percent of grains. Plagioclase predominates over K-feldspars in many lithic arenites. Plagioclase is typically sodic, ranging in composition from about An₁₅ to An₃₅ (albite to andesine). Among the K-feldspars, orthoclase appears to be more common than microcline.

Rock fragments are clearly the most distinctive feature of lithic arenites. Both stable fragments (e.g. chert) and unstable fragments may be present. Although detrital chert is included with quartz in some sandstone classifications, chert is nonetheless a rock fragment (e.g. Fig. 4.17). Many lithic arenites contain only minor amounts of chert; however, chert concentrations ranging to 75 percent or more have been reported.

It is, of course, the presence of abundant unstable, fine-grained rock fragments that particularly characterize lithic arenites. The abundance of these rock fragments may range from less than 10 percent to as much as 80 percent, but abundances of 20 to 40 percent are more typical. Volcanic rock fragments (e.g. Fig. 4.18) are especially common in lithic arenites derived from magmatic-arc settings. Granite and other coarse plutonic igneous rock fragments are reported in some lithic arenites, but generally in very minor amounts. Common metamorphic rock fragments include slate, phyllite, and schist (Fig. 4.19). Coarser crystalline gneiss fragments are much less common, as are serpentinite fragments.

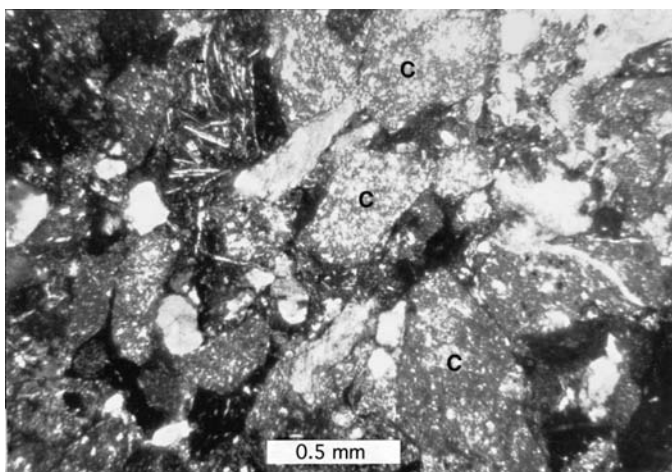


Figure 4.17 Detrital chert grains (C) in a chert-rich lithic arenite. Otter Point Formation (Jurassic), southwest Oregon. Crossed nicols. (Sample courtesy of R. L. Lent.)

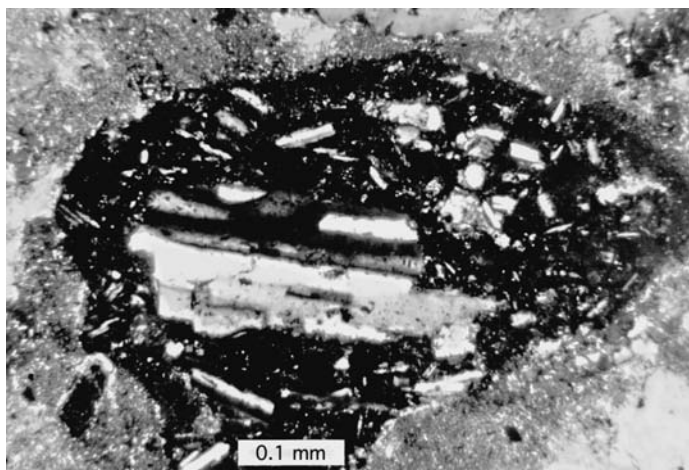


Figure 4.18 Large volcanic clast showing plagioclase laths in a glassy groundmass. Miocene volcanoclastic sandstones, ODP Leg 127, Site 796, Japan Sea (depth 283 m below seafloor). Crossed nicols.

Sedimentary rock fragments include fine-grained sandstone (Fig. 4.20), siltstone, shale or mudstone (Fig. 4.21), and, less commonly, carbonates. Owing to the large variety of rock fragments that may be present in lithic sandstones, some workers have suggested subdividing these sandstones on the basis of rock-fragment type (e.g. Folk, 1974, p. 129). This procedure yields such special names as volcanic arenite, phyllarenite, chert arenite, and calclithite (composed predominantly of carbonate clasts), depending upon rock-fragment composition.

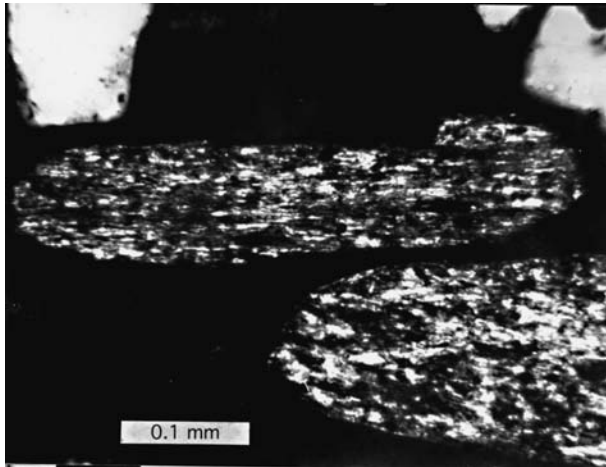


Figure 4.19 Large metamorphic fragments (fine schist/phyllite), modern shelf sediment, Taiwan Strait. Crossed nicols.

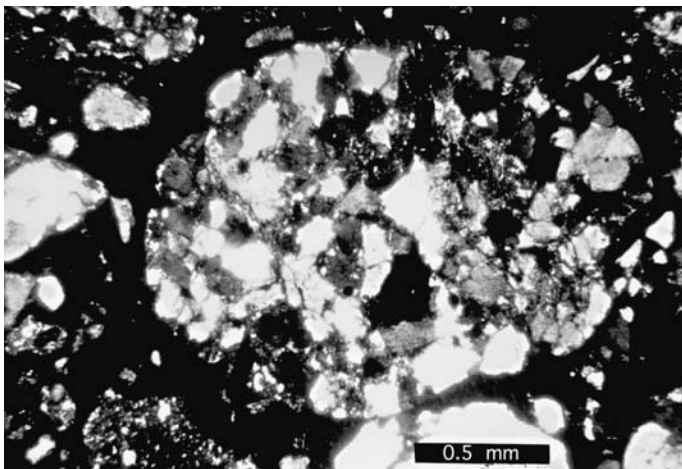


Figure 4.20 Large well-rounded sandstone clast, modern shelf sediment, Taiwan Strait. Crossed nicols.

Micas are absent or very scarce in some lithic arenites; however, they are very abundant in others, particularly some fluvial sandstones. Rarely, mica values exceeding 10 percent have been reported. Muscovite appears to be somewhat more common than biotite. Heavy minerals are present in lithic arenites in amounts ranging from traces to more than 10 percent. Although some lithic arenites contain mainly ultrastable zircon, tourmaline, and rutile, most contain a variety of unstable heavy minerals. These less-stable heavy minerals may include epidote, sphene, garnet, hornblende, glaucophane, clinopyroxenes,

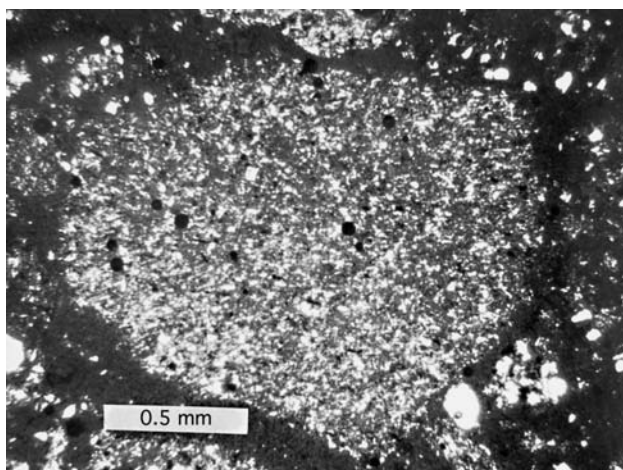


Figure 4.21 Silty mudstone clast, modern shelf sediment, Taiwan Strait. Crossed nicols.

orthopyroxenes, apatite, fluorite, pumpellyite, clinozoisite, laumontite, lawsonite, cordierite, magnetite, pyrite, leucoxene, chromite, and corundum. Thus, the ZTR index of these sandstones is generally low compared to that of quartz arenites. Many lithic arenites of Devonian or younger age contain charcoal fragments or opaque organic material that is probably mostly macerated plant debris. In some lithic arenites, fine organic matter is concentrated in thin laminae that give the sandstones a laminated appearance.

Cements and matrix

Some lithic arenites contain no visible cements, whereas others contain cements in amounts ranging to more than 30 percent of total constituents. Carbonate cements appear to be most common and may include calcite, dolomite, and siderite. Silica cement (quartz overgrowths) is moderately abundant in some lithic arenites. Other common cements are chlorite, clay minerals, iron oxides, and pyrite. The matrix content of lithic arenites ranges from trace amounts to as much as 40 percent, although most contain less than 20 percent matrix.

As discussed, clay matrix and clay cements are difficult to distinguish under a petrographic microscope, unless the clays are fairly coarse grained and exhibit distinctive cement textures such as the drusy texture shown in Fig. 4.9. This problem of identification is compounded owing to the authigenic origin of much matrix. So-called authigenic matrix that fills original pore space or pore space created by dissolution of cement or framework grains is, in fact, cement, although it may not be recognizable as such under a petrographic microscope. Other authigenic matrix forms by replacing framework grains or cements. Finally, some authigenic matrix is simply original detrital or infiltrated matrix that has undergone recrystallization.

Lithic arenites deposited in fluvial or nearshore marine environments may have less matrix on the average than deeper-water, graywacke-type lithic arenites. This difference may simply reflect different diagenetic histories rather than significant differences in

original, detrital matrix content. Therefore, we should be extremely careful about making environmental interpretation on the basis of matrix content of sandstones.

Texture

Many lithic sandstones are coarse-grained; however, the grain size of these rocks may range from very fine sand to very coarse sand or granules. Classified according to Folk's (1951) textural maturity classification, most lithic arenites are texturally immature owing to their high matrix content. If we ignore matrix as being largely authigenic and classify them on the basis of the sorting and rounding characteristics of the framework grains, they are mainly submature to mature. Sorting of framework grains may range from well sorted to very poorly sorted. Although lithic arenites derived from sedimentary source rocks may contain moderately well-rounded quartz, or quartz with rounded outlines beneath inherited overgrowths, the roundness of quartz in most lithic arenites tends to range between angular to subrounded. Subangular quartz is probably most common. Lithic fragments and other framework grains in lithic arenites are also commonly subangular to subrounded. Few lithic arenites are composed predominantly of well-rounded grains.

Chemical composition

The chemical composition of lithic arenites is quite variable, and the composition of some lithic arenites is very similar to that of some feldspathic arenites. Silicon dioxide values are moderate and commonly range between 50 to 70 percent, whereas Al_2O_3 values tend to be high and commonly exceed 10 percent. Iron, potassium, and magnesium values are moderately high also. The high Al, Fe, K, and Mg concentrations may reflect the generally high clay content of lithic arenites. Argast and Donnelly (1987) suggest that Al_2O_3 , K_2O , Fe_2O_3 , and MgO all tend to be enriched in the fine-grained, phyllosilicate-rich fraction of sandstones, whereas SiO_2 and Na_2O concentrations are related to the coarser-grained, tectosilicate fraction. The Na_2O content is probably strongly correlated to the albitic composition of sodium-rich plagioclase feldspars. Magnesium content can be affected by the presence of detrital dolomite clasts and dolomite cements, and calcium abundance is affected by detrital limestone clasts and calcite cements.

Origin and field characteristics

The high content of unstable rock fragments and the moderately high feldspar content of lithic arenites suggest that they are derived from rugged, high-relief source areas. Detritus is stripped rapidly from these elevated areas before weathering processes can destroy unstable clasts and other framework grains. Furthermore, most lithic arenites contain fine-grained clasts derived from source regions composed mostly of fine-grained rocks, that is, volcanic rocks, schists, phyllites, slates, fine-grained sandstones, shales, and limestones. Source areas with these characteristics occur primarily in orogenic belts located along the suture zones of collision plates and in magmatic arcs (e.g. Dickinson, 1985). Lithic arenites are probably derived only rarely from continental-block provenances, which typically yield quartz arenites and feldspathic arenites.

Lithic arenites derived from recycled orogen provenances that formed by collision of continental blocks may be deposited in proximate alluvial fans or other fluvial environments. They are light-gray, “salt-and-pepper,” or light-brown sandstones that display bedding characteristics ranging from evenly bedded to irregular, laterally discontinuous. Both tabular and trough stratification may be prominent. Scour-and-fill structures, current lamination, and ripple marks are common sedimentary structures. Many beds may be highly micaceous. Fluvial lithic arenites are commonly associated with thin shales and conglomerates and may be locally very coarse grained.

In some settings, deposition can take place in marine foreland basins adjacent to foldthrust belts. Alternatively, lithic detritus may be transported by large rivers off the continent into deltaic or shallow, pericontinental shelf environments. Lithic arenites deposited in deltaic environments can have many characteristics in common with alluvial deposits, but the deltaic sands tend to be somewhat better sorted and more evenly bedded. They may be interbedded with shales containing marine fossils or with tidal flat or marsh deposits. Lithic arenites deposited in shallow-marine environments are commonly more evenly bedded and laterally persistent than fluvial and deltaic sandstones. Horizontal laminations and both tabular and trough cross-bedding may be common. Some units may display hummocky cross-stratification. Ripple marks are common, especially oscillation ripples. Marine fossils may be present and bioturbation structures can be scarce to abundant. Macroscopic plant fragments may be locally abundant in marine lithic arenites of Devonian age or younger. Shallow-marine shelf arenites may be interbedded with shelf muds that are commonly bioturbated also.

Lithic arenites derived from magmatic-arc settings are typically enriched in volcanic rock fragments and plagioclase feldspars. Lithic detritus may be deposited in nonmarine settings within intra-arc basins, but most is probably carried by rivers to coastal areas. There, much of it is retransported into deeper water by turbidity currents or other sediment gravity-flow mechanisms. Ultimately, this detritus is deposited in forearc basins, backarc basins, or subduction-zone trenches. Lithic arenites deposited in these settings are particularly likely to undergo deep burial and incipient metamorphism, leading to development of characteristics generally ascribed to graywackes. They are typically dark gray, dark green, or black, well indurated and well bedded. The bedding may be repetitious or rhythmic (Fig. 4.22) and laterally extensive. Individual sandstone beds may display distinct vertical size grading and Bouma sequences. Lithic arenites of turbidite origin are typically interbedded with pelagic clays and may also be associated with resedimented conglomerates, bedded cherts, and submarine basalts.

Examples

Lithic arenites are very abundant in the geologic record. Examples of lithic arenites include the Mississippian Mauch Chunk Formation of Pennsylvania, sandstones of the Carboniferous Trenchard Group in England, some Cretaceous and Jurassic sandstones of the southern Rocky Mountains of Canada, and some sandstones of the Jurassic Morrison Formation in the Colorado Plateau. Probable deltaic lithic arenites in these tables include the Oligocene

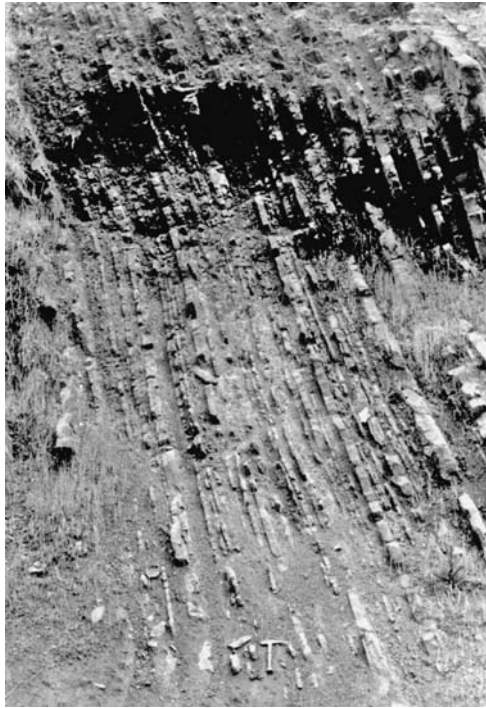


Figure 4.22 Rhythmic bedding in thin, graded lithic arenites of the Roseburg Formation (Eocene), southern Oregon Coast Range. The beds are tilted at an angle of about 70 degrees. Note the hammer for scale.

Frio Formation of Texas and the Triassic Ivishak Formation in Alaska. Shallow-marine lithic arenites include the Cretaceous Shannon Sandstone of Wyoming, the Eocene Bushnell Rock Member of the Lookingglass Formation in Oregon (fluvial to shallow marine), and the North Peak and Glenure formations of New Zealand. Overall, turbidites are probably the most abundant type of lithic sandstones.

4.7 Volcaniclastic sandstones

4.7.1 Introduction

The term volcaniclastic is applied to all siliciclastic sedimentary rocks enriched in volcanic fragments regardless of the mechanism that produced the fragments. Volcaniclastic deposits can be emplaced or deposited in any environment, on land, under water, or under ice, and may be mixed in any significant proportion with nonvolcanic fragments. Volcaniclastic deposits thus include both epiclastic sedimentary rocks, made up of products generated by fragmentation of pre-existing volcanic rocks owing to weathering and erosion, and rocks formed by primary

volcanic processes. Primary volcanic processes include **pyroclastic** (explosive) eruptions and **autoclastic** processes, e.g. fragmentation of magma that flows into water. Both processes generate fragmented products that are deposited contemporaneously with fragmentation.

Volcaniclastic rocks composed of abundant sand-size, epiclastic volcanic clasts are simply volcanic-derived epiclastic sandstones. These sandstones are studied and classified as any other epiclastic sandstones and differ from other sandstones primarily in their high content of volcanic-derived particles. They classify as either lithic arenites or feldspathic arenites, depending upon feldspar/rock fragment ratios. Sand-size volcaniclastic rocks that form by primary volcanic processes are called **tuffs** and are commonly regarded to be igneous rocks rather than sedimentary rocks. Such rocks are not, however, wholly igneous. They originate by igneous processes (e.g. magmatic explosions) but they are deposited by sedimentary processes (e.g. airfall). Owing to their mixed origin, the classification and genetic affinities of these rocks are intriguing problems. Additional information about the processes that form volcaniclastic sediments may be found in numerous sources, including Cas and Wright (1987), Leyrit and Montenat (2000), and White and Rigs (2001).

4.7.2 Classification

As mentioned, both epiclastic volcanic detritus and redeposited pyroclastic detritus (as well as nonreworked pyroclastic detritus) form volcaniclastic deposits. When volcaniclastic sandstones are classified on the basis of particle composition, they classify as lithic arenites (wackes) or feldspathic arenites (wackes). Typically, volcanic clasts exceed feldspars; however, plagioclase feldspars may be more abundant than volcanic clasts in some volcaniclastic sandstones. Owing to their high content of unstable volcanic rock fragments that can alter diagenetically to form matrix, most epiclastic volcaniclastic sandstones are wackes rather than arenites. Some volcaniclastic sandstones, such as sandstones deposited as lahars, may also contain detrital matrix.

4.7.3 Petrographic characteristics of volcaniclastic sandstones

The compositional features that particularly distinguish volcaniclastic sediments, whether composed of pyroclastic or epiclastic detritus, are their content of particles derived from volcanic sources. Particles generated as a direct result of volcanic action are called pyroclasts. Three principal kinds of **pyroclasts** are recognized: glassy fragments, crystals, and lithic fragments.

1. **Glassy fragments** are fragments consisting of partially recrystallized to unrecrystallized, consolidated pieces of erupted magma. These glass fragments are transparent in thin section in ordinary light and isotropic under crossed nicols. Glasses may have other colors such as red, yellow, and black depending upon impurities and the oxidation state of iron in the glasses. More viscous, silicic to intermediate lavas give rise to highly vesicular magmas that during explosive eruptions yield pumice fragments of various sizes. Sand-size pumice fragments (Fig. 4.23) are called **pumice ash**. Magmatic explosions cause fragmentation of pumice vesicle walls or bubble walls, producing angular, ash-size glass particles called **shards**. Magmatically produced glass shards tend to have

“Y” and cusped shapes (Fig. 4.24) and may become plastically deformed and welded if they are still hot enough when deposited.

2. **Crystals**, both entire crystals and angular fragments of crystals, occur in many pyroclastic deposits. Broken crystals may be particularly abundant. Crystals of plagioclase feldspar are most common and may display zoning (Fig. 4.25). Also, pyroxene and amphibole crystals are common in some tuffs. If quartz crystals are present they generally show the slight rounding and embayment typical of volcanic quartz. Fragments of glassy material may remain attached to the crystals as blebs or crusts. Most such crystals are phenocrysts derived by magmatic or phreatomagmatic explosive disruption of porphyritic magmas. Less commonly, crystals or crystal fragments may be derived by fragmentation of accessory or accidental lithic fragments.
3. **Lithic fragments** are the denser, generally nonvesicular, nonglassy volcanic fragments in pyroclastic deposits. Some glass may be present within the fragments as interstitial material between small crystals. A variety of rock-fragment textures may be present, including fragments with small oriented laths (Fig. 4.26A), small unoriented laths (Fig. 4.26B), large phenocrysts set in a fine-grained matrix (Fig. 4.26C), and both large phenocrysts and small laths in a fine groundmass (Fig. 4.26D).

Epiclasts are crystals, crystal fragments, glass fragments, and rock fragments that have been released from pre-existing volcanic rock by weathering or erosion and transported from their place of origin by gravity, air, water, or ice (Schmid, 1981). It can be difficult to differentiate between epiclasts and pyroclasts. Pettijohn *et al.* (1987, p. 192) suggest that the following features constitute criteria that can be used to identify pyroclasts.

1. Euhedral feldspars, many of which are broken, are commonly zoned and generally oscillatory
2. Volcanic quartz, which is generally rounded or embayed owing to magmatic resorption
3. Minerals such as olivine and pyroxenes that are not commonly abundant in epiclastic sandstones
4. Glassy fragments
5. Low quartz content, and high (euhedral) feldspar to quartz ratio.

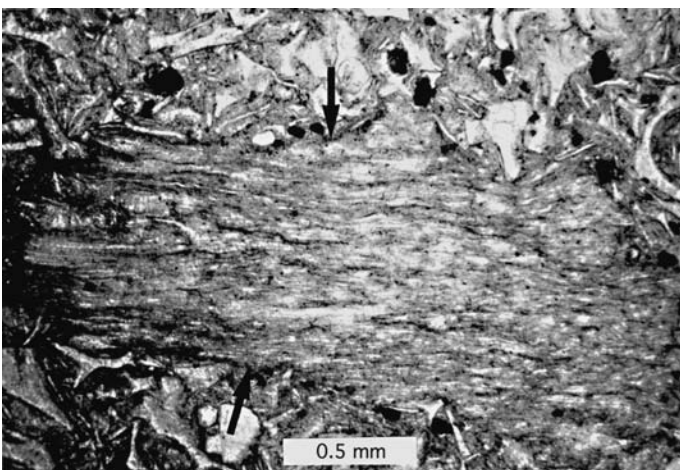


Figure 4.23 Large pumice fragment (arrows) surrounded by small glass shards. Colestin Formation (Eocene–Oligocene), southern Oregon. Ordinary light. (Sample courtesy of E. A. Bestland.)

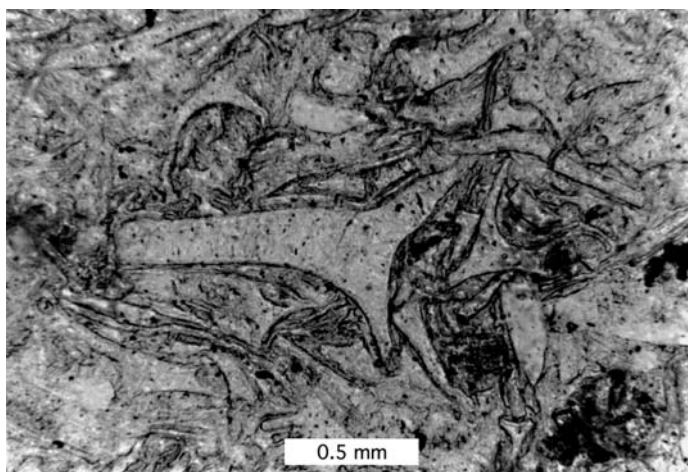


Figure 4.24 Glass shards in a volcaniclastic deposit. Note large Y-shaped cleat near center of photograph. Colestin Formation (Eocene–Oligocene), southern Oregon. Ordinary light. (Sample courtesy of E. A. Bestland.)

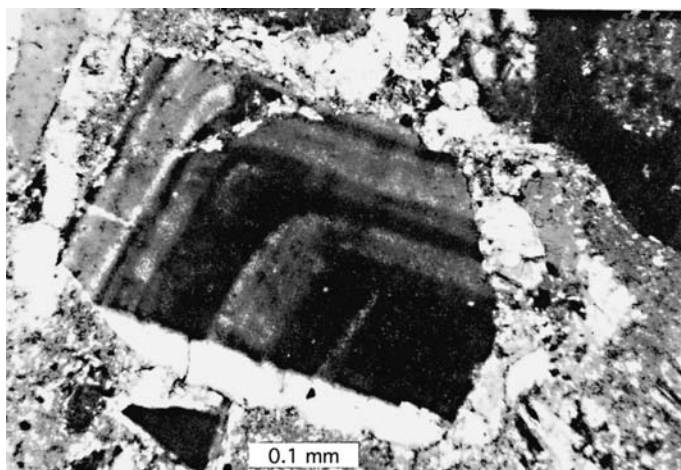


Figure 4.25 Broken, oscillatory zoned plagioclase grain. Miocene deep-sea sandstone, ODP Leg 127, Site 796, Japan Sea (depth 250 m below seafloor).

4.7.4 Alteration of volcaniclastic sandstones

Volcaniclastic sandstones contain a variety of unstable constituents (fine-grained lithic fragments, glassy fragments, mafic minerals, plagioclase feldspars) that alter readily during diagenesis (Fisher and Schmincke, 1984, ch. 12). Glass is particularly susceptible to alteration. It typically alters to smectite clay minerals, zeolite minerals, or silica minerals. Devitrification of silicic glass can generate microcrystalline textures that resemble

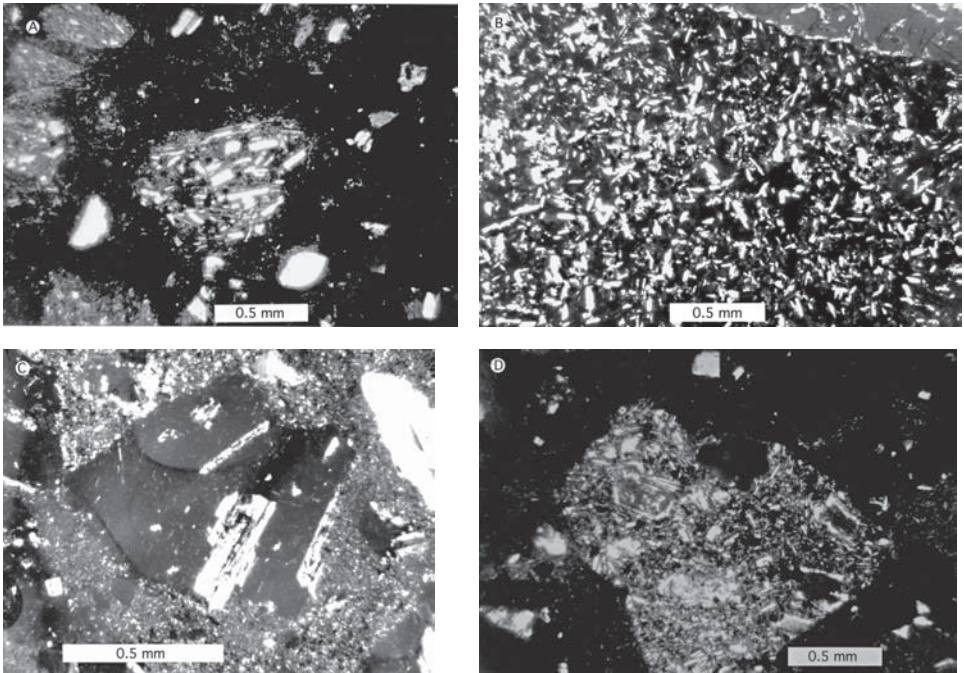


Figure 4.26 Crossed-nicols photomicrographs of typical volcanic rock fragments in volcaniclastic sediments. A. Small lithic fragment (center of photograph) containing very small, mainly oriented plagioclase laths. B. Large lithic fragment containing numerous small, unoriented plagioclase laths. C. Lithic fragment (center of photograph) containing large phenocrysts in a glassy groundmass. D. Lithic fragment containing both large phenocrysts and small, unoriented phenocrysts. Samples A, C, D from Miocene deep-sea sandstone, ODP Leg 127, Japan Sea. Sample B from Colestin Formation (Eocene–Oligocene), southern Oregon, courtesy of E. A. Bestland.

sedimentary chert. Such fragments may be extremely difficult to distinguish from chert unless distinctive euhedral crystals, such as feldspar laths, are preserved in the fragments. Also, glass can be replaced by minerals such as zeolites or calcite. Alteration of glass, feldspars, and lithic fragments can produce large amounts of authigenic clay matrix/cement. Silica cement may be present also as chalcedony or opal. Finally, squeezing of soft volcanic grains can produce pseudomatrix. These diagenetic changes in volcaniclastic sandstones make identification of original constituents difficult and differentiation of volcanic clasts from matrix a challenging task.

4.7.5 Occurrence and field characteristics

Volcaniclastic sandstones are common throughout the geologic record. Accurate measurements of the overall abundance of volcaniclastic sediments are not available; however, the volume of such ancient sediments is believed to be large (Fisher and Schmincke, 1984, p. 3).



Figure 4.27 Well-bedded Quaternary andesitic airfall pyroclastic deposits. The uppermost layers are draped over previously formed deposits along an irregular erosional surface. The beds are not folded; the inclined layers accumulated at the attitudes shown in the photograph. Oshima Island, Japan. (Photograph courtesy of A. R. McBirney.)

They occur preferentially in rock successions deposited in convergent-margin, magmatic-arc settings, including trenches, forearc basins, backarc basins, and intra arc basins. Epiclastic and reworked volcanoclastic sediments can be deposited by various fluid-flow and sediment gravity-flow processes in both continental and marine environments. Many ancient epiclastic or redeposited pyroclastic volcanoclastic sandstones appear to be turbidites that are associated with deeper-water deposits such as pelagic shales and cherts.

Pyroclastic detritus can also be deposited in both subaerial and subaqueous environments. Deposition of pyroclastic deposits is probably most common on land, including deposition in lakes. Ancient pyroclastic deposits are commonly closely associated with lava flows. Airfall, flows, and surges may generate well-bedded sequences of deposits (Fig. 4.27) that can appear very similar to epiclastic deposits. See Pettijohn *et al.* (1987, table 6.4, p. 224 and table 6.6, p. 236) for some distinguishing characteristics of pyroclastic deposits and redeposited volcanoclastic deposits. Pyroclastic deposits may contain graded beds (normal, reverse, complex grading), cross-beds, massive beds, and thin, parallel beds. Other sedimentary structures include antidunes, chute-and-pool structures, convolute bedding, load casts, and mudcracks

4.8 Miscellaneous sandstones

As indicated in preceding sections, the framework grains in epiclastic and volcanoclastic sandstones are dominantly quartz, feldspars, and rock fragments. Rock-fragment composition

can be quite varied. Most clasts are pieces of fine-grained igneous rocks, silicic metamorphic rocks, or siliciclastic sedimentary rocks; however, fragments of limestone, dolomite, and chert are common also. Occasionally, we find sandstones that contain significant amounts of framework constituents other than quartz, feldspars, and common rock fragments. These constituents may include heavy minerals such as magnetite, ilmenite, zircon, and rutile that were probably concentrated by placer-forming processes, as on beaches. Rarely, unusual rock fragments such as serpentinite fragments may make up a substantial fraction of the framework grains. Sand-size fragments of intrabasinal precipitates such as carbonate grains (ooids, pellets, intraclasts, fossils) can be abundant in some sandstones. Sandstones enriched in carbonate grains are called **calcareneous sandstones**. **Greensands**, sandstones containing significant amounts of glauconite, are moderately common in the geologic record, especially along unconformity surfaces. **Phosphatic sandstones** containing appreciable amounts of phosphatic skeletal fragments (Chapter 12), ooids, etc. occur also but are much less common.

Further reading

- Adams, A. E., W. S. Mackenzie, and C. Guilford, 1984, *Atlas of Sedimentary Rocks Under the Microscope*: John Wiley and Sons, New York, NY.
- Cas, R. A. F. and J. V. Wright, 1987, *Volcanic Successions: Modern and Ancient*: Allen and Unwin, London.
- Leyrit, H. and C. Montenat (eds.), 2000, *Volcaniclastic Rocks, From Magmas to Sediments*: Gordon and Breach Science Publishers, Amsterdam.
- Lindholm, R. C., 1987, *A Practical Approach to Sedimentology*: Allen and Unwin, London.
- Mackenzie, W. S. and C. Guilford, 1980, *Atlas of Rock-Forming Minerals in Thin Section*: John Wiley and Sons, New York, NY.
- Mange, M. A. and D. T. Wright (eds.), 2007, *Heavy Minerals in Use: Developments in Sedimentology* 58.
- Pettijohn, F. J., P. E. Potter, and R. Siever, 1987, *Sand and Sandstone*, 2nd edn., Springer-Verlag, New York, NY.
- Scholle, P. A., 1979, *A Color Illustrated Guide to Constituents, Textures, Cements, and Porosities of Sandstones and Associated Rocks*: AAPG Memoir 28.

5

Conglomerates

5.1 Introduction

Siliciclastic sedimentary rocks that consist predominantly of gravel-size (> 2 mm) clasts are called conglomerates. The Latin-derived term **rudite** is also sometimes used for these rocks. Conglomerates are common rocks in stratigraphic sequences of all ages, but make up less than about one percent by weight of the total sedimentary rock mass (Garrels and McKenzie, 1971, p. 40). Geologists have focused a level of attention on conglomerates, judged by the number of published papers, quite out of proportion to their relative abundance. This focus stems from their usefulness in tectonic and provenance analysis (Chapter 7) and the growing interest of sedimentologists in the rather specialized depositional environments of conglomerates. Also, some conglomerates serve as reservoir rocks for oil and gas.

The framework grains of conglomerates are composed mainly of rock fragments (clasts) rather than individual mineral grains. These clasts may consist of any kind of rock. Some conglomerates are composed almost entirely of highly durable clasts of quartzite, chert, or vein quartz. Others are composed of a variety of clasts, some of which, limestone and shale clasts for example, may be unstable or weakly durable. Conglomerates may contain various amounts of matrix, which commonly consists of clay- or sand-size particles or a mixture of clay and sand.

Owing to their coarse grain size, conglomerates do not lend themselves readily to study in the laboratory. They are studied primarily in the field, by a variety of techniques. Clast counts, which consist of identifying several hundred randomly chosen clasts from a given outcrop, are used to determine clast composition. Size and sorting of clasts can be determined by measuring the dimensions of individual pebbles with a caliper. Some shape parameters such as sphericity can be derived also from these size measurements. Roundness is commonly determined by visual estimates. Conglomerate beds exposed in three-dimensional outcrops can be studied to determine aspects of fabric such as fabric support (clast-supported versus matrix-supported), the long-axis orientation of clasts, and the imbrication dips of clasts. All of these textural elements are useful in environmental interpretation.

In this chapter, we examine the composition, textures, and structures of conglomerates. Further, we see how some of these properties can be used as a basis for conglomerate classification and as tools for environmental analysis. Finally, some generalized depositional models for conglomerates are presented and discussed.

5.2 Definition of conglomerates

In contrast to sandstones, conglomerates contain a substantial fraction of gravel-size (>2 mm) particles. The percentage of gravel-size particles required to distinguish a conglomerate from a sandstone or mudstone (shale) is arguable. Folk (1974, p. 28) sets the boundary between gravel and gravelly mud or gravelly sand at 30 percent gravel. That is, he considers a deposit with as little as 30 percent gravel-size fragments to be a gravel. On the other hand, Gilbert (Williams *et al.*, 1982, p. 330) indicates that a sedimentary rock must contain more than 50 percent gravel-size fragments to be called a conglomerate. Siliciclastic sedimentary rocks that contain fewer than 50 percent gravel-size clasts (possibly fewer than 30 percent according to Folk's usage) are conglomeratic sandstones or conglomeratic mudstones. Some geologists use the terms pebbly sandstone or pebbly mudstone to describe such sandstones or mudstones, although Gilbert reserves these terms for rocks with less than about 25 percent gravel-size clasts. Crowell (1957) suggested the term **pebbly mudstone** for any poorly sorted sedimentary rock composed of dispersed pebbles in an abundant mudstone matrix. The term "pebbly" is not an appropriate adjective for all such rocks with sparse clasts, however, because many of these rocks contain larger clasts (cobbles or boulders). Because of this somewhat confusing terminology for conglomeratic rocks that contain considerable mud or sand matrix, Flint *et al.* (1960) proposed the term **diamictite** for nonsorted to poorly sorted, siliciclastic sedimentary rocks that contain larger particles of any size in a muddy matrix

Thus, there are two kinds of rudites: (1) conglomerates with low to moderate amounts of matrix, and (2) conglomerates with abundant matrix (diamictites). Although the term diamictite is often applied to poorly sorted glacial deposits, it may be used for any sedimentary rock having the characteristics described. Flint (1971, p. 154) indicates that the term diamictite can be used "for nonsorted terrigenous sediments and rocks containing a wide range of particle sizes, regardless of genesis."

Unfortunately, we don't know exactly what "abundant matrix" means when applied to diamictites. Flint *et al.* (1960) did not specify the minimum amount of matrix that characterizes a diamictite. Rather than characterizing conglomerates on the basis of matrix content alone, perhaps a better approach is to make distinction on the basis of fabric support. If mud or sand matrix is so abundant that the clasts in a rudite or gravelly sediment do not form a supporting framework, the fabric is commonly referred to as **matrix-supported** (Fig. 5.1). Rudites or gravelly sediments that contain so little matrix that the gravel-size framework grains touch and thus form a supporting framework are called **clast-supported** (Fig. 5.2). (To avoid unnecessary confusion regarding diamictites, throughout the remainder of this chapter all rudites will be called conglomerates, which can be either clast-supported or matrix-supported.)

Because fabric support depends upon clast shape as well as upon the relative abundance of framework clasts and matrix, there is no fixed percentage of matrix that characterizes a clast-supported fabric versus a matrix-supported fabric. To determine the kind of fabric support in a gravel deposit or in a consolidated rock, one must commonly examine the deposit in



Figure 5.1 Matrix-supported fabric in conglomerates of the Bushnell Rock Member of the Lookingglass Formation (Eocene), southern Oregon Coast Range. Note that the large clasts appear to “float” in the mud–sand matrix.



Figure 5.2 Clast-supported fabric in terrace gravels of the Umpqua River, southwest Oregon. Clasts are in contact and thus form a supporting framework. Hammer head for scale.

a three-dimensional outcrop. Clasts that do not appear to touch in a two-dimensional outcrop may actually touch in three dimensions. Furthermore, clast-supported fabrics may grade to matrix-supported fabrics within the same depositional unit. Careful, detailed field examination of three-dimensional outcrops of gravel deposits or ancient conglomerates and diamictites is the only way to determine fabric support.

The gravel-size material in conglomerates consists mainly of rounded to subrounded rock fragments (clasts). By contrast, **breccias** are aggregates of angular, gravel-size fragments.

Table 5.1 *Fundamental genetic types of conglomerates and breccias*

Major types	Subtypes	Origin of clasts
Epiclastic conglomerate and breccia	Extraformational conglomerate and breccia	Breakdown of older rocks of any kind through the processes of weathering and erosion; deposition by fluid flows (water, ice) and sediment gravity flows
	Intraformational conglomerate and breccia	Penecontemporaneous fragmentation of weakly consolidated sedimentary beds; deposition by fluid flows and sediment gravity flows
Volcanic breccia	Pyroclastic breccia	Explosive volcanic eruptions, either magmatic or phreatic (steam) eruptions; deposited by airfalls or pyroclastic flows
	Autobreccia	Breakup of viscous, partially congealed lava owing to continued movement of the lava
	Hyaloclastic breccia	Shattering of hot, coherent magma into glassy fragments owing to contact with water, snow, or water-saturated sediment (quench fragmentation)
Cataclastic breccia	Landslide and slump breccia	Breakup of rock owing to tensile stresses and impact during sliding and slumping of rock masses
	Tectonic breccia: fault, fold, crush breccia	Breakage of brittle rock as a result of crustal movements
	Collapse breccia	Breakage of brittle rock owing to collapse into an opening created by solution or other processes
Solution breccia		Insoluble fragments that remain after solution of more soluble material; e.g. chert clasts concentrated by solution of limestone
Meteorite-impact breccia		Shattering of rock owing to meteorite impact

Source: Modified from Pettijohn, 1975, p. 165.

The particles in breccias are distinguished from those in conglomerates by their sharp edges and unworn corners, although no specified roundness limit for breccias is in common use. Many breccias, such as volcanic and tectonic breccias, are nonsedimentary in origin. Table 5.1 lists the major kinds of conglomerates and breccias, classified on the basis of origin.

The most common kinds of rudites are **extraformational, epiclastic conglomerates and breccias**. These rocks are called extraformational because they are composed of clasts that originated outside the formation itself. They are called **epiclastic** because they are generated by breakdown of older rocks through the processes of weathering and erosion. Thus, they are formed by the same kinds of processes that create epiclastic sandstones.

Intraformational conglomerates and breccias are deposits that formed by penecontemporaneous fragmentation of weakly consolidated beds and subsequent redeposition of the

resulting fragments within the same general depositional unit. Sedimentary processes, such as storm waves or mass flows, that bring about fragmentation and redeposition of clasts to create intraformational conglomerates and breccias are probably very short-term events, possibly requiring only a few hours or days. These intraformational deposits commonly occur as thin units that are generally localized in extent. The fragments in these deposits may be well rounded or angular depending upon the amount of transport and reworking. Very commonly, they are flat or disc-shaped, giving rise to the term **flat-pebble conglomerate**. Flat-pebble conglomerates characterized by flattened pebbles stacked virtually on edge, owing to strong current activity, are called **edgewise conglomerates**. The most common intraformational conglomerates and breccias are those formed of (1) limestone or dolomite clasts in a limestone or sandy limestone matrix and (2) shale (mudstone) clasts in a sandy matrix (Pettijohn, 1975, p. 184). In this book, epiclastic sedimentary breccias are considered to be a kind of angular conglomerate and are not further differentiated from conglomerates.

Many breccias are generated by nonsedimentary processes such as volcanism. **Volcanic breccias** are formed by primary volcanic processes that may include explosive volcanism, autobrecciation of partially congealed lavas, or quench fragmentation of hot magmas that come into contact with water, snow, or water-saturated sediment. (Note: Volcanic conglomerates made up of clasts formed by weathering and erosion of older volcanic rocks are epiclastic conglomerates.) Less-common breccias are those that form through the processes of cataclasis or collapse (**cataclastic breccias**) and solution of soluble rocks such as limestone or salt, leaving insoluble gravel-size residues (**solution breccias**). **Meteorite-impact breccias** are even less common.

Although nonsedimentary breccias and intraformational conglomerates are interesting, our concern in this chapter is primarily with the more common and abundant extraformational, epiclastic conglomerates. Therefore, most of the remaining part of this chapter deals with these conglomerates. A very short discussion of volcanic breccias and agglomerates is included near the end of the chapter. Readers who wish a more extended discussion of breccias may wish to consult Laznicka (1988).

5.3 **Composition of epiclastic conglomerates**

5.3.1 *Composition of framework clasts*

Gravel-size particles are the framework grains of conglomerates. Conglomerates may contain gravel-size pieces of individual minerals such as vein quartz; however, the framework fraction of most conglomerates consists of rock fragments (clasts). Virtually any kind of igneous, metamorphic, or sedimentary clast may be present in a conglomerate, depending upon source rocks and depositional conditions. Some conglomerates are made up of only the most stable and durable types of clasts, that is, quartzite, chert, or vein-quartz clasts. The term **oligmict conglomerate** is often applied to stable conglomerates composed mainly of a single clast type, as opposed to **polymict conglomerates**, which contain an assortment of clasts. Polymict conglomerates made up of a mixture of largely unstable or

metastable clasts such as basalt, limestone, shale, and phyllite are commonly called **petromict conglomerates**.

Some conglomerates that are enriched in quartzose clasts may be first-cycle deposits (i.e., not recycled from an older generation of conglomerates) that formed by erosion of a quartzite, quartz arenite, or chert-nodule limestone source. Others were probably derived from mixed parent-rock sources that included less-stable rock types. Continued recycling of mixed ultrastable and unstable clasts through several generations of conglomerates leads ultimately to selective destruction of the less-stable clasts and concentration of stable, quartzose clasts. Petromict conglomerates, and oligomict conglomerates made up of weakly durable clasts such as limestone and basalt, are more likely than conglomerates enriched in quartzose clasts to be first-cycle deposits. The clast composition of first-cycle conglomerates depends upon both the composition of the source rocks and the nature and intensity of the transport and depositional processes. These processes may destroy some very weakly durable clasts even in a single depositional cycle.

In addition to these factors, the clast composition of conglomerate deposits may be a function also of sorting by clast size. As a result of weathering, some parent rocks typically yield large clasts, whereas others break down to yield smaller fragments. For example, metaquartzites and dense, volcanic-flow rocks such as rhyolite tend to yield large fragments whose sizes are determined by the thickness of bedding and spacing of joints, whereas shales and argillites yield clasts in the finer pebble sizes owing to their fissile nature and closely spaced joint patterns in outcrop (Blatt, 1982, p. 144). Furthermore, less-durable fragments such as shale clasts tend to break into still finer-sized clasts during transport, whereas metaquartzite and rhyolite are more durable. Thus, the clasts of a given size in a conglomerate may be biased toward a particular rock type. Meaningful comparison of conglomerate composition from one unit to another requires that comparison be made between units of comparable clast size.

Other than the distinction made here between oligomict and petromict conglomerates, few generalities can be stated about clast composition. Almost any combination of clast types is possible in conglomerates, as shown in [Table 5.2](#). Note from this table that conglomerates may be made up of various mixtures of igneous, sedimentary, and metamorphic clasts, or they may be composed dominantly of a single clast type. For example, some conglomerates are composed dominantly of volcanic clasts, others of metamorphic quartzite clasts, and still others of sedimentary chert, limestone, or dolomite clasts. For additional examples of conglomerate compositions see Seiders and Blome (1988).

5.3.2 Composition of matrix and cements

The matrix of conglomerates is composed mainly of clay- and sand-size particles. In contrast to the upper size limit of about 30 microns set for the matrix in sandstones, no grain-size limit has been established for the matrix of conglomerates. Conglomerate matrix is simply the finer material that fills the interstitial spaces among gravel-size clasts. Any kind of mineral or small rock fragment, including glassy fragments, can be present as matrix. Thus,

Table 5.2 *Clast composition of some North American conglomerates*

Clast type	Range of values (%)	Average value (%)
Quartzite	<1–95	21
Chert	<1–95	17
Vein quartz	<1–20	2
Basalt/Andesite	<1–90	17
Rhyolite/Dacite	<1–75	10
Granite/Diorite	<1–15	5
Metavolcanics	<1–55	7
Metasediments (undifferentiated)	<1–10	2
Schists/Argillite	<1–30	4
Sandstone/Siltstone	<1–50	15
Shale	<1–48	4
Conglomerate	<1–6	1
Limestone/Dolomite	<1–90	13
Other	<1–10	2

Based on data from 17 localities, mostly in western USA (See Boggs, 1992, p. 216 for sources)

the matrix may consist of various kinds of clay minerals and fine micas and/or silt- or sand-size quartz, feldspars, rock fragments, heavy minerals, and so on. The matrix itself may be cemented with quartz, calcite, hematite, clay, or other cements. Together, these cements and matrix materials bind the framework grains of the conglomerates.

5.4 Texture

5.4.1 *Matrix content and fabric support*

High-energy processes, such as fluvial and beach processes, that transport and deposit gravels may remove most fine-size detritus and deposit gravels with little sand or mud matrix. On the other hand, gravels transported by glaciers and sediment-gravity-flow processes such as debris flows may contain abundant matrix. In fact, many gravel deposits that originate by these processes may contain more muddy matrix than framework clasts. Thus, as mentioned, some gravel fabrics are matrix-supported.

Conglomerates that contain essentially no matrix (voids among pebbles unfilled) are called **openwork** conglomerates (Pettijohn, 1975, p. 157). Openwork conglomerates are uncommon, in contrast to many sandstones that are deposited with open pores. That is, the pores of many sandstones are filled at the time of deposition only by fluids and not by matrix. Thus, in contrast to sandstones, conglomerates tend to have two size modes, one in the gravel-size range (the framework grains) and one in the sand- to mud-size range (the matrix grains).

5.4.2 Clast shape and orientation

The shape and orientation of sedimentary particles are discussed in detail in [Chapter 2](#). The discussion in [Chapter 2](#) applies to the particles in conglomerates as well as those in sandstones; however, the shapes and orientations of particles in conglomerates may differ in some respects from those of associated sandstones. For example, gravel-size particles can become moderately rounded with comparatively short distances of stream transport, whereas sand-size particles undergo very little rounding. Therefore, clasts in a fluvial conglomerate may be well rounded, whereas grains in associated sandstones may be subangular to angular (Pettijohn, 1975, p. 163). The form (sphericity) of conglomerate clasts tends to be related to the shapes of the initial rock fragments released from the parent rocks. Parent rocks with a schistose or fissile fabric are likely to release tabular or disc-shaped fragments, whereas more-massive rocks such as metaquartzite tend to release more-equant-shaped clasts. Clast shape may, of course, be subsequently modified to some extent during transport owing to abrasion and clast breakage.

Because many conglomerate clasts do have an elongated or tabular shape, these clasts may assume a preferred orientation during transport and deposition. For example, elongated, gravel-size clasts tend to become oriented transverse to current flow ([Fig. 2.21D](#)) during stream transport, whereas sand-size grains are more likely to become oriented parallel to current flow. Tabular and elongated clasts also tend to develop an imbricated or shingled fabric under strong unidirectional currents ([Fig. 2.21E](#); see also [Fig. 5.7](#)). For more details on particle orientation, see [Section 2.3.8](#).

5.5 Sedimentary structures in conglomerates

Many of the sedimentary structures described in [Chapter 3](#) do not occur in conglomerates, which tend to have restricted suites of structures. Many conglomerates are massive (structureless); however, crude to well-developed planar horizontal or inclined stratification is moderately common. Tabular and trough cross-bedding is also present in some conglomerates, such as fluvial conglomerates; however, cross-bedding is much less common in conglomerates than in sandstones. Conglomerates may be nongraded, or they may display normal, inverse, or normal-to-inverse size grading. Other structures include gravel-filled scours and channels, and gravel lenses. Conglomerates may be associated with sandstones that display a much greater variety of sedimentary structures.

5.6 Descriptive classification of conglomerates

5.6.1 General statement

In spite of the strong interest that geologists have in coarse-grained sedimentary rocks, we lack an adequate system for formally classifying conglomerates. Instead of formal names for conglomerates, geologists commonly use a variety of informal names. Some of these names are based on composition of the clasts (e.g. quartzite conglomerates), others on grain size

(e.g. pebble conglomerates), and still others on presumed depositional environment or depositional process (e.g. fluvial conglomerates, debris-flow conglomerates). Pettijohn's (1975) classification is probably the best known of the few published conglomerate classifications, but it appears to be little used.

The paucity of formal conglomerate classifications stands in sharp contrast to the more than 50 classifications for sandstones that have been proposed (Friedman and Sanders, 1978, p. 190). Although sandstones may be overclassified, there appears to be a need for an adequate conglomerate classification. One reason that few conglomerate classifications have been proposed may be because conglomerates are not as easily classified as sandstones. For example, the many kinds of framework clasts that can be present in conglomerates make it difficult to reduce clast lithologies to three principal kinds. Thus, in contrast to classification of sandstones, it is not easy to plot the clast composition of conglomerates on a ternary classification diagram.

5.6.2 Classification by relative clast stability

One way to deal with the composition of conglomerates for the purpose of classification is to place clasts into two groups on the basis of relative clast stability: (1) **ultrastable clasts** (quartzite, chert, vein quartz), and (2) **metastable and unstable clasts** (all other clasts). Thus, on the basis of clast stability, we recognize two kinds of conglomerates. Conglomerates made up of framework grains that consist dominantly of ultrastable clasts (>~90 percent) are **quartzose conglomerates**. Conglomerates that contain fewer ultrastable clasts are **petromict conglomerates**. As indicated in Section 5.3.1, the term petromict conglomerate is in common use for conglomerates containing abundant unstable or metastable clasts.

The compositional boundary between quartzose and petromict conglomerates is commonly placed at 90 percent stable clasts. This 90 percent boundary is arbitrary; however, it does agree with the boundary between stable grains and unstable grains set in some sandstone classifications. Also, it coincides with the boundary suggested by Pettijohn (1975, p. 165) in his conglomerate classification.

Classifying conglomerates on the basis of clast stability has some important genetic significance. For example, some quartzose conglomerates probably originate as a result of intense chemical weathering of source rocks such as chert-nodule limestones. Others form as a result of prolonged transport or multiple recycling of clasts, processes that mechanically eliminate less-durable clasts. By contrast, petromict conglomerates are more likely to be first-cycle deposits that originate under less-intensive weathering conditions or that undergo less-prolonged transport and abrasion. Thus, the proposed stability classification has important interpretative value.

5.6.3 Classification by clast lithology

Although classification of conglomerates on the basis of clast stability is useful, as discussed, it reveals little about the actual clast lithology of conglomerates. Because conglomerates can contain a wide variety of clast types (Table 5.2), it is often desirable in the study of

Conglomerates

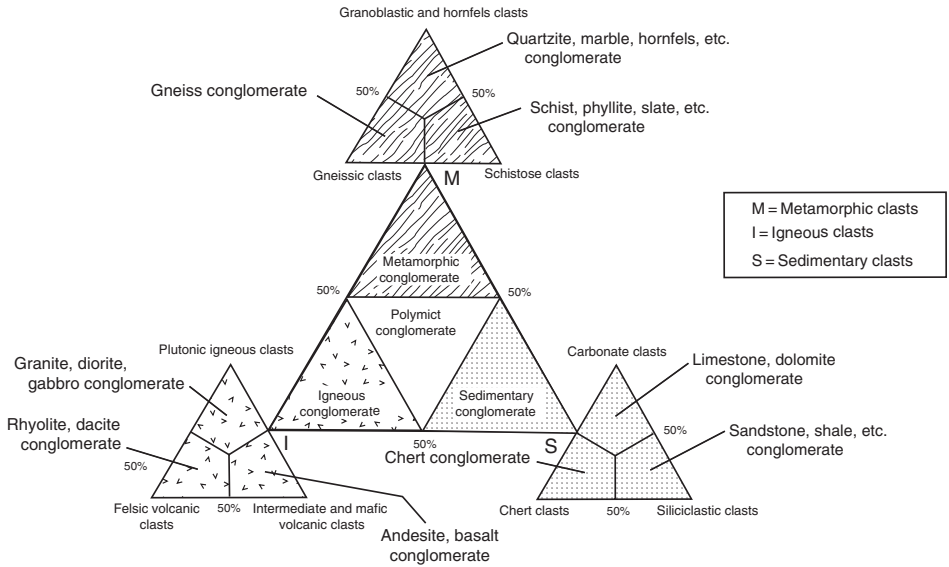


Figure 5.3 Classification of conglomerates on the basis of clast lithology. Note that conglomerates can be either clast-supported or matrix-supported.

conglomerates to focus on clast composition rather than on clast stability, particularly in source-rock studies.

For classification purposes, conglomerate clasts can be grouped into three fundamental kinds: igneous, metamorphic, and sedimentary. Admittedly, some subjectivity may be involved in assigning clasts to these genetic groups; however, clast identification is commonly rather easy. The relative abundance of the different kinds of clasts (e.g. basalt, schist, sandstone) in a conglomerate is established in the field by clast counts. Once composition has been determined, clasts are grouped by genetic type (igneous, metamorphic, sedimentary) as end members of a classification triangle. Thus, all clasts, including ultrastable clasts, are normalized in terms of these three fundamental end members.

Figure 5.3 shows how conglomerates can be classified on the basis of these end-member clast types. The classification triangle in Fig. 5.3 is divided into four fields to yield four kinds of conglomerates: **metamorphic (clast) conglomerates**, **igneous (clast) conglomerates**, **sedimentary (clast) conglomerates**, and **polymict conglomerates**. The term polymict can be applied informally to all conglomerates containing clasts of mixed lithology; however, it is used in a formal sense in this classification to denote conglomerates made up of roughly subequal amounts of metamorphic, igneous, and sedimentary clasts. Although this classification is largely descriptive, these conglomerate names obviously have some provenance significance because the terms identify major genetic categories of source rocks from which conglomerates are derived.

To arrive at the actual name of a conglomerate on the basis of dominant clast lithology requires that daughter triangles be erected on the basic classification diagram, as shown in

Fig. 5.3. For conglomerates that fall into the metamorphic, igneous, or sedimentary fields, the clasts are renormalized in the daughter triangle to 100 percent metamorphic, igneous, or sedimentary clasts, as appropriate. Clast composition is then plotted on the corresponding daughter triangle. Thus, sedimentary conglomerates, for example, could be classified as limestone or dolomite conglomerates, sandstone conglomerates, chert conglomerates, and so on, depending upon the relative percentages of various kinds of sedimentary clasts. Metamorphic conglomerates include schist conglomerates, gneiss conglomerates, quartzite conglomerates, and so on. Igneous conglomerates include granite conglomerates, basalt conglomerates, and so on. Informal names such as limestone conglomerate have been in use for years. This recommended classification simply formalizes the classification procedure and places some definite compositional limits on each kind of conglomerate on the basis of clast types. Note that polymict conglomerates, which contain roughly equal amounts of metamorphic, igneous, and sedimentary clasts, are not further classified by specific lithologic types.

In verbal descriptions of conglomerates, the stability class name can be combined, if desired, with the appropriate lithologic name (derived from the classification diagram) to provide additional clarification of the composition. Thus, for example, a chert conglomerate might be called a quartzose chert conglomerate if it contains more than 90 percent stable clasts, or a petromict chert conglomerate if it contains fewer than 90 percent stable clasts and chert is the dominant clast type.

5.6.4 Classification by clast size

Finally, terms for the relative sizes of clasts in a conglomerate can be used as adjectives that are added to appropriate compositional terms, if desired. Thus, we could have a cobble-rich quartzose conglomerate, a boulder-rich petromict conglomerate, and so on.

5.7 Occurrence of quartzose and petromict conglomerates

5.7.1 General statement

Conglomerates occur in sedimentary successions of all ages from Precambrian to Holocene and on all continents of the world. The clasts that make up conglomerates are derived from many kinds of igneous, metamorphic, and sedimentary source rocks. These clasts can be transported and deposited by a variety of fluid-flow and sediment-gravity-flow processes. Space does not permit detailed discussion of conglomerate occurrence; however, a brief discussion of quartzose and petromict conglomerates and some generalities about their sources are given below.

5.7.2 Quartzose conglomerates

Quartzose conglomerates, which consist dominantly of metaquartzite, vein-quartz, or chert clasts, are derived from metasedimentary, sedimentary, and some igneous rocks. As

suggested by Pettijohn (1975, p. 166), these clasts are a residuum concentrated by destruction of a much larger volume of rock. Quartzite clasts are derived from metasedimentary sequences containing quartzite beds. Less-stable metasedimentary clasts such as argillite, slate, and schist, originally present in such metasedimentary sequences, must have been destroyed by weathering, erosion, and sediment transport. Quartz-filled veins occur broadly scattered through mainly igneous and metamorphic rocks. Concentrations of vein-quartz clasts in quartzose conglomerates implies destruction of large bodies of such primary igneous or metamorphic rock. Likewise, the concentration of chert clasts in a conglomerate implies destruction of large volumes of chert-nodule limestone to yield a chert-clast concentrate. Some chert clasts may, of course, be derived also by erosion of bedded chert deposits.

Such wholesale destruction of rock masses to yield relatively small concentrates of quartzose clasts implies either extremely intensive chemical weathering or vigorous transport that mechanically destroyed less durable clasts. More than one cycle of weathering and transport could be involved. The source rocks that yield quartzose clasts are most likely to occur in recycled orogen or continental block provenances ([Chapter 1](#)). Because quartzose clasts represent only a small fraction of a much larger original body of rock, the total volume of quartzose conglomerates is commonly small. They tend to occur as scattered pebbles, thin, pebbly layers, or lenses of pebbles in dominantly sandstone units (Pettijohn, 1975, p. 166). They appear to be largely of fluvial, particularly braided-stream, origin, but marine, wave-worked quartzose conglomerates also exist.

Examples of quartzose conglomerates are known from throughout the world in sedimentary units ranging in age from Precambrian to Tertiary. Precambrian examples include the jasper-bearing Lorrain quartzites (Huronian) of Ontario, and Paleozoic examples include parts of the Silurian Tuscarora Quartzite and the Devonian Chemung and Mississippian Pocono formations of the US central Appalachians. Mesozoic and Tertiary examples include quartzose conglomerates in the Cretaceous Hornbrook Formation and Mississippian Bragdon Formation of the northern Klamath Mountains of northern California, the Tertiary Brandywine upland gravels of Maryland, and the Lafayette upland gravels of western Kentucky. Many quartzose conglomerates also occur in Tertiary successions in the US Rocky Mountains (e.g. Kraus, 1984). Some stratigraphic characteristics of these conglomerates are illustrated in [Fig. 5.4](#). Additional examples are discussed by Pettijohn (1975, p. 166). This tabulation of examples is by no means comprehensive.

5.7.3 Petromict conglomerates

As discussed, petromict conglomerates contain significant amounts of metastable rock fragments. Most are polymictic conglomerates, made up of a variety of metastable clasts. They may be derived from many different types of plutonic igneous, volcanic, metamorphic, or sedimentary rock. As shown in [Table 5.2](#), the clasts in a given conglomerate unit may be dominantly volcanic, dominantly metamorphic, or dominantly sedimentary, depending upon the source-rock lithology. Conglomerates composed dominantly of plutonic igneous

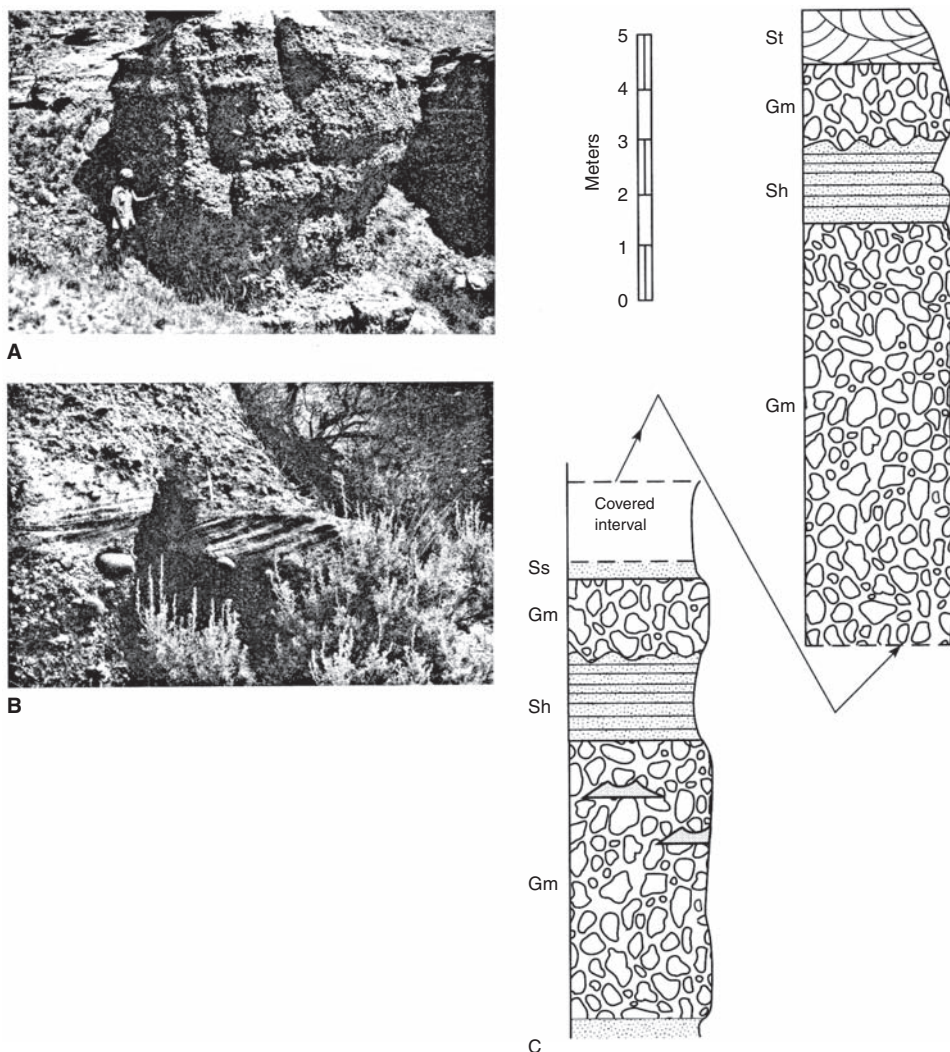


Figure 5.4 Massive or horizontally stratified conglomerate facies assemblage in Tertiary quartzite conglomerates of Wyoming. A. Crude horizontal stratification in gravel facies. B. Large-scale planar cross-stratification as a lens in the gravel facies. C. Stratigraphic section of part of the gravel facies assemblage; St= cross-stratified sandstone, Gm= massive or crudely stratified gravel, Sh= horizontally laminated sandstone, Ss= sandstone with broad, shallow scours. (From Kraus, M.J., 1984, *Sedimentology and tectonic setting of early Tertiary quartzitic conglomerate, northwest Wyoming*, in Koster, E.H. and R.J. Steele, (eds.), *Sedimentology of Gravels and Conglomerates*: Canadian Society of Petroleum Geologists Memoir 10, Fig. 8, p. 210, reprinted by permission.)

clasts appear to be uncommon, probably because plutonic rocks such as granites tend to disintegrate into sand-size fragments rather than forming larger blocks. Among petromict conglomerates containing significant amounts of sedimentary clasts, clasts of siliciclastic sedimentary rock are generally more common than clasts of carbonate rocks. On the other hand, some conglomerates are composed mainly of carbonate clasts (Table 5.2). Owing to their lesser stability compared to quartzose clasts, the clasts of petromict conglomerates are more likely than quartzose clasts to be of first-cycle origin. Nonetheless, the fact that some petromict conglomerates contain clasts of a previous generation of petromict conglomerates shows that some metastable clasts can survive recycling.

The volume of ancient petromict conglomerates is far greater than that of quartzose conglomerates. The petromict conglomerates form the truly great conglomerate bodies of the geologic record, and they may reach thicknesses of thousands of meters. Some conglomerates composed mainly of volcanic clasts form especially thick sequences. The preservation and accumulation of such thick sequences of metastable clasts, particularly clasts of highly soluble limestone or dolomite, imply rapid erosion of sharply elevated highlands (or areas of active volcanism in the case of volcanic conglomerates). Alternatively, some petromict conglomerates, such as some limestone conglomerates, may have accumulated at lower elevations but under very cold conditions where glacial activity provided the erosion mechanism. In any case, the metastable clasts of petromict conglomerates must have been stripped from source areas before chemical weathering processes could bring about solution or promote disintegration to sand-size particles. Furthermore, they must have been transported only short distances from the source, or they were transported by processes that did not mechanically destroy the clasts. Petromict conglomerates can accumulate in any tectonic provenance (continental block, recycled orogen, or magmatic arc) where the requisite conditions that allow their preservation are met. They are deposited in environments ranging from fluvial through shallow-marine to deep-marine, although the bulk of the truly thick petromict conglomerate bodies are probably nonmarine.

Examples of petromict conglomerates in the geologic record are so numerous and so varied that a listing of occurrences is essentially pointless. Examples could be cited from sedimentary sequences of all ages and from all continents of the world. See, for example, Seiders and Blome (1988). Space does not permit extended discussion of specific examples, but one example of a mixed-clast conglomerate in the Miocene Kotanbetsu Formation of Hokkaido, Japan is shown in Fig. 5.5.

5.8 Conglomerate properties and depositional environments

Descriptive classification of conglomerates (Fig. 5.3) is useful as a means of identifying the compositional differences among conglomerates and in relating clast composition to sediment sources (provenance). On the other hand, many conglomerate workers focus on study of depositional environments and are thus interested in the properties of conglomerates that relate to depositional origin. They are commonly more concerned with the textural and structural properties of conglomerates than with clast composition. Instead of

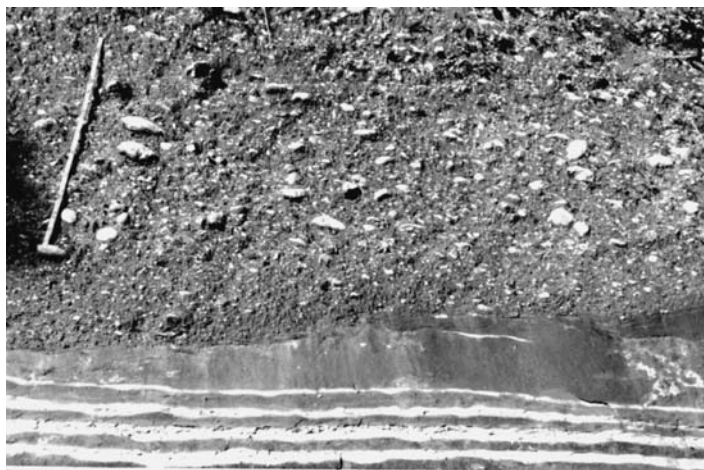


Figure 5.5 Polymict conglomerates of the Miocene Kotanbetsu Formation of Hokkaido, Japan. This facies displays inverse-to-normal grading and overlies finer-grained turbidite units. The vertical scale is 100 cm long. (From Okada, H. and S. K. Tandon, 1984, Resedimented conglomerates in a Miocene collision suture, Hokkaido, Japan, in Koster, E. H. and R. J. Steele, (eds.), *Sedimentology of Gravels and Conglomerates*: Canadian Society of Petroleum Geologists Memoir 10, Fig. 9, p. 419, reprinted by permission. Photograph courtesy of H. Okada.)

discussing and classifying conglomerates on the basis of clast lithology, they are more likely to classify them on the basis of presumed depositional origin. Thus, they may refer to a particular conglomerate as a wave-worked conglomerate, a resedimented conglomerate, and so on.

The textural and structural characteristics of conglomerates are generated owing to deposition under a particular set of environmental conditions. Thus, a goal of many conglomerate studies is to identify the paleoenvironments of conglomerates on the basis of these characteristic properties. Gravels are deposited in modern environments ranging from fluvial to deep-marine by a variety of fluid-flow, ice-flow and rafting, and sediment-gravity-flow processes. We assume that ancient conglomerates were deposited in similar environments and that the characteristics of ancient conglomerates and modern gravels deposited in similar environments are also similar. The scope of this book does not allow detailed discussion of depositional environments. Readers who wish more background knowledge of depositional environments may turn to a variety of sources; see, for example, Boggs (2006, ch. 8–11) and references therein.

Each environment in which conglomerate is deposited is characterized by a particular set of depositional processes, which produces conglomerates with distinctive textures and sedimentary structures that reflect depositional setting and depositional process. This relationship is summarized in [Table 5.3](#). Conglomerates in this table are grouped according to presumed depositional processes and the probable environment in which these processes operated.

Table 5.3 *Major transport/depositional processes and depositional environments of conglomerates*

Transport mechanism	Type of flow or depositional process	Suggested conglomerate name based on process	Depositional environment	Environmental name
	Sheetflood flow in shallow braided channels	Sheetflood conglomerate	Alluvial fans, proglacial outwash fans, subglacial zones, fan deltas	Braided-stream conglomerate
	Channelized flow in deeper fluvial channels	Streamflow conglomerate	Entrenched channels in alluvial and outwash fans, subglacial channels, channels of nonfan streams, subaerial delta/fan-delta distributaries	Alluvial-fan conglomerate, fluvial channel conglomerate, deltaic conglomerate, fan-delta conglomerate, glaciofluvial conglomerate
Fluid (water) flow	Wave upwash and backwash	Wave-worked conglomerate	Marine beachface, possibly lacustrine beachface	Beachface conglomerate
	Shoreward movement of wave bore; flow of longshore and rip currents, storm surges	Wave-, storm-, and current-worked conglomerate	Marine shoreface, possibly lacustrine shoreface	Shoreface conglomerate, shelf conglomerate
	Tidal-current flow, largely in channels	Tide-worked conglomerate	Marine nearshore environments, especially in tidal channels	Tidal conglomerate

Ice flow	Subaerial ice melt and glacial overriding Subaqueous ice meltout, meltwater (traction) underflow, ice rafting	Meltout/lodgment conglomerate Subaqueous meltout conglomerate	Meltout zones of grounded glaciers Proglacial lakes, proglacial marine environments, including deltaic environments	Glacial conglomerate Glaciomarine conglomerate, glaciolacustrine conglomerate
Sediment gravity flow	Subaerial debris flow Subaqueous debris flow Density-modified grain flow High-density turbidity-current flow	Subaerial debris-flow conglomerate Subaqueous debris-flow conglomerate Subaqueous grain-flow conglomerate Turbidite conglomerate	Alluvial fans, proglacial outwash fans, glacier margins Subaqueous outwash plains, marine and lacustrine deltas and fan deltas, submarine channels and fans	Alluvial-fan conglomerate, proglacial conglomerate, Deltaic conglomerate, fan-delta conglomerate, submarine-fan conglomerate

Resedimented conglomerate



Figure 5.6 Poorly graded, massive to crudely stratified sheetflood conglomerate, Port Orford Formation (Early Pleistocene), southern Oregon coast.

Table 5.3 divides conglomerates into nine fundamental types: sheetflood (braided-stream) conglomerate, streamflow conglomerate, wave-worked conglomerate, wave-, storm-, and current-worked conglomerate, tide-worked conglomerate, meltout/lodgment conglomerate, subaqueous meltout conglomerate, subaerial debris-flow conglomerate, and resedimented conglomerate. Resedimented conglomerates are further divided into subaqueous debris-flow conglomerates, subaqueous grain-flow conglomerates, and turbidite conglomerates. The distinguishing characteristics of each of the conglomerate types listed in **Table 5.3** are discussed briefly below.

Sheetflood (braided-stream) conglomerates are deposited in shallow, braided streams where stream-energy is commonly high and discharge may be episodic. (See Smith *et al.*, 2006, for extended coverage of braided rivers.) Deposits are dominantly clast-supported, with a matrix of silt or sand. Individual beds are generally nongraded, but vertical facies sequences typically display a fining-upward trend. Stratification in sheetflood conglomerates is common, ranging from crudely developed to well developed, and may be either planar or cross-bedded. Clasts commonly display upstream-dipping imbrication and transverse long-axis orientation. **Figure 5.6** is an example of a crudely planar stratified sheetflood conglomerate.

Streamflow conglomerates are deposited by channelized flow in deeper fluvial channels. They are also typically clast supported, and silt/sand matrix may range from rare to abundant. They display unimodal clast orientation with dominant upstream imbrication dips



Figure 5.7 Well-imbricated, grain-supported streamflow gravels in terrace deposits of the Umpqua River, southwest Oregon. The arrow shows direction of stream flow.

(Fig. 5.7) and transverse long-axis orientation. They also display fair size-sorting of clasts, although they may contain some very large clasts, and clasts are generally well rounded. They commonly exhibit abundant cross-stratification.

Wave-worked (beachface) conglomerates occur in nearshore environments where wave energy is sufficient to transport and rework gravels supplied by fluvial input or coastal erosion. The constant reworking of clasts in the surf zone tends to produce well-sorted, well-rounded gravel deposits. Deposits are typically clast supported with a sand matrix; however, on dominantly sand beaches clasts may occur as thin gravel layers in a dominantly sand section. Beachface conglomerates are particularly characterized by an abundance of disc-shaped clasts, generally good sorting of clasts, well-developed seaward-dipping imbrication, and gentle seaward stratification (Fig. 5.8). Figure 5.9 shows typical characteristics of beachface gravels on a modern beach.

Wave-, storm-, and current-worked (shoreface and shelf) conglomerates are deposited on the shoreface and shelf, which lies immediately seaward of the beachface. Gravels are reworked by waves as well as by longshore and rip currents. Conglomerates deposited in this environment are characterized by poor to moderate sorting, and fabrics range from clast-supported to (sand) matrix-supported. Individual beds tend to be sharp-based and range to 1 m or more in thickness. Beds can be cross-bedded, structureless, normally graded, or imbricated in lower portions. Clasts commonly show bimodal dip directions. Shoreface deposits may be gravel dominated (Fig. 5.10) or consist of sands with interbedded, thin, gravelly layers (Fig. 5.11).

Tide-worked conglomerates are not well represented, or at least not well known, in the ancient sedimentary record. Tide-worked surface gravels have been reported from modern marine shelf environments (see review by Phillips, 1984). Phillips also describes tide-worked conglomerates in the basal Santa Margarita Sandstone in central California that may be

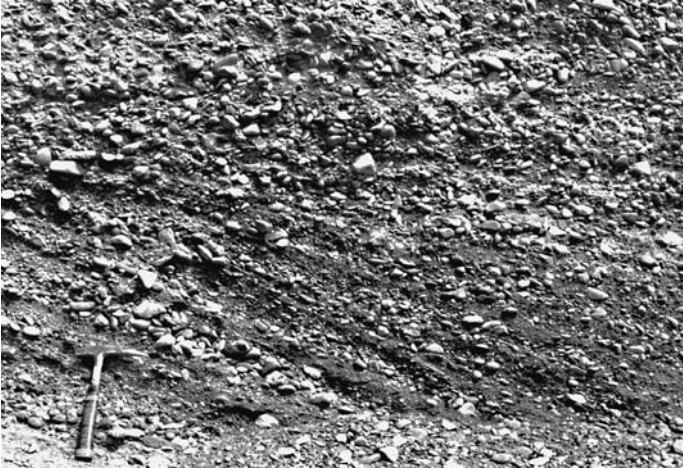


Figure 5.8 Stratification in Pleistocene beachface gravels, Cape Blanco, southern Oregon coast.



Figure 5.9 Moderately well-sorted, well-rounded, clast-supported modern beach gravels, southern Oregon coast. Note also the imbrication of the clasts.

representative of ancient tide-worked conglomerates. The Santa Margarita conglomerates are commonly matrix-supported but are clast-supported in part; clasts are moderately to poorly sorted and shape ranges from rounded to well rounded. Grading ranges from nongraded to normal or inverse. Stratification ranges from tabular to trough cross-bedded. Units display a general fining-upward trend, with clasts diminishing upward in both size and abundance. [Figure 5.12](#) shows some of the characteristics of the conglomerate.

Meltout/lodgment conglomerates are deposited subaerially; they consist of materials dropped by melting of grounded glaciers to form poorly sorted, matrix-rich gravelly

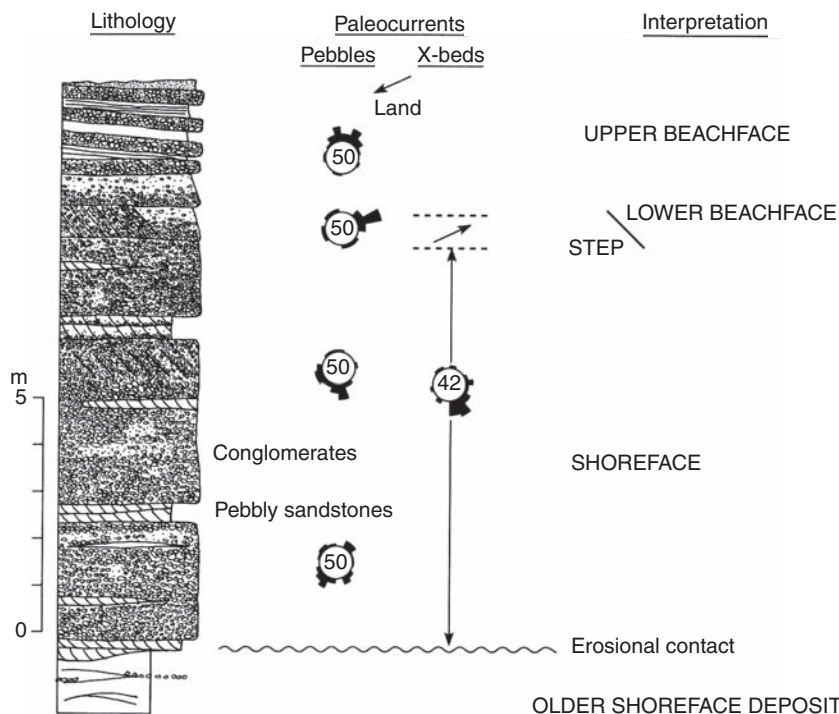


Figure 5.10 Characteristics of a gravel-dominated shoreface sequence in the Baytree Member of the Cardium Formation (Cretaceous), Alberta, Canada. Numbers inside the paleocurrent rose diagrams refer to numbers of measurements. (From Hart, B.S. and A.G. Plint, 1989, Gravelly shoreface deposits: a comparison of modern and ancient facies sequences: *Sedimentology*, **36**, Fig. 4, p. 556, reprinted by permission of Elsevier Science Publishers.)

deposits that are called till or glacial diamictite. They are commonly matrix-supported and very poorly sorted. Clast size can range to meter-size boulders. Some clasts may be faceted or striated. Long dimension of clasts is commonly parallel to ice-flow direction; clasts display little or no imbrication. Deposits are commonly massive, but may contain lenses or beds of stratified, better-sorted material. They may be succeeded upward by stratified, finer-grained glaciofluvial or glaciolacustrine deposits. Figure 5.13 shows some characteristics of these glacial conglomerates.

Subaqueous meltout conglomerates, also referred to as **aquatillites**, form in either lacustrine or marine environments owing to deposition from melting, gravel-charged ice. Deposition may occur as a traction carpet created by dense underflows of meltwater issuing from subglacial tunnels at the front of retreating ice or by direct meltout of ice-rafted material from floating ice. Conglomerates deposited in these environments are dominantly matrix-supported and poorly sorted; however, traction underflow deposits may be better sorted than subaerial meltout/lodgment conglomerates. Clasts can range from angular to well rounded, depending upon source, and may be striated, polished, and faceted.

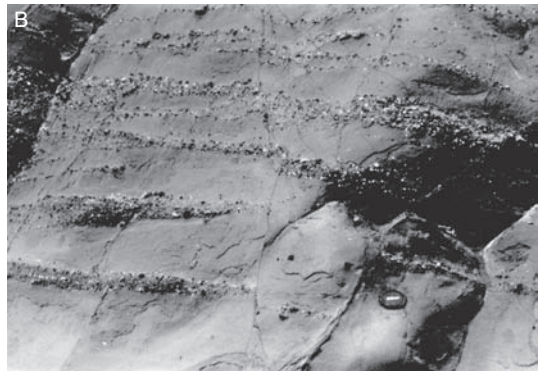
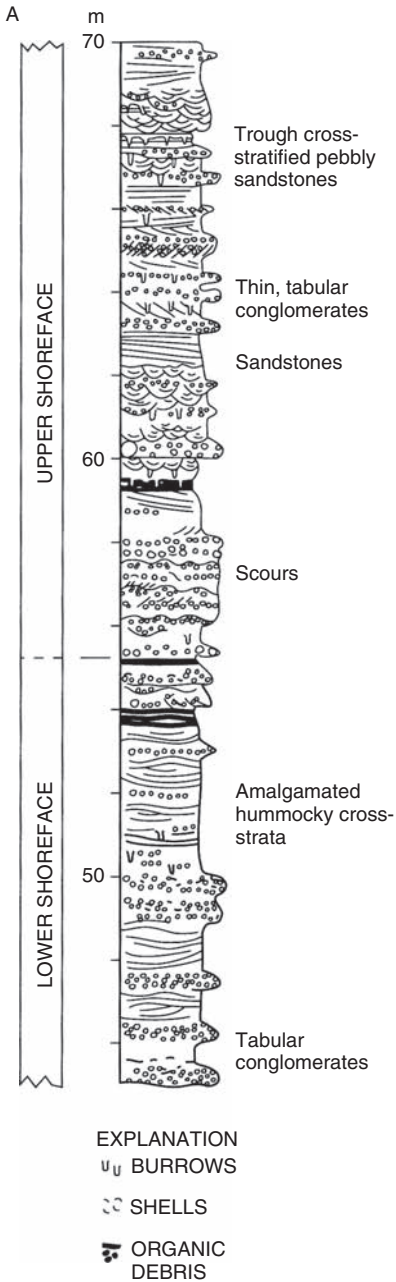


Figure 5.11 A. Schematic representation of wave- and current-dominated (shoreface) conglomerates in sandstones of Floras Lake (Miocene), southwestern Oregon. (From Leithold, E. L. and J. Bourgeois, 1984, Characteristics of coarse-grained sequences deposited in nearshore, wave-dominated environments – examples from the Miocene of southwestern Oregon: *Sedimentology*, **31**, Fig. 3, p. 572, reprinted by permission of Elsevier Science Publishers.) B. Shoreface conglomerates in sandstones of Floras Lake (Miocene), southwest Oregon. This example shows low-angle, cross-stratified, thin conglomerate beds in a sand-dominated unit.

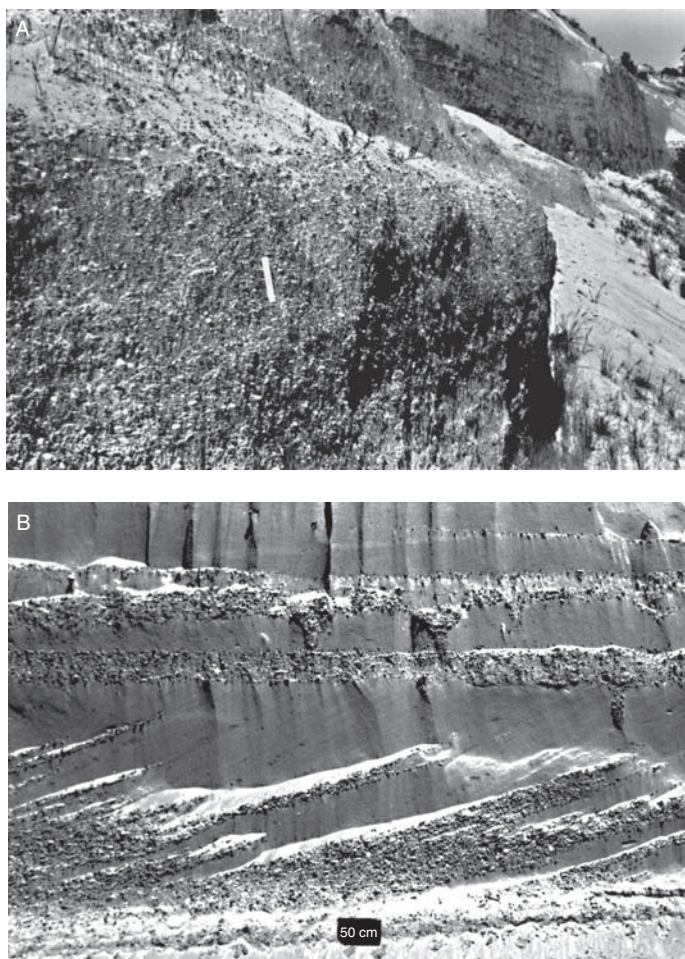


Figure 5.12 A. Large-scale (> 5m thick) trough cross-beds in conglomerates of the basal Santa Margarita Sandstone (Miocene), Santa Cruz Mountains, California. Ruler scale = 20 cm. B. Conglomerate and sand cross-beds in the Santa Margarita Sandstone. Scale bar = 50 cm. (Photographs courtesy of R. L. Phillips.)

Orientation of dropstones (stones that drop from melting ice) is generally random unless the stones are reworked by bottom currents. The deposits of traction underflows show parallel-to-current-flow long-axis trends, with up-current imbrication dips. Dropstone deposits are generally massive; underflow deposits may show crude horizontal stratification. Conglomerate units may be associated with better-stratified pebbly sands and silts that display cross-bedding and ripple cross-lamination. They commonly show no pronounced vertical grain-size trends but may pass upward into finer-grained sediments that formed as an ice front retreated. They differ from subaerial ice-meltout conglomerates by having clast-supported fabrics in some units and better sorting and better-developed stratification, particularly in underflow deposits.



Figure 5.13 Erosional pinnacles formed of massive, unstratified glacial meltout/lodgment conglomerate. Valley of Herron, Switzerland. (Photograph courtesy of E. M. Baldwin.)

Subaerial debris-flow conglomerates are generated by debris flows on land, particularly on alluvial fans and proglacial outwash fans. Subaerial debris flows are sediment gravity flows composed of gravel-size particles and characterized by the presence of a cohesive matrix of clay particles and fine sand. Such flows are capable of transporting material of widely varying sizes, including very large clasts. Thus, deposits tend to be matrix-supported and poorly sorted, and thicker units generally have larger clasts.

Subaerial debris-flow deposits are commonly nongraded, but some units may display either inverse or normal grading. Clasts in the deposits generally show no preferred orientation, although flow-parallel orientation may be present. They commonly exhibit no internal stratification, but they may be crudely layered owing to a succession of deposits (e.g. Fig. 5.14). Conglomerate units may be capped by a thin layer of tightly packed gravel, possibly overlain by stratified, stream-reworked (?) sandstone. The principal distinguishing characteristics of subaerial debris-flow deposits are illustrated schematically in Fig. 5.15.

The term, **resedimented conglomerate**, has been applied to conglomerates formed by remobilizing sedimentary material that had a previous history of deposition in a fluvial, lacustrine, coastal, or shelf setting, and which was subsequently retransported into generally deeper water (e.g. Howell and Normark, 1982). Retransport takes place by some kind of massflow process. Lowe (1982) identified three kinds of massflows that are capable of transporting gravel into deeper water: subaqueous debris flows, density-modified grain flows, and high-density turbidity currents. For a brief discussion of these types of mass flows, see Boggs (2006, ch. 2).

A close genetic relation exists between these three types of mass flows, and these flow types probably form a continuum. Both subaqueous debris flows and grain flows can likely evolve into fully turbulent turbidity currents with downslope mixing and dilution. Because of this close relationship in depositional process, it can be difficult to differentiate the

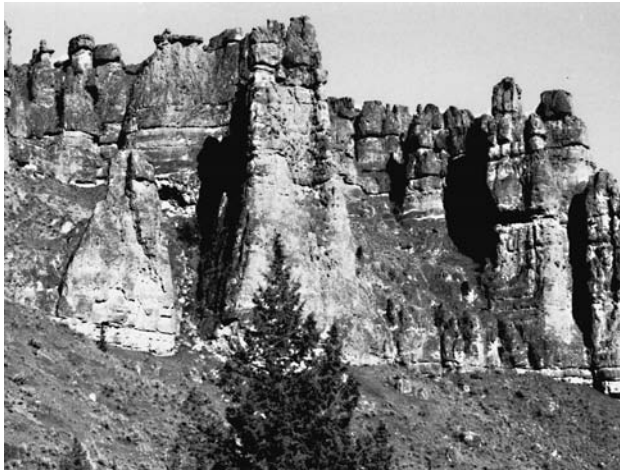


Figure 5.14 Massive to crudely stratified subaerial debris-flow conglomerate. Clarno Formation (Eocene–Oligocene), eastern Oregon. (Photograph courtesy of G. J. Retallack.)

deposits of these three types of flows – the deposits probably also form a continuum. Subaqueous mass flows can occur both in marine settings and in lakes, including glacially influenced marine settings and lakes.

The principal characteristics of subaqueous debris-flow conglomerates, subaqueous grain-flow conglomerates, and turbidite conglomerates are listed in [Table 5.4](#). Note that many similarities, as well as differences, exist in the characteristics of these conglomerates. The characteristics of subaqueous debris-flow conglomerates are further illustrated in [Fig. 5.16](#). Compare this figure with [Fig. 5.15](#) to see differences between subaerial and subaqueous debris-flow conglomerates.

5.9 Volcaniclastic conglomerates and breccias

The composition, classification, and origin of volcaniclastic sediments, with particular emphasis on volcaniclastic sandstones, are discussed in [Chapter 4](#). Volcaniclastic deposits composed mainly of gravel-size volcanic clasts of epiclastic origin are best regarded as volcanic-derived, epiclastic conglomerates or breccias. They are classified and interpreted as any other epiclastic conglomerate. Coarse volcaniclastic deposits of primary volcanic origin are classified differently. Pyroclastic particles ranging in size from 2 to 64 mm are called **lapilli**. Particles coarser than 64 mm are called **blocks**, if angular, and **bombs** if round and fluidally shaped. The lithified deposits formed from these coarse pyroclastic particles are called **lapillistone**, **pyroclastic breccia**, and **agglomerate (bombs)**.

As discussed in [Chapter 4](#), coarse pyroclasts are produced by explosive eruptions and may be deposited by pyroclastic fall, pyroclastic flow, or pyroclastic surge. Intrusion of lava or magma into water, ice, or wet sediment can lead to granulation or shattering of the lava into angular fragments, producing so-called **hyaloclastites**. Debris flows or mud

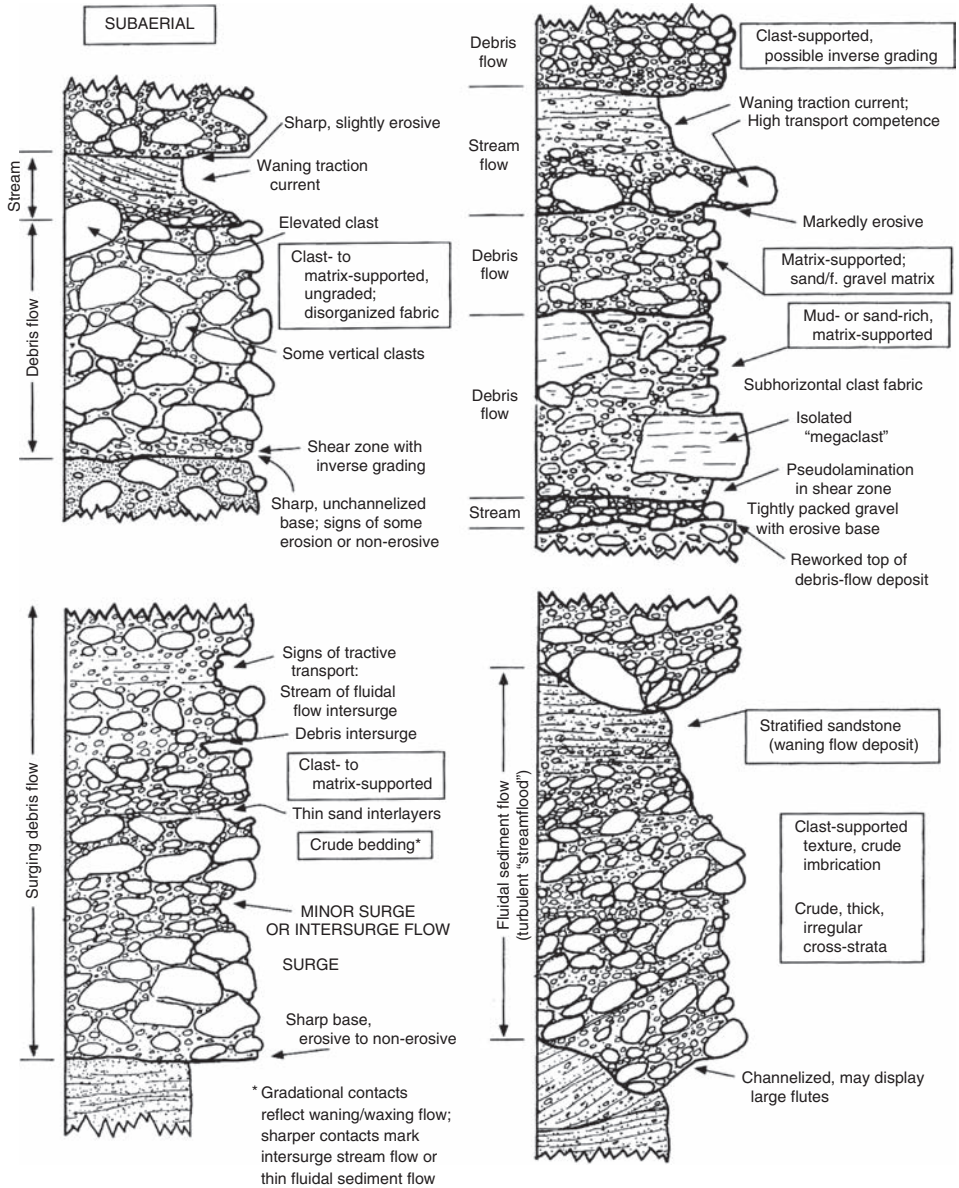


Figure 5.15 Schematic sections illustrating typical features of subaerial debris-flow deposits. (From Nemeč, W. and R.J. Steel, 1984, Alluvial and coastal conglomerates: their significance and some comments on gravelly mudflow deposits, in Koster, E. H. and R.J. Steel, (eds.), *Sedimentology of Gravels and Conglomerates*: Canadian Society of Petroleum Geologists Memoir 10, Fig. 15, p. 15, reprinted by permission.)

Table 5.4 *Characteristics of resedimented conglomerates*

	Subaqueous debris-flow conglomerates	Subaqueous grain-flow conglomerates	Turbidite conglomerates
Fabric support	Clast-supported to matrix-supported; matrix may increase upward within beds	Clast-supported with sand, silt, or clay matrix	Clast-supported to matrix-supported; matrix may increase upward within beds
Texture	Sorting generally poor; pebble roundness variable depending upon source; poor correlation between clast size and bed thickness	Sorting moderate to poor; clast roundness variable	Sorting poor to moderate; variable clast roundness; fossils in associated shales (mudstones)
Vertical size grading	Typically nongraded, but may display inverse, inverse-to-normal, or normal grading	Inverse grading especially common, but may be nongraded or normally graded	Normal grading particularly common; inverse, complex, or nongraded less common
Clast orientation	Poorly developed, but better than in subaerial debris-flow conglomerates	Imbrication common; long axes of clasts dominantly oriented in flow-parallel direction	Upflow imbrication common; long axes dominantly oriented in flow-parallel direction
Stratification	Poor internal stratification; may overlie stratified granule sandstones or contain thin mud/silt interbeds, possibly with wave-generated structures	Crude stratification on a large scale; may be separated by sandstone interbeds; internally, conglomerate units lack stratification; associated sandstones planar-laminated or cross-laminated	Horizontally stratified to trough cross-bedded, more rarely massive; channel deposits more massive than nonchannel deposits
Vertical facies sequences	Sequences that fine upward to sandy capping beds common; common tendency toward upward increase in matrix content	May become finer grained upward, grading to sand cappings	Fining- and thinning-upward sequences most common; rare coarsening-upward sequences; may pass upward into a sand capping

flows may retransport pyroclastic materials down the slopes of volcanoes to produce lahar deposits.

If neither the epiclastic nor the primary volcanic origin of coarse volcaniclastic deposits can be established, these coarse materials are referred to simply as volcanic conglomerates or breccias, as appropriate. Extended discussion of the characteristics of coarse pyroclastic

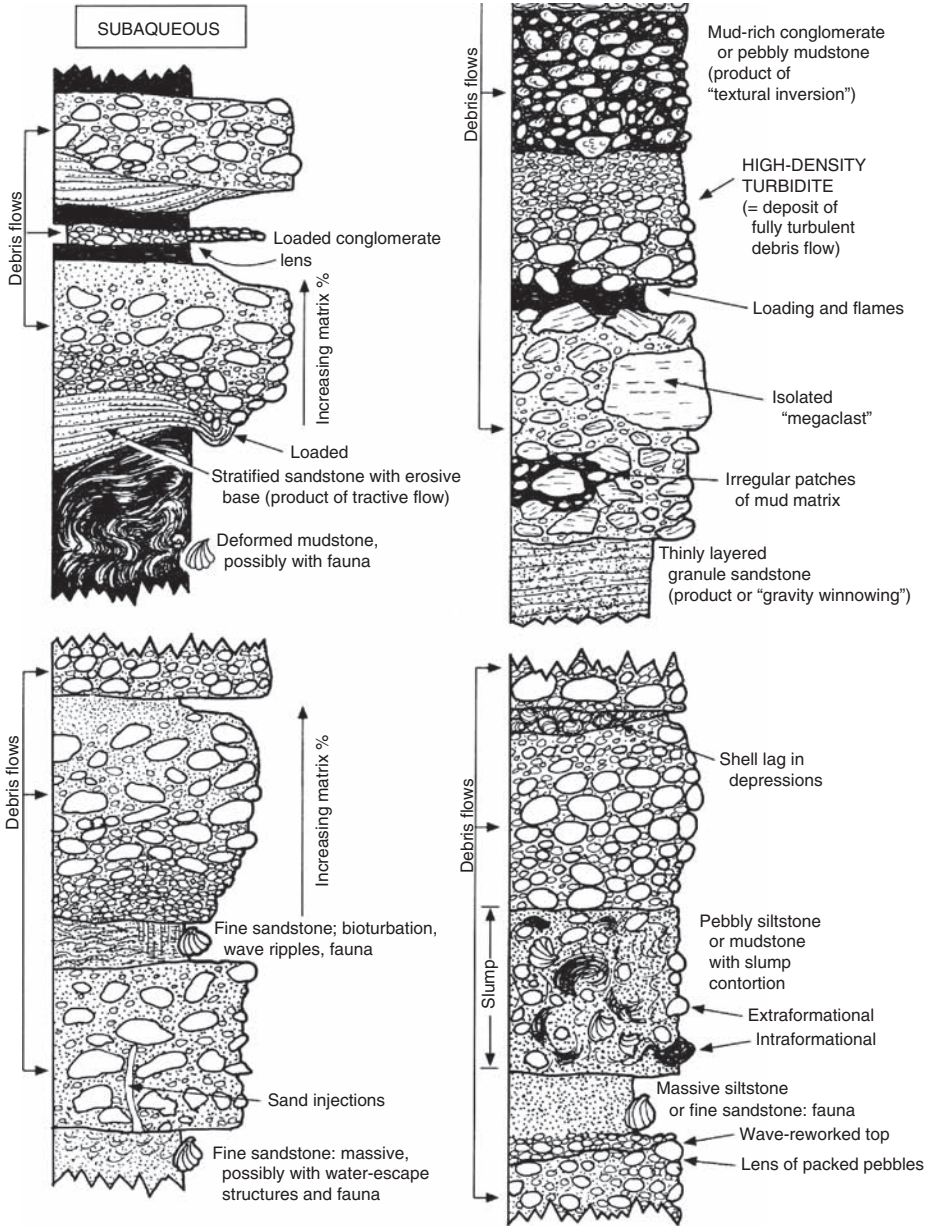


Figure 5.16 Schematic sections illustrating typical features of subaqueous debris-flow conglomerates. (From Nemec, W. and R. J. Steel, 1984, Alluvial and coastal conglomerates: their significance and some comments on gravelly mudflow deposits, in Koster, E. H. and R. J. Steel, (eds.), *Sedimentology of Gravels and Conglomerates*: Canadian Society of Petroleum Geologists Memoir 10, Fig. 16, p. 17, reprinted by permission.)

deposits is beyond the scope of this book. Readers are referred to Cas and Wright (1987), Fisher and Schmincke (1984), and Leyrit and Montenat (2000) for further details of these deposits.

Further reading

- Koster, E. H. and R. H. Steel (eds.), 1984, *Sedimentology of Gravels and Conglomerates*: Canadian Society of Petroleum Geologists Memoir 10.
- Miall, A. D., 1996, *The Geology of Fluvial Deposits*: Springer-Verlag, Berlin. (See sections dealing with gravel-bed rivers and gravel lithofacies.)

6

Mudstones and shales

6.1 Introduction

Fine-grained, siliciclastic sedimentary rocks, composed mainly of particles smaller than ~62 microns (coarse silt and finer), make up approximately 50 percent of all sedimentary rocks in the stratigraphic record (Chapter 1). Thus, they are about twice as abundant as sandstones and conglomerates combined. These fine-grained rocks are known by a variety of names, including lutites, siltstones, mudstones, mudrocks, claystones, and shales. Tourtelot (1960) reviews in detail the history of fine-sediment terminology. He points out (p. 342) that historically the term shale has been used in two ways: (1) in a restricted sense to mean a laminated clayey rock and (2) as a broad, group name for all fine-grained siliciclastic rocks. He concludes that it is acceptable practice to include both these meanings for shale, and, therefore, that shale is the appropriate class name for fine-grained rocks, of equal standing with sandstones and limestones as group names.

Certainly our comprehension is broad enough to include two meanings of the word “shale”: First, the reasonably precise meaning of “laminated clayey rock” to which the origin of the word entitles it, and second, the meaning of the “general class of fine-grained rocks,” which our historical use of the word bequeaths to it.

Although some geologists (e.g. Potter *et al.*, 1980, p. 15) have agreed with Tourtelot’s conclusion that shale is an acceptable class name for all fine-grained rocks, others (e.g. Lundegard and Samuels, 1980; Spears, 1980; Stow and Piper, 1984) consider the dual use of the term in this way to be confusing. They favor using the term mudrock as a group name for fine-grained sedimentary rocks and prefer to reserve the term shale for use in its more restricted sense to mean a laminated or fissile fine-grained rock. Potter *et al.* (2005) appear to have swung toward this point of view in their most recent book. They now recommend **mudstone** as the general, class name for fine-grained rocks (equivalent in usage to sandstone and limestone, i.e. it has a “stone” ending); they restrict the term shale to obviously fissile varieties. See also Macquaker and Adams (2003), who likewise appear to favor mudstone as the class name. Although I (reluctantly) recognize Potter *et al.*’s (2005) restricted usage, it is difficult to overcome the long-held tendency to refer to all fine-grained rocks as shales.

Geologists in the past have focused less attention overall on mudstones than on sandstones. Probably this is so because mudstones are more difficult to study owing to their fine grain size and because they contain fewer interesting textures and structures. For example, petrographic analysis of all but the very coarsest-grained mudstones is quite difficult. The mineralogy of finer-grained mudstones must be determined by X-ray diffractometer techniques, the scanning electron microscope, or other techniques that are commonly time consuming and often quite expensive. Furthermore, mudstones and shales not uncommonly occur as thick, repetitive sequences of thin- to medium-bedded rocks that may contain few visible sedimentary structures or textural features of interest. They can be pretty monotonous to work with in the field. Also, many fine-grained units are poorly exposed and difficult to observe.

The study of fine-grained siliciclastic sedimentary rocks has thus lagged somewhat behind that of coarser-grained rocks. Nonetheless, geologists have a strong interest in mudstones, as evidenced by the extensive literature available on these fine-grained rocks. See, for example, the bibliography of mudstones cited in Schieber *et al.* (1998). Information about fine-grained sediments, including recent, unconsolidated sediments, has been accumulating rapidly since the late 1960s, owing in part to research involved in the Deep-Sea Drilling Project (DSDP) and Ocean Drilling Program (ODP) and to the interest of petroleum geologists in fine-grained rocks as possible source rocks for petroleum. Geologists are interested in such aspects of fine-grained sediments as their source (provenance), modes of transport (e.g. surface currents, bottom currents, nepheloid plumes, turbidity currents and other mass movements), depositional environments, and organic content (petroleum source potential). To evaluate the genetic significance of mudstones requires that we have knowledge of their textures, structures, mineralogy, chemistry, and fossil content. In this chapter, we examine some of the characteristic properties of mudstones, discuss their classification, and briefly describe their origins and occurrences.

6.2 **Methods of study**

Owing to their fine grain size, mudstones require somewhat different methods of study than do sandstones and conglomerates. Detailed discussion of these techniques is outside the scope of this book, but may be found in several sources, including O'Brien and Slatt (1990) and Schieber and Zimmerle (1998). Fabrics in mudstones, such as the fine-scale laminae in shales, are studied by using X-radiography techniques (e.g. O'Brien and Slatt, 1990, p. 8), as well as by using the scanning electron microscope and the petrographic microscope. Particle orientation can also be determined by electron microscopy and image analysis (e.g. Tovey *et al.*, 1995).

Because of their fine grain size, the minerals in mudstones (especially clay minerals) are difficult to study with a petrographic microscope. Therefore, mineralogy is determined by using X-ray powder methods or by backscattered electron microscopy (e.g. Krinsley *et al.*, 1998). The chemical composition of mudstones can be analyzed by wet-chemical methods or by a variety of instrumental techniques, including electron probe microanalysis (EPMA),

secondary-ion mass spectrometry (SIMS), and laser-ablation–inductively coupled plasma mass spectrometry (LA-ICP-MS). See Boggs and Krinsley (2006, pp. 37–46) for a brief description of these instrumental techniques.

6.3 Physical characteristics of mudstones and shales

6.3.1 *Texture*

Grain size

Few published data on the sizes of particles in mudstones and shales are available. Data compiled by Picard (1971) for a small number of analyses of ancient shales indicate that these samples contain about 80 percent silt, 17 percent clay, and 3 percent sand. Pettijohn (1975, p. 262) suggests that the average shale contains about two parts silt and one part clay. We don't know how representative these values are of mudstones and shales in general. It is likely that the grain size of fine-grained rocks varies widely.

Texturally, clay is defined as all material finer than 4 microns; silt ranges in size from 4 to 63 microns; sand ranges from 63 microns to 2 mm. The sizes of fine, unconsolidated particles can be determined by using a number of instrumental techniques, which are based mainly on measuring the settling velocity of particles in water (see discussion in Boggs, 2006, p. 54). These methods cannot be used to measure the grain sizes of particles in mudstones and shales, which generally cannot be disaggregated to yield individual particles. The sizes of grains in consolidated rocks can be measured by using an electron microscope (e.g. Fig. 6.1); however, this is an expensive procedure that is seldom done. The difficulty of determining the sizes of particles in mudstones may account for the fact that comprehensive data on the grain size of these rocks have not been published.

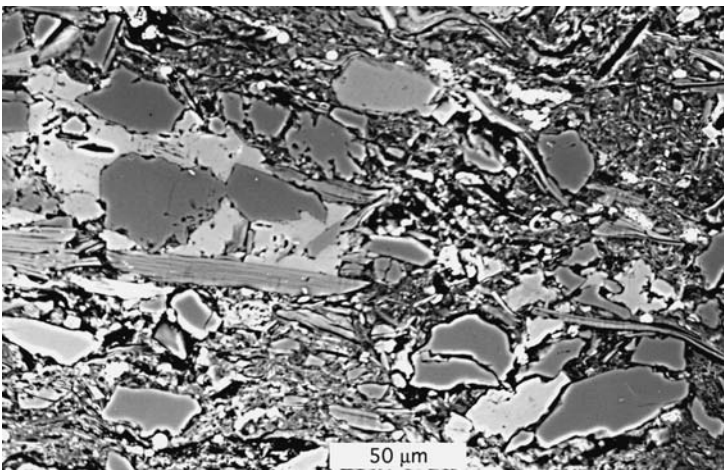


Figure 6.1 Electron microscope photograph of a mudstone containing various-sized grains of quartz (blocky) and clay minerals (flaky). Photograph courtesy of David Krinsley.



Figure 6.2 Electron micrograph of kaolinite clay minerals magnified 4700 \times . Note the platy or flaky appearance of the pseudo-hexagonal kaolinite crystals, which are arranged in this specimen in distinct “books.”

Particle shape

The shapes of the small particles that make up mudstones, unlike the shapes of sand-size and larger particles, are little modified by sediment erosion and transport. For example, Kuenen (1959, 1960) demonstrated that very small quartz particles ($< \sim 0.1$ mm) do not become rounded very effectively by any type of eolian or stream transport. Therefore, the shapes of fine-silt- and clay-size particles in mudstones reflect mainly the original shapes of the detrital particles, largely unmodified by transport abrasion, or they reflect the shapes of minerals generated during diagenesis. Thus, most particles in mudstones are very angular. Many particles, especially clay minerals and fine micas, have very low sphericity. Electron microscopy (e.g. Sudo *et al.*, 1981) reveals that most clay minerals have platy, flaky, or acicular shapes (e.g. Fig. 6.2). Some investigators (e.g. Ehrlich and Chin, 1980; Mazzullo *et al.*, 1982) have used Fourier shape analysis (Chapter 2) to study the shapes of quartz silt as a clue to provenance. Otherwise, few efforts appear to have been made to relate the shapes of fine particles in mudstones to their genesis.

6.3.2 Microfabric

Because shales contain high concentrations of clay minerals that have platy or flaky shapes, these rocks may exhibit microfabrics resulting from the preferred orientation of flaky clay minerals. Clay fabric is defined as the orientation and arrangement or spatial distribution of the solid particles (in fine-grained sediments) and the particle-to-particle relationships (Bennett *et al.*, 1991a). The microstructures of fine-grained sediments are explored in depth in the compendium volume edited by Bennett *et al.*, 1991b, which contains 59 papers by different authors.

Three kinds of depositional and diagenetic processes and mechanisms may operate to produce clay and shale microfabrics: physicochemical, bioorganic, and burial-diagenesis (Bennett *et al.*, 1991a). In turn, **physicochemical processes** take place by three mechanisms: **electrochemical** (forces that hold particles together internally and that bind particles), **thermochemical** (forces arising from temperature and temperature differences, e.g. Brownian motion, freezing of water), and **interface dynamics** (differential motion of settling particles under the influence of gravity, differential flow of water masses of differing density, impact of particles on sediment interface, flow at the interface, and microroughness of the interface). **Bioorganic processes** represent the effects of living organisms on sediment properties and are brought about by **biomechanical** (bioturbation), **biophysical** (aggregation or agglutination of particles by organic processes), and **biochemical** (chemical production and destruction of chemical entities, e.g. production of gases by organisms) mechanisms. **Burial-diagenesis** processes that can affect shale microfacies take place by **mass gravity mechanisms** (mechanical rearrangement of particles owing to overburden stresses) and **cementation** and other diagenetic phenomena.

The interplay of these processes determines the clay-particle fabric. The elements of clay fabric are illustrated in Fig. 6.3, which depicts the various kinds of particle associations in clay suspensions. Thus, clay particles may be deflocculated and randomly dispersed, be edge-to-edge flocculated, edge-to-face flocculated, etc.

The kind of orientation (face-to-face?) that produces **fissility** in shales is of particular interest. Bates and Jackson (1980) define fissility as the property possessed by some rocks of splitting easily into thin layers along closely spaced, roughly planar, and approximately parallel surfaces (e.g. Fig. 6.4). The term fissile is used in two ways to mean (1) capable of being easily split along closely spaced planes, i.e. possessing fissility, and (2) frequency of splitting, i.e. the thickness of layers between fissile planes or planes of parting.

Potter *et al.* (1980) use the term fissile to indicate a class of parting, with parting defined as the tendency of a rock to split along lamination or bedding – a tendency greatly enhanced by weathering. The relationship of parting to bedding and lamination is shown in Table 6.1, as modified by Potter *et al.* from earlier schemes of Alling (1945), Ingram (1954), and McKee and Weir (1953). Table 6.1 shows that fissile is a subdivision of parting and that a fissile parting is thinner than a lamina (laminae are strata less than 10 mm thick); that is, fissile partings range in thickness from 0.5 mm to 1.0 mm. Parting thinner than 0.5 mm is referred to as **papery**, and parting thicker than 1 mm is **platy**, **flaggy**, or **slabby**, depending upon thickness.

Thus, in summary, a fissile fine-grained rock is one that tends to split relatively easily into thin, approximately parallel layers that range in thickness from about 0.5 mm to 1.0 mm. Shales that split into thinner layers are called papery shales, and those that split into thicker units are platy, flaggy, or slabby shales depending upon thickness of the parting, as shown in Table 6.1. Potter *et al.* (1980) suggest that the clay and organic contents of shales decrease and the sand, silt, and carbonate content increases as thickness of parting units increases.

The cause of fissility in shales is a topic of long-standing interest, which is, as yet, not fully resolved. Moon and Hurst (1984) suggest that the geochemistry of the environment

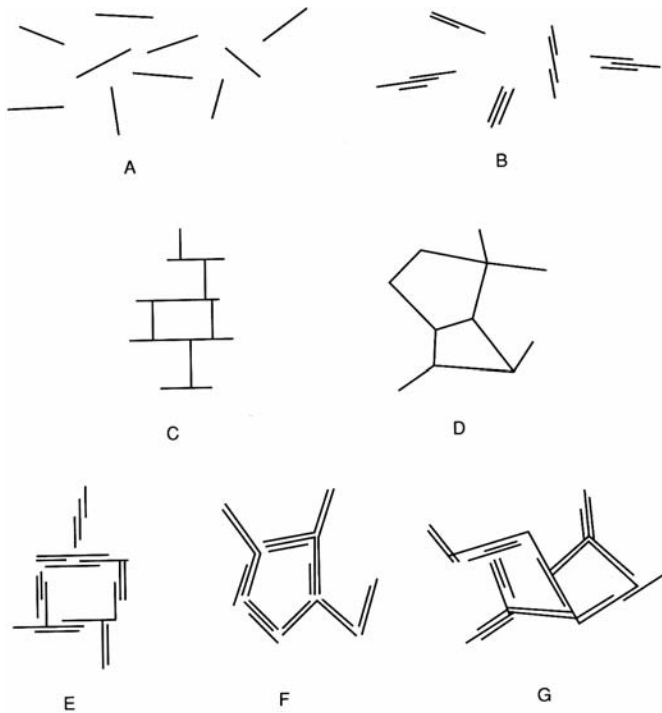


Figure 6.3 Kinds and terminology of particle associations in clay suspensions: (A) dispersed and deflocculated, (B) aggregated but deflocculated (face-to-face association, or parallel or oriented aggregation), (C) edge-to-face flocculated but dispersed, (D) edge-to-edge flocculated but dispersed, (E) edge-to-face flocculated and aggregated, (F) edge-to-edge flocculated and aggregated, (G) edge-to-face and edge-to-edge flocculated and aggregated. (From van Olphen, H., 1977, *An Introduction to Clay Colloid Chemistry*, 2nd edn.: John Wiley and Sons, New York, NY, Fig. 23, p. 97: reprinted by permission.)



Figure 6.4 Laminated shale (pre-Mississippian), Arctic National Wildlife Refuge, Alaska.

Table 6.1 *Stratification and parting in shales*

Thickness	Stratification		Parting	Composition
30 cm	Thin	Bedding	Slabby	↓ Clay and organic content ————— Sand, silt, and carbonate content ↑
3 cm	Very thin			
10 mm	Thick	Lamination	Flaggy	
5 mm	Medium		Platy	
1 mm	Thin		Fissile	
0.5 mm	Very thin		Papery	

Source: Potter, P. E., *et al.*, 1980, *Sedimentology of Shale*, Table 1.3, p. 16, reprinted by permission of Springer-Verlag, Berlin.

may be the crucial factor in producing fissility. In particular, the presence or absence of peptizing or dispersing agents in the water determines if clay sediments reach the bottom as dispersed, single plates or as flocs. Organic substances are suggested by Moon and Hurst to be the main peptizing agents. In anoxic environments where organic compounds are abundant, the peptizing qualities of these organic substances cause dispersion of flocs or prevent flocs from forming in the first place. Thus, clay settles as single plates. In oxic environments where peptizing agents are absent, clay settles as flocs (Fig. 6.5). Domains form (exactly how is not yet clear) in the freshly deposited sediment. [Domains are microscopic or submicroscopic regions within which the clay particles are in parallel array (Aylmore and Quirk, 1960).] These domains are randomly oriented in oxic sediments and more or less parallel oriented in anoxic sediments.

Lithification causes additional alignment or parallel orientation of the domains in the muds deposited in anoxic environments, producing fissility. Lithification does not destroy the random orientation of domains in muds of oxic environments, although the domains become more closely packed. Thus, muds deposited in oxic environments form nonfissile mudstones. As Byers suggested as long ago as 1974, oriented fabrics produced in anoxic environments would likely be preserved owing to limited bioturbation in such toxic environments.

Curtis *et al.* (1980) proposed that preferred orientation in clay-rich sediments results mainly from compaction strain. They suggested that fissility is not due to clay-mineral orientation but

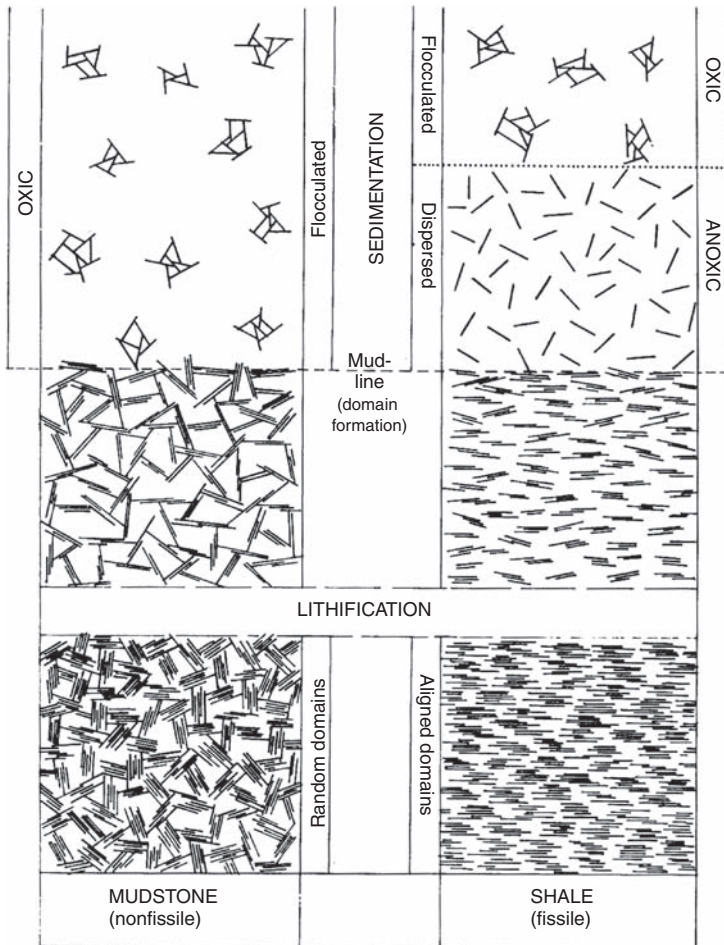


Figure 6.5 Schematic representation of major microstructural changes that occur in clay sediments during deposition and lithification. (From Moon, C.F. and C.W. Hurst, 1984, *Fabrics of muds and shales: an overview*, in Stow, D.A.V. and D.J.W. Piper, (eds.), *Fine-Grained Sediments: Deep-Water Processes and Facies*: Blackwell Scientific, Oxford. Fig. 5, p. 588, reprinted by permission.)

instead is related to fine-scale lamination. They suggested further that the degree to which clay mineral orientation can be attained is limited by the presence of nonplaty minerals such as quartz, which prevent planar fabric development in their immediate vicinity. A problem in ascribing clay-mineral orientation to postdepositional compaction is that shales which do not display oriented fabrics can occur stratigraphically below other shale units that do display oriented fabrics.

As pointed out by Bennett *et al.* (1991b), one of the important goals in the study of fine-grained sediments is use of their fabric signatures as clues to ancient environments and processes. Unfortunately, the relationship between fabrics and depositional environments is

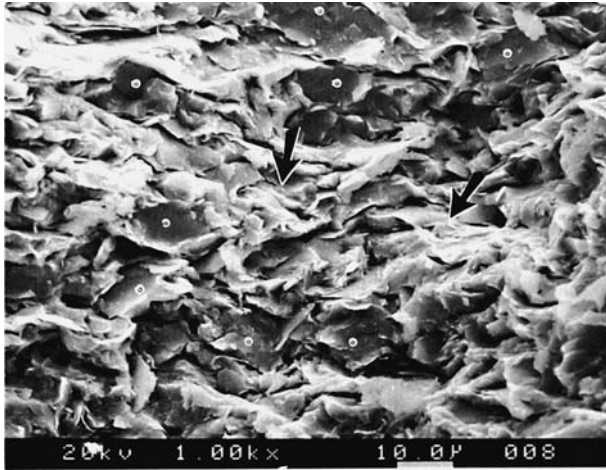


Figure 6.6 SEM photomicrograph of the Willowvale unit – shallow-water facies (gray shale), Verona, New York. The random orientation (bioturbated fabric) shows a mixture of platy clay minerals (arrows) and abundant silt-size quartz grains (small white dots). [From O’Brien, N. R., C. E. Brett, and M. J. Woodard, 1998, Shale fabric as a clue to sedimentary process – Example from the Williamson–Willowvale shales (Silurian), New York, in Schieber, J., W. Zimmerle, and P. Sethi (eds.), *Shales and Mudstones II* : Schweizerbart’sche Verlagsbuchhandlung, Stuttgart, p. 60, Fig. 5, reproduced by permission.)

complex and not easily generalized. An example of this kind of relationship is provided by O’Brien *et al.* (1998), who describe the random orientation of clay flakes in the oxic shallow-water, bioturbated, facies of the Williamson Shale (Fig. 6.6), and compares this lack of orientation to the high degree of preferred flake orientation in deep-water, anoxic facies of the equivalent formation (Fig. 6.7). Additional examples are described in Bennett *et al.* (1991b).

6.3.3 Sedimentary structures

The characteristics and origins of most common structures that occur in sedimentary rocks are described in Chapter 3. Many of these structures are present in mudstones and shales, including parallel stratification, massive bedding, graded bedding, flaser bedding, ripple marks, convolute lamination, trace fossils and bioturbation structures, mud cracks, concretions, cone-in-cone structures, and color banding. In addition to these so-called “macro-structures,” millimeter-scale structures may be present that require use of petrographic imaging or X-radiography techniques to recognize. See, for example, Kuehl *et al.* (1991) for a description of some of these fine-scale structures such as micro-cross-laminations and graded laminae.

Readers are referred to Chapter 3 for details of these various sedimentary structures. With the exception of laminae, they are not further discussed here. Because of the prevalence of

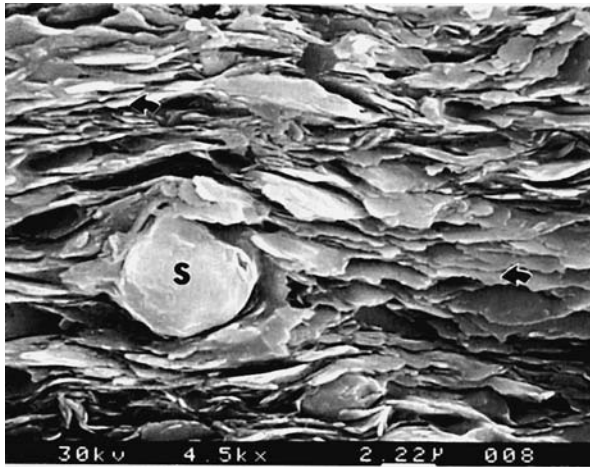


Figure 6.7 SEM photomicrograph of the fabric of the Williamson Shale – basinward facies (black shale portion), Palmer’s Glen, New York. Note the abundant parallel clay flakes (arrow) and the rare silt grain (S). [From O’Brien, N. R., C. E. Brett, and M. J. Woodard, 1998, Shale fabric as a clue to sedimentary process – Example from the Williamson–Willowvale shales (Silurian), New York, in Schieber, J., W. Zimmerle, and P. Sethi (eds.), *Shales and Mudstones II: Schweizerbart’sche Verlagsbuchhandlung, Stuttgart*, p. 64, Fig 8B, reproduced by permission.]

parallel-laminated stratification in many shales, the relationship of laminae to fissile partings, and the use of lamination as a criterion in the classification of shales, some additional discussion of lamination is given here.

As discussed in [Chapter 3](#), **laminae** are defined as strata having a thickness less than 10 mm. Laminae may or may not display fissility. They are produced by short-lived fluctuations in depositional conditions that cause variations in grain size, content of clay and organic material, mineral composition, or microfossil or fecal-pellet content of sediment. Laminae produced by alternating layers of finer- and coarser-grained sediments are probably most abundant overall in sedimentary rocks; however, laminae that contain concentrations of organic matter are common also in some shales. [Figure 6.8](#) shows the fairly typical appearance of laminated shale in outcrop. A close-up view of shale laminae is provided in [Fig. 6.9](#).

Parallel laminae are known to form both by deposition from suspension and by traction currents. Most laminae in shales are probably deposited in some manner from suspension. Possible suspension mechanisms may include: (1) slow suspension settling in lakes, where levels of organic activity are commonly low – the formation of varves, for example; (2) sedimentation on some parts of deltas, where abundant fine sediment that is periodically supplied by distributaries leads to rapid deposition; (3) deposition on tidal flats in response to fluctuations in energy levels and sediment supply during tidal cycles; (4) deposition in subtidal shelf areas where thin sand layers that accumulate owing to storm activity may alternate with thin mud laminae formed during periods of slower accumulation;



Figure 6.8 Laminated shales in the Lincoln Peak Fm. (Cambrian), east side of Schell Creek Range, Nevada.

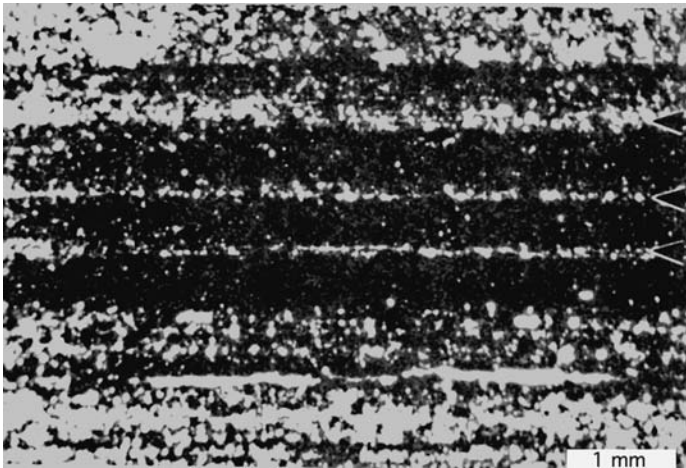


Figure 6.9 Fine laminations in Devonian black shales, New York. Fine organic material is concentrated in the thicker, darker layers. Thin silt laminae (arrows) separate the organic-rich layers. (After O'Brien, N., 1989, Origin of lamination in Middle and Upper Devonian black shale, New York State: *Northeastern Geol.*, **11**, p. 161, Fig. 2C. Photograph courtesy of N. O'Brien.)

(5) surface-wave activity that causes resuspension of shelf muds; (6) slow sedimentation in deep-sea pelagic or hemipelagic environments by deposition from nepheloid layers; and (7) deposition in deep water by turbidity currents, which results from a combination of suspension settling and near-bottom current shear.

The specific characteristics of lamination may have environmental significance. For example, O'Brien (1990) reports three styles of lamination (fine, thick, and wavy laminated) in Lower Jurassic shales from Yorkshire, Great Britain. He relates these different kinds of lamination to deposition under changing water depths and energy conditions during marine transgression. Schieber (1991) interprets wavy-crinkly carbonaceous laminae in Precambrian shales of Montana as microbial mat deposits. Genger and Sethi (1998) report millimeter-scale to centimeter-scale laminae in black shales of the Mid-Continent region, USA, which they relate to paleoenvironmental changes and sea-level fluctuations. Additional examples of the paleoenvironmental significance of lamination are discussed in Schieber *et al.* (1998) and Potter *et al.* (2005).

6.4 Composition

6.4.1 Mineralogy

Bulk-mineral composition

Clay minerals, fine-size micas, quartz, and feldspars are the most abundant minerals in mudstones and shales. A variety of other minerals may occur in these rocks in minor quantities, including zeolites, iron oxides, heavy minerals, carbonates, sulfates, and sulfides, as well as fine-size organic matter (Table 6.2). Because of the difficulties involved in petrographic analysis of fine sediments, most investigators have concentrated on the clay mineralogy of shales, which can be determined fairly easily by X-ray diffraction methods. Quantitative to semiquantitative determination of fine quartz, feldspars, and other minerals in shales can be made also by X-ray diffraction methods (e.g. Suryanarayana and Norton, 1998), with a scanning electron microscope equipped with an energy-dispersive X-ray unit (e.g. Goldstein *et al.*, 2003), or with an electron probe microanalyzer (e.g. Reed and Romanenko, 1995). Also, quartz, feldspars, and other nonclay minerals can be separated from clay minerals in shales by chemical techniques (Blatt *et al.*, 1982), allowing these nonclay minerals to be studied more effectively by petrographic methods. See also Wiegmann *et al.* (1982) for a discussion of methods of determining the complete mineral composition of shales.

In spite of the availability of these analytical techniques, relatively few quantitative analyses of the bulk composition of shales and mudstones have been reported. Some available data are summarized in Table 6.3. Note that the average contents of quartz in the shales listed in this table range from about 15 to 54 percent. Average values of feldspar (K-feldspar plus plagioclase) content range from less than 1 percent to more than 15 percent. Average clay-mineral abundances range between about 17 and 57 percent. The abundances of calcite, dolomite, siderite, and pyrite, which are secondary minerals (cements and replacement minerals), are relatively low in most shales.

Readers should keep in mind that the variations in mineral abundances shown in Table 6.3 may be due to several factors. For example, mineral composition is known to vary markedly with grain size. Quartz tends to be more abundant in coarser-grained mudstones and shales, whereas clay minerals are more abundant in finer-grained mudstones and shales.

Table 6.2 *Principal constituents in shales and mudstones*

Constituents	Remarks
<i>Silicate minerals</i>	
Quartz	Makes up 20 to 30 percent of the average shale; probably mostly detrital; chalcedony and biogenic opal-A and opal-CT may also be present
Feldspars	Commonly less abundant than quartz; plagioclase generally more abundant than alkali feldspars
Zeolites	Commonly present as an alteration product of volcanic glass; phillipsite and clinoptilolite are common zeolites in modern marine sediments
<i>Clay minerals</i>	
Kaolinite (7 Å)	Forms under strongly leaching conditions: abundant rainfall, good drainage, acid waters; in marine basin tends to be concentrated nearshore
Smectite–illite–muscovite (10 Å and greater)	Smectite is a hydrated, expandable clay; common in soils and as an alteration product of volcanic glass; alters to illite during burial; illite is the most abundant clay mineral in shales; derived mainly from pre-existing shales; alters to muscovite during diagenesis; muscovite may also be detrital
Chlorite, corrensite, and vermiculite	Chlorite forms particularly during burial diagenesis; second in abundance only to illite in Paleozoic and older shales; during burial, vermiculite may convert to corrensite and finally to chlorite
Sepiolite and attapulgite	Magnesium-rich clays that form under special conditions where pore waters are rich in Mg, e.g. saline lakes
<i>Oxides and hydroxides</i>	
Iron oxides	Hematite most common in shales, but goethite or limonite may be more common in modern muds; commonly present as coatings on clay minerals; may be converted to pyrite or siderite in reducing environments
Gibbsite	Consists of $\text{Al}(\text{OH})_3$; may be associated with kaolinite in marine shales derived from the weathering of tropical landmasses
<i>Carbonates</i>	
Calcite	More common in marine than nonmarine shales
Dolomite	An important cementing agent in some shales
Siderite and ankerite	Occur in shales most commonly as concretions
<i>Sulfur minerals</i>	
Sulfates: gypsum, anhydrite, and barite	Occur as concretions in shales and may indicate the presence of hypersaline conditions during or after deposition
Sulfides	Mainly the iron sulfides pyrite and marcasite; these sulfides are most abundant in marine shales and indicate reducing conditions either at the time of deposition or during diagenesis

Table 6.2 (cont.)

Constituents	Remarks
<i>Other constituents</i>	
Apatite	Occurs particularly as nodules in marine shales that accumulated slowly in areas of high organic productivity (see Chapter 12)
Volcanic glass	Common in modern continental and marine muds in areas of volcanic activity; converts to zeolites and smectites during burial diagenesis
Heavy minerals	Occur in shales, but little is known about patterns of occurrence and relative abundance
<i>Organic substances</i>	
Discrete and structured organic particles	Mostly palynomorphs or small coaly fragments (vitrinite) (see Chapter 13)
Kerogen	Occurs in all shales except red ones; see Chapter 13 for the characteristics of kerogen

Source: Drawn mainly from Potter *et al.*, 1980, pp. 47–49.

A considerable amount of the variation shown in Table 6.3 could be due to this factor alone. Mineral composition may vary also owing to tectonic setting or depositional environment. For example, Bhatia (1985) reports that quartz ranges from a low of 17 percent in passive-margin shales to as much as 46 percent in shales deposited in oceanic island arcs, whereas clay-mineral abundance ranges from 20 percent in oceanic island-arc shales to more than 75 percent in passive-margin shales. Blatt and Totten (1981) report significant variation in the quartz content of marine shales as a function of distance from shoreline: 47 percent quartz at a distance of 60 km from shore versus 11 percent quartz at a distance of 270 km.

Because so many different factors may affect the mineral composition of mudstones and shales, it is difficult to generalize about their average composition. Many additional data are needed to better define their bulk mineralogy. The values shown in Table 6.3 suggest, however, that the average quartz content of mudstones and shales may be about 35 percent, average feldspar content about 5 percent, and average clay-mineral content approximately 35 percent. Note, however, that clay minerals make up nearly half of the minerals in some mudstones and shales.

Clay-mineral composition

Because clay minerals form such a significant fraction of most mudstones and shales, some additional discussion of the clay minerals is desirable. Clay minerals belong to the group of silicate minerals known as **phyllosilicates**. They are characterized particularly by SiO_4^{4-} ionic groups in combination with metallic cations. The SiO_4^{4-} groups consist of a silicon atom surrounded by four oxygen atoms in a tetrahedral configuration. Therefore, they are called **silica tetrahedra** or **silicon–oxygen tetrahedra**. Silica tetrahedra can be linked together to form indefinitely extending tetrahedral sheets.

Table 6.3 Average percent mineral composition of shales of different ages

Age	Number of analyses	Clay minerals	Quartz	Potassium feldspar	Plagioclase feldspar	Calcite	Dolomite	Siderite	Pyrite	Other minerals	Organic carbon
Quaternary	5	29.9	42.3	12.4	–	6.6	2.4	–	5.6	–	0.9
Pliocene	4	56.5	14.6	5.7	11.9	3.2	–	2.9	1.8	<1.0	2.6
Miocene	9	25.3	34.1	7.4	11.7	14.6	1.2	–	1.9	2.4	1.4
Oligocene	4	33.7	53.5	3.0	–	5.5	–	–	–	4.0	0.4
Eocene	11	40.2	34.6	2.0	8.1	3.8	4.6	1.7	1.6	–	3.5
Cretaceous	9	27.4	52.9	3.6	1.6	2.9	7.9	0.1	1.6	–	2.0
Jurassic	10	34.7	21.9	0.6	4.4	14.6	1.6	0.4	10.9	–	10.9
Triassic	9	29.4	45.9	10.7	0.7	3.7	4.1	5.1	–	–	0.3
Permian	1	17.0	28.0	4.0	8.0	–	1.0	–	–	42.0	0.2
Pennsylvanian	7	48.9	32.6	0.8	6.2	1.4	2.1	3.4	3.5	–	1.0
Mississippian	3	57.2	29.1	0.4	2.9	–	–	0.6	5.1	–	4.7
Devonian	22	41.8	47.1	0.6	–	2.0	1.3	0.3	3.3	–	3.7
Ordovician	2	44.9	32.2	<1.0	6.3	9.8	0.5	0.5	3.4	–	1.5
Misc. ages	29	47.8	33.1	<1.0	5.5	5.2	2.3	0.8	3.1	–	4.5

Note: Values adjusted to 100% for shales of each age.

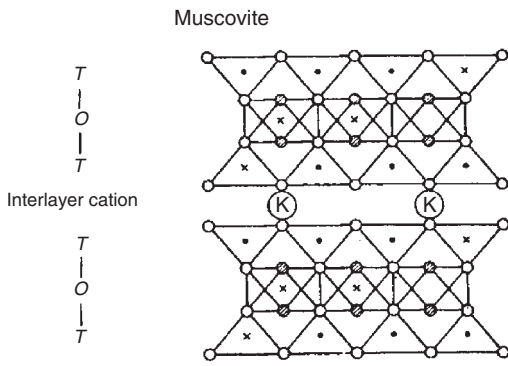
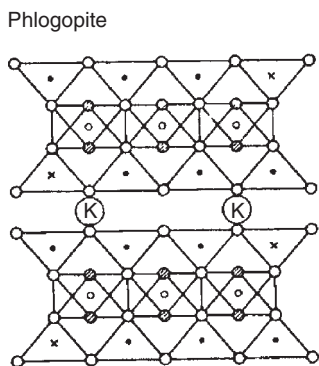
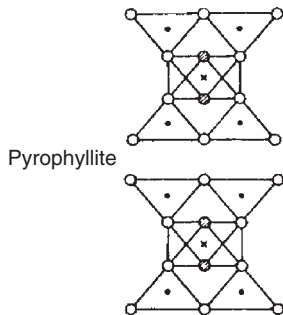
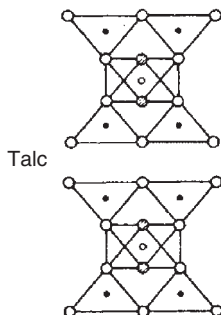
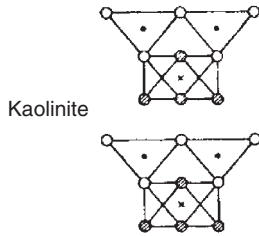
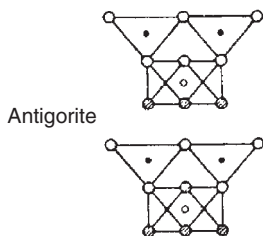
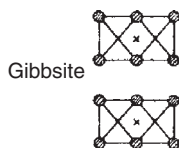
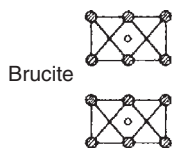
Source: O'Brien, N. R. and R. M. Slatt, 1990, *Argillaceous Rock Atlas*, Springer-Verlag, New York, NY, Table 1, pp. 124–125.

Phyllosilicates also contain groups of OH^- ions joined with cations (aluminum, magnesium, iron) in a sixfold coordination, leading to an **octahedral** configuration. These octahedra can be linked to form octahedral sheets. Tetrahedral sheets are often referred to as T layers and octahedral sheets are called O layers. All phyllosilicate minerals are formed by various combinations of T layers and O layers, as illustrated schematically in Fig. 6.10.

Some phyllosilicates have a one-layer (1:1), or T-O structure. Examples are **kaolinite** (dioctahedral) and **antigorite** (trioctahedral) (Fig. 6.10). Individual T-O layers are joined to other T-O layers by relatively weak van der Waals bonds, which accounts for the good cleavage of these phyllosilicates. Other phyllosilicates have a two-layer (2:1), or T-O-T, structure in which individual T-O-T layers are likewise bonded to each other by weak van der Waals bonds. Examples are **pyrophyllite** (dioctahedral) and **talc** (trioctahedral). Other clay minerals are derived from this basic T-O-T structure by substitution of trivalent aluminum ions for some tetravalent silicon ions in the cation sites of tetrahedral sheets. Each substitution of an aluminum ion results in creation of a free negative charge on the surface of the T-O-T sheet. For example, if an aluminum ion is substituted for every fourth silicon ion in the pyrophyllite structure, a

Trioctahedral

Di-octahedral



O = Octahedral
T = Tetrahedral

○ = Oxygen
⊗ = Hydroxyl
● = Silicon
× = Aluminium
◊ = Magnesium

Figure 6.10 Schematic representation of the linking of T and O layers to form clay minerals and micas. (From Klein, C. and C. S. Hurlbut, Jr. 1985, *Manual of Mineralogy*, 20th edn.: John Wiley and Sons, New York, NY, Fig. 11.69, p. 421. Reprinted by permission.)

univalent negative charge results. A univalent cation (K) can be bound in the interlayer position to balance this charge, yielding the **true micas** (see the muscovite structure in Fig. 6.10). Similarly, substitution of one aluminum ion for every fourth silicon ion in the trioctahedral talc structure, and binding of an interlayer potassium ion, yields **phlogopite**. Binding sodium rather than potassium in the interlayer position of talc yields **paragonite**.

Smectite clay minerals such as montmorillonite are derived from the pyrophyllite structure by insertion of sheets of molecular water containing exchangeable cations between pyrophyllite T-O-T layers. Similarly, **vermiculite** is derived from the talc structure by interlamination of sheets of water molecules. **Illite** has a composition somewhat intermediate between smectite and the true micas. It is derived by random substitution of aluminum for silicon in tetrahedral sites of pyrophyllite and introduction of some molecular water containing potassium between pyrophyllite T-O-T layers. **Chlorites** consist of two layers of talc separated by a brucite-like octahedral layer or two layers of pyrophyllite separated by a gibbsite-like octahedral layer. For discussion of the derivation of other phyllosilicates see Klein and Hurlbut (2002).

Classification and identification of clay minerals

The clay minerals and related phyllosilicates can be divided into a few distinct groups on the basis of layer type and cation content of the octahedral sheet (dioctahedral or trioctahedral; Table 6.4). Subdivision of these basic groups into subgroups and species is made on the basis of layer charge, type of interlayer material, type of layer stacking, chemical composition, and type of component layers and nature of stacking (ordered, random) for mixed-layer clays (Eslinger and Pevear, 1988, pp. 2–10). The clay minerals are a complex group of minerals, and detailed discussion of these minerals and their distinguishing characteristics is beyond the scope of this book. Readers are referred to specialized works on clay minerals such as Velde (1995) and Meunier (2005) for additional information.

Our primary concern in this book is with the more common clay mineral groups: kaolin or kaolinite, smectite (particularly montmorillonite), the true micas (especially muscovite, biotite, illite), and chlorite. Mixed-layer clay minerals, chlorite/smectite or illite/smectite, are also common constituents of shales and mudstones.

6.4.2 Chemical composition

The principal minerals that occur in shales and mudstones are indicated in Table 6.2. The relative abundance of the major minerals (Table 6.3), in turn, determines the chemical composition of these rocks. Table 6.5 shows the average chemical composition of selected shales and mudstones from North America and Russia.

As shown in Table 6.5, SiO₂ is most abundant chemical constituent in shales and mudstones. The SiO₂ content of these fine-grained rocks is influenced by all silicate minerals present but it is particularly affected by quartz, which is an abundant constituent of most shales and mudstones. Aluminum is the second most abundant chemical constituent. The Al₂O₃ content is related particularly to feldspar and clay-mineral abundance. Owing to the generally

Table 6.4 *Classification of clay minerals*

Layer type	Interlayer material	Group	Subgroup	Species (examples)
1:1	None or H ₂ O only	Serpentine–kaolin ($x \sim 0$)	Serpentine	Chrysotile, lizardite, berthierine
			Kaolin	Kaolinite, dickite, nacrite, halloysite
2:1	None	Talc–pyrophyllite ($x \sim 0$)	Talc	Talc, willemseite
			Pyrophyllite	Pyrophyllite
	Hydrated exchangeable cations	Smectite ($x \sim 0.2-0.6$)	Saponite	Saponite, hectorite, saunonite, stevensite, etc.
			Montmorillonite	Montmorillonite, beidellite, nontronite
	Hydrated exchangeable cations	Vermiculite ($x \sim 0.6-0.9$)	Trioctahedral vermiculite	Trioctahedral vermiculite
			Diocahedral vermiculite	Diocahedral vermiculite
	Nonhydrated cations	True mica ($x \sim 0.5-1.0$)	Trioctahedral true mica	Phlogopite, biotite, lepidolite, annite
			Diocahedral true mica	Muscovite, illite, glauconite, paragonite, celadonite
	Nonhydrated cations	Brittle mica ($x \sim 2.0$)	Trioctahedral brittle mica	Clintonite
			Diocahedral brittle mica	Margarite
Hydroxide	Chlorite (x variable)	Trioctahedral chlorite	Clinochlore, chamosite, nimite, pennantite	
		Diocahedral chlorite	Donbassite	
2:1 Mixed-layer (regular)	Variable	None	None	Hydrobiotite, rectorite, corrensite, aliettite, tosudite, kulkeite
Modulated 1:1 layer	None	No group name ($x \sim 0$)	No subgroup name	Antigorite, greenalite
Modulated 2:1 layer	Hydrated exchangeable cations	Sepiolite–palygorskite (x variable)	Sepiolite	Sepiolite, loughlinitite
			Palygorskite	Palygorskite
	Variable	No group name (x variable)	No subgroup name	Minnesotaite, stilpnomelane, zussmanite

x = layer charge/O₁₀ (OH)₂

Source: Eslinger, E. and D. Pevear, 1988, *Clay Minerals*: See. Econ. Paleontologists and Mineralogists Short Course Notes 22. Table 2.1, pp. 2–12, reprinted by permission of SEPM, Tulsa, OK.

Table 6.5 Average chemical composition of selected shales and mudstones reported in the literature

	1	2	3	4	5	6	7	8	9	10	11	12	13
SiO ₂	60.65	64.80	59.75	56.78	67.78	64.09	66.90	63.04	62.13	65.47	64.21	64.10	40–73
Al ₂ O ₃	17.53	16.90	17.79	16.89	16.59	16.65	16.67	18.63	18.11	16.11	17.02	17.70	13–32
Fe ₂ O ₃	7.11	–	–	–	–	–	–	–	–	–	–	2.70	
FeO	–	5.66	5.59	6.56	4.11	6.03	5.87	7.66	7.33	5.85	6.71	4.05	2–20
MgO	2.04	2.86	4.02	4.56	3.38	2.54	2.59	2.60	3.57	2.50	2.70	2.65	<1–6
CaO	0.52	3.63	6.10	8.91	3.91	5.65	0.53	1.31	2.22	4.10	3.44	1.88	<1–6
Na ₂ O	1.47	1.14	0.72	0.77	0.98	1.27	1.50	1.02	2.68	2.80	1.44	1.91	<0.1–5
K ₂ O	3.28	3.97	4.82	4.38	2.44	2.73	4.97	4.57	2.92	2.37	3.58	3.60	<1–11
TiO ₂	0.97	0.70	0.98	0.92	0.70	0.82	0.78	0.94	0.78	0.49	0.72	0.86	
P ₂ O ₅	0.13	0.13	0.12	0.13	0.10	0.12	0.14	0.10	0.17	–	–	–	
MnO	0.10	0.06		0.08		0.07	0.06	0.12	1.10	0.07	0.05	–	<0.1–0.3

Source:

- (1) Moore, 1978 (Pennsylvanian shale, Illinois Basin)
- (2) Gromet *et al.*, 1984 (North American shale composite)
- (3) Ronov and Migdisov, 1971 (average North American Paleozoic shale)
- (4) Ronov and Migdisov, 1971 (average Russian Paleozoic shale)
- (5) Ronov and Migdisov, 1971 (average North American Mesozoic shale)
- (6) Ronov and Migdisov, 1971 (average Russian Mesozoic shale)
- (7) Cameron and Garrels, 1980 (average Canadian Proterozoic shale)
- (8) Ronov and Migdisov, 1971 (average Russian Proterozoic shale)
- (9) Cameron and Garrels, 1980 (average Canadian Archean shale)
- (10) Ronov and Migdisov, 1971 (average Archean shale)
- (11) Clark, 1924 (average shale)
- (12) Shaw, 1956 (compilation of 155 analyses of shale)
- (13) Melson *et al.*, 1998, (ranges of values compiled from 102 analyses of shales from 34 geological formations)

high abundance of clay minerals in shales and mudstones, these minerals have a strong influence on shale chemistry. The aluminum content of kaolinites is particularly high; therefore, shales that contain exceptionally high aluminum (>20 percent Al₂O₃), called **high alumina shales**, are likely to contain high percentages of clay minerals, especially kaolinite.

The oxides K₂O and MgO each make up less than 5 percent of average shale. Potassium and magnesium abundance in shales and mudstones is particularly affected by clay-mineral abundance, although some magnesium may be supplied by dolomite, and potassium is contained in potassium feldspars. Shales containing more than 5 percent K₂O are comparatively rare. These **potassic shales** have been suggested to owe their high potassium content to the presence of authigenic K-feldspars. Sodium oxide, Na₂O, makes up about 1–3 percent of average shale. Sodium abundance is related both to clay minerals (e.g. smectites) and to the content of sodium plagioclase.

The average abundance of iron oxides ($\text{Fe}_2\text{O}_3 + \text{FeO}$) in shales and mudstones is commonly between about 5 and 10 percent. Iron is supplied by iron oxide minerals (hematite, limonite, goethite), some fine micas and clay minerals, e.g. biotite, smectites, and chlorite, and the carbonate minerals siderite and ankerite. Also, substantial amounts of iron in some organic-rich shales are contained in sulfide minerals (pyrite, marcasite). Shales containing more than about 15 percent iron oxides are called **ferruginous shales** or **ferriferous shales**.

Table 6.5 shows that the CaO content of shales and mudstones ranges from less than 1 percent to almost 10 percent. Calcium in shales and mudstones is derived from calcium-rich plagioclase and from carbonate minerals, particularly calcite and dolomite. Calcium is contained also in some of the clay minerals and in gypsum and anhydrite. Shales particularly enriched in carbonates are called **calcareous shales**.

Oxides of titanium and phosphorus make up less than 1 percent each of average shales and mudstones. Although the P_2O_5 content of shales is commonly less than about 0.2 percent, some so-called **phosphatic shales** contain substantially greater abundances. Phosphatic shales that contain more than about 20 percent P_2O_5 are called **phosphorites**. The origin of phosphorites is discussed in Chapter 12. In addition to major elements, shales and mudstones contain a variety of trace elements: B, Ba, Ga, Cr, V, Li, Ni, Co, Cu, Sc, Zr, Sr, Pb, and a host of others. The trace-element abundance of shales has a complex relationship to provenance, depositional environments, and diagenesis.

Because chemical composition is a direct function of mineralogy, and mineral composition varies with grain size, the major-element chemical composition of shales and mudstones is related also to grain size. Coarser-grained shales and mudstones contain more quartz than do finer-grained ones and thus tend to have a higher SiO_2 content. Finer-grained shales and mudstones contain higher percentages of clay minerals, resulting particularly in aluminum enrichment and lower SiO_2 concentrations. Calcium, magnesium, and potassium tend also to be concentrated in the finer fraction of shales and mudstones; however, calcium and magnesium content can be strongly influenced by secondary carbonate cements that may be particularly abundant in coarser-grained mudstones and shales.

6.4.3 Organic-matter content of shales and mudrocks

Most of the organic matter in shales is fine-size sapropel, which consists largely of the remains of phytoplankton, zooplankton, spores, pollen, and the macerated fragments of higher plants. During burial and diagenesis, this organic matter goes through a series of complex changes, brought about by combined biochemical and chemical attack. These diagenetic processes destroy much of the organic matter and convert the remainder to an insoluble substance called kerogen. Most of the organic matter in shales consists of kerogen. Additional details about the origin of kerogen, as well as discussion of the chemical and isotope composition of organic matter, are given in Chapter 13.

Most sedimentary rocks deposited under aqueous conditions contain some organic material. Data compiled by Tissot and Welte (1984, p. 97) show that average relative abundance of organic carbon in shales and mudstones, reported by various workers, ranges between about

1.0 and 2.2 percent. Some black shales contain considerably greater amounts than this average, ranging to 10 percent or more. Sedimentary rocks that are exceptionally rich in organic carbon are discussed in [Chapter 13](#). The abundance of organic matter in sedimentary rocks depends upon a number of factors, including grain size of the sediment, depositional environment, and sediment mineralogy. These factors are examined further in [Chapter 13](#).

6.5 Color of mudstones and shales

Mudstones and shales may have a variety of colors ranging through red, brown, yellow, green, light gray, and dark gray to black. An excellent discussion of the causes of colors in shales is given by Potter *et al.* (1980, p. 53). The colors of shales appear to be a function mainly of the carbon content and the oxidation state of iron in the shales. The progression of colors from light gray through dark gray to black correlates with increasing carbon content of shales, whereas variations in color from red through purple to greenish gray correlate with decreasing ratios of $\text{Fe}^{3+}/\text{Fe}^{2+}$. The oxidation state of iron appears to be much more important in determining the color of sediments (Fe^{3+} iron gives red colors, Fe^{2+} iron gives green colors) than the total amount of iron present in the rocks. On the other hand, a few studies have shown that there is less iron in some greenish or gray sediments than in associated red sediments. The oxidation state of iron is controlled by the amount of organic matter in sediments, which can furnish electrons to drive iron into the reduced state. Therefore, green or greenish-gray shales tend to have a higher organic matter content (less organic matter is destroyed by oxidation) than red or yellow shales.

Color is associated in a very general way with depositional conditions. That is, black shales tend to form in relatively deep, restricted basins where reducing conditions prevail and abundant organic matter is preserved. Alternatively, they form in some shallow-water, tidal-flat and estuarine environments where organic matter is abundant. Red shales are characteristic of oxidizing environments. Such environments occur particularly in continental settings. Red muds accumulate also in deep-sea basins where sedimentation rates are low, and the muds are thus in contact with oxidizing bottom waters for long periods of time. The colors of muds that prevail at the time of deposition can be changed during burial diagenesis and uplift if the sediments are brought into a different chemical environment. Thus, the ferric iron (Fe^{3+}) that characterizes red shales at the time of deposition may subsequently be reduced to ferrous iron (Fe^{2+}) during diagenesis to yield green shales. Likewise, green shales can be changed to red shales after deposition if initial reducing conditions are subsequently followed by oxidizing conditions. Because color can be affected so markedly by diagenesis, it is not a reliable indicator of depositional conditions.

6.6 Classification of mudstones and shales

Classification of sandstones and conglomerates is based primarily on the mineralogy or particle composition of these rocks, although texture (matrix abundance) is used as a secondary classification parameter in some classifications. By contrast, classification of shales and

mudstones on the basis of mineralogy has generally been regarded as impractical because of the difficulty in obtaining quantitative data on shale composition owing to their fine grain size. Thus, proposed classifications are based mainly on texture (grain size) and structure (lamination).

Many geologists are content to use informal names for mudstones and shales that reflect properties such as color (red shales, green shales, black shales), organic content (carbonaceous shales), or relative abundance of particular kinds of cementing materials or chemical constituents (calcareous shales, ferriferous shales, high-alumina shales, phosphatic shales, siliceous shales). Nonetheless, a few formal classifications for fine-grained rocks do exist.

Most proposed classifications of fine-grained rocks are based upon the relative abundance of silt-size and clay-size particles in these rocks and upon the presence or absence of lamination or fissility. An example of classification on the basis of grain size is shown in Fig. 6.11. Potter *et al.* (2005, p. 256) and Macquaker and Adams (2003) discuss other examples. The classification of Potter *et al.* (1980, p. 14), reproduced here as Table 6.6, is an example of a classification that uses both grain size and lamination as classification parameters. These authors suggest that other properties of shales and mudstones such as mineralogy, color, fossil content, and types of organic constituents can be used as adjectival modifiers for the basis textural names shown in Table 6.6.

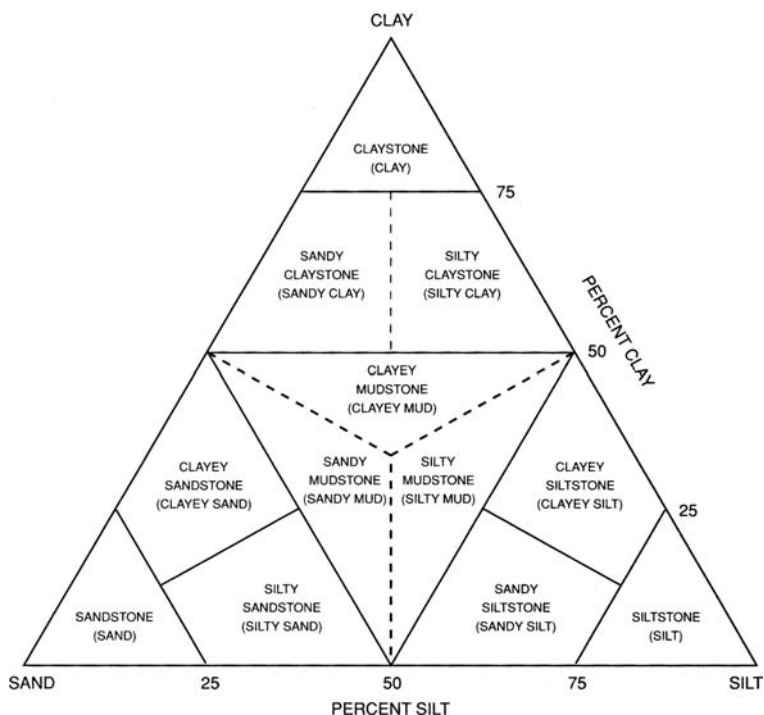


Figure 6.11 Textural classification of fine-grained rocks and sediments. (From Picard, M. D., 1971, Classification of fine-grained sedimentary rocks: *J. Sediment. Petrol.*, **41**, Fig. 3, p. 185. Reprinted by permission of Society for Sedimentary Geology, Tulsa, OK.)

Table 6.6 *Textural classification of shales*

Percentage clay-size constituents			0–32	33–65	66–100
Field adjective			Gritty	Loamy	Fat or slick
Nonindurated	Beds	Greater than 10 mm	Bedded silt	Bedded mud	Bedded claymud
	Laminae	Less than 10 mm	Laminated silt	Laminated mud	Laminated claymud
Indurated	Beds	Greater than 10 mm	Bedded siltstone	Mudstone	Claystone
	Laminae	Less than 10 mm	Laminated siltstone	Mudshale	Clayshale
Metamorphosed		Degree of metamorphism Low ↓ High	Quartz argillite	Argillite	
			Quartz slate	Slate	
			Phyllite and/or mica schist		

Source: Potter, P. E. *et al.*, 1980, *Sedimentology of Shale*, Table 1.2, p. 16, reprinted by permission of Springer-Verlag, New York, NY.

6.7 Distribution and significance of mudstones and shales

6.7.1 Occurrence in time and space

As mentioned in the chapter introduction, mudstones and shales make up about 50 percent of all sedimentary rocks. Most of these mudstones and shales are of marine origin. They occur in stratigraphic successions of all ages and on all continents of the world. Ronov

(1983) indicates that shales have been the dominant sedimentary rock deposited throughout most of geologic time (Fig. 1.3). Their overall abundance in the geologic record reflects the high average abundance of fine-grained material generated by the processes of weathering and erosion (which are related to elevated landmasses and high rainfall); the general availability through time of oceanic and interior basins to serve as catchment areas for fine sediment; and the relative efficiency of transporting agencies such as bottom currents, turbidity currents, suspension transport mechanisms, nepheloid transport mechanisms, and wind for movement of fine sediment to more distal parts of depositional basins.

The wide distribution of mudstones and shales in space and time suggests that the environments that favor deposition of fine sediment are common and that they have recurred throughout time. Mudstones and shales are not especially characteristic of any particular geologic time. They are abundant in rocks of all ages; however, their geographic distribution varies as a function of age. Thus, their relative abundances reflect changing patterns of land and sea through time. The relative abundances of mudstones and shales in stratigraphic successions of a particular age are related to depositional setting. The thickest shale and mudstone sections tend to occur in sedimentary successions that were deposited in mobile, marine basins. Nonetheless, moderate thicknesses of nonmarine mudstones and shales (some oil shales, for example) can occur in stratigraphic successions deposited in interior basins, either in lacustrine or alluvial basins.

Potter *et al.* (2005, p. 78) suggest that ancient muddy sediments were deposited particularly in meander and anastomosing stream systems on continents, in interdistributary portions of deltas, in some quiet-water transitional-marine coastal environments such as lagoons and estuaries, and in many low-energy marine environments on the shelf, slope, and deep ocean floor.

Fine-grained sediment may be deposited on land by wind to form loess or other eolian deposits; however, most fine, siliciclastic sediment is deposited in water. Deposition takes place mainly in quiet water, below wave base, at water depths ranging from tens of meters to thousands of meters. As mentioned above, such low-energy environments can be present in a variety of depositional settings on continents (i.e. lakes, alluvial piedmonts or plains, river floodplains), in transitional marine environments (deltas, estuaries, lagoons, tidal flats), on the shallow-marine shelf and the continental slope, and in deeper-marine basins. In continental settings, fine sediment is transported in suspension by wind and by stream flow. It may also be transported, together with sand and gravel, by glacial ice and by mass-transport processes (mud flows, debris flows, turbidity currents in lakes). Fine sediment that is delivered to the ocean by any of these processes can be retransported further seaward by several mechanisms that may include storm-generated waves and currents, suspension transport in near-surface plumes, near-bottom nepheloid transport, turbidity currents, and bottom currents, as mentioned. Overall, turbidity currents are probably the most important mechanism for moving large quantities of fine sediment to distal parts of deep basins. Wind may also transport fine sediment from land to distant regions of the ocean and may be the principal mechanism for transport of pelagic sediment. See Boggs (2006) for discussion of sediment transport processes.

Within the depositional environment, deposition of fine sediment takes place by slow gravity settling of dispersed single particles or by more-rapid settling of clay flocs. Organisms may

aid in deposition of fine sediment by pelletizing muds and by creating baffles or other features (e.g. algal mats) that trap and hold fine sediment.

Mudstones and shales deposited in a given depositional environment acquire characteristic properties (geometry, lithology, facies associations, textures, structures, fossil content) that may allow them to be distinguished from mudstones and shales of other environments. Thus, they may be important paleoenvironmental indicators. See Potter *et al.* (1980, table 1.9) for a useful summary of the characteristic properties of mudstones and shales deposited in major environments. Further discussion of muddy depositional systems may be found in many published sources, such as Potter *et al.* (2005, ch. 5) and several papers in Schieber *et al.* (1998, vol. 1).

6.7.2 Significance of mudstone and shale occurrence

The presence of thick units of mudstones or shales in ancient stratigraphic sequences implies derivation of fine-grained sediment from large-volume land masses that were weathered and eroded under generally humid, high-rainfall conditions. Furthermore, the presence of mudstones and shales in a stratigraphic section suggests deposition in a quiet-water paleoenvironment. Most thick units were deposited in marine basins and tend to be laterally extensive. Individual marine mudstone and shale beds may be relatively thin, but they can commonly be traced laterally for considerable distances. By contrast, associated sandstone, conglomerate, or limestone facies are generally more restricted in their lateral extent. Therefore, many mudstone and shale beds make excellent stratigraphic markers. In comparison to marine mudstones and shales, shale and mudstone sequences deposited in nonmarine settings tend to be thinner overall and laterally less extensive.

As discussed, mudstones and shales may display lithologic characteristics, sedimentary structures, fossil content, organic content, geochemical characteristics, and facies associations that have environmental significance. Furthermore, mudstones and shales, or facies closely associated with these rocks, may contain directional sedimentary structures that are useful as paleocurrent indicators. Clay minerals and feldspars in fine-grained rocks may have some importance as provenance indicators, although these rocks are generally less useful than sandstones in provenance studies (Chapter 7). Finally, mudstones and shales have considerable economic significance as source beds for petroleum and natural gas. Careful geochemical evaluation of the amount and types of kerogen in fine-grained rocks (Chapter 13) is now routine procedure in petroleum exploration programs.

Thus, in summary, mudstones and shales have paleoclimatic, paleoenvironmental, provenance, and economic significance. They deserve greater attention in future sedimentological studies than they have received in the past.

6.8 Examples

Because mudstones and shales are so common in sedimentary successions of all ages and on all continents, examples of these rocks are numerous. Geologists from any continent can readily compile an extensive list of mudstone and shale formation names. Some mudstones

and shales are internationally “famous” owing to their lithologic makeup, thickness and geographic extent, fossil content, or tectonic and stratigraphic significance, or to their economic potential as oil source beds or sites of copper mineralization or other mineralization. Examples include the Precambrian Figtree shales of South Africa, known for their early fossils; the Middle Cambrian Burgess Shale of British Columbia, famous for its preserved remains of soft-bodied organisms; the Silurian Gothlandian shales that extend throughout western Europe and much of northern Africa and the Persian Gulf; the organic-rich Devonian to Mississippian black shales (Ohio Shale, New Albany Shale, Chattanooga Shale, etc.) that cover much of the central and eastern parts of North America; the Permian Kupferschiefer of western Europe, known for its mineralization of copper, lead, and zinc; the Cretaceous Mowery Shale of the western interior of the United States, a thick, siliceous shale that is believed to be a major source bed for oil; and the Eocene Green River Oil Shale of Utah, Colorado, and Wyoming (USA), a well-known oil shale/mudstone that has high kerogen content with significant recoverable oil potential. These, and some other world-famous shales/mudstones, are pointed out by Potter *et al.* (1980, p. 83).

Further reading

- Bennett, R. H., W. R. Bryant, and M. H. Hulbert, 1991, *Microstructures of Fine-Grained Sediments*: Springer-Verlag, New York, NY.
- Chamley, H., 1989, *Clay Sedimentology*: Springer-Verlag, Berlin.
- Eslinger, E. and D. Pevear, 1988, *Clay Minerals for Petroleum Geologists and Engineers*: SEPM Short Course Notes 22.
- O’Brien, N. R. and R. M. Slatt, 1990, *Argillaceous Rock Atlas*: Springer-Verlag, New York, NY.
- Potter, P. E., J. B. Maynard, and W. A. Pryor, 1980, *Sedimentology of Shale*: Springer-Verlag, New York, NY.
- Potter, P. E., J. B. Maynard, and P. J. Depetris, 2005, *Mud and Mudstones*: Springer-Verlag, Berlin.
- Schieber, J., W. Zimmerle, and P. S. Sethi, 1998, *Shales and Mudstones I and II*: E. Schweizerbart’sche Verlagsbuchhandlung, Stuttgart, vol. 1; vol. 2.
- Stow, D. A. V. and D. J. W. Piper (eds.), 1984, *Fine-Grained Sediments: Deep-Water Processes and Facies*: Geological Society Special Publication 15.
- Velde, B., 1995, *Mineralogy of Clays*: Springer-Verlag, Berlin.
- Weaver, C. E., 1989, *Clays, Muds, and Shales*: Elsevier, Amsterdam.
- Wignall, P. B., 1994, *Black Shales*: Clarendon Press, Oxford.

Provenance of siliciclastic sedimentary rocks

7.1 Introduction

In the preceding chapters, I characterized sedimentary rocks in terms of their physical and chemical properties. Such characterization is not, however, the principal reason that we normally undertake research on sedimentary rocks. Determining the physical and chemical properties of these rocks is simply a means to a more important end, which is to reconstruct the history of the rocks. Our ultimate aim in studying siliciclastic sedimentary rocks is to develop a fuller understanding of (1) the source(s) of the particles that make up the rocks, (2) the erosion and transport mechanisms that moved the particles from source areas to depositional sites, (3) the depositional setting and depositional processes responsible for sedimentation of the particles (the depositional environment), and (4) the physical and chemical conditions of the burial environment and the diagenetic changes that occur in siliciclastic sediment during burial and uplift. These objectives, in turn, are important to the broader goal of developing reliable paleogeographic models of Earth for particular times in the past. Some studies have a further purpose of evaluating siliciclastic sedimentary rocks in terms of their economic potential as reservoir rocks for oil and gas, source beds for petroleum, host rocks for ore mineralization, groundwater aquifers, and so on.

In this chapter, we deal with one of these important objectives of geologic research, understanding the sources of siliciclastic sediment. We commonly refer to sediment source as provenance. The term **provenance** is derived from the French **provenir**, meaning to originate or come forth (Pettijohn *et al.*, 1987, p. 254). The term is also spelled provenience. Words such as source area and sourceland are sometimes used as synonyms for provenance. As the word provenance is commonly used by sedimentologists today, however, it has a broader meaning than just source area. The meaning of provenance has been extended to encompass the location of the source area (how far away was it and in what direction?), its size or volume, the lithology of the parent source rocks, the tectonic setting or the source area, and the climate and relief of the source area. Provenance studies are especially important to our understanding of paleogeography. When coupled with studies of depositional environments, they help us interpret the relative positions of ancient oceans and highlands at given times in the geologic past. From such studies, we are able to reconstruct the location, size, and lithologic composition of mountain systems

that have long since vanished. We may even be able to make intelligent guesses about the climate and relief of these highlands, as well as the tectonic setting in which the source area lay.

Most early studies of provenance focused on determining the lithology of parent source rocks, as interpreted from the particulate components of sandstones and conglomerates. Many investigators also sought to identify the locations of source areas on the basis of paleocurrent analysis of directional sedimentary structures and by mapping grain-size or grain-shape trends. Beginning in the 1970s, emphasis shifted to interpretation of tectonic setting in terms of plate-tectonic concepts; that is, characterization of source areas as magmatic arcs, collision orogens, or continental blocks. Only a few studies have focused on interpreting climate and relief of source area, possibly owing to the fact that such interpretations are difficult to make and their reliability is somewhat tenuous. Most provenance studies have involved analysis of sandstones or conglomerates; relatively few studies of shale provenance have been published. In this chapter, we examine some of the tools and techniques that sedimentologists use to interpret provenance.

7.2 Tools for provenance analysis

7.2.1 General statement

The most important features of siliciclastic sedimentary rocks upon which provenance interpretations are based are (1) the mineralogy and chemical composition of the detrital components in the rocks, from which we read source-rock lithology and tectonic setting, and (2) the presence of directional features in the rocks (sedimentary structures and particle size and shape gradients) that allow interpretation of paleocurrent patterns. Other characteristics of siliciclastic deposits useful in provenance analysis include the paleomagnetic characteristics of the rocks, which help establish the paleolatitude of the source area; vertical and lateral facies relationships of stratigraphic units, which are related to sediment transport directions; and the overall thickness and volume of siliciclastic units, which reflect to some degree the size of source area (Fig. 7.1).

7.2.2 Composition of detrital constituents

The mineralogy of the detrital particles in siliciclastic sedimentary rocks furnishes the primary evidence for the lithology of the parent rocks in the source area. Our knowledge of the lithology of vanished ancient mountain systems rests mainly on analysis of detrital framework modes of siliciclastic deposits derived from these mountains. Mineralogy also provides our most useful evidence for interpreting tectonic setting because source-rock lithology is linked fundamentally to tectonic setting. Detrital mineralogy may also provide limited insight into climatic conditions on the basis of the assumption that mineralogic maturity of sediments is determined in part by selective destruction of minerals at weathering sites. Weathering under very cold or very dry conditions presumably allows preservation

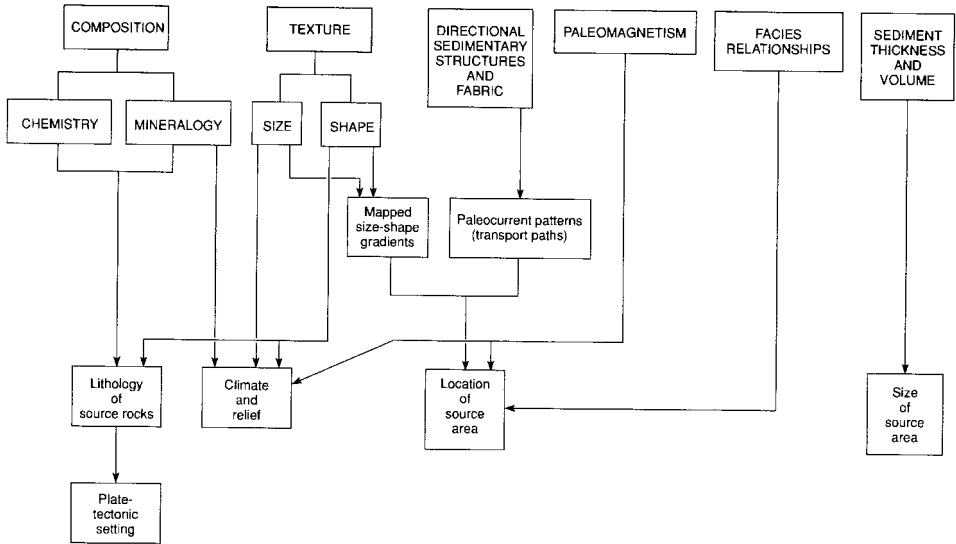


Figure 7.1 Properties of sedimentary rocks and their relationship to provenance.

of unstable minerals, whereas intense weathering under hot, humid conditions does not. Thus, detrital minerals provide some clues to climate. Chemical composition of minerals, particularly their trace-element chemistry, may aid also in identifying the lithology of source rocks. The cathodoluminescence characteristics of some minerals, particularly quartz, have significant value in source-rock interpretation (see Boggs and Krinsley, 2006, ch. 4).

7.2.3 Textures and structures

The textures and structures of siliciclastic sedimentary rocks provide the most direct evidence for location of source areas. Mapping grain-size trends and grain-shape trends together with evidence derived from directional sedimentary structures such as flute casts and cross-beds allows interpretation of paleocurrent directions. Thus, textural and structural data help fix the general direction in which the source area was located. Grain-size and -shape data may also provide some insight into the climate and relief of source areas, under the assumption that the nature and intensity of weathering can affect the sizes of particles released from source rocks. High-relief source areas tend to promote more-rapid erosion, and thus derivation of coarser particles, than low-relief source areas where slower erosion allows more time for size reduction by weathering processes. On the other hand, the grain size of sediments is a function of numerous complex variables, such as size sorting during sediment transport, and is not easily related to climate and relief. In terms of grain shape, intense rounding of grains, for example, could point to eolian activity and desert conditions in source areas.

7.2.4 *Thickness and volume of siliciclastic units*

The existence of vanished mountain systems and other highlands that acted as sediment sources in the past is known only indirectly from the preserved record of sediments stripped from these highlands and deposited in nearby or distant basins. The overall size of these vanished highlands can be estimated roughly from the volume of siliciclastic sediments preserved in the basins. Such estimates are indeed rough because the source area may have included considerable volumes of soluble rocks such as limestones. Also, much mud-size sediment derived from the source area may have been transported to and dispersed within distal areas where it cannot readily be tied to a particular source area.

7.2.5 *Paleomagnetism*

The magnetic inclination preserved in iron-bearing minerals in rocks of any kind is now used routinely as a tool for interpreting the paleolatitude at which rocks formed. [See, for example, Tauxe (2002) for information about paleomagnetism.] When applied to siliciclastic sedimentary rocks, a knowledge of paleolatitude allows geologists to determine if the rocks are now located in the same latitude in which they were deposited. If they are not, they are part of a displaced or exotic terrane. In such a case, the sedimentary rocks may (or may not) have been rifted away from their source area, which could now exist at some completely different location with respect to the depositional basin. A knowledge of the paleolatitude at which the sediments were deposited can be useful also in interpreting the climate of the source area or at least in constraining interpretations of climate on the basis of other factors.

7.2.6 *Facies relationships*

When displayed in maps and cross-sections, vertical and lateral facies relationships allow interpretation of source directions. Facies-relationships maps can be related to directional features such as cross-bedding and thus to paleoslope. Clastic ratio maps or sand-clay ratio maps, for example, give a clear indication of the general source direction of clastic detritus. Examination of a series of stratigraphic units of different ages can reveal the persistence, or lack of persistence, of a particular source area or can show geographic shifts in major sediment-dispersal centers as a function of time.

7.3 *Locating source areas*

7.3.1 *Paleocurrent analysis*

Methods for determining the relative positions of ancient source areas and depositional basins are based primarily on paleocurrent analysis of sedimentary rocks derived from these source areas. Paleocurrent indicators help establish paleoslope and paleotransport directions, which, in turn, reveal the direction in which the source area lay with respect to the depositional basin. Overall, the most useful paleocurrent indicators are probably the various

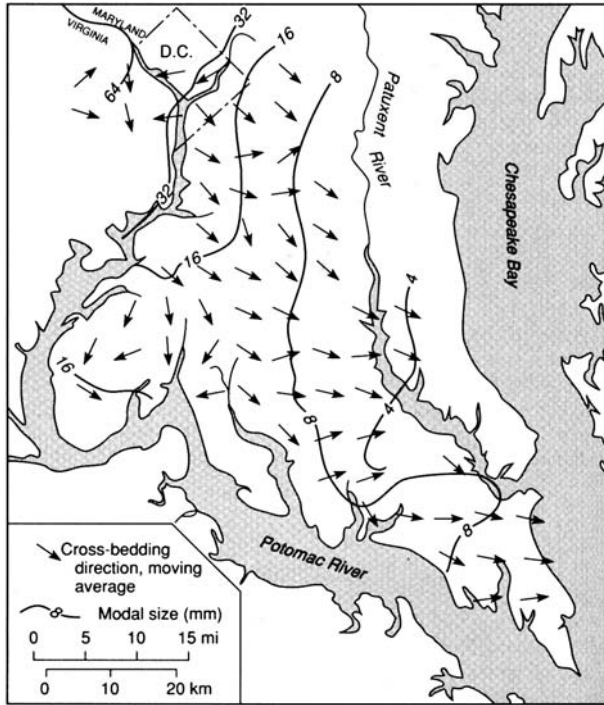


Figure 7.2 Example of the use of paleocurrent data to locate sediment source areas. Brandywine gravel of Maryland. (From Potter, P. E. and F. J. Pettijohn, 1977, *Paleocurrent and Basin Analysis*, Fig. 8–9, p. 282, reprinted by permission of Springer-Verlag, Berlin.)

kinds of directional sedimentary structures such as flute casts, ripple marks, and cross-beds. Methods of measuring the orientation of directional structures and presentation of directional data are discussed in [Section 3.7.2](#). Fabric elements of sediments such as long-axis orientation and imbrication of pebbles also have directional significance ([Section 2.3.8](#)). When paleocurrent data are plotted on maps such as that shown in [Fig. 7.2](#), the relative position of the source area with respect to the depositional basin may be clearly indicated.

7.3.2 Mapping scalar properties

In the absence of directional sedimentary structures or fabric elements, mapping the presence of distinctive minerals or pebbles of a particular lithology may point toward the source area. Such maps may reveal dispersal patterns and thus sediment source directions. Mapping the grain-size distributions within sandstone or conglomeratic deposits may likewise have directional significance. In conglomeratic rocks, grain-size distribution maps are typically based on maximum clast size, which is commonly given as the mean intermediate clast diameter of the ten largest clasts measured at each sample point. In sandy sediments, maps of either mean or maximum grain size may be prepared. If one works under the general assumption that sediments become

finer grained away from the source, grain-size distribution maps may reveal distinctive grain-size trends that point toward the sediment source area. Figure 7.2 shows contours of modal grain size as well as paleocurrent patterns. Note in this example that grain-size change and paleocurrent vectors indicate that the source area lay to the west of the map area.

Mapping grain shape (roundness, sphericity, form) to establish grain-shape trends is another possible technique to identify sediment dispersal directions. When such techniques are applied to pebbles, we might expect as a gross approximation that pebble roundness would increase in the direction of sediment transport. Further, particle form and sphericity might change also as a result of shape sorting and possibly abrasion during sediment transport. For example, roller-shaped and equant-shaped pebbles might be expected to outrun disc- and blade-shaped pebbles. Problems arising from factors such as pebble recycling, pebble breakage, and addition in fluvial systems of sediment from downstream tributaries and uncertainties about the relative effects of current shape sorting and abrasion on the shapes of pebbles all weaken the reliability of interpretations based on such techniques. These common shape techniques do not work well with sand-size particles because gross properties such as roundness and sphericity of sand-size quartz are not greatly affected by stream transport. More-sophisticated techniques for determining the shapes of quartz sand and silt by using Fourier shape analysis (Chapter 2) appear to hold greater promise for detecting meaningful downcurrent changes in particle shape.

Facies relationships that can be expressed in terms of thickness or lithologic character of various lithofacies can be mapped also. Such maps may be used as further evidence for sediment dispersal patterns and thus source-area location. Lithofacies-thickness (isopach) maps, maps that show the ratio of siliciclastic constituents to nonsiliciclastic constituents (clastic ratio maps), sand–shale ratio maps, facies maps that show the geographic distribution of major lithofacies types, and so on all provide evidence of sediment dispersal patterns (see Boggs, 2006, ch. 16).

7.3.3 Studies of paleomagnetism

As mentioned, the paleomagnetic characteristics of sedimentary rocks can be used to determine the paleolatitude of the depositional basin. Assuming that source areas are located within a few degrees of latitude to depositional basins, paleomagnetic evidence can be used to at least approximately locate the paleolatitude of source areas. Such evidence is particularly important in working with displaced terranes that may have been transported thousands of kilometers from their original location and may even have been rifted away from their source areas.

7.4 Factors that affect the composition of siliciclastic sedimentary rocks and provenance interpretation

7.4.1 General statement

Research on provenance analysis has focused especially on the particle framework composition of siliciclastic sedimentary rocks as a tool for interpreting lithology and

tectonic setting of source areas. It has long been recognized, however, that the composition of these rocks is controlled by more than the composition of the source rocks alone. Source-rock composition is certainly the first-order control on sediment composition, but the original composition may be severely modified by several factors, particularly (1) climate and relief of the source region, which control chemical weathering and erosion; (2) the nature of the sediment-transport process (including sediment recycling), which can affect composition by selective destruction of less-stable grains and selective sorting on the basis of size, shape, and specific gravity; (3) the depositional environment, where further selective grain destruction and sorting may take place, as well as mixing of sediment from different sources; and finally (4) diagenetic processes that may result in partial or complete dissolution of less-stable grains or their replacement by other minerals.

The factors that control sediment composition are summarized graphically in Fig. 7.3. As indicated by Johnsson (1993), the processes of sediment erosion, transport, deposition, and burial are intimately interlinked, which creates a complex web of feedback mechanisms that control sediment composition. For example, tectonic setting controls the slope and relief of the source area, which in turn control the duration time of sediment residence on slopes and thus the time available for chemical weathering processes to alter or destroy less-stable minerals. Realistic provenance interpretation requires that we recognize the many factors other than composition of parent source rocks that can affect sediment composition.

7.4.2 Effects of climate and relief

Climate (rainfall, temperature) and relief (elevation differences, slope angle) exert direct controls on the intensity and duration of weathering. It has long been recognized (e.g. Goldich, 1938) that the common rock-forming minerals have different stabilities with respect to chemical weathering processes. Minerals that crystallize at high temperatures (e.g., olivine, pyroxenes, amphiboles, calcium plagioclase) are less stable under chemical weathering conditions than minerals that crystallize at lower temperatures (e.g. sodium plagioclase, potassium feldspars, muscovite, quartz). Thus, chemical weathering processes act to selectively destroy less-stable minerals, which biases our ability to interpret provenance correctly from the surviving mineral assemblages in sediments.

We recognize in a general way that warm, humid climates increase weathering intensity and bring about, in a given period of time, greater destruction of parent-rock minerals than do very cold or very dry climates. Also, it is commonly accepted that low relief and gentle slopes promote chemical weathering because the duration of weathering is longer on gentle slopes. On the other hand, high relief and steep slopes favor erosion and rapid removal of minerals from the weathering environment before they are severely altered by weathering processes. See Dutta and Wheat (1993) for a case study of climatic and tectonic controls on sandstone composition.

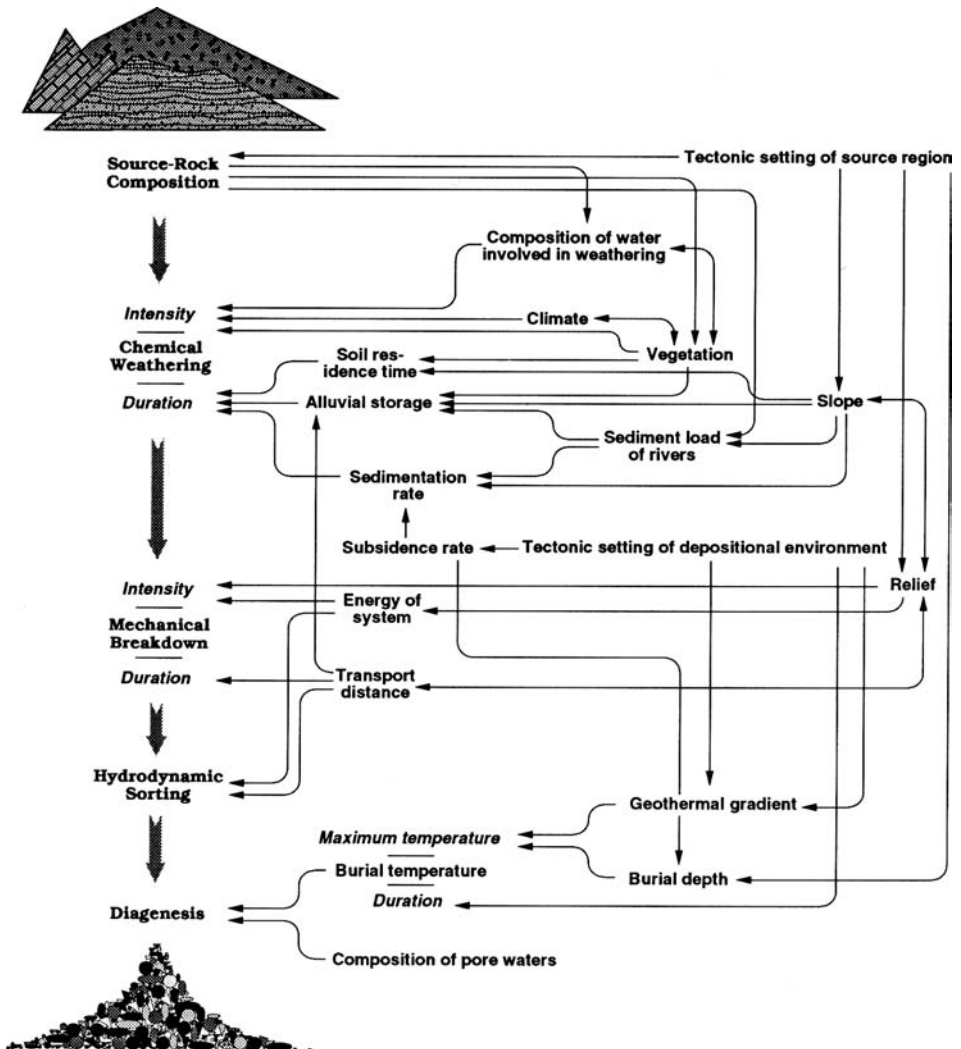


Figure 7.3 Schematic representation of the system controlling the composition of siliciclastic sediments. Arrows indicate parameters that exert influence on each other. (From Johnsson, M. J., 1993, The system controlling the composition of clastic sediments, in Johnsson, M. J. and A. Basu (eds.), *Processes Controlling the Composition of Clastic Sediments*: Geological Society of America Special Paper 284, Fig. 1, p. 11, reproduced by permission of the Geological Society of America.)

7.4.3 Effects of sediment transport

Sediment transport is the crucial link between source and depositional areas. Transport affects the composition of sediment in a variety of ways depending upon the mode of transport. Transport of sediment by current flow is a selective process. Particles are separated into a suspension load and a bedload, and within the bedload, gravels tend to be

separated from sand. These processes thus bring about sorting of particles by size, shape, and density. Obviously, such sorting changes the mix of particle compositions that was initially fed into the transport system. For example, current transport causes most clay minerals and other very fine minerals to become separated from coarser-grained quartz, feldspars, and rock fragments. Furthermore, gravel, which is composed mainly of rock fragments, tends to become separated from sand-size fragments. Additional sorting occurs within the sand fraction owing to shape and density differences of grains. To illustrate, heavy minerals become sorted by density into different size groups, resulting in fine-size, dense heavy minerals being transported along with hydraulically equivalent, coarser-grained quartz and feldspar. Even the composition of pebbles may be affected by size sorting during transport. For example, the clast composition of coarse gravels on river point bars can differ significantly from the clast composition of fine gravels on the same bars.

Current transport also causes significant abrasion of gravel-size detritus, as well as mechanical shattering and breaking owing to impact. Abrasion and impact shattering thus tend to selectively destroy mechanically weak or soft grains. Abrasion of sand-size grains during current transport is not extremely significant, apparently owing to the cushioning effect of water. Transport of sediment under waves, particularly in the littoral zone, may be even more effective than current flow in selective sorting of sediments because prolonged reworking by waves provides a greater opportunity for sorting than does the unidirectional movement of currents. Transport of sediment by ice or sediment gravity flows, such as turbidity currents, commonly produces less selective sorting by size and density and possibly less mechanical destruction than does current transport. Nonetheless, these transport processes have some effect on particle composition, e.g. abrasion by ice transport and sorting by size in the graded beds of turbidites.

Further, chemical weathering may continue to affect the composition of mineral assemblages after removal from the weathering environment. During transport, for example, sediment may be stored temporarily in alluvial deposits such as floodplains, point bars, and terraces (e.g. Johnsson, 1993). Even after deposition, chemical weathering may continue unless sediment is deposited rapidly and isolated from the weathering environment.

7.4.4 Effects of the depositional environment

Depending upon the depositional setting, sediments may or may not undergo additional modification within the depositional environment. Sediments deposited rapidly by fluvial processes or mass flows – on alluvial fans, for example – may undergo little further change before burial. By contrast, sediments brought into the littoral zone may undergo significant change within the beach environment before final deposition takes place. The littoral zone acts as a filter, holding back sands and gravels and allowing muds to pass outward onto the shelf. If sands and gravels do not bypass the shelf by resedimentation transport (mass transport) down submarine canyons that head up close to shore, they may be held within the littoral zone for long periods of time, where they are subject to intensive reworking by wave swash and longshore currents. Such intensive reworking could ultimately erase initial

compositional differences in sands, leading to high compositional maturity (quartz arenites) and effectively removing much of the compositional evidence of provenance.

On the other hand, under conditions where several streams carrying sediments of diverse composition empty onto a shelf, these sediments may become mixed by littoral transport processes or storm surges. Such mixing creates deposits with compositions that are extremely difficult to link to a single source area. Bioturbation within the depositional environment may also mix sediments of diverse origins, further complicating provenance analysis. Sediment transported off the shelf into deeper water probably does not undergo very much additional change, except perhaps some bioturbation, once it reaches its final depositional site. For an example of compositional controls in depositional systems, see Kairo *et al.* (1993).

7.4.5 Effects of diagenesis

Finally, sediments become subjected to changed geochemical conditions within the burial environment that can produce profound postdepositional modifications in composition. Metastable grains may be destroyed completely by dissolution, or they may be replaced by another mineral (e.g. the replacement of quartz by calcite) or altered to another mineral (e.g. the alteration of feldspars to clay minerals or micas). See McBride (1984) for a more extended discussion of the diagenetic processes that affect provenance determinations in sandstones. These changes are also discussed in [Chapter 8](#). They can result in selective destruction of less-stable constituents and thus significant loss in provenance information.

Collectively, the changes brought about in the composition of sediment by weathering and erosion, transport, reworking at the depositional site, and diagenesis can be significant. Obviously, provenance analysis requires that we be alert to the possibility of such changes and that we eschew negative evidence. That is, we cannot use the absence of particular constituents as a guide to provenance interpretation; we can use only their presence. The fact that feldspars and heavy minerals may be absent or scarce in a sandstone, for example, does not mean that they were necessarily absent or scarce in the source rocks. In practice, we may tend to forget this principle, but we do it at our peril.

7.5 Provenance of sandstones

7.5.1 Interpreting source-rock lithology

Introduction

Most research on provenance of siliciclastic sedimentary rocks has focused on sandstones. Much of this research has been concerned with attempts to interpret source-rock lithology from detrital mineral assemblages. Petrographic analysis of quartz, feldspars, micas, heavy minerals, and rock fragments forms the basis for most such studies; however, investigators are now turning also to supplementary techniques such as cathodoluminescence microscopy and geochemical studies of trace elements and isotopes in detrital minerals. Do the major

kinds of igneous, metamorphic, and sedimentary rocks contain uniquely different suites of minerals that provide a distinctive provenance signature? Are these characteristics preserved in sediments? Let's examine what is known about this interesting topic.

Reading provenance from the properties of quartz

General statement

Because quartz is the most abundant constituent in most sandstones, and essentially the only constituent of some sandstones, geologists have been intrigued by the potential provenance significance of quartz since the early years of petrographic study (e.g. Sorby, 1880; Mackie, 1896). These early studies focused particularly on the provenance significance of inclusions in quartz, although the possible provenance significance of undulatory extinction was also recognized quite early (Gilligan, 1919). In the United States, Krynine, in 1940 and in a series of later papers, appears to be the first worker to make in-depth studies of the properties of quartz (inclusions, undulatory extinction, polycrystallinity, nature of subgrain contacts, grain shape) as provenance indicators. Krynine proposed a genetic classification of quartz based on these properties that is still cited (e.g. Folk, 1974, p. 70). The properties of quartz that have been considered by subsequent workers to have possible provenance significance include inclusions, undulatory extinction, polycrystallinity, nature of subgrain contacts, grain shape or crystal shape, trace-element composition, and cathodoluminescence properties.

Quartz inclusions

Inclusions in quartz include both fluid and mineral inclusions (Section 4.2.1). Krynine (1940), drawing on earlier studies, apparently had considerable confidence in his ability to trace quartz grains to their source on the basis of inclusions and patterns of undulatory extinction. Since Krynine's time, little additional research has been focused on quartz inclusions. R. L. Folk, in the various editions of his well-known petrology textbook (e.g. Folk, 1974), suggests that quartz grains so crowded with bubbles (vacuoles) as to appear milky in reflected light come from hydrothermal veins. Otherwise, liquid inclusions do not appear to have much provenance significance. Volcanic quartz is believed to be nearly water-clear and contains almost no inclusions of any type. Quartz of other origins can contain varying amounts of mineral inclusions and bubbles. The relative abundance of mineral inclusions in these grains does not appear to be diagnostic. Only if the inclusions consist of a mineral that is in itself provenance-diagnostic, such as kyanite or sillimanite that form only in metamorphic rocks, do mineral inclusions have provenance value. Altogether, given what seems to be our present state of knowledge, quartz inclusions appear to have very limited value in provenance interpretation.

Undulatory extinction and polycrystallinity

Undulatory extinction and the polycrystalline nature of some quartz grains (Section 4.2.1) have received considerable attention as potential provenance indicators of quartz. Krynine (1940) and Folk (1974, and earlier editions of his textbook) used the degree of undulatory

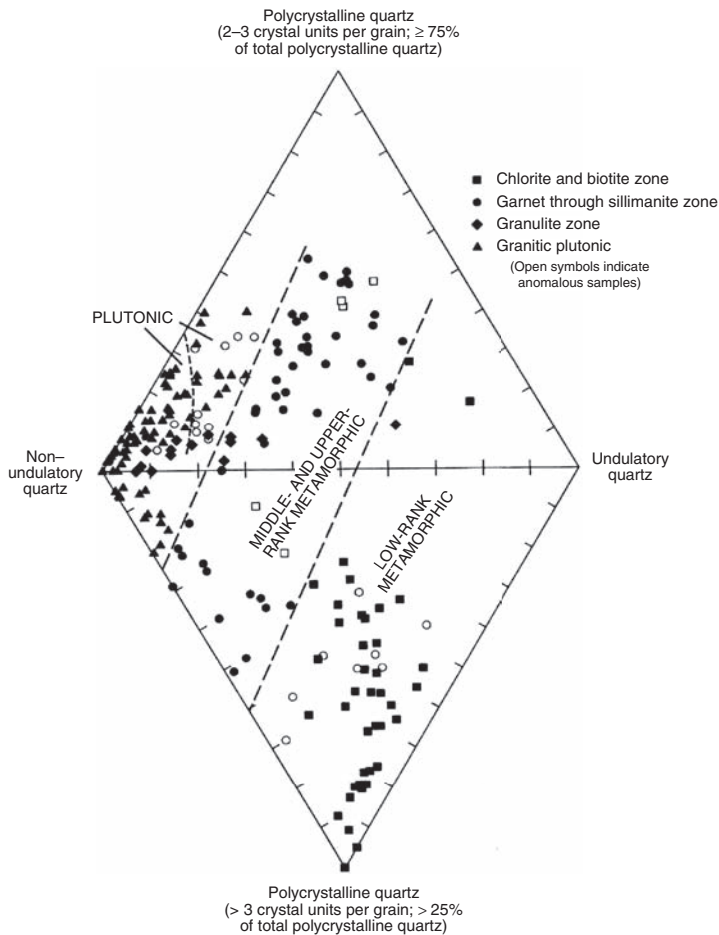


Figure 7.4 A four-variable plot of the nature of quartz populations in Holocene sands derived from source areas indicated by symbols. (From Basu, A. *et al.*, 1975, Reevaluation of the use of undulatory extinction and polycrystallinity in detrital quartz for provenance interpretation: *J. Sediment. Petrol.*, 45, Fig. 6, p. 879, reprinted by permission of SEPM, Tulsa, OK.)

extinction and the nature of polycrystalline grains to assign quartz to various presumed igneous and metamorphic parent rocks. These authors suggested that most highly undulose quartz (undulose extinction $> \sim 5$ degrees) is diagnostic of metamorphic rocks and non-undulose quartz is diagnostic of igneous rocks. Polycrystalline quartz was considered to be most indicative of metamorphic origin.

Basu *et al.* (1975) reexamined the validity of undulatory extinction as a provenance tool by analyzing a large number of samples from plutonic igneous and metamorphic rocks. They concluded that undulatory extinction and polycrystallinity can be used to distinguish plutonic quartz from low-rank metamorphic quartz in first-cycle sands. Their findings are summarized in Fig. 7.4. In this figure, the percentages of nonundulatory, undulatory, and

polycrystalline quartz in rock samples from known source rocks are plotted on a double-triangle diagram. If more than 75 percent of the polycrystalline quartz grains are composed of either two or three crystal units, the values are plotted on the upper triangle. If more than 25 percent of the polycrystalline grains consist of three or more crystal units, they are plotted on the lower triangle.

The data allow subdivision of the diagram into three provenance fields: low-rank metamorphic, middle- and upper-rank metamorphic, and plutonic. It is necessary to emphasize that some overlap between the fields occurs and that use of this method is limited to first-cycle sediments. The method does not work for provenance analysis of recycled, compositionally mature quartz arenites. Also, study must be confined to quartz grains that fall within a narrow size range. Basu *et al.* studied grains within the size range of 0.25–0.50 mm.

Cathodoluminescence characteristics of quartz

When a mineral such as quartz or feldspar is bombarded by a stream of high-energy electrons in a suitable instrument (e.g. a scanning electron microscope), particles of light (photons) are emitted. This phenomenon is called **cathodoluminescence** (CL). Most photons have wavelengths in the visible-light range of the electromagnetic spectrum; however, emissions may occur also in the near-ultraviolet and infrared. See Boggs and Krinsley (2006) for a detailed explanation of the causes of cathodoluminescence and the factors that affect the wavelength (and thus color) of CL photons and the intensity of CL emissions. Boggs and Krinsley also explore in depth the applications of cathodoluminescence imaging to study of sedimentary rocks. One of the more important applications is to provenance analysis, particularly study of the CL characteristics of quartz as a provenance tool. Cathodoluminescence images of quartz display two kinds of characteristics that may have provenance significance: color and fabric (or texture).

Cathodoluminescence color of quartz

As mentioned, cathodoluminescence results from the emission of photons in the ultraviolet, visible, and infrared range of the electromagnetic spectrum. In the visible range, luminescence occurs in a variety of colors (blue, violet, red, brown, green), depending upon the material bombarded. Cathodoluminescence color cannot be observed directly in most scanning electron microscopes but may be observed by using a special cathodoluminescence stage attached to an optical microscope (see Boggs and Krinsley, 2006, p. 20). As discussed by Boggs and Krinsley, CL emissions are related to the presence of electron traps, which are caused by structural (lattice) defects in a crystal or by the presence of foreign ions, such as Li^+ and Na^+ , in interstitial positions. Because lattice defects and impurity ions may vary considerably in quartz of different origins, CL colors may likewise vary. Thus, cathodoluminescence color is reputed to have potential for distinguishing the provenance of quartz.

Several researchers have investigated and reported the relationship between CL color and provenance. Although these various workers differ slightly in their interpretation of CL color versus provenance, general agreement appears to be solidifying with respect to the following relationships (Götze and Zimmerle, 2000, p. 65):

blue to violet CL:	plutonic quartz, as well as quartz phenocrysts in volcanic rock, and high-grade metamorphic quartz
red CL:	matrix quartz in volcanic rocks
brown CL:	quartz from regionally metamorphosed rocks
no CL or weakly luminescent:	authigenic quartz
short-lived green or blue CL:	hydrothermal and pegmatitic quartz

Boggs *et al.* (2002) demonstrated, however, that there is considerable overlap in CL colors among volcanic, plutonic, metamorphic, and hydrothermal quartz. We suggest that this overlap casts doubt on the practicality of using CL color as a provenance indicator.

Experience has shown that the CL color of quartz shifts with prolonged exposure to a beam of high-energy electrons during analysis. This color shift may have provenance significance. According to Götte *et al.* (2001), for example, light blue → bluish violet = igneous quartz, blue → brown = metamorphic/hydrothermal quartz, dark green → brown = hydrothermal quartz. Götte and Richter (2006) combined CL microscopy with digital image analysis and spectroscopic analysis to make a quantitative evaluation of CL color shift in mature (quartz-rich) sandstones. They were able in one study to identify up to 25 different quartz types, reflecting a highly variable provenance with plutonic, low-grade metamorphic, and sedimentary source rocks.

Cathodoluminescence fabric analysis of quartz

Geologists have known for some time that CL images of quartz reveal internal fabrics or textures such as zoning and healed fractures (e.g. Krinsley and Tovey, 1978; Milliken, 1994; Seyedolali *et al.*, 1997; Bernet and Bassett, 2005; Boggs and Krinsley, 2006). Milliken (1994) and Seyedolali *et al.* (1997) were among the first workers to point out that these features may have provenance significance. Cathodoluminescence textures and fabrics of quartz that convey provenance information are listed and briefly described in Table 7.1. These features are discussed in detail, along with presentation of appropriate CL images, in Boggs and Krinsley (2006). Only a brief review of the provenance significance of CL imaging is given here.

Volcanic quartz is particularly characterized by the presence of CL zoning (e.g. Fig. 7.5). Zoned fabrics can range from distinct, fine-scale oscillatory-type zoning to more ill-defined, complex zoning, such as that shown in Fig. 7.5. Zoned grains display bright-CL and dark-CL bands; boundaries between these bands range from sharp to indistinct. Cathodoluminescence images of volcanic quartz may (or may not) also display embayments and glass inclusions. Late-stage, open (cooling?), fractures may be present; healed fractures are uncommon. Most volcanic quartz exhibits CL zoning; however, Bernet and Bassett (2005) report significant amounts of (CL) unzoned quartz in some New Zealand volcanic rocks.

Plutonic quartz may likewise display CL zoning; however, most plutonic quartz does not. The most characteristic CL feature of plutonic quartz is the presence of dark-CL streaks and patches, informally dubbed “spiders” by Boggs and Krinsley (2006). Also, plutonic quartz commonly displays healed fractures in CL images. Figure 7.6 shows a fairly typical CL image of a plutonic quartz grain. Plutonic quartz that does display CL zoning also displays spiders and healed fractures, which distinguishes it from volcanic quartz.

Table 7.1 *Distinctive characteristics of quartz grains revealed by SEM–CL microscopy*

Feature	Description	Quartz source	Comments
Zoning	Typically displays oscillatory-type zoning with concentric bands oriented parallel to grain edges; less commonly, nonconcentric bands extend across grains parallel or at an angle to grain boundaries; bands range in width from 1 to >50 μm	Volcanic and plutonic rocks, hydrothermal veins	Particularly well developed in volcanic quartz; present in some plutonic quartz; zoned hydrothermal quartz commonly displays a complex pattern of small-scale zoned crystals that may include sector zoning
Healed fractures	Distinct, black (dark CL) lines (<5–> 20 μm wide) strongly resembling fractures; may have diverse orientations; not visible in BSE images	Plutonic and metamorphic rocks, hydrothermal veins	Particularly common in plutonic quartz; less common in metamorphic quartz, rare in volcanic quartz
Open fractures	CL-dark or CL-bright lines (depending upon epoxy resin used in sample preparation); visible in BSE images; various thicknesses and orientations	Any kind of source rock	Late-stage features that may be present in any kind of quartz, including volcanic quartz; have little provenance significance
Deformation lamellae	CL-dark, curved–straight, semiparallel lines that occur in one or more sets with various spacings; sets may extend across entire grain	Tectonically deformed metamorphic rocks	Apparently related to line defects in crystal structure generated as a result of deformation
Shock lamellae (planar deformation features)	Thin, dark-CL lines that occur in sets within which lines are essentially parallel; two or more sets oriented at different angles may be present	Shocked crystalline and sedimentary rocks	Present in quartz from meteorite or cometary impact structures and some system boundaries; may occur in feldspars
Dark-CL streaks and patches (“spiders”)	Broad (> 10 μm) black (dark-CL) elongated streaks with irregular boundaries and large (~10 to >100 μm), black patches; commonly occur with healed fractures	Plutonic rocks, high-grade metamorphic rocks, hydrothermal veins	Particularly characteristic of plutonic quartz; occur rarely in high-grade metamorphic rocks; absent (or very rare) in volcanic quartz
Indistinct mottling	Irregular CL intensity across grains, producing a mottled pattern	Metamorphic rocks, some volcanic rocks	Most common in metamorphic quartz
Nondifferential (homogeneous) CL	Grains display nearly uniform CL (little difference in CL intensity)	Metamorphic rocks, some volcanic rocks	Most common in metamorphic quartz

Source: Boggs and Krinsley, 2006, Table 4.3, p. 60.

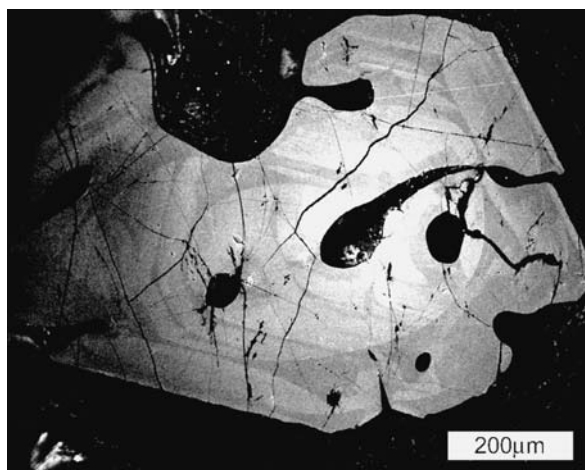


Figure 7.5 Cathodoluminescence zoned and embayed quartz in Triassic-Jurassic(?) rocks, New Zealand. Note also the dark-CL melt inclusions within the grain. Photograph courtesy of Professor Gordon Goles (deceased).

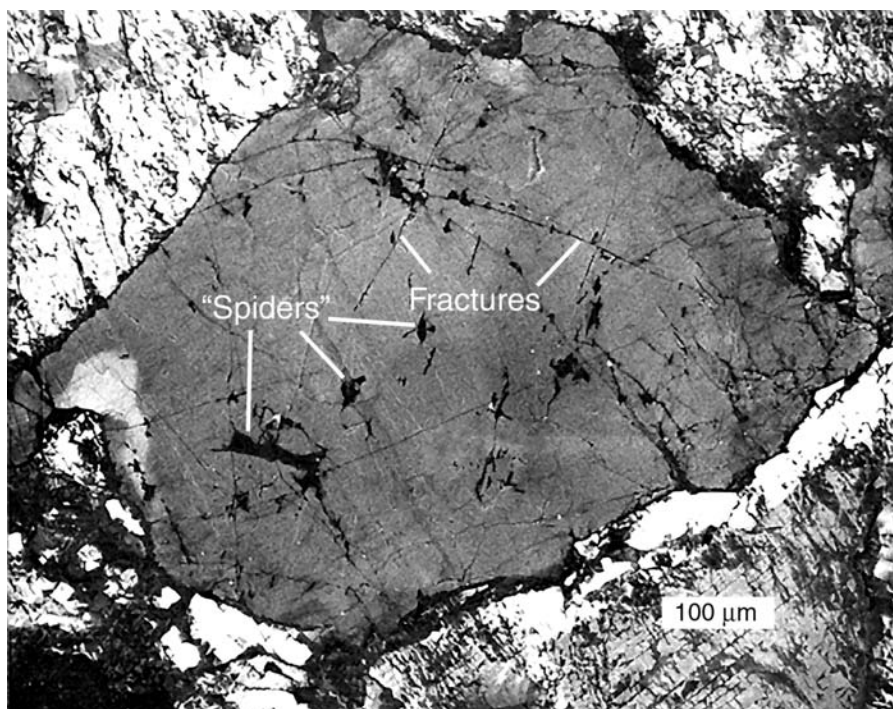


Figure 7.6 Cathodoluminescence image of a plutonic quartz grain, which displays dark-CL streaks and patches ("spiders") and healed fractures. Squamish Granodiorite (Cretaceous), British Columbia, Canada. Sample courtesy of J.K. Russell. (After Boggs, S. and D. Krinsley, 2006, *Application of Cathodoluminescence Imaging to the Study of Sedimentary Rocks*: Cambridge University Press, Fig. 4.5, p. 65, reproduced by permission.)

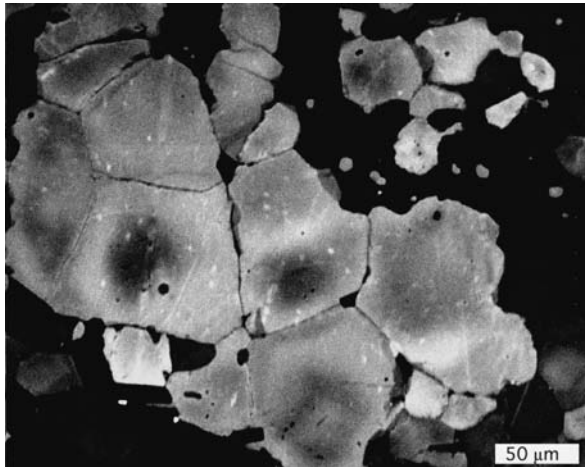


Figure 7.7 Cathodoluminescence image of metamorphic quartz showing mottled texture. Contact-metamorphosed hornfels, Japan. Specimen courtesy of Professor Hideo Kagami.

Metamorphic quartz can originate within a variety of metamorphic rocks, which formed under a wide range of temperatures, pressures, and interstitial fluid conditions. In spite of its diverse origin, empirical studies (e.g. Seyedolali *et al.*, 1997; Boggs and Krinsley, 2006) show that metamorphic quartz commonly displays only two characteristic CL signatures: mottled texture and homogeneous (nondifferential) texture. Mottled texture, illustrated in Fig. 7.7, may be caused by incomplete recrystallization or annealing accompanying metamorphism or it may be the result of deformation during metamorphism. Bernet and Bassett (2005) report a correlation between patchy/mottled CL and strong undulose extinction arising from increasing deformation. They found this texture in both low- to medium-grade and medium- to high-grade metamorphic quartz.

Metamorphic quartz that displays essentially homogeneous CL is also common (e.g. Fig. 7.8). Boggs and Krinsley (2006, p. 74) report that two contrasting types of metamorphic quartz grains may display homogeneous CL: bright-CL grains and dark-CL grains. Homogeneous bright-CL grains apparently form by recrystallization at high temperatures. The conditions under which dark-CL grains originate are more difficult to identify. They presumably form at lower temperatures, possibly as a result of significant physical deformation in some cases.

Provenance significance of feldspars

Introduction

Feldspars are generally very scarce or absent in quartz arenites; however, they are common constituents of most other sandstones. Several properties of feldspars make them useful provenance indicators. First, because feldspars are chemically and mechanically less stable than quartz, they are less likely to be recycled. Some feldspars may indeed be recycled, depending upon conditions; however, the presence of moderately abundant feldspars in a

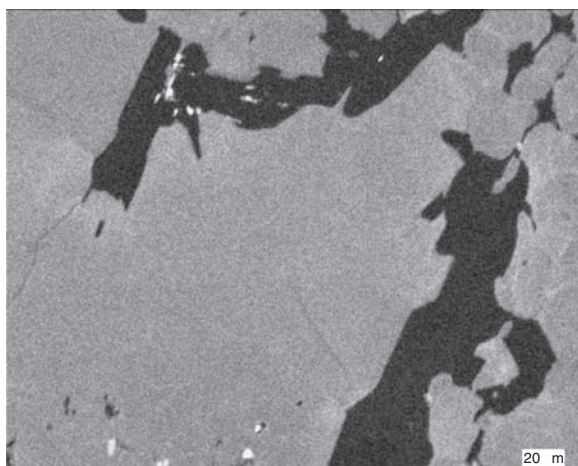


Figure 7.8 Cathodoluminescence image of metamorphic quartz showing homogeneous texture. Contact-metamorphosed hornfels, Japan. Specimen courtesy of Professor Hideo Kagami.

sandstone suggests derivation from crystalline source rocks. Thus, feldspars are more likely than quartz to provide information about first-generation source rocks. Both the mineralogy and chemistry of feldspars may have provenance significance. For example, microcline tends to be derived from felsic igneous or metamorphic rocks and calcic plagioclase from basic igneous or metamorphic rocks. Also, the chemical composition of feldspars is known to be a function of source rocks. The presence of zoning and twinning in plagioclase feldspars is likewise related to source-rock type. Let's examine some of these properties of feldspars to evaluate their usefulness and limitations in provenance studies.

Feldspar mineralogy

A particular type of feldspar may be derived from more than one kind of igneous or metamorphic rock. Therefore, feldspar mineralogy provides only a crude guide to provenance. Nonetheless, it is useful to see how feldspar mineralogy is related to source conditions.

The **potassium–sodium (alkali) feldspars** are essential constituents of felsic igneous rocks, pegmatites, and many felsic and intermediate gneisses (Deer *et al.*, 1992, pp. 391–395). The feldspar in plutonic felsic rocks and high-grade metamorphic rocks is commonly orthoclase and microcline, including perthitic (~1 mm-size exsolved lamellae) orthoclase, and microcline. In volcanic rocks it is sanidine and anorthoclase, including cryptoperthitic (1–5 micron-size exsolved lamellae). The feldspars occur as phenocrysts and as part of the groundmass. [Note: Parsons *et al.* (2005) refer to optically visible intergrowths as microperthite and suboptical intergrowths (< 1 mm in scale) as cryptoperthite.] Parsons *et al.* (2005) provide a richly illustrated atlas of alkali feldspar microtextures, as they appear in backscattered electron (BSE) images. They suggest, for example, that BSE images of volcanic sanidines are bright and featureless, whereas granitic alkali feldspars display visible, regular lenticular to irregular perthitic lamellae in BSE images.

Plagioclase feldspars are particularly common in volcanic rocks, where they occur as both phenocrysts and in the groundmass. They may be abundant also in some plutonic igneous and metamorphic rocks. Plagioclase in igneous rocks can have a wide range of compositions from calcium-rich (e.g. in basalts) to sodium-rich (e.g. in rhyolites), depending upon the composition of the host rock. Plagioclase in metamorphic rocks may also have a wide compositional range depending upon the metamorphic grade and chemical composition of the host rock (Deer *et al.*, 1992, p. 452). Unfortunately, plagioclase can become albitized during diagenesis, which effectively erases the parent-rock composition signature.

Zoning of feldspars

Although zoning can be present in some plagioclase porphyroblasts in metamorphic rocks (e.g. Deer *et al.*, 1963, p. 149), most zoned feldspars occur in igneous rocks. Thus, the presence of zoning in feldspars can generally be regarded to signify igneous origin. Both plagioclase and potassium–sodium feldspars can be zoned; however, zoning in plagioclase appears to be more common than that in the alkali feldspars. Only zoned plagioclase has received much attention as a potential provenance indicator. Zoned crystals commonly have calcium-rich cores and more sodic margins. In some zoned plagioclase crystals, the cores may be as calcic as An_{80} and margins as sodic as An_{45} . Other zoned plagioclase crystals may display only minor compositional changes between cores and margins.

Two general styles of zoning are recognized. **Oscillatory zoning** appears under crossed polarizing prisms as successive thin bands of alternating extinction and as bright and dark bands in BSE images (Fig. 7.9). **Progressive zoning** is more poorly defined and appears as a broad wave of extinction with or without sharp lines of demarcation. Thus, oscillatory zoning is fine-scale zoning, and progressive zoning is characterized by coarse, indefinite texture. Chemical zoning in feldspars can be studied by a variety of instrumental methods, such as electron probe microanalysis, as well as by optical methods.

Only a few published papers appear to have concentrated specifically on the use of zoning in feldspars as a provenance indicator. In an older, but comprehensive paper, Pittman (1963) examined specimens of volcanic, plutonic igneous, hypabyssal, and metamorphic rocks to establish the proportion of zoned to nonzoned plagioclase in these rocks. He also examined zoning in plagioclase grains in several sandstones whose provenance had been established by other means. He concluded that (1) the presence of any kind of zoning in a plagioclase grain is strongly indicative of igneous origin, (2) oscillatory zoning in detrital plagioclase grains is indicative of a volcanic or hypabyssal source, (3) progressive zoning has no value in distinguishing between a volcanic–hypabyssal and plutonic igneous source, (4) metamorphic plagioclases tend to be unzoned; however, the absence of zoning does not necessarily indicate metamorphic origin because much volcanic–hypabyssal and plutonic igneous plagioclase is unzoned also. Therefore, it is not safe to draw provenance inferences from unzoned plagioclase.

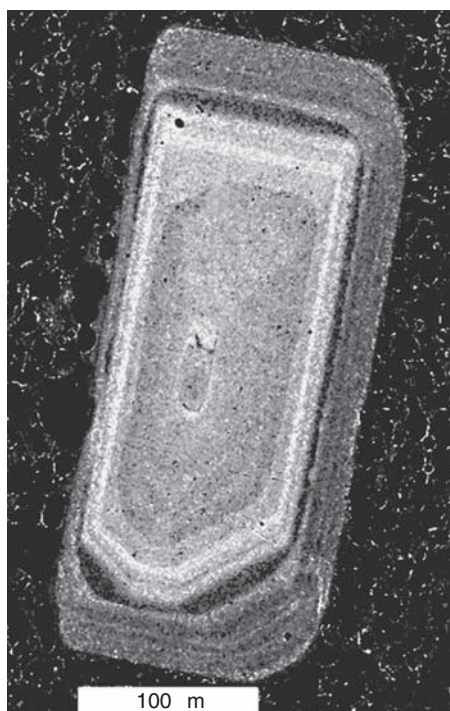


Figure 7.9 Backscattered electron (BSE) micrograph of a large, compositionally zoned plagioclase grain crystallized during the eruption of Mt. St. Helens (Washington, USA) in 1980. Photograph courtesy of Kathy Cashman, University of Oregon.

Feldspar twinning

Some investigators have suggested that the relative abundance and types of twinning in feldspars, particularly in plagioclase, has provenance significance. **A-twins** are twinned according to the albite, pericline, and accline laws. **C-twins** include crystals twinned according essentially to all the other twin laws (Manebach, Baveno, parallel, complex). Readers who may be a bit rusty with respect to twins and twin laws may wish to consult a standard mineralogy text such as Klein and Hurlbut (2002) for a review of twin laws.

Most interest in feldspar twinning as a provenance tool appears to date back to the 1950s and 1960s. For example, Gorai (1951) concludes from his study that C-twins are characteristic of volcanic and plutonic igneous rocks, although they may occur in very minor amounts in hornfels. A-twins occur in both igneous and metamorphic rocks, but are relatively less abundant in hornfelsic rocks. Volcanic rocks may contain C-twins, A-twins, and untwinned plagioclase. Metamorphic rocks contain mainly untwinned plagioclase and A-twins, and the abundance of twinned plagioclase appears to increase with increasing grain size. Helmold (1985) discusses the usefulness and limitations of twinning in provenance applications; however, little information has appeared in the more recent literature about the provenance significance of feldspar twinning.

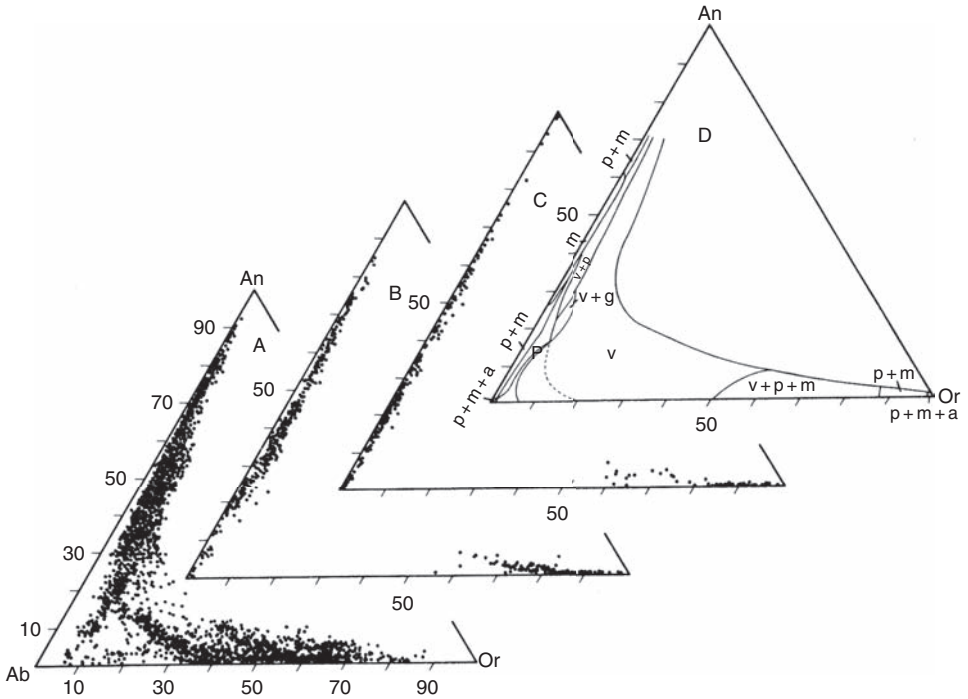


Figure 7.10 Chemical composition of feldspars as determined by approximately 5300 electron probe microanalyses. A. Composition of feldspars from volcanic rocks. B. Composition of plutonic feldspars. C. Composition of feldspars from metamorphic rocks. D. Composition range of eight groups of feldspar. v = volcanic; p = plutonic; m = metamorphic; v + g = volcanic or granophyre; v + p = volcanic or plutonic; p + m = plutonic or metamorphic; v + p + m = volcanic, plutonic, or metamorphic; p + m + a = plutonic, metamorphic, or authigenic. (After Trevena, A. S. and W. P. Nash, 1981, An electron microprobe study of detrital feldspar: *J. Sediment. Petrol.*, **36**, Fig. 1, p. 138, reprinted by permission of Society for Sedimentary Geology, Tulsa, OK.)

Feldspar chemistry

The electron probe microanalyzer has proven to be a highly useful tool for studying the chemical composition of individual feldspar (and other mineral) grains. Probably the most comprehensive studies of detrital feldspar composition are those of Trevena and Nash (1979, 1981). These authors compiled, from numerous sources, nearly 5000 electron microprobe analyses of plagioclase alkali feldspars. They carried out these analyses on a variety of volcanic, plutonic igneous, and metamorphic rocks. The results of their compilation are shown in Fig. 7.10. In this figure, chemical composition is plotted on triangular composition diagrams in terms of An (Ca), Ab (Na), Or (K) end members. Diagram A shows the composition of volcanic feldspars, B the composition of plutonic feldspars, and C the composition of metamorphic feldspars. Diagram D summarizes the ranges of all the provenance groups.

Figure 7.10 shows that feldspars from volcanic rocks have a wide range of compositions, whereas the composition of feldspars from plutonic and metamorphic rocks is somewhat more restricted. Trevena and Nash conclude that detrital alkali feldspars more sodic than 50 weight percent albite molecule are derived almost exclusively from volcanic sources. Alkali feldspars more potassic than 87 percent orthoclase molecule are derived from metamorphic and plutonic rocks. The potassium content of volcanic plagioclase increases significantly as sodium content increases. For the more sodic detrital plagioclase, this relationship allows discrimination between volcanic plagioclase and plagioclase derived from plutonic and metamorphic rocks.

Trevena and Nash (1981) suggest that other chemical elements in feldspars may have some provenance value. For example, detrital plagioclase of volcanic origin generally contains more iron and strontium than does nonvolcanic plagioclase. On the whole, however, the trace-element composition of feldspars has received little attention as a tool for provenance analysis. Some recent work has focused on use of Pb (lead) isotopes in detrital feldspar grains in provenance studies (e.g. McLennan *et al.*, 2003); however, this work appears to be aimed mainly at analysis of provenance terranes rather than source-rock interpretation.

Discussion of feldspar as a provenance indicator

Feldspars are one of the most useful detrital minerals as indicators of source-rock lithology. Source-rock interpretation is made on the basis of feldspar mineralogy, zoning, twinning, and chemical composition. Figure 7.11 summarizes the relationship between some of these important properties of plagioclase and its source rocks. The reliability of provenance interpretation is enhanced if interpretation is based on as many properties of feldspars as possible and practical.

The reliability of provenance interpretation can be seriously affected, however, by changes in the original feldspar composition brought about by the processes of weathering, transportation (abrasion and impact), and diagenesis, as discussed in preceding parts of this chapter. See, also, Johnsson and Basu (1993). We can't simply assume, in making provenance interpretation of siliciclastic sedimentary rocks, that the modal composition of detrital sediments faithfully reflects the composition of the source rocks. We must be aware, and take into consideration, the impact on composition brought about by the processes of weathering, sediment transport, and diagenesis.

Heavy minerals

Provenance interpretation from heavy-mineral petrography

Section 4.2.1 briefly describes the procedures used in petrographic analysis of heavy minerals. Two general approaches are used in provenance interpretation of heavy-mineral petrographic data. The first is to interpret source-rock lithology on the basis of assemblages of heavy minerals, under the assumption that each major kind of source rock yields a distinctive suite of heavy minerals (Table 7.2). To use this approach, it must be further assumed that the heavy-mineral assemblages that occur in detrital sedimentary rocks accurately reflect those originally present in the parent rocks. This assumption may be far from valid. Because heavy minerals have a wide range of chemical stabilities (Table 7.3), they are subject to selective



Figure 7.11 Summary of provenance-significant properties of plagioclase as determined with a standard petrographic microscope. Unbroken lines indicate more-probable sources of minerals. (From Pittman, E. D., 1970, Plagioclase feldspars as an indicator of provenance in sedimentary rocks: *J. Sediment. Petrol.*, **40**, Fig. 5, p. 596, reprinted by permission of the Society for Sedimentary Geology, Tulsa, OK.)

Table 7.2 *Heavy-mineral suites characteristic of principal kinds of source rocks*

Association	Source
Apatite, biotite, brookite, hornblende, monazite, muscovite, rutile, titanite, tourmaline (pink variety), zircon	Acid igneous rocks
Cassiterite, dumortierite, fluorite, garnet, monazite, muscovite, topaz, tourmaline (blue variety), wolframite, xenotime	Granite pegmatites
Augite, chromite, diopside, hypersthene, ilmenite, magnetite, olivine, picotite, pleonaste	Basic igneous rocks
Andalusite, chondrodite, corundum, garnet, phlogopite, staurolite, topaz, vesuvianite, wollastonite, zoisite	Contact metamorphic rocks
Andalusite, chloritoid, epidote, garnet, glaucophane, kyanite, sillimanite, staurolite, titanite, zoisite-clinozoisite	Dynamothermal metamorphic rocks
Barite, iron ores, leucoxene, rutile, tourmaline (rounded grains), zircon (rounded grains)	Reworked sediments

Source: After Feo-Codecido, G., 1956, Heavy mineral techniques and their application to Venezuelan stratigraphy: *Am. Assoc. Petrol. Geol. Bull.*, **40**, p. 979, as modified by Pettijohn *et al.*, 1987, p. 261, reprinted by permission of Springer-Verlag, New York.

Table 7.3 *Relative stabilities of heavy minerals under conditions of weathering and intrastratal solution during diagenesis; stability increases downward in the columns*

Surface weathering (A)	Intrastratal solution	
	Epidiagenesis (meteoric zone) (B)	Anadiagenesis (deep burial) (C)
Olivine	Olivine, pyroxene	Olivine, pyroxene
Apatite	Amphibole	Andalusite, sillimanite
Pyroxene	Sphene	Amphibole
Garnet	Apatite	Epidote
Amphibole	Epidote, garnet	Sphene
Kyanite	Chloritoid, spinel	Kyanite
Staurolite	Staurolite	Staurolite
Monazite	Kyanite	Garnet
Tourmaline	Andalusite, sillimanite, tourmaline	Apatite, chloritoid, spinel
Rutile	Rutile, zircon	Rutile, tourmaline, zircon
Zircon		

Source: Column (A) based on Goldich (1938), Dryden and Dryden (1946), and Sindowski (1949). Information in columns (B) and (C) from Morton (1985).

chemical destruction during weathering and diagenesis. Heavy minerals also have differential stabilities with respect to mechanical destruction during transport, and they are subject to selective sorting by size and shape during transport. See Morton and Hallsworth (1999) for more detailed discussion of this topic.

Assume for the moment that variations in heavy-mineral abundances owing to selective transport are insignificant and that one is dealing with an extensive suite of heavy minerals that has not been severely affected by weathering or diagenesis. That is, the heavy-mineral suite contains abundant unstable heavy minerals, showing that the effects of weathering and diagenesis must be minimal. How can provenance of sediment be determined on the basis of such a complex suite of minerals? The current trend in heavy-mineral analysis is to utilize some kind of statistical factor analysis, such as Q-mode factor analysis, to provide a reduction of variables and an objective classification of samples. See, for example, Mezzadri and Saccani (1989).

The second method of using heavy minerals in provenance studies, which avoids problems imposed by hydraulic fractionation and stability relationships, is to work with a single heavy mineral or heavy-mineral group. Such studies are called varietal studies. Different varieties of a given heavy mineral are distinguished on the basis of color, shape, inclusions, or geochemistry. In an early example of this approach, Krynine (1946) divided tourmalines into four main provenance types: (1) granitic tourmaline – dark brown, green, pink; small- or medium-size idiomorphic crystals, commonly full of bubbles and cavities; (2) pegmatitic or vein tourmaline – blue, with pleochroism in shades of mauve and lavender; large crystals; inclusions rare; (3) metamorphic tourmaline – colors variable, brown, pink, green, colorless; generally small crystals; may contain black, carbonaceous inclusions; and (4) sedimentary authigenic tourmaline – shows authigenic overgrowths that are typically colorless to very pale blue.

Subsequent provenance studies of varietal heavy minerals have employed more sophisticated techniques, such as identifying trace elements in individual heavy minerals by electron probe microanalysis. For example, Grigsby (1990) utilized step-wise discriminant function analysis to determine that TiO_2 , MgO , V_2O_3 , and Al_2O_3 could discriminate among detrital magnetite grains from felsic plutonic and volcanic, intermediate volcanic, and mafic plutonic parent rocks. In a more recent study, Zack *et al.* (2004) established that the Al, Si, V, Cr, Fe, Zr, Nb, and W content of rutile in upstate New York sedimentary rocks, determined by electron probe microanalysis, could be used to identify metapelitic, metabasitic, and high-grade gneissic source rocks – and to interpret characteristics of tectonic terranes. Numerous similar studies are reported in the published literature; see, for example, Morton (1991).

Ages of heavy minerals

A slightly different provenance approach is to determine the ages of detrital heavy mineral species by radiometric techniques. These ages can then be correlated to the ages of known crystalline rocks, thereby establishing the ages of the ultimate, although not necessarily the last, source of the sediments. Such data place age constraints upon the choice of possible source rocks for a given sedimentary deposit.

Zircon is perhaps the most common heavy mineral used in such studies. Cathodoluminescence techniques (e.g. Boggs and Krinsley, 2006, p. 79) are used to select different zones within zircon for dating. Uranium–lead dating is commonly carried out by using a SHRIMP (Sensitive High-Resolution Ion Microprobe) mass spectrometer to determine ages of individual zircon grains. Once the age of a zircon grain has been established, the grain may be traced to a still-existing source terrane of known age. See Lease *et al.* (2007) and numerous references therein for examples of the application of this technique.

Provenance significance of rock fragments

Detrital rock fragments in sandstones and conglomerates provide the most unequivocal evidence of source-rock lithology. There can be little doubt that a volcanic rock fragment indicates ultimate derivation from a volcanic source, a phyllite or schist clast must have come from a metamorphic parent rock, a limestone fragment indicates a limestone source rock, and so on. Therefore, rock fragments are valuable source-rock indicators in conglomerates and some sandstones, e.g. lithic arenites and many feldspathic arenites. With the exception of chert grains, rock fragments are scarce in most quartz arenites. Petrologic studies that include plotting the relative proportion of various kinds of rock fragments can be extremely valuable adjuncts to other provenance tools in source-rock or source-terrane analysis.

Although rock fragments are excellent source-rock indicators, several problems may arise in their use. The first of these is the problem of rock-fragment identification (see Table 4.5). Differentiating between chert and some felsic rock fragments or silicified volcanic rock fragments can be especially difficult. A second problem in interpretation arises from differences in chemical and mechanical stability of rock fragments that can result in selective destruction of less-stable fragments during weathering, transport, and diagenesis. A stability ranking for the various kinds of rock fragments has not yet been established by well-controlled research. Nonetheless, we know that certain kinds of rock fragments are less stable than others. For example, carbonate fragments are easily susceptible to solution in acidic surface waters or formation waters, and even some siliciclastic rock fragments such as volcanic clasts can be replaced or otherwise destroyed during diagenesis.

Further, some rock fragments such as shale, slate, and phyllite fragments may be mechanically destroyed by abrasion and impact during transport and deposition unless they are well cemented. Selective destruction of rock fragments, by whatever means, obviously biases the final assemblage of rock fragments in sandstones and weakens source-rock interpretation. To put it another way, we cannot be sure that chemically unstable or weakly durable source rocks were absent in a source area just because clasts of these rocks are absent in a sandstone. Conversely, because stable rock fragments such as chert and metaquartzite can be recycled, their presence in a sandstone may not indicate that quartzite and chert were present in the proximate source area.

The final problem has to do with the inherent relationship of parent-rock grain size and size of rock fragments. Only fine-size parent rocks yield substantial quantities of rock fragments of sand size. Therefore, coarse-grained parent rocks are poorly represented by rock fragments in sandstones. Establishing the relative abundance of various kinds of rock

fragments in a sandstone does not necessarily establish the relative importance of equivalent source rocks in the source area.

Whole-rock geochemistry as a source-rock indicator

Several studies have appeared in the geological literature that utilize whole-rock geochemistry in provenance analysis. These studies attempt to correlate the chemical composition of sandstones, expressed as abundances of certain major or minor elements or ratios of elemental abundances, to the chemical composition of appropriate source rocks. Such studies appear to allow identification of source rocks only in terms of rather broad compositional types. They may not have the resolving power of detrital mineralogy to identify specific source-rock types. In particular, they may not be able to determine in a given sandstone unit that mixing of sediment from two or more distinct sources has occurred. Also, chemical composition is affected by grain size of the sediments. In general, whole-rock geochemistry appears to be a more effective tool for evaluating tectonic setting than a tool for interpreting source-rock lithology. See Briggs *et al.* (2004), and references therein, for examples of whole-rock chemistry applied to provenance analysis.

7.5.2 Interpreting tectonic setting

Introduction

Preceding [Section 7.5.1](#) describes the methods and problems involved in interpreting source-rock lithology on the basis of detrital mineralogy and geochemistry. Interpreting source-rock lithology is, however, only part of the process of provenance analysis. To develop a fuller understanding of provenance and paleogeography requires that we understand also the relationship between source area, depositional basin, and the regional tectonic framework. Geologists have long had an interest in this relationship between tectonics and sedimentation. In North America, the role of tectonics in sedimentation was championed particularly by Krynine in the 1940s (e.g. Krynine, 1943). Interest was rekindled in the early 1960s with the development of the concept of plate tectonics. Research on the relationship of sediment composition and tectonics has continued extremely active since that time.

The basis for interpreting tectonic setting is the assumption that detrital mineralogy and geochemistry reflect not only source-rock lithology but also the general plate-tectonic setting. Plate-tectonic setting encompasses two features: (1) **major provenance terranes** (cratonic blocks, volcanic-arc systems, collision belts) and (2) **types of plate boundaries** (passive or rifted continental margins, active or orogenic continental margins, transform-fault margins). Presumably, each major plate-tectonic setting generates distinctive suites of source rocks. Erosion of these source rocks furnishes sediment to a variety of depositional basins located in different positions with respect to plate boundaries, e.g. foreland basins, backarc basins, forearc basins, intraarc basins, trenches ([Chapter 1](#)). The modal composition of quartz, feldspars, and rock fragments deposited in these basins, and possibly the geochemistry of the sediments as well, are putatively accurate reflectors of provenance terranes

that vary with plate-tectonic setting. This idea was pursued in the early 1970s by a small number of investigators (Dickinson and Rich, 1972; Crook, 1974; Schwab, 1975). It was developed most fully and perhaps stated most elegantly by Dickinson and Suczek (1979). Since that time, the concept has been reevaluated and applied by numerous workers.

Interpreting provenance terranes from sandstone detrital modes

General concept

Dickinson and Suczek (1979), Dickinson *et al.* (1983), and Dickinson (1985, 1988) suggest that all tectonic provenances can be grouped under three main types: continental blocks, magmatic arcs, and recycled orogens. Each of these provenance settings includes distinctive groupings of source rocks that shed sediments into associated basins.

Continental-block setting

Included in this category of provenances are major shields and platforms, as well as locally upfaulted basement blocks. Major shields, or **craton interior provenances**, are composed dominantly of basement rocks consisting of largely felsic plutonic igneous and metamorphic rock. Associated platform successions may include abundant sedimentary rocks. Sands derived from craton interiors are typically quartzose sands containing minor feldspars, reflecting multiple recycling and perhaps intense weathering and long distances of transport on cratons of low relief. K-feldspar to plagioclase ratios tend to be high. Thus, craton interior provenances yield largely quartz arenites, although some lithic arenites could be derived from positive areas located marginally to continental blocks. Sediments derived from cratons are deposited in local basins within the craton, in foreland basins, or along rifted continental margins in shelf, slope, or deeper-water environments. (See Boggs, 2006, chapter 16, for discussion of sedimentary basins.) Fault-bounded, **uplifted basement blocks** typically consist of granitic rocks and gneisses. High relief on these blocks results in rapid erosion, which generates relatively coarse feldspathic arenites and arkoses. Some blocks may have an initial cover of sedimentary or metamorphic rocks that can yield lithic arenites. Sediments from uplifted basement blocks are commonly deposited without much transport in nearby interior basins.

Magmatic-arc settings

Magmatic arcs consist of volcanic highlands located along active island arcs or on some continental margins. Some magmatic arcs, such as the Japan arc, may not have a continuous volcanic cover and may be associated with igneous, metamorphic, and sedimentary rocks. Magmatic arcs along continental margins that become deeply eroded or dissected may also expose deep-seated plutonic rocks. Young, **undissected arcs** tend to have a nearly continuous cover of volcanic rocks. Therefore, largely volcanoclastic debris is shed from undissected arcs (Dickinson and Suczek, 1979). This debris consists mainly of plagioclase feldspars and volcanic lithic fragments, many of which contain plagioclase phenocrysts. If quartz is present, it is volcanic quartz. Thus, sandstones derived from undissected magmatic arcs are almost exclusively volcanic lithic arenites. Sediment may be deposited in backarc

basins, forearc basins, intraarc basins, or trenches. **Dissected arcs** that expose deep-seated plutonic rocks shed a mixture of volcanic and plutonic detritus and under some conditions may even shed metamorphic or sedimentary detritus. Thus, K-feldspars and plutonic quartz may be present in this detritus along with volcanoclastic material. Sandstones derived from dissected arcs are thus less (volcanic) lithic-rich than those from undissected arcs.

Recycled-orogen settings

Recycled orogens are source regions created by upfolding or upfaulting of sedimentary or metasedimentary terranes, allowing detritus from these rocks to be recycled to associated basins. Many recycled orogens were formed by collision of terranes that were once separate continental blocks. This process creates uplift and welds the terranes together along a suture zone (collision-orogen provenances). **Collision orogens** are composed dominantly of nappes and thrust sheets of sedimentary and metasedimentary rocks, but may include subordinate amounts of plutonic or volcanic rocks, or even ophiolitic mélanges. Therefore, complex suites of sediments can be derived from such orogens. Dickinson and Suczek (1979) suggest that typical sandstones are composed of recycled sedimentary materials, have intermediate quartz contents, and contain an abundance of sedimentary–metasedimentary lithic fragments. Less-typical sandstones derived from collision orogens are quartz arenites, feldspathic arenites, and chert-rich sandstones. Sediments shed from collision orogens may be shed into foreland basins or may be transported longitudinally into adjacent ocean basins. Some recycled orogens are foreland uplifts associated with foreland fold-thrust belts. These **foreland uplift provenances** may contain a complex variety of source rocks, including siliciclastic sediments, carbonate rocks, metasediments, plutonic rocks in exposed basement blocks, and volcanic rocks. Thus, a variety of sandstone types can be derived from foreland uplifts, some of which may be indistinguishable from sandstones derived from continental blocks, collision orogens, or even subduction complexes (below). Dickinson and Suczek (1979) suggest that the most characteristic sandstones couple moderately high quartz contents with strikingly high feldspar content.

Finally, orogens consisting of uplifted subduction complexes composed of oceanic sediments and lavas are called **subduction-complex provenances**. Source rocks in these orogens may include deformed ophiolitic materials, greenstones, chert, argillite, graywackes, and limestones, which are exposed as constituents of mélanges, thrust sheets, and isoclinal folds formed by deformation within the subduction zone (Dickinson and Suczek, 1979). Sediments may be shed away from the subduction complex into forearc basins or into the adjacent trench. According to Dickinson and Suczek, the key signal for recognizing sandstones derived from subduction complexes is an abundance of chert, which, in their samples, greatly exceeded combined quartz and feldspar. They caution, however, that sandstones derived from subduction complexes containing abundant sandy source rocks may have a much weaker chert signal. Also, mixing of detritus from subduction-complex orogens, magmatic arcs, and collision orogens is possible.

Discussion

The principal petrographic characteristics of sediments derived from these major types of tectonic provenances are summarized in [Table 7.4](#). These are generalized characteristics,

Table 7.4 Framework composition of sandstones as related to tectonic provenance

Tectonic provenance	Derived sediment			Influence of climate and transport	
	Source rocks	Sand	Gravel		
Continental block					
A. Craton interior	Granitic and gneissic basement; subordinate sedimentary and metasedimentary rock from marginal belts	Quartz arenites and minor arkoses; high ratio of K-feldspar to plagioclase; minor lithic arenites	Minor quartzite(?); most clasts probably do not survive transport (?)	Platform settings, interior basins, foreland basins, passive continental margins and bordering oceans	Severe under humid conditions and long transport
B. Uplifted basement blocks	Granitic and gneissic basement plus sedimentary or metasedimentary cover; possible volcanic rocks	Feldspathic arenites and arkoses; minor sedimentary/metasedimentary or volcanic lithic arenites	Granite and gneiss clasts; minor sedimentary/metasedimentary, or clasts	Fault-bounded interior basins formed by incipient rifting or wrench faulting	Probably minimal owing to rapid erosion and short transport distance
Magmatic arc					
A. Undissected	Mainly andesitic to basaltic volcanic rocks	Lithic arenites composed of volcanic rock fragments and plagioclase grains; minor volcanic quartz	Andesite or basalt clasts	Forearc, backarc, and intraarc basins; trenches; possibly abyssal-plain basins	Probably minimal owing to rapid erosion and short transport distance
B. Dissected	Andesitic to basaltic volcanic rocks; plutonic igneous, metaigneous(?)	Mixtures of volcanic-derived rock fragments and plagioclase plus K-feldspar and quartz from plutonic sources	Andesite, basalt, plutonic igneous, or metaigneous clasts	Same as undissected arcs	Moderate effect of climate(?); minimal effect of transport

Table 7.4 (cont.)

Tectonic provenance	Source rocks	Derived sediment		Type of depositional basin	Influence of climate and transport
		Sand	Gravel		
Recycled orogen					
A. Subduction complexes	Ophiolite sequences (ultramafic rocks, volcanic rocks, chert); greenstones; argillites, graywackes; limestones; blueschists	Chert a key component (may exceed combined quartz and feldspar); may include sedimentary, ultramafic, volcanic rock fragments	Chert, greenstone, argillite, sandstone, limestone, serpentine	Forearc basins, trenches; possibly abyssal-plain basins	Probably minimal owing to rapid erosion and short transport distance
B. Collision orogens	Mainly sedimentary and metasedimentary rocks; subordinate ophiolite sequences, plutonic basement rocks, volcanic rocks	Intermediate quartz content; high quartz/feldspar ratio; abundant sedimentary and metasedimentary clasts, which may include chert from mélangé terranes or nodular lime-stones	Sedimentary and metasedimentary clasts, minor plutonic igneous, volcanic clasts, chert	Remnant ocean basins, foreland basins, basins developed along suture belts	Probably moderate to minimal
C. Foreland uplifts	Mainly sedimentary successions within fold-thrust belts; minor plutonic igneous, and metamorphic (?) rocks	Most diagnostic is high quartz with low feldspar content, but variable association of quartz, feldspar, chert	Sedimentary clasts, chert, minor plutonic igneous or metamorphic clasts	Mainly in foreland basins	Probably moderate to minimal

Source: Adapted from Dickinson, W. R. and C. Suczek, 1979, Plate tectonics and sandstone composition: *Am. Assoc. Petr. Geol. Bull.*, **63**, 2164–2182.

and readers should be aware that some overlap occurs in the characteristics of sediments derived from different provenances.

Knowing the major kinds of sediments derived from each major tectonic setting, it should be possible to interpret from the mineral composition of sandstones their probable tectonic provenance. Dickinson and Suczek tested this idea by plotting on triangular composition diagrams the framework modal composition of a large number of sandstones whose provenance was reasonably well known. Plots were made using various combinations of total quartz, feldspar, and unstable rock fragments, monocrystalline quartz, polycrystalline quartz, volcanic rock fragments, sedimentary rock fragments, plagioclase, and K-feldspar. These plots demonstrated that most sands from each major provenance setting formed well-defined clusters on the plots, although some individual samples plotted outside the clusters. The fact that gradational and overlapping field boundaries occur is not surprising, given the overlapping types of source rocks that occur in the major tectonic settings. On the basis of these sample studies, Dickinson *et al.* (1983) and Dickinson (1985) subsequently constructed generalized provenance plots for framework modes of detrital sandstones showing provisional subdivisions according to inferred tectonic provenance type. Two of these plots are shown in Fig. 7.12.

Ingersoll (1990) expanded upon this concept of actualistic sandstone petrofacies models – that is, models based upon petrographic data obtained from locally derived sands of known provenance and used to discriminate compositions statistically according to their source rocks. Ancient petrofacies are then compared to these “actualistic” petrofacies to better constrain provenance and paleotectonic reconstructions. Ingersoll suggests that this approach can be applied on a first-order scale (specific source rocks), second-order scale (source regions within a given tectonic setting), and third-order scale (continents and ocean basins).

Plate boundaries and detrital modes of sandstones

Can the nature of plate boundaries and the major kinds of depositional basins be interpreted on the basis of sandstone compositional modes? Dickinson and Valloni (1980) and Maynard *et al.* (1982) analyzed turbidite sands collected from a wide variety of sites on the modern ocean floor to examine the relationship of sandstone composition to known plate settings. The geographic position of the samples allowed them to be related to specific continental margins or oceanic island chains. The mean detrital framework modes of the sands were plotted on QFL (quartz/feldspar/lithic grains) and related diagrams to see if each major type of plate boundary shed sands with recognizable and distinctive provenance signature. Dickinson and Valloni's (1980) results are shown in Table 7.5. They report that sands derived from rifted continental margins have the highest quartz content and lowest percentage of lithic fragments. Plagioclase content is generally lower than in active-margin sands or those derived from oceanic island chains. Sands from active or orogenic continental margins are consistently less quartzose than those from rifted margins but contain more quartz than those derived from island chains. The proportion of polycrystalline to monocrystalline quartz is higher in sands derived from orogenic settings than in those from rifted-margin settings. Sands derived from intraplate, oceanic island chains generally lack quartz, contain

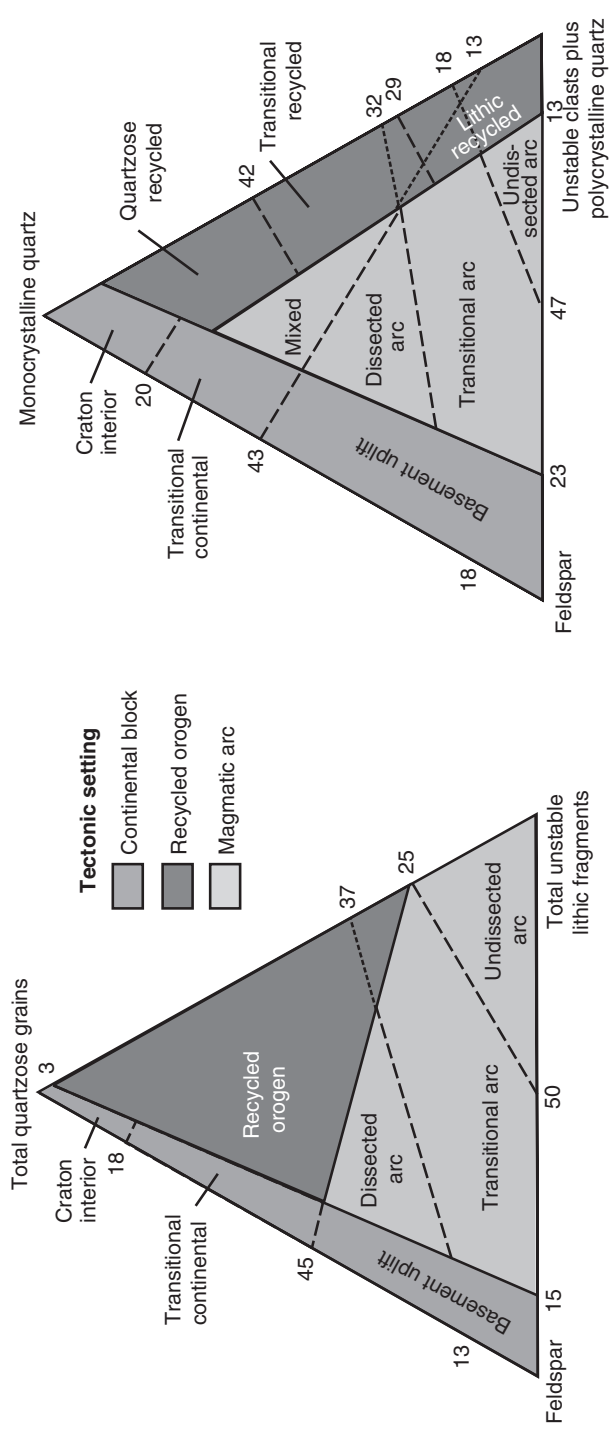


Figure 7.12 Relationship between framework composition of sandstones and tectonic settings, as indicated in Table 7.4. (After Dickinson, W. R. *et al.*, 1983, Provenance of North American sandstones in relation to tectonic setting: *Geol. Soc. Am. Bull.*, **94**, Fig. 1, p. 223.)

Table 7.5 *Composition of sandstone detrital constituents as a function of major types of plate boundaries*

	Rifted margin	Active margin	Island chain
Quartz content	Highest	Intermediate	Lowest
Polycrystalline/monocrystalline quartz ratio	Lowest	Highest	Little quartz
Plagioclase content	Lowest	High	High
K-feldspar content	Highest(?)	Intermediate	Little or none
Lithic-fragment content	Lowest	Intermediate	Highest(?)

Source: Dickinson, W. R. and R. Valloni, 1980, Plate settings and provenance of sands in modern ocean basins: *Geology*, **8**, 82–86.

plagioclase but little or no K-feldspar, and contain abundant lithic fragments that are almost exclusively volcanic clasts.

Maynard *et al.* (1982) conclude that sands derived from rifted, or trailing-edge, margins typically have more than 40 percent quartz, whereas those from active-margin settings (backarc, forearc, continental-margin arc, strike-slip) have less than 40 percent. Among active-margin settings, sands from intraocean forearc basins are composed dominantly of volcanic rock fragments, whereas those from strike-slip-related settings have a significantly lower proportion of volcanic grains in the rock fragments. Sands from other arc-related settings overlap considerably in composition. All share the characteristics of low quartz and high proportions of volcanic rock fragments; however, basins lying on the oceanic side of continental margin arcs and backarc basins of island arcs contain sands of almost identical composition.

Reliability of framework-mode provenance models

The sandstone modal framework plots described above provide other workers with convenient and potentially powerful models for evaluating tectonic setting. The tectonic provenance of any sandstone can presumably be interpreted simply by reference to these plots. Just how reliable are these models for provenance analysis? Judging by the number of papers utilizing this provenance technique that have now appeared in print, the models have received widespread acceptance. There is always a danger, however, with any fairly simple and elegant model that provisional or tentative field boundaries or conclusions become fixed boundaries or conclusions once the model is published. Subsequent workers tend to ascribe to the model a degree of rigor that was never actually intended by the authors. Therefore, it is necessary to be aware that in the application of these provenance models, as with any model, exceptions can occur.

Interpretations based on modal composition may not always agree with interpretations made on the basis of stratigraphic and structural relationships. For example, Mack (1984) points out four categories of sandstones that may plot in error on provenance framework diagrams: (1) sandstones deposited during the transition between tectonic regimes may be

derived, in part, from relict source rocks; (2) sandstones enriched in detrital quartz owing to weathering and/or depositional reworking may lead to inaccurate interpretation of tectonic setting from compositional data; (3) sandstones deposited in tectonic settings as yet unrepresented on the provenance diagram may plot between the provenance fields or overlap existing fields; and (4) sandstones containing abundant detrital carbonate rock fragments may affect the location of data points on provenance diagrams. Schwab (1981) applied Dickinson and Valloni's (1980) model based on study of sands from the modern ocean to evaluation of ancient sandstones in the French–Italian Alps. He found general support for the model, but underscored the necessity for defining the relationship between sandstone mineralogy and plate-tectonic setting more specifically. Girty *et al.* (1988) also sound a cautionary note about use of the model when sand or sandstone samples are from a limited geographic area and when metavolcanics are suspected in the provenance. Also, there is some disagreement among provenance workers about the use of the so-called Gazzi–Dickinson point-counting method versus the conventional point-counting method in provenance studies (Ingersoll *et al.*, 1984; Suttner and Basu, 1985). (In the Gazzi–Dickinson method, large, recognizable crystals within a rock fragment are identified and counted as that crystal – e.g. plagioclase – rather than the grain being counted as a rock fragment.) Even Dickinson (1988, p. 3) cautions against overextension of these models when he points out that petrofacies of mixed provenance are common because dispersal paths connecting sediment sources to basins of deposition may be complex. “Consequently, the geodynamic relations of different types of sedimentary basins as revealed by their overall morphology, structural relations, and depositional systems do not predict reliably the nature of the petrofacies that some basins contain.”

Further insight into potential problems involved in use of tectonic-provenance plots, is provided in the discussion of Dickinson and Ingersoll (1990) and Johnsson and Stallard (1990). Recently, Weltje (2006) made a rigorous statistical evaluation of Dickinson's sandstone provenance model. Weltje's analysis may be a bit difficult to follow for the “statistically impaired,” like myself; however, he gives the Dickinson model a mixed review. “Results indicate that differences between the grand means of each of the three provenance associations (continental block, magmatic arc and recycled orogen) are highly significant, whereas overall inferential success ratios range from 64% to 78% in the four ternary systems studied. Current methods of dealing with sands of mixed provenance are unsatisfactory.” In spite of its limitations, it is likely that Dickinson's model will continue to be popular with geologists.

Interpreting tectonic setting from sandstone geochemistry

Although most studies of tectonic setting have relied on interpretations based upon sandstone mineralogy, several studies have shown that major and trace-element geochemistry also reflect provenance differences that depend upon tectonic setting (e.g. Bhatia and Crook, 1986; Roser and Korsch, 1986; Skilbeck and Cawood, 1994). Both trace elements (particularly relatively immobile elements such as La, Y, Th, Zr, Hf, Nb, Ti, and Sc) and major elements have proven to be useful in studies of tectonic setting.

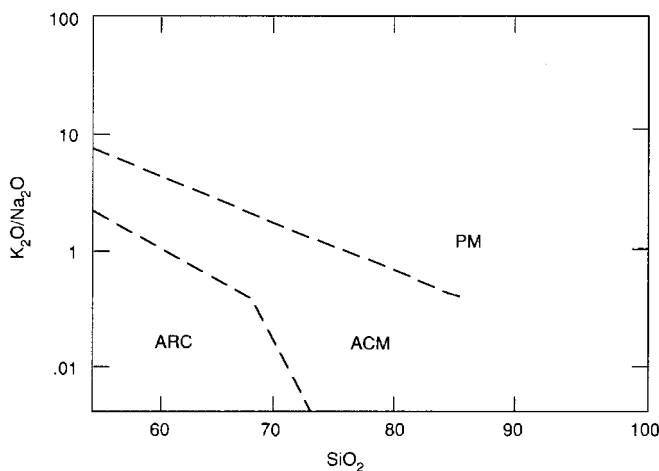


Figure 7.13 Chemical model for discriminating tectonic setting of sandstones and argillites on the basis of K_2O/Na_2O ratios and SiO_2 content. ARC= oceanic-island-arc margin, ACM= active continental margin, PM= passive margin. (After Roser, B. P. and R. J. Korsch, 1986, Determination of tectonic setting of sandstone–mudstone suites using SiO_2 content and K_2O/Na_2O ratios: *J. Geol.*, **94**, Fig. 2, p. 638, reprinted by permission of University of Chicago Press.)

The SiO_2 content and K_2O/Na_2O ratios in sandstones appear to be particularly sensitive indicators of geotectonic setting. For example, Roser and Korsch (1986) present a chemical model, based on K_2O/Na_2O ratios and SiO_2 content, for discriminating tectonic setting (Fig. 7.13). By using these chemical parameters, they were able to discriminate among samples from three major tectonic settings: passive margin (PM), active continental margin (ACM), and oceanic-island-arc margin (ARC). Some overlaps occur between the composition fields shown in Fig. 7.13, but overall the discriminating power of the technique appears to be reasonably good.

As an example of trace-element studies, Bhatia and Crook (1986) used Th, La, and Sc to discriminate between tectonic settings in New Zealand. Thallium and lanthanum are typically higher in rhyolites, whereas scandium is typically higher in basic igneous rocks. Thus, in Th–La–Sc plots, rocks that plot in the oceanic-island-arc field are generally more basic than those that plot in the continental-arc field, which are generally more silicic.

Further applications of these geochemical techniques to study of tectonic settings in New Zealand were made by Briggs *et al.* (2004). The results of their study, summarized in Fig. 7.14, show that New Zealand sedimentary rocks were deposited in Late Triassic–Late Jurassic time. The K_2O/Na_2O versus SiO_2 plots indicate that the sediments were derived mainly from oceanic-island-arc (ARC) and active-continental-margin (ACM) settings. The La–Th–Sc plots indicate oceanic-island-arc and continental-island-arc settings. These examples of the relation of sandstone geochemistry to tectonic setting are by no means comprehensive. They simply serve to illustrate the general principle that tectonic setting can be read from sandstone whole-rock geochemistry.

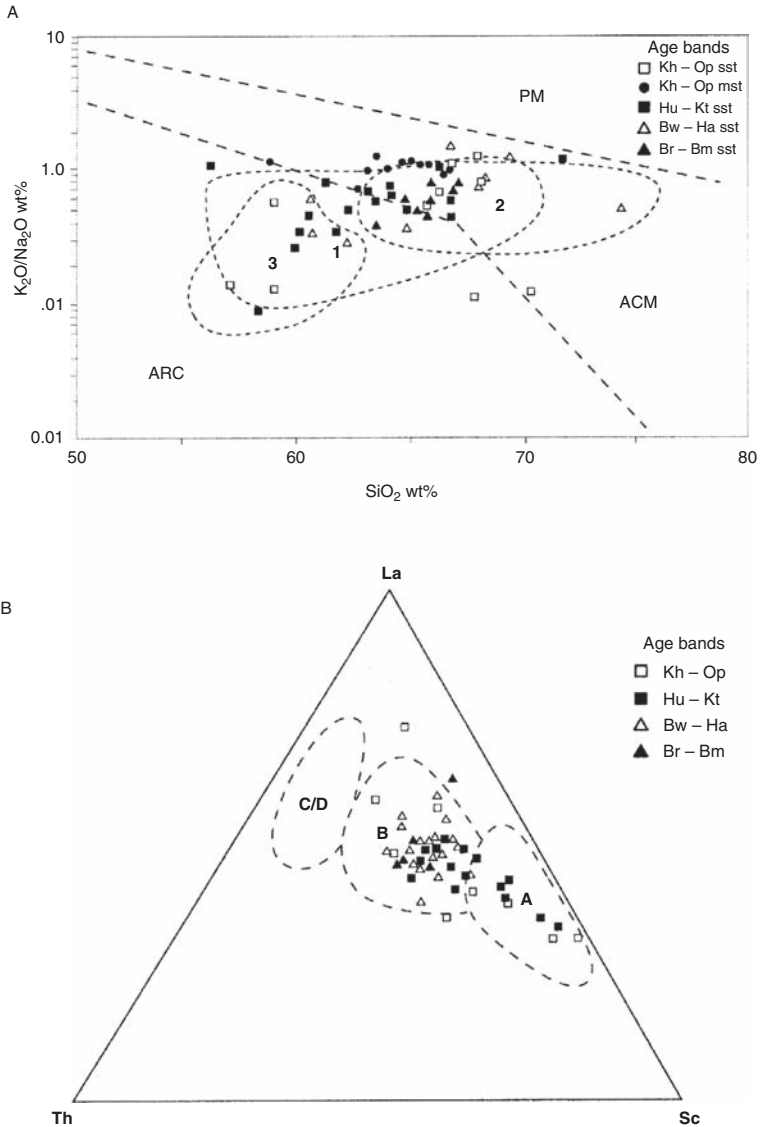


Figure 7.14 Tectonic setting of Murihiku rocks in the North Island, New Zealand, based on geochemical composition of the rocks. **A.** SiO_2 versus K_2O/Na_2O diagram plotted according to ages of sediment. Kh–Op=Mid–Late Jurassic; Hu–Kt=Early–Mid Jurassic; Bw–Ha=Late Triassic – Early Jurassic; Br–Bm=Late Triassic. Provenance fields after Roser and Korsch (1986). ARC=oceanic island arc; ACM=active continental margin; PM=passive continental margin. Compositional fields for Southland Syncline Murihiku rocks after Roser and Korsch (1986) are also shown (dotted envelopes): 1, Middle Triassic; 2, Late Triassic; 3, all Jurassic.: sst=sandstone; mst=mudstone. **B.** A Th–La–Sc diagram plotted according to ages. Provenance fields after Bhatia and Crook (1986). A, oceanic island arc; B, continental island arc; C, active continental margin; D, passive margin. (After Briggs *et al.*, 2004, Provenance history of a Late Triassic–Jurassic Gondwana margin forearc basin, Murihiku Terrane, North Island, New Zealand: Petrographic and geochemical constraints: *New Zealand J. Geol. Geophys.*, **47**, Fig. 5, p. 598, reproduced by permission.)

7.5.3 Interpreting climate and relief of source areas

Interpreting climate from petrographic data

Climate, through its influence on weathering processes, can have a significant effect on the ultimate composition of sandstones and thus on provenance interpretation. Hot, humid climates promote alteration and destruction of less-stable minerals and rock fragments, whereas very cold or very dry climates favor preservation of these less-stable constituents. Furthermore, conditions of low relief and gentle slopes enhance chemical weathering because particles are eroded from such areas slowly. By contrast, high relief and steep slopes promote rapid erosion of detritus before it is significantly weathered. Are the effects of climate sufficiently strong that they leave a climatic “signature” on detrital mineral assemblages that we can read? That is, can we determine from the petrographic characteristics of sandstones what the climate and relief of the source area might have been?

Perhaps the most straightforward attempt to interpret source-area climate and relief from detrital mineralogy is that of Folk (1974, p. 85). Folk suggests that climate and relief of ancient source areas can be evaluated on the basis of the relative size and degree of rounding of quartz and feldspar. That is, smaller size of feldspar grains relative to quartz grains and a high degree of rounding of both feldspar and quartz indicates prolonged reworking in source areas of low relief and intense weathering under hot, humid conditions. The simplicity of Folk’s concept is appealing; however, it is probably oversimplified, and it is certainly difficult to apply in practice. For example, grain roundness may be inherited from a previous sedimentary cycle and feldspars can become altered during diagenesis as well as during weathering.

Is it possible on the basis of sandstone mineralogy to develop reliable criteria for interpreting source-area climatic conditions that overcome these difficulties? Several investigators have attempted to clarify the relationship between climate and sandstone mineralogy by studying the composition of Holocene sands released from similar kinds of source rocks undergoing weathering under different climatic conditions (e.g. Young *et al.*, 1975; Grantham and Velbel, 1988; Mack and Jerzykiewicz, 1989). A second approach is to study the composition of ancient sandstones that formed under climatic conditions that are known on the basis of independent paleoclimatic evidence (e.g. Suttner and Dutta, 1986).

Investigators using the first approach attempt to set up a sampling program by which source rock lithology, relief, and sediment transport are as invariable as possible, with climate being the only major variable. Variations in the composition of first-cycle Holocene sands released from similar source rocks under these conditions, should thus reflect differences in climate. For example, Young *et al.* (1975) studied composition versus size of first-cycle sands derived from metamorphic and plutonic rocks in semiarid and humid climates. They conclude that regardless of crystalline source-rock type, weathering in semiarid climates generates greater amounts of rock fragments, feldspars, and accessory minerals. Weathering in humid climates produces relatively more polycrystalline and monocrystalline quartz because less-stable minerals and rock fragments are more easily destroyed by vigorous chemical weathering under humid conditions. See also Basu (1976) and Suttner *et al.* (1981).

Suttner and Dutta (1986) extrapolated these techniques developed with Holocene sands to study of ancient sandstones. These authors suggest that systematic variations in compositional maturity can be related to changing climatic conditions during deposition. For example, compositional maturity of Gondwana sandstones, from base to top of the group, increases progressively from immature to mature to submature to supermature. Suttner and Dutta link this change to the changing paleoclimate of India (glacial, arid → temperate, humid → warm, semiarid → warm, humid) associated with the Permian to Triassic drift of India through different latitudinal zones and the overall change in global climate.

As another example of this approach, Mack and Jerzykiewicz (1989) suggest that the ratio of volcanic rock fragments to plagioclase plus volcanic rock fragments (RFP index) and the ratio of volcanic rock fragments to accessory minerals plus volcanic rock fragments (RFA index) can be used as a paleoclimate indicator. They present data that show that the RFP and RFA indices are statistically lower in sandstones derived from humid regions than in those derived from regions with a semiarid climate. This difference reflects a greater degree of chemical breakdown of the parent rock and gravel- and sand-sized rock fragments, and release of monocrystalline grains, in humid climates.

There are many factors that make paleoclimate interpretation from sandstone composition data very tenuous. The techniques discussed above appear to work only for first-cycle sediments derived from crystalline plutonic or metamorphic rocks that have been transported relatively short distances, deposited in nonmarine environments without significant reworking, and that have undergone relatively little diagenetic alteration. Sediment recycling, extensive reworking in a marine environment, and extensive diagenetic alteration can all apparently destroy the climate signature. The problem of distinguishing between the effects of paleoweathering and diagenesis are considered at length by Velbel and Saad (1991). These authors concluded that “only long-term average paleoclimate conditions are preserved in sandstone detrital framework modes.” Further, “the framework petrographic signatures of paleoclimate can be discerned only in unglaciated sequences from mature extensional tectonic settings on continental plates, only in sedimentary basins with mild late-diagenetic histories, and only for those modern-ancient pairs [ancient sediment vs. modern sediment derived from the same tectonic setting] where the modern climate is more humid than the inferred ancient climate.”

Interpreting relief and slope

Estimating the relief of source areas is even more tenuous than estimating climate. Although geologists have generally accepted the dictum that rugged relief results in generation of coarser-grained, fresher detritus than that formed under conditions of low relief, that belief appears to be based largely on intuitive reasoning rather than actual research. Little quantitative work has apparently been done to evaluate the effects of relief on sandstone composition. Basu (1985) suggests that it is actually slope angle, not relief, that controls the residence time of sediment in soil horizons. If slopes are greater than the angle of repose of sediment, the effects of such steep slopes on rapid removal of soils could presumably mask all effects of climate even under the most humid, hot climatic conditions.

Grantham and Velbel (1988) provide some additional insight into this problem. These authors suggest that rock fragments are the most sensitive indicators of cumulative weathering effects. They maintain that abundance of rock fragments in detritus entering a fluvial transport system does not correlate directly with climate but, instead, correlates with total or cumulative chemical weathering in the source area. Total chemical weathering is, in turn, a function in part of duration of weathering. Duration of weathering is measured as the relief ratio (maximum relief divided by maximum length of each watershed) and is related to the total time weathering fluids and weatherable minerals and rock fragments are in contact. Because of higher rates of erosion, high slopes have shorter mineral-fluid times and overall shorter durations of weathering.

Chemical weathering is a function also of intensity of weathering, measured as effective precipitation (stream discharge per watershed unit area). Grantham and Velbel express the relationship between total chemical weathering and these duration and intensity factors as

$$\text{Cumulative chemical weathering index} = \text{Effective precipitation} \times \frac{1}{\text{Relief ratio}}$$

They conclude that soils in watersheds with low relief ratios and high discharge per unit area experience the most extensive chemical weathering; therefore, sediments derived from these source areas contain the lowest percentages of rock fragments. Thus, both climate and topographic slope affect sediment composition, and it may be difficult to separate the effects of these two variables.

We can perhaps conclude from this discussion that high relief, or more accurately steep slopes, promote preservation of rock fragments, which appear to be the most sensitive indicators of weathering conditions. Rock fragments are preserved relatively less well on low slopes that experience high rainfall. If slopes are very high, exceeding the angle of repose, then, presumably, abundant rock fragments will be preserved even under high-rainfall conditions. The relative abundance of rock fragments in a first-cycle sandstone is thus a rough indicator of slope conditions. These relationships have not been quantified, however, and provide only the roughest sort of guide to topographic relief and slope of source areas. We are still a long way from developing a full understanding of the relationship between climate, slope, and sandstone composition.

7.6 Provenance of conglomerates

7.6.1 General statement

Most published provenance studies deal with sandstones, probably because sandstones are much more abundant than conglomerates and are easier to study than shales and mudstones. When conglomerates are present in a stratigraphic section, however, they commonly provide more-reliable provenance interpretation than do sandstones. Conglomerates are composed mainly of rock fragments, which typically preserve textures and structures that

make identification of the parent rock quite easy. Thus, the coarse clasts in conglomerates can be readily traced to specific kinds of plutonic igneous, volcanic, metamorphic, or sedimentary source rocks. This virtually unequivocal interpretation of source-rock lithology from conglomerate clasts stands in sharp contrast to provenance interpretation from sandstones, in which minerals such as quartz, feldspars, and micas may be derived from a variety of source rocks.

Interpretation of provenance from conglomerates is not, however, without problems because depositional assemblages of clasts may not faithfully represent the types and proportions of parent rocks in the source area. A variety of factors may account for these differences. Blatt (1982, p. 144) points out, for example, that the initial size of rock fragments differs with different lithologies owing to factors such as different petrophysical properties (degree of cementation, fissility, foliation) of source rocks, thickness of bedding, and spacing of joints. Thus, for example, well-cemented quartzite tends to weather into larger blocks than does granite or shale. A strong relationship exists between clast composition and clast size; thus, gravels may become sorted by size and composition during transport. For example, Boggs (1969) reports that analysis of coarse- and fine-gravel populations from the same point bar in the Sixes River, southwest Oregon, shows that sandstone, siltstone, and argillite fragments occur preferentially in the fine population, whereas conglomerate, volcanic, schist, phyllite, and greenstone clasts occur preferentially in the coarser population.

It is extremely important to keep this size-composition relationship in mind during provenance analysis because fine gravels derived from a particular source region may have a distinctly different composition than coarse gravels derived from the same region. The problems caused by differential susceptibility of different kinds of rock fragments to destruction by chemical weathering and mechanical destruction during transport cause additional difficulties in interpretation. Blatt (1982, fig. 5.1) shows, for example, that detectible destruction of soft gravel clasts such as sandstone, limestone, and schist can occur during fluvial transport in distances of as little as 15 km. Abbott and Peterson (1978) experimentally determined the relative durability of clasts to abrasion during transport as shown in Fig. 7.15.

Thus, relative clast stability, and the susceptibility of clasts to destruction during weathering and transport, are important factors that must be considered in interpretation of provenance from conglomerates. Nonetheless, because the particles in conglomerates are typically deposited closer to their source areas than are sand-size particles, they generally survive better than sand-size particles that commonly undergo much longer distances of transport. Thus, on the whole, conglomerates make more reliable provenance indicators than do sandstones. Clearly, however, it is necessary to be cautious about interpreting provenance from compositionally mature conglomerates made up mainly of ultradurable clasts. Such conglomerates may have been recycled from an earlier generation of conglomerates, or they may have undergone sufficient transport to selectively remove less-durable clasts. Conglomerates made up of mixed populations of clasts that include moderately or weakly durable types are more likely to be first-cycle deposits and can generally be more safely used for provenance determination.

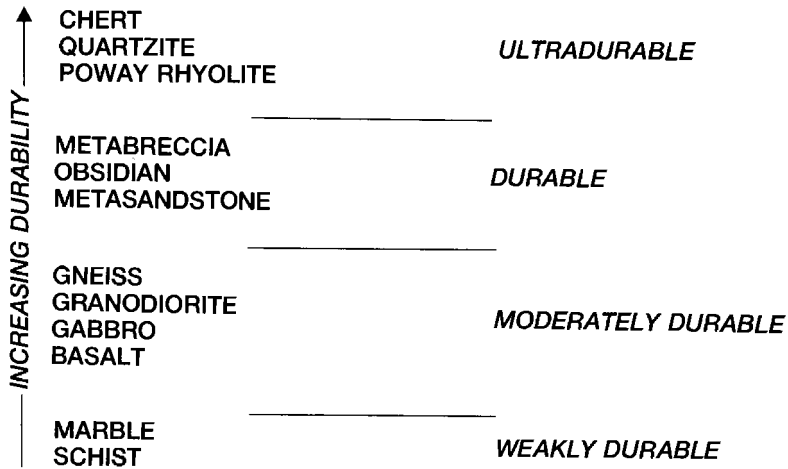


Figure 7.15 Abrasion durability scale for clasts. (From Abbott, P.L., and G.L. Peterson, 1978, Effect of abrasion durability on conglomerate clast populations: examples from Cretaceous and

7.6.2 Interpreting source-rock lithology from conglomerates

Basic procedure

Interpreting source-rock lithology from conglomerates is a comparatively straightforward process. First, due regard must be given to the problems imposed by clast size and selective destruction of clasts, as discussed above. The relative abundance of various kinds of clasts in a conglomerate is established by means of random pebble counts or clast counts, which is the rough equivalent of determining sandstone composition by thin-section modal point counts. Statistical treatment of these clast-composition data then allows interpretation of the approximate relative abundance or importance of various kinds of source rocks.

Lithologic provenance modeling

In areas where source rocks are preserved, a technique called “provenance modeling” can be used to identify matches between actual compositions of conglomerates and hypothetical compositions modeled from preserved source sections (Graham *et al.*, 1986; Decelles, 1988). This technique can be used only where some part of all the source rocks remains intact; that is, the full range of source units is at least partially preserved. It cannot be used if the source region has been so severely eroded that some of the potential source rocks are missing and thus not available for examination.

The steps involved in provenance modeling, as described by Graham *et al.* (1986), are shown in Fig. 7.16. The initial steps include determining the thickness of gravel-yielding

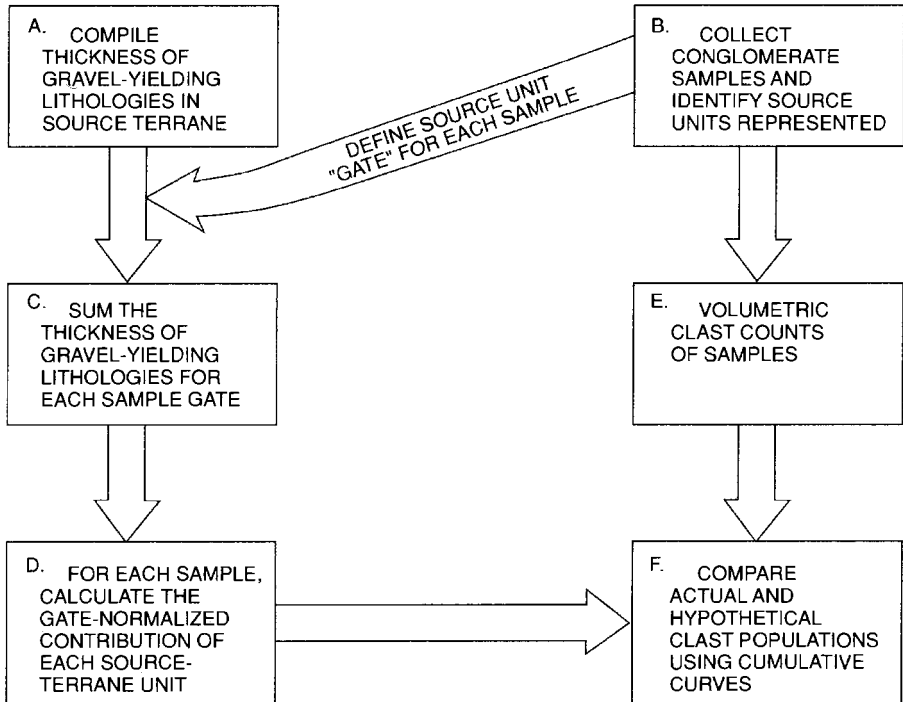


Figure 7.16 Schematic representation of the successive steps involved in provenance modeling of conglomerates. (From Graham, S.A. *et al.*, 1986, Provenance modeling as a technique for analysing source terrane evolution and controls on foreland sedimentation, in Allen, P.A. and

lithologies in the source area and making volumetric clast counts of samples of the conglomerate unit derived from this source area. The final step in the modeling process is to compare the calculated relative abundances of clasts with the actual relative abundances obtained by clast counts. This comparison can be made by plotting both the calculated relative clast abundance and the measured relative clast abundance on the same cumulative-curve diagram or histogram, as illustrated in Fig. 7.17.

If the final step demonstrates a close correlation between hypothetical relative abundance curves and actual curves, then we can assume with reasonable confidence that the relative abundance of the various kinds of clasts in the conglomerate adequately represents the relative abundance of these particular lithologies in the source region and that the provenance of the clasts has been correctly identified. If the relative abundance curves do not closely coincide, then some other explanation is required. This explanation might be that some lithologies present in the source area were selectively destroyed by weathering or transport processes. Alternatively, the conglomerates may not have been derived from the presumed source region or not entirely from that source region. Thus, the technique of

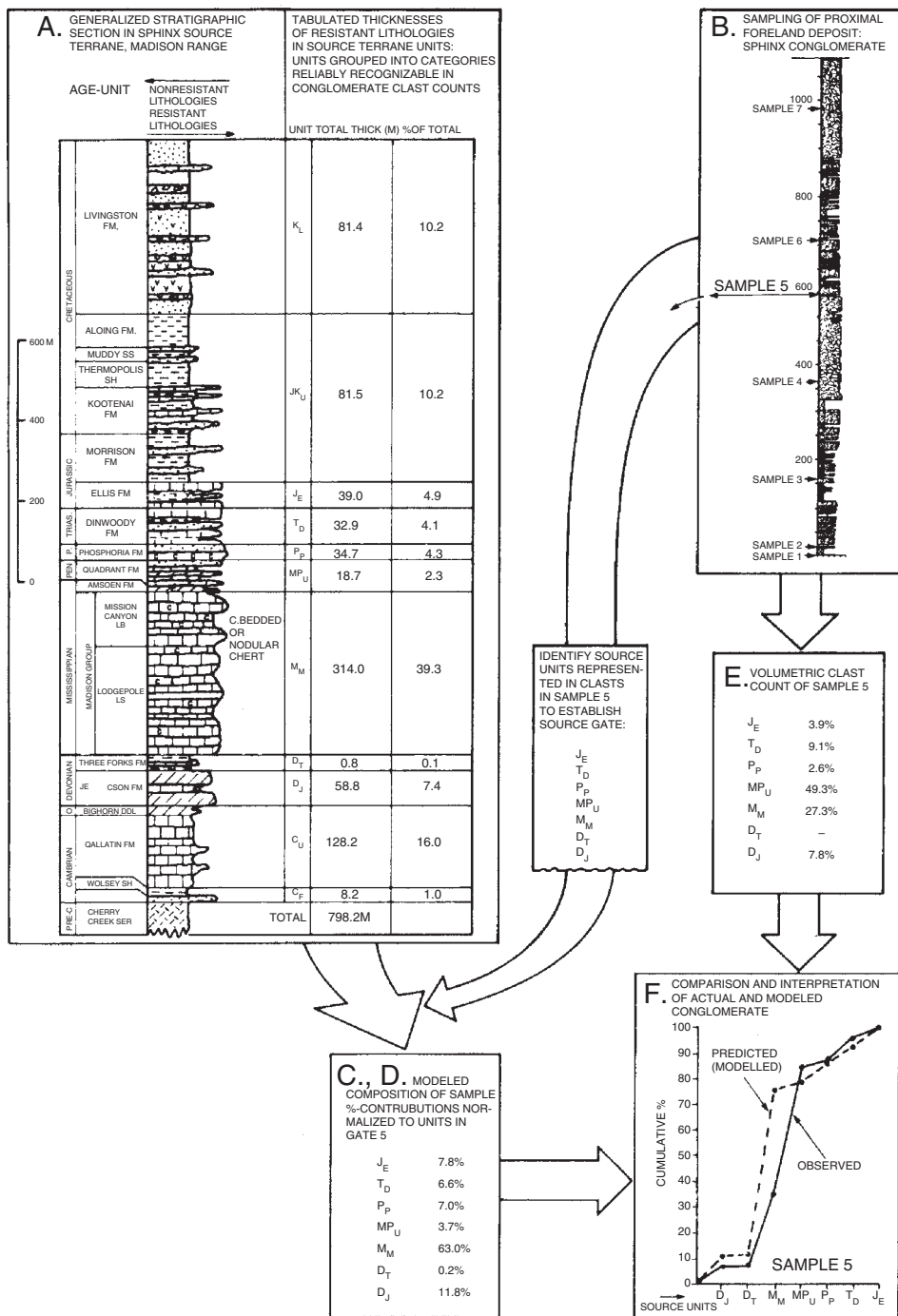


Figure 7.17 See next page for caption.

lithologic provenance modeling, when circumstances permit its application, should provide a more reliable means of relating conglomerate clast composition to a particular provenance than simple observation of clast-count data.

7.6.3 Interpreting tectonic setting from conglomerates

The process of interpreting tectonic setting from conglomerate compositional data is much the same as that used in interpreting tectonic setting from sandstone compositional data. That is, if we know the types of source rocks that are unique to each major tectonic setting, we should be able from clast-count data to interpret, at least approximately, the tectonic setting. Table 7.4 lists the major tectonic provenances, the major kinds of source rocks that occur in each provenance, the principal kinds of sand-size and gravel-size sediment that are derived from these source rocks, and the kinds of depositional basins in which these materials are deposited. No one has put together for conglomerates the kinds of provenance diagrams used by Dickinson and Suczek (1979) to study the tectonic setting of sandstones; however, Table 7.4 provides a rough guide to tectonic setting. For example, a predominance of volcanic clasts in a conglomerate suggests a magmatic-arc provenance, an abundance of sedimentary or metasedimentary clasts indicates a probable recycled-orogen provenance, and abundant granitic and gneissic clasts are most likely derived from uplifted basement blocks. For an application of this principle, see Herbig and Stattegger (1989).

A recent trend in provenance evaluation of conglomerates involves isotopic (age-dating) and geochemical analysis of conglomerate clasts. The general principles of these techniques are laid out in *Detrital Thermochronology* by Bernet and Spiegel (2004). Several workers, such as Dunkl *et al.* (1998), Brügel *et al.* (2004), and Wandres *et al.* (2004), discuss specific applications of geochemical techniques to provenance interpretation of conglomerate clasts.

The work by Wandres *et al.* is an admirably comprehensive and detailed example of such an application. These authors used X-ray fluorescence to obtain major and trace-element compositions, instrument neutron activation analysis (INAA) to analyze for rare-earth elements, and Sr–Nd isotopic analysis and SHRIMP U–Pb zircon dating methods to estimate ages of igneous and sedimentary clasts in New Zealand conglomerates. The results of their study allowed them to establish approximate ages of the source terranes from which

Caption for Figure 7.17 An example of the provenance-modeling technique as applied to the Sphinx Conglomerate (Cretaceous) in Montana. A. The Phanerozoic stratigraphic section that was recycled into the Sphinx Conglomerate. B–F. These show how one sample (Sample 5) is tracked through the modeling process. (From Graham, S. A., *et al.*, 1986, Provenance modeling as a technique for analysing source terrane evolution and controls on foreland sedimentation, in Allen, P. A. and P. Homewood (eds.), *Forelands Basins*: Blackwell Scientific, Oxford, Fig. 3, p. 428, reprinted by permission.)

the conglomerate clasts were derived and broadly characterize the igneous protosources of the terranes, as well as drawing some inferences about magmatic processes.

7.7 Provenance of shales and mudstones

Shales and mudstones are the most abundant kind of sedimentary rock. Nonetheless, geologists appear to be less interested in the provenance of these rocks than in that of sandstones and conglomerates – presumably because their fine grain size makes them more difficult to study petrographically. Two methods for studying shale provenance are commonly used. First, because most shales contain some silt- or sand-size particles, larger particles of quartz, feldspar, and heavy minerals can be studied by the same methods used to evaluate the provenance of sandstones. For example, Blatt and Caprara (1985) and Jones and Blatt (1984) studied feldspar in shales as provenance indicators.

The second method for studying shale provenance employs whole-rock geochemical analysis to determine rare-earth and trace-element abundances. Sethi *et al.* (1998) point out that whereas certain elements such as Na, Mg, Ca, U, and Rb are easily affected by weathering and diagenesis, rare-earth elements (REEs) are highly resistant to fractionation during weathering and diagenesis. “The low solubilities of the REEs and short residence times in the ocean allow for them to be faithfully preserved in terrigenous sediments and validate their use as accurate indicators of provenance.” Thus, numerous studies have been published in which the rare-earth composition of shales and mudstones is used as a technique for provenance interpretation. Most of these studies focus on identifying rather broad aspects of provenance terranes rather than interpreting specific source-rock lithologies.

For example, McLennan *et al.* (1990, 1993) analyzed shales and matrix-rich sands from a number of tectonic settings: continental trailing edge, continental collision, strike slip, backarc, continental arc, and forearc. They recognized five provenance components on the basis of geochemistry and Nd-isotopic composition: (1) Old Upper Continental Crust (old igneous/metamorphic terranes); (2) Recycled Sedimentary Rocks; (3) Young Undifferentiated Arc (young volcanic/plutonic source that has *not* experienced plagioclase fractionation); (4) Young Differentiated Arc (young volcanic/plutonic source that has experienced plagioclase fractionation); and (5) various exotic components (e.g. ophiolites). Table 7.6 summarizes some of the geochemical and Nd-isotopic characteristics of these terranes (provenances).

7.8 Concluding remarks

Interpretation of the provenance of sediments and sedimentary rocks is an important goal of many geologic studies. Most provenance studies focus on sandstones and conglomerates; however, the provenance of shales and mudstones is receiving increasing attention.

Table 7.6 Summary of geochemical and Nd-isotopic characteristics of terrane (provenance) types*

Terrane type	$\epsilon_{\text{Nd}}^{\dagger}$	Eu/Eu*	Th/Sc	Th/U	Other
Old Upper Continental Crust (OUC)	≤ -10	$\approx 0.60-0.70$	≈ 1.0	>3.8 (shales)	Evolved major-element composition (e.g. high Si/Al, CIA); high LILE abundances; uniform compositions
Recycled sedimentary rocks (RSR)	≤ -10	$\approx 0.60-0.70$	≥ 1.0		Evidence of heavy-mineral concentration from trace elements (e.g. Zr, Hf for zircon, REE for monazite)
Young Undifferentiated Arc (YUA)	$\geq +5$	≈ 1.0	< 1.0	< 3.0	Unevolved major-element compositions (e.g. low Si/Al, CIA); low LILE abundances; variable compositions
Young Differentiated Arc (YDA)	$\geq +5$	$\approx 0.50-0.90$	Variable	Variable	Evolved major-element composition (e.g. high Si/Al, CIA); high LILE abundances; variable compositions
Exotic components	Chemical and/or isotopic signature depends on the nature of the component; e.g. very high Mg, Cr, Ni, V, and Cr/V would be distinctive of ophiolite sources.				

* ϵ_{Nd} represents deviations of the $^{143}\text{Nd}/^{144}\text{Nd}$ ratio in parts per 10^4 from average chondritic meteorites; Eu* is a theoretical value for Eu, assuming no chondrite-normalized Eu anomaly; CIA is the mean Chemical Index of Alteration; LILE refers to lithophile elements. (After McLennan *et al.*, 1993, Table 1, p. 23.)

† The ϵ_{Nd} values are for modern sediments only. Distinctions between terrane types would persist for older sedimentary rocks but would be increasingly less pronounced with age. Exact values would depend on sedimentation age.

Comprehensive provenance study includes evaluation and interpretation of source-rock lithology, location and nature of the tectonic setting (provenance terranes), topographic relief and slope of source areas, as well as the climate of the source region. A variety of tools and techniques are used in provenance study, including petrographic microscopy, electron microscopy, cathodoluminescence imaging, geochemical and isotope analysis of individual mineral grains, and whole-rock geochemistry. Provenance analysis dates back to the late 1800s (e.g. Sorby, 1880; Mackie, 1896) and has been an active area of research since at least the 1940s. There is every reason to believe that significant interest in provenance will continue in the future.

Further reading

- Bahlberg, H. and P. A. Lloyd (eds.), 1999, Advanced techniques in provenance analysis of sedimentary rocks: *Sedimentary Geol.*, **124** (Special Issue)
- Bernet, M. and C. Spiegel (eds.), 2004, *Detrital Thermochronology – Provenance Analysis, Exhumation, and Landscape Evolution of Mountain Belts*: Geological Society of American Special Paper 378.
- Boggs, S, Jr. and D. Krinsley, 2006, *Application of Cathodoluminescence Imaging to the Study of Sedimentary Rocks*: Cambridge University Press, Cambridge.
- Johnsson, M. J. and A. Basu (eds.), 1993, *Processes Controlling the Composition of Clastic Sediments*: Geological Society of America Special Paper 284.
- Zuffa, G. G. (ed.), 1984, *Provenance of Arenites*: Reidel, Dordrecht.

8

Diagenesis of sandstones and shales

8.1 Introduction

Petrologic study of siliciclastic sedimentary rocks commonly focuses on interpretation of sediment provenance and depositional paleoenvironments. It may aim also at evaluating the economic significance of these sediments as source rocks or reservoir rocks for petroleum or as hosts for ore deposits. Discussion in previous chapters suggests that genetic interpretations can be compromised by postdepositional changes in composition or texture brought about by diagenetic processes. Provenance interpretation, in particular, can be severely affected by diagenetic processes that selectively remove feldspars, heavy minerals, or rock fragments by intrastratal solution. Diagenesis may also play an extremely important role in postdepositional modification of porosity, causing either decrease in porosity as a result of compaction and cementation or increase in porosity owing to solution processes. Thus, the economic importance of a particular sandstone body as a reservoir rock for petroleum, for example, may very well depend as much upon the diagenetic history of the sandstone as upon its original depositional characteristics. Therefore, to avoid erroneous interpretations of petrogenesis or costly errors in economic evaluations, it is necessary to understand as much as possible about the diagenetic processes that can affect siliciclastic sedimentary rocks. We are concerned not only with the nature of diagenetic processes but also with the types of changes that are produced in the rocks as a result of these processes. That is, we strive to recognize the diagenetic characteristics of siliciclastic rocks and to differentiate these diagenetic features from original depositional characteristics.

Diagenesis in the broadest sense encompasses all of the processes that act to modify sediment after deposition. Diagenesis may begin very early after deposition by processes such as biogenic reworking of unconsolidated sediment or cementation of grains at or near the sediment–water interface. It continues throughout burial and may extend into the uplift stage when a sediment pile is uplifted after burial. During the early stages of diagenesis, sediments undergo compaction, water expulsion, thinning of beds, and porosity loss. Concomitant and subsequent modifications may include cementation by various minerals such as quartz and carbonates, formation of other authigenic minerals, including clay minerals, and dissolution of less-stable minerals. These diagenetic processes bring about important physical, mineralogical, and chemical changes in original depositional

assemblages. The net effect of diagenetic modifications is to move initially incompatible assemblages of siliciclastic minerals toward conditions of chemical equilibrium that are more in adjustment with the diagenetic environment. Our ability to extract genetic information from ancient siliciclastic sedimentary rocks is strongly dependent upon our ability to understand these diagenetic changes and to reconstruct the postdepositional histories of these rocks.

Early studies of diagenesis focused on petrographic examination of thin sections and the evidence of compaction, cementation, dissolution, and so on that could be read from petrographic study. Petrographic examination remains the mainstay of diagenetic study; however, it has been increasingly supplemented since the 1960s by use of the electron microscope, cathodoluminescence petrography, X-ray diffraction analysis, electron microprobe analysis, and various techniques for geochemical evaluation, including isotope studies. In this chapter, we explore some of the more important aspects of siliciclastic sediment diagenesis.

8.2 Diagenetic stages and regimes

Diagenesis takes place during burial at depths ranging from the depositional interface to perhaps 15 km or more. Thus, the pressure–temperature conditions under which diagenesis occurs essentially extend from those that characterize weathering to those that characterize metamorphism. There are no clear-cut boundaries on either end of this scale, although diagenesis is commonly regarded to take place at temperatures below about 200–250 °C and at pressures below ~5 kb (Fig. 8.1).

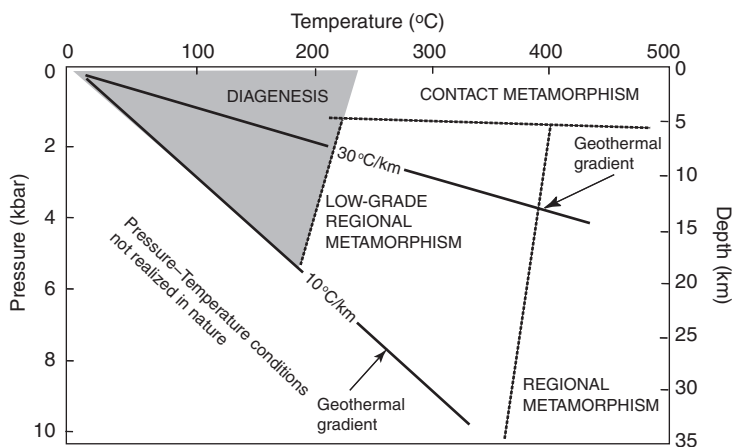


Figure 8.1 Pressure–temperature diagram relating diagenesis to metamorphic regimes and typical pressure–temperature gradients in Earth’s crust. The 10 °C/km geothermal gradient is typical of stable cratons; the 30 °C/km gradient is typical of rifted sedimentary basins. [Modified from Worden, R. H. and S. D. Burley, *Sandstone diagenesis: The evolution of sand to stone*, in Burley, S. D. and R. H. Worden (eds.), 2003, *Sandstone Diagenesis: Recent and Ancient*: Blackwell, Malden, MA, Fig. 1, p. 3, reproduced by permission.]

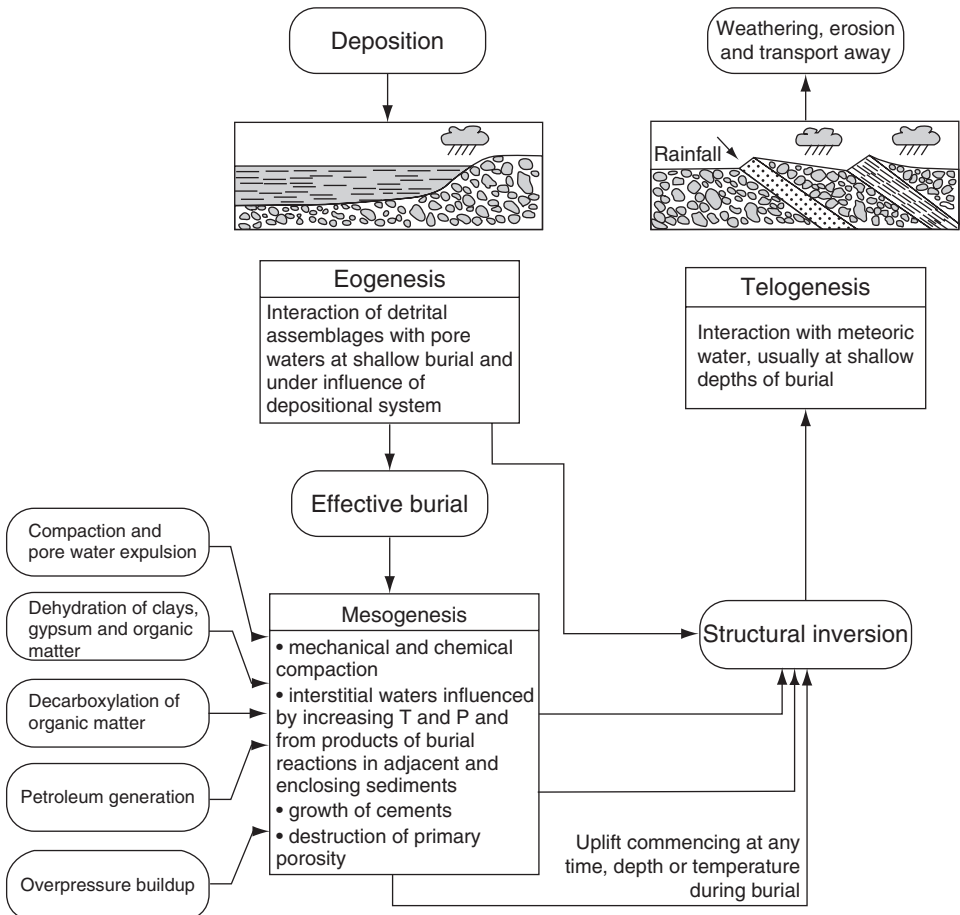


Figure 8.2 Flow chart illustrating the links between the regimes of diagenesis. Structural inversion refers to uplift. [From Worden, R. H. and S. D. Burley, 2003, *Sandstone diagenesis: The evolution of sand to stone*, in Burley, S. D. and R. H. Worden (eds.), *Sandstone Diagenesis: Recent and Ancient*: Blackwell, Malden, MA, Fig. 4, p. 7, reproduced by permission.]

Various investigators have suggested that diagenesis proceeds through three to six recognizable stages (Choquette and Pray, 1970; Dunoyer de Segonzac, 1970; Schmidt and McDonald, 1979; Dapples, 1979; Fairbridge, 1983; Singer and Müller, 1983; Burley *et al.*, 1985; Pettijohn *et al.*, 1987, p. 426). Perhaps the most widely accepted stages are those of Choquette and Pray (1970), who used the terms **eogenetic**, **mesogenetic**, and **telogenetic** to indicate the times of early burial, deeper burial, and late-stage erosion. Worden and Burley (2003) refer to these stages simply as eogenesis, mesogenesis, and telogenesis (Fig. 8.2). **Eogenesis** refers to the earliest stage of diagenesis, which takes place at very shallow depths (a few meters to tens of meters) largely under the conditions of the depositional environment. **Mesogenesis** is diagenesis that takes place during deeper burial under conditions of

increasing temperature and pressure and changed pore-water compositions. **Telogenesis** refers to late-stage diagenesis that accompanies or follows uplift of previously buried sediment into the regime of meteoric waters. Sediments that are still deeply buried in sedimentary basins (never uplifted) have not, of course, undergone telogenesis.

Whatever the terminology used to describe different diagenetic stages, it is clear that siliciclastic sediments undergo sequential changes with burial that occur as a result of biogenic activity, higher pressures and temperatures, and changed pore-water compositions. These diagenetic changes include postdepositional mixing of sediment owing to bioturbation; rearrangement of grain packing and loss of porosity as a result of compaction from sediment loading; loss of porosity through cementation; partial or complete destruction of some framework grains owing to pressure solution; destruction of some framework-grain cements or matrix by dissolution, creating secondary porosity; replacement of some minerals by others; and clay-mineral authigenesis. These processes are discussed in the remaining part of this chapter.

8.3 Diagenetic reactions in the eogenetic realm (Depositional-environment-related diagenesis)

8.3.1 General statement

The **eogenetic regime** is the depositional environment. Nonmarine environmental conditions range from arid-oxidizing to wet-reducing pore waters, and marine environments may be characterized by either oxidizing or reducing pore waters. Important biological and chemical/mineralogical diagenetic changes may occur during this early stage, with the course of mineralogical diagenesis determined by the specific Eh, pH, and chemical composition of the pore waters.

8.3.2 Bioturbation and compaction

Organisms rework sediment at or near the depositional interface through various crawling, boring, burrowing, and sediment-ingesting activities. These activities may extend from the depositional interface to depths of several tens of centimeters, resulting in churning or mixing sediment to various degrees. Bioturbation causes extensive destruction of primary sedimentary structures and textural patterns, thereby bringing about loss of important environmental information. Only sediments deposited in toxic or anoxic environments, or those deposited so rapidly that organisms do not have time to rework them, appear to escape bioturbation. As a result of their activities, organisms may destroy primary depositional features and create in their place a variety of traces such as mottled bedding, burrows, tracks, trails, and so on (Fig. 8.3). These features are referred to as trace fossils.

Although bioturbation can destroy primary depositional features such as lamination, it probably has little effect on the composition of siliciclastic sediment, except possibly



Figure 8.3 Mottled bedding in a core of highly bioturbated, deep-sea mud (Quaternary), Japan Sea. Ocean Drilling Program Leg 127, Site 795, 74 m below seafloor. (Photograph courtesy of Ocean Drilling Program, Texas A & M University.)

under those conditions where sediment in one layer is mixed by bioturbation with sediment of a different composition in another layer. Such mixing may also affect textural patterns if sediments of different grain size or shape are mixed. Organisms in deep burrows may bring about interchange of pore waters with overlying seawater; however, the effect of this process on composition of the sediment is probably inconsequential. Also, bioturbation may act locally to alter the porosity and permeability of sediments, but subsequent changes in porosity owing to compaction during deeper burial in the mesogenetic zone overshadow the effects of bioturbation. Except for destruction of sedimentary structures, which can be substantial, and minor changes in texture owing to mixing of sediments of different sizes or shapes, bioturbation probably does not greatly modify the characteristics of sediments. For a mathematical treatment of bioturbation effects, see Berner (1980, p. 42).

Minor lithification of sediment may take place in the eogenetic environment owing to cementation. On the other hand, little physical compaction ensues because of shallow burial depths and lack of overburden pressure. Compaction effects are considered in greater detail below under discussion of diagenesis in the mesogenetic zone.

8.3.3 Chemical and biochemical reactions

The nature and extent of diagenetic reactions in the eogenetic realm depend upon the depositional environment. Most sediment is deposited in the marine environment; however, some sediment is deposited in nonmarine environments where conditions may range from warm and humid to hot and arid. Pore waters of the sediment may thus be characterized by a range of Eh, pH, and salinity conditions, depending upon the environment.

The initial pore waters of shallow sediments deposited in marine environments tend to have high salinities (about that of average seawater, 35 o/oo), alkaline pHs, redox potentials that range from oxic to anoxic, and moderately high concentrations of bicarbonate and sulfate. Fine organic matter may be preserved in fine-grained marine sediments and become involved in diagenetic reactions, contributing reaction products to the pore waters.

Initially, siliciclastic sediments deposited in nonmarine settings have dominantly fresh pore waters; acid or alkaline pHs, depending upon environmental conditions; and oxic to slightly anoxic redox conditions. Bicarbonate may be abundant, but sulfate content of pore waters is generally much lower than that of marine sediments. Nonmarine sediments deposited in areas characterized by warm, humid climates and intense chemical weathering in source areas tend to have acidic pore waters with relatively high concentrations of dissolved chemical species (Burley *et al.*, 1985), although concentrations are much lower than those in pore waters of marine sediments. Fine organic matter tends to be preserved in the anoxic sediments in this environment and thus affects diagenetic reactions.

Under the conditions described above, eogenetic reactions in marine sediments are dominated by dissolution of unstable, fine-grained components and formation of characteristic new minerals. The formation of pyrite in the zone of sulfate reduction (owing to the reaction of hydrogen sulfide with iron-bearing minerals such as iron oxides, chlorite, and biotite) is particularly characteristic. Other important reactions include formation of authigenic iron-rich chlorites or chamosite, glauconite, illite/smectite clay minerals, and precipitation of K-feldspar overgrowths, quartz overgrowths, and carbonate cements. The commonly reported order of formation of these minerals is precipitation of pyrite, chlorite (in anoxic pore waters), illite/smectite (in oxygenated pore waters), followed by precipitation of quartz and feldspar overgrowths and, finally, precipitation of carbonate cements (Burley *et al.*, 1985). In marine sediments deposited in evaporite basins, the increased ionic concentration of the pore waters may lead to precipitation of sulfates, zeolites, and possibly smectite clays in addition to carbonates (Bjørlykke, 1983).

Bacterial activity plays an important role in diagenetic reactions at shallow depths, especially in shales and mudstones (e.g. Curtis, 1980; Clayton, 1994). Bacterial oxidation of organic matter ($\text{CH}_2\text{O} + \text{O}_2 \rightarrow \text{H}^+ + \text{HCO}_3^-$) in oxic sediments at very shallow burial depths generates bicarbonate ions, together with some ammonia and phosphates. At slightly greater depths, oxygen is depleted and reducing conditions prevail. In this zone, bacterial sulfate reduction ($2\text{CH}_2\text{O} + \text{SO}_4^{2-} \rightarrow 2\text{HCO}_3^- + \text{H}_2\text{S}$) is a dominant process. This process leads to formation of bicarbonate and hydrogen sulfide, with consequent reduction in pH. Adequate seawater sulfate to sustain sulfate-reducing bacteria apparently does not diffuse

downward below a depth of about 10 m. Therefore, below that depth, sulfate reduction gives way to fermentation ($2\text{CH}_2\text{O} + \text{H}_2\text{O} \rightarrow \text{CH}_4 + \text{HCO}_3^- + \text{H}^+$). Fermentation produces methane, bicarbonate ions, and hydrogen ions.

The organic processes described apply particularly to organic-rich marine shales and are less important in organic-poor sandstones. The reaction products of shale diagenesis (bicarbonates, hydrogen, hydrogen sulfide) can, however, be expelled from shales into associated sandstones and thereby affect the course of sandstone diagenesis.

Owing to lower salinities of pore waters in general, low concentrations of SO_4^{2-} , and the general prevalence of oxidizing conditions, early diagenetic reactions in nonmarine sediments differ somewhat from those in marine sediments. A number of diagenetic reactions occur that can include partial to complete dissolution of unstable heavy minerals, feldspars, and rock fragments, partial replacements of rock fragments or silicate minerals by illitic or montmorillonitic clays, and precipitation of authigenic feldspars, quartz, zeolites, clay minerals (mainly montmorillonite or mixed-layer illite–montmorillonite), iron oxides, and calcite. For example, much of the hematite that occurs in redbeds may be generated authigenically under these kinds of conditions (Walker *et al.*, 1978). Mechanical infiltration of clays into sandy sediments may also occur during the early stages of diagenesis (e.g. Dunn, 1992).

8.4 Diagenetic reactions in the mesogenetic zone (Burial diagenesis)

8.4.1 General statement

The **mesogenetic regime** is the environment of deeper burial. Little further change occurs in the sediment after the eogenetic stage until it is brought into an environment of increased temperature and changed pore-water composition. Elevated temperatures add energy to the reacting system, lowering reaction barriers and increasing reaction rates. Large-scale, deep circulation of pore fluids having different compositions and Eh, pH characteristics than those of the depositional environment causes transport of large quantities of dissolved constituents, bringing about major regional diagenetic changes. Significant physical (compaction) and chemical/mineralogical changes take place in siliciclastic sediment within the mesogenetic regime.

8.4.2 Factors affecting diagenesis in the mesogenetic regime

General statement

The principal factors that drive diagenetic reactions in the mesogenetic regime are increased temperature and pressure, changed pore-water composition, and the presence of fine organic material. These factors bring about both physical changes (e.g. compaction and porosity loss) and chemical/mineralogical changes (e.g. precipitation of cements, dissolution of minerals, replacement of minerals) that tend to bring the sediments into equilibrium with the diagenetic environment.

Increased temperature

Increase in temperature with deeper burial has several important effects on diagenesis. First, it causes an increase in the rate at which chemical reactions occur. The rate of chemical reactions is known to increase exponentially with increasing temperature. An increase in temperature of 10 °C can double or perhaps triple the reaction rate (e.g. Hunt, 1979, p. 127). Thus, mineral phases that were stable or metastable under eogenetic temperature conditions may become unstable with greater burial depth. Among other things, increasing temperature favors formation of denser, less-hydrous minerals. Increase in temperature also causes an increase in the solubility of most common minerals except the carbonate minerals. Therefore, pore waters are capable of dissolving more silica at higher temperatures. On the other hand, increasing temperature causes a decrease in the solubility of carbonate minerals, which are more likely to precipitate at greater burial depths and higher temperatures unless the pH decreases.

Some cations such as Mg^{2+} and Fe^{2+} are strongly hydrated at surface temperatures. Therefore, these cations do not readily enter the carbonate mineral lattice at low temperatures (the well-documented reluctance of dolomite to form in seawater at low temperatures except at high Mg/Ca ratios, for example). With increase in burial temperature to 60 °C or more, these ions become less hydrated and thus can form iron and magnesium carbonates in pore waters with relatively low Mg/Ca ratios. Thus, carbonate cements precipitated during mesodiagenesis commonly include iron- and magnesium-rich varieties (dolomite, ankerite, siderite).

Increased pressure

Increasing geostatic pressure with deeper burial is important because the solubility of minerals increases with increasing stress at grain contacts (following Reicke's principle). In sandstones, this increase in solubility leads to pressure solution of grains at contact points. Therefore, pressure solution can bring about significant increase in silica concentration in pore waters. The silica dissolved by pressure solution may quickly reprecipitate locally on grain surfaces that face open pores, or it may migrate to more distant areas before reprecipitation occurs. In addition to furnishing a source of silica for cementation, pressure solution, together with compaction caused by overburden pressure, reduces porosity and brings about some overall thinning of beds.

Changed pore-water composition

Changes in pore-water composition during mesodiagenesis may strongly influence dissolution and precipitation reactions. Pore-water composition can change as a result of a variety of processes, including chemical reaction of pore waters with clay minerals or other minerals, and large-scale circulation of formation waters.

For example, the alteration of smectite clays to illite at burial depths corresponding to temperatures of about 55 °C to 200 °C, is a common diagenetic process (dehydration) that releases water. This reaction also releases silica, sodium, calcium, iron, magnesium

and other ions into solution, thereby changing the chemical composition of the pore waters.

Pore-water composition can also be changed by downward migration of fresh waters from surface outcrops under a regional hydrodynamic gradient, basin-wide circulation of fluids owing to thermal convection, and upward migration of pore waters expelled by compaction (e.g. Bjørlykke, 1994; see also Montañez *et al.*, 1997, for extended discussion of basin-wide fluid flow). These processes may result in saline pore waters of buried formations being replaced by fresh water (downward migration) or, alternatively, replaced by even more saline waters brought upward from depth. Geologists have long recognized that the salinity of subsurface waters increases with increasing depth in many depositional basins. One of the most interesting ideas advanced to explain this trend involves circulating waters and a kind of reverse osmosis process called **salt sieving**, originally pointed out by White (1965). As pore waters migrate from sandstones through fine sediments containing clay minerals such as smectite and illite, the fine sediments act as semipermeable membranes. They allow uncharged water particles to pass through unimpeded but filter out and retain dissolved ions. Thus, water in sandstones on the inflow side of the membranes retains ions and becomes increasingly saline in time, whereas water on the outflow side (that has passed through the clay membranes) contains relatively few ions.

Presence of organic matter

Diagenesis in the mesogenetic zone cannot be fully evaluated without considering the role of organic matter. As discussed in Section 8.3.3, bacterial oxidation of organic matter and bacterial sulfate reduction in the presence of organic matter are dominant processes at very shallow burial depths. At greater depths, sulfate reduction gives way to fermentation, which produces methane, bicarbonate ions, and hydrogen ions. Bacterial fermentation may extend to depths corresponding to a maximum temperature of about 75–80 °C. Commonly, this depth is less than 1 km, but the depth can be greater where the geothermal gradient is low (Tissot and Welte, 1984, p. 202).

During burial, organic matter is initially altered mainly by microbial activity, but it subsequently undergoes additional chemical changes owing to processes such as polymerization, polycondensation (formation of humic and fulvic acids by combination of organic molecules), and insolubilization (conversion of humic and fulvic acids to insoluble humin). These processes convert the organic matter into a highly complex geopolymer called **kerogen** (Tissot and Welte, 1984, p. 90; Clayton, 1994), which may be a precursor to petroleum generation.

As part of its complex organic structure, kerogen contains carbonylic and phenolic functional groups. These functional groups may undergo thermal and oxidative cracking at temperatures below about 80 °C to form soluble organic acids (e.g. carboxylic acids and phenols) in associated shales and mudstones (a process recognized early by Carothers and Kharaka, 1979). Presumably, these organic acids are expelled from the shales during clay-mineral dewatering (smectite/illite transition) and make their way into associated

sandstones. As temperatures increase into the range of 120–200 °C with further burial, carboxylic acid anions are destroyed by thermal decarboxylation, as in the reaction



or



Thus, at temperatures ranging between about 80 °C and 120 °C, organic acids predominate in the pore waters of sandstones, whereas between temperatures of about 120 °C and 160 °C decarboxylation gradually destroys most of the carboxylic acids, releasing CO₂ in the process and increasing the partial pressure of CO₂.

The result of these organic reactions strongly affects the solubility of both carbonates and aluminosilicates because they tend to produce acidic pore waters in sediments. Thus, as temperatures increase progressively with depth during mesogenesis, dissolution of both carbonates (e.g. carbonate cements) and some silicate minerals such as feldspars may occur in response to organic–inorganic interactions.

8.4.3 Major diagenetic processes

Compaction

Causes of compaction

Compaction is the lessening of sediment volume, and concomitant decrease in porosity, brought about by grain rearrangement and other processes that result from sediment loading and tectonic forces. In regions of folding and thrust faulting, the compactive stresses resulting from tectonic forces may be greater than those resulting from sediment loading, thereby causing overprinting of burial compaction. In particular, tectonic stresses may result in fracturing of grains. On the whole, however, the overburden weight creates the major stress that causes compaction of sediments. The overburden weight results mainly from the weight of the sediment or rock mass. The average change in geostatic pressure with depth, the geostatic gradient, is about 244 bar/km (Fig. 8.4). Thus, at a depth of 10 km, for example, the geostatic or rock pressure is roughly 2.5 kbar. The average change in fluid pressure with depth, the hydrostatic gradient, is about 104 bar/km. At 10 km depth, the hydrostatic pressure is thus about 1.0 kbar.

The effective stress, the grain-to-grain stress, arises from the balance between the geostatic and hydrostatic pressures. It is equal to the geostatic pressure minus the pore-water pressure, a relationship known as Terzaghi's law (e.g. Giles, 1997, p. 153). The effective stress is reduced by increasing fluid overpressure (fluid pressure greater than the weight of the fluid column), which may be due to application of stresses to compressible rocks (e.g. Swarbrick *et al.*, 2002). If the fluid pressure approaches the geostatic pressure, the effective stress will approach zero (Bjørlykke, 1983).

Temperature also influences compaction by promoting pressure solution of grains (Houseknecht, 1984). Further, temperature decreases resistance of grains to deforming stresses.

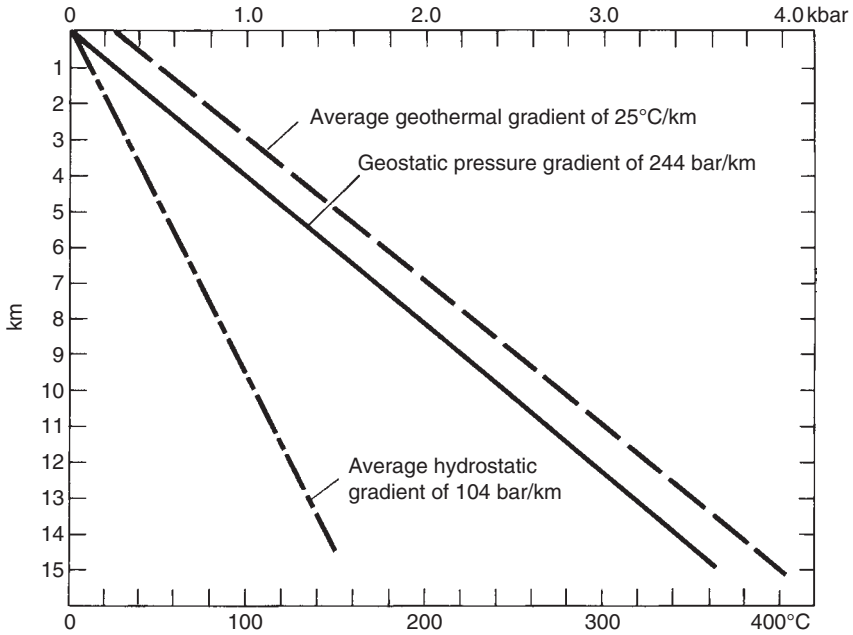


Figure 8.4 Average geostatic pressure gradient, hydrostatic pressure gradient, and geothermal gradient in sedimentary basins.

Compaction of sands

Newly deposited, unconsolidated sand has high porosity and a loosely packed fabric. Under sediment loading, the fabric becomes more tightly packed and porosity is reduced. We recognize that compaction of sands can involve (1) mechanical rearrangement of grains into tighter packing owing to slippage of grains past each other at points of contact, (2) bending of flexible grains such as micas, (3) ductile and plastic deformation, particularly of malleable grains such as rock fragments, (4) brittle fracture, particularly of carbonate shell material but possibly silicate grains also, and (5) pressure solution of quartz and other minerals (e.g. Wilson and McBride, 1988). The first four of these processes produce purely mechanical changes in packing. The fifth, pressure solution, is often referred to as chemical compaction because it also involves solution at grain contacts.

The compactability of sands is a complex function of numerous variables, the most important of which are grain size and sorting, grain shape, grain orientation, composition, matrix content, and cements. Holbrook (2002) suggests that average mineral ionic bond strength (which controls mineral hardness, solubility, and plastic compaction) and electrostatic repulsive forces in clay minerals are also important factors.

Reduction of porosity, which has an important effect on basin-wide circulation of formation waters, as well as the storage and transmission of economically important subsurface fluids (petroleum, groundwater), is one of the most thoroughly researched aspects of compaction.

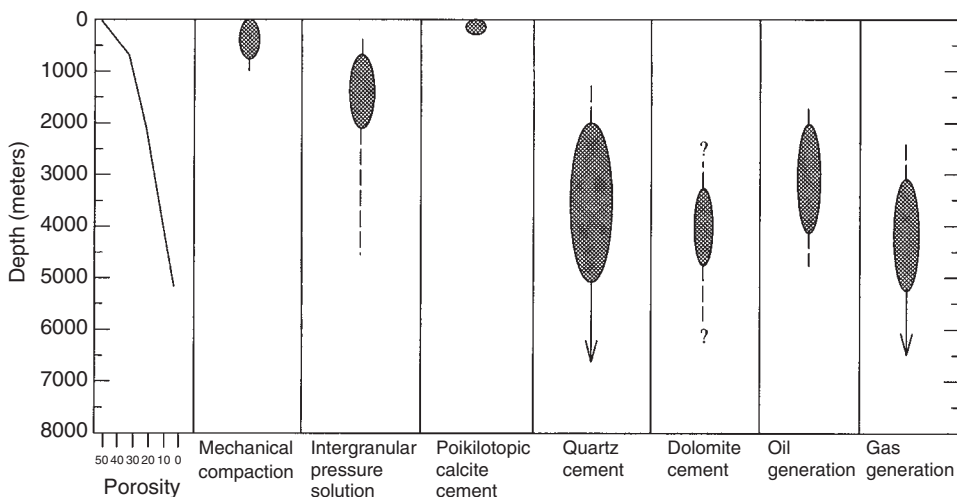


Figure 8.5 Summary diagram showing depth ranges at which mechanical compaction, pressure solution, and cementation reduce porosity in quartzose sandstones. Note that porosity is reduced from approximately 50 percent at the surface to virtually zero at a burial depth of about 5000 m. This diagram also shows the approximate depths at which oil and gas are generated in the subsurface. [From Stone, W. N. and R. Siever, 1996, Quantifying compaction, pressure solution, and quartz cementation in moderately- and deeply-buried quartzose sandstones from the greater Green River Basin, Wyoming, in Crossey, L. J., R. Loucks, and M. W. Totten (eds.), *Siliciclastic Diagenesis and Fluid Flow*: SEPM Special Publication 55, Fig. 5, p. 134. Reproduced by permission.]

Theoretical considerations show that even-sized spheres packed into the loosest arrangement (cubic packing) have a porosity of 47.6 percent. Simple rearrangement of the spheres to yield the tightest packing (rhombohedral packing) reduces the porosity to 26 percent (Graton and Fraser, 1935). The grains in natural sands are neither spheres nor even-sized grains. Therefore, neither the initial porosity of noncompacted sands nor the porosity loss that these sands undergo owing to tighter packing can be predicted theoretically.

Empirical studies show that porosity of loosely consolidated sands in the depositional environment may range from about 35 to 50 percent (e.g. Stone and Siever, 1996). Loss of porosity during burial diagenesis is commonly plotted as compaction curves, which show porosity loss as a function of burial depth (Fig. 8.5). Porosity is lost as a result of both mechanical compaction and pressure solution. (Pressure solution occurs at the contact point between grains, e.g. quartz, where grain solubility increases owing to pressure.)

Qualitative visual evidence of compaction is provided by bent mica flakes, deformation of ductile grains, and fractured grains. Figure 8.6 illustrates compaction effects in terms of volume loss owing to ductile and flexible grain deformation, as well as to pressure solution (note sutured contact). Cementation by quartz or other minerals, to be discussed, also reduces porosity. The combined effects of mechanical compaction, pressure solution, and cementation can reduce porosity to less than 2 percent at a burial depth of 5000 m (Stone and Siever, 1996). Note in Fig. 8.5 that mechanical compaction occurs at burial depths to about

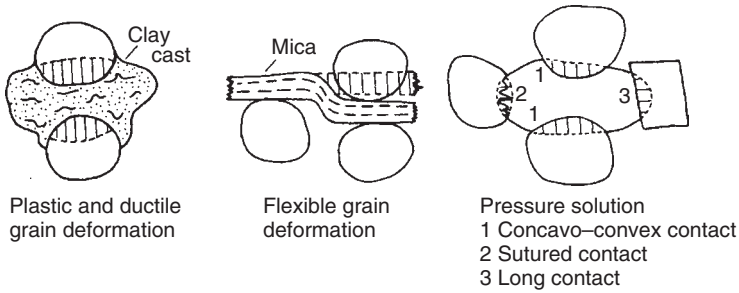


Figure 8.6 Schematic representation of textural criteria used to estimate volume loss in sandstones owing to compaction. The hachured areas indicate rock volume lost by grain deformation and pressure solution. (From Wilson, J. C. and E. F. McBride, 1988, *Compaction and porosity evolution of Pliocene sandstones, Ventura Basin, California: Am. Assoc. Petrol. Geol. Bull.*, 72, Fig. 10, p. 679, reprinted by permission of AAPG, Tulsa, OK.)

1000 m, pressure solution is operative at burial depths between about 500 and 4500 m, and cementation can take place to depths of about 6000 m.

Compaction of muds

Owing to the dominance of platy, flaky, or acicular clay minerals in muds, the initial porosity of muddy sediment is considerably higher than that of sands. Recent clay muds from the ocean floor and lake bottoms may have porosities as high as 70–90 percent, corresponding to water content of 50–80 percent (Singer and Müller, 1983).

Compaction during burial sharply reduces the porosity of muds. Porosity of muddy sediments may be reduced by compaction to values less than 20 percent at burial depths ranging from ~1 km to 3 km, however, some porosity (5–10%) may persist to depths of 6 km or more (e.g. Dzevanishir *et al.*, 1986). Loss of porosity by compaction is accompanied by expulsion of pore water and thinning of beds.

Cementation

Introduction

As discussed in Section 8.3, precipitation reactions can begin during eogenesis, resulting in formation of authigenic clay minerals, K-feldspar overgrowths, quartz overgrowths, and carbonate cements at shallow burial depths. Cementation continues during various stages of mesogenesis and may even occur under some conditions of telogenesis. Cementation plays a major role in reducing porosity in sandstones, and it can also affect compaction of sediments. For example, early-formed cements that fill the pore spaces of a sandstone or shale before significant compaction tend to inhibit further compaction of the sediment. Also, early cementation can restrict subsequent movement of fluids through sediments. Identification of cements and interpretation of the paragenetic sequence of cementation is, therefore, an essential step in diagenetic study. Petroleum geologists concerned with the reservoir properties of sandstones are particularly interested in cementation phenomena because of the adverse effect of

cementation on porosity of sandstones. Much of the primary porosity of sandstones may be destroyed at burial depths of about 5 km by a combination of cementation and compaction.

Minerals that commonly occur as cements in siliciclastic rocks include quartz, chalcedony, opal, K-feldspars and albite, calcite, aragonite, dolomite, siderite, ankerite, hematite, goethite (limonite), pyrite, gypsum, anhydrite, barite, chlorite and other clay minerals, zeolites, tourmaline, and zircon. Of these, silica, carbonate, and clay minerals are by far the most important and abundant cements, although zeolites may be abundant in some volcanoclastic sediments.

Carbonate cementation

Carbonate cements occur in all types of sandstones as well as in many shales and mudstones (e.g. Morad, 1998a). They appear to be most typical of quartz arenites, but they are also quite common in many feldspathic arenites (e.g. Morad *et al.*, 1990). Paleozoic and Precambrian lithic arenites (graywackes) generally contain little or no carbonate cement; however, carbonate cements are abundant in many Cenozoic and Mesozoic graywackes (Pettijohn *et al.*, 1987, p. 448). Older graywackes tend to have pore spaces filled with clay-mineral alteration products rather than with carbonate cements. Carbonate cements may occur as uniform pore fillings over large areas of a rock unit (e.g. Fig 8.7). Alternatively, their distribution can be very patchy. Well-cemented zones can grade to poorly cemented zones over distances of a few meters. Carbonate cement can occur also as lenses or stringers or as concretions (see Fig. 3.39). Carbonate concretions are a particularly common feature of some shales and mudstones. The patchy distribution of carbonate cements may reflect initially patchy carbonate precipitation, or it may be due to subsequent partial removal of more evenly distributed cement owing to dissolution during burial or outcrop exposure.

Calcite is the principal carbonate cement in siliciclastic sediments. Dolomite, ankerite (ferroan dolomite), siderite, and aragonite occur also; however, aragonite exists primarily in very young rocks.

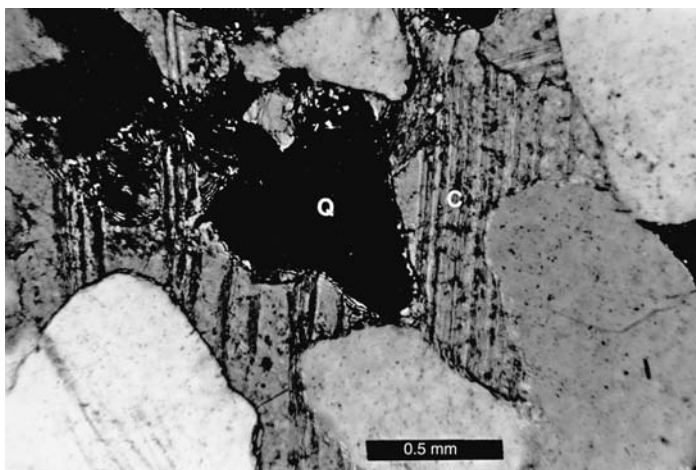
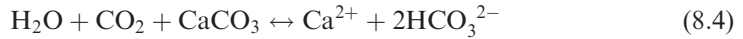


Figure 8.7 Poikilitic calcite cement (C) enclosing a quartz grain (Q). Quartz-rich example of Mauch Chunk Sandstone (Mississippian), Pennsylvania. Crossed nicols.

As discussed, both precipitation and dissolution of carbonate minerals can take place during diagenesis. Carbonate equilibrium is expressed by the relationship



Precipitation occurs when the solubility of calcium carbonate in pore waters decreases in a carbonate-saturated system. Solubility may decrease as a result of increase in the activity (concentration) of calcium or bicarbonate ions, increase in temperature, or decrease in ΣCO_2 . In a pore-water system that is not externally buffered, solubility of calcium carbonate minerals is dependent upon the CO_2 pressure, and pH depends upon ΣCO_2 ($\text{H}_2\text{CO}_3 + \text{HCO}_3^- + \text{CO}_3^{2-}$). If ΣCO_2 decreases, the pH increases, causing carbonate precipitation and vice versa. If the system is externally buffered, such as by organic acids, then the pH does not depend upon ΣCO_2 . Under these conditions, carbonate precipitation may occur as a result of increasing ΣCO_2 while the externally buffered system is at a constant pH (see discussion under "Presence of organic matter" in [Section 8.4.2](#)).

Source of carbonate

In the cementation processes described above, bicarbonate ions are supplied by organic reactions of some type (see also Morad, 1998b). To form calcite cements, a source of calcium must also be available. Dolomite precipitation further requires a source of magnesium, and ankerite and siderite precipitation require a source of iron. The content of these cations in original seawater is inadequate to supply all the Ca, Mg, and Fe needed for cementation during diagenesis. As many workers have pointed out, precipitation of carbonate cement from static pore waters can supply only a minute amount of cement. A steady contribution of both cations and anions must be renewed in pore water for cementation to proceed and fill a pore space. Berner (1980, p. 124) suggests that 300,000 pore volumes of water are needed to fill one volume of pore space completely. In a sandstone that contains fossils, dissolution of skeletal grains composed of aragonite, calcite, or high-magnesian calcite can furnish important amounts of bicarbonate, calcium, and magnesium.

Bicarbonate ions and cations can be supplied also by dissolution of limestones or dolomites in stratigraphic sections containing interbedded siliciclastic and carbonate rocks. In this regard, export of calcium carbonate from limestones undergoing pressure solution may be an important process. Additional Ca, Mg, and Fe are supplied by reactions with silicate minerals, such as conversion of smectite to illite and dissolution of calcium feldspars and ferromagnesian minerals. Under geologic conditions where downward circulating groundwaters move through mafic volcanic rocks, significant amounts of Ca, Mg, and Fe can be supplied by alteration of these rocks. Finally, carbonate cements precipitated in one part of a sediment pile may be dissolved and redistributed by advective transfer to other parts of the pile.

Carbonate-cement textures

Carbonate cements are commonly easy to recognize with a petrographic microscope. They may fill pore spaces among detrital grains with a mosaic of fine crystals, or a pore may be filled

with a single large crystal. In fact, a single crystal may grow large enough to surround several detrital grains to produce a poikilotopic texture, as shown in Fig. 8.7. Locally, where carbonate cement is abundant, displacive crystallization of the cement (Folk, 1965) may occur, forcing the detrital grains apart into a loosely packed fabric. Although some skepticism has been expressed about the occurrence of displacive calcite, displacive calcite in caliche profiles in sandstones has been reported more recently by Saigal and Walton (1988) and Braithwaite (1989). Partial replacement of silicate grains by carbonate cement can further enlarge the area of the cement. Where crystallization occurs within pores containing interstitial clays, the clays may be engulfed by and disbursed within the cement. Dolomite and iron carbonates may occur as distinct rhombs, which allows them to be distinguished from calcite. If they do not exhibit rhombic shape, it is very difficult to differentiate optically among the carbonate cements unless thin sections are stained for carbonates.

Silica cementation

Silica cements are common in both sandstones and shales. In sandstones, they typically occur in arenites with little or no matrix, but silica cement can occur in rocks containing matrix. Dutton and Diggs (1990) show that the volume of quartz cement in sandstones tends to decrease exponentially with increasing matrix content of the sandstones (Fig. 8.8). Silica cement most commonly takes the form of optically continuous overgrowths on quartz grains (e.g. Fig. 4.1). Such overgrowths are especially typical of silica-cemented quartz arenites, but they can be present also in quartz-rich feldspathic and lithic arenites. They rarely occur on the quartz grains of wackes such as turbidite sandstones. Quartz overgrowths appear to be relatively uncommon in modern sands (Pettijohn *et al.*, 1987, p. 452).

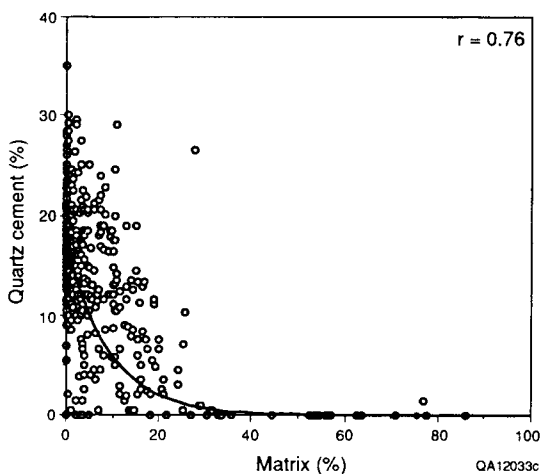


Figure 8.8 Exponential decrease in quartz cement as a function of increasing matrix content in Travis Peak (Cretaceous) sandstones, east Texas. (From Dutton, S. P. and T. N. Diggs, 1990, History of quartz cementation in Lower Cretaceous Travis Peak Formation, east Texas: *J. Sediment. Petrol.*, **60**, Fig. 5, p. 195, Reprinted by permission of Society for Sedimentary Geology, Tulsa, OK.]

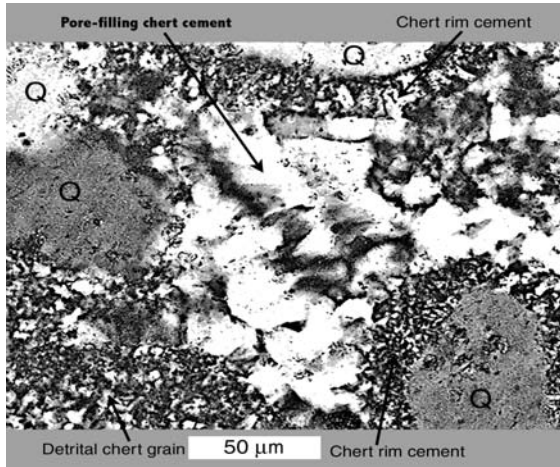


Figure 8.9 Petrographic image (crossed nicols) of microquartz cement filling space among four quartz grains (Q) and one detrital chert grain (lower left corner). Note isopachous chert–cement rims around some quartz grains. The sample is from a chert-cemented sandstone interbed in the Jefferson City Dolomite (Early Ordovician), Missouri. (From Boggs, S. and D. Krinsley, 2006, *Application of Cathodoluminescence Imaging to Study of Sedimentary Rocks*: Cambridge University Press, Fig. 5.10, p. 100, reproduced by permission.)

Opal and chalcedony or microquartz (chert) are less-common silica cements. Opal occurs primarily in Tertiary and younger sediments. Opal cement is most common in volcanoclastic sequences, but has been reported also from feldspathic sandstones (e.g. the Ogallala Formation of Kansas, Franks and Swineford, 1959). Chalcedony or microquartz cement generally does not occur in quartz arenites but may be common in sandstones with subwacke texture (Dapples, 1979). According to Dapples, microquartz (chert) can occur as either (a) an epitaxial cement on quartz grains that show interpenetration boundaries or (b) as intergrowths in small masses of interstitial or matrix clay. As the sandstone framework approaches that of a wacke, the latter type of cement is likely to be the kind of quartz cement present. Figures 8.9 and 8.10 provide an example of a microquartz-cemented sandstone. Some silica cement may consist of opal-CT (cristobalite–tridymite), which is an intermediate diagenetic stage between opal-A and quartz (chert).

Silica solubility

Precipitation of silica cements requires that the pore waters of sediments be supersaturated with respect to quartz or opal. The precipitation of enough cement to fill pore spaces further requires that large volumes of water circulate through the sediments. The excess silica in the pore water of a single pore can precipitate only a minute amount of silica. Once precipitation has occurred, no further cementation can take place until the water in the pore is replaced by new water supersaturated with silica. Thus, the process of filling a pore with cement demands that silica-supersaturated water circulate through the pore many times, a process that takes a very long period of time.

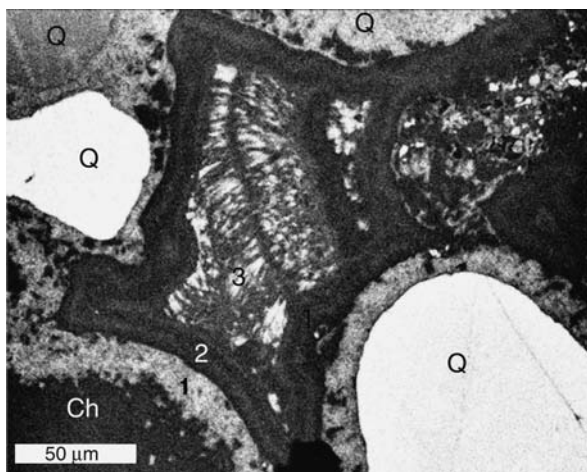


Figure 8.10 Cathodoluminescence (CL) image of the same microquartz cement shown in Fig. 8.9. Note that three generations of chert and microquartz cement (labeled 1, 2, 3) are clearly revealed in the CL image. (From Boggs, S. and D. Krinsley, 2006, *Application of Cathodoluminescence Imaging to Study of Sedimentary Rocks*: Cambridge University Press, Fig. 5.11, p. 102, reproduced by permission.)

The solubility of silica minerals is a function of the pH, hydrostatic pressure, temperature, and the crystallinity of the mineral. At pH values above about 9.0–9.5, the solubility of silica increases sharply; however, at lower values, pH has relatively little effect on silica solubility. Below a pH of about 9.5, undissociated orthosilicic acid (H_4SiO_4) is the main silica species present; above 9.5, H_3SiO_4^- is the main species. Most pore waters are buffered at a pH of around 8.0. Values greater than 9.0 occur only in some groundwaters associated with altering volcanic sequences, alkaline lakes in arid regions, and sabkha environments. Therefore, pH probably does not exert an important control on silica solubility under most diagenetic conditions. Solubility increases with increasing hydrostatic pressure. In seawater, this increase is about 35 percent at 1 kbar (Willey, 1974, p. 242).

The equilibrium solubility of quartz at 25 °C was determined by several early investigators to be about 6 ppm (e.g. Fournier, 1983). Amorphous silica (opal-A) was reported to have a much higher solubility of about 120–140 ppm (Siever, 1957) and opal-CT a solubility of about 70 ppm (Fournier and Rowe, 1962). Quartz solubility was reexamined by Rimstidt (1997), who determined that the solubility of quartz at 25 °C is actually 11.5 ppm, about twice the previously accepted value.

Silica solubility increases markedly with increasing temperature, as shown in Fig. 8.11. For example, the solubility of quartz at 150 °C is more than 10 times that at 25 °C. Thus, temperature appears to exert the major control on the solubility of the SiO_2 minerals. Given that quartz has a lower solubility than amorphous silica (e.g. opal), we would logically expect that quartz, with its lower solubility, precipitates in preference to opal unless concentrations of silica in pore waters are exceedingly high. On the other hand, experimental work shows that quartz precipitates very slowly; therefore, pore waters supersaturated with respect to quartz can persist for long

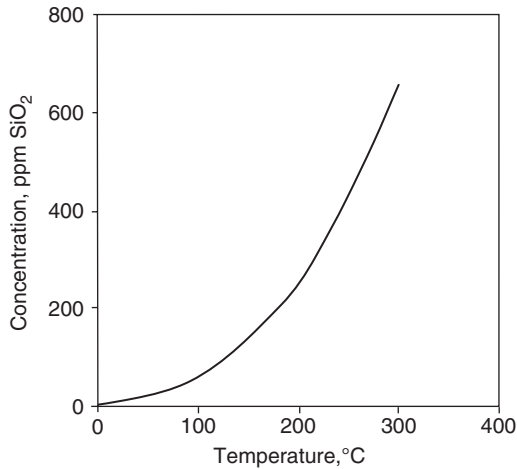


Figure 8.11 Graph showing the solubility of quartz at temperatures ranging from 0 to 300 °C. (After Rimstidt, J. D., 1997, Quartz solubility at low temperatures: *Geochim. Cosmochim. Acta*, **61**, Fig. 3, p. 2555, reproduced by permission of Elsevier Science Ltd.)

periods of time before precipitation occurs. Pore waters in shallow sediments buried to a few hundred meters depth have been reported to have concentrations of dissolved SiO₂ as high as 80 ppm, well above the equilibrium solubility of quartz (e.g. Gieskes *et al.*, 1983). The properties, behavior, and occurrence of silica in the geologic realm are reviewed in several books; see, for example, Heaney *et al.* (1994).

Timing of quartz cementation

Factors of interest in evaluating silica precipitation during diagenesis include the timing of cementation, mechanisms for precipitating silica, and sources of silica. Most silica cementation probably occurs during eodiagenesis and early mesodiagenesis. For example, Dutton and Diggs (1990) used oxygen isotope data to interpret that quartz cements were precipitated in the Cretaceous Travis Peak Formation of Texas (USA) at burial depths of 1 to 1.5 km and temperatures of 55–75 °C. Although most silica cementation likely occurs at moderately shallow burial depths and low temperatures, some workers report formation of overgrowths at much greater depths and higher temperatures. Surdam *et al.* (1989a) suggest, for example, that quartz overgrowths can be precipitated at temperatures ranging to about 80 °C during early stages of mesogenesis and also at temperatures between 160 and 200 °C during late mesogenesis. On the basis of fluid-inclusion studies, Girard *et al.* (1989) report that quartz overgrowths found in Lower Cretaceous arkoses of the Angora margin formed at temperatures ranging between 128 and 158 °C. Also, Walderhaug (1990) interpreted the temperature of formation of quartz overgrowths from subsurface sandstones from offshore Norway to lie between 90 and 118 °C. With deeper burial and progressively increasing temperature, concomitant increase in solubility of silica requires that pore waters contain much higher saturations of silica than that in shallow pore waters before quartz precipitation can occur.

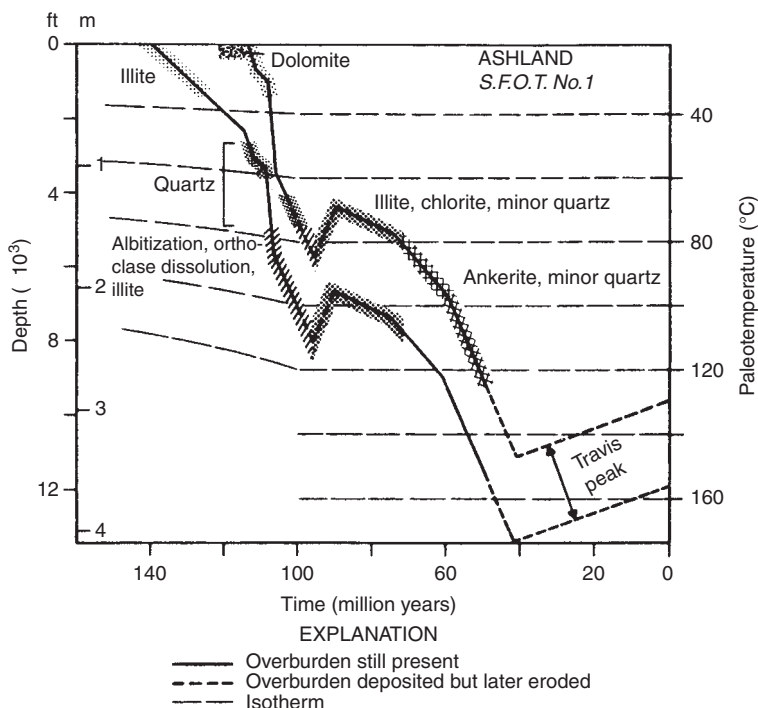


Figure 8.12 Burial-history curves for the top and base of the Travis Peak Formation (Cretaceous), east Texas (Ashland S.F.O.T. No. 1 oil well). Interpreted times at which quartz precipitation and other major diagenetic events occurred are shown as a function of burial depth and paleotemperature. (From Dutton, S. P. and T. N. Diggs, 1990, History of quartz cementation in Lower Cretaceous Travis Peak Formation, east Texas: *J. Sediment. Petrol.*, **60**, Fig. 3, p. 194, reprinted by permission of Society for Sedimentary Geology, Tulsa, OK.)

The timing of cementation in sandstones is commonly depicted in burial-history curves, which show the interpreted time of cementation as a function of burial depth and paleotemperature. Figure 8.12 is an example of this kind of plot; constructed for the Cretaceous Travis Peak Formation in east Texas (USA), this figure shows that the major phase of quartz cementation in this formation occurred at a burial depth between about 0.75 and 1.5 km and at temperatures of about 50–75 °C. Minor quartz cementation also took place at depths ranging to about 2 km. Several kinds of data are used to construct burial-depth curves of this type. Burial depths are estimated by using present-day thicknesses of stratigraphic units, which are corrected for compaction. The thicknesses of eroded strata are estimated from vitrinite reflectance measurements. (For an explanation of vitrinite reflectance, see Boggs, 2006, p. 585.) Paleotemperatures are estimated from oxygen isotope data, fluid-inclusion data, and/or vitrinite reflectance data, or from heat-flow extension models. Ages are determined by radiocarbon dating methods, for example, K/Ar ages of diagenetic illite (e.g. Lee *et al.*, 1989).

To provide an adequate explanation for precipitation of silica overgrowths at high burial temperatures requires that we identify both mechanisms for precipitation and a viable source for the silica. These topics are discussed below.

Mechanisms of silica precipitation

Mechanisms that have been suggested for quartz precipitation in sandstones include (1) cooling a hot, saturated solution, (2) lowering pore pressure, (3) mixing silica-saturated fluid with more saline formation waters at a given temperature and pressure, (4) lowering the pH of the saturated solution, (5) evaporating an undersaturated solution, and (6) semimembrane osmosis through a clay-rich shale layer (Leder and Park, 1986). As mentioned, pH probably has little effect on precipitation under normal diagenetic conditions; however, any mechanism that increases silica concentration in pore waters above the equilibrium concentration can presumably cause precipitation.

Many workers have suggested that cooling of saturated solutions may be a major mechanism of quartz precipitation. For example, Leder and Park (1986) propose a model for quartz cementation that requires basin-wide circulation of silica-saturated fluids driven by thermal convection or hydrostatic head. Silica is dissolved in downward-migrating waters as they encounter progressively higher temperatures. As the continuously circulating fluids that dissolved silica on their downward migration move upward toward the basin edges, they cool and precipitate quartz in pore spaces. Diffusion from deeper regions of warmer temperature to shallower formations at cooler temperature can also transfer silica upward, although this process is probably less effective than convection. Cooling of circulating pore waters offers a reasonable explanation for late-stage quartz precipitation at moderate or shallow burial depths; however, it appears difficult to apply this mechanism to precipitation of quartz at temperatures of 160 °C or more. Presumably, some local silica source would have to be present that could supply enough silica to drive pore-water saturations above the critical level needed for quartz precipitation.

Silica sources

The source of silica for quartz cementation during diagenesis has been the subject of considerable discussion and surmise. All of the following have been mentioned as possible mechanisms to supply the needed silica: (1) dissolution of silica by meteoric waters during subaerial weathering, (2) dissolution of the opaline skeletons of organisms such as diatoms and radiolarians, (3) dissolution of silica from quartz grains by circulating pore waters flowing over quartz grains in sandstones, (4) pressure solution of quartz grains, and (5) release of silica by mineral reactions, including clay-mineral reactions, dissolution of feldspars, and alteration of volcanic fragments, glass, and mafic minerals.

At the low temperatures typical of shallow burial in the eogenetic regime, precipitation of quartz could occur in pore waters containing as little as about 13 ppm dissolved silica (average concentrations in nonmarine surface waters). Thus, at very shallow burial depths in nonmarine environments or where telogenetic uplift brings sediments near the surface, adequate silica for quartz precipitation may be present in meteoric waters, although large volumes of such dilute water would have to pass through the sediment pores to precipitate a

significant amount of quartz cement. On the other hand, marine waters contain an average silica concentration of only about 1 ppm, well below the solubility of quartz. Therefore, silica would have to be supplied from a source other than the original seawater in order for quartz cementation to take place during early burial in marine environments.

Pressure solution of quartz grains at points of contact and various mineral reactions that release silica appear to be the most important sources of silica for quartz cementation at intermediate and deeper depths in the mesogenetic regime. There is, however, disagreement among workers about the relative importance of pressure solution and mineral reactions in supplying silica. Stone and Siever (1996) provided some insight into this problem by making a quantitative study of silica cements in quartzose sandstones in the Green River Basin, Wyoming. These authors report that intergranular pressure solution provided enough silica for 4 percent quartz overgrowths; stylolitization provided an average of 2 percent quartz overgrowths. Feldspar dissolution, carbonate replacement, and clay-mineral transformations together provided an additional 1.6 percent. The internal silica sources thus produced a total of 7.6 percent quartz overgrowths. Because the typical Green River Basin quartzose sandstone contains 17.4 percent quartz cement, an average of 9.8 percent quartz cement must have been provided by external silica sources. Presumably, silica from outside sources is provided through basin-wide fluid circulation, as discussed above.

Opal and microquartz (chert) cement

Because of its high solubility, opal is a comparatively rare cement in sandstones except in some volcanoclastic sequences where the opal is derived from alteration of volcanic glass. Microquartz (chert) cements are also much less common than quartz overgrowths, but they do occur in lithic arenites and even in some quartz arenites. Microquartz (chert) cement can occur both as a syntaxial rim on quartz grains and as a mosaic of chert deposited within pore space (e.g. Figs. 8.9 and 8.10). Although chert cement can conceivably precipitate directly from pore waters, more likely it precipitates initially as opal-A or opal-CT. Opal-CT has a lower solubility (~ 70 ppm SiO_2) than opal-A (120–140 ppm), and thus in silica-enriched pore waters opal-CT may form in preference to quartz because it apparently precipitates more rapidly than quartz. Opal-CT subsequently transforms to microcrystalline quartz (chert). In highly enriched pore waters, opal-A may be the initial cement, which subsequently inverts and recrystallizes first to opal-CT and then to microquartz. In volcanogenic sequences, the silica in opal and microquartz is derived locally by alteration of volcanic glass and other volcanic products, as mentioned.

Microquartz (chert) cements in quartz arenites, which are rarely associated with volcanoclastic rocks, must have a different source. Pettijohn *et al.* (1987, p. 455) reason, however, that the source must nevertheless be nearby. Owing to the relative rapidity of precipitation of opaline silica phases, the silica would not remain in pore waters over long distances of transport. They suggest that the source may be soil waters in lateritic terrains, which are known to precipitate opal in the lower parts of soil zones. Precipitation of opal/microquartz cements may thus occur in sandstones at shallow depths below lateritic soils, i.e. below weathering surfaces that ultimately become unconformities.

Cementation by other minerals

Carbonate and silica cements are by far the most common cements in sandstones; however, numerous other minerals may be present as cements, generally in minor amounts. Sulfate cements (gypsum, anhydrite, barite) are present in some sandstones, particularly those deposited in evaporitic environments, where gypsum is precipitated as a cement at shallow burial depths. Late-stage anhydrite may precipitate at greater burial depths if an adequate source of SO_4^{2-} ions are available in subsurface brines. Authigenic iron oxides (hematite and goethite) are derived by oxidation of iron-bearing minerals (such as biotite) in oxic pore waters. Iron oxides act as pigments that coat detrital grains, form halos around ferromagnesian minerals, pervade and stain clay matrix, or be disseminated within calcite cement. Authigenic hematite may be abundant in some redbeds (e.g. Walker, 1974).

Feldspar cements occur primarily as overgrowths on detrital feldspar grains, either on K-feldspar or albite grains (e.g. Fig. 8.13). Although not abundant, feldspar cement is most common in feldspathic and volcanoclastic sandstones and is less common in quartz arenites and lithic arenites. Overgrowths may form both during eogenesis and some stages of mesogenesis. The geochemical conditions that favor precipitation of feldspar overgrowths include an adequate concentration of dissolved silica and Na^+ and K^+ ions in pore waters, and moderately high temperatures (Kastner and Siever, 1979).

Clay minerals (e.g. smectite, illite, kaolinite, chlorite) are common cementing materials in many lithic arenites and volcanoclastic sandstones. Clay-mineral cements may display drusy texture within pores, as shown in Fig. 4.9, or pores may be completely filled with fibrous (chlorite) or platy/flaky (kaolinite) clay minerals (Fig. 8.14). For extended

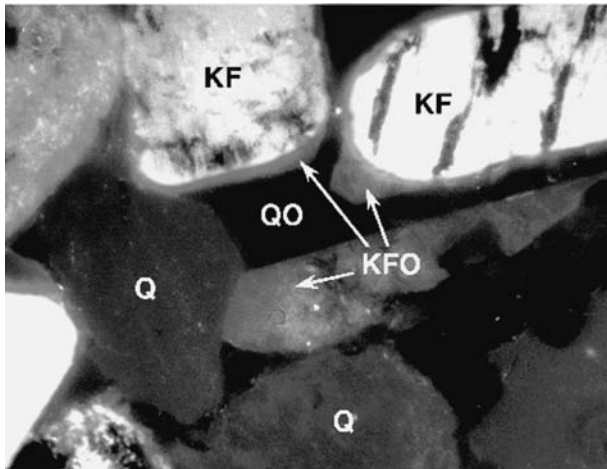


Figure 8.13 Cathodoluminescence image of K-feldspar (microcline) overgrowths (KFO) on detrital feldspars (KF). Q = quartz; QO = quartz overgrowth. Triassic “Buntsandstein” of southwestern Germany. [From Richter, D. K. *et al.*, 2003, Progress in application of cathodoluminescence (CL) in sedimentary petrology: *Mineral. Petrol.* 79, Plate 2, Fig. h, p. 131. Reproduced by permission of Springer-Verlag. Photograph courtesy of Thomas Götte.]

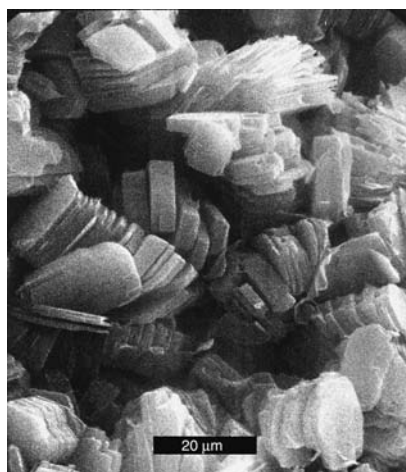


Figure 8.14 Secondary scanning electron photograph of platy kaolinite crystals arranged in “books.” within a core of Miocene sandstone, Japan Sea. [From Boggs, S., Jr., and A. Seyedolali, 1992, Diagenetic albitization, zeolitization, and replacement in Miocene sandstones, Sites 796, 797, and 799, Japan Sea, in Pisciotto, K. A., J. C. Ingle, Jr., M. T. von Breyman, *et al.* (eds.), *Proceedings of the Ocean Drilling Program, Scientific Results: ODP*, College Station, TX, vol. 127/128, part 1, Fig. 22, p. 144.]

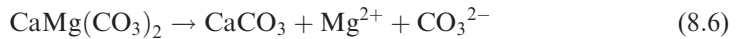
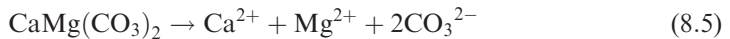
discussion of clay minerals in sandstones, with numerous photographic plates, see *Origin, Diagenesis, and Petrophysics of Clay Minerals in Sandstones* edited by Houseknecht and Pittman (1992). Less-common minerals that may be present as cements in sandstones include zeolites, tourmaline, zircon, and pyrite.

Dissolution and porosity enhancement

Introduction

Dissolution of certain mineral phases is mentioned in various parts of the preceding discussion of cementation. Dissolution of minerals, rock fragments, and skeletal materials during weathering and diagenesis accounts for much of the dissolved silica and carbonate required for cementation. Further, dissolution processes are responsible for producing most of the secondary porosity in sandstones, particularly at depths below 2–3 km, by removal of cements and framework grains. The development of secondary porosity in sandstones is a subject of paramount importance to petroleum geologists evaluating the oil potential of reservoir rocks, and extensive research has been done since the 1960s to evaluate the porosity effects of dissolution. As a result of dissolution processes, low-stability minerals such as calcium plagioclase and mafic minerals are destroyed, leading to mineral assemblages biased toward more-stable minerals. Interpretation of such biased assemblages is a major problem and challenge in provenance analysis, as discussed in [Chapter 7](#). Therefore, an understanding of dissolution and other diagenetic processes is vital to provenance interpretation. Dissolution also plays a part in other diagenetic processes such as replacement and recrystallization. In this section, we look further at the processes of dissolution and their effect in particular on mineral composition and porosity.

The process of dissolution consists of removal in solution of all or part of previously existing minerals, leaving void spaces in the rocks. Solution of some minerals such as calcite (CaCO_3) and quartz (SiO_2) occurs by simple **congruent dissolution**, which involves complete, homogeneous dissolution of parts of the mineral. This process leaves the remaining part unchanged in composition. That is, the material dissolved from the mineral has the same composition as the mineral. **Incongruent dissolution** is a selective solution process that causes the undissolved part of a mineral to be altered in composition. In other words, the more soluble parts of a mineral dissolve in greater amounts. For example, dolomite is thought to dissolve congruently at surface temperatures (Equation 8.5) but dissolves incongruently, at least in part, at higher temperatures (Equation 8.6; Krauskopf, 1979, p. 72).



Note in Equation 8.6 that the original dolomite is eventually converted to calcite by selective dissolution and removal of Mg^{2+} . Other examples of incongruent dissolution include the alteration of K-feldspar to kaolinite and the alteration of volcanic glass to smectite. Incongruent dissolution reactions are extremely important in the formation of authigenic clays. An excellent, short discussion of partial or incongruent dissolution is given in Pettijohn *et al.* (1987, pp. 439–442).

Dissolution may take place in pure water, water with dissolved carbon dioxide, water of variable salinity containing dissolved cations and anions, and water containing various kinds of organic acids. Dissolution occurs when the solubility of a particular mineral is exceeded under a given set of Eh, pH, temperature, and salinity conditions. For example, the stability of most silicate minerals decreases with increasing temperature, whereas the stability of carbonate minerals increases with increasing temperature. The stability of some minerals, such as the carbonate minerals, is further controlled by pH. Calcite and aragonite, for example, are stable at pH values above about 7.8 but undergo solution under acidic conditions. Calcite and aragonite are also more soluble in waters of high salinity than in fresh water. The oxidation potential Eh may exert an important control on the stability of some minerals such as hematite and magnetite. The presence of organic acids in pore waters may promote dissolution of minerals such as feldspars and mafic minerals by forming soluble chelates with the metal ions in the minerals.

Intrastratal solution of framework grains

Dissolution can affect both minerals and rock fragments including K-feldspars, plagioclase, muscovite, biotite, unstable heavy minerals, carbonate rock fragments, volcanic rock fragments, and chert. Even quartz may undergo solution along strained zones and microcrystalline boundaries. Only the ultrastable heavy minerals zircon, tourmaline, and rutile appear to resist dissolution (McBride, 1984). Dissolution of detrital grains or cements can be partial or complete. Partial dissolution of mineral grains can often be recognized by jagged or embayed boundaries. If grains are completely dissolved, no evidence remains of the grain identity unless the void left by the dissolved grain has a distinctive shape, such as the rhombic shape of dolomite, that is preserved by subsequent filling with clay minerals or

other cements. Alteration of feldspars or glass shards to clay minerals by incongruent solution can also be recognized if the distinctive feldspar or shard shape is preserved.

The selective dissolution of less-stable framework grains or parts of grains during diagenesis is called **intrastratal solution**. The problem that complete dissolution of less-stable grains creates for provenance analysis has been recognized at least since the 1940s. Pettijohn (1941) reported a statistical tendency for older sedimentary rocks to have fewer heavy minerals, a less-varied suite of heavy minerals, and a greater ratio of ultrastable (zircon, tourmaline, rutile) to less-stable heavy minerals than younger rocks. He attributed these characteristics to intrastratal solution. Although alternative explanations for this trend, involving progressive unroofing of a sedimentary–metamorphic–plutonic igneous source, have been offered, Pettijohn's views have generally been vindicated by subsequent work. For example, Morton (1984) suggests that intrastratal solution can alter a diverse suite of heavy minerals consisting of 20 or more species to one containing only zircon, rutile, and tourmaline. Similar observations are reported by Milliken and Mack (1990). Dissolution proceeds according to the relative stabilities of the minerals, with least-stable minerals undergoing dissolution first (see Table 7.3, Chapter 7, for the relative stabilities of common heavy minerals). Morton (1984) suggests that the relative order of stability is controlled by composition of the interstitial waters but that the limits of persistence of particular heavy minerals is a function of pore-fluid temperatures, rate of water migration, and geologic time.

Feldspars may also be destroyed by dissolution during diagenesis. For example, Wilkinson *et al.* (2001) reported significant loss of K-feldspar with burial in three rift and two passive-margin settings in the North Sea and the US Gulf coast. Initial K-feldspar content of up to 30 volume percent was reduced to less than 5 percent at burial depths of 1.5 to 4.5 km. Owing to dissolution, sandstones that were arkoses at shallow depth became sub-arkoses or quartz arenites at greater depth. Obviously, feldspar dissolution has serious negative implications for provenance interpretation of deeply buried sandstones. See Montañez *et al.* (1997) for additional discussion of feldspar dissolution in sandstones.

Decementation

In addition to dissolution of framework grains in sandstones and shales, cements precipitated during an earlier stage of diagenesis may be removed during a later stage. This process is called **decementation**. Decementation operates primarily on carbonate cements, and may result in complete or partial removal of previously formed cements. Obviously, dissolution of carbonate cements requires a change in the geochemical conditions of the diagenetic environment from that present at the time of carbonate precipitation.

Decrease in pH, decrease in temperature, or increase in salinity could be responsible for the change. Many workers have suggested that decrease in pH with greater burial occurs as a result of the formation of organic acids and decarboxylation reactions accompanying the maturation of organic matter (Section 8.3.3). The salinity of pore water is known to increase at an almost linear rate with increasing burial depth. Increase in salinity could cause carbonate decementation, provided that increase in carbonate stability owing to increased temperature did not overwhelm the effects of increased salinity. The reverse situation is true

during uplift of sediments. Decreased temperature favors decementation, but decrease in pore-water salinity works against decementation. On the other hand, uplift may bring the rocks within the zone of meteoric recharge, where decementation can proceed rapidly in acidic meteoric waters. If cements are completely removed during decementation, no evidence of the former presence of the cement remains, and decementation cannot be documented. Remnants of the former cement may be preserved, however, as evidence of decementation. Petrographic studies suggest that multiple episodes of cementation and decementation may occur during burial and uplift of a sediment pile.

Porosity evolution owing to dissolution

Aside from the potential loss of provenance information resulting from dissolution, dissolution also has a strong effect on the evolution of porosity during diagenesis. Decementation and destruction of framework grains in sandstones obviously create secondary porosity; however, not all dissolution reactions necessarily create porosity. For example, incongruent dissolution of K-feldspar to form kaolinite may result in *in situ* formation of kaolinite with little or no increase in porosity. Pressure solution of quartz grains at contact points, admittedly a special kind of solution, reduces rather than increases porosity. Pressure solution causes interpenetration of quartz grains and therefore increased compaction and overall thinning of beds. Compaction owing to pressure solution is often called chemical compaction. Furthermore, as discussed in the preceding section, much of the silica released by pressure solution may be subsequently reprecipitated as quartz overgrowths, further reducing porosity.

In an early paper, Schmidt and McDonald (1979) reported that primary intergranular porosity in sandstones is reduced to essentially zero at burial depths of about 3 km by a combination of mechanical and chemical compaction. They suggested that the amount of secondary porosity owing to intrastatal solution and decementation increases concomitantly with decrease in primary porosity, and becomes especially important below about 3 km. Ultimately, secondary porosity declines and gradually decreases to nearly zero at about 8 km depth.

Subsequently, secondary porosity in sandstones has been reevaluated and reported by numerous researchers, e.g. Shanmugam (1984), Milliken (1989), Surdom *et al.* (1989a), Giles and De Boer (1990), and Wilkinson *et al.* (2001). As mentioned above, Wilkinson *et al.* examined dissolution of K-feldspar as a function of burial depth. Accompanying changes in porosity with burial depth are shown in Fig. 8.15. Note from this figure that primary porosity decreases sharply below a depth of about 2.5 km, whereas secondary porosity increases – and persists to depths exceeding 5 km. Eventually, of course, almost all porosity is destroyed by compaction and cementation at greater depths.

Replacement

Nature of process

Replacement involves the dissolution of one mineral and essentially simultaneous precipitation of another mineral in its place. This statement does not mean that a large mineral is

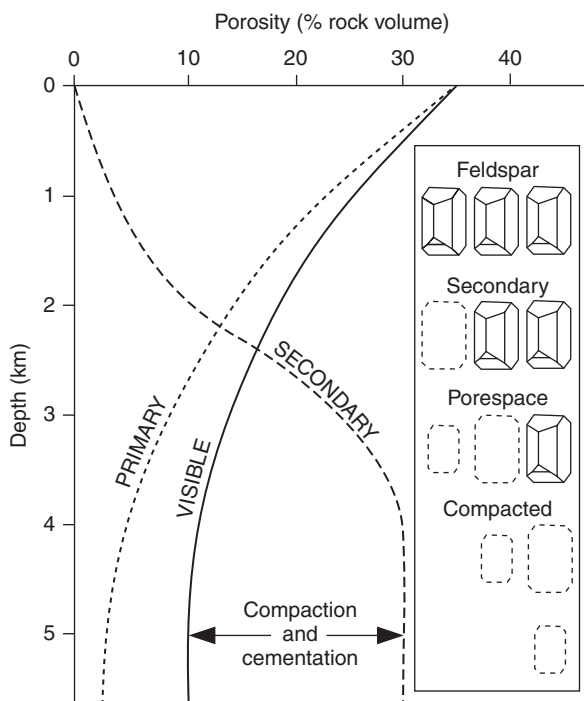


Figure 8.15 Graph showing decline in feldspar and primary porosity with burial depth, and concomitant increase in secondary porosity. The total porosity generated is never visible at any one time because of the continuing compaction of both primary and secondary porosity. (From Wilkinson, M., K. L. Milliken, and R. S. Haszeldine, 2001, Systematic destruction of K-feldspar in deeply buried rift and passive margin sandstones: *J. Geol. Soc. London*, **158**, Fig. 3, p. 682, reproduced by permission.)

dissolved rapidly and another instantly deposited in its place. Rather, dissolution and reprecipitation may take place over a long period of time, with the guest mineral gradually replacing the host. Replacement reactions appear to take place within a very thin film of solution. Within this film, ions in a mineral undergoing solution diffuse outward into open pore water while the replacing ions diffuse from the pore water onto the freshly dissolved surface (precipitation surface).

Formerly, it was assumed that replacement can occur only under geochemical conditions in which pore fluids are undersaturated with respect to the host mineral undergoing replacement and are supersaturated with respect to the guest mineral doing the replacing. Maliva and Siever (1988a) propose, however, that undersaturation with respect to the bulk host phase is not necessarily a prerequisite for replacement. They suggest that replacement can occur by a **force of crystallization-controlled mechanism** along thin films that have only diffusional access to bulk pore waters in equilibrium with the bulk host sediments. All that is required for replacement is a sufficient degree of local supersaturation with respect to the authigenic mineral phase, and suitable conditions in the rock for initial crystal nucleation.

Replacement appears to take place without any volume change between the replaced and replacing minerals. Owing to the nature of the replacement process, delicate textures and structures present in the original mineral may be faithfully preserved in the replacement mineral. Well-known examples of such preservation are petrified wood and carbonate fossils replaced by chert.

Replacement, as described, is not the same process as dissolution followed later by precipitation. The latter process first produces a cavity, which is subsequently filled by precipitation of another mineral. Is there also a difference between replacement and alteration by incongruent solution? Incongruent solution may preserve the outline or shape of a grain but does not preserve its internal texture, e.g. alteration of K-feldspar to kaolinite. Clearly, many petrographers nonetheless consider the alteration of feldspars to clay minerals to be a type of replacement process, although kaolinitization of feldspar (and mica) may be accompanied by large increases in volume (McBride, 1984). Petrographic observations show that replacement of one mineral by another may begin along the outside edge of a grain, at the center of the grain, or in some position in between.

Common replacement minerals

Many kinds of minerals may be involved in replacement reactions, including the silica minerals, carbonates, feldspars, clay minerals, sulfates, halides, zeolites, pyrite, and iron oxides. Common replacement events include replacement of carbonate minerals by micro-quartz (chert), replacement of chert by carbonate minerals, replacement of feldspars and quartz by carbonate minerals (Fig. 8.16), replacement of clay matrix by carbonate

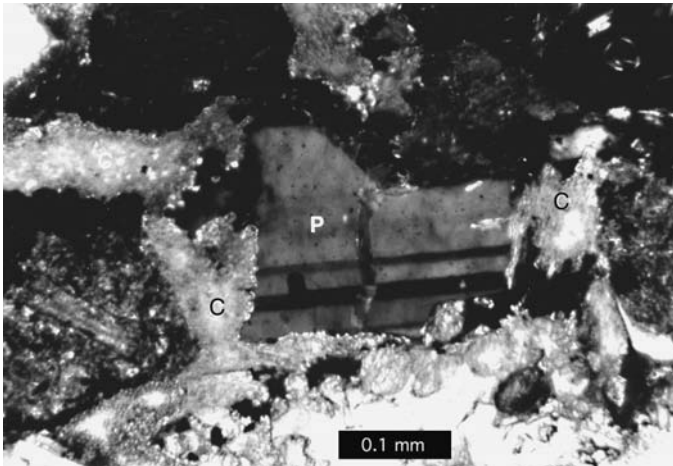


Figure 8.16 Twinned plagioclase grain (P) strongly embayed by replacement calcite (C), Miocene sandstone, Japan Sea. [From Boggs, S., Jr. and A. Seyedolali, 1992, Diagenetic albitization, zeolitization, and replacement in Miocene sandstones, Sites 796, 797, and 799, Japan Sea, in Pisciotto, K. A., J. C. Ingle, Jr., M. T. von Breyman *et al.* (eds.), *Proceedings of the Ocean Drilling Program, Scientific Results*, vol. 127/128, part 1, Fig. 26, p. 146.]

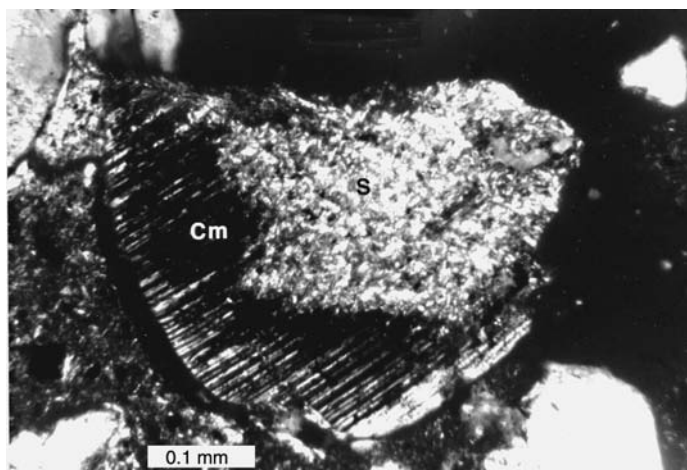
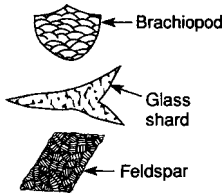
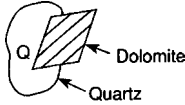
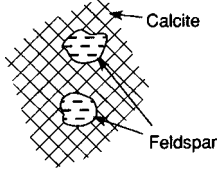
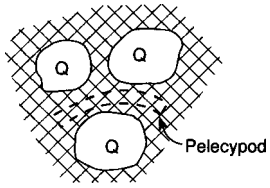
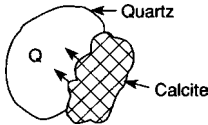
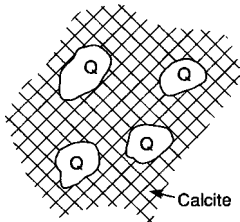


Figure 8.17 Broken, twinned plagioclase grain partially replaced by sericite (S) and dark-colored clay minerals (Cm), Miocene sandstone, Japan Sea. [From Boggs, S., Jr. and A. Seyedolali, 1992, Diagenetic albitization, zeolitization, and replacement in Miocene sandstones, Sites 796, 797, and 799, Japan Sea, in Pisciotto, K. A., J. C. Ingle, Jr., M. T. von Breymann, *et al.* (eds.), *Proceedings of the Ocean Drilling Program, Scientific Results*, vol. 127/128, part 1, Fig. 24, p. 145.]

minerals, and replacement of feldspars, rock fragments, and ferromagnesian minerals by clay minerals (Fig. 8.17), albitization of plagioclase and K-feldspar (see below), replacement of feldspars and volcanic rock fragments with zeolites in volcanoclastic sequences, and replacement of feldspars by evaporite minerals such as anhydrite in sandstones associated with evaporites. Although less common, feldspars can also be replaced by quartz. For example, Morad and Aldahan (1987) report extensive replacement of feldspars by quartz in Proterozoic sandstones of Sweden and Norway. Also, some clay minerals, muscovite, and some zeolites can be replaced by Na-feldspar or K-feldspar. Probably, the most characteristic replacement events in sandstones are replacement of silicate minerals by calcite or dolomite, replacement (loosely) of feldspars by clay minerals, and albitization of feldspars.

The major problems in studying paragenetic sequences of replacement minerals are (1) to recognize that replacement has occurred, and (2) to determine which mineral has replaced which. It is not always easy to tell which is the guest mineral and which is the host. Furthermore, if a grain is completely replaced, the identity of the original grain is lost unless the replacement process produces an identifiable pseudomorph. Table 8.1 lists some useful criteria for identifying replacement textures and distinguishing between host and guest minerals. Readers are cautioned, however, that replacement events can be very complex and can involve several stages of replacement by different minerals, as well as reversals in replacement between two minerals. Therefore, it may be very difficult to identify all stages of replacement, and extremely careful study may be required to sort out the replacement sequence.

Table 8.1 *Criteria for recognizing replacement textures*

Texture/ composition	Criterion	Examples	Appearance
Illogical mineral composition (pseudomorphs)	Shape of grain does not fit mineralogy	Calcareous shell replaced by microquartz (chert) or anhydrite; volcanic glass shard replaced by smectite; feldspar replaced by kaolinite	
Automorphic penetration	Cross-cutting relationship; one mineral clearly cuts across or transects the boundary of another	Quartz or feldspar grain cut by calcite or dolomite crystal	
Preservation of unreplaced relic of host grain	Remnant of host mineral appears to "float" in the surrounding replacement mineral	Remnant of a feldspar grain within a larger mass of calcite; feldspar remnants have the same optical orientation	
Ghost or phantom structure	Recognizable "ghosts" of original grain (best seen in plane polarized light)	Ghosts of carbonate fossils in dolomite or calcite cement; most common in carbonate rocks	
Caries texture	Bitelike embayments of guest mineral into host mineral	Calcite replacing quartz grain along edges (caution: don't confuse simple overlap of grains having irregular boundaries with replacement along grain boundaries)	
Abnormally loose packing	Abnormally large numbers of detrital grains that appear to be "floating"; i.e. large patches of a rock are not grain-supported	Quartz grains that appear to "float" in calcite; calcite has replaced the original mineral that occupied the space among the quartz grains	

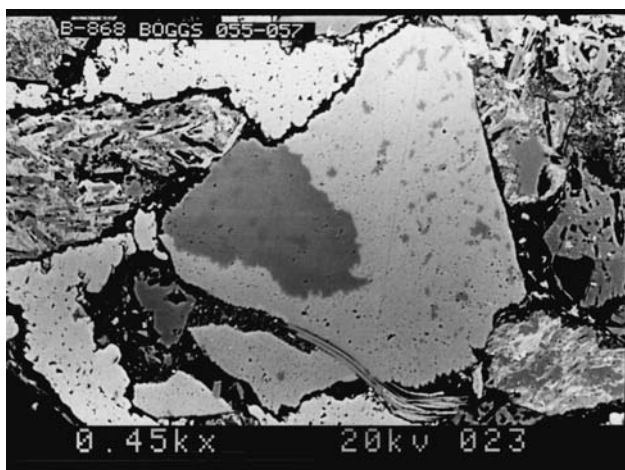


Figure 8.18 Partially albitized plagioclase grain (center of photograph), as revealed by backscattered electron microscopy (BSE). The dark patches are albitized areas. Miocene deep-sea sandstone, Japan Sea. Ocean Drilling Program Leg 127, Site 797. (Photograph courtesy of David Krinsley.)

Albitization

The albitization of feldspars is a special kind of replacement process that involves replacement of calcic plagioclase or K-feldspar with sodic plagioclase (albite). This process produces changes in feldspars that are not always detected during petrographic study. Although many workers have reported albitization of feldspars, the fact that no distinction is made between the different plagioclase feldspars during many routine petrographic studies means that albitization may go unrecognized. Unless a distinctive albitization texture is produced during diagenesis, or unless composition is analyzed by a suitable instrument such as the electron probe microanalyzer, albitization may not be detected. Partial albitization of K-feldspar grains or the presence of “chessboard” texture (Walker, 1984) is an indication of albitization. Distinctive patterns of albitization (Fig. 8.18) may also be revealed by backscattered electron microscopy (e.g. Morad *et al.*, 1990). Exceptionally high abundance of albite in a sandstone also suggests albitization. More routine use of the electron probe microanalyzer and backscattered electron microscopy in diagenesis studies is increasing the chance of identifying albitized feldspars.

Both Ca-bearing plagioclase and K-feldspar may undergo albitization. Most investigators suggest that albitization occurs at temperatures on the order of 100–150 °C (Milliken *et al.*, 1981; Boles, 1982; Surdam *et al.*, 1989a). On the other hand, albitization has also been reported to take place at temperatures as low as 70–100 °C (e.g. Morad *et al.*, 1990; Aagaard *et al.*, 1990). Albitization of feldspars may occur by direct replacement by albite, or through intermediate stages that involve initial replacement of feldspars by calcite, anhydrite, or other minerals, followed by replacement of these minerals with albite (e.g. Walker, 1984). Albitization may also occur by partial

dissolution of detrital feldspars, followed by precipitation of albite in dissolution voids (Milliken, 1989).

Effects of replacement

Replacement processes, like dissolution processes, can affect the porosity of formations as well as influencing interpretations of provenance on the basis of detrital mineralogy. Porosity is affected mainly by alteration of feldspars, rock fragments, and micas to clay minerals, with a concomitant increase in volume, which tend to plug pores and reduce porosity. Loss of provenance information arises from complete replacement of grains so that the identity of the original grain is in doubt. Complete alteration of feldspars and other detrital grains to clay minerals, complete replacement of feldspars or other grains by carbonate minerals, and complete albitization of feldspars are probably the most important replacement processes that cause loss of provenance information and misinterpretation of provenance. Albitization of K-feldspars, for example, may result in the complete disappearance of K-feldspars from a formation or stratigraphic unit with concomitant increase in the content of sodic plagioclase. If albitization goes undetected, interpretation of provenance on the basis of feldspars can give very misleading results.

Recrystallization and inversion

The term **recrystallization**, as used in this book, refers to change in size or shape of crystals of a given mineral, without accompanying change in chemical composition or mineralogy. **Inversion** is a more complex kind of recrystallization in which one polymorph of a mineral changes to another polymorph without change in chemical composition, e.g. the transformation of aragonite (CaCO_3) to calcite (CaCO_3). Folk (1965) suggested the term **neomorphism** to cover both recrystallization and inversion.

Recrystallization of a substance represents a change from a less-stable to a more-stable form of the substance. The driving force behind recrystallization is the tendency toward a minimum in the Gibbs free energy of the chemical system (Pettijohn *et al.*, 1987, p. 438). Most commonly, this tendency drives recrystallization in the direction of increasing crystal size. That is, small crystals recrystallize to larger crystals, a process sometimes referred to as **aggrading recrystallization** or **aggrading neomorphism**. The opposite process, recrystallization of large crystals to small crystals, has been reported, particularly in carbonate rocks, however, **degrading recrystallization** is not common and is poorly understood. Recrystallization energetics also drive inversion of less-stable polymorphs to more-stable forms.

Simple recrystallization involving only a change in size or shape of grains is an important process in carbonate rocks (Chapter 11). Recrystallization is generally regarded to be relatively unimportant in siliciclastic rocks; however, Ji and Mainprice (1990) report extensive recrystallization in plagioclase crystals that have undergone metamorphism. A kind of inversion process that takes place in the presence of fluids occurs in both kinds of rocks. This process, which is actually a solution reprecipitation process, is most common in CaCO_3 and SiO_2 minerals. Alteration of metastable aragonite to calcite is particularly

common in carbonate rocks (Chapter 11). Because such alteration takes place comparatively rapidly under aqueous conditions, aragonite rarely occurs in rocks older than the Tertiary. Nonetheless, aragonite has been reported in older rocks, e.g. Pennsylvanian rocks. It commonly occurs in older rocks under some kind of special conditions where the aragonite has been prevented from reacting with pore fluids. For example, aragonite in shells may be preserved by asphalt coatings (Brand, 1989). Polymorphic transformation of aragonite to calcite has minor significance in sandstones and shales, where it is limited mainly to alteration and recrystallization of aragonite fossils and cements.

Transformation of the SiO_2 polymorphs from opal-A to opal-CT to quartz (chert) is a common diagenetic process in muddy sediments that contain significant quantities of opaline skeletal remains, e.g. deep-sea diatom or radiolarian oozes. Sandstones commonly contain few opaline skeletal remains, but they may contain opal-A or opal-CT cements, particularly sandstones in volcanoclastic rocks. Opal cements subsequently transform to microcrystalline quartz (chert). The conversion of opal-A to microcrystalline quartz is controlled by both temperature and time. That is, conversion proceeds at a faster rate in areas having high geothermal gradients and high sedimentation rates than in areas with lower rates (Siever, 1983). The rate of conversion depends also upon the nature of the starting material and the solution chemistry, particularly the availability of Mg^{2+} and OH^- ions, which form magnesium hydroxide compounds that serve as a nucleus for crystallization of opal-CT (Kastner and Gieskes, 1983). Opal inversion is a solution-precipitation process. Opal-A first dissolves to yield solutions rich in silica. The silica then flocculates to yield opal-CT, which becomes increasingly ordered before dissolving to yield pore waters of low silica concentration. Slow growth of quartz takes place from these waters (Williams and Crerar, 1985). Identification of opal-A, opal-CT, and quartz phases commonly requires X-ray diffraction techniques.

Clay-mineral authigenesis

Although diagenetic reactions affecting clay minerals are discussed in several preceding sections, it may be well at this point to summarize the various processes that involve clay-mineral authigenesis. Diagenetic changes that affect clay minerals include alteration of nonclay-mineral precursor minerals such as feldspars and volcanic glass to produce clay minerals, alteration of one kind of clay mineral to another, and precipitation of clay minerals into pore spaces where no obvious precursor mineral is present. Preceding discussion indicates that clay-mineral diagenesis is influenced by temperature and by organic and inorganic reactions that affect pore-water composition. Increasing temperature generally promotes clay-mineral diagenesis, although some clay minerals such as kaolinite are known to form at both low and high temperatures.

Table 8.2 summarizes some common clay-mineral diagenetic changes that occur in sandstones and shales. Reactions involving kaolinite and smectite are particularly important. For additional information about clay minerals in sandstones and clay-mineral diagenesis, see Houseknecht and Pittman (1992).

Table 8.2. Some important clay-mineral diagenetic reactions in sandstones and shales

Precursor mineral	Mineral formed	Chemical reaction	Diagenetic stage	Approx temp. of reaction	Remarks
K-feldspars*	Kaolinite	$2\text{KAlSi}_3\text{O}_8 + 2\text{H}^+ + 9\text{H}_2\text{O} \rightarrow \text{Al}_2\text{Si}_2\text{O}_5(\text{OH})_4 + 4(\text{H}_4\text{SiO}_4) + 2\text{K}^+$	Eogenesis, telogenesis	< ~25 °C	Silicic acid and K ⁺ released
Ca-plagioclase	Kaolinite	$\text{CaAl}_2\text{Si}_2\text{O}_8 + 2\text{H}^+ + \text{H}_2\text{O} \rightarrow \text{Al}_2\text{Si}_2\text{O}_5(\text{OH})_4 + \text{Ca}^{2+}$	Eogenesis, telogenesis	< ~25 °C	Ca ²⁺ released
Kaolinite	K-feldspar	$\text{Al}_2\text{Si}_2\text{O}_5(\text{OH})_4 + 4(\text{H}_4\text{SiO}_4) + 2\text{K}^+ \rightarrow 2\text{KAlSi}_3\text{O}_8 + 2\text{H}^+ + 9\text{H}_2\text{O}$	Mesogenesis	< ~150 °C(?)	Silicic acid, K ⁺ added; H ₂ O, H ⁺ released
Kaolinite	Ca-plagioclase	$\text{Al}_2\text{Si}_2\text{O}_5(\text{OH})_4 + \text{Ca}^{2+} \rightarrow \text{CaAl}_2\text{Si}_2\text{O}_8 + 2\text{H}^+ + \text{H}_2\text{O}$	Mesogenesis	< ~150 °C	Ca ²⁺ added; H ₂ O, H ⁺ released
Kaolinite	Muscovite (or illite**)	$3\text{Al}_2\text{Si}_2\text{O}_5(\text{OH})_4 + 2\text{K}^+ \rightarrow 2\text{KAl}_3\text{Si}_3\text{O}_{10}(\text{OH})_2 + 2\text{H}^+ + \text{H}_2\text{O}$	Mesogenesis	~120–150 °C	K ⁺ added; H ⁺ , H ₂ O released
Smectite	Illite	$\text{Smectite} + 4.5\text{K}^+ + 8\text{Al}^{3+} \rightarrow \text{illite} + \text{Na}^+ + 2\text{Ca}^{2+} + 2.5\text{Fe}^{3+} + 2\text{Mg}^{2+} + 3\text{Si}^{4+} + 10\text{H}_2\text{O}$	Mesogenesis	~55–200 + °C	Smectite dominant at < ~100 °C; mixed-layer S/I occurs at ~100–200 °C; illite dominant at > ~200 °C; H ₂ O released
Smectite	Chlorite	$\text{Smectite} + (\text{Fe}^{2+}, \text{Fe}^{3+}) \rightarrow (\text{Mg}, \text{Al}, \text{Fe})_6[\text{Si}, \text{Al}]_4\text{O}_{10}(\text{OH})_8 + \text{SiO}_2 + \text{Na}^+ + \text{Ca}^{2+} + \text{H}_2\text{O}$ (not balanced)	Mesogenesis	~55–200 + °C	Chlorite dominant at > 200 °C
Volcanic glass	Na-smectite	$\text{Na}_2\text{KCaAl}_5\text{Si}_{11}\text{O}_{32} + \text{MgSiO}_3 + \text{H}_2\text{O} + 4\text{H}^+ + 4\text{HCO}_3^- \rightarrow \text{Na}(\text{Al}_5\text{Mg})\text{Si}_{12}\text{O}_{30}(\text{OH})_6 + \text{Na}^+ + \text{Ca}^{2+} + 4\text{HCO}_3^-$	Eogenesis, mesogenesis	< 25–150 + °C	Mg ²⁺ , SiO ₂ , H ₂ O added; Na ⁺ , Ca ²⁺ released
Illite (or muscovite)	Glaucanite	$\text{Illite} + (\text{Fe}^{2+}, \text{Fe}^{3+}) \rightarrow \text{glaucanite} + \text{K}^+ + \text{Al}_2\text{O}_3$ (not balanced)	Eogenesis, mesogenesis	< ~50 °C	Fe ²⁺ , Fe ³⁺ added; K ⁺ , Al ₂ O ₃ released
Muscovite	K-feldspar	$\text{KAl}_3\text{Si}_3\text{O}_{10}(\text{OH})_2 + 2\text{K}^+ + 6(\text{H}_4\text{SiO}_4) \rightarrow 3\text{KAlSi}_3\text{O}_8 + 12\text{H}_2\text{O} + 2\text{H}^+$	Mesogenesis	< ~150 °C (?)	Silicic acid, K ⁺ added; H ₂ O, H ⁺ released
Na–Al smectite	Na-feldspar	$\text{Na}(\text{Al}_5\text{Mg})\text{Si}_{12}\text{O}_{30}(\text{OH})_6 + 4\text{Na}^+ + 3(\text{H}_4\text{SiO}_4) \rightarrow 5\text{NaAlSi}_3\text{O}_8 + 8\text{H}_2\text{O} + 2\text{H}^+ + \text{Mg}^{2+}$	Mesogenesis	< ~150 °C (?)	Silicic acid, Na ⁺ added; H ₂ O, H ⁺ , Mg ²⁺ released
Na–Al smectite	K-feldspar	$\text{Na}(\text{Al}_5\text{Mg})\text{Si}_{12}\text{O}_{30}(\text{OH})_6 + 5\text{K}^+ + 3(\text{H}_4\text{SiO}_4) \rightarrow 5\text{KAlSi}_3\text{O}_8 + 8\text{H}_2\text{O} + 2\text{H}^+ + \text{Na}^+ + \text{Mg}^{2+}$	Mesogenesis	< ~150 °C	Silicic acid, K ⁺ added; H ₂ O, H ⁺ , Na ⁺ , Mg ²⁺ released
Kaolinite + K-feldspar	Illite + quartz	$\text{Al}_2\text{Si}_2\text{O}_5(\text{OH})_4 + \text{KAlSi}_3\text{O}_8 \rightarrow \text{KAl}_3\text{Si}_3\text{O}_{10}(\text{OH})_2 + 2\text{SiO}_2 + \text{H}_2\text{O}$	Mesogenesis	~120–150 °C	H ₂ O released
Pore waters	Kaolinite	$\text{Al}_2\text{O}_3 + 2\text{SiO}_2 + 2\text{H}_2\text{O} \rightarrow \text{Al}_2\text{Si}_2\text{O}_5(\text{OH})_4$	Eogenesis, telogenesis	< ~25 °C	No obvious precursor; kaolinite precipitated in pore space

* Alteration of Na-feldspar proceeds by same reaction but with release of Na⁺. ** Reaction shown is for muscovite; to form illite requires addition of more K⁺ and SiO₂. Source: Data from Bjørlykke, 1983, Boles and Franks, 1979, Kastner and Stever, 1979, Pettijohn *et al.*, 1987, and Lee *et al.*, 1989.

The burial diagenesis of clay minerals is often depicted in burial-history curves such as that shown in Fig. 8.12. Many studies of clay-mineral diagenesis are now being carried out as multidisciplinary studies that may include also investigation of other authigenic minerals such as quartz, feldspar, and carbonate cements. Techniques for such multidisciplinary studies include petrography, K/Ar dating, oxygen and carbon isotope measurements, and fluid-inclusion studies. These techniques provide information on the timing and temperature of formation of authigenic mineral phases and on the nature and origin of the diagenetic fluids. See Girard *et al.* (1989) for a good example of this approach.

Clay-mineral reactions are obviously most important in shales, which contain large amounts of clay minerals. Most sandstones probably contain little detrital clay, except possibly infiltrated clay; however, alteration of feldspars, ferromagnesian minerals, and volcanic glass can lead to formation of substantial quantities of authigenic clay minerals. Also, pore waters generated in shale sequences can migrate into associated sandstones and thereby affect the course of diagenesis in the sandstones, as noted. Thus, clay-mineral reactions are an important aspect of diagenesis in both shales and sandstones. These reactions proceed as a function of pore-water compositions and temperature. Time is also a factor in clay-mineral diagenesis; several workers have pointed out, for example, that there is a statistical increase in illite and chlorite with increasing age. On the other hand, drastic diagenetic changes in clay minerals have been reported in rocks as young as late Tertiary (e.g. Ramseyer and Boles, 1986). The correlation between clay-mineral diagenesis and time may thus be more apparent than real. Older rocks may simply have had a statistically higher chance of being subjected to the kinds of temperatures required for diagenesis. The geothermal gradient and residence time of diagenetically active temperature may be more important than actual geologic age (e.g. Chamley, 1989).

Zeolite authigenesis

Sedimentary zeolites occur in a variety of environments including (1) closed hydrologic systems such as saline, alkaline lakes, (2) saline, alkaline soils and land surfaces, (3) open hydrologic systems where groundwaters can percolate freely, particularly in nonmarine settings, (4) deep-sea sediments, (5) hydrothermal alteration zones, and (6) burial diagenesis or metamorphic environments (Hay, 1981). The principal zeolites that occur in sedimentary rocks are shown in Table 8.3; as shown, zeolites are hydrated aluminosilicates. Structurally, they are composed of a three-dimensional network of SiO_4^{4-} tetrahedra, like the feldspars, but the structure is much more open than that of the feldspars.

Zeolites that occur in alkaline lake deposits form at shallow depths and low temperatures. Zeolites common in this environment include analcime, chabazite, clinoptilolite, erionite, mordenite, and phillipsite (Surdam, 1981). In deep-sea sediments, zeolites can also occur at shallow depths at relatively low temperatures in clays and volcanoclastic sediments (e.g. Boggs and Seyedolali, 1992). Phillipsite and clinoptilolite are most common, with analcime next in abundance (e.g. Fig. 8.19). Erionite, natrolite, and mordenite occur only rarely. These zeolites form by reaction of volcanic glass with pore waters, possibly with addition of biogenic silica (Hay, 1981).

Table 8.3 Common zeolite minerals in sedimentary rocks

Zeolite	Typical formula	Crystal system	Habit in sedimentary rocks
Analcime	$\text{Na}_2(\text{Al}_2\text{Si}_4\text{O}_{12}) \cdot 2\text{H}_2\text{O}$	Cubic	Trapezohedra
Chabazite	$\text{Ca}(\text{Al}_2\text{Si}_4\text{O}_{12}) \cdot 6\text{H}_2\text{O}$	Hexagonal	Rhombs
Clinoptilolite	$(\text{Na}_2\text{K}_2)(\text{Al}_2\text{Si}_{10}\text{O}_{20}) \cdot 8\text{H}_2\text{O}$	Monoclinic	Laths and plates
Erionite	$(\text{Na}_2\text{K}_2, \text{Ca}, \text{Mg})_{4.5}(\text{Al}_9\text{Si}_{27}\text{O}_{72}) \cdot 27\text{H}_2\text{O}$	Hexagonal	Hexagonal rods and bundles of rods
Ferrierite	$(\text{Na}_2\text{Mg}_2)(\text{Al}_6\text{Si}_{30}\text{O}_{72}) \cdot 18\text{H}_2\text{O}$	Orthorhombic	Laths and rods
Heulandite	$\text{Ca}_3\text{Na}_2\text{Al}_8\text{Si}_{28}\text{O}_{72} \cdot 24\text{H}_2\text{O}$	Monoclinic	Laths
Laumontite	$\text{Ca}(\text{Al}_2\text{Si}_4\text{O}_{12}) \cdot 4\text{H}_2\text{O}$	Monoclinic	Laths
Mordenite	$(\text{Na}_2\text{K}_2\text{Ca})(\text{Al}_2\text{Si}_{10}\text{O}_{24}) \cdot 7\text{H}_2\text{O}$	Orthorhombic	Needles and fibers
Natrolite	$\text{Na}_2(\text{Al}_2\text{Si}_3\text{O}_{10}) \cdot 2\text{H}_2\text{O}$	Orthorhombic	—
Phillipsite	$(1/2\text{Ca}, \text{Na}, \text{K})_3(\text{Al}_3\text{Si}_5\text{O}_{16}) \cdot 6\text{H}_2\text{O}$	Orthorhombic	Rods and laths
Wairakite	$\text{Ca}(\text{Al}_2\text{Si}_4\text{O}_{12}) \cdot 2\text{H}_2\text{O}$	Monoclinic	—

Note: Zeolites are colorless or white when pure but may be colored by iron oxides or other impurities.

Source: Data from Deer *et al.*, 1966, and Mumpton, 1981.

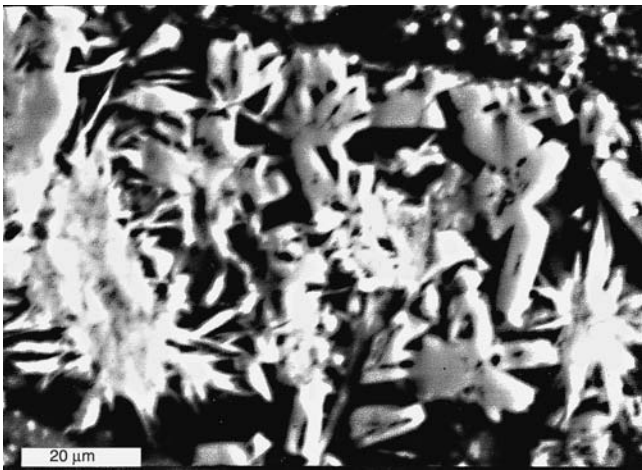


Figure 8.19 Backscattered electron micrograph of stellate clusters and tabular crystals of analcime, which forms pseudomorphs after clinoptilolite or heulandite. Miocene deep-sea sediment, Japan Sea. (From Boggs, S., Jr. and A. Seyedolali, 1992, Diagenetic albitization, zeolitization, and replacement in Miocene sandstones, Sites 796, 797, and 799, Japan Sea, in Pisciotto, K. A., J. C. Ingle, Jr., M. T. von Breyman, *et al.* (eds.), *Proceedings of the Ocean Drilling Program, Scientific Results*, vol. 127/128, part 1, Fig. 19, p. 143.]

Volcaniclastic sediments buried to greater depths in open hydrologic systems, in either marine or nonmarine environments, typically undergo extensive alteration to zeolites. Zeolitization occurs particularly in thick sequences of volcaniclastic deposits, in which zeolites may occur in zones as a function of burial depth and temperature. Sediments at shallower depths are

characterized by a diagenetic mineral assemblage that may include mordenite, clinoptilolite, heulandite, phillipsite, and smectite. Zeolites in moderately to deeply buried volcanoclastic sediments may include analcime, laumontite, and wairakite, together with lawsonite, prehenite, and pumpellyite. Zeolites may be absent from the most deeply buried volcanogenic deposits, which contain instead an albite–chlorite–quartz assemblage that formed by alteration of zeolites. Also, one zeolite may transform to another during burial diagenesis. For example, Ogihara and Iijima (1989) report that clinoptilolite has transformed to heulandite at burial depths of 1710–1770 m in some Cretaceous marine strata in Japan.

The diagenetic formation of zeolites in volcanoclastic sequences takes place by alteration of plagioclase, volcanic glass, and volcanic lithic fragments. Clay minerals and biogenic silica may also be involved in some reactions. Plagioclase may alter partially or completely to zeolites or albite or develop clay rims. Glass shards and volcanic lithic fragments may be replaced by zeolites or clay minerals. Zeolites may also precipitate as cements in pore spaces. Three principal kinds of reactions occur in the diagenetic process: (1) hydration, (2) formation of carbonates (carbonatization), and (3) dehydration (Surdam and Boles, 1979). Hydration and carbonate formation occur during the early stages of diagenesis, whereas dehydration occurs during later diagenesis. According to Surdam and Boles, zeolite diagenesis in volcanogenic sediments can take place over a broad range of temperatures from about 10 °C to 200+ °C, with the upper limit of pressure and temperature being about 3 kbar pressure and 300 °C temperature.

Hydration is commonly the earliest diagenetic reaction and may be recognized petrographically by features such as hydration rims on plagioclase or glass fragments. The reaction is either

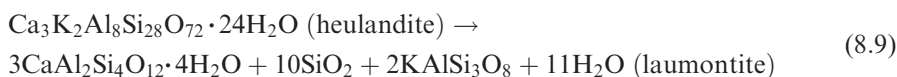


or

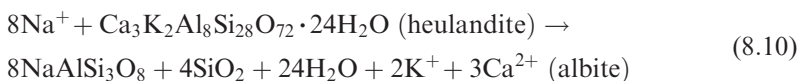


Hydration reactions may be accompanied by addition of SiO₂, which could be supplied by replacement of quartz. Hydration commonly causes significant reduction in porosity and permeability of the sediments owing to increase in volume of the zeolites. The hydration process may release Ca²⁺, which can combine with HCO₃[−] to form early carbonate cements if a source of bicarbonate is available. These carbonate cements further reduce porosity and permeability.

Dehydration reactions occur during later diagenesis and higher burial temperatures. These reactions may involve alteration of one zeolite to another or alteration of a zeolite to a different kind of mineral. For example, heulandite can dehydrate to laumontite (Surdam and Boles, 1979):



or heulandite can dehydrate to albite



Large quantities of water are released during these dehydration reactions, along with silica and cations such as calcium, sodium, and potassium.

Surdam and Boles (1979) suggest that temperature may be overemphasized in zeolite diagenesis and that fluid flow and pore-water composition may be as significant as depth of burial in controlling the distribution of diagenetic minerals in volcanoclastic deposits. Fluid effects are especially important during early diagenesis when the fluid-to-grain ratio is high, and during later stages, when dehydration and fracturing are important.

Vavra (1989) provides an example of the influence of multiple variables in zeolite diagenesis. He reports that zeolite-facies mineral assemblages are an important authigenic component of feldspathic arenites and volcanic lithic arenites in Triassic sandstones of the central Transantarctic Mountains, Antarctica. The mineral assemblages include heulandite, mordenite, and analcime, as well as smectite, chlorite, and quartz. Vavra interprets that this mineral suite formed at shallow burial depths and moderately low temperatures by reaction between sediments and groundwater. With deeper burial, zeolite-facies minerals were subjected to higher temperatures associated with Jurassic diabase intrusions. Under these conditions, fluid-rock reactions resulted in conversion of smectite to mixed-layer illite/smectite and produced albite, laumontite, prehnite, epidote, and chlorite. Vavra suggests that the diagenetic reactions in this sandstone were controlled by a combination of parent-rock composition, fluid chemistry, permeability, and temperature.

The diagenetic changes that occur in volcanogenic sediments from the early to late stages of diagenesis are summarized in Fig. 8.20.

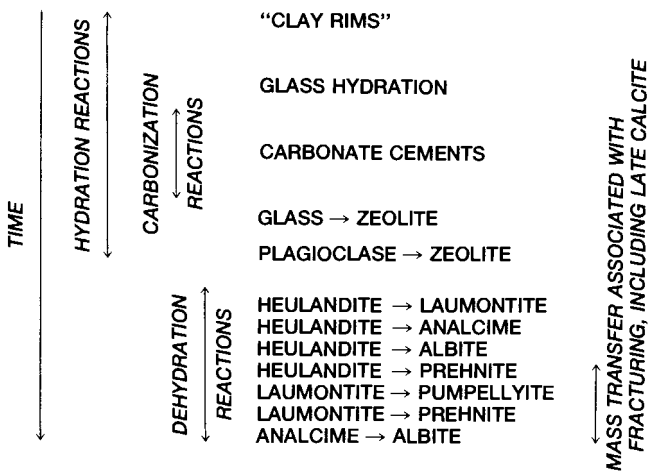


Figure 8.20 Descriptive framework for zeolitization and other diagenetic changes in volcanoclastic sediments. (From Surdam, R. C. and J. R. Boles, 1979, *Aspects of Diagenesis*: SEPM Special Publication 26, Fig. 17, p. 241, reprinted by permission of the Society for Sedimentary Geology, Tulsa, OK).

Oxidation of ferromagnesian minerals

Oxidation of iron-rich volcanic fragments and ferromagnesian minerals such as magnetite, biotite, and pyroxenes is a common diagenetic process. Oxidation initially produces goethite (limonite), which dehydrates with age to hematite. The iron oxides may alter and obscure the original detrital ferromagnesian grains so thoroughly that they cannot be recognized. Also, the oxides may migrate outward from the grain to form a surrounding halo, or they may invade and coat adjacent grains, making them difficult to identify. Much, if not most, of the hematite in ancient redbeds may be the product of diagenetic alteration of ferromagnesian minerals. Oxidation of ferromagnesian grains occurs particularly at shallow burial depths in the presence of oxic meteoric waters, but can occur at any depth where oxidizing waters are present. Destruction of detrital grains by oxidation is thus most common during eogenesis and telogenesis.

Ages of diagenetic events

In the preceding sections, the timing of diagenetic events is discussed in terms of relative stages of diagenesis: eogenesis, mesogenesis, telogenesis; early, middle, late diagenesis; shallow, moderate, deep burial, and so on. The relative timing of events in a diagenetic paragenetic sequence is usually established by petrographic study of compaction, cementation, and replacement textures as well as by knowledge of the pressure–temperature stability fields of the various diagenetic minerals. The timing of porosity enhancement and loss is of special interest to petroleum geologists, who try to construct predictive models for evaluating the timing of diagenetic events (e.g. Surdam *et al.*, 1989b).

In addition to relative dating of diagenetic events, geologists are increasingly interested in determining the absolute timing of such events. There is also increasing interest in relating the timing of diagenetic events to large-scale geologic phenomena such as periods of emergence, rapid sedimentation, and faulting (e.g. Lundegard, 1989). Determining the absolute age of a diagenetic event requires that the absolute age of characteristic diagenetic minerals be determined. Absolute ages are determined by isolating authigenic minerals whose ages can be established by using standard techniques of geochronology that involve dating by radiometric methods. A common technique is to determine the ages of authigenic illite and glauconite by using the potassium/argon method. The ages of overgrowths on potassium feldspars may also be determined by this technique. Alternatively, the $^{40}\text{Ar}/^{39}\text{Ar}$ method can be used to determine ages of these minerals, and the potassium/calcium method may be used for dating feldspar cements. Rubidium/strontium dating of illite and $^{87}\text{Sr}/^{86}\text{Sr}$ dating of cements such as marine carbonate cements are less common techniques.

Paleomagnetic methods have also been applied to determining the ages of authigenic iron oxides in redbeds or in sedimentary units that have experienced solution of iron carbonates with subsequent reprecipitation of iron oxides. The age resolution of such methods is generally not very good, and the paleomagnetic scale for rocks older than the Jurassic is not as well established as that for younger rocks. For a review of these diagenetic dating techniques and their limitations, see Lundegard (1989). As discussed in preceding sections of this chapter, ages determined by the above methods are often combined with information obtained by petrography, isotope analysis, and fluid-inclusion studies to produce burial-history curves (e.g. Fig. 8.12).

8.5 Diagenetic reactions in the telogenetic zone (uplift and exposure-related diagenesis)

Uplift and exposure of the sediment pile brings sediments into the **telogenetic regime**, characterized by lowered pressures and temperatures and by generally oxidizing, meteoric pore waters. Mineral assemblages formed under high temperatures and pressures during mesogenesis tend to become unstable under the changed conditions of telogenesis. Mesogenetic pore waters may be flushed and replaced by meteoric waters of low salinity that are commonly oxidizing and acidic, although alkaline meteoric waters may exist under some conditions. Diagenetic mineral assemblages formed during mesogenesis may become unstable under these changed conditions and may undergo dissolution or alteration. Also, original detrital mineral assemblages can undergo further diagenesis. Telogenetic modifications of mineral assemblages may occur at some depth below Earth's surface, but within the zone of meteoric water circulation, or they may occur at the surface by weathering processes. They may include dissolution of previously formed cements or framework grains (creating porosity), or *in situ* alteration of framework grains to clay minerals (occluding porosity). Alternatively, depending upon the nature of pore waters, silica or carbonate cements can be precipitated. For example, carbonate cements can be precipitated in the vadose zone by evaporative pumping under climatic conditions that favor evaporation (Surdam *et al.*, 1989b).

Observed diagenetic changes that have been attributed to telogenetic modification include oxidation and destruction of organic matter, oxidation of iron carbonates to form iron oxides and eventually hematite, oxidation of sulfides to form sulfates such as gypsum, dissolution of pyroxenes, amphiboles, and other heavy minerals during weathering, and alteration of detrital feldspars to kaolinite. Detrital feldspars are also reported to alter to illite and authigenic K-feldspars. Other telogenetic changes may include alteration of chlorite to vermiculite and dissolution of iron oxides and carbonates.

Telogenesis may, therefore, modify previously formed diagenetic mineral assemblages, or it may produce changes in original detrital mineral assemblages that escaped modification during eogenesis and mesogenesis. Thus, telogenesis may cause additional loss of information about detrital mineral composition and loss of information about eogenetic and mesogenetic authigenic mineral assemblages. Furthermore, it may either enhance or reduce porosity, depending upon the specific conditions of the telogenetic environment.

Further reading

- Burley, S. D. and R. H. Worden, 2003, *Sandstone Diagenesis: Recent and Ancient*: Blackwell, Malden, MA.
- Crossey, L. J., R. Loucks, and M. E. Totten (eds.), 1996, *Siliciclastic Diagenesis and Fluid Flow: Concepts and Applications*: SEPM Special Publication 55.
- Giles, M. R., 1997, *Diagenesis: a Quantitative Perspective: Implications for Basin Modelling and Rock Property Prediction*: Kluwer, Dordrecht.

- Houseknecht, D. W. and E. D. Pittman, 1992, *Origin, Diagenesis, and Petrophysics of Clay Minerals in Sandstones*: SEPM Special Publication 47.
- Huffman, A. and G. Bowers (eds.), 2002, *Pressure Regimes in Sedimentary Basins and their Prediction*: AAPG Memoir 76.
- McDonald, D. A. and R. C. Surdam (eds.), 1984, *Clastic Diagenesis*: AAPG Memoir 37.
- McIlreath, I. A. and D. W. Morrow, 1990, *Diagenesis*: Geological Association of Canada, Memorial University of Newfoundland.
- Moñtanez, I. P., J. M. Gregg, and K. L. Shelton (eds.), 1997, *Basin-Wide Diagenetic Patterns: Integrated Petrologic, Geochemical, and Hydrologic Considerations*: SEPM Special Publication 57.
- Morad, S. (ed.), 1998, *Carbonate Cementation in Sandstones: Distribution Patterns and Geochemical Evolution*: International Association of Sedimentologists Special Publication 26.
- Morad, S., 1998, Carbonate cementation in sandstones: Distribution patterns and geochemical evolution, in Morad, S. (ed.), *Carbonate Cementation in Sandstones: Distribution Patterns and Geochemical Evolution*: International Association of Sedimentologists Special Publication 26, pp. 1–26.
- Parker, A. and B. W. Sellwood (eds.), 1994, *Quantitative Diagenesis: Recent Developments and Applications to Reservoir Geology*: Kluwer, Dordrecht.
- Stonecipher, S. A., 2000, *Applied Sandstone Diagenesis: Practical Petrographic Solutions for a Variety of Common Exploration, Development, and Production Problems*: SEPM Short Course Notes 50.
- Wolf, K. H. and G. V. Chilingar (eds.), 1992, *Diagenesis, III*: Elsevier, New York, NY.
- Wolf, K. H. and G. V. Chilingar (eds.), 1994, *Diagenesis, IV*: Elsevier, New York, NY.

Part III

Carbonate sedimentary rocks



Pennsylvanian-age limestones, Goosenecks of the San Juan River, Utah

9

Limestones

9.1 Introduction

As indicated in [Chapter 1](#), carbonate rocks make up about one-fifth to one-quarter of all sedimentary rocks in the stratigraphic record. They occur in many Precambrian assemblages and in all geologic systems from the Cambrian to the Quaternary. Both limestone and dolomite are well represented in the stratigraphic record. Dolomite is the dominant carbonate rock in Precambrian and Paleozoic sequences, whereas limestone is dominant in carbonate units of Mesozoic and Cenozoic age (Ronov, 1983).

On the basis of their abundance alone, about the same as that of sandstones, carbonate rocks are obviously an important group of rocks. They are important for other reasons as well. They contain much of the fossil record of past life forms, and they are replete with structures and textures that provide invaluable insight into environmental conditions of the past. Aside from their intrinsic value as indicators of Earth history, they also have considerable economic significance. They are used for a variety of agricultural and industrial purposes, they make good building stone, they serve as reservoir rocks for more than one-third of the world's petroleum reserves, and they are hosts to certain kinds of ore deposits such as epigenetic lead and zinc deposits.

The microscopic study of carbonate rocks dates back to the beginning of petrographic analysis. The science of petrography was initiated by an English geologist named Henry Clifton Sorby, who began petrographic analysis in about 1851 with the study of limestones. Other historically interesting early studies of carbonate rocks include investigation of carbonate sediments in the Bahamas by Black (1933) and Cayeux's (1935) classic work on the carbonate rocks of France. Modern study of carbonate sediments and depositional processes is generally regarded to have begun in the 1950s with the publications of Newell *et al.* (1951), Illing (1954), and Ginsburg (1956) dealing with modern carbonate sediments in the Bahamas and Florida Bay. Since the 1950s, the pace of research on carbonate rocks has accelerated. Dozens of books and many hundreds of research papers, in many languages, that are devoted to carbonate rocks are now available. A few of the more pertinent of these volumes are listed under Further reading at the end of this chapter.

With so much information available, a great deal is obviously known about the characteristics of carbonate rocks and the conditions under which they form. Nonetheless, field and

laboratory research on carbonates continues to be extremely active. Microscopic petrography remains the primary tool for petrologic analysis of carbonate rocks; however, standard petrography is being increasingly supplemented by use of more sophisticated tools such as scanning electron microscopy (SEM), cathodoluminescence (CL) imaging, electron probe microanalysis (EPMA), secondary-ion mass spectrometry (SIMS), and laser-ablation–inductively coupled plasma mass spectrometry (LA–ICP–MS). See Boggs and Kinsley (2006, ch. 3) for a brief discussion of these and other instrumental techniques. Tucker (1988) provides a somewhat dated, but more detailed, review of many important techniques in sedimentology. Computers and statistics are being increasingly used also for evaluation and interpretation of the vast amounts of data generated by these research tools.

In this chapter, we examine the mineralogy, chemical composition, and characteristic textures and structures of limestones. Also, we see how these features are used in classification. Further, we examine the petrographic characteristics of the principal kinds of limestones and explore these characteristics as a basis for interpreting the depositional environments of ancient limestones. The characteristics and origins of dolomite are discussed in Chapter 10, and the diagenesis of carbonate rocks is covered in Chapter 11.

9.2 Mineralogy

9.2.1 Principal carbonate groups

Carbonate rocks are so called because they are composed primarily of carbonate minerals. These minerals, in turn, derive their identity from the carbonate anion (CO_3^{2-}), which is a fundamental part of their structure. The CO_3^{2-} carbonate anion combines with cations such as Ca^{2+} , Mg^{2+} , Fe^{2+} , Mn^{2+} , and Zn^{2+} to form the common carbonate minerals (Table 9.1). A large number of other, little-known minerals also contain the CO_3^{2-} anion (see Frye, 1981). In many of these lesser-known minerals, the carbonate anion is present along with other anions, such as Cl^- , SO_4^{2-} , OH^- , F^- , and PO_4^{2-} , and many of the minerals are hydrated. Most of these uncommon minerals do not occur in sedimentary rocks, and they are not considered further in this book. A few of the carbonate phosphate minerals such as carbonate fluorapatite [$\text{Ca}_5(\text{PO}_4, \text{CO}_3)3\text{F}$] and carbonate hydroxyapatite [$\text{Ca}_5(\text{PO}_4, \text{CO}_3)3\text{OH}$] are discussed in Chapter 12.

The common carbonate minerals fall into three main groups: the **calcite group**, the **dolomite group**, and the **aragonite group** (Table 9.1). Minerals in the calcite and dolomite group belong to the rhombohedral (trigonal) crystal system, and those in the aragonite group belong to the orthorhombic system. Dolomite-group minerals differ from calcite-group minerals in that they are double carbonates. That is, they contain Mg^{2+} and/or Fe^{2+} in addition to Ca^{2+} . The rhombohedral carbonates have sixfold coordination. In calcite minerals, the atoms are arranged such that layers containing Ca, Mg, Mn, Fe, or Zn atoms alternate with layers of carbonate atoms, with the layers being equidistant along the z-axis. The triangular CO_3^{2-} groups have identical orientation within a given layer, but the orientation is reversed in alternate layers. Each oxygen ion in the calcite structure has two Ca^{2+} ions (or other

Table 9.1 *Common carbonate minerals*

Mineral	Crystal system	Formula	Substitutions	Indicatrix	Distinguishing characteristics	Remarks
<i>Calcite group</i>						
Calcite	Rhombohedral (trigonal)	CaCO ₃	Mg for Ca common; also small amounts of Fe ²⁺ and Mn for Ca	Uniaxial (-)	Lower birefringence than other rhombohedral carbonates; twin lamellae more common; lamellae parallel to edge or the long diagonal of the cleavage rhomb	Dominant mineral of limestones, especially in rocks older than the Tertiary
Magnesite	Rhombohedral (trigonal)	MgCO ₃	Fe ²⁺ for Mg; complete solid-solution series with siderite; minor Mn and Ca for Mg	Uniaxial (-)	Lacks twin lamellae; marked change in relief with rotation; Fe varieties yellow or brown	Uncommon in sedimentary rocks, but occurs in some evaporite deposits
Rhodochrosite	Rhombohedral (trigonal)	MnCO ₃	Fe ²⁺ for Mn; complete solid-solution series with siderite; also, Ca for Mn	Uniaxial (-)	Pink color (if present); association with other Mn-bearing minerals	Uncommon in sedimentary rocks; may occur in Mn-rich sediments associated with siderite and Fe-silicates
Siderite	Rhombohedral (trigonal)	FeCO ₃	Complete solid-solution series between siderite and magnesite and siderite and rhodochrosite	Uniaxial (-)	Yellow-brown or brown color; higher indices than other rhombohedral carbonates	Occurs as cements and concretions in shales and sandstones; common in ironstone deposits; also in carbonate rocks altered by Fe-bearing solutions
Smithsonite	Rhombohedral (trigonal)	ZnCO ₃	Fe ²⁺ and Mn for Zn; minor Ca, Mg, Cd, Cu, Co, Pb for Zn	Uniaxial (-)	Dirty, yellow-brown color	Uncommon in sedimentary rocks; occurs in association with Zn ores in limestones

Table 9.1 (cont.)

Mineral	Crystal system	Formula	Substitutions	Indicatrix	Distinguishing characteristics	Remarks
<i>Dolomite group</i>						
Dolomite	Rhombohedral (trigonal)	$\text{CaMg}(\text{CO}_3)_2$	Fe^{2+} for Mg; forms solid-solution series with ankerite; minor Mn for Mg	Uniaxial (-)	Commonly forms euhedral rhombs; may be stained with Fe-oxides; higher indices than calcite; twin lamellae may be parallel to both long and short diagonals of rhomb	Dominant mineral of dolomites; commonly associated with calcite or evaporite minerals
Ankerite	Rhombohedral (trigonal)	$\text{Ca}(\text{Mg,Fe,Mn})(\text{CO}_3)_2$	Limited solid-solution series with dolomite; also Mn for Mg or Fe^{2+}	Uniaxial (-)	Like dolomite; distinguished from magnesite by presence of twin lamellae	Much less common than dolomite; occurs in Fe-rich sediments as disseminated grains or concretions
<i>Aragonite group</i>						
Aragonite	Orthorhombic	CaCO_3	Small amounts of Sr or Pb for Ca	Biaxial (-) $2V = 18^\circ$	Distinguished from calcite by lack of rhombohedral cleavage, biaxial character, and slightly higher indices	Common mineral in recent carbonate sediments; alters readily to calcite
Cerussite	Orthorhombic	PbCO_3		Biaxial (-) $2V = 9^\circ$	White color; adamantine luster	Occurs in supergene lead ores
Strontianite	Orthorhombic	SrCO_3	Ca, Ba for Sr	Biaxial (-) $2V = 7-10^\circ$	Higher $2V$ than aragonite	Occurs in veins in some limestones
Witherite	Orthorhombic	BaCO_3	Minor Ca, Sr, Mg for Ba	Biaxial (-) $2V = 16^\circ$	Optically similar to aragonite	Occurs in veins associated with galena ore

Note: Common features of most carbonate minerals: high birefringence, change of relief with rotation, colorless in thin section.
Source: Data from multiple sources.

cation) as nearest neighbors. In dolomite minerals, the cation layers alternate; that is, layers of Ca^{2+} ions alternate with layers of Mg^{2+} (or Fe^{2+}) ions. Orthorhombic carbonates have a ninefold coordination (three cations for each oxygen). In aragonite-group carbonates, the CO_3^{2-} groups do not lie midway between Ca (or Pb, Sr, Ba) layers. Further, they are rotated 30 degrees to right or left so that each oxygen atom has three neighboring Ca (or other cation) atoms. For further details on the structure of the carbonate minerals see Reeder (1983), Speer (1983), and Tucker and Wright (1990, p. 284).

Cations with smaller ionic radii (Mg^{2+} , Zn^{2+} , Fe^{2+} , Mn^{2+}) tend to favor sixfold coordination, whereas those with larger ionic radii (Sr^{2+} , Pb^{2+} , Ba^{2+}) favor ninefold coordination. The radius of the calcium ion is intermediate in size between these smaller and larger ions; therefore, Ca^{2+} can enter into a sixfold coordination to form rhombohedral CaCO_3 (calcite) or into a ninefold coordination to form orthorhombic CaCO_3 (aragonite). Aragonite is the less-stable polymorph and transforms in time to calcite. More details of aragonite to calcite transformation are given in Chapter 11.

Among the carbonate minerals listed in Table 9.1, only calcite, dolomite, and aragonite are volumetrically important minerals in limestones and dolomites. Furthermore, aragonite is important only in Cenozoic-age carbonate rocks and modern carbonate sediments. Siderite and ankerite are common as cements and concretions in some sedimentary rocks but rarely form important parts of carbonate units. The other carbonate minerals in Table 9.1 occur so rarely in carbonate rocks that they receive little further mention in this chapter.

9.2.2 Ion substitution in carbonate minerals

Because the common cations in carbonate minerals have the same charge and similar ionic radii, substitution of cations is common. Solid-solution series exist between many of the end-member series (Table 9.1). Substitution of Mg^{2+} (ionic radius 0.072 nm) for Ca^{2+} (ionic radius 0.100 nm) is particularly common. On the other hand, the larger Ca^{2+} ion does not readily substitute for Mg^{2+} . In the calcite structure, disordered cation substitution of Mg^{2+} for Ca^{2+} can occur, up to several mole percent MgCO_3 . Calcite containing more than about 4 mol% MgCO_3 (5 mol% according to some authors) is commonly called **magnesian calcite** or **high-magnesian calcite** (Mg-calcite). Some magnesian calcites may contain as much as 30 mol% MgCO_3 (Veizer, 1983). Calcite with less than about 4 mol% MgCO_3 is called **low-magnesian calcite** or simply **calcite**. Less commonly, Fe^{2+} can substitute for Ca^{2+} or Mg^{2+} in calcite to form **ferroan calcite**, and minor amounts of Mn^{2+} can also substitute for Ca^{2+} . High-magnesian calcite is metastable with respect to calcite and may lose its Mg in time and alter to calcite. Alternatively, if exposed to magnesium-rich pore waters, high-magnesian calcite can gain additional Mg and be replaced by dolomite.

Magnesium does not commonly replace calcium in aragonite, although the aragonitic skeletons of some organisms incorporate Mg during growth. Small amounts of Sr or Pb may substitute for Ca in aragonite. In dolomite, ferrous iron (ionic radius 0.078 nm) may substitute for Mg in a limited solid-solution series with up to 70 mol% $\text{CaFe}(\text{CO}_3)$, although the compound $\text{CaFe}(\text{CO}_3)$ does not occur naturally (Scoffin, 1987, p. 5). The more iron-rich

phase of dolomite is called ankerite and the less iron-rich ferroan dolomite. The iron in dolomites may give the mineral a brownish color in outcrops and hand specimens. Small amounts of Mn can also replace Mg in dolomite.

9.2.3 Identification of carbonate minerals

Because calcite, aragonite, and dolomite are the dominant minerals in carbonate rocks, it is important to identify these minerals in petrologic study. Some distinguishing features of the carbonate minerals are listed in [Table 9.1](#). Nonetheless, it is often difficult to distinguish among these minerals in hand specimens and thin sections. Identification can be greatly aided by staining and etching techniques. For example, aragonite is stained black with Fiegl's solution ($\text{Ag}_2\text{SO}_4 + \text{MnSO}_4$), whereas calcite remains unstained. Calcite is stained red in a solution of Alizarin red S and dilute HCl, whereas dolomite remains unstained. Dolomite and high-magnesian calcite can be stained yellow in an alkaline solution of Titan yellow. Also, dolomite can be distinguished from calcite by etching. For details of these methods, see Miller (1988). The carbonate minerals can be differentiated also by X-ray diffraction methods.

9.2.4 Mineralogy of carbonate-secreting organisms

The skeletal remains of calcium carbonate-secreting organisms are volumetrically important components of many limestones. These skeletal remains may consist of aragonite, calcite, or high-magnesian calcite containing as much as 30 mole percent MgCO_3 . For example, most molluscs are composed of aragonite, although some (e.g. some gastropods) are composed of low-magnesian calcite. Echinoderms are composed of high-magnesian calcite, and foraminifers are composed of low- or high-magnesian calcite. Some groups of organisms may build skeleton of both aragonite and calcite. A few organisms, e.g. diatoms and radiolarians, secrete skeletons composed of silica. See Flügel (2004, p. 103) for further details about the dominant mineralogy of the major groups of carbonate-secreting organisms.

Note that the mineral composition of calcareous organisms may change with burial diagenesis. Aragonite in skeletal grains transforms to calcite with time and, as indicated, high-magnesian calcite may either lose Mg and alter to low-magnesian calcite or gain Mg to form dolomite.

9.2.5 Noncarbonate components

Carbonate rocks commonly contain various amounts of noncarbonate minerals, but generally less than about 5 percent. Noncarbonate minerals may include common silicate minerals such as quartz, chalcedony or microquartz, feldspars, micas, clay minerals, and heavy minerals. Clay minerals are particularly abundant constituents of some carbonates. Other minerals reported in carbonate rocks include fluorite, celestite, zeolites, iron oxides, barite, gypsum, anhydrite, and pyrite. Most noncarbonate minerals in limestones and dolomites are probably of detrital origin; however, some minerals such as chalcedony, pyrite, iron oxides, and anhydrite may form

during carbonate diagenesis. To facilitate study, noncarbonate minerals are commonly separated from carbonate constituents by acid treatment. Thus, they are usually referred to as **insoluble residues**; however, not all noncarbonate constituents are insoluble in acids.

Carbonate rocks may also contain fine-size plant or animal organic matter. The mean organic content of carbonate rocks is only about 0.2 percent (Hunt, 1979, p. 265); however, carbonate sediments deposited under some conditions contain significantly higher amounts of organic material.

9.3 Chemical and isotope composition

9.3.1 Elemental composition

Limestones contain one major cation, Ca^{2+} , and one minor cation, Mg^{2+} . Numerous other cations may be present in limestones in trace amounts. The most abundant of these trace cations are silicon, aluminum, iron, potassium, manganese, strontium, sodium, phosphorus, titanium, and boron. The major anion in carbonate rocks is CO_3^{2-} , but significant amounts of SO_4^{2-} , OH^- , F^- , and Cl^- may also be present.

The major-element composition of carbonate rocks is a function of the kinds and amounts of carbonate minerals (Table 9.1), fossils (see Scholle and Ulmer-Scholle, 2003), and noncarbonate constituents present in the rocks. Major elements occur in all carbonate minerals and fossils. On the other hand, trace elements such as B, P, Mg, Ni, Cu, Fe, Zn, Mn, V, Na, U, Sr, Pb, K, and Ba are particularly concentrated in skeletal material. Cations with large ionic radii, such as strontium and, to a lesser extent, barium, lead, and uranium, commonly show higher concentrations in aragonite than in calcite. Elements with small ionic radii, such as magnesium, manganese, iron, nickel, and phosphorus tend to be concentrated in calcite (Milliman, 1974, p. 142). Magnesium appears to interfere with precipitation of aragonite; therefore, the magnesium content of most aragonites is reported to be less than about 0.5 percent. As discussed in Section 9.2, the magnesium content of calcite may be low ($< \sim 4$ mol% MgCO_3) or high (up to 30 or more mol% MgCO_3). For further details on the factors that affect incorporation of trace elements into carbonate materials see Veizer (1983) and Morse and Mackenzie (1990). Many trace elements, such as Si, Al, Na, K, Ti, Mn, Fe, and Ba, probably owe their presence in carbonate rocks mainly to the content of noncarbonate constituents in these rocks.

9.3.2 Stable-isotope composition

General principles

The most important stable isotopes in carbonate rocks are isotopes of oxygen and carbon. The relative abundance of these isotopes is shown in Table 9.2. Note that oxygen has three stable isotopes; however, ^{18}O and ^{16}O are most abundant and are the principal oxygen isotopes used in isotope studies. Carbon has only two stable isotopes, ^{13}C and ^{12}C , but it has an additional radioactive isotope (^{14}C). The isotope composition of geologic materials is commonly expressed as ratios of the isotopes rather than actual abundances of the isotopes. The isotope

Table 9.2 *Relative abundances of natural stable isotopes of oxygen and carbon*

Element	Atomic number	Isotope	Relative isotopic abundances (percent)
O	8	16	99.757
		17	0.038
		18	0.205
C	6	12	98.93
		13	1.07

Source: *CRC Handbook of Chemistry and Physics*, 87th edn. (2006–2007).

ratio of a sample is compared to that in an arbitrary standard, and the isotope composition of the sample is expressed as per mil (parts per thousand) deviation from that of the standard. Thus, the oxygen isotope composition of carbonates is given as the ratio of $^{18}\text{O}/^{16}\text{O}$ in a carbonate sample compared to that of the standard, and is expressed as

$$\delta^{18}\text{O} = \frac{[(^{18}\text{O}/^{16}\text{O})_{\text{sample}} - (^{18}\text{O}/^{16}\text{O})_{\text{standard}}]}{(^{18}\text{O}/^{16}\text{O})_{\text{standard}}} \times 1000 \quad (9.1)$$

The carbon isotope composition of carbonates is expressed as the ratio of $^{12}\text{C}/^{13}\text{C}$ with reference to a standard in the same manner that oxygen isotopes are expressed.

The standard for both oxygen and carbon isotopes was originally the University of Chicago PDB Standard, which is the isotope composition of a fossil belemnite from the Cretaceous Pee Dee Formation of South Carolina. The supply of this standard is now exhausted; however, substitute standards have been prepared (PDB II and PDB III), as reported by Sharp (2007, p. 24). Even though the supply of the original sample of PDB is exhausted, PDB remains the standard for reporting all carbon isotopes and most oxygen isotopes.

Oxygen isotope abundances are also reported relative to a sample of ocean water called SMOW (Standard Mean Ocean Water). This standard is also referred to as V-SMOW, where V stands for Vienna, the location of the ocean-water sample. See Sharp (2007, pp. 24–25) for discussion of problems involved with reference standards.

Oxygen isotopes

The oxygen isotope composition of carbonate minerals is a function primarily of the isotope composition and temperature of the water in which the minerals are precipitated. Additional oxygen isotope fractionation is dependent upon the mineralogical form of CaCO_3 minerals, their Mg content, and upon biological processes – called the vital effect.

The $\delta^{18}\text{O}$ isotope composition of meteoric waters can range widely from about +5 to –30‰ (Faure and Mensing, 2005, p. 700). These variations are controlled mainly by

evaporation–condensation processes related to geographic latitude and altitude. Because most carbonates are precipitated in warm regions, calcites precipitated in equilibrium with meteoric waters typically have $\delta^{18}\text{O}$ values of about -4‰ (Anderson and Arthur, 1983). The average $\delta^{18}\text{O}$ composition of seawater is approximately 0‰ ; however, $\delta^{18}\text{O}$ values in surface ocean waters may range from about -1‰ to $+1\text{‰}$ depending upon salinity. Values of $\delta^{18}\text{O}$ display an almost linear increase with increasing salinity.

When water evaporates at the surface of the ocean, the lighter ^{16}O isotopes are preferentially removed in the water vapor, leaving the heavier ^{18}O in the ocean. This isotopic fractionation process thus causes water vapor to be depleted in ^{18}O with respect to the seawater from which it evaporates. When ^{18}O -depleted moisture falls in polar regions, it is locked up as ice on land and is prevented from returning quickly to the ocean. Because of this retention of light-oxygen water in the ice caps, the ocean becomes progressively enriched in ^{18}O as ^{18}O -depleted ice caps build up during a glacial stage. Thus, marine carbonates that precipitate in the ocean during a glacial stage, particularly biogenic carbonates such as foraminifers, will be enriched in ^{18}O relative to those that precipitate during times when the climate is warmer and ice caps on land are absent or smaller. Melting of ice caps, with consequent return of light-oxygen water to the ocean is reflected by a decrease in $\delta^{18}\text{O}$ values in marine biogenic carbonates. Savin and Yeh (1981) suggest that complete melting of global ice caps could produce depletion in the average $\delta^{18}\text{O}$ of the whole ocean by -0.8 to -1.3‰ relative to that of the present ocean.

The equilibrium fractionation of oxygen isotopes is strongly affected by temperature. The relationship between ocean temperature and oxygen isotope composition was determined by Epstein *et al.* (1953) to be

$$T(^{\circ}\text{C}) = 16.9 - 4.2(\delta_{\text{c}} - \delta_{\text{w}}) + 0.13(\delta_{\text{c}} - \delta_{\text{w}})^2 \quad (9.2)$$

where δ_{c} = equilibrium oxygen isotope composition of calcite and δ_{w} = oxygen isotope composition of the water from which the calcite was precipitated. This equation has become the classic temperature equation (Sharp, 2007, p. 126). [Note: A more recent version of the equation relating isotopic fractionation to temperature, in which temperature is expressed in kelvins, is given by Kim and O'Neil (1997)]. A graphical plot of Epstein *et al.*'s equation is shown in Fig. 9.1. Owing to the relationship depicted in this figure, the oxygen isotope composition of carbonates can be used as a tool to determine ocean paleotemperatures, provided that the salinity of the water can also be determined. If the paleosalinity can be determined by some independent method, a correction for the departure of $\delta^{18}\text{O}$ from values of normal marine waters can be made (Railsback *et al.*, 1989). Note that $\delta^{18}\text{O}$ values decrease as temperature increases.

Organisms that secrete calcium carbonate can cause additional fractionation of oxygen isotopes, the so-called **vital effect** (see Faure and Mensing, 2005, p. 707). These effects can bring about either positive or negative deviations from inorganic equilibrium, and must be considered when evaluating the isotopic composition of carbonate shells.

Veizer *et al.* (1999) demonstrate that $\delta^{18}\text{O}$ in the ocean shows a general increase in $\delta^{18}\text{O}$ values from about -8‰ to 0‰ PDB from Cambrian time to the present. Second-order oscillations of ~ 150 million years duration, which are related to cold intervals, are superimposed on this general trend (Fig. 9.2). Veizer *et al.* suggest that this long-term trend of

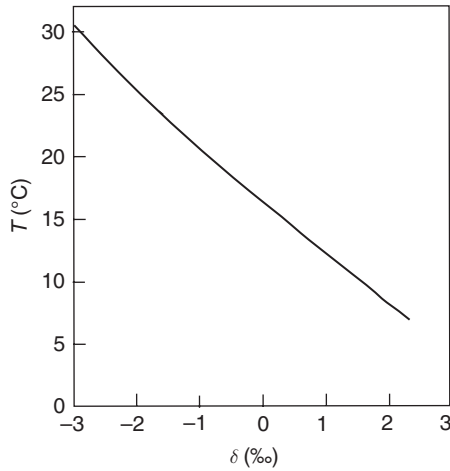


Figure 9.1 Oxygen isotope temperature scale, plotted from Epstein *et al.*'s data for determining the fractionation factor for carbonate-water. The x-axis ($\delta\text{‰}$) refers to the $(\delta_c - \delta_w)$ for Equation 9.2; Temp. ($^{\circ}\text{C}$) is the measured water temperature. (After Epstein, S. *et al.*, 1953, Revised carbonate-water isotopic temperature scale: *Geol. Soc. Am. Bull.*, **64**, Fig. 9, p. 1324, reproduced by permission.)

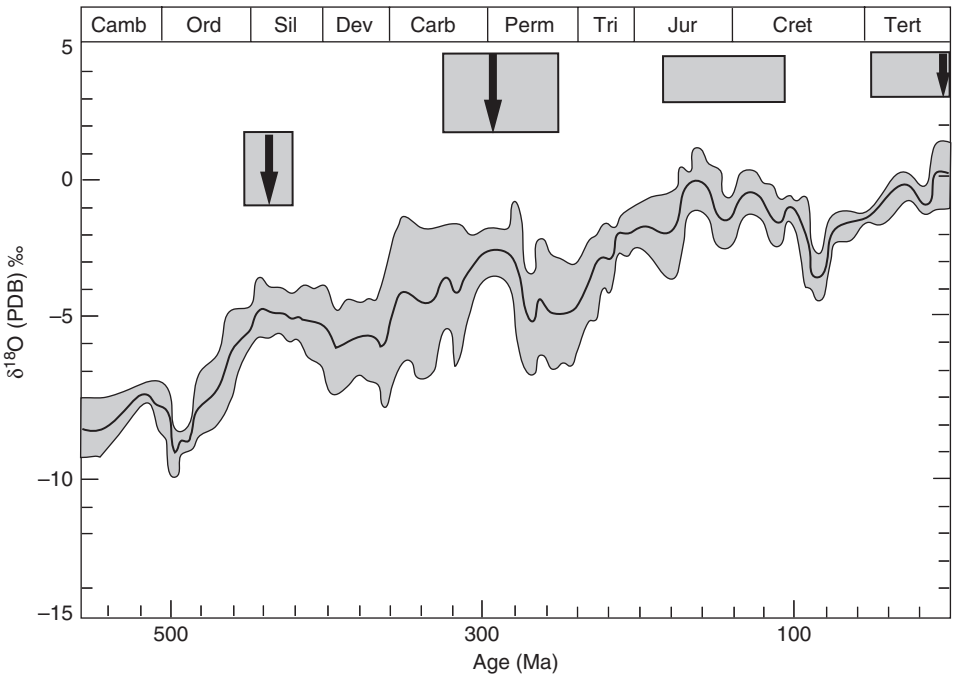


Figure 9.2 Variations in oxygen isotope ratios in low-magnesian carbonate (fossil) shells during Phanerozoic time. One standard deviation (1σ) uncertainties are shown as the shaded region around the heavy central line. Cold periods are indicated by the shaded boxes above the curve; times of glaciation are shown by heavy arrows. Note that cold periods correspond to higher $\delta^{18}\text{O}$ values. (After Veizer, J. *et al.*, 1999, $^{87}\text{Sr}/^{86}\text{Sr}$, $\delta^{13}\text{C}$ and $\delta^{18}\text{O}$ evolution of Phanerozoic seawater: *Chem. Geol.*, **161**, Fig. 13, p. 75, reproduced by permission of Elsevier Science.)

increasing $\delta^{18}\text{O}$ with time is a function of both tectonic factors and biologically mediated redox balance of carbon and sulfur cycles.

Carbon isotopes

The carbon isotope composition of carbonate sediments is influenced primarily by the isotope composition of the water from which carbonate minerals precipitate and to a lesser extent by temperature and biogenic fractionation. The $\delta^{13}\text{C}$ values in carbonates reflect the $^{13}\text{C}/^{12}\text{C}$ ratio of CO_2 dissolved in water. This ratio, in turn, is a reflection of the source of carbon in the CO_2 . The $\delta^{13}\text{C}$ of total dissolved carbon (TDC) in meteoric waters may range from highly negative values to positive values (Veizer, 1983), although negative values are most characteristic.

Values of $\delta^{13}\text{C}$ in the total dissolved carbon of ocean water are commonly higher than those in meteoric waters, with average values of approximately +1‰. Surficial ocean waters are generally isotopically heavier than this average and deep waters are lighter (Kroopnick, 1980). The $\delta^{13}\text{C}$ of ocean water is affected by runoff of isotopically light water from the continents, but the change toward lighter carbon with depth probably reflects the residence time of deep-water masses in the ocean. Carbon-13 is depleted in deep-water masses that have long residence times near the ocean bottom, owing to oxidation of low- $\delta^{13}\text{C}$ marine organic matter that sinks from the surface. Oxidation of this low- $\delta^{13}\text{C}$ organic matter leads to production of low- $\delta^{13}\text{C}$ dissolved bicarbonate (HCO_3^-), which is then used by organisms to build shells. Respiration by bottom-dwelling organisms may also cause a decrease in $\delta^{13}\text{C}$ of deep-bottom waters. The $\delta^{13}\text{C}$ values of ocean waters may vary latitudinally as well as with depth. Surface waters in regions of upwelling in the zone of equatorial divergence tend to have lighter values and midlatitude areas have heavier values, which reflect variations in organic productivity, rates of upwelling and down sinking of waters, CO_2 invasion and evasion, and temperature (Veizer, 1983).

The carbon isotope composition of carbonates is affected also by temperature in a manner similar to that in which oxygen isotopes are affected. The temperature fractionation effect is not nearly so strong, however, and carbon isotopes are not commonly used in paleotemperature studies. Thus, because fractionation during carbonate precipitation is relatively insensitive to temperature, $\delta^{13}\text{C}$ values of ancient marine carbonates reflect the $\delta^{13}\text{C}$ value of dissolved *inorganic* carbon in the past. On the other hand, *biogenic* fractionation can cause large deviations in $\delta^{13}\text{C}$ values from inorganic equilibrium values, commonly resulting in much lower (more negative) values than equilibrium values. See Sharp (2007, p. 162) for extended discussion of the vital effect on dissolved carbon.

9.3.3 Stable-isotope composition of carbonate sediments and fossils

Owing to the various factors that influence the oxygen and carbon isotope composition of skeletal and inorganic carbonates, wide variations in the isotopic composition of natural carbonates occur. For example, freshwater carbonates tend to have negative $\delta^{13}\text{C}$ and $\delta^{18}\text{O}$ values whereas marine carbonates tend to have positive values. The

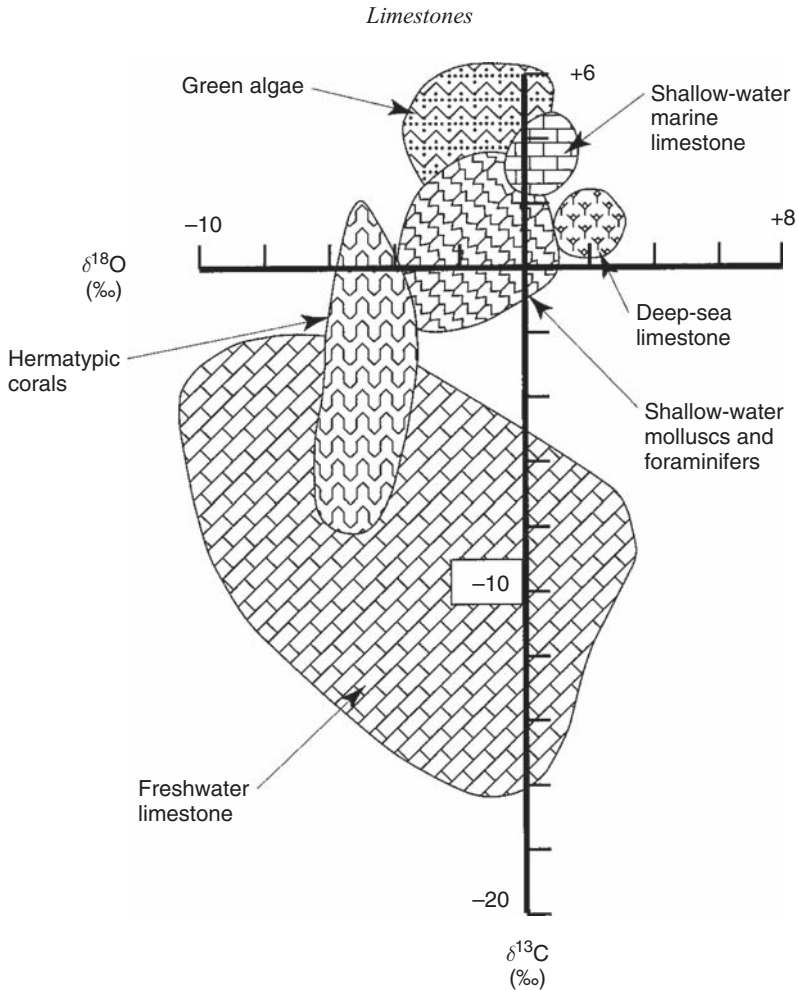


Figure 9.3 Distribution of $\delta^{18}\text{O}$ and $\delta^{13}\text{C}$ values in various types of marine carbonates. (After Milliman, J.D., 1974, *Marine Carbonates*: Springer-Verlag, Berlin Fig. 19, p. 33, reprinted by permission.)

distribution of $\delta^{13}\text{C}$ and $\delta^{18}\text{O}$ values in various kinds of Quaternary carbonates is summarized in Figure 9.3.

As is the case with oxygen isotopes (shown in Fig. 9.2), carbon isotope values of marine carbonates vary as a function of time (Fig. 9.4). The $\delta^{13}\text{C}$ curve for Phanerozoic time shows a general increase from about $-1 \pm 1\text{‰}$ to $+4 \pm 2\text{‰}$ PDB during the Paleozoic, an abrupt drop of 2‰ at the Permian/Triassic transition, and oscillations around $+2\text{‰}$ in the course of the Mesozoic and Cenozoic. Higher-order oscillations are superimposed on this general trend. Veizer *et al.* (1999) indicate that these changes reflect changes in the carbon isotopic composition of the oceans with time and not diagenesis. They suggest that the changes indicate a unified exogenic (litho-, hydro-, atmo-, biosphere) system driven by tectonics via its control of (bio)geochemical cycles.

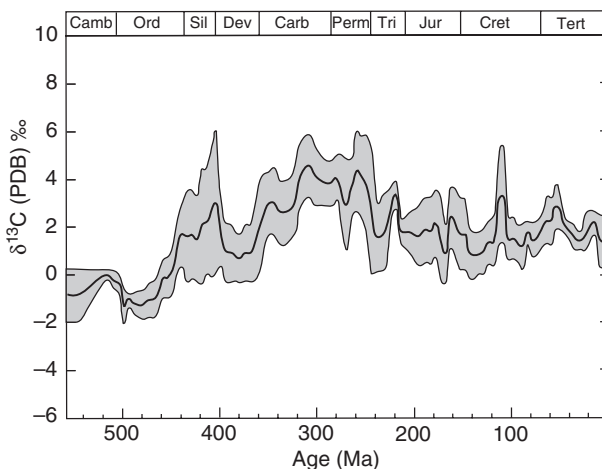


Figure 9.4 Variations of $\delta^{13}\text{C}$ values in marine carbonates, based on analysis of low-magnesian carbonate shells. One standard deviation (1σ) uncertainties are shown as the shaded region around the heavy central line. (After Veizer *et al.*, 1999, $^{87}\text{Sr}/^{86}\text{Sr}$, $\delta^{13}\text{C}$ and $\delta^{18}\text{O}$ evolution of Phanerozoic seawater: *Chem. Geol.*, (161, Fig. 10, p. 72, reproduced by permission of Elsevier Science.)

9.3.4 Radiogenic isotopes in carbonate rocks

In addition to the stable isotopes of oxygen and carbon, carbonates may contain several radiogenic isotopes, including carbon-14, thorium-230, protactinium-231, and strontium-87. Carbon-14, thorium-230, and protactinium-231 isotopes, in particular, have proven to be useful for direct determination of the ages of young carbonate sediments. For a brief discussion of the usefulness and limitations of these dating techniques see Boggs (2006, ch. 15).

9.4 Major components of limestones

9.4.1 General statement

As discussed in Chapters 4 and 5, sandstones consist dominantly of various kinds of sand- and silt-size silicate grains with various amounts of fine, siliciclastic mud matrix and secondary cements, including carbonate cements. The mineralogy of carbonate rocks is almost totally different from that of sandstones, but many limestones resemble sandstones texturally in that they consist of various kinds of sand- and silt-size carbonate grains and various amounts of fine lime mud matrix and carbonate cements. (Note: some limestones are texturally similar to siliciclastic mudstones; they are composed dominantly or entirely of lime mud and contain few or no silt- or sand-size carbonate grains.)

Although limestones commonly contain only one or two dominant minerals, in contrast to sandstones, several distinct kinds of carbonate grains are recognized. Most of these grains are not single crystals but are composite grains made up of large numbers of small calcite or aragonite crystals. Folk (1962) proposed the term **allochem** to cover all of these organized









PELOIDS			Small micritic grains, commonly without internal structure. Subrounded, spherical, ovoid or irregular in shape. Size between <math><0.02</math> and about 1 mm, commonly 0.10 to 0.50 mm.
COATED GRAINS	CORTOIDS		Rounded skeletal grains and other grains covered by a thin micrite envelope. Boundary between the central grain and the envelope indistinct. Size between <math><1</math> mm to a few centimeters.
	ONCOIDS		Large and small grains consisting of a more or less distinct nucleus (e.g. a fossil) and a thick cortex formed by irregular, non-concentric, partially overlapping micritic laminae. Laminae may exhibit biogenic structures. No tendency to increase sphericity during growth. Size from <math><1</math> mm to a few decimeters.
	OIDS		Spherical or ovoid grains, consisting of smooth and regular laminae formed as successive concentric coatings around a nucleus. Laminae may exhibit tangential and radial microfabrics. Size between 0.20 and about 2 mm, commonly between 0.5 and 1 mm.
	PISOIDS		Large subspherical and irregularly shaped grains, consisting of a mostly non-biogenic nucleus and a thick cortex formed by conspicuously, often densely spaced laminae exhibiting tangential and radial microfabrics. PISOIDS occur as isolated grains or are incorporated in crusts. Size generally >2 mm, up to >1 cm.
GRAIN AGGREGATES			Compound grains consisting of two or more originally separated particles (e.g. ooids, skeletal grains) that have been bound and cemented together, forming grape-like or rounded lumps. Intergrain spaces filled with micrite or spar. Outline irregular lobular or rounded. Size 0.5 to more than 2 mm.
CLASTS			Synsedimentary or postsedimentary lime clasts, reworked partly consolidated carbonate sediment or already lithified material. Shape and size are highly variable: angular to rounded. Size ranges between <math><0.2</math> mm and several decimeters. Very small clasts are hardly distinguishable from peloids.
SKELETAL GRAINS			Fragmented or complete skeletons of organisms. Size from 0.05 mm to many centimeters.

Figure 9.5 Descriptive terminology of the major kinds of carbonate grains. (After Flügel, E., 2004, *Microfacies of Carbonate Rocks*: Springer-Verlag, Berlin, Fig. 4.7, p. 100, reproduced by permission.)

carbonate aggregates that make up the bulk of many limestones. The principal kinds of carbonate grains are illustrated and briefly described in Fig. 9.5. They include both non-skeletal grains (e.g. lithoclasts, ooids) and skeletal grains (fossil and fossil fragments). Further description and discussion of carbonate grains are provided by Flügel (2004). Excellent color photographs of carbonate grains may be found in Adams and Mackenzie (1998) and Scholle and Ulmer-Scholle (2003).

9.4.2 Carbonate grains

Peloids

Peloids are spherical, ovoid, or rod-shaped, mainly silt-sized carbonate grains that commonly lack definite internal structure (Fig. 9.6). They are generally dark gray to black owing to contained organic material and may or may not have a thin, dark outer rim. The most common size of peloids ranges from about 0.05 to 0.20 mm, although some are much larger. Peloids are composed mainly of fine micrite 2 to 5 microns in size, but larger crystals may be present. They are commonly well sorted and they may occur in clusters.

Many peloids, especially those with well-rounded, symmetrical shapes, are thought to be of fecal origin. These peloids are commonly called **pellets**. Fecal pellets are produced

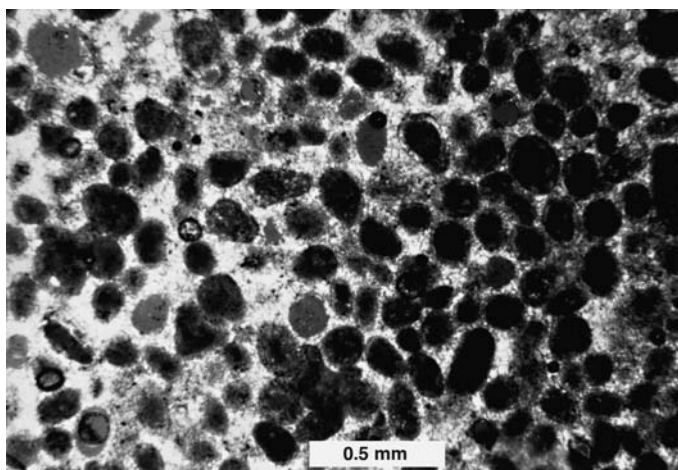


Figure 9.6 Peloids and a few small coated grains cemented by sparry calcite cement. Specimen source unknown. Crossed nicols.

by a variety of organisms that ingest fine carbonate mud while feeding on organic-rich sediments. The pellets are shaped in the guts of these organisms and then extruded. Fecal pellets are produced by organisms such as crustaceans, holothurians, brachiopods, amphineurans, pelecypods, gastropods, ostracods, copepods, decapods, echinoderms, tunicates, worms, and even fish. Each kind of organism tends to produce pellets of a distinctive shape and size. Although most fecal pellets are structureless, some may have a sieve-like internal structure formed by cylindrical holes parallel to the long dimension of the pellet. These holes may be filled with sparry cement, giving the pellets a speckled appearance in thin sections. Other pellets may have lamella-like or ring-like internal structures. Although most fecal pellets in ancient carbonate rocks are small, the pellets of some modern organisms may exceed 5 mm. Most pellets appear to be produced by organisms living in quiet, marine water with muddy bottoms. Thus, pellets in ancient limestones occur most commonly in muddy limestones (micrites), and their presence suggests deposition in low-energy environments.

Not all marine peloids are fecal pellets. Some are believed to form by carbonate encrustation around filaments of cyanobacteria, endolithic algae, or fragments of other algae. Indistinct algal structures may still be present in these algal peloids. Still others are suggested to form as a result of bacterial activity, by replacement by repeated nucleation (chemical precipitation) around centers of growth, by crystal growth on nuclei of clastic origin, and by spontaneous nucleation of microcrystalline calcite. Some peloids, referred to as **pseudopeloids**, may simply be small rounded intraclasts, formed by reworking of semi-consolidated carbonate mud or mud aggregates. Others may represent bioclasts or ooids that have been totally micritized by boring organisms or possibly by recrystallization. Compared to fecal pellets, these various nonfecal peloids tend to be characterized by poorer sorting, more-irregular shapes, and diverse sizes (0.02 mm to > 2 mm).

Coated grains: ooids, oncoids, and cortoids

Definition

Coated grain is a general term used for all carbonate grains composed of a **nucleus** surrounded by an enclosing layer or layers commonly called the **cortex** (see Peryt, 1983a, p. 3). Various kinds of coated grains are recognized, largely on the basis of the structure of the cortex. Coated grains are divided into four broad groups: ooids, oncoids, cortoids, and pisoids.

Ooids

Calcareous ooids are small, more or less spherical to oval carbonate particles, which are characterized by the presence of concentric laminae that coat a nucleus. The nucleus may be a skeletal fragment, peloid, smaller ooid, or even a siliciclastic grain such as a quartz grain. Most ooids are sand- to silt-size particles. They range in size from about 0.1 mm to more than 2 mm, with 0.5 mm to 1 mm being most common. Carbonate grains that are structurally similar to ooids but are larger than about 2 mm are called **pisoids** (to be discussed).

Ooids are white to cream in color and commonly have a pearly luster if formed in agitated water. Quiet-water ooids may have a dull luster. Ooids are distinguished especially by the presence of concentric, accretionary layers or laminae.

Ooids that consists of numerous laminae are regarded to be **mature** or **normal ooids** (Fig. 9.7). Those that have only a few laminae are called **superficial ooids** (Fig. 9.8), following the usage of Illing (1954). Carozzi (1960, p. 238) restricts the term superficial ooid to those ooids having only a single accretionary layer; however, most workers appear to prefer the definition of Illing. Richter (1983a) suggests that ooids are distinguished by the following general characteristics: (1) they are formed of a cortex and a nucleus of variable composition and size, (2) the cortex is smoothly laminated, (3) the laminae are either concentric or they are thinner on points of stronger curvature of the nucleus, and vice-versa, thus increasing the sphericity of the ooid during its growth, and (4) constructive biogenic structures are lacking.

With respect to structure of the cortex, carbonate workers distinguish three principal kinds of primary ooids (Fig 9.9): (1) ooids in which crystals are arranged tangentially within layers, (2) ooids with radially arranged crystals (Fig. 9.10), and (3) micritic or microsparitic ooids with randomly oriented crystals. In addition, secondary fabrics occur in some ooids. These diagenetic fabrics may include radial structures as well as oomoldic and *in situ* calcitized fabrics. See Flügel (2004, p. 148) for additional examples of unusual ooids. Ooids vary also in mineral composition. Most modern-Holocene marine ooids are composed of aragonite, although some are composed of Mg-calcite. Most modern nonmarine ooids are composed of calcite. Most ancient ooids are also composed of calcite, presumably owing to diagenetic alteration of aragonite or Mg-calcite.

Ooids form by accretionary processes whereby CaCO_3 is precipitated onto the surface of a nucleus in water saturated to supersaturated with calcium bicarbonate. Water agitation appears to be important to growth of ooids, particularly tangential ooids which commonly have highly spherical forms and polished surfaces. As discussed, however, some ooids can form under quiet-water conditions. Quiet-water ooids are more likely to have a radial

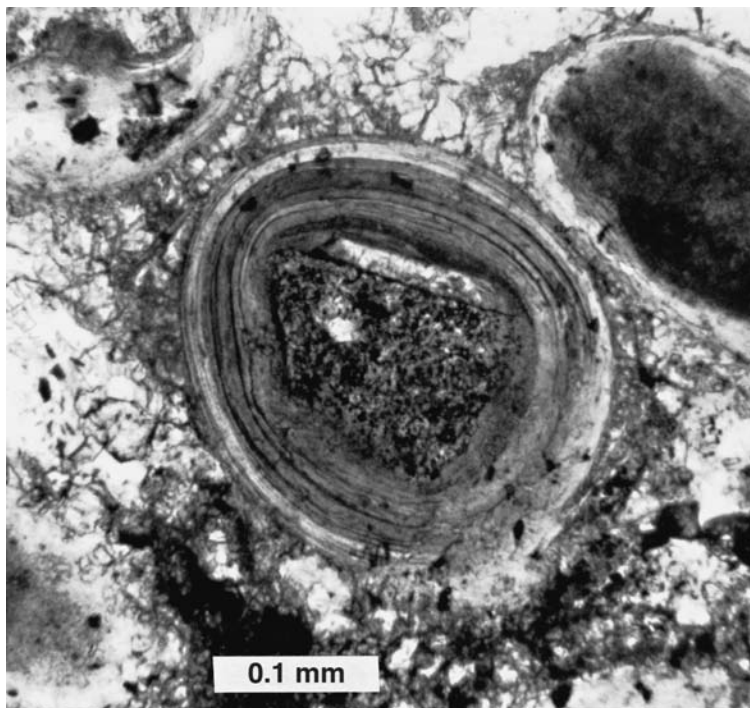


Figure 9.7 Ooid (center of photograph) made up of numerous thin, concentric layers surrounding an intraclast (nucleus). Tertiary limestone, Spain. Ordinary light photograph. (Specimen courtesy of P. D. Snavley.)

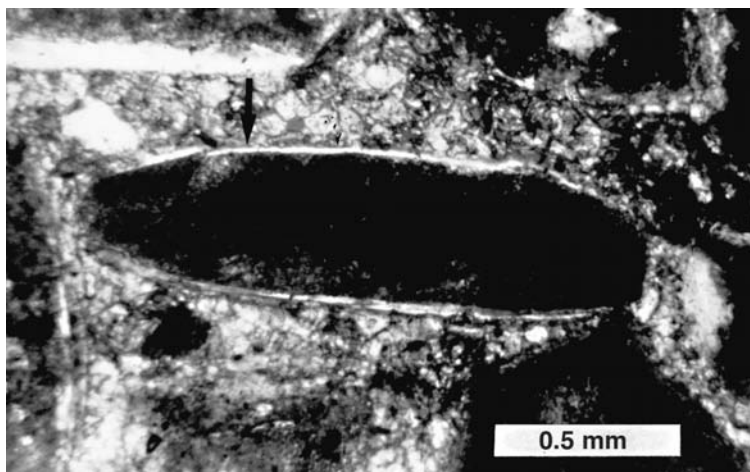


Figure 9.8 Superficial ooid (arrow) that displays a single thin layer or coat around a large micritic nucleus. Tertiary limestone, Spain. Crossed nicols. (Specimen courtesy of P. D. Snavley.)

Structural type	Primary ooids			Diagenetically altered ooids	
	Aragonite	Mg-calcite	Calcite	Calcite	
1 TANGENTIAL	Marine lacustrine/hypersaline thermal	?	Caliche	?	
2 RADIAL	Marine lacustrine/hypersaline	Marine	Cave pearls lacustrine fluvial	Mg-calcite	Calcite
3 RANDOM	Marine	?	Lacustrine caliche	Mg-calcite or Aragonite	Calcite Calcite
4 OOMOLDIC		Tangential structure	Nucleus	Aragonite	Dissolution Calcite cement
5 PSEUDOSPAR	Random structure	Radial structure		Aragonite	Calcite

Figure 9.9 Principal kinds of carbonate ooids. The inset (dashed rectangle) shows details of tangential, radial, and random structure of the cortex. [Modified from Richer, D. K., 1983a, *Calcareous ooids: a synopsis*, in Peryt, T. M. (ed.), *Coated Grains*: Springer-Verlag, Berlin, [Fig. 1, p. 75, reproduced by permission.]

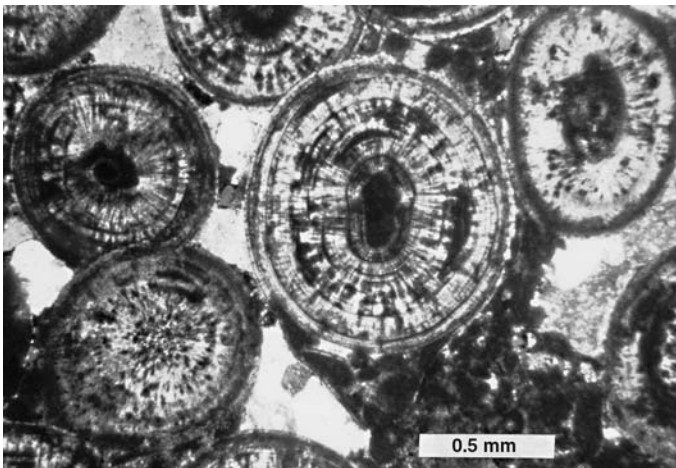


Figure 9.10 Radial ooids of marine origin. Devonian limestone, Canada. Crossed nicols.



Figure 9.11 Large oncooids exposed on a weathered limestone surface. Wasatch Formation (Eocene), Utah. (Photograph courtesy of H. P. Buchheim.)

structure, less-spherical form, and less-polished surfaces. Ooids occur most commonly on shallow carbonate platforms, but can be deposited in a wide variety of environments from fluvial to deep-marine, owing in some cases to retransport. Ooids may contain organic matter such as the remains of blue-green algae (cyanobacteria), fungi, and bacteria. Although there has been much speculation about the possible role of organisms in the formation of ooids, there is no conclusive evidence that organisms do in fact influence their formation. Ooids appears to form primarily by inorganic processes.

Oncoids

Coated grains more irregular in shape than ooids, and with more irregular laminae, are called oncooids (Fig. 9.11). Oncoids are also generally larger than ooids, commonly ranging from <2 mm to > 10 mm. They form in both nonmarine and marine environments. Many authors restrict the term oncooid to grains of cyanobacterial and bacterial origin (see Peryt, 1983a). Others (e.g. Richter, 1983b) include also as oncooids carbonate grains encrusted by red algae and bryozoans. Also, irregularly layered, coated grains without organic structures (such as spongiostromate oncooids) and nodules in vadose environments (so-called vadoids in pedo-rites) are considered by some workers to be oncooids. Most oncooids that form through the activities of encrusting organisms are a type of stromatolite, corresponding to Type SS (discrete spheroids) of Logan *et al.* (1964).

Oncoids have some kind of nucleus, which is surrounded by layers composed mainly of fine micrite but that may contain silt- or sand-size noncarbonate detrital grains. These layers form through the activities of organisms such as cyanobacteria that cause the formation of successive layers around the nucleus as the nucleus is shifted about in agitated water. The layers may be wavy or crinkly. Logan *et al.* recognize three subtypes of algal oncooids on the basis of layer structure and shape (Fig. 9.12):

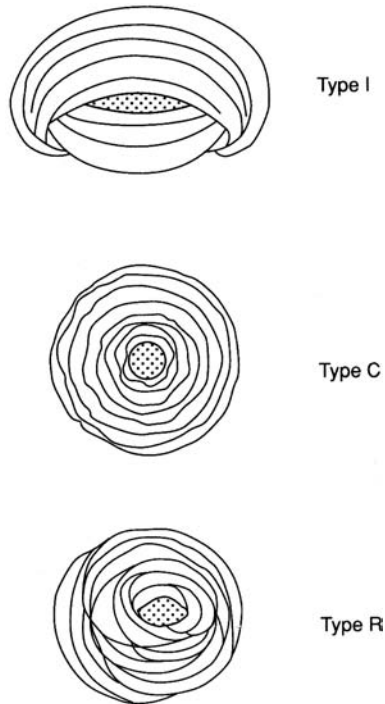


Figure 9.12 Principal types of algal oncooids. Type I: inverted, stacked; Type C: concentrically stacked; Type R: randomly stacked. The patterns indicate successive growth stages. (After Logan B. W., R. Rezak, and R. N. Ginsburg, 1964, Classification and environmental significance of algal stromatolites: *J. Geol.*, 72, Fig. 4, p. 76, reproduced by permission of University of Chicago Press.)

1. **Type I – inverted, stacked.** These oncooids form when growth of layers on one side of a nucleus is interrupted, and the oncoid is overturned. This step is followed by partial dissolution or erosion of the grain. A second oncoid then grows on top of the first.
2. **Type C – concentrically stacked.** Layers are arranged concentrically around the nucleus; thus, these grains may resemble pisoids. The shape of the oncoid is governed by the shape of the nucleus.
3. **Type R – randomly stacked.** Domed-shaped layers grow at different rates as the oncoid is occasionally moved by waves or currents, producing the random stacking.

Oncoids of different origin may have somewhat different shapes from those illustrated in Fig. 9.12. For additional information on oncooids see Flügel (2004, ch. 4) and the more than one dozen papers on this subject in Peryt (1983b).

Cortoids

Some coated grains consist of fossils, ooids, or peloids coated with a thin envelope of generally dark colored micrite (Fig. 9.13), commonly consisting of crystals 2 to 5 microns in size. Flügel (1982, p. 160) called these grains cortoids, after the word cortex (Latin for bark).

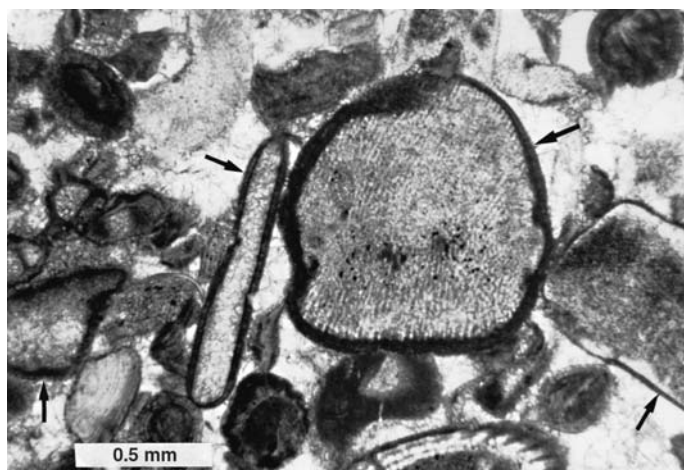


Figure 9.13 Micrite envelopes (arrows) developed around echinoderms and other fossil fragments. Renault Formation (Mississippian), Missouri. Crossed nicols.

The micrite envelopes may originate by several processes, which can include destructive micritization related to the activities of microboring organisms, constructive development of envelopes by epilithic organisms (organisms that live on or attached to rocks or other stony matter), and partial dissolution and recrystallization (Flügel, 2004, p. 120). Cortoids may resemble superficial ooids that have only a single layer around a nucleus; however, superficial ooids are characterized by a thin concentric layer that forms by accretionary processes rather than by micritization of the nucleus.

Pisoids

Pisoids are coated grains that resemble ooids; however, they differ in their internal structure, are generally less uniform in shape, and are commonly larger (several millimeters to centimeters). Most are nonmarine in origin. Those formed in the groundwater vadose zone are called **vadoids** (e.g. Fig. 9.14); those formed in caves are **cave pearls**. The characteristics and origins of pisoids are discussed in detail in Peryt (1983b, pp. 437–560) and Flügel (2004, ch. 4).

Lithoclasts

General statement

Carbonate lithoclasts are detrital fragments of carbonate rock produced by disintegration of pre-existing carbonate rock or sediment, either within or outside a depositional basin. They are also sometimes called **limeclasts**. Lithoclasts may range in size from very fine sand to pebbles or even boulders. They tend to be well rounded, but may also be subrounded, subangular, or angular. Very small lithoclasts may be confused with large peloids. Two kinds of lithoclasts are recognized on the basis of origin: intraclasts and extraclasts.

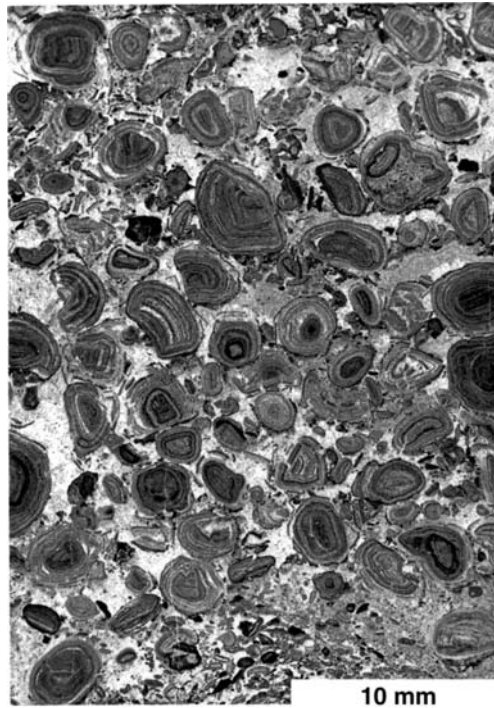


Figure 9.14 Nonmarine pisolites from the vadose zone (vadoids), Upper Triassic, Croatia. [From Peryt, T. M., 1983, Vadoids, in Peryt, T. M. (ed.), *Coated Grains*, Springer-Verlag, Berlin, Fig. 2, p. 441, reproduced by permission.]

Intraclasts

Some lithoclasts originate within a depositional basin by fragmentation of penecontemporaneous, commonly weakly cemented, carbonate sediment. Small pieces of this sediment are eroded from the seafloor and redeposited at or near the original area of deposition. Lithoclasts having this origin are called intraclasts. Folk (1962) suggests that intraclasts may range in origin from fragments reworked from the immediate seafloor perhaps a few days after deposition to fragments torn by deeper erosion of sediment buried perhaps a few meters below the surface, as long as the sediment is still unconsolidated. Figure 9.15 illustrates typical intraclasts.

Although most intraclasts are probably produced by physical disruption of penecontemporaneous sediment by normal waves, storm waves, or currents, some intraclasts may form by other mechanisms. These mechanisms could include organic activity on the surface of sediment, burrowing or boring activity within sediment, and local sliding of weakly consolidated sediment (Flügel, 1982, p. 164). Two mechanisms for producing intraclasts that are regarded to be particularly common are (1) erosion of lithified beachrock within the intertidal and supratidal zones, and (2) disruption of desiccated and cracked supratidal, partially lithified calcareous muds, to produce lime-mud clasts. Intraclasts produced by erosion of surface sediment almost immediately after it is deposited are plastic and easily

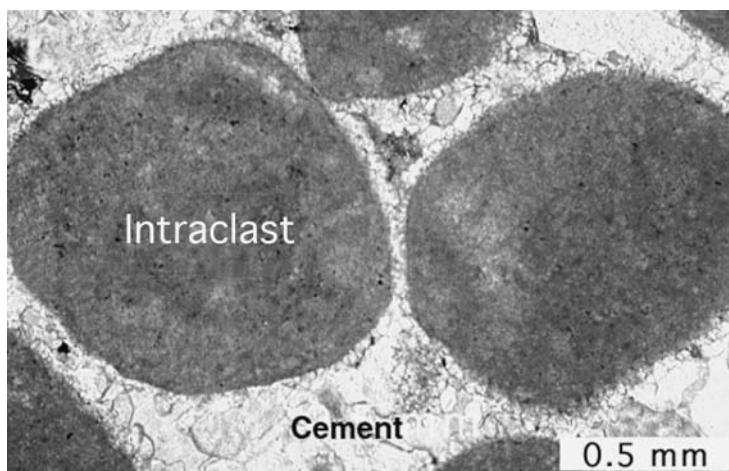


Figure 9.15 Well-rounded intraclasts (produced in a high-energy environment), cemented with sparry calcite cement. Devonian limestone, Canada.

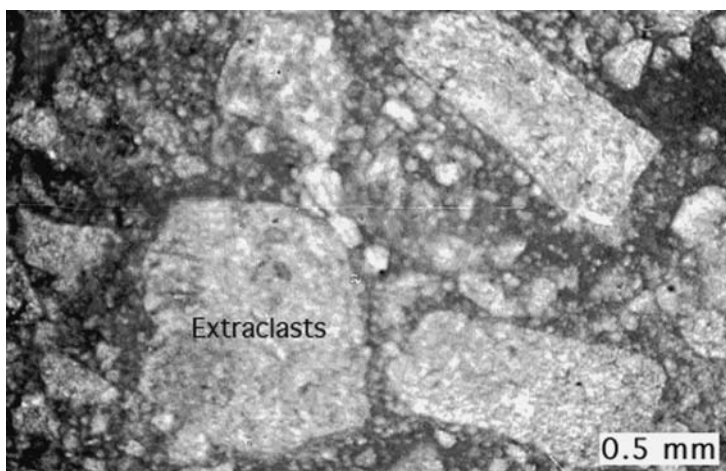


Figure 9.16 Angular to subrounded lithoclasts in a lime-mud (dark) matrix. Calville Limestone (Permian), Nevada.

deformed upon redeposition. Erosion of more deeply buried sediment produces better consolidated clasts that are more likely to preserve their shape when redeposited.

Extraclasts

Lithoclasts generated by erosion of much older, lithified carbonate rock exposed on land (outside the depositional basin in which the clasts accumulate) are called extraclasts. They are simply carbonate rock fragments (Fig. 9.16). Because intraclasts and extraclasts differ

Table 9.3 *Distinguishing characteristics of extraclasts*

Characteristic	Description
Fossil content	May contain reworked, stratigraphically older fossils
Weathering features	Clasts have iron-stained, oxidized boundaries or rims
Inherited veins	May contain recrystallized veins inherited from parent rock
Nature of clast boundaries	Fossils or other grains within the clast possibly truncated at the extraclast boundary
Roundness	Clasts either conspicuously rounded or conspicuously angular
Compaction effects	Extraclasts lack compaction features, whereas intraclasts may show evidence of postdepositional compaction
Diagenetic textures	Extraclasts containing cementation or recrystallization textures that differ from associated carbonate grains
Associated noncarbonate grains	Tend to be associated with detrital chert or sandstone fragments

From multiple sources.

fundamentally in origin, it is important in genetic studies to distinguish between the two. Intraclasts yield information about the depositional basin, such as the presence of bottom currents and the consolidation state of the sea bottom. Lithoclasts have little environmental significance but yield information about the source area (provenance). Table 9.3 lists some of the features of extraclasts that distinguish them from intraclasts. In spite of this list of criteria, it is often extremely difficult to distinguish between extraclasts and intraclasts. If the lithoclasts lack recognizable fossils (which is common) or if they show no evidence of weathering or lack recrystallized veins (which is also common), it may be impossible to differentiate unequivocally between lithoclasts. Nonetheless, it is important to try.

Aggregate grains and lumps

Aggregate grains are irregularly shaped carbonate grains that consist of two or more carbonate fragments joined together by a micritic (lime-mud) matrix. Aggregate grains were first described by Illing (1954) who called them lumps. Illing identified three major subtypes of lumps: (1) grapestones – aggregates resembling in shape a bunch of grapes, (2) botryoidal lumps – grapestones with superficial ooid coatings, and (3) encrusting lumps – lumps smoother than grapestones and with hollow interiors. Milliman (1974, p. 42) suggests that these three types of lumps form a continuum rather than representing discrete grain types, and he proposes use of the term **aggregate grain** to cover all of these types. Purdy (1963) previously suggested using the term **grapestone** to include all of Illings' lumps except botryoidal lumps, which he calls cryptocrystalline grains (lumps). Milliman (1974, p. 42) distinguished between aggregate grains and lumps on the basis of the micrite-matrix content of the grains. That is, micrite matrix makes up less than half of aggregate grains but more than half of lumps.

Aggregate grains and lumps are mud aggregates that form *in situ* by agglutination of adjacent carbonate grains such as peloids, ooids, and skeletal fragments. Physical, chemical,

and biologic processes all appear to have a role in the agglutination process. Winland and Matthews (1974) propose that initial binding is accomplished by algae and encrusting foraminifers. Later, cementation and infilling of the aggregates occurs owing to continued growth of these organisms within the aggregates and to filling of internal voids by chemical or biochemical precipitation of cement. Tucker and Wright (1990, p. 12) suggest that lumps evolve from grapestones by continued cementation and micritization of grains (Fig. 9.17). (The term chasmoliths used in Fig. 9.17 refers to microorganisms that live in holes not of their own creation. Endoliths are organisms that bore into grains and micritize them.)

Where the organism that encrusts aggregate grains is recognizable, such as coralline algae or encrusting foraminifers, Milliman (1974, p. 44) suggests that the aggregate grains be classified as skeletal. Winland and Matthews (1974) suggest that aggregate grains form under conditions where there is a supply of firm carbonate grains, uneven water turbulence, high water circulation rates, and very low sedimentation rates. Some aggregate grains may closely resemble intraclasts. In fact, some workers regard these grains as a type of intraclast. Aggregate grains are particularly common in the modern ocean in the Bahama area. They have also been reported from shallow, brackish water of tidal zones and some sea-marginal hypersaline pools. Aggregate grains are not particularly common in ancient limestones, probably because of the limiting environmental conditions under which they form. Also, unless the aggregates undergo very early cementation, their shapes and textures may be obliterated by compaction during burial.

Skeletal grains (bioclasts)

Skeletal grains are among the most abundant and important kinds of grains that occur in limestones of Phanerozoic age. Skeletal grains may consist of whole fossil organisms, angular fragments of fossils, or fragments rounded to various degrees by abrasion. Skeletal grains may occur with other kinds of carbonate grains or they may constitute the only kind of carbonate grains in a particular limestone. Some limestones are composed almost entirely of skeletal remains, which are cemented together with a small amount of micrite or sparry calcite cement. The kinds of skeletal grains that occur in limestones encompass essentially the entire spectrum of organisms that secrete hard parts; however, the relative abundance of various kinds of skeletal remains has varied through time. Figure 9.18 illustrates the relative importance of the principal kinds of calcareous marine organisms that formed carbonate sediments during Phanerozoic time. Note that some groups of organisms achieved their maximum development as carbonate-sediment producers during the Paleozoic, others during the Mesozoic and Cenozoic. Figure 9.18 does not include all organisms that contribute to formation of carbonate sediment. Omitted here, for example, are the cyanobacteria that do not themselves calcify, but which play an extremely important role in trapping and binding fine carbonate sediment to form stromatolites.

As mentioned, most skeletal grains are composed of aragonite, calcite, or magnesian calcite (see Flügel, 2004, p. 103). Vertebrate remains, fish scales, conodonts, and the remains of a few invertebrate organisms such as inarticulate brachiopods are composed of calcium phosphate. Also, a few, e.g. diatoms and radiolarians, are composed of silica. The original composition of skeletal grains may be altered during diagenesis. Aragonite skeletons transform to calcite, and

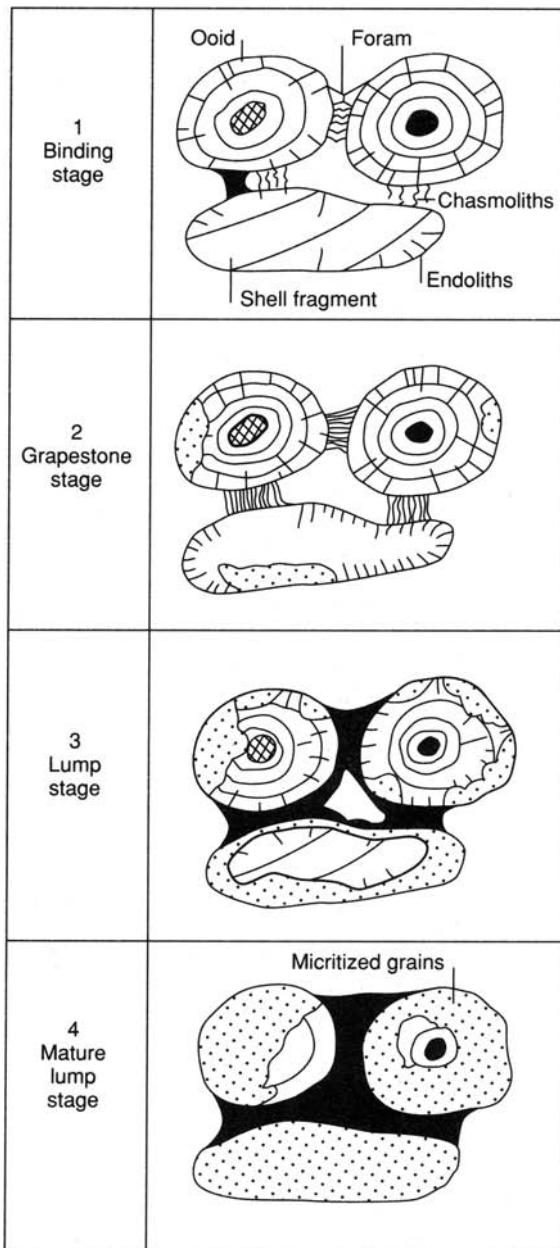


Figure 9.17 Stages in the formation of aggregate grains. Stage 1: carbonate grains are bound together by foraminifers, microbial filaments, and mucilage. Chasmolithic microorganisms occur between the grains, whereas endolithic forms bore into the carbonate substrates. Stage 2: calcification of the microbial braces occurs, typically by high-magnesian calcite, to form a cemented grapestone. Progressive micritization (conversion to lime mud) of carbonate grains takes place. Stage 3: increased cementation at grain contacts, by microbially induced precipitation, fills depressions to create smoother relief. Stage 4: filling of any central cavity to form a dense, heavily micritized and matrix-rich aggregate. Some replacement of the high-magnesian calcite components by aragonite may also occur. (After Tucker, M. E. and V.P. Wright, 1990, *Carbonate Sedimentology*: Blackwell Scientific, Oxford, Fig. 1.8, p. 12, reproduced by permission.)

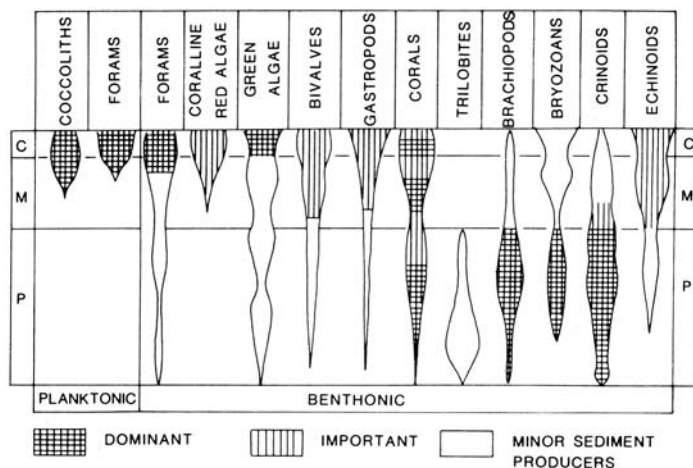


Figure 9.18 The approximate diversity, abundance, and relative importance of various calcareous marine organisms as sediment producers. P, Paleozoic; M, Mesozoic; C, Cenozoic. (After Wilkinson, B. H., 1979, *Biom mineralization, paleoceanography, and evolution of calcareous marine organisms: Geol.*, 7, Fig. 1, p. 526. Published by Geological Society of America, Boulder, CO.)

high-magnesian calcite grains may alter to calcite or become dolomitized. Carbonate skeletal grains may also undergo replacement by silica.

Each kind of organism that lived in the past was adapted to a particular set of ecological conditions. Because this was so, fossils yield vital information about environmental conditions such as water depth, salinity, turbidity, and energy levels. Therefore, it is extremely important in petrologic studies of carbonate rocks to identify each skeletal grain. Identifying skeletal grains in thin sections can be an extremely challenging task, even for relatively experienced researchers. In many cases, only fragments of the original shell are preserved, and these fragments may be cut at various angles in the plane of the thin section. For example, a fragment of a brachiopod spine may have an outline that appears in thin section to be a circle, an oval, or an elongated rectangle, depending upon the orientation of the thin-section cut. Also, different organisms may appear quite similar in small fragments of thin-section size. Fragments of corals and bryozoans, for example, can be quite difficult to differentiate.

Beginning carbonate petrographers can generally benefit from some kind of identification guide to help cut through the maze of confusing forms that fossils present in thin section. Fortunately, photographic atlases are available that show plates, some in color, of all the major fossil groups as they appear in thin section (e.g. Adams and MacKenzie, 1998; Scholle and Ulmer-Scholle, 2003). Space requirements in this book do not allow inclusion of numerous figures to illustrate all the major groups of fossil organisms. Figures 9.19 through 9.21 provide examples of a few kinds of skeletal grains that are common in limestones.

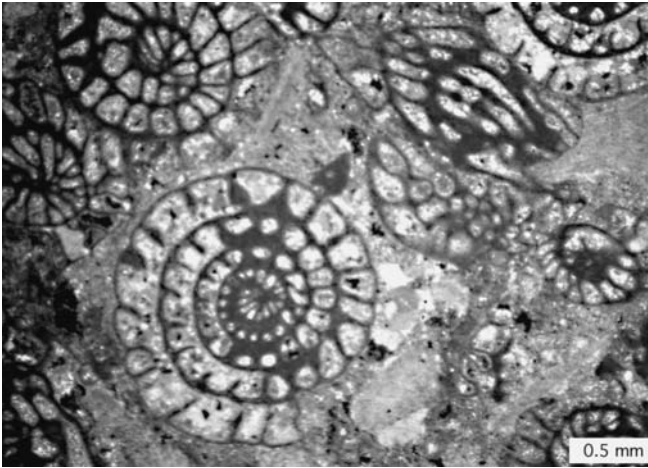


Figure 9.19 *Fusulinid* foraminifers as they appear in thin section. Both cross-sectional and longitudinal views are shown. Morgan Formation (Pennsylvanian), Colorado. Crossed nicols photomicrograph.

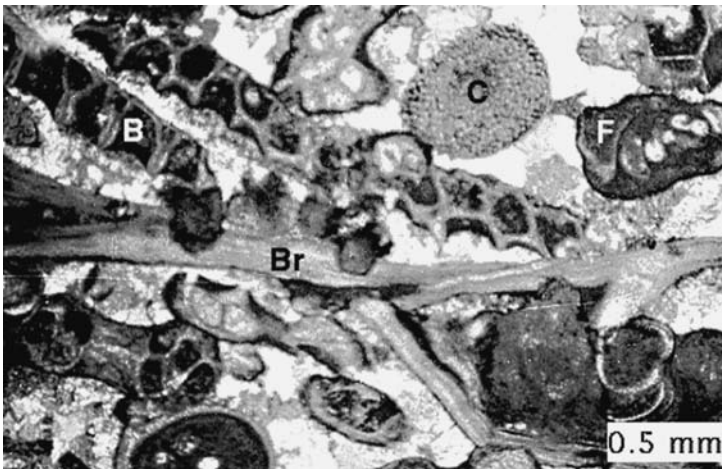


Figure 9.20 Mixed skeletal grains cemented with sparry calcite (white). C, crinoid; B, bryozoan; Br, brachiopod. Salem Formation (Mississippian), Missouri. Crossed nicols photomicrograph.

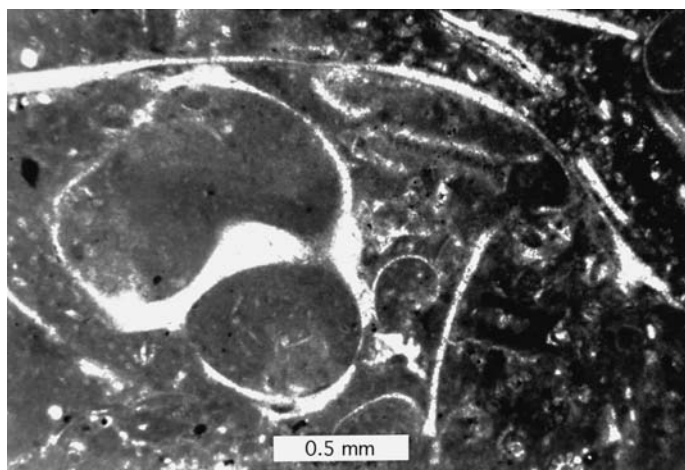


Figure 9.21 Gastropod shell and other mollusc fragments (white) surrounded by dark lime mud (micrite). Edwards Limestone (Cretaceous), Texas. Crossed nicols.

9.4.3 Microcrystalline carbonate (lime mud)

Although many limestones are composed dominantly of carbonate grains (allochems), few if any limestones are made up entirely of sand–silt-size grains. The remaining part of the rock is composed either of sparry calcite cement (described in the [next section](#)) or microcrystalline calcite or aragonite, commonly referred to as **lime mud**. Texturally, lime mud is analogous to the clay-size matrix in siliciclastic sedimentary rocks and to siliciclastic mudstones. In modern carbonate environments, lime muds are composed mainly of aragonite needles about 1–5 microns in length. In ancient limestones, they consist of similar sized, but more equant, crystals of calcite. Lime muds may also contain a few percent clay-size, noncarbonate impurities such as clay minerals, quartz, feldspar, and organic matter. Folk (1959) proposed the term **micrite** as a contraction for microcrystalline calcite; this term has been universally adopted to signify very fine-grained carbonate sediment. It is used loosely to include all carbonate mud, including aragonite muds; that is, all microcrystalline carbonate. Micrite has a grayish to brownish, subtranslucent appearance under the microscope (Fig. 9.22). It is generally easily distinguished from carbonate grains by its finer size and from sparry calcite, which is coarser grained and more translucent. Although micrite typically occurs as a matrix among carbonate grains, some limestones are composed almost entirely of micrite. Such a limestone is texturally analogous to a siliciclastic shale or mudstone.

The presence of substantial micrite in a limestone is commonly interpreted to indicate deposition under fairly low-energy conditions, where little winnowing of fine mud takes place. Deposition in agitated water is suggested to cause removal of micrite, leaving mud-free carbonate grains that may later become cemented by sparry calcite. This long-standing dogma must be reexamined, however, in light of the discovery that micrite can precipitate internally in cavities and sediment pores below the sediment–water interface.

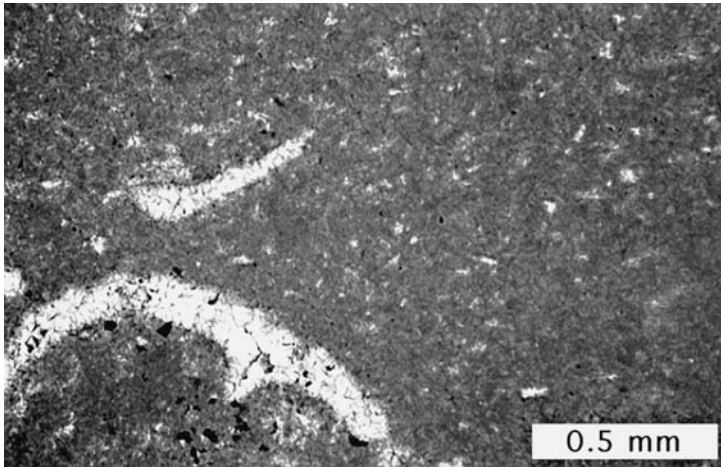
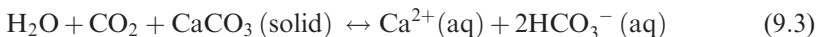


Figure 9.22 Photomicrograph of a limestone composed dominantly of micrite, with a few skeletal fragments (white). Plattin Limestone (Ordovician), Missouri. Crossed nicols.

The precipitation of cements with microcrystalline texture has been recognized since the mid 1960s (Reid *et al.*, 1990). Initially, micrite cement was thought to precipitate internally in the same manner as spar cement (discussed below) by successive growth of crystals on the walls of cavities. It is now recognized that micrite can also nucleate in suspension within cavities and settle on cavity floors. Furthermore, repeated nucleation can result in formation of peloids. Thus, there are two kinds of micrite: **seafloor micrite**, which is deposited at the sediment–water interface, and **internal micrite**, which accumulates inside cavities and intergranular pores (Fig. 9.23). Carbonate deposits, including high-energy deposits such as oolites, may thus contain micrite that is not related to depositional conditions. Therefore, we must exercise considerable caution in interpreting environments of limestone deposition on the basis of micrite/grain ratios. Pore-filling micrite that exhibits peloidal or clotted textures, or that occurs in limestones that exhibit evidence of submarine lithification (Chapter 11), may very likely be internal micrite.

The origin of seafloor micrite (microcrystalline aragonite and calcite mud) presents an interesting problem. Theoretical considerations of carbonate equilibria suggest that CaCO_3 should precipitate inorganically under conditions of supersaturation. The equilibrium relationship for CaCO_3 in water and dissolved carbon dioxide is



Loss of CO_2 owing to heating, pressure decrease, photosynthesis, or other reasons disturbs this equilibrium, causing the reaction to shift to the left. This reaction is easily demonstrated in the laboratory. Nonetheless, it has now been adequately established that calcite does not precipitate freely in the presence of Mg in seawater. Aragonite nucleation is also inhibited, apparently by the presence of organophosphatic compounds (see discussion in Boggs, 2006, p. 176).

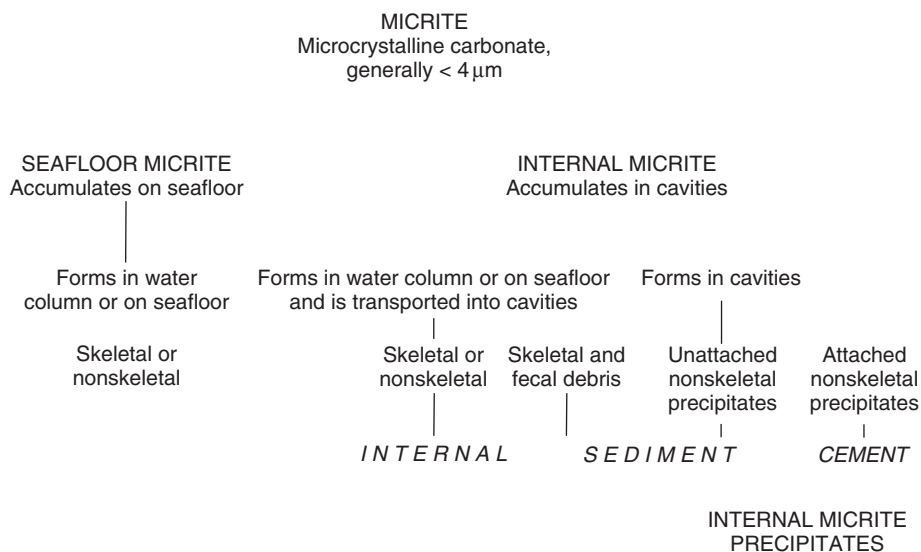


Figure 9.23 Classification of microcrystalline carbonate (micrite) on the basis of sites of deposition. Seafloor micrite accumulates at the sediment–water interface during deposition and reflects depositional energy and textural maturity of sediments. Internal micrite accumulates below the depositional interface during diagenesis and is unrelated to environments of deposition. (From Reid, R. P., I. G. MacIntyre, and N. P. James, 1990, Internal precipitation of microcrystalline carbonate: a fundamental problem for sedimentologists: *Sediment. Geol.*, **68**, Fig. 1, p. 164, reprinted by permission of Elsevier Science Publishers, Amsterdam.)

Questions about the inorganic precipitation of CaCO_3 have long been tied in with questions about the origin of whittings. **Whittings** are drifting clouds of seawater that appear milky because of suspended carbonate crystals (mainly aragonite and Mg-calcite). The presence of these whittings in modern carbonate environments such as the Bahama Banks has been suggested by some authors to be proof of inorganic precipitation of CaCO_3 . On the other hand, some observers have attributed the whittings to the action of bottom-feeding fish that stir up sediment or to resuspension of bottom mud by wave action. Recent studies suggest that microbially mediated precipitation owing to photosynthesizing microalgae or cyanobacteria is the likely origin of whittings (e.g. Robbins *et al.*, 1997; Yates and Robbins, 2001).

A great deal of the lime mud in the geologic record may have been produced in some other ways through the activities of organisms. Photosynthesis by algae and other plants (as mentioned), and bacterial action and decomposition of organic matter may promote micrite precipitation by changing the water chemistry. It is likely, however, that much organically related micrite is produced in a more direct manner by organisms. A principal source of lime mud may be the tiny aragonite needles contained within some green and red algae. When these organisms die, chemical and bacterial decomposition of their soft tissue releases the aragonite needles to the seafloor (e.g. Macintyre and Reid, 1995).

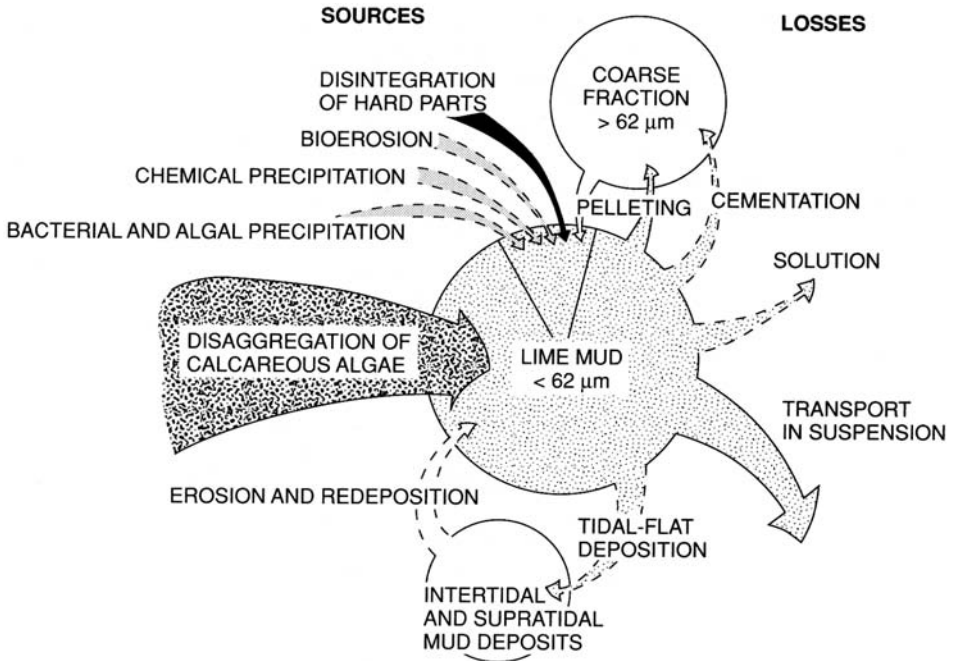


Figure 9.24 Multiple origin of lime mud in the Bight of Abaco, Bahamas. (After Neumann, A. C. and L. S. Land, 1975, Lime mud deposition and calcareous algae in the Bight of Abaco, Bahamas: a budget: *J. Sediment. Petrol.*, **45**, Fig. 4, p. 796, reprinted by permission of the Society for Sedimentary Geology, Tulsa, OK.)

Other mechanisms for production of fine carbonate sediment, many of which are organically related, include (1) disintegration of the hard parts of invertebrates, (2) breakdown of skeletal grains and other material owing to bioerosion by organisms such as parrot fish, (3) boring of carbonate grains or substrate by endolithic algae, fungi, and invertebrates, (4) physical abrasion of larger particles, and (5) production of micrite-size skeletal tests by microorganisms and nannoorganisms. Many of these processes, as they are thought to operate in the Bahamas, are illustrated diagrammatically in Fig. 9.24. The width of the arrows in this figure suggests the relative lime-mud contribution by each of these processes, as interpreted by Neumann and Land (1975). Shinn *et al.* (1989) suggest that inorganic precipitation of lime mud is more important and disintegration of calcareous algae is less important than indicated by this diagram.

9.4.4 Sparry calcite

The third major constituent of limestones, in addition to carbonate grains and micrite, is sparry calcite. Crystals of sparry calcite are large (0.02–0.1 mm) compared to micrite crystals and appear clear or white when viewed in plane light under a polarizing microscope.

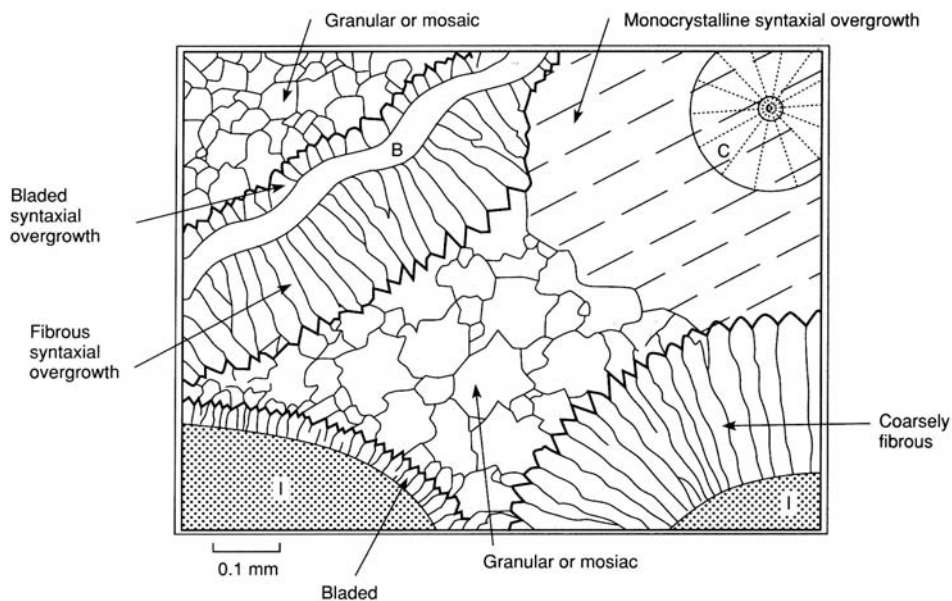


Figure 9.25 Some important types of sparry calcite cement fabrics in limestones. B = brachiopod, C = crinoid, I = intraclast. The change from bladed crystals to larger, granular crystals in the lower left corner of the figure illustrates “drusy” fabric. (After Folk, R. L., 1965, *Some aspects of recrystallization in ancient limestones*, in Pray, L. C. and R. Murray (eds.), *Dolomitization and Limestone Diagenesis*: SEPM Special Publication 13, Fig. 6, p. 27, reprinted by permission of the Society for Sedimentary Geology, Tulsa, OK.]

They are distinguished from micrite by their larger size and clarity and from carbonate grains by their crystalline shapes and lack of internal microstructures.

Much of the sparry calcite in limestones occurs as a cement that fills interstitial space among carbonate grains. Sparry calcite cement is particularly common in grain-rich limestones, such as oolites, that were deposited in agitated water that prevented micrite from filling pore spaces. Therefore, as mentioned, the presence of significant amounts of sparry calcite cement in a limestone is commonly interpreted to indicate deposition of the limestone in agitated water. This criterion should be applied with caution, however, because much pore space in limestones can be secondary – produced by dissolution during diagenesis. Sparry calcite cement that fills secondary pores has no relationship to depositional conditions.

Sparry calcite can form a variety of cementation fabrics, and several distinctive types of cement are recognized. The most common types are **granular or mosaic cement**, which is composed of nearly equant crystals; **fibrous cement**, either coarsely or finely fibrous; **bladed cement**; and **syntaxial cement** (overgrowths) – see Fig. 9.25. The most common syntaxial overgrowths are monocrystalline overgrowths around echinoderm fragments, which consist of plates composed of a single calcite crystal. Monocrystalline overgrowths are in optical continuity with these single-crystal echinoderm plates. These syntaxial cement

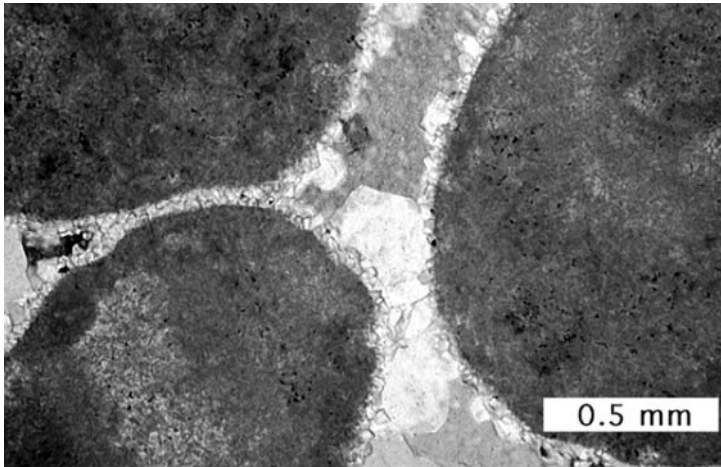


Figure 9.26 Sparry calcite cementing rounded (dark) intraclasts. The cement displays drusy texture: small calcite crystals, oriented with their long dimensions perpendicular to the clast surfaces, grade outward from the margins of the clasts into larger, randomly oriented calcite crystals. Devonian limestone, Canada. Crossed nicols.

rims are analogous to the overgrowths on quartz grains. Syntaxial overgrowths are also known to occur on brachiopod and mollusk fragments, foraminifer tests, and corals. Overgrowths of this type consist of bladed crusts, and the individual bladed crystals are in optical continuity with foundation crystals in the fossils (Scoffin, 1987, p. 127.)

Euhedral to anhedral, bladed or coarsely fibrous crystals that are oriented perpendicular to carbonate grain surfaces may display an increase in grain size toward the center of the pore or cavity and a concomitant change to more equant, granular crystals. This distinctive pore-filling fabric is commonly referred to as drusy cement. **Drusy fabric** is illustrated in Fig. 9.25 by the change from small bladed to larger granular crystals in the lower left corner of the figure. Figure 9.26 also illustrates drusy fabric. Depending upon the conditions of their origin, sparry cements may take on a number of other fabrics, such as isopachous and botryoidal. These cement fabrics are discussed further in Chapter 11.

Not all sparry calcite in limestones is cement that formed by precipitation into a pore or other cavity. Some sparry calcite, referred to as **neospar**, originates through recrystallization of micrite or carbonate grains (Fig. 9.27). This kind of sparry calcite does not fill pore space; therefore, its presence has no value in interpreting depositional conditions. It is important in petrologic studies to differentiate sparry calcite formed by recrystallization processes from sparry calcite cement. Although recrystallized sparry calcite does not commonly form a drusy fabric, it can mimic most of the other type of cement mentioned above. Therefore, differentiating between sparry calcite cement and recrystallization spar is a major problem in carbonate petrology. Further details are given in Chapter 11.

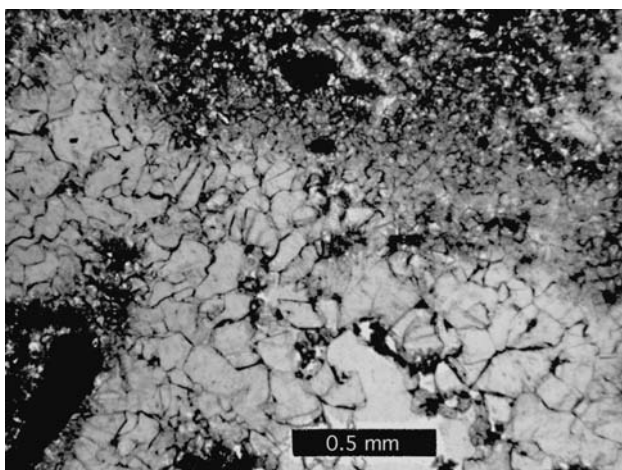


Figure 9.27 Coarse neospar (large, clear crystals) formed by recrystallization of micrite (dark). Note the indistinct boundary between the neospar and the “dirty” incipiently recrystallized micrite. Robinson Limestone (Pennsylvanian), Colorado. Ordinary light.

9.5 Classification of carbonate rocks

9.5.1 Available classifications

Classifications for carbonate rocks have not proliferated quite to the extent of sandstone classifications. Nonetheless, twenty or so carbonate classifications have appeared in print since the early 1960s. Somewhat more than half of these classifications are in English-language journals or books.

Publication in 1959 and 1962 of Folk’s largely descriptive classification marked the beginning of modern limestone classification. Folk’s classification is based on the relative abundance of three constituents: carbonate grains, lime mud (micrite), and sparry calcite cement. In the same volume in which Folk published his 1962 classification, Dunham (1962) published a classification based on depositional textures: (1) grain packing and the abundance of carbonate grains relative to micrite; and (2) depositional binding of grains. Folk and Dunham’s classifications have stood the test of time, being still in use after more than 50 years; however, some modifications to the classifications have been suggested by other workers. These classifications are considered in further detail below.

9.5.2 Folk’s classification (1962)

Folk’s classification is applicable primarily to thin-section analysis. It is not an easy classification to use in the field. Use of the classification requires a definite knowledge of the kinds and abundances of carbonate grains (allochems) and the relative abundance of micrite and sparry calcite cement. The classification (Table 9.4) is hierarchal and requires that the user proceed through a number of definite steps.

Table 9.4 Classification of carbonate rocks according to Folk (1962)

Limestones, partly dolomitized limestones		Replacement dolomitites		
		>10% Allochems Allochemical rocks	<10% Allochems Microcrystalline rocks	
Sparry calcite cement > micro- crystalline ooze matrix	Microcrystalline ooze matrix >sparry calcite cement	Undis- turbed bioherm rocks	Allochem ghosts	No allochem ghosts
Sparry allochemical rocks	Microcrystalline allochemical rocks	Biothite	Finely crystalline intraclastic dolomite, etc.	Medium crystalline dolomite
Intrasparrudite Intrasparite	Intramicrodite* Intramicrocite*	Most abundant allochem	Aphanocrystalline biogenic dolomite, etc.	Very finely crystalline pellet dolomite, etc.
Oosparrudite Oosparite	Oomicrodite* Oomicrocite*	Micrite; if disturbed, dismicrite; if primary,	Pellets: pelletiferous micrite	etc.
Bioparrudite Bioparite	Biopelmicrodite Biopelmicrocite	Pellets: pelletiferous micrite	Pellets: pelletiferous micrite	etc.
Intra- > 25% Clasts	Ooids > 25%	Volume ratio of fossils to pellets	Pellets: pelletiferous micrite	etc.
Ooids > 25%	Volume ratio of fossils to pellets	Micrite; if disturbed, dismicrite; if primary,	Pellets: pelletiferous micrite	etc.
Ooids > 25%	Volume ratio of fossils to pellets	Micrite; if disturbed, dismicrite; if primary,	Pellets: pelletiferous micrite	etc.
Ooids > 25%	Volume ratio of fossils to pellets	Micrite; if disturbed, dismicrite; if primary,	Pellets: pelletiferous micrite	etc.

Note: Names and symbols in the body of the table refer to limestones. If the rock contains more than 10 percent replacement dolomite, prefix the term "dolomitized" to the rock name. The upper name in each box refers to calcitrichites (median allochem size larger than 1.0 mm); the lower name refers to all rocks with median allochem size smaller than 1.0 mm. Grain size and quantity of ooze matrix, cements, or terrige- nous grains are ignored.

*Designates rare rock types.

Source: Folk, R. L., 1962, Spectral subdivision of limestone types, in W. E. Ham (ed.), Classification of Carbonate Rocks, AAPG Memoir 1, Table 1, p. 70, reprinted by permission of AAPG, Tulsa, OK.

		Allochemical rocks		Orthochemical rocks
		I	II	III
		SPARRY CALCITE CEMENT	MICROCRYSTALLINE CALCITE MATRIX	MICROCRYSTALLINE CALCITE LACKING ALLOCHEMS
Allochem composition	INTRACLASTS (i)	<i>INTRASPARITE</i>	<i>INTRAMICRITE</i>	<i>MICRITE</i>
	OOIDS (o)	<i>OOSPARITE</i>	<i>OOMICRITE</i>	<i>DISMICRITE</i>
	FOSSILS (b)	<i>BIOSPARITE</i>	<i>BIOMICRITE</i>	Autochthonous reef rocks IV
	PELLETS (p)	<i>PELSPARITE</i>	<i>PELMICRITE</i>	<i>BIOLITHITE</i>
			Sparry calcite Microcrystalline calcite	

Figure 9.28 Schematic representation of the constituents that form the basis for Folk's classification of carbonate rocks (Table 9.4). [After Folk, R. L., 1962, Spectral subdivision of limestone types, in Ham, W. E. (ed.), *Classification of Carbonate Rocks*: AAPG Memoir 1, Fig. 3, p. 71, reproduced by permission of AAPG, Tulsa, OK.]

Classification is made by first determining the relative abundance of carbonate grains (allochems) vs. micrite plus sparry calcite cement. Further subdivision is then made on the basis of the relative abundance of the various types of carbonate grains (Fig. 9.28) and the relative abundance of micrite plus sparry calcite cement. Note, as mentioned, that the classification is hierarchal (e.g. >25% intraclasts, <25% intraclasts; >25% ooids, <25% ooids). Classification in this manner yields a bipartite name that reflects both the major types of carbonate grains in the limestone and the relative abundance of micrite and sparry calcite cement. For example, an **oosparite** is an ooid-rich rock cemented with sparry calcite cement that contains little micrite, whereas an **oomicrite** is an ooid-rich limestone in which micrite is abundant and sparry calcite is subordinate. Additional textural information can be added by use of the textural maturity terms shown in Fig. 9.29. Thus, a **packed oomicrite** indicates a grain-supported oolitic limestone, and a **sparse oomicrite** is an oolitic rock with a mud-supported fabric.

Note that Folk's classification can also be used to classify dolomite rock, if "ghosts" of the original allochems are still identifiable in the dolomite. If the dolomite formed by replacement of a limestone, the assigned name depends upon the presence or absence of

Percent allochems	OVER 2/3 LIME-MUD MATRIX				SUBSEQUAL SPAR AND LIME MUD	OVER 2/3 SPAR CEMENT		
	0–1%	1–10%	10–50%	OVER 50%		SORTING POOR	SORTING GOOD	ROUNDED AND ABRADED
Representative rock terms	MICRITE AND DISMICRITE	FOSSILIFEROUS MICRITE	SPARSE BIOMICRITE	PACKED BIOMICRITE	POORLY WASHED BIOSPARITE	BIOSPARITE	BIOSPARITE	BIOSPARITE
Terminology	<i>Micrite and dismicrite</i>	<i>Fossiliferous micrite</i>	<i>Biomicroite</i>		<i>Biosparite</i>			
Terrigenous analogues	<i>Claystone</i>		<i>Sandy claystone</i>	<i>Clayey or immature sandstone</i>	<i>Submature sandstone</i>	<i>Mature sandstone</i>	<i>Supermature sandstone</i>	

Lime-mud matrix
 Sparry calcite cement

Figure 9.29 Textural classification of carbonate sediments on the basis of relative abundance of lime-mud matrix and sparry calcite cement and on the abundance and sorting of carbonate grains (allochems). [After Folk, R. L., 1962, Spectral subdivision of limestone types, in Ham, W. E. (Ed.), *Classification of Carbonate Rocks*: AAPG Memoir 1, Fig. 4, p. 76, reproduced by permission of AAPG, Tulsa, OK.]

recognizable “ghosts” of carbonate grains, e.g. **oolitic dolomite**, or simply **medium crystalline dolomite**. He suggests that fine-grained primary dolomites be called **dolomicrite**. See [Chapter 10](#) for more details on dolomites and dolomite classification.

Folk’s carbonate classification is a workable classification and appears to be widely used; however, it has some problems. For one thing, the original classification makes no provisions for oncolites, which can be abundant in some limestones. Also, he does not include extraclasts in the classification. Because of the difficulty frequently experienced in differentiating extraclasts from intraclasts, most workers probably lump them together with intraclasts. Thus, use of the term intraclast can be misleading. Likewise, no special provision is made for aggregate grains or lumps. Folk appears to consider these grains a type of intraclast. The classification of some dolomites as primary dolomite is a judgment call. Whether or not some dolomites are primary is a problem not yet adequately resolved. This problem is discussed in detail in [Chapter 10](#). Finally, Folk’s use of sparry calcite cement as a classification parameter departs from the practice of many other classifiers, who do not use authigenic minerals in classification. The difficulty in differentiating sparry calcite of recrystallization origin from sparry calcite cement makes the use of sparry calcite cement in classification a particular problem.

To overcome some of these problems, Strohmenger and Wirsing (1991) proposed a modification of Folk classification (Fig. 9.30). The term “pellet” is replaced by the more general term “peloid,” and oncoids are introduced as a fifth type of allochem. This introduction requires some change in the volumetric allochem proportions: 25% has been changed to 20% (or 40% in the case of fossils/peloids). They also propose to call a rock with $\geq 20\%$ extraclasts an extramicrite (extramicrudite) or an extrasparite (extrasparudite), depending upon the size of the components and the micrite/sparite ratio.

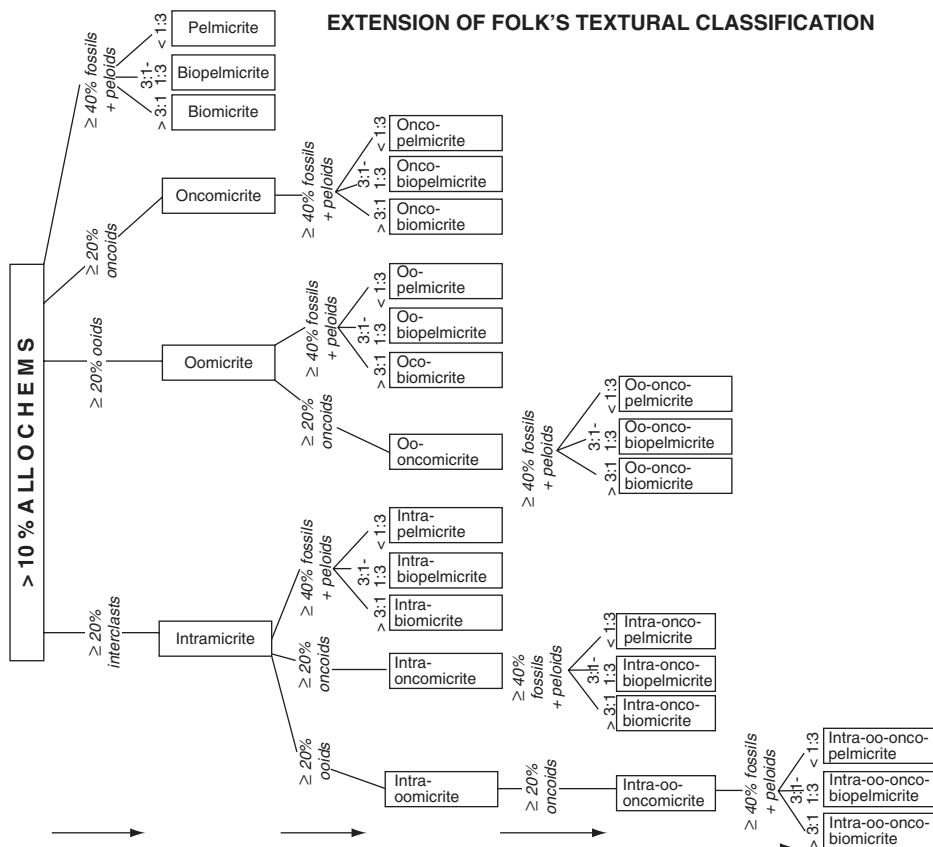


Figure 9.30 Modified Folk classification. [After Strohmenger, C. and G. Wirsing , 1991, A proposed extension of Folk's (1959, 1962) textural classification of carbonate rocks: *Carbonate Evaporite*, 6, Fig. 2, p. 25, (as rearranged slightly by Flügel , 2004, p. 360), reproduced by permission of Northeastern Science Foundation.]

9.5.3 Dunham's classification (1962)

Dunham (1962) took a different approach to classification by focusing upon depositional limestone textures rather than upon the identity of specific kinds of carbonate grains (Table 9.5A). He considers two aspects of texture: (1) grain packing and the relative abundance of grains and micrite and (2) depositional binding of grains. To use this classification the user must first determine if the original constituents of the limestone were or were not bound together at the time of deposition. For rocks composed of components not bound together during deposition (i.e. components deposited as discrete grains or crystals), the rocks are further divided into those that contain lime mud (micrite) and those that lack mud. Rocks that contain lime mud are either mud-supported or grain-supported. Determining the type of fabric support can be a problem, and the fabric must be visualized as it might appear in three dimensions and not simply as it appears in the two dimensions of a thin-section plane.

Table 9.5 *Classification of limestone according to depositional textures*

A		DEPOSITIONAL TEXTURE RECOGNIZABLE		DEPOSITIONAL TEXTURE NOT RECOGNIZABLE	
Original components not bound together during deposition		Contains mud (particles of clay and fine silt size)		Original components were bound together during deposition . . . as shown by intergrown skeletal matter, lamination contrary to gravity, or sedimentation	
		Mud-supported	Grain-supported	organic or questionably organic matter and are too large to be interstices.	
Less than 10% grains	More than 10% grains	WACKSTONE	PACKSTONE	BOUNDSTONE	
MUDSTONE			GRAINSTONE		
Lacks mud and is grain-supported					
B		ALLOCTHONOUS LIMESTONE Original components not organically bound during deposition		AUTOCHTHONOUS LIMESTONE Original components organically bound during deposition	
Less than 10% > 2 mm components		Greater than 10% > 2mm components		By organisms that build a rigid framework	
Contains lime mud (< 0.03 mm)		No lime mud		By organisms that act as baffles	
Mud-supported		Grain-supported			
Less than 10% grains (> 0.03 mm < 2 mm)	Greater than 10% grains (> 2 mm)	Matrix-supported		By organisms that encrust and bind	
MUDSTONE	WACKSTONE	PACKSTONE	GRAINSTONE	BOUNDSTONE	
				FRAMESTONE	BAFFLESTONE
				RUDSTONE	BINDSTONE

Source: A. After Dunham, R. J., 1962, Classification of carbonate rocks according to depositional textures, in Ham, W. E., ed., *Classification of Carbonate Rocks*, AAPG, Memoir 1, Table 1, p. 117, reprinted by permission of AAPG, Tulsa, OK, B. after Dunham, R. J., 1962, as modified by Embry, E. F., III and J. E. Klovan, 1972, Absolute water depth limits of late Devonian paleoecological zones, *Geol. Bulletin* 441, Fig. 5, p. 676, reprinted by permission.

Mud-supported limestones are **mudstones** (i.e. lime mudstones) if they contain less than 10 percent carbonate grains and **wackestones** if they contain more than 10 percent grains. Grain-supported limestones that contain some micrite mud matrix are **packstones**. Grain-supported limestones that lack mud matrix are **grainstones**. Dunham uses the term boundstone for limestones composed of components bound together at the time of deposition. This name is roughly equivalent to Folk's biolithite, and can include stromatolitic limestones as well as coral-reef and similar limestones.

Embry and Klovan (1972) modified Dunham's classification by subdividing limestones composed of originally unbound constituents into two groups on the basis of carbonate grain size. This modified classification scheme places more emphasis on limestone conglomerates (Table 9.5B). Thus, they recognize two kinds of limestones on the basis of grain size: limestones that contain less than 10 percent >2 mm-size grains and those that contain greater than 10 percent >2 mm-size grains. Names for limestones containing less than 10 percent >2 mm-size grains are the same as those used by Dunham. Embry and Klovan added two new names for rocks composed of more than 10 percent >2 mm-size grains: **floatstone** for matrix-supported limestones and **rudstone** for component (grain)-supported limestones. They also divided Dunham's boundstone into three subcategories on the basis of the presumed kind of organisms that built the limestones: **framestone** – built by organisms that construct rigid frameworks (i.e. *in situ*, massive organisms such as corals that build rigid, three-dimensional frameworks), **bindstone** – built by organisms that encrust and bind (these organisms do not build a three-dimensional framework), and **bafflestone** – formed by organisms that act as baffles (i.e. stalk-shaped organisms that acted as baffles at the time of deposition). This added subdivision of boundstone into three genetic categories constitutes mixing of genetic and descriptive parameters in the same classification. Such a subdivision may be difficult to make in practice, and it is certainly subjective. It may be preferable to stick with the name boundstone unless you are certain of the types of organisms that formed the boundstone. See Wright (1992) for yet another proposed modification of the Dunham classification.

The Folk and Dunham classifications are described herein in some detail because they appear to be the classifications most widely used by carbonate petrographers today, even though they were originally proposed more than a halfcentury ago. As mentioned, numerous other classifications for carbonate rocks have been published; see the bibliography of classifications provided by Flügel (2004, p. 268).

9.5.4 Classification of mixed carbonate and siliciclastic sediments

Most carbonate rocks contain only a small percentage of noncarbonate, siliciclastic constituents. On the other hand, some carbonate rocks contain significant percentages of siliciclastic constituents, just as some siliciclastic sedimentary rocks contain high concentrations of carbonate constituents. Although such mixed sediments are not abundant in the geologic record, they are common enough (see Doyle and Roberts, 1988) to create problems when we try to classify them using classification schemes designed for limestones and sandstones.

See Mount (1985) and Zuffa (1980) for classification schemes that deal with mixed carbonate and siliciclastic sediments.

9.6 Structures and textures in limestones

9.6.1 Structures also common to siliciclastic rocks

Although limestones are intrabasinal rocks, composed mainly of constituents precipitated in some manner from water, most carbonate grains in limestones undergo some transport before final deposition. Transport may occur by a variety of mechanisms, including tidal currents, longshore currents, wave action in shoaling zones, and turbidity currents. Accordingly, many ancient limestones display sedimentary structures that appear very similar to those that occur in siliciclastic sedimentary rocks. These structures may include (1) physically produced features such as cross-beds, lamination, ripple marks, and graded bedding, (2) deformation structures such as convolute lamination and synsedimentary folds, and (3) biogenically produced structures such as mottled bedding and other trace fossils. The textures of carbonate grains (size, shape, arrangement) may also be affected by transport processes, although shapes and sizes of some kinds of carbonate grains are determined mainly by their origin and not by transport and abrasion processes (e.g. whole fossils, ooids, pellets). See the richly illustrated volume by Demicco and Hardie (1994), for further discussion of these structures.

9.6.2 Special structures

In addition to these common kinds of sedimentary structures and textures, limestones may contain some special structures and textures that are not common or that do not occur in siliciclastic rocks. The most important of these special characteristics are listed and briefly described in Table 9.6. Further details are provided below.

Cryptalgal fabrics

Cryptalgal fabrics are fabrics in carbonate rocks believed to be biosedimentary structures that originated through the sediment-binding and/or mineral-precipitating activities of blue-green algae (cyanobacteria) and bacteria (Monty, 1976). Table 9.7 summarizes the principal kinds of cryptalgal fabrics. Layered (laminated) cryptalgal structures are best known because they include **stromatolites**. Stromatolites are hemispherical structures (domal, club-shaped, columnar) characterized by generally nonplanar laminations ranging to a few millimeters in thickness (Table 9.8; Fig. 9.31). They generally have well-defined, three-dimensional boundaries and all except oncolites grow attached to the substrate. Logan *et al.* (1964) divide stromatolites into a few fundamental types on the basis of the shapes of the hemispheres and the presence or absence of linking structures between hemispheres (Table 9.8).

Logan *et al.* suggest that the change from laterally linked hemispheroids to discrete, vertically stacked hemispheroids to discrete spheroids shown in Table 9.8 indicates an

Table 9.6 *Special kinds of structures and textures in limestones*

Structure or texture	Description and origin
Cryptalgal fabric	Layered and unlayered biosedimentary structure that originated through the sediment-binding and/or mineral-precipitating activities of blue-green algae (cyanobacteria) and bacteria
Stromatactis	Evenly to irregularly distributed subhorizontal voids, generally in carbonate muds, several millimeters to centimeters in size, with a nearly flat bottom and a convex-upward upper surface with an irregular, digitate roof; filled with sparry calcite cement or micrite
Birdseye structure	Similar to stromatactis but smaller, commonly 1–3 mm, and shapes may be spherical, oval, elongated, or irregular
Geopetal fabric	A structure displayed inside the cavities of fossils or beneath convex-up shells, formed by partial infilling by micrite, creating a nearly flat floor, with the remaining, upper part of the cavity filled with sparry calcite cement; allows top and bottom of beds to be differentiated
Tepee structure	Structure that resembles an inverted, depressed V in cross-section; occurs in marine, peritidal, lacustrine, and caliche environments; these arched-up antiforms are generated in carbonate hardgrounds owing to expansion caused by cementation or by fracturing and fracture fill by sediment or cement
Nodular structure	Nodules ranging in size to several centimeters that occur in a matrix of micrite and clay; particularly common in deep-water carbonates; origin probably early diagenetic, but poorly understood
Stylolites	Suturelike seams in carbonate rocks marked by irregular and interlocking penetration of the two sides; caused by pressure solution
Bioherm	Large-scale, moundlike or lenslike mass built by sedentary organisms; i.e., reefs and banks

increasing energy spectrum. That is, laterally linked hemispheroids are deposited under the lowest-energy conditions and discrete spheroids under the highest-energy conditions. Buekes and Lowe (1989) describe four morphological types of stromatolites from Archean carbonate rocks of South Africa, which they also relate to environmental conditions: stratiform, domal, columnar, and conical stromatolites. They suggest that stratiform stromatolites formed in upper intertidal, domal stromatolites formed in middle intertidal, columnar stromatolites formed in lower intertidal, and conical stromatolites formed in high-energy, subtidal channel environments.

Cryptalgal laminites lack the hemispherical form of stromatolites. They are laterally continuous stratiform deposits that are characterized by subcontinuous planar lamination ranging from less than a millimeter to several centimeters (Monty, 1976).

Monty (1976) discusses a variety of mechanisms that may be responsible for the development of laminated cryptalgal fabrics, including (1) diurnal differences in algal growth, (2) alternation between preferred vertical and preferred horizontal growth patterns of

Table 9.7 *Principal kinds of cryptalgal structures and fabrics*

I. LAMINATED FABRIC – characterizes stromatolites, oncolites, and cryptalgal laminites	
A. Laminated fabric – prominent laminations separated by distinct physical discontinuities	
B. Laminoid fabric – lacks distinct laminae, but contains more or less horizontal structures that outline an overall layering; three principal kinds of structures:	
1. Laminoid fenestral fabric – repetitive, elongate cavities or fenestrae	
2. Laminoid boundstone fabric – fabric arising from orientation of elongate particles parallel to the overall lineation that pervades the cryptalgal body; presumably formed by binding of particles by successive algal mat surfaces	
3. Lenticular laminoid fabric – fabric created by irregular juxtaposition and superposition of algal cushions or mats much smaller than the width of the stromatoid	
II. NONLAYERED FABRIC	
A. Thrombolitic fabric – centimeter-sized patches or clots of micrite with rare clastic particles, separated by spaces filled with sparry calcite; may occur together with algal filaments; may be indistinctly laminated in part (Aitken, 1967)	
B. Massive fabric – shows no internal lineation or spatial organization of particles; may be difficult to identify as cryptalgal	
C. Radial fabric – shows radial growth of calcified algal filaments; may be interrupted in places by concentric layers, but overall fabric is nonlayered	

Source: After Monty, 1976.

Table 9.8 *Structure of hemispherical stromatolites showing examples of laterally linked hemispheroids, vertically stacked hemispheroids, and discrete spheroids*


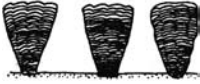



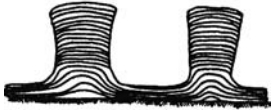


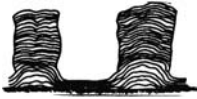
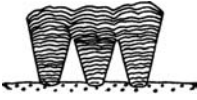
Types	Description	Vertical section of stromatolite structure
Laterally linked hemispheroids	Space-linked hemispheroids with close-linked hemispheroids as a microstructure in the constituent laminae	
Discrete, vertically stacked hemispheroids	Discrete, vertically stacked hemispheroids composed of close-linked hemispheroidal laminae on a microscale	
Discrete spheroids	Spheroidal structures consisting of inverted, stacked hemispheroids	
	Spheroidal structures consisting of concentrically stacked hemispheroids	
	Spheroidal structures consisting of randomly stacked hemispheroids	

Table 9.8 (cont.)

Types	Description	Vertical section of stromatolite structure
Combination forms	Initial space-linked hemispheroids passing into discrete, vertically stacked hemispheroids with upward growth of structures	
	Initial discrete, vertically stacked hemispheroids passing into close-linked hemispheroids by upward growth	
	Alternation of discrete, vertically stacked hemispheroids and space-linked hemispheroids due to periodic sediment infilling of interstructure spaces	
	Initial space-linked hemispheroids passing into discrete, vertically stacked hemispheroids; both with laminae of close-linked hemispheroids	
	Initial discrete, vertically stacked hemispheroids passing into close-linked hemispheroids; both with laminae of close-linked hemispheroids	

Source: After Logan, B. W., R. Rezak, and R. N. Ginsburg, 1964, Classification and environmental significance of algal stromatolites: *J. Geol.* 72. Fig. 4, p. 76, and Fig. 5, p. 78, reprinted by permission of University of Chicago Press.

the algal filaments, (3) different growth rates of various algal species within the algal mat, (4) growth of algal layers inside a mat (rather than at the surface of the mat), (5) periodic calcification of algal mats by poorly understood processes, (6) precipitation of carbonate crystals with different crystal habits, (7) periodic enrichment in various mineral compounds (e.g. Fe and Mn), (8) periodic influx of detrital particles (sand, silt, mud, organic matter), (9) periodic inorganic cementation owing to changes in geochemical conditions, (10) different reaction of laminae during diagenesis, resulting in alternating dolomitic and calcitic laminae, (11) alignment of detrital particles and agglutination by algae, and (12) formation of fenestral fabrics owing to separation of algal mats because of gas-bubble formation or shrinkage.



Figure 9.31 Stromatolites in limestones of the Helena Formation (Precambrian), Glacier National Park, Montana.

Best known of the **nonlayered cryptalgal fabrics** are **thrombolites**. Thrombolite fabrics are characterized by millimeter- and centimeter-size patches or clots of micrite separated by spaces filled either with sparry calcite cement or silt- and sand-sized sediment (Aitken, 1967; Kennard and James, 1986). Microscopic algal filaments may be present in the clots. Thrombolite fabrics are generally nonlayered but may be indistinctly laminated in part. Thrombolites are believed to form as a result of oxidation of dead colonies of algae, intergrowth and coalescence of colonies of algae, or internal dissolution of a calcified algal mass. According to Kennard and James (1986), “the individual mesoscopic clots (mesoclots) within thrombolites are interpreted as discrete colonies or growth forms of calcified, internally poorly differentiated, and coccoid-dominated microbial communities.” Kennard and James suggest that thrombolites form a continuum with stromatolites. That is, thrombolites grade through **undifferentiated boundstones** to stromatolites. Thrombolites occur primarily in Cambrian and Lower Ordovician rocks.

Massive fabrics may develop as a result of more or less continuous entrapment and agglutination of detrital particles, rapid sedimentation of detrital particles compared to algal growth, invasion and binding of previously deposited sediment by algae, continuous precipitation of carbonate in growing mucilaginous algal masses or diatom mats, or obliteration of original laminated or thrombolitic fabrics during diagenesis. **Radial fabrics** apparently form by radial growth of calcified algal filaments. For further description of these structures and their modes of origin see Monty (1976).

Stromatactis

Stromatactis cavities are particularly common in Paleozoic carbonate mudstones and wackestones associated with reefs and banks. These spar-filled cavities have a smooth base and an irregularly digitate roof, tend to occur in swarms, and have a reticulate (network) distribution

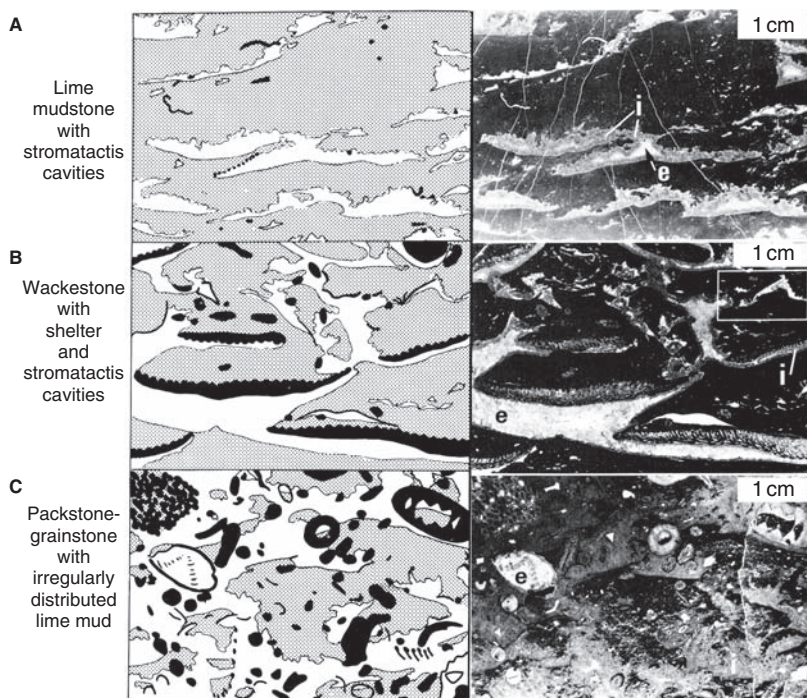


Figure 9.32 Thin-section photomicrographs and equivalent line drawings of stromatactis cavities in Devonian limestones, eastern Victoria, Australia. A. Lime mud with abundant stromatactis cavities. B. Skeletal wackestone with abundant stromatactis and shelter cavities (cavities under fossils). C. Packstone–grainstone with irregularly distributed lime mud. In the photographs, (i) refers to first-generation, inclusion-filled cement, and (e) refers to second-generation, clear, equant cement. In the line drawings, lime mud is patterned, skeletal elements are black, and cement-filled cavities are left blank. [After Wallace, M. W., 1987, The role of internal erosion and sedimentation in the formation of stromatactis mudstones and associated lithologies: *J. Sediment. Petrol.*, **57**, Fig. 3, p. 697, reproduced by permission of the Society for Sedimentary Geology, Tulsa, OK.]

(Bathurst, 1982). Figure 9.32 illustrates the typical shapes of stromatactis cavities with their sediment-filled floors and spar-filled upper parts. Although well known from numerous limestone units, the origin of these structures is problematic and controversial. Wallace (1987) cites some of the different viewpoints on origin and provides a short bibliography of pertinent papers on this subject. Origin of the structures has variously been linked to organisms in some way, such as decay of soft-bodied organisms, burrowing and bioturbation activities of crustaceans, diagenetic alteration and cementation of sponge networks, recrystallization of algae and bryozoans, and microbial accretion. Numerous inorganic processes have also been postulated, including slumping, dewatering and collapse, dynamic metamorphism, recrystallization of carbonate mud, pressure solution, and submarine crust formation.

On the basis of studies of limestones in eastern Victoria, Australia, Wallace (1987) proposes that the structures he studied formed by a process of internal erosion and sedimentation

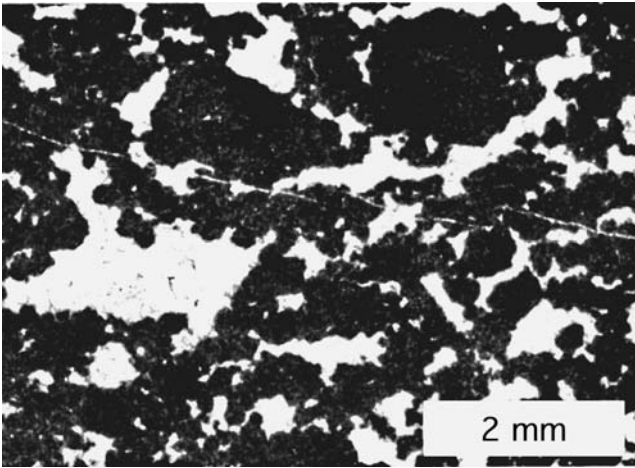


Figure 9.33 Photomicrograph of birdseye structure in a micritic limestone. El Abra Limestone (Cret.), northeastern Mexico. [After Griffith, Pitcher, and Rice, 1969, Quantitative environmental analysis of a Lower Cretaceous reef complex, in G. M. Friedman (ed.), *Depositional Environments in Carbonate Rocks*: SEPM Special Publication 14, Fig. 10A, p. 126, reproduced by permission of the Society for Sedimentary Geology, Tulsa, OK.]

(internal reworking) that took place immediately below the sediment–water interface. Carbonate mud was eroded from the roofs of existing cavities and redeposited on the floors. This process left a digitate, erosional roof in each cavity and created a smooth floor that migrated upward as the cavity was filled with internal sediment. The unfilled part of the cavity above the floor subsequently filled with sparry cement. This postulated erosional–depositional process requires that a precursor cavity system be present to initiate the process of internal erosion. How such a precursor system of cavities may have formed is not clear.

Birdseye structure

This term was apparently introduced by Ham (1952) to describe small, spar-filled voids in micritic limestones of Oklahoma. These structures (Fig. 9.33) superficially resemble stromatolites, but differ in some important respects. They are smaller (commonly about 1–3 mm), have shapes ranging from irregular to spherical or oval, lack internal sediment-constructed floors, and generally occur irregularly distributed or arranged in patterns parallel to bedding, rather than in reticulate patterns. Mechanisms for producing the birdseye cavities suggested by various investigators include creation of voids in algal mats by decay of the algae, escape of gas bubbles from decaying organic matter, bioturbation by small organisms, formation of pores by desiccation of carbonate mud in tidal zones, trapping of air bubbles in muds during temporary subaerial exposure, leaching of anhydrite nodules, and selective recrystallization during diagenesis.

Geopetal fabrics

Geopetal fabrics resemble stromatolites to the extent that they are cavities with nearly smooth, sediment-constructed floors that are filled above the floors with sparry calcite

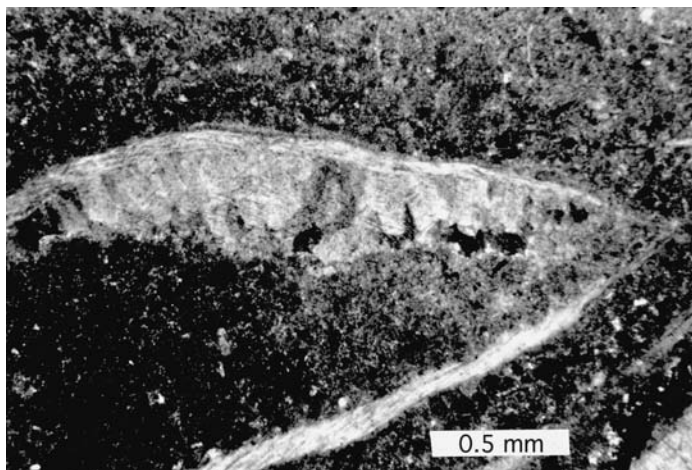


Figure 9.34 Geopetal fabric inside a brachiopod shell. Micrite fills the lower part of the shell; sparry calcite cement fills the uppermost part. The top of the bed is toward the top of the photomicrograph. Devonian limestone, Alaska. Crossed nicols.

cement. They differ, however, in that the cavities occur either within whole fossils or underneath convex-upward fossil shells such as mollusk and brachiopod shells (Fig. 9.34). These structures are also called shelter cavities and may occur in association with stromatolites. They form by precipitation or infiltration of micrite into or beneath a fossil shell, followed by precipitation of sparry calcite cement in the uppermost part of the cavity. Many geopetal structures are large enough to be easily seen in outcrops, where they provide useful indicators of tops and bottoms of beds.

Tepee structures

Tepee structures are small- to large-scale polygons with upturned antiform margins that resemble an inverted, depressed V (Fig. 9.35). These structures have been reported from submarine hardgrounds (a zone at the seafloor that has been lithified to form a hardened surface owing to early cementation and encrustation by sessile organisms and that is commonly bored by organisms and encrusted by solution), and from lacustrine and caliche environments. Tepee structures occur as buckled margins of saucerlike megapolygons. They form when the surface area of carbonate crusts expands by some mechanism, causing the hardened sediment to crumple and form a pattern of megapolygons with upturned antiform margins. Submarine tepees occur mainly in shallow-water, subtidal, intertidal, and supratidal environments. They occur also in peritidal environments as well as in lacustrine and caliche environments. Although all tepees are apparently caused by expansion, the causes of expansion (e.g. force of crystallization owing to filling of fractures; wetting and drying) are different in different environmental settings (see Kendall and Warren, 1987).



Figure 9.35 Tepee structure in limestone. Yates Formation (Permian), New Mexico. Note hammer for scale. (Photograph courtesy of Earl McBride.)

Nodular structures

Limestones composed of nodules set in a micritic, or less commonly, carbonate sand matrix occur in many ancient carbonate sequences. They appear to be particularly common in deeper-water deposits, but they have been reported also from shallower-water deposits (e.g. Noble and Howells, 1974). The nodules can range in size from less than a centimeter to tens of centimeters and in shape from rounded, subelliptical forms to irregular, elongated sausagelike forms. Nodular structure may be confined to relatively thin units within a limestone body or they may make up a substantial fraction of the overall sequence, as shown in Fig. 9.36. Many, but not all, nodular structures are associated with hardgrounds (see Chapter 11) or incipient hardgrounds (Kennedy and Garrison, 1975). Most theories advanced to explain the formation of nodular structure assume *in situ* early submarine cementation aided perhaps by compaction, pressure solution, or slumping. In a study of modern nodular carbonate sediments from the Bahamas, Mullins *et al.* (1980) call on a combination of physical (bottom currents), chemical, and biological (burrowing) processes, and *in situ* submarine cementation to explain nodule formation.

Stylolites

Stylolites are suturelike seams in sedimentary rocks marked by irregular and commonly interlocking penetration of the two sides of the seam. They are most common in carbonate



Figure 9.36 Rhythmically bedded nodular chalks (Cretaceous), Ballard Cliffs, Swanage, Dorset, England. (From Kennedy, W.J. and R.E. Garrison, 1975, Morphology and genesis of nodular chalks and hardgrounds in the Upper Cretaceous of southern England: *Sedimentology*, **22**, Fig. 13, p. 322, reproduced by permission of Elsevier Science Publishers, Amsterdam.)

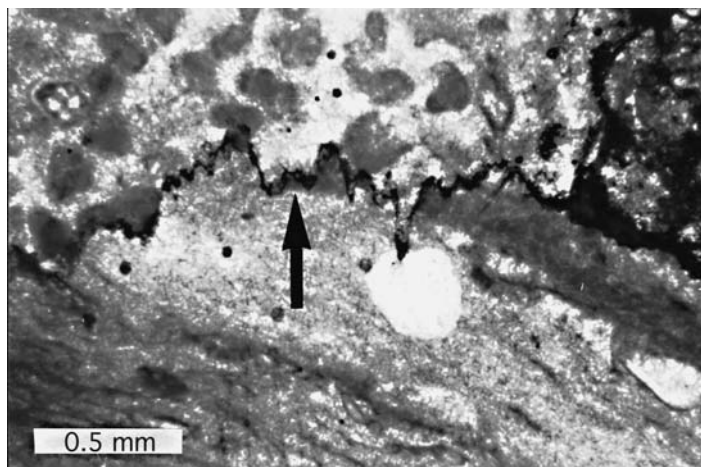


Figure 9.37 Microstylolite (arrow) in limestones of the Wadleigh Formation (Devonian), Alaska. Ordinary-light photomicrograph.

rocks but occur also in some sandstones and quartzites. Stylolite seams in limestones are characterized by concentrations of insoluble residues that may consist of clay minerals, other fine-size silicate minerals, iron oxides, or fine-size organic matter. Stylolites may occur on a microscale (grain-to-grain suturing), a somewhat larger scale where they cut across grains, micrite, and possibly cement (Fig. 9.37), or on a much larger scale. Stylolites are commonly oriented parallel to bedding planes, but they may occur at an angle to bedding



Figure 9.38 A small stromatolitic bioherm enclosed in thin beds of carbonate mudstone that bend around the bioherm from both above and below. Upper Cambrian Conococeague Limestone, western Maryland. (From Demicco, R. V. and L. A. Hardie, 1994, *Sedimentary Structures and Early Diagenetic Features of Shallow Marine Carbonate Deposits*: SEPM Atlas Series 1, Fig. 60, p. 79, reproduced by permission of the Society for Sedimentary Geology, Tulsa, OK.)

planes or even perpendicular to bedding. Stylolites are believed to form as a result of pressure solution, although the exact manner in which pressure solution works to produce the seams is poorly understood. Because stylolites are essentially diagenetic structures, they are discussed further in [Chapter 11](#).

Bioherms

Bioherms are large, lenslike or moundlike bodies of carbonate rock that consist largely of the remains of sedentary organisms and that are enclosed in rocks of different lithology or character (Fig. 9.38). They range in size from a few centimeters, across, such as the one shown in Fig. 9.38, to huge structures several hundred meters across. Some bioherms are composed of colonial organisms that constructed a rigid framework or core around which the bioherm accreted. Such a bioherm is called a **reef**. Some bioherms do not contain a framework core but are simply built of organisms that piled up in place as they died. Is this type of bioherm also a reef? Opinions differ. Many geologists call a bioherm that lacks a framework core a bank, mound, or mudmound, or use the nongenetic term **carbonate buildup** rather than calling it a reef. See Longman (1981) for some insight into this problem. In any case, bioherms are common in Phanerozoic-age carbonate rocks, and they represent a type of structure not found in siliciclastic sedimentary rocks. Although most bioherms are composed in part of organic remains, the kinds of organisms that built bioherms has varied through time. The earliest bioherm builders in Cambrian time were the archaeocyathids. These organisms have been succeeded through time as mound builders by organisms such as stromatoporoids, algae, bryozoans, rudists, and corals (James, 1983). Most modern framework-core reefs are built by corals.

9.7 Carbonate microfacies and marine depositional environments

9.7.1 Microfacies analysis

The term **microfacies** refers to sedimentary facies that can be studied and characterized in small sections of a rock. The name is generally applied to characteristics that can be determined by study of thin sections with a petrographic microscope or by similar methods. Flügel (2004, p. 1) defines a microfacies as “the total of all paleontological and sedimentological data which can be described and classified in thin sections, peels, polished slabs or rock samples.” According to Carozzi (1989, p. 24), a carbonate microfacies is “the total of the mineralogic, paleontologic, textural, diagenetic, geochemical, and petrophysical features of a carbonate rock.” Carozzi (p. 24) also reviews the history of the microfacies concept. Microfacies analysis can be carried out by a variety of analytical techniques including chemical, isotope, and X-ray diffraction analysis, scanning electron microscopy, cathodoluminescence microscopy, and paleontological techniques. Nonetheless, petrographic microscopic analysis has always been, and remains, the primary method for microfacies study.

The purpose of microfacies analysis is to provide a detailed inventory of carbonate rock characteristics (carbonate grain types, kinds and growth forms of fossils, size and shape of grains, nature of micrite, cement, particle fabrics) that can subsequently be related to depositional conditions. Thus, the ultimate aim of microfacies analysis is environmental interpretation. Microfacies analysis begins in the field with collection of samples. It then moves to the laboratory, where thin sections are prepared for study, which includes both qualitative and detailed quantitative analysis. Such analysis commonly includes determination of (1) the relative abundance of the main constituents (grains, matrix, cements), (2) shapes, sizes, sorting, and other characteristics of the carbonate grains, including types of fossil organisms, (3) nature of the matrix, (4) kinds of cements, and (5) nature of the fabric (grain-support, mud-support, bioturbation, etc.).

To insure that important characteristics of the rock are not overlooked during analysis, it is generally advisable to use a checklist of some type. Published checklists include those of Flügel (1982, p. 394), Flügel (2004, p. 59), and Wilson (1975, p. 60). Owing to the large number of criteria observed during microfacies analysis, statistical methods are commonly used to test the validity of the data and to reduce the data to a more manageable level that can be used in environmental interpretation. Cluster and factor analysis are among the most commonly used statistical techniques (e.g. Carozzi, 1989, pp. 30–31). A final classification of each thin section into distinct microfacies types is reached at the end of statistical analysis.

9.7.2 Standard microfacies types

Flügel (1982, 2004) and Wilson (1975), in particular, have advocated use of carbonate microfacies data to establish a restricted number of major microfacies types that serve as models for all carbonate microfacies, regardless of the ages of the carbonate rocks. These microfacies are referred to as standard microfacies types. They can be grouped into facies “belts” or zones, which are then used to build a generalized depositional model for carbonate

rocks. Carozzi (1989, p. 33) disagrees with this approach and suggests that there is essentially an infinite number of depositional models. Thus, he regards the concept of standard microfacies types to be a “premature oversimplification” and suggests that such oversimplification even contradicts the purpose of microfacies techniques, “which is merely to unravel and explain the variety rather than to standardize the results into a rigid framework before its time.” Even Flügel (1982, p. 403) cautions that standard microfacies types should not be overrated, and Wilson (1975, p. 64) acknowledges that organization of microfacies into a limited number of categories is an oversimplification.

Granted that the concept of standard microfacies may be an oversimplification, it is nonetheless a useful simplification. It provides a kind of standard to which we can compare our own analytical results; this can be exceedingly helpful in initial environmental interpretation. Virtually everyone agrees that many depositional environments are complex and cannot be adequately represented by a simple model; however, if we exercise good judgment and common sense in use of models such as standard microfacies types, they can be invaluable aids in environmental interpretation. With these cautions in mind, let’s take a look at Wilson’s standard microfacies types.

Wilson (1975, p. 64) proposed 24 standard microfacies (SMF) types. He selected names for these standard microfacies on the basis of major kinds of carbonate grains, paleontologic data, micrite abundance, and carbonate fabrics, using the textural classification of Dunham (1962) or Embry and Klovan (1972), as appropriate (Table 9.9). Note in this table that SMFs 25 and 26 are added from Flügel (2004, p. 681); also some terms in the table are not covered in these classifications, e.g. **calcsiltite** (a rock composed of carbonate grains of silt size) and **bioclasts** (fossil fragments). Flügel (2004, pp. 683–711) provides an extremely useful set of photographic plates that illustrate each of these 26 standard microfacies types.

These standard microfacies types represent the most common kinds of carbonate microfacies; however, experience in working with carbonate rocks has shown that not every microfacies fits neatly into one of these categories. Students using these standard microfacies types as models should be prepared to accept the likelihood that some microfacies may contain elements of more than one of these standard types, or may not fit any of the types exactly. Considering the wide variety and complexity of carbonate environments and the variations in fossil organisms and other geologic factors that have occurred with time, we could hardly expect anything else. These inconsistencies are likely to be frustrating for beginning students, but become less of a problem as experience is gained in study of carbonate rocks.

9.7.3 *Depositional environments and facies zones*

Limestones in the modern ocean are deposited in several kinds of platform/shelf environments, which include rimmed platforms, open shelves, ramps, isolated platforms, and epeiric platforms (Fig. 9.39). We assume that ancient limestones were deposited in similar environments.

Wilson (1975, pp. 26–27) suggested a general model for carbonate deposits (based on the rimmed platform setting in Fig. 9.39), which encompasses nine major facies belts or **facies zones** corresponding to nine major carbonate environments. These facies zones are shown in

Table 9.9 *Standard carbonate microfacies types*

SMF		
No.	Name	Distinguishing characteristics
1	Spiculite	Dark, organic-rich, clayey mudstone or wackestone containing silt-sized spicules; spicules commonly oriented, generally siliceous monaxons, commonly replaced by calcite
2	Microbioclastic calcisiltite	Small bioclasts and peloids with a fine grainstone or packstone texture; mm-scale ripple cross-lamination common
3	Pelagic mudstone or wackestone	Micritic matrix with scattered fine sand- or silt-size grain composed of pelagic microfossils (e.g. radiolarians or globigerinids) or megafauna (e.g. graptolites or thin-shelled bivalves)
4	Microbreccia or bioclastic–lithoclastic packstone	Worn grains of originally robust character; may consist of locally derived bioclasts and/or previously cemented lithoclasts; may also include quartz, chert, or other kinds of carbonate fragments; commonly graded
5	Bioclastic grainstone–packstone or floatstone	Composed mainly of bioclasts derived from organisms inhabiting reef top and flanks; geopetal fillings and infiltrated fine sediment in shelter cavities common
6	Reef rudstone	Large bioclasts of reef-top or reef-flank organisms; no matrix material
7	Boundstone	Composed of <i>in situ</i> sessile organisms. May be called framestone if composed of massive upright and robust forms, bindstone if composed of encrusting lamellar mats enclosing and constructing cavities and encrusting micrite layers, and bafflestone if composed of delicate, complex, frond-like forms; commonly, micrite clotted or vaguely pelleted
8	Whole-fossil wackestone	Sessile organisms rooted in micrite, which contains only a few scattered bioclasts; well-preserved infauna and epifauna
9	Bioclastic wackestone or bioclastic micrite	Micritic sediment containing fragments of diverse organisms jumbled and homogenized through bioturbation; bioclasts may be micritized
10	Packstone–wackestone with coated and worn bioclasts in micrite	Sediment displays textural inversion; i.e. grains show evidence of formation in high-energy environment but contain mud matrix
11	Grainstone with coated bioclasts in sparry cement	Bioclasts cemented with sparry cement; bioclasts may be micritized
12	Coquina, bioclastic grainstone or rudstone	A shell hash in which certain types of organisms dominate (e.g., dasyclads, shells, or crinoids); lacks mud matrix
13	Oncoid biosparite grainstone	Composed mainly of oncoids in sparry cement

Table 9.9 (*cont.*)

SMF		
No.	Name	Distinguishing characteristics
14	Lags	Coated and worn particles; may include ooids and peloids that are blackened and iron-stained; with phosphate; may also include allochthonous lithoclasts
15	Oolite, ooid grainstone	Well-sorted, well-formed, multiple-coated ooids ranging from 0.5 to 1.5 mm in diameter; fabric commonly overpacked; invariably cross-bedded
16	Pelsparite or peloidal grainstone	Probable fecal pellets; may be admixed with concentrated ostracod tests or foraminifers; may contain centimeter-thick graded laminae and fenestral fabric
17	Grapestone pelsparite or grainstone	Mixed facies of isolated peloids, agglutinated peloids, and aggregate grains (grapstones and lumps); may include some coated grains
18	Foraminiferal or dasycladacean grainstone	Consists of concentrations of tests, commonly mixed with peloids
19	Loferite	Laminated to bioturbated, pelleted lime mudstone–wackestone; may grade to pelsparite with fenestral fabric; ostracod–peloid assemblage common in mudstones; may also include micrite with scattered foraminifers, gastropods, and algae
20	Algal stromatolite mudstone	Stromatolites
21	Spongiostrome	Tufted algal fabric in fine lime-mud sediment
22	Micrite with large oncoids	Wackestone or floatstone containing oncoids
23	Unlaminated, homogeneous, unfossiliferous pure micrite	Micrite; may contain crystals of evaporitic minerals
24	Rudstone or floatstone with coarse lithoclasts and/or bioclasts	Clasts commonly consist of unfossiliferous micrite or calcisiltite, and may have an edgewise or imbricate arrangement; may be cross-bedded; matrix sparse
25	Laminated evaporite–carbonate mudstone	
26	Pisoid cementstone, rudstone or packstone	

Source: Wilson, 1975, pp. 64–69, with additions (SMF 25, 26) by Flügel, 2004, p. 681.

Fig. 9.40, which includes an additional zone (10) added by Flügel (2004, p. 662). The major characteristics of the facies zone are as follows:

1. Facies zone 1 – dark shales and carbonate mudstones; deposited in deeper-water basin environment, commonly below the oxygenation level
2. Facies zone 2 – very fossiliferous limestones with shale interbeds; deposited on the open-sea shelf below storm-wave base but above the oxygenation level

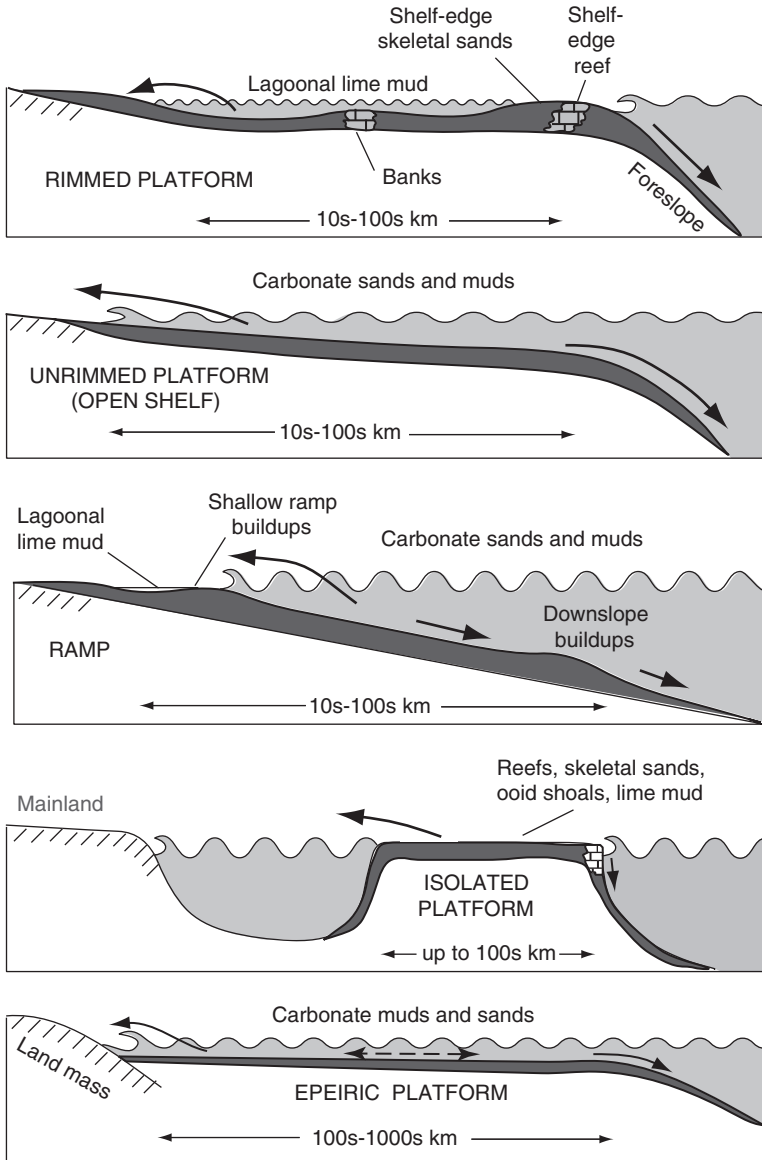


Figure 9.39 Schematic representation of principal kinds of marine platform/shelf carbonate environments. [From Boggs, S., 2006, *Principles of Sedimentology and Stratigraphy*, 4th edn., and Fig. 11.2, p. 369, based on James and Kendall (1992) and Wright and Burchette (1996). Reproduced by permission of Prentice-Hall, Upper Saddle River, N. J.]

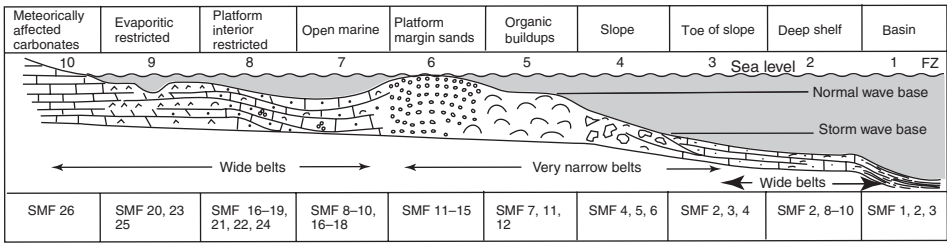


Figure 9.40 Facies zones (FZ) and standard microfacies (SMF) types of the Wilson model for describing a rimmed carbonate platform. [After Wilson, J. E., 1975, *Carbonate Facies in Geologic History*: Springer-Verlag, New York, NY, Fig. XII-1, p. 351, with additions from Flügel, 2004, p. 662, reproduced by permission.]

- Facies zone 3 – fine-grained, graded to nongraded limestones, possibly containing exotic blocks derived from the foreslope; deposited on the toe of the foreslope
- Facies zone 4 – fine- to coarse-grained limestone with breccia and exotic blocks, deposited on the foreslope seaward of the platform edge; carbonate debris derived from facies zone 5.
- Facies zone 5 – organic buildups (reefs and other bioherms) composed of various kinds of boundstones, particularly framestones; commonly make up the edge or rim of the carbonate platform, but may not be present on all carbonate platforms
- Facies zone 6 – winnowed, sorted carbonate sands (calcarenites) composed particularly of skeletal grains derived from facies belts 4 and 5; ooids also common; deposited in very shallow water immediately landward of organic buildups or, if no buildups present, at the very edge of the platform
- Facies zone 7 – mixed carbonate deposits that may include carbonate sands derived from belt 6, wackestones, mudstones; possible interbeds of shale or silt; patch reefs or other bioherms may be present; deposited in shallow water on the open-shelf platform where water circulation is normal
- Facies zone 8 – bioclastic wackestones, lithoclastic and bioclastic sands, pelleted carbonate mudstones, stromatolites, interbeds of shale or silt; deposited in shallow water on inner platform where water circulation may be restricted
- Facies zone 9 – nodular dolomites and anhydrites (on platforms where evaporative conditions exist); stromatolites; siliciclastic muds or silts; deposited in intertidal to supratidal zone
- Facies zone 10 – limestones in subaerial or subaquatic settings that have been affected by meteoric waters under meteoric–vadose and marine–vadose conditions

Note from Fig. 9.40 that each facies zone is characterized by a few standard microfacies types; however a particular standard microfacies type can appear in more than one facies zone.

The facies zones shown in Fig. 9.40 are based on the rimmed platform model (Fig. 9.39), as mentioned. Flügel (2004, p. 661) points out that this model is overcomplete, and that platforms with a reduced number of facies zones are the common case. See Flügel (2004, pp. 664–670) for discussion of facies zones on ramps, unrimmed platforms, and epeiric platforms. As suggested by Figs. 9.39 and 9.40, limestones are deposited in a variety of marine environments. From the shoreline outward, these environments may range from the supratidal through the shallow subtidal, open-shelf lagoon, platform margin (carbonate

sands or carbonate buildups), and slope to the deep-marine basin environment. Within these environments, a variety of depositional processes operate to generate, transport, and deposit sediment. These processes may include those that are mainly chemical (e.g. inorganic precipitation of ooids and lime mud), mainly biochemical (e.g. secretion of CaCO_3 by organisms to build skeletal elements, decomposition of calcareous algae to release aragonite needles, organic production of pellets, micritization of skeletal grains by endolithic algae and fungi), and mainly physical (e.g. erosion of semiconsolidated lime mud to generate intraclasts, physical breakdown of larger particles, transport and deposition of terrigenous grains). Thus, depending upon the environment and the process or processes involved, the many kinds of limestones discussed in preceding sections of this chapter are generated. Environmental analysis is not the major focus of this book; therefore, I do not provide here greater coverage of marine carbonate depositional environments and depositional processes than that discussed above. The subject of carbonate environments is so extensive in scope that the entire book could be devoted to that subject alone. In fact, several books dealing with carbonate environments are available. For a short summary of carbonate environments and depositional processes, see Boggs (2006, ch. 11).

9.7.4 Chemistry of marine carbonate deposition

Regardless of the specific marine depositional environment, the formation of carbonate sediment involves chemical processes in some way. Although some of these processes may be biogenically induced, and mechanical processes may erode and transport carbonate sediment, chemistry remains a first-order control on the formation of carbonate deposits. As discussed in Section 9.2, aragonite, calcite, and magnesian calcite are the dominant minerals in limestones. What chemical factors are particularly important to precipitation of these minerals? Let's begin an answer to this question by examining the **calcium carbonate solubility product**, which is related to CO_2 partial pressure, temperature, and salinity.

The equilibrium solubility product (K) of calcium carbonate is the ionic activity solubility product of calcium and carbonate in any solution that is in equilibrium with calcium carbonate, as shown by the relationship

$$K = \frac{a_{\text{Ca}^{2+}} \times a_{\text{CO}_3^{2-}}}{a_{\text{CaCO}_3}} \quad (9.4)$$

The terms Ca^{2+} and CO_3^{2-} refer to the activities of Ca^{2+} and CO_3^{2-} ions in the aqueous solution, and CaCO_3 refers to the activity of CaCO_3 in the carbonate phase. Activities are a function of concentration, and the relation between activity and concentration is

$$\alpha = X \quad (9.5)$$

where X for solid phases (e.g. CaCO_3) is the mole fraction (number of moles of a component divided by the total number of moles of all components in solid solution) of

the pure end member in the solid solution. For aqueous species, it is expressed as the concentration of the ion in the electrolyte solution (e.g. mol kg⁻¹ or mol L⁻¹). The term γ is the rational activity coefficient (see Berner, 1971, p. 21, for an equation for calculating calcium activity). For pure end-member composition, $\gamma = 1$ and $X_{\text{CaCO}_3} = 1$. For very dilute solutions, activity and concentration are approximately the same.

The solubility product (K) is the value measured at equilibrium or calculated by use of the equation

$$\Delta G = -RT \ln K \quad (9.6)$$

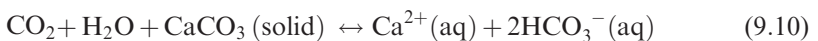
where ΔG refers to change in Gibbs free energy, R is the gas constant (8.314 J mol⁻¹ K⁻¹), T is absolute temperature (Kelvin), and \ln is natural logarithm. Gibbs free energy (G) = $H - TS$, where H is enthalpy = $U + PV$, U is internal energy, P is pressure, V is volume, T is temperature (Kelvin), and S is entropy.

The calcium carbonate solubility product is a constant for a given set of conditions, but varies as a function of CO₂ partial pressure, temperature, and salinity. The solubility product increases with rising partial pressure of CO₂ and increasing salinity, but decreases with increasing temperature. In practical terms, this relationship means that aragonite and calcite are most likely to precipitate under conditions of (1) low CO₂ partial pressure, (2) low salinity, and (3) high temperature. Further, the solubilities of aragonite and calcite under a given set of conditions are not the same. Aragonite (and Mg-calcite) is generally more soluble than calcite; however, calcite may not precipitate in preference to aragonite owing to the presence of specific inhibitors in seawater (e.g. Mg).

The amount of dissolved carbon dioxide in seawater exerts a major control on the solubility of calcium carbonate, as indicated by the following equilibrium relations:



The interaction between CO₂, H₂O, and **solid** CaCO₃ can be summarized as



The dissociation of H₂CO₃ and HCO₃⁻ in seawater can be expressed approximately by the following equations:

$$K'1 = \frac{[\text{H}^+][\text{HCO}_3^-]}{[\text{H}_2\text{CO}_3]} \quad (9.11)$$

$$K'2 = \frac{[\text{H}^+][\text{CO}_3^{2-}]}{[\text{HCO}_3^-]} \quad (9.12)$$

where $K'1$ and $K'2$ are apparent dissociation constants (which change with temperature, pressure, and salinity), and brackets denote concentration. The following

equations show the relation of pH to the carbon dioxide/water system (Milliman, 1974, p. 9):

$$\text{pH} = \text{p}K'1 + \log \frac{[\text{HCO}_3^-]}{[\text{H}_2\text{CO}_3]} \quad (9.13)$$

$$\text{pH} = \text{p}K'2 + \log \frac{[\text{CO}_3^{2-}]}{[\text{HCO}_3^-]} \quad (9.14)$$

where p refers to negative logarithm. At pH values less than 7.5, the main CO_2 species are H_2CO_3 and HCO_3^- and Equation 9.13 approximates the system. At pH values greater than 7.5 the dominant species are HCO_3^- and CO_3^{2-} and Equation 9.14 applies.

Clearly, the amount of CO_2 dissolved in seawater affects the pH of the water. The decrease in pH with increasing CO_2 partial pressure is not, however, a linear function because the high alkalinity of seawater tends to buffer the seawater system. Carbonate alkalinity (CA) is defined as

$$\text{CA} = [\text{HCO}_3^-] + 2[\text{CO}_3^{2-}] \quad (9.15)$$

For each mole of water and dissolved CO_2 that react, some yield H^+ and HCO_3^- . Owing to the high alkalinity of seawater, however, a high proportion of the dissolved CO_2 may form undissociated H_2CO_3 . Also, some of the CO_2 is held in CO_3^{2-} . Thus, the addition of n moles of CO_2 may not release $2n$ moles of H^+ , as predicted by Equations 9.7–9.9, but a much smaller quantity. Therefore, the pH of seawater may change less than theoretical considerations predict with respect to changes in partial pressure of CO_2 . Values of pH for seawater rarely fall outside the range of 7.8 to 8.3. On the other hand, freshwaters are poorly buffered and may show much larger changes of pH with variations in CO_2 partial pressure.

Nonetheless, CO_2 partial pressure exerts a very important control on carbonate solubility, and any process that removes CO_2 from seawater alters its carbonate equilibrium and may bring about carbonate precipitation (Equation 9.10). Thus, loss of CO_2 owing to increased temperature, decreased pressure (water agitation), or photosynthesis can theoretically cause precipitation of CaCO_3 .

Although a great deal of the carbonate sediment in the geologic record is probably related to organic activity in some way, an important fraction of this sediment may be of abiotic (inorganic) origin. Conventional wisdom has it that both the composition and crystal habit of abiotic carbonate minerals are influenced by the Mg/Ca ratio of the water. Precipitation from waters with low Mg/Ca ratios, such as meteoric waters, is thought to produce equant crystals of low-magnesian calcite. By contrast, precipitation from waters with high Mg/Ca ratios, such as seawater or hypersaline brines, is thought to form acicular or elongate crystals of mainly high-magnesian calcite and/or aragonite. Given and Wilkinson (1985) maintain, however, that many exceptions to this pattern occur in modern carbonate environments.

All this is by way of pointing out that the influence of Mg/Ca ratios on the mineralogy, composition, and morphology of abiotic carbonate minerals is an important and controversial problem. Some investigators (e.g. Mucci and Morse, 1983) suggest that the Mg/Ca ratio of the water is the primary factor that determines whether abiotic carbonate minerals are

calcite, high-magnesian calcite, or aragonite. Several workers in addition to Mucci and Morris (e.g. Berner, 1975; Reddy and Wang, 1980) have suggested that Mg^{2+} strongly inhibits the precipitation of calcite and that aragonite or Mg-calcite preferentially precipitates in the presence of Mg^{2+} in seawater. Some growth inhibitors may also affect aragonite precipitation. For example, Berner *et al.* (1978) demonstrated experimentally that organic compounds found in natural humic and fulvic acids or in phosphatic compounds can form thin organophosphatic coatings on aragonite seed nuclei, which inhibit nuclei growth and prevent or delay aragonite precipitation.

On the other hand, Given and Wilkinson (1985) suggest that mineralogy, composition, and morphology are controlled largely by the kinetics of surface nucleation and the amount of reactants, principally carbonate ions, at growth sites. That is, Mg/Ca ratios only indirectly control the precipitated phases. They suggest that equant crystals form under conditions where CO_3^{2-} ion concentration and/or rates of fluid flow are low. Under these conditions, growth sites on precipitating crystals are starved of carbonate ions, *c*-axis growth is retarded, and an equant crystal results. Where carbonate ions are abundant and/or rates of fluid flow are high, *c*-axis growth is enhanced and an acicular or elongate crystal results. Furthermore, they maintain that the magnesium content of calcite is also controlled by crystal-growth rates. At high CO_3^{2-} concentration and rapid crystal-growth rates, acicular high-magnesian calcite forms. At lower CO_3^{2-} concentrations and lower-crystal growth rates, low-magnesian calcite forms. Finally, they suggest that aragonite precipitation is favored when rates of reactant supply are high, whereas calcite forms when rates are low. Morse (1985) takes strong exception to Given and Wilkinson's stance that carbonate-ion concentration and crystal-growth rates are the dominant factors controlling the carbonate mineral phases precipitated. He regards this hypothesis as largely incorrect and unsupported by experimental and observational data. Possibly, both kinetics and Mg/Ca ratios influence the precipitation of abiotic carbonates.

9.8 Nonmarine carbonates

9.8.1 Introduction

Because most carbonate rocks in the stratigraphic record are of marine origin, the preceding sections of this chapter have focused almost exclusively on marine limestones. Carbonate rocks also form in a variety of nonmarine settings, including lakes, streams, marshes, springs, caves, soils, and dune environments. The volume of these nonmarine or terrestrial carbonates is small, but they are an interesting addition to the overall carbonate record. Also, when they can be identified in ancient deposits, they make useful paleoenvironmental indicators. Therefore, a very brief description of the principal kinds of nonmarine carbonate rocks is given here.

9.8.2 Lacustrine carbonates

Carbonate sediments occur in some freshwater lakes such as Lake Zürich and Lake Constance in Europe, as well as in saline lakes such as Great Salt Lake, Utah and the

ephemeral playa lakes of Death Valley, California. The principal carbonate mineral formed in freshwater lakes is low-Mg calcite. The deposits of saline lakes may include low-Mg calcite, high-Mg calcite, and protodolomite (Chapter 10). Aragonite and magnesite (MgCO_3) may also occur in lake sediments but are uncommon minerals. Differences in the mineralogy and composition of these lacustrine carbonate minerals have commonly been regarded to reflect variations in Mg/Ca ratios of the lake water. That is, low-Mg calcite forms at low Mg/Ca ratios (< 2), high-Mg calcite forms at high Mg/Ca ratios (2–12), and aragonite and magnesite form at very high Mg/Ca ratios (> 12). As discussed above, however, Given and Wilkinson (1985) maintain that carbonate-ion availability and crystal-growth rate may also be important considerations. Deposits of saline lakes with very high alkalinity may include some rare carbonate minerals that commonly do not occur in marine environments; e.g. vaterite ($\mu\text{-CaCO}_3$), monohydrocalcite ($\text{CaCO}_3 \cdot \text{H}_2\text{O}$), trona ($\text{NaHCO}_3 \cdot \text{Na}_2\text{CO}_3 \cdot 2\text{H}_2\text{O}$), nahcolite (NaHCO_3), and natron ($\text{Na}_2\text{CO}_3 \cdot 10\text{H}_2\text{O}$).

Lacustrine carbonate sediments may include **abiotic precipitates**, **algal carbonates**, and **carbonate shell accumulations**. These carbonate materials may be mixed to various degrees with organic matter; biogenic silica (mainly diatom frustules); fine, detrital siliciclastics; and evaporite minerals. Abiotic precipitation is probably important mainly in saline lakes in areas where evaporation rates are high. Under these conditions, both loss of water and loss of CO_2 can trigger precipitation of calcite and Mg-calcite. Important quantities of detrital silt and clay may occur with the carbonate minerals, as well as evaporitic minerals such as gypsum and halite. In ephemeral lakes such as playa lakes, variations in influx of terrigenous detritus may be reflected in alternating layers of mud and salts, with various amounts of carbonate minerals. In freshwater lakes, precipitation of low-magnesian calcite probably occurs largely as a result of CO_2 loss owing to high surface-water temperatures and the photosynthetic activities of planktonic algae. Again, influx of detrital clay and silt may be significant, and this detritus may mix with carbonate sediment to form chalky or marly deposits. Alternatively, terrigenous detritus may be so abundant that it completely masks or swamps carbonate sediment.

In some lakes, varves consisting of alternating thin layers of calcite-rich and clay-rich sediments may be present, reflecting variations in depositional conditions from summer to winter. In addition to their role in photosynthesis, algae may also form stromatolites and oncolites in both freshwater and saline lakes. Some algae such as *Chara* produce calcareous tubes and round, calcified reproductive bodies that become part of the carbonate sediment. Rooted, aquatic plants may induce precipitation of carbonate, which may cover the plants with a heavy carbonate crust. Nonmarine invertebrates such as ostracods, molluscs, and gastropods are common in many lakes and may generate shell deposits in the marginal areas of the lakes. These deposits commonly make up only a small volume of the overall carbonate sediments. Ooids are present in some saline lakes, e.g. Great Salt Lake, Utah, and one occurrence of low-Mg ooids in a freshwater lake (Higgins Lake, Michigan) has also been reported. For an excellent short review of carbonate deposition in lakes, see Dean and Fouch (1983); see also Tucker and Wright (1990, pp. 164–190.)

9.8.3 Carbonates in rivers, streams, and springs

Only a very small volume of carbonate sediment forms in the flowing water of rivers, streams, and springs. Commonly, such water is too undersaturated with calcium carbonate to precipitate carbonate minerals; however, saturation may occur in waters that drain regions underlain by carbonate rocks. Carbonate precipitated from streams and cold-water springs commonly consists of low-Mg calcite, whereas precipitates from hot springs may also include aragonite. The terminology of carbonate sediments formed in these freshwater environments is a bit confusing. The general name for all of these deposits is **travertine**. On the other hand, some authors apply the name travertine only to the more massive, dense, finely crystalline varieties of these deposits. These carbonates range in color from tan to white or cream, and some may be banded (Fig. 9.41). The more porous, spongy, or cellular varieties of these freshwater carbonates (e.g. Fig. 9.42), which commonly form as encrustations on plant remains, are called **tufa**. Pedley (1990) defines tufa as “cool water deposits of highly porous or spongy freshwater carbonate rich in microphytic and macrophytic growth, leaves and woody tissue.” Some workers use the term **calcareous sinter** to refer to both travertine and tufa; however, Flügel (2004, pp. 734–735) suggests that sinter is predominantly inorganic in origin and is characterized by well-developed lamination and lack of porosity.

Precipitation of travertine occurs predominantly in springs and spring-fed lakes and at waterfalls or cascades. Chafetz and Folk (1984) suggest that, morphologically, travertines can occur as (1) waterfall or cascade deposits, (2) lake-fill accumulations, (3) sloping mounds, fans, or cones, (4) terraced mounds, and (5) fissure ridges. Precipitation of travertine requires that groundwaters or streams be supersaturated with calcium carbonate with respect to calcite and supersaturated in CO_2 with respect to air. Precipitation can occur in cold-water springs owing to loss of CO_2 resulting from higher temperatures at the mouth of the spring and

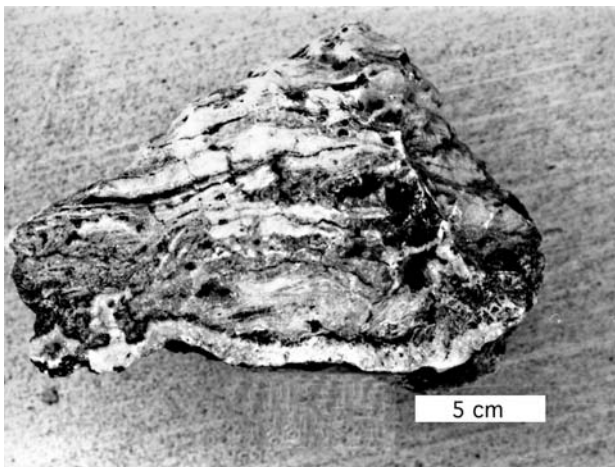


Figure 9.41 Crudely banded travertine. Unknown location. (Specimen furnished by R. A. Linder.)

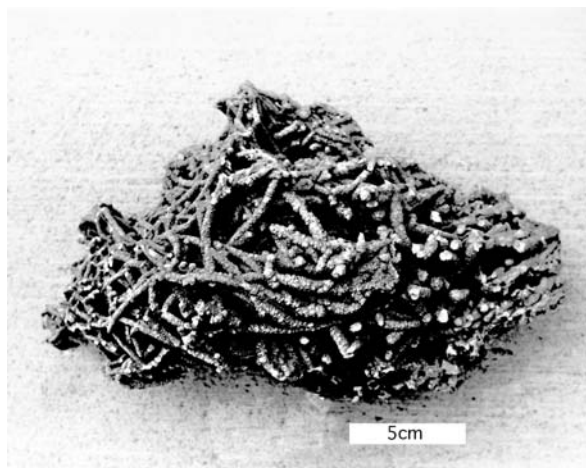


Figure 9.42 Tufa formed in a hot spring, Nevada, USA. (University of Oregon collection.)

exposure of spring water to the atmosphere (decrease in pressure). Agitation of water in the springs and photosynthesis by plants are additional factors in CO_2 loss. In hot springs, evaporation of water around the mouths of the springs may also play a role in CO_2 loss. Away from the mouths of springs, photosynthesis by blue-green algae (cyanobacteria) and mosses are more important factors in CO_2 loss. Tufas apparently form as a result of precipitation of calcite onto plants such as mosses and algae. Chafetz and Folk (1984) conclude that bacteria are also important agents in precipitation of travertines. Precipitation of travertine at waterfalls results from CO_2 loss as a result of decreased pressure arising from strong water agitation (Julia, 1983) and possibly also from photosynthesis by algae and mosses. These plants become calcified by the travertine, resulting in an irregular tangle of plant molds and inorganic crusts and cements. For further discussion of tufa and travertine, see Pedley (1990), Heimann and Sass (1989), and Flügel (2004, pp. 14–18).

Thus, depending upon their specific mode of origin, travertine forms a wide variety of deposits. These deposits may range from vertical sheets built by incrustations of mosses in hanging springs and cascades to horizontal sheets formed in pools and dams. Travertine includes varieties that are relatively dense and massive; relatively dense and banded; and porous, spongy, cellular, or laminated owing to encrustation on algae, mosses, and other plants. In addition to layered travertine, ooids have been reported from the agitated waters of some hot springs. Ancient travertine commonly occurs in association with sedimentary strata or alluvium but occur also in some volcanic and granitic terrains.

9.8.4 *Speleothem (cave) carbonates*

Carbon dioxide-rich groundwaters that migrate through carbonate formations dissolve away parts of the formations and create solution pipes, sinks, and caves. The geomorphological

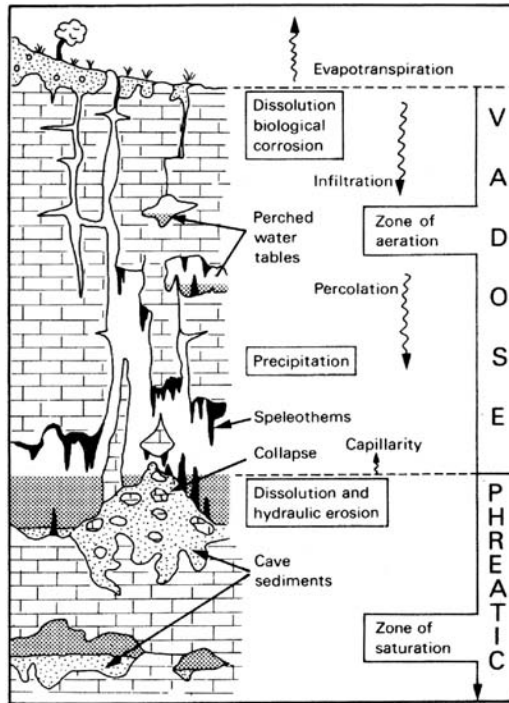


Figure 9.43 Features of a mature karst profile. The vadose zone is the groundwater zone of aeration, and the phreatic zone is the zone of saturation where pore space is filled with water. Note that speleothems occur especially in the vadose zone, whereas collapse breccias and other cave sediments are common in the phreatic zone. [After Esteban, M. and C. F. Klappa, 1983, Subaerial exposure environment, in Scholle, P.A., D.G. Bebout, and C.H. Moore. (eds.), *Carbonate Depositional Environments*: AAPG Memoir 33, Fig. 5, p. 4, as modified by Scoffin, T.P., 1987, *Carbonate Sediments and Rocks*: Blackie, Glasgow Fig. 12.1, p. 147. Reproduced by permission of AAPG, Tulsa, OK.)

features resulting from such solution activity are referred to as **karst** features (Fig. 9.43). The characteristics of karsts are explored in detail in the multi-authored volume, *Perspectives on Karst Geomorphology, Hydrology, and Geochemistry*, edited by Harmon and Wicks (2006).

When carbonate- and CO_2 -saturated groundwater enters air-filled caves, carbonate precipitation occurs on a massive scale owing to loss of CO_2 , probably as a result of decreased pressure and evaporation. Therefore, caves in carbonate terrains are the sites of extensive carbonate deposits, which are referred to collectively as **speleothems**. These deposits may take the form of **stalactites** (conical projection hanging from the roof, formed by dripping water), **stalagmites** (conical dripstone projecting upward from the floor), laminated **flowstones** (formed by flowing water), and **globoids** (cave pearls or cave pisolites formed by precipitation of carbonate as concentric layers around a nucleus). For example, Jones and MacDonald (1989) report cave pisolites up to 8 cm long that formed in rimstone pools in

a cave on Grand Cayman. They suggest that these pisoids formed by a combination of inorganic precipitation and organic processes (calcification of filamentous microorganisms). Caves may also contain collapse breccia consisting of carbonate blocks that have fallen from cave roofs (Fig. 9.43). The various processes by which speleothems form are thoroughly discussed in *Speleogenesis*, a monograph edited by Klimchouk *et al.* (2000).

9.8.5 Caliche (calcrete) carbonates

Soils in arid to semiarid regions, especially those developed on underlying carbonate rocks, may become so enriched in calcium carbonate that they form a caliche or calcrete deposit. Genetically, caliche is defined as a fine-grained, chalky to well-cemented, low-magnesian calcite deposit that formed as a soil in or on pre-existing sediments, soils, or rocks. Esteban and Klappa (1983) suggest, however, as a more useful descriptive definition that “caliche is a vertically zoned, subhorizontal to horizontal carbonate deposit, developed normally with four rock types: (1) massive-chalky, (2) nodular-crumbly, (3) platy or sheet-like, and (4) compact crust or hardpan.” An idealized caliche profile is shown in Fig. 9.44. Esteban and Klappa stress that many variations of this profile exist and that the only consistent relation is that the massive-chalky rock grades downward into the original rock or sediment

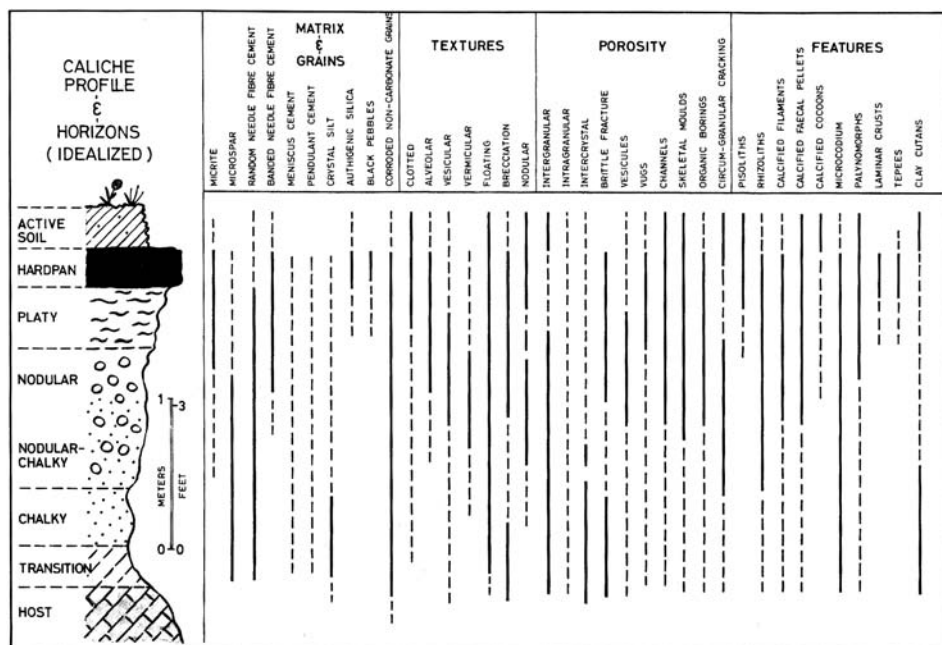


Figure 9.44 Idealized caliche profile and the distribution of major characteristics within the profile. [After Esteban, M. and C.F. Klappa, 1983, Subaerial exposure environment, in Scholle, P. A., D. G. Bebout, and C. H. Moore (eds.), *Carbonate Depositional Environments*: AAPG Memoir 33, Fig. 7, p. 5, reproduced by permission of AAPG, Tulsa, OK.]

through a transition zone. These caliche profiles may extend downward below the soil surface for distances ranging from < 1 m to a few tens of meters.

Soils are formed on carbonate bedrock by physical and chemical weathering processes that result in concentration of insoluble residues from the bedrock. Note: ancient soils are called paleosols (e.g. Retallack, 1997). Calcium carbonate accumulates in the upper soil profile owing to evaporation of carbonate-saturated pore waters drawn to the surface by capillary action. Continued carbonate precipitation and downward mobilization result in formation of a **hardpan**, which is well indurated, lacks visible porosity, and is more resistant to weathering than underlying horizons. This hardpan may contain rhizoliths (root traces) and pisoids; macroscopically it may appear massive or structureless, laminated, brecciated, or nodular.

Platy caliche, which is characterized by horizontal to subhorizontal, platy, wavy, or thinly bedded habit, commonly occurs immediately below the hardpan. Platy caliche may also contain rhizoliths but is more friable and has greater porosity than the hardpan. It probably represents an immature stage in hardpan development. Searl (1989) reports an unusual occurrence of extensive sheetlike and fan developments of columnar calcite within and immediately below hardpan layers in some south Wales calcretes. Individual crystals in this columnar calcite range to 30 cm long. **Nodular caliche** is made up of silt- to pebble-size nodular structures called glaebules, which consist of concentrations of CaCO_3 intermixed in a less carbonate-rich matrix. **Chalky caliche** is generally unconsolidated (non-cemented) and is characterized by the presence of cream to white, silt-size calcite grains. Chalky caliche tends to be homogeneous and structureless. It grades upward into nodular caliche and downward through a transition zone to the host material. Vertical variations in carbonate grains and matrix, textures, porosity, and other features of caliches are summarized in Fig. 9.44. Although the carbonate mineral in most calcretes is calcite, soil profiles cemented with dolomite are also known (e.g. Khalaf, 1990). Such dolomite-cemented profiles are referred to as **dolocretes**.

9.8.6 Eolian carbonates

Wind-blown carbonate sands, referred to as carbonate **eolinites**, occur adjacent to carbonate shorelines. Less commonly, they occur also along the margins of some saline lakes. They consist mainly of sand-size skeletal grains and ooids that were blown inland from carbonate beaches. Much of the land surface of Bermuda, for example, consists of carbonate dune sands, and they are also common on the Bahama islands. Carbonate dune sands exhibit the same general kinds of textures and structures as those occurring in siliciclastic dune deposits. Thus, they are characterized by generally well-rounded, well-sorted grains and may display large-scale, high-angle cross-stratification. The carbonate grains may be bonded with calcite cement. Ancient carbonate eolinites may be difficult to differentiate from carbonate beach sands. If present, terrestrial fossils (land snails, pollen, other plant remains), root traces (rhizoids or rhizoconcretions), and the remains of paleosols are diagnostic.

9.8.7 Other nonmarine carbonates

Palustrine carbonates form in marsh or marsh-like environments by repeated drying of the sediments in carbonate swamps bordering lakes or in episodically drying shallow lakes. They are micritic and display a wide range of exposure features, including brecciated, clotted, and peloidal fabrics. These features are associated with vesicular porosities and structures related to root activity and wetting and drying cycles (e.g. Armenteros and Huerta, 2006). Palustrine carbonates may be interbedded with siliciclastic claystones, marls, sandstones, and coals.

Peritidal carbonates are deposited in the zone between maximum high tide and maximum low tide in marginal marine and shoreline depositional environments. Deposition is controlled by a number of factors (tidal range, wave energy, sediment supply) that include periodic desiccation (Tucker and Wright, 1990, pp. 137–164). The characteristics of peritidal carbonates include fine-scale laminations, desiccation structures, tepee structures, microbial/algal mats, fenestral fabrics, mud intraclasts, skeletal remains, and vadose pisoids (Flügel, 2004, p. 749).

Further reading

- Adams, A. E. and W. S. MacKenzie, 1998, *A Color Atlas of Carbonate Sediments and Rocks Under the Microscope*: John Wiley and Sons, New York, NY.
- Alonso-Zarza, A. M. and L. H. Tanner (eds.), 2006, *Paleoenvironmental Record and Applications of Calcretes and Palustrine Carbonates*: Geological Society of America Special Paper 416.
- Carozzi, A. V., 1989, *Carbonate Rock Depositional Models – A Microfacies Approach*: Prentice-Hall, Englewood Cliffs, NJ.
- Demicco, R. V. and L. A. Hardie, 1994, *Sedimentary Structures and Early Diagenetic Features of Shallow Marine Carbonate Deposits*: SEPM Atlas Series 1.
- Faure, G. and T. M. Mensing, 2005, *Isotopes: Principles and Applications*, 3rd edn.: John Wiley and Sons, Hoboken, NJ.
- Flügel, E., 2004, *Microfacies of Carbonate Rocks: Analysis, Interpretation and Application*: Springer-Verlag, Berlin.
- Hoefs, J., 1997, *Stable Isotope Geochemistry*, 4th edn.: Springer-Verlag, Berlin.
- Keith, B. D. and C. W. Zuppann (eds.), 1993, *Mississippian Oolites and Modern Analogs*: AAPG Studies in Geology 35.
- Morse, J. W. and F. T. Mackenzie, 1990, *Geochemistry of Sedimentary Carbonates*: Elsevier, Amsterdam.
- Peryt, T. (ed.), 1983, *Coated Grains*: Springer-Verlag, Berlin.
- Scholle, P. A. and D. S. Ulmer-Scholle, 2003, *A Color Guide to the Petrography of Carbonate Rocks: Grains, Textures, Porosity, Diagenesis*: AAPG Memoir 77.
- Sharp, Z., 2007, *Principles of Stable Isotope Geochemistry*: Prentice-Hall, Upper Saddle River, NJ.
- Tucker, M. E. and V. P. Wright, 1990, *Carbonate Sedimentology*: Blackwell Scientific, Oxford.

10

Dolomites

10.1 Introduction

Carbonate rocks range in age from Holocene to Precambrian. The mass of Precambrian carbonate rocks is much smaller than that of Phanerozoic carbonates, which are particularly abundant in stratigraphic sequences of Paleozoic age. Carbonate rocks less than about 100 million years old are dominantly calcium carbonates with a low Mg/Ca ratio consistent with the ratio that would be expected if the rocks formed mainly by accumulation of carbonate skeletal debris. The Mg/Ca ratio rises sharply, but irregularly, with increasing age in carbonate rocks older than about 100 million years. Thus, it has been a commonly accepted tenet that dolomites make up an increasing proportion of carbonate rocks with increasing age and that the average composition of Precambrian carbonate rocks approaches that of the mineral dolomite (Garrels and Mackenzie, 1971, p. 237). This long-accepted view that dolomites increase in abundance relative to other carbonates with increasing age was challenged by Given and Wilkinson (1987). These authors maintain that whereas dolomites do change in relative abundance through time, these changes do not correlate directly with age. Rather, they say that increased amounts of dolomite formation correlate to periods of sea-level highs and continental flooding. In turn, this viewpoint has been challenged by others (e.g. Zenger 1989). Secular variations in dolomite abundance during the Phanerozoic remain a controversial topic; see discussion in Machel (2004).

Whatever the true story of relative abundance, dolomites are an extremely intriguing group of rocks, and they have considerable economic significance as reservoir rocks for petroleum. Certainly, few kinds of sedimentary rocks have generated so much interest and controversy among geologists and geochemists with regard to their origin. Most ancient dolomites are relatively thick, coarse-crystalline, porous to nonporous, massive rocks, many of which appear to have formed through pervasive dolomitization (replacement and recrystallization) of precursor limestones. On the other hand, dolomites that form in modern environments, as well as some ancient dolomites, tend to be thinner and finer-crystalline and otherwise lack distinctive evidence of massive dolomitization. The origin of these fine-grained dolomites, as well as the mechanisms responsible for large-scale, pervasive dolomitization of ancient limestones, has been hotly debated by geologists for well over half a century.

In this chapter, we examine first the mineralogy, textures, and structures of dolomites. We then take a look at some current ideas and controversies regarding the origin of dolomite.

10.2 Mineralogy of dolomites

10.2.1 Stoichiometric vs. nonstoichiometric dolomite

As shown in Table 9.1, only two minerals belong to the dolomite group: **dolomite** $[\text{CaMg}(\text{CO}_3)_2]$ and **ankerite** $[\text{Ca}(\text{Mg, Fe, Mn})(\text{CO}_3)_2]$. Dolomite forms a limited solid-solution series with ankerite. Perfectly ordered dolomite $[\text{CaMg}(\text{CO}_3)_2]$, in which calcium and magnesium have equal molar proportions, is called **stoichiometric** dolomite. In this ideal dolomite, a plane of CO_3 ions alternates first with a plane of Ca ions, then with a plane of Mg ions (i.e. $\text{CO}_3\text{-Ca-CO}_3\text{-Mg-CO}_3$, and so on), with the *c*-axis of the crystal oriented perpendicular to the stacked planes. Oxide analysis of an ideal dolomite yields 21.9 percent MgO, 30.4 percent CaO, and 47.7 percent CO_2 by weight (Blatt *et al.*, 1980, p. 510). As described by Land (1985), ideal dolomite is the most stable form in which CaCO_3 and MgCO_3 can combine under sedimentary conditions.

Thermodynamically, ideal dolomite has the lowest free energy possible for any combination of subequal amounts of CaCO_3 and MgCO_3 that can be combined under these conditions. Thus, ideal dolomite is the least soluble form in which subequal amounts of these materials can be combined. Any changes in the ideal structure or composition raise the free energy of the crystal and make it more soluble.

Ideal dolomite is rare in the geologic record. Many natural dolomites, particularly modern or Holocene dolomites, are poorly ordered **protodolomite** with an excess of calcium. Although less common, magnesium-rich dolomite is known also. The reported composition of naturally occurring dolomite ranges from about $\text{Ca}_{1.16}\text{Mg}_{0.84}(\text{CO}_3)_2$ to about $\text{Ca}_{0.96}\text{Mg}_{1.04}(\text{CO}_3)_2$ (Land, 1985). The structure of protodolomite may have faultlike steps or dislocations, and trace elements such as Na and Sr may be common in the crystal lattice owing to substitution for Ca or Mg. Isomorphous substitution of divalent ions, particularly ferrous iron, for calcium or magnesium (Table 9.1) is a further reason for departure of natural dolomites from ideal composition.

Land (1985) points out that the very young dolomite that occurs in Holocene environments is poorly ordered, but that it displays at least partial ordering. Crystals are only a few micrometers in size and consist of aggregates of submicrometer crystals that have generally similar orientation to that of neighboring crystals. They have numerous structural defects of various kinds, and great variation in the degree of ordering and calcium enrichment can exist within the crystals. Thus, the crystal structures are highly strained and inhomogeneous, and they are further characterized by a high degree of trace-element substitution. This kind of structurally and compositionally inhomogeneous dolomite is unstable to metastable, and it dissolves or alters much more readily than does more highly ordered dolomite. Metastable phases of dolomite have the potential to achieve a more stable state by undergoing structural or compositional changes with time. Thus, most older Phanerozoic dolomites and Precambrian dolomites are more highly ordered than is Holocene protodolomite.

According to Land, the most common kind of sedimentary dolomite, which is especially characteristic of post-Paleozoic sequences, is **calcium-rich dolomite** that exhibits a lamellar

structure when examined by transmission electron microscopy and electron diffraction. This type of dolomite represents a more stable phase than Holocene dolomite but is still metastable and dissolves more rapidly than ideal dolomite. Continued stabilization of this dolomite can occur through time as a result of solution–reprecipitation, which gradually moves it toward a more ordered state.

Finally, a third common kind of sedimentary dolomite is “**nearly stoichiometric, well-ordered dolomite**,” which is known mostly from Paleozoic and Precambrian sequences. Nonetheless, it is still less well ordered than ideal, stoichiometric dolomite and it is characterized by numerous structural defects, especially various kinds of faultlike features. The density of these structural defects is much less common, however, than in the two preceding kinds of dolomite. Even this “nearly stoichiometric” dolomite is less stable than ideal dolomite owing to the strained and broken bonds associated with the structural defects.

10.2.2 Identifying dolomite in thin section

Dolomite and calcite commonly occur together in many carbonate rocks. Dolomite can be readily identified by X-ray diffraction techniques, but because both dolomite and calcite are uniaxial negative minerals, they may be difficult to distinguish optically. Nesse (1986, p. 144) lists the following criteria that may be used to help make the distinction:

1. Dolomite is more likely to form euhedral crystals than is calcite.
2. Calcite is more likely to be twinned than is dolomite.
3. Twin lamellae in calcite may be parallel or oblique to the long diagonal of the crystal or parallel to the edges of cleavage rhombs but not parallel to the short diagonal. Twin lamellae in dolomite may be parallel to either the long or short diagonals of cleavage rhombs (Fig. 10.1).
4. Dolomite has higher refractive indices, higher specific gravity, and is less reactive in cold, dilute HCl.
5. Dolomite may be colorless, cloudy, or stained by iron oxides, whereas calcite is commonly colorless.

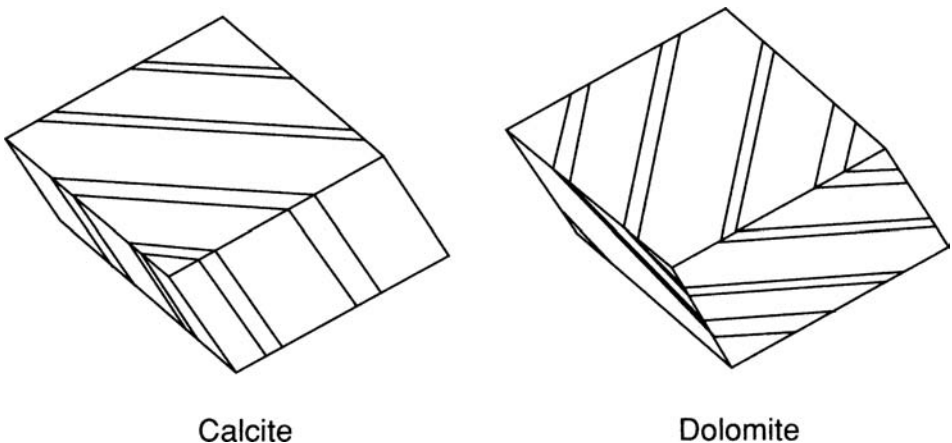


Figure 10.1 Orientation of twin lamellae in calcite and dolomite. (From Nesse, W. D., 1986, *Introduction to Optical Mineralogy*: Oxford University Press, New York, NY, Fig. 10.3, p. 139, reprinted by permission.)

In addition to these criteria, several procedures are available for staining carbonate rocks that allow distinction between dolomite and calcite. For a review of these techniques, see Miller (1988).

10.3 Dolomite textures

Dolomites may be composed of crystals of nearly uniform size (**unimodal size distribution**) or crystals of various sizes (**polymodal size distribution**). Dolomite can occur either as rhomb-shaped euhedral to subhedral crystals or as nonrhombic, commonly anhedral crystals. Rhomb-shaped dolomite commonly displays straight compromise boundaries between crystals and is referred to as **planar dolomite** by Sibley and Gregg (1987), who originally called it **idiotopic dolomite** (Gregg and Sibley, 1984). (A compromise boundary is a surface of contact, not corresponding to a crystal face, between two mutually growing but differently oriented crystals.) Anhedral, nonrhombic dolomite is called **nonplanar dolomite** (originally called **xenotopic dolomite** by Gregg and Sibley, 1984). Boundaries between crystals in nonplanar dolomite are mostly curved, lobate, serrated, or indistinct. On the basis of textural characteristics, Gregg and Sibley (1984) and Sibley and Gregg (1987) divide planar dolomite (or idiotopic dolomite) into four subcategories and nonplanar dolomite (xenotopic dolomite) into three subcategories (Fig. 10.2).

Planar-euhedral dolomite is made up of loosely packed but crystal-supported, well-formed rhombs. The intercrystalline spaces among crystals may be filled with another mineral such as calcite, or the spaces may be empty (porous). The texture of porous dolomites of this type is sometimes referred to as **sucrosic** (sugary). **Planar-subhedral dolomite** has subhedral to anhedral crystals and very low porosity. Dolomites of this type have straight boundaries (Fig. 10.3A) and large numbers of preserved crystal-face junctions. Crystal-face junctions form where straight boundaries between two crystals meet at a distinct angle that is less than about 160° . **Planar void-filling dolomite** consists of euhedral dolomite crystals with terminations that project into open spaces. Such dolomite may be a cement, but it may form also by replacement of the margins of a carbonate grain, with subsequent dissolution of the center of the grain. Alternatively, it could form by replacement of a precursor cement. Some dolomite rhombs may appear to “float” in a limestone (micrite) matrix. Such matrix-supported dolomites are called **planar-porphrotopic**.

Nonplanar-anhedral dolomite is characterized by mainly anhedral crystals with curved, lobate, serrated, or indistinct intercrystalline boundaries (Fig. 10.3B). Inclusions may be abundant in the crystals, and they commonly display undulatory extinction. Nonplanar-anhedral dolomite may be confused with planar-subhedral dolomite; however, the presence of irregular crystal boundaries and the scarcity of crystal-face junctions help to distinguish the two.

Nonplanar void-filling dolomite is irregular-shaped or saddle-shaped dolomite that fills open space. **Saddle dolomite**, described by Radke and Mathis (1980), is a variety of dolomite with a warped crystal lattice that is characterized by curved crystal faces and cleavage and by sweeping extinction (Fig. 10.4). Saddle dolomite crystals of cement origin

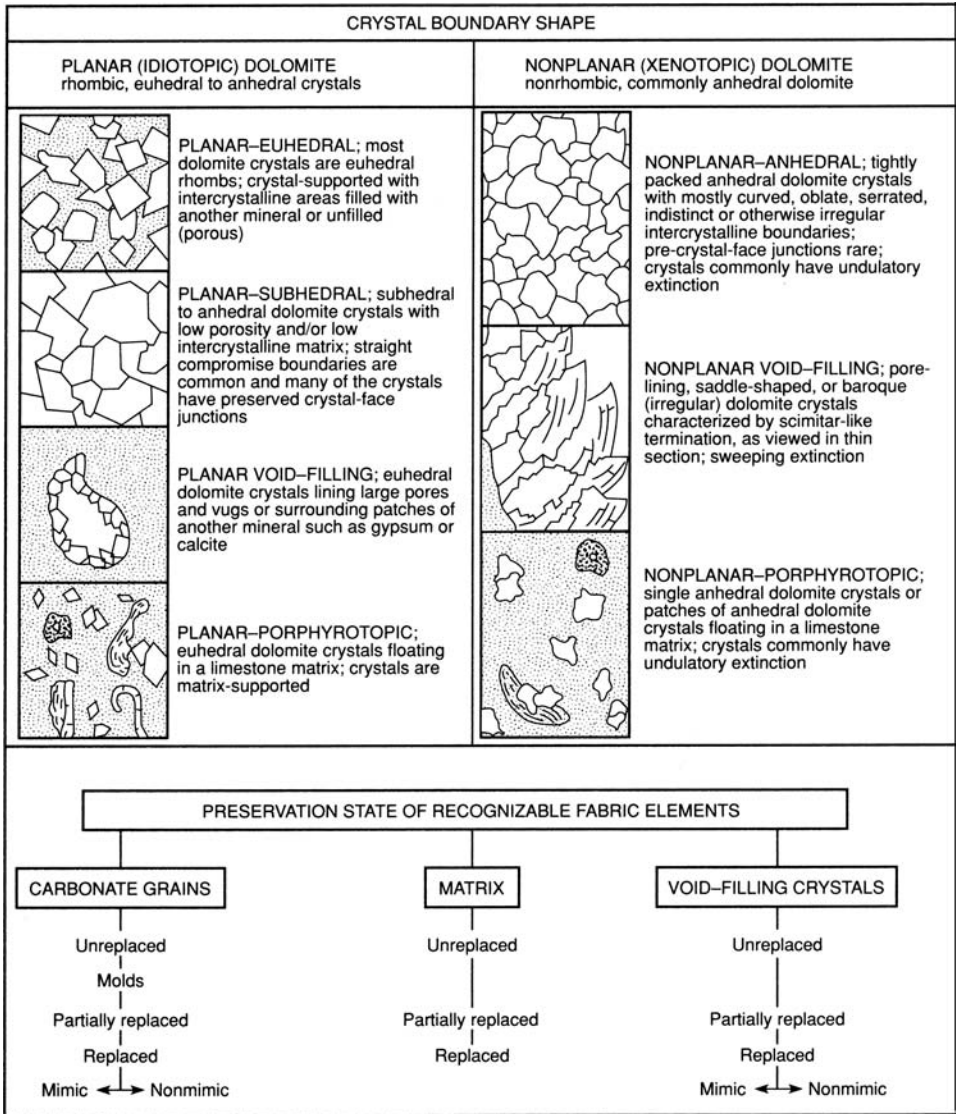


Figure 10.2 Classification of dolomite textures. See text for further explanation. [After Gregg, J. M. and D. F. Sibley, 1984, Epigenetic dolomitization and the origin of xenotopic dolomite texture: *J. Sediment. Petrol.*, **54**, Fig 6, p. 913, and Sibley, D.F. and J.M. Gregg, 1987, Classification of dolomite rock textures: *J. Sediment. Petrol.*, **57**, Fig. 1, p. 968; figures reprinted by permission of SEPM, Tulsa, OK.]

have long, curved edges leading to pointed terminations, resembling somewhat a Persian scimitar.

Nonplanar-porphyrotopic dolomite is similar to planar-porphyrotopic dolomite except that the crystals are mainly anhedral. The crystals probably form by replacing micritic

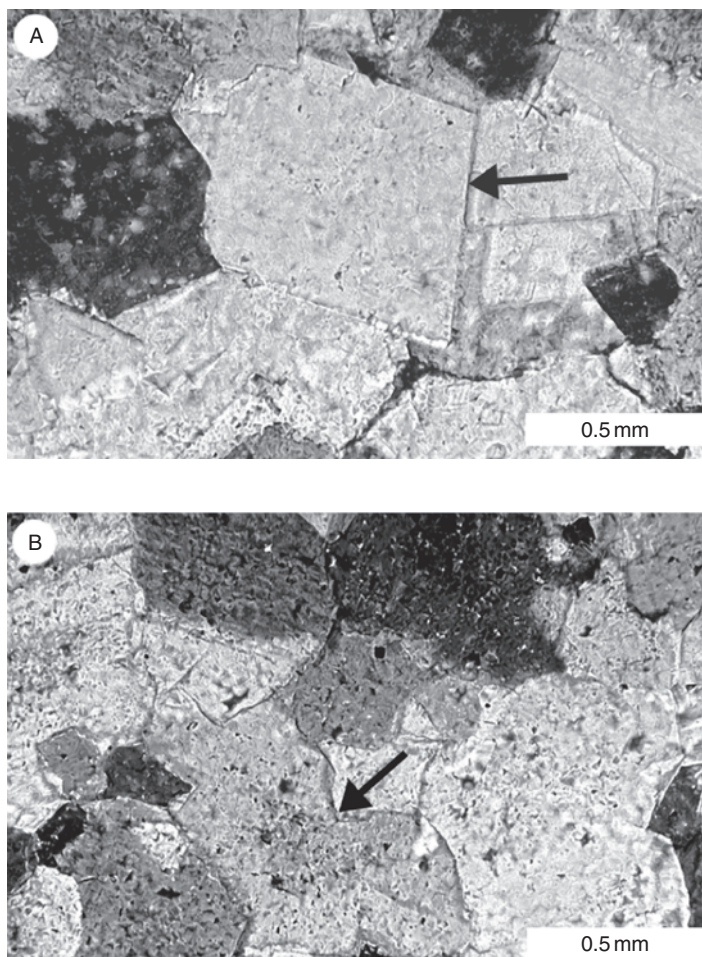


Figure 10.3 Photomicrograph of dolomite crystals: A. Planar dolomite exhibiting euhedral crystals with planar faces (arrow), Bonneterre Formation (Cambrian), Missouri. B. Nonplanar dolomite, with curved or irregular faces, Davis Formation (Cambrian), Missouri. Crossed nicols.

limestones or other limestones. Note: Wright (2001) proposed an additional, **transitional**, textural type in which planar and nonplanar crystals appear side by side.

Dolomites of replacement origin may preserve original carbonate textures to various degrees. Therefore, description of dolomite texture may include characteristics of original carbonate grains, matrix (micrite), and void-filling crystals. As illustrated in Fig. 10.2, carbonate grains may be unreplaced, may be dissolved leaving molds, or may be replaced to various degrees. If carbonate grains are completely replaced, they may be replaced **mimically** or **nonmimically**. Mimic replacement refers to preservation of the form and internal structure of a carbonate grain and generally occurs only if replacement is by many

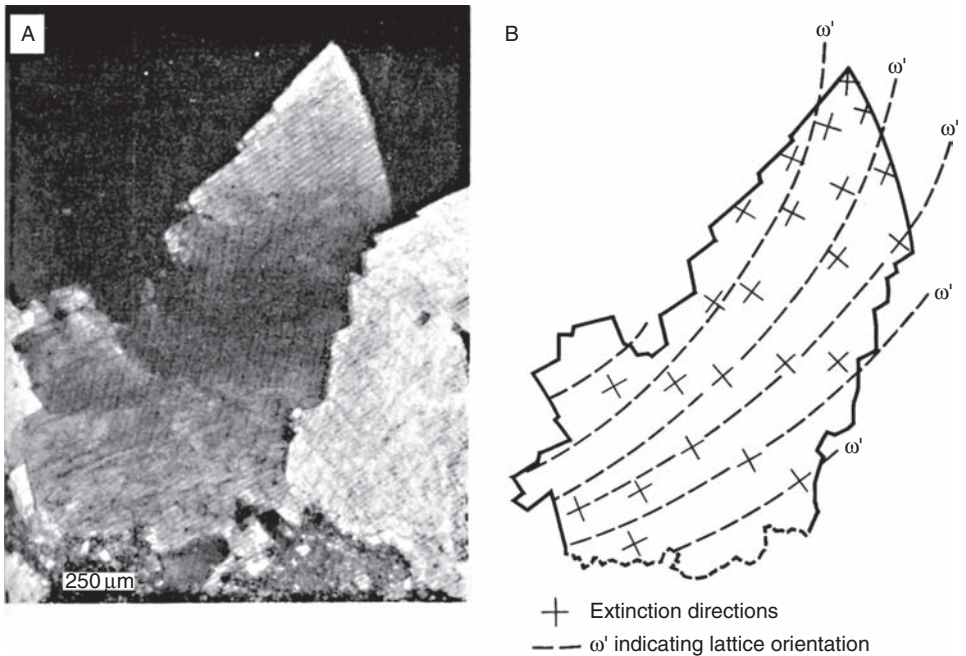


Figure 10.4 Saddle dolomite. A. Photomicrograph of speckle-form dolomite with only part of the crystal in complete extinction. The boundary with the adjacent crystal (right side) has a zigzag appearance. B. Sketch of same crystal. Directions of extinction (crosses) are plotted within the crystal with interpolated ω' traces (dashed lines), which indicate distorted lattice planes. The direction of optimum crystal growth coincides with the region of greatest lattice divergence. (From Radke, B. M. and R. L. Mathis, 1980, On the formation and occurrence of saddle dolomite: *J. Sediment. Petrol.*, **50**, Fig. 3, p. 1153, reprinted by permission of SEPM, Tulsa, OK.]

small dolomite crystals. Nonmimic replacement may preserve the form but not the internal structure of a carbonate grain (Fig. 10.5). If the form of the grain is completely destroyed during replacement, of course no evidence of replacement remains. In many dolomites, only very faint outlines of original carbonate grains remain; these are referred to as **ghosts**. Figure 10.5 illustrates how ghost textures may form in dolomites. Matrix and original void-filling crystals may also be replaced partially or completely.

Gregg and Sibley (1984) proposed that dolomite texture is related to temperature of formation. Below some critical temperature that lies between about 50 °C to 100 °C, called the **critical roughening temperature**, dolomite crystal growth produces dominantly euhedral crystals, resulting in planar textures. Growth of dolomite crystals above this temperature may produce anhedral crystals, resulting in nonplanar texture, although planar crystals can apparently also form above this temperature for reasons not clearly understood. By contrast, calcite has a critical roughening temperature below about 25 °C. Therefore, calcite crystals are commonly anhedral. It is not completely certain, however, if a critical roughening temperature exists for replacive dolomites (Braithwaite, 1991). See also Machel (2004) and Gregg (2004).

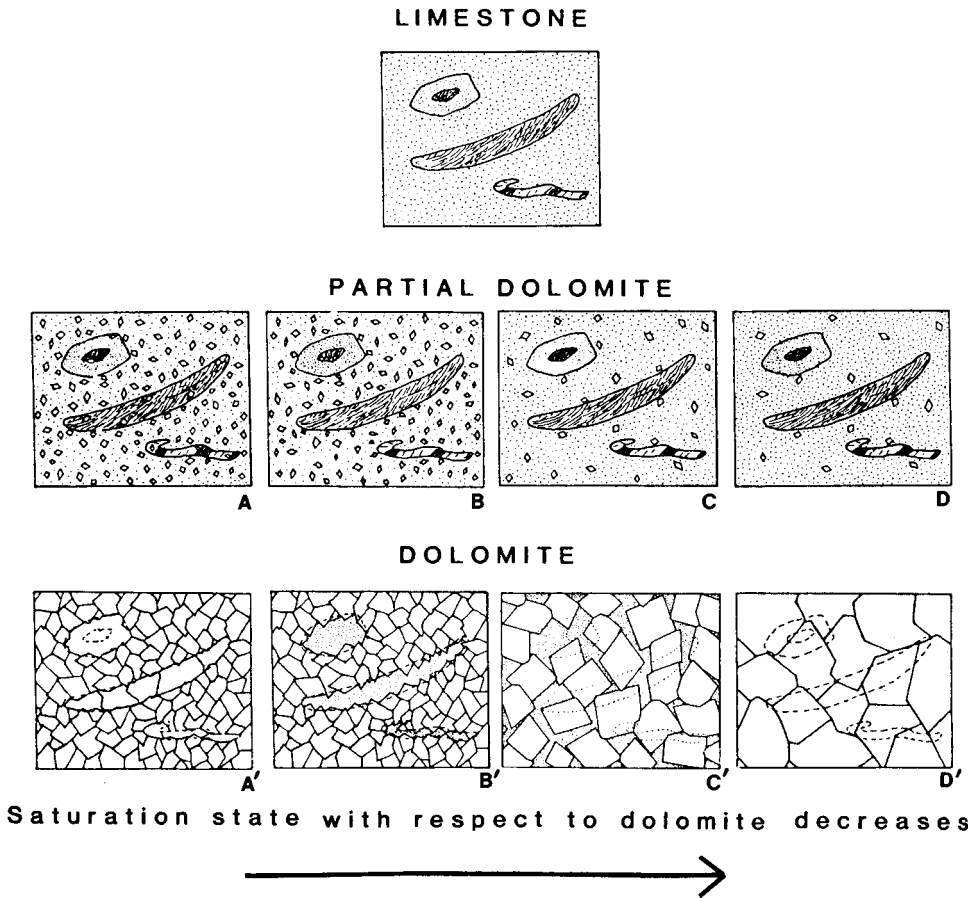


Figure 10.5 Replacement of carbonate grains and the formation of carbonate grain ghosts in planar dolomite. Note that the overall texture is related to the saturation state of the dolomitizing fluids with respect to dolomite, which decreases to the right in the diagram. D and D' represents a condition where saturation state is low but residence time in the dolomitizing solution is long, resulting in a low-porosity dolomite. Note also that A' has mimically replaced crinoid and nonmimically replaced brachiopod and trilobite fragments. B' has molds, and C' and D' have ghosts of the fossil grains. [After Sibley, D. F. and J. M. Gregg, 1987, Classification of dolomite rock textures: *J. Sediment. Petrol.*, 57, Fig. 11, p. 974, reprinted by permission of SEPM, Tulsa, OK.]

10.4 Zoned dolomite

Many rhombic dolomite crystals have a cloudy, rhombic central zone surrounded by a clear rim (Fig. 10.6). These crystals are often referred to as zoned dolomite. The cloudy centers of the crystals result from the presence of inclusions, which may be bubbles or unreplaced inclusions of calcite or other minerals, whereas the clear rims are nearly inclusion free. These “zoned crystals” may form by replacement of a CaCO_3 precursor such as a micritic

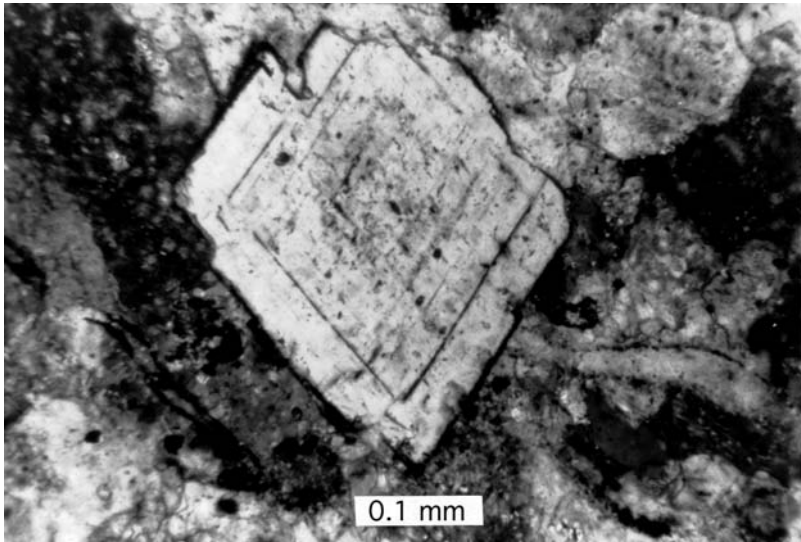


Figure 10.6 Zoned dolomite crystal showing a clouded center and an almost clear rim. Paleozoic limestone, Great Basin, USA. Crossed nicols.

limestone, or they may grow into open pore space. Where they form within a precursor limestone, the cloudy centers represent replacement of the precursor CaCO_3 . The clear rims must have formed in empty pore space around the margins of the cloudy rhombs. The empty space may be created by dissolution of CaCO_3 from just beyond the limits of the cloudy replacement rhombs. The CaCO_3 dissolved from the immediately surrounding area is then reprecipitated syntaxially in the newly created space around the cloudy rhomb. Clear syntaxial rims may also form in optical continuity on dolomite crystals that project into voids. These syntaxial rims may either enlarge earlier-formed clear rims or produce clear dolomite rims on pre-existing cloudy crystals.

In addition to these so-called zoned dolomites, some dolomites exhibit fine-scale internal zoning that results from differences in composition, particularly iron composition. Ferrous iron is common in many dolomite crystals as a substitute for magnesium. If this ferrous iron is subsequently oxidized to ferric iron (hematite), it is visible with a standard petrographic microscope. Thus, some dolomite crystals may contain concentric, alternating zones of red, iron-rich and clear, iron-poor dolomite that mark growth stages of the rhomb (Blatt, 1982, p. 313). Because iron does not so readily substitute for calcium, calcite does not show this type of visible zoning. Dolomite crystals that may not display visible zoning under a petrographic microscope, may show well-developed fine-scale zoning when viewed by cathodoluminescence (Fig. 10.7).

Reeder and Prosky (1986) attribute this type of zoning to systematic compositional differences between nonequivalent growth sectors in dolomite rhombs and refer to it as **sector zoning**. They report that growth sectors forming under $\{1120\}$ crystal faces are

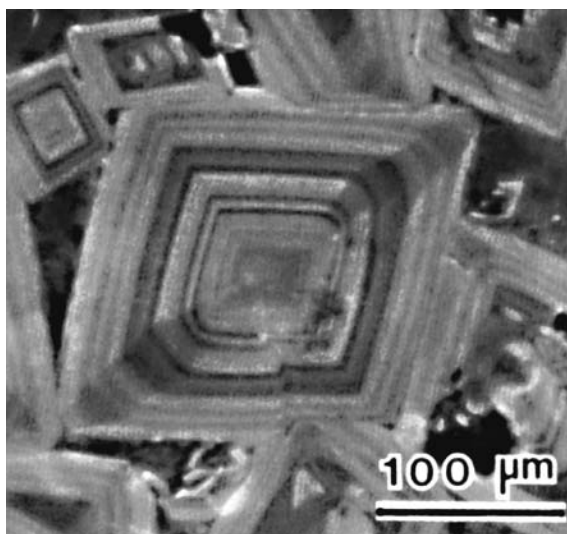


Figure 10.7 Compositional sector zoning in dolomite crystals as revealed by cathodoluminescence. [From Reeder, R. J. and J. L. Prosky, 1986, Compositional sector zoning in dolomite: *J. Sediment. Petrol.*, **56**, Fig. 2, p. 239, reprinted by permission of SEPM, Tulsa, OK.]

enriched in Fe and Mg and slightly enriched in Mn relative to sectors forming under $\{1014\}$ faces. Furthermore, transmission electron microscopy shows that growth microstructures differ within these different growth sectors. Reasons for these compositional and structural differences are poorly understood, but may be related to differences in growth rate, atomic configuration at the growing surface, and mechanisms of growth. Dolomite crystals may also exhibit syntaxial overgrowths (e.g. Machel, 2004), although overgrowths are not as common on dolomite crystals as on calcite crystals such as on echinoderm fragments.

10.5 Mottled and zebra structure

Some dolomites display a distinctive mottled structure, particularly on weathered surfaces. The mottles range in shape from tubular to highly irregular, including anastomosing networks. In general, mottling appears to be the result of incomplete dolomitization; however, various kinds of processes or conditions have been suggested to account for the differential dolomitization. Mottles oriented approximately parallel to bedding surfaces of the precursor limestone probably represent selective dolomitization along zones of higher porosity and permeability. Tubular-shaped mottles may be relict borings or other organic traces. Very irregular mottles that cut indiscriminately across preserved stratification in limestones and that are not associated with obvious fracture systems are more difficult to explain. They may be diagenetic, but the mechanism responsible for isolation of the patches is not well understood. Kirkham (2004) suggests that mottled Jurassic-age dolomite in the Arabian Gulf is due to concentrations of microcrystalline iron sulfate owing to the activities of sulfate-reducing bacteria.

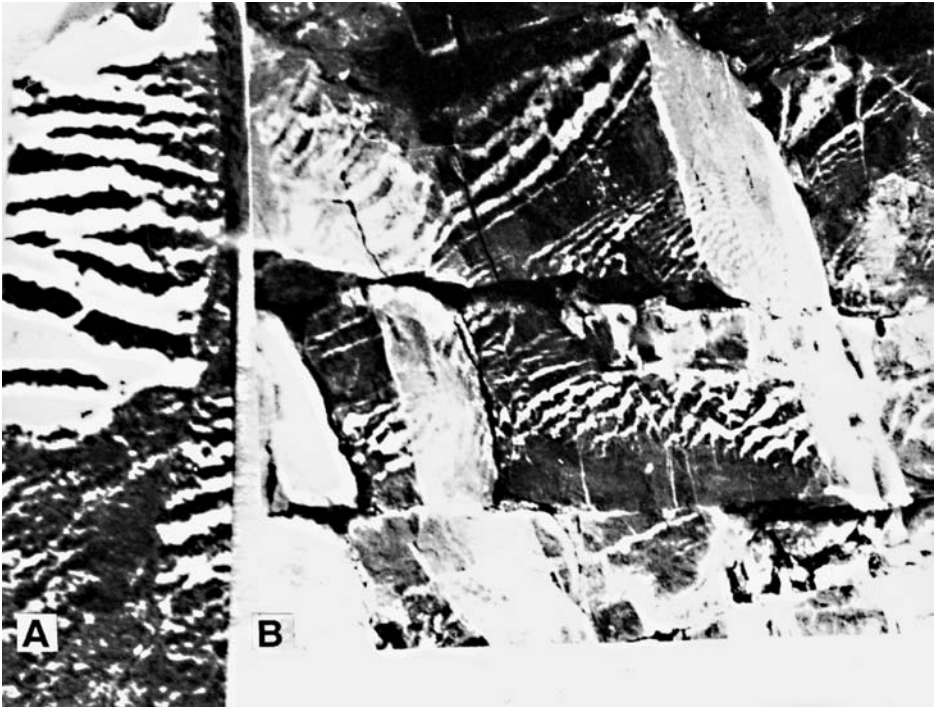


Figure 10.8 Zebra structure in dolomite, possibly caused by expansion during a precursor phase of evaporite precipitation. Width of specimen 35 mm. [From Beales, F. W. and J. L. Hardy, 1980, Criteria for recognition of diverse dolomite types with emphasis on studies of host rocks for Mississippi Valley-type ore deposits, in Zenger, D. H., J. B. Dunham, and R.L. Ethington (eds.), *Concepts and Models of Dolomitization*: SEPM Special Publication 28, Fig. 3, p. 206, reprinted by permission of SEPM, Tulsa, OK.]

Zebra structure is a term used to describe some dolomites that display conspicuous, somewhat irregular light and dark bands, which are commonly oriented parallel to bedding. The light-colored bands range in color from light gray to white and are typically coarse-grained, and may be vuggy (porous). The darker bands are generally fine-grained. Zebra structure has commonly been reported from altered dolomites associated with sedimentary ore deposits and evaporites. Beales and Hardy (1980) suggest that the zebra structure (Fig. 10.8) they describe in dolomites from Mississippi-Valley-type lead/zinc ore deposits is a type of expansion structure. Allegedly, displacive precipitation of gypsum resulted in expansion and brecciation of the host rock. Subsequent dissolution of the gypsum created open spaces that were later filled by white, sparry dolomite. The origin of zebra dolomite is, however, controversial. It may involve more than one mechanism, including repeated fracturing or some kind of geochemical self organization (e.g. Krug *et al.*, 1996).

10.6 Origin of dolomite

10.6.1 The dolomite problem

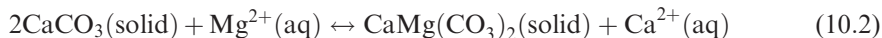
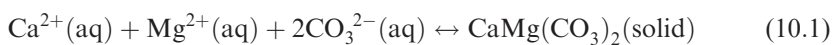
As mentioned in the introduction to this chapter, dolomites are common rocks in the geologic record and appear to form an increasing proportion of carbonate rocks with increasing age. Dolomites have been studied for two hundred years, but their origin is still enigmatic and controversial. The so-called “dolomite problem” arises in part from the fact that geochemists have not yet successfully precipitated well-ordered, stoichiometric dolomite in the laboratory at the normal temperatures ($\sim 25^\circ\text{C}$) and pressure ($\sim 1\text{ atm}$) that occur at Earth's surface. One worker (Land, 1998) ran an experiment for 32 years without precipitating dolomite. Elevated temperatures in excess of 100°C are required to precipitate a well-ordered dolomite in the laboratory. At normal temperatures of about 25°C , only calcium-rich, poorly ordered protodolomite forms.

Nonetheless, nearly stoichiometric dolomite is common in the geologic record. The reluctance of such dolomite to precipitate under normal surface conditions has given rise to numerous theories to explain the occurrence of nearly stoichiometric dolomite in the rock record. Some dolomites preserve relict or ghost limestone textures such as fossils or ooids. Other dolomites are known to grade fairly abruptly to limestone along a boundary that cuts across bedding planes. These dolomites clearly formed by replacement processes, with the mineral dolomite replacing calcite, Mg-calcite, or aragonite. Presumably, replacement occurred as Mg-bearing subsurface waters migrated through the carbonate sediments, possibly over periods of tens to hundreds of millions of years. Determining how extensive, thick sequences of ancient dolomites formed is also part of the dolomite problem.

In contrast to these obvious replacement dolomites, many dolomites do not contain visible relict textures, leaving their origin open to speculation. Did these dolomites form as a primary dolomite precipitate in spite of the failure of laboratory experiments to precipitate dolomite at surface temperatures? Alternatively, were they originally precipitated as CaCO_3 , which quickly altered, partially or entirely, to dolomite before burial or at very shallow burial depths? Or did they form much later by replacing a precursor limestone such as a micrite that contained few recognizable textures or structures? A dolomite formed by replacing such a featureless limestone would presumably contain no relict limestone textures.

10.6.2 Chemical considerations

The chemical reactions of interest with respect to dolomite formation are



Equation 10.1 represents primary precipitation of dolomite, and Equation 10.2 is an equation commonly used to represent dolomite replacement of calcite or aragonite.

(Note: The reaction shown in Equation 10.2 is only one of a dozen or more reactions that have been proposed to represent the replacement of CaCO_3 by dolomite; see Machel and Mountjoy, 1986, and Machel, 2004.)

Some investigators have suggested that certain dolomites are indeed primary precipitates that formed by the reaction indicated in Equation 10.1. Is there any way to determine unequivocally if a particular dolomite formed as a primary precipitate? Unfortunately, the answer appears to be no; however, let's take a look at modern dolomites, some of which are suggested to be primary precipitates. Prior to about the middle 1940s, few occurrences of dolomite were known in modern environments. Thus, little support for the concept of primary precipitation could be gained from modern occurrences. Subsequently, dolomite has been reported from numerous modern localities, including some in Russia, South Australia, the Persian Gulf, the Bahamas, Bonaire Island off the Venezuela mainland, the Florida Keys, the Canary Islands, Deep Springs Lake, California, and Elk Lake, Minnesota. Ages of these dolomites range to about 10,000 years, although most are less than 3000 years old. Mole percent MgCO_3 ranges from about 30 to 50, but is commonly less than 45. Therefore, most modern dolomite is protodolomite.

Experimental studies of oxygen isotopes in coexisting dolomite and calcite samples from some of these deposits have been made in an effort to confirm or disprove primary origin. Experimental data extrapolated from high temperature to low temperature suggest that at 25 °C primary precipitates of dolomite should be enriched, with respect to coexisting calcite, by detectable amounts of heavy oxygen (higher $\delta^{18}\text{O}$ values). Unfortunately, isotope studies of modern dolomites have failed consistently to produce the results predicted by these experimental data. Consequently, many geologists and geochemists now apparently believe that only an insignificant amount of ancient dolomite is truly the product of primary precipitation at or above the sediment–water interface. The relative importance of primary dolomite in the geologic record is far from settled, but much of the recent work focuses on the problem of penecontemporaneous dolomitization of precursor calcium carbonate. That is, it attempts to determine the conditions that are required to bring about dolomitization of aragonite or calcite over short periods of time such as a few years to a few thousands of years.

The requirements for dolomite formation, along with possible mechanisms of dolomitization, have been reviewed by numerous workers: e.g. Machel and Mountjoy (1986), Usdowski (1994), Land (1998), Arvidson and Mackenzie (1999), and Machel (2004). The formation of dolomite has to be considered in terms of both thermodynamics and kinetics. Thermodynamic considerations include the $\text{Ca}^{2+}/\text{Mg}^{2+}$ ratio, $\text{Ca}^{2+}/\text{CO}_3^{2-}$ ratio, and temperature, which define the CaCO_3 and $\text{CaMg}(\text{CO}_3)_2$ thermodynamic stability fields in the system calcite–dolomite–water. Dolomite formation is thermodynamically favored in solutions of (1) low $\text{Ca}^{2+}/\text{Mg}^{2+}$ ratios, (2) low $\text{Ca}^{2+}/\text{CO}_3^{2-}$ ratios (high carbonate alkalinity), (3) high temperatures, (4) salinities higher or lower than that of seawater (Fig. 10.9A), and (5) where fluids suddenly release CO_2 (Machel, 2004).

The failure of well-ordered, stoichiometric dolomite to precipitate from seawater at surface temperatures is generally attributed to kinetic factors (i.e. rates of change in the

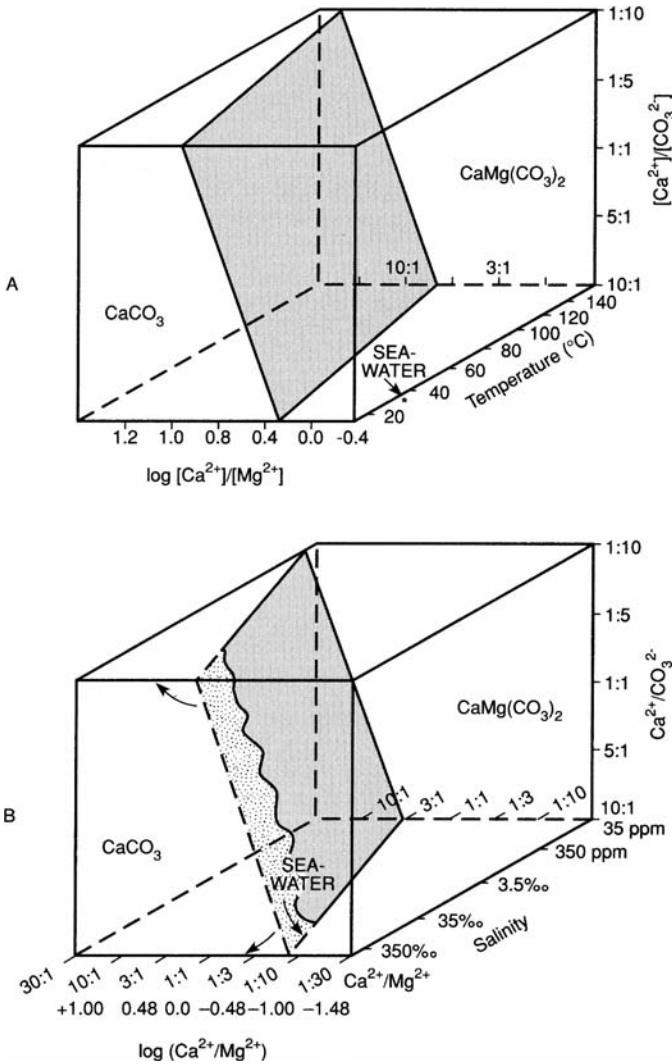


Figure 10.9 Thermodynamic (A) and kinetic (B) stability diagrams for the system calcite–dolomite–water. The ionic ratios (square brackets) in diagram A are activity ratios; seawater plots in the dolomite field, on the basal plane just outside the diagram (asterisk). The exact inclination of the stability field boundary (stippled) is not known. In diagram B, seawater plots just in the calcite field. At salinities higher than about 35 ‰, the field boundary (stippled) is probably bent toward higher $\text{Ca}^{2+}/\text{Mg}^{2+}$ ratios (in the direction of the arrows, wider stippled area). (After Machel, H.-G. and E. W. Mountjoy, 1986, Chemistry and environments of dolomitization – a reappraisal: *Earth Sci. Rev.*, **23**, Figs. 2 and 3, p. 184, reprinted by permission.)

concentration of reactants), such as $\text{Ca}^{2+}/\text{Mg}^{2+}$ ratios, $\text{Ca}^{2+}/\text{CO}_3^{2-}$ ratios, and salinity. These factors may be used to construct a kinetic stability diagram (Fig. 10.9B). This diagram suggests that dolomite is kinetically favored by low $\text{Ca}^{2+}/\text{Mg}^{2+}$ ratios, low $\text{Ca}^{2+}/\text{CO}_3^{2-}$ ratios, and low salinity. It is also favored by higher temperatures, because the calcite–dolomite field boundary

shifts toward higher $\text{Ca}^{2+}/\text{Mg}^{2+}$ ratios with increasing temperature. In fact, at temperatures in excess of about 100°C most kinetic inhibitors become ineffective (Machel and Mountjoy, 1986).

10.6.3 Dolomite models – Introduction

Theoretically, dolomites can form in three different ways (Machel, 2003): (1) by **dolomitization**, which is the replacement of CaCO_3 by $\text{CaMg}(\text{CO}_3)_2$, (2) by **dolomite cementation**, which is precipitation of dolomite from aqueous solution in primary or secondary pore spaces, and (3) by precipitation from aqueous solution to form sedimentary deposits (“**primary dolomite**”). The volume of dolomite cement is small compared to the total volume of dolomite, and primary dolomite appears to be rare and restricted to some evaporitic lagoonal and/or lacustrine settings. Thus, the great bulk of dolomite in the geologic record apparently formed by dolomitization (replacement). Consequently, published discussion of the origin of dolomite has focused on mechanisms of dolomitization.

Several models to explain the origin of dolomites have been proposed; see, for example, discussion by Braithwaite (1991), Budd (1997), Machel (2003, 2004), and Warren (2000). According to Machel (2004), dolomite models must fulfill three specific criteria:

1. *thermodynamic*: there must be supersaturation for dolomite, with variable saturation states for calcite and aragonite; replacement dolomite requires undersaturation with respect to calcium carbonate; otherwise there will be dolomite cementation;
2. *kinetic*: the rate of dolomite formation must be equal to or greater than the rate of calcium carbonate dissolution, otherwise there will be significant dissolution porosity;
3. *hydrologic*: there must be long-lasting pore-water flow, preferably with high magnesium content (or, alternatively, magnesium supply via diffusion from seawater).

Two kinds of dolomite are recognized on the basis of the timing and nature of dolomite formation: (1) syndepositional (penecontemporaneous) and (2) postdepositional.

Penecontemporaneous dolomites form while the host sediments are in their original depositional setting; that is, they form under the geochemical conditions of the depositional environment. Known examples are mainly of Holocene age, although a few examples of older penecontemporaneous dolomites have been reported. They form (in small amounts) primarily in shallow-marine to supratidal environments and mainly by direct precipitation from normal or evaporated seawater (e.g. Budd, 1997). They occur as thin layers and lenses in sabkhas, salinas, and evaporative lagoons/lakes (e.g. Last, 1990), and as supratidal crusts and fine-crystalline cements and replacements in peritidal sediments (e.g. Machel, 2003).

Small quantities of penecontemporaneous dolomites are reported to form also in deeper-water, hemipelagic to pelagic settings (Lumsden, 1988). For example, Miocene hemipelagic carbonates on the margin of the Great Bahama Bank are partially dolomitized to depths ranging from 50–500 m subsea. The dolomites occur as primary void-filling cements and as replacements of micritic sediments, red algae, and echinoderm grains (Swart and Melim, 2000).

The origin of penecontemporaneous dolomites in both shallow-water/supratidal and hemipelagic/pelagic settings appears to be influenced by bacterial sulfate reduction and/or methano-genesis (e.g. Vasconcelos and McKenzie, 1997; Mazzullo, 2000). The exact role that bacteria play in reducing the kinetic barriers to dolomitization is poorly understood, although reduction of magnesium- and calcium-hydration barriers, increase in alkalinity, and changes in pH may be involved (Machel, 2004).

Postdepositional dolomites form after deposition has ceased and the host carbonates have been removed from the zone of active sedimentation. Removal from the sedimentation zone may occur by sediment progradation, burial, uplift, eustatic sea-level change or any combination of these factors. Postdepositional dolomites form at various burial depths, ranging from a few meters to thousands of meters, where pore-water chemistries differ significantly from those of the depositional environment. Dolomitization in the deeper subsurface requires adequate porosity and permeability of the sediments to allow fluids to circulate, and an efficient “pump” for driving fluid circulation. According to Machel (2003), almost all extensive dolostones are postdepositional.

As mentioned, a number of models have been proposed to explain the origin of dolomite. The more important models are illustrated in Fig. 10.10 and further discussed below. Note that these are all models for dolomitization, which implies formation of dolomite by replacement and, to a lesser extent, by cementation.

10.6.4 Basic dolomite models

Reflux model

Many, but certainly not all, of the known occurrences of modern or Holocene dolomites are in hypersaline environments such as the sabkhas of the Persian Gulf and the supratidal zones of arid climates. Under these strongly evaporative conditions where rates of evaporation exceed rates of precipitation, seawater beneath the sediment surface becomes concentrated by evaporation. Therefore, hypersaline environments have salinities greater than that of normal seawater. Evaporative concentration leads to precipitation of aragonite and gypsum, which preferentially removes Ca^{2+} from the water and increases the Mg/Ca ratio. The Mg/Ca ratio in normal seawater is about 5:1. When this ratio rises to a sufficiently high level owing to evaporation, possibly in excess of 10:1, dolomite presumably forms. Most dolomites formed from evaporated seawater are postdepositional and form by way of reflux; a few are penecontemporaneous and form in sabkhas, as mentioned above (Machel, 2004).

Adams and Rhodes (1960) proposed that seawater concentrated by evaporation as dense brines in surface ponds or bays (lagoonal and shallow-marine settings) behind barriers such as a reef would sink downward through earlier-deposited calcium carbonate sediment and thus displace less dense seawater in the pores of the sediment (see Fig. 10.10A). Flushing of large volumes of this magnesium-rich brine through the underlying sediment would putatively bring about dolomitization, a process they referred to as **seepage refluxion**. During this process, Mg^{2+} replaces Ca^{2+} in CaCO_3 minerals, releasing Ca^{2+} in solution.

Dolomitization model	Source of Mg ²⁺	Delivery mechanism	Hydrological model	Predicted dolomite patterns
A. Reflux dolomitization	Seawater	Storm recharge, evaporative pumping density-driven flow		
B. Mixing-zone (Dorag) dolomitization	Seawater	Tidal pumping		
C1. Seawater dolomitization	Normal seawater	Slope convection ($K_V > K_H$)		
C2. Seawater dolomitization	Normal seawater	Slope convection ($K_H > K_V$)		
D1. Burial dolomitization (local scale)	Basinal shales	Compaction-driven flow		
D2. Burial dolomitization (regional scale)	Various subsurface fluids	Tectonic expulsion topography-driven flow		
D3. Burial dolomitization (regional scale)	Various subsurface fluids	Thermo-density convection		
D4. Burial dolomitization (local and regional scales)	Various subsurface fluids	Tectonic reactivation of faults (seismic pumping)		

Figure 10.10 Dolomitization models, illustrated as groundwater flow systems and predicted dolomitization patterns. Examples show incomplete dolomitization of carbonate platforms or reefs; i.e. they represent early phases of dolomitization. Arrows denote flow directions (K_V = vertical permeability; K_H = horizontal permeability); dashed lines show isotherms (lines connecting points of equal temperature). Predicted dolomitization patterns are shaded. (After Wilson, E. N., L. A. Hordie and O. M. Philips (1990), Dolomitization front geometry, fluid flow patterns, and the origin of massive dolomite: The Triassic Latemar buildup, northern Italy: *Am. J. Sci.*, **290**, Fig., 13, p. 765, as modified by Machel, 2004, Concepts and models of dolomitization: a critical reappraisal, in Braithwaite, C. J. R., G. Rizzi, and G. Darke (eds.), *The Geometry and Petrogenesis of Dolomite Hydrocarbon Reservoirs*: Geological Society of London, Special Publication 235, Fig 19, p. 40, reproduced by permission of American Journal of Science.)

The reflux model has subsequently become very popular, and has been invoked to explain pervasive dolomitization on a large, sometimes unrealistic, scale. Numerical modeling studies by Jones and Rostron (2000) and Jones *et al.* (2002, 2003, 2004) demonstrate that *active reflux* can take place to depths of several hundred meters. Jones *et al.* (2002) further suggest that *latent reflux* can continue after cessation of brine generation at the platform top. Latent reflux is presumably driven by the greater density of earlier generated brines, which causes the brines to continue to sink and disperse laterally even after brine generation stops. Also, normal seawater “sucked” in from above through the platform top adds to the refluxing fluid. Machel (2004) points out that both active and latent refluxing brines exit at or near the platform margin. Therefore, reflux dolomitization is confined to the platform and cannot be invoked to explain dolomitization beyond the platform margin, e.g. on a basin-wide scale, as suggested by some workers.

Sabkha model

Sabkhas are coastal supratidal mudflats that are common in arid regions such as the Arabian Gulf. Evaporite minerals precipitate displacively within sabkha sediments, which consist of carbonates and possibly siliciclastics, in a capillary zone above a saline water table. Upward flow of water from the saturated groundwater zone replaces the water lost by capillary evaporation, a process referred to as **evaporative pumping** (e.g. Hsü and Siegenthaler, 1969). Water lost from sabkha sediments (water table) by evaporation is replaced by storm-driven seawater. Magnesium for dolomitization is supplied by this seawater, which is propelled periodically onto the lower supratidal zone and along remnant tidal channels. The salinity of seawater is elevated significantly beyond gypsum saturation on and within the supratidal flats. The resulting brines then reflux through the sabkha sediment similar to downward flow in the reflux model.

The sabkha on the Trucial Coast of Abu Dhabi Sabkha dolomite is perhaps the best-known example of sabkha dolomitization. Dolomite forms in a narrow (1–1.5 km) zone next to the strandline and in flooded tidal channels that extend further landward, as a cement and by replacement of aragonite. Dolomite is restricted to the upper 1–2 m of the sediment (Machel, 2004).

Mixing-zone model

Some modern/Holocene dolomites and most ancient dolomites are not directly associated with evaporites. Therefore, the hypersaline (reflux and sabkha) models do not appear to be appropriate for these dolomites. Hanshaw and others (1971) proposed that dolomitization could occur from brackish groundwaters that were produced through mixing of seawater-derived brines and freshwater (e.g. Fig. 10.10B). Such low-salinity groundwaters could be saturated with respect to dolomite at Mg/Ca ratios as low as 1:1. Subsequently, this concept was further developed by Badiozamani (1973), Land (1973), and Folk and Land (1975). The mixing-zone model, or variations thereof, has been referred to also as the **Dorag model** (Badiozamani, 1973) and the **schizohaline model** (Folk and Land, 1975).

The fundamental concept underlying the Dorag model is explained in detail by Badiozamani on the basis of thermodynamic calculations. Mixing of meteoric waters with seawater causes undersaturation with respect to calcite, whereas dolomite saturation increases, resulting in replacement of CaCO_3 by dolomite. Folk and Land (1975) maintain (in their schizohaline model) that in solutions of low salinity and low ionic strength, dolomite can apparently form at Mg/Ca ratios as low as 1:1. When seawater or evaporated brine with high Mg/Ca ratios is diluted by mixing with freshwater (schizohaline environment), the mixture will retain the high Mg/Ca ratio (low Ca/Mg ratio) but not the high salinity of the saline water. Thus, these mixed waters putatively become special waters capable of forming ordered dolomite. According to Folk and Land, dolomite formed from dilute solutions is perfectly clear with plane, mirror-like faces, (so called **limpid dolomite**) and is more resistant to solution than ordinary dolomite.

In spite of initial acceptance of the mixing-zone model by many workers, and its application in some cases to explain pervasive dolomitization of entire carbonate platforms, the model appears to have fallen into disrepute. Machel (2004) suggests that the mixing-zone model has been highly overrated and that not a single location in the world has been shown to be extensively dolomitized in a freshwater–seawater mixing zone. (See also Melim *et al.*, 2004) Rather, the dominant diagenetic process in most mixing zones is extensive dissolution of calcium carbonate, up to the dimension of caves, not formation of dolomite. If dolomite forms at all, it is in minuscule amounts. The main role of coastal-mixing zones may be that of a hydrologic pump for seawater dolomitization (discussed below), instead of a geochemical environment favorable for dolomitization (Machel and Mountjoy, 1990). See also comments by Melim *et al.* (2004).

Seawater dolomitization model

In all of the above models, some kind of “special” water (i.e. seawater modified in some way) is required for dolomitization. On the other hand, a few authors have proposed that dolomitization can take place in normal, unmodified seawater if a sufficient volume of seawater can be passed through the sediment (e.g. Carballo and Land, 1984; Carballo *et al.*, 1987; Saller, 1984; Sass and Katz, 1982). Dolomitization can presumably occur only when active pumping of magnesium-bearing water takes place. Simply immersing carbonate sediments in static fluids, whether they are hypersaline, normal marine, or mixed marine–meteoric, rarely appears to nucleate dolomite, much less generate significant volumes of dolomite (Land, 1985). On the other hand, if large volumes of water are forced through the sediment so that each pore volume of water in the sediment is constantly being renewed with new water, then dolomitization can presumably occur (models C1 and C2, Fig. 10.10). Movement of large volumes of water through the sediment provides a constant source of magnesium and removes replaced calcium and other ions that might “poison” the dolomite crystal structure. Thus, any mechanism that provides a means of forcing large amounts of water through the sediment can presumably bring about dolomitization (see Fig. 10.10C).

As an example, Carballo *et al.* (1987) report an area of Sugarloaf Key, Florida, where seawater is forced upward and downward through Holocene carbonate mud during rise and

fall of seawater accompanying spring tides, a process they call **tidal pumping**. Owing to the large volume of seawater driven through the sediment by this mechanism, large quantities of magnesium are imported into the sediment, and pore fluids are constantly being replaced by new fluids. Under these conditions, dolomite is forming in the sediment even though little or no evaporation of the seawater has occurred. Carballo *et al.* suggest that dolomite forms both by precipitation as a cement and by later replacement of pre-existing crystallites. The results of this study thus clearly imply that normal seawater can act as a dolomite-forming fluid, without the requirement of magnesium concentration through evaporation, if enough seawater is forced through sediment. If hypersaline waters are available, movement of these waters could also bring about dolomitization. Thus, a continuous spectrum of dolomitization may exist from normal-marine subtidal to hypersaline-subaerial (Machel and Mountjoy, 1986).

The Cenozoic dolomites of the Bahama platform are probably the best-studied examples of seawater dolomitization. Postdepositional dolomitization is driven by circulation of saline groundwater (seawater composition) through the Bahama sediments. In addition to tidal pumping mentioned above, large-scale circulation of seawater takes place by thermal convection and density reflux (Whitaker *et al.*, 1994). In this regard, seawater dolomitization is similar in some respects to burial dolomitization described below. In fact, Machel (2003) suggests that Bahama dolomites represent a hybrid regarding classification. The dolomitizing solution is nearly normal seawater, yet thermal convection, as a hydrologic system and drive for dolomitization is better classified under burial (subsurface) models.

Intermediate- to deep-burial dolomitization models

General statement

Let us return to the problem of explaining the relatively thick, massive, widespread dolomites that constitute most of dolomite in the geologic record. Did these dolomites form either by direct precipitation or by dolomitization through one or more of the mechanisms discussed in the above models? Alternatively, did they form much later, perhaps millions to hundreds of millions of years later, by intermediate to deep subsurface dolomitization of precursor limestones? If so, how did these dolomites form? Part of the “dolomite problem” involves coming up with a satisfactory explanation to account for the large amounts of magnesium that had to be imported into pre-existing calcium carbonate sediments to bring about such dolomitization. Further, the mechanism has to account also for removal of the calcium and other ions released by the dolomite replacement process. Because seawater is the only common and abundant magnesium-rich fluid on Earth, seawater (logically) must have furnished the primary source of magnesium for dolomitization. Under some circumstances, seawater may have been modified in some way (e.g. surface evaporation, mixing with meteoric waters, mixing with basement hydrothermal fluids, subsurface evolution by salt-sieving, dissolution of buried salt, reaction with mineral phases, clay mineral dewatering to produce connate brines); however, such modification to increase magnesium concentration may not be necessary. In fact, some subsurface waters derived from seawater may be depleted in magnesium relative to seawater. If a sufficient volume of essentially normal seawater can be forced through carbonate sediment, presumably dolomitization can occur.

Thus, seemingly, the problem of pervasive subsurface dolomitization boils down to finding suitable mechanisms for large-scale, mass transport of seawater through subsurface carbonate formations (see Fig. 10.10D). This problem is complicated by the fact that subsurface formations exhibit significant variations in porosity and permeability. Effective, large-scale dolomitization could occur only where an effective seawater circulation mechanism was present and where the carbonate precursor rocks had sufficient permeability and porosity to allow entry and passage of the dolomitizing waters. Perhaps these requisite conditions provide an explanation for the fact that not all carbonate rocks are dolomitized. It may be reasonable to ask, given hundreds of millions of years of burial history, why aren't all ancient limestones dolomitized? Machel and Mountjoy (1986) point out that the problem of proving subsurface dolomitization is twofold. First, we have to come up with a water circulation mechanism that can account for the magnesium supplied to the limestones. Then we have to exclude near-surface dolomitization as the mechanism of dolomitization and, instead, establish that dolomitization took place in the subsurface. The latter step may be very difficult to do.

Land (1985) suggests that most dolomite must form relatively early in the depositional and burial history of sediment when seawater or seawater-derived fluids can be actively pumped. On the other hand, several investigators have proposed a deeper, subsurface origin for some dolomites on the basis of petrographic, geochemical, or other evidence. For example, some dolomitization coincides with the formation of stylolites by pressure solution. Also, some dolomite may undergo more than one stage of dolomitization. For example, Gregg and Shelton (1990) propose two stages of dolomitization in dolomites of the Bonneterre and Davis formations of southeastern Missouri (USA). Planar dolomite formed by early diagenesis of cryptalgalaminites, and nonplanar dolomite formed by late-stage neomorphism (recrystallization) of planar dolomite and by dolomitization of peloid mudstones.

In any case, if intermediate to deep subsurface dolomitization was important in the past, some mechanism or mechanisms had to operate that forced large quantities of water through precursor carbonate sediment. The principal mechanisms proposed for moving Mg-bearing waters through subsurface carbonates include (1) compaction-driven flow, (2) topography-driven flow, and (3) thermal convection (Machel, 2004; Whitaker *et al.*, 2004). Hydrothermal (pertaining to hot water) flow has also been suggested; however, hydrothermal flow is probably important only locally and in association with faults, fractures, and localized heat sources. (Note: hydrothermal dolomite may occur in association with sedimentary ore deposits.) One or more of the other three mechanisms probably accounts for larger-scale fluid movement.

Compaction-driven flow

Burial compaction of sediments owing to sediment loading raises pore pressures in sediments and drives fluid flow upward and laterally. Flow resulting from burial compaction occurs at fairly shallow depths, probably less than 1000 m, above the zone where porosity and permeability are reduced by cementation and solution-compaction. Although compaction

flow may account for some dolomitization, many authors have pointed out that such flow cannot form massive dolomites over large regions. Owing to the limited volume of these fluids, there is simply not enough magnesium in the fluids per unit volume of overlying strata to account for widespread dolomitization. Locally, where faults or other characteristics of the strata may funnel compaction flow into limited bodies of carbonates such as reefs, such flow may be responsible for dolomitization. Because burial compaction takes place at relatively shallow depths, dolomitization by (burial) compaction-driven fluids must occur relatively early during basin subsidence.

Compaction may also be caused by tectonic loading and compression during orogenic events such as thrust faulting. Oliver (1986) likens this compactional system to a giant “squeegee,” which can allegedly drive fluids over tens to hundreds of kilometers. Again, however, compactional water from a large-volume source must be channeled through a small cross-section of permeable rocks or along permeable faults or fractures for enough magnesium to be present for extensive dolomitization (Whitaker *et al.*, 2004).

Topography-driven flow

Topography-driven flow refers to flow of subsurface fluids downward and upward within a basin by gravity owing to the presence of a hydraulic head, the magnitude of which is determined by the elevation of the meteoric recharge area for the subsurface formations (e.g. Garven and Freeze, 1984). Such flow probably takes place to some extent in all sedimentary basins. The depth within the basin to which flow extends, the lateral distance of flow (possibly as much as several hundreds of kilometers), and the velocity of flow depend upon both the hydraulic head and the permeability distribution in the subsurface formations. The general conditions for such flow are shown schematically in Fig. 10.11. By this

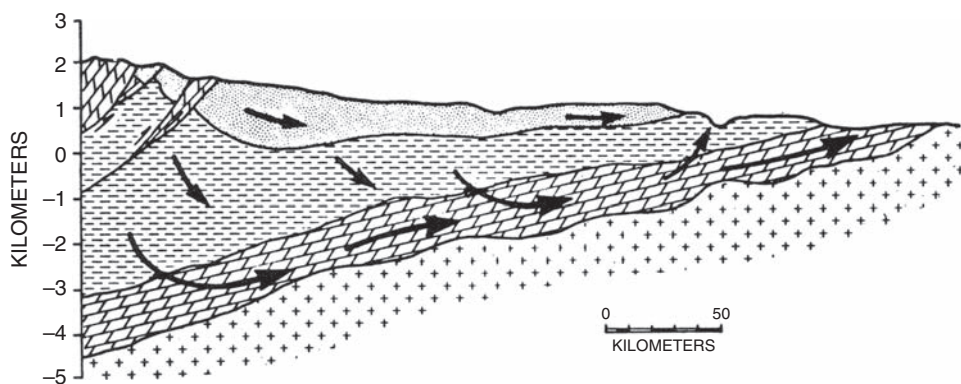


Figure 10.11 Conceptual model of topography-driven fluid flow in a sedimentary basin. Flow is driven by the hydraulic head of fluid resulting from meteoric recharge. The geometry of the flow system (arrows) is controlled by the water-table configuration and the permeability distribution in subsurface formations. (From Garvin, G. and R. A. Freeze, 1984, Theoretical analysis of the role of groundwater flow in the genesis of stratabound ore deposits: *Am. J. Sci.*, **284**, Fig. 3, p. 1091, reprinted by permission.)

mechanism of flow, enormous quantities of meteoric waters could be driven to considerable depths down along one side of a basin, to the extent allowed by permeability of the formations, and up again along the other side.

To be effective as a dolomitizing medium, the meteoric waters must acquire adequate magnesium en route. Some magnesium might be released by pressure solution of dolomite or Mg-calcite, but this Mg would not be new Mg. Solution of salt deposits containing Mg-bearing salts (polyhalite, carnallite, kieserite) could also supply magnesium, but the volume of these salts is probably small. Further, magnesium may be released during clay-mineral diagenesis; however, much of the released Mg may be taken up locally in forming new authigenic minerals such as chlorite. Thus, it is possible that gravity-driven fluid flow is a self-limiting process with respect to its dolomitization potential owing to limited supply of magnesium.

On the other hand, some published studies lend support to the potential importance of this process. For example, Gregg (1985) invoked topography-driven flow to explain dolomitization of a sheet of dolomite about 6 m thick in the Cambrian Bonnetterre Formation of Missouri, which extends over an area of about 17,000 km². Also, Yao and Demicco (1995) suggest that dolomitization of Cambro-Ordovician carbonates in the southern Canadian Rocky Mountains was mediated by topography-driven flow. Conversely, other workers have questioned the significance of topography-driven flow as a mechanism to bring about pervasive dolomitization (e.g. Hardie, 1987; Machel, 2004; Whitaker *et al.*, 2004). They suggest that insufficient evidence is available to demonstrate that the flow systems contained enough magnesium for regional dolomitization.

Thermal convection-driven flow

Thermal convection refers to movement of fluids in “cells” owing to spacial variations in temperature. Warming of fluids decreases their density and sets up a drive that moves less-dense, warmer fluids upward and laterally into circular cells. Variations in temperature may be due to such factors as elevated heat flux in the vicinity of igneous intrusions, differences in temperature of warm waters on ocean platforms and cold ocean waters, and even differences in thermal conductivity of different kinds of sediments (Machel, 2004).

Thermal convection within cells is classified as **open**, **closed** (Fig. 10.12), or **mixed**. Kohout (1967) proposed open-cell circulation of the type shown in Fig. 10.12B, subsequently referred to as **Kohout convection**, to explain thermal convection beneath the Florida Platform, Gulf of Mexico. Cold seawater enters the platform at depths of as much as 3000 m under the Straits of Florida. This water is prevented from moving downward by a geothermal barrier, which forces the seawater to move laterally toward the platform interior. There, it discharges back to the sea through numerous geothermal springs. Because the cell is open to the ocean, normal seawater enters the system to provide adequate magnesium for dolomitization. Within closed cells (Fig. 10.12C), however, the restricted supply of magnesium creates a severe limitation to dolomitization unless the cells interact with forced convection (Figs. 10.12A and B), a style of flow called **mixed convection** (Raffensperger and Vlassopolous, 1999).

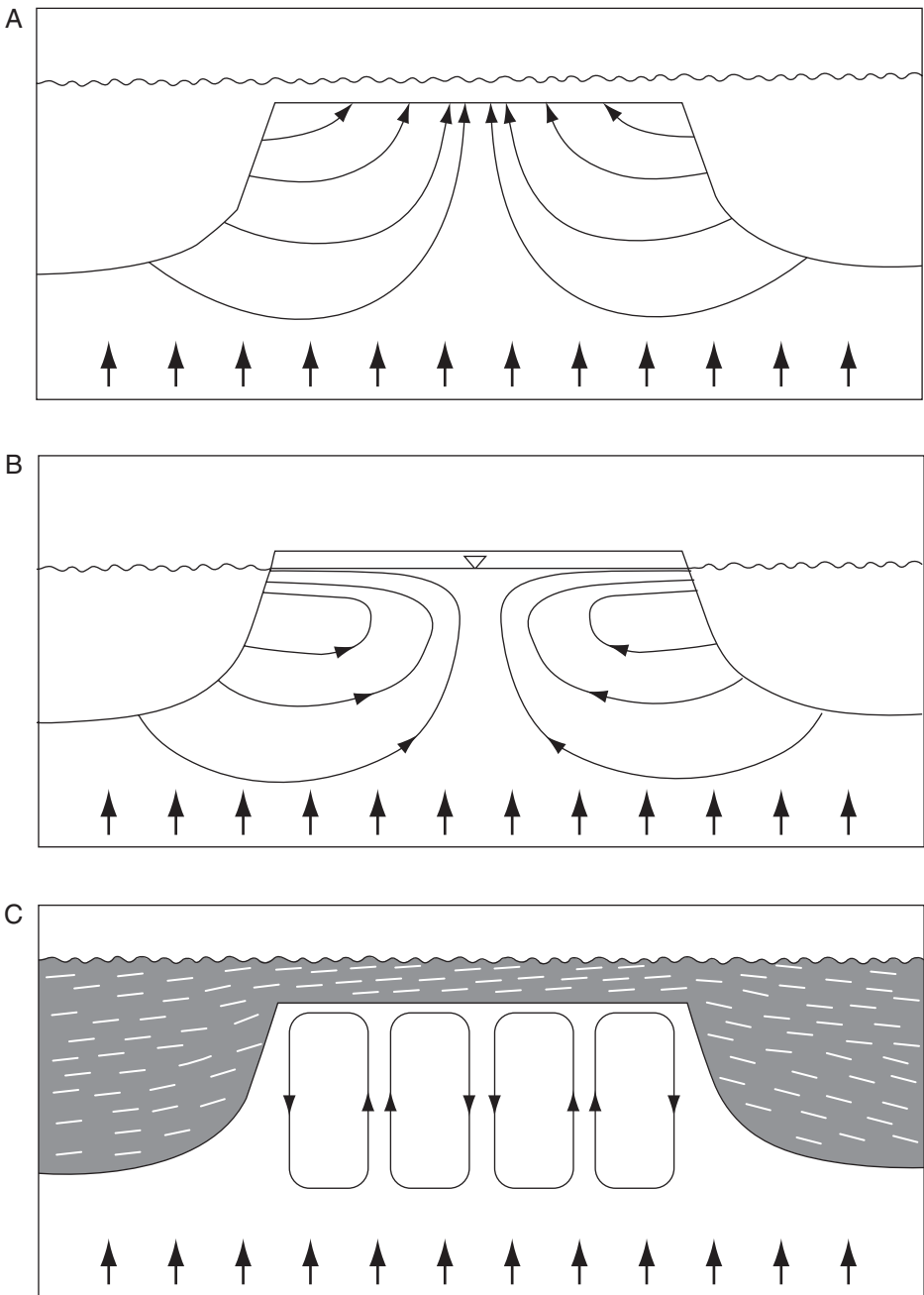


Figure 10.12 Thermal convection in an isolated carbonate platform driven by geothermal heating: (A) submerged platform, (B) emergent platform, (C) convection in a platform buried beneath low-permeability sediments. (A) and (B) show “forced convection” in open cells ; (C) illustrates “free convection” in closed cells. (From Whitaker, F.F.P.L. Smart, and G.D. Jones, 2004, Dolomitization from conceptual to numerical models, in Braithwaite, C.J.R., G. Rizzi, and G. Darke (eds), *The Geometry and Petrogenesis of Dolomite Hydrocarbon Reservoirs*: Geological Society of London Special Publication 235, Fig. 2, p. 103, reproduced by permission.)

10.6.5 Discussion and summary

Dolomites form by precipitation of $\text{CaMg}(\text{CO}_3)_2$ from solution (primary dolomite), by dolomite cementation in pore spaces of sediment, and by replacement (dolomitization) of precursor carbonate sediment (CaCO_3) with $\text{CaMg}(\text{CO}_3)_2$. Primary precipitation and dolomite cementation account for only a minor amount of dolomite; replacement apparently generated most of the dolomite in the geologic record. Dolomites can form penecontemporaneously, while the host sediments are still in their original depositional setting, or postdepositionally after the host carbonate sediments have been removed from the zone of active sedimentation. Most dolomite is postdepositional.

The formation of postdepositional dolomite by replacement requires circulation of large volumes of magnesium-rich fluid through porous and permeable precursor carbonate sediments. As illustrated in Fig. 10.10, models for dolomitization that have been invoked to fulfill this requirement fall into four basic categories: (1) reflux dolomitization, which occurs in hypersaline environments, (2) mixing-zone (mixed freshwater and seawater) dolomitization, (3) seawater dolomitization at shallow and near-surface burial depths, and (4) burial dolomitization at intermediate–deep depths.

Fluid circulation in the reflux model is provided by downward flow, through underlying sediment, of brines generated within hypersaline environments in lagoonal or shallow-marine settings. These brines are denser than seawater and are enriched in magnesium. Reflux flow can apparently extend to depths of several hundreds of meters or deeper. Reflux flow of these chemically evolved brines appears to be an effective dolomitizing mechanism, and has been invoked to explain dolomitization on a scale ranging from small to platform-wide.

Mixing of seawater and freshwater takes place within sediments in coastal zones where saline formation waters are mixed through a transition zone with overlying, seaward-flowing meteoric waters that form a lens above the saline formation waters. These mixed waters were initially considered capable of bringing about extensive dolomitization; however, the mixing-zone model has now been largely discounted.

Normal, unmodified, seawater can mediate dolomitization when large volumes of seawater are circulated through carbonate sediments. Seawater can be circulated through sediments at near-surface and shallow burial depths by tidal pumping and thermal convection in open convection cells, referred to as **forced** convection. In the deeper subsurface, circulation is driven by compaction (both by sediment loading and tectonically induced stresses), thermal convection in closed cells, and topography-driven flow.

The effectiveness of compaction flow in dolomitization is constrained by the small volume of fluids expelled by compaction. Within closed thermal convection, the restricted supply of magnesium also creates a limit to dolomitization unless the cells interact with forced convection. Topography-driven flow forces meteoric water through the sediments. To be effective as a dolomitizing medium, this water must first acquire magnesium in route by such mechanisms as solution of Mg-bearing carbonate minerals and Mg-bearing salt deposits, and release of magnesium during clay-mineral diagenesis.

Higher temperatures tend to overcome the effects of the various factors that inhibit dolomite formation. Thus, temperature has a strong effect on dolomitization. Environments with temperatures greater than about 50 °C (subsurface and hydrothermal environments) appear to enhance dolomitization.

10.6.6 Examples

It may be instructive for students at this point to examine some published case histories of various dolomite formations. The literature on dolomites is so extensive that it is not practical in this book to select and summarize representative case histories other than those discussed in preceding sections of this chapter. In fact, it is difficult to define what “representative” means when applied to dolomites. Therefore, students are encouraged to delve into some of this available literature on their own. A good place to start is with the further reading listed below. Also, articles on dolomites regularly appear in many geological journals. In particular, examine recent issues of the *Journal of Sedimentary Petrology*, *Sedimentology*, and *Sedimentary Geology*. Exposure to original research literature of this type allows students to gain insights into the viewpoints of a variety of researchers, viewpoints that are not filtered through the biases of textbook writers such as myself.

Further reading

- Allen, J. R. and W. D. Wiggins, 1993, *Dolomite Reservoirs: Geochemical Techniques for Evaluating Origin and Distribution*: AAPC Continuing Education Course Notes Series; No. 36, various pagings.
- Bernasconi, S. M., 1994, *Geochemical and Microbial Controls on Dolomite Formation in Anoxic Environments: A Case Study from the Middle Triassic (Ticino, Switzerland)*: E. Schweizerbart sche Verlagsbuchhandlung, Stuttgart.
- Braithwaite, C. J. R., G. Rizzi, and G. Darke (eds.), 2004, *The Geometry and Petrogenesis of Dolomite Hydrocarbon Reservoirs*: Geological Society Special Publication 235.
- Purser, B. M., Tucker, and D. Zenger (eds.), 1994, *Dolomites: a Volume in Honour of Dolomieu*: Blackwell Scientific, Oxford.
- Shukla, V. and P. A. Baker (eds), 1988, *Sedimentology and Geochemistry of Dolostones*: SEPM Special Publication 43.
- Zenger, D. H., J. B. Dunham, and R. L. Ethington, 1980, *Concepts and Models of Dolomitization*: SEPM Special Publication 28.

11

Diagenesis of carbonate rocks

11.1 Introduction

Chapter 8 discusses the processes that bring about diagenesis of siliciclastic sediments. In that chapter, the terms eodiagenesis, mesodiagenesis, and telodiagenesis are used to describe the stages of diagenesis that occur in siliciclastic sediments as they are progressively buried and subsequently uplifted. Significant differences exist between siliciclastic and carbonate sediments; therefore, the course of diagenesis differs in these two fundamentally different kinds of rocks. To illustrate, carbonate sediments are intrabasinal deposits, which are precipitated in some manner from the water in which they are deposited. Thus, initially, carbonate minerals are more or less in chemical equilibrium with the waters of their depositional environment. By contrast, siliciclastic sediments are brought into the depositional basin from outside. Further, carbonate sediments are composed of only a very few major minerals (aragonite, calcite, dolomite) in contrast to a much larger variety of minerals and rock fragments that may be present in siliciclastic sedimentary rocks. Carbonate minerals are more susceptible in general to diagenetic changes such as dissolution, recrystallization, and replacement than are most silicate minerals. Also, they are generally more easily broken down by physical processes, and they are much more susceptible to attack by organisms that may crush or shatter shells or that may bore into carbonate grains or shells.

Nonetheless, carbonate sediments proceed in a general way through the same diagenetic regimes as siliciclastic sediments. That is, carbonate sediments go through early (shallow-burial), middle (deep-burial), and possibly late (uplift and unroofing) stages of diagenesis. In terms of time and burial depth, these stages are similar to the eodiagenetic, mesodiagenetic, and telodiagenetic stages of siliciclastic diagenesis. In fact, the terms eogenetic, mesogenetic, and telogenetic were introduced by Choquette and Pray (1970) to designate zones of carbonate diagenesis. There are, however, significant differences between carbonate and siliciclastic sediments with respect to the nature of the diagenetic processes that occur in each of these stages. We cannot simply import the concepts developed for siliciclastic diagenesis to explain carbonate diagenesis. The ultimate result of burial diagenesis of siliciclastic sediments is to move initially incompatible assemblages of largely silicate minerals toward a state of greater equilibrium with their burial conditions of pressure, temperature, and pore-fluid compositions. These processes may thus produce important changes in mineral composition, but they rarely,

if ever, result in wholesale, pervasive alteration or replacement of depositional mineral assemblages. By contrast, carbonate sediments may undergo pervasive changes involving aragonite calcitization, recrystallization, and replacement that may bring about complete or nearly complete change in depositional mineralogy. For example, an initial aragonite mud may alter entirely to calcite (micrite) during early diagenesis and burial. In turn, the calcite may conceivably be replaced completely or nearly completely by dolomite at a later time. Also, cementation tends to be a more important process in carbonate rocks than in siliciclastic rocks.

Pervasive alteration of carbonate sediments not only changes the mineralogy of the sediments, but it may also destroy or severely modify depositional textures (e.g. carbonate grains, micrite). Thus, important environmental information may be lost. Further, the diagenesis of carbonate sediments may produce marked changes in porosity. Porosity is enhanced by dissolution processes and reduced by compaction and cementation. Because of the marked susceptibility of carbonate sediments to diagenetic alteration, special care must be taken in the study of carbonate rocks to recognize and identify features of diagenetic origin. Unless diagenetic features are differentiated from depositional features, the validity of genetic interpretations may be severely compromised.

In this chapter, we take an in-depth look at carbonate diagenesis. We begin by discussing early diagenesis in the seafloor environment, where carbonate sediments may be affected by biologic as well as by chemical and physical processes. Many carbonate sediments are subsequently exposed to meteoric conditions, either before or after deep burial. Significant diagenetic change takes place in carbonates in this environment under the influence of dilute, chemically aggressive meteoric pore waters. We then follow the course of diagenesis during deep burial. During burial diagenesis, increased pressure, increased temperature, and changed pore-water compositions are the important factors that bring about diagenetic change.

11.2 Regimes of carbonate diagenesis

As discussed in [Chapter 10](#), most carbonate sediments originate in marine environments. Therefore, this discussion of carbonate diagenesis focuses on the diagenesis of marine carbonates. Nonmarine carbonates also undergo diagenesis; however, diagenetic effects are generally less severe in nonmarine carbonates because they are composed of more stable carbonate minerals (mainly low-magnesian calcite) than are marine carbonates. [Figure 11.1](#) illustrates schematically the principal environments of carbonate diagenesis. We recognize three major regimes of diagenesis (James and Choquette, 1983a):

1. **The seafloor and shallow-marine subsurface** regime includes the seafloor and the very near-surface environment, that is, the eogenetic zone of Choquette and Pray (1970). It is characterized mainly by marine waters of normal salinity, although hypersaline waters are present in evaporative environments. Mixed marine–meteoric waters may be present also at the strandline and in the shallow subsurface at the mixing interface between the marine realm and the meteoric realm ([Fig. 11.1](#)).
2. **The meteoric regime** is distinguished by the presence of freshwater. It includes the unsaturated, vadose zone above the water table and the phreatic zone, or saturated zone, below the water table. As mentioned, a zone of mixed marine–meteoric water exists between the meteoric and marine

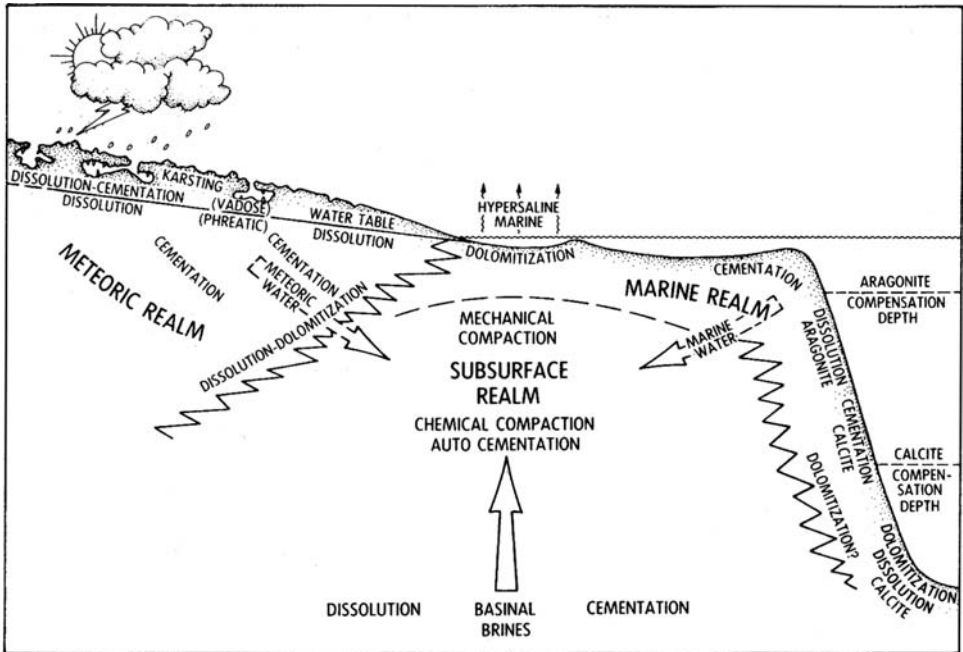


Figure 11.1 The principal environments in which postdepositional modification of carbonate sediments occur. The dominant processes that operate in each diagenetic realm are also indicated. See text for details. (From Moore, C. H., 1989, *Carbonate Diagenesis and Porosity*. Developments in Sedimentology 46, Fig. 3.1, p. 44, reprinted by permission of Elsevier Science Publishers, Amsterdam.)

realms. Nonmarine carbonates originate in the meteoric regime. Marine carbonates may be brought into this regime, at least for a short time, in three ways: (a) by falling sea level, (b) by progressive sediment filling of a shallow carbonate basin (which produces a shallowing-upward sequence) until the sediment interface is at or above sea level, and (c) by late-stage uplift and unroofing of a deeply buried carbonate complex. Thus, the meteoric regime may include both the eogenetic and telogenetic zones of Choquette and Pray.

3. **The deep subsurface** is referred to as the **marine phreatic** or **deep phreatic** zone by some authors. In the deep subsurface, sediment pores are filled with waters that were either marine or meteoric waters in the beginning. The composition of deep pore waters is commonly different, however, from either marine or meteoric waters owing to burial modifications. The deep subsurface is the mesogenetic zone of Choquette and Pray.

11.3 Diagenesis on the seafloor

11.3.1 Biogenic processes

As discussed in [Chapter 9](#), organisms participate in a variety of ways in generating carbonate deposits. After carbonate sediments are deposited, however, organisms can degrade and

break down skeletal grains and other carbonate materials. This organic degradation is actually a kind of sediment-forming process because it results in the production of finer-grained sediment. Nonetheless, it is included here as a type of very early diagenesis because it brings about modification of previously formed sediment.

The most important kind of biogenetic modification of sediment is caused by the boring activities of organisms. A variety of organisms are capable of boring into carbonate substrates. Microborings are produced by endolithic organisms (organisms that live in minute burrows) such as fungi, bacteria, and green, blue-green, and possibly red algae. Macroborings are formed by larger organisms, including sponges, mollusks, worms, echinoids, and crustaceans. Boring by algae, fungi, and bacteria is a particularly important process for modifying skeletal material and carbonate grains. Boring by photosynthesizing algae is confined to the photic zone and operates most effectively in the upper part of this zone at water depths less than about 70–100 m. On the other hand, the activities of fungi are believed to extend to depths of 500 m or more, and heterotrophic (nonphotosynthesizing) algae and bacteria may be present to abyssal depths (e.g. Friedman *et al.*, 1971).

Boring of carbonate grains by endolithic fungi and algae is commonly most intense in shallow-water tropical areas. Very fine-grained aragonite and/or high-magnesian calcite (Mg-calcite) is then precipitated into the holes left by these organisms. If boring activities are prolonged and intense, the entire surface of a grain may become infested by these aragonite- or Mg-calcite-filled borings, resulting in the formation of a thin coat of micrite around the grain. This coating is called a **micrite envelope** (Bathurst, 1966). The cortoids described in [Chapter 9](#) probably formed in this way. Even more intensive boring may result in complete micritization of the grain, with the result that all internal textures are destroyed and a kind of peloid is created. In colder and deeper waters, boring by endoliths may also be fairly intense. Because these waters are not commonly saturated with CaCO_3 , however, the vacated borings do not fill with precipitated CaCO_3 . Under these conditions, rather than forming a micrite envelope, continued boring eventually results in breakdown of the skeletal materials into finer-grained particles.

In addition to boring activities, organisms may contribute to carbonate destruction in the marine environment in some other ways: (1) predators such as fish including rays that eat shelled invertebrates break down the shells into smaller fragments, (2) predators attack and kill living substrate such as coral polyps, hastening the post-mortem invasion by boring organisms, (3) grazing organisms such as gastropods, echinoids, and fish attack and erode calcareous substrate, including reefs, and (4) browsing organisms such as holothurians and gastropods ingest carbonate sediment and pass it through their digestive mechanisms (e.g. Milliman, 1974, p. 258). This last process may cause some erosion and dissolution of carbonate particles, although its overall effect is believed to be quite minimal. The bioturbation activities of organisms can churn up carbonate sediment, resulting in textural mixing and destruction of sedimentary structures such as laminations. Furthermore, mixing of sediments near the sediment–water interface may cause some change in pore-water chemistry by mixing interstitial pore waters with overlying bottom waters. If the bottom water is undersaturated, such mixing could result in dissolution or etching of carbonate grains brought in contact with these waters as a result of bioturbation.

11.3.2 Carbonate cementation and dissolution

General conditions affecting cementation and dissolution

Carbonate sediments precipitated directly in the marine environment consist primarily of aragonite and Mg-calcite, although small amounts of low-magnesian calcite may also form. Dolomite also occurs in some modern marine environments, as mentioned in [Chapter 10](#). Much of the carbonate in marine environments consists of the remains of CaCO_3 -secreting organisms; however, the carbonate mineralogy of skeletal tests is different for different groups of organisms.

For example, most molluscs are composed of aragonite, although some (e.g. some gastropods) are composed of low-magnesian calcite. Echinoderms are composed of high-magnesian calcite, and foraminifers are composed of low- or high-magnesian calcite. Some groups of organisms may build skeletons of both aragonite and calcite (e.g. some sponges). A few organisms, such as diatoms and radiolarians, secrete skeletons composed of silica. See Flügel (2004, p. 103) for further details.

In the depositional environment, marine carbonates are exposed to either normal-marine or hypersaline waters. Most carbonate sediments are deposited in tropical waters where temperatures commonly exceed about 18 °C; however, carbonate deposits composed mainly of shell remains occur also in temperate waters and even in some colder waters. Some carbonate sediments (e.g. pelagic oozes, carbonate turbidites) are deposited in deep water where bottom waters are quite cold and pressures are high. The diagenetic behavior of carbonate minerals in marine waters is influenced by the chemistry of the water (carbonate saturated or undersaturated) and by the relative solubilities of the carbonate minerals that make up skeletal grains and other carbonates. The relative solubility of the carbonate minerals is a function of mineralogy and the Mg content of magnesian calcite. Very high magnesian calcite (> 12 mol% MgCO_3) is most soluble, followed by aragonite and Mg-calcite with about 12 mol % MgCO_3 . In turn, aragonite and 12 mol% Mg-calcite are more soluble than Mg-calcite with less than 12 mol% MgCO_3 , and low-magnesian calcite (4 mol% MgCO_3 or less) is least soluble (James and Choquette, 1984). Dolomite is even less soluble than the CaCO_3 minerals. The rate of dissolution of dolomite is about 100 times slower than that of calcite and aragonite (Busenberg and Plummer, 1986).

The solubilities of all these minerals vary as a function of temperature and pressure (water depth). Solubilities decrease with increasing temperature and increase with increasing pressure of seawater. Therefore, seawaters can range in composition from those that are highly saturated with respect to calcium carbonate (surface waters in tropical regions) to those that are undersaturated (cold surface waters in high latitudes and deep bottom waters). Typical variations in temperature with depth in the modern tropical ocean are shown in [Fig. 11.2](#), which also shows relative solubility curves for aragonite and calcite in terms of percent carbonate in sediments. Note that the aragonite **lysocline**, the zone of abrupt increase in aragonite solubility, occurs at a much shallower depth than the calcite lysocline. The aragonite and calcite **compensation depths** refer to the depths below which these minerals dissolve faster than they are accumulating. Therefore, these minerals do not occur on the ocean floor below these depths. On the

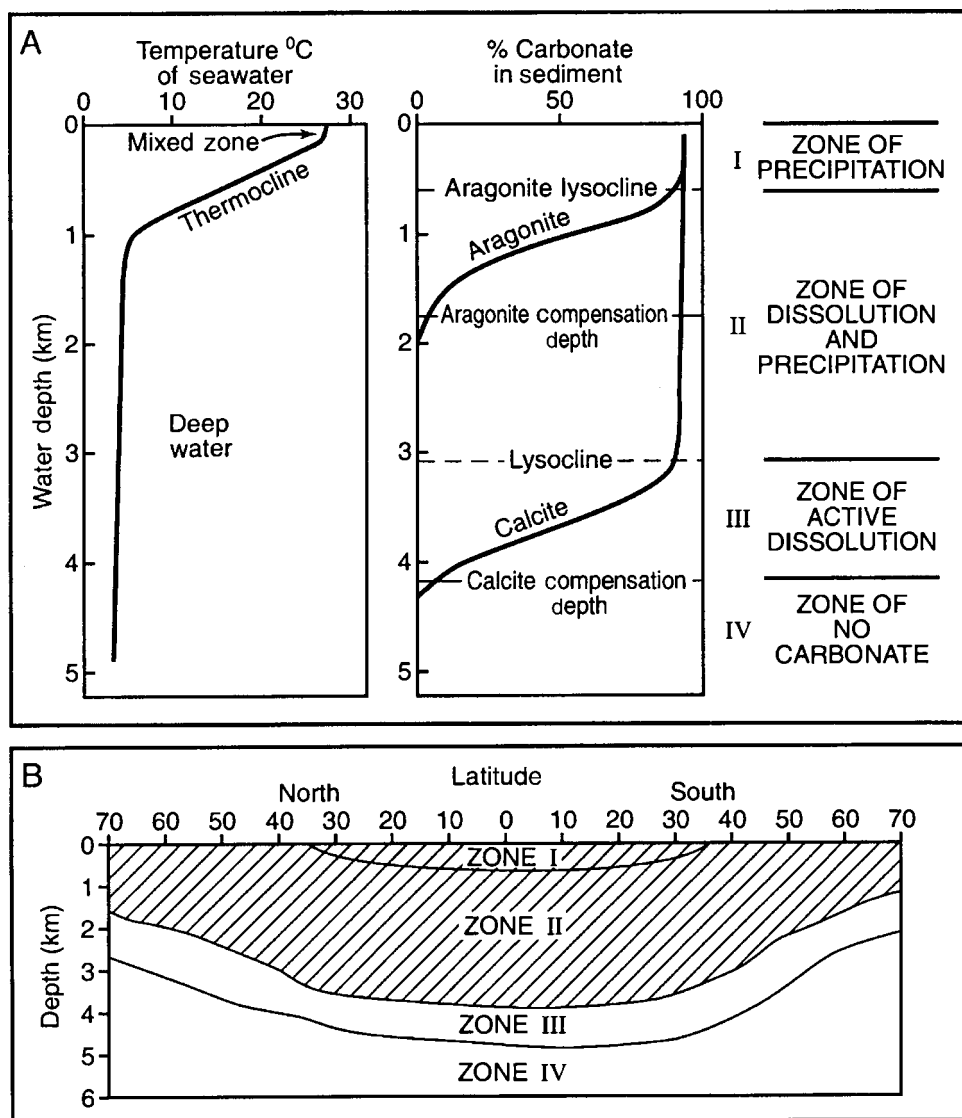


Figure 11.2 Generalized plots showing variations in seawater temperature with water depth and the relative positions of the aragonite and calcite lysoclines and compensation depths. Major zones of seafloor diagenesis are plotted to the right. (From James N. P. and P. W. Choquette, 1983b, Diagenesis 6. Limestones – The sea floor diagenetic environment: *Geosci. Can.*, **10**, Fig. 1, p. 163 and Fig. 2, p. 164, reprinted by permission of the Geological Association of Canada.)

average, the aragonite compensation depth in the modern ocean is shallower by about 3 km than the calcite compensation depth (CCD) (James and Choquette, 1983b).

James and Choquette (1983b) differentiate four carbonate “diagenetic” depth zones in the modern ocean. The conditions for carbonate diagenesis are approximately the same within

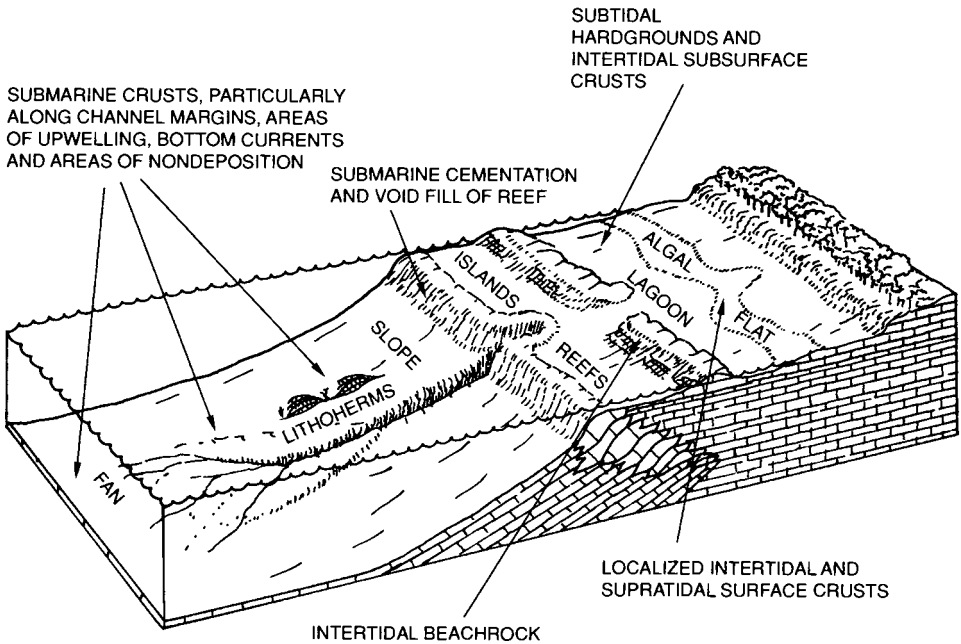


Figure 11.3 Major sites of carbonate cementation on the seafloor. (Modified slightly from Harris, P. M., C. G. St. C. Kendall and I. Lerche, 1985, Carbonate cementation – a brief review, in *Carbonate Cements: Paleontologists and Mineralogists Special Publication 36*, Fig. 3, p. 83, reprinted by permission of SEPM, Tulsa, OK.)

each of these zones, but differ between zones. Zone I (Fig. 11.2) is the **zone of precipitation**, which occurs mainly in shallow tropical to subtropical settings. The average lower depth limit of this zone in the tropics is about 1000 m, and the lower limit rises to the surface at about 35 degrees north and south latitude. In this zone, precipitation of cements (primarily aragonite and Mg-calcite) predominate and little or no dissolution occurs. Zone II is a **zone of partial dissolution** of carbonates. It lies below the aragonite lysocline in tropical to subtropical regions, but occurs at the ocean surface at latitudes higher than about 35 degrees. Little inorganic precipitation of aragonite or Mg-calcite takes place in this zone; but dissolution, particularly of aragonite and Mg-calcite, can occur. Zone III is the **zone of active dissolution**, which lies between the calcite lysocline and the calcite compensation depth (CCD). It may shallow to near the surface in polar seas. Zone IV is the **zone of no carbonate**, which occurs below the CCD. Dissolution is predominant in this zone, and no carbonate is accumulating.

Cementation

Sites of marine cementation

The major sites of carbonate cementation on the seafloor are indicated in Fig. 11.3. Early marine cementation occurs primarily in the warm, shallow waters of Zone I (Fig. 11.2). Some cements may form in cold shelf waters and deeper waters of Zone II, but cementation

appears to be very minor. High-magnesian calcite is apparently the most common marine cement overall, but aragonite is common also in waters of slightly elevated salinity (James and Ginsburg, 1979). Early cementation can occur within pores or cavities in carbonate grains lying loose on the seafloor or buried to very shallow depths below the sediment interface, without cementing these particles together. The inner cavities of shells and other skeletal grains and microborings in the surfaces of skeletal grains appear to be particularly favorable sites for such early cementation. For example, early cementation inside pellets, grapestones (lumps), and possibly ooids results in early hardening of these grains.

Cements may also be precipitated between carbonate grains to create lithified substrate. The best conditions for cementation of grains appear to be in areas where good water circulation or turbulence furnishes a constant supply of CaCO_3 -saturated fluid that can be pumped or forced through the surface and near-surface sediments by waves, currents, or tides. Because each pore volume of seawater contains only a minute amount of dissolved CaCO_3 , and only a small percentage of this CaCO_3 may precipitate, the pore fluids must be constantly renewed for a pore to fill with cement. Thus, as many as 10,000 to 100,000 pore volumes of seawater may be required to fill a pore with carbonate cement (see discussion by Scholle and Halley, 1985). An additional requirement for cementation of grains is that the substrate must be well enough stabilized to allow cementation to occur before grains are remobilized by waves or currents.

Platform-margin reefs, especially those on windward margins, are areas of the carbonate platform where these requisite conditions, particularly strong water turbulence, are met particularly well. Thus, in a matter of tens to thousands of years, some reefs may become well cemented (James and Choquette, 1983b). Platform-margin carbonate sand shoals, where grains inside the shoals are at rest or are bound by algae, may also become well cemented to form **hardgrounds** (Bathurst, 1975, several sections). Hardgrounds in modern carbonate environments have been reported in numerous areas, including the margins of the Persian Gulf, the Bahama Platform, and Sharks Bay in western Australia. Hardgrounds have also been reported in ancient carbonate sequences, where they may occur as part of ooid-bearing platform-margin sequences, within coarse grainstones in normal-marine cratonic sequences, and as the terminal phases of shallowing-upward sequences (Moore, 1989, p. 88). Typical characteristics of hardgrounds are illustrated in Fig 11.4 ; they include the presence of an abraded, commonly irregularly bored surface. This surface may be marked also by the presence of encrusting fossils and intraclasts derived from the hardground and may be stained by manganese.

Some strandline sands may also become lithified by cementation to form beachrock (see Fig. 11.3). Beachrock consists of carbonate-cemented layers of beach sand that dip seaward at about the same angle as the beach sediments. It may be composed mainly of cemented carbonate sands, but quartz or volcanic sands may also form beachrock. Presumably, the beach sand is stabilized owing to binding by algae, fungi, or roots for a long enough period for cementation to occur (Strasser *et al.*, 1989). High turbulence in the littoral zone furnishes a constant supply of CaCO_3 -rich waters. Mixing of meteoric water and seawater in strandline sediments may be an additional factor causing cement precipitation to form beachrock,

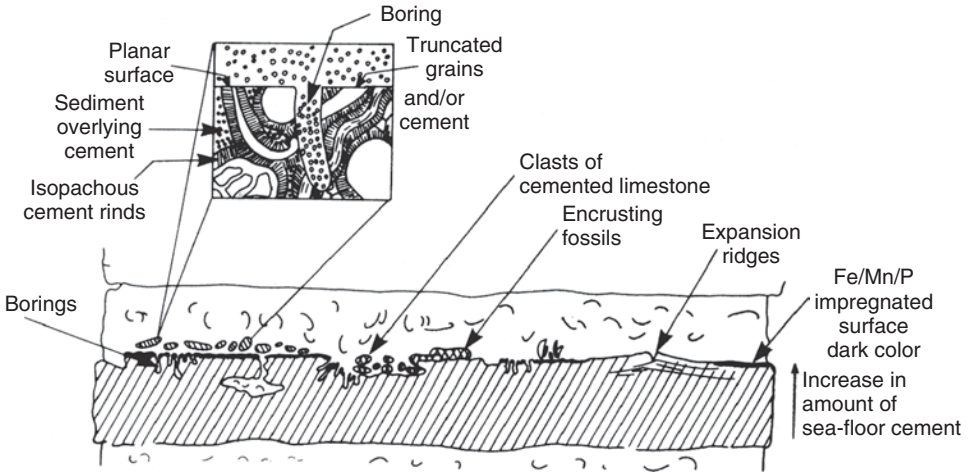


Figure 11.4 Distinguishing characteristics of seafloor hardgrounds. (From James N.P. and P.W. Choquette, 1983b, Diagenesis 6. Limestones – The sea floor diagenetic environment: *Geosci. Can.*, **10**, Fig. 12, p. 172, reprinted by permission of the Geological Association of Canada.)

although CO_2 degassing owing to water turbulence is probably a more important factor. Localized formation of carbonate crusts may occur also in algal mats and on other sediment in the intertidal and supratidal zones (Fig. 11.3).

Thus, reefs, platform-margin sand shoals, and strandline deposits are favored areas for early seafloor cementation. On the other hand, most sediments of shallow carbonate platforms are not cemented. This lack of cementation is especially evident in muddy sediments in shelf lagoons, where sluggish water movements, continuous bioturbation, and reducing conditions apparently discourage cementation.

Calcite or Mg-calcite cemented hardgrounds may occur also in deeper water on the upper parts of platform-margin slopes and on the deeper seafloor in areas swept by bottom currents. These areas are within the zone of aragonite dissolution or partial dissolution, but above the zone of calcite dissolution. For example, Neumann *et al.* (1977) describe lithified carbonate mounds in the Straits of Florida that occur at water depths of about 600–700 m. These mounds, which they refer to as **lithoherms** (see Fig. 11.3), rise as much as 50 m above the bottom. They are composed of ahermatypic corals and crinoids that are lithified by numerous superimposed, Mg-calcite cemented crusts. An additional example of a deep-marine lithified sediment was reported by Schlanger and James (1978). These authors describe lithified Bahamian peri-platform oozes in the Tongue of the Ocean at water depths of 700–1960 m. Lithification apparently took place by alteration of aragonite to low-magnesian calcite, dissolution of aragonite, and subsequent precipitation of calcite in the resulting voids. Submarine carbonate crusts may also occur on other parts of the deeper seafloor along some submarine channel margins, in areas of upwelling, and in areas of nondeposition (Fig. 11.3). The tops of some seamounts are also sites of carbonate cementation.

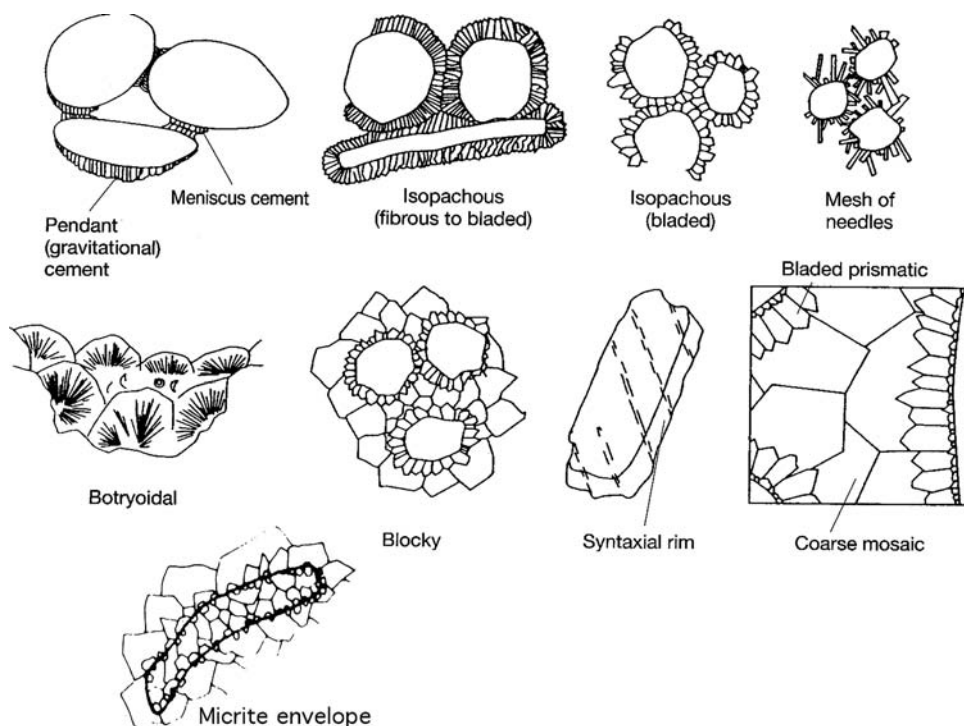


Figure 11.5 Principal kinds of cements that form in carbonate rocks. Marine (seafloor) diagenetic environments are characterized particularly by aragonitic meniscus and pendant cements (in beachrock), isopachous cement, needle cement, and botryoidal cement. Meteoric-realm cements are composed dominantly of calcite and include meniscus, pendant, and micrite-envelope cements in the vadose zone and isopachous, blocky, and syntaxial-rim cements in the phreatic zone. Cements in the subsurface burial realm are also mainly calcite and include syntaxial rims, bladed-prismatic, and coarse-mosaic types. (Modified from James, N.P. and P.W. Choquette, 1983b, Diagenesis 6. Limestones – The seafloor diagenetic environment: *Geosci. Can.*, **10**, Fig. 3, p. 165; James, N.P. and P.W. Choquette, 1984, Diagenesis 9. Limestones – The meteoric diagenetic environment: *Geosci. Can.*, **11**, Fig. 24, p. 177; Choquette, P.W. and N.P. James, 1987, Diagenesis of limestones – 30 The deep burial environment: *Geosci. Can.*, **14**, Fig. 21, p. 16.)

Types of marine cements

High-magnesian calcite and aragonite are the dominant kinds of shallow-marine cements, although dolomite may act as a cement in some environments (Chapter 10). High-magnesian calcite can occur as micrite-size crystals that form very thin rinds around grains or fill pore spaces among grains. As a pore filler, micrite is not strictly a cement, as it may not bind grains together. Some micrite cements may have a peloidal structure. Micrite cements have been reported from beachrock, within Bahamian grapestones, in Bahamian hardgrounds (e.g. Moore, 1989, p. 77), and in reefs. Magnesian calcite can occur also as **fibrous to bladed crystals** that form much thicker rinds (Fig. 11.5). Aragonite cement commonly occurs as **fibrous rinds** around skeletal grains and other carbonate grains. These crusts are

often called **isopachous rinds** because they have approximately equal thickness. Fibrous to bladed aragonite or Mg-calcite cement is common in beachrock. Some fibrous cement in beachrock occurs only at grain contacts where a meniscus of water would be held by capillary forces as interstitial water drained from the beach sand during low tide. This cement is called **meniscus cement** (Dunham, 1971). Nonisopachous fibrous cement in beachrock that appears to sag downward under grains is called **pendant** or **gravitational cement**. Aragonite may also occur as an intergranular **mesh of needlelike crystals** that grow with random orientation into pore space, or as fibrous-radial crystals that have a **botryoidal** form. Both of these forms can occur in forereef environments, for example.

The subject of carbonate cementation and carbonate cements is of broad interest to geologists, especially petroleum geologists who are concerned with the inhibiting effects of cementation on carbonate porosity. Therefore, numerous research papers have addressed this topic and at least two books have been devoted to carbonate cements (Schneidermann and Harris, 1985; Bricker, 1971). Many outstanding color photographs of carbonate cements are available in Scholle and Ulmer-Scholle (2003).

Dissolution

As discussed above, seawater becomes undersaturated in carbonate at depth in the ocean and at colder temperatures in shallow water at high latitudes. Thus, dissolution may begin in diagenetic Zone II (Fig. 11.2). It accelerates in Zone III, and becomes complete in Zone IV (below the CCD). The relative rate of dissolution is determined by the water geochemistry and the carbonate mineralogy. As mentioned, very high-magnesian calcite is more soluble than aragonite, which is more soluble than Mg-calcite. In turn, Mg-calcite is more soluble than calcite, and dolomite is least soluble. Thus, selective solution of carbonate materials can take place, bringing about relative enrichment of the more stable carbonate phases, particularly calcite.

Obviously, most dissolution of carbonate on the seafloor takes place outside the warm shallow waters of Zone I, which is the zone of precipitation and cementation. It follows also that very little carbonate sediment is generated outside of Zone I except skeletal grains. Therefore, most carbonate sediments in deeper water and at higher latitudes in shallow water are composed dominantly of skeletal grains. Skeletal grains in deep water include the remains of planktonic organisms such as foraminifers, pteropods, and coccoliths. Skeletal deposits in shallow temperate and colder waters consist mainly of the remains of benthonic organisms (e.g. benthonic foraminifers, calcareous red algae, bryozoans, mollusks, echinoderms). Although few carbonate sediments other than skeletal materials originate in deeper water, shallow-water carbonate grains and mud may be carried off platforms into deeper water by sediment gravity flows. Also, carbonate muds may be swept off platforms in suspension to settle as peri-platform oozes.

Deeper waters may be undersaturated with respect to aragonite and possibly high-magnesian calcite. Therefore, depending upon their composition, selective dissolution of carbonate materials can occur. In the case of planktonic organisms, pteropods are composed of aragonite, but foraminifers and coccoliths are composed of calcite. Thus, pteropods will

dissolve at a shallower depth than foraminifers and coccoliths but these organisms will also disappear below the CCD. Organisms in temperate waters tend to be composed mainly of calcite. Therefore, their remains are relatively stable on the seafloor. Nonetheless, shells can become visibly etched in these waters. If shells are heavily bored by endolithic organisms, solution can aid in breaking down these shells to smaller pieces. Very little clay-size carbonate (micrite) occurs in temperate and high-latitude waters, probably because very little if any inorganic precipitation of fine carbonate takes place in these waters. Fine-size carbonate no doubt does occur by skeletal breakdown, but its scarcity in cold temperate waters suggests that it is destroyed by dissolution. Carbonate grains and lime mud transported from shallow platforms to deeper waters is also subject to dissolution. The relative importance of this dissolution obviously depends upon the mineralogy of the sediment and the saturation state of the water in which redeposition occurs. For example, an aragonite mud transported into deep, undersaturated water may dissolve, followed by precipitation of low-magnesian calcite. On the other hand, fragments of corals or bryozoans, composed mainly of calcite, would have a better chance of surviving dissolution unless they were transported below the CCD. Owing to its slow rate of solubility, some dolomite can presumably survive dissolution below the CCD.

11.3.3 Marine neomorphism

Neomorphism is a term used by Folk (1965) to cover the combined processes of inversion and recrystallization. **Inversion** is the change of one mineral to its polymorph (e.g. aragonite to calcite). The term, as applied to the transformation of aragonite to calcite, appears to have been used in the past with somewhat different meanings. Apparently, its correct meaning is the transformation of aragonite to calcite in the solid (dry) state. Transformation in the solid state proceeds by Ca–O bond destruction and reformation and requires temperatures on the order of 300 °C to 600 °C (Carlson, 1983). Inversion (in the solid state) probably does not occur in the diagenetic environment. Most diagenetic transformation of aragonite takes place in the presence of fluids. Under these conditions, transformation appears to proceed by solution of aragonite and essentially simultaneous precipitation of calcite. The transformation takes place across a thin film of water nanometers to micrometers in thickness (e.g. Wardlaw *et al.*, 1978). As submicroscopic voids are created on one side of the film by dissolution of aragonite, calcite moves through the film to precipitate in these voids. Thus, the alteration of aragonite to calcite by this process is a special kind of replacement. Many geologists today refer to this fine-scale process simply as **calcitization**. For clarity in this book, I refer to the transformation of aragonite to calcite in the wet state as **polymorphic transformation**.

Trace elements, particularly strontium, tend to be partitioned into and become concentrated in calcite during the process of polymorphic transformation. This type of calcitization may preserve relict aragonite textures, which may be outlined by relics of organic matter or other insoluble material (Sandberg, 1983). For example, relict shell structures of aragonite fossils may still be visible, even though a mosaic of calcite crystals cross-cut the original

fabric. Calcitization of aragonite can be accomplished also by larger-scale aragonite dissolution that produces visible pores, owing to solution of fossils, carbonate grains, or cements, followed by precipitation of calcite cement in the resulting molds. In this case, cementation may occur soon after formation of the molds or much later than the time of mold formation. This process, strictly speaking, is not polymorphic transformation but dissolution/cementation. It produces essentially the same mineralogical results as polymorphic transformation, but primary aragonite textures are not preserved.

Recrystallization is primarily a change in size or shape of crystals (e.g. increase or decrease in the size of calcite crystals) where no change in mineral composition takes place. Thus, the “replacement” of small calcite crystals by larger calcite crystals (no change in mineralogy) is recrystallization. The change of high-magnesian calcite to low-magnesian calcite is also recrystallization according to Folk (1965), but not according to Bathurst (1975, p. 475). Further, Bathurst (1975, p. 476) states that recrystallization in the dry state is unknown in carbonate diagenesis and that only “wet recrystallization” is important.

Because it is often very difficult to tell the difference (with a normal polarizing microscope) between solution–precipitation processes and recrystallization, Folk (1965) proposed what he called a comprehensive term of ignorance, **neomorphism**, to cover all transformations between one mineral and itself or a polymorph. Thus, neomorphism includes the polymorphic transformation of aragonite to calcite, alteration of Mg-calcite to calcite, and recrystallization. Note that neomorphism takes place without change in the major chemical composition, although trace-element and isotope composition may change. Typically, neomorphism results in an increase in crystal size of carbonate minerals (aggrading neomorphism).

Neomorphism appears to be a relatively unimportant process in the shallow, warm waters of diagenetic Zone I on the seafloor. Rare occurrence of Mg-calcite foraminifers and coralline algae that alter to aragonite have been reported. Also, aragonite cements may partially replace aragonitic mollusk shells, and parts of aragonitic cements and skeletons may change to Mg-calcite (see discussion by James and Choquette, 1983b); however, neomorphism in this zone seems to be uncommon. On the other hand, carbonate grains and sediments transported into deeper water or pelagic shells settling into such water may undergo some aggrading neomorphism, which commonly involves alteration of Mg-calcite or aragonite to low-magnesian calcite. An example is the alteration of aragonite to calcite in Bahamian peri-platform oozes reported by Schlanger and James (1978). Examples of neomorphic alteration of skeletal debris have been reported also from the deep foreereef off North Jamaica and on deep banks in the Gulf of Mexico (Scoffin, 1987, p. 105). Most of these examples appear to occur in areas of low sedimentation and prolonged exposure to cold seawater.

11.4 Diagenesis in the meteoric environment

11.4.1 Geochemical constraints

As mentioned, carbonate sediments initially deposited in the marine environment can be brought into contact with meteoric waters in at least three ways: (1) complete sediment

filling of a shallow carbonate basin (platform setting) to or above sea level, i.e. shoaling upward, (2) falling sea level, which exposes previously formed carbonates, and (3) late-stage uplift and unroofing of older carbonates, which brings them into the zone of meteoric water. Because of the common tendency for shallow-marine carbonates to shoal upward to sea level, or to be exposed by falling sea level, meteoric diagenesis dominates the diagenesis of most shallow-marine carbonate sequences (Land, 1986).

Although meteoric waters may exhibit a wide range of saturation states, they are commonly undersaturated with respect to most carbonate minerals. Thus, aragonite and Mg-calcite deposited under marine conditions can undergo significant alteration when brought under the influence of dilute, acidic meteoric waters. This alteration can include both dissolution and neomorphism to low-magnesian calcite. Although low-magnesian calcite is more stable (less soluble) than aragonite and Mg-calcite in meteoric waters, owing to the low Mg/Ca ratios and salinities of these waters, calcite may also undergo partial or complete dissolution in meteoric waters. Many meteoric waters are strongly acidic and undersaturated with respect to CaCO_3 owing to their high content of dissolved CO_2 derived by atmospheric interchange and solution from the soils through which they pass. Thus, even calcite may not escape alteration in such strongly “aggressive” meteoric waters. Dissolution may occur by simple corrosion (dissolution by rainwater), organic corrosion (dissolution owing to increased CO_2 from decaying organic matter in soils), mixing corrosion (resulting from mixing of different meteoric waters or mixing of meteoric water with connate water or seawater), and hydrostatic corrosion (owing to increased hydrostatic pressure with depth below the water table). See the discussion by James and Choquette (1984).

Although low-magnesian calcite can dissolve in meteoric waters under some conditions, as stated, precipitation of low-magnesian calcite is a more common process in the meteoric diagenetic environment than is dissolution. Precipitation occurs when waters become oversaturated with respect to calcite. According to James and Choquette (1984), precipitation may be either water controlled or mineral controlled. **Water-controlled precipitation** takes place under conditions of oversaturation owing to removal of CO_2 from the system. Carbon dioxide may be removed by heating (including evaporation), pressure loss (e.g. waters emerging into a cave or the atmosphere), or photosynthesis. Calcite will precipitate from oversaturated waters if it can, but may be inhibited from precipitation by kinetic factors or the presence of ions such as Mg^{2+} , SO_4^- , or PO_4^{3-} . If inhibited, the saturation state will rise until a thermodynamic drive is reached that is sufficient to overcome the kinetic problem. **Mineral-controlled precipitation** involves dissolution of more-soluble aragonite and Mg-calcite, which results in oversaturation with respect to calcite. Precipitation of calcite follows. In this process, calcite is never dissolved because oversaturation is achieved and maintained by dissolution of aragonite and Mg-calcite. On the other hand, kinetics may prevent calcite from precipitating as rapidly as the rate of dissolution of aragonite or Mg-calcite. For example, Schmalz (1967) estimated that the rate of aragonite dissolution in fresh meteoric water is 100 times greater than the rate of calcite precipitation. For a more detailed look at the dissolution and growth kinetics of calcite and aragonite, see Busenberg

and Plummer (1986). Thus, meteoric waters may become several times oversaturated with respect to calcite owing to the slowness of calcite to precipitate. The new calcite can precipitate in open voids as cement between grains or within grains, or it can precipitate on a microscale inside particles, replacing the original aragonite or Mg-calcite.

This discussion suggests that mineral-controlled precipitation can eventually lead to wholesale alteration in carbonate mineralogy, with metastable aragonite and Mg-calcite being “replaced” by calcite. On the other hand, carbonate sediments that originally contained little aragonite may undergo only slight cementation during meteoric diagenesis. For example, James and Bone (1989) report that the Gambler Limestone of southern Australia, a cool-water limestone composed dominantly of bryozoans, has undergone very little cementation in 10 million years of diagenesis in the meteoric environment. They conclude from the characteristics of this limestone that meteoric cementation is effective only for carbonate sediments that originally contained abundant aragonite particles.

11.4.2 Diagenesis in the vadose zone

General conditions

Longman (1980) suggests that the vadose zone (Fig. 11.1) can be divided into two parts, which represent the end members of a continuous spectrum: (1) the soil zone, or zone of solution, and (2) the zone of precipitation or capillary fringe zone. Thickness of these zones may vary considerably, particularly as a function of climate. The boundaries between the zones are gradational and may fluctuate abruptly in response to rainfall. Also, the zone of precipitation may be absent under some conditions. Solution and neomorphism tend to proceed rapidly under humid conditions but much more slowly in dry regions. Much rainwater moves through the vadose zone fairly slowly by gravity percolation or vadose seepage. Water can also move through the zone by vadose flow, which involves relatively rapid flow by way of joints, large fissures, or sinkholes.

Dissolution

In the vadose zone of the meteoric environment (Fig. 11.1), both air and water may be present in the pores, but the pores are not completely filled (saturated) with water. Chemically aggressive meteoric water percolating (seeping) or flowing down through the vadose zone within a body of emerged marine carbonate sediment will initially cause extensive solution of aragonite and Mg-calcite and may also dissolve calcite. If the sediments are composed entirely of calcite, little further dissolution or precipitation may occur once the vadose waters reach saturation with respect to CaCO_3 . Exceptions to this generality are possible if the calcite grains are very small, mixing of meteoric waters (vadose seepage and vadose flow) occurs, or degassing of CO_2 takes place owing to exposure to the atmosphere (in caves) or increased temperatures. If, however, the sediments are composed of a mixture of aragonite, Mg-calcite, and calcite, the vadose waters continue to bring about dissolution owing to mineral-controlled processes that stem from differences in solubility

(James and Choquette, 1984). Thus, extensive dissolution of aragonite and Mg-calcite can occur, with concomitant precipitation of calcite.

Alteration of Mg-calcite to calcite

Owing to its lower solubility, Mg-calcite alters to calcite through a solution–reprecipitation process. Magnesian-calcite dissolves incongruently (Bathurst, 1980) and, presumably, the most MgCO_3 -rich parts of skeletal grains dissolve first. As MgCO_3 is dissolved, calcite is simultaneously precipitated onto the existing calcite crystal lattice and preserves the original crystallographic orientation. Because this process is fabric-preserving, calcite crystals formed by alteration of Mg-calcite appear essentially identical to the precursor Mg-calcite under a polarizing microscope. Analysis of the iron content of the calcite is required to determine if it formed by alteration of Mg-calcite. Calcite precipitated from seawater does not contain iron, whereas Mg-calcite does. Thus, an iron-rich low-magnesian calcite must have formed by alteration of a Mg-calcite precursor (Richter and Füchtbauer, 1978).

Neomorphism of aragonite to calcite

Aragonite can invert to calcite in the solid (dry) state at high temperatures; however, this process probably does not occur during sediment diagenesis. In the presence of fluids in the vadose zone, aragonite readily alters to calcite by solution–reprecipitation. As discussed, alteration can take place either on a microscale (replacement), which is fabric-preserving, or on a macroscale that involves solution and mold formation and possible filling of the molds by calcite cement. The difference between these two processes is illustrated diagrammatically in Fig. 11.6. This figure shows that microscale dissolution and reprecipitation is fabric preserving and results in no secondary porosity. By contrast, macroscale dissolution may create molds (moldic porosity) that are not all immediately filled by calcite precipitation. In this case, the CaCO_3 in solution may be precipitated as calcite cement in other pore space further downflow. It is commonly believed, however, that extensive moldic porosity does not occur in the vadose zone. Because aragonite is generally more abundant than Mg-calcite in shallow-water carbonate deposits, alteration of aragonite to calcite in the vadose zone is a volumetrically important process.

Calcite cementation

In addition to precipitation of calcite in the process of microscale alteration of Mg-calcite and aragonite in the vadose zone, calcite is precipitated as a coarse cement into larger holes created by dissolution of these minerals. Calcite may also precipitate inside grains such as fossils and in open pore space among grains (James and Choquette, 1984). This calcite cement tends to form equant crystals. Because pore spaces are not completely filled with water, however, the cement commonly does not surround grains or completely fill pores. Typically, it takes the form of meniscus or pendant (stalactitic) cement (Fig. 11.5). Thus, it may resemble in form cements precipitated in the marine vadose zone (i.e. in beachrock); however, vadose cement is composed of calcite whereas beachrock cement is composed of Mg-calcite or aragonite. If cementation is prolonged, pores may be completely filled with cement, and the characteristic meniscus or pendant shapes may be lost.

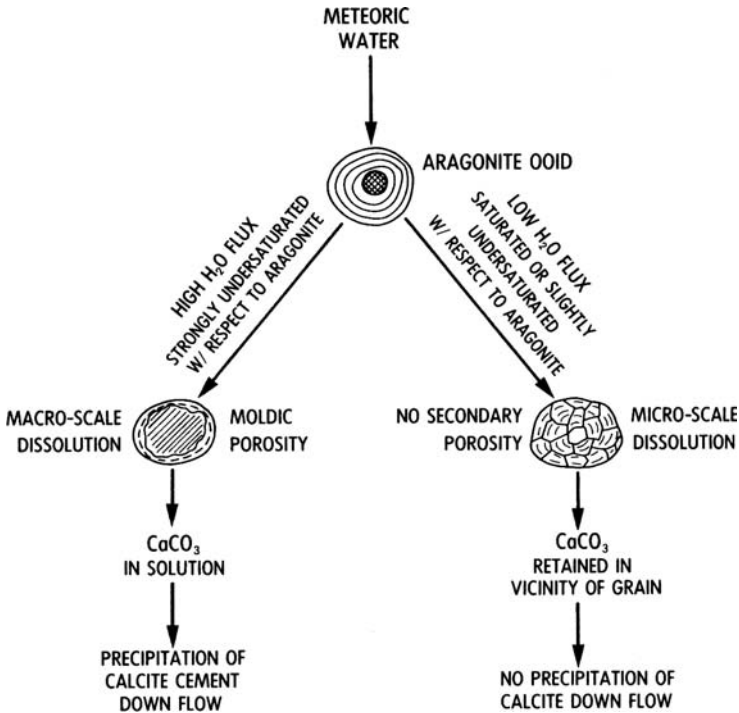


Figure 11.6 Schematic diagram illustrating the difference between microscale dissolution (fabric-preserving) and macroscale dissolution (fabric-destructive). Hydrologic and geochemical conditions that influence these pathways of diagenesis are indicated. (From Moore, C. H., 1989, *Carbonate Diagenesis and Porosity: Developments in Sedimentology* 46, Fig. 6.6, p. 170, reprinted by permission of Elsevier Science Publishers, Amsterdam.)

Micrite-envelope cement forms in voids created by complete dissolution of carbonate grains (probably aragonite grains) that had an original low-magnesian calcite micrite envelope. During dissolution, this envelope or rind resists solution and thus acts as a mold (Scoffin, 1987, p. 111; Tucker and Wright, 1990, p. 13). Subsequent filling of the mold by blocky, low-magnesian calcite cement gives the micrite cement pattern illustrated in Fig. 11.5. Syntaxial (epitaxial) overgrowths on echinoderm fragments may also occur in the vadose environment. In finer-grained sediment, where capillary forces are greater and vadose water is held longer, calcite cementation may be more pervasive than in coarser sediment.

11.4.3 Diagenesis in the phreatic zone

Hydrologic characteristics

The freshwater phreatic zone lies below the vadose zone, and all pore space in this zone is filled with meteoric water. The top of the zone is the water table, and the base is a zone of

mixing with underlying water. This underlying water is normal seawater in areas near the coast but it is subsurface formation water (connate water) in more inland areas. Water enters the phreatic zone either by vadose seepage or by direct vadose flow through fractures or sinks from lakes, streams, or runoff. Thus, waters of quite different chemical character may be present (and may mix) in the phreatic zone. Water in the phreatic zone moves in a subhorizontal direction toward some outlet or discharge area.

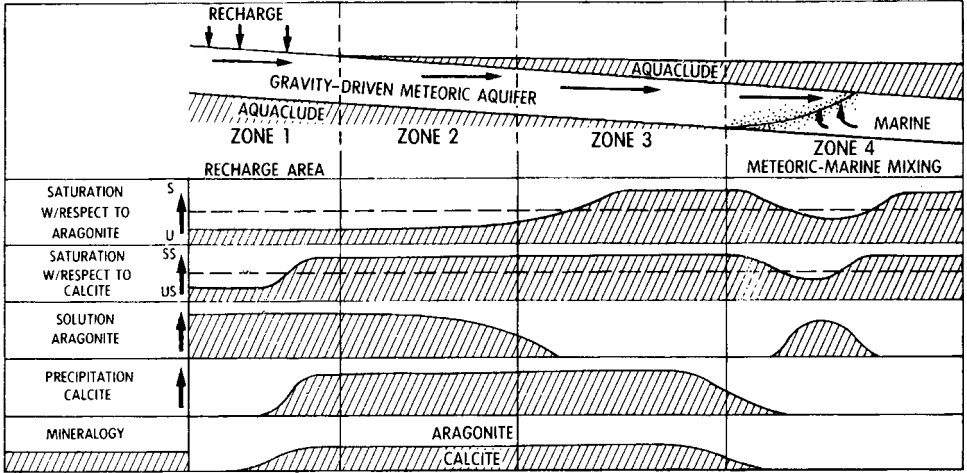
Diagenetic processes

Because the phreatic zone is buried below the water table and is not accessible for direct examination, observation of carbonate sediments in this zone can be had only from cores. Therefore, much less is known about diagenesis in the phreatic zone than in the vadose zone. Longman (1980) proposed an ideal model for freshwater phreatic diagenesis, in which he assumed that phreatic waters become increasingly saturated with CaCO_3 with increasing depth. According to this model, dissolution predominates in the shallower parts of the phreatic zone, and cementation (or no diagenetic activity) occurs in the deeper part. Because this model is based on inference, it remains to be tested.

Diagenetic processes are more intense in the phreatic zone, where grains are constantly surrounded by water and where water flow through sediment is more constant than in the vadose zone, where water flow is ephemeral. Furthermore, the water table itself is a zone of particularly intense activity (James and Choquette, 1984; Moore, 1989, p. 181). If aggressive CO_2 -rich waters are still undersaturated when they reach the water table, particularly those arriving directly from the surface by vadose flow, dissolution will be concentrated along the water table. Many caves in carbonate deposits occur at the water table. On the other hand, if CO_2 degassing is active along the water table, cementation can occur. Furthermore, below the water table, mixing of waters having different carbon dioxide levels and CaCO_3 saturation states may bring about either dissolution or precipitation, depending upon the characteristics of the mixed waters. Thus, it is not easy to pinpoint specific zones of dissolution or precipitation in the phreatic zone.

In any case, metastable sediments appear to alter rapidly in the phreatic zone and to become better calcitized and lithified than the same kinds of sediments in the overlying vadose zone (James and Choquette, 1984). Furthermore, the rate of stabilization of aragonite and Mg-calcite appears to be faster in regional meteoric aquifer systems than in those hydrologic systems on small carbonate islands where there is a local floating meteoric water lens. Presumably, this difference exists because most of the water on small islands arrives by seepage from the vadose zone, whereas large volumes of water can enter regional aquifer systems by vadose flow. Also, there is more active movement of water through the system. With respect to island phreatic systems, Moore (1989, p. 185) suggests that dissolution of aragonite, creation of moldic porosity, and precipitation of calcite are all most active in the upper part of the phreatic zone. Aragonite dissolution diminishes downward toward the mixing zone, and the percentages of calcite cement and moldic porosity also decrease downward. Moore (1989, p. 195; 2001, p. 215) proposes a much more complex model for diagenesis within a regional aquifer system where the aquifer is confined

A. Immature stage



B. Mature stage

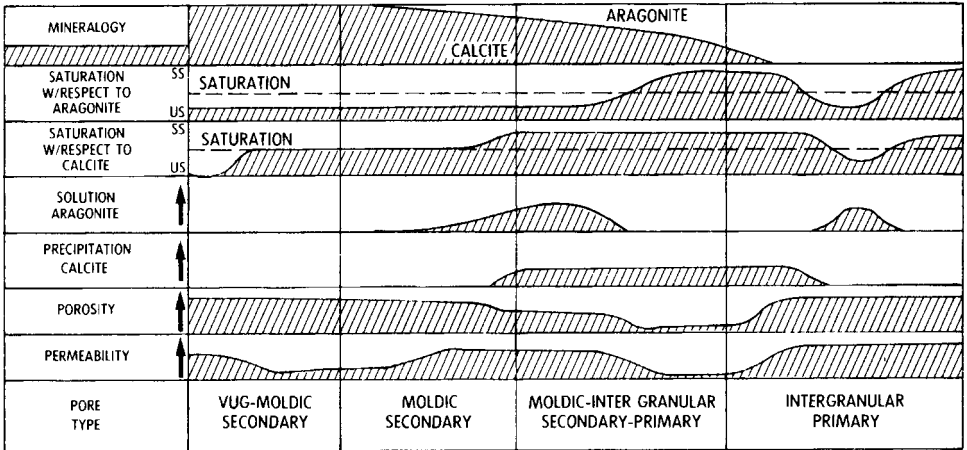


Figure 11.7 Postulated diagenetic model for a gravity-driven, confined meteoric aquifer system (top of diagram). Water moves from Zone 1 (recharge area) toward Zone 4 (mixing zone). Note that in the early, immature stage of diagenesis aragonite is still present in the recharge area. In the more advanced, mature stage, aragonite has been destroyed by dissolution and calcite is present in the recharge area. (From Moore, C. H., 1989, *Carbonate Diagenesis and Porosity: Developments in Sedimentology* 46, Fig. 7.12, p. 195, reprinted by permission of Elsevier Science Publishers, Amsterdam.)

between nonpermeable layers (aquacludes). According to this model (Fig. 11.7), aragonite is initially present (immature stage) in the recharge area, and aragonite dissolution and concomitant calcite precipitation are very active processes. In the mature stage, aragonite is gone from the recharge area (but is still present in downflow areas), and aragonite dissolution and calcite precipitation are greatly reduced. Considerable porosity is present in the sediments in the mature stage.

Phreatic cements

Because phreatic cements are precipitated in pores that are completely filled with water, in contrast to vadose pores, meniscus and pendant cements do not occur. Instead, isopachous cements and blocky cements are dominant (Fig. 11.5). Crystal size of phreatic cements tends to be somewhat larger than that of vadose cements. Syntaxial overgrowths of echinoderms may also be very common.

11.4.4 Diagenesis in the mixing zone

The base of the freshwater phreatic zone is the interface between freshwater and underlying more saline waters (Fig. 11.1). In coastal regions and small islands, this underlying water is normal seawater. In more inland settings, it is connate formation waters that may be greatly modified from original seawater or freshwater. Because there is mixing of freshwater and more-saline water across the interface, this zone is referred to as a mixing zone.

Geologists have generated considerable interest in the mixing zone as a possible site for dolomitization. As discussed in Chapter 10, however, the original thermodynamic underpinnings of the mixing-zone dolomite theory are now being questioned. Furthermore, little dolomite actually occurs in most modern mixing zones. With respect to the behavior of CaCO_3 in the mixing zone, dissolution appears to be more important than precipitation. The presence of caves that form in carbonate rocks at the mixing zone supports this conclusion. James and Choquette (1984) suggest that solution is likely favored in the upper, more-dilute parts of the mixing zone. Precipitation of calcite, if it occurs, is more likely to take place in the lower part of the zone. Furthermore, calcite cement may become more magnesium-rich further down in the mixing zone.

11.4.5 Diagenesis in the telogenetic meteoric environment

The preceding discussion of meteoric diagenesis deals with marine carbonates exposed to meteoric waters owing to shoaling upward (basin filling) or falling sea level. These young sediments consist mainly of Mg-calcite and aragonite; therefore, they are highly susceptible to dissolution and calcification in the meteoric environment owing to mineral-controlled dissolution–precipitation reactions (James and Choquette, 1984). Old carbonate sediments that have been deeply buried and subsequently exhumed by uplift and unroofing may also be exposed to and altered by meteoric waters (telogenesis). These older sediments may have been exposed initially to meteoric diagenesis, or they may have been buried directly without exposure to meteoric waters. In either case, subsequent burial diagenesis (next section) likely converted original Mg-calcite or aragonite sediments to calcite or possibly dolomite. Therefore, when these mineralogically stabilized carbonates arrive in the telogenetic zone, their late-stage diagenesis by meteoric waters differs from that of unstabilized Mg-calcitic and aragonitic sediment.

During telogenesis, dissolution in both the freshwater vadose and phreatic zones is the dominant diagenetic process. Dissolution probably takes place mainly in chemically aggressive

waters charged with soil-derived CO₂, but may also occur in mixed meteoric and saline waters. In relatively humid climates, dissolution can lead to extensive karstification (Fig. 9.43). Solution during karst development generates openings of all sizes, from tiny solution pores called **vugs** to large caves and caverns. Several recent books have been published that describe the characteristics of karsts; see, for example, Harmon and Wicks (2006). Because carbonates in the telogenetic zone are already stabilized, mineral-controlled solution–precipitation does not occur. Aggressive meteoric waters will dissolve calcite (or dolomite) until they become saturated with respect to calcite (or dolomite). Once the waters are saturated, little further dissolution or precipitation will occur. If saturation is achieved at shallow depth, cavity formation and porosity enhancement will extend only to shallow depths. Also, little additional cementation will occur within sediment pores in the downflow direction as saturated waters move through the rock. Of course, precipitation may occur in caves, springs, etc., as described in Chapter 9. Thus, other than extensive solution in the zone of unsaturated, aggressive meteoric waters, the effects of diagenesis of old, stabilized carbonates in the meteoric zone is much less pronounced than the diagenesis of immature, unstabilized carbonates described in the preceding section. Carbonate telogenesis, as well as the diagenesis of unstabilized carbonates, is also much less pronounced in arid and semiarid climates than in humid climates.

11.5 Diagenesis in the deep-burial environment

11.5.1 Introduction

As discussed in preceding sections, many carbonate sediments undergo early diagenesis on the seafloor, owing largely to cementation by aragonite and Mg-calcite. These sediments may subsequently be subjected to additional diagenesis in the meteoric environment, where dissolution of aragonite and Mg-calcite and precipitation of calcite are dominant processes. Carbonate sediments previously modified by diagenesis on the seafloor or in the meteoric zone, as well as carbonates that may have escaped seafloor lithification or meteoric diagenesis, are ultimately buried. It is in this deeper-burial zone (Fig. 11.1) below the reach of surface-related processes – the mesogenetic diagenetic regime – that carbonates have their longest residence times. Therefore, there is ample opportunity in the deep-burial environment for additional diagenesis to occur. Choquette and James (1987) point out that lithification on the seafloor can take place very rapidly in as little as 10¹ to 10⁴ years, and diagenesis in the meteoric environment can involve time intervals on the order of 10³ to 10⁵ years. On the other hand, diagenesis in the deep-burial environment may continue over tens to hundreds of millions of years (10⁶–10⁸ years), although the rate of diagenetic change drops off rapidly with increasing depth and time.

Deep burial subjects carbonate sediments to increased temperature, lithostatic pressure, and hydrostatic pressure and brings them into contact with pore waters that differ in composition from those on the seafloor or in the meteoric environment. Under these changed conditions, carbonate sediments undergo compaction and physical reorientation of grains, as well as chemical alteration, through the processes of cementation, dissolution,

and neomorphism. The exact course of diagenesis in the deep-burial environment depends upon several factors, including the mineralogy of the starting material (aragonite, Mg-calcite, or low-magnesian calcite), grain size and texture of the sediment, porosity and permeability, composition of pore fluids, and the temperature and pressure of the deep-burial regime. These factors are explored further below.

11.5.2 Factors influencing burial diagenesis

Initial mineralogy and grain size

Carbonate sediments previously altered in the meteoric zone are mineralogically stabilized to various degrees; that is, aragonite and Mg-calcite have already been converted totally or mainly to low-magnesian calcite or dolomite. Such sediments have a relatively low diagenetic potential to further generate calcite during diagenesis (Scholle and Halley, 1985). By contrast, carbonate sediments composed mainly of aragonite and Mg-calcite have a much higher potential to generate calcite cements through dissolution and reprecipitation processes. Thus, initially, chemical diagenesis of mineralogically stabilized carbonate sediments in the burial environments likely proceeds at a slower rate than that of unstabilized sediments. Because rates of diagenesis decrease with increasing time and burial depths, however, these rates may tend to equalize after a time.

Fine-grained sediments have higher surface-area to volume ratio than do coarse-grained sediments. Because of this higher reactive surface area, chemical diagenetic processes involving solution–reprecipitation and recrystallization (neomorphism) tend to proceed faster in fine-grained sediments than in coarser sediments. Fine-grained sediments may also undergo compaction more readily than will coarser sediments. On the other hand, fine-grained sediments have low permeability (although porosity may be high), which limits the passage of fluids through the sediments. Coarser-grained sediments may have lower porosity than do finer sediments, but commonly have much better permeability. Thus, grain size and permeability tend to have inverse effects on chemical diagenesis.

Pore-fluid composition

Marine carbonate sediments that escape diagenesis in the meteoric zone have initial pore fluids that are normal seawater. The pore fluids of carbonate sediments in the meteoric environment are composed of freshwater in the vadose and phreatic zones; the freshwater becomes mixed with more-saline waters in the mixing zone. With deeper burial, the chemical composition, pH, and Eh of pore waters may change significantly. These changes can be brought about by several processes, including rock–mineral reactions, dissolution of evaporites, shale dewatering (with waters derived from associated shales imported into carbonate sediments), decarboxylation of organic matter, and salt-sieving. Most waters in the deep-burial environment are more saline than seawater and may have different chemistries (Chapter 8 and 10). In many depositional basins, there is a general trend of increasing salinity with depth. In other basins, the waters are less saline than

seawater, apparently owing to mixing of meteoric, marine, and perhaps basinal waters (Stoesser and Moore, 1983).

Pore-water composition and pH have an extremely important influence on diagenetic processes such as dissolution, pressure solution, cementation, dolomitization (Chapter 10), and neomorphism. As discussed in preceding parts of this book, pore fluids must move continuously through sediments for significant dissolution or precipitation to occur. In the shallower parts of the deep-burial environment, gravity-driven fluid flow predominates. In deeper parts of basins, large-scale basin circulation driven by thermal processes such as Kohout circulation may be important (Chapters 8 and 10). Thus, fluids may move either downward or upward through sediments depending upon specific conditions of the basin. In the later stages of carbonate diagenesis, porosity tends to be destroyed by compaction and cementation, and the volume of water available for diagenesis is diminished. As the volume is decreased and flux through the rock is slowed, the diagenetic system changes from an open-water-dominated system to a closed-rock-dominated system (Prezbindowski, 1985). In some carbonate systems, liquid hydrocarbons may be present in pore waters at some stage. These hydrocarbons are believed to inhibit pressure solution as well as the formation of cements.

Temperature

The average geothermal gradient in sedimentary basins is about 25 °C/km (Fig. 8.4). Wide variations in geothermal gradients are possible in different basins, ranging from as low as 10 °C/km to as high as 35 °C/km. As suggested in Chapter 8, increasing temperature causes an increase in the rate of most chemical reactions. On the other hand, increasing temperature causes a significant decrease in the solubility of calcite and other carbonate minerals. Thus, the effect of temperature increase is to favor precipitation of carbonate cements and dolomitization during deeper burial. By contrast, the solubility of most silicate minerals, including chalcedony and quartz, increases with increasing temperature.

Increasing temperature combined with increasing pressure can bring about the dewatering (dehydration) of certain minerals, releasing waters that may affect carbonate diagenesis. Examples include the dewatering of smectite (Chapter 8), the conversion of gypsum to anhydrite, the transformation of opal-A to quartz, and the dehydration of hydrous iron oxides (limonite) to hematite. Finally, temperature is involved in the conversion of organic matter to organic acids, kerogen, and hydrocarbons (thermal maturation) during burial diagenesis (Chapter 8). Although many of these dewatering processes are more likely to occur in siliciclastic sedimentary rocks than in carbonates, waters released from siliciclastic rocks may move laterally or vertically into carbonate sediments.

Pressure

Both geostatic pressure and hydrostatic pressure increase linearly with increasing burial depth (Fig. 8.4). The geostatic pressure gradient in a limestone basin would be slightly less steep than the average gradient shown in Fig. 8.4 because limestone is less dense than siliciclastic rocks. Sediments undergoing burial may be affected also by directed pressures

related to tectonic stresses. The net pressure on sedimentary particles in the burial environment is the difference between lithostatic pressure and hydrostatic pressure. This pressure difference creates strain, which is relieved by dissolution and is the force that drives pressure solution or chemical compaction (Choquette and James, 1987).

Hydrostatic pressures at a particular depth are typically much lower than geostatic pressures (commonly less than about one-half). On the other hand, pore fluids trapped in sediments during compaction or in sediments subjected to tectonic stresses may develop abnormally high hydrostatic pressures. Petroleum geologists refer to such sediments as being **overpressured** or **geopressured**. Abnormally high fluid pressures can affect the diagenesis of carbonates in at least two ways. First, they may retard both mechanical and chemical compaction, thereby preventing porosity loss. Overpressured zones may also isolate pore fluids from surrounding diagenetic waters, retarding fluid and ion transfer and possibly preventing or significantly slowing cementation. These factors may explain the preservation of unusually high porosities reported in some deeply buried carbonate oil reservoirs (e.g. Feazel and Schatzinger, 1985).

11.5.3 Diagenetic processes in the deep-burial environment

Physical compaction

Grain packing and reorientation

Newly deposited, watery carbonate sediments commonly have very high initial porosities. Depending upon the grain size and nature of the carbonate particles, initial porosity may range from about 40 to more than 80 percent. Unless these sediments undergo very early cementation and lithification on the seafloor, significant porosity reduction and concomitant thinning of beds occur during burial diagenesis. Muddy carbonate sediments (lime muds and wackestones) commonly have the highest porosity; therefore, compaction effects are typically greatest for these sediments. A considerable amount of porosity reduction occurs very early during burial simply by grain settling, repacking, and reorientation that accompany early dewatering. This process continues until a grain-supported framework is established, which may occur within a few meters or so below the seafloor (Choquette and James, 1987). The actual amount of porosity lost in this process depends upon the nature of the sediment. Porosity loss may be as little as 10 percent (e.g. from 80 percent to 70 percent) in grain-rich sediments such as foraminiferal oozes to 40 percent (e.g. 80 percent to 40 percent) in mud-rich sediments.

Grain deformation

With deeper burial and progressively higher overburden pressure, carbonate grains are packed even more tightly. Eventually, overburden stresses result in grain deformation by brittle fracturing and breakage and by plastic or ductile squeezing. Significant additional reduction in porosity accompanies this process. To illustrate, Shinn and Robbin (1983) conducted *in situ* compaction experiments on cores of modern carbonate sediments that

have porosities ranging from 47 to 83 percent (mostly 60–75 percent). Porosities after compaction were reduced to as little as 29 percent (mostly 35–45 percent) of original porosities. Further, thickness of the cores was reduced to as little as 27 percent (mostly 30–65 percent) of original thickness. Shinn and Robbin report that most compaction effects occurred at pressures equivalent to burial depths less than about 1000 ft (305 m). Increasing loads to an equivalent of more than 10,000 ft (3400 m) of burial depth did not significantly increase compaction or reduce sediment core length but did produce some chemical compaction (pressure solution). These experimental results suggest that significant compaction of carbonate sediments, with accompanying porosity loss and thinning of beds, can occur at burial depths less than 300 m. In fact, Shinn and Robbin (1983) conclude that at burial depths of as little as 100 m, compaction of marine lime sediments can reduce their depositional thickness by one-half with accompanying porosity losses of 50–60 percent of original pore volumes.

Effects of physical compaction

In addition to porosity loss and bed thinning, numerous other effects accompany physical compaction. As enumerated by Shinn and Robbin (1983) and Choquette and James (1987) these effects include (1) squeezing and deformation of organic matter into wispy, “stylolite-like” layers that drape over rigid grains, (2) mashing of sediment-filled circular burrows to produce ellipsoidal structures, (3) flattening of pellets or other grains, (4) rotation of shells or other grains into tighter packing, (5) crushing of shells, ooids, or other grains and fracturing of micrite envelopes (particularly in grain-supported carbonates), (6) obliteration of pellets and birdseye or fenestral voids in sediments that were not lithified by early cementation, (7) thinning of laminae between and draping over early concretions, (8) production of swirling structures, and (9) conversion of grain-poor lime mud or wackestone (mud-supported) to packstone (grain-supported). This last effect occurs as a result of grains in an originally mud-supported fabric being forced together by compaction until they touch (Shinn and Robbin, 1983).

The extent of porosity loss, bed thinning, and other mechanical compaction effects is related to the degree of early cementation in the sediments. If extensive intergranular cementation takes place in either the seafloor or shallow meteoric diagenetic environments, compaction effects are moderated (e.g. Moore, 2001, p. 300). Soft grains such as pellets may preserve their shapes, and less overall thinning of beds occurs. Porosity loss owing to compaction is also less significant, although porosity is obviously reduced by cementation.

Chemical compaction (pressure solution)

Nature of the process

Chemical compaction of siliciclastic sediments owing to pressure solution is discussed in [Chapter 8](#). As pointed out in that chapter, grain-to-grain pressure solution at the contact points of individual grains can result in the formation of interpenetrating or sutured contacts.

On a larger scale, pressure-solution seams called **stylolites** can develop. Pressure solution appears to be a much more prevalent process in carbonate rocks than in siliciclastic rocks, and a great variety of both microstylolites and larger-scale stylolites are common features of carbonates.

Pressure solution begins after mechanical compaction is essentially complete and a stable grain framework has been created. Load or tectonic stress transmitted to grain-contact points or surfaces causes dissolution at the contact. Solid calcium carbonate is changed to liquid, creating a solution film (Robin, 1978). Calcium and bicarbonate ions released into solution move away from the stressed contact point or surface by solution transfer or diffusion toward adjacent areas of lower stress (i.e. pores). These ions may be reprecipitated locally as calcite cement, or they may remain dissolved in the pore waters and move to more-distant sites. Because pressure solution following mechanical compaction results in additional porosity loss and bed thinning, the process was referred to by Lloyd (1977) as **chemical compaction**.

Factors affecting chemical compaction

As suggested, pressure solution begins after mechanical compaction has established a stable grain framework, so load or tectonic stresses can be transmitted from grain to grain. Pressure solution is most easily visualized in grain-rich limestones such as oolites; however, it occurs also in mud-dominated limestones. Numerous factors are believed to influence the magnitude of chemical compaction, either to enhance or retard compaction. These factors include burial depth and/or tectonic stress, carbonate mineralogy, the presence of insolubles such as clay minerals, composition of pore waters, the presence of liquid hydrocarbons, and elevated pore pressures (Choquette and James, 1987; Feazel and Schatzinger, 1985; Moore, 2001, p. 305).

Geologists frequently state that pressure solution begins at burial depths as shallow as 200 m. Moore (2001, p. 305) points out, however, that the depth at which pressure solution begins depends upon many factors in addition to load stress, including tectonic stress arising from folding or faulting. The onset of chemical compaction has actually been reported by various authors to occur at depths ranging from less than 200 m to as much as 1500 m. One reason for such variation may be carbonate mineralogy. Carbonates composed of metastable aragonite or Mg-calcite should be more susceptible to chemical compaction than stable calcite sediments such as deep-sea pelagic carbonates or dolomite. Insolubles such as clay minerals and fine organic matter apparently also play an important role in pressure solution (Choquette and James, 1987; Sassen *et al.*, 1987; Wanless, 1979); stylolites appear unlikely to develop in carbonates that do not contain any insolubles. Magnesium-poor meteoric waters are regarded to be chemically more aggressive in promoting pressure solution than marine pore waters; thus, reports of very shallow chemical compaction may be related to meteoric pore waters. By contrast, the early introduction of hydrocarbons into pore space may retard or shut down chemical compaction (Feazel and Schatzinger, 1985). Finally, elevated pore pressures in geopressured zones reduce stress at grain contacts and also retard chemical compaction.

Effects of chemical compaction

The most obvious effect of pressure solution is the formation of stylolites and solution seams. Creation of these features is accompanied by reduction in bulk volume of the rocks and resultant loss of porosity. For example, Coogan and Manus (1975) suggest that grain-rich limestone with about 40 percent original porosity may experience as much as a 30 percent volume loss owing to pressure solution (volume loss calculated by measuring accumulated amplitudes of megascopic stylolites). Original porosity is thus reduced to about 25 percent. If approximately 4 percent cement originating from pressure solution is formed during this process, the final porosity is about 21 percent. These figures may not apply to all limestones, but they indicate that volume reduction and porosity loss can be significant. Furthermore, volume reduction by pressure solution may continue even after essentially all porosity is lost (Choquette and James, 1987).

Stylolites and related features have long been recognized as the product of pressure solution, and several early classifications for stylolites were proposed (e.g. Park and Schot, 1968; Trurnit, 1968). A stylolite is a kind of **sutured seam** that is characterized by a jagged surface, is generally coated by insolubles such as clay minerals or organic matter, and is made up of interlocking pillars, sockets, and variously shaped teeth (Choquette and James, 1987). Stylolites occur as single or multiple features (swarms of stylolites), and their amplitude may range from small to large (Fig. 11.8). Sutured seams thus include both megastylolites with amplitudes exceeding 1 cm (Fig. 11.9) and microstylolites between individual grains, in which the amplitude of the interpenetrating contacts between grains is less than 0.25 mm (e.g. Fig. 11.10). Stylolites are typically oriented parallel to depositional bedding; however, they can occur also at various angles to bedding and thus create reticulate or nodule-bounding patterns.

Since publication of these early classifications of stylolites, additional solution features have been recognized, including **nonsutured seams**, and additional classifications have been suggested by several authors (Buxton and Sibley, 1981; Garrison and Kennedy, 1977; Logan and Semeniuk, 1976; Koepnick, 1984; Wanless, 1979). For example, Wanless (1979) suggests that relatively clean limestones with resistant units will form sutured seams (stylolites) and grain-contact sutures. On the other hand, pressure solution of limestones enriched in insolubles (>10 percent clay, quartz, organic matter) will concentrate insolubles as a film, producing nonsutured seams (Fig. 11.11). These nonsutured seams have been given various names including clay seams, wispy laminae, wavy laminae, microstylolites, and pseudo-stylolites. Nonsutured seams may occur as single clay-film surfaces or as anastomosing swarms of wispy seams oriented parallel to bedding. They may occur also in nonparallel, reticulate orientation producing a pattern of closely spaced nodules referred to as **fitted fabric** (Wanless, 1979; Buxton and Sibley, 1981). Logan and Semeniuk (1976) refer to this reticulate fabric as **stylobreccia**. Fitted fabric (see Fig. 11.8) appears to occur particularly in poorly cemented grainstones, but may occur also in packstones and wackestones (Buxton and Sibley, 1981). Pressure solution apparently starts at grain contacts; microstylolites then propagate irregularly through the rock to create a fitted-fabric network (Choquette and James, 1987).

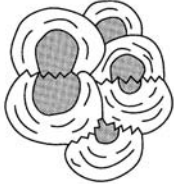
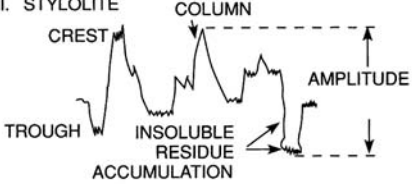
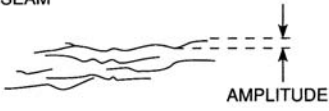

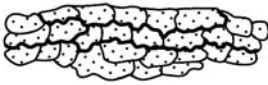
<p>I. MICROSTYLOLITE</p> 	<p>PRESSURE SOLUTION FEATURE</p> <ol style="list-style-type: none"> 1. Sutured contacts between interpenetrating grains 2. Amplitude < 0.25 mm 3. Minor insoluble residue
<p>II. STYLOLITE</p> 	<ol style="list-style-type: none"> 1. Sutured surface of interpenetrating columns 2. Laterally continuous surface on core scale 3. Amplitude ≥ 1 cm 4. Variable insoluble residue accumulation among surfaces and along individual surfaces
<p>III. WISPY SEAM</p> 	<ol style="list-style-type: none"> 1. Converging and diverging sutured to undulose surfaces 2. Individual surfaces laterally discontinuous on core scale 3. Individual surface amplitude < 1 cm 4. Insoluble residue accumulation along individual surfaces ≤ 1 mm
<p>IV. SOLUTION SEAM</p> 	<ol style="list-style-type: none"> 1. Undulose surfaces 2. Laterally continuous on core scale 3. Insoluble residue accumulation ≥ 1 mm
<p>V. FITTED FABRIC</p> 	<ol style="list-style-type: none"> 1. Reticulate network of microstylolites 2. Dissolution features occur pervasively throughout a zone 3. Thickness of zone ranges from millimeters to several centimeters

Figure 11.8 Principal kinds of pressure solution features in carbonate rocks. (Modified from Koepnick, R.B., 1984, Distribution and vertical permeability of stylolites within a Lower Cretaceous carbonate reservoir, Abu Dhabi, United Arab Emirates, in *Stylolites and Associated Phenomena – Relevance to Hydrocarbon Reservoirs*: Abu Dhabi National Reservoir Research Foundation Special Publication, Abu Dhabi Fig. 1, p. 262, with additions by C.H. Moore, 1989, *Carbonate Diagenesis and Porosity*: Developments in Sedimentology 55, Fig. 9.7, p. 248; reprinted by permission of Elsevier Science Publishers, Amsterdam.

Cementation

Nature of the process

Much of the research on carbonate diagenesis carried out since the 1950s has concentrated on study of Holocene and Pleistocene carbonates. Significant evidence of cementation in these rocks, believed to have taken place in the seafloor and meteoric burial environments,



Figure 11.9 Well-developed, sutured stylolites in limestone. Cretaceous limestone, Calcare Massiccio, Italy. (Photograph courtesy of E. F. McBride.)



Figure 11.10 Sutured contact or microstylolite (arrow) between two crinoid fragments, formed as a result of pressure solution (chemical compaction), Middle Mississippian limestone, Oklahoma.

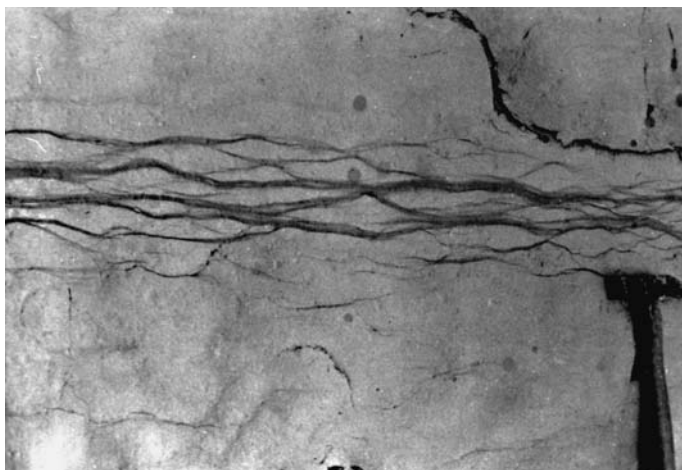


Figure 11.11 Nonsutured stylolite seams in limestone, Middle Chalk (Cretaceous), Compton Bay, Isle of Wight, Hampshire, Southern England. (From Garrison, R. E. and W. J. Kennedy, 1977, Origin of solution seams and flaser structures in Upper Cretaceous chalks of southern England: *Sediment. Geol.*, 19, Fig. 8, p. 117, reprinted by permission of Elsevier Science Publishers, Amsterdam.)

has been reported in the literature. Consequently, geologists frequently assert that most cementation must occur at shallow depths. On the other hand, Scholle and Halley (1985), as well as many other geologists (see discussion by Choquette and James, 1987), argue that much of the cementation in carbonate rocks takes place in moderately deep to very deep subsurface settings (mesodiagenetic environments). Clearly, all cements in deep-water carbonates such as chalks that were never exposed to meteoric waters must be of deep-burial origin. A growing body of evidence obtained by petrographic, cathodoluminescence, stable-isotope, and fluid-inclusion study suggests that much of the cement in ancient peritidal, shallow-marine, and platform-margin limestone may also have formed during deep-burial diagenesis.

The factors that control dissolution and precipitation of carbonates at depth are complex and poorly understood. Unless carbonate sediments escape mineralogical stabilization in the seafloor or meteoric environment, the subsurface fluids in contact with carbonate minerals may be more or less in equilibrium with CaCO_3 . Thus, there may be no strong geochemical “drive” to bring about either dissolution or cementation. Nonetheless, much available evidence indicates that deep-burial dissolution and cementation must occur. What, then, drives these processes, particularly cementation? Temperature, pressure (particularly as it affects carbon dioxide partial pressure, P_{CO_2}), salinity, and ion composition of pore waters must be major factors that influence dissolution and cementation. Other factors that may affect these processes include grain size, fabric, mineralogy, porosity, and permeability. In turn, these variables affect rates of fluid flow (flux). It is difficult to know exactly which combination of factors actually leads to cementation. Factors that favor cementation

(or solution–reprecipitation) are suggested to include metastable mineralogy, highly oversaturated pore waters, high porosity and permeability (which enable high rates of fluid flow), increase in temperature, decrease in carbon dioxide partial pressure (P_{CO_2}), and pressure solution (Feazel and Schatzinger, 1985; Choquette and James, 1987).

Increasing temperature in the range of 25 °C to 200 °C may decrease the solubility of calcite in water by up to two orders of magnitude (Sharp and Kennedy, 1965) and thus promote cementation. On the other hand, accompanying increase in pressure probably counteracts some of this decrease. Nonetheless, temperature increase must be important. In a discussion of chalk cementation in Deep Sea Drilling Project (DSDP) cores, Wetzel (1989) reports that cement content of chalks doubles in sediments that have experienced temperatures four times higher. Fluid-inclusion studies suggest that deep-burial cement may be precipitated from CaCO_3 -saturated pore waters ranging from brackish to highly saline (10–100 ‰). As discussed elsewhere in this book, tens of thousands to hundreds of thousands of pore volumes of water must pass through a pore to precipitate a significant amount of cement. Thus, oversaturation with respect to calcite and relatively high fluid flux favor cementation. It is probable, however, that fluid flux under many subsurface conditions is quite small. Degassing of CO_2 , owing to escape from deep-burial zones to the shallow subsurface along faults or fractures, is a potentially important but unproven mechanism for enabling cementation (Choquette and James, 1987).

If we accept the premise that a significant volume of calcite (or dolomite) cement may be precipitated in the deep-burial environment, then we must identify an adequate source of CaCO_3 to provide the cement. The mechanism for supplying deep-burial CaCO_3 most frequently mentioned (e.g. Scholle and Halley, 1985) is pressure solution. Moore (1989, p. 261) points out, however, that an enormous amount of carbonate section must be removed by pressure solution to furnish a small amount of cement. He suggests that CaCO_3 derived by local pressure solution must be supplemented from other sources. Possibly, it may be imported from other, adjacent subsurface carbonate units likewise undergoing pressure solution. Alternatively, late dissolution of limestones or dolomites by pore fluids made aggressive by organic acids and CO_2 generated during organic matter diagenesis (see Chapter 8) may furnish additional CaCO_3 .

Characteristics of burial cements

As mentioned, burial cements occur in both deep-water chalks and coarser-grained shallow-water carbonates. Cements in chalks are composed of very fine crystals (1–10 microns) and are best studied with the scanning electron microscope. Burial carbonate cements in coarser-grained carbonates can include clear, coarse calcite as well as dolomite. The general characteristics of these cements are summarized by Choquette and James (1987). They are commonly enriched in iron and manganese, depleted in strontium, and depleted in ^{18}O compared to shallow-burial cements. Cathodoluminescence is dull, the cements may or may not show compositional zonation, and fluid inclusions (containing both a gas and liquid phase) and hydrocarbon inclusions are common (Sellwood *et al.*, 1989). The principal kinds of cement are as follows.

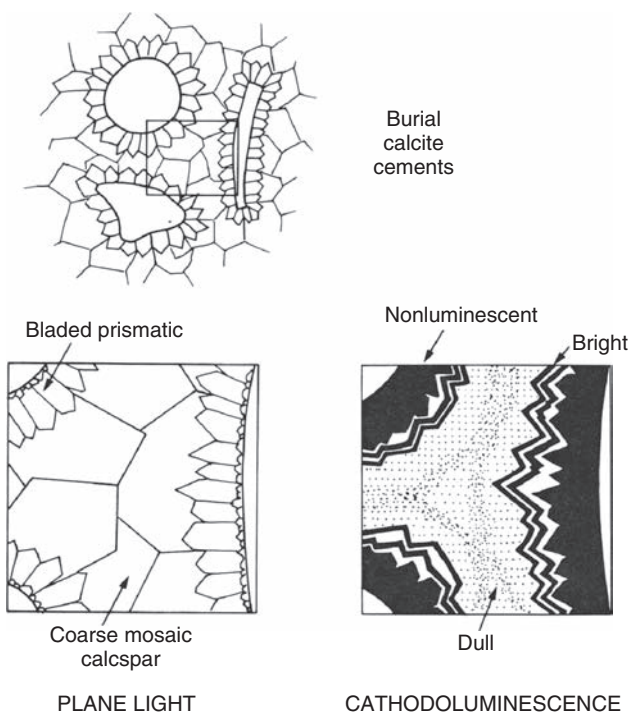


Figure 11.12 Schematic representation of principal kinds of deep-burial cements. Cements analyzed by cathodoluminescence imaging may display luminescent banding, with luminescence of bands ranging from nonluminescent through bright to dull. These bands reflect differences in Fe and Mn content of the cements that may indicate different generations of cement. See subsequent discussion of cement stratigraphy for details. (From Choquette, P.W. and N.P. James, 1987, Diagenesis of limestones – 3. The deep burial environment: *Geosci. Can.*, **14**, Fig. 21, p. 16, reprinted by permission of the Geological Association of Canada.)

1. **Bladed-prismatic calcite** consist of elongate, scalenohedral crystals a few tens of micrometers across and up to a few hundreds of micrometers long. They typically grow directly on grain surfaces or on top of an earlier generation of marine cements (Figs. 11.12, 11.13).
2. **Coarse mosaic calcspar**, commonly much coarser than bladed-prismatic calcite, typically consists of plane-sided, equant crystals (Figs. 11.12). Where present with bladed-prismatic calcite, it is typically younger than the bladed calcite.
3. **Poikilitic calcite** cement consists of millimeter-size crystals that are large enough to enclose several carbonate grains (Fig. 11.14).
4. **Coarse dolomite** cements consist of clear-to-turbid, coarse crystals that may include planar (xenotopic) dolomite, saddle dolomite, and baroque dolomite. See Chapter 10 for additional description of these dolomites and the conditions under which they form.
5. **Coarse anhydrite cement** occurs in some buried limestones. These cements generally occur in limestones that are associated with evaporite deposits.

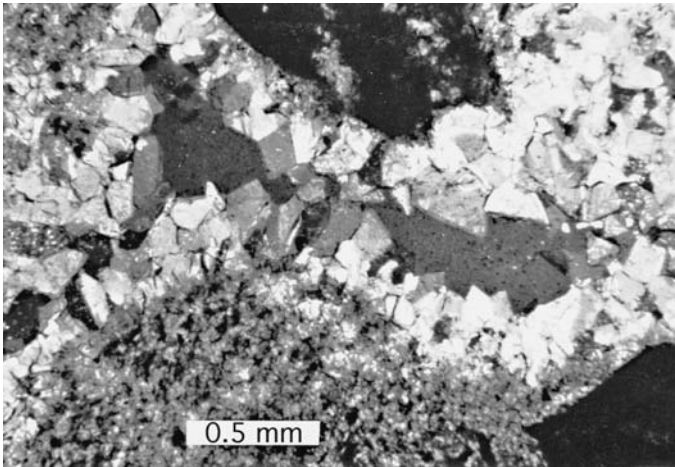


Figure 11.13 Bladed-prismatic calcite lining margins of a cavity and grading inward to mosaic calcite toward the center of the cavity. The cavity is incompletely filled with cement. Robinson Limestone (Pennsylvanian), Colorado. Crossed nicols.

It may be possible to differentiate burial cements from earlier-formed cements on the basis of careful petrographic examination. Evidence for late-burial origin are discussed by Moore (1985), Choquette and James (1987), and Sellwood *et al.* (1989). Cements are considered to be “late-stage” if cement crystals (1) cross-cut other features known to be formed by burial diagenesis, such as stylolites or other pressure-solution seams (Fig. 11.14), (2) heal fractured grains or spalled ooid cortices, (3) enclose compacted grains (the poikilotopic calcite in Fig. 11.14) or fill compaction pores, indicating that cementation postdates physical or chemical compaction, (4) fill late-stage tectonic fractures, or fill dissolution pore spaces that were created by solution of grains and early-burial cements, and (5) enclose solid hydrocarbons such as asphalt or pyrobitumens that themselves were formed during deep-burial diagenesis.

Differentiating cement fabrics from neomorphic fabrics

In addition to the problem of differentiating between early and late cement, it is also necessary to differentiate between cement and neomorphic calcite. Differentiating sparry calcite cement from neomorphic spar is one of the most troublesome problems in carbonate petrology. The fabric of neomorphic spar, which is formed by polymorphic transformation and recrystallization (discussed below), can strongly resemble that of some cements. Because misidentification of neomorphic spar for cement can lead to errors in interpreting depositional and diagenetic history, it is important to distinguish between the two. Unfortunately, avoiding misidentification is easier said than done. Bathurst (1975, p. 417) lists some 17 different characteristics of cements that help to distinguish them from neomorphic spar. These criteria, with additions from other sources, are summarized in Table 11.1. They should be compared with Table 11.2, which summarizes the distinguishing characteristics of neomorphic calcite.

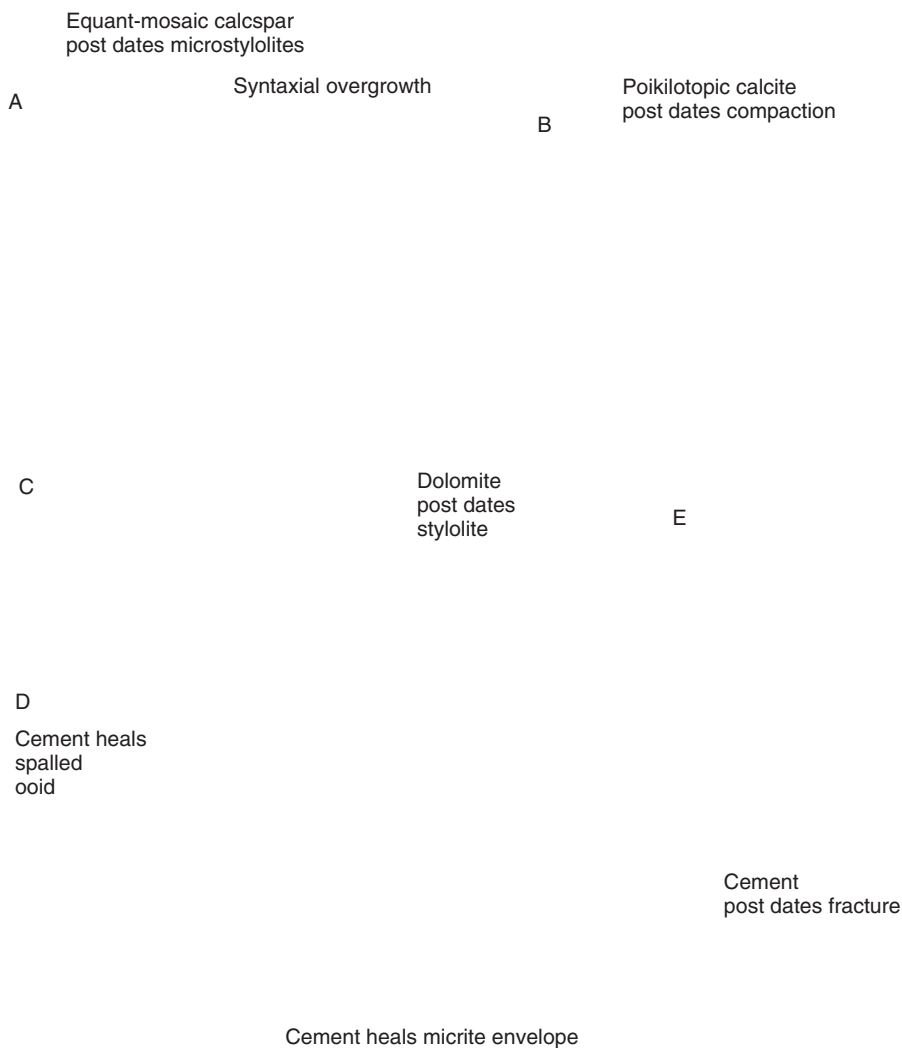


Figure 11.14 Examples of criteria that suggest late-burial cementation. A. Syntaxial overgrowth encloses microstylolites formed during a preceding stage of chemical compaction. B. Calcite poikilotopically encompasses grains packed and broken during physical compaction. C. Cement crystals cut across stylolites formed during chemical compaction. D. Ooids or micrite envelopes broken during compaction are healed by cement. E. Cement fills late-stage tectonic fractures. (From Choquette, P. W. and N. P. James, 1987, Diagenesis of limestones – 3. The deep burial environment: *Geosci. Can.*, **14**, Fig. 24, p. 18, reprinted by permission of the Geological Association of Canada.)

Geochemistry and isotope composition of deep-burial cements

Burial cements, including both calcite and late-burial saddle dolomite, are commonly enriched in iron and manganese but have low strontium concentrations. Iron and manganese enrichment apparently reflects the progressive enrichment of iron and manganese in

Table 11.1 *Distinguishing characteristics of sparry calcite cement*

<ul style="list-style-type: none"> ● Two or more distinct generations of spar are present (unlikely in neomorphic spar); the spar is commonly clear and free of relict structures or impurities. ● The cement encrusts free surfaces such as the surfaces of carbonate grains or molds. ● Crystals of the cement mosaic have a preferred orientation of longest diameters normal to the initial substrate on which they grew; size of the crystals increases away from the initial substrate, and crystals tend to become larger, more blocky, and less well oriented (drusy fabric) ● Cement fabrics are characterized by a high percentage of enfacial junctions (an enfacial junction is a triple junction between three crystals where one of the angles is 180 degrees), and boundaries between crystals are mainly plane interfaces. ● Spar fabrics that occur in association with particles composed of micrite (e.g. pellets or micrite envelopes) that are not themselves altered to neomorphic spar are likely to be cements. ● Contacts between spar and carbonate particles are sharp. ● Spar lines a cavity that is incompletely filled, or spar occupies the upper part of a cavity, the whole lower part of which is filled with more or less flat-topped, mechanically deposited micrite (geopetal structure). ● The presence of distinctly banded zones within crystals, as revealed by staining or cathodoluminescence; such zones would be uncommon in neomorphic spar.
--

Source: Bathurst, R. G. C., 1975, and other sources. Compare with Table 11.2.

concentrated subsurface brines owing to rock–water interactions with siliciclastic rocks and evaporites, and low strontium concentrations may reflect the slow rate of precipitation of deep-burial calcite and dolomite (Moore, 2001, p. 310).

Because oxygen isotope fractionation is affected by temperature, oxygen isotopes should theoretically show progressively decreasing $\delta^{18}\text{O}$ values with increasing burial (Choquette and James, 1987; Moore, 2001). Choquette and James (1987) suggest, for example, that $\delta^{18}\text{O}$ isotope compositions should hypothetically show a more or less steady decrease from values of about 0‰ in the meteoric zone to values as low as –10 to –12‰ with deep burial. This hypothetical trend reflects increasing temperatures of the precipitating waters. A number of empirical studies lend support to this general hypothetical trend. As subsurface waters become increasingly hotter with burial, however, the $\delta^{18}\text{O}$ composition of the waters themselves become increasingly higher. Heydari and Moore (1988) and Moore (2001) have shown that the progressive decrease in $\delta^{18}\text{O}$ values in cements may ultimately be buffered and even reversed, by the increasingly high $\delta^{18}\text{O}$ values of deep pore fluids. Thus, the isotopic composition of cements precipitated at temperatures in excess of about 150 °C may be higher than for those precipitated at lower burial temperatures (e.g. 40 °C–100 °C).

Carbon isotope composition changes also with deep burial; however, most studies indicate that $\delta^{14}\text{C}$ values decline only slightly with burial depth. Moore (2001, p. 311) suggests that the reason most subsurface cements show little variation in carbon isotope composition is because the cement is rock buffered owing to chemical compaction. On the

Table 11.2 *Distinguishing characteristics of neomorphic calcite*

- Radial-fibrous fabrics are present.
- Neomorphic spar embays (nibbles) detrital micrite; embayments tend to be sawtoothed; relicts of micrite may appear as wisps or threads in spar.
- Spar transects skeletal grains, ooids, or other carbonate grains; grains may be only partially replaced by spar, preserving some of the internal structure of the grain (e.g. the fibrous structure of aragonitic fossils), or they may be replaced entirely, thus preserving only the outline or form of the grain.
- Crystal size of spar may vary irregularly and patchily from place to place; however, equigranular fabrics also occur.
- The presence of undigested silt, clay, or organic matter trapped in spar, or the presence of dusty relicts of earlier cement fringes; sparry calcite cement is commonly free of such cloudy impurities.
- Abnormally loose packing (floating relicts), as shown by patches of micrite, skeletal grains, or other carbonate grains entirely surrounded by spar; this criterion must be used with caution because grains that do not appear to be in contact in the two-dimensional plane of a thin section may actually be in contact in three dimensions, in which case the spar may be cement.
- Patches of spar in the midst of homogeneous micrite may indicate neomorphic spar; however, such patches may also form by filling of small burrows, gas-bubble holes, etc. by sparry calcite cement.
- Intercrystalline boundaries tend to be curved or wavy, in contrast to the plane boundaries typical of sparry calcite cements.
- Neomorphic spar displays few enfacial junctions between crystals in contrast to cement spar, which commonly contains high percentages of enfacial junctions.
- Neomorphic syntaxial rims may contain cloudy impurities, display sawtoothed margins, or transect adjacent carbonate grains; syntaxial rims surrounded by micrite may appear to be neomorphic; however, cathodoluminescence study may reveal that the rims formed by displacive crystallization or by filling of solution cavities around grains.
- Cathodoluminescence may show relicts of earlier cement fabrics or other replaced fabrics.
- Crystals may be separated by concentrations of impurities that were expelled by growing crystals and displaced to line compromise boundaries.

Source: Bathurst R.G.C., 1975, 1983, and other sources. Compare with Table 11.1.

other hand, increasing volumes of light carbon (^{12}C) generated as a by-product of hydrocarbon maturation, may bring about slight depletion in $\delta^{14}\text{C}$ values.

Cement stratigraphy

As discussed, carbonate cements can be precipitated in the seafloor, meteoric, or deep-burial diagenetic environments. During the progressive burial and diagenesis of a given carbonate deposit, one generation of cement may be deposited in the seafloor environment, another in the meteoric environment, and still another in the deep-burial environment. With careful study, it may be possible to detect each of these generations of cement. For example, it may be possible within single pores or adjacent pores in a limestone to identify a marine seafloor cement (oldest), a vadose cement (younger), and a meteoric phreatic cement (youngest). Alternatively, the cement sequence might consist of a

beachrock cement (oldest), a vadose cement (younger), and a deep-burial cement (youngest). This technique of studying successive generations of cement, referred to as **cement stratigraphy**, was introduced by Evamy (1969) and was first applied in cathodoluminescence studies by Meyers (1974). The technique has subsequently been employed by numerous investigators as a tool for unraveling the burial history of limestones.

In some samples, different generations of cements may be tentatively identified simply by petrographic analysis; for example, a cloudy seafloor cement (oldest) may be present with a clear meteoric cement (youngest). Most cement stratigraphy requires more-detailed study that may involve staining, cathodoluminescence (CL) imaging, ultraviolet microscopy, trace-element analysis, and fluid-inclusion studies. To illustrate, staining with potassium ferricyanide can reveal differences in ferrous iron content of calcite or dolomite. These differences may reflect changes in oxidizing conditions of the precipitating fluid, such as a change from the meteoric to the deep-burial environment.

The most heavily used tool in cement stratigraphy is cathodoluminescence imaging (Machel, 2000). The cathodoluminescence intensity (brightness) of carbonate cements is mainly a function of the concentrations of Mn^{2+} ions, which activate cathodoluminescence, and Fe^{2+} ions, which quench cathodoluminescence. The concentration levels of divalent Mn and Fe in cements are, in turn, related particularly to the redox conditions of the depositional and diagenetic environments. It is commonly reported in cement stratigraphy studies that cements display a trend from oldest to youngest cements of (1) nonluminescence to (2) bright luminescence to (3) dull luminescence (Fig. 11.12). This trend is interpreted to signify progressive change during burial from well-oxidized conditions that (1) inhibit the uptake of Mn^{2+} and Fe^{2+} (no luminescence) to (2) reducing conditions that favor uptake of Mn^{2+} but keep Fe^{2+} locked up in interactions with organic matter and sulfates (bright luminescence) to (3) deeper-burial reducing conditions where Fe^{2+} is available to quench luminescence (dull luminescence). Figure 11.15 provides an example of the use of CL imaging to identify several generations of cement in a cement-filled cavity. See Boggs and Krinsley (2006, pp. 120–129) for extended discussion of cement stratigraphy and its applications.

Neomorphism

As discussed in Section 11.3.3, neomorphism refers to diagenetic changes that take place owing to polymorphic transformation (solution–reprecipitation) and/or recrystallization (Folk, 1965). Neomorphism does not include formation of a solution cavity (mold) and subsequent refilling by cement. Neomorphism typically produces an increase in crystal size, referred to as **aggrading neomorphism**. Folk proposes that aggrading neomorphism can occur either by gradual enlargement of all crystals (coalescive neomorphism) or by growth of a few large crystals in a static groundmass (porphyroid neomorphism). The end result is the same (Fig. 11.16).

Folk suggests that a decrease in crystal size is also possible and refers to such a decrease as **degrading neomorphism** (grain diminution of other authors). A putative example of degrading neomorphism is the partial or complete alteration of an echinoderm fragment (single calcite crystal) to a mosaic of small crystals. Degrading neomorphism is not a

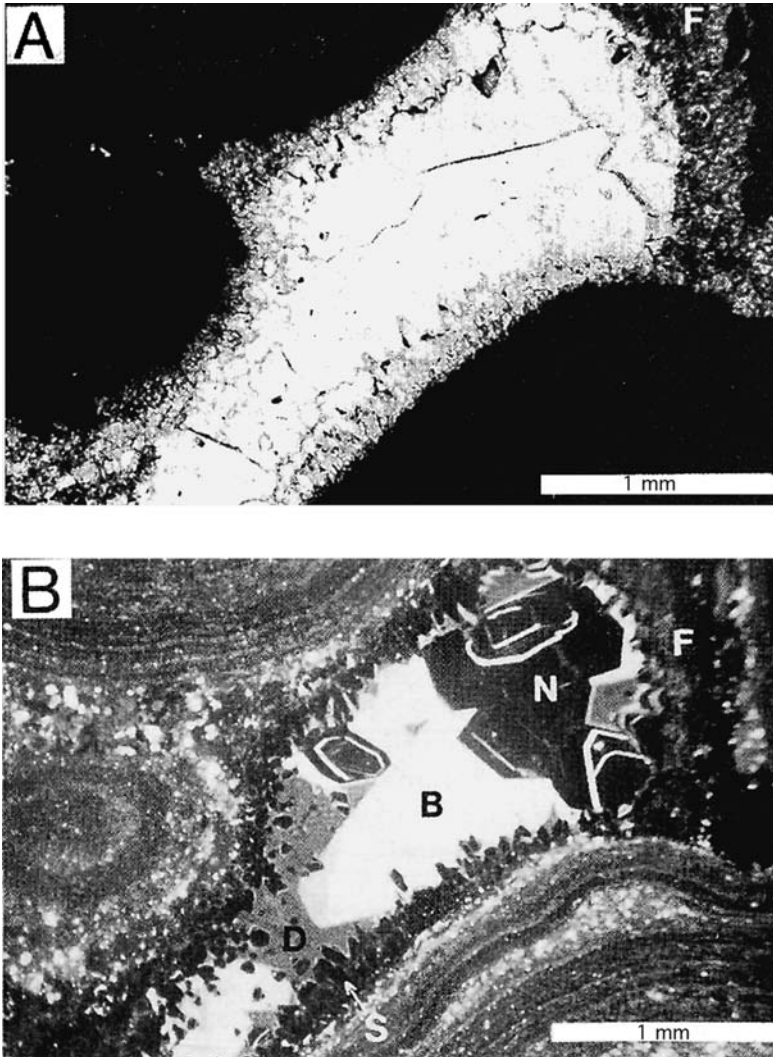


Figure 11.15 A. Thin-section photomicrograph (plane-polarized light) of a cement-filled cavity in a pisoid limestone, filled by a fibrous meniscus cement (F) and a clear cement. B. Cathodoluminescence image of the same area in (A). (F) is patchy, low-intensity meniscus cement. Nonluminescent, elongated crystals (S) rim the cavity. The clear, equant cement consists of an early nonluminescent cement (N) overgrown by a brightly luminescent cement (B) that, in turn, is overgrown by a dully luminescent cement (D). Pillara Limestone (Devonian), Western Australia. (From Wallace, M. W. C. Kerans, P. E. Playford, and A. McManus, 1991, Burial diagenesis in the Upper Devonian reef complexes of the Geikie Gorge Region, Canning Basin, Western Australia: *Am. Assoc. Petr. Geol. Bull.* **75**, Fig. 6A, B, p. 1023. Reproduced by permission.)

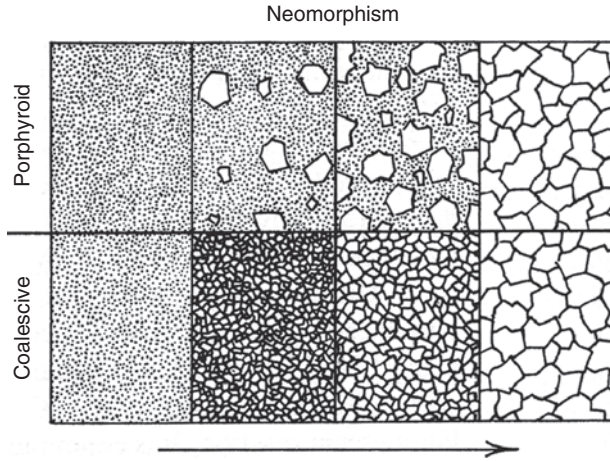


Figure 11.16 Schematic illustration of porphyroid and coalescive aggrading neomorphism. (From Folk, R. L., 1965, Some aspects of recrystallization in ancient limestones, in Pray, L. C. and R. C. Murray (eds.), *Dolomitization and Limestone Diagenesis*, SEDM Special Publication 13, Fig. 3, p. 22, reprinted by permission of SEPM, Tulsa, OK.)

common process but may occur under stressed or low-metamorphic conditions according to Flügel, 2004 (p. 321).

Three kinds of aggrading neomorphism are important in carbonates (Folk, 1965): (1) change of aragonite crystals in a lime mud to 1–3 micron-size calcite (micrite), (2) more advanced neomorphism of mud-size carbonate to 5–20 micron-size **microspar**, and (3) further neomorphism of mud, micrite, fossils, or other carbonate grains to coarse sparry or fibrous calcite, called **pseudospar**, with crystal size ranging to several tenths of millimeters. Presumably, wet recrystallization is the dominant process causing formation of microspar and pseudospar; however, wet polymorphic transformation of aragonite to calcite or solution–reprecipitation involving Mg-calcite are probably also involved for those carbonates that have not been completely stabilized mineralogically. Such metastable materials might include marine carbonate sediments that were never exposed to meteoric diagenesis, fossils containing aragonite or Mg-calcite, or previously formed aragonitic or Mg-calcitic cements. Burial neomorphism is probably affected by the same factors discussed above under cementation, that is, increasing temperature and pressure, metastable mineralogy, and pore-fluid flux.

Folk (1965) suggests that the driving force behind recrystallization may involve several factors including (a) energy of a phase transformation, (b) solution of tiny grains or projections, and precipitation about a larger nucleus, (c) pressure solution, (d) energy of a strained crystal lattice, and (e) surface tension caused by crystal boundary curvature. In a discussion of the instability of micrometer-size fabrics and the drive toward formation of coarser fabrics, Bathurst (1975, p. 349) suggests that some mud-size crystals are so small as to be supersoluble. Small crystals have a greater density of edges per unit surface area and thus a greater concentration of unneutralized bonds, and many crystals have residual elastic

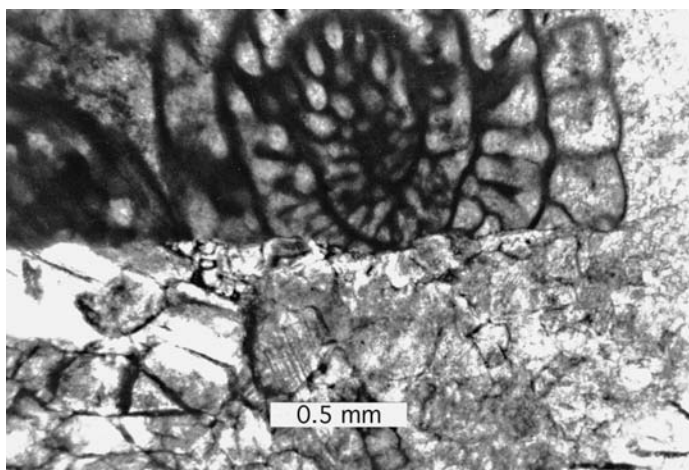


Figure 11.17 Photomicrograph of Fusulinid foraminifer (top) cut in half owing to recrystallization to neomorphic spar (bottom half of photograph). Pennsylvanian limestone, Paradox Basin, Utah. Crossed nicols.

strain and are thus more soluble. The presence of metastable aragonite and Mg-calcite is likewise an important factor. See also discussion by Morse and Mackenzie (1990, p. 391).

As mentioned, neomorphism appears to be a relatively minor process in the seafloor diagenetic environment. Considerable neomorphism does occur in the meteoric burial environment where aragonite and Mg-calcite are altered to calcite. Change in crystal shape and increase in crystal size accompany this stabilization process. Neomorphism is probably an important process also in the deep-burial diagenetic environment, given the long periods of time involved in burial diagenesis. A major problem in evaluating the overall significance of deep-burial neomorphism is the difficulty in differentiating neomorphic calcite from calcite cement, as mentioned. With respect to neomorphism, Bathurst (1975, p. 483) states that “the process yields a sparry calcite that is always difficult to distinguish, sometimes impossible to distinguish, from the sparry calcite of cement.” Neomorphism can produce at least three kinds of crystal fabrics:

1. **Granular fabrics** appear as a mosaic of crystals, with crystal size ranging upward from about 4 microns to 50–100 microns (Fig. 11.17). Crystal size may vary irregularly and patchily from place to place, although equigranular fabrics can also occur.
2. **Radial-fibrous fabrics** occur in which crystals are arranged in subspherical, stellate masses (Fig. 11.18). Commonly, the center of the masses consists of equigranular microspar (5 to 10 microns in size) surrounded by coarser elongate crystals with their axis radially distributed; elongate crystals may taper toward the center of the stellate structure (Bathurst, 1975, p. 484).
3. **Syntaxial rims** are alleged to occur on skeletal grains owing to neomorphism of surrounding micrite. Syntaxial rims are most common on echinoderm fragments but may occur also on coarse crystals in the walls of brachiopod or mollusk shells. These syntaxial rims may closely resemble syntaxial-rim cements.

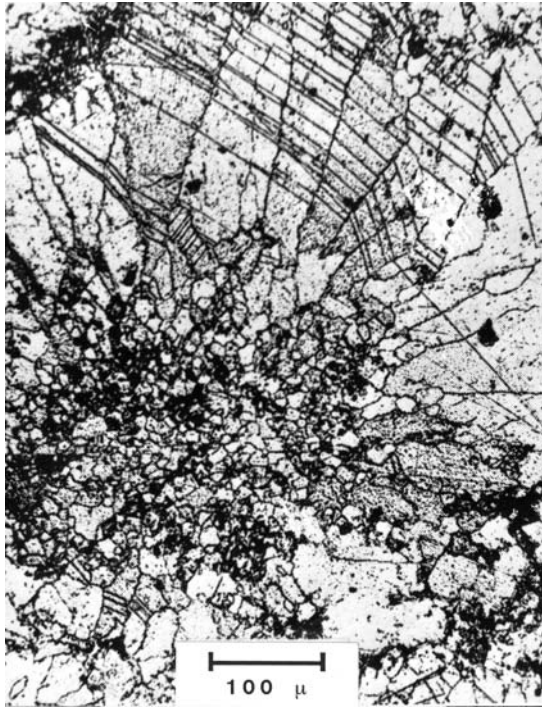


Figure 11.18 Stellate neomorphic fabric formed by alteration of a biomicrite. Note equigranular microspar in the core of the stellate mass. Carboniferous limestone, Derbyshire, England. Ordinary light. (From Bathurst, R. G. C., 1975, *Carbonate Sediments and their Diagenesis*: Elsevier, Amsterdam, Fig. 332, p. 479, reprinted by permission.)

Neomorphic spar may replace detrital micrite, carbonate grains, or an earlier generation of aragonite, Mg-calcite, or calcite cement. The problem of differentiating between neomorphic spar and sparry calcite cement is a very difficult one in carbonate petrology because many cement fabrics mimic neomorphic fabrics. As mentioned by Bathurst above, it may be impossible in some cases to make the distinction. Nonetheless, Bathurst (1975, pp. 484–493, 1983) provides a number of criteria that he believes characterize neomorphic spar. The principal criteria are summarized in Table 11.2. Compare this table with Table 11.1, which lists the distinguishing features of cements. No single criterion in Table 11.2 can be regarded as unequivocal proof of the neomorphic origin of spar, however, and it is wise to apply as many of the criteria as possible.

Interpretation of syntaxial rims as neomorphic replacements of micrite is particularly troublesome. Petrographic criteria may support a neomorphic origin for syntaxial rims in a particular deposit, whereas cathodoluminescence studies may indicate a different origin. For example, Walkden and Berry (1984) restudied the origin of syntaxial rims in Lower Carboniferous limestones in Great Britain that were previously considered to be of

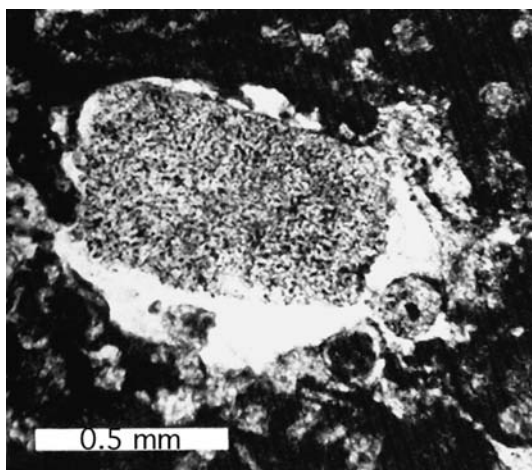


Figure 11.19 Syntaxial overgrowth (bright) surrounding a large crinoid grain. Plane-light photomicrograph. (Modified from Walkden, G. M., and J. R. Berry, 1984, Syntaxial overgrowths in muddy crinoidal limestones: cathodoluminescence sheds new light on an old problem: *Sedimentology*, **31**, Fig. 2, p. 253, reproduced by permission of Blackwell Publishing, Inc.)

neomorphic origin. On the basis of cathodoluminescence analysis, however, they conclude that the rims formed by passive cementation into solution voids that formed around echinoderm fragments during diagenesis (Fig. 11.19). In another cathodoluminescence study of syntaxial rims in limestones, Maliva (1989) concludes that the rims formed by displacive crystal growth that simply pushed aside the enclosing micrite. Thus, it appears that interpreting the origin of syntaxial rims on fossils must be approached with caution.

Replacement

Replacement involves the dissolution of one mineral and the nearly simultaneous precipitation of another mineral **of different composition** in its place. Thus, the process of replacement is similar to the process of wet polymorphic transformation, but it involves minerals of different composition. Many kinds of mineral may replace carbonate minerals during diagenesis, including chert, pyrite, hematite, apatite, anhydrite, and dolomite. As discussed in [Chapter 10](#), dolomite can replace aragonite or calcite on a massive scale, resulting in pervasive dolomitization of limestone sequences. Other than dolomite, chert is probably the most common replacement mineral in carbonate rocks. Bodies of replacement chert may range in size from micrometer-size patches within carbonate grains to centimeter-size nodules and lenses that engulf both carbonate grains and micrite. Replacement may be either fabric-destructive or fabric-preserving. For example, replacement of fossils by chert very commonly preserves the fine textural details of the fossils. On the other hand, much replacement of aragonite or calcite by dolomite is fabric-destructive ([Chapter 10](#)).

Replacement can occur in all diagenetic environments. Dolomite, for example, may replace calcium carbonate in both shallow-burial and deep-burial environments. Replacement of

carbonates by chert is not common on the seafloor but can occur in both the meteoric and deep-burial environments. Maliva and Siever (1989b) report chertification of Paleozoic carbonates at burial depths ranging from 30 to 1000 m. In carbonate–evaporite sequences, replacement of carbonate minerals by anhydrite at depth is known to be a common process.

Conventional wisdom holds that replacement can occur in any environment that favors the dissolution of calcium carbonate and the precipitation of the guest mineral and where an adequate source of magnesium, silica, iron, sulfate, etc. is available to form the precipitating mineral. Most investigators have assumed that replacement occurs in a diagenetic environment in which the bulk pore waters of the sediment or rock undergoing replacement are supersaturated with respect to the guest (replacing) mineral and undersaturated with respect to the bulk host (replaced) mineral, whose free surfaces are in contact with pore waters. Maliva and Siever (1988a) make the extremely interesting suggestion, however, that undersaturation with respect to the bulk host phase is not necessarily a prerequisite for replacement. They propose that diagenetic replacement can occur by a **force of crystallization-controlled mechanism** along thin films that have only diffusional access to bulk pore waters in equilibrium with the bulk host sediments. According to this model, “nonhydrostatic stresses resulting from authigenic crystal growth are principally responsible for local host-phase dissolution at authigenic-host phase contacts.” All that is required for replacement is a sufficient degree of local supersaturation with respect to the authigenic mineral phase and suitable conditions in the rock for initial crystal nucleation. The degree of saturation of the bulk pore water with respect to the host mineral being replaced is of secondary importance. Maliva and Siever maintain that nonhydrostatic stresses resulting from authigenic crystal growth are sufficient for host-mineral dissolution. They developed this model originally to explain silicification of fossils in limestones (Maliva and Siever, 1988b) but suggest that it may also be applied to replacement of detrital quartz by carbonate minerals and replacement of carbonate minerals by dolomite. Replacement of carbonate minerals by silica may be highly selective, with silica quite commonly replacing fossils and other carbonate grains such as ooids in preference to micrite (e.g. Maliva and Siever, 1988b).

Significant silicification of carbonates requires an adequate source of silica. Dissolution of siliceous sponge spicules is commonly postulated to be the principal mechanism for supplying silica. Otherwise, silica must come from sources outside carbonate formations. Generally, it is extremely difficult to identify the source of silica in a given carbonate unit. The silica–carbonate replacement reaction is known to be a reversible one. At some stages during diagenesis, silica can replace carbonate, and subsequently be itself replaced by carbonate. In turn, the replacing carbonate may be partially or completely replaced by silica at a later stage. Assuming that Maliva and Siever’s (1988a) “force of crystallization” theory is correct, these reversals may be governed mainly by varying silica concentrations in pore waters.

Carbonate replacement can generally be recognized by careful petrographic examination. Criteria for recognizing replacement textures are discussed in [Chapter 8](#) and illustrated in [Table 8.1](#). Illogical mineral composition (pseudomorphs), cross-cutting relationships, and caries texture (bitelike embayments into the host mineral) are particularly useful criteria.

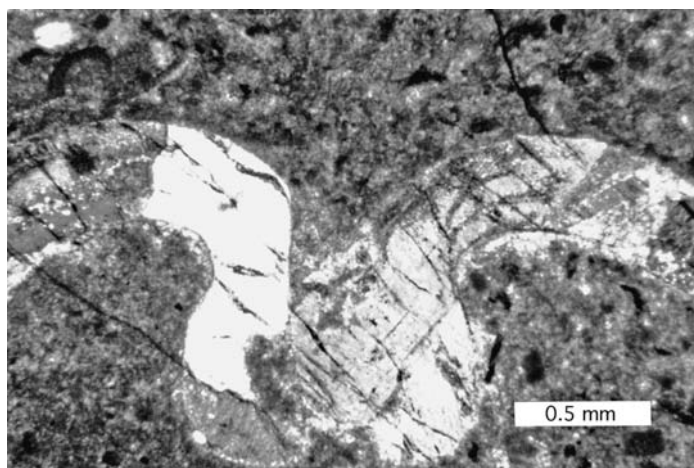


Figure 11.20 Section of a brachiopod shell almost completely replaced by coarse anhydrite. An example of illogical mineral composition as a clue to recognition of replacement fabrics. Pennsylvanian limestone, Paradox Basin, Utah. Crossed nicols.

Figure 11.20 shows an example of illogical mineral composition (a fossil shell replaced by anhydrite), and Fig. 11.21 illustrates caries texture (bitelike replacement).

Dissolution

Deeply buried carbonate rocks have presumably been mineralogically stabilized owing to dolomitization, neomorphism, and cementation. Therefore, few highly soluble phases should be present. Nonetheless, dissolution in the deep-burial environment does occur. Two factors may account for deep-burial dissolution: (1) Subtle differences in the relative solubilities of stabilized carbonates may exist owing to factors such as crystal size, trace-element and organic-matter content, and microporosity. In general, biogenic calcite is more soluble than calcitized aragonite or Mg-calcite, which are more soluble than calcite cement (Choquette and James, 1987). (2) Decarboxylation of organic matter during maturation may release sufficient CO_2 and organic acid into pore fluids to cause dissolution (see Chapter 8, Section 8.4.2).

Thus, dissolution may be fabric selective, with preferential removal of less-stable biogenic calcite and possibly calcitized carbonate grains. On the other hand, dissolution may be nonfabric selective if CO_2 and organic acid levels in pore waters are high enough. In nonfabric-selective dissolution, dissolution begins in interparticle or intergranular pores, which are enlarged by dissolution into large vugs. These enlarged vugs are rounded, and they cut across all textural elements, including carbonate grains, late-burial cements, and stylolites. This cross-cutting relationship of solution pores is the best evidence of deep-burial dissolution. Because decarboxylation processes take place at burial temperatures just below those required to form liquid hydrocarbons, decarboxylation-driven dissolution may create important amounts of secondary porosity in carbonate reservoirs for storage of petroleum.



Figure 11.21 A foraminifer partially replaced by chert (arrow). Salem Formation (Mississippian), Missouri.





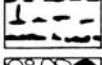










11.6 Evolution of porosity in carbonate rocks

11.6.1 Introduction

Because carbonate rocks contain more than one-third of the world's petroleum reserves, the porosity of carbonate rocks is an important subject to petroleum geologists. The porosity and permeability of sedimentary rocks influence the migration of petroleum, and the porosity of reservoir rocks determines the amount of petroleum that can be stored in a given petroleum trap. Thus, the origin, evolution, and preservation of porosity in carbonate rocks has considerable economic significance in addition to being a subject of scientific interest. Analysis and interpretation of carbonate porosity require some knowledge of porosity classification as well as an understanding of the origin and evolution of porosity. These topics are discussed very briefly in this section. Useful books dealing with carbonate petrology include Budd *et al.* (1995), Lucia (1999), Moore (1989, 2001), and Scholle and Ulmer-Scholle (2003).

11.6.2 Classification and origin of carbonate porosity

Numerous classifications of porosity have been proposed (see bibliography in Scholle and Ulmer-Scholle, 2003, p. 294); however, most geologists worldwide use the porosity classification of Choquette and Pray (1970) to describe carbonate porosity. This classification (Fig. 11.22)

BASIC POROSITY TYPES			
FABRIC SELECTIVE		NOT FABRIC SELECTIVE	
	INTERPARTICLE	BP	
	INTRAPARTICLE	WP	
	INTERCRYSTAL	BC	
	MOLDIC	MO	
	FENESTRAL	FE	
	SHELTER	SH	
	GROWTH-FRAMEWORK	GF	
			 FRACTURE FR
			 CHANNEL* CH
			 VUG* VUG
			 CAVERN* CV
<p style="text-align: center; margin: 0;">*Cavern applies to man-sized or larger pores of channel or vug shapes.</p>			
FABRIC SELECTIVE OR NOT			
	BRECCIA BR		BORING BO
			BURROW BU
			SHRINKAGE SK

MODIFYING TERMS			
GENETIC MODIFIERS		SIZE* MODIFIERS	
PROCESS	DIRECTION OR STAGE	CLASSES	
SOLUTION	s	ENLARGED	x
CEMENTATION	c	REDUCED	r
INTERNAL SEDIMENT	i	FILLED	f
TIME OF FORMATION			
PRIMARY		P	
pre-depositional		Pp	
depositional		Pd	
SECONDARY		S	
eogenetic		Se	
mesogenetic		Sm	
telogenetic		St	
<p style="margin: 0;">Use size prefixes with basic porosity types: mesovug msVUG small mesomold smsMO microinterparticle mcBP</p>			
<p style="margin: 0;">*For regular-shaped pores smaller than cavern size. †Measures refer to average pore diameter of a single pore or the range in size of a pore assemblage. For tubular pores use average cross-section. For platy pores use width and note shape.</p>			
<p style="margin: 0;">Genetic modifiers are combined as follows:</p>			
PROCESS + DIRECTION + TIME			
<p style="margin: 0;">EXAMPLES: solution-enlarged sx cement-reduced primary crP sediment-filled eogenetic ifSe</p>			
ABUNDANCE MODIFIERS			
percent porosity		(15%)	
or			
ratio of porosity types		(1:2)	
or			
ratio and percent		(1:2) (15%)	

Figure 11.22 Classification of porosity in carbonate rocks. (From Choquette, P. W. and L. C. Pray, 1970, Geologic nomenclature and classification of porosity in sedimentary carbonates: *Am. Assoc. Pet. Geol. Bull.*, 54, Fig. 2, p. 224, reprinted by permission of AAPG, Tulsa, OK.)

divides porosity into three basic types: fabric selective, not fabric selective, and fabric selective or not. **Fabric-selective** porosity includes interparticle porosity (pore space among grains), intraparticle porosity (pore space within grains), fenestral porosity (irregular, elongated openings commonly oriented parallel to bedding), intercrystalline porosity (pore space among crystals), moldic porosity (solution molds), shelter porosity (pore space beneath umbrellalike fossils or other grains), and growth-framework porosity (porosity within reef frameworks or similar structures).

Most of these fundamental kinds of fabric-selective porosity are generated as a result of depositional processes and are thus kinds of **primary porosity**. Porosity that results from diagenetic processes is secondary porosity. Moldic porosity is entirely of secondary origin, and most intercrystalline porosity is probably also secondary. Interparticle pores are initially primary but can be enlarged by secondary solution processes. Some intraparticle porosity may also be generated by dissolution, and dissolution processes are probably involved to some extent in the formation of fenestral porosity (Chapter 9).

Porosity that is **not fabric selective** is entirely of secondary origin and forms as a result of fracturing and/or solution. **Fabric selective or not porosity** includes both primary and secondary types. Breccia porosity probably forms mainly by secondary processes that involve solution collapse or tectonism. Boring and burrow porosity form by primary (biogenic) processes, but porosity can subsequently be modified by cementation and decementation (solution). Shrinkage porosity is formed primarily by secondary processes.

Choquette and Pray (1970) include modifying terms in their classification (Fig. 11.22) that allow expression of pore size, abundance, and origin. Although the genetic modifiers are useful, some are so subjective that they may be difficult to apply (e.g. eogenetic, mesogenetic, telogenetic).

11.6.3 Changes in carbonate porosity with deep burial

As discussed in preceding sections of this chapter, carbonate sediments undergo various diagenetic modifications during burial that either reduce or enhance porosity. Mechanical compaction, chemical compaction, and cementation reduce porosity, whereas dissolution increases porosity. Uncompacted carbonate sediments may have initial porosities ranging from about 40 to 80 percent. By contrast, the final porosity of carbonate rocks may range from nearly zero to a few percent. Values of 5–15 percent are common in reservoir facies (Choquette and Pray, 1970). Clearly, the overall effect of burial diagenesis is to reduce the porosity of carbonate sediments to low levels. Deeply buried carbonate rocks that undergo late-stage uplift into the telogenetic zone may, of course, develop enhanced porosity owing to dissolution of carbonate grains or previously formed cements by chemically aggressive meteoric waters.

Several workers have constructed empirical depth–porosity curves on the basis of data derived from deep wells. See, for example, the porosity–depth curves for chalks in North America and Europe by Choquette and Pray (1970), the porosity–depth plots for south Florida limestones by Schmoker and Halley (1982), and several plots discussed by Moore (2001,

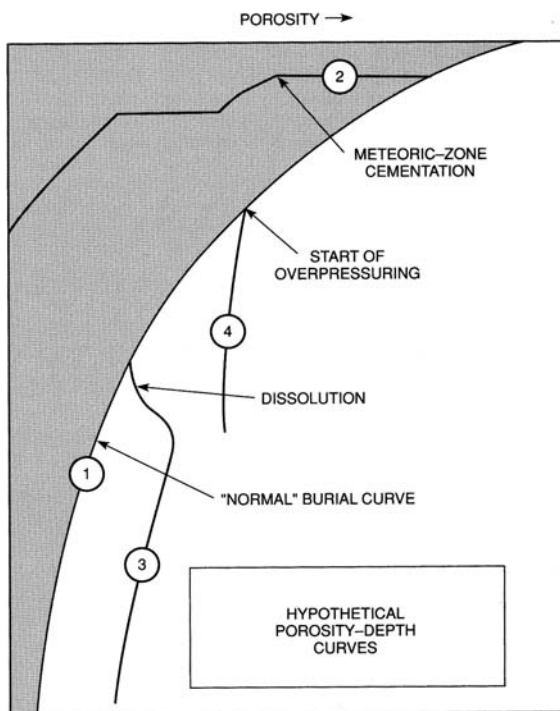


Figure 11.23 Hypothetical curve illustrating (1) a so-called “normal” porosity–depth relationship for fine-grained sediments with marine pore waters, (2) cementation in the meteoric zone (horizontal segments) alternating with burial in marine pore waters, (3) reversal of normal porosity–depth trend owing to dissolution in the deep subsurface, followed by resumption of normal burial, and (4) arrested porosity reduction owing to abnormally high pore pressure. (From Choquette, P. W. and N. P. James, 1987, Diagenesis 12. Diagenesis in limestones – 3. The deep burial environment: *Geosci. Can.*, **14**, Fig. 33, p. 23, reprinted by permission of the Geological Association of Canada.)

p. 298). These curves typically show a nonlinear, exponential trend of decreasing porosity with increasing depth. Typically, they show that initially high porosity values are reduced to values of about 10–20 percent at burial depths of about 3 km and to less than 5 percent at depths of about 6 km. The shapes of these curves are normally considered to be due mainly to mechanical and chemical compaction; however, many of the factors discussed in preceding sections of this chapter, especially cementation, must also affect the shapes of the curves.

Choquette and James (1987) generated a hypothetical porosity–depth curve that schematically illustrates how these various factors can affect porosity during burial (Fig. 11.23). Note that considerable deviation from a “normal” exponential curve (curve 1) can occur as a result of meteoric-zone cementation, overpressuring, and deep-burial dissolution. Curve 2 is a curve for chalk or lime mud subjected to early meteoric or possibly marine cementation, (3) is a curve that might be expected if solution is created at considerable depth, and (4) is a curve that might result from overpressuring.

11.7 Summary statement

Carbonate sediments are susceptible during diagenesis to a number of processes that can alter both their composition and physical properties. Diagenesis begins on the seafloor before sediments have undergone significant burial. Early diagenesis includes biogenetic alteration, such as boring of shell fragments by fungi and algae and mixing of sediment by organisms (bioturbation), as well as physico-chemical changes (e.g. cementation and dissolution). Cementation in warmer waters brings about minor lithification of sediments, which can include development of hardgrounds in shallow water and precipitation of carbonate crusts at water depths down to a few hundred meters. On the other hand, less-stable minerals such as aragonite may undergo at least partial dissolution in the presence of CO₂-rich colder waters at high latitudes and deeper depths.

After deposition in shallow-water environments, carbonate sediments can subsequently be brought into contact with meteoric waters by complete filling of shallow-water basins to or above sea level, by falling sea level, or by late-stage tectonic uplift. Under meteoric conditions, aragonite and Mg-calcite may undergo dissolution in the presence of acidic, CO₂-charged waters. On the other hand, precipitation of calcite can occur if waters become saturated with CaCO₃ with respect to calcite or if CO₂ is lost through warming of the water or photosynthesis. Neomorphism of aragonite to calcite may also occur. The general effect of diagenesis in the meteoric zone is to stabilize the mineral assemblage by destroying less-stable aragonite and low-magnesian calcite and concomitantly generating stable high-magnesian calcite.

Thus, carbonate sediments that first go through a stage of meteoric diagenesis arrive in the deep-burial diagenetic environment already stabilized. Carbonate sediments that undergo burial directly, without going through a stage of meteoric diagenesis, still contain aragonite and low-magnesian calcite. Further chemical diagenesis in the deep-burial environment of unstabilized mineral assemblages may proceed more rapidly than that of stabilized assemblages; however, both will undergo additional diagenetic change under the influence of increased temperatures and pressures and changed pore-water compositions.

Diagenetic processes in the deep-burial environment include physical and chemical compaction, cementation, dissolution, and neomorphism. Physical compaction produces a number of effects on carbonate sediments, such as breakage of fossil shells and deformation of soft grains; however, its most important effect is reduction in porosity of the sediment. Initial porosities ranging from 40–80 percent can be reduced to values well below 10 percent at great depth. Chemical compaction (pressure solution) produces stylolites on a local scale and, on a larger scale, causes extensive loss of porosity and thinning of beds.

Somewhat paradoxically, both cementation and dissolution occur in the burial environment depending upon burial conditions. Factors that favor cementation include increase in temperature, oversaturated pore waters, and decrease in CO₂ partial pressure. Factors that favor dissolution include increased rock pressure (pressure solution), undersaturated pore fluids, and chemically aggressive pore fluids owing to dissolved CO₂ and organic acids generated by diagenesis of organic matter. Neomorphic changes, such as alteration of

aragonite and low-magnesian calcite to high-magnesian calcite, and increase in crystal size owing to recrystallization are also common in the burial environment.

Further reading

- Adams, A. E. and W. S. MacKenzie, 1998, *A Color Atlas of Carbonate Sediments and Rocks Under the Microscope*: John Wiley and Sons, New York, NY.
- Bathurst, G. C., 1993, Microfabrics in carbonate diagenesis: A critical look at forty years in research. In Rezak, R. and D. L. Lavoie (eds.), *Carbonate Microfabrics*: Springer-Verlag, New York, NY, pp. 3–14.
- Demico, R. V. and L. A. Hardie, 1994, *Sedimentary Structures and Early Diagenetic Features of Shallow Marine Carbonate Deposits*: SEPM Atlas Series 1.
- Moore, C. H., 2001, *Carbonate Reservoirs: Porosity Evolution and Diagenesis in a Sequence Stratigraphic Framework*: Developments in Sedimentology 55.
- Morse, J. W. and F. T. Mackenzie, 1990, *Geochemistry of Sedimentary Carbonates*: Elsevier, Amsterdam, chs. 6–8.
- Scholle, P. A. and D. S. Ulmer-Scholle, 2003, *A Color Guide to the Petrography of Carbonate Rocks: Grains, Textures, Porosity, Diagenesis*: AAPG Memoir 77.
- Sellwood, B. W., 1994, Principles of carbonate diagenesis, in Parker, A. and B. W. Sellwood (eds.), *Quantitative Diagenesis: Recent Developments and Applications to Reservoir Geology*: Kluwer, Dordrecht, pp. 1–32.
- Tucker, M. E. and R. G. C. Bathurst (eds.), 1990, *Carbonate Diagenesis*: Blackwell Scientific, Oxford.
- Tucker, M. E. and V. P. Wright, 1990, *Carbonate Sedimentology*: Blackwell Scientific, Oxford, ch. 7.

Part IV

Other chemical/biochemical sedimentary rocks and carbonaceous sedimentary rocks



Triassic bedded chert exposed along the Kiso River, Japan

12

Evaporites, cherts, iron-rich sedimentary rocks, and phosphorites

12.1 Introduction

This chapter deals with the chemical/biochemical rocks other than carbonates. Thus, it discusses evaporites, the siliceous sedimentary rocks (cherts), iron-rich sedimentary rocks (iron-formations and ironstones), and phosphorites. Volumetrically, these rocks are far less abundant than siliciclastic sedimentary rocks and carbonate rocks. If we add the percentages of shale, sandstone, and carbonate rocks calculated or measured by various authors such as Ronov *et al.* (1980), the unaccounted volume of total sedimentary rocks that can be attributed to these chemical/biochemical rocks appears to be no more than about 2 percent. The small volume of these rocks is not, however, a measure of their importance or the interest that we have in them. All of the sedimentary rocks discussed in this chapter have considerable economic significance. Evaporite deposits such as gypsum, halite (rock salt), and trona are mined for a variety of industrial and agricultural purposes, iron-rich sedimentary rocks are the source of most of our iron ores, phosphorites are extremely important sources of fertilizers and other chemicals, and the siliceous sedimentary rocks have some economic value, e.g. in the semiconductor industry.

In addition to their economic importance, all of the rocks discussed in this chapter are intrinsically interesting owing to their compositions and origins. The origin of many of these rocks is still enigmatic even after many years of study. For example, we are still unsure of the depositional mechanisms that account for the formation of the iron-rich sedimentary rocks, nor do we have a fully satisfactory explanation for the source or sources of the vast amount of iron locked up in these deposits. Also, there are many unanswered questions about the origin of phosphorites and the processes by which phosphorus becomes so highly concentrated in phosphate deposits. We understand somewhat better the origin of evaporites and cherts; nonetheless, we certainly do not have all the answers.

In this chapter we take a look at each of these interesting and economically significant kinds of sedimentary rocks. Space limitations do not permit analysis and discussion of each of these groups of rocks in the detail accorded the siliciclastic sedimentary rocks and carbonates. Accordingly, I do not place undue stress on the petrographic characteristics of these rocks. Nonetheless, I have tried to provide enough details about their mineralogy, chemical compositions, and other properties to give readers a reasonable understanding of

their principal characteristics. I also discuss some of the more interesting and enigmatic aspects of their origin, and alternate points of view about origin are presented where appropriate. An extensive list of additional readings is provided at the end of the chapter for those readers who wish to explore the properties of these rocks in greater detail.

12.2 Evaporites

12.2.1 Introduction

We use the term evaporites to include all those sedimentary rocks formed by evaporation of saline waters. Sedimentary rocks containing evaporite minerals are common in the geologic record. Evaporite deposits occur in rocks as old as early Precambrian, where they are preserved mainly as pseudomorphs rather than as the actual salt. Extensive accumulations of evaporite minerals are very common in Phanerozoic stratigraphic sequences. Evaporite deposition was especially widespread and important during the Late Cambrian, Permian, Jurassic, and Miocene. Lesser accumulations took place during the Silurian, Devonian, Triassic, and Eocene (Ronov *et al.*, 1980). Although evaporites make up less than about 2 percent of the sediments deposited on the world's platforms during Phanerozoic time, evaporites were deposited quite rapidly when they were forming. As much as 100 m of evaporites could be deposited in about 1000 years when conditions were right (Schreiber and Hsü, 1980); this rate is two or three orders of magnitude higher than the rate at which most other shelf sediments are deposited. One of the thickest known deposits of evaporites is the Late Miocene Mediterranean Messinian evaporite sequence, which may exceed 2 km in thickness. The Messinian evaporites are believed to have been deposited in less than 200,000 years.

Although the bulk of ancient evaporite deposits were probably deposited under marine or marginal-marine conditions, evaporites were also deposited at various times in the past in nonmarine settings. Deposition in continental settings was particularly important during early phases of the Triassic–Jurassic rifting of Pangea, when the basal deposits in the Atlantic and Gulf Coast basins, and in many other rift basins, were formed (Schreiber, 1988a). Evaporites are also forming today in many parts of the world where rates of evaporation exceed water input. Many of these areas lie in nonmarine settings within continental masses. Although evaporite deposition is most common in warm areas of the world, evaporites are forming at present in arid portions of the Arctic and Antarctic. On the other hand, evaporite deposition is much slower in colder regions than in warmer regions. Also, depositional rates for evaporites in nonmarine settings are slower than those in marine-fed basins because the feed waters for nonmarine basins are initially very dilute (Schreiber, 1988a). Marine evaporites tend to be thicker and more laterally extensive than nonmarine evaporites and are generally of greater geologic interest.

Evaporite salts have been mined and used by humans for more than 5000 years (Warren, 2006, p. 791). Halite, gypsum, trona, and other salts are currently used for a variety of industrial and agricultural purposes. In addition to their commercial value, evaporites are associated with carbonate rocks in many major oil fields of the world. Squeezing and

remobilization of salt deposits creates petroleum traps in association with salt domes; subsurface solution of evaporite cements in carbonate and siliciclastic rocks can create important amounts of secondary porosity in these rocks; and evaporite caprocks form seals over many petroleum traps that prevent the petroleum from escaping.

12.2.2 Composition

Major minerals

Evaporite deposits are composed dominantly of varying proportions of halite (NaCl), anhydrite (CaSO₄) and gypsum (CaSO₄·2H₂O), although numerous other minerals may be present in minor amounts. Approximately 80 minerals in total have been reported from evaporite deposits (Stewart, 1963). About 60 of the more important minerals are listed, together with their chemical compositions, in Table 12.1 (Warren, 2006, p. 3). Gypsum is more abundant than anhydrite in modern evaporite deposits (Dean, 1982); however, anhydrite is more abundant than gypsum in deposits buried to depths exceeding about 610 m owing to dewatering of gypsum and its conversion to anhydrite.

Evaporite minerals display a variety of crystal forms, as illustrated in Fig. 12.1. Halite crystals include cubes with depressed faces, skeletal hopper crystals and pyramidal hopper crystals and toothlike forms. Gypsum and anhydrite crystals also take a variety of forms that include single crystals, radial clusters of crystals, and numerous types of complex twinned crystals. As mentioned, evaporites can form in both marine and nonmarine environments. Owing to differences in the dissolved mineral composition of the feed waters, different suites of minerals tend to form in the two environments. See Warren (2006, ch. 2) for discussion of marine vs. nonmarine brines, and Hardie (1984) for discussion of the characteristics of marine and nonmarine evaporites.

Marine evaporite minerals

Because marine evaporites are precipitated from seawater, the mineral composition of marine evaporites in various deposits tends to be relatively constant. Seawater has an average salinity of about 35 parts per thousand (‰). Although 12 elements are present in seawater in amounts greater than 1 ppm (0.001 parts per thousand) (Braitsch, 1971), Cl⁻ (18.98%), Na⁺ (10.56%), SO₄²⁻ (2.65%), Mg²⁺ (1.27%), Ca²⁺ (0.40%), K⁺ (0.38%), and HCO₃⁻ (0.14%) make up the bulk of the dissolved solids in seawater. Trace elements, present in amounts ranging from about 65 ppm to 1 ppm, include Br⁻, Sr²⁺, B³⁺, F⁻, and H₄SiO₄.

Excluding the carbonate minerals, most of which are not evaporites, the most common marine evaporite minerals are the calcium sulfate minerals gypsum and anhydrite. Halite is next in abundance, followed by the potash salts (sylvite, carnallite, langbeinite, polyhalite, kainite) and the magnesium sulfate kieserite. The common marine evaporite minerals can be grouped on the basis of chemical composition into chlorides, sulfates, and carbonates (Table 12.2). Note that the anions (Cl⁻, SO₄²⁻, CO₃²⁻) are combined with the cations Na⁺, K⁺, Mg²⁺, or Ca²⁺ to form the various minerals. Evaporite deposits may also contain various amounts of impurities such as clay minerals, quartz, feldspar, or sulfur.

Table 12.1 Major evaporite minerals

Mineral	Formula	Mineral	Formula
Anhydrite	CaSO ₄	Leonhardtite	MgSO ₄ · 4H ₂ O
Antarcticite	CaCl ₂ · 6H ₂ O	Leonite	MgSO ₄ · K ₂ SO ₄ · 4H ₂ O
Aphthitalite (glaserite)	K ₂ SO ₄ · (Na,K)SO ₄	Loewite	2MgSO ₄ · 2Na ₂ SO ₄ · 5H ₂ O
Aragonite **	CaCO ₃	Mg-calcite**	(Mg _x Ca _{1-x})CO ₃
Bassanite	CaSO ₄ · 1/2H ₂ O	Magnesite**	MgCO ₃
Bischofite	MgCl ₂ · 6H ₂ O	Meyerhoffite	Ca ₂ B ₅ O ₁₁ · 7H ₂ O
Bloedite (astrakanite)	Na ₂ SO ₄ · MgSO ₄ · 4H ₂ O	Mirabilite	Na ₂ SO ₄ · 10H ₂ O
Borax (tincal)	Na ₂ B ₄ O ₇ · 10H ₂ O	Nahcolite	NaHCO ₃
Boracite	Mg ₃ B ₇ O ₁₃ · Cl	Natron	Na ₂ CO ₃ · 10H ₂ O
Burkeite	Na ₂ CO ₃ · 2Na ₂ SO ₄	Nitratite (soda nitre)	NaNO ₃
Calcite**	CaCO ₃	Nitre (salt petre)	KNO ₃
Carnallite	MgCl ₂ · KCl · 6H ₂ O	Pentahydrate	MgSO ₄ · 5H ₂ O
Colemanite	Ca ₂ B ₅ O ₁₁ · 5H ₂ O	Pirssonite	CaCO ₃ · Na ₂ CO ₃ · 2H ₂ O
Darapskite	NaSO ₄ · NaNO ₃ · H ₂ O	Polyhalite	2CaSO ₄ · MgSO ₄ · K ₂ SO ₄ · H ₂ O
Dolomite**	Ca _(1+x) Mg _(1-x) (CO ₃) ₂	Proberite	NaCaB ₅ O ₉ · 5H ₂ O
Epsomite	MgSO ₄ · 7H ₂ O	Priceite (pandermite)	CaB ₄ O ₁₀ · 7H ₂ O
Ferronatrite	3NaSO ₄ · Fe ₂ (SO ₄) ₃ · 6H ₂ O	Rinneite	FeCl ₂ · NaCl · 3KCl
Gaylussite	CaCO ₃ · Na ₂ CO ₃ · 5H ₂ O	Sanderite	MgSO ₄ · 2H ₂ O
Glauberite	CaSO ₄ · Na ₂ SO ₄	Schoenite (picromerite)	MgSO ₄ · K ₂ SO ₄ · 6H ₂ O
Gypsum	CaSO ₄ · 2H ₂ O	Shortite	2CaCO ₃ · Na ₂ CO ₃
Halite	NaCl	Sylvite	KCl
Hanksite	9Na ₂ SO ₄ · 2Na ₂ CO ₃ · KCl	Syngenite	CaSO ₄ · K ₂ SO ₄ · H ₂ O
Hexahydrate	MgSO ₄ · 6H ₂ O	Tachyhydrate	CaCl ₂ · 2MgCl ₂ · 12H ₂ O
Howlite	H ₅ Ca ₂ SiB ₅ O ₁₄	Thenardite	Na ₂ SO ₄
Ikaite**	CaCO ₃ · 6H ₂ O	Thermonatrite	NaCO ₃ · H ₂ O
Inyoite	Ca ₂ B ₆ O ₁₁ · 13H ₂ O	Tincalconite	Na ₂ B ₄ O ₇ · 5H ₂ O
Kainite	4MgSO ₄ · 4KCl · 11H ₂ O	Trona	NaHCO ₃ · Na ₂ CO ₃ · 2H ₂ O
Kernite	Na ₂ B ₄ O ₇ · 4H ₂ O	Tychite	2MgCO ₃ · 2NaCO ₃ · Na ₂ SO ₄
Kieserite	MgSO ₄ · H ₂ O	Ulexite	NaCaB ₅ O ₉ · 5H ₂ O
Langbeinite	2MgSO ₄ · K ₂ SO ₄	Van'thoffite	MgSO ₄ · 3Na ₂ SO ₄

Less-saline alkaline earth carbonates or evaporitic carbonates are indicated by **, the remainder are more-saline evaporite salts. Less-common evaporite minerals, such as borates, iodates, nitrates, and zeolites are not listed. (After Warren, J., 2006, *Evaporites: Sediments, Resources, and Hydrocarbons*: Springer-Verlag, Berlin, Table 1.1, p. 3. Reproduced by permission.)


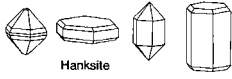
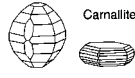

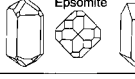
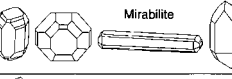

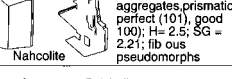


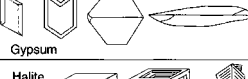
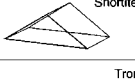


	Orthorhombic; Massive granular, stumpy prisms, flat plates; Perfect (001) and good (010) cleavage; H=3.0-3.6; SG = 2.9-3.0; Tasteless		Hexagonal; tabular or prismatic; good (001), uneven fracture. Weakly effervescent in dilute acid; H = 3.0 - 3.5; SG = 2.56; Deliquescent; Salty taste
	Orthorhombic; Massive, coarsely crystalline, bipyramids; Flare as euhedral crystals that tend to be barrel shaped; No cleavage, conchoidal fracture; H = 1.0-2.5; SG = 1.6; Very bitter taste, very hygroscopic or deliquescent		Stable at temperatures = 0°C then converts to calcite. Extensive deposits about coldwater springs in saline lakes (Mono lake) and relict in Lake Lahontan. Previously known as pseudogaylussite, thinoite, devil's horn calcite.
	Orthorhombic; Botryoidal, granular, fibrous; Perfect (010), distinct (011); H = 1.63-1.67; SG = 1.75; Sharp taste, deliquescent, only stable below 27°C; In dry air quickly loses water and turns to powder.		Monoclinic; Prismatic, tabular, acicular, granular fibrous, massive; perfect (001) also (001) (010) (011), conchoidal, H = 1.5 - 2.0; SG = 1.49; Taste cool then weakly saline and bitter; disintegrates to powdery thenardite on exposure.
	Monoclinic; Individual crystals dispersed in clay host in playa. In Venezuelan lakes called clavos or nails; (110) perfect, conchoidal; H = 2.5-3; SG = 1.99. React with acid; Calcite replacement common		Monoclinic; friable aggregates; prismatic; perfect (101), good (100); H = 2.5; SG = 2.21; fibrous pseudomorphs
	Monoclinic; tabular parallel to c, tabular by extension of (111), prismatic, good (001) poor (110) conchoidal; H = 2.5 - 3.0; SG = 2.7 - 2.85; Slightly saline taste. On hydration converts to gypsum and mirabilite; typically slushy, crumbly.		Monoclinic; crystalline to granular aggregates; efflorescences; (001) distinct, conchoidal; H = 1-1.5; SG = 1.48; Melts to thenardite in air
	Monoclinic; Plates, needles, fibres, massive (alabaster), swallowtail and palmate twins; Perfect (010) good (111) (100); H = 2.0; SG = 2.3-2.4; Tasteless		Triclinic; Prismatic, massive, massive fibrous, lamellar, Good (100); H = 2.5 - 3.5; SG 2.78; Tasteless; Alters to gypsum in contact with humid air.
	Cubic; Perfect cleavage, conchoidal; Cubes, hoppers, rats, fibrous; H = 2.5; SG = 2.1 - 2.2; Salty taste		Orthorhombic; wedge shaped crystals; distinct (010), conchoidal; H = 3.0; SG = 2.60; Secondary alteration salt in trona depositing regions
			Monoclinic; typically fibrous nodular or columnar massive; (100) perfect, uneven to subconchoidal fracture; H = 2.5 - 3.0; SG = 2.14; taste alkaline; Effervesces in acids

Figure 12.1 Characteristic shapes and physical properties of some common evaporite minerals. (From Warren, J., 1999, *Evaporites: Their Evolution and Economics*: Blackwell Science, Oxford, Fig. 4.33, p. 148, reproduced by permission.)

Table 12.2 Classification of marine evaporites on the basis of mineral composition

Mineral class	Mineral name	Chemical composition	Rock name
Chlorides	Halite	NaCl	Halite; rock salt
	Sylvite	KCl	Potash salts
	Carnallite	$\text{KMgCl}_3 \cdot 6\text{H}_2\text{O}$	
Sulfates	Langbeinite	$\text{K}_2\text{Mg}_2(\text{SO}_4)_3$	Potash salts
	Polyhalite	$\text{K}_2\text{Ca}_2\text{Mg}(\text{SO}_4)_4 \cdot \text{H}_2\text{O}$	
	Kainite	$4\text{MgSO}_4 \cdot 4\text{KCl} \cdot 11\text{H}_2\text{O}$	
	Anhydrite	CaSO_4	Anhydrite; anhydrock
	Gypsum	$\text{CaSO}_4 \cdot 2\text{H}_2\text{O}$	Gypsum; gyprock
	Kieserite	$\text{MgSO}_4 \cdot \text{H}_2\text{O}$	—
Carbonates	Calcite	CaCO_3	Limestone
	Magnesite	MgCO_3	—
	Dolomite	$\text{CaMg}(\text{CO}_3)_2$	Dolomite; dolostone

Nonmarine evaporites

Nonmarine evaporites form from waters that were originally river water or groundwater. The chemistries of these original waters can be highly variable, depending upon the lithology of the rocks with which they interact. For example, rivers that flow across limestones are commonly enriched in Ca^{2+} and HCO_3^- , whereas those that flow across igneous and metamorphic rocks tend to be enriched in silica, Ca^{2+} , and Na^+ . Because of these differences in original water chemistry, more diverse suites of minerals typify nonmarine evaporite deposits than typify marine deposits (Harvie *et al.*, 1982). Thus, many nonmarine deposits contain evaporite minerals that are not common in marine evaporites. These minerals may include trona, mirabilite, glauberite, borax, epsomite, thenardite, gaylussite and bloedite (see Table 12.1). On the other hand, nonmarine deposits may also contain anhydrite, gypsum, and halite and may even be composed dominantly of these minerals. Therefore, it may not always be easy to distinguish between marine and nonmarine evaporites on the basis of mineralogy.

12.2.3 Classification of evaporites

Evaporites can be classified informally into marine and nonmarine types on the basis of origin; however, this is a subjective call and may not always be easy to make. They can be further classified as chlorides, sulfates, and carbonates on the basis of mineralogy, as shown in Table 12.2. Other than these simple, informal classifications, no general classification scheme for evaporite rocks as a whole appears to exist. Only a few rock names have been given to evaporite deposits, and these names are applied on the basis of the dominant mineral in the deposits. Rocks composed mainly of halite are called halite or **rock salt**. Rocks made up dominantly of gypsum or anhydrite are simply called gypsum or anhydrite, although some geologists use the names **rock gypsum** or **rock anhydrite**. Less commonly they are called gyprock and anhydrock. Few evaporite beds are composed dominantly of minerals other than the calcium sulfates and halite. No formal names have been proposed for rocks enriched in other evaporite minerals, although the term potash salts is used informally for potassium-rich evaporites.

As indicated, most evaporite deposits consist of either anhydrite/gypsum or halite. I know of no formal scheme for subdividing halite (rock salt) into subtypes; however, Maiklem *et al.* (1969) proposed a useful scheme for the structural classification of anhydrites. Many anhydrites are characterized by distorted fabrics that result from volume changes owing to dehydration of gypsum and rehydration of anhydrite during diagenesis. Maiklem *et al.* (1969) propose a structural classification for anhydrite on the basis of fabric and bedding. This classification divides anhydrites into about two dozen structural types, which can be lumped into three fundamental structural groups: nodular anhydrites, laminated anhydrites, and massive anhydrites.

Nodular anhydrite consists of irregularly shaped lumps of anhydrite that are partly or completely separated from each other by a salt or carbonate matrix (Fig. 12.2). **Mosaic anhydrite** is a type of nodular anhydrite in which the anhydrite masses or lumps are

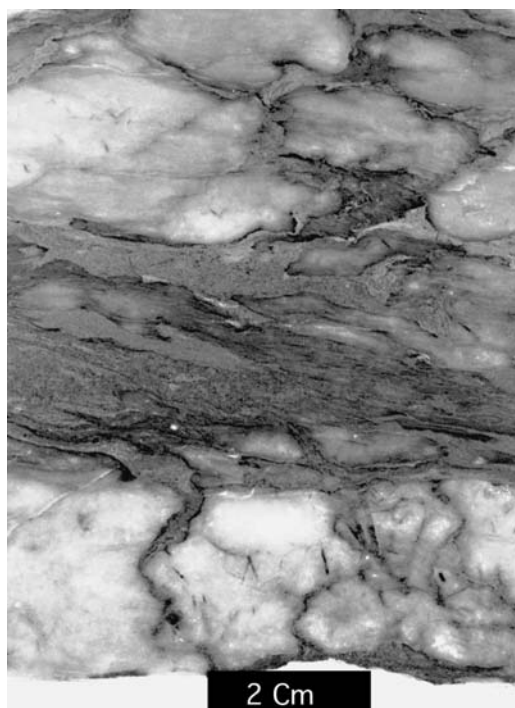


Figure 12.2 Nodular anhydrite in a core sample of the Buckner Anhydrite (Jurassic), Texas. Dark-colored carbonate separates and surrounds lighter-colored anhydrite nodules.

approximately equidimensional and are separated by very thin stringers of dark carbonate mud or clay. The formation of nodular anhydrite begins by displacive growth of gypsum in carbonate or clayey sediments. Subsequently, gypsum crystals alter to anhydrite pseudomorphs, which continue to enlarge by addition of Ca^{2+} and SO_4^{2-} from an external source. This displacive growth ultimately results in segregation of the anhydrite into nodular masses. **Chickenwire structure** is a term used for a particular type of mosaic or nodular anhydrite that consists of slightly elongated, irregular polygonal masses of anhydrite separated by thin dark stringers of other minerals such as carbonate or clay minerals (Fig. 12.3). This structure apparently forms when growing nodules ultimately coalesce and interfere. Most of the enclosing sediment is pushed aside and what remains forms thin stringers between the nodules (Shearman, 1982).

Laminated anhydrites, sometimes called laminites, consist of thin, nearly white anhydrite or gypsum laminations that alternate with dark-gray or black laminae rich in dolomite or organic matter (Fig. 12.4). The laminae are commonly only a few millimeters thick and rarely attain a thickness of one centimeter. Many thin laminae are remarkably uniform with sharp planar contacts that can be traced laterally for long distances. Some are reported to be traceable for distances of 290 km (Anderson and Kirkland, 1966). Laminites may comprise vertical sequences hundreds of meters thick in which hundreds

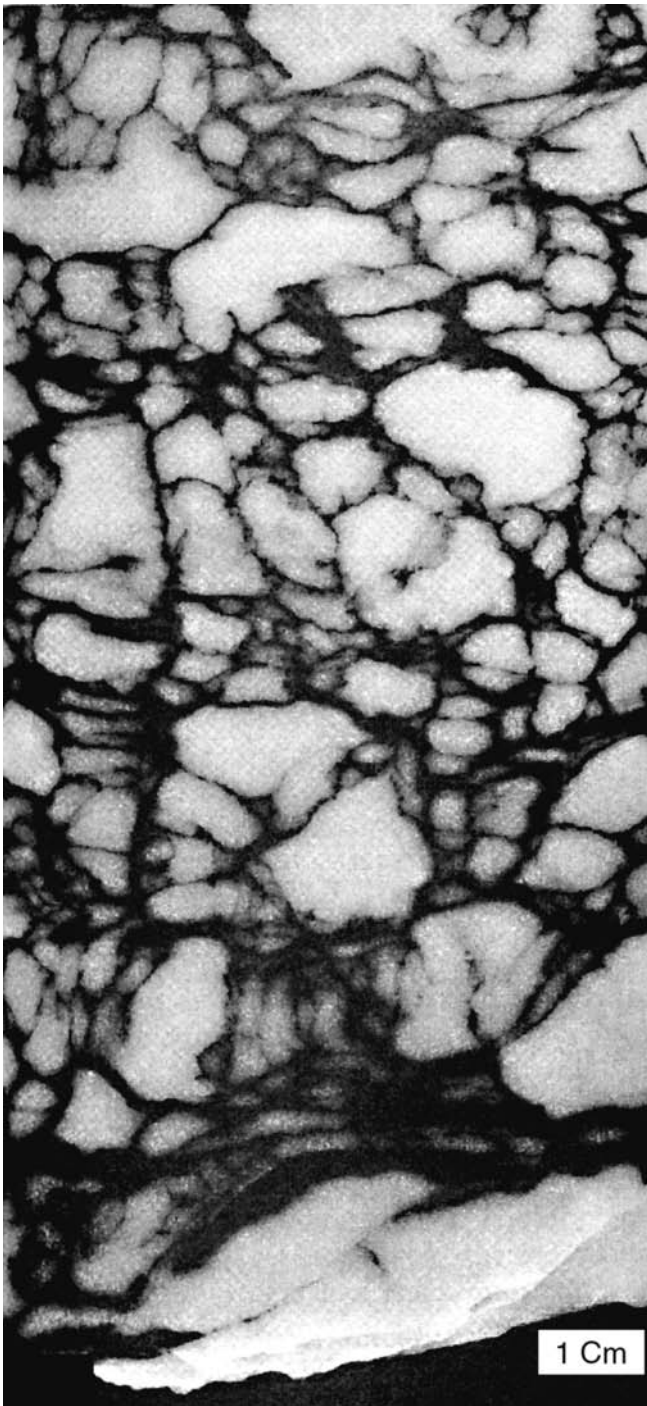


Figure 12.3 Chickenwire nodular structure in anhydrite. Evaporite series of the Lower Lias (Jurassic), Aquitaine Basin, southwest France. (From Bouroullec, J., 1981, Sequential study of the top of the evaporitic series of the Lower Lias in a well in the Aquitaine Basin (Auch 1), southwestern France, in *Chambre Syndical de la Recherche et de la Production du Pétrole et du Gaz Naturel* (eds.), *Evaporite Deposits: Illustration and Interpretation of Some Environmental Sequences*, Pl. 36, p. 157, reprinted by permission of Editions Technip, Paris, and Gulf Publishing Co., Houston, TX. Photograph courtesy of J. Bouroullec.)

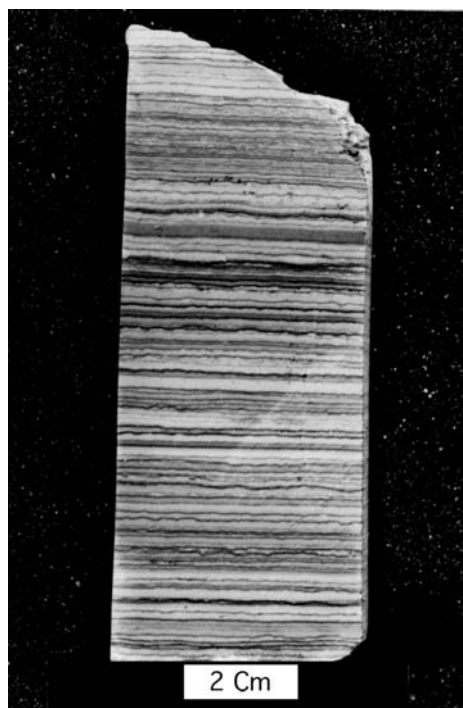


Figure 12.4 Laminated evaporite from the Prairie Evaporite (Devonian), Canada.

of thousands of laminae are present. Laterally persistent laminae are believed to form by precipitation of evaporites in quiet water below wave base. They could presumably form either in a shallow-water area protected in some manner from strong bottom currents and wave agitation or in a deeper-water environment. Alternating light and dark pairs of bands in laminated evaporites may represent annual varves resulting from seasonal changes in water chemistry and temperature or they may represent cyclic changes or disturbances of longer duration. Laminae of anhydrite can occur with thicker layers of halite, producing laminated halite.

Some laminated anhydrite may form by coalescence of growing anhydrite nodules, which expand laterally until they merge into a continuous layer. Layers formed by this mechanism are thicker, less distinct, and less continuous than laminae formed by precipitation. A special type of contorted layering that has resulted from coalescing nodules has been observed in some modern sabkha deposits where continued growth of nodules creates a demand for space. The lateral pressures that result from this demand cause the layers to become contorted, forming ropy bedding or **enterolithic structures** (Fig. 12.5).

Massive anhydrite is anhydrite that lacks perceptible internal structures. True, completely massive anhydrite is less common than nodular and laminated anhydrite, and its origin is poorly understood. Presumably, it represents sustained, uniform conditions of



Figure 12.5 Enterolithic structure in nodular gypsum of the Granada Basin, southern Spain. (Photograph courtesy of J. M. Rouchy.)



Figure 12.6 Massive, white gypsum in the Minturn Formation (Pennsylvanian), exposed in a bluff in north-central Colorado, USA.

deposition. Haney and Briggs (1964) suggest that massive anhydrite forms by evaporation at brine salinities of approximately 200–275‰, just below the salinities at which halite begins to precipitate. Figure 12.6 shows an outcrop of massive gypsum (rehydrated anhydrite) preserved under relatively dry climatic conditions.

12.2.4 *Deposition of evaporites*

Evaporation sequence

Ocean water has an average salinity of about 35‰. When ocean water is evaporated in the laboratory, evaporite minerals are precipitated in a definite sequence that was first demonstrated by Usiglio in 1848 (reported in Clarke, 1924). Minor quantities of carbonate minerals begin to form when the original volume of seawater is reduced by evaporation to about one-half, and brine concentration is about twice that of seawater. Gypsum appears when the original volume has been reduced to about 20 percent. At this point, the brine has a concentration of about four to five times that of normal seawater (130–160‰). Halite begins to form when the water volume reaches approximately 10 percent of the original volume, or 11 to 12 times the brine concentration of seawater (340–360‰). Magnesium and potassium salts are deposited when less than about 5 percent of the original volume of water remains; at that point, brine concentration may be more than 60 times that of seawater. See also McCaffrey *et al.* (1987).

The same general sequence of evaporite minerals occurs in natural evaporite deposits, although many discrepancies exist between the theoretical sequences predicted on the basis of laboratory experiments and the sequences actually observed in the rock record. In general, the proportion of CaSO_4 (gypsum and anhydrite) is greater and the proportion of late-stage Na–Mg–K sulfates and chlorides is less in natural deposits than that predicted from theoretical considerations. This early-sulfate excess and late-sulfate deficiency is commonly attributed to incomplete cycles of evaporation, with brines containing most of the dissolved Na, Mg, and K continually being refluxed out of the basin. Diagenesis may also contribute to differences between theoretical and observed successions of evaporites. For more-extended discussion of this subject, see Dean (1982) and Hardie (1984).

Many marine evaporite deposits are quite thick, some exceeding 2 km, yet it has long been recognized that evaporation of a column of seawater 1000 m thick will produce only about 14 to 15 m of evaporites. Evaporation of all the water of the Mediterranean Sea, for example, would yield a mean thickness of evaporites of only about 60 m. Obviously, special geologic conditions operating over a long period of time are required to deposit thick sequences of natural evaporites. The basic requirements for deposition of marine evaporites are a relatively arid climate, where rates of evaporation exceed rates of precipitation, and partial isolation of the depositional basin from the open ocean. Isolation is achieved by means of some type of barrier that restricts free circulation of ocean water into and out of the basin. Under these restricted conditions, the brines formed by evaporation are prevented from returning to the open ocean, allowing them to become concentrated to the point where evaporite minerals are precipitated. Nonmarine evaporites form, of course, under different conditions. Nonetheless, they also require strongly evaporative conditions and a plentiful supply of water for thick deposits to form.

Physical processes in deposition of evaporites

Although we tend to regard evaporite deposits as simply the products of chemical precipitation owing to evaporation, many evaporite deposits are not just passive chemical

precipitates. The evaporite minerals have, in fact, been transported and reworked in the same way as the constituents of siliciclastic deposits and carbonate deposits. Transport can occur by normal fluid-flow processes or by mass-transport processes such as slumps and turbidity currents. Therefore, evaporite deposits may display clastic textures, including both normal and reverse size grading and various types of sedimentary structures such as cross-bedding and ripple marks.

Depositional models for evaporite

Dominance of modern subaerial and shallow-water environments

Modern evaporites are accumulating in a variety of nonmarine and marginal-marine settings, as indicated in Fig. 12.7. Note from this figure that modern evaporites form in sabkhas, salinas, and interdune environments. All of these settings are in subaerial or shallow subaqueous environments. This subaerial to very shallow-water origin of modern evaporites stands in sharp contrast to the apparent environment of many ancient evaporites. Many thick sequences of ancient marine evaporites appear to have formed in laterally

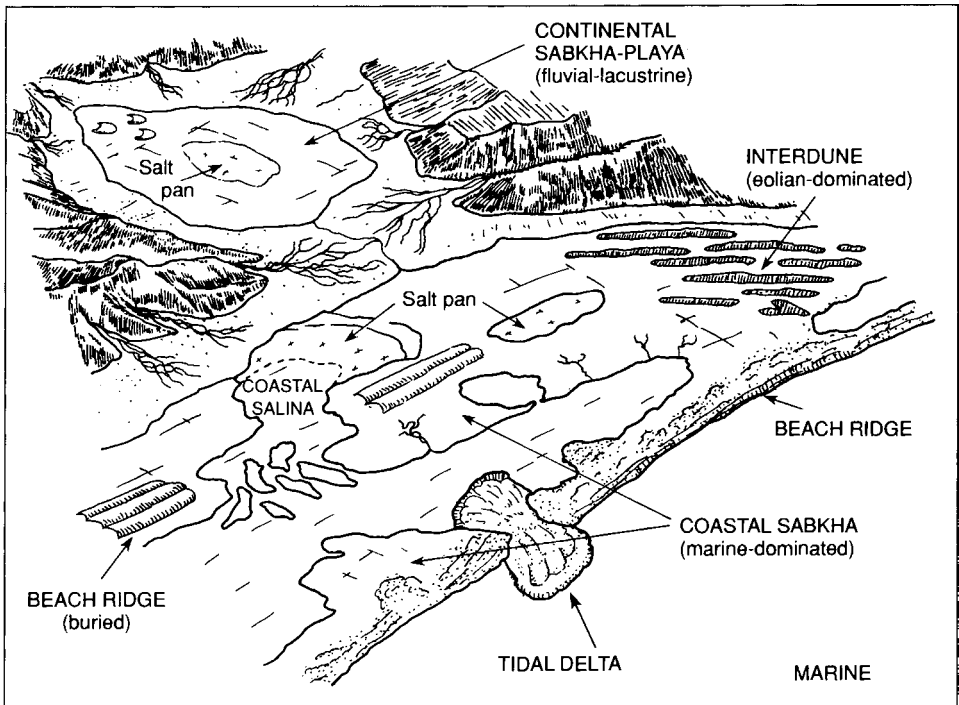


Figure 12.7 Principal settings in which modern evaporite deposits are accumulating. (From Kendall, A. C., 1984, *Evaporites*, in Walker, R. G. (ed.), *Facies Models: Geoscience Canada Reprint Series 1*, Fig. 1, p. 260, as modified slightly by Warren, 1989, reprinted by permission of the Geological Association of Canada.)

extensive, shallow- to deep-water basins, for which there are no modern equivalents. Thus, the Principle of Uniformitarianism cannot be strictly applied in the case of evaporites because the present range of evaporite environments is clearly not an adequate guide to evaporite environments of the past.

Subaerial evaporites

Many modern evaporites accumulate in **sabkhas** or salt flats. Sabkhas are for the most part subaerial mud flats in which evaporites form, although they may be covered at times by ephemeral shallow water. Modern sabkhas have been described in many parts of the world but are particularly well known in the Persian Gulf (Warren, 2006, p. 139). Warren describes the sabkhas as “extensive, barren, salt-encrusted, and periodically flooded, coastal and inland mudflats.” According to Hanford (1981), sabkhas can occur in both continental settings (nonmarine sediments and continental groundwaters) and marginal-marine settings (marine sediments and mainly marine-derived groundwaters). In continental environments, they occur in inland areas in fluvial-lacustrine (playa)-dominated settings and in eolian-dominated, interdune settings (Fig. 12.7). In the marginal-marine environment, they occur as coastal sabkhas in the intertidal and supratidal zones. Sabkhas commonly do not consist entirely or even dominantly of evaporites. Sabkha sediments are composed of a combination of evaporite minerals and carbonate and/or terrigenous clastic sediments. Evaporite minerals may form both at the surface of sabkhas and displacively within sabkha sediments, creating distorted fabrics, as mentioned.

Shallow subaqueous evaporites

Shallow subaqueous evaporites accumulate in the marginal-marine environment in coastal lakes called **salinas** (Warren and Kendall, 1985; Warren, 2006, p. 221). Modern salinas are particularly common in southern and western Australia, but they occur also around the margins of the Mediterranean, Black, and Red seas. Salinas typically occur in carbonate environments, commonly in depressions within coastal carbonate dunes or in association with carbonate reefs. Gypsum appears to be the most common evaporite mineral in most salinas; however, some (e.g. Lake Macleod, Australia) are filled with halite. The stratigraphic record suggests that many ancient shallow subaqueous evaporites were deposited on broad platforms that were far more extensive laterally than any evaporite environments known today. Thus, modern salinas are probably not adequate models for these ancient platform evaporites. Subaqueous evaporites occur also in lacustrine settings in continental basins. Lake Magadi in the African Rift is probably the best-documented modern example. Trona ($\text{NaHCO}_3 \cdot \text{Na}_2\text{CO}_3 \cdot 2\text{H}_2\text{O}$) and sodium silicate minerals such as magadiite [$\text{NaSi}_7\text{O}_{13}(\text{OH})_3 \cdot \text{H}_2\text{O}$] are characteristic deposits of this lake.

Deep-water evaporites

With the possible exception of the Dead Sea in the Middle East, no modern examples of deep-water evaporite basins exist. Therefore, models for deep-water evaporites are based on theoretical considerations and study of presumed ancient deep-water evaporites. Deep-water

evaporites are putatively characterized by thin bedding and lamination and lateral continuity of beds and laminae. Strata are composed predominantly of laminar evaporitic carbonate, sulfate, and halite. They occur in sections tens to hundreds of meters thick that can be correlated over tens to hundreds of kilometers (Schreiber *et al.*, 1986). Although most deep-water evaporites probably formed mainly by *in situ* precipitation, some appear to be turbidites. These evaporite turbidites are composed dominantly of gypsum or carbonate and gypsum, although rare halite turbidites have also been reported. Evaporite turbidites occupy the deepest portions of ancient evaporite basins. They apparently formed by rapid precipitation in the shallow areas of evaporite basins, resulting in unstable marginal accumulations that were subsequently redeposited downslope by turbidity currents.

Shallow-water vs. deep-water evaporites

As mentioned, most ancient evaporite deposits appear to have accumulated in platform or basin-wide settings that extended for tens to hundreds of kilometers. Basinwide evaporites are thick, and they contain textural evidence indicating deposition in a variety of environments ranging from deep-water to platform to continental. Some textural and structural differences in continental, coastal-sabkha, and subaqueous evaporites are illustrated in Fig. 12.8. These textural criteria should be used with caution, however, because similar kinds of features can form in different environments. For example, nodular anhydrites have been observed in many modern coastal sabkhas; therefore, many geologists assume that nodular anhydrites found in ancient evaporite deposits also signify deposition under sub-aerial, sabkha conditions. Dean *et al.* (1975) point out, however, that nodular anhydrites and laminated anhydrites, which both form in standing water, occur together in some environments. This association is taken to mean that nodular anhydrites can also form in deeper-water environments. Apparently, all that is needed for formation of nodular anhydrite is growth of crystals in mud in contact with highly saline brines, which can occur in deep or shallow standing water as well as in a sabkha environment. Also, note from Fig. 12.8 that laminated evaporites can form in both shallow and deep water.

Kendall (1984) suggests that ancient basins containing thick sequences of bedded evaporites are of three subtypes (Fig. 12.9). The **deep-water, deep-basin model** for ancient basin evaporites assumes existence of a deep basin separated from the open ocean by some type of sill. The sill acts as a barrier to prevent free interchange of water in the basin with the open ocean but allows enough water into the basin to replenish that lost by evaporation. Seaward escape of some brine allows a particular concentration of brine to be maintained for a long time, leading to thick deposits of certain evaporite minerals such as gypsum. The **shallow-water, shallow-basin model** assumes concentration of brines in a shallow, silled basin but allows for accumulation of great thicknesses of evaporites owing to continued subsidence of the floor of the basin. The **shallow-water, deep-basin model** requires that the brine level in the basin be reduced below the level of the sill, a process called **evaporative drawdown**, with recharge of water from the open ocean taking place only by seepage through the sill or by periodic overflow of the sill. Total desiccation of the floors of such basins could presumably occur periodically, allowing the evaporative process to go to



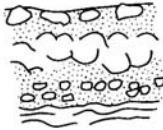





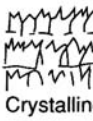

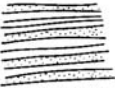



CONTINENTAL	Subaerial and lacustrine	SULFATE		SALT	
			Continental sabkha		PLAYA LAKE and COASTAL POND (as in subaqueous)
COASTAL SABKHA	Vadose and shallow phreatic			Displacive halite	
SUBAQUEOUS	Shallow	Increasing turbulence →			
			Laminated		Cross-laminated and rippled
	Shelf		Crystalline with carbonate		Wavy, anastomosing beds
		Crystalline			
Deep		mm-laminated		Debris flows	
				Turbidites	

Figure 12.8 Summary of evaporite textures and structures characteristic of major evaporite environments. [After Kendall, A.C., 1984, Evaporites, in Walker, R.G. (ed.), *Facies Models: Geoscience Canada Reprint Series 1*, Fig. 2, p. 261. Modified from Schreiber *et al.*, 1976, and subsequently modified by Warren, 1989. Reprinted by permission of Geological Association of Canada.]

completion, thereby depositing a complete evaporite sequence, including magnesium and potassium salts.

12.2.5 Diagenesis of evaporites

Evaporites are particularly prone to burial alteration and undergo a variety of diagenetic modifications that may include dehydration of gypsum and rehydration of anhydrite, dissolution, cementation, recrystallization, replacement, calcitization of sulfates owing to

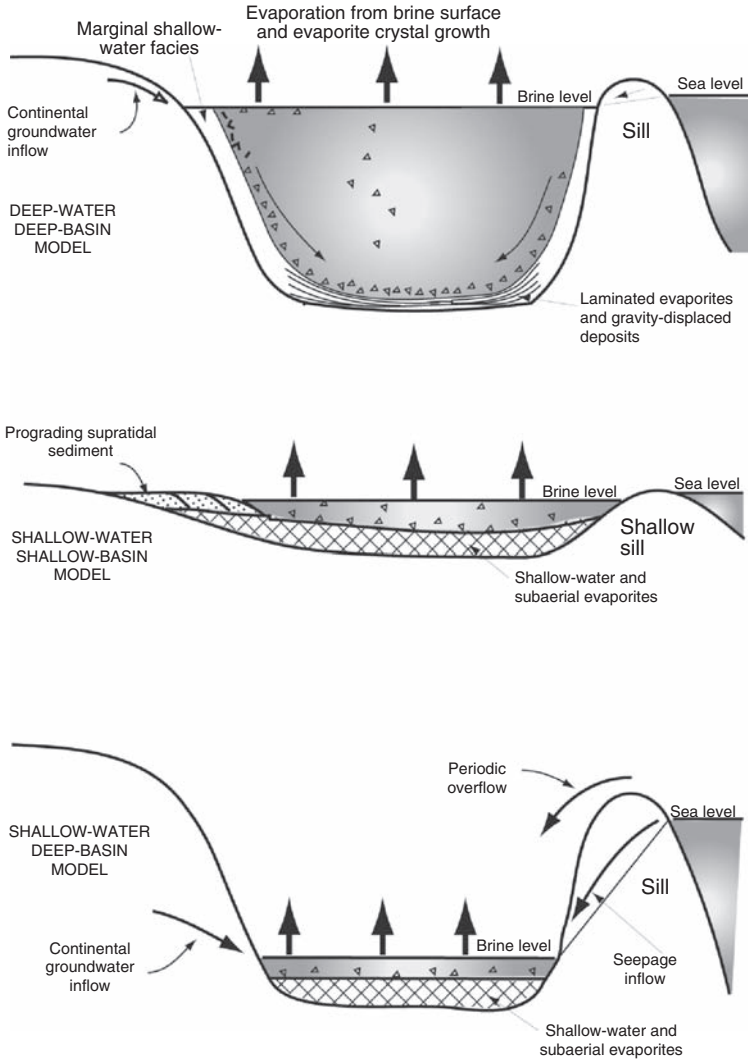


Figure 12.9 Schematic diagram illustrating three models for deposition of marine evaporites in basins where water circulation is restricted by the presence of a sill. [Modified from Kendall, A. C., 1979, Subaqueous evaporites, in R. G. Walker (ed.), *Facies Models: Geoscience Canada Reprint Series 1*, Fig. 17, p. 170, reprinted by permission of the Geological Association of Canada.]

bacterial processes, and deformation (Hardie, 1984; Schreiber, 1988b; Warren, 2006, p. 38, 85). The conversion of gypsum to anhydrite and back again is particularly important. With burial, gypsum is transformed to anhydrite at temperatures above 60°C, with a volume loss in water of about 38 percent. Exhumation of buried anhydrite results in rehydration with accompanying increase in volume. These volume changes and

hydration and rehydration reactions account for a considerable amount of the deformation in evaporites (development of nodules, enterolithic structures, etc.), as discussed. Owing to their low yield strengths, evaporites respond to burial and tectonic pressures by plastic deformation. Deformation may take place as a result of pressure solution, the formation of spaced cleavage, or by folding and diapirism (Schreiber, 1988b). The scale of deformation can range from millimeter-scale pygmatic folds to kilometer-scale salt diapirs.

Although considerable diagenesis of evaporite deposits may take place at moderate burial depths, some diagenetic changes can occur very early during diagenesis and at very shallow depths. For example, Casas and Lowenstein (1989) report that dissolution and cementation reactions in some modern California and Mexico saline-pan halites are essentially complete within the first 45 m of burial. Also, Hussain and Warren (1989) describe the early diagenetic formation of nodular and enterolithic gypsum in the vadose zone (unsaturated groundwater zone above the water table) in playa deposits of west Texas. Diagenetic processes include: dissolution and replacement of gypsum by halite or dolomite at depths of only 1–2 m; early-diagenetic enlargement and coalescence of gypsum crystals to create nodules within laminated host sediment; diffuse growth of nodules in the lower vadose zone to create chickenwire textures; and growth of gypsum in the upper vadose zone to form enterolithic bands.

12.2.6 Ancient evaporite deposits

As mentioned, evaporite deposits are common in the rock record and are particularly abundant in stratigraphic sequences of Late Cambrian, Permian, Jurassic, and Miocene ages. As also mentioned, most ancient evaporites appear to be of marine origin. They accumulated on a vertical and lateral scale far exceeding anything known in modern evaporite deposits. Many of these extensive platform and basin-wide ancient evaporite sequences have been intensively studied in sediment cores and in mine exposures. Particularly well-studied examples of ancient basinal evaporites include the Miocene Messinian of the Mediterranean region exceeding 2 km in thickness, the Permian Zechstein of the North Sea area also exceeding 2 km in thickness, Upper Silurian evaporites in the Michigan Basin (USA) exceeding 600 m in thickness, and evaporite deposits of the Permian Delaware Basin of west Texas and New Mexico that exceed 1 km in thickness. Evaporite deposits of the Delaware Basin are especially characterized by their striking lateral continuity.

Although not as common and abundant as marine evaporites, ancient nonmarine evaporites are also recognized. Putative ancient sabkha evaporites have been reported from many formations, including the Permian San Andreas Formation of west Texas, the Permian Lower Clear Fork Formation in the Palo Duro Basin of the Texas Panhandle, the Ordovician Red River Formation in the Williston Basin along the USA–Canadian border, the Permian Upper Minnelusa Formation in Wyoming, and formations in rift basins such as those of the East African and Baikal rifts. The literature on ancient evaporite deposits is voluminous. Readers who wish more information about ancient evaporites should consult

the list of additional readings at the end of this chapter. These books contain extensive lists of references to published articles on evaporites.

12.3 Siliceous sedimentary rocks (cherts)

12.3.1 Introduction

Siliceous sedimentary rocks are fine-grained, dense, commonly very hard rocks composed dominantly of the SiO_2 minerals quartz, chalcedony, and opal. Most siliceous rocks also contain minor amounts of impurities such as clay minerals, hematite, calcite, dolomite, and organic matter. **Chert** is the general group name used for siliceous sedimentary rocks. Cherts are common but not abundant rocks in the geologic record. Overall, they probably make up less than 1 percent of all sedimentary rocks, but they are represented in stratigraphic sequences ranging in age from Precambrian to Quaternary. Also, they are forming today as siliceous oozes in some parts of the modern ocean. Most ancient chert occurs as bedded deposits in association with generally deep-water sediments such as pelagic shales and turbidites. Bedded cherts are common in ophiolite and subduction complexes, and many bedded chert sequences are quite thick. Chert occurs also as nodules and stringers in shallow-water limestones of all ages, where it forms diagenetically as a replacement for carbonate minerals. Rare shallow-water bedded cherts have also been reported (e.g. Ledesma-Vázquez *et al.*, 1997). Rocks such as shales that are highly cemented with silica are also a kind of siliceous sedimentary rock; however, these rocks are not considered in this discussion.

In this section, we examine the mineralogy and chemical composition of cherts, briefly discuss the principal kinds of cherts, and consider some of the problems involved in their origin. The origin and common occurrence of bedded cherts in ancient subduction complexes is of great interest to geologists concerned with aspects of Earth history such as paleogeography, paleoceanographic circulation patterns, and plate tectonics. Siliceous rocks also have some economic significance. Silicon is used in the semiconductor and computer industries, and it is used also for making glass and related products such as fire bricks. Furthermore, siliceous deposits occur in association with important economic deposits of other minerals, including Precambrian iron ores, uranium deposits, manganese deposits, and phosphorite deposits. Many petroleum deposits also occur in association with siliceous rocks, which may be source rocks and possibly even reservoir rocks for petroleum. Developing a better understanding of the origin of chert may help to understand the origin of these other, economically significant, deposits.

12.3.2 Mineralogy and texture

Quartz is the primary mineral of siliceous deposits; however, other SiO_2 minerals in these deposits can include chalcedonic quartz, amorphous silica (opal-A), and disordered cristobalite and tridymite (opal-CT). Opal-CT is low-temperature cristobalite disordered by interlayered tridymite lattices (terminology of Jones and Segnit, 1971). As indicated, we

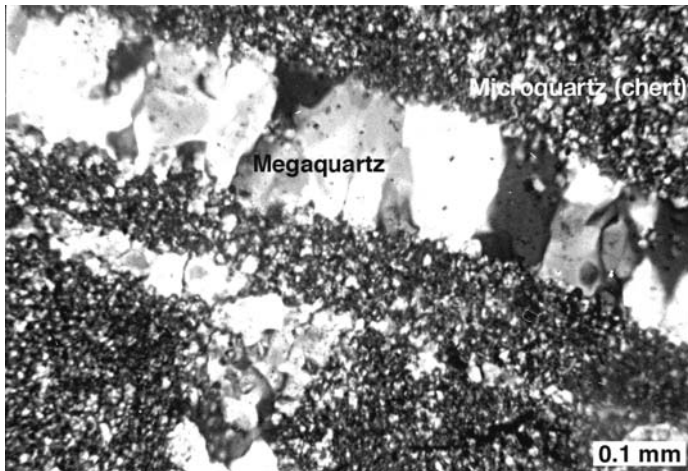


Figure 12.10 Fine-textured, nearly equigranular microquartz (chert) cut by a vein of much coarser megaquartz. Source of specimen unknown. Cross-polarized light.

commonly use the group name chert to cover all rocks formed of these minerals. Opal-A is primarily of biogenic origin and forms the tests of siliceous plankton and the spines of some sponges. Skeletal opal-A is metastable and converts in time to opal-CT and finally quartz. Nonetheless, unaltered opal-A organic remains are present in some cherts, particularly those of Cenozoic age, suggesting a biogenic origin for these cherts. All gradations may be present in chert deposits – from pure opal to pure quartz chert, depending upon the age of the deposits and the conditions of burial.

Texturally, the quartz that forms cherts can be divided into three main types: (1) **microquartz**, consisting of nearly equidimensional grains of quartz less than about 20 microns in size (Fig. 12.10), (2) **megaquartz**, composed of equant to elongated grains greater than 20 microns (Fig. 12.10), and (3) **chalcedonic quartz**, forming sheaflike bundles of radiating, thin crystals about 0.1 mm long (Fig. 12.11; Folk, 1974). In most chalcedonic quartz, the elongated fibers have negative elongation, with the *c*-axis being perpendicular to the length of the fibers, and the crystals are said to be length-fast. In some chalcedony, however, the *c*-axes are parallel to the fibers and the chalcedony is thus length-slow. Folk and Pittman (1971) found a strong correlation between length-slow chalcedony and the presence of evaporites or former evaporites. The chalcedony can occur as pseudomorphs of gypsum and anhydrite or in nodules that closely resemble the chickenwire structure of nodular evaporites. Folk and Pittman point out, however, that not all chalcedony in evaporites is length-slow and note also that some length-slow chalcedony has been found in basic igneous rocks. Therefore, length-slow chalcedony is not an infallible indicator of vanished evaporites. Hattori (1989) reports length-slow chalcedony from the Mino Terrane in Japan. In this terrane, it occurs as vein minerals or replaces carbonates that Hattori interprets to have formed in an evaporative environment. Hattori cautions, however, that length-slow

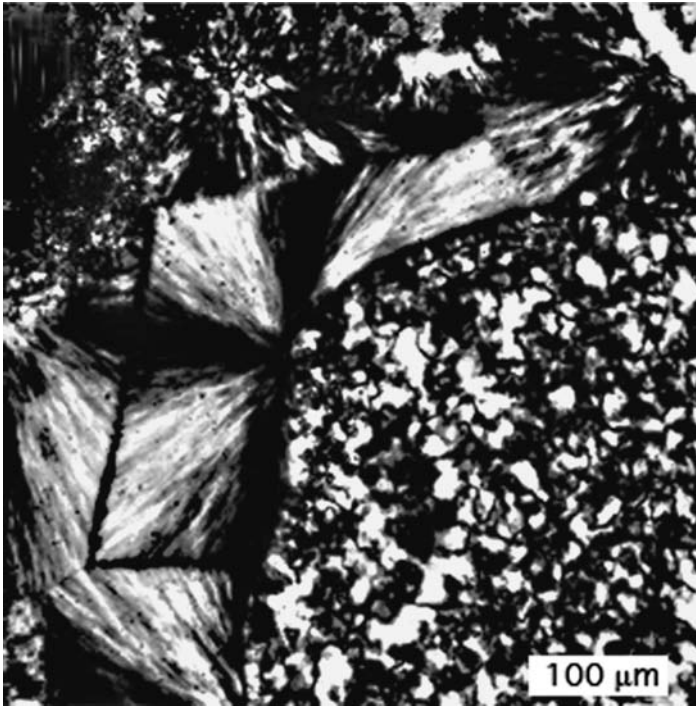


Figure 12.11 Sperulitic (radial-fibrous) chalcedony cement (lower left corner) and microquartz (lower right corner) in a chert deposit from the Gunflint Formation (Precambrian), Ontario, Canada. Cross-polarized light. (From Maliva, R.G., A.H. Knoll, and B.M. Simonson, 2005, Secular changes in the Precambrian silica cycle: Insights from chert petrology: *Geol. Soc. Am. Bull.*, 117, Fig. 4D, p. 840, reproduced by permission.)

chalcedony can be confused in thin section with length-slow colorless chlorite or flamboyant quartz. He recommends that it be identified by determining the chemical composition, crystal structure, and fibrous nature by electron microprobe, X-ray diffraction, and scanning electron microscope, respectively.

As mentioned, many cherts contain recognizable remains of siliceous organisms, including radiolarians, diatoms, silicoflagellates, and sponge spicules (e.g. Fig. 12.12). Some cherts contain no preserved remains of siliceous organisms, but may contain constituents such as detrital clays and other siliciclastic minerals, pyroclastic particles, and organic matter. They may also contain authigenic minerals such as silica cement, clay minerals, hematite, pyrite, and magnetite.

12.3.3 Chemical composition

Cherts are composed dominantly of SiO_2 but can include minor amounts of Al, Fe, Mn, Ca, Na, K, Mg, Ni, Cu, Ti, Sr, and Ba. The amount of SiO_2 varies markedly in different types of

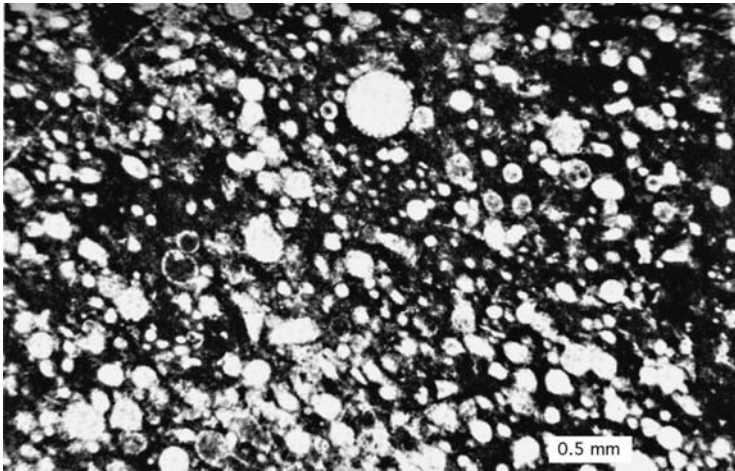


Figure 12.12. Photomicrograph showing moderately well-preserved radiolarians in chert from the Otter Point Formation (Jurassic), Oregon. Plane-polarized light. (Photograph courtesy of Robert Lent.)

cherts, ranging from more than 99 percent in very pure cherts such as the Arkansas Novaculite (Cressman, 1962) to less than 65 percent in some nodular cherts. Aluminum is commonly the second-most abundant element in cherts, followed by Fe, Mg or K, Ca and Na. Cherts may also contain trace amounts of rare-earth elements such as cerium (Ce) and europium (Eu).

Jones and Murchey (1986) suggest that the chemical elements in cherts are derived from four possible sources: biogenic, detrital, hydrogenous (precipitated or absorbed from seawater), and hydrothermal. Siliceous organisms furnish the major source of Si, and Ca may be derived in part from calcareous organisms. Detrital impurities furnish additional Si, as well as Al, Ti, Ca, Mg, K, and Na. In areas of high volcanic activity such as backarc basins and seamounts, significant amounts of K and Mg may be furnished in detrital components (Hein *et al.*, 1983). The hydrogenous elements may include Fe, Mn, Ni, and Cu. Elements that may be contributed from hydrothermal fluids in areas of high heat flow such as oceanic spreading centers include Fe, Mn, and Ba.

12.3.4 Principal kinds of cherts

Varieties of chert

Although chert is the general group name for siliceous sedimentary rocks composed dominantly of SiO_2 minerals, several names are applied to various varieties of chert. **Flint** is used both as a synonym for chert and as a varietal name for chert, particularly chert that occurs as nodules in Cretaceous chalks. **Jasper** is a variety of chert colored red by impurities of disseminated hematite. Jasper that is interbedded with hematite in Precambrian iron formations is called **jaspilite**. **Novaculite** is a very dense, fine-grained, even-textured chert that occurs mainly in mid-Paleozoic rocks of the Arkansas, Oklahoma, Texas region of south central United States.

Porcellanite is a term used for fine-grained siliceous rocks with a texture and fracture resembling that of unglazed porcelain. The term is often used by chert workers for cherts having this character that are composed mainly of opal-CT. **Siliceous sinter** is porous, low-density, light-colored siliceous rock deposited by waters of hot springs and geysers. Although most siliceous rocks consist dominantly of chert, some have a high content of detrital clays or micrite. These impure cherts grade compositionally into siliceous shales or siliceous limestones.

Bedded vs. nodular chert

General statement

Cherts can be divided on the basis of gross morphology into bedded cherts and nodular cherts. Most bedded cherts are further distinguished by their content of siliceous organisms of various kinds. Mineralogy is not used as a basis for classifying cherts because these rocks are all composed mainly of SiO₂ minerals. The principal distinguishing characteristics of bedded and nodular cherts are described below.

Bedded chert

Bedded chert consists of layers of nearly pure chert, ranging to several centimeters in thickness, that are commonly interbedded with millimeter-thick partings or laminae of siliceous shale (Fig. 12.13). Bedding may be even and uniform or may show pinching and swelling. These rhythmically bedded deposits are also referred to as **ribbon cherts**. Many chert beds lack internal sedimentary structures; however, graded bedding, cross-bedding, ripple marks, sole markings, convolute layers, and soft-sediment folds have been reported in some cherts. The presence of these structures indicates that mechanical transport was involved in the deposition of these rocks, quite possibly transport by turbidity currents. Bedded cherts are commonly associated with ophiolitic rocks such as submarine volcanic flows or pillowed greenstones, tuffs, pelagic limestones, shales or argillites, and siliciclastic or carbonate turbidites. As indicated, many bedded cherts are composed dominantly of the remains of siliceous organisms, which are commonly altered to various degrees by solution and recrystallization. Bedded cherts can be subdivided on the basis of type and abundance of siliceous organic constituents into four principal types:

1. **Diatomaceous deposits** include both diatomites and diatomaceous cherts. **Diatomites** are light-colored, soft, friable siliceous rocks composed chiefly of the opaline frustules of diatoms, a unicellular aquatic plant related to the algae. Thus, they are fossil diatomaceous oozes. Diatomites of both marine and lacustrine origin are recognized. Marine diatomites are commonly associated with sandstones, volcanic tuffs, mudstones or clay shales, impure limestones (marls), and, less commonly, gypsum. Lacustrine diatomites are almost invariably associated with volcanic rocks. **Diatomaceous chert** consists of beds and lenses of diatomite that have well-developed silica cement or groundmass that has converted the diatomite into dense, hard chert. Beds of diatomaceous chert comprising strata several hundred meters in thickness have been reported from some sedimentary sequences such as the Miocene Monterey Formation of California (Garrison *et al.*, 1981), which may reach a thickness in some areas of as much as 2000 m. Marine diatomaceous deposits occur in rocks as old as the Cretaceous, and nonmarine deposits are reported from rocks as old as the Eocene (Barron, 1987).



Figure 12.13 Thin, well-bedded cherts in the Mino Belt Group (Triassic), near Inuyama, Honshu, Japan.

Note that these so-called diatomaceous cherts or diatom cherts are composed of diatoms cemented by silica and that the diatoms still consist mainly of opal-A. When diatomaceous deposits are converted to quartz chert during diagenesis (discussed below), the diatoms commonly do not survive. Therefore, quartz cherts containing recognizable diatoms are rare. Hein *et al.* (1990) reported the first known example of such chert from Eocene deposits on Adak Island, Alaska. They propose that diatoms were preserved in this quartz chert because early and rapid alteration of ubiquitous volcanic glass in the section released silica and saturated the pore waters with respect to opal-A.

2. **Radiolarian deposits** consist dominantly of the remains of radiolarians, which are marine planktonic protozoans with a latticelike skeletal framework. Radiolarian deposits can be divided into radiolarite and radiolarian chert. **Radiolarite** is the comparatively hard, fine-grained, chertlike equivalent of radiolarian ooze, that is, indurated radiolarian ooze. **Radiolarian chert** is well-bedded, microcrystalline radiolarite that has a well-developed siliceous cement or groundmass. Because radiolarians are more robust and contain less surface area than diatoms, radiolarians tend to survive silica diagenesis. Therefore, they are common components of many bedded quartz cherts (Hein *et al.*, 1990). Radiolarian cherts are commonly associated with tuffs, mafic volcanic rocks such as pillow basalts, pelagic limestones, and turbidite sandstones that are believed to indicate a deep-water origin. On the other hand, some radiolarian cherts are associated with micritic limestones and other rocks that suggest deposition at shallower depths of perhaps 200–1000 m (Iijima *et al.*, 1979).
3. **Siliceous spicule deposits** include spicularite (spiculite), a siliceous rock composed principally of the siliceous spicules of invertebrate organisms, particularly sponges. Spicularite is loosely cemented in contrast to spicular chert, which is hard and dense. Spicular cherts are mainly marine in

origin and occur associated with glauconitic sandstones, black shales, dolomite, argillaceous limestones, and phosphorites. They are not generally associated with volcanic rocks and are probably deposited mainly in relatively shallow water a few hundred meters deep.

4. **Bedded cherts containing few or no siliceous skeletal remains** have been described by many authors. Some of these reported occurrences of barren cherts may simply be the result of inadequate microscopic examination of the cherts, which might be found upon closer examination to contain siliceous organisms. Others have been examined closely and clearly contain few siliceous organisms. Cherts in this latter group include most cherts associated with the Precambrian iron-formations, as well as many Phanerozoic-age cherts such as the Mississippian-Devonian-age Arkansas Novaculite of Arkansas and Oklahoma and the Caballos Novaculite of Texas. Except for the absence of skeletal remains, these cherts resemble radiolarian cherts both megascopically and in their lithologic associations (Cressman, 1962). Some of these cherts are probably radiolarian cherts that have undergone such severe diagenesis that no recognizable radiolarians remain. Others, particularly Precambrian cherts, may have some other origin. For example, cherts in the Precambrian Barberton Greenschist Belt of South Africa formed by silicification (replacement) of volcanic rocks, biogenic sediments, and evaporites (Lowe, 1999).

Nodular cherts

Nodular cherts are subspheroidal masses, lenses, or irregular layers or bodies that range in size from a few centimeters to several tens of centimeters (Fig. 12.14). They commonly lack internal structures, but some nodular cherts contain silicified fossils or relict structures such as bedding. Colors of these cherts range from green to tan and black. They typically occur in shelf-type carbonate rocks where they tend to be concentrated along certain horizons parallel to bedding. More rarely, they occur in sandstones and mudrocks, lacustrine sediments, and evaporites. They have also been encountered in cores of deep-sea sediment

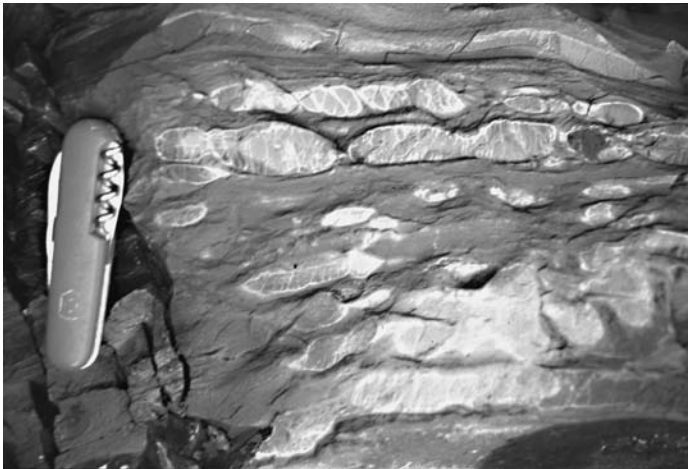


Figure 12.14 Nodular chert in limestones of the Helena Formation (Precambrian), Glacier National Park, Montana. (From Boggs, S., Jr., 2006, *Principles of Sedimentology and Stratigraphy*, 4th edn.: Prentice-Hall, Upper Saddle River, NJ, Fig. 7.11, p. 210, reproduced by permission.)

recovered during Deep Sea Drilling Project (DSDP) and Ocean Drilling Program (ODP) coring in the open ocean. Nodular cherts originate mainly by diagenetic replacement. In carbonate rocks, nodular chert can replace micrite as well as fossils and other carbonate grains; such chert occurs in both limestones and dolomites. Diagenetic origin is clearly demonstrated in many nodules by the presence of partly or wholly silicified remains of calcareous fossils or ooids, burrow fillings, algal structures, etc. (e.g. Gao and Land, 1991). Nodular cherts can also replace anhydrite, pelagic clays, and, rarely, sandstones. See Maliva and Siever (1989a) for discussion of the mechanisms by which nodular cherts form.

12.3.5 Deposition of chert

Silica solubility

The solubility of solid SiO_2 at 25 °C in distilled water is ~11 ppm for quartz and ~116 ppm for amorphous or noncrystalline varieties of silica such as opal (Rimstidt, 1997; Gunnarsson and Arnórsson, 2000). Silica solubility is affected particularly by temperature. Solubility increases markedly with increasing temperature; solubility at 100 °C is approximately three times that at 25 °C (Fig. 12.15). Solubility is also affected by pH. Although solubility

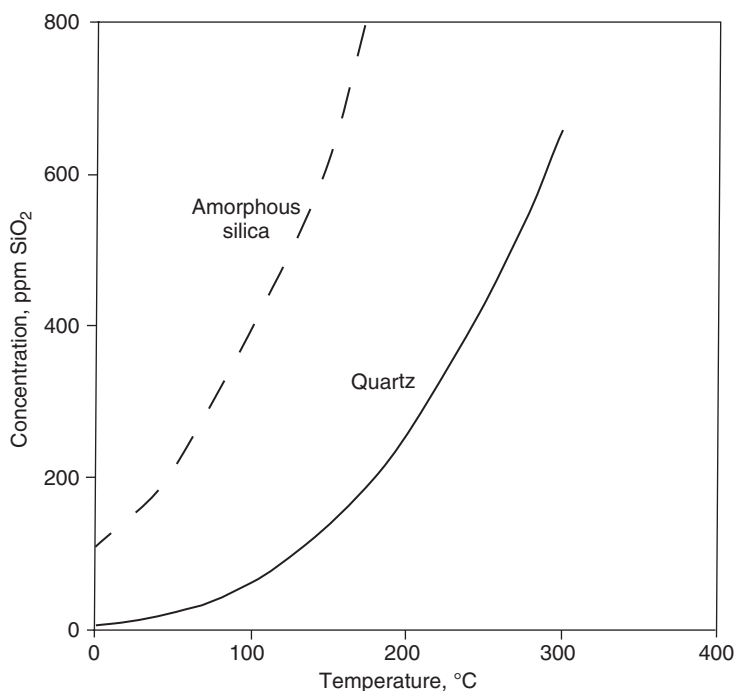


Figure 12.15 Graph showing the solubility of quartz and amorphous silica in water as a function of temperature. The quartz curve is from Rimstidt (1997) and is based on values determined experimentally by Rimstidt plus values reported in the literature. The amorphous silica curve is drawn from data in Gunnarsson and Arnórsson (2000)

changes very little with increase in pH up to about pH 9, it rises sharply at pH values above 9 (e.g. Dove and Rimstidt, 1994; Walther, 2005, p. 205).

Silica concentrations in seawater

Silica is transported in riverwater to the modern ocean as silicic acid (H_4SiO_4) in concentrations averaging about 13 ppm SiO_2 . In addition, silica is added to the oceans through reaction of seawater with hot volcanic rocks along midocean ridges and by low-temperature alteration of oceanic basalts and detrital silicate particles on the seafloor. Some silica may also escape from silica-enriched pore waters of pelagic sediments on the seafloor. These silica sources are summarized in Fig. 12.16. Despite contributions of silica from these various sources, the silica concentration in seawater is quite low. Surface waters are particularly depleted in silica (commonly <0.01 ppm SiO_2). Silica concentration increases downward in the ocean to a maximum of about 11 ppm below a depth of about 2 km. The average dissolved silica content of the ocean is only 1 ppm (Heath, 1974). The variations in silica concentration with depth reflect uptake of silica near the surface by phytoplankton and regeneration of silica at depth owing to dissolution of the silicon tests of phytoplankton.

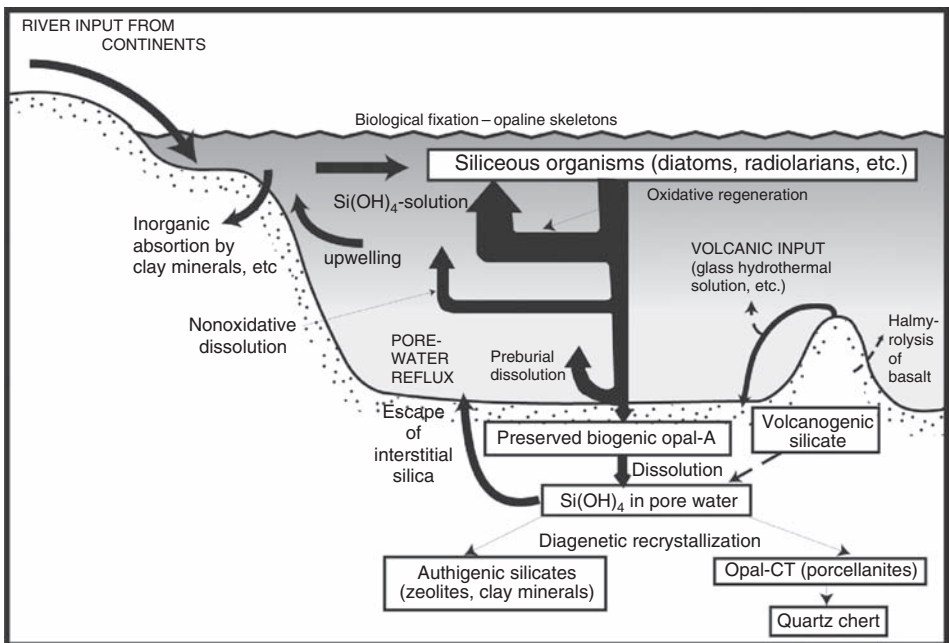


Figure 12.16 Sources of dissolved silica in seawater. {After Riech, V. and U. von Rad, 1979, Silica diagenesis in the Atlantic Ocean: Diagenetic potential and transformations, in Talwani M., W. Hay, and W.B.F. Ryan (eds.), *Deep Drilling Results in the Atlantic Ocean: Continental Margins and Paleoenvironment*: American Geophysical Union, Maurice Ewing Series 3, Fig. 2, p. 322, modified from Heath, G. R., 1974, Dissolved silica and deep-sea sediments, in Hay, W. W. (ed.), *Studies in Paleo-Oceanography*: SEPM Special Publication 20, Fig. 7, p. 81, reprinted by permission of SEPM, Tulsa, OK.)

The difference between the average silica content of rivers and that of modern seawater thus reflects biogenic removal of silica to construct skeletal tests of diatoms, radiolarians, and other siliceous organisms. Most of the silica in these tests redissolves upon the death of the organisms; however, a small amount (perhaps 1–10 percent) reaches the bottom sediments (Calvert, 1974).

Precipitation of chert from seawater

Biogenic removal of silica

Seawater in the modern ocean, with an average dissolved silica content of only 1 ppm, is grossly undersaturated with respect to silica. Once silica is in solution under a given set of temperature and pH conditions, it does not appear to crystallize readily to form quartz even from solutions that have silica concentrations exceeding the solubility of quartz (~11 ppm at 25 °C). Therefore, it is unlikely that chalcedony or microquartz (chert) can be precipitated directly by inorganic processes from highly undersaturated ocean water. Microcrystalline quartz might be precipitated in some local basins where waters are saturated with silica, owing perhaps to dissolution of volcanic ash. Some silica may be removed from seawater in the open ocean by adsorption onto clay minerals or other silicate particles (Heath, 1974); however, such processes cannot account for the many bedded sequences of nearly pure chert that occur in the geologic record.

Removal of silica from ocean water by silica-secreting organisms to build opaline skeletal structures appears to be the only mechanism capable of large-scale silica extraction from undersaturated seawater. This biologic process has operated since at least early Paleozoic time to regulate the balance of silica in the ocean. **Radiolarians** (Cambrian/Ordovician–Holocene), **diatoms** (Jurassic?–Holocene), and **silicoflagellates** (Cretaceous–Holocene) are microplankton that build skeletons of opaline silica. These siliceous microplankton have apparently been abundant enough in the ocean during Phanerozoic time to extract most of the silica delivered to the oceans by rock weathering, etc. Diatoms are probably responsible for the bulk of silica extraction from ocean waters in the modern ocean (Calvert, 1983); however, radiolarians were the most important silica-secreting organisms in the Phanerozoic oceans of Jurassic and older age. Heath (1974) calculates that the residence time for dissolved silica in the ocean ranges from 200 to 300 years for biologic utilization to 11,000–16,000 years for incorporation into the geologic record – a very short time from a geologic point of view.

While silica-secreting organisms are alive, their siliceous skeletons are protected by an organic coating that prevents them from dissolving in highly undersaturated and corrosive seawater. After death, this coating is destroyed by biochemical decomposition and the opaline skeletons began to undergo dissolution. In areas of the ocean where siliceous organisms flourish (zones of upwelling), the rate of production of siliceous skeletons may be so high that they cannot all be dissolved as rapidly as they are produced. Under such conditions, a sufficient number of the siliceous skeletons may survive total dissolution to accumulate on the seafloor as siliceous oozes (sediments containing more than about two-thirds siliceous skeletal material). After burial by additional siliceous ooze or clayey

sediment, these opaline skeletal materials continue to undergo solution; however, the dissolving silica is trapped in the pore spaces of the sediment and cannot all escape back to the open ocean. The pore waters thus become increasingly enriched in silica. Silica concentrations exceeding 120 ppm are reported in pore fluids extracted from some deep-sea cores recovered at some DSDP sites (e.g. Gieskes, 1983). Such pore waters are saturated to supersaturated with respect to silica, and cherts are thought to precipitate slowly from these concentrated interstitial solutions. Thus, the formation of cherts is in part a sedimentation process involving the depositional concentration of biogenic opaline tests and in part a diagenetic process with crystallization, and recrystallization, of the chert taking place after sediment burial.

The formation of quartz cherts from the remains of siliceous organisms composed of opal-A is a solution–reprecipitation process. The process is illustrated diagrammatically in Fig. 12.17. Biogenic opal-A typically does not convert directly to quartz chert. Instead, it commonly goes through an intermediate phase in which metastable opal-CT precipitates from pore waters that are saturated with silica owing to dissolution of opal-A. Skeletal opal-A first dissolves to yield solutions high in silica. The silica then flocculates to yield opal-CT. In turn, opal-CT is converted into microquartz also by solution–reprecipitation. Finally, microquartz is transformed to megaquartz as burial temperatures approach those of metamorphism. Megaquartz, as well as fibrous quartz, can also form at lower temperatures in small amounts as cavity and fracture fillings.

Opal-CT may occur in open spaces in sediments as **lepispheres**, which are 5–20 micron spherulitic aggregates of blade-shaped crystals (Wise and Kelts, 1972). It can occur also as nonspherulitic blades, as rim cements and overgrowths, and as a massive cement (Maliva and Siever, 1988b). As mentioned, chert composed of opal-CT is referred to by many silica workers as porcellanite.

The rates of diagenetic evolution of silica from biogenic opal-A to opal-CT and finally to quartz chert are controlled by several physico-chemical factors. Temperature is commonly considered to be a particularly important control, with increasing temperature promoting an increased rate of transformation. Siever (1983) stresses the importance of temperature and sedimentation rates on silica diagenesis. He suggests that the conversion process can require a few millions of years to tens of millions of years, depending upon conditions. Faster rates of transformation occur where rates of sedimentation and burial are high because sediment is quickly buried to depths where high temperatures bring about rapid transformation. Much longer time is required for transformation of opal-A to opal-CT under conditions of slow sedimentation and a low geothermal gradient than under conditions of rapid sedimentation and a high geothermal gradient.

Kastner and Gieskes (1983) have demonstrated that the rate of transformation of opal-A to quartz also depends upon the nature of the opal starting material and the presence of magnesium hydroxide compounds, which serve as a nucleus for the crystallization of opal-CT. Williams *et al.* (1985) conclude that increasing surface-to-volume ratio of siliceous particles – a ratio that increases with decreasing particle size – results in greater solubility of opal and an increase in the rate of transformation. These authors also suggest that under

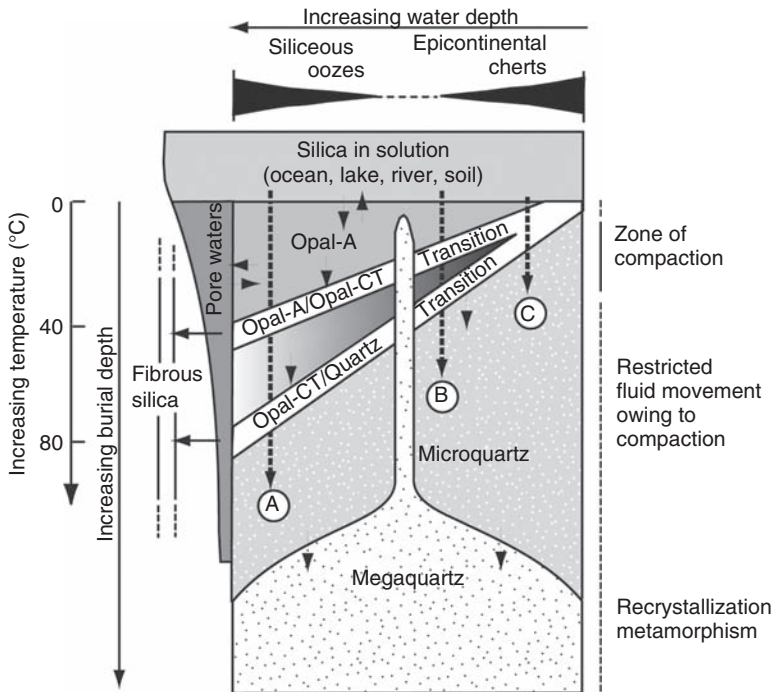


Figure 12.17 Schematic diagram showing major silica phases and their possible diagenetic transformations. Vertical dimension represents qualitative burial depth with associated increase in temperature and loss of porosity and permeability. Horizontal dimension represents qualitative water depth of the initial environment. In general, deep-sea siliceous oozes lie to the left of the diagram, whereas epicontinental deposits lie toward the right. Diagenetic path A represents silica initially deposited as opal-A (diatoms, radiolarians), which subsequently transforms to opal-CT and then microquartz by means of solution–reprecipitation steps. Path C represents early diagenetic cherts in which microquartz forms during shallow burial. B represents a possible pathway for chert formation under conditions intermediate between A and C. Megaquartz forms by metamorphic recrystallization of microquartz or by direct growth into voids (suggested by the “spike”) at any stage of burial. Fibrous silica can grow in vugs and fractures at all burial depths. (After Knauth, L. P., 1994, *Petrogenesis of chert*, in Heaney, P. J., C. T. Prewitt, and G. V. Gibbs (eds.), *Silica: Physical Behavior, Geochemistry and Materials Applications*; Mineralogical Society of America Reviews in Mineralogy 29, Fig. 4, p. 239, reproduced by permission.)

some conditions opal-A can transform directly to quartz chert without going through the intermediate opal-CT stage (path C in Fig. 12.17).

According to Maliva *et al.* (2005), three major secular changes in chert deposition are recognized in the geologic record. One of these took place during Precambrian time (discussed below); two occurred during the Phanerozoic. The earliest Phanerozoic change occurred during Cambro-Ordovician time, when a transition from inorganic silica precipitation of the Precambrian to biologically dominated deposition of the Phanerozoic took place. Another major change took place in Late Cretaceous to Paleocene time when diatoms

shifted the main locus of silica deposition from the shallow shelf to deep shelf and oceanic environments.

Nonbiogenic cherts

The origin of bedded, ribbon cherts that contain no siliceous organic remains is poorly understood. Direct, inorganic precipitation of amorphous silica has been reported in some ephemeral Australian lakes (Peterson and von der Borch, 1965). Pleistocene cherts from alkaline Lake Magadi, Kenya, are also believed to form inorganically by early replacement of sodium silicate precursors – magadiite, $\text{NaSi}_7\text{O}_{13}(\text{OH})_3 \cdot 3\text{H}_2\text{O}$, and/or kenyaite, $\text{NaSi}_{11}\text{O}_{20} \cdot 5(\text{OH}) \cdot 3\text{H}_2\text{O}$ (Schubel and Simonson, 1990). Until recently, no similar occurrences have been reported in the open-marine environment that could help explain the presence of widespread nonfossiliferous chert deposits such as the Arkansas Novaculite. The scarcity of radiolarians and sponge spicules in the Arkansas Novaculite and similar Phanerozoic-age cherts does not, however, preclude the possibility that these cherts were formed by organisms. They could have been derived from siliceous oozes that were subsequently almost completely dissolved and recrystallized, leaving few or no recognizable siliceous organic remains (Weaver and Wise, 1974).

The origin of Precambrian bedded cherts is a particular problem. Siliceous organisms are not definitely known to have existed in Precambrian time. Scattered remnants of possible siliceous planktonic organisms have been reported from Precambrian cherts by some investigators (e.g. LaBerge, 1973); however, geologists disagree about the biogenic origin of these structures. More recently, LaBerge *et al.* (1987) reported the common presence of spheroids in many Precambrian cherts associated with iron-formations. One type is about 30 microns in diameter and has a double-wall structure (Fig. 12.18). LaBerge *et al.* believe that these structures may represent the remains of an organism that had a siliceous frustule. If these structures indeed represent the remains of siliceous organisms, the origin of Precambrian cherts takes on a new dimension. Until the existence of Precambrian siliceous organisms is definitely proven, however, we have to assume that Precambrian cherts were formed mainly by inorganic precipitation. The source of the silica that was required to saturate Precambrian ocean waters to the point of quartz precipitation is not definitely known.

It appears likely that concentration of silica in the Proterozoic (Precambrian) ocean was higher than that in the modern ocean. Higher concentrations may have been related to greater hydrothermal flux to the ocean or to high rates of chemical weathering on land (Maliva *et al.*, 2005). These authors suggest that cherts associated with Proterozoic iron-formations formed to a large degree by primary silica precipitation (as opposed to replacement of a carbonate or other mineral precursor) in marine peritidal to subtidal environments. Presumably, silica was precipitated by chemical (inorganic) processes, although bacteria may have played some role in precipitation (Maliva *et al.*, 1989).

On the other hand, some Precambrian cherts apparently formed by replacement of precursor sediments. For example, Lowe (1999) suggests that Precambrian cherts in the Swaziland Supergroup in the Barberton Greenschist Belt of South Africa formed by

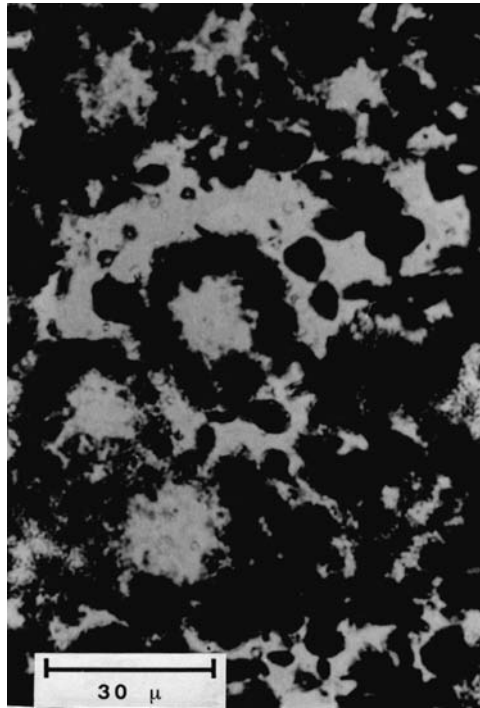


Figure 12.18 Spheroidal structures of problematical silica-secreting organisms in 3.5 billion-year-old iron-formations from the Pilbara region, western Australia. The structures are pigmented by submicrometer hematite dust. [From LaBerge, G. L., E. I. Robbins, and T.-M. Han, 1987, A model for the biological precipitation of Precambrian iron-formations, in Appel, P. W. V. and G. L. LaBerge (eds.), *Precambrian Iron-Formations*, Theophrastus Publications, Athens, Fig. 11C, p. 86, reprinted by permission.]

silicification (replacement) of volcanoclastic and pyroclastic deposits, terrigenous sandstones and shales, biogenic sediments (algal mats), and evaporites.

12.3.6 Replacement chert

In addition to its occurrence as bedded chert, chert can also occur in the form of small nodules, lenses, or thin, discontinuous beds (Fig. 12.14). Nodular cherts are especially common in carbonate rocks but occur also in evaporites and siliciclastic rocks. Relict textures in these nodular cherts suggest that most are formed by diagenetic replacement. For example, Hein and Karl (1983) suggest that open-ocean cherts recovered from DSDP cores formed by volume-for-volume replacement of carbonates (chalk) and clay, as shown by preservation of burrows and other sedimentary structures. Chert nodules and lenses nucleate among local concentrations of magnesium compounds (Kastner *et al.*, 1977), apparently because magnesium hydroxide nuclei aid in the formation of opal-CT lepispheres. The nodules grow until all the local biogenic silica in the host sediments is dissolved. Silica dissolved from opaline skeletal

grains is precipitated initially as opal-CT, which is converted to quartz chert with increasing time and temperature. Maliva and Siever (1988c) refer to this mechanism for forming deep-sea nodular cherts as a maturation process whereby chert evolves from originally dispersed biogenic opal-A through an intermediate stage to quartz porcellanite or chert. These cherts are typically characterized by quartz-replaced lepispheres, which provide good textural evidence for an opal-CT precursor. Hein and Karl (1983) stress that these open-ocean or deep-ocean replacement cherts are not analogous to bedded cherts or ribbon cherts (described above), which form in orogenic belts near continental margins.

Replacement cherts also occur in shallow, platform carbonate rocks. Knauth (1979) suggests that the mixing zone where meteoric groundwaters mix with seawater in a coastal area may be a particularly favorable geochemical environment for chert replacement of carbonates. Silica is supplied in this environment by the dissolution of sponge spicules or other forms of biogenic opal-A within the sediment pile and is then transported into the zone of mixing where replacement of CaCO_3 occurs. Presumably, opal-A is first transformed to opal-CT, which then replaces the carbonate and is later diagenetically altered to quartz chert.

Alternatively, the carbonate could be replaced directly by quartz. Maliva and Siever (1989b) report the presence of quartz-replaced lepispheres in several Mesozoic and Paleozoic nodular cherts in shelf limestone formations. They suggest that quartz-replaced lepispheres in these cherts indicate formation by a maturation process similar to that for deep-sea cherts. Nodular cherts formed by direct replacement of limestone by quartz are distinguished by absence of quartz-replaced lepispheres and a coarser (>10 microns) crystal size. The necessary geochemical conditions for replacement of carbonate by chert are discussed in [Chapter 11](#). Nodular cherts have also been reported to form by silica replacement of anhydrite, with the silica again being derived by dissolution of biogenic opal (Chowns and Elkins, 1974) and by selective replacement of carbonate grainstones, burrow fillings, and algal structures, as well as evaporite nodules (Gao and Land, 1991).

12.3.7 Ancient cherts

Bedded cherts or ribbon cherts occur in sedimentary sequences ranging in age from Precambrian to Neogene. Hein and Parrish (1987) provide a particularly useful compilation of bedded chert deposits from all parts of the world. In this compilation, they inventory a total of 306 chert deposits and indicate that this list is not completely comprehensive. Although bedded chert deposits occur in geologic systems of all ages, they are particularly abundant in Jurassic to Neogene rocks, moderately abundant in Devonian and Carboniferous rocks, and lowest in Silurian and Cambrian deposits ([Fig. 12.19](#)). Ancient chert deposits are also unevenly distributed with respect to paleolatitude. The greatest majority of them are concentrated between 0 and 30 degrees latitude ([Fig. 12.20](#)). This latitude range encompasses the equatorial–oceanic divergence and west-coast upwelling zones. Presumably, the greatest productivity of siliceous plankton took place in these zones of upwelling. Note from [Fig. 12.20](#), however, that the distribution by latitude is not uniform through time. Apparently, different paleoceanographic circulation patterns existed before the assembly of Pangaea, during Pangaea’s existence, and after its

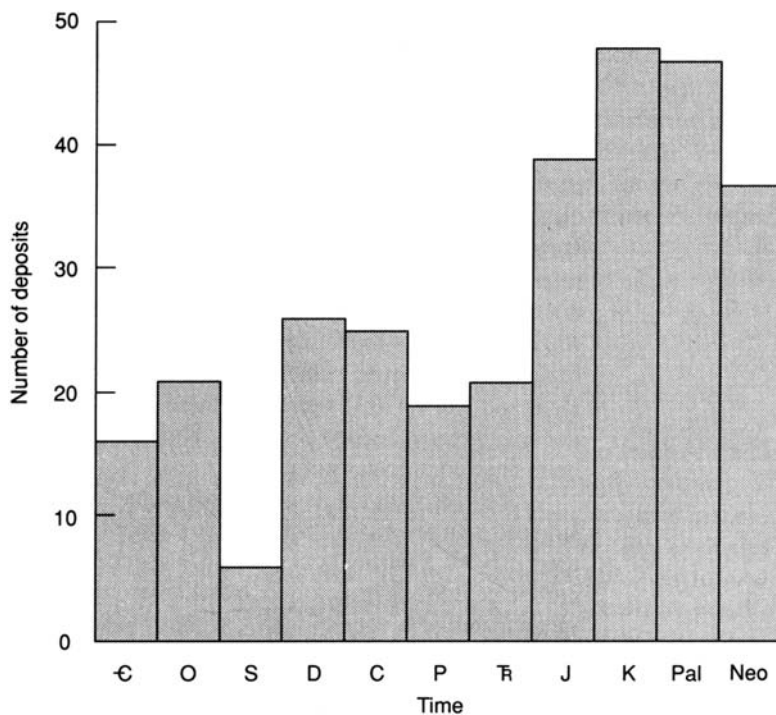


Figure 12.19 Distribution of chert through time. [After Hein, J. R. and J. T. Parrish, 1987, Distribution of siliceous deposits in space and time, in Hein, J. R. (ed.), *Siliceous Sedimentary Rock-Hosted Ores and Petroleum*, Fig. 2-1, p. 15. Copyright 1987 by Van Nostrand Reinhold. All rights reserved.]

breakup (Hein and Parrish, 1987). Because chert deposits are apparently related to paleoceanographic circulation patterns and zones of upwelling, there is considerable interest in chert deposits as clues to ancient ocean-circulation patterns.

Chert deposits are particularly common around the margins of the Pacific and in the Tethys region (the Alpine-Himalayan orogenic belt extending from the Caribbean region to the Indonesian region). Hein and Parrish's (1987) compilation of chert deposits indicates that the greatest number of chert deposits occur in the United States (about 22% of total deposits) and the Former Soviet Union (14 percent of total deposits). Chert deposits are moderately abundant in Japan, Canada, Malaysia, Mexico, Indonesia, and Australia. Cherts occur also in many other countries, including China, Great Britain, Peru, Chile, Antarctica, France, Italy, Greece, Spain, New Zealand, Central and South America, Turkey, the former Yugoslavia, Bulgaria, India, the Philippines, and Germany. *Siliceous Deposits in the Pacific Region*, edited by Iijima *et al.* (1983), and *Siliceous Deposits of the Tethys and Pacific Regions*, edited by Hein and Obradović (1989), are useful publications that describe many of the chert deposits of these regions.

The ancient chert deposits inventoried by Hein and Parrish (1987) include many examples of diatomites, radiolarites, radiolarian cherts, and some spiculites. Also included are cherts that

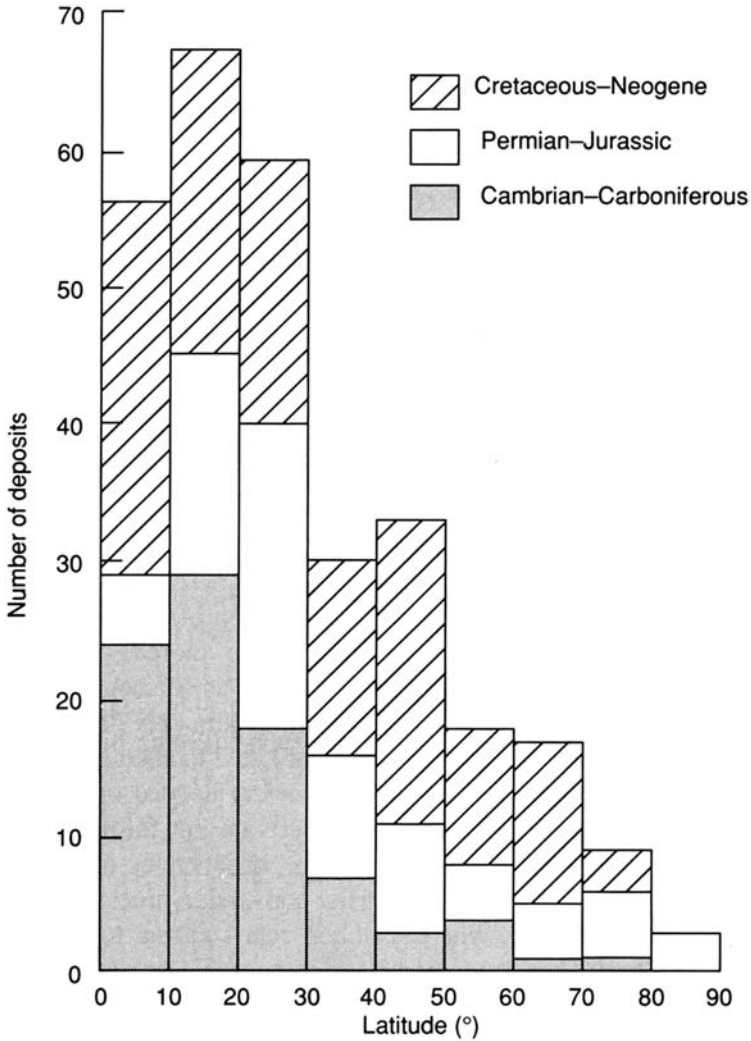


Figure 12.20 Paleolatitude distribution of chert through time. [After Hein, J. R. and J. T. Parrish, 1987, Distribution of siliceous deposits in space and time, in Hein, J. R. (ed.), *Siliceous Sedimentary Rock-Hosted Ores and Petroleum*, Fig. 2-3, p. 17. Copyright 1987 by Van Nostrand Reinhold. All rights reserved.]

contain less-abundant remains of siliceous organisms. Bedded chert deposits occur in association with a wide variety of sedimentary rocks, including limestone, dolomite, shale, sandstone and siltstones (including graywackes), conglomerate, phosphates, iron-formations, argillite, slate, schist, marble, quartzite, greenstone, tuff, basalt, ophiolite, pillow lavas, and ultramafic rocks.

Although most ancient bedded cherts, with the possible exception of Precambrian cherts, are believed to be of biogenic origin, the origin of bedded chert or ribbon chert is still something of an enigma. As mentioned, it seems reasonably clear now that the deep-sea

cherts encountered during the Deep Sea Drilling Project and the more recent Ocean Drilling Program are not true analogs of ancient bedded cherts. These deep-sea or open-sea cherts form by replacement of carbonates or clays, with silica furnished by dissolution of local siliceous organisms. They lack the rhythmic bedding of ribbon cherts, make up only a small percentage of the carbonate or clay sequences in which they occur, and occur as lenses, nodules, or stringers on a millimeter or centimeter scale.

By contrast, ribbon cherts make up at least 50 percent of sequences composed also of basalt, shale, sandstone, or other rock and consist of beds ranging to tens of centimeters thick and that extend laterally for tens of meters or more (Hein and Karl, 1983). Ribbon chert sequences must have been deposited initially as siliceous oozes or as turbidites composed mostly of siliceous organisms with various amounts of admixed clay. The siliceous oozes or turbidites were subsequently converted to chert by diagenetic recrystallization, as described. A key difference between ancient bedded or ribbon cherts and DSDP and ODP cherts appears to be that ribbon cherts do not form by diagenetic replacement of carbonate or clay. Instead, the whole mass of siliceous ooze deposits is transformed to chert by the opal-A to opal-CT to quartz conversion process. Also, DSDP and ODP cherts occur in the open ocean, whereas ribbon cherts appear to have formed mainly in continental-margin settings in orogenic belt sequences. These settings may include backarc basins such as the Bering, Philippine, and Japan seas; small ocean basins with transform-fault-dominated spreading centers (spreading basins rather than spreading ridges) such as the Gulf of California; and silled basins that are locally isolated from terrigenous material such as the wrench basins of the California continental borderland (Hein and Parrish, 1987).

12.4 Iron-rich sedimentary rocks

12.4.1 Introduction

Small amounts of iron occur in nearly all sedimentary rocks – about 4.8 percent in the average shale, 2.4 percent in the average sandstones, and 0.4 percent in the average limestones (Blatt, 1982). Sedimentary rocks that contain more than about 15 percent iron, corresponding to 21.3 percent Fe_2O_3 or 19.4 percent FeO , are considered to be iron rich. Although iron-bearing minerals occur in sedimentary rocks of all ages, true iron-rich rocks are very unevenly distributed by age in the geologic record. Most iron-rich sedimentary rocks were deposited during three major time periods: the Precambrian, the early Paleozoic, and the Jurassic and Cretaceous.

Iron-rich sedimentary rocks make up only a very small fraction (<1 percent) of the sedimentary rocks in the geologic record; however, their enormous economic significance greatly overshadows their relatively minor abundance. Most of the world's currently mined iron ore comes from sedimentary deposits, primarily Precambrian banded, cherty iron-formations. These banded iron deposits have iron contents ranging from about 24 to 40 percent (James and Trendall, 1982). They are located primarily in the shield areas of the major continental masses including North and South America, Africa, India, Russia, and Australia.

The iron-rich sedimentary rocks are an enigmatic group of rocks from the standpoint of their temporal and spatial distribution and origin. We do not fully understand why these rocks were deposited mainly during the three time periods mentioned, and we have many

other questions concerning their origin. For example, what special depositional conditions existed during these time periods that were not present during other times? What was the source of the vast quantities of iron now locked up in sedimentary rocks of these ages? What was the mechanism of iron transport, and under what conditions was the iron deposited? We will examine these questions in this section, along with discussion of the physical and chemical characteristics of the iron-rich sedimentary rocks.

12.4.2 Principal kinds of iron-rich sedimentary rocks

The classification of iron-rich sedimentary rocks is a contentious subject (Trendall, 1983) and a variety of names, many of local origin, are applied to these rocks. Dimroth (1979) suggests that all iron-rich rocks can be grouped into three broad categories of deposits on the basis of composition and physical characteristics: detrital chemical iron-rich sediments, iron-rich shales, and miscellaneous iron-rich deposits (Table 12.3). The iron-rich shales and

Table 12.3 *Principal classes of iron-rich sedimentary rocks*

I. Detrital chemical iron-rich sediments
A. Cherty iron-formation
Texture: analogous to limestone texture
Composition: iron-rich chert containing hematite, magnetite, siderite, ankerite, or (predominantly alumina-poor) silicates as predominating iron minerals; relatively poor in Al and P
B. Minette-type ironstone (aluminous iron-formation)
Texture: analogous to limestone texture
Composition: aluminous iron silicates (chamosite, chlorite, stilpnomelane), iron oxides, and carbonates; relatively rich in Al and P
II. Iron-rich shales
C. Pyritic shales
Bituminous shales containing nodules or laminae of pyrite; grade into massive pyrite bodies by coalescence of pyrite laminae and nodules
D. Siderite-rich shales
Bituminous shales with siderite concretions; grade into massive siderite bodies by coalescence of concretions
III. Miscellaneous iron-rich deposits
E. Iron-rich laterites
F. Bog iron ores
G. Manganese nodules and oceanic iron crusts
H. Iron-rich muds precipitated from hydrothermal brines, Lahn-Dill-type iron oxide ores, and stratiform, volcanogenic sulfide deposits
I. Placers of magnetite, hematite, or ilmenite sand

Source: Modified slightly from Dimroth, E., 1979, Models of physical sedimentation of iron formations, in Walker, R. G. (ed.), *Facies Models*: Geoscience Canada Reprint Series 1. Table I, p. 175, reprinted by permission of Geological Association of Canada.

miscellaneous types of iron-rich rocks rarely form deposits of economic significance and are volumetrically unimportant compared to the detrital chemical sediments. The nomenclature problem applies primarily to these last rocks. James (1966, 1992) proposed that these rocks be divided into two principal types: iron-formation and ironstone. He used the term **iron-formation** to include iron-rich rocks of largely Precambrian age and **ironstone** for rocks of mainly Phanerozoic age. James (1992) defines iron-formation as “ a chemical sediment, typically thin-bedded or laminated, containing 15 percent or more iron of sedimentary origin, commonly but not necessarily containing layers of chert.” Ironstones also contain ~15 percent or more iron but they are non-cherty, lack the laminated or thin-bedded structure typical of iron-formation, have a distinctly lower content of silica, and typically have oolitic textures.

12.4.3 Iron-formations

Distribution

James and Trendall (1982) indicate that iron-formations are primarily of Precambrian age, but range in age from early Precambrian to Devonian. A few deposits of even younger age (Mesozoic and Cenozoic) have also been reported (Ohmoto *et al.*, 2006). Three periods of peak deposition are recognized: mid Archean (3400–2900 my), early Proterozoic (2000–2500 my), and late Proterozoic (750–500 my). The geographic distribution of most of the more important deposits is shown in Fig. 12.21 and listed in Table 12.4; see also Ohmoto *et al.* (2006, table 1). Note that these deposits occur on the major Precambrian cratons of Earth and that one iron-formation characterized as a *very large* deposit occurs in each of the continents listed in Table 12.4. Approximately 90 percent of the preserved iron-formations in the world are contained in these five large deposits (James and Trendall, 1982).

Characteristics

Sedimentary structures

Banded iron-formations consist of distinctively banded sequences (Fig. 12.22) composed of layers enriched in iron alternating with layers rich in chert. Banding occurs at a variety of scales. In some iron-formations, millimeter-scale concentrations of iron-bearing minerals define **microbands** within centimeter-scale **mesobands** of chert (terminology of Trendall and Blockley, 1970). In turn, chert mesobands are separated by mesobands of iron-rich materials called **chert matrix**. These microbands and mesobands can occur within larger-scale bands (macrobands) ranging from 20 m to 500 m or more (Fig. 12.23). The bands tend to be laterally continuous for long distances. In the Hamersley Basin of Western Australia, for example, the banding is laterally continuous over the entire estimated 150,000 km² original depositional area of the basin (James and Trendall, 1982).

Gole and Klein (1981) suggest that microbanding, in the strict sense described above (illustrated in Fig. 12.24E, F), is not common; lamination is more commonly expressed by alternating 0.1–2.0 mm thick laminae of different iron-bearing minerals (Fig. 12.24C, D). Laminated iron formations may also include other small-scale structures such as chert pods,

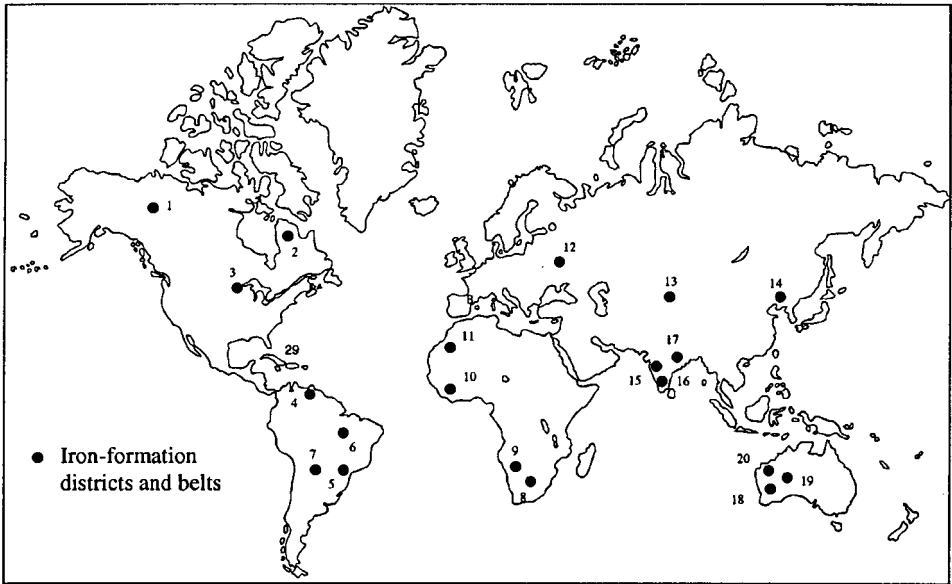


Figure 12.21 World distribution of most major iron-formation belts and districts. Canada: Raritan (1); Labrador Trough (2); USA–Canada: Lake Superior region (3); Venezuela: Imataca Complex (4); Brazil: Quadrilátero Ferrífero (5); Serra dos Carajás (6); Urucum (7); South Africa: Transvaal–Griquatown belt (8); Namibia: Damara belt (9); West Africa: Liberian Shield (10); Mauritania: Ijil Group (11); USSR (former): Krivoy Rog and Kursk Magnetic Anomaly (12); Baykal region (13); Anshan (14); India: Goa (15); Karnataka (16); Bihar–Orissa belt (17); Australia: Yilgarn Block greenstone belts (18); Napperu Basin (19); Hamersley Basin (20). (After Misra K. C., 2000, *Understanding Mineral Deposits*: Kluwer, Dordrecht, Fig. 15.1, p. 663, reproduced by permission.)

macules (spots or knots), and small spherical nodules. Some iron-formations have oolitic and granular textures (Fig. 12.24A, B), which James and Trendall (1982) refer to as **granule iron-formation**. These iron-formations, which occur mainly in Proterozoic sequences (Gole and Klein, 1981), appear to be less well laminated than other iron-formations, although they may be laminated in part. The textures of these iron-formations resemble those of limestones. Dimroth (1979) recognizes textural types in iron-formations equivalent to micritic, pelleted, intraclastic, oolitic, pisolitic, and stromatolitic limestone textures. Other sedimentary structures reported from banded iron-formations include cross-bedding, graded bedding, load casts, ripple marks, erosion channels, shrinkage cracks, and slump structures. These structures show that many of the constituents of iron-formations must have undergone mechanical transport and deposition.

Mineralogy and geochemistry

On the basis of relative abundance of major iron-bearing minerals, James (1966, 1992) defined four principal kinds of iron-rich sedimentary rocks, which he referred to as facies:

Table 12.4 *Estimated initial size and age of selected cherty, banded iron-formations*

	Area (may include more than one stratigraphic unit)	Class	Estimated age* (my)
Africa	Damara Belt, Namibia	Moderate	650 (590–720)
	Shushong Group, Botswana	Small	1875 (1750–2000)
	Ijil Group, Mauritania	Moderate	2100 (1700–2500)
	Transvaal-Griquatown, S. Africa	Very large	2263 (2095–2643)
	Witwatersrand, S. Africa	Small	2720 (2643–2800)
	Liberian Shield, Liberia-Sierra Leone	Large	3050 (2750–3350)
	Pongola beds, Swaziland-S. Africa	Moderate	3100 (2850–3350)
	Swaziland Supergroup, Swaziland-S. Africa	Small	3200 (3000–3400)
Australia	Nabberu Basin	Large	2150 (1700–2600)
	Middleback Range	Moderate	2200 (1780–2600)
	Hamersley Range	Very large	2500 (2350–2650)
Eurasia	Altai region, Kazakhstan, W. Siberia	Moderate	375 (350–400)
	Maly Khinghan-Uda, Far East USSR	Large	550 (500–800?)
	Central Finland	Moderate	2085 ± 45
	Krivoy Rog-KMA, USSR	Very large	2250 (1900–2600)
	Bihar-Orissa, India	Large	3025 (2900–3150)
	Belozorysky-Konski, Ukraine, USSR	Moderate	3250 (3100–3400)
North America	Raritan Group, western Canada	Moderate	700 (550–850)
	Yavapai Series, southwest USA	Small	1795 (1775–1820)
	Lake Superior, USA	Large	1975 (1850–2100)
	Labrador Trough and extensions, Canada	Very large	2175 (1850–2500)
	Michipicoten, Canada-Vermilion, USA	Moderate	2725 (2700–2750)
	Beartooth Mountains, Montana, USA	Small	2920 (2700–3140)
	Isua, Greenland	Small	>3760 ± 70
South America	Morro du Urucum-Mutun, Brazil-Bolivia	Moderate	600? (450–900)
	Minas Gerais, Brazil	Very large	2350 (2000–2700)
	Imataca Complex, Venezuela	Large	3400 (3100–3700)

* In the absence of other data, the assigned age is the arithmetic mean of the age limits given in brackets. *Source:* James, H. L. and A. F. Trendall, 1982, Banded iron formation: Distribution in time and paleoenvironmental significance, in Holland, H. D. and M. Schidlowski (eds.), *Mineral Deposits and the Evolution of the Biosphere*. Table 1, p. 202, reprinted by permission of Springer-Verlag, Berlin.

(1) oxides, (2) silicates, (3) carbonates, and (4) sulfides. The principal minerals in each of these facies are shown in Table 12.5. Note that the chemistry of iron-formations is dominated by SiO₂ and Fe (Table 12.6), which can be expressed as Fe₂O₃, FeO, and FeS₂. Gole and Klein (1981) show that the average chemical composition of iron-formations is about 45–50 percent SiO₂, 13–27 percent Fe₂O₃, 17–25 percent FeO (29–32 percent total Fe), 3–6 percent MgO, 2–7 percent CaO, 1–2 percent Al₂O₃, and less than 1 percent each of TiO₂, MnO, Na₂O, K₂O, P₂O₅, S, and C.

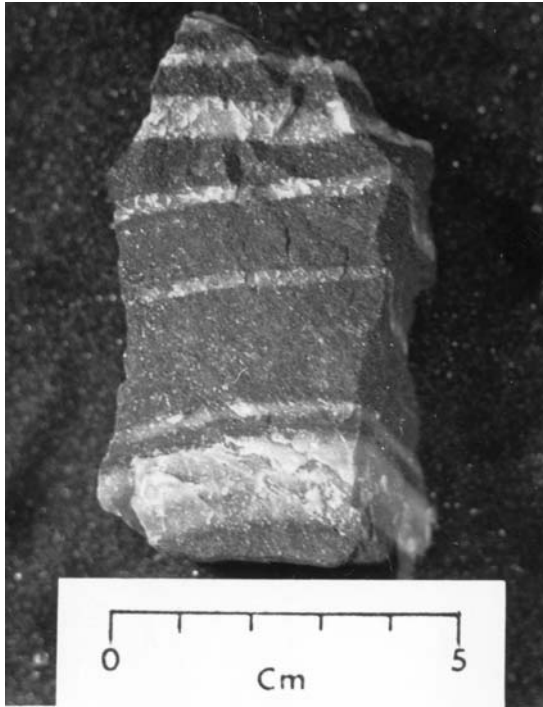


Figure 12.22 Banded iron-formation from the Negaunee Iron Formation (Precambrian), Michigan. The light-colored bands are chert; dark layers are iron-rich units. Length 8 cm. (Specimen furnished by M. H. Reed.)

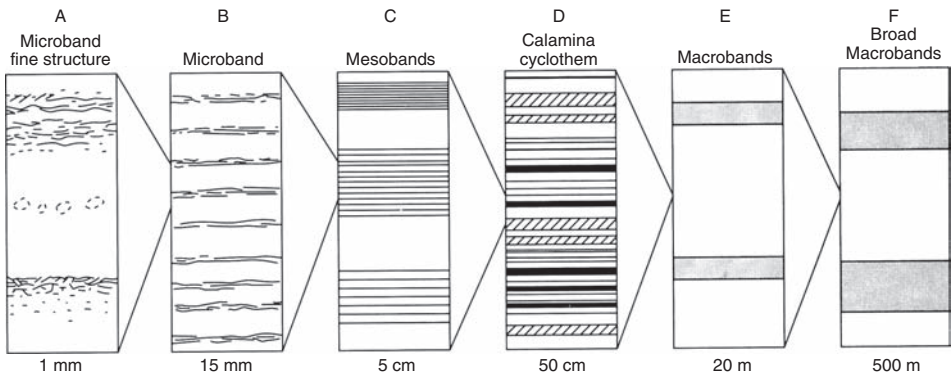


Figure 12.23 Various scales of banding in banded iron-formations of the Hamersley Basin, Western Australia. A shows the fine structure within the microbands illustrated in B, which are defined by iron-rich minerals. In C, microbanded chert mesobands of different microband interval are represented, separated by chert matrix (blank pattern). D shows a regular cyclicality of different chert types, which occur within the larger cyclothem shown in E and F. [From James, H. L. and A. F. Trendall, 1982, Banded iron formation: Distribution in time and paleoenvironmental significance, in Holland, H. D. and M. Schidlowski (eds.), *Mineral Deposits and the Evolution of the Biosphere*, Springer-Verlag, Berlin, Fig. 2, p. 209, reprinted by permission.]

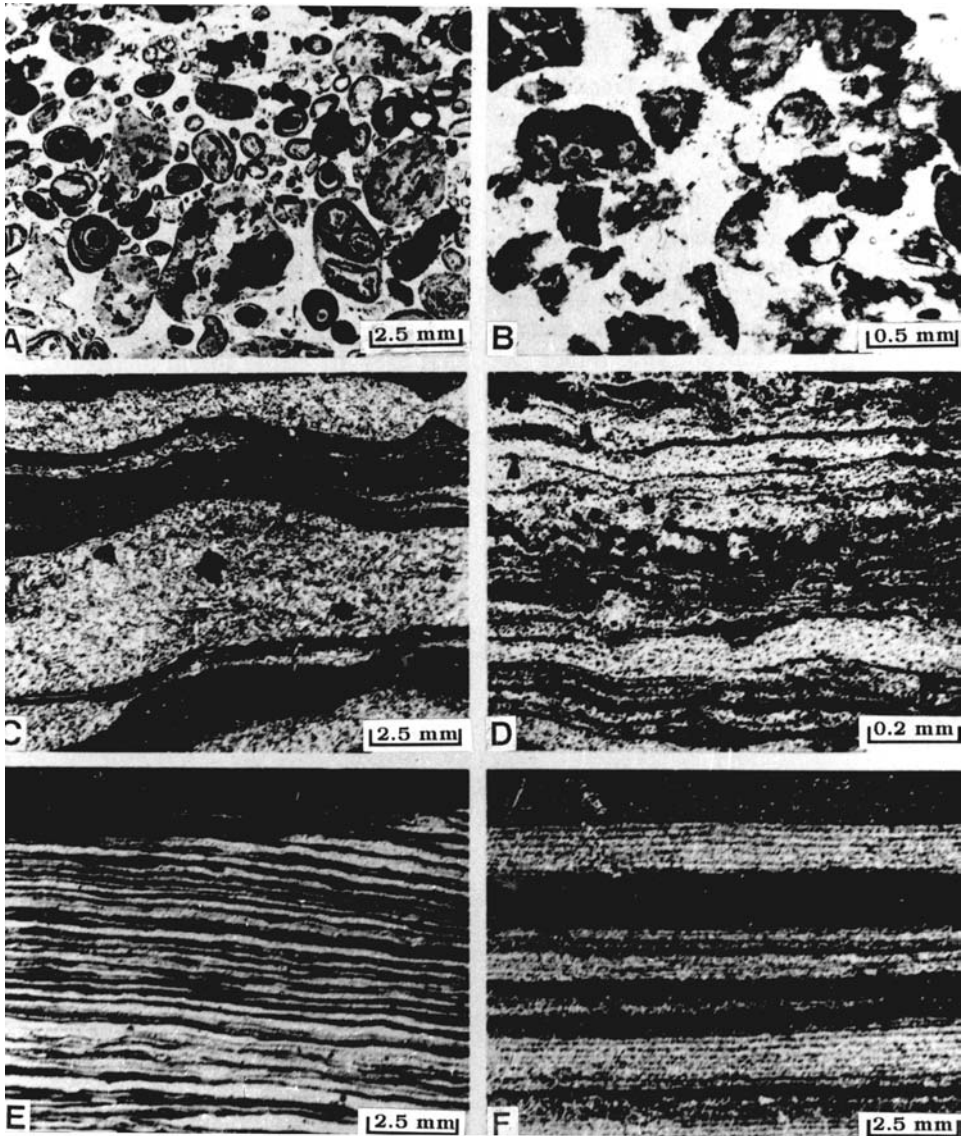


Figure 12.24 Photographs of granule texture and small-scale banding in Precambrian banded iron-formations. A. Ooids and granules composed of magnetite, chert, minor carbonate, and stilpnomelane in a chert-rich matrix (Sokoman Iron Formation, Labrador Trough). B. Granules of minnesotaite, greenalite, stilpnomelane, siderite, and minor magnetite in a chert-rich matrix (Biwabik Iron Formation, Minnesota). C. Laminae in a minnesotaite-stilpnomelane-quartz-minor magnetite assemblage (Negaunee Iron Formation, northern Michigan). D. Microbands defined by quartz, magnetite, and minor siderite, ankerite, and chlorite (Negaunee Iron Formation). E. Microbanding in a quartz-magnetite mesoband (Joffre Member of the Hamersley Group, Western Australia). F. Alternating massive and microbanded mesobands in a magnetite-quartz-minor grunerite-bearing iron-formation, metamorphosed to amphibolite grade (Forrestania area, Archean Yilgarn Block, Western Australia). (From Gole, M.J. and C. Klein, 1981, *Banded iron-formation through much of Precambrian time: J. Geol.*, **89**, Fig. 2, p. 174, reprinted by permission of the University of Chicago Press.)

Table 12.5 *Principal features of iron-formation facies*

Facies	Iron minerals*	Fe contents (wt %)	Lithology	Distinctive features
Oxide				
Hematitic	Specular hematite (Magnetite)	30–40	Thin-bedded to wavy bedded alternation of bluish black hematite and gray or reddish chert	Specularite content; oolitic in many districts
	Magnetitic			
Magnetitic	Magnetite (Minnesotaite) (Stilpnomelane) (Greenalite) (Siderite)	25–35	Heavy dark rock, evenly bedded to irregularly bedded; layers of magnetite alternate with dark chert and mixtures of silicates and siderite	Strongly magnetic
Silicate	Minnesotaite Stilpnomelane (Magnetite) (Siderite) (Greenalite) (Chamosite) (Chlorite)	20–30	Light to dark green rock, generally laminated or even-bedded, but in some districts wavy to irregularly bedded; commonly interlayered with magnetitic oxide facies or carbonate facies	Commonly magnetic; may be granule-bearing
Carbonate	Siderite (Stilpnomelane) (Minnesotaite) (Magnetite) (Pyrite)	20–30	Light to dark gray, evenly bedded or laminated alternation of siderite and chert	Generally non-magnetic; stylolites common
Sulfide	Pyrite (Siderite) (Greenalite)	15–25	Laminated to thinly layered black carbonaceous argillite; chert rare	“Graphitic”

* In rocks of low metamorphic grade; common but non-essential minerals in parentheses.

Source: James, H. L., 1992, Precambrian iron-formations: Nature, origin, and mineralogic evolution from sedimentation to metamorphism, in K. H Wolf and G. V. Chilingarian (eds), *Diagenesis III*, Developments in Sedimentology 47, Table 11-1, p. 548,

Associated facies

Iron-formations occur in association with a wide variety of other rock types, and there appears to be no consistent lithologic association in rock units either below or above iron-formations (Gole and Klein, 1981). Iron-formations commonly occur within sequences of siliciclastic sedimentary rocks, and cherty iron-formations can grade into slightly cherty iron-rich sandstones, siltstones, and shales. They may also be present in association with limestones and dolomites, quartzite, argillite, schist, volcanic rocks, and ultramafic rocks. Volcanic rocks appear to be particularly common in Archean banded iron-formation

Table 12.6 *Chemical composition of sedimentary facies of iron-formations*

	Oxide facies	Silicate facies	Carbonate facies	Sulfide facies
Fe	37.80	26.5	21.23	20.0
FeO	2.10	28.9	22.22	2.35
Fe ₂ O ₃	51.69	5.6	5.74	–
FeS ₂	–	–	–	38.70
SiO ₂	42.89	50.7	48.72	36.67
Al ₂ O ₃	0.42	0.4	0.15	6.90
Mn	0.3	0.4	0.50	0.001
P	0.03	–	0.07	0.09
CaO	0.1	0.1	4.60	0.13
MgO	+	4.2	0.84	0.65
K ₂ O	+	–	+	1.81
Na ₂ O	+	–	0.01	0.26
TiO ₂	+	+	+	0.39
CO ₂	–	5.1	14.10	–
S	–	+	2.76	–
SO ₃	–	–	–	2.60
C	–	+	++	7.60
H ₂ O ⁺	0.43	5.2	2.67	1.25

Note: += trace; ++ = larger trace; – = not present.

Source: Eichler, J., 1976, Origin of Precambrian banded iron-formations, in Wolf, K. H. (ed.), *Handbook of Strata-Bound and Stratiform Ore Deposits*, v. 7. Table VI, p. 187, reprinted by permission of Elsevier Science Publishers, Amsterdam.

sequences, although they occur also in Proterozoic sequences. On the other hand, carbonate rocks are comparatively rare in Archean sequences.

Principal kinds of iron-formations

Various attempts have been made to classify iron-formations into a few specific, representative types. For example, Gross (1965) divided iron-formations into Algoma-type and Superior-type. According to him, **Algoma-type** iron-formations are intimately associated with various volcanic rocks. They are thinly banded or laminated, lack oolitic or granular textures, and commonly extend laterally for only a few kilometers. By contrast, Gross suggested that **Superior-type** iron-formations are not associated with volcanic rocks but commonly occur with quartzite, black carbonaceous shale, conglomerate, dolomite, massive chert, chert breccia, and argillite. They contain granular and oolitic textures, and commonly extend laterally for hundreds of kilometers. Button *et al.* (1982) list **Raritan-type** deposits as a third kind of iron-formation. These deposits occur in several basins of late Precambrian age and are associated in part with glacial deposits. Deposits of significant dimensions occur in the Raritan Group of northwestern Canada and in the Morro du Urucum

region of western Brazil and eastern Bolivia. Button *et al.* suggest that these deposits are somewhat richer in iron than are normal iron-formations.

Unfortunately, there is lack of agreement among the experts with respect to classifying particular iron-formations. For example, Trendall (1983) does not agree with the practice of classifying most iron-formations into two major types: Algoma and Superior. He maintains that “this demonstrably subjective distinction is not only inadequate to accommodate, without distortion, many major iron-formations of the world, but imposes an artificial two-fold division not present in the complex spectrum of rocks it seeks to cover.” See also discussion by James (1992, p. 559).

12.4.4 Ironstones

Ironstones are dominantly Phanerozoic-age sedimentary deposits. They occur mainly in early Paleozoic and Jurassic–Cretaceous rocks, but they range in age from Pliocene to middle Precambrian. The age distribution of Phanerozoic oolitic ironstones is shown in Fig. 12.25.

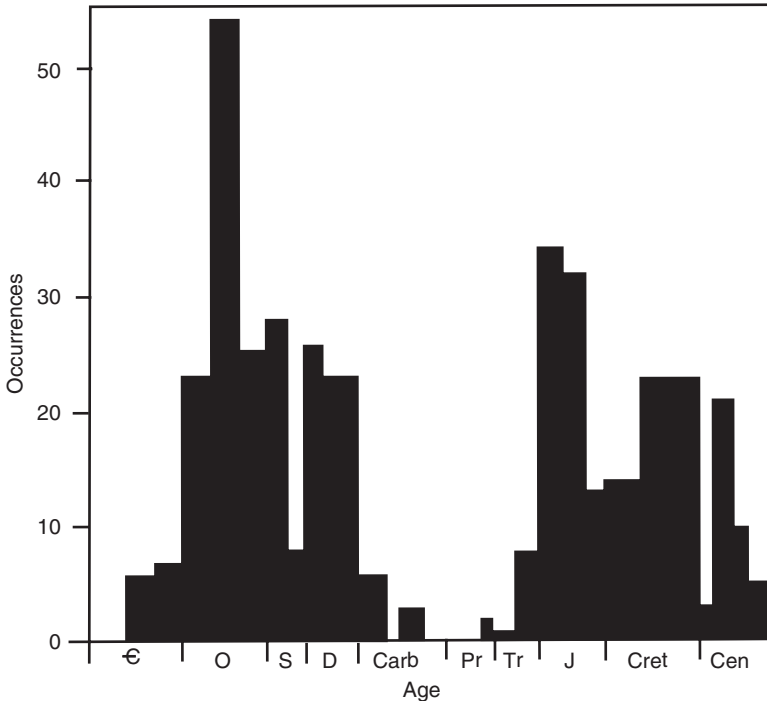


Figure 12.25 Histogram of the stratigraphic distribution of Phanerozoic ironstones. (After Van Houten, F. B., 2000, Ooidal ironstones and phosphorites – A comparison from a stratigrapher’s view, in Glenn, C. R., L. Prévôt-Lucas, and J. Lucas (eds.), *Marine Authigenesis: From Global to Microbial*: SEPM Special Publication 66, Fig. 1, p. 127. Reprinted by permission of the Society for Sedimentary Geology, Tulsa, OK.)



Figure 12.26 Hematitic oolitic Clinton ironstone (lower part of photograph) of the Keefer Member of the Mifflintown Formation (Silurian), Pennsylvania. Limestone beds overlie the ironstones. (Photograph courtesy of T. Schuster.)

They are present on all the major continents but relatively few deposits of Cambrian age or Carboniferous–Triassic age occur on any continent.

The volume of preserved ironstones is much less than that of the iron-formations, although they are locally important, as mentioned. Ironstones form thin, massive, or poorly banded sequences (Fig. 12.26), a few meters to a few tens of meters thick, in sharp contrast to the much thicker, well-banded iron-formations. They generally have an oolitic texture (Fig. 12.27), and they may contain fossils that have been partly or completely replaced by iron minerals. Van Houten (1982) suggests two major ironstone facies: (1) sandy and shelly shallow-marine sediments with abundant pellets of glauconite, and (2) ferric oxide–chamosite (mostly 7Å iron-rich clay minerals) oolite; ferric oxides can include both hematite and goethite. These two facies can be associated, and (locally) oolitic deposits may replace glauconite facies vertically or interfinger with them laterally. Hematite is the main iron-bearing mineral in red deposits, and berthierine (similar to chamosite) and siderite predominate in green deposits (Harder, 1989). Most of the ferric oxide–chamosite oolites accumulated during early Ordovician to late Devonian and early Jurassic to middle Cenozoic time (Van Houten, 1982).

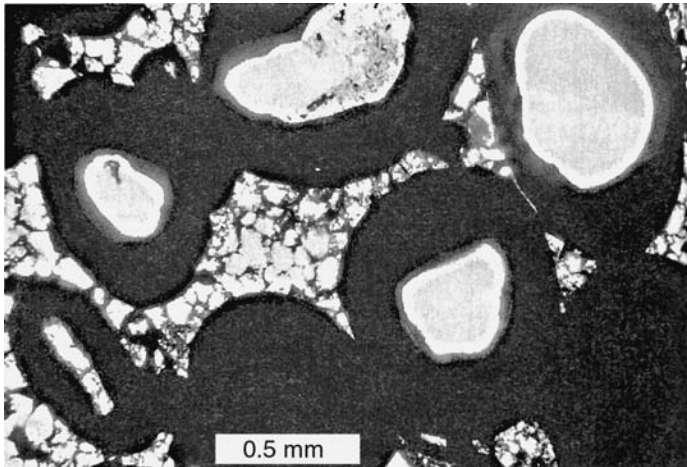


Figure 12.27 Ironstone ooids with quartz nuclei, cemented with sparry calcite cement. Clinton Formation (Silurian), New York. Ordinary light.

Nonferrous minerals in ironstones may include detrital quartz, calcite, dolomite, authigenic phosphorite, and authigenic chert. As mentioned, ironstones are commonly poorly banded; however, they may contain a variety of other sedimentary structures. These structures can include cross-bedding, ripple marks, scour-and-fill structures, rip-up clasts, and burrows. Structures such as cross-beds and ripple marks indicate that mechanical transport of grains was involved in the origin of these deposits.

Ironstones are commonly interbedded with carbonates, mudrocks, and fine-grained sandstones of shelf to shallow-marine origin. Many occur in deltaic sequences. On the other hand, some ironstones occur in association with deeper-water mudstones or marly limestones. See Young and Taylor (1989) for additional details of the mineralogy and geochemistry of ironstones, and Van Houten (2000) for information about geographic and age distribution.

12.4.5 Iron-rich shales

Pyritic black shales occur in association with both Precambrian iron-formations and Phanerozoic ironstones. They commonly form thin beds in which sulfide content may range as high as 75 percent. Pyrite occurs disseminated in these black carbonaceous shales and in some limestones. It occurs also as nodules, laminae, and as a replacement of fossil fragments and other iron minerals. Pyrite-rich layers have also been reported in some limestones. **Siderite-rich shales** (clay ironstones) occur primarily in association with other iron-rich deposits. They are also present in the coal measures of both Great Britain and the United States. Siderite occurs disseminated in the mudrocks or as flattened nodules and more or less continuous beds.

12.4.6 Miscellaneous iron-rich deposits

Bog-iron ores are minor accumulations of iron-rich sediments that occur particularly in small freshwater lakes of high altitude. They range from hard, oolitic, pisolitic, and concretionary forms to soft, earthy types. **Iron-rich laterites** are residual iron-rich deposits that form as a product of intense chemical weathering. They are basically highly weathered soils in which iron is enriched. **Manganese crusts and nodules** are widely distributed on the modern seafloor in parts of the Pacific, Atlantic, and Indian oceans in areas where sedimentation rates are low. They have also been reported from ancient sedimentary deposits in association with such oceanic sediments as red shales, cherts, and pelagic limestones. Both iron-rich (15–20 percent Fe) and iron-poor (less than about 6 percent Fe) varieties of manganese nodules are known. These nodules contain variable amounts of Cu, Co, Ni, Cr, and V in addition to manganese and iron.

Metalliferous sediments occur in oceanic settings, particularly near active mid-ocean spreading ridges. They are believed to form by precipitation from metal-rich hydrothermal fluids that have become enriched through contact and interaction with hot basaltic rocks. These sediments are enriched in Fe, Mn, Cu, Pb, Zn, Co, Ni, Cr, and V. Metal-enriched sediments have also been reported from some ancient sedimentary deposits in association with submarine pillow basalts and ophiolite sequences of ocean crustal rocks.

Heavy-mineral placers are sedimentary deposits that form by mechanical concentration of mineral particles of high specific gravity, commonly in beach or alluvial environments. Magnetite, ilmenite, and hematite sands are common constituents of placers, particularly beach and marine placers. Placers are local accumulations that occur mainly in Pleistocene- to Holocene-age sediments and that commonly do not exceed 1 to 2 m in thickness. Marine placer deposits containing about 5 percent iron ore have been mined off the southern tip of Kyushu, Japan for many years (Mero, 1965), and offshore placers containing up to 10 percent magnetite and ilmenite have been reported off the southeastern coast of Taiwan (Boggs, 1975). Beach placers containing ilmenite have been exploited commercially in Australia since about 1965 (Hails, 1976). “Fossil” placer deposits are comparatively rare, although thin, heavy-mineral laminae are common in some ancient beach deposits. Hails (1976) reports that outcrops of ilmenite- and magnetite-bearing placers of Cretaceous age are exposed discontinuously through New Mexico, Colorado, Wyoming, and Montana subparallel to the Rocky Mountains.

12.4.7 Origin of iron-rich sedimentary rocks

Introduction

The origin of iron-rich sedimentary rocks is an enigmatic topic that has been debated by geologists for well over a century. The number of papers written about the origin of iron-rich sediments is probably exceeded only by the number written about the origin of dolomite, which is equally enigmatic. Because there is no modern analog for the iron-rich sediments, depositional models for these sediments have to be formulated mainly

on the basis of the ancient record. Geologists with access to the same data may draw different inferences from these data; therefore, numerous models for the origin of iron-rich sedimentary rocks have been advanced – none of which has gained complete acceptance. Most of the controversy focuses on the origin of iron-formations, which form the bulk of the iron-rich rocks.

A number of important questions are involved in the debate about the origin of iron-formations and ironstones. Why, for example, are cherty, banded iron-formations confined primarily to the Precambrian? Why are iron-formations and ironstones not forming today? What is the source of the vast amount of iron locked up in the known iron-rich deposits? Was volcanism involved in some way in the formation of some or all of these iron deposits? How was iron transported from its source to the depositional site, and what was the depositional environment in which iron-rich sediments accumulated?

Modern depositional environments of iron-bearing minerals

There are no modern counterparts to the ancient environments that presumably favored widespread deposition of iron-rich sediments to produce iron-formations and ironstones, but iron-bearing minerals are being deposited on a small scale in a variety of modern environments. Iron sulfides, particularly pyrite (FeS_2), are forming in black muds that accumulate under reducing conditions in stagnant ocean basins, tidal flats, and organic-rich lakes. Iron sulfides are also accumulating around the vents of hot springs located on the crests of mid-ocean ridges. Chamosite, a complex Fe–Mg–Al silicate, has been reported in modern sediments at water depths as great as 150 m in the Orinoco and Niger deltas and on the ocean floor off Guinea, Gabon, Sarawak, and in the Malacca Straits. Glauconite is a K–Mg–Fe–Al silicate mineral that has been reported from Monterey Bay, California, and from various other parts of the ocean at water depths ranging down to about 2000 m.

Iron oxides such as goethite (FeOOH) are accumulating in some modern lakes and bogs and as ooids on the floor of the North Sea. Iron-rich ooids and peloids have also been reported off the northeast coast of Venezuela, in muddy deposits on the Orinoco Delta, and off the Amazon Delta (e.g. Van Houten, 2000). Manganese nodules, which contain manganese, copper, cobalt, nickel and other metals in addition to iron, occur in both seawater and freshwater. They are particularly widespread in the Pacific Ocean at water depths of about 4–5 km. On the whole, modern examples of iron-rich sediments are small and fairly rare; they provide few clues to the depositional conditions that favored generation of massive ancient iron deposits.

The problem of iron solubility

The dissolution of iron from source areas and its subsequent transport and deposition to form iron-rich deposits are governed by the Eh and pH of the environment. Iron in the oxidized or ferric (Fe^{3+}) state is much less soluble than iron in the reduced or ferrous (Fe^{2+}) state (Fig. 12.28). Ferric iron is soluble only at pH values less than about 4, which rarely occur under natural conditions. Oxidation potential–pH diagrams such as Fig. 12.28 can be used in

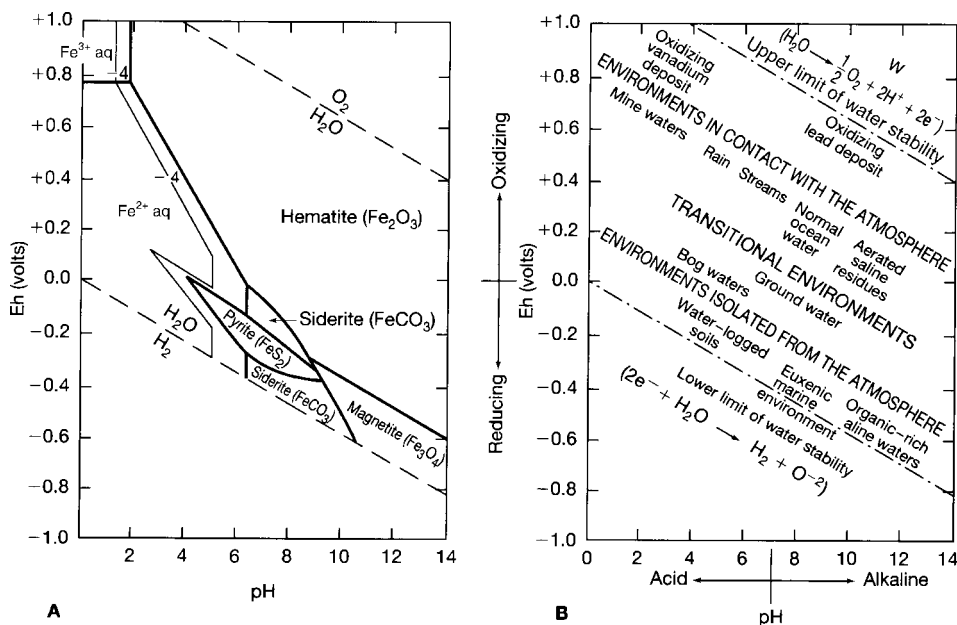


Figure 12.28 A. Eh–pH diagram showing the stability fields of the common iron minerals, sulfides, and carbonates in water at 25 °C and 1 atm total pressure. Total dissolved sulfur = 10^{-6} ; total dissolved carbonate = 10^0 . B. Graph showing Eh and pH of waters in some natural environments. (A. After Garrels, R. M. and C. L. Crist, 1965, *Solutions, Minerals, and Equilibria*: Harper and Row, New York, Fig. 7.21, p. 224, reprinted by permission. B. after Blatt, H., G. V. Middleton, and R. Murray, 1980, *Origin of Sedimentary Rocks*, 2nd edn.: Prentice-Hall, Upper Saddle River, NJ, Fig. 6.12, p. 241, reprinted by permission, based on data from Baas Becking L. G. M., *et al.*, 1960, Limits of the natural environment in terms of pH and oxidation-reduction potentials: *J. Geol.*, **68**, pp. 243–284.)

a general way to predict the stability of iron-bearing minerals and serve to illustrate that Eh is commonly more important than pH in determining the solubility of iron and the kind of iron-bearing mineral that will be deposited under given conditions. For example, hematite (Fe_2O_3) is precipitated under oxidizing conditions at the pH levels commonly found in the ocean and surface waters, siderite (FeCO_3) forms under moderately reducing conditions, and pyrite (FeS_2) forms under moderate to strong reducing conditions.

On the other hand, the iron geochemistry of natural systems is far more complex than the simplified conditions assumed in constructing Eh–pH diagrams, and such diagrams are of only limited use in environmental interpretations. Many problems are associated with the formation of sedimentary iron deposits, and the mechanisms by which transport and deposition of iron occurred in the past to form iron-formations and ironstones are still controversial. One of the principal problems stems from the fact that iron tends to be insoluble in the oxidized or Fe^{3+} state. Assume for a moment that subaerial weathering of iron-rich minerals is the major source of iron for iron-formations. Given that oxidized iron is largely insoluble, how can large quantities of iron be taken into solution and transported

from subaerial weathering sites under the oxidizing conditions that commonly prevail in streams and rivers?

This problem of solution and transport of iron under oxidizing conditions prompted some early workers (Lepp and Goldich, 1964; Cloud, 1973; Lepp, 1987) to postulate that low oxygen levels existed during the Precambrian which allowed great quantities of iron to be transported in the soluble, reduced state (Fe^{2+}) to marine basins. Presumably, local oxidizing conditions existed within some parts of broad, shallow-marine basins, owing to photosynthetically generated oxygen, where the iron was oxidized to the insoluble ferric state (Fe^{3+}) and precipitated. In any case, this argument cannot be used to explain the solution and transport of iron during the Phanerozoic when an oxidizing atmosphere clearly existed.

Models for deposition of iron-formations

Introduction

Three principal aspects of the iron problems have to be addressed to account for the formation of iron-rich rocks: (1) the source of the iron, (2) transport of iron to the depositional basin in a soluble state, presumably under reducing conditions, and (3) episodic precipitation of the iron within the basin. The origin of iron-formations was summarized recently by Trendall (2002) and Simonson (2003), and has been discussed by others too numerous to list. Many early hypotheses were offered to explain the origin of iron-formations: i.e. replacement of carbonates, deposition in large lakes, deposition in association with Precambrian evaporites, precipitation in oxygen oases, deposition as biogenic oozes (see review in Simonson, 2003). Ohmoto *et al.* (2006) also discuss several early models for the origin of iron-formations.

Most of these early hypotheses have been discounted. Opinion now appears to be solidifying around the hypothesis that: (1) the source of the iron lay within the ocean, not on land, (2) iron was transported in solution from the ocean source to depositional basins in a stratified ocean, and (3) deposition took place in marine basins by processes not fully understood but that likely included microbial mediation.

Source of iron

Early workers assumed that the iron in iron-formations was derived by weathering of iron-bearing minerals on land. The low atmospheric oxygen levels that apparently existed during the Precambrian putatively allowed great quantities of iron to be transported in rivers, in the soluble, reduced (Fe^{2+}) state, to marine basins. The subsequent discovery of hydrothermal systems along mid-ocean ridges, where iron was being dissolved from hot, basaltic rocks, shifted attention to the ocean as the source of iron (e.g. Simonson, 1985, 2003; Isley, 1995). That is, iron was supplied by submarine reaction of outpouring lava and hydrothermal activity from hot springs located along mid-ocean ridges. Iron may also have been supplied by leaching of cooled mantle rock on the ocean floor during the Precambrian before the rocks were covered by a protective mantle of abyssal sediment (Trendall, 2002). Calculations by Trendall suggest that these oceanic processes could generate an average

content of iron in the Precambrian oceans of ~10 ppm, enough to account for the iron in iron-formation deposits.

Iron transport in the ocean

Many investigators have suggested that the marine basins in which iron was deposited had a stratified water column. That is, they had an upper, oxygen-rich layer and an intermediate to deep oxygen-poor (anoxic) layer. Reasons for stratification of the water column are poorly understood (Simonson, 2003), but ferrous iron supplied by hydrothermal systems and dissolved from ocean-floor rocks was concentrated in the anoxic layer. Deep- to intermediate-water containing dissolved iron may have moved upward to shallower depths on continental shelves owing to upwelling or it may have spread laterally as a plume from high-standing mid-ocean ridges (Isley, 1995).

Depositional basins and depositional processes

Like so many other aspects of the origin of iron-formations, the conditions and processes responsible for precipitation of iron deposits are poorly understood. The large size of many iron-formation deposits suggests that some very large depositional basins were present on Precambrian continental margins. Precipitation of iron in these shallower-water basins may have occurred by interaction between the anoxic bottom-water layer and the upper oxygen-rich layer, with the oxygen content of the upper water being responsible for precipitation of iron hydroxides and/or oxides owing to oxidization of soluble Fe^{2+} to insoluble Fe^{3+} (Buekes and Klein, 1992). On the other hand, there is growing evidence (e.g. from isotopic studies) that microbes may have played an important role in precipitation of the iron (e.g. Beard *et al.*, 1999). Microbes extract iron from solution and metabolize it (e.g. through iron reduction) to provide cell energy, after which it is immediately precipitated as a waste product (Brown, 2006). Photosynthetic production of oxygen by aerobic microbes may also mediate iron precipitation (Trendall, 2002).

Chert layers and banding

The abundance of chert in banded iron-formations suggests that the silica content of Precambrian ocean was much higher than that of the modern ocean (e.g. Siever, 1992), which may reflect the absence of silica-secreting organisms in Precambrian time that removed silica from the ocean. The cause of the banding (alternate deposition of layers of chert and layers of iron-rich minerals) is controversial. Several hypotheses have been advanced (e.g. variations in magmatic activity along mid-ocean ridges that affected iron supply; seasonal and climatic variations); however, no widely accepted explanation for the banding has been advanced. See discussion in Trendall (2002).

Cessation of iron-formation deposition

Significant iron-formation deposition ceased near the end of the Precambrian. Two processes have been suggested to explain the disappearance of significant iron-formations from

the post-Precambrian stratigraphic record. This change is generally attributed to a dramatic rise in atmospheric oxygen levels in late Precambrian time, presumably resulting in oxygen enrichment of the anoxic bottom layer, thereby dramatically reducing iron solubility in bottom water. Alternatively, the change may be the result of an increase in concentration of dissolved sulfide (e.g. Anbar and Knoll, 2002). In any case, some change in ocean chemistry prevented the storage and/or long-distance transport of dissolved iron after Precambrian time (Simonson, 2003).

Deposition of ironstones

The age distribution of ironstones is shown in Fig. 12.25. As mentioned, most ironstone deposits are quite small compared to the giant iron-formation deposits. According to Petranek and Van Houten (1997), ironstones were deposited in marine deltaic, nearshore, and shallow offshore environments. Some, so-called “concentrated” ironstones are 3–4 m thick and contain 60–70 percent ooids. Other “lean” ironstones are typically 5–25 cm thick and generally contain less than 30 percent ooids and peloids scattered in iron-rich mudstone (Bhattacharyya, 1989).

Most ironstone deposits are Phanerozoic in age. They commonly contain kaolinite, hematite, berthierine or chamosite, siderite, and apatite with calcite (Van Houten, 2000). According to Van Houten, the chemical components of ironstones were initially derived from deeply weathered uplands and fed by rivers into shallow seas with very little detrital clastic sediments. (Van Houten doesn’t explain how the iron was transported by rivers under the oxidizing conditions that existed in the Phanerozoic atmosphere.) The ironstones were first laid down as ferric oxide and kaolinite ooids and peloids in clay mud. Subsequently, they may have been reworked by oceanic currents or basinal-current upwelling to form winnowed layers.

The source of the iron in ironstones has also been attributed to exhalation of hot, iron-rich fluids from hydrothermal systems in the ocean, as is the case for iron in iron-formations. For example, Kimberley (1994) describes iron-rich ooids on the seafloor at Cape Mala Pascua, Venezuela, and links the iron to exhalation of hot fluids from deep source areas in the ocean. Sturesson *et al.* (1999) suggest a very different source for the iron in iron-rich ooids of Ordovician age from Russia and Estonia. These authors propose that hydrolysis and dissolution of glass in volcanic ash provided the iron for the ooids.

12.5 Sedimentary phosphorites

12.5.1 Introduction

Phosphorites are sedimentary deposits containing more than about 15–20 percent P_2O_5 . Thus, they are significantly enriched in phosphorus over most other types of sedimentary rocks. The phosphorous content of average shales is about 0.11–0.17 percent P_2O_5 , the average sandstone contains about 0.08–0.16 percent P_2O_5 , and the average limestone about 0.03–0.7 percent P_2O_5 (McKelvey, 1973). Shales, sandstones, or limestones that contain

less than 20 percent P_2O_5 but which are enriched in phosphorus over that found in average sediments are referred to as phosphatic, e.g. phosphatic shale. Phosphorus-rich sedimentary rocks are called by a variety of names – **phosphate rock**, **rock phosphate**, **phosphates**, **phosphatites**, and **phosphorites**. Not all of these terms have exactly the same meaning, however, and geologists do not agree about which is most appropriate as a name for phosphorus-rich sedimentary rocks. In this book, the term phosphorite is used with the meaning given at the beginning of this paragraph.

The total volume of sedimentary phosphates in the geologic record is quite small; however, sedimentary phosphorites are of special economic interest. They contribute about 82 percent of the world's production of phosphate rock, and make up about 96 percent of the world's total resources of phosphate rock (Notholt *et al.*, 1989). The remaining phosphate resources are in igneous rocks. The most important production at this time comes from rocks of Miocene–Pliocene, Upper Cretaceous–Eocene, and Permian ages in the USA and from Cambrian rocks in the (former) USSR and China. Sedimentary phosphates occur in rocks of all ages from Precambrian to Holocene. Modern phosphorites also occur as nodules on some parts of the ocean floor. The origin of phosphorites is perhaps less enigmatic than that of iron-rich sedimentary rocks; nonetheless, many aspects of their origin are still poorly understood. For example, modern ocean water contains only about 70 parts per billion (ppb) phosphorus, but some ancient phosphorite deposits contain 30–40 percent P_2O_5 . These values represent a concentration factor of up to two million times as great as the phosphorus content of the ocean, and are 200–300 times greater than the P_2O_5 content of average sedimentary rock. We are left to ponder the special depositional conditions that must have existed to produce such significant enrichment. Also, we do not have a clear understanding of why phosphorites accumulated in so much greater volumes at certain times in the geologic past than they are accumulating in the modern ocean.

12.5.2 Occurrence and distribution

Most phosphate deposits occur in marine sedimentary sequences. They have been reported in rocks of all ages and on all continents, although they are unevenly distributed in space and time. Figure 12.29 shows the geographic and age distribution of the major phosphorite deposits on land. Phosphorites occur in numerous Archean and Proterozoic (Precambrian) formations (Van Houten, 2000), as well as in Phanerozoic deposits. In fact, according to Northolt and Sheldon (1986), the greatest global phosphogenic episode in geologic history occurred in Late Precambrian and Cambrian time. Figure 12.30 provides details of the age distribution of Phanerozoic deposits. Phosphorite deposition appears to have been particularly prevalent during the Late Proterozoic and Cambrian in central and southeast Asia; the Ordovician in Australia, North America, and parts of Europe; the Permian in North America; the Jurassic and Early Cretaceous in eastern Europe; the Late Cretaceous to Eocene in the Tethyan Province of the Middle East and North Africa; and the Miocene of southeastern North America (Cook, 1976; Van Houten, 2000). In the United States, for

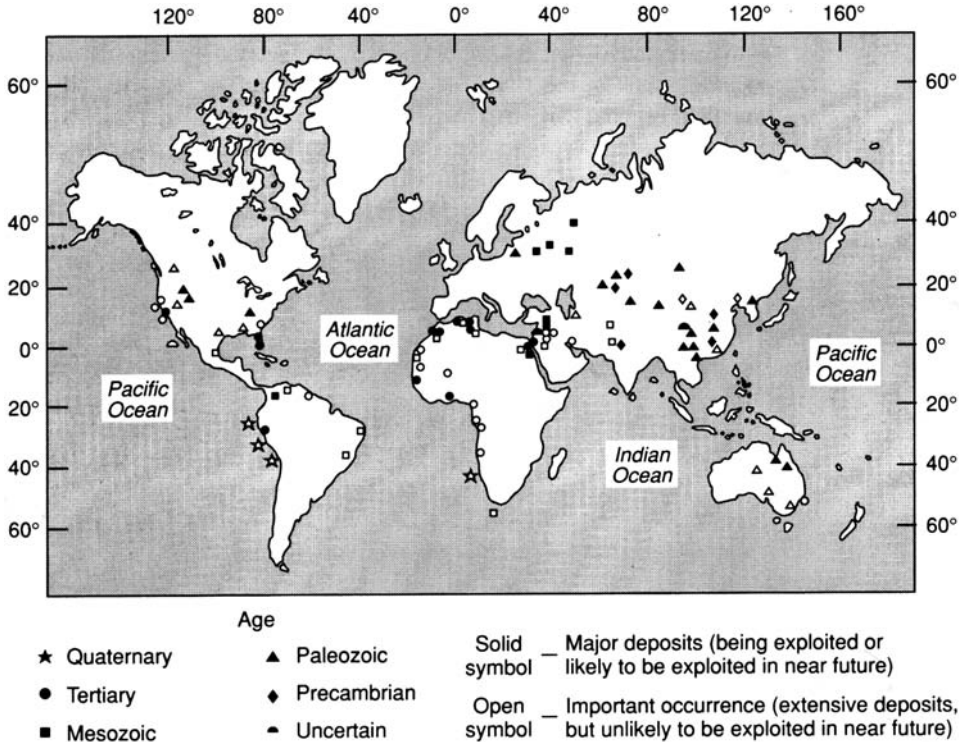


Figure 12.29 Worldwide distribution of major sedimentary phosphorite deposits. (After Cook, P. J., 1976, Sedimentary phosphate deposits, in Wolf, K. H. (ed.), *Handbook of Strata-Bound and Stratiform Ore Deposits*, Elsevier, Amsterdam, Fig. 1, p. 505, reprinted by permission.)

example, deposits containing more than 20 percent P_2O_5 occur in Florida, Georgia, and North Carolina (Miocene–Pliocene), the Western Phosphate Field in Idaho (Permian), and in Utah (Carboniferous). Most ancient phosphorite deposits appear to have accumulated at latitudes between about 0 and 40 degrees. It is not fully understood why phosphorite deposition was favored at low latitudes, although it is widely believed that upwelling in the ocean played a major role in the origin of these deposits.

Deposits of phosphate nodules and phosphatic sediments occur also on the present ocean floor, mainly at depths less than about 400 m and mostly in the vicinity of coastlines (Fig. 12.31). They are concentrated particularly off the coasts of southern California and Baja California, eastern United States, Peru and Chile, and southwest Africa. They occur also on the floor of the Pacific, Indian, and Atlantic oceans and on some seamounts (Baturin, 1982; Benninger and Hein, 2000). Most of these phosphate nodule accumulations are deposits older than the Holocene that formed on the seafloor more than 700,000 years ago (Kolodny and Kaplan, 1970). Some modern phosphate nodules are now forming on the ocean floor in a few places such as the Peru–Chile continental margin (Burnett and Froelich,

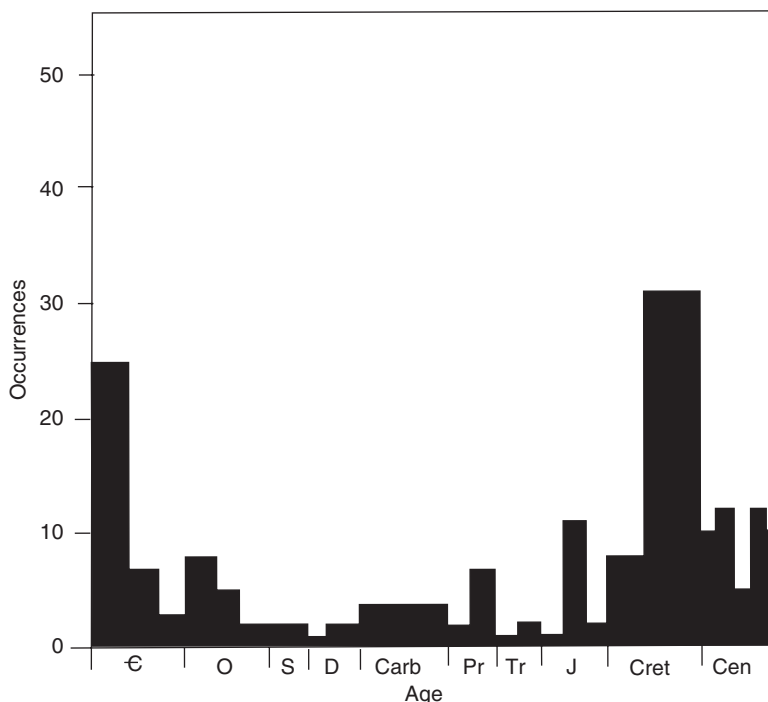


Figure 12.30 Histogram of the stratigraphic distribution of Phanerozoic phosphorites. (After Van Houten, F. B., 2000, Ooidal ironstones and phosphorites – A comparison from a stratigrapher’s view, in Glenn, C. R., L. Prévôt-Lucas, and J. Lucas (eds.), *Marine Authigenesis: From Global to Microbial*: SEPM Special Publication 66, Fig. 1, p. 127. Reprinted by permission of the Society for Sedimentary Geology, Tulsa, OK.)

1988) and the Nambian shelf off southwest Africa (Baturin, 2000). Holocene-age phosphate nodules have also been reported from estuarine environments (Cullen *et al.*, 1990).

12.5.3 Stratigraphic characteristics

In ancient phosphorite deposits, phosphate-rich layers typically occur interbedded with carbonate rocks, mudrocks, or chert. A characteristic feature of many major phosphorite accumulations is the triple association of phosphate, chert, and sediments containing abundant organic carbon. The phosphatic beds of some deposits are lenticular over short distances, whereas others are very uniform in lithology and thickness over hundreds of square kilometers. Phosphatic rocks commonly grade regionally into nonphosphatic sedimentary rocks of the same age.

One of the best-studied examples of an ancient phosphorite deposit is the Permian-age Phosphoria Formation of western Wyoming and Idaho (Fig. 12.32). This formation is several hundred meters thick. Phosphatic members of the formation reach

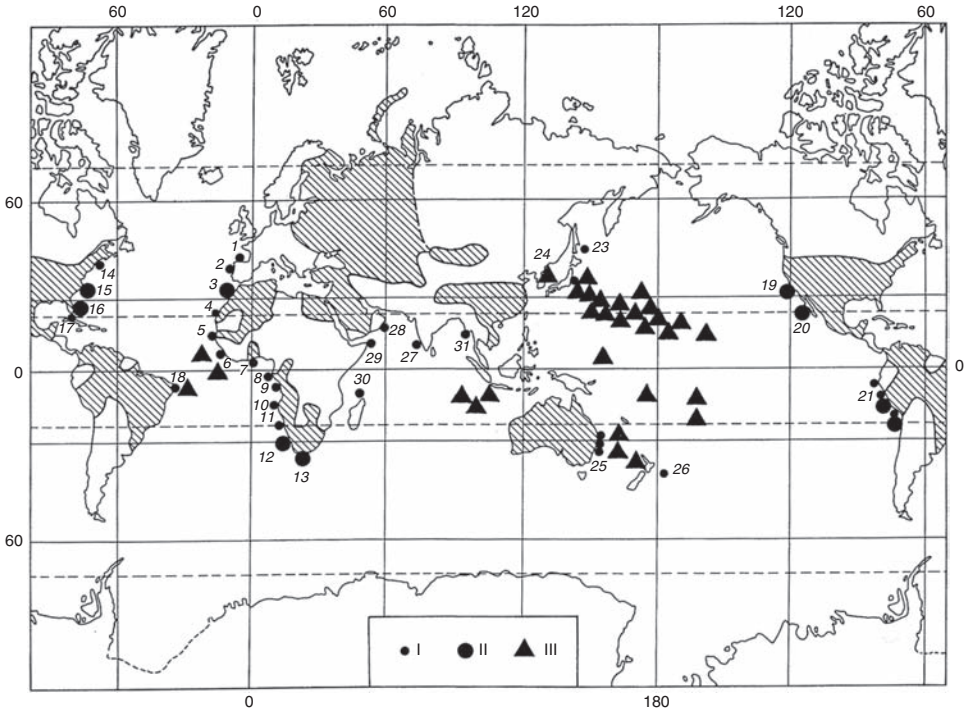


Figure 12.31 Distribution of phosphorites over the world ocean. I isolated samples and small occurrences of phosphorites; II significant resources of phosphorites; III phosphorites on subsea mountains (seamounts). Numbers refer to specific localities on continental margins, shelves, and slopes. Hatched areas may have considerable phosphorite resources on land. (From Baturin, G.N., 1998, Phosphorites, in Marfunin, A. S. (ed.), *Advanced Mineralogy*: Springer-Verlag, Berlin, vol. 3, Fig. 57, p. 228, reproduced by permission.)

30–35 m in thickness and cover an area of thousands of square kilometers. Additional information about the stratigraphic characteristics of major phosphate deposits of the world is available in Notholt *et al.* (1989) and Glenn *et al.* (2000).

12.5.4 Composition of phosphorites

Sedimentary phosphates are composed of phosphate minerals, all of which are varieties of apatite. The principal varieties are fluorapatite $[\text{Ca}_5(\text{PO}_4)_3\text{F}]$, chlorapatite $[\text{Ca}_5(\text{PO}_4)_3\text{Cl}]$, and hydroxyapatite $[\text{Ca}_5(\text{PO}_4)_3\text{OH}]$. Most sedimentary phosphates are carbonate hydroxyl fluorapatites in which up to 10 percent carbonate ions can be substituted for phosphate ions to yield the general formula $\text{Ca}_{10}(\text{PO}_4, \text{CO}_3)_6\text{F}_{2-3}$. Many other substitutions of both cations and anions in the fluorapatite structure are possible. See Nathan (1984), McClellan and Van Kauwenbergh (1990), and Knudsen and Gunter (2002) for additional details. These carbonate hydroxyl fluorapatites are commonly called **francolite**. Although more than 300 phosphate minerals are known, francolite is virtually the only phosphate mineral that occurs in unweathered marine

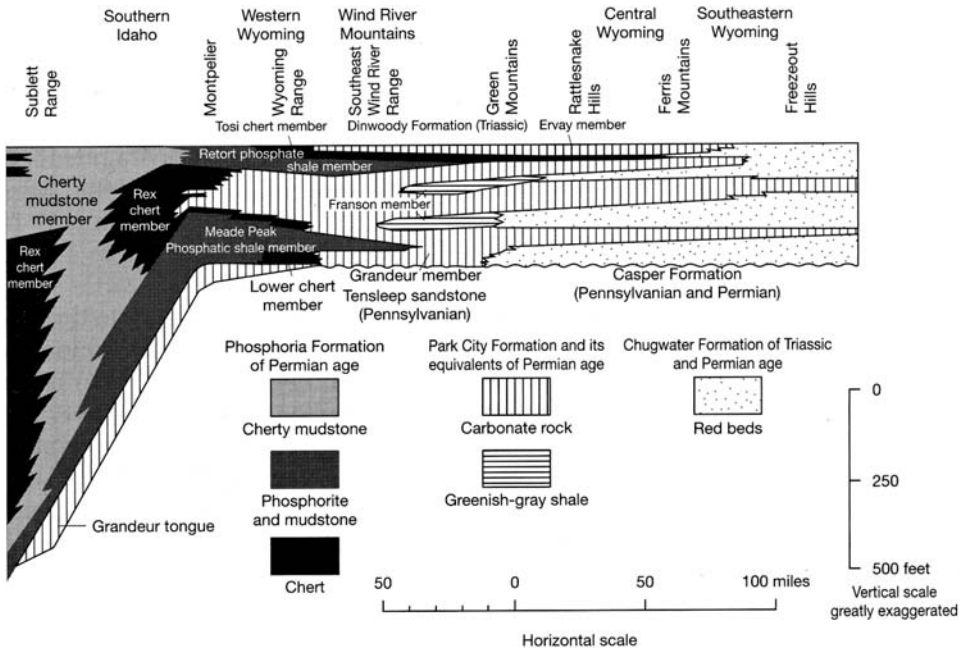


Figure 12.32 Stratigraphic relations of the phosphatic Phosphoria Formation (Permian), Park City Formation (Permian), and Chugwater Formation (Triassic) of Idaho and Wyoming. Note in particular the Retort phosphatic shale member and the Meade Peak phosphatic shale member. (After Sheldon, R. P., 1989, Phosphorite formations, western United States, in Northolt A. J. G., R. P. Sheldon, and D. F. Davidson (eds.), *Phosphate Deposits of the World*, 2: Cambridge University Press, Cambridge, Fig. 8.1, p. 54, reproduced by permission.)

phosphorites. Note: francolite is not a formal mineral name; some workers prefer to use the name **carbonate-fluorapatite** (CAF) instead. The wastebasket term **collophane** is often used for sedimentary apatites for which the exact chemical composition has not been determined.

Phosphorites commonly also contain some detrital quartz and authigenic chert. Opal-CT may also be present. The common association of cherts, carbonates, and organic-rich shales with phosphorites has already been mentioned. Both calcite and dolomite may occur in phosphorites, and dolomite may be particularly abundant. Glauconite, illite, montmorillonite, and zeolites, especially clinoptilolite, may also be present in some deposits. Organic matter is a characteristic constituent of many phosphorites (Nathan, 1984).

The chemistry of phosphorites is dominated by phosphorus, silicon (which is present in minerals other than apatite), and calcium. Slansky (1986, p. 70) shows that the abundance of these elements in 20 phosphorites ranging in age from Precambrian to Holocene is $P_2O_5 = 22\text{--}39$ percent; $SiO_2 = <1\text{--}25$ percent, and $CaO = 43\text{--}53$ percent. Other common constituents include Al_2O_3 ($<1\text{--}5$ percent); Fe_2O_3 ($<1\text{--}4$ percent); MgO ($<1\text{--}6$ percent); Na_2O (<1 percent); K_2O (<1 percent); F ($1\text{--}4$ percent); Cl (<1 percent); SO_3 ($0\text{--}11$ percent); and organic carbon ($0\text{--}2$ percent). Many trace elements, such as Ag, Cd, Mo, Se, Sr, U, Yu, Zn,

as well as the rare-earth elements may also be present in phosphorites in amounts commonly exceeding their average compositions in seawater, the crust, and the average shale (Nathan, 1984). See also Notholt *et al.* (1989) and McClellan and Van Kauwenbergh (1990).

12.5.5 Petrographic characteristics and classification of phosphates

Phosphorites have textures that resemble those in limestones. Thus, they may contain ooids, peloids, fossils (bioclasts), and clasts. These grains are, of course, composed of apatite rather than calcite. Some phosphorites lack distinctive granular textures and are composed instead of fine, micrite-like, textureless colophane. Cook (1976) refers to this kind of phosphorite as **phospholuite**. Sedimentary apatites are quite commonly cryptocrystalline; that is, the crystals are too small to be visible under the petrographic microscope. Thus, in polarized light they appear as brownish isotropic material; however, when crystal size increases above a few micrometers their birefringence appears (Slansky, 1986, p. 41). Phosphatic grains such as pellets may contain inclusions of organic matter, clay minerals, silt-size detrital grains, and pyrite. The abundant organic matter in phosphorites contributes to their color, which is commonly dark brown to black.

Peloidal or pelletal phosphorites are particularly common, e.g. the phosphates of the Permian Phosphoria Formation, USA (Sheldon, 1989), and many other phosphorite deposits. Some peloids are essentially structureless (e.g. Fig. 12.33), whereas others contain a nucleus of some type. Still others are compound, grapestone-like particles. Some peloids

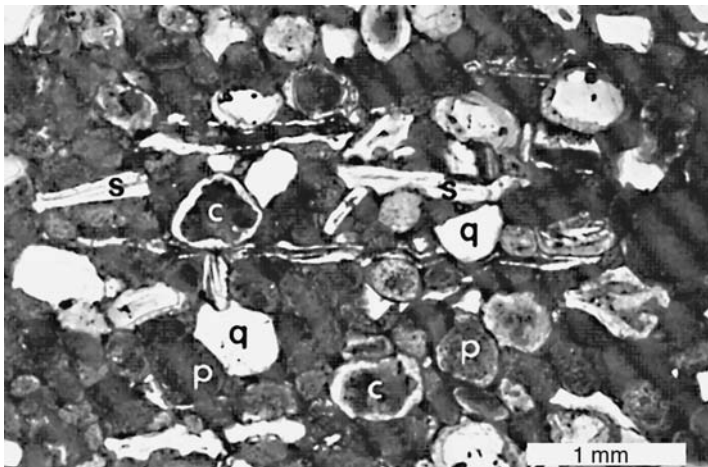


Figure 12.33 Thin-section photomicrograph (crossed nicols) of quartz-bearing phosphorite from the Meade Peak Formation (Permian) of Utah. c = phosphatic coated grains, s = abundant phosphatic shelly debris, p = phosphatic peloids, and q = reworked quartz. [From Hendrix, M. S. and C. W. Beyers, 2000, Stratigraphy and sedimentology of Permian strata, Uinta Mountains, Utah: Allostratigraphic controls on the accumulation of economic phosphate, in Glenn, C. R., L. Prévôt-Lucas, and J. Lucas (eds.), *Marine Authigenesis: From Global to Microbial*: SEPM Special Publication 66, Fig. 4D, p. 355, reproduced by permission of the Society for Sedimentary Geology, Tulsa, OK.]

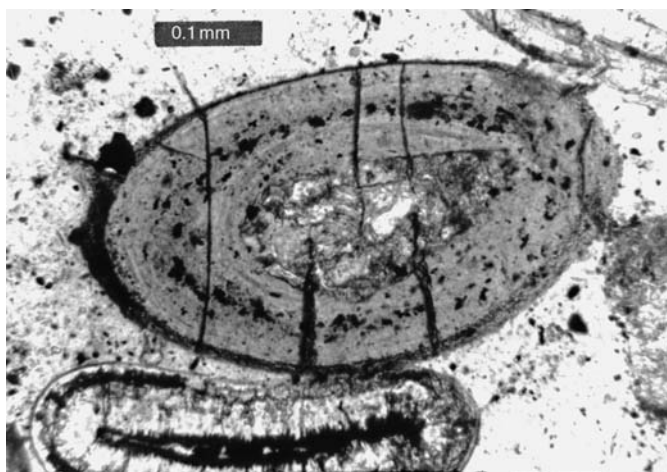


Figure 12.34 Brown-colored, phosphatic ooid in a phosphorite. Phosphoria Formation (Permian), northern Rocky Mountains. Plane-polarized light.

may be of fecal origin (i.e. they are fecal pellets); however, such an origin apparently remains uncertain. Peloids may contain various kinds of fossils such as foraminiferal or radiolarian tests, as well as quartz, clay minerals, and organic matter, as mentioned. Peloidal phosphates may also include ooids that contain a nucleus and display well-developed concentric layering (Fig. 12.34). Ooids are less common in phosphorites than peloids but may make up most of the phosphatized grains in some deposits, e.g. phosphatic ooids in the Lower Jurassic of central England (Horton *et al.*, 1980). Phosphatized fossils or fragments of originally phosphatic shells (Fig. 12.33) may in some cases form a significant part of phosphorite deposits. Fossils may include both invertebrate and vertebrate remains. Lithoclasts consisting of reworked fragments of pre-existing phosphorites also occur in some deposits, e.g. Miocene phosphorites of Florida (Riggs, 1980).

Most grains in phosphorites are sand size; however, particles greater than 2 mm may occur. These large grains are commonly referred to as nodules and can range in size from 2 mm to several tens of centimeters. Like nodules in limestones, they can be spherical, lenticular, or flattened parallel to bedding.

No scheme for naming and classifying of phosphorites on the basis of texture appears to be in wide use at this time. Because phosphorites have textures similar to those in limestones (e.g. peloidal, oolitic, fossiliferous), some geologists have suggested using modified limestone classifications to distinguish different kinds of phosphorites. Slansky (1986) advocated using a classification system based, to some extent, on Folk's (1962) limestone classification. Cook and Shergold (1986) and Trappe (2001) suggested adopting Dunham's (1962) carbonate classification (modified by Embry and Klován, 1971). Use of these modified carbonate classification schemes yields names such as **wackestone phosphorite** (Cook and Shergold) and **phosclast wackestone** (Trappe) – names that don't exactly trip off the tongue.

12.5.6 Principal kinds of phosphate deposits

In addition to petrographic classification, phosphorite deposits can be divided into groups on the basis of bedding characteristics and the principal types of phosphate materials that make up the deposits. Five principal groups have been identified:

1. **Bedded phosphorites** form distinct beds of variable thickness, commonly interbedded and interfingering with carbonaceous mudrocks, cherts, and carbonate rocks. The phosphorite occurs as peloids, ooids, pisoids, phosphatized fossils and skeletal fragments, and cements. A classic example of a bedded phosphate deposit is the Permian Phosphoria Formation of the northwestern United States (Fig. 12.32). This formation has a total thickness of 420 m and extends over an area of about 350,000 km² (McKelvey *et al.*, 1959; Sheldon, 1989; Herring, 1995). Bedded phosphates are believed to form in shelf areas associated with zones of upwelling in the ocean.
2. **Bioclastic phosphorites** are a special type of bedded phosphate deposit composed largely of vertebrate skeletal fragments such as fish bones, shark teeth, fish scales, coprolites, etc. The Rhaetic Bone Bed (Upper Triassic) of western England (Greensmith, 1989, p. 213) provides an example. Deposits composed mainly of invertebrate fossil remains such as phosphatized bivalve shells are also known. These phosphate-bearing organic materials commonly become further enriched in P₂O₅ during diagenesis and may be cemented by phosphate minerals. See, for example, Schwennicke *et al.* (2000).
3. **Nodular phosphates** are brownish to black, spherical to irregular-shaped nodules ranging in size from a few centimeters to a meter or more. Internal structure of phosphate nodules ranges from homogeneous (structureless) to layered or concentrically banded. Phosphatic grains, pellets, shark teeth, and other fossils may occur within the nodules. Phosphate nodules are particularly common in many Neogene to Holocene deposits of the world (Burnette and Riggs, 1990). They are forming today in zones of upwelling in the ocean, e.g. the Peru continental margin (Burnett and Froelich, 1988) and the upper west Florida slope (Fountain and McClellan, 2000). Some ancient phosphorite nodules may be of diagenetic origin, and some are relict features of disconformity and unconformity surfaces.
4. **Pebble-bed phosphorites** are composed of phosphatic nodules, phosphatized limestone fragments, or phosphatic fossils that have been mechanically concentrated by reworking of earlier-formed phosphate deposits. A good example of this type of deposit is the Miocene and Quaternary river-pebble and land-pebble deposits of Florida (Cathcart, 1989).
5. **Guano deposits** are composed of the excrement of birds and possibly bats that has been leached to form an insoluble residue of calcium phosphate. Guano occurs today on small oceanic islands in the Eastern Pacific and the West Indies. Guano deposits are not important in the geologic record.

12.5.7 Deposition of phosphorites

Chemical and biochemical processes

As mentioned, the principal phosphate minerals in sedimentary rocks are various varieties of carbonate-apatites, of which carbonate-fluorapatite (CAF) is most common. The conditions that favor precipitation of calcium carbonate also favor formation of carbonate-apatite, although carbonate-apatite can precipitate at values of pH possibly as low as 7.0 whereas calcium carbonates generally do not precipitate below a pH of about 7.5 (Bentor, 1980).

Carbonate-apatite precipitation also appears to be favored by slightly reducing conditions. The factors affecting phosphate solubility are not thoroughly understood, however, and the solubility of carbonate-apatite has not been definitely established. It is not definitely known if the ocean is saturated with carbonate-apatite, although it is believed that it is very near saturation (Kolodny, 1981). The average concentration of phosphorus in the ocean is 70 ppb (parts per billion) (Gulbrandsen and Roberson, 1973) compared to 20 ppb in average riverwater. The concentration of phosphorus in ocean water ranges from only a few ppb in surface waters, which are strongly depleted by biologic uptake, to values of 50–100 ppb at depths greater than about 200–400 m.

Phosphorus is removed from seawater in several ways. Some phosphorus is precipitated along with calcium carbonate minerals during deposition of limestones; however, the average limestone contains only about 0.04 percent P_2O_5 . Phosphorus is also removed from ocean water by concentration in the tissues of organisms, but this phosphorus is returned to the ocean when organisms die unless they are quickly buried by sediment before decay of the organic tissue is complete. Some phosphorus may be removed from seawater by incorporation into metalliferous sediments as a result of adsorption onto metallic minerals such as iron hydroxides. Finally, phosphorus is removed from ocean water in some manner to form marine apatite deposits. We are particularly interested in this last process because the major problem associated with phosphorite deposition is identifying a mechanism that can explain how trace amounts of phosphorus in seawater can be concentrated to form phosphorite deposits.

A secondary or replacement origin has been suggested for some phosphorite deposits to account for this enrichment. On the other hand, the preservation in many other phosphorite deposits of clastic textures and primary sedimentary structures such as cross-bedding and laminations indicates that these sediments are primary deposits. Several geologists who made early studies of phosphorite deposits suggested an association between phosphorite deposition and areas of upwelling in the oceans. (Upwelling brings nutrient-rich cold water from deeper parts of the ocean up into near-surface waters.) Studies of the distribution of ancient phosphorites show that most occur in lower latitudes in the trade-wind belts along one side of a basin where deeper water could have upwelled adjacent to a continent. Most phosphate nodule deposits on the modern ocean floor (Fig. 12.31) also occur in areas of upwelling.

Early ideas on upwelling and phosphorite deposition assumed that inorganic precipitation of apatite occurred as cold, deep, phosphate-rich waters welled up onto a shallow shelf. Under these postulated conditions, carbon dioxide would be lost from the upwelling waters owing to pressure decrease, warming, or photosynthesis, causing pH to increase and carbonate-apatite precipitation to occur. It has now been suggested, however, that Mg^{2+} ions in seawater have an inhibiting effect on the growth of carbonate-apatite crystals in much the same way that they inhibit the precipitation of calcite (Martens and Harris, 1970). Inhibition is caused by the smaller Mg^{2+} ion replacing Ca^{2+} in the apatite structure. On the other hand, Gulbrandsen *et al.* (1984) demonstrated that given enough time, seven years in their experiment, apatite could crystallize from solutions containing Mg^{2+} , raising some

question about the efficacy of Mg^{2+} inhibition under natural conditions. Also, most or all of the phosphorus brought to surface waters by upwelling currents is quickly used up by organisms that utilize phosphate as one of the essential nutrients needed for organic growth. Rapid biologic utilization prevents phosphate levels in the ocean from rising to the point of saturation. This factor, together with possible Mg^{2+} inhibition, seems to rule out the direct inorganic precipitation of apatite from open-ocean water as a major process in phosphogenesis.

Nonetheless, biologic utilization of phosphate to build soft body tissue appears to provide the answer to the problem of phosphate concentration in sediments. Modern phosphate nodules are forming in areas of oceanic upwelling where a steady supply of phosphate brought from the large deep-ocean reservoir allows continuous growth of organisms in large numbers. After death, organisms and organic debris not consumed by scavengers pile up on the ocean floor under reducing conditions where decay is inhibited. These organic materials include the remains of phytoplankton and zooplankton, coprolites (feces), and the bones and scales of fish. Under the toxic, reducing conditions of the seafloor, some of the soft body tissue is thus preserved long enough to be buried and incorporated into accumulating sediment. Perhaps about 1–2 percent of the total phosphorus involved in primary productivity in upwelling zones is ultimately incorporated into the sediments in this way (Baturin, 1982).

Slow decay of body tissue after burial, probably aided by bacterial processes, releases phosphorus to the interstitial waters of the sediment. Studies of the chemistry of interstitial waters in sediments where modern phosphate nodules are forming, and in other areas of the seafloor where organic-rich sediments are accumulating under reducing conditions, have turned up phosphorus concentrations in the interstitial waters of these sediments ranging from 1400 ppb to as much as 7500 ppb (Bentor, 1980; Froelich *et al.*, 1988). At such high concentrations of phosphorus in interstitial waters, the waters are supersaturated with respect to calcium phosphate. The phosphate thus begins to precipitate out on the surface of siliceous organisms, carbonate grains, particles of organic matter, fish scales and bones, siliciclastic mineral grains, or older phosphate particles (Baturin, 1982). Phosphorite nodules thus form **within** the sediments by diagenetic reactions between organic-rich sediments and their phosphate-enriched interstitial waters.

Froelich *et al.* (1988) report that carbonate-fluorapatite is precipitating from pore waters in the upper few centimeters of organic-carbon-rich muds on the Peru continental margin. They suggest that the mechanism of phosphate release may be linked to dissolution of fish debris or the presence of microbial mats in surficial sediments. Magnesium concentrations in the pore waters are nearly the same as that of seawater. Thus, for reasons that are poorly understood, magnesium depletion is apparently not a prerequisite for carbonate-fluorapatite precipitation in these sediments. In the Peru continental-margin sediments, phosphatic minerals precipitate only at very shallow depths. Below a depth of a few centimeters, excessive carbonate-ion concentration and diminished reactive iron and sulfate compositions favor dolomite formation, and preclude further precipitation of phosphatic minerals (Glenn and Arthur, 1988). Glenn and Arthur suggest that precipitation of phosphatic

minerals in the Peru sediments may be influenced in some poorly understood way by filamentous bacteria and chemical absorption of clays into organic compounds.

Phosphatized bacterial remains have been reported in phosphorites by several investigators (e.g. Lamboy, 1990), raising the possibility that bacteria play some direct role in the origin of phosphorites. Baturin (2000) states that “phosphatization seems impossible without bacterial participation,” however, he suggests that the role of bacteria is not in the direct precipitation of phosphate. Rather, the bacteria act to decompose organic material, reduce sulfate, and mobilize soluble phosphate. “Enrichment of dissolved phosphate is the main prerequisite for phosphate deposition and diagenetic accretion.”

Physical processes in deposition

The presence of clastic textures and primary depositional sedimentary structures in some phosphorite deposits seems inconsistent with this proposed diagenetic concentration mechanism. Therefore, Kolodny (1980) suggested a two-stage process for the origin of ancient phosphorite deposits. In the first stage, apatite forms diagenetically in stagnant, reducing basins by phosphorus mobilization in interstitial waters in the manner postulated for formation of modern phosphate nodules. The final stage involves reworking and enrichment of these diagenetically formed nodules by mechanical concentration processes. This stage is characterized by oxidizing conditions, and concentration presumably takes place in a high-energy environment during lower stands of sea level. This final stage, during which the original diagenetically formed phosphorite sediments are mechanically reworked under shallow-water conditions, accounts for the clastic textures and primary sedimentary structures found in many ancient phosphorites.

Support for this concept of mechanical concentration is provided by Glenn and Arthur (1990) in a study of major phosphorite deposits of Egypt. They report that phosphorite grains that were precipitated initially in reducing shales have been mechanically reworked and concentrated. Reworking occurred as a result of sea-level fall and delta progradation. Further, phosphorites in some of the deposits were concentrated into giant phosphorite sand waves owing to storm waves and tidal processes.

In summary, upwelling of phosphate-rich waters from deeper parts of the ocean and biologic utilization of the phosphate in soft body tissue appear to be important factors in the origin of phosphorite deposits. Phosphorus is deposited on the seafloor in organic detritus and buried with accumulating sediment. Phosphate becomes concentrated in the pore waters of sediment during slow decay of the phosphate-bearing, soft-bodied organisms and other organic detritus. Carbonate-apatite precipitates diagenetically from these phosphate-enriched pore waters by some process not yet fully understood to form gel-like, gradually hardening, phosphate concretions. Subsequently, these diagenetic deposits are reworked mechanically owing to lowered sea levels, allowing final concentration and deposition of phosphatic sediments by waves and currents. These processes are summarized diagrammatically in Fig. 12.35.

Other models

This postulated cold- and deep-water upwelling model for formation of phosphorite deposits is a plausible hypothesis, but it has some flaws. It does not, for example, explain why phosphorites

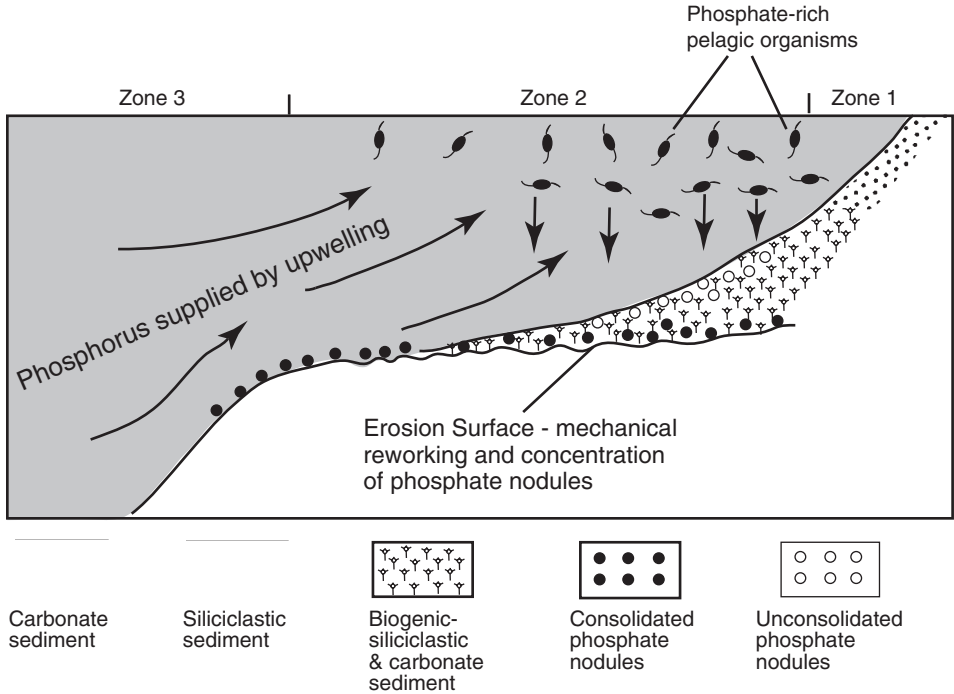


Figure 12.35 Schematic illustration of phosphorite deposition in areas of upwelling on open ocean shelves. Near-shore, shallow-water siliciclastic deposits form in Zone 1. Zone 2 is the zone where high contents of phosphate-rich biogenic detritus accumulate in sediments owing to deposition of pelagic organisms; phosphate nodules form in this zone by diagenetic processes, followed by reworking of phosphate-rich sediments during lowered sea level. Zone 3 is a deeper-water zone of carbonate sediments with local phosphate nodules. (After Baturin, G. N., 1982, *Phosphorites on the SeaFloor: Origin, Composition, and Distribution*: Elsevier, Amsterdam, Fig. 5.4, p. 227, reprinted by permission.)

accumulated on a much vaster scale at some times in the geologic past than at present. Bentor (1980) postulates that some additional mechanism, not realized or understood at the present time, may have been important in the past. Hiatt and Budd (2003) suggest that the cold- and deep-water model is not feasible to explain the giant phosphorus deposits in the Permian Phosphoria Formation of the western USA (Fig. 12.32). Instead, they propose a model that visualizes deposition of phosphorite in shallow-shelf areas (water depths < 200 m to very shallow). An oxygen-depleted, nutrient-rich, intermediate water mass (rather than a deep-water mass) entered the Phosphoria Sea and was driven to the surface and seaward by coastal upwelling. High biological productivity in mid-shelf position caused high organic particulate flux to the seafloor, where bacterial respiration consumed all dissolved oxygen. Regeneration of phosphorus provided a supply of nutrients to inner-shelf settings where phosphogenesis occurred under low-oxygen conditions.

Research on the origin of phosphorites is still very much in a state of flux. Interested readers may wish to consult some of the additional phosphorite readings suggested below.

Further reading***Evaporites***

- Busson, G. and B. C. Schreiber (eds.), 1997, *Sedimentary Deposition in Rift and Foreland Basins in France and Spain*: Columbia University Press, New York, NY. (Focus primarily on evaporites.)
- Melvin, J. L. (ed.), 1991, *Evaporites, Petroleum and Mineral Resources*: Elsevier, Amsterdam.
- Schreiber, B. C. (ed.), 1988, *Evaporites and Hydrocarbons*: Columbia University Press, New York, NY.
- Usdowski, E. and M. Dietzel, 1998, *Atlas and Data of Solid-Solution Equilibria of Marine Evaporites*: Springer-Verlag, Berlin.
- Warren, J., 1999, *Evaporites: Their Evolution and Economics*: Blackwell Science, Oxford.
- Warren, J., 2006, *Evaporites: Sediments, Resources, and Hydrocarbons*: Springer-Verlag, Berlin.

Siliceous sedimentary rocks

- Heaney, P. J., C. T. Prewitt, and G. V. Gibbs (eds.), 1994, *Silica: Physical Behavior, Geochemistry and Materials Applications*: Mineralogical Society of America Reviews in Mineralogy 29.
- Hein, J. R. (ed.), 1987, *Siliceous Sedimentary Rock-Hosted Ores and Petroleum*: Van Nostrand Reinhold, New York, NY.
- Hein, J. R. and J. Obradović (eds.), 1989, *Siliceous Deposits of the Tethys and Pacific Regions*: Springer-Verlag, New York, NY.
- Iijima, A., J. R. Hein, and R. Siever (eds.), 1983, *Siliceous Deposits in the Pacific Region*: Developments in Sedimentology 36.
- Lowe, D. R. and G. R. Byerly, 1999, *Geologic Evolution of the Barberton Greenstone Belt*: South Africa Geological Society of America Special Paper 329 (includes several papers that discuss Precambrian chert.)

Iron-rich sedimentary rocks

- Appel, P. W. U. and G. L. LaBerge, 1987, *Precambrian Iron-Formations*: Theophrastus Publications, Athens.
- Kesler, S. E. and H. Ohmoto (eds.), 2006, *Evolution of Early Earth's Atmosphere, Hydrosphere, and Biosphere – Constraints from Ore Deposits*: Geological Society of America Memoir 198. See chs. 13–17.
- Melnik, Y. P., 1982, *Precambrian Banded Iron-Formations*: Developments in Precambrian Geology 5. (Translated from the Russian by Dorothy B. Vitaliano.)
- Misra, K. C., 2000, *Understanding Mineral Deposits*: Kluwer, Dordrecht,. See ch. 15.
- Petránek, J. and F. B. Van Houten, 1997, *Phanerozoic Ooidal Ironstones*: Czech Geological Survey Special Paper 7.
- Trendall, A. F. and R. C. Morris (eds.), 1983, *Iron-Formation Facts and Problems*: Developments in Precambrian Geology 6.
- Van Houten, F. B. and D. P. Bhattacharyya, 1982, Phanerozoic oolitic ironstone – Facies models and distribution in space and time: *Rev. Earth Planet. Sci.*, **10**.
- Young, T. P. and W. E. G. Taylor (eds), 1989, *Phanerozoic Ironstones*: Geological Society Special Publication 46.

Phosphorites

- Baturin, G. N. and C. W. Finkl, Jr., 1982, *Phosphorites on the Sea Floor; Origin Composition and Distribution*: Developments in Sedimentology 33 (Translated from the Russian by Dorothy B. Vitaliano.)
- Bentor, Y. K. (ed.), 1980, *Marine Phosphorites: Geochemistry, Occurrence, Genesis*: SEPM Special Publication 29.
- Burnett, W. C. and P. N. Froelich (eds., special issue), 1988, The origin of marine phosphorites: The results of the R. V. Robert D. Conrad Cruise 23–06 to the Peru shelf: *Mari. Geol.*, **80**, 181–346.
- Burnett, W. C. and S. R. Riggs (eds.), 1990, *Phosphate Deposits of the World, 3: Neogene to Modern Phosphorites*: Cambridge University Press, Cambridge.
- Cook, P. J. and J. H. Shergold (eds.), 1986, *Phosphate Deposits of the World, 1: Proterozoic and Cambrian Phosphorites*: Cambridge University Press, Cambridge.
- Glenn, C. R., L. Prévôt-Lucas, and J. Lucas (eds.), 2000, *Marine Authigenesis: From Global to Microbial*: Society for Sedimentary Geology Special Publication 66 (Contains numerous papers devoted to phosphorites.)
- Kohn, M. J., J. Rakovan, and J. M. Hughes (eds.), 2002, *Phosphates: Geochemical, Geobiological, and Material Importance*: Reviews in Mineralogy and Geochemistry 36.
- Northolt, A. J. G., R. P. Sheldon, and D. F. Davidson (eds.), 1989, *Phosphate Deposits of the World, 2: Phosphate Rock Resources*: Cambridge University Press, Cambridge.
- Northolt, A. J. G. and I. Jarvis (eds.), 1990, *Phosphorite Research and Development*: The Geological Society of London, Bath.
- Slansky, M., 1986, *Geology of Sedimentary Phosphates*: North Oxford Academic Publishers, London.

13

Carbonaceous sedimentary rocks

13.1 Introduction

Most sedimentary rocks, including rocks of Precambrian age, contain at least a small amount of organic matter consisting of the preserved residue of plant or animal tissue. The average content of organic matter in sedimentary rocks is about 2.1 weight percent in mudrocks, 0.29 percent in limestones, and 0.05 percent in sandstones (Degens, 1965). The average in all sedimentary rocks is about 1.5 percent. Organic matter contains about 50–60 percent carbon; therefore, the average sedimentary rock contains about 1 percent organic carbon. A few special types of sedimentary rocks have significantly more organic material than these average rocks. Black shales and other organic-rich and bituminous mudrocks typically contain 3 to 10 or more percent by weight of organic matter. Some oil shales contain even higher percentages, ranging to 25 percent or more, and coals may be composed of more than 70 percent organic matter. Certain solid hydrocarbon accumulations, such as asphalt and bitumen deposits formed from petroleum by oxidation and loss of volatiles, constitute another example of a sedimentary deposit greatly enriched in organic carbon. In fact, even liquid petroleum can be thought of as a special kind of organic-rich deposit although it is clearly not rock. Sedimentary rocks containing significant enrichment in organic matter over average sediments are called carbonaceous sedimentary rocks. The amount of organic matter required to designate a sediment as carbonaceous is not firmly established. Shales or carbonate rocks with at least 10 percent organic matter are probably called carbonaceous sedimentary rocks by many geologists, and rocks with 3–10 percent organic matter are regarded as organic rich. The carbon in carbonaceous sedimentary rocks is believed to be almost entirely of organic origin, although a few scientists maintain that petroleum may originate by inorganic processes.

The overall abundance of carbonaceous sedimentary rocks is not accurately known, although the volume of economically significant carbonaceous rocks is probably less than 1 percent of the total sediment volume. These rocks are, however, extremely valuable. Most kinds of highly organic-rich carbonaceous sediments are either currently exploited for fossil fuels, or they have potential value as an energy source. Currently, coal and petroleum (including natural gas) are the principal kinds of fossil fuels. Oil shales or kerogen shales contain significant volumes of organic matter that can be converted to petroleum through

heating. Oil shales may thus be exploited in the future as coal and petroleum resources diminish. Less organic-rich rocks, such as black shales that contain about 3–10 percent organic matter, currently have little economic potential.

In addition to their economic or potentially economic value, organic-rich sedimentary rocks have considerable scientific interest. The unusually high concentrations of organic matter in these rocks point toward some kind of exceptional environmental and sediment-burial conditions. It appears likely, for example, that anoxic conditions in the world's oceans that favored preservation of organic matter, may have been much more widespread during some periods in Earth's history than at present. Thus, the carbonaceous sedimentary rocks may provide valuable insight into Earth's paleoenvironments.

In this chapter, we examine briefly the distribution, characteristics, and origins of the major kinds of carbonaceous sedimentary rocks. Because of the extraordinary economic significance of these deposits, the literature on carbonaceous rocks is voluminous, particularly the literature concerning petroleum and coal. I make no attempt in this short chapter to provide comprehensive treatment of the occurrence and characteristics of coal, oil shale, and petroleum. Several references listed under Further reading provide interested readers with a starting point for further literature research.

13.2 Characteristics of organic matter in carbonaceous sedimentary rocks

13.2.1 *Principal kinds of organic matter*

Organic content of carbonaceous sedimentary rocks is the characteristic that particularly distinguishes them from other sedimentary rocks. Therefore, in the study of carbonaceous rocks, it is essential to develop some understanding of the physical and chemical attributes of this organic matter. Three basic kinds of organic matter accumulate in subaerial and subaqueous environments: humus, peat, and sapropel. Soil **humus** is plant organic matter that accumulates in soils to form a number of decay products such as humic and fulvic acids. Most soil humus is eventually oxidized and destroyed; thus, little is preserved in sedimentary rocks. **Peat** is also humic organic matter, but peat accumulates in freshwater or brackish-water swamps and bogs, where stagnant, anaerobic conditions prevent total oxidation and bacterial decay. Therefore, some peat that accumulates under these conditions can be preserved in sediments, e.g. in coals and shales. **Sapropel** is fine organic matter that accumulates subaqueously in lakes, lagoons, and marine basins where oxygen levels are moderately low. It consists largely of the remains of phytoplankton and zooplankton and of spores, pollen, and macerated fragments of higher plants.

It is often difficult to differentiate accurately between the types of organic matter found in ancient sediments, but both humic and sapropelic types are recognized. Humic organic matter is the chief constituent of most coals, although a few coals are composed of sapropel. The organic material that occurs in shales is sapropelic; however, it is so finely disseminated and altered that it is difficult to identify. The organic matter in shales is not the same as the original organic material deposited in the parent mud. The original organic material has been changed by a complex

diagenetic process involving chemical and biochemical degradation, yielding an insoluble organic substance called **kerogen**. Among other things, kerogen is believed to be the precursor material of petroleum, which is derived from kerogen by natural thermal or thermocatalytic cracking (Section 13.3.4). Kerogen is insoluble in both aqueous alkaline solvents and common organic solvents. Some organic material in sediments is soluble in and extractable by organic solvents. This material is called **bitumen**. In ancient shales, kerogen makes up 80 to 99 percent of the organic matter; the rest is bitumen (Tissot and Welte, 1984, p. 132).

13.2.2 Chemical structure of kerogen

Kerogen consists of masses of almost completely macerated organic debris, which is chiefly plant remains such as algae, spores, spore coats, pollen, resins, and waxes. The chemical structure of kerogen is complex. According to Tissot and Welte (1984, p. 148), the structure consists of nuclei cross-linked by chainlike bridges. The nuclei themselves consist of stacks, made up of two to four essentially parallel aromatic sheets, each containing less than 10 condensed aromatic rings (see Fig. 13.1 for an example of an aromatic ring). Some of the rings may be heterocycles containing nitrogen, sulfur, and possibly oxygen. A heterocyclic compound is one in which one or more of the carbon atoms in the ring are replaced by an atom of another element such as nitrogen, sulfur, or oxygen. The nuclei may also contain naphthenic rings, alkyl chains substituted on the aromatic rings, and various functional groups (Fig. 13.1). The bridges that are cross-linked to the nuclei may consist of a variety of organic structures, including linear or branched aliphatic chains, which are attached to the nuclei as substituents, and oxygen or sulfur functional groups such as ketones, esters, ethers, sulfides, and disulfides. Alkyl groups, which are formed from aliphatic chains by removal of a hydrogen atom, are commonly represented by the symbol R (Fig. 13.1). An aliphatic chain R may be combined with a functional group such as an ester to form part of a bridge structure. Also, various functional groups such as hydroxyl, carboxyl, or methoxyl may be substituted on nuclei or chains.

On the basis of chemical composition, Tissot and Welte (1984, p. 151) classify kerogen into three major types. **Type I kerogen** has high initial H/C and low O/C ratios. It is rich in aliphatic structures and thus in hydrogen. Algal kerogens belong in this group. **Type II kerogen** has relatively high H/C and low O/C ratios, but polyaromatic nuclei and heteroatomic ketone and carboxylic acid groups are more prevalent than they are in Type I kerogen. Ester bonds are important. Sulfur is present also in substantial amounts, located in heterocycles and as a sulfide bond. Type II kerogen is apparently derived from phytoplankton, zooplankton, bacteria, etc. deposited in marine environments under reducing conditions. **Type III kerogen** has relatively low initial H/C and high initial O/C ratios. Polyaromatic nuclei and heteroatomic ketone and carboxylic acid groups are more important than in Type II. No ester groups occur, but noncarbonyl oxygen may be included in ether bonds. Type III kerogen is believed to be derived mainly from terrestrial plants and contains much identifiable vegetal debris. Tissot and Welte (1984, p. 155) identify also a **residual type** of organic matter characterized by abnormally low H/C ratios associated with high O/C ratios. This type of organic matter has abundant aromatic nuclei and oxygen-containing

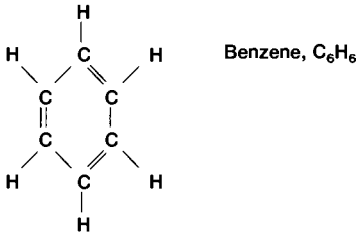
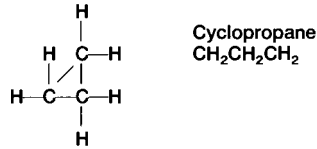
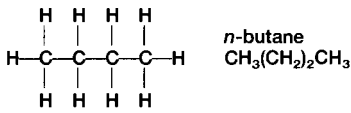
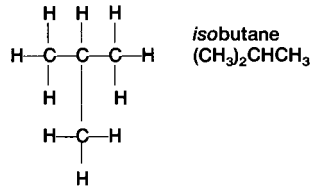
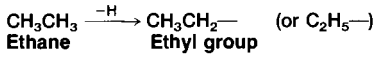
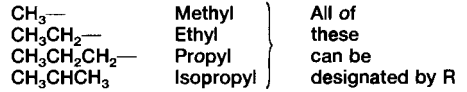
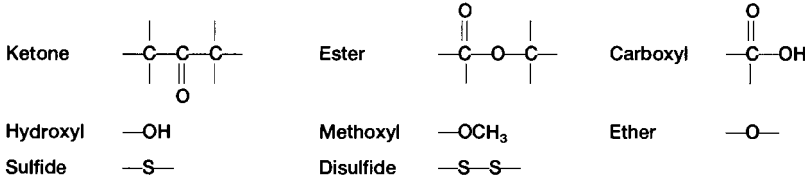
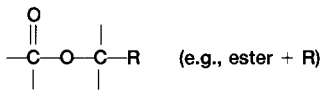
Aromatic ring**Napthenic ring****Linear aliphatic chain****Branched aliphatic chain****Alkyl group****Alkyl groups represented by symbol R****Functional groups****Aliphatic chain R with a functional group**

Figure 13.1 Examples of organic structural groups that may occur in kerogen. Note that alkyl groups are formed from aliphatic chains by removal of a hydrogen atom. For convenience, alkyl groups are often represented by the symbol R. A functional group such as an ester can be combined with an aliphatic chain R.

groups, but aliphatic chains are absent. It is characterized by coaly fragments of oxidized organic matter or charcoal. For additional discussion of kerogen, see Durand (1980), Hunt (1996), and Welte *et al.* (1997).

13.2.3 Elemental chemistry of organic matter

The elemental chemistry of organic matter is relatively simple. It consists dominantly of carbon, with lesser amounts of hydrogen, oxygen, nitrogen, and sulfur. Data shown in

Table 13.1 Average elemental composition of kerogen in shales from North America and Europe and the composition of coals from Germany and Yugoslavia

Kerogen type	Weight percent				
	C	H	O	N	S
Type I	78.8	8.8	7.7	2.0	2.7
Type II	77.8	6.8	10.5	2.2	2.7
Type III	82.5	4.6	10.5	2.1	0.2
C					
O Lignite	68.6	5.1	21.2	2.6	2.5
A Bituminous	88.3	5.0	3.9	2.0	0.8
L Anthracite	91.3	3.2	3.2	1.8	0.5

Source: Tissot and Welte, 1984, p. 141.

Table 13.1 suggest that the average weight percent carbon in typical kerogen ranges between about 78 and 83. Hydrogen abundance ranges from about 5 to 9 percent, oxygen from 8 to 11 percent, nitrogen about 2 percent, and sulfur from about 0.2 to 3 percent. Ranges among individual kerogens are greater than those shown by these average values.

Elemental composition is related to kerogen type and diagenetic history. Type I kerogen tends to be high in hydrogen and relatively low in oxygen, whereas Type III kerogen is high in oxygen and relatively low in hydrogen. Type II kerogen has high oxygen and intermediate hydrogen abundance. Thermal maturation or coalification of organic material results in a relative loss of oxygen and hydrogen and a relative enrichment in carbon.

13.2.4 Stable isotope chemistry

The elemental chemistry of organic matter provides some insight into the origin of kerogen, but it is not of significant value in evaluating the depositional environment or diagenetic history of the organic matter in carbonaceous sedimentary rocks. On the other hand, geologists and geochemists are showing growing interest in use of isotope geochemistry of organic matter as possible tools for characterizing organic matter and for analyzing its depositional and diagenetic history.

The general principles of isotope geochemistry are discussed briefly in Section 9.3. Potentially useful stable isotopes in the study of organic matter include those of carbon, oxygen, hydrogen, nitrogen, and sulfur. Carbon isotopes are expressed as $\delta^{13}\text{C}$ [the deviation in parts per mil (‰) of the ratio of $^{13}\text{C}/^{12}\text{C}$ in a sample compared to that of a standard]. Similarly, oxygen isotopes are expressed as $\delta^{18}\text{O}$ (ratio of $^{18}\text{O}/^{16}\text{O}$ in a sample compared to a standard), hydrogen isotopes are expressed as δD (ratio of $^2\text{D}/^1\text{H}$ in a sample compared to a standard, where D is deuterium), nitrogen is expressed as $\delta^{15}\text{N}$ (ratio of $^{15}\text{N}/^{14}\text{N}$ in a sample compared to a standard), and sulfur isotopes are expressed as $\delta^{34}\text{S}$ (ratio of $^{34}\text{S}/^{32}\text{S}$ in a sample compared to a standard).

Carbon isotopes are of particular interest owing to the possibility that they can be used for chemostratigraphic and environmental interpretations. A number of factors affect the reliability of such interpretations, however, including mixing of organic matter from different sources, sediment reworking, and thermal degradation during diagenesis (e.g. Popp *et al.*, 1997). Readers interested in isotope geochemistry are urged to consult additional references on this subject, such as Hoefs (2004) and Valley and Cole (2001).

13.3 Major kinds of carbonaceous sedimentary rocks

13.3.1 General statement

The dominant organic constituents of carbonaceous sediments are humic and sapropelic organic matter. The nonorganic constituents are either siliciclastic grains or carbonate materials. Carbonaceous sediments can be classified, on the basis of relative abundance of these constituents and the kinds of organic matter that compose the constituents (humic vs. sapropelic), into three basic types of organic-rich rocks: coal, oil shale, and asphaltic substances (Fig. 13.2). Asphaltic substances are formed from sapropelic organic material

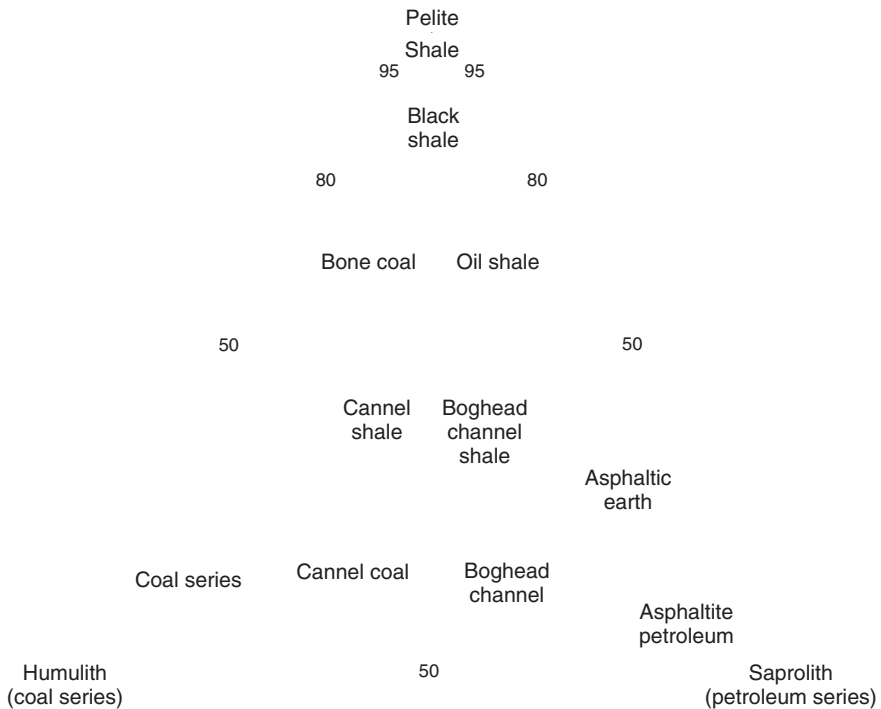


Figure 13.2 Classification and nomenclature of carbonaceous sediments on the basis of relative abundance of humic organic constituents (humulith), sapropelic organic constituents (saprolith), and fine-grained terrigenous constituents (pelite). (From Pettijohn, F. J., 1975, *Sedimentary Rocks*, 3rd edn.: Harper and Row, New York, NY. Fig. 11.37, p. 445, reprinted by permission.)

that has undergone a complex process of change and maturation during burial. The origin of petroleum and asphaltic substances is discussed in [Sections 13.3.4](#) and [13.3.5](#).

13.3.2 Coals

Nature and distribution

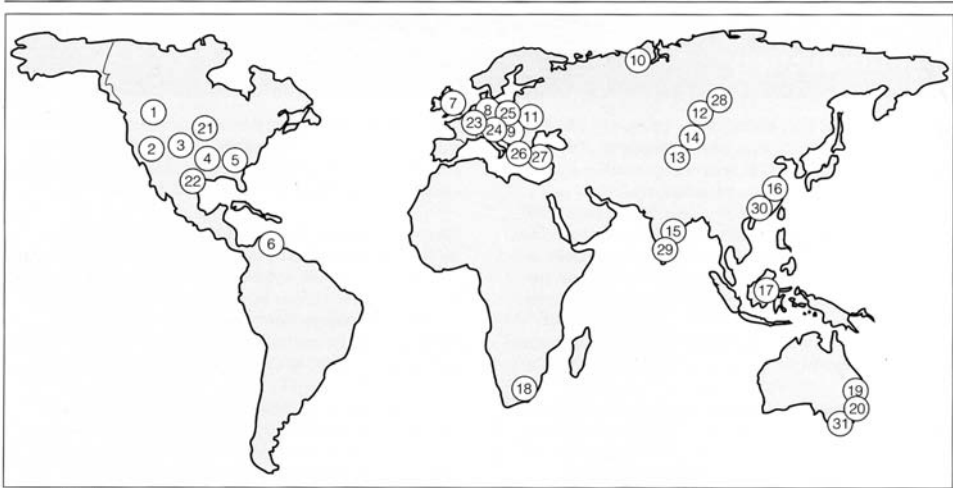
Coals are a carbon-rich type of carbonaceous sediment. They are composed dominantly of combustible organic matter but contain variable amounts of impurities (ash) that are largely siliciclastic materials. The amount of ash that coals can contain and still retain the name of coal is not precisely fixed. Some very impure coals (bone coals) may contain 70–80 percent ash, but most coals have less than 50 percent ash by weight. Most coals are humic coals, although a few are sapropelic coals that are made up mostly of spores, algae, and fine plant debris. Cannel coals and boghead coals are sapropelic coals. Coals are defined in various ways, but a commonly accepted definition is that of Schopf (1956).

Coal is a readily combustible rock containing more than 50 percent by weight and more than 70 percent by volume of carbonaceous material, formed from compaction or induration of variously altered plant remains similar to those of peaty deposits. Differences in the kinds of plant materials (type), in degree of metamorphism (rank), and range of impurities (grade), are characteristic of the varieties of coal.

Although the overall volume of coal is quite small, coals are widely distributed geographically. They occur in sedimentary rocks ranging in age from Precambrian to Tertiary, and peat analogs of coal occur in Quaternary sediments. Coal is reported in Precambrian rocks as old as 1700 million years in the Michigamme Slate of Michigan (Tyler *et al.*, 1957). This coal is probably algal coal. Coals did not become common until the development of woody land plants in the Devonian (Pettijohn, 1975, p. 451). The first extensive coal deposits occur in rocks of Carboniferous age. Throughout the world as a whole, coals occur in scattered localities in all of the post-Devonian geologic systems, although they tend to be more abundant in some systems, particularly the Carboniferous. In the United States, coals are most common in rocks of Pennsylvanian, Cretaceous, and Tertiary ages. Data compiled by Walker (2000) show that the major coal resources of the world occur in China, the United States, Russia, Germany, India, Australia, South Africa, and Poland. The remaining coal resources are scattered among about a dozen other countries of the world ([Fig. 13.3](#)).

Classification

Fourteen or more approaches to classification of coals are in use (Elliott and Yohe, 1981). Perhaps the most common and important method is classification by **rank** ([Table 13.2](#)), which is based on volatile matter and calorific value. Rank is a function of the degree of coalification or carbonification (increase in organic carbon) attained by a given coal owing to burial and metamorphism. **Peat** is often included in a tabulation of coals, but peat is

**Hard coal**

- 1 Western Canada
- 2 Western USA
- 3 Powder River basin, USA
- 4 Illinois basin, USA
- 5 Appalachia, USA
- 6 Guajira, Colombia
- 7 East Pennine, UK
- 8 Ruhr, Germany
- 9 Upper Silesia, Poland/Czech Republic
- 10 Pechora, Russia

- 11 Donetsk, Ukraine/Russia
- 12 Kuznetsk, Russia
- 13 Karaganda, Kazakhstan
- 14 Ekibastuz, Kazakhstan
- 15 Jharia/Raniganj, India
- 16 Eastern China
- 17 Kalimantan, Indonesia
- 18 Karoo, South Africa
- 19 Bowen basin, Australia
- 20 Sydney basin Australia

Lignite

- 21 Great Plains, USA/Canada
- 22 Gulf Coast, USA
- 23 Rhineland, Germany
- 24 Bohemia, Czech Republic
- 25 Poland
- 26 Greece
- 27 Turkey
- 28 Kansk-Achinsk, Russia
- 29 Neyveli, India
- 30 China
- 31 Victoria, Australia

Figure 13.3 Location of the world's major hard coal (bituminous, anthracite) and lignite basins. (From Walker, S., 2000, *Major Coalfields of the World: IEA Coal Research: The Clean Coal Centre, London*, Fig. 1, p. 8, reproduced by permission.)

actually not a true coal. Peat consists of unconsolidated, semicarbonized plant remains with high moisture content. **Lignite** or brown coal is the lowest-rank coal. Lignites are brown to brownish black coals that have high moisture content and commonly retain many of the structures of the original woody plant fragments. They are dominantly Cretaceous or Tertiary in age. **Bituminous coals** are hard, black coals that contain lower amounts of volatiles and less moisture than lignite and have a higher carbon content. They commonly display thin layers consisting of alternating bright and dull bands (Fig. 13.4). **Subbituminous** coal has properties intermediate between those of lignite and bituminous coal. **Anthracite** is a hard, black, dense coal that contains more than 90 percent carbon. It is a bright, shiny rock that breaks with conchoidal fracture, such as the fractures in broken glass. Bituminous coals and anthracite are largely of Mississippian and Pennsylvanian (Carboniferous) ages. **Cannel coal** and **boghead coal** are nonbanded, dull, black coals that also break with conchoidal fracture; however, they have bituminous rank and much higher volatile content than does anthracite. Cannel coal is composed of conspicuous percentages of spores. Boghead coals are composed dominantly of nonspore algal remains. **Bone coal** is very impure coal with high ash content.

Table 13.2 ASTM classification of coals by rank^A

Class	Group	Fixed carbon limits (percent)(dry, mineral-matter-free basis)		Volatile matter limits (percent) (dry mineral-matter-free basis)		Calorific value limits (Btu per pound) (moist ^B mineral-matter-free basis)		Agglomerating character
		Equal or greater than	Less than	Greater than	Equal or less than	Equal or greater than	Less than	
I. Anthracite	1. Meta-anthracite	98	2	Nonagglomerating
	2. Anthracite	92	98	2	8	
	3. Semianthracite ^C	86	92	8	14	
II. Bituminous	1. Low-volatile bituminous coal	78	86	14	22	Commonly agglomerating ^E
	2. Medium-volatile bituminous coal	69	78	22	31	
	3. High-volatile A bituminous coal	...	69	31	...	14 000 ^D	...	
	4. High-volatile B bituminous coal	13 000 ^D	14 000	
	5. High-volatile C bituminous coal	11 500	13 000	
III. Subbituminous	1. Subbituminous A coal	10 500	11 500	Agglomerating
	2. Subbituminous B coal	9 500	10 500	
	3. Subbituminous C coal	8 300	9 500	
IV. Lignite	1. Lignite A	6 300	8 300	Nonagglomerating
	2. Lignite B	6 300	

^AThis classification does not include a few coals, principally nonbanded varieties, which have unusual physical and chemical properties and which come within the limits of fixed carbon or calorific value of the high-volatile bituminous and subbituminous ranks. All of these coals either contain less than 48 % dry, mineral-matter-free fixed carbon or have more than 15,500 moist, mineral-matter-free British thermal units per pound.

^BMoist refers to coal containing its natural inherent moisture but not including visible water on the surface of the coal.

^CIf agglomerating, classify in low-volatile group of the bituminous class.

^DCoals having 69 percent or more fixed carbon on the dry, mineral-matter-free basis shall be classified according to fixed carbon, regardless of calorific value.

^EIt is recognized that there may be nonagglomerating varieties in these groups of the bituminous class, and that there are notable exceptions in high-volatile C bituminous group.

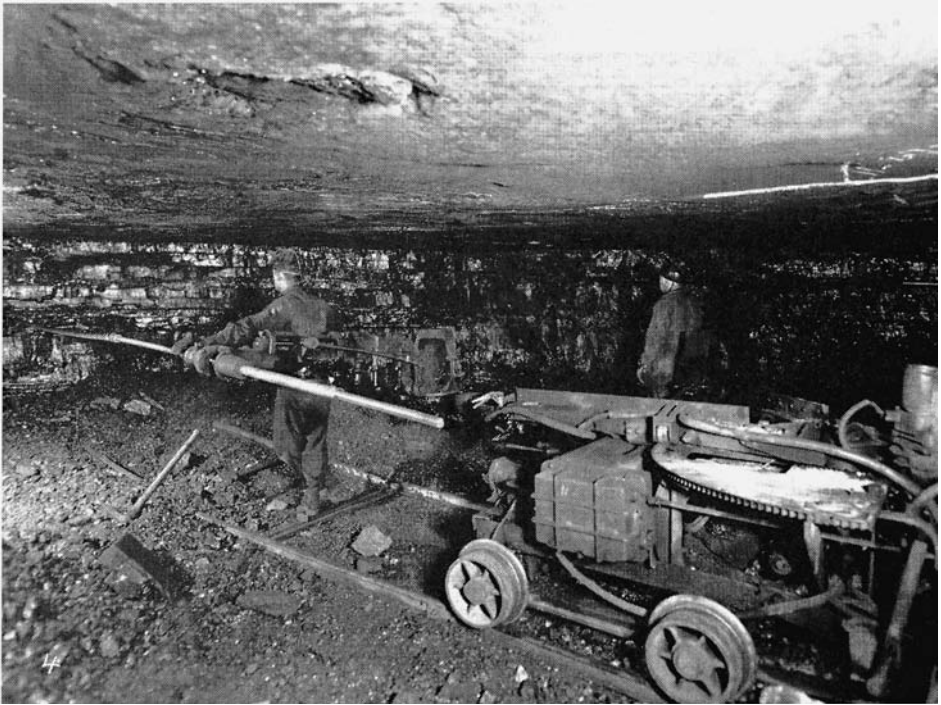


Figure 13.4 Layered and banded bituminous coal, Cedar Grove Seam (Pennsylvanian), Logan County, West Virginia. Thickness of the coal seam is about 2.3 m. [Photograph courtesy of Island Creek Coal Co.] (From Boggs, S., 2006, *Principles of Sedimentology and Stratigraphy*, 4th edn.,: Prentice-Hall, Upper Saddle River, NJ, Fig. 7.22, p. 232, reproduced by permission.)

Petrography of coals

Coals are not homogeneous materials, but instead are made up of various components somewhat analogous to the minerals of inorganic rocks. Coals can thus be classified also on the basis of megascopic textural appearance and their recognizable petrographic or microscopic constituents. Transmitted-light microscopes can be used to study coals up to the rank of low-volatile bituminous. At higher-rank levels, the organic material becomes opaque, and effective study requires use of incident (reflected) light. Incident light microscopy is most commonly used in coal petrography because it can be used to analyze coals over the complete rank from peat to anthracite and graphite (Bustin *et al.*, 1985).

Stopes (1919) recognized four types of coal, now called **lithotypes**, on the basis of megascopic appearance. These four lithotypes, called **vitrain**, **clarain**, **durain**, and **fusain**, comprise millimeter-thick bands or layers of humic coal. They are briefly described in [Table 13.3](#) and illustrated in [Fig. 13.5](#). Under the microscope, coal can be seen to consist of several kinds of organic units that are single fragments of plant debris, or in some cases the organic units are fragments consisting of more than one type of plant tissue. Stopes (1935)

Table 13.3 *Principal coal lithotypes and macerals***Lithotypes**

- Vitrain** – brilliant, glossy, vitreous, black coal, bands 3–5 mm thick; breaks with a conchoidal fracture; clean to touch.
- Clarin** – smooth fracture with pronounced gloss; dull intercalations or striations; small-scale sublamination within layers give surface a silky luster; the most common macroscopic constituent of humic coals.
- Durain** – occurs in bands a few cm thick; firm, somewhat granular texture; broken surfaces have a fine lumpy or matte texture; characterized by lack of luster, gray to brownish black color, and earthy appearance.
- Fusain** – soft, black; resembles common charcoal; occurs chiefly as irregular wedges; friable and porous if not mineralized.

Macerals

- Vitrinites** – originated as wood or bark; a major humic constituent of bright coals. Subtypes:
- Collinite** – structureless or nearly structureless; commonly occurs as a matrix or impregnating material for fragments of other macerals.
- Tellinite** – derived from cell-wall material of bark and wood and preserves some of the cellular texture.
- Inertinites** – composed of woody tissues, fungal remains, or fine organic debris of uncertain origin; relatively high carbon content. Subtypes:
- Fusinite** – cell structures composed of carbonized or oxidized cell walls and hollow lumens (the space bounded by the wall of an organ) that are commonly mineral filled; characteristic of fusain.
- Semifusinite** – a transitional state between fusinite and vitrinite.
- Schlerotinite** – composed of the remains of fungal schlerotia (a hardened mass of tubular filaments or threads) or altered resins; characterized by oval shape and varying size.
- Micronite** (< 10 μm) and **macronite** (10–100 μm) – structureless, opaque, granular macerals derived from fine-grained organic detritus.
- Inertodetrinite** – finely divided, structureless, clastic form of inertinite in which fragments of various kinds of inertinite macerals occur as dispersed particles.
- Liptinites** (exinites) – originate from spores, cuticles, resins, and algae; can be recognized from shapes and structures unless original constituents are compacted and squashed. Subtypes:
- Sporinite** – composed of the remains of yellow, translucent bodies (spore exines) that are commonly flattened parallel to bedding.
- Cutinite** – formed from macerated fragments of cuticles (layers covering the outer wall of a plant's epidermal cells).
- Resinite** – the remains of plant resins and waxes; occur as isolated rounded to oval or spindle-shaped, reddish, translucent bodies, or as diffuse impregnations, or as fillings in cell cavities.
- Alginite** – composed of the remains of algal bodies; serrated, oval shape; characteristic of boghead coal.

Source: Boggs, S., Jr., 2006, *Principles of Sedimentology and Stratigraphy*, 4th edn., Prentice Hall, Table 7.4, p. 233, reproduced by permission.

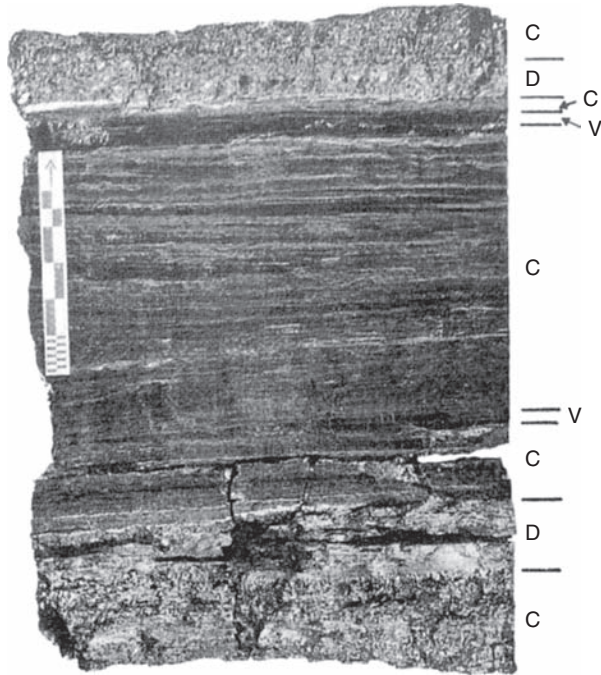


Figure 13.5 Bituminous coal showing examples of three lithotypes: V, vitrain; C, clarain; and D, durain. The small subdivision of the scale = 1 cm. (From Bustin, R. M. *et al.*, 1985, *Coal Petrology, Its Principles, Methods, and Applications*: Geological Association of Canada Short Course Notes 3, Pl. 6A, p. 51, reprinted by permission.)

suggested the name **maceral** for these organic units as a parallel word for the term mineral used for the constituents of inorganic rocks. The starting materials for macerals are woody tissues, bark, fungi, spores, and so on; however, these materials are not always recognizable in coals. Macerals are divided into three major groups: **vitrinite**, **inertinite**, and **liptinite**. The characteristics of these macerals and their most common subtypes are summarized in [Table 13.3](#). Macerals are further discussed by Scott (2002); some representative examples are shown in [Fig. 13.6](#).

The macerals in coals are identified on the basis of reflectivity, anisotropy, morphology, relief, and size. Under the reflecting microscope, liptinites appear dark gray with low reflectivity. Vitrinites are medium-gray, medium-reflecting, and inertinites are light-gray to white, high-reflecting. Anisotropy is defined as maximum reflectance minus minimum reflectance. Macerals of the liptinite and inertinite groups are, in general, isotropic. With increasing rank, coal becomes distinctly anisotropic (Bustin *et al.*, 1985). Shape or form, size, and internal structures are used to distinguish macerals if reflectance is too similar to permit identification. Macerals may also have differences in relief when viewed in incident light owing to differences in hardness. Inertinite macerals commonly show positive relief, and liptinite macerals may also show positive relief compared to the vitrinite matrix.

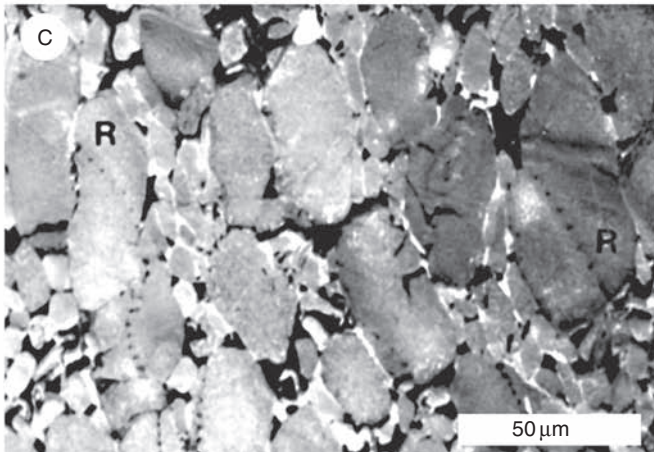
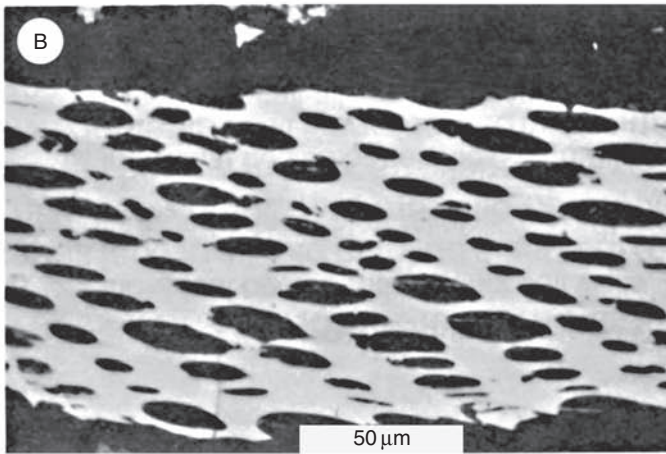
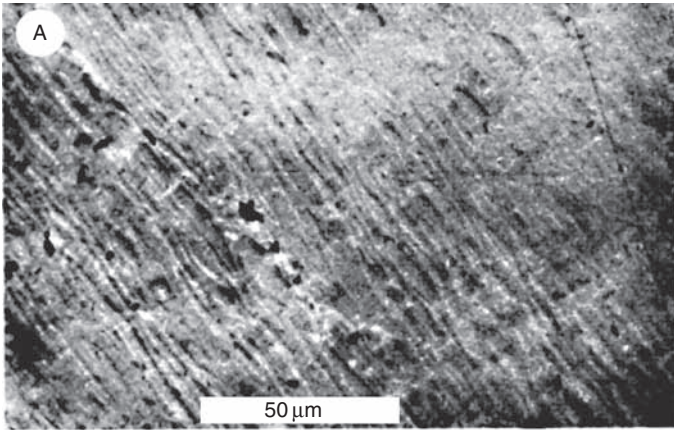


Figure 13.6 Examples of coal macerals, as illustrated in reflected-light photographs: A – telinite, a vitrinite maceral; B – fusinite, an inertinite maceral; and C – resinite (R), a liptinite maceral. (After Bustin, R. M. *et al.*, 1985, *Coal Petrology, Its Principles, Methods, and Applications*: Geological Association of Canada Short Course Notes 3., Pl. 3, Fig. 5, p. 41; Pl. 4, Fig. 2a, p. 45; Pl. 5, Fig. 1, p. 47, reprinted by permission.)

Etching the surface of coals with a strong oxidizing agent is also a common technique in coal petrography. Etching enhances differences among macerals and makes them easier to identify. Fluorescence microscopy involves irradiation of coals with blue light or ultraviolet light, which causes the coals to luminesce or fluoresce. The presence or absence of fluorescence and the fluorescence colors can be used to identify the different macerals.

Coal petrology is a highly specialized kind of petrography and is not pursued in detail here. Several references are available to readers who may wish more information about this complex subject. See, for example, Bustin *et al.* (1985), Crelling and Dutcher (1980), International Committee for Coal Petrology (1971, 1975), Stach *et al.* (1982), Ting (1982), and Ward (1984). A 2008 computer link to Internet resources dealing with coal petrology is provided at www.mineralogie.uni-wuerzburg.de/links/petrology/coal.html

Origin of coal

As suggested, coals consist primarily of humic organic material that is mainly the degraded, but not highly degraded, remains of higher plants. Rare coals are composed of sapropels, that is, mainly spores and pollen. Because land plants did not become well established until the Devonian, older coals, such as Precambrian coals, must be composed largely of algal remains, as mentioned. Land plants did not become truly abundant until the Carboniferous; therefore, the first major coal deposits occur in rocks of Carboniferous age.

The origin of coal requires two major conditions: a favorable climate for plant growth and an environment in which preservation of organic matter is favored. Climate influences the rate of plant growth, and warm, wet, tropical to subtropical climates are most favorable to rapid growth. Rates of accumulation of peat of as much as 4 mm per year under some tropical climates (e.g. Anderson, 1964) have been reported. On the other hand, the decomposition rate of plant debris is quite fast under these climatic conditions. Plants grow more slowly in cool, dry climates, but organic matter decomposes at a slower rate. Coal can form only where the rate of plant accumulation is greater than the rate of decomposition. Although we tend to think of coals as being the deposits of warm, humid climates, coals can also form in cold climates. Ancient coals were deposited at all latitudes from the equator to polar regions, with the majority forming in midlatitudes (McCabe, 1984). Accumulating plant debris is most likely to be preserved in depositional environments where oxidation of the organic matter is inhibited owing to rapid burial in a subsiding swampy area where the water table is close to the peat surface. For thick coal seams to develop, these conditions must exist for a geologically long period of time. That is, the coal swamps must not be destroyed by major environmental changes such as a marine transgression or a rapid influx of terrigenous clastics. The most favorable depositional environments appear to be transitional-marine (paralic) settings such as back-barrier environments, deltas, and coastal and interdelta plains. See Cobb and Cecil (1993) for additional examples of coal-forming environments.

The conversion of humic organic matter to coal results from both biochemical and geochemical processes. Organic matter is transformed progressively from peat through lignite, subbituminous, and bituminous coals to semianthracite and anthracite coal.

Biochemical processes are involved in the coalification process up to the rank of bituminous coals (Bustin *et al.*, 1985). At very shallow burial depths, aerobic bacteria and fungi initiate decomposition of organic materials. According to Bustin *et al.*, the order of susceptibility of organic matter to decomposition is (1) protoplasm, (2) chlorophyll, (3) oils, (4) carbohydrates, (5) epidermis, seed coats, (6) pigments, (7) cuticles, (8) spore and pollen exines, (9) waxes, and (10) resins. Thus, organic residues such as cuticles, spores and pollen, waxes, and resins are most likely to be present in coals. With deeper burial and loss of oxygen, anaerobic microbes take over the process of biochemical decomposition, which continues to depths of tens of meters. During the biochemical stage of coalification, the more easily hydrolyzable organic compounds are converted to carbon dioxide, ammonia, methane gas, and water and are subsequently lost. Some of the remaining compounds are oxidized, apparently with the aid of microorganisms, to form humic acids. The remaining, non-oxidized material is incorporated into the peat, where it undergoes further biochemical change under reducing conditions. This process results ultimately in the formation of humin.

Some compaction occurs during biochemical conversion of organic matter, resulting in loss of moisture. With deeper burial, compaction and moisture loss continue, together with loss of oxygen, whereas carbon content increases. Overall volatile content (water, carbon dioxide, hydrogen) of coals decreases with increasing coalification; however, coals retain about 5–6 percent hydrogen into the semianthracite stage. A number of additional chemical changes occur that affect the structure of organic molecules. Compaction and volatile loss accompanying deep burial result in thinning of coal beds by a factor of as much as 30 to 1 (Ryer and Langer, 1980); that is, 30 m of original peat might produce only 1 m of coal. Temperature has a particularly important effect on the coalification process. The rank of coal tends to increase with depth owing to increase in temperature with depth. The formation of anthracite coals requires temperatures in excess of $\sim 200^{\circ}\text{C}$ (Daniels *et al.*, 1990). The time over which heating occurs appears to be important also. The rank of coal tends to increase with increasing time of heating.

As mentioned, coals form under climatic conditions that favor plant growth and in depositional environments where burial conditions favor preservation of organic material. Furthermore, the coal-forming environment had to be protected in some way from significant influx of detrital sediments. These conditions appear to be met best in swamps where organic matter can accumulate below water that is relatively stagnant and deficient in oxygen. To explain the low detrital content of coals, McCabe (1984) suggests three possibilities: (1) detrital minerals were leached away owing to the highly acid waters in some swamps, (2) the peat accumulated in raised or floating swamps, which are protected from clastic deposition, or (3) peats accumulated at times when the regional clastic supply was cut off for some reason during swamp development.

Coals occur dominantly in clastic depositional sequences, although thin limestones may be associated with some coals. In some coal-bearing sequences, the coals display a cyclic pattern of occurrence. Pennsylvanian coal sequences of the United States midcontinent region, for example, typically begin with an underclay or seatrock followed by coal. The coal is overlain by marine limestone and/or shale as well as by siltstone or sandstone, which,

in turn, are overlain by another underclay and coal, and so on. Some coals are overlain by lacustrine shales and freshwater limestones rather than by marine deposits, and still others are overlain by fluvial clastic sediments or even volcanic deposits.

Observation of cyclic coal sequences led in the early 1930s to the concept of coal **cyclothem**s, which were tied to marine transgressions and regressions. Considerable controversy arose over the tectonic vs. eustatic origin of these transgressions and regressions, a debate that continued particularly through the 1960s. Since the 1960s, interest in the cyclothem concept appears to have abated somewhat. Much of the more recent research on coal stratigraphy has focused on depositional environments and local controls on sedimentation patterns. Some geologists have proposed, for example, that we may be able to explain simple transgression and regression processes in cyclothem s by sedimentation processes associated with depositional events such as deltaic deposition. Thus, so the suggestion goes, it may not be necessary to invoke the classic concepts of major transgressions and regressions to explain coal cycles.

Klein and Willard (1989) reexamined the origin of Pennsylvanian coal-bearing cyclothem s of North America. They suggest that the transgressive and regressive cycles that affected North American cyclothem s were controlled by several factors. These factors include (1) flexural deformation during plate accretion into a supercontinent, (2) concomitant glaciation and eustatic sea-level change, and (3) associated episodic thrust loading and foreland-basin subsidence of small magnitude on progressively more rigid crust. Many ancient coals appear to have formed in coastal areas in deltaic, back-barrier, and fluvial settings. Others formed in intermontane fluvial-dominated or lacustrine-dominated environments (Rahmani and Flores, 1984). A recent development in the study of coals is examination of coal-bearing successions in a sequence-stratigraphic framework. See the papers offered in Pashin and Gastaido (2004) for examples of this approach.

Swampy environments large enough to form major coal deposits have existed since the Carboniferous (Fig. 13.7). Only the Triassic Period appears to have been a time when coal-forming processes were at a minimum. Note from Fig. 13.7 that most major coal deposits occur in the Northern Hemisphere; however, owing to plate movements some coals may have formed originally in different latitudes than those in which they now exist. As mentioned, coal deposits are widely distributed on the major continents of Earth. Major coal producers include China, the USA, Russia, Germany, and India. Thomas (1992, ch. 4) and Walker (2000) provide useful summaries of coal deposits in numerous countries throughout the world.

13.3.3 Oil shale

Definition and importance

The term “oil shale” is applied to fine-grained sedimentary rocks from which substantial quantities of oil can be derived by heating. Hutton (1995) defines oil shale as a sedimentary rock that contains organic matter (at least 5 weight percent) that, when retorted, produces sufficient oil to produce more energy than the energy required to produce the oil originally.

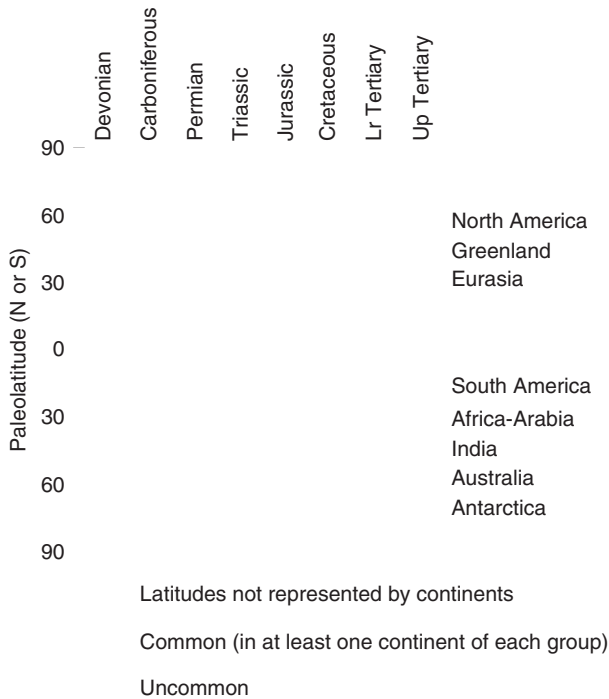


Figure 13.7 Distribution of coal deposits by paleolatitude. Since the Permian, the upper group of continents has been mainly in the Northern Hemisphere and the lower group in the Southern Hemisphere. (From McCabe, P. J., 1984, Depositional environment of coal and coal-bearing strata, in Rahmani, R. A. and R. M. Flores (eds.), *Sedimentology of Coal and Coal-Bearing Sequences*: International Association of Sedimentologists Special Publication 7, Fig. 7, p. 23, as modified from Habicht, J. K. A., 1979, *Paleoclimate, Paleomagnetism, and Continental drift*: Association of Petroleum Geologists Studies in Geology 9, Fig. 11, p. 15, reprinted by permission of Blackwell Scientific, Oxford, and AAPG, Tulsa, OK.)

The term is actually a misnomer in the sense that relatively little free oil occurs in these rocks, although small blebs, pockets, or veins of asphaltic bitumens may be present. This soluble bitumen fraction constitutes as much as 20 percent of the organic content of typical oil shales. The remaining 80 percent or more of organic substances is present in the form of kerogen, which yields oil when heated to a temperature of about 350 °C. The organic content of oil shales commonly does not exceed about 25 percent; the remaining part of the rock is composed of inorganic constituents, which are mainly silicate grains or carbonate minerals. Thus, an “oil shale” can actually be an organic-rich limestone as well as a shale.

Oil shales are of special interest to geologists and economists because of their potential to generate oil when refined into fuel at sufficiently high temperatures. Several countries have attempted to develop small oil-shale industries, including Australia, Brazil, New Zealand, Switzerland, Sweden, Estonia, Spain, China, Scotland, France, and South Africa. Peak development was reached immediately after World War II. Most oil-shale plants have now

closed, with the exception of some plants in the former Soviet Union and China (Tissot and Welte, 1984, p. 254). Relatively little commercial exploitation of oil shales has occurred, primarily because oil produced from oil shales cannot compete economically with petroleum. Also, many technological problems are associated with mining and extraction processes, as well as with disposal of the gigantic amounts of waste rock that would be created by surface retorting processes. Some observers believe that oil shales will be mined and utilized as a major source of fuel in the future as petroleum and natural gas supplies inevitably dwindle. Others are not so sure that large-scale exploitation of oil shales will ever become economically feasible. Only time will tell. At least 50 countries of the world have reserves of oil shale that have the potential to be exploited in the future (Russell, 1990, p. 4).

Oil shales are also of interest because of the information they convey about ancient depositional environments. To preserve such high levels of organic matter in shales and carbonate rocks requires unusual environmental conditions. Many oil-shale deposits may have been deposited in large lakes (see, for example Carrol and Wartes, 2003). Others formed in small lakes, bogs, and lagoons that may have been associated with coal-forming swamps. Still others probably formed in shallow seas on continental platforms and continental shelves where water circulation was restricted. Although geologists commonly assume that preservation of large quantities of organic matter requires both high rates of organic productivity and anoxic conditions, Pederson and Calvert (1990) dispute the requirement for anoxia in the case of organic-rich marine sediments. They suggest that high rates of organic productivity is the fundamental control on accumulation of organic-rich facies in the ocean and marginal seas – not the presence or absence of anoxia.

Age, distribution, and abundance

Oil shales range in age mainly from Cambrian to Tertiary. To my knowledge, the only oil shales of Precambrian age are the Nonesuch shales of Michigan and Wisconsin (USA), which contain very minor amounts of organic matter (Russell, 1990, p. 98). Some Quaternary-age deposits contain organic debris that can yield oil (Duncan, 1976). Oil shales are widespread geographically. They occur in at least 50 countries (Russell, 1990, p. 4), although they are concentrated especially in the United States (see Fig. 13.8), Europe, and the former Soviet Union. Cambrian and Ordovician deposits occur particularly in northern Europe, northern Asia, and east-central United States and Canada. Silurian–Devonian deposits are best developed in eastern and central United States, North Africa, and the central European USSR. Late Paleozoic oil shales occur on all the continents. Large deposits occur in southern Brazil, and smaller deposits are known in Scotland, France, Spain, South Africa, Australia, the USSR, Canada, Uruguay and southern Argentina, the northwestern United States and Alaska. Mesozoic oil shales also occur on all continents, except Australia, in such widely scattered areas as central Africa (Zaire), northern and eastern Asia, the Middle East, Europe, Alaska, central Canada, and the western United States. Tertiary oil shales occur particularly in the western United States (Green River shales) as well as in New Zealand, Europe, the Andes Mountains of South America, the southern parts of the former Soviet Union and eastern China, and some other countries.



Figure 13.8 Oil-shale deposits of the United States. (From Russell, P.L., 1990, *Oil Shales of the World: Their Origin, Occurrence and Exploration*: Pergamon Press, Oxford, Fig. 6.1, p. 83, reproduced by permission.)

The greatest reserves of oil shale occur in the United States, followed by Brazil, the Former Soviet Union, and Zaire. Much smaller but potentially economic reserves occur in a number of other countries, including Jordan, Morocco, Italy, China, Thailand, and northern and western Europe. Russell (1990, p. 4) estimates that the potential world supply of oil from oil shale is 2000 trillion barrels of in-place oil. He provides a brief description of the geology, reserves, and oil potential of all major world oil-shale deposits. The Green River Formation in Colorado, Utah, and Wyoming represents the world's largest single hydrocarbon resource (Russell, 1990, p. 86).

Composition and classification

According to Yen and Chilingar (1976), the average oil shale consists of 86 percent inorganic constituents (quartz, feldspars, clay minerals, carbonates, pyrite), 11 percent kerogen, and 3 percent soluble bitumen. The organic content of oil shales is the property that particularly distinguishes them from other shales. Organic constituents commonly do not exceed about 25 percent of the rock, but much higher values are present in some deposits. It is this content of organic matter that gives oil shales their economic significance. As mentioned, some of the organic material consists of soluble bitumens; however,

commonly more than 80 percent consists of kerogen. The elemental chemistry and chemical structure of kerogen are described in the preceding [Section 13.2](#).

As mentioned, not all oil shales are actually shales. Some are organic-rich siltstones, mudrocks, limestones, and impure coals. Three basic types are recognized: (1) **Carbonate-rich oil shales** are those in which the principal nonkerogen constituents are calcite, dolomite, ankerite, and variable amounts of siliciclastic silt. They are generally hard, tough, and resistant to weathering (Duncan, 1976). (2) **Silica-rich oil shales** are shales in which the main constituents apart from kerogen are fine-grained quartz, feldspar, and clay minerals. They may also contain chert, opal and phosphatic nodules. Siliceous oil shales are generally dark brown or black and are less resistant to weathering than the carbonate-rich shales. (3) **Cannel shale** is an oil shale that consists predominantly of organic matter that completely encloses other mineral grains. The organic matter is composed largely of algal remains. Hutton (1995) discusses various classification schemes for oil shales and suggests three types of oil shales on the basis of the liptinite macerals they contain: (1) **terrestrial oil shale** – composed of liptinite derived from terrestrial plants, (2) **lacustrine oil shale** – composed of liptinite derived from lacustrine (including brackish, saline or fresh-water) algae, and (3) **marine oil shale** – composed of liptinite derived from marine algae, acritarchs, and dinoflagellates.

The amount of oil that can be extracted from oil shales ranges from about 4 percent to more than 50 percent of the weight of the rock; that is, between 10 to 150 gallons of oil per ton of rock (Duncan, 1976). See Russell (1990) for specific yields from various oil-shale deposits of the world.

Origin

Oil shales form in environments where organic matter is abundant and anaerobic or reducing conditions prevent oxidation and total bacterial decomposition. They are deposited in both lacustrine (lake) and marine environments where the above conditions are met. As mentioned, the principal environments are (1) large lakes, (2) shallow seas or continental platforms and continental shelves in areas where water circulation was restricted and reducing or where weakly oxidizing conditions existed, and (3) small lakes, bogs, and lagoons associated with coal-producing swamps. The deposits of large lakes may range in composition from marls to argillaceous limestones. Probably the largest deposit of oil shale in the world, the Green River Shale in west-central United States, is a lake deposit. Sediments associated with lake deposits may include volcanoclastic sediments and evaporites. Oil-shale deposits in shallow seas consist mainly of siliciclastic sediments, although carbonates may also be present. In the United States, the Devonian black shales that extend over several states in the eastern midcontinent region are a good example of oil shales deposited in shallow seas. Oil shale deposits in small lakes or bogs may be associated with or overlie coal beds.

The main source of kerogen in major oil-shale deposits appears to be algal remains. The microstratification in many oil shales suggests recurring variations in the supply of organic remains and fine siliciclastic detritus. Oil shales formed in lakes or swamps may be associated with impure cannel- or boghead-type coal, tuffs and other volcanic rocks, or

even evaporites. Many oil shales deposited in large lakes are carbonate-rich types and tend to have high oil yields. Oil shales deposited in marine environments are characteristically the silica-rich type and have lower oil yields, although some Tertiary- and Mesozoic-age siliceous oil shales have rich oil yields. Oil shales extend over wide geographic areas and are commonly associated with limestones, cherts, sandstones, and phosphatic deposits.

13.3.4 Petroleum

Nature and composition

Petroleum is not a carbonaceous sedimentary rock, but it is a carbon-rich organic substance that occurs as liquid and gas accumulations predominantly in sandstones and carbonate rocks. Therefore, a very brief discussion of petroleum is included here with the carbonaceous sedimentary rocks. Petroleum and natural gas constitute the most important source of energy in the world today. For that reason, the factors that govern the availability of petroleum are of much more than academic interest. Major oil companies, world governments, politicians, and the average citizen are all vitally concerned with the petroleum supply. To say that the course of world political and economic events in the near future will be governed in a major way by the availability of petroleum is not too strong a statement. Until an adequate alternative source of energy is developed, the fate of the world's nations may very well depend upon who has and who does not have access to abundant, cheap supplies of petroleum.

Liquid petroleum is composed dominantly of carbon (about 85 percent) and hydrogen (about 13 percent). It also contains an average of about 1.5 percent sulfur, 0.5 percent nitrogen, and 0.5 percent oxygen (Hunt, 1996, p. 24). Despite its simple elemental chemical composition, the molecular structure of petroleum can be exceedingly complex. The molecules in petroleum range from the simple methane gas molecule (CH_4) with a molecular weight of 16 to molecules with molecular weights in the thousands. Several hundred different hydrocarbons have been recorded in natural crude oils; however, all hydrocarbons can be grouped into a few basic classes or series having common molecular structural form. These structural forms are complex and are not explained in detail here, but the main hydrocarbon series are:

1. **Paraffins (alkanes)** – open-chain molecules with single covalent bonds between carbon atoms (Fig. 13.9).
2. **Napthenes (cycloparaffins)** – closed-ring molecules with single covalent bonds between carbon atoms (Fig. 13.10).
3. **Aromatics (arenes)** – one or more benzene-ring structures with double covalent bonds between some carbon atoms (Fig. 13.11).

Most natural gases as well as many liquid petroleum products belong to the paraffin series of hydrocarbons. Most naphthene hydrocarbons are liquid petroleum products, although two naphthenes occur as gases at normal temperatures. The aromatics, which are named for their strong aromatic odor, are liquid petroleum products. They commonly make up only a small percentage of the petroleum in natural crude oils.

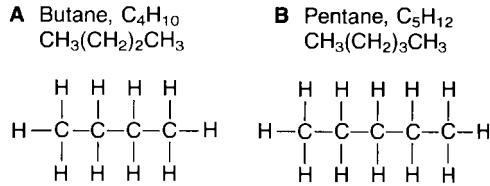


Figure 13.9 Schematic structure of paraffin hydrocarbons having the general formula $C_n H_{2n+2}$, where n refers to the number of carbon or hydrogen atoms. A. Butane. B. Pentane.

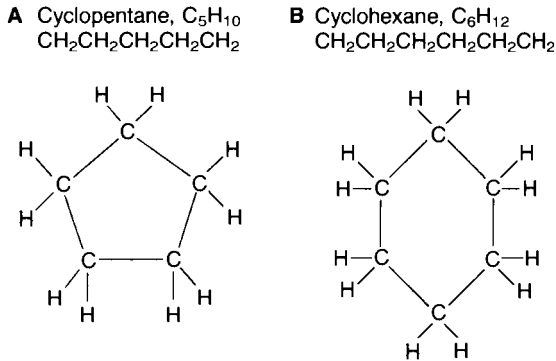


Figure 13.10 Schematic structure of naphthene (cycloparaffin) hydrocarbons having the general formula $C_n H_{2n}$. A. Cyclopentane. B. Cyclohexane.

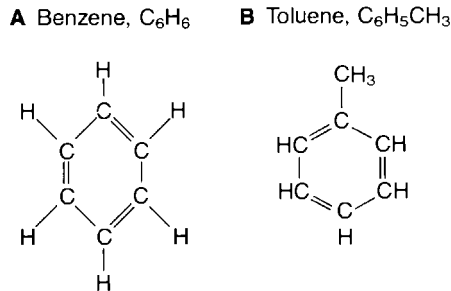


Figure 13.11 Schematic structure of aromatic hydrocarbons having the general formula $C_n H_{2n-6}$. A. Benzene. B. Toluene.

Occurrence and distribution of petroleum

Commercial accumulations of petroleum can occur in any kind of rock that contains sufficient porosity to permit storage of economically significant quantities of petroleum. Most oil deposits occur in sedimentary rocks, particularly sandstones and carbonate rocks. Roughly 55 percent of the world supply of petroleum and 75 percent of its natural gas occur in sandstones. About 45 percent of world petroleum reserves and 25 percent of natural-gas

reserves occur in carbonate rocks. Very small amounts of petroleum may occur in other kinds of sedimentary rocks and even in some fractured igneous or metamorphic rocks. Petroleum deposits are located in all the world's continents, but they are concentrated in four main areas: (1) the Middle East (Persian Gulf Basin), (2) the northern and western sides of the Gulf of Mexico and the south side of the Caribbean, (3) the flanks of the Ouachita Mountains in the United States, and (4) the flanks of the Ural Mountains in the former Soviet Union. These four areas account for nearly three-fourths of the world's oil and two-thirds of its natural gas. The major oil-producing countries of the world in terms of proven reserves of petroleum are the Middle East countries of Saudi Arabia, Iraq, Iran, Abu Dhabi, and Kuwait. These Middle East countries are followed by the former Soviet Union, Venezuela, Mexico, the United States, and Libya. Petroleum occurs in rocks of all ages, although very little occurs in Precambrian or Quaternary rocks. Roughly 60 percent of the world's reserves of petroleum are in rocks of Mesozoic (especially Cretaceous) age. About 30 percent occurs in rocks of Tertiary age and 8–10 percent in rocks of Paleozoic age.

Petroleum deposits accumulate within some kind of trap. A trap is a structural or stratigraphic feature of a rock into which oil or gas can easily migrate but from which it is difficult to escape. Three common types of petroleum traps are anticlines, faults, and stratigraphic pinchouts (Fig. 13.12). Petroleum occurs within the pores of sedimentary strata along with water. Owing to its lower specific gravity, it tends to rise upward and accumulate above the

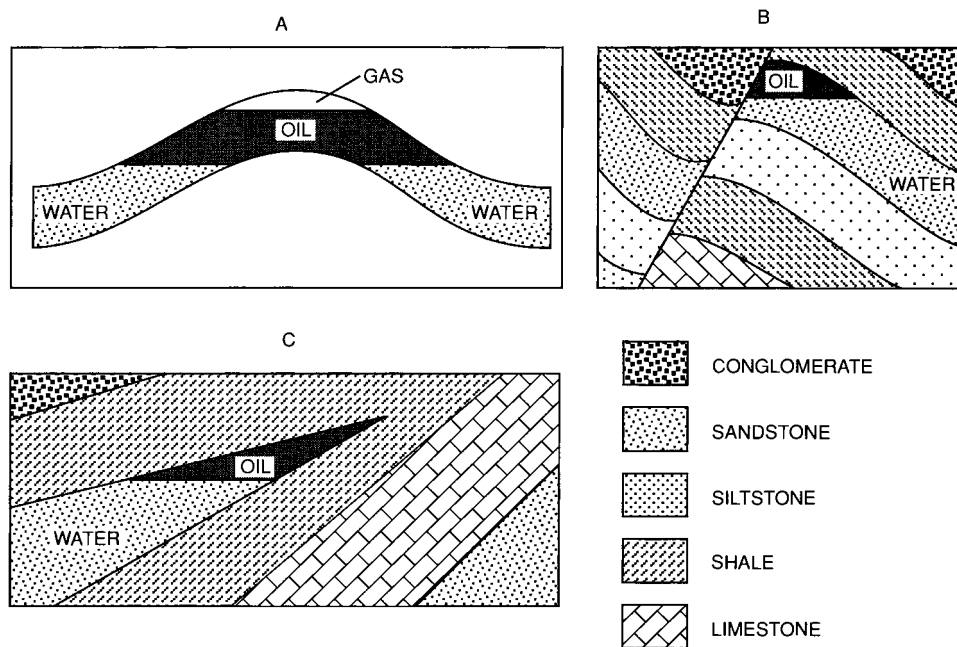


Figure 13.12 Schematic representation of three kinds of petroleum traps. A. Anticlinal trap. B. Fault trap, with an impermeable fault gouge or mineral seal along the fault. C. Stratigraphic (pinchout) trap.

water. Thus, petroleum will rise to the crest of a structure such as an anticline. If the sedimentary layer in which petroleum accumulates is overlain by an impermeable layer such as shale or evaporites, the petroleum cannot escape upward beyond the crest of the trap. Thus, it will accumulate until it fills the closed area of the trap (Fig. 13.12). The search for petroleum deposits centers particularly around locating traps, which may or may not be filled with petroleum. Because traps are located deep beneath the surface, seismic prospecting methods must commonly be used to locate the traps.

Origin of petroleum

Most geologists believe that petroleum is of organic origin and that it formed from organic matter by a complex maturation process during sediment diagenesis. On the other hand, a small but respected number of scientists firmly believe that petroleum can originate by inorganic processes, probably within the upper mantle. Decades of oil-well drilling have not completely resolved this difference of opinion. Owing to the overwhelming weight of evidence that favors an organic origin, however, I discuss the origin of petroleum in this book only from the organic-origin point of view. It is highly probable that petroleum forms from plant and animal organic matter by a complex maturation process during sediment burial. The transformation of organic matter to petroleum involves initial microbial alteration and subsequent thermal alteration and cracking. Most organic matter produced by plants and animals is destroyed by oxidation and organisms. Only a small percentage of the organic matter created through time, perhaps 1 percent, needs to have been preserved, however, to account for the known petroleum deposits. Organic matter that is deposited along with fine-grained sediments in reducing environments has commonly been regarded to have the best chance of preservation, although, as mentioned, Pederson and Calvert (1990) suggest that anoxic conditions are not required if rates of organic productivity are high. Thus, the source materials for petroleum are believed to be contained primarily in organic-rich shales and fine-grained carbonate rocks that were deposited under conditions of high organic productivity by marine phytoplankton (plants) and zooplankton (animals) – probably in some kind of restricted or low-oxygen environment.

During burial, organic matter undergoes complex changes as it proceeds through three main stages of transformation, commonly referred to by petroleum geologists as diagenesis, catagenesis, and metagenesis. During **diagenesis**, which takes place at burial depths of tens to hundreds of meters and at temperatures below about 50°C, organic **biopolymers** (carbohydrates, proteins, lipids, lignin, and other highly organized organic substances) are degraded by microbial activity. This biochemical process results in formation of individual organic compounds, called **monomers**, such as sugars, amino acids, fatty acids, and phenols. Microbial degradation also results in production of a small amount of methane gas. These microbial reactions occur particularly in clays and muds deposited in either reducing or oxic environments where rapid burial prevents the organic matter from being destroyed completely by oxidation. With deeper burial, these monomers undergo additional change owing to polymerization and condensation. Polymerization is the combining of simple molecules to form more complex molecules, and condensation is the combining of

two or more molecules to form a larger molecule, with loss of another molecule such as H_2O . Through condensation and polymerization, monomers are gradually converted to **geopolymers**, which are humic and fulvic acids together with humin. (Humic and fulvic acids are complex, high-molecular-weight organic compounds. Humic acid is soluble in alkaline solutions but is precipitated by acidification. Fulvic acid is soluble in both acid and base; humin is insoluble in both acid and base.) A small amount of aromatic and naphthenic hydrocarbons may also be generated during this stage owing to additional chemical processes such as decarboxylation and hydrogen disproportionation (loss of hydrogen from some molecules and enrichment in others). With further condensation and insolubilization (conversion of soluble humic and fulvic acids to insoluble humin), the geopolymers are converted into kerogen. This diagenetic process is illustrated schematically in Fig. 13.13. As shown in this figure, some hydrocarbonlike organic substances such as lipids may go through the diagenesis stage with only minor degradation. For additional insight into the pathways of condensation leading to generation of kerogen, see Horsfield (1997).

Once formed, kerogen is highly stable and can persist at moderately low temperatures for hundreds of millions of years. As discussed above, kerogen is the principal kind of organic matter preserved in oil shales. On the other hand, with increasing temperature accompanying deeper burial, kerogen can undergo thermal degradation to form liquid hydrocarbons. This process, referred to as **catagenesis**, takes place at burial depths exceeding about 1000 m and at temperatures of about 50–150 °C and pressures of 300–1500 bar. Catagenesis involves the cracking (breaking of carbon to carbon bonds) of kerogen and other complex, high-molecular-weight compounds to form hydrocarbons. At the low end of the temperature range (up to about 125 °C), thermocatalytic cracking (in the presence of a catalyst such as smectite clay) probably predominates. At higher temperatures, thermal cracking, which does not require a catalyst, predominates. Thus, during catagenesis, low- to medium-molecular-weight hydrocarbons are formed at lower temperatures, with lighter hydrocarbons and some methane forming at the high end of the temperature range above about 120 °C. Above 120 °C, some previously formed liquid hydrocarbons may also be cracked to methane.

In many oil-producing basins, the maturation of organic matter may not proceed beyond the catagenesis stage. If deeper burial occurs, with temperatures exceeding about 150–200 °C, the maturation process enters the **metagenesis** stage. In the temperature range of metagenesis, liquid hydrocarbons are no longer formed. Some methane may continue to be generated to burial depths corresponding to temperatures of about 250 °C. At higher temperatures, any remaining organic matter is converted to anthracitic and graphitic materials. Also, liquid petroleum may be destroyed to form methane plus solid hydrocarbons (discussed below) and graphite. The above discussion is based on information in Tissot and Welte (1984, pp. 69–92), Hunt (1979, ch. 4), Hunt (1996, ch. 5), and Horsfield (1997).

After petroleum has formed from organic source materials at substantial burial depths, it migrates by processes not yet fully understood from the fine-grained source rocks into associated coarser-grained, porous, and permeable sandstone or carbonate rocks. The petroleum then migrates, possibly along with water, up the regional dip of the basin within these “carrier beds” until it reaches a trap. There, it slowly accumulates until it may fill the trap.

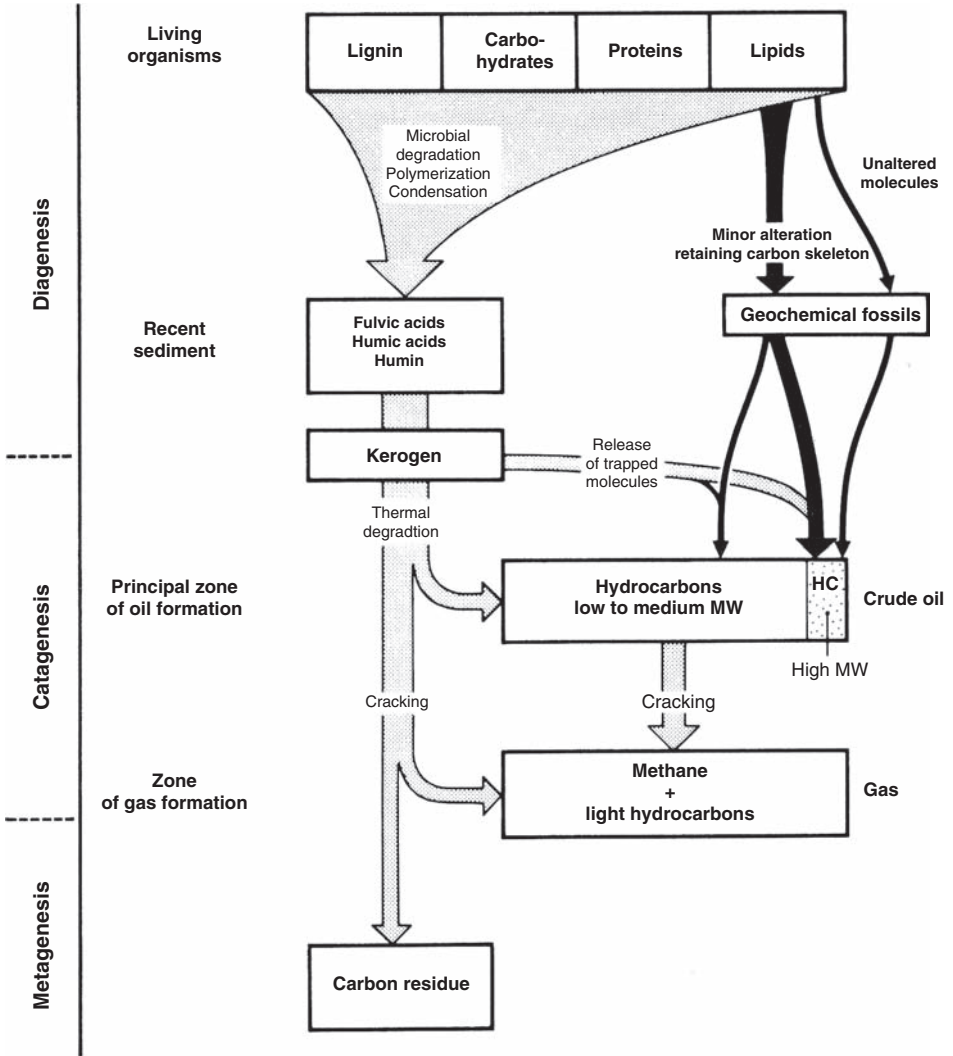


Figure 13.13 Schematic illustration of the sequential conversion of organic matter in living substances to fulvic and humic acids, kerogen, and hydrocarbons, Note that some petroleumlike hydrocarbons in lipids undergo only minor alteration during diagenesis and are thus referred to as geochemical fossils. HC=hydrocarbons; MW=molecular weight. (From Tissot, B. P. and D. H. Welte, 1984, *Petroleum Formation and Occurrence*, 2nd edn.: Springer-Verlag, Berlin, Fig. II.3.1, p. 94, reprinted by permission).

The above discussion outlines the fundamental concept of petroleum origin that appears to be most widely accepted by petroleum geologists today. Nonetheless, many problems and questions remain regarding the origin of petroleum and its migration from shale source rocks into permeable and porous sandstone or carbonate reservoir rocks. The subject of petroleum

geology constitutes an entire field of research in itself, and many ideas regarding the origin of petroleum are controversial.

13.3.5 Solid hydrocarbons

Introduction

These substances are hydrocarbons such as natural asphalts and mineral waxes that occur in a semisolid or solid state. Most solid hydrocarbons probably formed from liquid petroleum that were subjected to loss of volatiles, oxidation, and biologic degradation after seepage to the surface. Bacterial degradation can putatively occur also at depth in subsurface reservoirs (e.g. Meyer *et al.*, 2007). Solid hydrocarbons occur as seepages, as surface accumulations, as impregnations occupying the pore spaces of sandstones or other sedimentary rock, and in veins and dikes. They are black or dark brown and have a characteristic odor of pitch or paraffin. Some solid hydrocarbons are combustible and thus have commercial value as fuels. Others are infusible. All solid hydrocarbons are of interest to petroleum geologists, however, because their presence at the surface is an indication of petroleum at depth in a region. Also, study of their occurrence may help to solve the problems related to the origin and alteration of petroleum.

Composition and occurrence

Solid hydrocarbons have roughly the same elemental chemical composition as liquid petroleum, but the percentage of carbon and hydrogen tend to be somewhat lower and the content of sulfur, nitrogen, and oxygen somewhat higher. They are divided into four main varieties or series based on fusibility (melting temperature) and solubility in carbon disulfide (CS₂), an organic solvent (Fig. 13.14): asphalts, asphaltites, natural mineral waxes, pyrobitumens.

Asphalts are soft, semisolid bitumens that occur as seeps, surface pools, or as viscous impregnations in sediments. They are dark colored, plastic to fairly hard, easily fusible, and soluble in carbon disulfide. Varietal names for asphalts from different areas are shown in Fig. 13.14. Asphalts are commonly associated with active oil seeps. The most important economic accumulations of asphalts are in so-called **tar sands**. Tar-sand deposits occur in many parts of the world and a few are large enough (e.g. the Athabasca tar sands of Canada) to have considerable economic significance. Major deposits of natural bitumens occur in North America, South America, Transcaucasia, and Russia. Smaller deposits are present in Europe, Africa, and East and Southeast Asia. According to Meyer *et al.* (2007), 5500 billion barrels of oil (equivalent) are present in these major and minor deposits.

Asphaltites occur primarily in dikes and veins that cut sediment beds. They are harder and denser than asphalts and melt at higher temperatures. They are largely soluble in carbon disulfide. Names applied to varieties of asphaltites that differ slightly in density, fusibility, and solubility are **gilsonite**, **glance pitch**, and **grahamite**. In the United States, deposits of asphaltites are known from Utah and Oklahoma. Other deposits occur in Peru, Argentina, Cuba, Trinidad, Mexico, the Dead Sea area, and the former Soviet Union.

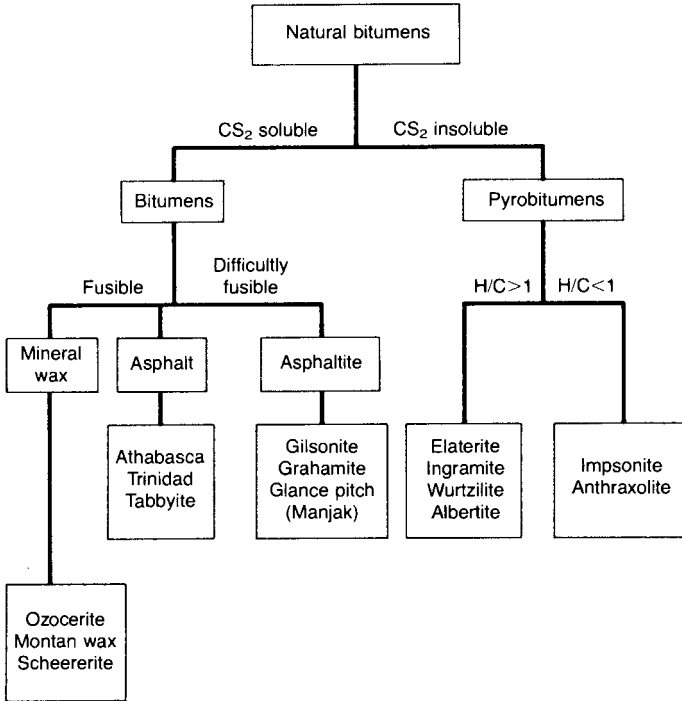


Figure 13.14 Terminology of principal kinds of naturally occurring solid hydrocarbons. (From J. M. Hunt, 1979, *Petroleum Geochemistry and Geology*: W. H. Freeman, San Francisco, CA, Fig. 8.28, p. 400, reproduced by permission.)

Native mineral waxes are solid, waxy, light-colored substances that consist largely of paraffinic hydrocarbons of high molecular weight. They represent the residuum of high-wax oils exposed at the surface. The most important native mineral wax is **ozocerite**, which consists of veinlike deposits of greenish or brown wax. **Montan wax** is an extract obtained from some kinds of brown coals or lignites. Mineral waxes are fusible and soluble in carbon disulfide.

Pyrobitumens occur in dikes and veins like asphaltites but are infusible and largely insoluble in carbon disulfide. They also tend to have higher sulfur content than other solid hydrocarbons. Several varieties of pyrobitumens are recognized. Softer forms include **elaterite**, a soft elastic substance rather like India rubber, and **wurtzilite**. More-indurated forms are **albertite**, a black, solid bitumen with a brilliant jetlike luster and conchoidal fracture, **ingramite**, and the metamorphosed pyrobitumens **impsonite** and **anthraxolite**. Owing to their infusibility, pyrobitumens do not have commercial value as fuels.

For additional details of the characteristics of solid hydrocarbons see Hunt (1979, pp. 398–404). Hunt (1996, various pages) further discusses bitumens and some of the other more important solid hydrocarbons.

Further reading

- Bustin, R. M., A. R. Cameron, D. A. Grieve, and W. D. Kalkreuth, 1985, *Coal Petrology, Its Principles, Methods, and Applications*, 2nd edn.: Geological Association of Canada Short Course Notes 3.
- Cobb, J. C. and C. B. Cecil (eds.), 1993, *Modern and Ancient Coal-Forming Environments*: Geological Society of America Special Paper 286.
- Hunt, J. M., 1996, *Petroleum Geochemistry and Geology*, 2nd edn.: W. H. Freeman, New York, NY.
- Pashin, J. C. and R. A. Gastaldo, 2004, *Sequence Stratigraphy, Paleoclimate, and Tectonics of Coal-Bearing Strata*: American Association of Petroleum Geology Studies in Geology.
- Rahmani, R. A. and R. M. Flores (eds.), 1984, *Sedimentology of Coal and Coal-Bearing Sequences*: International Association of Sedimentologists Special Publication 7.
- Russell, P. L., 1990, *Oil Shales of the World: Their Origin, Occurrence and Exploitation*: Pergamon Press, Oxford.
- Snape, C. (ed.), 1995, *Composition, Geochemistry and Conversion of Oil Shales*: Kluwer, Dordrecht.
- Thomas, L., 1992, *Handbook of Practical Coal Geology*: John Wiley and Sons, Chichester.
- Tissot, B. P. and D. H. Welte, 1984, *Petroleum Formation and Occurrence*, 2nd edn.: Springer-Verlag, Berlin.
- Walker, S., 2000, *Major Coalfields of the World*: IEA Coal Research, The Clean Coal Centre, London.
- Welte, D. H., B. Horsfield, and D. R. Baker (eds.), 1997, *Petroleum and Basin Evolution: Insights from Petroleum Geochemistry, Geology and Basin Modeling*: Springer-Verlag, Berlin.

References

- Aagaard, P., P. K. Egeberg, G. C. Saigal, S. Morad, and K. Bjørlykke, 1990, Diagenetic albitization of detrital K-feldspars in Jurassic, lower Cretaceous and Tertiary clastic reservoir rocks from offshore Norway, II. Formation water chemistry and kinetic considerations: *J. Sediment. Petrol.* **60**, 575–81.
- Abbott, P. L. and G. L. Peterson, 1978, Effect of abrasion durability on conglomerate clast populations: examples from Cretaceous and Eocene conglomerates of the San Diego area, California: *J. Sediment. Petrol.*, **48**, 31–42.
- Adams, A. E. and W. S. MacKenzie, 1998, *A Color Atlas of Carbonate Sediments and Rocks under the Microscope*: John Wiley and Sons, New York, NY.
- Adams, A. E., W. S. Mackenzie, and C. Guilford, 1984, *Atlas of Sedimentary Rocks Under the Microscope*: John Wiley and Sons, New York, NY.
- Adams, J. E. and M. L. Rhodes, 1960, Dolomitization by seepage refluxion: *Am. Assoc. Pet. Geol. Bull.*, **44**, 1912–1921.
- Agrawal, Y. C., I. N. McCave, and J. B. Riley, 1991, Laser-diffraction size analysis, in Syvitski, J. P. M. (ed.), 1991, *Principles, Methods, and Application of Particle Size Analysis*: Cambridge University Press, Cambridge, pp. 119–128.
- Aitken, J. D., 1967, Classification and environmental significance of cryptalgal limestones and dolomites, with illustrations from the Cambrian and Ordovician of southwestern Alberta: *J. Sediment. Petrol.*, **37**, 1163–1178.
- Allen, J. R. L., 1968, *Current Ripples: Their Relation to Patterns of Water Motion*: North Holland, Amsterdam.
- Allen, J. R. L., 1982, *Sedimentary Structures – Their Character and Physical Basis*: Elsevier, Amsterdam, vol. I; vol. II.
- Allen, P. A. and J. R. Allen, 2005, *Basin Analysis: Principles and Applications*, 2nd edn.: Blackwell Publishing, Malden, MA.
- Allen, P., 1945, Sedimentary variations: some new facts and theories: *J. Sediment. Petrol.*, **15**, 75–83.
- Alling, H. L., 1945, Use of microlithologies as illustrated by some New York sedimentary rocks: *Geol. Soc. Am. Bull.*, **56**, 737–756.
- Anbar, A. D. and A. H. Knoll, 2002, Proterozoic ocean chemistry and evolution: A bioinorganic bridge?: *Science*, **297**, 1137–1142.
- Anderson, J. A. R., 1964, The structure and development of peat swamps of Sarawak and Brunei: *J. Tropical Geog.*, **18**, 7–16.
- Anderson, R. Y. and D. W. Kirkland, 1966, Intrabasin varve correlation: *Geol. Soc. Am. Bull.*, **77**, 241–256.
- Anderson, T. F. and M. A. Arthur, 1983, Stable isotopes of oxygen and carbon and their application to sedimentologic and paleoenvironmental problems, in Arthur, M. A.

- T. F. Anderson, I. R. Kaplan *et al.* (eds.), *Stable Isotopes in Sedimentary Geology*: SEPM Short Course Notes 10, pp. 1–1 to 1–151.
- Archer, J. B., 1984, Clastic intrusions in deep-sea fan deposits of the Rosroe Formation, Lower Ordovician, western Ireland: *J. Sediment. Petrol.*, **54**, 1197–1205.
- Argast, S. and T. W. Donnelly, 1987, The chemical discrimination of clastic sedimentary components: *J. Sediment. Petrol.*, **57**, 813–823.
- Armenteros, I. and P. Huerta, 2006, The role of clastic sediment influx in the formation of calcrete and palustrine facies: A response to paleogeographic and climatic conditions in the southeastern Tertiary Duerco Basin (northern Spain), in Alonso-Zarza, A. M. and L. H. Tanner (eds.), 2006, *Paleoenvironmental Record and Applications of Calcretes and Palustrine Carbonates*: Geological Society of America Special Paper 416, pp. 119–132.
- Arnott, R. W. C. and B. M. Hand, 1989, Bedforms, primary structures and grain fabrics in the presence of suspended sediment rain: *J. Sediment. Petrol.*, **59**, 1062–1069.
- Arvidson, R. S. and F. T. Mackenzie, 1999, The dolomite problem: control of precipitation kinetics by temperature and saturation state: *Am. J. Sci.*, **299**, 257–288.
- Ashley, G. M. (chairperson), 1990, Classification of large-scale subaqueous bedforms: a new look at an old problem: *J. Sediment. Petrol.*, **60**, 160–172.
- Asquith, G. and D. Krygowski, 2004, *Basic Well Log Analysis*, 2nd edn.: American Association of Petroleum Geology, Tulsa, OK.
- Assaad, F., P. E. LaMoreau, and T. H. Hughes (eds.), 2004, *Field Methods for Geologists and Hydrogeologists*: Springer-Verlag, Berlin.
- Aylmore, L. A. G. and J. P. Quirk, 1960, Domain or turbostratic structure of clays: *Nature*, **187**, 1046–1048.
- Badiozamani, K., 1973, The Dorag dolomitization model – application to the Middle Ordovician of Wisconsin: *J. Sediment. Petrol.*, **43**, 965–984.
- Bagnold, R. A. and O. Barndorff-Nielsen, 1980, The pattern of natural size distribution: *Sedimentology*, **27**, 199–207.
- Barndorff-Nielsen, O., 1977, Exponentially decreasing distributions for the logarithm of particle size: *Proc. Royal Soc. London A.*, **353**, 401–419.
- Barndorff-Nielsen, O., K. Dalsgaard, C. Halgreen, *et al.*, 1982, Variation in particle size distribution over a small dune: *Sedimentology*, **29**, 53–65.
- Barrett, P. J., 1980, The shape of rock particles: a critical review: *Sedimentology*, **27**, 291–303.
- Barron, J. A., 1987, Diatomite: Environmental and geologic factors affecting its distribution, in J. R. Hein (ed.), *Siliceous Sedimentary Rock – Hosted Ores and Petroleum*: Van Nostrand Reinhold Co., New York, NY, pp. 164–178.
- Basu, A., 1976, Petrology of Holocene fluvial sand derived from plutonic source rocks: implications to paleoclimate interpretation: *J. Sediment. Petrol.*, **46**, 694–709.
- Basu, A., 1985, Influence of climate and relief on compositions of sand released at source areas, in Zuffa, G. G. (ed.), *Provenance of Arenites*: Reidel, Dordrecht, pp. 1–18.
- Basu, A., S. W. Young, L. J. Suttner, W. C. James, and G. H. Mack, 1975, Re-evaluation of the use of undulatory extinction and polycrystallinity in detrital quartz for provenance interpretation: *J. Sediment. Petrol.*, **45**, 873–882.
- Bates R. L. and J. A. Jackson (eds.), 1980, *Glossary of Geology*, 2nd edn.: American Geological Institute, Falls Church, VA.
- Bathurst, R. G. C., 1966, Boring algae, micrite envelopes and lithification of molluscan biosparites: *Geol. J.*, **5**, 15–32.

- Bathurst, R. G. C., 1975, *Carbonate Sediments and their Diagenesis*, 2nd edn.: Elsevier, Amsterdam.
- Bathurst, R. G. C., 1980, Lithification of carbonate sediments: *Sci. Prog.*, **66**, 451–471.
- Bathurst, R. G. C., 1982, Genesis of stromatactis cavities between submarine crusts in Paleozoic carbonate mud buildups: *J. Geol. Soc. London*, **139**, 165–181.
- Bathurst, R. G. C., 1983, Neomorphic spar versus cement in some Jurassic grainstones: Significance for evaluation of porosity evolution and compaction: *J. Geol. Soc. London*, **140**, 229–237.
- Baturin, G. N., 1982, *Phosphorites on the Seafloor: Origin, Composition, and Distribution*: Elsevier, Amsterdam.
- Baturin, G. N., 2000, Formation and evolution of phosphorite grains and nodules on the Namibian shelf, from Recent to Pleistocene, in Glenn G. R. L., L. Prévôt-Lucas, and J. Lucas (eds.), *Marine Authigenesis: From Global to Microbial*: SEPM Special Publication 66, pp. 185–199.
- Beales, F. W. and J. L. Hardy, 1980, Criteria for the recognition of diverse dolomite types with an emphasis on studies on host rocks for Mississippi Valley-type ore deposits, in D. H. Zenger, J. B. Dunham, and R. L. Ethington (eds.), *Concepts and Models of Dolomitization*: SEPM Special Publication 28, pp. 197–213.
- Beard, B. L., C. M. Johnson, L. Cox *et al.*, 1999, Iron isotope biosignatures: *Science*, **285**, 1889–1892.
- Bennett, R. H., N. R. O'Brien, and M. H. Hulbert, 1991a, Determinants of clay and shale microfabric signatures: Processes and mechanisms, in Bennett, R. H., N. R. O'Brien, and M. H. Hulbert (eds.), *Microstructures of Fine-Grained Sediments*: Springer-Verlag, New York, NY, pp. 5–32.
- Bennett, R. H., N. R. O'Brien, and M. H. Hulbert (eds.), 1991b, *Microstructures of Fine-Grained Sediments*: Springer-Verlag, New York, NY.
- Benninger, L. M. and J. R. Hein, 2000, Diagenetic evolution of seamount phosphorite, in Glenn *et al.* (eds.), *Marine Authigenesis: From Global to Microbial*: SEPM Special Publication 66, pp. 245–256.
- Bentor, Y. K. (ed.), 1980, *Marine Phosphorites – Geochemistry, Occurrence, Genesis*: SEPM Special Publication 29.
- Berner, R. A., 1971, *Principles of Chemical Sedimentology*: McGraw-Hill, New York, NY.
- Berner, R. A., 1975, The role of magnesium in crystal growth of aragonite from sea water: *Geochim. Cosmochim. Acta*, **39**, 489–505.
- Berner, R. A., 1980, *Early Diagenesis*: Princeton University Press, Princeton, NJ.
- Berner, R. A., J. T. Westrich, R. Graber, J. Smith, and C. S. Martens, 1978, Inhibition of aragonite precipitation from supersaturated seawater: A laboratory and field study: *Am. J. Sci.*, **278**, 816–837.
- Bernet, M. and K. Bassett, 2005, Provenance analysis by single quartz grain SEM-CL/optical microscopy: *J. Sediment. Res.*, **75**, 492–499.
- Bernet, M. and C. Spiegel (eds.), 2004, *Detrital Thermochronology – Provenance Analysis, Exhumation, and Landscape Evolution of Mountain Belts*: Geological Society of America Special Paper 378.
- Beuselinck, L., 1998, Grain-size analysis by laser diffractometry; comparison with the sieve-pipette method: *Catena Giessen*, **32**, 193–208.
- Bhatia, M. R., 1983, Plate tectonics and geochemical composition of sandstones: *J. Geol.*, **91**, 611–627.

- Bhatia, M. R., 1985, Composition and classification of Paleozoic flysch mudrocks of eastern Australia: Implications in provenance and tectonic setting interpretation: *Sed. Geol.*, **41**, 249–268.
- Bhatia, M. R. and K. A. W. Crook, 1986, Trace element characteristics of greywackes and tectonic setting discrimination of sedimentary basins: *Contrib. Mineralogy Petrol.*, **92**, 181–193.
- Bhattacharyya, A., 2000, *Analysis of Sedimentary Successions: A Field Manual*: A. A. Balkema, Rotterdam.
- Bhattacharyya, D. P., 1989, Concentrated and lean oolites: Examples from the Nubia Formation at Aswan, Egypt, and significance of the oolite types in ironstone genesis, in Young, T. P. and W. E. G. Taylor (eds.), *Phanerozoic Ironstones*: Geological Society Special Publication 46, pp. 93–103.
- Bjørlykke, K., 1983, Diagenetic reactions in sandstones, in A. Parker and B. W. Sellwood (eds.), *Sediment Diagenesis*: Reidel, Dordrecht, pp. 169–213.
- Bjørlykke, K., 1994, Pore-water flow and mass transfer of solids in solution in sedimentary basins, in Parker, A. and B. W. Sellwood (eds.), *Quantitative Diagenesis: Recent Developments and Applications to Reservoir Geology*: Kluwer Academic Publishing, Dordrecht, pp. 189–221.
- Black, M., 1933, The precipitation of calcium carbonate on the Great Bahama Bank: *Geol. Mag.*, **70**, 455–466.
- Blatt, H., 1982, *Sedimentary Petrology*: W. H. Freeman, San Francisco, CA.
- Blatt, H. and J. R. Caprara, 1985, Feldspar dispersal patterns in shales of the Vanoss formation (Pennsylvanian), south-central Oklahoma: *J. Sediment. Petrol.*, **55**, 548–552.
- Blatt, H. and M. W. Totten, 1981, Detrital quartz as an indicator of distance from shore in marine mudrocks: *J. Sediment. Petrol.*, **51**, 1259–1266.
- Blatt, H., G. Middleton, and R. Murray, 1980, *Origin of Sedimentary Rocks*, 2nd edn.: Prentice-Hall, Englewood Cliffs, NJ.
- Blatt, H., R. L. Jones, and R. G. Charles, 1982, Separation of quartz and feldspars from mudrocks: *J. Sediment. Petrol.*, **52**, 660–662.
- Blott, S. J., D. J. Croft, K. Pye, S. E. Saye, and H. E. Wilson, 2004, Particle size analysis by laser diffraction, in Pye, K. and D. J. Croft (eds.), *Forensic Geoscience: Principles, Techniques and Applications*: Geological Society Special Publication 232, pp. 63–73.
- Boggs, S., Jr., 1969, Relationship of size and composition in pebble counts: *J. Sediment. Petrol.*, **39**, 1243–1246.
- Boggs, S., Jr., 1972, Petrography and geochemistry of rhombic calcite pseudomorphs from mid-Tertiary mudstones of the Pacific Northwest, USA: *Sedimentology*, **19**, 219–235.
- Boggs, S., Jr., 1975, Seabed resources of the Taiwan continental shelf: *Acta Oceanographica Taiwanica*, **5**, 1–18.
- Boggs, S., Jr., 1992, *Petrology of Sedimentary Rocks*: Macmillan Publishing Co., New York, NY.
- Boggs, S., Jr., 2006, *Principles of Sedimentology and Stratigraphy*, 4th edn.: Prentice Hall, Upper Saddle River, NJ.
- Boggs, S., Jr. and D. Kinsley, 2006, *Application of Cathodoluminescence Imaging to the Study of Sedimentary Rocks*: Cambridge University Press, Cambridge.
- Boggs, S., Jr. and A. Seyedolali, 1992, Diagenetic albittization, zeolitization, and replacement in Miocene sandstones, Sites 796, 797, and 799, Japan Sea, in Pisciotto, K. A., J. C. Ingle, Jr., M. T. von Breyman, et al. (eds.), *Proceedings of the Ocean*

- Drilling Program, Scientific Results*: ODP, College Station, TX, vol. 127/128, part 1, pp. 131–151.
- Boggs, S., Jr., Y.-I. Kwon, G. G. Goles *et al.* 2002, Is quartz cathodoluminescence color a reliable provenance tool? A quantitative examination: *J. Sediment. Res.*, **72**, 408–415.
- Boles, J. R., 1982, Albitization of plagioclase, Gulf Coast Tertiary: *Am. J. Sci.*, **282**, 165–180.
- Boles, J. R. and S. G. Franks, 1979, Clay diagenesis in Wilcox Sandstones of southwest Texas: implications of smectite diagenesis on sandstone cementation: *J. Sediment. Petrol.*, **49**, 55–70.
- Bond, G. C. and J. C. Devay, 1980, Pre-upper Devonian quartzose sandstones in the Shoo Fly formation northern California – Petrology, provenance and implications for regional tectonics: *J. Geol.*, **88**, 285–308.
- Bouma, A. H., 1962, *Sedimentology of Some Flysch Deposits*: Elsevier, Amsterdam.
- Braithwaite, C. J. R., 1989, Displacive calcite and grain breakage in sandstones: *J. Sediment. Petrol.*, **59**, 258–266.
- Braithwaite, C. J. R., 1991, Dolomites, a review of origins, geometry and textures: *Trans. Royal Soc. Edinburgh, Earth Sciences*, **82**, 99–112.
- Braitsch, O., 1971, *Salt Deposits: Their Origin and Composition*: Springer-Verlag, Berlin.
- Brand, J., 1989, Aragonite–calcite transformation based on Pennsylvanian molluscs: *Geol. Soc. Am. Bull.*, **101**, 377–390.
- Bricker, O. P. (ed.), 1971, *Carbonate Cements*: Johns Hopkins Press, Baltimore, MD.
- Briggs, R. M., M. P. Middleton, and C. S. Nelson, 2004, Provenance history of a Late Triassic–Jurassic Gondwana margin forearc basin, Murihiku Terrane, North Island, New Zealand: Petrographic and geochemical constraints: *New Zealand J. Geol. Geophys.*, **47**, 589–602.
- Bromley, R. G., 1996, *Trace Fossils: Biology, Taphonomy, and Applications*, 2nd edn.: Chapman and Hall, London.
- Brown, D. A., 2006, Microbial mediation of iron mobilization and deposition in iron formations since the early Precambrian, in Kesler, S. E. and H. Ohmoto (eds.), *Evolution of Early Earth's Atmosphere, Hydrosphere, and Biosphere – Constraints from Ore Deposits*: Geological Society of America Memoir 198, pp. 239–256.
- Brügel, A., I. Dunkl, W. Frisch, J. Kuhlemann, and K. Balogh, 2004, Geochemistry and geochronology of gneiss pebbles from foreland molasse conglomerates: Geodynamic and paleogeographic implications for the Oligo-Miocene evolution of the Eastern Alps: *J. Geol.*, **111**, 543–563.
- Budd, D. A., 1997, Cenozoic dolomites of carbonate islands: Their attributes and origin: *Earth Sci. Rev.*, **42**, 1–47.
- Budd, D. A., A. H. Saller, and P. M. Harris (eds.), 1995, *Unconformities and Porosity in Carbonate Strata*: AAPG Memoir 63.
- Buekes, N. J. and C. Klein, 1992, Models for iron-formation deposition, in Schopf, J. W. and C. Klein (eds.), *The Proterozoic Biosphere*: Cambridge University Press, Cambridge.
- Buekes, N. J. and D. R. Lowe, 1989, Environmental control on diverse stromatolite morphologies in the 3000 My Pongola Supergroup, South Africa: *Sedimentology*, **36**, 383–397.
- Burger, H. and W. Skala, 1976, Comparison of sieve and thin-section technique by a Monte-Carlo model: *Comput. Geosci.*, **2**, 123–139.
- Burley, S. D., J. D. Kantorowicz, and B. Waugh, 1985, Clastic diagenesis, in Brenchley, P. J. and B. P. J. Williams (eds.), *Sedimentology, Recent Developments and Applied Aspects*: Blackwell Scientific Publishing, Oxford, pp. 189–226.

- Burnett, W. C. and P. N. Froelich (eds., special issue), 1988, The origin of marine phosphorites: The results of the R. V. Robert D. Conrad Cruise 23–06 to the Peru shelf: *Mar. Geol.*, **80**, 181–346.
- Burnett, W. C. and S. R. Riggs (eds.), 1990, *Phosphate Deposits of the World, 3: Neogene to Modern Phosphorites*: Cambridge University Press, Cambridge.
- Burst, J. F., 1965, Subaqueously formed shrinkage cracks in clay: *J. Sediment. Petrol.*, **35**, 348–353.
- Busby, C. J. and R. V. Ingersoll (eds.), 1995, *Tectonics of Sedimentary Basins*: Blackwell Science, Cambridge, MA.
- Busenberg, E. and L. N. Plummer, 1986, A comparative study of the dissolution and crystal growth kinetics of calcite and aragonite, in F. A. Mumpton (ed.), *Studies in Diagenesis*: US Geological Survey Bulletin 1578, pp. 139–168.
- Bustin, R. M., A. R. Cameron, D. A. Grieve, and W. D. Kalkreuth, 1985, *Coal Petrology, its Principles, Methods, and Applications*: Geological Association of Canada Short Course Notes V. 3.
- Button, A., T. D. Brock, P. J. Cook *et al.*, 1982, Sedimentary iron deposits, evaporites, and phosphorites, in H. D. Holland and M. Schidlowski (eds.), *Mineral Deposits and Evolution of the Biosphere*: Springer-Verlag, New York, NY, pp. 259–273.
- Buxton, T. M. and D. F. Sibley, 1981, Pressure solution features in shallow buried limestones: *J. Sediment. Petrol.*, **51**, 19–26.
- Byers, C. W., 1974, Shale fissility: relation to bioturbation: *Sedimentology*, **21**, 479–484.
- Calvert, S. E., 1974, Deposition and diagenesis of silica in marine waters, in K. J. Hsü and H. C. Jenkyns (eds.), *Pelagic Sediments: on Land and Under the Sea*: International Association of Sedimentologists, Special Publication 1 pp. 273–299.
- Calvert, S. E., 1983, Sedimentary geochemistry of silicon, in R. R. Aston (ed.), *Silicon Geochemistry and Biogeochemistry*: Academic Press, London, pp. 143–186.
- Cameron, E. M. and R. M. Garrels, 1980, Geochemical composition of some Precambrian shales from the Canadian Shield: *Chem. Geol.*, **28**, 181–197.
- Campbell, C. V., 1966, Truncated wave-ripple laminae: *J. Sediment. Petrol.*, **36**, 820–828.
- Campbell, C. V., 1967, Lamina, laminaset, bed and bedset: *Sedimentology*, **8**, 7–26.
- Carballo, J. D. and L. S. Land, 1984, Holocene dolomitization of supratidal sediments by active tidal pumping, Sugarloaf Key, Florida (abs.): *Am. Assoc. Pet. Geol. Bull.*, **68**, 459.
- Carballo, J. D., L. S. Land, and D. E. Miser, 1987, Holocene dolomitization of supratidal sediments by active tidal pumping, Sugarloaf Key, Florida: *J. Sediment. Petrol.*, **57**, 153–165.
- Carlson, W. D., 1983, The polymorphs of CaCO₃ and the aragonite–calcite transformation, in R. J. Reeder (ed.), *Carbonates: Mineralogy and Chemistry*: Mineralogical Society of America Reviews in Mineralogy 11, pp. 191–225.
- Caroll, A. R. and M. A. Wartes, 2003, Organic carbon burial by large Permian lakes, northwest China, in Chan, M. S. and A. W. Archer (eds.), *Extreme Depositional Environments: Mega End Members in Geologic Time*: Geological Society of America Special Paper 370, pp. 91–104.
- Carothers, W. W. and Y. K. Kharaka, 1979, Aliphatic acid anions in oil-field waters – implications for origin of natural gas: *Am. Assoc. Pet. Geol. Bull.*, **62**, 2441–2453.
- Carozzi, A. V., 1960, *Microscopic Sedimentary Petrography*: John Wiley and Sons, New York, NY.
- Carozzi, A. V., 1989, *Carbonate Rock Depositional Models – A Microfacies Approach*: Prentice-Hall, Englewood Cliffs, NJ.

- Carstens, H., 1985, Early diagenetic cone-in-cone structures in pyrite concretions: *J. Sediment. Petrol.*, **55**, 105–108.
- Carver, R. E., 1971, *Procedures in Sedimentary Petrology*: John Wiley and Sons, New York, NY.
- Cas, R. A. F. and J. V. Wright, 1987, *Volcanic Successions: Modern and Ancient*: Allen and Unwin, London.
- Casas, E. and T. K. Lowenstein, 1989, Diagenesis of saline pan halites: Comparison of petrographic features of modern, Quaternary, and Permian halites: *J. Sediment. Petrol.*, **59**, 724–739.
- Cathcart, J. B., 1989, The phosphate deposits of Florida with a note on the deposits in Georgia and South Carolina, USA, in Northolt, A. J. G., R. P. Sheldon, and D. F. Davidson (eds.), *Phosphorite Deposits of the World, 2: Phosphate Rock Resources*: Cambridge University Press, Cambridge, pp. 62–70.
- Cayeux, L., 1935, *Les Roches Sédimentaires de France: Roches Carbonatées*: Masson et Cie, Paris.
- Chafetz, H. S. and R. L. Folk, 1984, Travertines: Depositional morphology and the bacterially constructed constituents: *J. Sediment. Petrol.*, **54**, 289–316.
- Chamley, H., 1989, *Clay Sedimentology*: Springer-Verlag, Berlin.
- Cheel, R. and D. A. Leckie, 1993, Hummocky cross-stratification, in Wright, P. V. (ed.), *Sedimentology Review 1*, Blackwell Scientific Publications, Oxford, pp. 103–122.
- Choquette, P. W. and N. P. James, 1987, Diagenesis in limestones – 3. The deep burial environment: *Geosci. Can.*, **14**, 3–35.
- Choquette, P. W. and L. C. Pray, 1970, Geologic nomenclature and classification of porosity in sedimentary carbonates: *Am. Assoc. Pet. Geol. Bull.*, **54**, 207–250.
- Chowns, T. M. and J. E. Elkins, 1974, The origin of quartz geodes and cauliflower cherts through the silicification of anhydrite nodules: *J. Sediment. Petrol.*, **44**, 885–903.
- Christiansen, C., 1984, *A Comparison of Sediment. Parameters from Log Probability Plots and Log-Log Plots of the Same Sediments*: Geoskrifter 20.
- Christiansen, C. and D. Hartmann, 1991, The hyperbolic distribution, in Syvitski, J. P. M. (ed.), 1991, *Principles, Methods, and Application of Particle Size Analysis*: Cambridge University Press, Cambridge, pp. 237–248.
- Clark, F. W., 1924, *The Data of Geochemistry*, 5th edn.: US Geological Survey Bulletin 770.
- Clark, M. W., 1981, Quantitative shape analysis: a review: *J. Math. Geol.*, **13**, 303–320.
- Clark, M. W., 1987, Image analysis of clastic particles, in Marshall, J. R. (ed.), *Clastic Particles*: Van Nostrand Reinhold, New York, NY, pp. 256–266.
- Clayton, C. J., 1994, Microbial and organic processes, in Parker, A. and B. W. Sellwood (eds.), *Quantitative Diagenesis: Recent Developments and Applications to Reservoir Geology*: Kluwer, Dordrecht, pp. 125–160.
- Cloud, P. E., 1973, Paleocological significance of banded iron formations: *Econ. Geol.*, **68**, 1135–1143.
- Coakley, J. P. and J. P. M. Syvitski, 1991, SediGraph technique, in Syvitski, J. P. M. (ed.), 1991, *Principles, Methods, and Application of Particle Size Analysis*: Cambridge University Press, Cambridge, pp. 129–142.
- Cobb, J. C. and C. B. Cecil, 1993, *Modern and Ancient Coal-Forming Environments*: Geological Society of America Special Paper 286.
- Collinson, J. D., 1970, Bedforms of the Tana River, Norway: *Geogr. Ann.*, **52A**, 31–55.
- Collinson, J. D. and D. B. Thompson, 1989, *Sedimentary Structures*, 2nd edn.: Chapman and Hall, London.

- Coogan, A. H. and R. W. Manus, 1975, Compaction and diagenesis of carbonate sands, in Chilingarian, G. V. and K. H. Wolf (eds.), *Compaction of Coarse-Grained Sediments I. Developments in Sedimentology 18A*: Elsevier, New York, NY, pp. 79–166.
- Cook, P. J., 1976, Sedimentary phosphate deposits, in Wolf, K. H. (ed.), *Handbook of Strata-Bound and Stratiform Ore Deposits*: Elsevier, Amsterdam, vol. 7, pp. 506–536.
- Cook, P. J. and J. H. Shergold, 1986, Proterozoic and Cambrian phosphorites – Nature and origin, in Cook, P. J. and J. H. Shergold (eds.), *Phosphate Deposits of the World, 1: Proterozoic and Cambrian Phosphorites*: Cambridge University Press, Cambridge, pp. 369–386.
- Crelling, J. C. and R. R. Dutcher, 1980, Principles and Applications of Coal Petrology: SEPM Short Course Notes 8.
- Cressman, E. R., 1962, *Nondetrital Siliceous Sediments*: US Geological Survey Professional Paper 440-T.
- Crimes, T. P., 1975, The stratigraphal significance of trace fossils, in Crimes, T. P. and J. C. Harper (eds.), *The Study of Trace Fossils*: Springer-Verlag, Berlin.
- Crook, K. A. W., 1960, Petrology of Parry Group, Upper Devonian–Lower Carboniferous, Tamworth–Nundel District, New South Wales: *J. Sediment. Petrol.*, **30**, 538–552.
- Crook, K. A. W., 1970, Graywackes, in *Encyclopaedia Britannica 10*: Encyclopaedia Britannica, Chicago.
- Crook, K. A. W., 1974, Lithogenesis and geotectonics: The significance of compositional variation in flysch arenites (graywackes), in Dott, R. H. Jr. and R. H. Shaver (eds.), *Modern and Ancient Geosynclinal Sedimentation*: SEPM Special Publication 19, pp. 304–310.
- Crowell, J. C., 1957, Origin of pebbly mudstones: *Geol. Soc. Am. Bull.*, **68**, 993–1009.
- Cullen, D. J., G. A. Challis, and G. W. Drummond, 1990, Late Holocene estuarine phosphogenesis in Raglan Harbour, New Zealand: *Sedimentology*, **37**, 847–857.
- Curtis, C. D., 1980, Diagenetic alteration in black shales: *J. Geol. Soc. London*, **137**, 189–194.
- Curtis, C. D., S. R. Lipshie, G. Oertel, and M. J. Pearson, 1980, Clay orientation in some Upper Carboniferous mudrocks, its relationship to quartz content and some inferences about fissility, porosity and compaction history: *Sedimentology*, **17**, 333–339.
- Daniels, E. J., S. P. Altaner, S. Marshak, and J. R. Eggleson, 1990, Hydrothermal alteration in anthracite in eastern Pennsylvania: Implications for the mechanisms of anthracite formation: *Geology*, **18**, 247–250.
- Dapples, E. C., 1979, Diagenesis of sandstones, in Larsen, G. and G. V. Chilingar (eds.), *Diagenesis in Sediments and Sedimentary Rocks*: Elsevier, Amsterdam, pp. 31–97.
- Dauphas, N., N. L. Cates, S. J. Mojzsis, and V. Busigny, 2007, Identification of chemical sedimentary protoliths using iron isotopes in the > 3750 Ma Nuvvuagittuq supracrustal belt, Canada: *Earth Planet. Sci. Lett.*, **254**, 358–376.
- Dean, W. E., 1982, Theoretical versus observed successions from evaporation of seawater, in W. E. Dean and B. C. Schreiber (eds.), *Marine Evaporites*: SEPM Short Course Notes 4, pp. 74–85.
- Dean, W. E. and T. D. Fouch, 1983, Lacustrine environment, in Scholle, P. A., D. G. Bebout, and C. H. Moore, 1983, *Carbonate Depositional Environments*: AAPG Memoir 33, pp. 97–130.
- Dean, W. E., G. R. Davies, and R. Y. Anderson, 1975, Sedimentological significance of nodular and laminated anhydrite: *Geology*, **3**, 367–372.

- Decelles, P. G., 1988, Lithologic provenance modeling applied to the Late Cretaceous synorogenic Echo Canyon Conglomerate, Utah: A case of multiple source areas: *Geology*, **16**, 1039–1043.
- Deer, W. A., R. A. Howie, and J. Zussman, 1963, *Rock-Forming Minerals, Framework Silicates*: John Wiley and Sons, New York, vol. 4.
- Deer, W. A., R. A. Howie, and J. Zussman, 1966, *An Introduction to the Rock-Forming Minerals*: Longman, London.
- Deer, W. A., R. A. Howie, and J. Zussman, 1992, *An Introduction to the Rock-Forming Minerals*, 2nd edn.: Longman, London, John Wiley and Sons, New York, NY.
- Deer, W. A., R. A. Howie, and J. Zussman, 1997, *Rock-Forming Minerals*, 2nd edn., Geological Society London, London, vols. 3A, 4A, and 4B.
- Degens, E. T., 1965, *Geochemistry of Sediments*: Prentice-Hall, Englewood Cliffs, NJ.
- Demico, R. V. and L. A. Hardie, 1994, *Sedimentary Structures and Early Diagenetic Features of Shallow Marine Carbonate Deposits*: SEPM Atlas Series 1.
- Dickinson, W. R., 1970, Interpreting detrital modes of graywacke and arkose: *J. Sediment. Petrol.*, **40**, 695–707.
- Dickinson, W. R., 1974, Plate tectonics and sedimentation, in Dickinson, W. R. (ed.), *Tectonics and Sedimentation*: Society of Economic Paleontologists and Mineralogists Special Publication 22, pp. 1–27.
- Dickinson, W. R., 1976, *Plate Tectonic Evolution of Sedimentary Basins*: American Association of Petroleum Geologists Continuing Education Course Notes, Series 1.
- Dickinson, W. R., 1985, Interpreting provenance relations from detrital modes of sandstones, in Zuffa, G. G. (ed.), *Provenance of Arenites*: Reidel, Dordrecht, pp. 333–361.
- Dickinson, W. R., 1988, Provenance and sediment dispersal in relation to paleotectonics and paleogeography of sedimentary basins, in Kleinspehn, K. L. and C. Paola (eds.), *New Perspectives in Basin Analysis*: Springer-Verlag, New York, NY, pp. 3–25.
- Dickinson, W. R. and R. V. Ingersoll, 1990, Physiographic controls on the composition of sediments derived from volcanic and sedimentary terrains on Barro Colorado Island, Panama – Discussion: *J. Sediment. Petrol.*, **60**, 797–798.
- Dickinson, W. R. and E. I. Rich, 1972, Petrologic intervals and petrofacies in the Great Valley Sequence, Sacramento Valley, California: *Geol. Soc. Am. Bull.*, **83**, 3007–3024.
- Dickinson, W. R. and C. Suczek, 1979, Plate tectonics and sandstone compositions: *Am. Assoc. Pet. Geol. Bull.*, **63**, 2164–2182.
- Dickinson, W. R. and R. Valloni, 1980, Plate settings and provenance of sands in modern ocean basins: *Geology*, **8**, 82–86.
- Dickinson, W. R., L. S. Beard, G. R. Brakenridge, et al., 1983, Provenance of North American Phanerozoic sandstones in relation to tectonic setting: *Geol. Soc. Am. Bull.*, **94**, 222–235.
- Diepenbroek, M., A. Bartholomä, and H. Ibbken, 1992, How round is round? A new approach to the topic ‘roundness’ by Fourier grain shape analysis: *Sedimentology*, **39**, 411–422.
- Dimroth, E., 1979, Models of physical sedimentation of iron formations, in R. G. Walker (ed.), *Facies Models*: Geoscience Canada Reprint Series 1, pp. 159–174.
- Dobkins, J. E. and R. L. Folk, 1970, Shape development on Tahiti-Nui: *J. Sediment. Petrol.*, **40**, 1167–1203.
- Donovan, S. K., 1994, *The Palaeobiology of Trace Fossils*: John Hopkins Press, Baltimore, MD.

- Dove, P. M. and J. D. Rimstidt, 1994, Silica–water interactions, in Heaney, P. J., C. T. Prewitt, and G. V. Gibbs (eds.), *Silica: Physical Behavior, Geochemistry and Materials Applications*: Mineralogical Society of America Reviews in Mineralogy 29.
- Doyle, L. J. and H. H. Roberts, 1988, *Carbonate–Clastic Transitions*: Elsevier, Amsterdam.
- Doyle, L. J., K. L. Carder, and R. G. Stewart, 1983, The hydraulic equivalence of micas: *J. Sediment. Petrol.*, **53**, 643–648.
- Dryden, L. and C. Dryden, 1946, Comparative rates of weathering of some common heavy minerals: *J. Sediment. Petrol.*, **16**, 91–96.
- Duke, W. L., R. W. C. Arnott, and R. J. Cheel, 1991, Shelf sandstone and hummocky cross-stratification: New insights on a stormy debate: *Geology*, **19**, 625–628.
- Duncan, D. C., 1976, Geologic setting of oil-shale deposits and world prospects, in Yen, T. F. and G. V. Chilingarian (eds.), *Oil Shale*: Elsevier, Amsterdam, pp. 13–26.
- Dunham, R. J., 1962, Classification of carbonate rocks according to depositional texture, in Ham, W. E. (ed.), *Classification of Carbonate Rocks*: AAPG Memoir 1, pp. 108–121.
- Dunham, R. J., 1971, Meniscus cement, in O. P. Bricker (ed.), *Carbonate Cements*: Johns Hopkins University Studies in Geology 19, pp. 297–300.
- Dunkl, I., W. Frisch, J. Kuhlemann, and A. Brügel, 1998, Pebble-population-dating: A new method for provenance analysis: *Terra Nostra*, **98**, 45.
- Dunn, T. L., 1992, Infiltrated material in Cretaceous, volcanic sandstones, San Jorge Basin, Argentina, in Houseknecht, D. W., E. D. Pittman, and B. H. Lidz (eds.), *Origin, Diagenesis, and Clay Minerals in Sandstones*: Society for Sedimentary Geology Special Publication 47, pp. 159–174.
- Dunoyer de Segonzac, G., 1970, The transformation of clay minerals during diagenesis and low-grade metamorphism: A review: *Sedimentology*, **15**, 281–346.
- Durand B. (ed.), 1980, *Kerogen*: Editions Technip, Paris.
- Dutta, P. K. and R. W. Wheat, 1993, Climatic and tectonic controls on sandstone composition in the Permo-Triassic Sydney Foreland Basin, Eastern Australia, in Johnson, M. J. and A. Basu (eds.), *Processes Controlling the Composition of Clastic Sediments*: Geological Society of America Special Paper 284, pp. 187–202.
- Dutton, S. P. and T. N. Diggs, 1990, History of quartz cementation in the Lower Cretaceous Travis Peak Formation, east Texas: *J. Sediment. Petrol.*, **60**, 191–202.
- Dzevanshir, R. D., L. A. Buryakovskiy, and G. V. Chilingarian, 1986, Simple quantitative evaluation of porosity of argillaceous sediments at various depths of burial: *Sediment. Geol.*, **46**, 169–175.
- Dzulnyski, S. and E. K. Walton, 1965, *Sedimentary Features of Flysch and Graywacke*: Developments in Sedimentology 7.
- Ehrlich, R. and M. Chin, 1980, Fourier grain-shape analysis: a new tool for sourcing and tracking abyssal silts: *Mar. Geol.*, **38**, 219–231.
- Ehrlich, R. and B. Weinberg, 1970, An exact method for characterization of grain shape: *J. Sediment. Petrol.*, **40**, 205–212.
- Ehrlich, R., P. J. Brown, J. M. Yarus, and R. S. Przygocki, 1980, The origin of shape frequency distributions and the relationship between size and shape: *J. Sediment. Petrol.*, **50**, 475–484.
- Ehrlich, R., S. J. Crabtree, S. K. Kennedy, and R. L. Cannon, 1984, Petrographic image analysis, I. Analysis of reservoir pore complexes: *J. Sediment. Petrol.*, **54**, 1365–1378.
- Ehrlich, R., S. K. Kennedy, and C. D. Brotherhood, 1987, Respective roles of Fourier and SEM techniques in analyzing sedimentary quartz, in Marshall, J. R. (ed.), *Clastic Particles*, Van Nostrand Reinhold, New York, NY, pp. 292–301.

- Elliott, M. A. and G. R. Yohe, 1981, The coal industry and coal research and development in perspective, in Elliott, M. A. (ed.), *Chemistry of Coal Utilization, Second Supplementary Volume*: Wiley Interscience, New York, NY, pp. 1–54.
- Embry, A. F. and J. E. Klovan, 1971, A late Devonian reef tract on the northeastern Banks Island, N. W. T.: *Canada Pet. Geol. Bull.*, **19**, 730–781.
- Embry, A. F. and J. E. Klovan, 1972, Absolute water depth limits of late Devonian paleoecological zones: *Geol. Rundsch.*, **61**, 672–686.
- Epstein, S., R. Buchsbaum, H. A. Lowenstam, and H. C. Urey, 1953, Revised carbonate–water isotopic temperature scale: *Geol. Soc. Am. Bull.*, **64**, 1315–1326.
- Eslinger, E. and D. Pevear, 1988, *Clay Minerals for Petroleum Geologists and Engineers*: SEPM Short Course Notes 22.
- Esteban, M. and C. F. Klappa, 1983, Subaerial exposure environment, in Scholle, P. A., D. G. Bebout, and C. H. Moore (eds.), *Carbonate Depositional Environments*: AAPG Memoir 33, pp. 1–54.
- Evamy, B. D., 1969, The precipitational environment and correlation of some calcite cements deduced from artificial staining: *J. Sediment. Petrol.*, **39**, 787–821.
- Fairbridge, R. W., 1983, Syndiagenesis–anadiagenesis–epidiagenesis: phases in lithogenesis, in G. Larsen and G. V. Chilingar (eds.), *Diagenesis in Sediments and Sedimentary Rocks, 2*: Elsevier, Amsterdam, pp. 17–113.
- Faure, G. and T. M. Mensing, 2005, *Isotopes: Principles and Applications*, 3rd edn.: John Wiley and Sons, Hoboken, NJ.
- Feazel, C. T. and R. A. Schatzinger, 1985, Prevention of carbonate cementation in petroleum reservoirs, in Schneidermann, N. and P. M. Harris (eds.), *Carbonate Cements*: SEPM Special Publication 36, pp. 97–106.
- Ferree, R. A., D. W. Jordan, R. S. Kertes, K. M. Savage, and P. M. Potter, 1988, Comparative petrographic maturity of river and beach sand, and origin of quartz arenites: *J. Geol. Educ.*, **36**, 79–87.
- Fieller, N. R. J., D. D. Gilbertson, and W. Olbricht, 1984, A new method for environmental analysis of particle size distribution data from shoreline sediments: *Nature*, **311**, 648–651.
- Fisher, R. V. and H. -U. Schmincke, 1984, *Pyroclastic Rocks*: Springer-Verlag, Berlin.
- Flint, R. F., 1971, *Glacial and Quaternary Geology*: John Wiley and Sons, New York, NY.
- Flint, R. F., J. E. Sanders, and J. Rodgers, 1960, Diamictite, a substitute term for symmictite: *Geol. Soc. Am. Bull.*, **71**, 1809–1810.
- Flügel, E., 1982, *Microfacies Analysis of Limestones*: Springer-Verlag, Berlin.
- Flügel, E., 2004, *Microfacies of Carbonate Rocks: Analysis, Interpretation and Applications*: Springer-Verlag, Berlin.
- Folk, R. L., 1951, Stages of textural maturity in sedimentary rocks: *J. Sediment. Petrol.*, **21**, 127–130.
- Folk, R. L., 1959, Practical petrographic classification of limestones: *Am Assoc. Pet. Geol. Bull.*, **43**, 1–38.
- Folk, R. L., 1962, Spectral subdivision of limestone types, in Ham, W. E. (ed.), *Classification of Carbonate Rocks*: AAPG Memoir 1, pp. 62–84.
- Folk, R. L., 1965, Some aspects of recrystallization in ancient limestones, in Pray, L. C. and R. C. Murray (eds.), *Dolomitization and Limestone Diagenesis*: SEPM Special Publication 13, pp. 14–48.
- Folk, R. L., 1968, Bimodal supermature sandstones. Product of the desert floor. *XXIII Internat. Geol. Cong. Proc.* **8**, 9–32.
- Folk, R. L., 1974, *Petrology of Sedimentary Rocks*: Hemphill Publishing Co., Austin, TX.

- Folk, R. L. and L. S. Land, 1975, Mg/Ca ratio and salinity: Two controls over crystallization of dolomite: *Am. Assoc. Pet. Geol. Bull.*, **59**, 60–68.
- Folk, R. L. and J. S. Pittman, 1971, Length-slow chalcedony: A new testament for vanished evaporites: *J. Sediment. Petrol.*, **41**, 1045–1058.
- Folk, R. L. and W. C. Ward, 1957, Brazos River bar: A study in the significance of grain-size parameters: *J. Sediment. Petrol.*, **27**, 3–26.
- Forrest, J. and N. R. Clark, 1989, Characterizing grain size distributions: evaluation of a new approach using multivariate extension of entropy analysis: *Sedimentology*, **36**, 711–722.
- Fountain, K. B. and G. H. McClellan, 2000, Mineralogical and geochemical evidence for the origin of phosphorite nodules on the upper West Florida slope, in Glenn, C. R., L. Prévôt-Lucas, and J. Lucas (eds.), *Marine Authigenesis: From Global to Microbial*: SEPM Special Publication, 66 pp. 201–220.
- Fournier, R. D. and J. J. Rowe, 1962, The solubility of cristobalite along the three-phase curve, gas plus liquid plus cristobalite: *Am Mineral.*, **47**, 897–902.
- Fournier, R. O., 1983, A method of calculating quartz solubility in aqueous sodium chloride solutions: *Geochim. Cosmochim. Acta*, **47**, 579–586.
- Francus, P., 1998, An image-analysis technique to measure grain-size variation in thin sections of soft clastic sediment: *Sediment. Geol.*, **121**, 289–298.
- Franks, P. C., 1969, Nature, origin, and significance of cone-in-cone structures in the Kiowa Formation (Early Cretaceous), North-Central Kansas: *J. Sediment. Petrol.*, **39**, 1438–1454.
- Franks, P. C. and A. Swineford, 1959, Character and genesis of massive opal in Kimball Member, Ogallala Formation, Scott County, Kansas: *J. Sediment. Petrol.*, **29**, 186–196.
- Frey, R. W. and A. Seilacher, 1980, Uniformity in marine invertebrate ichnology: *Lethaea*, **13**, 183–207.
- Frey, R. W., S. G. Pemberton, and J. A. Fagerstrom, 1984, Morphological, ethological and environmental significance of the ichnogenera *Scoyenia* and *Ancorichnus*: *J. Paleontol.*, **58**, 511–528.
- Friedman, G. M., 1962, Comparison of moment measures for sieving and thin-section data in sedimentary petrological studies: *J. Sediment. Petrol.*, **32**, 15–25.
- Friedman, G. M., 1967, Dynamic processes and statistical parameters compared for size frequency distribution of beach and river sands: *J. Sediment. Petrol.*, **37**, 327–354.
- Friedman, G. M., 1979, Address of the retiring president of the International Association of Sedimentologists: Differences in size distributions of populations of particles among sands of various origins: *Sedimentology*, **26**, 3–32.
- Friedman, G. M. and J. E. Sanders, 1978, *Principles of Sedimentology*: John Wiley and Sons, New York, NY.
- Friedman, G. M., C. D. Gebelein, and J. E. Sanders, 1971, Micrite envelopes of carbonate grains are not exclusively of photosynthetic algal origin: *Sedimentology*, **16**, 89–96.
- Froelich, P. N., M. A. Arthur, W. C. Burnett, *et al.*, 1988, Early diagenesis of organic matter in Peru continental margin sediments: Phosphorite precipitation: *Mar. Geol.*, **80**, 309–343.
- Frye, K., 1981, *Encyclopedia of Mineralogy*: Hutchinson Ross Publishing, Stroudsburg.
- Full, W. E., R. Ehrlich, and S. K. Kennedy, 1984, Optimal configuration and information content of sets of frequency distributions: *J. Sediment. Petrol.*, **54**, 117–126.
- Galehouse, J. S., 1971, Sedimentation analysis, in Carver, R. E. (ed.), *Procedures in Sedimentary Petrology*: John Wiley and Sons, New York, NY, pp. 69–94.

- Gao, G. and L. S. Land, 1991, Nodular cherts from the Arbuckle Group, Slick Hills, SW Oklahoma: A combined field, petrographic and isotopic study: *Sedimentology*, **38**, 857–870.
- Garrels, R. M. and C. L. Christ, 1965, *Solutions, Minerals, and Equilibria*: Harper and Row, New York, NY.
- Garrels, R. M. and F. T. Mackenzie, 1971, *Evolution of Sedimentary Rocks*: W. W. Norton, New York, NY.
- Garrison, R. E. and W. J. Kennedy, 1977, Origin of solution seams and flaser structure in Upper Cretaceous chalks of southern England: *Sediment. Geol.*, **19**, 107–137.
- Garrison, R. E., R. B. Douglass, K. E. Pisciotto, C. M. Isaacs, and J. C. Ingle (eds.), 1981, *The Monterey Formation and Related Siliceous Rocks of California*: SEPM, Pacific Section, Los Angeles, CA.
- Garven, G. and R. A. Freeze, 1984, Theoretical analysis of the role of groundwater flow in the genesis of stratabound ore deposits: *Am. J. Sci.*, **284**, 1085–1174.
- Genger, D. and P. Sethi, 1998, A geochemical and sedimentological investigation of high-resolution environmental changes within the Late Pennsylvanian (Missourian) Eudora Core Black Shale of the Mid-Continent region, U.S.A., in Schieber, J., W. Zimmerle, and P. S. Sethi (eds.), 1998, *Shales and Mudstones I and II*: E. Schweizerbart'sche Verlagsbuchhandlung, Stuttgart, pp. 271–293.
- Gieskes, J. M., 1983, The chemistry of interstitial waters of deep sea sediments: Interpretations of deep sea drilling data, in Riley, J. P. and R. Chester (eds.), *Chemical Oceanography 8*: Academic Press, New York, pp. 221–269.
- Gieskes, J. M., H. Elderfield, and B. Nevsky, 1983, Interstitial water studies, Leg 65, Deep Sea Drilling Project, in Lewis, B. R. R., P. Robison *et al.* (eds.), *Initial Reports, DSDP 65*, US Government Printing Office, Washington, DC, pp. 441–449.
- Giles, M. R., 1997, *Diagenesis: A Quantitative Perspective – Implications for Basin Modelling and Rock Property Prediction*: Kluwer Academic, Dordrecht.
- Giles, M. R. and R. B. de Boer, 1990, Origin and significance of redistributional secondary porosity: *Mar. Pet. Geol.*, **7**, 378–397.
- Gilligan, A., 1919, The petrography of the Millstone Grit of Yorkshire: *Geol. Soc. London Q. J.*, **75**, 251–292.
- Ginsburg, R. N., 1956, Environmental relationships of grain size and constituent particles in some south Florida carbonate environments: *Am. Assoc. Pet. Geol. Bull.*, **40**, 2384–2387.
- Girard, J.-P., S. M. Savin, and J. L. Aronson, 1989, Diagenesis of the Lower Cretaceous arkoses of the Angola Margin: Petrologic, K/Ar dating and $^{18}\text{O}/^{16}\text{O}$ evidence: *J. Sediment. Petrol.*, **59**, 519–538.
- Girty, G. H., B. J. Mossman, and S. D. Pincus, 1988, Petrology of Holocene sand, Peninsular Ranges, California and Baja Norte, Mexico: Implications for provenance-discrimination models: *J. Sediment. Petrol.*, **58**, 881–887.
- Given, R. K. and B. H. Wilkinson, 1985, Kinetic control of morphology, composition, and mineralogy of abiotic sedimentary carbonates: *J. Sediment. Petrol.*, **55**, 109–119.
- Given, R. K. and B. H. Wilkinson, 1987, Dolomite abundance and stratigraphic age: Constraints on rates and mechanisms of Phanerozoic dolostone formation: *J. Sediment. Petrol.*, **57**, 1068–1078.
- Glenn, C. R., L. Prévôt-Lucas, and J. Lucas (eds.), 2000, *Marine Authigenesis: From Global to Microbial*: Society for Sedimentary Geology. Special Publication 66. (Contains numerous papers devoted to phosphorites.)

- Glenn, C. R. and M. A. Arthur, 1988, Petrology and major element geochemistry of Peru margin phosphorites and associated diagenetic minerals: authigenesis in modern organic-rich sediments: *Mar. Geol.*, **80**, 231–267.
- Glenn, C. R. and M. A. Arthur, 1990, Anatomy and Origin of a Cretaceous phosphorite-greensand giant, Egypt: *Sedimentology*, **37**, 123–154.
- Goldich, S. S., 1938, A study in rock weathering: *J. Geol.*, **46**, 17–58.
- Goldstein, J. I., D. E. Newbury, P. Echlin *et al.*, 2003, *Scanning Electron Microscopy and X-Ray Microanalysis*, 3rd edn., Kluwer Academic/Plenum, New York, NY.
- Gole, M. J. and C. Klein, 1981, Banded iron-formations through much of Precambrian time: *J. Geol.*, **89**, 169–183.
- Gorai, M., 1951, Petrological studies on plagioclase twins: *Am Mineral.*, **36**, 884–901.
- Götte, T. and D. K. Richter, 2006, Cathodoluminescence characterization of quartz particles in mature arenites: *Sedimentology*, **53**, 1347–1359.
- Götte, T., R. D. Neuser and D. K. Richter, 2001, New parameters of quartz in sandstone-petrography: Cathodoluminescence (CL) – investigation of mature sands and sandstones of north-western Germany. Conference Abstracts, Cathodoluminescence in Geosciences: New insights from CL in combination with other techniques, Freiburg, September 6–8, pp. 38–39.
- Götze, J. and W. Zimmerle, 2000, *Quartz and Silica as Guide to Provenance in Sediments and Sedimentary Rocks: Contributions to Sedimentary Geology 21*, E. Schweizerbart'sche Verlagsbuchhandlung, Stuttgart.
- Graham, S. A., R. B. Tolson, P. G. Decelles, *et al.*, 1986, Provenance modeling as a technique for analysing source terrane evolution and controls on foreland sedimentation, in Allen, P. A. and P. Homewood (eds.), *Foreland Basins*: Blackwell Scientific, Oxford, pp. 425–436.
- Grantham, J. H. and M. A. Velbel, 1988, The influence of climate and topography on rock-fragment abundance in modern fluvial sands of the southern Blue Ridge Mountains, North Carolina: *J. Sediment. Petrol.*, **58**, 219–227.
- Graton, L. C. and H. J. Fraser, 1935, Systematic packing of spheres with particular relation to porosity and permeability: *J. Geol.*, **43**, 785–909.
- Greensmith, T. J., 1989, *Petrology of the Sedimentary Rocks*, 7th edn.: Unwin Hyman, London.
- Greenwood, B. and D. J. Sherman, 1986, Hummocky cross-stratification in the surf zone: flow parameters and bedding genesis: *Sedimentology*, **33**, 33–45.
- Gregg, J. M., 1985, Regional epigenetic dolomitization in the Bonneterre Dolomite (Cambrian), southeastern Missouri: *Geology*, **13**, 503–506.
- Gregg, J. M., 2004, Basin fluid flow, base-metal sulphide mineralization and the development of dolomite petroleum reservoirs, in Braithwaite, C. J. R., G. Rizzi, and G. Darke (eds.), *The Geometry and Petrogenesis of Dolomite Hydrocarbon Reservoirs*: Geological Society of London, Special Publication 235, pp. 157–175.
- Gregg, J. M. and K. L. Shelton, 1990, Dolomitization and dolomite neomorphism in the backreef facies of the Bonneterre and Davis formations (Cambrian), southeastern Missouri: *J. Sediment. Petrol.*, **60**, 549–562.
- Gregg, J. M. and D. F. Sibley, 1984, Epigenetic dolomitization and the origin of xenotopic dolomite texture: *J. Sediment. Petrol.*, **54**, 908–931.
- Grewal, K. S., G. D. Buchan, J. J. Clayton, and R. J. Mcpherson, 1991, *A Comparison of the Sedigraph and Pipette Methods for Soil Particle Size Analysis: Geological Society of New Zealand Miscellaneous Publication*, Lower Hutt, New Zealand.

- Griffith, J. C., 1967, *Scientific Methods in Analysis of Sediments*: McGraw-Hill, New York, NY.
- Griffiths, J. C., 1971, Problems of sampling in geoscience: *Trans. Inst. Min. Metall.*, **80**, B346–B356.
- Grigsby, J. D., 1990, Detrital magnetite as a provenance indicator: *J. Sediment. Petrol.*, **60**, 940–951.
- Gromet, L. P., R. F. Dymek, L. A. Haskin, and R. L. Korotev, 1984, The “North American shale composite”: Its compilation and major and trace element characteristics: *Geochim. Cosmochim. Acta*, **48**, 2469–2482.
- Gross, G. A., 1965, Geology of Iron Deposits in Canada I: General Geology and Evaluation of Iron Deposits: *Geological Survey of Canada, Economic Geology Report 22*.
- Gulbrandsen, R. A. and C. E. Roberson, 1973, Inorganic phosphorites in seawater Griffith, E. J. *et al.* (eds.), *Environmental Phosphorus Handbook*: John Wiley and Sons, New York, NY, ch. 5, pp. 117–140.
- Gulbrandsen, R. A., C. E. Roberson, and S. T. Neil, 1984, Time and crystallization of apatite in seawater: *Geochim. Cosmochim. Acta*, **48**, 213–218.
- Gunnarsson, I. and S. Arnórsson, 2000, Amorphous silica solubility and the thermodynamic properties of H_4SiO_4 in the range of 0° to 350°C at P_{sat} : *Geochim. Cosmochim. Acta*, **64**, 2295–2307.
- Hails, J. R., 1976, Placer deposits, in Wolf, K. H. (ed.), *Handbook of Strata-Bound and Stratiform Ore Deposits*, Elsevier, New York, NY, pp. 213–244.
- Hallam, A., 1981, *Facies Interpretation and the Stratigraphic Record*: W. H. Freeman, San Francisco, CA.
- Ham, W. E., 1952, Algal origin of the “Birdseye” limestones in the McLish Formation: *Okla. Acad. Sci., Proc.* **33**, 200–203.
- Haney, W. D. and L. I. Briggs, 1964, Cyclicity of textures in evaporite rocks of the Lucas Formation, in Merriam, D. F. (ed.), *Symposium on Cyclic Sedimentation*: Kansas Geological Survey Bulletin 169, vol. 1, pp. 191–197.
- Hanford, C. R., 1981, A process-sedimentary framework for characterizing recent and ancient sabkhas: *Sediment. Geol.*, **30**, 255–265.
- Hanshaw, B. B., W. E. Back, and R. G. Deike, 1971, A geochemical hypothesis for dolomitization of groundwater: *Econ. Geol.*, **66**, 710–724.
- Harder, H., 1989, Mineral genesis in ironstones: a model based upon laboratory experiments and petrographic observations, in Young, T. P. and W. E. G. Taylor (eds.), *Phanerozoic Ironstones*: The Geological Society, London, pp. 9–18.
- Hardie, L. A., 1984, Evaporites: marine or non-marine: *Am. J. Sci.*, **284**, 193–240.
- Hardie, L. A., 1987, Dolomitization: A critical view of some current views: *J. Sediment. Petrol.*, **57**, 166–183.
- Harmon, R. S. and C. M. Wicks (eds.), 2006, *Perspectives on Karst Geomorphology, Hydrology, and Geochemistry – A Tribute Volume to Derek C. Ford and William B. White*: Geological Society of America Special Paper 404.
- Harms, J. C., J. B. Southard, and R. G. Walker, 1982, *Structures and Sequences in Clastic Rocks*: SEPM Short Course 9.
- Harms, J. C., J. B. Southard, D. R. Spearing, and R. G. Walker, 1975, *Depositional Environments as Interpreted From Primary Sedimentary Structures and Stratification Sequences*: SEPM Short Course 2.
- Harvie, C. E., H. P. Euster, and J. M. Weare, 1982, Mineral equilibria in the six-component seawater system, Na–K–Mg–Ca– SO_4 –Cl– H_2O at 250°C , II: Composition of the saturated solutions: *Geochim. Cosmochim. Acta*, **46**, 1603–1618.

- Hasiotis, S. T., J. C. Van Wagoner, T. M. Demko, *et al.*, 2002, *Continental Trace Fossils*: SEPM. Short Course Notes 52.
- Hattori, I., 1989, Length-slow chalcedony in sedimentary rocks of the Mesozoic allochthonous terrane in central Japan and its use for tectonic synthesis, in Hein, J. R. and J. Obradović (eds.), *Siliceous Deposits of the Tethys and Pacific Regions*: Springer-Verlag, New York, NY, pp. 201–215.
- Hay, R. L., 1981, Geology of zeolites in sedimentary rocks, in Mumpton, F. A. (ed.), *Mineralogy and Geology of Natural Zeolites*: Mineralogical Society of America, Reviews in Mineralogy 4, pp. 53–64.
- Heaney, P. J., C. T. Prewitt, and G. V. Gibbs (eds.), 1994, *Silica: Physical Behavior, Geochemistry and Materials Applications*: Mineralogical Society of America, Reviews in Mineralogy 29.
- Heath, G. R., 1974, Dissolved silica and deep-sea sediments, in Hay, W. W. (ed.), *Studies in Paleo-Oceanography*: SEPM Special Publication 20, pp. 77–93.
- Hecht, C. A., 2004, Geomechanical models for clastic grain packing: *Pure Appl Geophys.*, **161**, 331–349.
- Heimann, A. and E. Sass, 1989, Travertines in the northern Hula Valley, Israel: *Sedimentology*, **36**, 95–108.
- Hein, J. R. and S. M. Karl, 1983, Comparisons between open-ocean and continental margin chert sequences, in Iijima, A., J. R. Hein, and R. Siever (eds.), *Siliceous Deposits in the Pacific Region*: Elsevier, Amsterdam, pp. 25–43.
- Hein, J. R. and J. Obradović (eds.), 1989, *Siliceous Deposits of the Tethys and Pacific Regions*: Springer-Verlag, New York, NY.
- Hein, J. R. and J. T. Parrish, 1987, Distribution of siliceous deposits in space and time, in Hein, J. R. (ed.), *Siliceous Sedimentary Rock – Hosted Ores and Petroleum*: Van Nostrand Reinhold, New York, NY, pp. 10–57.
- Hein, J. R., E. P. Kuijers, P. Denyer, and R. E. Sliney, 1983, Petrology and geochemistry of Cretaceous and Paleogene cherts from western Costa Rica, in Iijima, A., J. R. Hein, and R. Siever (eds.), *Siliceous Deposits in the Pacific Region*: Elsevier, Amsterdam, pp. 143–174.
- Hein, J. R., H.-W. Yeh, and J. A. Barron, 1990, Eocene diatom chert from Adak Island, Alaska: *J. Sediment. Petrol.*, **60**, 250–257.
- Helmold, K. P., 1985, Provenance of feldspathic sandstones – the effect of diagenesis on provenance interpretations: a review, in G. G. Zuffa (ed.), *Provenance of Arenites*: Reidel, Dordrecht, pp. 139–163.
- Herbig, H.-G. and K. Stattegger, 1989, Late Paleozoic heavy mineral and clast modes from the Betic Cordillera (southern Spain): transition from a passive to an active continental margin: *Sediment. Geol.*, **63**, 93–108.
- Herring, J. R., 1995, Permian phosphorites: A paradox of phosphogenesis, in Scholle, P. A., T. M. Peryt, and D. S. Ulmer-Scholle (eds.), *The Permian of Northern Pangea. Sedimentary Basins and Economic Resources*: Springer-Verlag, Berlin, pp. 292–312.
- Hesse, R. and S. K. Chough, 1980, The Northwest Atlantic mid-ocean channel of the Labrador Sea: II. Deposition of parallel laminated levee-muds from the viscous sublayer of low density turbidity currents: *Sedimentology*, **27**, 697–711.
- Heydari, E. and C. H. Moore, 1988, Oxygen isotope evolution of the Smackover pore waters, southeast Mississippi salt basin: *Geol. Soc. Am. Abst. Program*, **20**: A261.
- Hiatt, E. E. and D. A. Budd, 2003, Extreme paleoceanographic conditions in a Paleozoic oceanic upwelling system: Organic productivity and widespread phosphogenesis in the Permian Phosphoria Sea, in Chan, M. S. and A. W. Archer (eds.), *Extreme Depositional*

- Environments: Mega End Members in Geologic Time*: Geological Society of America Special Paper 370, pp. 245–264.
- Hoefs, J., 2004, *Stable Isotope Geochemistry*: Springer-Verlag, Berlin.
- Holbrook, P., 2002, The primary controls over sediment compaction, in Huffman, A. R. and G. L. Bowers (eds.), *Pressure Regimes in Sedimentary Basins and their Prediction*: AAPG Memoir 76, pp. 21–32.
- Horsfield, B., 1997, The bulk composition of first-formed petroleum in source rocks, in Welte, D. H., B. Horsfield, and D. R. Baker (eds.) *Petroleum and Basin Evolution*: Springer-Verlag, Berlin, pp. 337–402.
- Horton, A., H. C. Ivimey-Cook, R. K. Harrison, and B. R. Young, 1980, Phosphatic ooids in the Upper Lias (Lower Jurassic) of central England: *J. Geol. Soc. London*, **137**, 731–740.
- Houghton, H. F., 1980, Refined technique for staining plagioclase and alkali feldspars in thin section: *J. Sediment. Petrol.*, **50**, 629–631.
- Houseknecht, D. W., 1984, Influence of grain size and temperature on intergranular pressure solution, quartz cementation, and porosity in a quartzose sandstone: *J. Sediment. Petrol.*, **54**, 348–361.
- Houseknecht, D. W. and E. D. Pittman (eds.), 1992, *Origin, Diagenesis, and Petrophysics of Clay Minerals in Sandstones*: SEPM Special Publication 47.
- Howell, D. G. and W. R. Normark, 1982, Sedimentology of submarine fans, in Scholle, P. A. and D. Spearing (eds.), *Sandstone Depositional Environments*: AAPG Memoir 31, pp. 365–404.
- Hsü, K. J., 1989, *Physical Principles of Sedimentology*: Springer-Verlag, Berlin.
- Hsü, K. J. and C. Siegenthaler, 1969, Preliminary experiments and hydrodynamic movement induced by evaporation and their bearing on the dolomite problem: *Sedimentology*, **12**, 11–25.
- Hubert, J. F., 1962, A zircon–tourmaline–rutile maturity index and the interdependence of the composition of heavy mineral assemblages with the gross composition and texture of sandstones: *J. Sediment. Petrol.*, **32**, 440–450.
- Hunt, J. M., 1979, *Petroleum Geochemistry and Geology*: W.H. Freeman, San Francisco, CA.
- Hunt, J. M., 1996, *Petroleum Geochemistry and Geology*, 2nd edn.: W. H. Freeman, New York, NY.
- Hunter, R. E., 1967, The petrography of some Illinois Pleistocene and Recent sands: *Sediment. Geol.*, **1**, 57–75.
- Hussain, M. and J. K. Warren, 1989, Nodular and enterolithic gypsum: the “sabkatization” of Salt Flat Playa, west Texas: *Sediment. Geol.*, **64**, 13–24.
- Hutton, A. C., 1995, Organic petrography of oil shales, in Snape, C. (ed.), *Composition, Geochemistry and Conversion of Oil Shales*: Kluwer, Dordrecht, pp. 17–33.
- Iijima, A., H. Inagaki, and Y. Kakuwa, 1979, Nature and origin of the Paleogene cherts in the Setogawa Terrain, Shnizuoka, central Japan: *J. Fac. Sci., Univ. Tokyo*, **20**, 1–30.
- Iijima, A., J. R. Hein, and R. Siever (eds.), 1983, *Siliceous Deposits in the Pacific Region*: Developments in Sedimentology 36.
- Illenberger, W. K., 1991, Pebble shape (and size?): *J. Sediment. Petrol.*, **61**, 756–767.
- Illing, L. V., 1954, Bahaman calcareous sands: *Am. Assoc. Pet. Geol. Bull.*, **38**, 1–95.
- Ingersoll, R. V., 1988, Tectonics of sedimentary basins: *Geol. Soc. Am. Bull.*, **100**, 1704–1719.
- Ingersoll, R. V., 1990, Actualistic sandstone petrofacies: discriminating modern and ancient source rocks: *Geology*, **18**, 733–736.

- Ingersoll, R. V., T. D. Bullard, R. L. Ford, *et al.*, 1984, The effect of grain size on detrital modes: A test of the Gazzi–Dickinson point counting method: *J. Sediment. Petrol.*, **54**, 103–116.
- Ingram, R. L., 1954, Terminology for thickness of stratification and parting units in sedimentary rocks: *Geol. Soc. Am. Bull.*, **65**, 937–938.
- Ingram, R. L., 1971, Sieve analysis, in Carver, R. E. (ed.), *Procedures in Sedimentary Petrology*: John Wiley and Sons, New York, NY, pp. 49–67.
- International Committee for Coal Petrology, 1971, *International Handbook of Coal Petrography, 1st Supplement to 2nd Edition*: Centre National de la Recherche Scientifique, Paris.
- International Committee for Coal Petrology, 1975, *Analysis Subcommittee, Fluorescence Microscopy and Fluorescence Photometry*, in *International Handbook of Coal Petrography, 2nd Supplement to 2nd Edition*: Centre National de la Recherche Scientifique, Paris.
- Isley, A. E., 1995, Hydrothermal plumes and the delivery of iron to banded iron formations: *J. Geol.*, **103**, 169–185.
- James, H. L., 1966, *Chemistry of Iron-Rich Sedimentary Rocks: Data of Geochemistry*, 6th edn.: US Geological Survey Professional Paper 440-W.
- James, H. L., 1992, Precambrian iron-formations: Nature, origin, and mineralogic evolution from sedimentation to metamorphism, in Wolf K. H. and G. V. Chilingarian (eds.), *Diagenesis III: Developments in Sedimentology* 47, pp. 543–589.
- James, H. L. and A. F. Trendall, 1982, Banded iron formation: Distribution in time and paleoenvironmental significance, in Holland, H. D. and M. Schidlowski (eds.), *Mineral Deposits and the Evolution of the Biosphere*: Springer-Verlag, Berlin, pp. 199–218.
- James, N. P., 1983, Reef environment, in Scholle, P. A., D. G. Bebout, and C. H. Moore (eds.), *Carbonate Depositional Environments*: AAPG Memoir 33, pp. 345–440.
- James, N. P. and Y. Bone, 1989, Petrogenesis of Cenozoic, temperate water calcarenites, south Australia: A model for meteoric shallow burial diagenesis of shallow water calcite sediments: *J. Sediment. Petrol.*, **59**, 191–203.
- James, N. P. and P. W. Choquette, 1983a, Diagenesis 5. Limestones: Introduction: *Geosci. Can.*, **10**, 159–161.
- James, N. P. and P. W. Choquette, 1983b, Diagenesis 6. Limestones – The sea floor diagenetic environment: *Geosci. Can.*, **10**, 162–179.
- James, N. P. and P. W. Choquette, 1984, Diagenesis 9. Limestones – The meteoric diagenetic environment: *Geosci. Can.*, **11**, 161–194.
- James, N. P. and R. N. Ginsburg, 1979, *The Seaward Margin of Belize Barrier and Atoll Reefs*: International Association of Sedimentologists Special Publication 3.
- James, N. P. and A. C. Kendall, 1992, Introduction to carbonate and evaporite facies models, in Walker, R. G. and N. P. James (eds.), *Facies Models – Response to Sea Level Change*: Geological Association of Canada, St. Jouns, Newfoundland, pp. 265–276.
- James, W. C. and R. Q. Oaks Jr., 1977, Petrology of the Kinnikinic Quartzite (Middle Ordovician), east-central Idaho: *J. Sediment. Petrol.*, **47**, 1491–1511.
- Jerram, D. A., 2001, Visual comparators for degree of grain-size sorting in two and three dimensions: *Comput. Geosci.*, **27**, 485–492.
- Ji, S. and D. Mainprice, 1990, Recrystallization and fabric development in plagioclase: *J. Geol.*, **98**, 65–79.
- Johnson, M. R., 1994, Thin section grain size analysis revisited: *Sedimentology*, **41**, 985–999.

- Johnsson, M. J., 1993, The system controlling composition of clastic sediments, in Johnsson, M. J. and A. Basu (eds.), *Processes Controlling the Composition of Clastic Sediments*: Geological Society of America Special Paper 284, pp. 1–19.
- Johnsson, M. J. and A. Basu, 1993, *Processes Controlling the Composition of Clastic Sediments*: Geological Society of America Special Paper 284.
- Johnsson, M. J. and R. F. Stallard, 1990, Physiographic controls on the composition of sediments derived from volcanic and sedimentary terrains on Barro Colorado Island, Panama – Reply: *J. Sediment. Petrol.*, **60**, 799–801.
- Johnsson, M. J., R. F. Stallard, and R. H. Meade, 1988, First-cycle quartz arenites in the Orinoco River basin, Venezuela and Colombia: *J. Geol.*, **96**, 263–277.
- Jones, B. and R. W. MacDonald, 1989, Micro-organisms and crystal fabrics in cave pisoliths from Grand Cayman, British West Indies: *J. Sediment. Petrol.*, **59**, 387–396.
- Jones, D. L. and B. Murchev, 1986, Geologic significance of Paleozoic and Mesozoic radiolarian chert: *Ann. Rev. Earth Planet. Sci. Lett.*, **14**, 455–492.
- Jones, G. D. and B. J. Rostron, 2000, Analysis of flow constraints in regional-scale reflux dolomitization: Constant versus variable-flux hydrological models: *Bull. Can. Pet. Geol.*, **48**, 230–245.
- Jones, G. D., F. F. Whitaker, P. L. Smart, and W. E. Sanford, 2002, Fate of reflux brines in carbonate platforms: *Geology*, **30**, 371–374.
- Jones, G. D., P. L. Smart, F. F. Whitaker, B. J. Rostron, and H. G. Machel, 2003, Numerical modeling of reflux dolomitization in the Grosmont platform complex (Upper Devonian), Western Canada Sedimentary Basin: *Am. Assoc. Pet. Geol. Bull.*, **87**, 1273–1298.
- Jones, G. D., F. F. Whitaker, P. L. Smart, and W. E. Sanford, 2004, Numerical analysis of seawater circulation in carbonate platforms: II. The dynamic interaction between geothermal and brine reflux circulation: *Am. J. Sci.*, **304**, 250–284.
- Jones, J. B. and E. R. Segnit, 1971, The nature of opal I. Nomenclature and constituent phases. *J. Geol. Soc. Aust.*, **18**, 57–68.
- Jones, N. W. and F. D. Bloss, 1980, *Laboratory Manual for Optical Mineralogy*: Alpha Editions (Burgess International Group, Inc.), Edina, MI, variously paginated.
- Jones, R. L. and H. Blatt, 1984, Mineral dispersal patterns in the Pierre Shale: *J. Sediment. Petrol.*, **54**, 17–28.
- Julia, R., 1983, Travertines, in Scholle, P. A., D. G. Bebout, and C. H., Moore (eds.), *Carbonate Depositional Environments*: AAPG Memoir, pp. 64–72.
- Kahn, J. S., 1956, The analysis and distribution of the properties of packing in sand-size sediments I. On the measurement of packing in sandstones: *J. Geol.*, **64**, 385–395.
- Kairo, S., L. J. Suttner, and P. K. Dutta, 1993, Variability in sandstone composition as a function of depositional environments in coarse-grained delta systems, in Johnson, M. J. and A. Basu (eds.), *Processes Controlling the Composition of Clastic Sediments*: Geological Society of America Special Paper 284, pp. 263–284.
- Kastner, M. and J. M. Gieskes, 1983, Opal-A to opal-CT transformation: A kinetic study, in Iijima, A., J. R. Hein, and R. Siever (eds.), *Siliceous Deposits in the Pacific Region*: Developments in Sedimentology 36, pp. 211–228.
- Kastner, M. and R. Siever, 1979, Low temperature feldspars in sedimentary rocks: *Am. J. Sci.*, **279**, 435–479.
- Kastner, M., J. B. Keene, and J. M. Gieskes, 1977, Diagenesis of siliceous oozes – I. Chemical controls on the rate of opal-A to opal-CT transformation – an experimental study: *Geochim. Cosmochim. Acta*, **41**, 1041–1059.

- Kendall, A. C., 1984, Evaporites, in Walker, R. G. (ed.), *Facies Models*, 2nd edn., Geoscience Canada Reprint Series 1, pp. 259–296.
- Kendall, C. G. St. C. and J. Warren, 1987, A review of the origin and setting of tepees and their associated fabrics: *Sedimentology*, **34**, 1007–1027.
- Kennard, J. M. and N. P. James, 1986, Thrombolites and stromatolites: two distinct types of microbial structures: *Palaios*, **1**, 492–503.
- Kennedy, S. K. and J. Mazzullo, 1991, Image analysis method of grain size measurement, in Syvitski, J. P. M. (ed.), 1991, *Principles, Methods, and Application of Particle Size Analysis*: Cambridge University Press, Cambridge, pp. 76–87.
- Kennedy W. J. and R. E. Garrison, 1975, Morphology and genesis of nodular chalks and hardgrounds in the Upper Cretaceous of southern England: *Sedimentology*, **22**, 311–386.
- Khalaf, F. I., 1990, Occurrence of phreatic dolocrete within Tertiary clastic deposits of Kuwait, Arabian Gulf: *Sediment. Geol.*, **68**, 223–239.
- Kim, S.-T. and J. R. O’Neil, 1997, Equilibrium and nonequilibrium oxygen isotope effect in synthetic carbonates: *Geochim. Cosmochim. Acta*, **61**, 3461–3475.
- Kimberley, M. M., 1994, Debate about ironstones: has solute supply been surficial weathering, hydrothermal convection, or exhalation of deep fluids: *Terra Nova*, **6**, 116–132.
- Kirkham, A., 2004, Patterned dolomites: microbial origin and clues to vanished evaporites in the Arab Formation, Upper Jurassic, Arabian Gulf, in Braithwaite, C. J. R., G. Rizzi, and G. Darke (eds.), *The Geometry and Petrogenesis of Dolomite Hydrocarbon Reservoirs*: Geological Society of London Special Publication 235, pp. 301–308.
- Klein, C. and C. S. Hurlbut Jr., 2002, *The 22nd Edition of the Manual of Mineral Science (after James D. Dana)*: John Wiley and Sons, New York, NY.
- Klein, G. de V. and D. A. Willard, 1989, Origin of Pennsylvanian coal-bearing cyclothem of North America: *Geology*, **17**, 152–155.
- Klimchouk, A. B., D. C. Ford, A. N. Palmer, and W. Dreybrodt (eds.), 2000, *Speleogenesis: Evolution of Karst Aquifers*: National Speleological Society, Huntsville, AL.
- Knauth, L. P., 1979, A model for the origin of chert in limestone: *Geology*, **7**, 274–277.
- Knudsen, A. C. and M. E. Gunter, 2002, Sedimentary phosphorites – An example: Phosphoria Formation, Southeastern Idaho, U. S. A., in Kohn, M. L., J. Rakavan, J. M. Hughes *et al.* (eds.), *Phosphates – Geochemical, Geobiological, and Materials Importance*: Mineralogical Society of America Reviews in Mineralogy and Geochemistry 48, pp. 363–389.
- Koepnick, R. B., 1984, Distribution and vertical permeability of stylolites within a Lower Cretaceous carbonate reservoir, Abu Dhabi, U.A.E.. in *Stylolites and Associated Phenomena – Relevance to Hydrocarbon Reservoirs*: Abu Dhabi Reservoir Research Foundation Special Publication, Abu Dhabi, pp. 261–278.
- Kohout, F. A., 1967, Ground water flow and the geothermal regime of the Floridan Plateau: *Trans. Gulf Coast Assoc. Geol. Soc.*, **17**, 339–354.
- Kolodny, Y., 1980, The origin of phosphorite deposits in light of occurrences of Recent sea-floor phosphorites, in Bendor, Y. K. (ed.), *Marine Phosphorites*: SEPM Special Publication 29, p. 249.
- Kolodny, Y., 1981, Phosphorites, in Emiliani, C. (ed.), *The Ocean Lithosphere: the Sea*. John Wiley and Sons, New York, NY, vol. 7, pp. 981–1023.
- Kolodny, Y. and I. R. Kaplan, 1970, Uranium isotopes in sea floor phosphorites: *Geochim. Cosmochim. Acta*, **34**, 3–24.

- Konert, M., 1997, Comparison of laser grain size analysis with pipette and sieve analysis: A solution for underestimation of the clay fraction: *Sedimentology*, **44**, 523–35.
- Kraus, M. J., 1984, Sedimentology and tectonic setting of early Tertiary quartzite conglomerates, northwest Wyoming, in Koster, E. H. and R. J. Steel (eds.), *Sedimentology of Gravels and Conglomerates*: Canadian Society of Petroleum Geology Memoir 10, pp. 203–216.
- Krauskopf, K. B., 1979, *Introduction to Geochemistry*, 2nd edn.: McGraw-Hill, New York, NY.
- Krinsley, D. and J. Dornkamp, 1973, *Atlas of Quartz Sand Surface Textures*: Cambridge University Press, Cambridge.
- Krinsley, D. and N. K. Tovey, 1978, Cathodoluminescence in quartz sand grains: *Scan. Electron Microsc.*, **1**, 887–894.
- Krinsley, D. and P. Trusty, 1986, Sand grain surface textures, in Sieveking, G. De C. and M. B. Hart (eds.), *The Scientific Study of Flint and Chert*: Cambridge University Press, Cambridge, pp. 201–207.
- Krinsley, D. H., K. Pye, S. Boggs Jr., and N. K. Tovey, 1998, *Backscattered Scanning Electron Microscopy and Image Analysis of Sediments and Sedimentary Rocks*: Cambridge University Press, Cambridge.
- Kroopnick, P., 1980, The distribution of ^{13}C in the Atlantic Ocean: *Earth Planet. Sci. Lett.*, **49**, 469–484.
- Krug, H.-J., H. Brandstädter, and K. H. Jacob, 1996, Morphological instabilities in pattern formation by precipitation and crystallization processes: *Geol. Rundsch.*, **85**, 19–28.
- Krumbein, W. C., 1941, Measurement and geological significance of shape and roundness of sedimentary particles: *J. Sediment. Petrol.*, **11**, 64–72.
- Krynine, P. D., 1940, *Petrology and Genesis of the Third Bradford Sand*: Pennsylvania State College Mineral Industries Experimental Station, Bulletin 27.
- Krynine, P. D., 1943, *Diastrophism and the Evolution of Sedimentary Rocks*: Pennsylvania Mineral Industries Tech Paper 84-A.
- Krynine, P. D., 1946, The tourmaline group in sediments: *J. Geol.*, **54**, 65–87.
- Kuehl, S. A., T. M. Hairu, M. W. Sanford, C. A. Nittrouer, and D. J. DeMaster, 1991, Millimeter-scale sedimentary structure of fine-grained sediments: Examples from continental margin environments, in Bennett, R. H., N. R. O'Brien, and M. H. Hulbert (eds.), *Microstructures of Fine-Grained Sediments*: Springer-Verlag, New York, pp. 33–45.
- Kuenen, Ph. H., 1958, Experiments in geology: *Glasgow Geol. Soc. Trans.*, **23**, 1–28.
- Kuenen, Ph. H., 1959, Experimental abrasion, part 3, Fluvial action on sand: *Am J. Sci.*, **257**, 172–190.
- Kuenen, Ph. H., 1960, Experimental abrasion, part 4, Eolian action: *J. Geol.*, **68**, 427–449.
- LaBerge, G. L., 1973, Possible biological origin of Precambrian iron-formations: *Econ. Geol.*, **68**, 1098–1109.
- LaBerge, G. L., E. I. Robbins, and T. -M. Han, 1987, A model for the biological precipitation of Precambrian iron-formations – A: Geological evidence, in Appel, P. W. U. and G. L. LaBerge (eds.), *Precambrian Iron-Formations*: Theophrastus Publications, Athens, pp. 69–96.
- Lamboy, M., 1990, Microbial mediation in phosphatogenesis: New data from the Cretaceous phosphatic chalks of northern France, in Northolt, A. J. G., and I., Jarvis (eds.), 1990, *Phosphorite Research and Development*, Geological Society Special Publication 52, pp. 157–167.

- Land, L. S., 1973, Holocene meteoric dolomitization of Pleistocene limestones, North Jamaica: *Sedimentology*, **20**, 411–424.
- Land, L. S., 1985, The origin of massive dolomite: *J. Geol. Educ.*, **33**, 112–125.
- Land, L. S., 1986, Limestone diagenesis – some geochemical considerations, in Mumpton, F. A. (ed.), *Studies in Diagenesis*: US Geological Survey Bulletin 1578, pp. 129–137.
- Land, L. S., 1998, Failure to precipitate dolomite at 25 °C from dilute solutions despite 1000-fold over-saturation after 32 years: *Aquat. Geochem.*, **4**, 361–368.
- Last, W. M., 1990, Lacustrine dolomite – an overview of modern, Holocene, and Pleistocene occurrences: *Earth Sci. Rev.*, **27**, 221–263.
- Laznicka, P., 1988, *Breccias and Coarse Fragmentites: Petrology, Environments, Associations, Ores*: Elsevier, Amsterdam.
- Lease, R. O., D. W. Burbank, G. E. Gehrels, Z. Wang, and D. Yuan, 2007, Signature of mountain building: Detrital zircon U/Pb ages from northeastern Tibet: *Geology*, **35**, 239–242.
- Leder, F. and W. C. Park, 1986, Porosity reduction in sandstones by quartz overgrowths: *Am. Assoc. Pet. Geol. Bull.*, **70**, 1713–1728.
- Ledesma-Vázquez, J., R. W. Berry, M. E. Johnson, and S. Gutiérrez-Sánchez, 1997, El Mono Chert: A shallow-water chert from the Pliocene Infierno Formation, Baja California Sur, Mexico, in Johnson, M. E. and Ledesma-Vázquez, J. (eds.), *Pliocene Carbonates and Related Facies Flanking the Gulf of California, Baja California, Mexico*: Geological Society of America Special Paper 318, pp. 73–81.
- Lee, M., J. L. Aronson, and S. M. Savin, 1989, Timing and condition of Permian Rotliegende sandstone diagenesis, southern North Sea: K/Ar and oxygen isotopic data: *Am. Assoc. Pet. Geol. Bull.*, **73**, 195–215.
- Lepp, H., 1987, Chemistry and origin of Precambrian iron-formations, in Appel, P. W. U. and G. L. LaBerge (eds.), *Precambrian Iron-Formations*: Theophrastus Publications, Athens, pp. 3–30.
- Lepp, H. and S. S. Goldich, 1964, Origin of Precambrian iron-formation: *Econ. Geol.*, **58**, 1025–1061.
- Le Roux, J. P., 2004, A hydrodynamic classification of grain shapes: *J. Sediment. Res.*, **74**, 135–143.
- Lewis, D. W. and D. McConchie, 1994, *Analytical Sedimentology*: Chapman and Hall, New York, NY.
- Leyrit, H. and C. Montenat, 2000, *Volcaniclastic Rocks, From Magmas to Sediments*: Gordon and Beach Science Publishers, Amsterdam.
- Lindholm, R. C., 1987, *A Practical Approach to Sedimentology*: Allen and Unwin, London.
- Lloyd, R. M., 1977, Porosity reduction by chemical compaction – stable isotope model: *Am. Assoc. Pet. Geol. Bull.*, **61**, 809.
- Logan, B. R. and V. Semeniuk, 1976, *Dynamic Metamorphism: Processes and Products in Devonian Carbonate Rocks, Canning Basin, Western Australia*: Geological Society of Australia Special Publication 16.
- Logan, B. W., R. Rezak, and R. N. Ginsburg, 1964, Classification and environmental significance of algal stromatolites: *J. Geol.*, **72**, 68–83.
- Longman, M. W., 1980, Carbonate diagenetic textures from nearsurface diagenetic carbonates: *Am. Assoc. Pet. Geol. Bull.*, **64**, 461–487.
- Longman, M. W., 1981, A process approach to recognizing facies of reef complexes, in Toomey, D. F. (ed.), *European Fossil Reef Models*: SEPM Special Publication 30, pp. 9–40.

- Lowe, D. R., 1982, Sediment gravity flows: II. Depositional models with special reference to the deposits of high-density turbidity currents: *J. Sediment. Petrol.*, **52**, 279–297.
- Lowe, D. R., 1999, Petrology and sedimentology of cherts and related silicified sedimentary rocks in the Swaziland Supergroup, in Lowe, D. R. and G. R. Byerly (eds.), *Geologic Evolution of the Barberton Greenschist Belt, South Africa*: Geological Society of America Special Paper 329, pp. 83–114.
- Lowe, D. R. and R. D. LoPiccolo, 1974, The characteristics and origin of dish and pillar structures: *J. Sediment. Petrol.*, **44**, 484–501.
- Lucia, F. J., 1999, *Carbonate Reservoir Characterization*: Springer-Verlag, New York, NY.
- Lumsden, D. N., 1988, Characteristics of deep-marine dolomites: *J. Sediment. Res.*, **58**, 1023–1031.
- Lundegard, P. D., 1989, Temporal reconstruction of sandstone diagenetic histories, in Hutcheon, I. E. (ed.), *Burial Diagenesis*: Mineralogical Association of Canada Short Course Handbook 15, pp. 161–200.
- Lundegard, P. D. and N. D. Samuels, 1980, Field classification of fine-grained sedimentary rocks: *J. Sediment. Petrol.*, **50**, 781–786.
- Machel, H. G., 2000, Application of cathodoluminescence to carbonate diagenesis, in Pagel, M., V. Barbin, P. Blanc, and D. Ohnstedter (eds.): *Cathodoluminescence in Geosciences*, Springer-Verlag, Berlin, pp. 271–301.
- Machel, H. G., 2003, Dolomites and dolomitization, in Middleton, G. M., M. J. Church, M. Conglio, L. A. Hardie, and F. S. Longstaffe (eds.), *Encyclopedia of Sediments and Sedimentary Rocks*: Kluwer, Dordrecht, pp. 234–243.
- Machel, H. G., 2004, Concepts and models of dolomitization: a critical reappraisal, in Braithwaite, C. J. R., G. Rizzi, and G. Darke (eds.), *The Geometry and Petrogenesis of Dolomite Hydrocarbon Reservoirs*: Geological Society of London Special Publication 235, pp. 6–63.
- Machel, H. G. and E. W. Mountjoy, 1986, Chemistry and environments of dolomitization – A reappraisal: *Earth Sci. Rev.*, **23**, 175–222.
- Machel, H. G. and E. W. Mountjoy, 1990, Coastal mixing-zone dolomite, forward modeling, and massive dolomitization of platform-margin carbonates – Discussion: *J. Sediment. Petrol.*, **60**, 1008–1012.
- Macintyre, I. G. and R. P. Reid, 1995, Crystal alteration in a living calcareous alga (*Halimeda*): Implications for studies in skeletal diagenesis: *J. Sediment. Petrol.*, **A65**, 143–153.
- Mack, G. H., 1984, Exceptions to the relationship between plate tectonics and sandstone compositions: *J. Sediment. Petrol.*, **54**, 212–220.
- Mack, G. H. and T. Jerzykiewicz, 1989, Detrital modes of sand and sandstone derived from andesitic rocks as a paleoclimate indicator: *Sediment. Geol.*, **65**, 35–44.
- MacKenzie, W. S. and A. E. Adams, 1994, *A Colour Atlas of Rocks and Minerals in Thin Section*: Manson Publishing, London.
- Mackenzie, W. S. and C. Guilford, 1980, *Atlas of Rock-Forming Minerals in Thin Section*: John Wiley and Sons, New York, NY.
- Mackie, W., 1896, The sands and sandstones of eastern Moray: *Edinburgh Geol. Soc. Trans.*, **7**, 148–172.
- Macquaker, J. H. S. and A. E. Adams, 2003, Maximizing information from fine-grained sedimentary rocks: An inclusive nomenclature for mudstones: *J. Sediment. Res.*, **73**, 735–744.
- MacRae, N. D., 1995, Secondary-ion mass spectrometry and geology: *Can. Mineral.*, **33**, 219–236.

- Magwood, J. P. A., 1992, Ichnotaxonomy: A burrow by any other name?, in Maples, C. G. and R. W. West (eds.), *Trace Fossils: The Paleontological Society Short Courses in Paleontology* 5, pp. 15–33.
- Mahaney, W. C., 2002, *Atlas of Sand Grain Surface Textures and Applications*: Oxford University Press, New York, NY.
- Mahaney, W. C., A. Stewart, and V. Kalm, 2001, Quantification of SEM microtextures useful in sedimentary environmental discrimination: *Boreas*, **30**, 165–171.
- Maiklem, W. R., D. G. Bebolt, and R. P. Glaister, 1969, Classification of anhydrite – A practical approach: *Can. Pet. Geol. Bull.*, **17**, 194–233.
- Maliva, R. G., 1989, Displacive syntaxial overgrowths in open marine limestones: *J. Sediment. Petrol.*, **59**, 397–403.
- Maliva, R. G. and R. Siever, 1988a, Diagenetic replacement controlled by force of crystallization: *Geology*, **16**, 688–691.
- Maliva, R. G. and R. Siever, 1988b, Mechanisms and controls of silicification of fossils in limestone: *J. Geol.*, **96**, 387–398.
- Maliva, R. G. and R. Siever, 1988c, Pre-Cenozoic nodular cherts: evidence for opal–CT precursors and direct quartz replacement: *Am. J. Sci.*, **288**, 798–809.
- Maliva, R. G. and R. Siever, 1989a, Nodular chert formation in carbonate rocks: *J. Geol.*, **97**, 421–433.
- Maliva, R. G. and R. Siever, 1989b, Chertification histories of some Late Mesozoic and Middle Paleozoic platform carbonates: *Sedimentology*, **36**, 907–926.
- Maliva, R. G., A. H. Knoll, and R. Siever, 1989, Secular change in chert distribution: A reflection of evolving biological participation in the silica cycle: *Palaios*, **4**, 519–532.
- Maliva, R. G., A. H. Knoll, and B. M. Simonson, 2005, Secular changes in the Precambrian silica cycle: Insights from chert petrology: *Geol. Soc. Am. Bull.*, **117**, 835–845.
- Maples, C. G. and R. W. West (eds.), 1992, *Trace Fossils: The Paleontological Society Short Courses in Paleontology* 5.
- Martens, C. S. and R. C. Harris, 1970, Inhibition of apatite precipitation in marine environment by magnesium ions: *Geochim. Cosmochim. Acta*, **34**, 621–625.
- Matlack, K. S., D. W. Houseknecht and K. R. Applin, 1989, Emplacement of clay into sand by infiltration: *J. Sediment. Petrol.*, **59**, 77–87.
- Maynard, J. B., R. Valloni, and H.-S. Yu, 1982, Composition of modern deep-sea sands from arc-related basins, in Leggett, J. E. (ed.), *Trench-Forearc Geology: Sedimentation and Tectonics on Modern and Ancient Active Plate Margins*: Geological Society of London Special Publication 10, pp. 551–561.
- Mazzullo, J. and S. Magenheimer 1987, The original shapes of quartz sand grains: *J. Sediment. Petrol.*, **57**, 479–487.
- Mazzullo, J. M. and R. Ehrlich, 1983, Grain-shape variation in the St. Peter Sandstone: A record of eolian and fluvial sedimentation of an Early Paleozoic cratonic sheet sand: *J. Sediment. Petrol.*, **53**, 105–120.
- Mazzullo, J., D. Sims, and D. Cunningham, 1986, The effects of shape sorting and abrasion upon the shapes of fine quartz sand grains: *J. Sediment. Petrol.*, **56**, 45–56.
- Mazzullo, J., A. Alexander, T. Tieh, and D. Menglin, 1992, The effects of wind transport on the shapes of quartz silt grains: *J. Sediment. Petrol.*, **62**, 961–971.
- Mazzullo, S. J., 2000, Organogenic dolomitization in peritidal to deep sea sediments: *J. Sediment. Res.*, **70**, 10–23.
- Mazzullo, S. J., R. Ehrlich, and O. H. Pilkey, 1982, Local and distal origin of sands in the Hatteras abyssal plain: *Mar. Geol.*, **48**, 75–88.

- McBride, E. F., 1984, Diagenetic processes that affect provenance determinations in sandstone, in Zuffa, G. G. (ed.), *Provenance of Arenites*: Reidel, Dordrecht, pp. 95–113.
- McBride, E. F., T. N. Diggs, and J. C. Wilson, 1991, Compaction of Wilcox and Carrizo sandstones (Paleocene–Eocene) to 4420 M, Texas Gulf Coast: *J. Sediment. Petrol.*, **61**, 73–85.
- McCabe, P. J., 1984, Depositional environments of coal and coal-bearing strata, in Rahmani, R. A. and R. M. Flores (eds.), *Sedimentology of Coal and Coal-Bearing Sequences*: International Association of Sedimentologists Special Publication 7, pp. 13–42.
- McCaffrey, M. A., B. Lazar, and H. D. Holland, 1987, The evaporation path of seawater and the coprecipitation of Br^- and K^+ with halite: *J. Sediment. Petrol.*, **57**, 928–937.
- McCave, I. N., R. J. Bryant, H. F. Cook, and C. A. Coughanowr, 1986, Evaluation of a laser-diffraction size analyzer for use with natural sediments: *J. Sediment. Petrol.*, **56**, 561–564.
- McClellan, G. H. and S. J. Kauwenbergh, 1990, Mineralogy of sedimentary apatites, in Northolt, A. J. G. and I. Jarvis (eds.), *Phosphorite Research and Development*: Geological Society Special Publication 52, pp. 23–31.
- McIlroy, D., 2004, *The Application of Ichnology to Palaeoenvironmental and Stratigraphic Analysis*: Geological Society of London, London.
- McKee, E. D. and G. W. Weir, 1953, Terminology for stratification and cross-stratification in sedimentary rocks: *Geol. Soc. Am. Bull.*, **64**, 381–390.
- McKelvey V. E., 1973, Abundance and distribution of phosphorus in the lithosphere: in *Environmental Phosphorus Handbook*: Wiley, New York, pp. 13–31.
- McKelvey, V. E., J. S. Williams, R. P. Sheldon, E. R. Cressman, and T. M. Channey, 1959, *The Phosphoria, Park City, and Shedhorn Formations in the Western Phosphate Field*: US Geological Survey Professional Paper 313-A.
- McLennan, S. M., S. R. Taylor, M. T. McCulloch, and J. B. Maynard, 1990, Geochemical and Nd–Sr isotopic composition of deep-sea turbidites: Crustal evolution and plate tectonic associations: *Geochim. Cosmochim. Acta*, **54**, 2015–2050.
- McLennan, S. M., S. Hemming, D. K. McDaniel, and G. N. Hanson, 1993, Geochemical approaches to sedimentation, provenance, and tectonics, in Johnsson, M. J. and A. Basu (eds.), *Processes Controlling the Composition of Clastic Sediments*: Geological Society of America Special Paper 284, pp. 21–40.
- McLennan, S. M., B. Bock, S. R. Hemming, *et al.*, 2003, The role of provenance and sedimentary process in the geochemistry of sedimentary rocks, in Lentz, D. R. (ed.), *Geochemistry of Sediments and Sedimentary Rocks: Evolutionary Considerations to Mineral Deposit-Forming Environments*: Geological Association of Canada, GeoText 4, pp. 7–38.
- McTainsh, G. H., 1997, Particle size analysis of aeolian dusts, soils and sediments in very small quantities using a Coulter Multisizer: *Earth Surf. Proc. Land.*, **22**, 1207–1216.
- Melim, L. A., P. K. Swart, and G. P. Eberli, 2004, Mixing-zone diagenesis in the subsurface of Florida and the Bahamas: *J. Sediment. Res.*, **74**, 904–913.
- Melson, W. G., J. T. Haynes, T. O’Hearn, *et al.*, 1998, K-shales of the central Appalachian Paleozoic: Properties and origin, in Schieber, J., W. Zimmerle, and P. S. Sethi (eds.), 1998, *Shales and Mudstones II*: E. Schweizerbart’sche Verlagsbuchhandlung, Stuttgart, pp. 143–159.
- Mero, J. L., 1965, *The Mineral Resources of the Sea*: Elsevier, New York NY.
- Meunier, A., 2005, *Clays*: Springer-Verlag, Berlin.

- Meyer, R. F., E. D. Attanasi, and P. A. Freeman, 2007, *Heavy Oil and Natural Bitumen Resources in Geological Basins of the World*: US Geological Survey Open-File Report 2007–1084.
- Meyers, W. J., 1974, Carbonate cement stratigraphy of the Lake Valley Formation (Mississippian), Sacramento Mountains, New Mexico: *J. Sediment. Petrol.*, **44**, 837–861.
- Mezzadri, G. and E. Saccani, 1989, Heavy mineral distribution in Late Quaternary sediments of the southern Aegean Sea: Implications for provenance and sediment dispersal in sedimentary basins at active margins: *J. Sediment. Petrol.*, **59**, 412–422.
- Miall, A. D., 1990, *Principles of Sedimentary Basin Analysis*, 2nd edn.: Springer-Verlag, New York, NY.
- Miall, A. D., 2000, *Principles of Sedimentary Basin Analysis*, 3rd edn.: Springer-Verlag, New York, NY.
- Miller, J., 1988, Microscopical techniques: I. Slices, slides, stains and peels, in Tucker, M. (ed.), *Techniques in Sedimentology*: Blackwell Scientific, Oxford, pp. 86–107.
- Miller, W. (ed.), 2006, *Trace Fossils, Problems, Prospects*: Elsevier, Amsterdam.
- Milligan, T. G. and K. Kranck, 1991, Electroresistance particle size analyzers, in Syvitski, J. P. M. (ed.), 1991, *Principles, Methods, and Application of Particle Size Analysis*: Cambridge University Press, Cambridge, pp. 109–118.
- Milliken, K. L., 1989, Petrography and composition of authigenic feldspars, Oligocene Frio Formation, south Texas: *J. Sediment. Petrol.*, **59**, 361–374.
- Milliken, K. L., 1994, Cathodoluminescence textures and the origin of quartz silt in Oligocene mudrocks, south Texas: *J. Sediment. Res.*, **A64**, 567–571.
- Milliken, K. L. and L. E. Mack, 1990, Subsurface dissolution of heavy minerals, Frio Formation sandstones of the ancestral Rio Grande Province, south Texas: *Sediment. Geol.*, **68**, 187–199.
- Milliken, K. L., L. S. Land, and R. G. Loucks, 1981, History of burial diagenesis determined from isotopic geochemistry, Frio Formation, Brazoria County, Texas: *Am. Assoc. Pet. Geol. Bull.*, **65**, 1397–1413.
- Milliman, J. D., 1974, *Marine Carbonates*: Springer-Verlag, New York, NY.
- Milner, H. B., 1962, *Sedimentary Petrography*, 4th edn: George Allen and Unwin Ltd., London, vol. II.
- Monicard, R. P., 1980, *Properties of Reservoir Rocks: Core Analyses*: Gulf Publishing, Houston (Editions Technip: Paris).
- Montañez, I. P., J. M. Gregg, and K. L. Shelton, 1997, *Basin-Wide Diagenetic Patterns: Integrated Petrologic, Geochemical, and Hydrologic Considerations*: SEPM Special Publication 57.
- Monty, C. L. V., 1976, The origin and development of cryptalgal fabrics, in Walter, M. R. (ed.), *Stromatolites*: Elsevier, Amsterdam, pp. 193–249.
- Moon, C. F. and C. W. Hurst, 1984, Fabric of muds and shales: an overview, in Stow, D. A. V. and D. J. W. Piper (eds.), *Fine-Grained Sediments: Deep-Water Processes and Facies*: Geological Society Special Publication 15, pp. 579–593.
- Moore, C. H., 1985, Upper Jurassic subsurface cements: A case history, in Schneidermann, N. and P. M. Harris (eds.), *Carbonate Cements*: SEPM Special Publication 36, pp. 291–308.
- Moore, C. H., 1989, *Carbonate Diagenesis and Porosity*: Developments in Sedimentology 46.
- Moore, C. H., 2001, *Carbonate Reservoirs: Porosity Evolution and Diagenesis in a Sequence Stratigraphic Framework*: Developments in Sedimentology 55.

- Moore, D. M., 1978, A sample of the Purington Shale prepared as a geochemical standard: *J. Sediment. Petrol.*, **48**, 995–998.
- Morad, S. (ed.), 1998a, *Carbonate Cementation in Sandstones: Distribution Patterns and Geochemical Evolution*: International Association of Sedimentologists Special Publication 26.
- Morad, S., 1998b, Carbonate cementation in sandstones: Distribution patterns and geochemical evolution, in Morad, S. (ed.), 1998, *Carbonate Cementation in Sandstones: Distribution Patterns and Geochemical Evolution*: International Association of Sedimentologists Special Publication 26, pp. 1–26.
- Morad, S. and A. A. Aldahan, 1987, Diagenetic replacement of feldspars by quartz in sandstones: *J. Sediment. Petrol.*, **57**, 488–493.
- Morad, S., M. Bergan, R. Knarud, and J. P. Nystuen, 1990, Albitization of detrital plagioclase in Triassic reservoir sandstones from the Snorre Field, Norwegian North Sea: *J. Sediment. Petrol.*, **60**, 411–425.
- Moraes, M. A. S. and L. F. De Ros, 1990, Infiltrated clays in fluvial Jurassic sandstones of Recôncavo Basin, Northeastern Brazil: *J. Sediment. Petrol.*, **60**, 809–819.
- Morse, J. W., 1985, Kinetic control of morphology, composition, and mineralogy of abiotic sedimentary carbonates: Discussion: *J. Sediment. Petrol.*, **55**, 919–920.
- Morse, J. W. and F. T. Mackenzie, 1990, *Geochemistry of Sedimentary Carbonates*: Elsevier, Amsterdam.
- Morton, A. C., 1985, Heavy minerals in provenance studies, in Zuffa, G. G. (ed.), *Provenance of Arenites*: Reidel, Dordrecht, pp. 249–77.
- Morton, A. C., 1991, Geochemical studies of detrital heavy minerals and their application to provenance research, in Morton, A. C., S. P. Todd, and P. D. W. (eds.), *Development in Sedimentary Provenance Studies*: Geological Society of London Special Publication 57, pp. 31–45.
- Morton, A. C. and C. R. Hallsworth, 1999, Processes controlling the composition of heavy mineral assemblages in sandstones: *Sediment. Geol.*, **124**, 3–29.
- Mount, J., 1985, Mixed siliciclastic and carbonate sediments: A proposed first-order textural and compositional classification: *Sedimentology*, **32**, 435–442.
- Mucci, A. and J. W. Morse, 1983, The incorporation of Mg^{2+} and Sr^{2+} into calcite overgrowths: Influences of growth rate and solution composition: *Geochim. Cosmochim. Acta*, **47**, 217–233.
- Mullins, H. T., A. C. Neumann, R. J. Wilber, and M. R. Boardman, 1980, Nodular carbonate sediment on Bahamian slopes: Possible precursors to nodular limestones: *J. Sediment. Petrol.* **50**, 117–131.
- Mumpton, F. A., 1981, Natural zeolites, in Mumpton, F. A. (ed.), *Mineralogy and Geology of Natural Zeolites*: Mineralogical Society of America Reviews in Mineralogy 4, pp. 1–17.
- Nathan, Y., 1984, The mineralogy and geochemistry of phosphorites, in Nriagu, J. O. and P. B. Moore (eds.), *Phosphate Minerals*: Springer-Verlag, Berlin, pp. 275–291.
- Naylor, M. A., 1980, The origin of inverse grading in muddy debris flow deposits – a review: *J. Sediment. Petrol.*, **50**, 1111–1116.
- Nelson, C. H., 1982, Modern shallow-water graded sand layers from storm surges, Bering shelf: A mimic of Bouma sequences and turbidite systems: *J. Sediment. Petrol.*, **52**, 537–545.
- Nesse, W. D., 1986, *Introduction to Optical Mineralogy*: Oxford University Press, New York, NY.

- Neumann, A. C. and L. S. Land, 1975, Lime mud deposition and calcareous algae in the Bight of Abaco, Bahamas: A budget: *J. Sediment. Petrol.*, **45**, 763–786.
- Neumann, A. C., J. W. Kofoed, and G. H. Keller, 1977, Lithoherms in the Straits of Florida: *Geology*, **5**, 4–11.
- Newell, N. D., J. K. Rigby, A. J. Whitman, and J. S. Bradley, 1951, Shoal-water geology and environments, eastern Andros Island, Bahamas: *Am. Mus. Nat. Hist. Bull.*, **97**, 1–29.
- Noble, J. P. A. and K. D. M. Howells, 1974, Early marine lithification of the nodular limestones in the Silurian of New Brunswick: *Sedimentology*, **21**, 597–609.
- Notholt, A. J. and R. P. Sheldon, 1986, Proterozoic and Cambrian phosphorites – regional review: World resources, in Cook, P. J. and J. H. Shergold (eds.), *Phosphate Deposits of the World, 1. Proterozoic and Cambrian Phosphorites*: Cambridge University Press, Cambridge, pp. 9–19.
- Notholt, A. J. G., R. P. Sheldon, and D. F. Davidson (eds.), 1989, *Phosphate Deposits of the World, 2: Phosphate Rock Resources*: Cambridge University Press, Cambridge.
- O'Brien, N. R., 1990, Significance of lamination in Toarcian (Lower Jurassic) shales from Yorkshire, Great Britain: *Sediment. Geol.*, **67**, 25–34.
- O'Brien, N. R. and R. M. Slatt, 1990, *Argillaceous Rock Atlas*: Springer-Verlag, New York, NY.
- O'Brien, N. R., C. E. Brett, and M. J. Woodard, 1998, Shale fabrics as a clue to sedimentary processes – example from the Williamson–Willowvale shales (Silurian), New York, in Schieber, J., W. Zimmerle, and P. Sethi (eds.), *Shales and Mudstones II*: E. Schweizerbart'sche Verlagsbuchhandlung, Stuttgart, pp. 55–66.
- Odom, I. E., T. W. Doe, and R. H. Dott, Jr., 1976, Nature of feldspar–grain size relations in some quartz-rich sandstones: *J. Sediment. Petrol.*, **46**, 862–870.
- Ogihara, S. and A. Iijima, 1989, Clinoptilolite to heulandite transformation in burial diagenesis, in Jacobs, P. A. and R. A. Van Santen (eds.), *Zeolites: Facts, Figures, Future*: Elsevier, Amsterdam, pp. 491–500.
- Ohmoto, H., Y. Watanabe and K. E. Yamaguchi, 2006, Chemical and biological evolution of early Earth: Constraints from banded iron formations, in Kesler, S. E. and H. Ohmoto (eds.), *Evolution of Early Earth's Atmosphere, Hydrosphere, and Biosphere – Constraints from Ore Deposits*: Geological Society of America Memoir 198, pp. 291–331.
- Oliver, J., 1986, Fluids expelled tectonically from orogenic belts: Their role in hydrocarbon migration and other geologic phenomena: *Geology*, **14**, 99–102.
- Ondrick, C. W. and J. C. Griffith, 1969, Frequency distribution of elements in Rensselaer Graywacke, Troy, New York: *Geol. Soc. Am. Bull.*, **80**, 509–518.
- Orford, J. D. and W. B. Whalley, 1983, The use of fractal dimension to characterize irregular-shaped particles: *Sedimentology*, **30**, 655–668.
- Orford, J. D. and W. B. Whalley, 1987, The quantitative description of highly irregular sedimentary particles: the use of the fractal dimension, in J. R. Marshall (ed.), *Clastic Particles*, Van Nostrand Reinhold, New York, NY, pp. 267–280.
- Pandalai, H. S. and S. Basumallick, 1984, Packing in a clastic sediment: concepts and measurements: *Sediment. Geol.*, **39**, 87–93.
- Park, W. C. and E. H. Schot, 1968, Stylolitization in carbonate rocks, in Müller, G. and G. M. Friedman (eds.), *Carbonate Sedimentology in Central Europe*: Springer-Verlag, New York, NY, pp. 66–74.
- Parsons, I., P. Thompson, M. R. Lee, and N. Cayzer, 2005, Alkali feldspar microtextures as provenance indicators in siliciclastic rocks and their role in feldspar dissolution during transport and diagenesis: *J. Sediment. Res.*, **75**, 921–942.

- Pashin, J. C. and R. A. Gastaldo, 2004, *Sequence Stratigraphy, Paleoclimate, and Tectonics of Coal-Bearing Strata*: American Association of Petroleum Geology Studies in Geology 51.
- Pederson, T. F. and S. E. Calvert, 1990, Anoxia vs. productivity: what controls the formation of organic-carbon rich sediments and sedimentary rocks: *Am. Assoc. Pet. Geol. Bull.*, **74**, 454–466.
- Pedley, H.M., 1990, Classification and environmental models of cool freshwater tufas: *Sediment. Geol.*, **68**, 143–154.
- Peryt, T. M., 1983a, Classification of coated grains, in Peryt, T. M. (ed.), *Coated Grains*: Springer-Verlag, Berlin, pp. 3–6.
- Peryt, T. M. (ed.), 1983b, *Coated Grains*: Springer-Verlag, Berlin.
- Peterson, M. N. and C. C. von der Borch, 1965, Chert: Modern inorganic deposition in a carbonate-precipitating locality: *Science*, **149**, 1501–1503.
- Petránek, J. and F. B. Van Houten, 1997, *Phanerozoic Ooidal Ironstones*: Czech Geological Survey Special Paper 7.
- Pettijohn, F. J., 1941, Persistence of heavy minerals and geologic age: *J. Geol.*, **49**, 610–625.
- Pettijohn, F. J., 1963, Chemical composition of sandstones – excluding carbonate and volcanic sands, in *Data of Geochemistry*, 6th edn. US Geological Survey Professional Paper 440S.
- Pettijohn, F. J., 1975, *Sedimentary Rocks*, 3rd edn.: Harper and Row, New York, NY.
- Pettijohn, F. J. and P. E. Potter, 1964, *Atlas and Glossary of Primary Sedimentary Structures*: Springer-Verlag, New York, NY.
- Pettijohn, F. J., P. E. Potter, and R. Siever, 1987, *Sand and Sandstone*, 2nd edn.: Springer-Verlag, New York, NY.
- Phillips, R. L., 1984, Depositional features of Late Miocene, marine cross-bedded conglomerates, California, in Koster, E. H. and R. J. Steel (eds.), *Sedimentology of Gravels and Conglomerates*: Canadian Society of Petroleum Geology Memoir 10, pp. 345–358.
- Piazzola, J. and V. V. Cavaroc, 1991, Comparison of grain-size-distribution statistics determined by sieving and thin-section analyses: *J. Geol. Educ.*, **39**, 364–367.
- Picard, M. D., 1971, Classification of fine-grained sedimentary rocks: *J. Sediment Petrol.*, **41**, 179–195.
- Pickerill, R. K., 1994, Nomenclature and taxonomy of invertebrate trace fossils, in Hopkins, S. K. (ed.), *The Palaeobiology of Trace Fossils*: John Hopkins University Press, Baltimore, MD, pp. 3–42.
- Pittman, E. D., 1963, The use of zoned plagioclase as an indicator of provenance: *J. Sediment. Petrol.*, **33**, 380–386.
- Plummer, P. S. and V. A. Gostin, 1981, Shrinkage cracks: Desiccation or syneresis? *J. Sediment. Petrol.*, **51**, 1147–1156.
- Popp, B. N., P. Parekh, B. Tilbrook, R. R. Bidigare, and E. A. Laws, 1997, Organic carbon $\delta^{13}\text{C}$ variations in sedimentary rocks as chemostratigraphic and paleoenvironmental tools: *Paleogeogr., Paleoclim., Paleoecol.*, **132**, 119–132.
- Poppe, L. J., A. H. Eliason, and J. J. Fredricks, 1985, *APSAS – an Automated Particle Size Analysis System*: US. Geological Survey Circular 963.
- Potter, P. E. and F. J. Pettijohn, 1977, *Paleocurrents and Basin Analysis*, 2nd edn.: Springer-Verlag, New York.
- Potter, P. E., J. B. Maynard, and W. A. Pryor, 1980, *Sedimentology of Shale*: Springer-Verlag, New York.

- Potter, P. E., J. B. Maynard, and P. J. Depetris, 2005, *Mud and Mudstones*: Springer-Verlag, Berlin.
- Powers, M. C., 1953, A new roundness scale for sedimentary particles: *J. Sediment. Petrol.*, **23**, 117–119.
- Prezbindowski, D. R., 1985, Burial cementation – is it important? A case study, Stuart City Trend, south-central Texas, in Schneidermann, N. and P. M. Harris (eds.), *Carbonate Cements*, SEPM Special Publication 36, pp. 241–264.
- Prothero, D. R. and F. Schwab, 2004, *Sedimentary Geology: An Introduction to Sedimentary Rocks and Stratigraphy*, 2nd edn.: W. H. Freeman, New York.
- Purdy, E. G., 1963, Recent calcium carbonate facies of the Great Bahama Bank: *J. Geol.*, **71**, 334–355; 472–497.
- Pye, K., 1994, Shape sorting during wind transport of quartz silt grains – Discussion: *J. Sediment. Petrol.*, **A64**, 704–705.
- Radke, B. M. and R. L. Mathis, 1980, On the formation and occurrence of saddle dolomite: *J. Sediment. Petrol.*, **50**, 1149–1168.
- Raffensperger, J. P. and D. Vlassopoulos, 1999, The potential for free and mixed convection in sedimentary basins: *Hydrogeol. J.*, **7**, 505–520.
- Rahmani, R. A. and R. M. Flores (eds.), 1984, *Sedimentology of Coal and Coal-Bearing Sequences*: International Association of Sedimentologists Special Publication 7.
- Railsback, L. B., T. F. Anderson, S. C. Ackerly, and J. L. Cisne, 1989, Paleooceanographic modeling of temperature–salinity profiles from stable isotopic data: *Paleoceanography*, **4**, 585–591.
- Ramseyer, K. and J. R. Boles, 1986, Mixed-layer illite/smectite minerals in Tertiary sandstones and shales, San Joaquin basin, California: *Clays Clay Mins.*, **34**, 115–124.
- Reddy, M. M. and K. K. Wang, 1980, Crystallization of calcium carbonate in the presence of metal ions. I. Inhibition by magnesium ions at pH 8.8 and 25 °C: *J. Cryst. Growth*, **50**, 470–480.
- Reed, S. J. B. and Romanenko, 1995, Electron probe microanalysis, in Marfunin, A. S. (ed.), *Advanced Mineralogy, Methods and Instrumentations: Results and Recent Developments*: Springer-Verlag, Berlin, vol. 2, pp. 240–246.
- Reeder, R. J., 1983, Crystal chemistry of the rhombohedral carbonates, in Reeder, R. J. (ed.), *Carbonates: Mineralogy and Chemistry*: Mineralogical Society of America Reviews in Mineralogy 11, pp. 1–47.
- Reeder, R. J. and J. L. Prosky, 1986, Compositional sector zoning in dolomite: *J. Sediment. Petrol.*, **56**, 237–247.
- Reid, R. P., I. G. Macintyre, and N. P. James, 1990, Internal precipitation of microcrystalline carbonate: A fundamental problem for sedimentologists: *Sediment. Geol.*, **68**, 163–170.
- Reineck, H. E. and I. B. Singh, 1980, *Depositional Sedimentary Environments*, 2nd edn.: Springer-Verlag, Berlin.
- Retallack, G. J., 1997, *A Colour Guide to Paleosols*: John Wiley and Sons, Chichester.
- Ricci-Lucchi, F., 1995, *Sedimentographica: A Photographic Atlas of Sedimentary Structures*, 2nd edn.: Columbia University Press, New York.
- Richter, D. K., 1983a, Calcareous ooids: A synopsis, in Peryt, T. (ed.), *Coated Grains*, Springer-Verlag, Berlin, pp. 72–99.
- Richter, D. K., 1983b, Classification of coated grains: Discussion, in Peryt, T. (ed.), *Coated Grains*, Springer-Verlag, Berlin, pp. 7–8.

- Richter, D. K. and H. Füchtbauer, 1978, Ferroan calcite replacement indicates former magnesian calcite skeletons: *Sedimentology*, **25**, 843–861.
- Ridley, W. I. and F. E. Lichte, 1998, Major, trace, and ultratrace element analysis by laser ablation ICP-MS, in Shanks, W. C. and W. I. Ridley (eds.), *Applications of Microanalytical Techniques to Understanding Mineralizing Processes: Reviews in Economic Geology* 7, pp. 199–215.
- Riggs, S. R., 1980, Intraclast and pellet phosphorite sedimentation in the Miocene of Florida: *J. Geol. Soc. London*, **137**, 741–748.
- Rimstidt, J. D., 1997, Quartz solubility at low temperatures: *Geochim. Cosmochim. Acta*, **61**, 2553–2558.
- Rittenhouse, G., 1943, Transportation and deposition of heavy minerals: *Geol. Soc. Am. Bull.*, **54**, 1725–1780.
- Robbins, L. L., Y. Tao, and C. A. Evans, 1997, Temporal and spacial distribution of whittings on Great Bahama Bank and a new lime mud budget: *Geology*, **25**, 947–950.
- Robin, P. F., 1978, Pressure solution at grain-to-grain contacts: *Geochim. Cosmochim. Acta*, **42**, 1383–1389.
- Ronov, A. B., 1983, The Earth's Sedimentary Shell: AGI Reprint Series 5.
- Ronov, A. B. and A. A. Migdisov, 1971, Geochemical history of the crystalline basement and sedimentary cover of the Russian and North American platforms: *Sedimentology*, **16**, 137–185.
- Ronov, A. B., E. E. Khain, A. N. Balukhovskiy, and K. B. Seslavinsky, 1980, Quantitative analysis of Phanerozoic sedimentation: *Sediment. Geol.*, **25**, 311–325.
- Roser, B. P. and R. J. Korsch, 1986, Determination of tectonic setting of sandstone–mudstone suites using SiO₂ content and K₂O/Na₂O ratios: *J. Geol.*, **94**, 635–650.
- Russell, P. L., 1990, *Oil Shales of the World: Their Origin, Occurrence and Exploration*: Pergamon Press, Oxford.
- Ryer, T. A. and A. W. Langer, 1980, Thickness change involved in the peat-to-coal transformation for a bituminous coal of Cretaceous age in central Utah: *J. Sediment. Petrol.*, **50**, 987–992.
- Sagoe, K. -M. O. and G. S. Visher, 1977, Population breaks in grain-size distributions of sand – A theoretical model: *J. Sediment. Petrol.*, **47**, 285–310.
- Saigal, G. C. and E. K. Walton, 1988, On the occurrence of displacive calcite in Lower Old Red Sandstones of Carnoustie, eastern Scotland: *J. Sediment. Petrol.*, **58**, 131–135.
- Saller, A. H., 1984, Petrologic and geochemical constraints on the origin of subsurface dolomite: An example of dolomitization by normal seawater, Enewetak Atoll: *Geology*, **12**, 217–220.
- Sandberg, P. A., 1983, An oscillating trend in Phanerozoic non-skeletal carbonate mineralogy: *Nature*, **305**, 19–22.
- Sass, E. and A. Katz, 1982, The origin of platform dolomites: *Am. J. Sci.*, **282**, 1184–1213.
- Sassen, R., C. H. Moore, and F. C. Meendsen, 1987, Distribution of hydrocarbon source potential in the Jurassic Smackover Formation: *Org. Geochem.*, **11**, 379–383.
- Savin, S. M. and H. W. Yeh, 1981, Stable isotopes in ocean sediments, in C. Emiliani (ed.), *The Sea*: Wiley-Interscience, New York, NY, vol. 7, pp. 1521–1554.
- Schäfer, A. and T. Teyssen, 1987, Size, shape and orientation of grains in sands and sandstones – image analysis applied to rock thin-sections: *Sediment. Geol.*, **52**, 251–271.
- Schieber, J., 1991, Sedimentary structures: Textures and depositional settings of shales from the Lower Belt Supergroup, Mid-Proterozoic, Montana, U.S.A., in Bennett, R. H.,

- N. R. O'Brien, and M. H. Hulbert (eds.), *Microstructures of Fine-Grained Sediments*: Springer-Verlag, New York, NY, pp. 101–108.
- Schieber, J. and W. Zimmerle, 1998, Petrology of shales: A survey of technics, in Schieber, J., W. Zimmerle, and P. S. Sethi (eds.), *Shales and Mudstones I*: Schweizerbart'sche Verlagsbuchhandlung, Stuttgart, pp. 3–12.
- Schieber, J., W. Zimmerle, and P. S. Sethi (eds.), 1998, *Shales and Mudstones I and II*: E. Schweizerbart'sche Verlagsbuchhandlung, Stuttgart.
- Schlanger, W. and N. P. James, 1978, Low-magnesian calcite forming on the deep-sea floor, Tongue of the Ocean, Bahamas: *Sedimentology*, **25**, 675–702.
- Schmalz, R. F., 1967, Kinetics and diagenesis in carbonate sediments: *J. Sediment. Petrol.*, **37**, 60–68.
- Schmid, R., 1981, Descriptive nomenclature and classification of pyroclastic deposits and fragments: Recommendations of the IUGS Subcommittee on the Systematics of Igneous Rocks: *Geology*, **9**, 41–43.
- Schmidt, V. and D. A. McDonald, 1979, The role of secondary porosity in the course of sandstone diagenesis, in Scholle, P. A. and P. R. Schluger (eds.), *Aspects of Diagenesis*: SEPM Special Publication 26, pp. 175–207.
- Schmoker, J. W. and R. B. Halley, 1982, Carbonate porosity versus depth: A predictable relation for south Florida: *Am. Assoc. Pet. Geol. Bull.*, **66**, 2561–2570.
- Schneidermann, N. and P. M. Harris, 1985, *Carbonate Cements*: SEPM Special Publication 36.
- Scholle, P. A., 1978, *A Color Illustrated Guide to Carbonate Rock Constituents, Textures, Cements and Porosities*: AAPG Memoir 27.
- Scholle, P. A., 1979, *A Color Illustrated Guide to Constituents, Textures, Cements and Porosities of Sandstones and Associated Rocks*: AAPG Memoir 28.
- Scholle, P. A. and R. B. Halley, 1985, Burial diagenesis: out of sight out of mind, in Schneidermann, N. and P. M. Harris (eds.), *Carbonate Cements*: SEPM Special Publication 36, pp. 309–334.
- Scholle, P. A. and D. S. Ulmer-Scholle, 2003, *A Color Guide to the Petrography of Carbonate Rocks: Grains, Textures, Porosity, Diagenesis*: AAPG Memoir 77.
- Schopf, J. M., 1956, A definition of coal: *Econ. Geol.*, **51**, 521–527.
- Schreiber, B. C., 1988a, Introduction, in Schreiber, B. C. (ed.), *Evaporites and Hydrocarbons*: Columbia University Press, New York, NY, pp. 1–10.
- Schreiber, B. C., 1988b, Subaqueous evaporite deposition, in Schreiber, B. C. (ed.), *Evaporites and Hydrocarbons*: Columbia University Press, New York, NY, pp. 182–255.
- Schreiber, B. C. and K. J. Hsü, 1980, Evaporites, in Hobson, G. D. (ed.), *Developments in Petroleum Geology – 2*: Applied Science Publishers, Barking, pp. 87–138.
- Schreiber, B. C., G. M. Friedman, A. Decima, and E. Schreiber, 1976, Depositional environments of Upper Miocene (Messinian) evaporite deposits of the Sicilian basin: *Sedimentology*, **23**, 729–760.
- Schreiber, B. C., M. E. Tucker, and R. Till, 1986, Arid shorelines and evaporites, in Reading, H. G. (ed.), *Sedimentary Environments and Facies*: Blackwell Science, Oxford, pp. 189–228.
- Schubel, K. A. and B. M. Simonson, 1990, Petrography and diagenesis of cherts from Lake Magadi, Kenya: *J. Sediment. Petrol.*, **60**, 761–776.
- Schwab, F. L., 1975, Framework mineralogy and chemical composition of continental margin-type sandstone: *Geology*, **3**, 487–490.
- Schwab, F. L., 1981, Evolution of the Western Continental Margin, French–Italian Alps: Sandstone mineralogy as an index of plate tectonic setting: *J. Geol.*, **89**, 349–368.

- Szwarcz, H. P. and K. C. Shane, 1969, Measurement of particle shape by Fourier analysis: *Sedimentology*, **13**, 213–231.
- Schwennicke, T., H. Siegmund, and C. Jehl, 2000, Marine phosphogenesis in shallow-water environments: Cambrian, Tertiary, and Recent examples, in Glenn, C. R., L. Prévôt-Lucas, and J. Lucas (eds.), *Marine Authigenesis: From Global to Microbial*: SEPM Special Publication 66, pp. 481–498.
- Scoffin, T. P., 1987, *An Introduction to Carbonate Sediments and Rocks*: Blackie, Glasgow.
- Scott, A. C., 2002, Coal petrology and the origin of coal macerals: a way ahead?: *Int. J. Coal Geol.*, **50**, 119–134.
- Searl, A., 1989, Pedogenic columnar calcite from the Oolite Group (Lower Carboniferous), south Wales: *Sediment. Geol.*, **62**, 47–58.
- Sedimentation Seminar, 1981, Comparison of methods of size analysis for sands of the Amazon and Solemões rivers, Brazil and Peru: *Sedimentology*, **28**, 123–128.
- Seiders, V. M. and C. D. Blome, 1988, Implications of upper Mesozoic conglomerate for suspect terrane in western California and adjacent areas: *Geol. Soc. Am. Bull.*, **100**, 374–391.
- Seilacher, A., 1964, Biogenic sedimentary structures, in Imbrie, J. and N. D. Newell (eds.), *Approaches to Paleoecology*: John Wiley and Sons, New York, NY, pp. 296–315.
- Sellwood, B. W., T. J. Shepherd, M. R. Evans, and B. James, 1989, Origin of late cements in oolitic reservoir facies: a fluid inclusion and isotopic study (Mid-Jurassic, southern England): *Sediment. Geol.*, **61**, 223–237.
- Sethi, P. S., R. E. Hannigan, and E. L. Leithold, 1998, Rare-earth element chemistry of Cenomanian–Turonian shales of the North American Greenhorn Sea, Utah, in Schieber, J., W. Zimmerle, and P. Sethi (eds.), *Shales and Mudstones II*: E. Schweizerbart'sche Verlagsbuchhandlung, Stuttgart, pp. 195–208.
- Seyedolali, A., D. H. Kinsley, S. Boggs, Jr., et al., 1997, Provenance interpretation of quartz by scanning electron microscope – cathodoluminescence fabric analysis: *Geology*, **25**, 787–790.
- Shanmugam, G., 1984, Types of porosity in sandstones and their significance in interpreting provenance, in Zuffa, G. G. (ed.), *Provenance of Arenites*: Reidel, Dordrecht, pp. 115–137.
- Sharp, W. E. and G. C. Kennedy, 1965, The solution alteration of carbonate rocks, the effects of temperature and pressure: *J. Geol.*, **73**, 391–403.
- Sharp, Z., 2007, *Principles of Stable Isotope Geochemistry*: Prentice-Hall, Upper Saddle River, NJ.
- Shaw, D. M., 1956, Geochemistry of pelitic rocks. Part III: Major elements and general geochemistry: *Geol. Soc. Am. Bull.*, **67**, 919–934.
- Shearman, D. J., 1982, Evaporites of coastal sabkhas, in Dean, W. E. and B. C. Schreiber (eds.), *Marine Evaporites*: SEPM Short Course Notes 4, pp. 6–42.
- Shearman, D. J. and A. J. Smith, 1985, Ikaite, the parent mineral of jarrowite-type pseudomorphs: *Proc. Geologists Assoc.*, **96**, 305–314.
- Sheldon, R. P., 1989, Phosphorite deposits of the Phosphoria Formation, western United States, in Notholt, A. J. G., R. P. Sheldon, and D. F. Davidson (eds.), *Phosphate Deposits of the World, 2*: Cambridge University Press, Cambridge, pp. 53–61.
- Shinn, E. A. and D. M. Robbin, 1983, Mechanical and chemical compaction in fine-grained shallow-water limestones: *J. Sediment. Petrol.*, **53**, 595–618.
- Shinn, E. A., R. P. Steinen, B. H. Lidz, and P. K. Swart, 1989, Whitings, a sedimentologic dilemma: *J. Sediment. Petrol.*, **59**, 147–161.

- Sibley, D. F. and J. M. Gregg, 1987, Classification of dolomite rock textures: *J. Sediment. Petrol.*, **57**, 967–975.
- Siever, R., 1957, The silica budget in the sedimentary cycle: *Am. Mineral.*, **42**, 821–841.
- Siever, R., 1983, Evolution of chert at active and passive continental margins, in Iijima, A., J. R. Hein, and R. Siever (eds.), *Siliceous Deposits in the Pacific Region: Developments in Sedimentology* 36, pp. 7–24.
- Siever, R., 1992, The silica cycle in the Precambrian: *Geochim. Cosmochim. Acta*, **56**, 3265–3272.
- Simonson, B. M., 1985, Sedimentological constraints on the origins of Precambrian iron-formations: *Geol. Soc. Am. Bull.*, **96**, 244–252.
- Simonson, B. M., 2003, Origin and evolution of large Precambrian iron formations, in Chan, M. A. and A. W. Archer (eds.), *Extreme Depositional Environments: Mega End Members in Geologic Time*: Geological Society of America Special Paper 370, pp. 231–244.
- Sindowski, F. K. H., 1949, Results and problems of heavy mineral analysis in Germany: A review of sedimentological–petrological papers, 1936–1948: *J. Sediment. Petrol.*, **19**, 3–25.
- Singer, A. and G. Müller, 1983, Diagenesis in argillaceous sediments, in Larsen, G. and G. V. Chilingar (eds.), *Diagenesis in Sediments and Sedimentary Rocks, 2*: Elsevier, Amsterdam, pp. 115–212.
- Singer, J. K., J. B. Anderson, M. T. Ledbetter, *et al.*, 1988, An assessment of analytical techniques for the size analysis of fine-grained sediments: *J. Sediment. Petrol.*, **58**, 534–543.
- Skilbeck, C. G. and P. A. Cawood, 1994, Provenance history of a Carboniferous Gondwana margin forearc basin, New England Fold Belt, eastern Australia: modal and geochemical constraints: *Sediment. Geol.*, **93**, 107–133.
- Slansky, M., 1986, *Geology of Sedimentary Phosphates*: North Oxford Academic Publishers, London.
- Smith, G. H. S., J. L. Best, C. S. Bristow, and G. E. Petts (eds.), 2006, *Braided Rivers: Process, Deposits, Ecology and Management*: International Association of Sedimentologists Special Publication 36.
- Sneed, E. D. and R. L. Folk, 1958, Pebbles in the lower Colorado River, Texas – A study in particle morphogenesis: *J. Geol.*, **66**, 114–150.
- Sorby, H. C., 1880, On the structure and origin of non-calcareous stratified rocks: *Proc. Geol. Soc. London*, **36**, 46–92.
- Southard, J. B. and L. A. Boguchwal, 1990, Bed configurations in steady unidirectional water flows. Part 2. Synthesis of flume data: *J. Sediment. Petrol.*, **60**, 658–679.
- Spears, D. A., 1980, Toward a classification of shales: *J. Geol. Soc. London*, **137**, 125–129.
- Speer, J. A., 1983, Crystal chemistry and phase relations of orthorhombic carbonates, in Reeder, R. J. (ed.), *Carbonates: Mineralogy and Chemistry*: Mineralogical Society of America Reviews in Mineralogy 11, pp. 145–190.
- Sperazza, M., 2004, High-resolution particle size analysis of naturally occurring very fine-grained sediment through laser diffractometry: *J. Sediment. Res.*, **74**, 736–743.
- Stach, E., M. Th. Mackowsky, M. Teichmüller, *et al.*, 1982, *Coal Petrology*, 3rd edn.: Gebrüder Borntraeger, Berlin.
- Stauffer, P. H., 1967, Grain-flow deposits and their implications, Santa Ynez Mountains, California: *J. Sediment. Petrol.*, **37**, 487–508.

- Stein, R., 1985, Rapid grain-size analyses of clay and silt fraction by Sedigraph 5000D: Comparison with Coulter counter and Atterberg methods: *J. Sediment. Petrol.*, **55**, 590–593.
- Stewart, F. H., 1963, Marine evaporites, in Fleischer, M. (ed.), *Data of Geochemistry*: US Geological Survey Professional Paper 440-Y.
- Stoesser, R. K. and C. H. Moore, 1983, Chemical constraints and origins of four groups of Gulf Coast reservoir fluids: *Am. Assoc. Pet. Geol. Bull.*, **67**, 896–906.
- Stokes, S., C. S. Nelson, and T. R. Healy, 1989, Textural procedures for the environmental discrimination of late Neogene coastal sand deposits, southwest Auckland, New Zealand: *Sediment. Geol.*, **61**, 135–150.
- Stone, W. N. and R. Siever, 1996, Quantifying compaction, pressure solution and quartz cementation in moderately- and deeply-buried quartzose sandstones from the Greater Green River Basin, Wyoming, in Crossey, L. J., M. W. Totten, and P. A. Scholle (eds.), *Siliciclastic Diagenesis and Fluid Flow: Concepts and Applications*: SEPM Special Publication 55, pp. 129–150.
- Stopes, M. C., 1919, On the four visible ingredients in banded bituminous coal. Studies in the composition of coal: *Royal Soc. London Proc., Ser. B.*, **90**, 470–487.
- Stopes, M. C., 1935, On the petrology of banded bituminous coal: *Fuel London*, **14**, 4–13.
- Stow, D. A. V., 2005, *Sedimentary Rocks in the Field: A Color Guide*: Elsevier, Burlington, MA.
- Stow, D. A. V. and A. J. Bowen, 1980, A physical model for the transport and sorting of fine-grained sediment by turbidity currents: *Sedimentology*, **27**, 31–46.
- Stow, D. A. V. and D. J. W. Piper, 1984, Deep-water fine-grained sediments: history, methodology and terminology, in Stow, D. A. V. and D. J. W. Piper (eds.), *Fine-Grained Sediments*: Geological Society Special Publication 15, pp. 3–14.
- Strasser, A., E. Davaud, and Y. Jedouri, 1989, Carbonate cements in Holocene beachrock: Examples from Bahiret el Biban, southeastern Tunisia: *Sediment. Geol.*, **62**, 89–100.
- Strohmenger, C. and G. Wirsing, 1991, A proposed extension of Folk's textural classification of carbonate rocks: *Carbonate Evaporite*, **6**, 23–28.
- Sturesson, U., A. Dronov, and T. Saadre, 1999, Lower Ordovician iron ooids and associated oolitic clays in Russia and Estonia: A clue to the origin of iron oolites: *Sediment. Geol.*, **123**, 63–80.
- Sudo, T., S. Shimoda, H. Yotsumoto, and S. Aita, 1981, *Electron Micrographs of Clay Minerals*: Elsevier, Amsterdam.
- Suess, E., W. Balzer, K.-F. Hesse, *et al.*, 1982, Calcium carbonate hexahydrate from organic-rich sediments of the Antarctic Shelf: Precursor of Glendonites: *Science*, **1216**, 1128–1131.
- Sugisaki, R., 1984, Relation between chemical composition and sedimentation rate of Pacific ocean-floor sediments deposited since the middle Cretaceous: Basic evidence for chemical constraints on depositional environments of ancient sediments: *J. Geol.*, **92**, 235–260.
- Surdam, R. C., 1981, Zeolites in closed hydrologic systems, in Mumpton, F. A. (ed.), *Mineralogy and Geology of Natural Zeolites*: Mineralogical Society of America Reviews in Mineralogy 4, pp. 65–91.
- Surdam, R. C. and J. R. Boles, 1979, Diagenesis of volcanic sandstones, in Scholle, P. A. and P. R. Schluger (eds.), *Aspects of Diagenesis*: SEPM Special Publication 26, pp. 227–242.
- Surdam, R. C., L. J. Crossey, E. S. Hagen, and H. P. Heasler, 1989a, Organic–inorganic interactions and sandstone diagenesis: *Am. Assoc. Pet. Geol. Bull.*, **73**, 1–23.

- Surdam, R. C., T. L. Dunn, H. P. Heasler, and D. B. MacGowan, 1989b, Porosity evolution in sandstone/shale systems, in Hutcheon, I. E. (ed.), *Burial Diagenesis: Mineralogical Association of Canada Short Course Handbook 15*, pp. 61–134.
- Suryanarayana, C. and M. G. Norton, 1998, *X-Ray Diffraction: a Practical Approach*: Plenum Press, New York, NY.
- Suttner, L. J. and A. Basu, 1985, The effects of grain size on detrital modes: A test of the Gazzi–Dickinson point-counting method: *J. Sediment. Petrol.*, **55**, 616–617.
- Suttner, L. J. and P. K. Dutta, 1986, Alluvial sandstone composition and paleoclimate, I. Framework mineralogy: *J. Sediment. Petrol.*, **56**, 329–345.
- Suttner, L. J., A. Basu, and G. H. Mack, 1981, Climate and the origin of quartz arenites: *J. Sediment. Petrol.*, **51**, 1235–1246.
- Sutton, R. G. and T. L. Lewis, 1966, Regional patterns of cross-laminae and convolution in a single bed: *J. Sediment. Petrol.*, **36**, 225–229.
- Swanson, F. J., 1972, Morphogenesis and shape sorting of coarse sediment in the Elk River, Southwestern Oregon: Unpublished Ph.D dissertation, University of Oregon, OR.
- Swarbrick, R. E., M. J. Osborne, and G. S. Yardley, 2002, Comparison of overpressure magnitude resulting from main generating mechanisms, in Huffman, A. R. and G. L. Bowers (eds.), *Pressure Regimes in Sedimentary Basins and Their Prediction: AAPG Memoir 76*, pp. 1–12.
- Swart, P. K. and L. A. Melim, 2000, The origin of dolomites in Tertiary sediments from the margin of Great Bahama Bank: *J. Sediment. Res.*, **70**, 738–748.
- Swift, D. J. P., J. R. Schubel, and R. E. Sheldon, 1972, Size analysis of fine-grained suspended sediments: a review: *J. Sediment. Petrol.*, **42**, 122–134.
- Syvitski, J. P. M. (ed.), 1991a, Applications, in *Principles, Methods, and Application of Particle Size Analysis*: Cambridge University Press, Cambridge, p. 281.
- Syvitski, J. P. M., 1991b Factor analysis of size frequency distributions: Significance of factor solutions based on simulation experiments, in Syvitski, J. P. M. (ed.), 1991, *Principles, Methods, and Application of Particle Size Analysis*: Cambridge University Press, Cambridge, pp. 249–263.
- Syvitski, J. P. M., K. W. Asprey, and D. A. Clattenburg, 1991, Principles, design, and calibration of settling tubes, in Syvitski, J. P. M. (ed.), *Principles, Methods, and Application of Particle Size Analysis*: Cambridge University Press, Cambridge, pp. 45–63.
- Tauxe, L., 2002, *Paleomagnetic Principles and Practice*: Kluwer, Dordrecht.
- Telford, R. W., M. Lyons, J. D. Orford, W. B. Whalley, and D. Q. M. Fay, 1987, A low-cost, microcomputer-based image analyzing system for characterization of particle outline morphology, in Marshall, J. R. (ed.), *Clastic Particles*: Van Nostrand Reinhold, New York, NY, pp. 281–289.
- Thomas, L., 1992, *Handbook of Practical Coal Geology*: John Wiley and Sons, Chichester.
- Thompson, S. K., 2002, *Sampling*, 2nd edn.: John Wiley and Sons, New York.
- Ting, F. T. C., 1982, Coal macerals, in Meyers, R. A. (ed.), *Coal Structure*: Academic Press, New York, NY, pp. 7–49.
- Tissot, B. P. and D. H. Welte, 1984, *Petroleum Formation and Occurrence*, 2nd edn.: Springer-Verlag, Berlin.
- Tolstov, G. P., 1976, *Fourier Series*: Dover Publishers, New York.
- Torley, R. F., 2001, Results of a new method of Fourier grain-shape analysis of detrital quartz grains in sediments from Jackson County, Oregon: *Oreg. Geol.*, **63**, 60–64.
- Tourtelet, H. A., 1960, Origin and use of the word “shale”: *Am. J. Sci.*, **258-A** (Bradley Volume) 335–343.

- Tovey, N. K., M. H. Hounslow, and J. M. Wang, 1995, Orientation analysis and its application in image analysis: *Adv. Imag. Elect. Phys.*, **93**, 219–329.
- Trappe, J., 2001, A nomenclature system for granular phosphate rock according to depositional texture: *Sediment. Geol.*, **145**, 135–150.
- Trendall, A. F., 1983, Introduction, in Trendall, A. F. and R. C. Mooris (eds.), *Iron-Formation: Facts and Problems*: Elsevier, Amsterdam, pp. 1–12.
- Trendall, A. F., 2002, The significance of iron-formation in the Precambrian record, in Wladyslaw, A. and P. L. Corcoran (eds.), *Precambrian Sedimentary Environments*: International Association of Sedimentologists Special Publication 33, pp. 33–66.
- Trendall, A. F. and J. G. Blockley, 1970, The iron formations of the Precambrian Hammersley Group, western Australia: *Geol. Surv. West. Aust. Bull.*, **119**, 1–136.
- Trevena, A. S. and W. P. Nash, 1979, Chemistry and provenance of detrital feldspars: *Geology*, **7**, 475–478.
- Trevena, A. S. and W. P. Nash, 1981, An electron microprobe study of detrital feldspar: *J. Sediment. Petrol.*, **51**, 137–150.
- Trurnit, P., 1968, Analysis of pressure-solution contacts and classification of pressure solution phenomena, in Müller, G. and G. M. Friedman (eds.), *Carbonate Sedimentology in Central Europe*: Springer-Verlag, New York, NY, pp. 75–84.
- Tucker, M. (ed.), 1988, *Techniques in Sedimentology*: Blackwell Scientific, Oxford.
- Tucker, M. E., 2003, *Sedimentary Rocks in the Field*: John Wiley and Sons, Chichester.
- Tucker, M. E. and V. P. Wright, 1990, *Carbonate Sedimentology*: Blackwell Scientific, Oxford.
- Tyler, S. A., E. S. Barghoorn, and L. P. Barrett, 1957, Anthracitic coal from Precambrian Upper Huronian black shale of the Iron River district, northern Michigan: *Geol. Soc. Am. Bull.*, **68**, 1293–1304.
- Uzdowski, E., 1994, Synthesis of dolomite and geochemical implications, in Purser, B. H., M. E. Tucker, and D. H. Zenger (eds.), *Dolomite – a Volume in Honour of Dolomieu*: International Association of Sedimentologists Special Publication 21, pp. 345–360.
- Valley, J. W. and D. R. Cole (eds.), 2001, *Stable Isotope Geochemistry*: Mineralogical Society of America Reviews in Mineralogy and Geochemistry 43.
- Van den Berg, E. H., V. F. Bense, and W. Schlager, 2003, Assessing textural variation in laminated sands using digital image analysis of thin sections: *J. Sediment. Res.*, **73**, 133–143.
- Van Houten, F. B., 1982, Phanerozoic oolitic ironstones – Geologic record and facies models: *Ann. Rev. Earth Planet. Sci.*, **10**, 441–457.
- Van Houten, F. B., 2000, Ooidal ironstones and phosphorites – A comparison from a stratigrapher's view, in Glen, C. R., L. Prévôt-Lucas, and J. Lucas (eds.), *Marine Authigenesis: From Global to Microbial*: SEPM Special Publication 66, pp. 127–132.
- Vasconcelos, C. and J. A. McKenzie, 1997, Microbial mediation of modern dolomite precipitation and diagenesis under anoxic conditions (Lagoa Vermelha, Rio de Janeiro, Brazil): *J. Sediment. Res.*, **67**, 378–390.
- Vavra, C. L., 1989, Mineral reactions and controls on zeolite-facies alterations in sandstones of the central Transantarctic Mountains, Antarctica: *J. Sediment. Petrol.*, **59**, 688–703.
- Veizer, J., 1983, Trace elements and isotopes in sedimentary rocks, in Reeder, R. J. (ed.), *Carbonates: Mineralogy and Chemistry*: Mineralogical Society of America Reviews in Mineralogy 11, pp. 265–299.
- Veizer, J., D. Ala, K. Azmy, et al., 1999, $^{87}\text{Sr}/^{86}\text{Sr}$, $\delta^{13}\text{C}$ and $\delta^{18}\text{O}$ evolution of Phanerozoic seawater: *Chem. Geol.*, **161**, 59–88.

- Velbel, M. A. and M. K. Saad, 1991, Paleoweathering or diagenesis as the principal modifier of sandstone framework composition? A case study from some Triassic rift-valley redbeds of eastern North America, in Morton, A. C., S. P. Todd, and P. W. D. Haughton (eds.), *Developments in Sedimentary Provenance Studies*: Geological Society Special Publication 57, pp. 91–99.
- Velde, B., 1995, *Mineralogy of Clays*: Springer-Verlag, Berlin.
- Vincent, P., 1986, Differentiation of modern beach and coastal dune sands – A logistic regression approach using parameters of the hyperbolic function: *Sediment. Geol.*, **49**, 167–176.
- Visher, G. S., 1969, Grain size distributions and depositional processes: *J. Sediment. Petrol.*, **39**, 1074–1106.
- Wadell, H., 1932, Volume, shape and roundness of rock particles: *J. Geol.*, **40**, 443–451.
- Walderhaug, O., 1990, A fluid inclusion study of quartz-cemented sandstones from offshore mid Norway: *J. Sediment. Petrol.*, **60**, 203–210.
- Walkden, G. M. and J. R. Berry, 1984, Syntaxial overgrowths in muddy crinoidal limestones: Cathodoluminescence sheds new light on an old problem: *Sedimentology*, **31**, 251–267.
- Walker, S., 2000, *Major Coalfields of the World*: IEA Coal Research, The Clean Coal Centre, London.
- Walker, R. G., 1984, Shelf and shallow marine sands, in Walker, R. G. (ed.), *Facies Models*, 2nd edn.: Geoscience Canada Reprint Series 1.
- Walker, T. R., 1974, Formation of red beds in moist tropical climates: A hypothesis: *Geol. Soc. Am. Bull.*, **85**, 633–638.
- Walker, T. R., 1984, Diagenetic albittization of potassium feldspars in arkosic sandstones: *J. Sediment. Petrol.*, **54**, 3–16.
- Walker, T. R., B. Waugh, and A. J. Grone, 1978, Diagenesis in first-cycle desert alluvium of Cenozoic age, southwestern United States and northwestern Mexico: *Geol. Soc. Am. Bull.*, **89**, 19–32.
- Wallace, M. W., 1987, The role of internal erosion and sedimentation in the formation of stromatactis mudstones and associated lithologies: *J. Sediment. Petrol.*, **57**, 695–700.
- Walther, J. V., 2005, *Essentials of Geochemistry*: Jones and Bartlett Publishers, Boston, MA.
- Wandres, A. M., J. D. Bradshaw, S. Weaver, et al., 2004, Provenance analysis using conglomerate clast lithologies: a case study from the Pahau terrane of New Zealand: *Sediment. Geol.*, **167**, 57–89.
- Wanless, H. R., 1979, Limestone response to stress: Pressure solution and dolomitization: *J. Sediment. Petrol.*, **49**, 437–462.
- Ward, C. R. (ed.), 1984, *Coal Geology and Coal Technology*: Blackwell Scientific, Melbourne.
- Wardlaw, N., A. Oldershaw, and M. Stout, 1978, Transformation of aragonite to calcite in a marine gastropod: *Can. J. Earth Sci.*, **15**, 1861–1866.
- Warren, J., 2000, Dolomite: occurrence, evolution and economically important associations: *Earth Sci. Rev.*, **52**, 1–81.
- Warren, J. K., 1989, *Evaporite Sedimentology*: Prentice-Hall, Englewood Cliffs, NJ.
- Warren, J. K., 2006, *Evaporites: Sediments, Resources, and Hydrocarbons*: Springer-Verlag, Berlin.
- Warren, J. K. and G. C. St. C. Kendall, 1985, Comparison of marine sabkhas (subaerial) and salina (subaqueous) evaporites: Modern and ancient: *Am. Assoc. Pet. Geol. Bull.*, **69**, 1013–1023.

- Weaver, M. and S. W. Wise, Jr., 1974, Opaline sediments of the southeastern coastal plain and Horizon A: Biogenic origin: *Science*, **184**, 899–901.
- Welte, D. H., B. Horsfield, and D. R. Baker (eds.), 1997, *Petroleum and Basin Evolution: Insights From Petroleum Geochemistry, Geology and Basin Modeling*: Springer-Verlag, Berlin.
- Weltje, G. J., 2006, Ternary sandstone composition and provenance: an evaluation of the “Dickinson model,” in Buccianti, A., G. Mateur-Figuras, and V. Pawlowsky-Glahn (eds.), *Compositional Data Analysis in the Geosciences: From Theory to Practice*: Geological Society of London Special Publication 264, pp. 79–99.
- Wentworth, C. K., 1922, A scale of grade and class terms for clastic sediments: *J. Geol.*, **30**, 377–392.
- Wetzel, A., 1989, Influence of heat flow on ooze/chalk cementation: Quantification from consolidation parameters in DSDP sites 504 and 505 sediments: *J. Sediment. Petrol.*, **59**, 539–547.
- Whalley, W. B. and J. D. Orford, 1986, Practical methods for analysing and quantifying two-dimensional images, in Sieveking, C. De C. and M. B. Hart (eds.), *The Scientific Study of Flint and Chert*: Cambridge University Press, Cambridge, pp. 235–242.
- Whitaker, F. F., P. L. Smart, V. C. Vahrenkamp, H. Nicholson, and R. A. Wogelius, 1994, Dolomitization by near-normal seawater? Field evidence from the Bahamas, in Purser, B., M. Tucker, and D. Zenger (eds.), *Dolomites – a Volume in Honour of Dolomieu*: International Association of Sedimentologists Special Publication 21, pp. 111–132.
- Whitaker, F. F., P. L. Smart, and G. D. Jones, 2004, Dolomitization: from conceptual to numerical models, in Braithwaite, C. J. R., G. Rizzi, and G. Darke (eds.), *The Geometry and Petrogenesis of Dolomite Hydrocarbon Reservoirs*: Geological Society of London Special Publication 235, pp. 99–139.
- White, D. E., 1965, Saline waters of sedimentary rocks, in Young, A. and J. E. Galley (eds.), *Fluids in Subsurface Environments*: AAPG Memoir 4, pp. 342–366.
- White, J. D. L. and N. R. Riggs (eds.), 2001, *Volcaniclastic Sedimentation in Lacustrine Settings*: International Association of Sedimentologists Special Publication 30.
- Wiegman, J., C. H. Horte, and G. Kranz, 1982, Determination of the complete mineral composition of clays, in van Olphen, H. and F. Veniale (eds.), *International Clay Conference 1981: Developments in Sedimentology* 35, pp. 365–372.
- Wilkinson, M., K. L. Milliken, and R. S. Haszeldine, 2001, Systematic destruction of K-feldspar in deeply buried rift and passive margin sandstones: *J. Geol. Soc. London*, **158**, 675–683.
- Willey, J. D. 1974, The effect of pressure on the solubility of amorphous silica in seawater at 0 °C: *Mar. Chem.*, **2**, 239–250.
- Williams, H., F. J. Turner, and C. M. Gilbert, 1982, *Petrography: An Introduction to the Study of Rocks in Thin Sections*, 2nd edn.: W. H. Freeman, San Francisco, CA.
- Williams, L. A. and D. A. Crerar, 1985, Silica diagenesis, II. General mechanisms: *J. Sediment. Petrol.*, **55**, 312–321.
- Williams, L. A., G. A. Parks, and D. A. Crerar, 1985, Silica diagenesis, I. Solubility controls: *J. Sediment. Petrol.*, **55**, 301–311.
- Wilson, J. C. and E. F. McBride, 1988, Compaction and porosity evaluation of Pliocene Sandstones, Ventura Basin, California: *Am. Assoc. Petrol. Geol. Bull.*, **72**, 664–681.
- Wilson, J. E., 1975, *Carbonate Facies in Geologic History*: Springer-Verlag, New York, NY.
- Winland, H. D. and R. K. Matthews, 1974, Origin and significance of grapestone, Bahama Island: *J. Sediment. Petrol.*, **44**, 921–927.

- Wise, S. W., Jr. and K. R. Kelts, 1972, Inferred diagenetic history of a weakly silicified deep sea chalk: *Gulf Coast Assoc. Geol. Soc. Trans.*, **22**, 177–203.
- Woodland, B. G., 1964, The nature and origin of cone-in-cone structure: *Fieldiana: Geol.*, **13**, 185–305.
- Worden, R. H. and S. D. Burley, 2003, Sandstone diagenesis: the evolution of sand to stone, in Burley, S. D. and R. H. Worden (eds.), *Sandstone Diagenesis: Recent and Ancient*: Blackwell, Malden, MA, pp. 3–44.
- Worden, R. H. and S. Morad (eds.), 2003, *Clay Mineral Cements in Sandstones*: International Association of Sedimentologists, Special Publication 34.
- Wright, V. P., 1992, A revised classification of limestones: *Sediment. Geol.*, **76**, 177–185.
- Wright, V. P. and T. P. Burchette, 1996, Shallow-water carbonate environments, in Reading, H. G. (ed.), *Sedimentary Environments: Processes, Facies and Stratigraphy*: Blackwell Science., Oxford, pp. 325–394.
- Wright, W. R., 2001, Dolomitization, fluid-flow and mineralization of the lower carboniferous rocks of the Irish Midlands and Dublin Basin: Unpublished Ph.D thesis, University College, Dublin (Cited in Machel, 2004.)
- Wyrwoll, K. -H. and G. K. Smyth, 1985, On using the log-hyperbolic distribution to describe the textural characteristics of eolian sediments: *J. Sediment. Petrol.*, **55**, 471–478.
- Yao, Q. and R. V. Demicco, 1995, Paleoflow patterns of dolomitizing fluids and paleohydrogeology of the southern Canadian Rocky Mountains: Evidence from dolomite geometry and numerical modeling: *Geology* **23**, 791–794.
- Yates, K. K. and L. L. Robbins, 2001, Microbial lime-mud production and its relation to climate change, in Gearhard, L. C., W. E. Harrison, and B. M. Hanson (eds.), *Geological Perspectives of Global Climate Change*: AAPG Studies in Geology 47, pp. 267–283.
- Yen, T. F. and G. V. Chilingar, 1976, Introduction to oil shales, in Yen, T. F. and G. V. Chilingarian (eds.), *Oil Shale*: Elsevier, Amsterdam, pp. 1–12.
- Young, S. W., 1976, Petrographic textures of detrital polycrystalline quartz as an aid to interpreting crystalline source rocks: *J. Sediment. Petrol.*, **46**, 595–603.
- Young, S. W., A. Basu, G. Mack, N. Darnell, and L. J. Suttner, 1975, Use of size-composition trends in Holocene soil and fluvial sand for paleoclimatic interpretation: Proceedings of the IXth International Congress on Sedimentation, Th. 1, Nice, France, July 6–13.
- Young, T. P. and W. E. G. Taylor (eds.), 1989, *Phanerozoic Ironstones*: The Geological Society Special Publication 46.
- Zack, T., H. von Eynatten, and A. Kronz, 2004, Rutile geochemistry and its potential use in quantitative provenance studies: *Sediment. Geol.*, **171**, 37–58.
- Zenger, D. H., 1989, Dolomite abundance and stratigraphic age: Constraints on rates and mechanisms of Phanerozoic dolostone formation – Discussion: *J. Sediment. Petrol.*, **59**, 162–164.
- Zingg, Th., 1935, Beiträge zur Schotteranalyse: *Schweiz. Mineral. Petrog. Mitt.*, **15**, 39–140.
- Zuffa, G. G., 1980, Hybrid arenites: Their composition and classification: *J. Sediment. Petrol.*, **50**, 21–29.

Index

- aggregate grains (carbonate), 5, 336, 337, 339, 350, 368
- albite, 121, 241, 281, 299, 300
- albitization, 287, 297, 299, 300
- amphiboles, 113, 124, 127, 148, 226, 308
- analcime, 303–306
- andalusite, 124, 243
- anhydrite, 290, 318, 463, 466, 467, 469, 474, 476
- ankerite, 136, 213, 275, 281, 318
- anorthoclase, 119, 120, 237
- anoxia, 200, 202, 203, 273, 511, 512, 528, 544, 550
- apatite, 105, 124, 243, 518–523
- aragonite, 281, 301, 314, 317, 319, 342, 343, 372, 374, 411–429, 446–449, 456, 457
- arkose, 141, 150, 151
- aulacogens, 14
- authigenic minerals, 129, 303, 307, 480

- bacterial activity, 273, 327
- bafflestone, 353, 367
- barite, 6, 106, 124, 148, 281, 290
- basin analysis, 18, 109
- basins, types of, 12–16, 246–248, 474, 476, 495
- beachrock, 415, 417–419
- bindstone, 353, 367
- bioherms, 364, 370
- bioturbation, 53, 99, 229, 271, 272, 416, 456
- birdseye structure, 355, 360
- bitumen, 6, 527, 529, 543, 553, 554
- böhm lamellae, 114, 115
- Bouma sequence, 70–72, 157
- boundstone, 353, 356, 367, 370
- breccias, 167–169, 189, 379
- burial-history curves, 287, 303, 307

- calcite, 314, 317–319, 327–330, 337–350, 371–380, 384, 388–396, 409–430, 438–451, 456, 457
- calcitization, 409, 419, 420, 475
- carbonaceous sedimentary rocks, 527–555
 - chemical composition of, 530
 - kerogen in, 529–530
 - kinds of, 532
 - organic matter in, 5, 528
- carbonate
 - grains, 59, 325–340
 - minerals, 314, 317–320
 - solubility, relative, 412
- carboxylic acid, 276, 277, 529
- caries texture, 129, 450
- catagenesis, 551
- cathodoluminescence, 111, 232–237, 444
- cement stratigraphy, 443, 444
- cements
 - carbonate, 148, 281–283, 414, 418, 438–440
 - quartz, 283–289
 - other, 290, 291
- chalcedony, 114, 117, 118, 281, 284, 478–480
- chamosite, 129, 273, 508, 512
- chemical compaction, 278, 431, 432, 433, 434, 456, 457
- chert
 - bedded, 478, 482–484, 492–495
 - chemical composition of, 480
 - deposition of, 485–491
 - mineralogy and texture of, 478–480
 - nodular, 484
 - replacement by, 491
 - varieties of, 481
- chickenwire structure, 467
- chlorite, 122, 123, 210
- clarin, 537
- clay minerals, 113, 123, 136, 205, 207, 210, 301, 303
- coal, 533–542
 - classification of, 533
 - macerals in, 538
 - origin of, 540–542
 - petrography of, 536
- conglomerates, 165–193
 - cement in, 170
 - classification of, 168, 172
 - composition of, 169
 - depositional environments of, 178
 - fabric support in, 166

- matrix in, 170
- occurrence of, 175
- open work, 171
- sedimentary structures in, 172
- corpuscle effect, 26, 40
- cyanobacteria, 91, 331, 354, 377
- cyclothem, 542
- decarboxylation, 277, 451, 551
- decementation, 293, 294
- diagenesis of carbonate rocks
 - diagenetic processes
 - biogenic activity, 410
 - cementation, 414, 423, 435
 - compaction (physical), 431, 432
 - dissolution, 291–294, 418, 422, 451, 454
 - neomorphism, 419, 420, 423, 444, 446
 - pressure solution *see* (chemical compaction)
 - replacement, 449, 450
 - diagenetic regimes, 409
 - deep-burial, 428
 - meteoric, 409, 420
 - mixing-zone, 409, 427
 - seafloor, 409, 410
 - variables affecting
 - mineralogy and grain size, 429
 - pore-fluid composition, 429
 - pressure, 430
 - temperature, 430
- diagenesis of Sandstones and Shales
 - ages of diagenetic events, 307
 - albitization, 299
 - bioturbation, 271
 - cementation, 280–291
 - chemical and biochemical reactions in, 273
 - clay-mineral authigenesis, 301
 - compaction, 277–280
 - dissolution, 291–294
 - eogenesis, 271–274
 - mesogenesis, 274–307
 - oxidation (of ferromagnesian minerals), 307
 - recrystallization and inversion, 300–301
 - replacement, 294–297
 - stages of diagenesis, 269
 - telogenesis, 308
 - zeolite authigenesis, 303–306
- diagenetic stages, 269
- diamictite, 166
- dissolution
 - congruent, 292
 - incongruent, 292, 294
- dolomites, 382–407
 - chemistry of, 393
 - dolomite problem, The, 393
 - mineralogy of, 383
 - models for origin of, 396–404
 - mottled, 391
 - protodolomite, 383
 - stoichiometry of, 383
 - texture of, 385
 - zoning of, 389
- dolomitization, 394–407
- drusy texture, 129–132, 345, 346
- durain, 536–538
- enterolithic structure, 469, 477
- eogenesis, 270, 271, 408
- eolinite (carbonate), 380
- epiclasts, 160
- epimatrix, 134
- evaporative pumping, 308, 399
- evaporative drawdown, 474
- evaporites, 462–478
 - ancient deposits of, 477
 - classification of, 466
 - deposition of, 471
 - depositional models for, 472
 - diagenesis of, 475
 - mineralogy of, 463–466
 - rates of deposition, 462
- extraclasts, 335, 336, 350
- fabric, 53–58
 - grain packing, 53
 - particle orientation, 54
- feldspars, general, 118–121
 - alkali (potassium), 118, 119, 237
 - chemistry of, 240
 - plagioclase, 119, 121, 122, 147, 238
 - twinning of, 239
 - zoning of, 237, 238
- feldspathic arenite, 146–151
- fermentation, 274, 276
- fissility, 198, 200
- flint, 481
- floatstone, 353
- fluid inclusion studies, 286, 303, 307, 437, 438, 444
- framestone, 353, 357
- francolite, 516, 517
- fusain, 536, 537
- garnet, 113, 124, 142, 148, 154, 243
- geopetal fabric, 131, 355, 360, 361
- geosynclines, 12
- glauconite, 6, 129, 273, 307, 505, 508, 517
- glaucofanite, 124, 154, 243
- goethite, 113, 136, 206, 213, 281, 290, 307, 505, 508

- grain shape, 36–49
 fourier shape analysis, 41–46
 methods of expressing, 36
 particle form, 38
 roundness, 40
 significance of, 46–48
 sphericity, 38
- grain size, 21–36
 grain-size scales, 21
 interpretation and significance of, 32–36
 methods of measuring, 23–32
- grainstone, 353, 367, 368, 415, 492
- grapestone, 336, 337, 368, 415
- graywacke, 141, 147, 151, 152, 157, 281
- greensands, 164
- gypsum, 290, 397, 399, 461, 463, 466, 467, 470, 471, 474, 476, 477
- halite, 463, 466, 469, 471, 474, 477
- hardgrounds, 361, 415, 416
- heavy minerals, 112, 123–125, 129, 137, 138, 148, 207, 241, 244, 293
- hematite, 496, 502, 505, 509, 512
- hornblende, 124, 154, 243
- hyaloclastites, 189
- hydraulic equivalent size, 123, 137
- hydraulic ratio, 137
- iron-rich sedimentary rocks, 495–512
 depositional models of, 510
 kinds of, 496
 iron formations, 497
 iron-rich shales, 506
 ironstones, 504
 origin of, 507
- isotopes
 carbon, 320, 323, 531, 532
 hydrogen, 531
 nitrogen (organic matter), 531
 oxygen, 319–321, 324, 442
 radiogenic, 325
 sulfur, 531
- jasper, 481
- kaolinite, 197, 206, 208, 290, 291, 301, 308
- kerogen, 213, 276, 529–531, 546, 551
- lahars, 58, 159
- limestones, 313–381
 carbonate grains in, kinds of, 326–339
 carbonate microfacies, 365–366
 chemical composition of, 319
 chemistry of deposition, 371–374
 classification of, 347–354
 depositional environments of, 366–369
 isotope composition of, 319–325
 micrite in, 341–344
 mineralogy of, 314–319
 nonmarine carbonates, 374–381
 ooids in, 328–331
 sparry calcite in, 344–346
 structures and textures in, 354–364
- limonite, 113, 124, 206, 213, 307, 430
- liptinite, 537, 538, 539, 546
- lithic arenite, 139, 141, 151–159, 247, 290
- lithoclasts, 333–336, 367, 368, 519
- lithoherm, 416
- lumps (carbonate), 336, 337, 350, 368, 415
- lysocline
 aragonite, 412, 414
 calcite, 412–414
- macerals, 537–540, 546
- magadiite, 473, 490
- magmatic are provenances, 11, 13, 156, 178, 221, 247, 248, 254
- magnetite, 113, 124, 148, 307, 496, 502, 507
- marcasite, 136, 206, 213
- matrix, 112, 129, 132, 134, 139, 143
- mesodiagenesis (mesogenesis), 270, 280, 286, 290, 307, 308, 408
- micas, 112, 113, 122, 123
- micrite (defined), 341–344
- micrite envelope, 333, 411, 432, 435
- micritization, 333, 337, 371, 411
- microcline, 119, 120, 147, 237, 290
- mudcracks, 101, 163
- mudstone (carbonate), 352, 353
- mudstones and Shales, 194–219
 chemical composition of, 210
 classification of, 214, 215
 definition of, 194
 fissility in, 198
 method of study, 195
 microfabrics in, 197
 mineralogy of, 205
 organic matter in, 213
 sedimentary structures in, 202
 textures of, 196
- muscovite, 112, 122, 123, 142, 206, 209
- neomorphism, 300, 419, 420, 423, 444, 446, 447
- oil Shale, 542–547
 composition and classification of, 545
 origin of, 546
- oncoids, 331, 332, 350
- ooids, 328–331

- opal, 115, 117, 142, 206, 284, 285, 289, 301, 478, 479, 488, 489, 492
- organic matter, 128, 213, 276, 319, 527–529, 531, 540, 542, 550
- orthoclase, 119, 120, 237
- orthomatrix, 134
- overpressured-fluid zones, 431
- packing (of grains), 53, 54, 278, 279, 431
- packstone, 353, 359, 367, 432
- paleocurrent analysis, 58, 109, 221, 223
- paleomagnetism, 223, 225
- pebbly mudstone, 166, 192
- pellets, 99, 326, 327, 349, 518, 519
- permeability, 59, 61, 62, 402, 429
- perthite, 119, 120, 237
- petroleum, 547–553
 - composition of, 547
 - occurrence and distribution of, 548
 - origin of, 550–553
- phi scale, 22, 23
- phreatic zone, 378, 409, 410, 424, 425, 427
- phosphorites, 213, 461, 512–526
 - classification of, 518
 - deposition of, 520–524
 - kinds of, 520
 - mineralogy of, 516, 219
 - occurrence of, 513
 - stratigraphic characteristics of, 515
- phyllosilicates, 207, 208, 210
- plagioclase *see* (Feldspar)
- plate tectonics, 12, 246, 478
- point counting, methods of, 59
- polymorphic transformation, 301, 419, 420, 440, 444, 446, 449
- porcellanite, 482, 488, 492
- porosity, 59–62
 - In carbonate rocks, 451–455
 - In siliciclastic rocks, 278–280
- pressure solution (chemical compaction), 275, 278, 279, 294, 432–438
- protodolomite, 393, 394
- protomatrix, 132, 134
- provenance, 220–267
 - climate and relief (analysis of), 257–259
 - conglomerates and, 259
 - factors affecting interpretation of, 225
 - modeling of, 261
 - paleocurrent analysis and, 223
 - paleomagnetism and, 225
 - sandstones and, 229
 - shales and, 265
 - source-rock lithology and, 229–246
 - tectonic setting, 246–255, 264
 - tools for analysis of, 221–223
- pseudomatrix, 134, 162
- pseudomorphs' 298, 450
- pyrite, 496, 506, 508
- pyrobitumins, 553, 554
- pyroclasts, 159, 160, 189
- pyroxenes, 113, 147, 160, 307, 308
- quartz (general), 114–117
 - monocrystalline, 115, 116, 142, 251, 258
 - nonundulose, 142
 - overgrowths on, 116, 155, 273, 280, 283, 286, 289, 294
 - polycrystalline, 115–117
 - undulose, 142, 231
- quartz arenite, 139, 141–149, 247
- reactivation surfaces, 76
- recycling of sedimentary rocks, 9–11, 124, 173, 178, 247
- reefs, 364, 415–417
- replacement, force of crystallization- controlled, 295, 450
- rock fragments, 113, 125–130
- rudstone, 353, 367, 368
- rutile (ZTR Index), 125, 142
- sabkhas, 399, 472–474
- saddle dolomite, 388, 441
- salinas, 472, 473
- salt sieving, 276
- sampling (field), 16, 17
- sand crystals, 106, 107
- sandstones, 111–164
 - authigenic minerals in, 129
 - cement in, 130, 142, 148, 155
 - chemical composition of, 111, 134–138
 - classification of, 138–141
 - composition, 111
 - detrital grains in, 112
 - matrix in, 129–134
 - mineralogy of, 112–126
 - particle composition, 112
- sanidine, 119, 120, 237
- sapropels, 6, 528
- scanning electron microscopy, 314, 365
- sedimentary structures, 63–109
 - amalgamated beds, 66
 - ball and pillow structures, 85
 - beds and bed sets, 64, 67
 - Bouma sequence, 70
 - bounce, brush, prod, roll, and skip marks, 94
 - channels, 90
 - concretions and nodules, 104
 - cone-in-cone structure, 107
 - convolute bedding and lamination, 84
 - cross-bedding, 74

- sedimentary structures (cont.)
- current crescents, 96
 - dish and pillar structures, 89
 - flame structures, 85
 - flaser and lenticular bedding, 77
 - flute casts, 95
 - graded bedding, 70
 - groove casts, 93
 - hummocky cross-stratification, 79
 - laminae, 64
 - laminated bedding, 67
 - load casts, 97
 - massive bedding, 73
 - mudcracks, 101
 - parting lineation, 102
 - reactivation surface, 76
 - ripple cross-lamination, 76
 - ripple marks, 80
 - rip-up clasts, 88
 - sandstone dikes and sills, 103
 - scour-and-fill structures, 90
 - sole markings, 92
 - sparry calcite, 344–346
 - stromatolites, 91, 354
 - stylolites, 107
 - syneresis cracks, 101
 - synsedimentary folds, 86
 - trace fossils, 98–101
- sedimentary textures, 21–62
- seepage refluxion, 397
- sericite, 113, 147, 149, 297
- shale dewatering, 272, 429
- shales *see* (mudstones and shales)
- shards, 127, 159–161, 293, 305
- siderite, 8, 496, 502
- silica
- cement, 155, 283, 284, 289, 290
 - solubility of, 284, 285, 485
 - source of, 288, 289, 486
- sinter, siliceous, 482
- skeletal grains, 326, 337
- smectite, 113, 210, 275, 282, 306
- solid hydrocarbons, 553–554
- asphaltites, 553
 - asphalts, 553
 - native mineral waxes, 554
 - pyrobitumens, 554
- sparry calcite cement, 344–346
- spicularite, 483
- Stokes' Law, 24
- stromatactis, 355–361
- stromatolites, 91, 92, 354, 355
- stylolites, 107, 433–436, 441
- surface texture, 37, 49–51
- syntaxial overgrowths, 142
- carbonates, 345, 346
 - quartz, 116, 283, 286
- telodiagenesis (telogenesis), 270, 271, 308, 408
- tepee structure, 355, 361, 362
- textural inversion, 144, 367
- textural maturity, 52, 53, 141, 156, 349
- thrombolites, 358
- trace fossils, 98–101
- travertine, 376, 377
- tridymite, 114, 115, 117
- tufa, 376, 377
- tuffs, 159, 160, 482
- turbidites, 70–73, 158, 474
- Udden – Wentworth grain-size scale, 21, 22
- undulatory extinction, 114, 115, 230, 231
- vadose zone, 308, 333, 378, 422–425, 477
- vitrain, 536–538
- vitrite, 537–539
- volcanic glass, 206, 207
- volcaniclastic sandstones, 158–163
- zebra dolomite, 391, 392
- zeolites, 206, 303, 305
- zircon, 124, 125, 148, 245, 265
- zoned dolomite, 389, 390
- ZTR index, 125, 142, 148, 155